DELHI POLYTECHNIC
LIBRARY

CLASS NO. 621.3

BOOK NO. K 285 E

ACCESSION NO. 21001

DELHI COLLEGE OF ENGINEERING
Kashmere Gate, Delhi

◆

LIBRARY

DATE DUE

For each day's delay after the due date a fine of **10** P. per Vol. shall be charged for the first week, and **50** P. per Vol. per day for subsequent day. Text Book Re. **1.00**

Borrower's No.	Date Due	Borrower's No.	Date Due

EXPERIMENTAL ELECTRICAL ENGINEERING

VOLUME II

ELECTRICAL LABORATORY EXPERIMENTS

An abridgment of "Experimental Electrical Engineering" by The Late Vladimir Karapetoff, arranged and revised by Boyd C. Dennison. 487 pages. 6 by 9¼. 332 figures.

EXPERIMENTAL ELECTRICAL ENGINEERING

Vol. I. By The Late Vladimir Karapetoff. Fourth Edition revised by Boyd C. Dennison. 781 pages. 6 by 9. 431 figures.

Vol. II. By The Late Vladimir Karapetoff. Fourth Edition—revised by Boyd C. Dennison. 814 pages. 6 by 9¼. 930 figures.

Published by
JOHN WILEY & SONS, Inc.

EXPERIMENTAL

ELECTRICAL ENGINEERING

AND

MANUAL FOR ELECTRICAL TESTING

FOR ENGINEERS AND FOR STUDENTS IN
ENGINEERING LABORATORIES

VOL. II

BY
The Late V. KARAPETOFF
Professor Emeritus of electrical engineering, Cornell University

REVISED BY
BOYD C. DENNISON
Professor of electrical engineering,
Carnegie Institute of Technology

FOURTH EDITION — COMPLETELY REVISED AND RESET

NEW YORK
JOHN WILEY & SONS, INC.
LONDON: CHAPMAN & HALL, LIMITED

COPYRIGHT, 1907, 1911, 1927,
BY
V. KARAPETOFF

First Edition entered at Stationers' Hall

COPYRIGHT, 1941,
BY
VLADIMIR KARAPETOFF AND BOYD C. DENNISON

All Rights Reserved

*This book or any part thereof must not
be reproduced in any form without
the written permission of the publisher.*

SECOND PRINTING OCTOBER, 1948

Printed in U. S. A.

PREFACE TO THE FOURTH EDITION

This volume undertakes a more advanced study of certain subjects introduced, in their simpler aspects, in Volume I, and, in addition, includes material on a-c bridges, single-phase and polyphase commutator machines, mercury-arc rectifiers, transmission lines, magnetic contactor control, oscillographs, electronic devices, wave analysis, and high-frequency measurements. A knowledge of the subject matter of Volume I is assumed as well as the ability to deal with vectors and vector operators. In the words of Professor Karapetoff in the Preface to the Third Edition:

" No apology is offered for the use of Vector Analysis in the theory of induction machines and commutator motors. . . . Only the scalar product of vectors is used, and the necessary theory is given in the text, making it unnecessary to refer to a special book on the subject. The simplification in the deduction of circular loci by this method lies in the fact that the mode of procedure is purely analytical and automatic, doing away with a hit-or-miss search for equal angles, similar triangles, etc.

" While the description of oscillographs is segregated in a chapter, the use of an oscillograph is either specified or implied in many experiments throughout the book. A thoughtful student should be encouraged to obtain the actual wave-forms of currents and voltages with which he is working, in order to understand the secondary phenomena involved and to save weary hours of disappointment trying to reconcile ammeter or voltmeter readings with a simplified theory."

In the Fourth Edition every department of the text has been carefully reviewed in an attempt to supplement and clarify the theory, to make the instructions for experiments more complete and helpful, and to bring to date literature references and descriptions of specific apparatus. In order that illustrations might be more effective and the appearance of the text more pleasing, some three hundred new drawings and cuts have been made. The important subject of symmetrical components has been expanded, and the method has been applied to the solution of numerical problems involving unsymmetrical loads and transformer banks, and motors operating under abnormal conditions.

Among the new methods and types of apparatus described and treated theoretically are the Allen and Gross fault locater for overhead lines, and the Crocker-Wheeler adjustable-speed a-c motor. The treatment of electronics and high-frequency measurements has been greatly expanded in this edition. Thanks are due to Professor R. T. Gabler for undertaking this portion of the work. Thanks are due also to Professor G. R. Patterson who made most of the new drawings, and to the General Electric Company, the Westinghouse Company, Western Electric Company, Electric Controller and Manufacturing Company, J. G. Biddle Company, RCA, General Radio Company, and others, who supplied cuts or made helpful suggestions.

B. C. DENNISON

CARNEGIE INSTITUTE OF TECHNOLOGY
PITTSBURGH, PA.
November 1, 1940

CONTENTS OF VOLUME II

CHAPTER XXVI

ELECTROSTATIC CAPACITANCE

ARTICLE TITLE PAGE

584. Physical Concept of Capacitance 1
585 Examples of Capacitors in Practice 2
586. Factors Determining the Capacitance of Condensers 3
587. Standard Condensers 3
588. Condensers in Series and in Parallel 6
589. Methods of Comparison of Capacitances 9
590. Defects in Condensers 9
591. Direct-Deflection Method of Comparison of Capacitances 10
592. Calibration of a Condenser by the Direct-Deflection Method 12
593. Method of Mixtures (Thomson Zero Method) 12
594. Comparison of Capacitances by the Method of Mixtures 14
595. Current-Time Curves for Capacitance and Resistance in Series 14
596. Determination of Capacitance from Loss of Charge 17
597. Electrolytic Condensers — Construction and Uses 18
598. Measurement of Capacitance in Electrolytic Condensers . 19
599. Test of an Electrolytic Condenser 20

CHAPTER XXVII

CAPACITANCE AND INDUCTANCE IN A-C CIRCUITS

600. Capacitance and Effect of Wave Form 21
601. Capacitive Reactance and Susceptance 22
602. Capacitance and Resistance in A-C Circuits 23
603. The Imperfect Condenser 27
604. Tests of an Imperfect Condenser 28
605. Capacitance and Inductance in Series and in Parallel 29
606. Parallel (Current) Resonance 29
607. Effect of Resistance upon Current Resonance 32
608. Capacitance and Inductance in Parallel, Current Resonance 34
609. Series or Voltage Resonance 35
610. Capacitance and Inductance in Series, Voltage Resonance 37

CHAPTER XXVIII

ALTERNATING-CURRENT BRIDGES

611. Alternating-Current Bridges 39
612 The General Balanced A-C Bridge 39
613. The Fundamental Equations of a Balanced Bridge 41
614. Comparison of Two Inductances by Means of an A-C Bridge 42
615 Comparison of Two Inductances by Means of an A-C Bridge 43

ARTICLE TITLE PAGE
616 The Capacitance Bridge 43
617 The Schering Impedance Bridge 46
618 Dawes and Hoover High-Voltage Bridge 47
619 Comparison of Two Capacitances 48
620 Comparison of a Capacitance with an Inductance 49
621 The Anderson Bridge 50
622 Comparison of an Inductance with a Capacitance 51
623 Mutual Inductance Bridges 51
624 Comparison of a Mutual Inductance with a Self-Inductance 52
625 Comparison of a Mutual Inductance with a Capacitance 52
626 Comparison of Two Mutual Inductances 53
627 Frequency Bridges 53
628 A Capacitance-Type Frequency Bridge 54
629 The Leeds and Northrup Frequency Control Bridge 54
630 Frequency Bridges with Mutual Inductance and Capacitance 57
631 Frequency Measurements with an A-C Bridge 58
632 Need of Shielding in A-C Bridges 58
633 The Wagner Ground 59

CHAPTER XXIX

VOLTAGE REGULATION OF SHORT TRANSMISSION LINES

634 Definitions of Long and Short Transmission Lines 62
635 Superiority of Three-Phase Lines 62
636 General Relations 63
637 Distributed and Concentrated Characteristics of Lines 65
638 Analytical Solutions 66
639 Examples of Calculations on Nominal 'π' Line 68
640 Graphical Methods of Calculating Transmission Line Performance 70
641 The Mershon Diagram 72
642 Voltage Regulation of a Transmission Line of Negligible Capacitance 74
643 Voltage Regulation of a Transmission Line with Concentrated Capacitance 74

CHAPTER XXX

VOLTAGE REGULATION OF LONG TRANSMISSION LINES

644 Distributed Constants of Long Lines 76
645 Fundamental Equations of the Long Transmission Line 78
646 Special Case of the Direct-Current Line 82
647 Tests of a D-C Line with Distributed Constants 82
648 The Physical Meaning of the Propagation Constant 83
649 Methods of Computation 84
650 Examples of Transmission-Line Calculations 85
651 Summary of Equations for the Long Line 86
652 Determination of Line Constants from No-Load and Short-Circuit Tests 89
653 Tests of an Experimental Long Line 90
654 Quarter-Wavelength and Half-Wavelength Lines 91
655 Study of Quarter-Wave and Half-Wave Lines 93

CHAPTER XXXI

GROUND DETECTORS AND INSULATION MEASUREMENTS

ARTICLE TITLE PAGE

656 Types of Insulation Faults 95

657 Ground Detectors 95

658 Electrostatic Ground Detectors 95

659 Neon-Tube and Vacuum-Tube Ground Detectors 98

660 Ground Detectors in Low-Voltage Systems 100

661 Study and Calibration of Ground Detectors 101

662 Insulation Resistance of a Wire, Cable, or Winding 102

663 Measurement of Insulation Resistance on a " Dead Line — Voltmeter Method 103

664 Measurement of Insulation Resistance on a " Live ' Line — Voltmeter Method 104

665 Insulation Measurements by Means of a Galvanometer 105

666 Insulation Measurements Using a Voltmeter and a Galvanometer 106

667 The Megger Insulation Tester 107

668 Details of the Megger Insulation Tester 108

669 Insulation Measurements with a " Megger " 111

670 The " Bridge-Meg " Resistance Tester 112

671 Resistance Measurements with a " Bridge-Meg ' 112

CHAPTER XXXII

FAULT LOCATION ON LINES

672 Fault Location on Lines 114

673 Methods of Fault Location 114

674 Single-Conductor Tests 115

675 Fault Location on a Single-Conductor Line 118

676 Loop Tests 118

677 Loop Tests Based upon the Drop-of-Potential Method 119

678 Fault Location by the Drop-of-Potential Loop Method 120

679. Bridge Loop Tests 121

680 Exercises with Murray and Varley Loops 123

681 The Jamison-Higgett Loop for High-Resistance Faults 123

682 Localization of Total Break by Capacitance Measurement 124

683 Fault Location by the Capacitance Method 125

684 Tracing-Current Methods 125

685 Induction Localizers 126

686 Bullard's Method of Tracing Faults 129

687. Fault Location by Tracing-Signal Current 131

688 A Resonance Method of Fault Location 131

689 Theory of Fault Location by Varying Frequency 132

690 Fault Location by the Method of Varying Frequencies 135

CHAPTER XXXIII

CURRENT AND VOLTAGE RELATIONS IN Y-CONNECTED POLYPHASE SYSTEMS

691 Current and Voltage Relations in Polyphase Y-Connected Systems 138

692 Uses and Advantages of the Three-Phase System. 138

ARTICLE TITLE PAGE
693. Y-Connected Three-Phase System 139
694. Current and Voltage Relations in a Symmetical and Balanced Y-System 141
695. Unsymmetrical Unbalanced Y-System — Current Notation 142
696. Voltage Notation 143
697. *The Cyclic Order of Subscripts* *144*
698. *Solution for Currents in Unbalanced Case; Equivalent Y and Delta* *144*
699 *Current and Voltage Relations in the Unsymmetrical Y-Connected Three-Phase System* *145*
700. Methods of Determining Phase Sequence or Phase Rotation .. 147
701 Determination of Phase Sequence in a Three-Phase System 149
702 Unbalanced Y-System; Neutral-Voltage Method 149
703. Methods Based on the Principle of Superposition 151
704. Superposition of a Reversed Neutral Voltage 152
705. A Graphical Example of the Use of the Neutral-Voltage Method 153
706. An Analytical Example of the Use of the Neutral-Voltage Method 155
707. Study of an Unbalanced Y-System by the Neutral-Voltage Method 157
708. Effect of Mutual Inductance 157

CHAPTER XXXIV

SYMMETRICAL COMPONENTS IN THE ANALYSIS OF UNBALANCED THREE-PHASE SYSTEMS

709. Method of Symmetrical Components .. 160
710. Principles Underlying the Resolution of an Unsymmetrical Three-Phase System of Vectors into Phase-Sequence Components 161
711. Analytical Determination of Positive-, Negative, and Zero-Sequence Components 163
712. General Case of the N-Phase System 164
713 Graphical Determination of Phase-Sequence Components 165
714. Phase-Sequence Components of Line Currents and Voltages in an Unsymmetrical Three-Phase System 166
715. Line Potential and Phase Potential Sequence Components 168
716. Symmetrical Components of Impedances 168
717. Solution of Problems Involving Unbalanced Y-Connected Loads 170
718. A Study of Symmetrical Components in an Unbalanced Y-Connected System 172

CHAPTER XXXV

METHODS OF MEASUREMENT IN SYMMETRICAL COMPONENTS

719. Unbalance Factor. .. 174
720. Phase-Sequence Voltmeters (a) Zero-Sequence Component Absent 174
721. Value of Positive-Sequence Component .. 175
722. Value of Negative-Sequence Component 176
723. Simultaneous Readings of Opposite Phase-Sequence Components 177
724. Measurement of the Zero-Sequence Component of Voltage 179
725. Study of Phase-Sequence Voltmeters 180
726. Measurement of Symmetrical Components of Current 180
727. Bridge-Type Sequence Network . 182

ARTICLE TITLE PAGE
728 Proof of the Bridge-Network 183
729 Measurement of Zero-Sequence Current 185
730 Measurement of Phase-Sequence Component Currents 185
731. Real and Reactive Power Due to Currents and Voltages of Positive and Negative Sequence . . 186
732. Proof That Positive-Sequence Currents and Negative-Sequence Voltages Give Zero Power .. 188
733. Resolution of Three-Phase Unbalanced Power into Components of Positive and Negative Sequence 188

CHAPTER XXXVI

POWER MEASUREMENTS IN THREE-PHASE SYSTEMS

734 Power Measurement in Three-Phase Circuits 190
735 The Three-Wattmeter Method 190
736 The Two-Wattmeter Method 192
737. The Watt-Ratio Curve 193
738 Supplementary Proof of the Two-Wattmeter Method 195
739 The Single-Wattmeter Method 196
740 Exercises with the Two-Wattmeter and Single-Wattmeter Methods 197
741 Reactive-Component Wattmeters 198
742 Measurement of Reactive Power in a Three-Phase System 202

CHAPTER XXXVII

THREE-PHASE DELTA, V-, AND T-CONNECTED SYSTEMS

743. Three-Phase Delta, V-, and T-Connected Systems 204
744 Delta Connection, Current and Voltage Notation 205
745. Relation between Delta and Y Currents in a Balanced System 206
746 Unbalanced Delta System 207
747. Study of Delta-Connected Systems 208
748 Equivalent Unbalanced Delta and Y Combinations 209
749. Study of Equivalent Y and Delta Impedances 211
750 V Connection 212
751. V Connection of Transformers 213
752 The General Case of Unbalanced V Connection 214
753 Electrical Relations in a V-Connected Three-Phase Circuit 216
754 T Connection .. 216
755. T Connection of Transformers.. 218
756 Parallel Delta- and T-Connected Transformer Banks — Symmetrical Component Solution 219
757 Electrical Relations in a T-Connected Three-Phase Circuit 221

CHAPTER XXXVIII

TWO-PHASE AND QUARTER-PHASE SYSTEMS

758 Two-Phase and Quarter-Phase Systems 222
759 Two-Phase, Three-Wire Systems 222
760. Electrical Relations in Two-Phase Systems.. . 225

ARTICLE TITLE PAGE
761. The Neutral-Voltage Method of Solution of Unbalanced Two-Phase Systems .. 226
762. Quarter-Phase Star-Connected Systems 226
763. Electrical Relations in Quarter-Phase Star-Connected Systems . 227
764. Quarter-Phase Mesh-Connected Systems .. 228
765. Electrical Relations in Quarter-Phase Mesh-Connected Systems 229

CHAPTER XXXIX

POLYPHASE TRANSFORMATIONS AND CONVERSIONS

766 Polyphase Transformations and Conversions 230
767. Three-Phase to Three-Phase Transformation 230
768. Exercises in Three-Phase to Three-Phase Transformation 232
769. Paralleling Three-Phase Transformers 233
770. Exercises in Paralleling Three-Phase Transformers 234
771 The T or Scott Connection 234
772. Unbalancing of Voltages with the Scott Connection 235
773. Study of the Scott Two-Phase to Three-Phase Transformation 236
774. Various Methods of Three-Phase to Two-Phase Transformation 237
775. Study of Various Two-Phase to Three-Phase Transformations 238
776. Six-Phase System .. 239
777. Electrical Relations in a Balanced Six-Phase System 240
778. Transformation from Three-Phase (or Two-Phase) to Six- and Twelve-Phase 240
779. Study of Transformations from Three-Phase and Two-Phase to Six-Phase 244
780. General Transformations of Polyphase Systems 245
781. Energy Relations in Polyphase Transformations 246
782. Transformation from Balanced Polyphase to Single-Phase System or Vice Versa .. 247

CHAPTER XL

HARMONICS IN POLYPHASE SYSTEMS

783. Harmonics in Polyphase Systems 249
784. Harmonics That Are Multiples of Three, or Triplen Harmonics 249
785. Oscillating Neutral 251
786 Harmonics Other Than Multiples of Three, or Non-Triplen Harmonics 252
787 Harmonics Caused by Saturation in Transformer Cores . 253
788. Triplen Harmonics in the Neutral Return 256
789. Harmonics in Y-Connected System 257
790. Triplen Harmonic Currents in Delta-Connected Windings 257
791. Triplen Harmonic Currents in a Delta-Connected Winding 259
792. Superposed Transmission over a Three-Phase Line 259
793. Superposition of Uniphase Transmission between Three-Phase Neutrals 260
794. Harmonics in a Symmetrical M-Phase System 261
795. Inductive Coordination between Power and Communication Circuits 261
796. Study of Inductive Interference between Power and Communication Circuits 261

CHAPTER XLI

PERFORMANCE DIAGRAMS OF NON-SALIENT-POLE MACHINES

ARTICLE TITLE PAGE
797. Performance Diagrams of Non-Salient-Pole Machines 263
798. Phase-Angle Notation 264
799. The Potier Diagram 265
800. Torque Angle and Synchronizing Power 268
801. Experimental Study of Potier Diagram 269
802. Unsaturated Machine 269
803. Locus Diagram of the Unsaturated Machine 271
804. Performance Characteristics of an Unsaturated Synchronous Machine 273
805. Saturated Machine 274
806. The Potieron 276
807. Synchronous Machine Charts Involving Circular Loci 277
808. Performance Characteristics of a Saturated Non-Salient-Pole Alternator 281

CHAPTER XLII

DIRECT AND TRANSVERSE ARMATURE REACTION IN SALIENT-POLE SYNCHRONOUS MACHINES

809. Purpose of the Chapter on Armature Reaction 282
810. The Magnetomotive Force of Alternating-Current Windings 282
811. Breadth and Pitch Factors 284
812. Example of the Effect of Distribution of the Winding upon the MMF Wave Form 285
813. Combined MMF of Distributed Polyphase Windings — Rotating Magnetic Field 286
814. Transverse Armature Reaction 288
815. Direct Armature Reaction 289
816. Direct and Transverse Components of Armature Current 290
817. Direct and Transverse Reaction Coefficients 291
818. Experimental Study of Armature Reaction 293
819. Measurement of Direct Reaction 296
820. Measurement of Transverse Reaction 297
821. Magnetic Leakage between Field Poles 298
822. Measurement of Pole Leakage in a Synchronous Machine 299

CHAPTER XLIII

PERFORMANCE DIAGRAMS OF SALIENT-POLE SYNCHRONOUS MACHINES

823. The Blondel Diagram 301
824. Special Cases of $\phi = 0$ and $\phi = -\theta$ 305
825. Comparison of Actual Performance with the Graphical Solution of the Blondel Diagram 306
826. Analytical Solution 307
827. Power as a Function of the Torque Angle 308
828. Comparison of Actual Performance with the Analytical Solution of the Blondel Diagram 309
829. The Blondelion 309
830. Performance at a Constant Field Current 309

ARTICLE TITLE PAGE
831. Locus Diagrams with Sectionalized Saturation Curve . 311
832. The Value of the Direct Reaction from the Straight-Line Saturation Curve 313
833. The Circle Diagram for Constant Terminal Voltage and Constant Armature Current — Sectionalized Saturation .. 313
834. Locus Diagrams for Constant Armature Current and Constant Excitation 315
835. The Locus at a Constant Terminal Voltage and Constant Field Current 316
836. Locus Diagram for Constant Power 316
837. Locus Diagrams of a Salient-Pole Synchronous Machine Studied in Connection with a Sectionalized Saturation Curve 317
838. Influence of the Armature Resistance 318
839. Correction for Variable Leakage Reactance .. 318

CHAPTER XLIV

THE SYNCHRONOUS MOTOR — OPERATING FEATURES

840. The Synchronous Machine as a Motor .. 323
841. Elementary Explanation of the Action of the Synchronous Motor 323
842. Performance Characteristics 325
843. Operation as a Synchronous Condenser 327
844. Theory of the Synchronous Motor V Curve 327
845. Proof that the Locus of the Current Vector Is a Circle .. 328
846. Circular Loci for Constant Mechanical Power 329
847. V Curves from the Circle Diagram . . 331
848. V Curves of a Synchronous Motor . .. 331
849. Example of the Synchronous Motor as a Synchronous Condenser 332
850. Improved Power Factor and Voltage Regulation by Means of a Synchronous Condenser 334
851. The Displacement Angle 334
852. Experimental Determination of the Torque Angle .. 336
853. Measurement of the Torque Angle in a Synchronous Machine 337
854. Hunting of Synchronous Machines 337
855. Damper Winding . 338
856. Study of Hunting of a Synchronous Motor 339
857. Starting of Synchronous Motors .. 339
858. Starting a Synchronous Motor by Means of an Auxiliary Induction Motor 340
859. Starting with a Squirrel-Cage Winding . 341
860. Exercises in Starting a Squirrel-Cage Synchronous Motor 342
861. Additional Methods of Starting Large Synchronous Motors 343
862. Theory of Starting and Pulling into Step 344
863. Induction-Start Synchronous Motors 344
864. Self-Excited Synchronous Induction Motor (Fynn-Weichsel) 345
865. Study of Fynn-Weichsel Self-Excited Synchronous Induction Motor. 347

CHAPTER XLV

THE SYNCHRONOUS CONVERTER — OPERATING FEATURES

866. The Synchronous Converter 350
867. General Description . 350
868. Induced Voltages . .. 352

ARTICLE TITLE PAGE
869. Ratio of No-Load Voltages in a Synchronous Converter.... 354
870. Ratios of Direct and Alternating Currents.... 354
871. Operation of the Rotary Converter.... 355
872. Armature Reaction in the Rotary Converter.... 356
873. Methods of Starting.... 358
874. Special Features of Starting.... 359
875. Practice in Starting Rotary Converters.... 360
876. Operation of the Synchronous Converter from the A-C Side.... 362

CHAPTER XLVI

THE SYNCHRONOUS CONVERTER (*Continued*)

877. Methods of Controlling Direct-Current Voltage.... 364
878. Combination of Series Field and Series Reactance.... 365
879. Compounding a Synchronous Converter by Means of Series Reactance 367
880. Synchronous-Booster Converter.... 368
881. Study of a Booster Converter.... 370
882. The I^2R Loss in a Converter Armature.... 370
883. Oscillographic Study of Armature Currents in a Synchronous Converter 373
884. High-Reluctance Commutating Poles.... 374
885. Other Means of Preventing Flashing.... 375
886. Hunting.... 375
886a. Hunting of a Synchronous Converter and Remedies Therefor.... 376

CHAPTER XLVII

THE APPROXIMATE CIRCLE DIAGRAM OF THE INDUCTION MOTOR

887. The Approximate Circle Diagram of the Polyphase Induction Motor.. 378
888. Proof of the Circular Locus of Currents in the Approximate Equivalent Circuit.... 378
889. Experimental Determination of the Current Locus in a Polyphase Induction Motor.... 379
890. Performance Items from the Circle Diagram.... 379
891. A Check upon the Relation between Slip and Rotor I^2R Loss.... 382
892. Rotor Ohmic and Effective Resistances.... 383
893. Special Scales for Use with the Circle Diagram.... 383
894. Some Other Methods of Predicting Induction Motor Performance.... 386
895. Effect of Rotor Resistance upon Motor Performance.... 388
896. Effects of Varying Applied Voltage.... 389
897. Effects of Changing Frequency.... 390
898. Speed Control of the Induction Motor by Tests and as Predicted from the Circle Diagram.... 392
899. The Induction Generator.... 393
900. Theory of the Induction Generator.... 394
901. The Circle Diagram of the Induction Generator.... 396
902. Load Characteristics of a Polyphase Induction Generator.... 396
903. Parallel Operation of Induction and Synchronous Generators.... 397
904. Braking of Induction Motors.... 397
905. Study of Various Methods of Braking Induction Motors.... 398

ARTICLE TITLE PAGE

906 The Performance of Polyphase Induction Motors on an Unsymmetrical Voltage Supply 399

907. Notation for Solution by Symmetrical Components 399

908. Analytical Solution of the Unbalanced Case 401

909 The Circle Diagram Applied to the Case of Unbalanced Voltages 402

910 Operation of a Polyphase Induction Motor on an Unsymmetrical Voltage Supply 403

APPENDIX Proof of the Circle Diagram Based on Fluxes and MMF's 404

CHAPTER XLVIII

THE EXACT CIRCLE DIAGRAM

911 The Exact Circle Diagram 407

912 Ho's Theorem 407

913 First Proof of Ho's Theorem 409

914. Second Proof of Ho's Theorem 410

915 Circle Diagram Derived from Ho's Theorem 411

916 Other Characteristic Quantities Derived from Ho's Theorem 413

917 Derivation of Induction Motor Characteristics from an Exact Circle Diagram 414

918 Equation of a Circle in Vector Algebra 415

919 Diagram of Currents and Fluxes, with Correction for the Ohmic Drop 417

920. A Proof of the Circle Based on Vector Algebra 418

921 Change from an Approximate to an Exact Circle Diagram 420

922 Effect of the Primary Resistance upon the Circle Diagram of the Polyphase Induction Motor 421

923 Bibliography on the Circle Diagram and Analytical Theory 421

CHAPTER XLIX

REGENERATIVE SPEED AND POWER-FACTOR CONTROL OF POLYPHASE INDUCTION MOTORS

924 Speed and Power-Factor Control of Polyphase Induction Motors 424

925 Cascade or Concatenation 424

926 Cumulative and Differential Cascade 425

927. Speed Control of Induction Motors by Concatenation 428

928 Speed Control by External EMF Applied to the Secondary 428

929. Explanation by Means of Equivalent Diagrams 429

930 Classification of Methods of Dynamic Speed Control 430

931 Electronic Speed Control . 434

932 Power-Factor Control 435

933 An External EMF Leading the Secondary Voltage 436

934 Explanation by Means of an Equivalent Diagram 437

935 Various Types of Commutating Machines 438

936 Generalized Rotary Converter 438

937. The Polyphase Commutator Machine 440

938 Commutator-Type Frequency Converter 441

939. The Commutator-Type Phase Advancer 443

940 The Self-Excited or Series-Excited Phase Advancer 444

ARTICLE TITLE PAGE

941 Separately Excited Phase Advancer 445
942. The Kapp Vibrator 446
943 An Experiment in Dynamic Speed Control 447

CHAPTER L

DIVERSE TOPICS ON ASYNCHRONOUS MACHINES

944 The Induction Machine as a Frequency Converter 450
945 Induction-Type Frequency Converter, Secondary Voltage and Frequency at No Load 452
946 General A-C Transformer under Load 452
947 Induction-Type Frequency Converter Load Test, Characteristics at Constant Primary Voltage 453
948 Induction-Type Frequency Converter, Characteristics at Constant Secondary Voltage (Compounding Curve) 454
949 The Operating Ranges of a General A-C Transformer 454
950 Induction Regulators 455
951 Single-Phase Induction Regulator 455
952 Automatic Operation — Line Drop Compensator and Contact-Making Voltmeter 457
953 Study of a Single-Phase Induction Regulator and Auxiliary Devices 458
954 Polyphase Induction Regulator 459
955 Study of a Polyphase Induction Regulator and Phase Shifter 460
956 Operation under Abnormal Conditions 460
957. Three-Phase Induction Motor with Single-Phase Rotor — Analysis by the Method of Symmetrical Components 461
958. The Equivalent Circuit for the Positive-Sequence Quantities 462
959 The Equivalent Circuit for Negative-Sequence Quantities. 463
960 The Combined Equivalent Circuit 464
961. Analytical Solution of the Equivalent Circuit 465
962 Operation at Voltages below and above the Rated Voltage 467
963 Effect of Voltage and Flux Harmonics 467
964 Fluctuating Load and Short-Circuit 468
965 Unsymmetrical Terminal Voltages 468
966 Characteristics of an Induction Machine 468
967. References 469

CHAPTER LI

THE SINGLE-PHASE INDUCTION MOTOR

968 The Single-Phase Induction Motor 470
969 Theory of Two Oppositely Rotating MMF's 470
970. Two Stators Acting on the Same Rotor 471
971 Operating Characteristics 472
972 The Secondary Copper Loss 474
973. Resolution of the Air-Gap Field in a Single-Phase Induction Motor into Two Revolving Components 474
974 Performance Characteristics of a Twin Polyphase Induction Motor Equivalent to a Single-Phase Machine 475

ARTICLE TITLE PAGE
975. The Calculation of the Performance of Single-Phase Induction Motors by the Method of Symmetrical Components........................ 475
976. Operation of a Three-Phase Induction Motor on Single-Phase Supply . 475
977. Numerical Example of a Three-Phase Motor on Single-Phase Supply.. 478
978. Performance of the Induction Motor Operating on Single-Phase, by Test and by Calculation.. 479
979. The Quadrature-Flux or Cross-Field Theory.......................... 480
980. Transformer and Rotational EMF's Induced in the Rotor........... 481
981. The Vector Diagram of the Single-Phase Induction Motor........... 482
982. Fundamental EMF Equations.. 484
983. Motor and Generator Action... 485
984. The Rotating Magnetic Field... 485
985. Performance Calculations.. 485
986. A Study of Vector Relations Involved in the Quadrature-Flux Theory of the Single-Phase Induction Motor............................. 486
987. The Circle Diagram Theory — The Five Fundamental Relations..... 487
988. The Five Fundamental Equations.. 488
989. Solution for the Primary Current... 490
990. An Equation of the Circular Locus....................................... 491
991. The Circle Diagram of a Single-Phase Induction Motor.............. 491
992. References.. 492

CHAPTER LII

SINGLE-PHASE COMMUTATOR-TYPE MOTORS

993. The Single-Phase Commutator-Type Motor.............................. 493
994. The Series Motor.. 494
995. Compensation of Armature Reaction..................................... 495
996. Difficulties in Commutation.. 496
997. Performance Characteristics... 498
998. Analytical Theory... 499
999. The Circle Diagram... 501
1000. Study of the Single-Phase Series Commutator Motor............... 501
1001. The Repulsion Motor.. 502
1002. The Principle of Action with Two Separate Field Windings......... 502
1003. Repulsion Motor with One Field Winding.............................. 504
1004. Conditions at Start... 505
1005. Analytical Theory and the Circle Diagram.............................. 506
1006. Study of the Single-Phase Repulsion Motor............................ 508
1007. Compensated Repulsion Motor... 508
1008. Properties of Armature Excitation... 509
1009. Analytical Theory... 510
1010. Study of the Compensated Repulsion Motor............................ 511
1011. Compensated Repulsion Motor with Brush Shift...................... 511
1012. Study of the Brush-Shifting Compensated Repulsion Motor.......... 513
1013. The Repulsion-Induction Motor.. 513
1014. Commutation Strips.. 515
1015. Vector Diagram and Improvement in Power Factor................... 515
1016. Study of the Single-Phase Repulsion-Induction Motor............... 517
1017. Shunt-Type Motors with Two Sets of Brushes......................... 517

ARTICLE TITLE PAGE
1018. Commutator-Type Induction Motor . 518
1019. Speed Control . .. 519
1020. Phase Compensation .. 520
1021. Starting and Reversing 521
1022. Study of the Single-Phase Commutator Motor of the Shunt Type with Two Sets of Brushes 522
1023 References 522

CHAPTER LIII

POLYPHASE COMMUTATOR MOTORS

1024 Polyphase Commutator Motors 523
1025. Arrangements of Parts and Electrical Connections 524
1026. The Diagram of MMF's 525
1027. The Diagram of EMF's 527
1028 Analytical Theory 529
1029 The Series-Connected Motor 530
1030 Study of a Polyphase Series Commutator Motor 531
1031. The Shunt-Connected Motor 532
1032. Study of a Polyphase Shunt-Connected Motor 533
1033. The Schrage Machine .. 533
1034. The Windings and Brush Shift 533
1035. The Magnitude and Phase of the EMF Impressed upon the Stator Winding at No Load 535
1036 Operating Characteristics 537
1037 The Starting Torque and Current 538
1038 The Vector Diagram of MMF's 538
1039 The Vector Diagram of EMF's .. 540
1040 Analytical Theory and the Circle Diagram 541
1041. Study of the Schrage Machine 542
1042. The Crocker-Wheeler Adjustable-Speed Induction Motor 542
1043 Operating Characteristics 543
1044. Rotor Induced EMF's 543
1045 Performance from the Equivalent Circuits 546
1046. Bibliography on A-C Commutator Motors 549

CHAPTER LIV

D-C MOTOR CONTROLLERS

1047. Magnetic Contactor Control for D-C Motors 551
1048. Functions of Magnetic Switches 551
1049. The Electromagnetic Contactor 553
1050. How to Read Contactor Diagrams . 554
1051. Elementary Exercises with Non-Automatic Magnetic Contactors 556
1052 Counter-EMF Method of Acceleration 557
1053. Current-Limit Methods of Acceleration, Series Lockout 557
1054. Current Limit by Series Relays . . 560
1055. Drop-across-Resistance Method .. 561
1056. Time-Limit Acceleration 562
1057. Overload and Under voltage Protection 566

ARTICLE TITLE PAGE

1058. Automatic Acceleration of a D-C Motor by Means of Magnetic Contactors 567
1059. Electronic Control Devices 568
1060. A Time Delay Relay 568
1061 A Thyratron Motor Speed Controller 570
1062 Control by Electronic Devices 571
1063 References 571

CHAPTER LV

CONTROLLERS FOR A-C MOTORS

1064 Polyphase Induction Motor Control 573
1065 Across-the-Line Starters 573
1066. Study of Across-the-Line Starters 576
1067. Primary-Resistance Starters — Manual 576
1068. Primary-Resistance Starters — Magnetic 577
1069 Study of Induction Motor Starters of the Primary-Resistance Type 578
1070 Reduced-Voltage Starters 578
1071. Manually Operated Auto-Starter 581
1072. Reduced-Voltage Starters of the Magnetic-Contactor Type 582
1073 Protection against Phase Failure and Phase Reversal 585
1074 Study of Induction-Motor Starters of the Auto-Transformer Type 585
1075 Rheostatic Control in the Secondary Circuit 586
1076 A Drum Controller 586
1077 Contactor-Type Controllers for Wound-Rotor Motors 588
1078 Details of an Automatic Contactor-Type Controller 588
1079 Liquid Rheostats and Slip Regulators 590
1080 Study of Induction-Motor Controllers of the Secondary-Resistance Type 593
1081 Automatic Starters for Synchronous Motors 594
1082 Typical Full-Voltage Starter 594
1083 Reduced-Voltage Starter for Synchronous Motors 597
1084 Study of Magnetic-Contactor Starters for Synchronous Motors 598
1085 References 598

CHAPTER LVI

MERCURY-ARC RECTIFIERS

1086 Mercury-Arc Rectifiers 600
1087 Fundamental Connections 600
1088 Unidirectional Conduction 602
1089 Internal Voltage Drop in a Mercury-Vapor Arc 604
1090 Means for Increasing Arc Stability 605
1091 External Current and Voltage Relations in the Single-Phase Mercury-Arc Rectifier 606
1092 Commercial Battery-Charging Rectifiers 607
1093 Load Test on a Single-Phase Mercury-Arc Rectifier 611
1094 Steel-Tank Rectifiers 612
1095. Effect of Number of Anodes 615
1096 Rectifiers in Parallel 616
1097 Elementary Current and Voltage Relations 618

ARTICLE TITLE PAGE
1098 Effect of Inductance in the Anode Circuits .. 620
1099. Voltage Control of Rectifiers .. 622
1100 Ignitron-Type Mercury-Arc Rectifier . .. 623
1101. Harmonics in the Rectified Waves 624
1102. Harmonic Components of the Anode Currents 626
1103. Study of Rectifier Wave Forms 627
1104 The Vreeland Oscillator .. 627
1105 Study of the Vreeland Oscillator 630
1106 References 630

CHAPTER LVII

THE OSCILLOGRAPH

1107. The Oscillograph 631
1108. Applications of the Oscillograph 631
1109. Classification of Oscillographs 632
1110. Electromagnetic Oscillograph 633
1111. The Galvanometer 633
1112. Optical System .. 634
1113. Recording Apparatus 635
1114. Electric Circuits 636
1115 String-Galvanometer Oscillograph 637
1116 Transient Visualizer 638
1117 Demonstration Oscillograph 639
1118 The Use of a Vacuum-Tube Amplifier with an Oscillograph 640
1119 Experimental Comparison of Vibrator Constants 641
1120 Study and Use of the Electromagnetic Oscillograph 642
1121 The Cathode-Ray Oscillograph . 643
1122 The Braun Tube (Cold-Cathode Oscillograph) 644
1123 Hot-Cathode Oscillograph 645
1124 Sweep-Frequency Control 647
1125. Study and Use of the Hot-Filament Cathode-Ray Oscillograph 648
1126 The Dufour-Type Cathode-Ray Oscillograph 649
1127 Modified Dufour-Type Oscillograph 650
1128. Norinder-Relay Oscillograph 651
1129 Timing Systems 652
1130 Study and Use of the Dufour-Type Cathode-Ray Oscillograph 653
1131 References to the Oscillograph 653

CHAPTER LVIII

HARMONIC ANALYSIS OF PERIODIC WAVES

1132. Harmonic Analysis of Periodic Waves 655
1133. Theory of the Fourier Series 656
1134. Waves with Odd Harmonics Only . 657
1135. Sine and Cosine Components of Harmonics 658
1136 Fundamental Rules Applying to Wave Analysis 660
1137. Determination of Coefficients A_n and B_n 661
1138 A Property of Equidistant Ordinates 662
1139 Sums of Sines and Cosines of Angles Differing by Equal Increments 663

ARTICLE TITLE PAGE
1140. Practical Methods of Harmonic Analysis 664
1141. Experimental Separation of Harmonics 664
1142. Instrumental and Mechanical Methods of Wave Analysis 665
1143. Analytical Methods of Wave Analysis 666
1144. Graphical Analysis of Periodic Waves 668
1145. Chaffee Simplified Method of Harmonic Analysis 668
1146. Practice in Analysis of Periodic Waves 672
APPENDIX. Tables for the Analysis of Periodic Waves 673

CHAPTER LIX

FUNDAMENTALS OF ELECTRONIC DEVICES

1147. Fundamentals of Electronic Devices 677
1148. Electrons in Metals 677
1149. Thermionic Emission 678
1150. Thermionic Cathodes 680
1151. Cathode Efficiencies 681
1152. Measurement of Emission Characteristics of Hot Cathodes 683
1153. Photoelectric Emission 684
1154. Color Response and Selective Effects 685
1155. Determination of the Characteristics of a Photoemissive Cell 686
1156. Motion of Ions and Electrons in Electric and Magnetic Fields 688
1157. Motion in a Uniform Electric Field 688
1158. Motion in a Uniform Magnetic Field 688
1159. Generalized Equations of Motion 689
1160. Motion in Combined Electric and Magnetic Fields 690
1161. Change of Electron Mass with Velocity 692
1162. Electron Optics 692
1163. Applications of the Equations of Motion 693
1164. The Magnetron 694
1165. Use of the Magnetron to Measure e/m or B 696
1166. High-Vacuum Diodes — Definition 697
1167. Plate Current-Voltage Relation 698
1168. Child's Law 699
1169. Types of High-Vacuum Diodes 700
1170. Measurement of Diode Parameters 701
1171. Rectification with the Diode 702
1172. Determination of Rectifier Regulation and Hum Percentage 704
1173. Rectifier Circuits 705
1174. Rectifier-Filter Design 706
1175. Test of a Three-Phase Rectifier Filter 709
1176. High-Vacuum Triodes 710
1177. Potential Distribution in a Triode 710
1178. Static Characteristic Curves 711
1179. Symbols Used in Electronic Theory 712
1180. Plate-Current Equation 713
1181. Triode Parameters 714
1182. Determination of Static Characteristics and Evaluation of Parameters of Triodes 715
1183. Dynamic Characteristics of Triodes 717

ARTICLE TITLE PAGE
1184. Triode Characteristics with an Impedance Load 719
1185. Measurement of Triode Parameters by the A-C Bridge Method 720
1186. Multielectrode Vacuum Tubes 723
1187. Determination of Static Characteristics of a Tetrode and a Pentode 726
1188. Beam Power Tubes 727
1189. Measurement of Multielectrode-Tube Parameters by A-C Methdds 728
1190. Class A Amplifiers 729
1191. Measurement of Gain of a Resistance-Capacitance Coupled Amplifier 732
1192. Amplifier Distortion 733
1193. Power Amplifiers 735
1194. Measurement of Power Output and of Distortion 736
1195. Gaseous Conduction 737
1196. Gaseous Rectifiers 744
1197. Voltage Drop through a Hot-Cathode Mercury-Vapor Tube 745
1198. Voltage Regulation and Hum in a Full-Wave Rectifier Using Phanotrons 745
1199. Grid-Controlled Rectifiers 746
1200. Grid Control Characteristics of a Thyratron Tube 747
1201. Determination of Control Characteristics of a Cold-Cathode Grid-Glow Tube 748
1202. Operation of Thyratrons with A-C Plate Voltage Supply 749
1203. Control of Plate Current in a Thyratron by Changing D-C Grid Voltage 751
1204. Control of Average Plate Current in a Thyratron by Changing the Phase of the A-C Grid Voltage 751
1205. Principle of the Mercury-Arc Rectifier 752
1206. Test of an Ignitron Controlled by a Thyratron 753
1207. Photoelectric Cells 754
1208. Characteristics of a Gas-Filled Phototube 756
1209. Characteristics of a Photovoltaic Cell 756
1210. Spectral Response of a Photocell 756

CHAPTER LX

HIGH-FREQUENCY MEASUREMENTS

1211. Introduction to High-Frequency Measurements 759
1212. Meters and Apparatus for High-Frequency Measurements 760
1213. Frequency Measurement 761
1214. Calibration of a Heterodyne Frequency Meter or Tuned-Circuit Wavemeter by a Standard-Frequency Source 769
1215. Methods of Measuring Frequencies in the Audio Range 771
1216. Calibration of an Audio-Frequency Oscillator 772
1217. Measurement of Ultra-High Frequencies 774
1218. Apparent Inductance in Iron-Cored Coils carrying Direct Current 774
1219. Measurement of Inductance in an Iron-Cored Coil 775
1220. Inductance Coils 777
1221. Measurement of Apparent Inductance, True Inductance and Capacitance of a Coil 779
1222. Condensers at High Frequencies 780
1223. Capacitance and Phase Angle of a Condenser by the Substitution Method 781
1224. Resistance of Conductors at High Frequencies 783

ARTICLE	TITLE	PAGE
1225.	Measurement of Resistance by Reactance Variation and Resistance Variation ..	784
1226.	Measurement of High Resistance at High Frequencies ..	786
1227.	Properties of Lines and Filters	787
1228.	Equivalent Networks.	790
1229.	Calibration of an Attenuator and Design of a Power-Level Indicator	792
1230.	Characteristics of Four-Terminal Networks ..	793
1231.	Electromechanical Systems	796
1232.	Measurements on a Telephone Receiver	798
1233.	Noise Measurement	799
1234.	Measurement and Analysis of Machinery Noise	800
1235.	Antenna Measurements	800
1236	Measurements of Antenna Impedance	802
1237.	Other Experiments	803
	INDEX	805

LIST OF EXPERIMENTS IN VOLUME II

CHAPTER XXVI

ELECTROSTATIC CAPACITANCE

EXPERIMENT PAGE

26-A. Calibration of a Condenser by the Direct-Deflection Method 12
26-B. Comparison of Capacitances by the Method of Mixtures 14
26-C. Determination of Capacitance from Loss of Charge 17
26-D. Test of an Electrolytic Condenser 20

CHAPTER XXVII

CAPACITANCE AND INDUCTANCE IN A-C CIRCUITS

27-A. Capacitance and Resistance in A-C Circuits 23
27-B. Tests of an Imperfect Condenser 28
27-C. Capacitance and Inductance in Parallel; Current Resonance 34
27-D. Capacitance and Inductance in Series; Voltage Resonance 37

CHAPTER XXVIII

ALTERNATING-CURRENT BRIDGES

28-A. Comparison of Two Inductances by Means of an A-C Bridge 43
28-B. Comparison of Two Capacitances 48
28-C. Comparison of an Inductance with a Capacitance 51
28-D. Comparison of a Mutual Inductance with a Self-Inductance 52
28-E. Comparison of a Mutual Inductance with a Capacitance 52
28-F. Comparison of Two Mutual Inductances 53
28-G. Frequency Measurements with an A-C Bridge 58

CHAPTER XXIX

VOLTAGE REGULATION OF SHORT AND MEDIUM-LENGTH TRANSMISSION LINES

29-A. Voltage Regulation of a Transmission Line of Negligible Capacitance . . 74
29-B. Voltage Regulation of a Transmission Line with Capacitance Concentrated at the Ends 74

CHAPTER XXX

VOLTAGE REGULATION OF LONG TRANSMISSION LINES

30-A. Tests of a Direct-Current Line with Distributed Constants 82
30-B. Tests of an Experimental Long Line 90
30-C. Study of Quarter-Wave and Half-Wave Lines 93

CHAPTER XXXI

GROUND DETECTORS AND INSULATION MEASUREMENTS ON ELECTRIC LINES

EXPERIMENT PAGE
31-A. Study and Calibration of Ground Detectors........................ 101
31-B. Insulation Measurements Using a Voltmeter and a Galvanometer....... 106
31-C. Insulation Measurements with a Megger Insulation Tester........... 111
31-D. Resistance Measurements with a " Bridge-Meg "................... 112

CHAPTER XXXII

FAULT LOCATION ON LINES

32-A. Fault Location on a Single-Conductor Line........................ 118
32-B. Fault Location by the Drop-of-Potential Loop Method.......... 120
32-C. Exercises with Murray and Varley Loops........................ 123
32-D. Fault Location by the Capacitance Method...................... 125
32-E. Fault Location by Tracing-Signal Current........................ 131
32-F. Fault Location by the Method of Varying Frequencies.............. 135

CHAPTER XXXIII

CURRENT AND VOLTAGE RELATIONS IN POLYPHASE Y-CONNECTED SYSTEMS

33-A. Current and Voltage Relations in a Balanced and Symmetrical Y-System 141
33-B. Current and Voltage Relations in an Unsymmetrical Y-Connected Three-Phase System.. 145
33-C. Determination of the Phase Sequence in a Three-Phase System...... 149
33-D. Study of an Unbalanced Y-System by the Neutral-Voltage Method.... 157

CHAPTER XXXIV

SYMMETRICAL COMPONENTS IN THE ANALYSIS OF UNBALANCED POLYPHASE SYSTEMS

34-A. Study of Symmetrical Components in an Unbalanced Y-Connected System.. 172

CHAPTER XXXV

METHODS OF MEASUREMENT IN SYMMETRICAL COMPONENTS

35-A. Study of Phase-Sequence Voltmeters.............................. 180
35-B. Measurement of Phase-Sequence Component Currents.............. 185
35-C. Resolution of Three-Phase Unbalanced Power into Components of Positive and of Negative Sequence.............................. 188

CHAPTER XXXVI

POWER MEASUREMENTS IN THREE-PHASE CIRCUITS

36-A. Exercises with the Two-Wattmeter and Single-Wattmeter Methods..... 197
36-B. Measurement of Reactive Power in a Three-Phase System........... 202

CHAPTER XXXVII

THREE-PHASE DELTA-, V-, AND T-CONNECTED SYSTEMS

EXPERIMENT PAGE
37-A. Study of Delta-Connected Systems.......... 208
37-B. Study of Equivalent Y and Delta Impedances 211
37-C. Electrical Relations in a V-Connected Three-Phase System.......... 216
37-D. Electrical Relations in a T-Connected Three-Phase System.......... 221

CHAPTER XXXVIII

TWO-PHASE AND QUARTER-PHASE SYSTEMS

38-A. Electrical Relations in Two-Phase Systems.......... 225
38-B. Electrical Relations in Quarter-Phase Star-Connected Systems.......... 227
38-C. Electrical Relations in Quarter-Phase Mesh-Connected Systems.......... 229

CHAPTER XXXIX

POLYPHASE TRANSFORMATIONS

39-A. Three-Phase to Three-Phase Transformation.......... 232
39-B. Exercises in Paralleling Three-Phase Transformers 234
39-C. Study of the Scott Two-Phase to Three-Phase Transformation.......... 236
39-D. Study of Various Two-Phase to Three-Phase Transformations.......... 238
39-E. Electrical Relations in a Balanced Six-Phase System.......... 240
39-F. Study of Transformations from Three-Phase to Two-Phase and Six-Phase.......... 244

CHAPTER XL

HARMONICS IN POLYPHASE SYSTEMS

40-A. Harmonics in Y-Connected Systems 257
40-B. Triplen Harmonic Currents in a Delta-Connected Winding 259
40-C. Superposition of Uniphase Transmission between Three-Phase Neutrals 260
40-D. Study of Inductive Interference between Power and Communication Circuits.......... 261

CHAPTER XLI

PERFORMANCE DIAGRAMS OF NON-SALIENT-POLE SYNCHRONOUS MACHINES

41-A. Experimental Study of the Potier Diagram 269
41-B. Performance Characteristics of an Unsaturated Synchronous Machine.. 273
41-C. Performance Characteristics of a Saturated Non-Salient-Pole Alternator 281

CHAPTER XLII

DIRECT AND TRANSVERSE ARMATURE REACTION IN SALIENT-POLE SYNCHRONOUS MACHINES

42-A. Measurement of Direct Armature Reaction.......... 296
42-B. Measurement of Transverse Armature Reaction.......... 297
42-C. Measurement of Pole Leakage in a Synchronous Machine.......... 300

CHAPTER XLIII

PERFORMANCE DIAGRAMS OF SALIENT-POLE SYNCHRONOUS MACHINES

EXPERIMENT PAGE
43-A. Comparison of Actual Performance with the Graphical Solution of the Blondel Diagram 306
43-B. Comparison of Actual Performance with Analytical Solution of the Blondel Diagram 309
43-C. Loss Diagrams of a Salient-Pole Synchronous Machine Studied in Connection with Sectionalized Saturation Curve 317

CHAPTER XLIV

THE SYNCHRONOUS MOTOR — OPERATING FEATURES

44-A. V-Curves of a Synchronous Motor 331
44-B. Improved Power Factor and Voltage Regulation by Means of a Synchronous Condenser 334
44-C. Measurement of the Torque Angle in a Synchronous Machine 337
44-D. Study of Hunting of a Synchronous Motor 339
44-E. Starting a Synchronous Motor by Means of an Auxiliary Induction Motor . 340
44-F Exercises in Starting a Squirrel-Cage Synchronous Motor 342
44-G. Study of the Fynn-Weichsel Self-Excited Synchronous Induction Motor 347

CHAPTER XLV

THE SYNCHRONOUS-CONVERTER — OPERATING FEATURES

45-A. Ratio of No-Load Voltages in a Synchronous Converter 354
45-B. Operation of the Rotary Converter from the D-C Side 355
45-C. Practice in Starting Rotary Converters 360
45-D. Operation of the Synchronous Converter from the A-C Side 362

CHAPTER XLVI

THE SYNCHRONOUS CONVERTER *(Continued)*

46-A. Compounding a Synchronous Converter by Means of a Series Reactance 367
46-B. Study of a Booster Converter 370
46-C. Oscillographic Study of Armature Currents in a Synchronous Converter 373
46-D. Hunting of a Synchronous Converter and Remedies Therefor 376

CHAPTER XLVII

THE APPROXIMATE CIRCLE DIAGRAM OF THE POLYPHASE INDUCTION MOTOR

47-A. Experimental Determination of the Current Locus in a Polyphase Induction Motor .. 379
47-B. A Check upon the Relation between Slip and Rotor I^2R Loss 382
47-C. Speed Control of the Induction Motor by Tests and as Predicted from the Circle Diagram .. 392
47-D. Load Characteristics of a Polyphase Induction Generator 396

EXPERIMENT PAGE
47-E. Parallel Operation of Induction and Synchronous Generators........ 397
47-F. Study of Various Methods of Braking the Induction Motor.......... 398
47-G. Operation of a Polyphase Induction Motor on an Unsymmetrical Voltage Supply.. 403

CHAPTER XLVIII

EXACT CIRCLE DIAGRAM OF THE POLYPHASE INDUCTION MOTOR

48-A. Derivation of Induction Motor Characteristics from an Exact Circle Diagram.. 414
48-B. Effect of the Primary Resistance upon the Circle Diagram of the Polyphase Induction Motor.................................... 421

CHAPTER XLIX

REGENERATIVE SPEED AND POWER-FACTOR CONTROL OF POLYPHASE INDUCTION MOTORS

49-A. Speed Control of Induction Motors by Concatenation........... .. 428
49-B. An Experiment in Dynamic Speed Control of Induction Motors 447

CHAPTER L

DIVERSE TOPICS ON INDUCTION MACHINES

50-A. Induction-Type Frequency Converter; Secondary Voltage and Frequency at No Load.. 452
50-B. Induction-Type Frequency Converter Load Test; Characteristics at Constant Primary Voltage.................................. 453
50-C. Induction-Type Frequency Converter; Load Characteristics at Constant Secondary Voltage................................... 454
50-D. The Operating Ranges of a General A-C Transformer.............. 454
50-E. Study of a Single-Phase Induction Regulator and Auxiliary Devices... 458
50-F. Study of a Polyphase Induction Regulator and Phase Shifter......... 460
50-G. Characteristics of an Induction Machine under Abnormal Conditions ... 468

CHAPTER LI

THE SINGLE-PHASE INDUCTION MOTOR

51-A. Resolution of the Air-Gap Field in a Single-Phase Induction Motor into Two Revolving Components................................ 474
51-B. Performance Characteristics of a Twin Polyphase Induction Motor Equivalent to a Single-Phase Machine........................ 475
51-C. Performance of the Induction Motor Operating on Single Phase, by Test and by Calculation... 479
51-D. A Study of Vector Relations Involved in the Quadrature-Flux Theory of the Single-Phase Induction Motor.......................... 486
51-E. The Circle Diagram of the Single-Phase Induction Motor........... 491

CHAPTER LII

SINGLE-PHASE COMMUTATOR-TYPE MOTORS

EXPERIMENT PAGE
52-A. Study of the Single-Phase Series Commutator Motor 501
52-B. Study of the Single-Phase Repulsion Motor. .. 508
52-C. Study of the Compensated Repulsion Motor .. 511
52-D. Study of the Brush-Shifting Compensated Repulsion Motor 513
52-E. Study of the Single-Phase Repulsion-Induction Motor 517

CHAPTER LIII

POLYPHASE COMMUTATOR MOTORS

53-A. Study of a Polyphase Series Commutator Motor 531
53-B. Study of a Polyphase Shunt-Connected Motor 533
53-C. Study of the Schrage Machine 542

CHAPTER LIV

MAGNETIC CONTACTOR CONTROL FOR D-C MOTORS

54-A Elementary Exercises with Non-Automatic Magnetic Contactors 556
54-B. Automatic Acceleration of a D-C Motor by Means of Magnetic Contactors 567
54-C Control by Electronic Devices 571

CHAPTER LV

CONTROLLERS FOR ALTERNATING-CURRENT MOTORS

55-A. Study of Across-the-Line Starters 576
55-B. Study of Induction Motor Starters of the Primary-Resistance Type 578
55-C. Study of Induction Motor Starters of the Auto-Transformer Type 585
55-D. Study of Induction Motor Controllers of the Secondary-Resistance Type 593
55-E Study of Synchronous Motor Starters 598

CHAPTER LVI

MERCURY-ARC RECTIFIERS

56-A Internal Voltage Drop in a Mercury-Vapor Arc 604
56-B. External Current and Voltage Relations in the Single-Phase Mercury-Arc Rectifier 606
56-C. Load Test on a Single-Phase Mercury-Arc Rectifier 611
56-D. Study of Rectifier Wave Forms 627
56-E. Study of the Vreeland Oscillator 630

CHAPTER LVII

THE OSCILLOGRAPH

57-A. Study and Use of the Electromagnetic Oscillograph . 642
57-B. Study and Use of the Hot-Filament Cathode-Ray Oscillograph 648
57-C. Study and Use of the Dufour-Type Cathode-Ray Oscillograph . . 653

CHAPTER LVIII

HARMONIC ANALYSIS OF PERIODIC WAVES

EXPERIMENT PAGE
58-A Practice in Analysis of Periodic Waves . 672

CHAPTER LIX

FUNDAMENTALS OF ELECTRONIC DEVICES

59-A Measurement of Emission Characteristics of Hot Cathodes 683
59-B. Determination of the Characteristics of a Photoemissive Cell 686
59-C Use of the Magnetron to Determine e/m and B 696
59-D Measurement of Diode Parameters 701
59-E Determination of Rectifier Regulation and Hum Percentage 704
59-F Test of a Three-Phase Rectifier Filter 709
59-G Determination of Static Characteristics and Evaluation of Parameters of Triodes 715
59-H Measurement of Triode Parameters by A-C Bridge Methods 720
59-I Determination of Static Characteristics of a Tetrode and a Pentode by Measurements on a Single Tube 726
59-J Measurement of Multielectrode Tube Parameters by A-C Methods 728
59-K Measurement of Gain of a Resistance-Capacitance Coupled Amplifier 732
59-L Measurement of Power Output and Distortion 736
59-M Measurement of the Voltage Drop through a Hot-Cathode Mercury-Vapor Tube 745
59-N Measurement of the Voltage Regulation and Hum Percentage in a Full-Wave Rectifier Using Phanotrons 745
59-O Determination of the Grid Control Characteristics of a Thyratron 747
59-P Determination of the Control Characteristics of a Cold-Cathode Grid-Glow Tube 748
59-Q Control of Average Plate Current in a Thyratron by Changing the D-C Grid Voltage 750
59-R Control of Average Plate Current of a Thyratron by Changing the Phase of the A-C Grid Voltage 751
59-S. Test of an Ignitron Controlled by a Thyratron 753
59-T. Determination of the Characteristics of a Gas-Filled Phototube 756
59-U Determination of the Characteristics of a Photovoltaic Cell 756
59-V Measurement of the Spectral Response of a Photocell 756

CHAPTER LX

HIGH-FREQUENCY MEASUREMENTS

60-A Calibration of a Heterodyne Frequency Meter or a Tuned-Circuit Wavemeter by a Standard-Frequency Source 769
60-B Calibration of an Audio-Frequency Oscillator Using a Standard-Frequency Source and a Cathode-Ray Oscillograph 772
60-C. Measurement of the Inductance of an Iron-Cored Coil Carrying Direct Current (Voltmeter Method) 775
60-D Measurement of the Apparent Inductance, True Inductance, and Capacitance of a Coil 779

EXPERIMENT PAGE

60-E. Measurement of the Capacitance and Phase Angle of a Condenser by the Substitution Method 781
60-F. Measurement of Resistance by Reactance Variation and Resistance Variation 784
60-G. Measurement of High Resistance (Low Conductance) at High Frequencies 786
60-H. Calibration of an Attenuator and Design of a Power-Level Indicator . . 792
60-I. Determination of the Characteristics of Four-Terminal Networks 793
60-J. Measurements on a Telephone Receiver 798
60-K. Measurement and Analysis of Machinery Noise 800
60-L. Measurement of Antenna Impedance 802

EXPERIMENTAL ELECTRICAL ENGINEERING

CHAPTER XXVI

ELECTROSTATIC CAPACITANCE

584. Physical Concept of Capacitance. — A capacitor (condenser) in general consists of two conductors, or plates, separated by a dielectric. Its principal characteristic is that, when the conductors are subjected to a difference of electrical potential, a displacement current flows into the dielectric, establishing there a state of stress.[1] This flow of electricity constitutes the charge in the condenser. The quantity of electricity displaced per unit of emf between the plates of the condenser is called its *capacitance*, the unit of which in the ampere-ohm system is the *farad*. A condenser is said to have a capacitance, C, of 1 farad if a charge, Q, of 1 coulomb (ampere-second) of electricity results from the application of a pressure, E, of 1 volt between the plates. Thus we have the fundamental relationship:

$$Q = CE \quad \ldots\ldots\ldots\ldots \quad (1)$$

Since the farad is too large a unit for practical uses, the *microfarad* (one-millionth of a farad) is more commonly used. In high-frequency circuits an even smaller unit, the millionth of a microfarad or micro-microfarad, is more suitable. The symbol for the microfarad is μf, for the micro-microfarad $\mu\mu$f.

Since the charge Q is the result of a current, i, flowing for a time t, one may write, in terms of instantaneous values:

$$q = \int i\,dt = C \times e \quad \ldots\ldots\ldots \quad (1a)$$

$$dq/dt = i = C\,de/dt \quad \ldots\ldots\ldots \quad (2)$$

---

[1] For a more detailed exposition of dielectric phenomena and the ampere-ohm system, see V. Karapetoff, "The Electric Circuit," pp. 143 and 215, McGraw-Hill Book Co.

Here i is the instantaneous charging current flowing into the condenser. Redefining the farad in terms of the current flow, one may say: *A condenser has a capacitance of 1 farad when a rate of change in applied potential of 1 volt per second results in a charging current of 1 ampere.* Since a change in sign of de/dt (eq. 2) means a reversal in direction of the current, i, it is evident that, when a capacitor is connected to a source of alternating emf, an alternating current flows in the circuit. Thus a capacitor is said to " pass " alternating current, but to constitute an open circuit to a steady d-c applied voltage. Alternating currents used in speech transmission in telephone circuits often have to " pass through capacitors." For a discussion of capacitance in a-c circuits see §600.

585. Examples of Capacitors in Practice. — Some of the important practical cases in which capacitance enters are as follows:

(1) In a long submarine telegraph cable the distributed capacitance is so great that an appreciable time elapses before the signal current reaches the far end of the cable. During the first few moments after the circuit is closed, all the current is used in charging the cable and in bringing it up to battery potential. This limits the speed of transmission of signals.

(2) In high-tension cables and in long overhead transmission lines capacitance has a noticeable effect on the distribution of potential along the line and may at times cause an abnormal voltage rise.

(3) Electrostatic capacitance in telephone lines considerably affects the quality of speech. To minimize this effect telephone lines are so constructed as to have as little capacitance as is feasible. Inductance in the form of " loading coils " inserted at intervals in long telephone lines is required to neutralize the effect of capacitance (§605).

(4) Condensers are useful in cases in which direct current must not flow through a certain part of the circuit although it must be possible for alternating current to pass with little opposition. The use of condensers in central-energy telephones is common.

(5) Condensers are an indispensable part of radio circuits, being necessary whenever it is desired to produce resonant conditions (§609) leading to electrical oscillations of a desired frequency.

(6) Capacitors are used in a-c power installations in parallel with low-power-factor inductive loads to improve the power factor of the system and the regulation and efficiency of transmission (§606).

(7) A condenser across a vibrating contact reduces sparking, by permitting a temporary flow of current as the contacts open. The Tirrill regulator (see Figs. 216 and 331) is an example of this application.

(8) Condensers are useful in special circuits for the purpose of eliminating higher harmonics (wave filters), for accentuating higher har-

monics in other cases of investigation, in the starting of single-phase (capacitor) motors, etc.

586. Factors Determining the Capacitance of Condensers. — The capacitance of a condenser varies directly with the area A of the opposing plates, with the dielectric constant (permittivity) K of the dielectric, and inversely with the distance D separating the plates. If the area of the plates is increased a larger volume of dielectric is subjected to the given electrostatic stress. Bringing the plates closer together by using thinner insulation increases the dielectric stress since the potential acting through unit thickness is thereby increased. K, the dielectric constant, states that the capacitance is K times the value it would have if air were the dielectric.

The capacitance of a plate-type condenser, when dimensions are in centimeters and C in microfarads, is

$$C = \frac{0.0886KA}{D \times 10^6} \quad . \; . \; . \; . \; . \; . \; . \; . \; . \; . \; . \quad (3)$$

With dimensions in inches

$$C = \frac{0.225K''A''}{D'' \times 10^6} \quad . \; . \; . \; . \; . \; . \; . \; . \; . \; . \; . \quad (4)$$

If there are p plates, each of area A'', and with alternate plates connected

$$C = \frac{0.225KA''(p - 1)}{D'' \times 10^6} \quad . \; . \; . \; . \; . \; . \; . \; . \; . \quad (5)$$

These equations hold rigidly only when D is small compared with A since otherwise the dielectric stress is not uniform over the entire plate (dielectric) area.

The dielectric properties of several insulating materials are given in the following table.[2]

587. Standard Condensers. — Except when used in very high-frequency circuits the values of capacitance required in condensers are too large to be obtained by means of two plates, unless the plates are given enormous dimensions. It therefore becomes necessary to use several plates (Fig. 432) connected alternately to the opposite terminals. An air-insulated condenser of this kind, shown in Fig. 433, has been used as a standard for measuring small capacitances and at low poten-

---

[2] Pender and McIlwain, "Electrical Engineers' Handbook," John Wiley & Sons; "Standard Handbook for Electrical Engineers," McGraw-Hill Book Co.

Material	Dielectric Constant *K*	Per Cent Power Factor	Dielectric Strength (volts/mil)
Asphalt (petroleum)	3.0	2.9	500
Beeswax (yellow)	2.9	2.94	250
Celluloid, clear	7.3	6.2	300–900
Glass (flint)	7.0	2.0	230–300
Gutta percha	3.0	1.8	....
Mica	6.6–8.7	0.01–0.04	500–1500
Paper	3.5	0.5	110–230
Parowax	1.9–2.5	0.03	300
Resin	2.7	0.29	
Rubber, hard	2.8–3.5	0.4–0.5	1000–2000
Shellac	3.0–3.7	0.8	...
Transformer oil	2.5	0.9–1.75	220
Varnished cloth	4.5–5.5	6.0	500–1300
Wood	3.0	2.5	100–350

tials. For larger values of capacitance, the plates must be brought much closer together, and their number greatly increased. Besides, it becomes necessary to use a dielectric other than air, since the thin metal sheets are not strong enough to support themselves. This also increases the capacitance of the condenser several times, because of the higher permittivity of dielectrics other than air (§586). In the selection of a dielectric it is necessary to consider not only its cost and dielectric strength, but also its permanence, absorption of electric charge, dielectric hysteresis loss, and leakage conductance (§590).

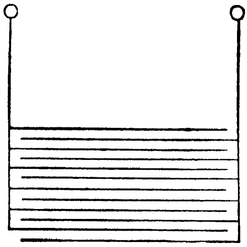
FIG. 432. Multiple-plate condenser.

Mica is used for insulation in standard condensers; also in those intended for high voltages. Such condensers consist of layers of tinfoil with sheets of mica between them. The whole is firmly pressed together in order to keep the distance between the plates, and consequently the capacitance, unaltered. A more satisfactory method is to have each sheet of mica coated chemically with a thin film of silver. A standard mica condenser is shown in Figs. 434*a* and 434*b*; it is subdivided into sections of 0.05, 0.05, 0.2, 0.2, and 0.5 microfarad. By combining these sections in series and in parallel, several values of capacitance may be obtained between 0.0192 and 1 microfarad (see the end of §588).

In some condensers of this type, knife switches, in place of plugs, are used to obtain various combinations of the sections, while for varying capacitance in small uniform steps, dial switches are used (Fig. 435*a*). In the dial-type condenser of Fig. 435*a* the lower dial switch controls 10

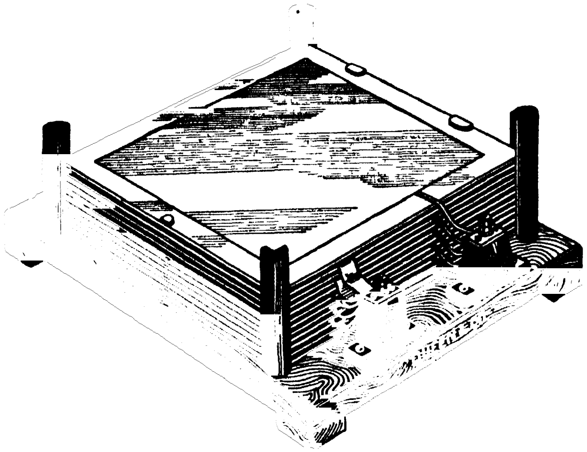

FIG. 433. A standard air condenser.

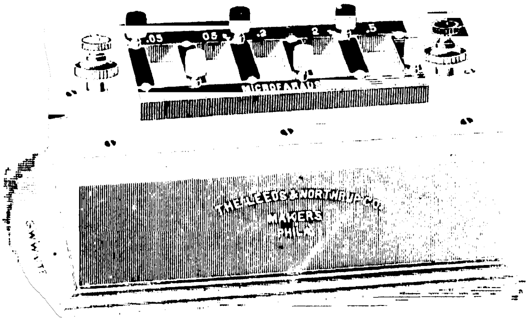

FIG. 434(*a*). An adjustable mica-insulated condenser.

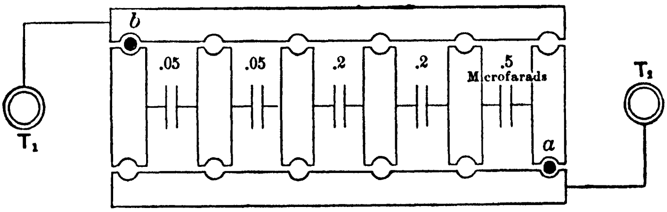

FIG. 434(*b*). Arrangement of sections in the condenser of Fig. 434(*a*).

points of 0.001 μf each, another dial switch 10 points of 0.01 μf each, and a third 10 points of 0.1 μf each. The capacitance can then be varied between 0.001 μf and 1.11 μf in steps of 0.001 μf. When an adjustable capacitance of small value is required an air-dielectric condenser with movable plates is used (Fig. 435*b*).

Mica condensers are quite expensive; therefore, where no great accuracy or high insulation is required, sheets of tinfoil are insulated with paper instead of mica. Each sheet of paper is dipped in hot paraffin during the construction, and the whole is immersed in paraffin after completion, in order to exclude air. This makes the condenser a solid mass and insures a constant distance between the sheets.[3]

588. Condensers in Series and in Parallel.—Condensers may be connected in series or in parallel, like resistances, and it is necessary to know how to calculate their combined capacitance.

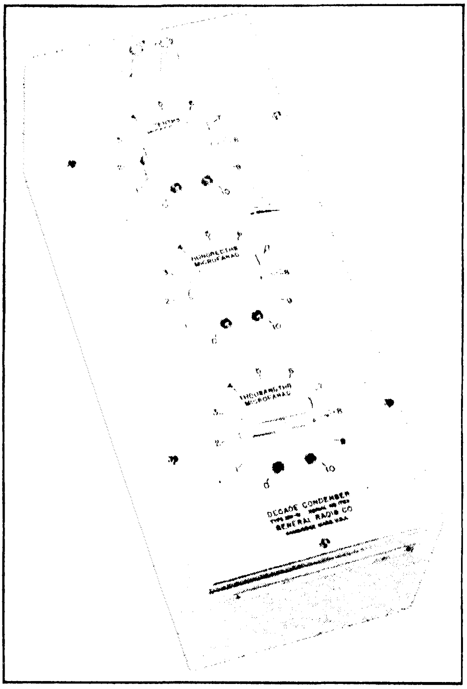

FIG. 435(*a*). Standard adjustable mica condenser — dial type.

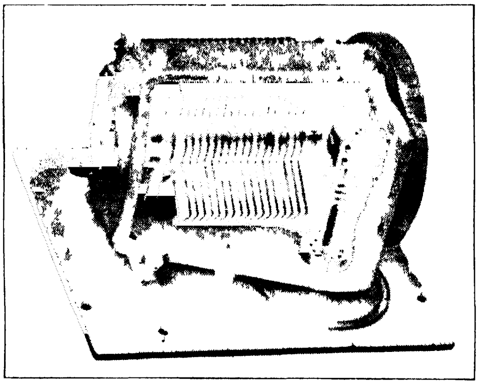

FIG. 435(*b*). Standard adjustable air condenser (General Radio Company).

(a) *Condensers in parallel.* Let several condensers (Fig. 436) of capacitances c_1, c_2, c_3, etc., respectively, be connected in parallel across a source of d-c voltage, E. The problem is to find the capacitance, C, of an equivalent condenser, that is, such a capacitance that at the same pressure, E, the same quantity of electricity will be displaced in it as in all the given condensers together. Let the quantities of electricity stored in the given condensers be q_1, q_2, q_3, etc. According to the definition of capacitance, eq. (1), we have:

---

[3] For a detailed description of standard condensers and their errors, see B. Hague, "Alternating Current Bridge Methods," Chapter III, Pitman & Sons, 1938. See also Balsbaugh and Moon, *Trans. A.I.E.E.*, vol. 52 (1933), p. 529.

$$q_1 = c_1E; \qquad q_2 = c_2E; \text{ etc.} \qquad (6)$$

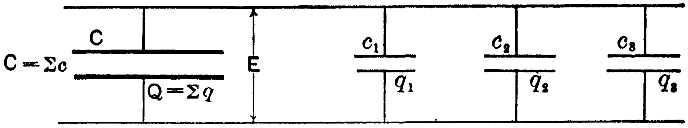

FIG. 436. Addition of capacitances in parallel.

For the equivalent condenser we must have:

$$q_1 + q_2 + \cdots = CE \qquad (7)$$

Substituting the values of the q's from eqs. (6) in eq. (7), we get:

$$C = \sum c \qquad (8)$$

In other words, the combined capacitance of condensers in parallel is equal to the sum of their capacitances. This result could have been foreseen from the physical concept of capacitance.

(b) *Condensers in series.* Condensers connected in series are shown in Fig. 437. The electric charge, or displacement, q, is the same in all of them, because electricity behaves like an incompressible fluid, and all the condensers together offer but one path for the displacement of a certain quantity of electricity between the line terminals. The problem is to find a single capacitance, C, such that it would cause the same displacement, q, at the same line voltage, E. Let the voltages across the given condensers be e_1, e_2, e_3, etc.; according to eq. (1), we then have:

$$q = c_1e_1 = c_2e_2 = c_3e_3 = \text{etc.} \qquad (9)$$

For the equivalent condenser:

$$q = CE = C(e_1 + e_2 + e_3 + \text{etc.}) \qquad (10)$$

Substituting the values of e_1, e_2, e_3, etc., from eqs. (9) in eq. (10), we find:

$$q = C(q/c_1 + q/c_2 + q/c_3 + \cdots)$$

or:

$$1/C = \sum(1/c) \qquad (11)$$

This can be expressed by saying that the sum of the reciprocals of two or more capacitances in series is equal to the reciprocal of the equivalent capacitance. Sometimes the reciprocal of the capacitance is called the *elastance* of a condenser. Therefore, eq. (11) expresses the fact that when condensers are connected in series their elastances are added. Equation (8) states that when condensers are connected in parallel their capacitances are added. Equations (9) and (10) show that the total voltage, E, is divided among the individual condensers inversely as their capacitances, or in direct proportion to their elastances. For similar laws concerning resistances and conductances, see §11.

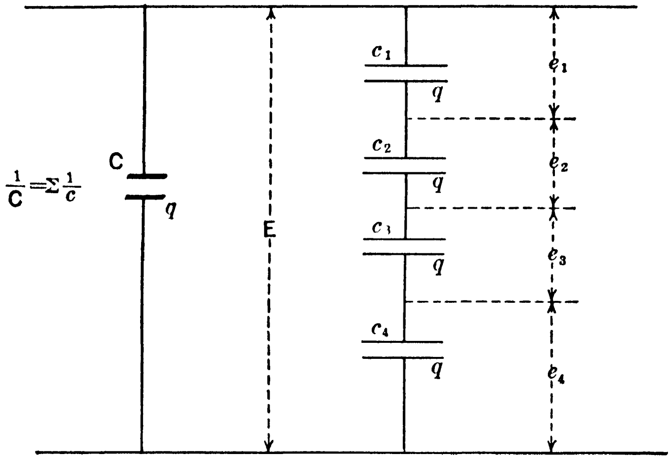

FIG. 437. Capacitances in series.

These results may be illustrated on the sectionalized condenser shown in Figs. 434*a* and 434*b*. The largest capacitance is obtained by connecting all the sections in parallel, with plugs inserted alternately in the two rows of holes, as in Fig. 434*a*. The smallest value of capacitance corresponds to all the sections in series, with plugs at *a* and *b* (Fig. 434*b*). Intermediate values are obtained by other suitable combinations of plugs. For example, to get 0.15 μf, two sections of 0.2 μf each are connected in series, which gives 0.1 μf.; then 0.05 μf is connected in parallel with them. With all the sections in series, we have:

$$1/C = 2/0.05 + 2/0.2 + 1/0.5 = 52\ \mu\text{f}^{-1}$$

or $C = 1/52\ \mu$f; this is the smallest value obtainable with this condenser. The largest capacitance, with all the sections in parallel, is:

$$0.5 + 2 \times 0.2 + 2 \times 0.05 = 1\ \mu\text{f}$$

589. Methods of Comparison of Capacitances. — From eq. (1) it is evident that the capacitance of any condenser may be determined by charging it to a known potential and then discharging it through a calibrated ballistic galvanometer (§179). From the galvanometer deflection, interpreted in coulombs, and the applied potential, the capacitance may be calculated.

The precision of this measurement depends upon the accuracy of galvanometer and voltmeter, as well as upon the skill of the observer. The time of charge and discharge is also important (§590). To avoid or reduce these errors most methods of measuring capacitances are based on a comparison of the capacitance under test with that of a standard condenser. The calibration of standard condensers themselves, by special precision methods, is outside the scope of this work.[4] The following methods of comparison are among those in use:

(1) Direct-deflection method;
(2) Method of mixtures;
(3) Thomson zero method;
(4) Loss of charge method;
(5) Bridge methods (Chapter XXVIII).

In addition, capacitance may be measured in terms of volts and amperes with sinusoidal alternating currents (impedance method). All these methods are described below.

Permittivity (the dielectric constant) can be determined by measuring the capacitance of a condenser of known dimensions. The principle is the same as in the determination of the resistivity of a material from the resistance of a conductor of known dimensions (§5). For relative determinations of permittivity, two condensers of identical dimensions may be used, one with dielectric of some standard material, the other employing the material under test. For liquids, the substitution method may be used, as in resistance measurements (§14).

590. Defects in Condensers. (a) *Absorption.* — In the discharge of a condenser having a solid dielectric there is an initial rush of the so-called "free charge" from the condenser, followed by a gradual flow of "absorbed" charge from the dielectric. Similarly, during the charge of a condenser the first rush of current supplies both the free charge and a portion of the absorbed charge, which latter is then completed by a diminishing current over a period of some seconds. Should the charging current be interrupted before the process of absorption is completed a portion of the free charge will be absorbed by the dielectric. It is evident, then, that the amount of the charge into or out of a given capacitor is a function of both potential and time, and any accurate method of testing a condenser must take this into account.

---

[4] Harvey L. Curtis, "Electrical Measurements," Chapter XIII, McGraw-Hill Book Co.

(b) *Dielectric hysteresis.*[5] When a condenser having a solid dielectric is subjected to a series of repeated charges and discharges, a heating of the dielectric takes place, showing that there is an actual energy loss (or transformation) within the dielectric. This loss is in addition to that accounted for by any actual flow of current through the finite, but very high, resistance of the dielectric. It is in the nature of molecular friction and is called *dielectric hysteresis.* The energy loss per cycle of charge and discharge is essentially proportional to the square of the applied potential.

(c) *Leakage.* Since the dielectric separating the plates of a condenser has finite resistance, as is true also of the materials and surfaces separating the terminals of the condenser, a minute current will flow continuously when the capacitor is subjected to a steady difference of potential. This leakage, or *conductance,* involves a further energy loss in the condenser. Surface resistance values, assuming that the surfaces are clean, are of the order of magnitude of 10^7 to 10^{14} ohms per cm^2 and are greatly affected by atmospheric humidity.

Volume resistivity values vary widely, characteristic values being from about 10^{13} to 10^{14} ohm-cm for mica, 2×10^8 ohm-cm for ivory, 10^{14} to 10^{17} ohm-cm for quartz, 2×10^9 ohm-cm for celluloid, 10^{15} ohm-cm for micanite, etc.[6] These values are greatly affected by temperature, and values are usually specified at 20°C. The equivalent circuit of the imperfect capacitor when used on a-c circuits is considered in §604.

591. Direct-Deflection Method of Comparison of Capacitances. — A standard capacitance C_1 and an unknown capacitance C_2 are arranged as in Fig. 438 so that either may be charged at will from a battery, *Ba*, of suitable potential, and then discharged through a ballistic galvanometer with proper shunt A. Comparison of the two deflections makes possible the determination of C_2. Suppose that the discharge of the condenser C_1 produces a deflection d_1, when the shunt A is set for a multiplying factor k_1. Similarly the discharge of C_2 gives a deflection d_2, with a multiplying factor k_2. Then, from eq. (1)

$$Q_1/Q_2 = (E_1C_1)/(E_2C_2) = (k_1d_1)/(k_2d_2) \quad . \quad . \quad . \quad . \quad . \quad (12)$$

---

[5] V. Karapetoff in "Standard Handbook for Electrical Engineers," Fifth Edition, sec. 2, McGraw-Hill Book Co.

[6] "Standard Handbook for Electrical Engineers," McGraw-Hill Book Co.

Therefore

$$C_2 = C_1(E_1/E_2)(d_2/d_1) \quad . \; . \; . \; . \; . \; . \; . \; . \; . \quad (13)$$

If the battery voltage is the same in the two condensers, as it would usually be, one may write

$$C_2 = C_1(d_2/d_1) \quad . \; . \; . \; . \; . \; . \; . \; . \; . \; . \; . \quad (14)$$

It is not essential that the ballistic galvanometer be calibrated for this test since the result depends only upon the ratio of the deflections, particularly if the damping of the galvanometer (§178) is the same for the two measurements, as it will be if the shunt, A, is of the Ayrton universal type.[7] When the capacitance of a long cable is measured by this method the copper conductor of the cable serves as one plate of the condenser and the lead sheath as the other. Since the sheath is grounded one terminal of the battery must also be grounded to complete the circuit. In order to increase the accuracy of the measurements, galvanometer deflections should be obtained at several values of battery voltage and plotted against these voltages as abscissas. From the two straight lines so obtained, the ratio k_1d_1/k_2d_2 can be computed. The more nearly the two capacitances are equal, the greater is the accuracy of results. When performing this experiment connect condensers, or sections of condensers, in series and in parallel, in order to check the relations derived in §588. Owing to the phenomenon of absorption the quantity of electricity obtained on discharge depends upon the duration of the charge. Moreover, repeated smaller discharges, due to the "absorbed charge," may be obtained after the first. Thus care should be exercised in charging and discharging condensers, especially long cables, and the effect of absorption, if any, should be noted.[8]

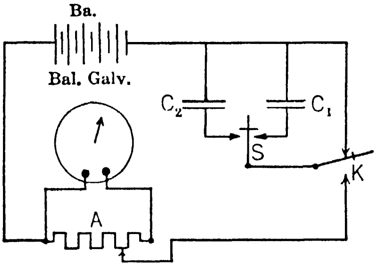

FIG. 438. Comparison of capacitances by the direct-deflection method.

---

[7] F. A. Laws, "Electrical Measurements," Second Edition, p. 43, McGraw-Hill Book Co.

[8] J. B. Whitehead, *Trans. A.I.E.E.*, vol. 45 (1926); V. Karapetoff, *A.I.E.E. Journal*, 1926, p. 236. F. A. Laws, "Electrical Measurements," Chapter VII, McGraw-Hill Book Co.

A charged condenser gradually loses its charge, partly through surface leakage, partly through internal equalization of opposite quantities of electricity, because the resistance of the dielectric is not infinite. Therefore, it is essential to discharge a condenser as soon as it is charged; or, if it is allowed to stand charged, this fact and the duration of the charge should be noted.

592. EXPERIMENT 26-A. — Calibration of a Condenser by the Direct-Deflection Method. — Arrange the apparatus as in Fig. 438, and compare the capacitance of one or more condensers with that of a standard condenser, following the procedure outlined in §591. If possible, in each case select a standard condenser which will give approximately the same deflection as is given by the unknown capacitance. Make sure that the battery voltage will not change between measurements on the standard and unknown capacitances. Take observations at several voltages so that curves of deflection against voltage may be taken.

Try the effect of varying the time of charge and discharge upon the values of capacitance obtained.

Change the position of the battery to one in which the galvanometer will deflect during charge, rather than discharge, of the condensers.

Comment upon the reliability of results and accuracy obtained. If the time of charge and discharge has been varied by known amounts, try to determine the values of C for instantaneous (zero time) of charge (geometric capacitance).

Where condensers have been tested in series and in parallel discuss the results obtained in comparison with theoretical values (§588).

593. Method of Mixtures (Thomson Zero Method). — In the method of mixtures, or cancellation, the following two principles are utilized: (1) the ratio of the capacitances is made equal to a ratio of resistances, which can be determined with great accuracy; (2) balance is obtained when the galvanometer deflection is zero, which adds to the accuracy of the method and makes it unnecessary to have a calibrated galvanometer. Three steps in the method are to be noted: In Fig. 439*a* the adjustable resistances R_1 and R_2 are connected across the battery and share its potential between them. C_1 (standard) and C_2 (unknown) are connected across R_1 and R_2 and are charged to potentials of values iR_1 and iR_2. In (*b*) the capacitors are connected in series with a resultant "mixing" or partial cancellation of their charges. In (*c*) the residual charges, if any, escape through the galvanometer.

If R_1 and R_2 have been so adjusted that the charges, $Q_1 = iR_1C_1$, and $Q_2 = iR_2C_2$, are equal, then, after "mixing," the resultant charge, $Q_1 - Q_2 = 0$, and there is no galvanometer deflection; in which case:

$$C_1iR_1 = C_2iR_2$$

or

$$C_2 = C_1(R_1/R_2) \quad \ldots \ldots \ldots \quad (15)$$

If the periods of mixing and of discharge are made sufficiently short, only the "free" charges (§590) are involved, and the method permits the determination of the so-called "geometric" capacitance of C_2. This eliminates the effects of absorption and leads to more accurate and consistent results.

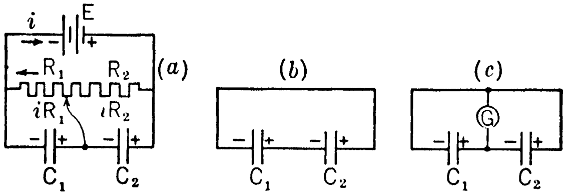

FIG. 439. Steps in the method of mixtures: (a) capacitors during charge; (b) period of mixture; (c) period of discharge.

A special three-pole double-throw switch is offered by one manufacturer (see Leeds & Northrup Co. Catalog EU2), so designed that when operated at a normal rate the charges are mixed and the galvanometer is in circuit for about 1/1000 second. (See Fig. 439.) The action is as follows:

1. The switch is thrown upward for charge.
2. The switch is thrown down, whereupon the outside blades first make contact (points 4 and 6), throwing the condensers in series and equalizing their charges.
3. The middle blade then makes contact with point 5 just before leaving contact with point 2, thus momentarily discharging the unequalized charge of the condensers.

The same switch may be used in the measurement of capacitance by the so-called "ballistic throw" method in which a certain capacitor is discharged instantaneously through a calibrated galvanometer and the unknown capacitance is determined (eq. 1) from the galvanometer reading and the value of the voltage at which the condenser was charged. Figure 441 illustrates this. In the charge position of the switch the condenser is placed across the battery. In the discharge position the condenser discharges momentarily through the galvanometer, i.e., while points 2 and 5 are still in contact.

594. EXPERIMENT 26-B. — Comparison of Capacitances by the Method of Mixtures. — Select resistors R_1 and R_2 with a sum equal to at least 1000 ohms. Using the special switch or its equivalent, arrange the equipment as in Fig. 440. Protect the galvanometer by a suitable shunt or series resistance. Having first set R_1 at a high and R_2 at a low value, close the switch first in the charge and then in the discharge position, noting direction of galvanometer deflection. Next set R_1 at a low and R_2 at a high value, and again note the direction of deflection.

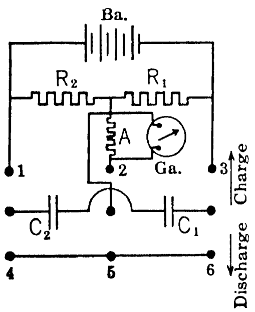

FIG. 440. Schematic diagram of the Leeds and Northrup switch in the method of mixtures.

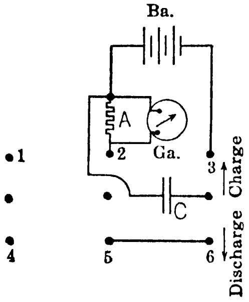

FIG. 441. The Leeds and Northrup geometric-capacitance switch used in the direct-reflection method.

If the two deflections are in opposite directions, the range of resistance values available will permit a balance. Now adjust R_1 and R_2 to give zero deflection even when the shunt A is set for maximum sensitivity. Note these values. See whether the results are affected by the speed of operation of the switch.

Repeat the experiment with different unknown capacitances. Determine the effect of the time of charge upon the consistency of results with different types of capacitors, as paper-insulated, mica-insulated, etc. Try also a length of lead-sheathed cable.

Having measured the capacitances of two or more condensers, determine the combined values which result when they are connected, first in series, then in parallel, and so check the relations of §588.

Discuss results obtained, and compare this method with the direct-deflection method (§591).

595. Current-Time Curves for Capacitance and Resistance in Series. — (a) *Growth of charge.* If a constant potential E is applied to a circuit containing a resistance R, and a de-energized capacitance C, in series (Fig. 442), one may write, for any time t after closing the switch upward:

$$E = Ri + 1/C \int i\,dt \quad . \; . \; . \; . \quad (16)$$

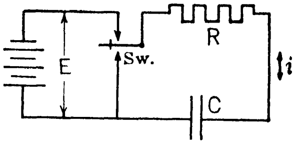

FIG. 442. Circuits for charge or discharge of a condenser through resistance.

Differentiating:

$$dE/dt = 0 = R\,di/dt + 1/C \quad . \; . \quad (17)$$

Rearranging:

$$di/i = -dt/RC \quad . \; . \; . \; . \; . \; . \; . \; . \; . \; . \quad (18)$$

By integration:

$$\log_e i = (-t/RC) + k \quad . \; . \; . \; . \; . \; . \; . \; . \quad (19)$$

or

$$i = e^{-t/RC+k} \quad . \; . \; . \; . \; . \; . \; . \; . \; . \; . \quad (20)$$

To evaluate k substitute $t = 0$, for which, since there is then no charge in the condenser, $\int i\,dt = 0$ (eq. 16) and $i_0 = E/R$. Therefore (eq. 20):

$$i_0 = E/R = e^k$$

so that the equation for current during the period of charge becomes:

$$i = (E/R)e^{-t/RC} \quad . \; . \; . \; . \; . \; . \; . \; . \; . \quad (21)$$

This might also be written:

$$\log_e i = \log_e (E/R) - t/RC \quad . \; . \; . \; . \; . \; . \quad (21a)$$

The value of the charge, q, in a condenser after a time t has elapsed, is derived from eq. (21). Since $i = dq/dt$,

$$q = \int_0^t i\,dt = E/R \int_0^t e^{-t/RC}\,dt$$

or

$$q = -CE(e^{\;t/RC})_0^t = -CE(e^{-t/RC} - 1)$$

Therefore

$$q = CE(1 - e^{-t/RC}) \quad . \; . \; . \; . \; . \; . \; . \; . \; . \quad (22)$$

while, since the potential across the condenser is q/C,

$$e = q/C = E(1 - e^{-t/RC}) \quad . \; . \; . \; . \; . \; . \; . \; . \quad (23)$$

Figure 443 shows the rise of potential with time in a 2-μf condenser in series with a 100,000-ohm resistance when 110 volts (d-c) is suddenly applied.

(b) *Loss of charge by leakage.* — If the switch in Fig. 442 is thrown downward after the condenser has become fully charged to the potential E, the condenser will lose its charge over a period of time in the form of a diminishing current through the resistance or "leak." Rewriting eq. (16) for this condition, and remembering that applied potential E is now zero,

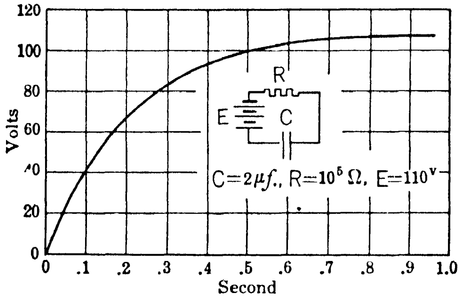

FIG. 443. Rise of condenser voltage during charge through resistance.

$$E = 0 = Ri + 1/C \int i\,dt \qquad (24)$$

Differentiating,

$$0 = R\,di/dt + i/C\,dt \qquad (25)$$

Or

$$di/i = -1/RC\,dt$$

Integrating,

$$\log_e i = -t/RC + k$$

Or

$$i = e^{-(t/RC+k)} \qquad (26)$$

At the beginning of the discharge, when $t = 0$, $i = I_0 = e^k$. But, since the condenser had been charged to the potential E, and at the beginning of discharge ($t = 0$), $E - RI_0 = 0$, or $I_0 = E/R$.

Therefore:

$$e^k = E/R$$

so that (eq. 26)

$$i = (E/R)e^{-t/RC} \qquad (27)$$

This is identical with eq. (21) for the current during the period of charge.

Rewriting eq. (27)

$$Ri/E = e^{-t/RC} \quad \ldots\ldots\ldots\ldots \quad (28)$$

but Ri, the drop across the resistance, equals the potential, e, of the condenser, so that one may write for eq. (28)

$$\log_e E/e = t/RC$$

or

$$RC \log_e E/e = t \quad \ldots\ldots\ldots\ldots \quad (29)$$

In terms of common logs,

$$2.303RC \log_{10} (E/e) = t \quad \ldots\ldots\ldots \quad (30)$$

Figure 444 is drawn to show the decreasing potential across a condenser which is losing its charge through a high resistance. Since charge $q = Ce$, this curve also shows how the charge decreases with time. In (*a*) the resistance is 1 megohm, and the voltage, initially 110 volts, drops to some 66 volts in 1 second. If a resistance of 1/10 megohm is placed across the condenser (curve *b*) it becomes practically completely discharged in 1 second.

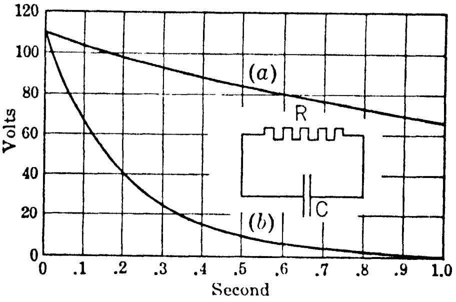

FIG. 444. Curves of condenser voltage during discharge through resistance: (*a*) $R = 10^6$ ohms; (*b*) $R = 10^5$ ohms ($C = 2\,\mu$f).

It is evident that the capacitance of a given condenser may be determined from the loss of charge (or potential) in a given time through a known high resistance (eq. 30). Unless the resistance of the condenser itself is infinitely great and surface leakage negligible the effect of these must be included in R. Instead of measuring the time for a given loss of charge, the time required to produce a certain charge through, say, an electron tube, may be measured.[9]

596. EXPERIMENT 26-C. — Determination of Capacitance from Loss of Charge. — The method is based on eq. (30). The condenser is charged at a certain voltage and immediately discharged through a ballistic galvanometer. Let the deflection be D. Then the condenser is charged to the same voltage, and a known high resistance, R (usually of the order of magnitude of megohms), is connected across its terminals. After a certain interval of time, t, the condenser is again discharged through the same ballistic galvanometer. Let the new deflection be d. Then, according to eq. (1), we have:

---

[9] Karolus and Reuss, *Physik. Zeit.*, vol. 22 (1921), p. 362.

$$E/e = D/d \quad . \; . \; . \; . \; . \; . \; . \; . \; . \; . \; . \quad (31)$$

Thus, in eq. (30), all the quantities except C are known, and C can be computed.

597. Electrolytic Condensers — Construction and Uses. — Electrolytic condensers usually employ aluminum or tantalum electrodes in a suitable electrolyte. Upon the electrodes a thin film of oxide or hydroxide is formed under the influence of an applied electrical potential. This film has a resistance up to several megohms per square centimeter of electrode area, the exact value depending upon the voltage applied during the formation of the film. Since the film, which together with a layer of minute gas bubbles constitutes the dielectric in this condenser, is extremely thin, the capacitance per unit of electrode area is higher than in any other type of condenser. According to Godsey[10] such a condenser using tantalum electrodes has a capacity of 0.2 μf per cm^2 when formed at 50 volts, and of 0.03 μf per cm^2 for a formation voltage of 300 volts (Fig. 445). Values for aluminum electrodes are lower. A typical aluminum condenser has a capacitance of 8 μf with an anode area of 72 in.^{2} and is formed to 450 volts. Some of the common electrolytes are potassium permanganate, sodium silicate, ammonium citrate, borax, and citric acid. Dielectric constants of the films have values of about 15 to 40, the presence of water in the film possibly accounting for these high values.

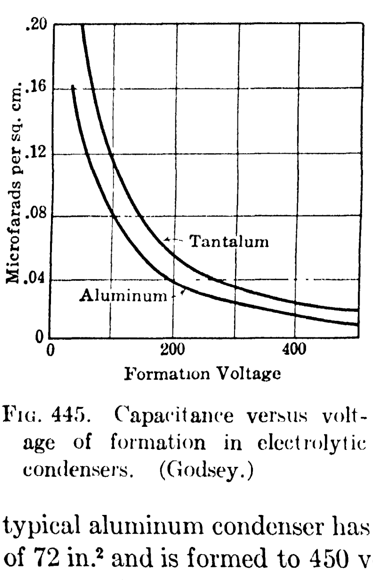

Fig. 445. Capacitance versus voltage of formation in electrolytic condensers. (Godsey.)

In the dry-type electrolytic condenser, the electrodes are thin sheets of aluminum, separated by a suitable gauze or other spacer impregnated with the electrolyte. The electrodes are rolled into compact form, and the whole is enclosed in a metal container. Capacitance of 2 μf, for a forming voltage of 300, is attained for 1 in.^{3} of volume.

Electrolytic condensers find their chief application in filters on the output of battery chargers in telephone service, for diminishing the arc at sparking contacts, as filters in the d-c power circuits of radio sets, and in the starting circuit of capacitor motors (see Chapter XXIII).

---

[10] *Trans. A.I.E.E.*, vol. 51, June 1932, p. 432.

598. Measurement of Capacitance in Electrolytic Condensers.—Since electrolytic condensers are most commonly used as filters in rectifier circuits, it is generally specified[11] that capacitance shall be measured with a d-c polarizing voltage 80 per cent of rated voltage and with a superposed a-c ripple voltage at 60 cycles of a value of 15 volts for capacitors rated 100 volts or higher. Such electrolytic condensers should have a leakage current at rated voltage of not more than 0.1 milliampere per microfarad of capacitance. The circuit of Fig. 446, due, except for minor changes, to Morecroft, permits the measurement of capacitance under the conditions stated. The electrolytic condenser, C, has a polarizing d-c potential impressed from the battery E_{dc} through a choke coil L. A 160-cycle a-c ripple voltage, E_{ac}, is superposed upon the polarizing voltage. A low-reactance (paper) condenser C_1 prevents direct current from flowing through the a-c source while the inductance, L, prevents alternating current from flowing through the battery. Voltmeter V_1 in series with a low-reactance paper condenser C_2 reads the a-c ripple voltage, while V_2 gives the polarizing voltage.

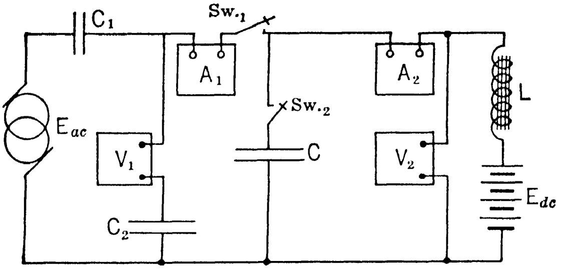

FIG. 446. Circuit for testing capacitance of electrolytic condensers under superposed d-c and a-c voltages (Morecroft).

The d-c milliammeter A_2 reads the leakage current of the condenser C, also that of C_2, which may be eliminated by opening switch Sw. The a-c ammeter A_1 reads the a-c current to C, also that through V_2 and the circuit of L and E_{dc}. V_2 may be temporarily open-circuited; the effect of L may be minimized by making its reactance, say, 50 times that of capacitor C.

Since (§600)

$$I_1 = 2\pi f C E_{ac}, \quad C = \frac{I_1}{2\pi f E_{ac}}$$

---

[11] "Electrical Engineers' Handbook," John Wiley & Sons, Third Edition, vol. V, sec. 4.

599. EXPERIMENT 26-D. — Test of an Electrolytic Condenser. — Arrange to test one or more electrolytic condensers as suggested in §598 at various values of polarizing d-c voltage, from zero to the maximum safe value, and at various values of superposed a-c potential. *If possible, determine the effect of temperature change.*

Devise a circuit including wattmeters to measure the losses in the capacitor under test, making sure that the wattmeter readings can be corrected for all other losses.

REFERENCES

1. V. KARAPETOFF, The Electric Circuit, McGraw-Hill Book Co., New York.
2. F. A. LAWS, Electrical Measurements, McGraw-Hill Book Co., 1937.
3. H. L. CURTIS, Electrical Measurements, McGraw-Hill Book Co., 1937.
4. A. W. SMITH, Electrical Measurements in Theory and Practice, McGraw-Hill Book Co., 1934.
5. W. R. SMYTHE and W. C. MICHELS, Advanced Electrical Measurements, Van Nostrand Co., 1932.
6. G. A. CAMPBELL, *Bell System Techn. Jour.*, vol. 1 (1922), p. 18, Direct capacity measurement.
7. F. W. GROVER, *Bur. Standards Bul.*, vol. 3 (1907), p. 371, Simultaneous measurement of capacity and power factor of condensers.
8. J. A. FLEMING and W. C. CLINTON, *Proc. Phys. Soc.* (London), vol. 18 (1901–03), p. 386, On the measurement of small capacitances and inductances.
9. E. B. ROSA and F. W. GROVER, *Bur. Standards Bul.*, vol. 1 (1904–05), p. 153, The absolute measurement of capacity.
10. H. L. CURTIS and CHAS. MOON, *Bur. Standards Sci. Paper*, 564, The absolute measurement of capacity by Maxwell's method.
11. H. H. RACE, *Trans. A.I.E.E.*, October 1928, p. 1044, The electrical characteristics of insulating materials.
12. H. BUMANN and J. PFAFFENBERGER, *A.E.G.Mitteil.* No. 11, p. 386, Direct-reading capacitance meter.
13. C. E. H. VON SOTHEN, *Elec. Eng'g*, September 1938, p. 505, Capacitors for power factor correction in industrial plants.

CHAPTER XXVII

CAPACITANCE AND INDUCTANCE IN A-C CIRCUITS

600. Capacitance and Wave Form. — (a) *Sine-form voltage impressed.* When a capacitor is connected to a source of alternating emf an alternating current flows in the circuit.[1] This result is obvious from the relation expressed in eq. (2), Chapter XXVI, namely, $dq/dt = i = C\,de/dt$. Thus, suppose that a sine-form voltage of amplitude E_m and frequency f is applied across a capacitor. Then

$$e = E_m \sin \omega t = E_m \sin 2\pi f t \quad . \; . \; . \; . \; . \; . \; . \quad (1)$$

It follows from eq. (2), Chapter XXVI, that

$$i = C\,de/dt = 2\pi f C E_m \cos 2\pi f t \quad . \; . \; . \; . \; . \; . \quad (2)$$

In terms of effective values

$$I = 2\pi f C E \quad . \; . \; . \; . \; . \; . \; . \; . \; . \; . \quad (3)$$

Thus the capacitor current is also sine-form. As shown by eqs. (1) and (2), the charging current in a condenser leads the voltage wave by 90 degrees. In terms of the vectors of current and voltage,

$$\dot{I} = 2\pi f C \dot{E} \underline{/90^\circ} \quad . \; . \; . \; . \; . \; . \; . \; . \; . \quad (4)$$

In this formula, if the capacitance is expressed in farads and the potential in volts, the current is in amperes. In practice, capacitance is usually stated in microfarads (1 μf is equal to 10^{-6} farad), whereupon

$$\dot{I} = 2\pi f C \dot{E}\, 10^{-6} \underline{/90^\circ} \quad . \; . \; . \; . \; . \; . \; . \; . \quad (5)$$

Using complex quantities, the foregoing formula may be written:

$$\dot{I} = j 2\pi f C \dot{E}\, 10^{-6} \quad . \; . \; . \; . \; . \; . \; . \; . \; . \; . \quad (6)$$

From formula (2) one may calculate the charging current of a known capacitance for a stated voltage and frequency. Conversely, from the measurements of current and voltage, the capacitance C may be calculated. This method of the measurement of capacitance is accurate only with loss-free (§590) condensers and with sinusoidal voltages, the presence of higher harmonics in the impressed voltage having a marked effect upon the value of the current.

---

[1] See V. Karapetoff, "The Electric Circuit," Chapters VI and XVIII, McGraw-Hill Book Co.

(b) *Non-sine-form voltage.* A non-sine-form periodic voltage wave is considered to consist of a fundamental wave of given frequency, plus harmonics (Chapter LVIII) of higher frequency. In waves symmetrical with reference to the axis of ordinates only odd harmonics are present, in addition to the fundamental. Such a voltage wave may be written:

$$e = E_1 \sin(\omega t + \alpha_1) + E_3 \sin 3(\omega t + \alpha_3) + E_5 \sin 5(\omega t + \alpha_5) + \cdots \quad (7)$$

From this it follows (eq. 2) that:

$$i = 2\pi fC\,[E_1 \cos(\omega t + \alpha_1) + 3E_3 \cos 3(\omega t + \alpha_3) + 5E_5 \cos 5(\omega t + \alpha_5) + \cdots] \quad . \quad . \quad . \quad . \quad . \quad . \quad (8)$$

Thus, it is seen that, if the fifth harmonic voltage has an amplitude equal to 10 per cent that of the fundamental, the fifth harmonic of charging current will be $0.1 \times 5 = 50$ per cent of the current due to the fundamental voltage. It should be remembered, however, that this does not mean a 50 per cent increase in the total current over the fundamental. If I_1, I_3, and I_5 are the amplitudes of the fundamental, third, and fifth harmonics of current, the effective value of the total current will be

$$I = \sqrt{(I_1^2 + I_3^2 + I_5^2)/2} \quad . \quad . \quad . \quad . \quad . \quad . \quad . \quad . \quad (9)$$

From eq. (9), if the third and fifth harmonic components of current were each 50 per cent of the fundamental, the resultant effective value of the combined current would be $\sqrt{1 + 0.5^2 + 0.5^2} = 1.2247$ times the effective value of the fundamental.

601. Capacitive Reactance and Susceptance. — Equation (3) shows that not only the capacitance but the expression $2\pi fC$, for a given voltage, determines the charging current of a condenser. The term $2\pi fC \times 10^{-6}$ is called the *capacitive susceptance.* Rewriting eq. (3) to give the voltage drop across a condenser

$$E = I \times 10^6/(2\pi fC) \quad . \quad . \quad . \quad . \quad . \quad . \quad . \quad . \quad . \quad (10)$$

Accordingly, we shall introduce the quantity:

$$x_c = 10^6/(2\pi fC) \quad . \quad . \quad . \quad . \quad . \quad . \quad . \quad . \quad . \quad . \quad (11)$$

and call x_c the *capacitive reactance* of the condenser, as distinguished from the inductive reactance $x = 2\pi fL$. Both are expressed in ohms. Capacitive susceptance is expressed in the reciprocal of ohms or *mhos.*

From eq. (11) it is seen that capacitive reactance varies inversely with frequency (Fig. 440), while capacitive susceptance is directly proportional to f (Fig. 447b).

When a resistor and a condenser are connected in series in an a-c circuit the resultant impedance is

$$z = r - jx_c \quad . \quad . \qquad . \qquad (12)$$

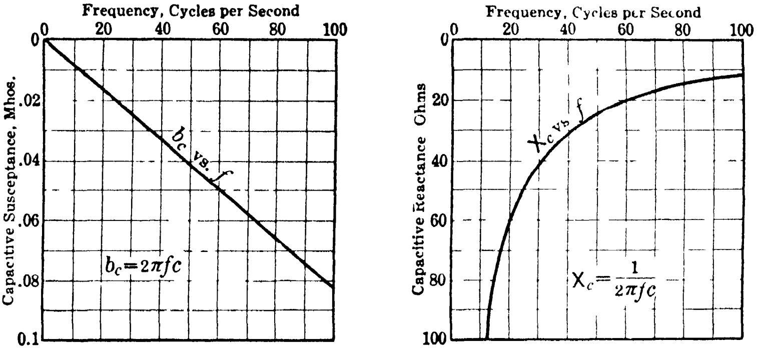

(a) (b)

FIG. 447. Effect of frequency upon capacitive reactance and susceptance.

The minus sign is necessary since, in a condenser, the voltage drop is 90 degrees behind the current, i.e., the current *leads* the voltage drop by 90 degrees.

When a resistance and a capacitance are connected in parallel the combined admittance becomes

$$y = g + jb \qquad (13)$$

where $g = 1/r$, and $b = 2\pi fC\ 10^{-6} = 1/x_c$.

The following experiment is intended to illustrate these relations.

602. EXPERIMENT 27-A. — Capacitance and Resistance in A-C Circuits. — Three conditions should be studied, namely: (a) capacitance across a circuit of variable voltage and frequency; (b) capacitance and resistance in series; and (c) capacitance and resistance in parallel.

(1) *Capacitance alone.* Connect a condenser of moderate capacitance, say 10 to 20 μf, to a source of variable voltage and frequency of substantially sine form. (a) Holding frequency constant, vary the voltage over a wide range, recording voltage, frequency, and current. (b) Holding the voltage constant, vary frequency over a considerable range, say from 40 to 80 cycles, and read as in (a). Connections are suggested in Fig. 448.

(2) *Capacitance and resistance in series.* Connect a capacitance and a resistance of roughly equal impedance at normal frequency in

series as in Fig. 450. If the capacitance is small, say 1 to 4 μf, a voltmeter may act as the resistance, as the current-measuring instrument, and as a voltmeter. (Note that at 60 cycles a capacitance of 2 μf has a reactance of $x_c = 10^6/(2\pi \times 60 \times 2) = 1320$ ohms.) Setting the voltage and speed of the alternator at desired values, connect the voltmeter in series with the condenser to read the current (equal to the voltmeter reading divided by its resistance), then throw the voltmeter across the line to read the voltage. Repeat at several values of voltage and frequency, above and below normal.

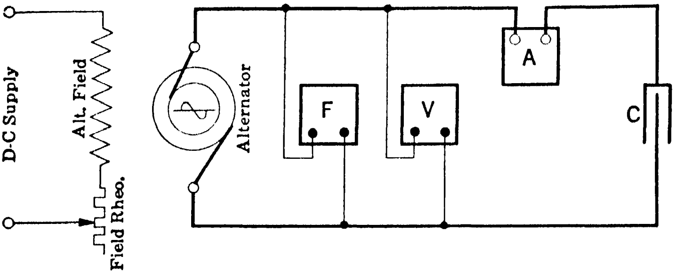

FIG. 448. Test of capacitance in an a-c circuit.

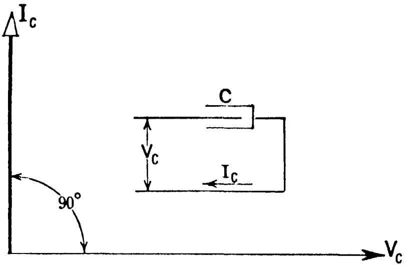

FIG. 449. Vector relations in a condenser on an a-c circuit.

If a condenser of, say, 100 μf is available the voltmeter may be connected alternately across the condenser and across a series resistance of about 20 ohms, since, at 100 volts and 60 cycles, the current in the circuit will be great enough to be practically unaffected by the shunting resistance of the voltmeter.

(3) *Capacitance and resistance in parallel.* Connect a condenser, C, suitable resistor, r, and meters as in Fig. 452. Holding frequency and voltage constant record watts, total current, A_1, resistor current, A_2, condenser current, A_3, voltage, and frequency. Repeat at higher and lower values of voltage, holding f constant; then at higher and lower

frequencies, holding voltage constant. Try opening the condenser circuit and note the effect upon the wattmeter reading and upon the total current.

Report. Run 1. (a) Plot amperes against volts at constant frequency. From the best straight line through the points calculate the capacitance, C, the capacitive reactance, x_c, and the capacitive susceptance, b. (Note that $b = I/E$.)

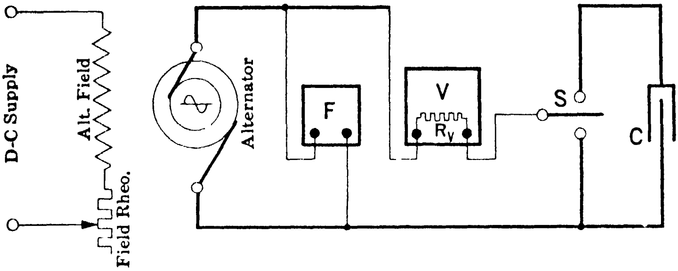

FIG. 450. Test of capacitance and resistance (voltmeter) in series.

(b) Plot current against frequency at constant voltage. Does it bear out the relation $I = 2\pi fCE\ 10^{-6}$? Calculate susceptance and reactance and plot against frequency. (See Fig. 447*a* and 447*b*.) Calculate C, and compare with the value found in (a).

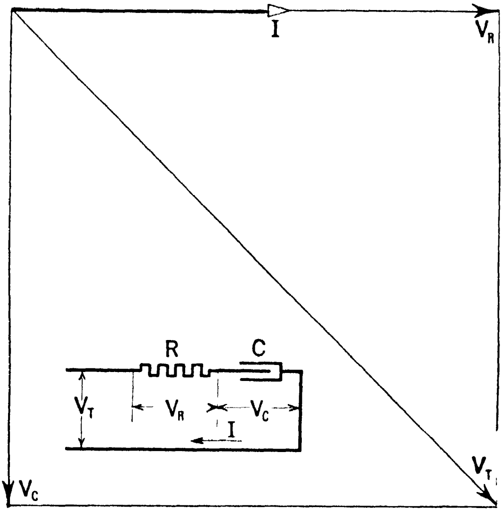

FIG. 451. Vector relations in a circuit containing resistance and capacitance in series.

Run 2. Calculate the capacitance, the resistance, the capacitive reactance and susceptance, and the total impedance $z = \sqrt{r^2 + x_c^2}$ for several sets of data, and compare z calculated above with that found as the ratio of the volts to the total current. Draw vector diagrams (Fig. 451) for two sets of readings with f constant, E variable, and again with E constant, f variable.

Run 3. Calculate capacitive susceptance ($b = I_3/E$), the resistance

r, conductance g, and total admittance $y = \sqrt{g^2 + b^2}$. Correct wattmeter readings for loss in the potential circuit if necessary, and determine the power factor, $\cos \theta = W/EI$, comparing it with the ratio g/y.

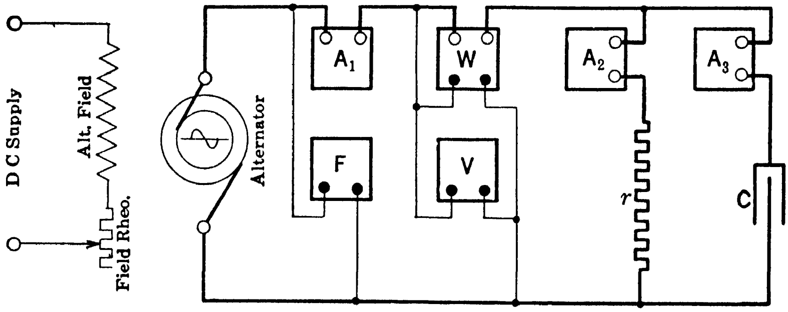

Fig. 452. Test of capacitance and resistance in parallel.

Assuming that total watts $= E^2/r$, compare the wattmeter readings (corrected) with values so calculated and explain differences.

Comment upon the power readings with C in and out of the circuit.

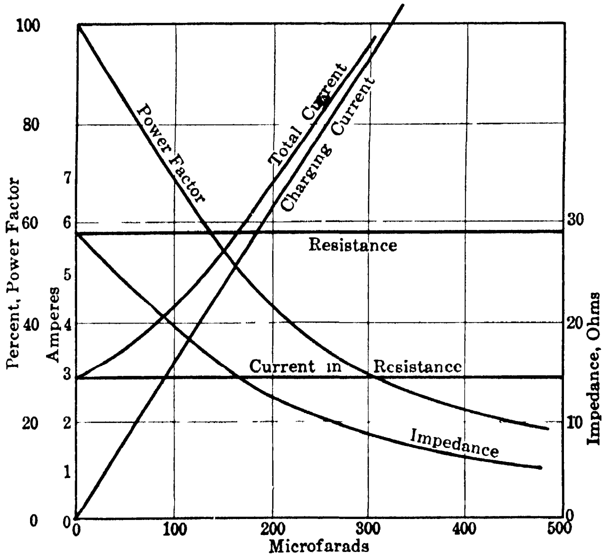

Fig. 453. Electrical relations with resistance and capacitance in parallel; voltage and frequency constant, capacitance variable.

Plot curves of readings and calculated values as functions of the variable frequency. Figure 453 shows similar curves but for C constant, f variable.

Draw vector diagrams at two values of voltage and at two values of frequency. Compare power factor from vector diagrams with the ratio W/EI.

603. The Imperfect Condenser. — In §590 it was stated that, owing to dielectric loss and leakage, the commercial condenser with solid dielectric could not be considered to be free from loss, i.e., as a pure capacitance. The effect of dielectric hysteresis becomes increasingly important as the frequency of the alternating emf impressed upon the condenser increases into the audio and radio ranges (Chapter LIX). Equation (6) indicated that alternating current and potential in a capacitance are in quadrature. This is not true of the imperfect capacitor which should be thought of as a perfect condenser of capacitance C_s in series with a resistance, R_s (Fig. 454*a*), or as a capacitance, C_p, in parallel with a resistance, R_p (Fig. 454*c*). A commercial condenser, then, will not pass a current leading the potential by 90 degrees, and therefore at zero power factor. The table in §586 gives characteristic power factors of several common dielectric materials used in the insulation of condensers.

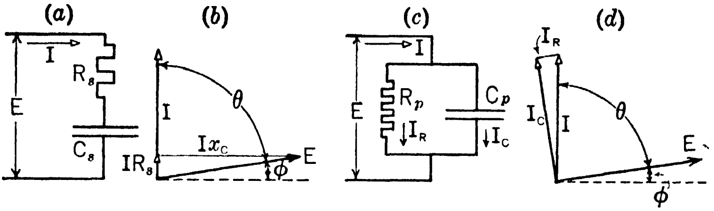

FIG. 454. Equivalent circuits and vector diagrams of the imperfect condenser.

Equivalent series resistance. Considering the loss in the condenser as due to a series resistance, R_s,

$$W = I^2R_s, \quad \text{or} \quad R_s = W/I^2 \tag{14}$$

The impedance of the condenser is then (eq. 12)

$$Z_s = R_s - jX_s = R_s - j\,10^6/(2\pi fC_s) \quad \ldots\ldots \tag{15}$$

where C_s is in microfarads. If $\cos\theta$ is the power factor

$$\tan\theta = X_s/R_s = 10^6/2\pi fC_sR_s \quad \ldots\ldots \tag{16}$$

Since θ is so nearly equal to 90 degrees, it is usual to evaluate the phase-defect angle, $\phi = 90° - \theta = \cot^{-1} X_s/R_s$ . . . . (17)

Therefore the phase-defect angle is given by the expression

$$\tan\phi = 2\pi fC_sR_s/10^6 \quad \ldots\ldots \tag{18}$$

If E is the total voltage (rms) across the defective condenser the fractional part, EX_s/R_s is the drop across the capacitance, C_s. Therefore (eq. 3)

$$I = (2\pi fC_s)/10^6 \cdot EX_s/Z_s \quad . \; . \; . \; . \; . \; . \; . \; . \quad (19)$$

But $X_s/Z_s = \sin\theta$. Solving for C_s:

$$C_s = I \times 10^6/(2\pi fE \sin\theta)$$

$$= I \times 10^6/(2\pi fE\sqrt{1 - \cos^2\theta}) \quad . \; . \; . \; . \; . \; . \quad (20)$$

In the test of such a condenser, if W, E, f, and I are known, then $\cos\theta = W/IE$ may be calculated, so that C_s is then found from eq. (20), and R_s from eq. (14).

Equivalent parallel resistance. In Fig. 454*c* the imperfect condenser is considered to consist of the pure capacitance C_p in parallel with the resistance R_p. From the theory of the parallel circuit, power loss is:

$$W = E^2/R_p, \qquad \text{or} \qquad R_p = E^2/W \quad . \; . \; . \; . \; . \; . \quad (21)$$

Expressing the admittance of the branched circuit in terms of conductance and susceptance (§597)

$$G = 1/R_p; \quad B = 2\pi fC_p/10^6; \quad \text{and} \quad Y = \sqrt{G^2 + B^2}$$

while

$$\cos\theta = G/Y, \quad \text{and} \quad \sin\theta = B/Y \quad . \; . \; . \; . \; . \quad (22)$$

Denoting by I_c the current through the pure capacitance (Fig. 454*c*),

$$I_c = EB = 2\pi fC_pE/10^6 \quad . \; . \; . \; . \; . \; . \; . \; . \; . \quad (23)$$

while total current is

$$I = EY \quad . \; . \; . \; . \; . \; . \; . \; . \; . \; . \; . \; . \quad (24)$$

Therefore: $I = (2\pi fC_pEY)/(B \times 10^6) = 2\pi fC_pE/(\sin\theta \times 10^6)$ (25)

or

$$C_p = I\sqrt{1 - \cos^2\theta} \times 10^6/(2\pi fE) \quad . \; . \; . \; . \; . \; . \; . \; . \; . \quad (26)$$

Equations (21) and (26) permit the determination of the equivalent resistance and capacitance of the imperfect condenser from measurements of current, potential, and loss when a sine-form emf wave of known frequency is impressed.

604. EXPERIMENT 27-B. — Tests of an Imperfect Condenser. — Although an accurate determination of the equivalent resistance and capacitance of an imperfect condenser requires a suitable a-c bridge and calibrated standards (see Chapter XXVIII), an attempt should be made to measure the losses of, say, a paper-insulated condenser, using as nearly as possible a pure sine wave of applied voltage, and carefully calibrated instruments of high sensitivity. The theory of §603 should be applied in calculating equivalent values, assuming first the series and then the parallel circuits for R and C.

605. Capacitance and Inductance in Series and in Parallel. — In Chapter VI, §138, it was shown that an inductance, L, in a circuit through which a sine-form current, $i = I_m \sin 2\pi ft$, was passing, caused a voltage drop

$$e = L\,di/dt = 2\pi fLI_m \cos 2\pi ft \quad . \; . \; . \; . \; . \; . \quad (27)$$

This voltage drop leads the current by 90 degrees, or, in vector terms,

$$\dot{E}_L = j2\pi fL\dot{I} = j\dot{I} \quad . \; . \; . \; . \; . \; . \; . \; . \; . \quad (28)$$

From eq. (6), the voltage drop across a capacitance in an a-c circuit is

$$E_c = -j\dot{I}/(2\pi fC) = -j\dot{I}x_c \quad . \; . \; . \; . \; . \; . \; . \quad (29)$$

From the above considerations it is evident that a capacitive reactance, x_c, may be considered as a negative inductive reactance so far as current-voltage relations are concerned. Therefore, when the two are in series, the result is the same as if a reactance equal to their difference $(x - x_c)$ were connected in the circuit. This equivalent or effective reactance may be of the nature of either component, depending upon whether $x_c > x$ or $x_c < x$.

When the two reactances are in parallel, they are combined according to the general rule for the combination of reactances or impedances in parallel (§§150 and 152), the opposite signs of x and x_c being kept in mind.

Because of the opposite effects of capacitance and inductance in an a-c circuit, the resulting voltage or current may be higher than if only one of them were present. This gives rise to a group of phenomena known as "electric resonance," which in some cases may be a disturbing factor in the operation of electrical apparatus, whereas in others it may be highly desirable. Some simple instances of resonance, observable at low frequencies, are discussed below.[2]

606. Parallel (Current) Resonance. — Let an inductance, L, and a capacitance, C, be connected in parallel to the same source of a-c energy (Fig. 455). Let the switch S_2 be open and S_1 closed. Let a current of, say, 5 amperes flow through the inductance, L, this current being practically in lagging quadrature with the applied voltage. Now let the switch S_1 be opened and S_2 closed, and let a current of, say, 4 amperes flow through the capacitance C. This current is practically in leading quadrature with the applied voltage (Fig. 456).

---

[2] See C. P. Steinmetz, "Transient Phenomena," and C. E. Magnusson, "Electric Transients," for phenomena taking place during transient conditions.

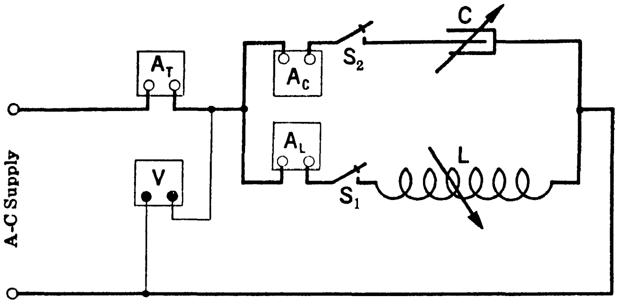

FIG. 455. Capacitance and inductance in parallel — conditions for current resonance.

Should both switches be closed simultaneously, the ammeter A_L will read 5 amperes, A_C will indicate 4 amperes, and the line ammeter, A_T, will show the geometric difference of the two, that is, about 1 ampere.

The above-described condition, when the resultant current is smaller than one or more of its components, is known as a *partial current resonance.* By properly adjusting the values of L and C, or the frequency of the supply, it is theoretically possible, provided that L and C are free from losses, to reduce the line current to zero, in which case the two component currents will be equal and opposite. Such a condition is called *perfect current resonance.* It takes place when, numerically:

$$x = x_c \quad . \; . \; . \quad (30)$$

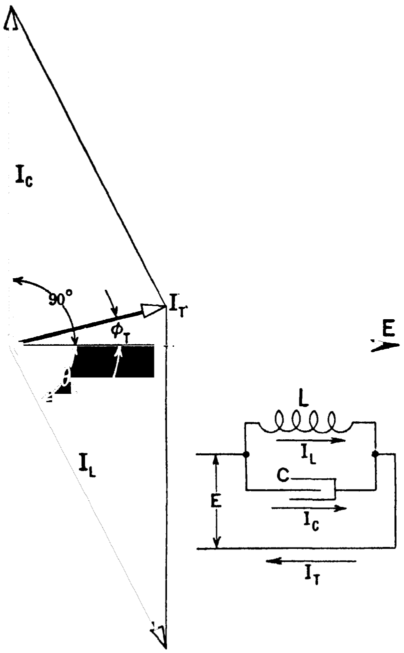

FIG. 456. Vector relations in a circuit having inductance and capacitance in parallel.

that is, when:

$$2\pi f L = 1/(2\pi f C) \quad . \; . \quad (31)$$

The latter relationship may be written in the form:

$$2\pi f \sqrt{LC} = 1 \quad . \; . \; . \; . \; . \; . \; . \; . \; . \; . \quad (32)$$

or

$$f = 1/2\pi\sqrt{LC} \quad . \; . \; . \; . \; . \; . \; . \; . \; . \; . \; . \quad (33)$$

In these expressions, f is the frequency of both currents, in cycles per second; L is the inductance in henrys; and C is the capacitance in farads. Equation (33) gives the *critical frequency* at which resonance will occur in the circuit.

In practice, the presence of unavoidable resistance makes it possible to obtain only an approximately perfect current resonance. The effect of varying capacitance is shown in Fig. 457. E is the applied voltage, and I_L is the (constant) current through the inductive reactance. Because there is some resistance, the current lags behind the voltage by less than 90 degrees. Theoretically, owing to imperfect dielectric the capacitive current I_c', leads the voltage by slightly less than 90 degrees, but the angle may be assumed to be 90 degrees. The geometric sum of these currents is the line current, I_T'. It lags behind the voltage whenever the inductive admittance happens to be higher than the capacitive admittance.

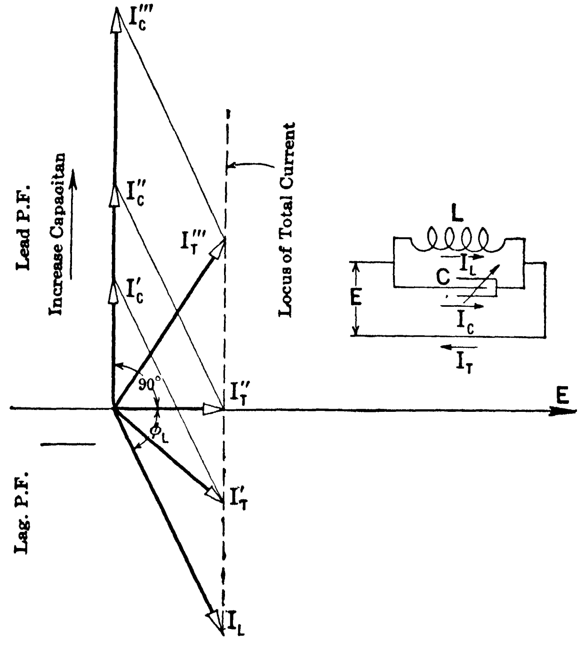

Fig. 457. A composite diagram for inductance and capacitance in parallel — capacitance variable.

Should the capacitance be increased so as to draw the current I_c'', the resultant line current would become I_T'', in phase with the voltage E, as if the whole circuit were non-inductive. This is the nearest approach to a perfect resonance possible with the given circuit. Should the capacitance be still further increased so as to draw the current I_c''', the line current, I_T''', becomes leading. The same relations are shown in Fig. 458 in the form of curves. As the capacitance is increased, the line current first drops, then increases again and becomes leading.

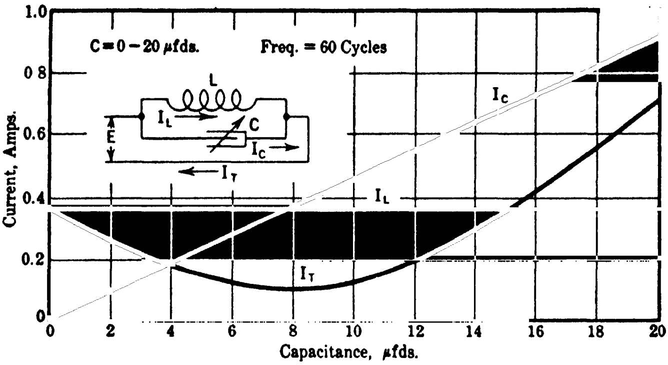

FIG. 458. Curves illustrating current resonance.

607. Effect of Resistance upon Current Resonance. — Case 1. Referring to Fig. 458, consider that the inductance coil has a resistance R, in addition to its inductance L, while the capacitance is free from losses. The current I_L in the inductive branch of the circuit will be

$$\dot{I}_L = \dot{E}/\sqrt{R^2 + \omega^2 L^2}\,\underline{/\tan^{-1} \omega L/R}\,. \tag{34}$$

In this branch $\cos \theta_L = R/\sqrt{R^2 + \omega^2 L^2}$

and $\sin \theta_L = \omega L/\sqrt{R^2 + \omega^2 L^2}$

where $\theta_L = \tan^{-1} \omega L/R$. Then,

$$\dot{I}_L = \frac{\dot{E}}{\sqrt{R^2 + \omega^2 L^2}} (\cos \theta_L - j \sin \theta_L)$$

$$= \dot{E}\left(\frac{R}{R^2 + \omega^2 L^2} - j\,\frac{\omega L}{R^2 + \omega^2 L^2}\right) \quad \ldots\ldots \tag{35}$$

In the capacitive branch of the circuit,

$$\dot{I}_c = j\omega C \quad \ldots\ldots\ldots\ldots \tag{36}$$

The total current $\dot{I}_T = \dot{I}_L + \dot{I}_c$

or

$$\dot{I}_T = \dot{E}\left[\frac{R}{R^2 + \omega^2 L^2} + j\left(\omega C - \frac{\omega L}{R^2 + \omega^2 L^2}\right)\right] \quad . . . \quad (37)$$

For the value of C which makes the power factor of the circuit unity,

$$\omega C - \omega L/(R^2 + \omega^2 L^2) = 0 \quad . . . . \quad (38)$$

Then

$$\dot{I}_T'' = ER/(R^2 + \omega^2 L^2) \quad . . . . \quad (39)$$

From eq. (38) the capacitance at which, for given values of f, R, and L, resonance occurs in the circuit is:

$$C = L/(R^2 + 4\pi^2 f^2 L^2) \quad . . . . \quad (40)$$

When R is negligible

$$C = 1/(4\pi^2 f^2 L) \quad . . . . \quad (41)$$

which agrees with eq. (33).

For fixed values of C, R, and L, resonance occurs at the frequency obtained by solving eq. (40), or

$$f = \frac{1}{2\pi}\sqrt{(1/LC) - R^2/L^2} \quad . . . . \quad (42)$$

Case 2. *Both inductance and capacitance are considered to possess appreciable series resistance* (Fig. 459). To determine the total current, in value and in phase relation, it is sufficient to find the separate admittances through the capacitive and inductive branches of the circuit and add them. The meanings of the various symbols are evident from an inspection of Fig. 459.

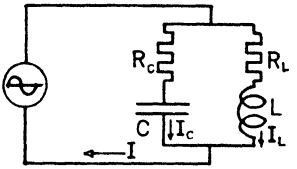

FIG. 459. Imperfect condenser in parallel with an imperfect inductance.

For the capacitive branch, the square of the impedance is

$$Z_c^2 = R_c^2 + 1/\omega^2 C^2 = (\omega^2 C^2 R_c^2 + 1)/\omega^2 C^2 \quad . . . . \quad (43)$$

The admittance of this branch

$$Y_c = G_c + jB_c = R_c/Z_c^2 + jX_c/Z_c^2$$

Remembering that $X_c = 1/\omega C$, and substituting for Z_c^2 from eq. (43),

$$Y_c = \frac{\omega^2 C^2 R_c}{\omega^2 C^2 R_c^2 + 1} + j\frac{\omega C}{\omega^2 C^2 R_c^2 + 1} \quad . . . . . \quad (44)$$

For the inductive branch

$$Z_L^2 = R_L^2 + \omega^2 L^2$$

and

$$Y_L = \frac{R_L}{Z_L^2} - \frac{jX_L}{Z_L^2} = \frac{R_L}{R_L^2 + \omega^2 L^2} - j\frac{\omega L}{R_L^2 + \omega^2 L^2} \quad . \; . \quad (45)$$

The total admittance,

$$Y_0 = Y_c + Y_L = \left(\frac{\omega^2 C^2 R_c}{\omega^2 C^2 R_c^2 + 1} + \frac{R_L}{R_L^2 + \omega^2 L^2}\right)$$
$$- j\left(\frac{\omega L}{R_L^2 + \omega^2 L^2} - \frac{\omega C}{\omega^2 C^2 R_c^2 + 1}\right) \quad . \; . \; . \quad (46)$$

For unity power factor (at resonance) the reactive term must vanish from eq. (46), or

$$\frac{\omega L}{R_L^2 + \omega^2 L^2} = \frac{\omega C}{\omega^2 C^2 R_c^2 + 1}$$

Solving

$$\omega^2 = (R_L^2 C - L)/LC(R_c^2 C - L) \quad . \; . \; . \; . \; . \quad (47)$$

Since $\omega = 2\pi f$, the resonant frequency f' becomes

$$f' = \frac{1}{2\pi}\sqrt{\frac{1}{LC}\,\frac{R_L^2 C - L}{R_c^2 C - L}} \quad . \; . \; . \; . \; . \; . \; . \; . \; . \quad (48)$$

For the case in which R_c is negligible eq. (48) reduces to eq. (42). For the case of resonance

$$I = E\left(\frac{\omega^2 C^2 R_c}{\omega^2 C^2 R_c^2 + 1} + \frac{R_L}{R_L^2 + \omega^2 L^2}\right) \quad . \; . \; . \; . \quad (49)$$

608. EXPERIMENT 27-C. — Capacitance and Inductance in Parallel; Current Resonance. — The connections are shown in Fig. 456. Instead of three ammeters, it may be more convenient to use one ammeter and a polyphase board (§60). The source of current must be as nearly sinusoidal as is feasible, for the reason explained at the end of §600. To make the conditions as simple as possible, first use an inductive coil without iron, or at least one in which the magnetic circuit is not saturated and has a large air-gap.

Run 1. (a) Close switch S_1, and, holding voltage and frequency constant, adjust the current through L to a desired value. Then close S_2 and increase the capacitance over the available range in approximately equal steps. For each value of C record the component currents,

I_L and I_c, total current I_T, volts, frequency, and watts. Note that the total current decreases and then increases again.

(b) Introduce resistance in series with the inductance and repeat the test.

(c) Shunt the condenser with a high resistance and repeat.

Run 2. Repeat the above test, varying the frequency over as wide a range as possible. If it is available use an oscillograph to record wave forms and phase relations. Note especially any evidence of oscillating current in the local circuit of L and C when E is suddenly changed.

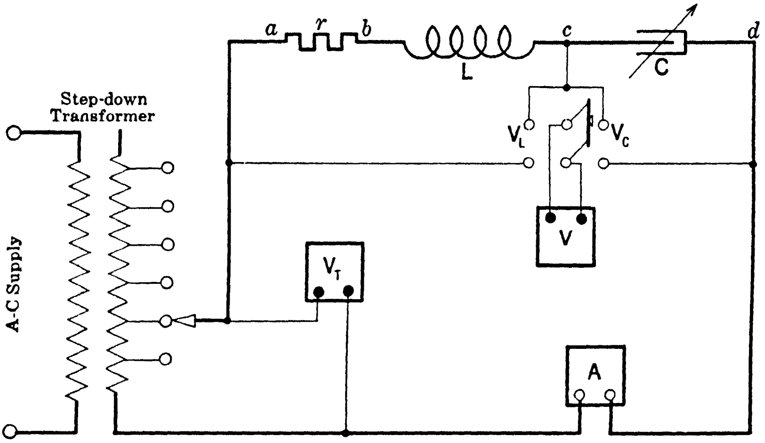

Fig. 460. Inductance and capacitance in series — voltage resonance.

Report. Make necessary calculations and plot the results as in Fig. 458. Draw vector diagrams at resonance and at either side of the resonant point (Fig. 457). Check the phase angles in the diagrams with those calculated from wattmeter readings.

Having determined the resistance and reactance of the coil, and the capacitive reactance of the condenser for a certain set of readings, calculate the total impedance of the circuit and compare with E/I. Check eq. (42) in §607 at resonance. Compare theoretical deductions and diagrams with the oscillograms.

609. Series or Voltage Resonance. — Let an inductance, L, and a capacitance, C, be connected in series as in Fig. 460. The resistance, r, is at first assumed to be negligible. Consider a certain current I to flow in the circuit. The voltage across a pure inductance, L, leads the current by 90 degrees; the voltage across the condenser lags behind it by the same amount. Hence the voltages across L and C are opposite and at least partially neutralize. Therefore the total voltage across the combination will be smaller than either. This condition is called *partial voltage resonance.* In the limiting case, when the two voltages are equal and opposite, there results *complete voltage resonance.* When such a condition occurs voltages dangerous to equipment and to life may result.

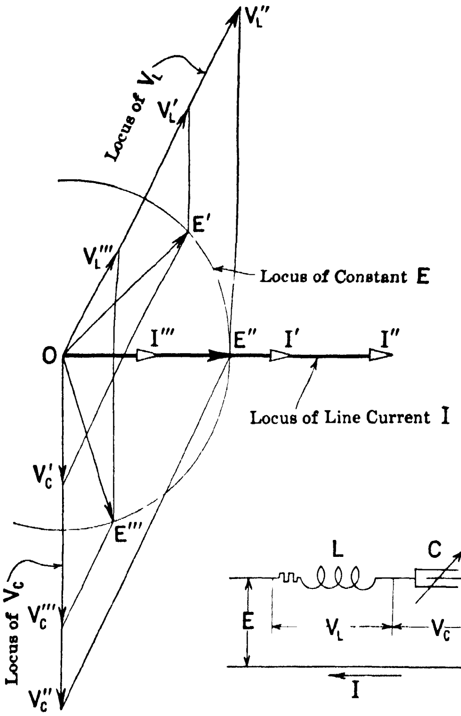

FIG. 461. Composite vector diagram for inductance and capacitance in series — capacitance variable.

Resonance is modified in practice by the unavoidable presence of some resistance, r (Fig. 460), which limits the current and the rise of potential. Assume the resistance and the inductive reactance to remain constant and the capacitance, C, to be gradually increased. This will cause the line current and the voltages to vary. Assume that line voltage is kept constant at a rather low value by using suitable taps on the step-down transformer.

Figure 461 shows the variation of the several vectors, when C is varied but L is held constant. In the polygon $OV_L'E'$, the current being variable but L constant, the impedance drop, OV_L, increases and decreases with the value of the current. The point E' moves on a circular arc drawn from O with the constant line voltage, E, as radius.

For small values of capacitance (large x_c) the figure assumes the position $OV_L'''E'''$, and the current is leading. At a certain value of capacitance the line voltage E'' is in phase with the current, as if the circuit contained resistance only. Similar relations are shown in the curves of Fig. 462, for x_c constant but x_L varying.

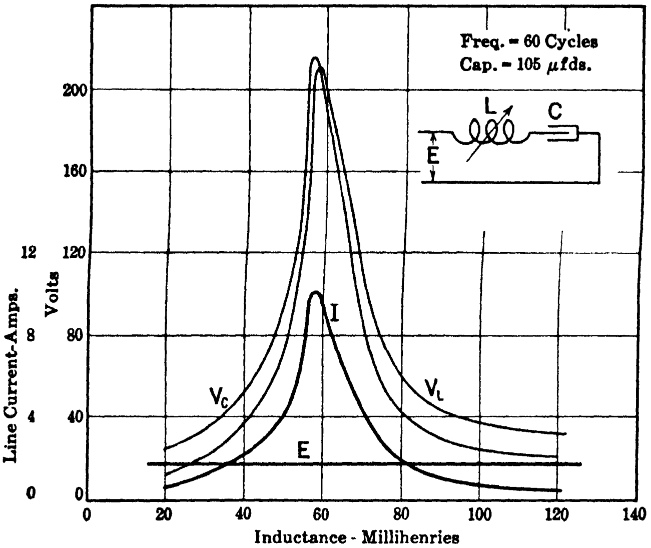

Fig. 462. Curves of voltage resonance — inductance variable.

610. EXPERIMENT 27-D. — Capacitance and Inductance in Series; Voltage Resonance. — The connections are shown in Fig. 460. The source of current should be as nearly sinusoidal as possible. Keep the supply voltage at a low enough value, introducing a step-down transformer if necessary, so that the current cannot exceed a safe value, even when $x_L = x_c$. (a) Connect in the circuit the minimum capacitance, using sufficient inductive reactance to have a rather small leading current. This corresponds to the left-hand end of the curves in Fig. 462. Increase the capacitance in steps, and at each step measure the voltages across L and across C; also the line voltage, power, and current. Maintain frequency constant. The voltage curve rises quite abruptly; therefore care should be exercised not to break down the insulation of the condenser. When the safe limit has been reached, open the circuit and reduce the reactance x_c (increase C) considerably beyond the resonance point, so as to have a small lagging current. Then approach the point of maximum resonance from the other side.

(b) Repeat this run with a fixed resistance equal to, say, 20 per cent of the impedance of the coil.

(c) Now set C at the value giving resonance; keep applied volts at the same value as before and vary the frequency over a wide range, reading as before.

Report. Plot curves as in Fig. 462 except that abscissas should be variable capacitance. Plot similar curves against frequency. Draw a diagram such as that shown in Fig. 461. Compare phase angles by diagram and from wattmeter readings. Note that the curves in (b) are more flat than those in (a). Explain.

REFERENCES

1. B. L. ROBERTSON and C. A. NICKLE, *Gen. Elec. Rev.*, August, 1930, Inductance and a simple laboratory means for its determination.

2. A. M. WIGGINS, *Elec. Jour.*, January, 1927, p. 20, Iron-core reactors with air gaps.

3. E. G. REED, *Elec. Jour.*, January, 1929, to August, 1929, inclusive, Alternating-current vector algebra.

4. V. PETROVSKY, *Gen. Elec. Rev.*, April, 1930, p. 215, Directed quantities in a plane space.

5. B. S. WILLIS, *Gen. Elec. Rev.*, April, 1931, Mechanical aids in the construction of vector diagrams.

6. SALTER, SHANKLIN, and WISEMAN, *Elec. Eng'g*, December, 1934, p. 1581, Resistance and reactance of three-conductor cables.

7. M. MALTI, Electric Circuit Analysis, John Wiley & Sons.

8. M. P. WEINBACH, Alternating-Current Circuits, Macmillan Co.

9. R. R. LAWRENCE, Principles of Alternating Circuits, McGraw-Hill Book Co.

10. F. M. COLEBROOK, Alternating Currents and Transients, McGraw-Hill Book Co.

11. A. E. CLAYTON, Alternating Currents, Longmans, Green & Co.

12. C. E. MAGNUSSON, Electric Transients, McGraw-Hill Book Co.

13. V. KARAPETOFF, The Electric Circuit, McGraw-Hill Book Co.

14. BRYANT and CORRELL, Alternating-Current Circuits, McGraw-Hill Book Co.

15. KERCHNER and CORCORAN, Alternating-Current Circuits, John Wiley & Sons.

CHAPTER XXVIII

ALTERNATING-CURRENT BRIDGES

611. The Wheatstone bridge, described in Chapter I for d-c resistance measurements, is also used with a-c currents for a comparison or relative measurement of self- and mutual inductances and capacitances. Since rapid and accurate testing of inductances and capacitances over a wide range has become of considerable practical importance, notably in the communication field, special bridges have been designed to enable such tests to be made with ease and accuracy. Such a device often consists of a plain four-arm Wheatstone bridge with resistance coils and with terminals by means of which any other coil or condenser can be connected in series or in parallel to any arm.[1]

A source of sinusoidal alternating current is used in the a-c bridge. At low frequencies, an ordinary sine-wave alternator, and for higher frequencies, an electrically operated tuning fork, may be used; at frequencies up to 4000 cycles per second, a Vreeland oscillator is very convenient. At still higher frequencies an electronic oscillator is employed. For a detector of electrical balance, a telephone receiver has been largely used where the frequencies are within the audible range. A vibration galvanometer (§45) is also useful within a certain range. A d-c galvanometer with a suitable rectifier can be used, and the heterodyne principle can be applied in the high-frequency range. With some of the measurements described below, the four resistances of the bridge have to be previously balanced on direct current; with other measurements this is not feasible.

612. The General Balanced A-C Bridge. — A general a-c bridge is shown in Fig. 463.[2] There are four impedances, Z_1, Z_2, Z_3, and Z_4, any one of which may contain either inductance or capacitance; some branches may have ohmic resistance only.

---

[1] Those interested in the subject of a-c bridges beyond the scope of this chapter will find detailed information in B. Hague's book, "Alternating-Current Bridge Methods," Pitman & Sons. Considerable information will also be found in E. M. Terry, "Advanced Laboratory Practice in Electricity and Magnetism," Chapters XI and XII, McGraw-Hill. For vibration galvanometers, see also A. E. Kennelly, "Electrical Vibration Instruments," Chapter XXII, Macmillan. Considerable information on the subject is also contained in descriptive technical catalogues of leading manufacturers of a-c bridges, galvanometers, oscillators, etc.

[2] V. Karapetoff, *Phil. Mag.*, vol. 44 (1922), p. 1024, The general a-c bridge.

Let the bridge be balanced on alternating current, that is, let the current in the galvanometer branch, *cd*, be equal to zero. The same current, I_u, is then flowing through both upper branches, Z_2 and Z_4.

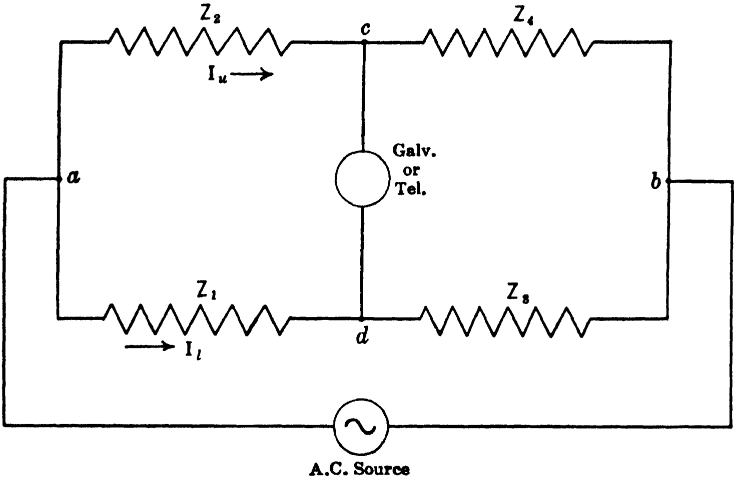

FIG. 463. Diagram of the general a-c bridge.

Let a current, I_l, flow through both lower branches, Z_1 and Z_3. (The subscripts *u* and *l* stand for "upper" and "lower," respectively.) The electrical relations are shown in Fig. 464, all four branches being assumed

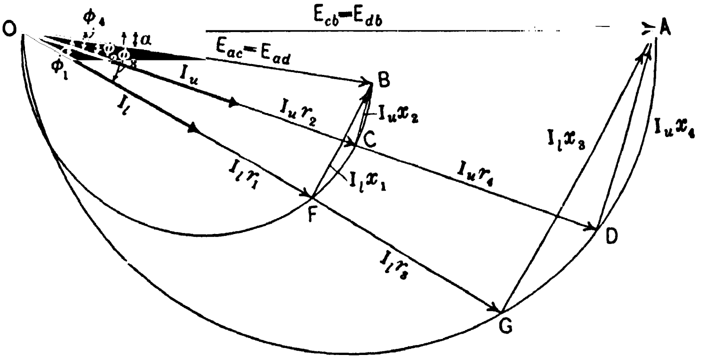

FIG. 464. Currents and voltages in a balanced a-c bridge.

to possess an inductive reactance and a resistance. Figure 464 is similar to Fig. 140 and expresses the following conditions: (1) The galvanometer current being equal to zero, the voltage between the points *a* and *c* (Fig. 463) is equal to that between *a* and *d*. Similarly, the voltage between c and b is equal to that between d and b. (2) The voltage drop in the branch 1 consists of the ohmic drop $I_l r_1$ in phase with the current I_l, and of the reactive drop, $I_l x_1$, in leading phase quadrature with the current. (3) Similar relationships hold true for the branches 2, 3, and 4. The corresponding phase angles are denoted by ϕ_1, ϕ_2, ϕ_3, and ϕ_4.

From this figure certain electrical relationships between the resistances and the inductances may be deduced, so that an unknown inductance may be computed in terms of the remaining quantities. If a capacitance is present, the corresponding reactance and the phase angle are assumed to be negative and plotted in the opposite direction (§601).

613. The Fundamental Equations of a Balanced A-C Bridge.—Although the analytical relationships between the individual resistances and reactances can be derived directly from the diagram shown in Fig. 464, a much more direct and concise way is by means of complex quantities. Denoting the impedances of the four branches by Z's, with the corresponding subscripts, we have:

$$I_u Z_2 = I_l Z_1 \quad \dots \dots \dots \quad (1)$$

$$I_l Z_3 = I_u Z_4 \quad \dots \dots \dots \quad (2)$$

Multiplying these equations, term by term, we get:

$$Z_2 Z_3 = Z_1 Z_4 \quad \dots \dots \dots \quad (3)$$

which is the fundamental equation of a balanced a-c bridge.

Let each branch consist of a resistance, r, in series with a reactance, x, the branches being distinguished by the corresponding subscripts. Then eq. (3) becomes:

$$(r_2 + jx_2)(r_3 + jx_3) = (r_1 + jx_1)(r_4 + jx_4) \quad \dots \quad (4)$$

Carrying out the multiplication and equating the real parts, also the imaginary parts, gives:

$$r_2 r_3 - x_2 x_3 = r_1 r_4 - x_1 x_4 \quad \dots \dots \dots \quad (5)$$

$$x_2 r_3 + r_2 x_3 = r_1 x_4 + x_1 r_4 \quad \dots \dots \dots \quad (6)$$

These expressions constitute the basis of several bridge measurements described below.

In some cases it is more convenient to use admittances, Y (§151), in place of the impedances, especially when a branch of the bridge consists of two paths in parallel. Equation (3) then becomes:

$$Y_2 Y_3 = Y_1 Y_4 \quad \dots \dots \dots \quad (7)$$

Equation (7) may be written:

$$(g_2 - jb_2)(g_3 - jb_3) = (g_1 - jb_1)(g_4 - jb_4) \qquad (8)$$

or, multiplying through and separating the real from the imaginary terms:

$$g_2g_3 - b_2b_3 = g_1g_4 - b_1b_4 \quad . \; . \; . \; . \; . \; . \; . \; . \quad (9)$$

$$b_2g_3 + g_2b_3 = b_1g_4 + g_1b_4 \quad . \; . \; . \; . \; . \; . \; . \; . \quad (10)$$

Cases are also possible in which there are two paths in parallel in one or more branches of the bridge, while in the remaining branches series connections are used. For example, if there is a parallel connection in branch 3, eq. (3) becomes:

$$Z_2/Y_3 = Z_1Z_4 \quad . \; . \; . \; . \; . \; . \; . \; . \; . \; . \quad (11)$$

This equation can be resolved into a real and an imaginary part, and two equations thus obtained, similar to eqs. (5) and (6), or (9) and (10).

The foregoing equations will now be applied to some practical bridge arrangements shown in Fig. 465.

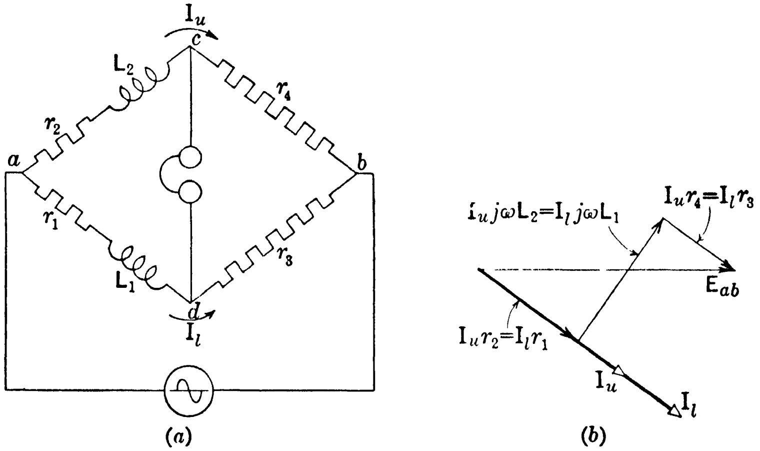

FIG. 465. The inductance bridge — connections and vector relations.

614. Comparison of Two Inductances by Means of an A-C Bridge (Inductance Bridge). — Figure 465*a* represents a special case of the bridge shown in Fig. 463. The branches 3 and 4 consist of non-inductive resistances only ($x_3 = x_4 = 0$), and the branches 1 and 2 contain some resistance as well as inductance. Let the bridge be first balanced on direct current, so that:

$$r_2r_3 = r_1r_4 \quad . \; . \; . \; . \; . \; . \; . \; . \; . \; . \; . \quad (12)$$

Then, with a-c balance, eq. (5) is also satisfied, and eq. (6) becomes:

$$x_2 r_3 = x_1 r_4 \quad . \quad . \quad . \quad . \quad . \quad . \quad . \quad . \quad . \quad . \quad . \quad (13)$$

or, since $x = 2\pi fL$:

$$x_1/x_2 = L_1/L_2 = r_3/r_4 = r_1/r_2 \quad . \quad . \quad . \quad . \quad . \quad . \quad . \quad (14)$$

In other words, when the bridge is balanced on direct as well as on alternating current, the ratio of the inductances or reactances is equal to that of the resistances. If one of the inductances is known, the other can be computed from the known ratio of the resistances.

615. EXPERIMENT 28-A. — Comparison of Two Inductances by Means of an A-C Bridge. — The method is described in the preceding section. A balance is first obtained with direct current so that eq. (12) is satisfied. Then a balance is obtained with alternating current, a variable standard inductance being used for L_1 or L_2, while the resistances are kept constant. When the bridge is balanced, eq. (14) holds true and the unknown inductance can be computed.

In addition to obtaining some practice in measurements, the student should investigate the following factors: (a) the advantages and the disadvantages of various a-c balance detectors (§611); (b) the influence of the frequency, eddy currents, and skin effect, upon the result; (c) the best source of alternating current and the disturbing effect of higher harmonics; (d) the best ratio of the resistances for maximum sensitiveness and accuracy; (e) the case in which the unknown inductance has an iron core, and the effect of saturation and core loss; (f) inaccuracy due to a mutual induction between the branches, or from an external circuit. In the report discuss the results obtained, and the limitations of the methods used. Draw vector diagrams to illustrate the relations involved.

616. The Capacitance Bridge. — Two forms of the a-c bridge for the comparison of capacitances will be considered, namely, the series-resistance and the parallel-resistance types.[3]

(1) *Series-resistance type.* Connections are shown in Fig. 466. Branches 3 and 4 consist of non-inductive resistances (ratio values). The capacitances C_1 and C_2, to be compared, are in branches 1 and 2, in series with adjustable standard resistances, r_1 and r_2. Owing to dielectric losses or leakage in the condensers the equivalent series resistances ρ_1 and ρ_2 are also shown in these branches (§603). Balance is obtained by adjusting r_3 and r_4, also r_1 and r_2. Calling $r_1 + \rho_1 = R_1$, and $r_2 + \rho_2 = R_2$, at balance

$$r_3(R_2 + 1/j\omega C_2) = r_4(R_1 + 1/j\omega C_1) \quad . \quad . \quad . \quad . \quad . \quad . \quad (15)$$

---

[3] B. Hague, " A-C Bridge Methods," Chapter IV, Pitman & Sons.

After multiplication

$$r_3R_2 - jr_3/\omega C_2 = r_4R_1 - jr_4/\omega C_1 \quad \ldots \ldots \quad (16)$$

Equating reals

$$r_3R_2 = r_4R_1 \quad \text{or} \quad R_2/R_1 = r_4/r_3 \quad \ldots \ldots \quad (17)$$

Also

$$r_3/\omega C_2 = r_4/\omega C_1 \quad \text{or} \quad C_2/C_1 = r_3/r_4 \quad \ldots \quad (18)$$

If the phase error of condenser C_1 is known the phase error of C_2 may be determined. From eqs. (17) and (18)

$$C_1R_1 = C_2R_2 \quad \text{or} \quad C_1(r_1 + \rho_1) = C_2(r_2 + \rho_2) \quad \ldots \quad (19)$$

Therefore

$$\omega C_1\rho_1 - \omega C_2\rho_2 = \omega C_2r_2 - \omega C_1r_1 \quad \ldots \ldots \quad (20)$$

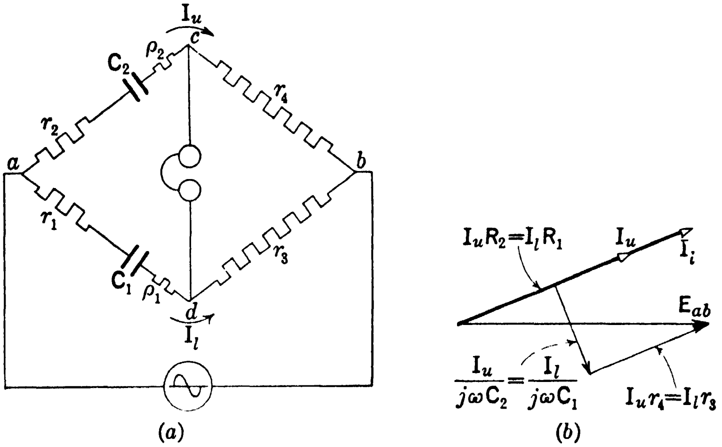

FIG. 466. The capacitance bridge; series-resistance type. (*a*) Connections; (*b*) vector relations.

With a resistance ρ_1 in series with a capacitance C_1 the impedance is $\rho_1 + 1/j\omega C_1$. The angle of phase error[4] is given by $\tan\theta_1 = \omega C_1\rho_1$, and $\tan\theta_2 = \omega C_2\rho_2$ so that, from eq. (20)

$$\tan\theta_2 - \tan\theta_1 = \omega C_1(r_1 - r_3r_2/r_4) \quad \ldots \ldots \quad (21)$$

or, since θ_2 and θ_1 are very small

$$\theta_2 - \theta_1 = \omega C_1(r_1 - r_3r_2/r_4) \quad \ldots \ldots \quad (22)$$

(2) *Parallel-resistance type.* When capacitances are connected in

---

[4] The phase angle, ϕ_1, of impedance, Z_1, $= \tan^{-1}\frac{x_1}{r_1}$, or $\tan\phi_1 = \frac{1}{\omega C_1\rho_1}$. Since the angle of phase error, θ_1, $= 90° - \phi_1$, $\tan\theta_1 = \omega C_1\rho_1$.

parallel with the resistances (Fig. 467), the fundamental equations, (9) and (10), are preferably used. Since $b_3 = b_4 = 0$, eq. (9) becomes:

$$g_2g_3 = g_1g_4 \quad . \; . \; . \quad . \; . \; . \; . \; . \; . \; . \quad (23)$$

and eq. (10) gives:

$$b_1/b_2 = C_1/C_2 = g_3/g_4 \quad . \; . \; . \; . \; . \; . \; . \quad (24)$$

In other words:

$$C_1/C_2 = r_4/r_3 = r_2/r_1 \quad . \; . \; . \; . \; . \; . \; . \quad (25)$$

Thus, when the bridge is balanced on direct current and on alternating current, the ratio of the capacitances is inversely that of the resistances. Here, again, it may be necessary to shunt the perfect condenser by a high resistance in order to balance it against an imperfect condenser.

To determine the equivalent capacitance and phase defect of an imperfect condenser this type of bridge may also be used. If r_1 and r_2 are adjustable standard resistances placed in parallel with C_1 and C_2 of which the equivalent shunting resistances due to dielectric losses are ρ_1 and ρ_2, then, calling $1/r_1 + 1/\rho_1 = g_1$ and $1/r_2 + 1/\rho_2 = g_2$, and remembering that b_3 and b_4 are each zero, while b_1 and b_2 are ωC_1 and ωC_2, respectively, one may write from eqs. (9) and (10)

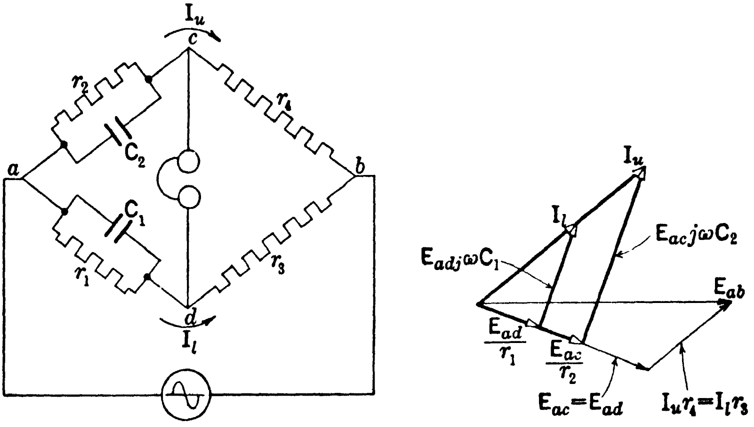

(a) (b)

FIG. 467. Capacitance bridge; parallel-resistance type. (a) Connections; (b) vector relations.

$$g_2g_3 = g_1g_4$$

and

$$b_2g_3 = b_1g_4 \quad . \; . \; . \; . \; . \; . \; . \; . \; . \; . \; . \quad (26)$$

or

$$(1/r_1 + 1/\rho_1)/(1/r_2 + 1/\rho_2) = \omega C_1/\omega C_2 \quad . \; . \; . \; . \quad (27)$$

Therefore

$$1/\omega C_1\rho_1 + 1/\omega C_1 r_1 = 1/\omega C_2\rho_2 + 1/\omega C_2 r_2 \quad . \; . \; . \; . \; (28)$$

Since the phase defect of a condenser and shunting equivalent resistance is measured by $\tan\theta = (1/\rho)/\omega C = 1/\omega C\rho$ from eq. (28) one may write

$$\tan\theta_2 - \tan\theta_1 = 1/\omega C_1 r_1 - 1/\omega C_2 r_2 \quad . \; . \; . \; . \; . \; (29)$$

or, approximately,

$$\theta_2 - \theta_1 = 1/\omega C_1 r_1 - 1/\omega C_2 r_2 \; . \; . \; . \; . \; . \; . \; . \; (30)$$

617. The Schering Impedance Bridge.[5] — A bridge which, in its more usual forms, has condensers in three arms and was developed primarily for high-voltage testing of bushings and determination of dielectric loss is called the Schering bridge. Its simplest form is shown in Fig. 468.

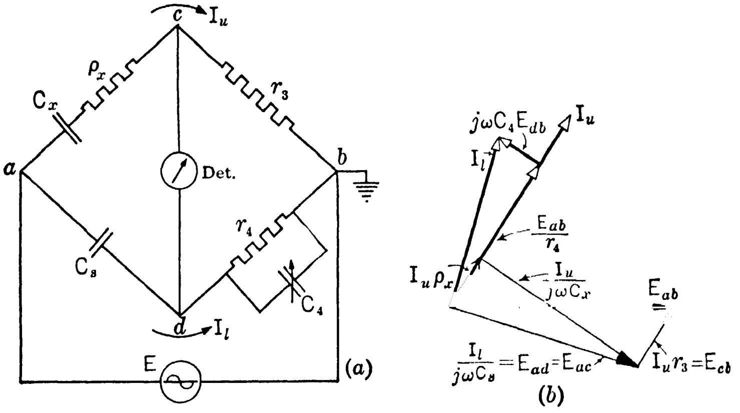

Fig. 468. Schering bridge used in test of high-voltage bushings. (a) Connections; (b) vector relations.

C_x and ρ_x are the capacitance and loss-equivalent resistance of the bushing under test. C_s is a standard air condenser assumed to be loss-free; r_3 and r_4 are pure resistances; C_4 is a variable air condenser. In a typical case C_s is about 100 $\mu\mu$f, with an impedance of 2.65×10^7 ohms at 60 cycles, the impedance of arm 4 is 1000 ohms, that is, the potential of r_4 and the adjustable capacitance C_4 above ground is low enough to be safely manipulated with proper insulating handles, unless there is a breakdown of C_x or C_s. Referring to Fig. 468*a*,

---

[5] For various forms of Schering bridge see F. A. Laws, " Electrical Measurements," Chapter VII, McGraw-Hill Book Co., or B. Hague, " A-C Bridge Methods," Chapter IV, Pitman & Sons. See also Hartshorn, *Beama*, 1923, vol. 13, p. 89; also B. Hague, *World Power*, August, 1925.

$$Z_x = \rho_x - j/\omega C_x, \quad Z_3 = r_3$$

$$Z_s = -j/\omega C_s, \quad Y_4 = (1/r_4) + j\omega C_4$$

At balance eq. (3) becomes

$$Z_x Z_4 = Z_s Z_3, \qquad \text{or} \qquad Z_x = Z_s Z_3 Y_4$$

Therefore

$$\rho_x - j/\omega C_x = (r_3 C_4/C_s) - jr_3/r_4 C_s \omega \quad . \; . \; . \; . \; . \quad (31)$$

Equating corresponding components

$$\rho_x = r_3 C_4/C_s \quad . \; . \; . \; . \; . \; . \; . \; . \; . \; . \; . \quad (32)$$

$$C_x = r_4 C_s/r_3 \; . \; . \; . \; . \; . \; . \; . \; . \; . \; . \; . \quad (33)$$

Power factor of the specimen = $\cot \theta$, approximately, or

$$\cos \theta = \rho_x \omega C_x = \omega C_4 r_4 \quad . \; . \; . \; . \; . \; . \; . \; . \; . \quad (34)$$

Since ρ_x is small compared with the reactance, $1/\omega C_x$, and since nearly the total voltage is across the test specimen,

$$I_u = \omega C_x E = \omega C_s E r_4/r_3$$

Power loss is, approximately,

$$W = EI_u \cos \theta = E^2 r_4{}^2 \omega^2 C_s C_4/r_3 \quad . \; . \; . \; . \; . \; . \quad (35)$$

618. Dawes and Hoover High-Voltage Bridge.[6] — A bridge especially adapted to the testing of high-voltage cables is shown in Fig. 469. C_x and ρ_x are the capacitance and series loss-equivalent resistance of the cable under test. C_s and ρ_s are the corresponding values of the standard condenser. $Z' = R' + j\omega L'$, and $Z'' = R'' + j\omega L''$, are the impedances of primary and secondary of a mutual inductance of coefficient M; r_3 and r_4 are adjustable resistances.

At balance the potential drops E_{ad} and $E_{ac'}$ must be equal, or

$$I_l(\rho_s - j/\omega C_s) = I_u(\rho_x - j/\omega C_x + Z' - j\omega M) \quad . \; . \; . \quad (36)$$

Similarly, since the drops E_{db} must equal $E_{c'b}$, or

$$I_l r_4 = I_u(r_3 + j\omega M) \quad . \; . \; . \; . \; . \; . \; . \; . \; . \; . \quad (37)$$

Dividing eq. (36) by eq. (37)

$$(\rho_s - j/\omega C_s)/r_4 = (\rho_x - j/\omega C_x + R' + j\omega L' - j\omega M)/(r_3 + j\omega M)$$

or

$$(\rho_s - j/\omega C_s)(r_3 + j\omega M) = r_4\,[\rho_x - j/\omega C_x + R' + j\omega(L' - M)]$$

---

[6] C. L. Dawes and P. L. Hoover, *Jour. A.I.E.E.*, 1926, pp. 337–347, Ionization in paper-insulated cables; also *ibid.*, 1929, pp. 3–7, 450–453.

Multiplying terms and equating corresponding components

$$\rho_x = (\rho_s r_3/r_4) + (M/C_s r_4) - R' \quad \ldots\ldots \quad (38)$$

and

$$1/C_x = (r_3/r_4 C_s) + \omega^2 [L' - M(1 + \rho_s/r_4)] \quad \ldots\ldots \quad (39)$$

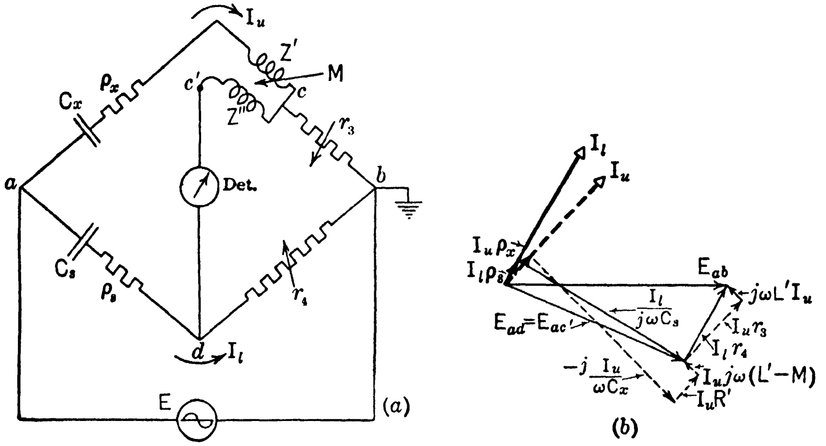

FIG. 469. Dawes-Hoover high-voltage bridge. (*a*) Connections; (*b*) vector relations.

These expressions may be simplified without great loss of accuracy by neglecting ρ_s of the standard condenser and ignoring $\omega^2(L' - M)$ in comparison with r_3/r_4C_s.

Then $\rho_x = (M/r_4C_s) - R' = M/r_4C_s$, approximately . . (40)

$$C_x = r_4C_s/r_3 \quad \ldots\ldots \quad (41)$$

Power factor of the sample, $\cos\theta = \omega C_x \rho_x = \omega M/r_3$, and $I_u = EC_x\omega$, nearly, so that

$$\text{Loss} = W = E^2\omega^2 MC_x/r_3 \quad \ldots\ldots \quad (42)$$

619. EXPERIMENT 28-B. — Comparison of Two Capacitances. — Several methods are described in the preceding sections. Two capacitances should be first compared in series with resistances and then in parallel with resistances (§616). It is left to the student to investigate theoretically and to try experimentally the case of one capacitance in series and the other in parallel with a resistance. The case of imperfect condensers and the influence of dielectric loss at high frequencies should also be investigated. Tests of bushings and of cables should be attempted with the Schering and Dawes-Hoover bridges, for which the question of "shielding" (§632) will have to be studied. For other tests, see the points mentioned in §615.

620. Comparison of a Capacitance with an Inductance. — The diagram of connections is shown in Fig. 470. Branches 1 and 4 consist of non-inductive resistances; branch 3 has a resistance in series with an inductance; and branch 2 consists of a non-inductive resistance shunted by a capacitance. Applying eq. (6), and replacing the given "parallel" quantities, r_2 and C_2, of the bridge by the equivalent "series" quantities, R_2 and X_2, we get:

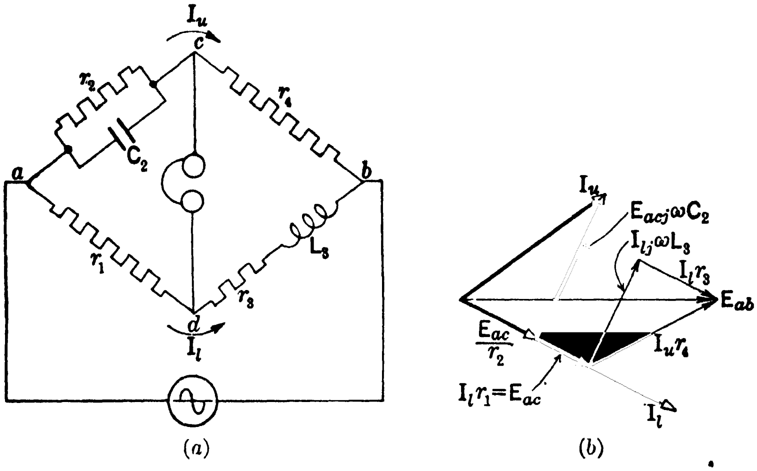

(a) (b)

FIG. 470. Comparison of capacitance with inductance — connections and vector relations.

$$X_2r_3 + R_2x_3 = 0 \quad . . . . (43)$$

or:

$$-X_2/R_2 = x_3/r_3 \quad . . . . (44)$$

According to the general theory of equivalent series and parallel circuits:

$$\tan \phi_2 = X_2/R_2 = b_2/g_2 = -\omega C_2/r_2^{-1} \quad . . . . (45)$$

Using this ratio in eq. (44) gives:

$$L_3 = C_2r_2r_3 \quad . . . . (46)$$

which is the desired relationship between C and L. However, this result is correct only provided that eq. (5) is also satisfied. It can be shown that this is equivalent to the requirement:

$$r_2r_3 = r_1r_4 \quad . . . . (47)$$

In other words, the bridge must also be balanced with direct current. The reader can check this statement by substituting eqs. (46) and (47) in eq. (5).

621. The Anderson Bridge. — When the values of L and C in the preceding method cannot be varied continually (in infinitesimal steps), the adjustment for an a-c balance may be somewhat tedious. In such cases the arrangement shown in Fig. 471, and known as Anderson's bridge, is more convenient. The condenser, instead of being connected directly across r_2, has an adjustable resistance, r_2', in series with it. The galvanometer, instead of being connected at c, is connected at c'.

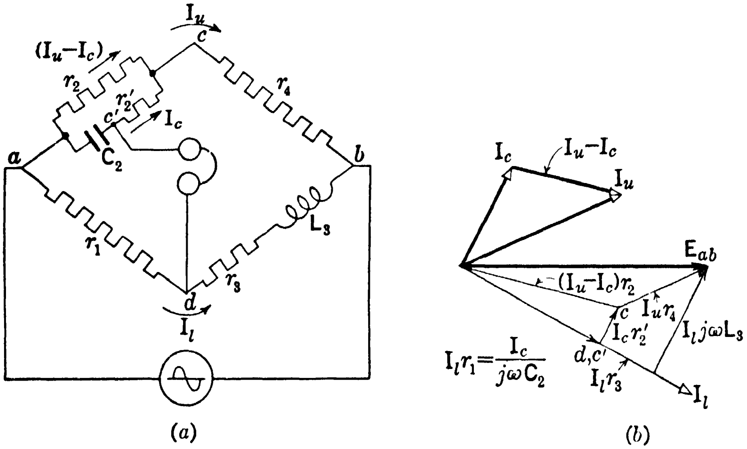

(a) (b)

FIG. 471. The Anderson bridge.

When the bridge is balanced, that is, when no alternating current is flowing through the galvanometer, the following three equations, in the complex notation, hold true:

$$(I_u - I_c)r_2 - I_c r_2' = I_l r_1 \quad \ldots\ldots\ldots \quad (48)$$

$$I_l(r_3 + j\omega L_3) = I_c r_2' + I_u r_4 \quad \ldots\ldots\ldots \quad (49)$$

$$I_c = I_l r_1 \cdot j\omega C_2 \quad \ldots\ldots\ldots\ldots\ldots \quad (50)$$

Equations (48) and (49) are generalized forms of eqs. (1) and (2) and become identical with them when $C_2 = 0$, that is, when $I_c = 0$. Substituting the value of I_c from eq. (50) in eqs. (48) and (49), we get:

$$I_u r_2 = I_l[r_1 + r_1(r_2 + r_2')j\omega C_2]; \quad I_l[r_3 + j\omega(L_3 - r_1 r_2' C_2)] = I_u r_4$$

When these equations are multiplied term by term, the currents I_u and I_l are eliminated and an equation is obtained corresponding to eq. (3). Equating the real and the imaginary parts, we get:

$$r_2 r_3 = r_1 r_4 \quad \ldots\ldots\ldots\ldots \quad (51)$$

$$L_3 = C_2\,[r_1 r_4 + r_2'(r_1 + r_3)] \quad \ldots\ldots\ldots \quad (52)$$

The first of these equations means that the bridge must first be balanced on direct current; then the relationship between L_3 and C_2 is expressed by eq. (52). When r_2' equals zero eq. (52) becomes identical with eq. (46), as it should be, since the two diagrams of connections become identical.

622. EXPERIMENT 28-C. — Comparison of an Inductance with a Capacitance. — The theory and the connections are explained in the two preceding sections. For the points to be investigated, see Experiments 28-A and 28-B.

MUTUAL-INDUCTANCE BRIDGES

623. The bridge shown in Fig. 472*a* is a further development of that shown in Fig. 463, differing from it by the addition of a mutual inductance, *M* (§156). Such a bridge is used for a comparison of a mutual inductance with a self-inductance or capacitance. Equations (1) and (2) become:

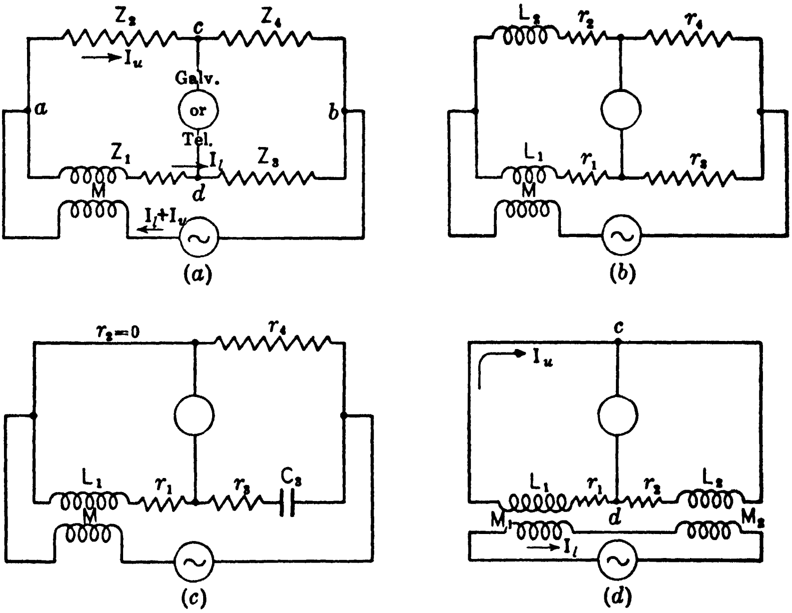

(*a*) (*b*) (*c*) (*d*)

Fig. 472. Mutual-inductance bridges.

$$I_u Z_2 = I_l Z_1 - (I_l + I_u) j x_m \quad . \; . \; . \; . \; . \; . \; . \quad (53)$$

$$I_l Z_3 = I_u Z_4 \quad . \; . \; . \; . \; . \; . \; . \; . \; . \; . \; . \; . \; . \quad (54)$$

$$x_m = \omega M \quad . \; . \; . \; . \; . \; . \; . \; . \; . \; . \; . \; . \; . \quad (55)$$

In these expressions x_m is the reactance corresponding to the mutual inductance, M. Eliminating I_u and I_l from eqs. (53) and (54), we get

$$(Z_2 + jx_m)Z_3 = (Z_1 - jx_m)Z_4 \quad . \quad . \quad . \quad . \quad . \quad . \quad . \quad (56)$$

This equation is similar to eq. (3) and becomes identical with it when $x_m = 0$. By analogy with eqs. (5) and (6), we may write directly:

$$r_2r_3 - (x_2 + x_m)x_3 = r_1r_4 - (x_1 - x_m)x_4 \quad . \quad . \quad . \quad . \quad (57)$$

$$(x_2 + x_m)r_3 + r_2x_3 = r_1x_4 + (x_1 - x_m)r_4 \quad . \quad . \quad . \quad . \quad (58)$$

These general relationships are applied below to two practical forms of such bridges.

624. EXPERIMENT 28-D. — Comparison of a Mutual Inductance with a Self-Inductance. — The diagram of connections is shown in Fig. 472*b*. In eqs. (57) and (58), put $x_3 = x_4 = 0$, whereupon the equations are simplified to:

$$r_2r_3 = r_1r_4$$

$$(x_2 + x_m)r_3 = (x_1 - x_m)r_4$$

or finally to:

$$r_1/r_2 = r_3/r_4 = (L_1 - M)/(L_2 + M) \quad . \quad . \quad . \quad . \quad . \quad (59)$$

The bridge is first balanced on direct current, and then on alternating current. One of the three quantities, L_1, L_2, or M, may be computed if the other two and the ratio of the resistances are known. For the points to be investigated experimentally, see §615.

625. EXPERIMENT 28-E. — Comparison of a Mutual Inductance with a Capacitance. — The diagram of connections is shown in Fig. 472*c*. If in eqs. (57) and (58) we put $r_2 = x_2 = x_4 = 0$, they become:

$$-x_mx_3 = r_1r_4$$

$$x_mr_3 = (x_1 - x_m)r_4$$

or, after reduction:

$$M = C_3r_1r_4 \quad . \quad . \quad . \quad . \quad . \quad . \quad . \quad . \quad . \quad . \quad . \quad (60)$$

$$M/(L_1 - M) = r_4/r_3 \quad . \quad . \quad . \quad . \quad . \quad . \quad . \quad . \quad . \quad (61)$$

This bridge cannot be balanced on direct current; when it is balanced on alternating current, eqs. (60) and (61) are satisfied and any two unknown quantities may be determined, when the remaining quantities are known. Ordinarily, this bridge is used for measuring C_3 by means of a known M. For the points to be investigated experimentally, see §§615 and 619.

3. **EXPERIMENT 28-F. — Comparison of Two Mutual Inductances.** — The diagram of connections is shown in Fig. 472*d*. When the galvanometer current is equal to zero, the points *c* and *d* are at the same potential. This means that the voltage induced by the current I_l in the secondary of the mutual inductance M_1 is completely used up in r_1 and L_1. Hence:

$$I_l j\omega M_1 = I_u(r_1 + j\omega L_1) \tag{62}$$

By analogy:

$$I_u(r_2 + j\omega L_2) = I_l j\omega M_2 \tag{63}$$

When these two equations are multiplied term by term, the two currents are eliminated, and we get:

$$M_1(r_2 + j\omega L_2) = M_2(r_1 + j\omega L_1) \tag{64}$$

from which:

$$M_1 r_2 = M_2 r_1, \quad \text{and} \quad M_1 L_2 = M_2 L_1$$

Consequently:

$$r_1/r_2 = L_1/L_2 = M_1/M_2 \tag{65}$$

Thus, when the bridge is balanced on alternating current, both conditions (65) are fulfilled simultaneously, and one of the mutual inductances can be computed in terms of the other. For the points to be investigated experimentally, see §615.

FREQUENCY BRIDGES

627. In the above-described bridges the arrangement of the parts is such that the frequency cancels out in the final equations, and the results are true within a wide range of frequencies. It is also possible to arrange the bridge of such combinations of resistance and capacitance,

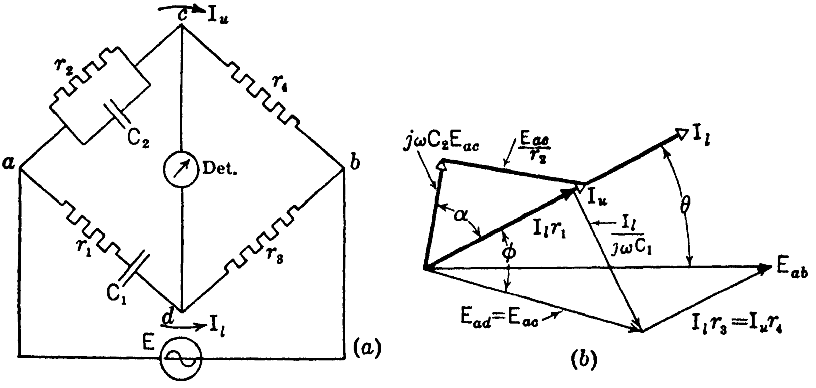

FIG. 473. A capacitance-type (Wien) frequency bridge. (*a*) Connections; (*b*) vector relations.

or of capacitance, resistance, and inductance, or mutual inductance, that a balance will be obtained at one frequency only, and be quite sensitive to changes of frequency. Such bridges are used to measure frequencies, or as a means toward the automatic control of frequency, as will be described below.

628. A Capacitance-Type Frequency Bridge. — Figure 473*a* shows the circuits and Fig. 473*b* the vector diagram of a frequency bridge formed of capacitances and resistances. When the bridge is balanced the voltage across *bc* is equal to that across *bd*, or $I_u r_4 = I_l r_3$. The resistances r_3 and r_4 being non-inductive, the currents I_u and I_l must be in phase with one another. This means that the voltages E_{ac} and E_{ad} must also be in phase. Consequently, the phase displacement angle θ_1 between I_l and E_{ad} is identical with the angle θ_2 between I_u and E_{ac}. These angles are expressed by the relations

$$\tan \theta_1 = x_1/r_1 = 1/\omega C_1 r_1 \qquad (66)$$

$$\tan \theta_2 = b_2/g_2 = \omega C_2 r_2 \qquad (67)$$

Since $\theta_1 = \theta_2$, it follows from eqs. (66) and (67) that

$$\omega^2 C_1 C_2 r_1 r_2 = 1 \qquad (68)$$

or

$$\omega = \sqrt{1/C_1 C_2 r_1 r_2}$$

and

$$f = \frac{1}{2\pi}\sqrt{1/C_1 C_2 r_1 r_2} \qquad (69)$$

From the general conditions for balance, namely, $Z_1 Z_4 = Z_2 Z_3$ (eq. 3) two equations result: eq. (68), and the relation $C_1 r_1 + C_2 r_2 = C_1 r_2 r_3 / r_4$. From the latter equation it follows that, if r_3 is made equal to r_4, and $r_2 = 2r_1$, balance is obtained when $C_1 = 2C_2$. Substituting these conditions in eq. (68) it follows that

$$2\pi f C_2 r_2 = 2\pi f C_1 r_1 = 1$$

or

$$f = 1/2\pi C_2 r_2 = 1/2\pi C_1 r_1 \qquad (70)$$

629. The Leeds and Northrup Frequency Control Bridge.[7] — Figure 474 shows a frequency bridge used in connection with a Leeds and Northrup automatic balancing device (§63) to maintain the frequency of an alternator constant, assuming a setting of the bridge such that it is balanced at a desired frequency, and the needle of the galvanometer in the central position. As soon as a change in frequency occurs, the galvanometer needle is deflected, owing to the unbalancing of the bridge, and moves to the right or left. Such a condition is shown in Fig. 474, where the raising of the pick-up arm, *A*, is seen to have lifted the lever arm L_1 and allowed the arm L_2 to drop. This tilts the rocking beam *B*, raising contact P_1 and lowering contact point P_2. With the rotation of the cams

---

[7] See Leeds and Northrup, *Bulletin* 161-A, 1936, "Automatic Frequency-Load Control for Interconnected Power Systems." Also see their catalog N-57-161, 1938.

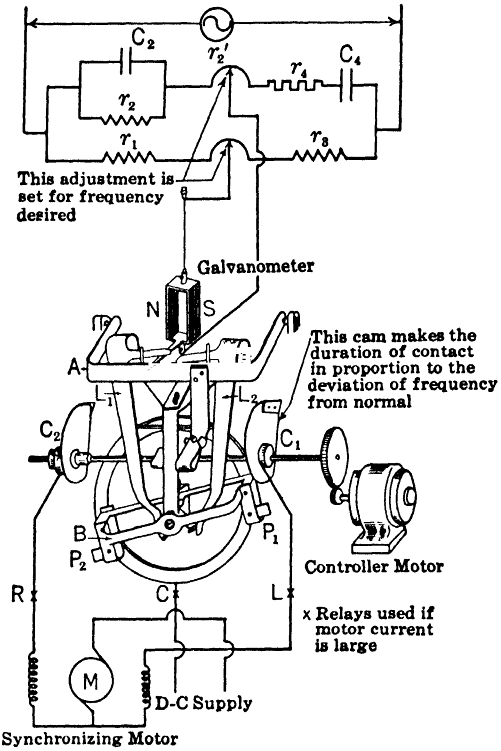
C₂
r₂'
C₄
r₄
r₂
r₁
r₃
This adjustment is set for frequency desired
Galvanometer
N
S
A
L₁
L₂
This cam makes the duration of contact in proportion to the deviation of frequency from normal
C₂
C₁
B
P₂
P₁
Controller Motor
R
C
L
x Relays used if motor current is large
M
D-C Supply
Synchronizing Motor

FIG. 474. Details of the Leeds and Northrup frequency bridge for automatic control of system frequency.

C_1 and C_2, which are driven by the controller motor, contact is completed for a longer or shorter time between C_1 and P_1 which energizes the " synchronizing motor " and causes it to rotate in the required direction and to increase or decrease the spring tension of the governor of the prime mover. This increases or decreases the speed of the set and so starts to correct the frequency of the unit. As long as the frequency is high or low by 1/100 cycle or more the bridge is unbalanced, the galvanometer deflects, and the control mechanism operates to restore correct frequency.

Referring to Fig. 475, where the bridge circuit is shown in detail, it is evident that at balance the potential drops across r_1 and r_3 are in phase.

Similarly the identical potential drops across Z_2 and Z_4 must be in phase, or $\tan\theta_2$ must equal $\tan\theta_4$. Consider the following equations:

$$Z_2 = r_2' + \frac{1}{1/r_2 + j\omega C_2} = \frac{r_2 + r_2' + j\omega C_2 r_2 r_2'}{1 + j\omega C_2 r_2} \quad . \; . \; . \quad (71)$$

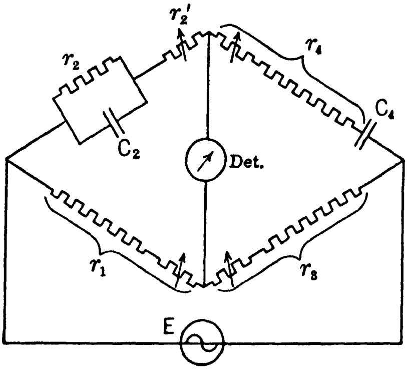

FIG. 475. Diagram of the Leeds and Northrup frequency-control bridge.

Rationalizing,

$$Z_2 = \frac{r_2 + r_2' + \omega^2 C_2^2 r_2^2 r_2'}{1 + \omega^2 C_2^2 r_2^2} - j\frac{\omega C_2 r_2^2}{1 + \omega^2 C_2^2 r_2^2}$$

Then $$\tan\theta_2 = \frac{\omega C_2 r_2^2}{r_2 + r_2' + \omega^2 C_2^2 r_2^2 r_2'} \quad . \; . \; . \; . \; . \; . \; . \; . \; . \; . \; . \quad (72)$$

Similarly $$Z_4 = r_4 + 1/j\omega C_4$$

$$\tan\theta_4 = 1/\omega C_4 r_4 \; . \; . \; . \; . \; . \; . \; . \; . \; . \; . \quad (73)$$

Equating $\tan\theta_2$ and $\tan\theta_4$

$$\frac{\omega C_2 r_2^2}{r_2 + r_2' + \omega^2 C_2^2 r_2^2 r_2'} = 1/\omega C_4 r_4$$

or, $$\omega^2 C_2 C_4 r_2^2 r_4 = r_2 + r_2' + \omega^2 C_2^2 r_2^2 r_2'$$

from which $$\omega^2 = \frac{r_2 + r_2'}{C_2 r_2^2 (C_4 r_4 - C_2 r_2')} \quad . \; . \; . \; . \; . \; . \; . \quad (74)$$

Since $C_2 r_2'$ is small compared with $C_4 r_4$

$$\omega^2 = \frac{r_2 + r_2'}{C_2 C_4 r_2^2 r_4}, \text{ nearly} \quad . \; . \; . \; . \; . \; . \; . \; . \quad (75)$$

or $$f = \frac{1}{2\pi}\sqrt{\frac{r_2 + r_2'}{C_2 C_4 r_2^2 r_4}} \quad . \; . \; . \; . \; . \; . \; . \; . \; . \quad (76)$$

Therefore, there is a definite frequency at which the bridge will balance, and, conversely, any departure from this frequency throws the bridge out of balance. Notice that the setting of the bridge is the more sensitive to changes in the adjusting resistance since an increase of r_2' means a decrease of r_4 and these resistances affect the critical frequency oppositely.

630. Frequency Bridges with Mutual Inductance and Capacitance. — A simple bridge of this kind is shown in Fig. 476*a*. In order to bring the current in the galvanometer branch to zero, the emf induced in the secondary of the mutual inductor must be equal and opposite to the voltage at the terminals of the condenser. Thus, the condition for a balance is:

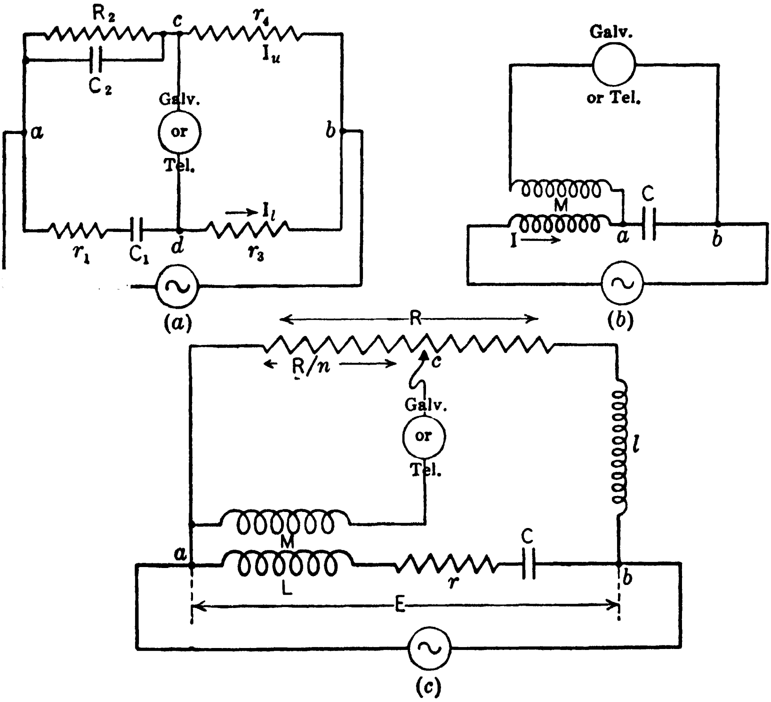

FIG. 476. Typical frequency bridges.

$$jI\omega M = jI/(\omega C) \quad . \ . \ . \ . \ . \ . \ . \ . \ . \ (77)$$

or:

$$2\pi f\sqrt{MC} = 1 \quad . \ . \ . \ . \ . \ . \ . \ . \ . \ . \ (78)$$

From this expression the frequency f may be computed when M and C are known.

A somewhat more elaborate bridge, based on the same principle, is shown in Fig. 476*b*. It differs from the preceding one mainly in having a high resistance, R, connected on the potentiometer principle. The galvanometer, or a telephone receiver, is connected to a point, c, of this resistance, the resistance ac being one nth part of the whole resistance, R. Another resistance, r, and a small inductance, l, are necessary for a balance. When the galvanometer current is zero, the voltage drop in the resistance R/n is equal to the emf induced in the secondary of the mutual inductor; hence:

$$E\frac{R/n}{R + j\omega l} = E\frac{-j\omega M}{r + j\omega L - j/(\omega C)} \quad . \quad . \quad . \quad . \quad . \quad (79)$$

In this expression E is the potential difference between the points a and b; this potential difference, divided by the impedance $(R + j\omega l)$ of the shunt circuit, gives the current through the resistance R. This current multiplied by the resistance R/n gives the voltage across R/n. The right-hand side of the equation has a similar meaning with respect to the main circuit. Equating the real and the imaginary parts, we get:

$$rR/n = (\omega)^2 lM$$

$$R/n\,[\omega L - (\omega C)^{-1}] = -R\omega M,$$

or, after simplification:

$$2\pi f\sqrt{C(L + nM)} = 1 \quad . \quad . \quad . \quad . \quad . \quad . \quad . \quad . \quad (80)$$

$$l = RrC\,[1 + L/(nM)] \quad . \quad . \quad . \quad . \quad . \quad . \quad . \quad . \quad (81)$$

The unknown frequency is computed from eq. (80), while eq. (81) gives the necessary relationship among the circuit constants.

Because of a larger number of circuit parts, this bridge admits of an easier adjustment within wide limits of frequencies, and does not require as large values of M and C as the bridge shown in Fig. 476*a*.

631. EXPERIMENT 28-G. — Frequency Measurements with an A-C Bridge. — Several types of bridges are described in §§628 to 630, and one or more of these should be investigated with respect to its range, accuracy, convenience, speed of adjustment, effect of stray fields, power loss in the condensers, etc. Make a study of commercial types of frequency-control devices and discuss the problem of time service from electric power systems, at least as far as the a-c bridge plays a part in such service.

632. Need of Shielding in A-C Bridges.[8] — In the various a-c bridges discussed in this chapter the assumption is made that the only capacitances or inductances present are those shown as elements in the bridge arms. Actually there is an electrostatic induction between every lead and element of the bridge and every other element or lead, as well as with reference to the earth and the observer's body. There is induction also between the bridge and the leads or load devices connected to the a-c power source, with both electromagnetic and electrostatic fields which introduce unwanted emf's in the bridge circuits. These fields also affect the telephone receiver or vibration galvanometer used as a detector. Even when the bridge is balanced there is a minimum of sound or vibration in the detector due to the above causes. Mutual inductance between inductors used in the bridge circuits may seriously alter the values involved. All these effects become greater as the frequency of the power source is increased.

---

[8] See F. A. Laws, "Electrical Measurements," Chapter VII.

If the observer's body, itself in contact with the earth or objects leading to earth, is at ground potential, and the telephone receiver is not at this potential, then, even when the bridge is balanced, there will be currents in the detector due to its electrostatic capacitance with reference to the observer, and to the potential of the detector with reference to earth. To minimize the difficulties arising from these conditions, a-c bridges must, in general, be carefully shielded, both in individual parts, and as a whole. Although this does not remove the admittances listed above, it does substitute fixed admittances for those which are variable, and makes it possible to secure a definite balance. Figure 477 is a typical shielded a-c bridge as described by Shackelton.[9] If possible the a-c power source used with the bridge should be of a frequency different from that of near-by power sources or their harmonics, and at final balance the detector should be at ground potential, say, through the use of a Wagner ground.

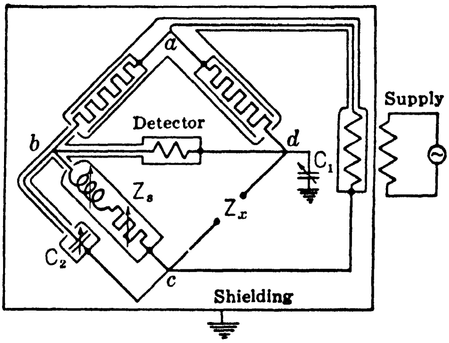

FIG. 477. Shielded inductive impedance bridge (Shackleton).

633. The Wagner Ground. — The Wagner earthing device, or ground,[10] Fig. 478, not only removes the head effect mentioned above, but also greatly reduces all earth capacitance influence upon the a-c bridge.

---

[9] W. J. Shackelton, "A Shielded Bridge for Inductive Impedance Measurements," *Trans. A.I.E.E.*, vol. 45 (1926), p. 1266.

[10] B. Hague, "A-C Bridge Methods," Chapter V, Pitman & Sons.

Thus, if the bridge is balanced (Fig. 478) so that c and d are at the same potential, but not at earth potential, currents from c and d to earth through the observer's head and body give a false indication in the telephone detector. In the Wagner ground variable impedances, Z_5 and Z_6, are placed across the a-c supply with their junction point, e, connected to ground. It is then possible, after the best obtainable balance of the bridge proper has been secured (switch *Sw* at d), to determine whether the detector is at ground potential by throwing the switch downward to e. By adjusting Z_5 and Z_6 and rebalancing the bridge until there is no indication in the detector for either position of the switch, it is possible to eliminate the effect of earth capacitance between the detector and ground and to secure a much more definite balance of the bridge than is possible without the use of the Wagner ground.

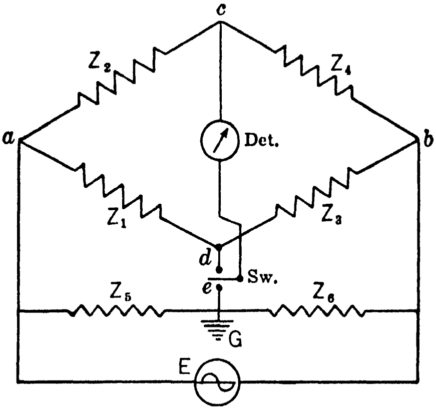

FIG. 478. A-c bridge with Wagner ground.

REFERENCES

1. S. I. REYNOLDS and H. H. RACE, *Gen. Elec. Rev.*, December, 1938, p. 529, Improved low-voltage a-c bridges for measuring properties of insulating materials.

2. A. L. BROWNLEE, *Elec. Jour.*, December, 1938, p. 467, Power factor measurement on cable insulation.

3. A. SERNER, *Wireless Eng'r*, vol. 14, February, 1937, p. 59, A new bridge for the direct measurement of impedance.

4. C. D. GREENTREE, *Elec. Eng'g*, June, 1937, p. 706, Vibration measuring instruments.

5. O. E. NÖLKE, *V.D.E.Fachberichte*, vol. 9, p. 191 (1937), A-C bridges and compensator connections with automatic balancing and recording.

6. A. WAHL, *A.E.G.Mitteil.* No. 11, p. 378, November, 1937, Frequency indicator.

7. R. F. FIELD, *Gen. Rad. Exper.*, vol. 10, March, 1936, Measurements at low frequency with the radio-frequency bridge.

8. *Gen. Rad. Exper.*, vol. 11, No. 7, December, 1936, An audio-frequency Schering bridge.

9. Balsbaugh, Kenney, and Herzenberg, *Elec. Eng'g,* March, 1935, p. 272, The M. I. T. power factor bridge and oil cell.

10. Ford and Reynolds, *Gen. Elec. Rev.*, February, 1933, p. 99, A-C bridges for measurements of electrical insulating materials.

11. L. Behr and A. J. Williams, Jr., *Proc. I.R.E.*, June, 1932, p. 969, The Campbell-Shackelton shielded ratio box.

12. A. C. Bartlett, *Jour. Sci. Instruments,* vol. 4, p. 33 (1926), Note on shielded non-inductive resistances.

13. J. G. Ferguson, *Trans. A.I.E.E.*, vol. 48 (1929), p. 1286, Shielding in high-frequency measurements.

14. Dawes, Hoover, and Reichard, *Trans. A.I.E.E.*, vol. 48 (1929), p. 1271, Some problems in dielectric loss measurements.

15. H. L. Curtis, *Trans. A.I.E.E.*, vol. 48 (1929), p. 1263, Shielding and guarding electrical apparatus used in measurements.

16. R. Davis, *Jour. Sci. Instruments,* vol. 5 (1928), pp. 305 and 354, The errors associated with high resistances in a-c measurements.

17. J. Cavallo, *Rev. gén. élec.*, vol. 17 (1925), p. 337, Quelques considérations de l'ordre pratique concernement l'employe du pont de Wheatstone en courant alternatif.

18. K. W. Wagner, *Elek. Zeits.*, vol. 32 (1911), p. 1001; vol. 33 (1912), p. 635, Zur Messung dielektrischer Verluste mit der Wechselstrombrücke.

19. V. Karapetoff, *Phil. Mag.*, vol. 44 (1922), p. 1024, The general a-c bridge.

20. F. A. Laws, Electrical Measurements, Chapter 7, McGraw-Hill Book Co.

21. B. Hague, A-C Bridge Methods, Pitman & Sons.

22. Smythe and Michels, Advanced Electrical Measurements, Chapter 8, Van Nostrand.

CHAPTER XXIX

VOLTAGE REGULATION OF SHORT AND MEDIUM-LENGTH TRANSMISSION LINES

634. Definitions. Long and Short Lines.—For the purposes of this discussion a short transmission line will be defined as one in which the distributed capacitance and leakage of the line are so low that, in the calculation of the performance of the line, these items may without serious error either be neglected altogether, or be considered as concentrated at certain points along the line. This is obviously not a question of the physical length of the line only, since a metal-sheathed or concentric cable will have a very high capacitance (and possibly leakance) as compared with an aerial line of the same length. Long lines will then be defined as those in which reasonable accuracy in calculations requires that inductance, capacitance, and leakance (if present) must be considered as distributed.

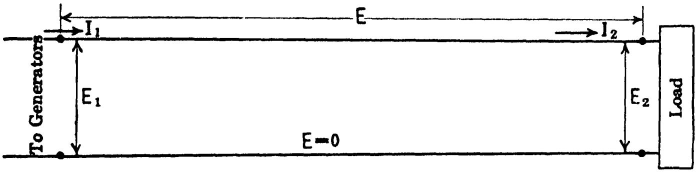

FIG. 479. A single-phase transmission line with ideal return conductor.

635. Superiority of Three-Phase Lines.—Transmission lines are usually built for operation with three-phase currents (Chapter XXXIII), rather than single-phase, first because three-phase generators are cheaper and have a better performance than single-phase machines, and second because less copper is required to transmit the same amount of power at a given voltage with the same loss. Assume a certain kva to be transmitted at a voltage kv between wires, over a single-phase line consisting of two conductors, each of resistance r_1. The line loss (I^2R) will be

$$\text{Loss}_1 = 2(\text{kva}/\text{kv})^2 \times r_1 = (\text{kva}/\text{kv})^2 \times 2\rho l/A_1,$$

since (§5, eq. 9) $r_1 = \rho l/A_1.$

For the three-phase case, the resistance per conductor being r_3, the loss will be (see Chapter XXXIII)

$$\text{Loss}_3 = 3\left(\frac{\text{kva}}{\sqrt{3}\text{kv}}\right)^2 \times r_3 = (\text{kva}/\text{kv})^2 \times \rho l/A_3$$

For the same loss in the two cases $A_1 = 2A_3$, or the conductors of the single-phase line must have twice the cross-sectional area of those for the three-phase line. The total volume and weight of copper will then compare as $2A_1/3A_3 = 4/3$, and the single-phase line will require 33 per cent more copper than the three-phase line. Of course there are other items of cost and performance not considered in this comparison.

636. General Relations. — When the three-phase voltages are symmetrical and the load is balanced, a three-phase line, for the purposes of computation of voltage drop and regulation, can be replaced by three single-phase lines with ideal return conductors (Fig. 479). For this reason, the whole treatment in this chapter is based on the single-phase transmission line.

The voltage at the generator end is denoted by E_1, that at the receiver end by E_2. Owing to the distributed capacitance and unavoidable leakage of the line, the generator current, I_1, is assumed to be different from the receiver current, I_2, as is actually the case in a long transmission line.

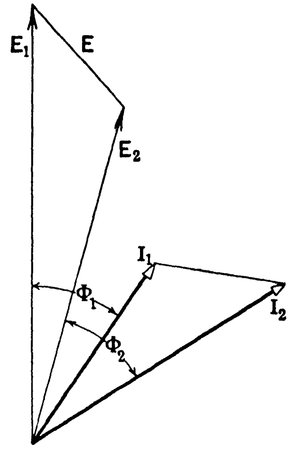

Fig. 480. Vectors of currents and voltages in the line of Fig. 479.

The vectorial relations are shown in Fig. 480. The voltage drop, E, due to the resistance and inductance of the line, causes the voltage E_2 at the receiver end to be different from the voltage E_1 at the generator end.

The voltage regulation of a transmission line at a certain load is equal to the arithmetical difference between the no-load and load voltages at the receiving end, divided by the load voltage, the impressed voltage at the sending end remaining constant.

The magnitude of the voltage drop, E, in a transmission line (Fig. 480) and its phase depend upon the following factors:

(1) The length of the line.

(2) The line constants per unit length, viz., the resistance, the inductance, the capacitance, and the leakage (or leakance).

(3) The transmission voltage.

(4) The frequency of the supply.

(5) The load current.

(6) The power factor of the load.

The values of the constants (resistance, inductive reactance, and capacitive admittance) for a transmission line may be calculated from the conductor size and spacing,[1] using the proper theoretical equations; but it is generally more convenient to select these values from the appropriate tables to be found in an electrical engineering handbook.[2] Brief tables are given here in order that the student may be able to select the approximate constants for an assumed line of a certain size and spacing of wire, and to duplicate these constants in a laboratory set-up for the purpose of checking experimentally the theoretical relations. These tables are made available through the courtesy of the Westinghouse Electric and Manufacturing Company from their " Notes and Data " for 1938. Series impedance per line $= r_a + j(x_a + x_d)$ ohms per mile. Shunt capacitive reactance to neutral $= x_a' + x_d'$ megohms per mile.

TABLE I

CHARACTERISTICS OF HARD-DRAWN* COPPER CONDUCTORS (at 60 cycles)

				x_a'	r_a	x_a
Conductor Size. B. and S. gauge	Number of Strands	Outside diameter, inches	Approx. Maximum Carrying Capacity, amperes	Shunt Capacitive Reactance at 1 ft, megohms per mile	Resistance, ohms per mile at 50° C	Inductive Reactance, ohms per mile at 1-ft spacing
0000	7	.522	484	.113	0.303	.504
000	7	.464	416	.117	0.382	.518
00	7	.414	359	.120	0.481	.532
0	7	.368	309	.124	0.607	.546
1	7	.328	266	.127	0.765	.560
2	7	.292	230	.131	0.964	.574
3	3	.285	202	.131	1.21	.585
4	3	.254	172	.135	1.52	.599
5	3	.226	150	.138	1.92	.613
6	3	.201	130	.142	2.42	.628
6	1	.162	123	.148	2.39	.637
7	1	.144	106	.152	3.01	.651
8	1	.129	92	.153	3.79	.665

* " Notes and Data," Westinghouse Electric and Manufacturing Co., 1938.

---

[1] See R. R. Lawrence, " Principles of Alternating Currents," Chapters 14 and 15, McGraw-Hill Book Co. Bryant and Correll, " Principles of Alternating Currents," Chapter XI, McGraw-Hill Book Co. L. F. Woodruff, " Principles of Electric Power Transmission and Distribution," Chapter 10, John Wiley & Sons.

[2] " Standard Handbook for Electrical Engineers," Sixth Edition, secs. 4, 14, and 15, McGraw-Hill Book Co. " Handbook for Electrical Engineers," Third Edition, John Wiley & Sons. " Handbook," Anaconda Copper Co. " Properties of A.C.S.R. Conductors," Aluminum Company of America.

TABLE II

Inductive Reactance Spacing Factors*

x_d vs conductor separation (at 60 cycles)

Feet	0	1	2	3	4	5	6	7	8	9
0	....	0	.084	.133	.168	.195	.217	.236	.252	.267
10	.279	.291	.302	.311	.320	.329	.336	.344	.351	.357
20	.364	.369	.375	.380	.386	.391	.395	.400	.404	.409
30	.413	.417	.421	.424	.428	.431	.435	.438	.441	.445

* "Notes and Data," Westinghouse Electric and Manufacturing Co., 1938.

TABLE III

Capacitive Reactance Spacing Factors (60 cycles)*

x_d' vs feet spacing

Feet	0	1	2	3	4	5	6	7	8	9
0	.....	0	.0206	.0326	.0411	.0478	.0532	.0577	.0617	.0652
10	.0683	.0711	.0737	.0761	.0783	.0804	.0823	.0841	.0858	.0874
20	.0889	.0903	.0917	.0930	.0943	.0955	.0967	.0978	.0989	.0999
30	.101	.102	.103	.104	.105	.106	.106	.107	.108	.109

* "Notes and Data," Westinghouse Electric and Manufacturing Co., 1938.

637. Distributed and Concentrated Characteristics of Lines. — Each infinitesimal element of a transmission line possesses resistance, inductance, and capacitance. Leakage conductance is present, chiefly at the insulators; but since there are a large number of insulators on a line of considerable length leakance is also assumed to be uniformly distributed along the line.

For this reason, if the line drop and voltage regulation of a long transmission or telephone line are to be accurately duplicated in the laboratory the apparatus should also possess distributed characteristics (r, x, and c). Circuits of this type are known as artificial transmission lines. In many problems the leakance may be neglected altogether, the line being assumed to possess a sufficiently high insulation resistance to the ground and between conductors. On a *short line*, operated at moderate frequency and voltage, the influence of capacitance may also be neglected. For lines of *medium length* the whole distributed capacitance may be replaced by an equal capacitance, C (or capacitive admittance Y_c), at the middle of the line, with one-half the line impedance,

$Z(= r + jx)$, on either side. This results in the *nominal "T" line* of Fig. 481*a*, for which the vector diagram is shown in Fig. 482*a*.

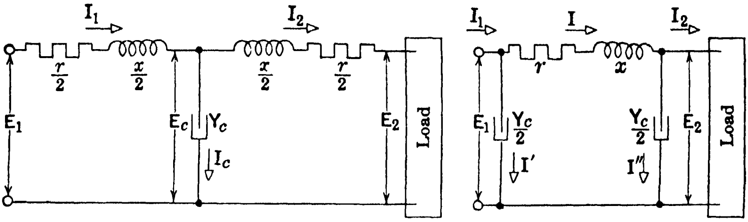

(*a*) (*b*)

FIG. 481. (*a*) Nominal T line; (*b*) nominal π line.

Likewise, one-half the capacitance or capacitive admittance may be placed at each end of the line with total line impedance, Z, between, giving the *nominal "π" line* of Fig. 481*b*, with vector diagrams as in Fig. 482*b*.

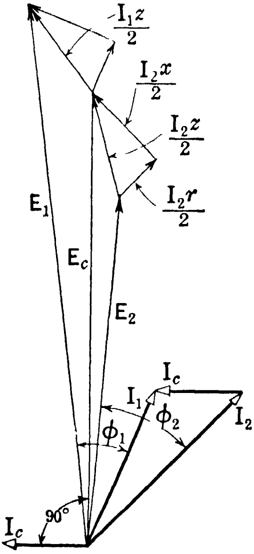

(*a*)

FIG. 482(*a*). Vector relations in the nominal T line.

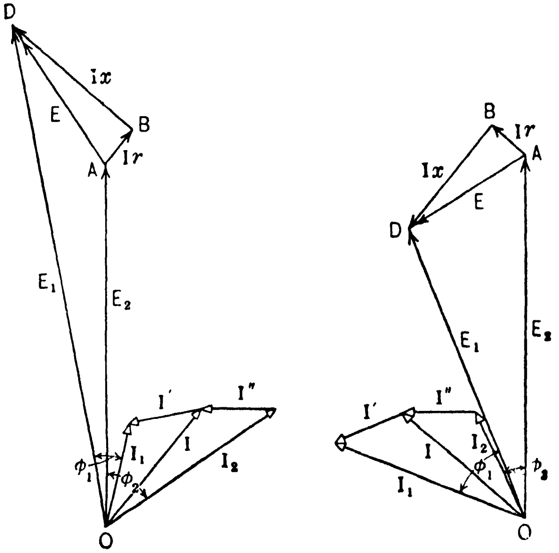

(*b*)

FIG. 482(*b*). Vector diagrams for the nominal π line for lagging and for leading current.

638. Analytical Solutions. — (a) *Nominal "T" line.* Inspection of Figs. 481*a* and 482*a* for the nominal "T" line leads to the following equations. In general the quantities involved are vectors (complex numbers).

Expressing E_1 in terms of the load voltage, E_2, and the several voltage drops

$$E_1 = E_2 + I_2Z/2 + (I_2 + E_cY_c)Z/2$$

But $$E_c = E_2 + I_2Z/2$$

Therefore $$E_1 = E_2(1 + Y_cZ/2) + I_2Z(1 + Y_cZ/4) \quad (1)$$
$$= AE_2 + BI_2 \quad (1a)[3]$$

or $$E_2 = [E_1 - I_2Z(1 + Y_cZ/4)]/(1 + Y_cZ/2) \quad (2)$$
$$= (E_1 - BI_2)/A \quad (2a)$$

Likewise $$I_1 = I_2 + I_c = I_2 + E_cY_c$$

or $$I_1 = I_2(1 + Y_cZ/2) + E_2Y_c \quad (3)$$
$$= AI_2 + CE_2 \quad (3a)$$

At no load, since $I_2 = 0$, eq. (2) gives, as the voltage at the receiver, for a given supply voltage E_1,

$$E_{20} = E_1/(1 + Y_cZ/2) \quad (4)$$
$$= E_1/A \quad (4a)$$

Regulation, as defined in §636, and expressing E_2 and E_{20} as simple numerical values, becomes

$$\text{Regulation} = (E_{20} - E_2)/E_2 \quad (5)$$

(b) *Nominal "π" line.* From Figs. 481*b* and 482*b* one may write

$$E_1 = E_2 + IZ$$

But $$I = I_2 + E_2Y_c/2$$

Therefore $$E_1 = E_2(1 + Y_cZ/2) + I_2Z \quad (6)$$
$$= A'E_2 + B'I_2 \quad (6a)$$

or $$E_2 = (E_1 - I_2Z)/(1 + Y_cZ/2) \quad (7)$$
$$= (E_1 - B'I_2)/A' \quad (7a)$$

Likewise $$I_1 = I_2 + E_2Y_c/2 + E_1Y_c/2 \quad (8)$$

Substituting the value of E_1 from eq. (6)

$$I_1 = I_2(1 + Y_cZ/2) + E_2Y_c(1 + Y_cZ/4) \quad (9)$$
$$= A'I_2 + C'E_2 \quad (9a)$$

---

[3] *A*, *B*, and *C* are complex circuit constants whose meaning is evident from eqs. (1) and (3); see §645.

or, in terms of E_1,

$$I_1 = I_2 + E_1 Y_c(1 + Y_c Z/4)/(1 + Y_c Z/2) \quad . \; . \; . \; . \quad (10)$$

$$= I_2 + E_1 C'/A' \quad . \; . \; . \; . \; . \; . \; . \; . \; . \; . \; . \; . \; . \; . \quad (10a)$$

From eq. (7) the receiver voltage at no load becomes

$$E_{20} = E_1/(1 + Y_c Z/2) \quad . \; . \; . \; . \; . \; . \; . \; . \quad (11)$$

$$= E_1/A' \quad . \; . \; . \; . \; . \; . \; . \; . \; . \; . \; . \; . \quad (11a)$$

Regulation is again calculated from eq. (5).

Steinmetz Equivalent Circuit. An approximate solution, but better than those of the nominal "T" or nominal "π" lines,[4] assumes the capacitance of the line lumped, ⅔ at the center and ⅙ at either end of the line. This results in the equations

$$E_1 = E_2(1 + Y_c Z/2 + Y_c^2 Z^2/36) + I_2 Z(1 + Y_c Z/6) \quad . \; . \; . \quad (12)$$

$$I_1 = I_2(1 + Y_c Z/2 + Y_c^2 Z^2/36) + E_2 Y_c(1 + 5 Y_c Z/36$$
$$+ Y_c^2 Z^2/216) \quad . \; . \; . \; . \; . \; . \; . \; . \; . \; . \; . \; . \; . \; . \; . \quad (13)$$

639. Examples of Calculations on the Nominal "π" Line. — A single-phase underground cable, 20 miles long, has a resistance of 17.1 ohms, an inductive reactance of 3 ohms (at 60 cycles), and a total capacitive admittance (susceptance) of $Y = 2\pi fC \times 10^{-6} = 2.28 \times 10^{-3}$ mho. The line delivers a load of 1500 kva, at 22,000 volts and at a power factor of 90 per cent, lagging. It is desired to determine the required voltage, E_1, at the sending end, and the regulation of the line when the load is thrown off but E_1 held constant.

Solution.

$$Z = 17.1 + j3, \quad Y_c/2 = j1.14/10^3, \quad I_2 = 1500/22 = 68.2 \text{ amperes}$$

Vectorially $I_2 = 68.2(0.9 - j0.436) = (61.3 - j29.7)$, $E_2 = 22{,}000 + j0$. From eq. (6)

$$E_1 = 22{,}000\,[1 + j1.14(17.1 + j3)/10^3] + (61.3 - j29.7)(17.1 + j3)$$
$$= 23{,}062 + j105 = 23{,}062\underline{/16'}$$

At no load, assuming E_1 held constant at 23,062 volts, by eq. (11)

$$E_{20} = 23{,}062/\,[1 + j1.14(17.1 + j3) \times 10^{-3}] = 23{,}150 \text{ volts}$$

$$\text{Regulation} = (23{,}150 - 22{,}000)/22{,}000 = 5.2 \text{ per cent}$$

---

[4] C. P. Steinmetz, "A-C Phenomena," Chapter 16.

From eq. (8)

$$I_1 = 61.3 - j29.7 + j1.14(22{,}000 + 23{,}062\underline{/16'}) \times 10^{-3}$$

$$= 61.3 + j21.7 = 65.2 \text{ amperes at 94 per cent power factor, leading}$$

Figure 483 shows the calculated performance of the above line at constant kilovolt-ampere load, varying power factor.

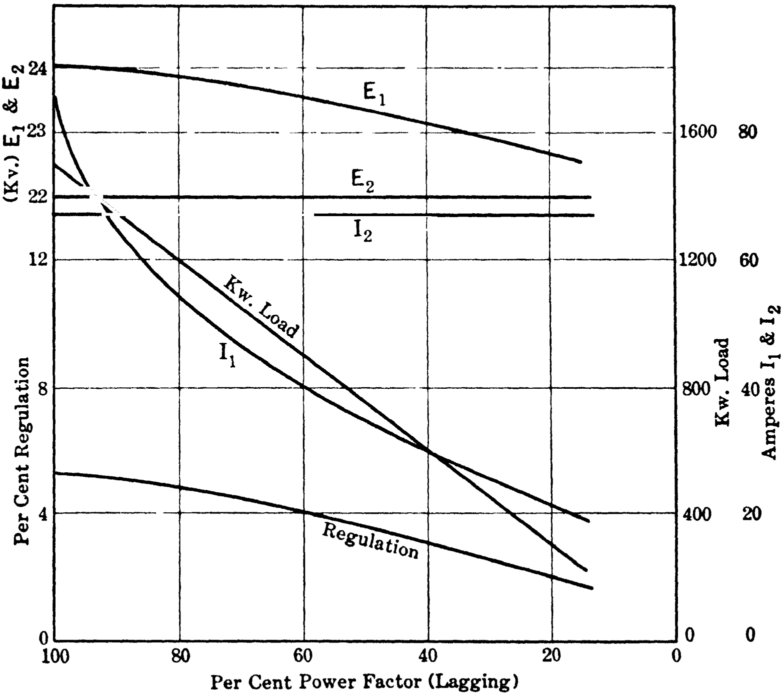

FIG. 483. Performance curves of a cable having high capacitance, low inductance — kva constant, power factor variable.

Since this line consists of a cable having concentric conductors, close together, it possesses a high capacitance and low inductance. A 20-mile aerial line made up of two 00 conductors spaced 3 feet apart, and having a resistance of 19.2 ohms, an inductive reactance of 26.8 ohms (see Tables I and II), and negligible capacitance yields the performance curves shown in Fig. 484. A comparison of the two sets of curves shows the effect of increased capacitance and of decreased inductance in the underground line.

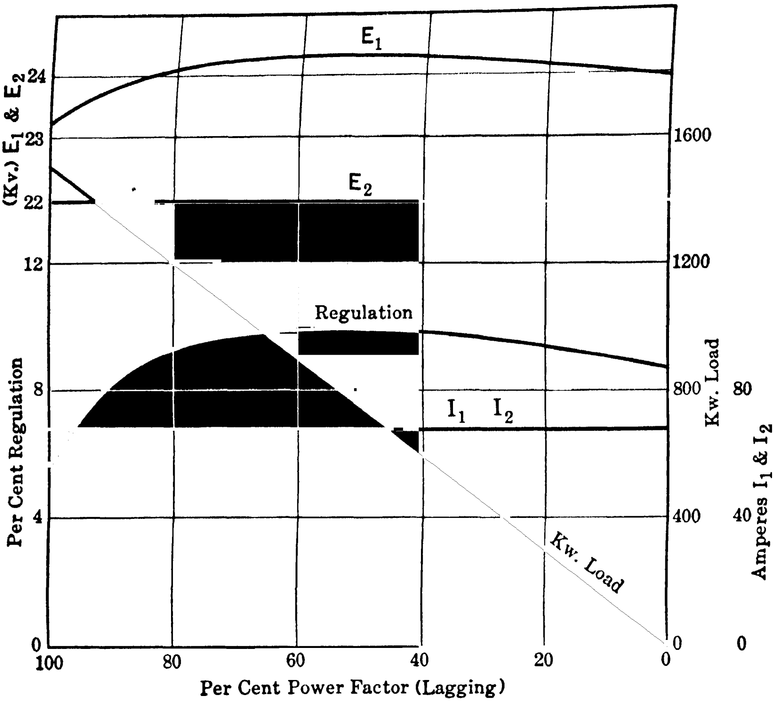

FIG. 484. Performance curves for a short line at constant kva, variable power factor.

640. Graphical Methods of Calculating Transmission-Line Performance. — The calculation of regulation on transmission lines in which the capacitance and leakance may be neglected is identical with that for transformers when the exciting current is neglected (Vol. I, §408), or of alternators by the A.I.E.E. method (Vol. I, §468). Evidently, then, Kapp's diagram (Vol. I, Fig. 286) and the synchronous impedance diagram (Vol. I, Fig. 339) apply to the short line.

A diagram for the transmission line of negligible capacitance, based on the Perrine-Baum diagram,[5] is shown in Fig. 485. Assume that a certain power is to be delivered at a fixed voltage E_2, over a line of resistance, R, and inductive reactance X. At 100 per cent power factor of the load the impedance drop, $IZ = O'a$, is added to E_2 to find the sending voltage, $E_1 = Oa$. Regulation is then $(E_1 - E_2)/E_2$. For the same power to be delivered at a power factor of 90 per cent leading, the impedance drop has the new value and position of $O'b$, $= O'a/\cos\theta$, at the angle θ ahead of $O'a$. The sending voltage is now Ob. The locus of the impedance vector (and of E_1) for the condition of constant load, at constant load voltage but variable power factor, is a straight line LL' perpendicular to $O'a$. By drawing a power factor semicircle about O' as center and with a radius of 100 per cent along $O'a$ extended, the determination of regulation at any desired power factor becomes very simple. Thus, for 80 per cent power factor, lagging, the perpendicular to $O'a$ from point 80 intersects the lagging power factor quadrant at p'. A straight line from p' to O' intersects the locus of IZ drop at c. Then $Oc = E_1$ and gives the regulation for this condition. Preferably the voltages and voltage drops should be in percentages with $E_2 = 100$ per cent. Arcs drawn with O as center through a, b, and c, etc., would intersect the line OO', extended, at distances giving the regulation directly to the scale of E_2. Thus $O'e$ is the per cent regulation at 80 per cent lagging power factor.

---

[5] "Standard Handbook for Electrical Engineers," Sixth Edition, sec. 14, McGraw-Hill Book Co.

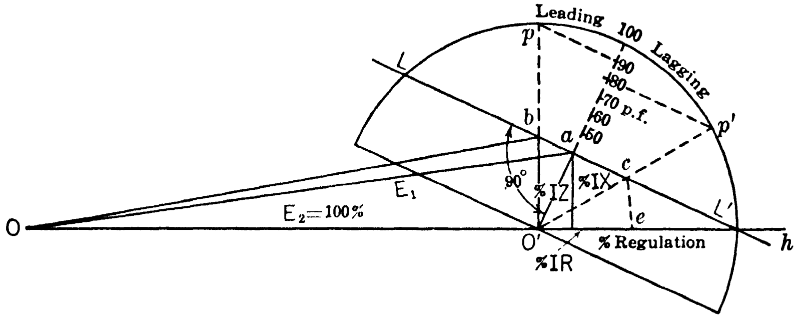

FIG. 485. Perrine-Baum regulation chart for constant load, varying power factor.

The diagram of Fig. 485 may be made to take account of charging current in a line of moderate length by considering one-half the charging capacitance concentrated at the receiving end of the line, as in the nominal " π " circuit (§638). The charging current of value $E_2Y_c/2$ is then subtracted from the (lagging) reactive component of the load current, giving a new value and power factor of the line current at the load end. Thus, the vector of the receiving line current is

$$I = I_2 \cos \theta - j(I_2 \sin \theta - E_2Y_c/2) \quad . \; . \; . \; . \; . \quad (14)$$

This current is at the angle θ' with reference to E_2. For a delivered power W at power factor $\cos \theta$ and voltage E_2

$$I = W/E_2 - j(W \sin \theta/E_2 \cos \theta - E_2Y_c/2) \quad . \; . \; . \quad (15)$$

and $$\tan\theta' = \frac{W\tan\theta/E_2 - E_2Y_c/2}{W/E_2} = \tan\theta - E_2^2Y_c/2W \quad . \quad . \quad (16)$$

By using cos θ′ in Fig. 485, regulation is found, taking into account the charging current of the line.

641. The Mershon Diagram. — A convenient diagram for the calculation of regulation where values are expressed in percentages so that a single diagram covers all ordinary cases is that of Mershon.[6] In Fig. 486 the familiar impedance-drop diagram is drawn for 90 per cent lagging power factor. The load current vector is shown along the line *Oh* which is divided in per cent of E_2. Circular arcs are drawn with center at *O* and radii from 100 per cent, up to, perhaps, 140 per cent. To determine

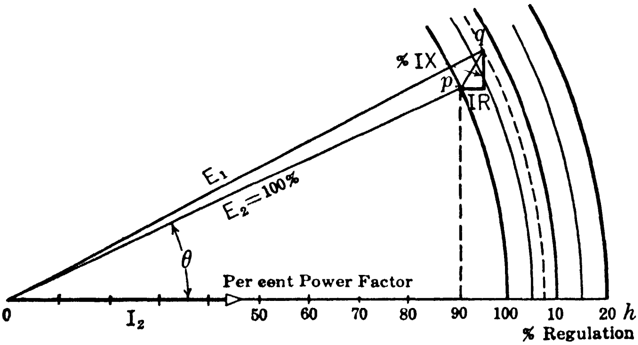

FIG. 486. The elementary Mershon diagram

regulation at the given value of current and at any desired power factor, E_2 (assumed 100 per cent) is located at the angle θ by drawing a vertical line from the desired power factor point on *Oh* upward to the 100 per cent circle, at *p*. From this point per cent *IR* drop is drawn to the right and then per cent *IX* drop upward (or downward for leading currents). *Oq* then gives the value of E_1, and per cent regulation is read by following the nearest circular arc down to the per cent regulation scale.

In actual use increased accuracy is obtained by using a large scale and drawing only that part of the chart from, say, 60 per cent power factor to 30 or 40 per cent regulation. Such a chart is given in Fig. 487.[7] The capacitance of the line may be taken into account in somewhat the same manner as in the Perrine-Baum diagram (eqs. 14 and 16). However, if the load current, *I*, is constant and its power factor varies, the impedance-drop triangle should be drawn for the line current (eq. 14) and at a point on the diagram corresponding to a power factor, $\cos \theta'$, obtained from the relation

---

[6] R. D. Mershon, *American Electrician*, vol. 9, p. 220.

[7] "Standard Handbook for Electrical Engineers," Sixth Edition, sec. 15, McGraw-Hill Book Co.

$$\tan \theta' = \frac{I_2 \sin \theta - E_2 Y_c/2}{I_2 \cos \theta} = \tan \theta - E_2 Y_c / 2 I_2 \cos \theta \quad . \quad . \quad (17)$$

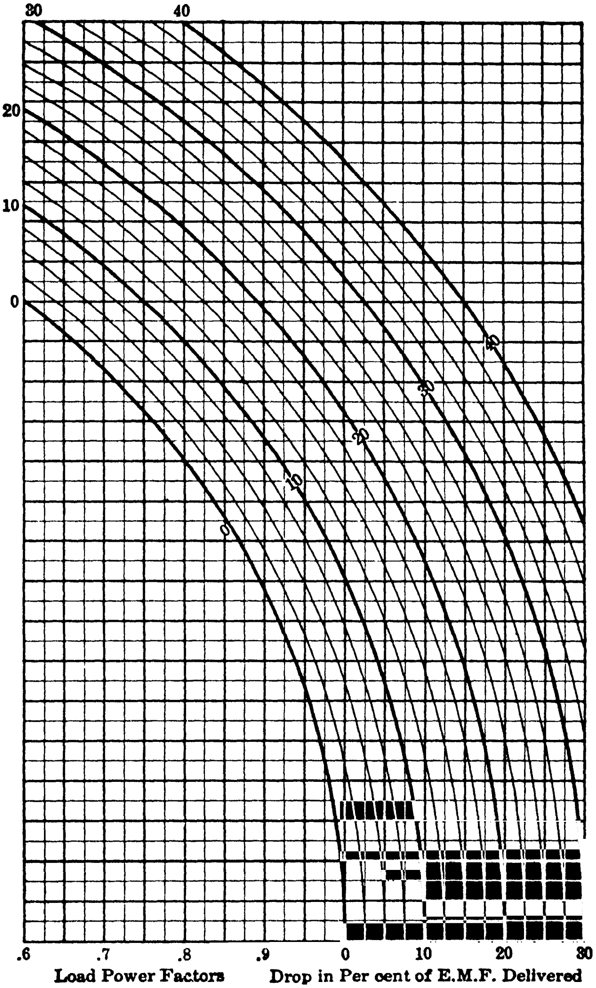

FIG. 487. Mershon chart for calculating regulation of a-c lines, etc.

Other diagrams for the calculation of transmission-line performance are available, one of the most comprehensive being that of Evans and Sels.[8] These are beyond the scope of this book. The reader is referred to the list of books and articles at the end of Chapter XXX.

[8] Evans and Sels, "Circle Diagrams for Transmission Systems," *Elec. Jour.*, December, 1921.

642. EXPERIMENT 29-A. — Voltage Regulation of a Transmission Line of Negligible Capacitance. — The purpose of the experiment is to *make a study of the influence of the following factors upon the voltage regulation of a line: (a) the magnitude of the load, (b) its power factor, (c) line constants, (d) frequency.* The transmission line in this case is represented by an adjustable resistance, r, in series with an adjustable inductive reactance, x. Provide a suitable load for which the power factor may be varied over a wide range. Adjust the line constants and load of rather low power factor so that the regulation is between 10 and 20 per cent, and with r and x nearly equal. Connect the necessary meters so as to read the generator and receiver volts and watts, the total line drop, the line current, separate drops across r and x, the power factor of the load. Keep the generator voltage and the power factor of the load constant, and reduce the load current in steps to zero. At each step read all the instruments. The data so obtained will illustrate the influence of factor (a) mentioned above.

In a similar manner, investigate the influence of factors (b), (c), and (d). In each case, keep all the factors constant, except the one under investigation. When varying the line constants, it is desirable to take measurements on a line of high resistance and low reactance, and vice versa, at both high and low values of the power factor of the load. If possible, arrange for a load with a leading current, by using either static condensers or an overexcited synchronous motor. Select a rather large inductive drop in the line and show that the receiver voltage may be higher than the generator voltage, and explain on the basis of the theory involved.

Report. Plot the results in the form of curves so as to bring out the influence of each factor as clearly as possible. Construct a few vector diagrams to show that the observed relations check with the theory, at least qualitatively. Show that the power loss in the line, the voltage drop, and the voltage regulation vary in a different manner with changes in the factors which enter into the problem.

643. EXPERIMENT 29-B. — Voltage Regulation of a Transmission Line with Capacitance Concentrated at the Ends. — The purpose of the experiment and the general directions are the same as in the preceding experiment, with the addition of the line capacitance, which is assumed to be concentrated at the ends (Fig. 488). The theory is explained in §§638 to 641.

Using the same total values of r, x, and C, imitate in turn the nominal "π," nominal "T," and Steinmetz equivalent circuits, testing each for performance, say, at constant kilovolt-amperes, variable power factor, and keeping E_1 (or E_2) constant. Take sufficient readings to be able to apply the theoretical equations for the several circuits and to check actual performance against that predicted.

State which equivalent circuit you would recommend for predicting the performance of a line of moderate length. Illustrate the method selected to predict the performance of a high-voltage line. Assume a certain amount of power to be delivered at a given voltage and power factor over an aerial (or underground) line of a certain length. (Example: 1000 kva, at 50,000 volts, 60 cycles, 80 per cent power factor, a distance of 50 miles with an energy loss of about 8 per cent.)

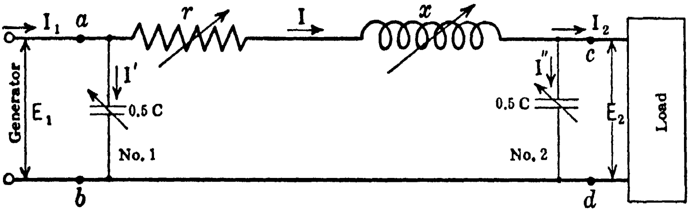

FIG. 488. Circuit of an artificial transmission line with concentrated capacitance, resistance, and inductance.

Select a conductor size and a spacing for aerial lines of perhaps 1 foot for each 10 kv. From the tables of §637 find the resistance, reactance, and capacitance per mile of line. Note that if the system is three-phase one deals with the volts to neutral and with the drop in one line.

From the above determined values predict the regulation of the line by the method selected.

Apply Mershon's diagram, the Perrine-Baum diagram, or the Dwight chart[9] for checking several of the above calculations.

---

[9] "Standard Handbook for Electrical Engineers," Sixth Edition, sec. 14, p. 1352, McGraw-Hill Book Co.

CHAPTER XXX

VOLTAGE REGULATION OF LONG TRANSMISSION LINES

644. Distributed Constants of Long Lines. — In the previous chapter an artificial electric line, consisting of a combination of resistances, inductances, and condensers, was made to represent, on a small scale, the performance of an actual line. Thus, the electrical behavior of the real line could be conveniently studied with accurate measuring instruments and without the complication of high voltages.

An actual transmission line is a " smooth " line, that is, its constants are uniformly distributed along its length. Each infinitesimal element of the line possesses resistance, inductance, and capacitance. The leakage conductance is mostly concentrated on insulators, but since there are a large number of towers or poles on a line of considerable length, and because of the comparatively small value of the leakage current, the leakance usually is also assumed to be uniformly distributed along the line. Consider an equivalent single-phase line with an ideal return conductor. The magnetic and electrostatic fluxes are somewhat as represented in Fig. 489, where the line consists of one conductor with ground return. In reality the fluxes produced by three-phase currents are of a much more complicated form.

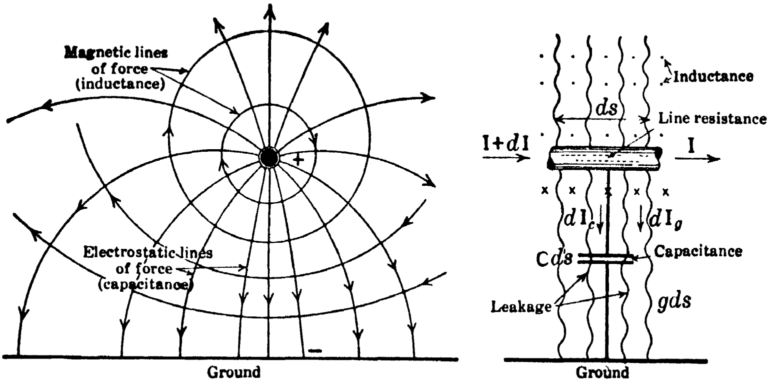
Magnetic lines of force (inductance)
+
Electrostatic lines of force (capacitance)
−
Ground
Inductance
ds
Line resistance
I+dI
I
dI_c
dI_g
Cds
Capacitance
Leakage
gds
Ground

FIG. 489. Representation of distributed inductance, capacitance, and leakance in a single-phase line with ground return.

In each element, ds, of the line, an infinitesimal current, dI_g, is lost through leakage. Another infinitesimal current, dI_c, goes to charge the capacitance of the line element when the voltage to the ground is increasing, and is given out by this capacitance during the parts of the cycle when the voltage is decreasing. Hence, at any instant the line current is different at different points of the line. In other words, the line current is a function not only of time, but of the distance along the line as well.

For this reason, if a long power-transmission or telephone line is to be accurately imitated in the laboratory, the apparatus must also possess distributed characteristics. Such characteristics are difficult to obtain in an artificial line, without making it unduly expensive and bulky. For this reason, most artificial lines are " lumpy," and consist of a finite number of series impedances and shunted admittances. Such a lumpy line represents the behavior of an actual smooth line only approximately, and the magnitude of the error depends upon the number of sections and upon the particular phenomenon studied. For certain low-frequency problems, a given lumpy line may represent a smooth line quite accurately, whereas for high-frequency oscillations and traveling waves it may give altogether misleading results.

In order to see this difference more clearly, the following analogy may be useful. Let it be desired to study the mechanical properties of a uniformly loaded string, stretched horizontally. Since it is difficult to realize such a uniform load, let a large number of weights, concentrated along the string, be used instead. Such a string will assume a static shape almost identical with a uniformly loaded one, and slow vibrations will also be practically the same for both. But if the purpose of the investigation is to study the propagation of rapid waves along the string, then the lumpiness will cause quite an appreciable error due to local reflections. Similarly, a lumpy electric line may represent steady low-frequency phenomena satisfactorily, but be entirely misleading for transient phenomena.

The constants of a lumpy line may be so chosen as to represent faithfully a smooth line at its terminals, but not at intermediate points. If a lumpy line is to cause the same voltage and current relations to exist as on a certain smooth line, say at the terminals and at two intermediate points, then the lumpy line must consist of at least three sections of proper constants.

A real transmission line may, at intervals, have concentrated loads, either shunted across it or inserted in series with it. Thus, branch lines constitute such shunted loads, while so-called loading coils used on telephone lines are an example of series loads. An artificial line should have proper terminals between sections to make it possible to insert such loads for an experimental study of their influence. The final theoretical formulas for smooth lines are given in §651.

645. Fundamental Equations of the Long Transmission Line. — An electric line with distributed resistance, capacitance, inductance, and leakance is shown schematically in Fig. 490. The formulas developed below refer to quantities *per phase* or *per conductor.* Therefore, the results can be applied to a system with any number of symmetrical phases. Let the uniformly distributed characteristics of the line, *per unit length,* be as follows:

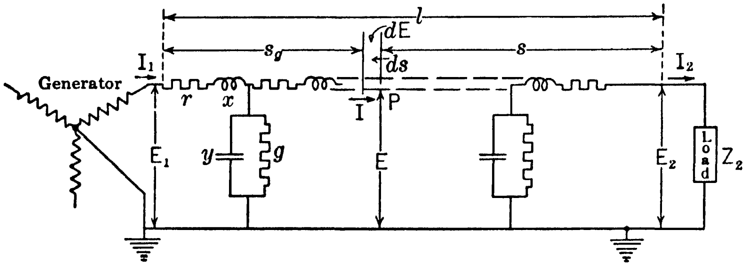

FIG. 490. A transmission line with distributed resistance, inductance, capacitance, and leakance.

Series resistance	r ohms per unit length of wire
Series inductive reactance	x ohms per unit length of wire
Shunt capacitive susceptance (to neutral)	b mhos per unit length of wire
Shunt leakage conductance (to neutral)	g mhos per unit length of wire
Series impedance $(r + jx)$	z ohms per unit length of wire
Shunt admittance to neutral $(g + jb)$	y mhos per unit length of wire

To derive the relationship between the current I, and the voltage E, at any point P on the line (Fig. 490) at a distance s from the receiver end, consider an infinitesimal element, ds, of the line. Its impedance is $z\,ds$, and its admittance is $y\,ds$, so that the drop in voltage and change in current in the element will be, respectively,

$$dE = Iz\,ds \quad \ldots\ldots\ldots\ldots \quad (1)$$

$$dI = Ey\,ds \quad \ldots\ldots\ldots\ldots \quad (2)$$

In these and the later equations, $z = r + j\omega L$ and $y = g + j\omega C$ are the series impedance and shunt admittance per conductor per unit length of the line.

Rewriting eqs. (1) and (2) in their more usual form,

$$dE/ds = zI \quad \ldots\ldots\ldots\ldots \quad (3)$$

$$dI/ds = yE \quad \ldots\ldots\ldots\ldots \quad (4)$$

Differentiating these equations with respect to s,

$$d^2E/ds^2 = z\,dI/ds \tag{5}$$

$$d^2I/ds^2 = y\,dE/ds \tag{6}$$

Substituting from eqs. (3) and (4) into (5) and (6) and transposing,

$$d^2E/ds^2 - zyE = 0 \tag{7}$$

$$d^2I/ds^2 - zyI = 0 \tag{8}$$

These are the fundamental differential equations of the transmission line and are of the standard form $d^2Y/dX^2 - aY = 0$. Equation (7) is integrated by letting

$$E = De^{\alpha s} \tag{9}$$

Differentiating (9) with respect to s

$$dE/ds = \alpha De^{\alpha} \tag{10}$$

$$d^2E/ds^2 = \alpha^2De^{\alpha} \tag{11}$$

Substituting from eqs. (10) and (11) into (7)

$$\alpha^2De^{\alpha s} - zyDe^{\alpha s} = 0 \tag{12}$$

or, $\alpha^2 - zy = 0$, giving for α the two roots of zy. That is,

$$\alpha_1 = \sqrt{zy}, \tag{13}$$

$$\alpha_2 = -\sqrt{zy} \tag{14}$$

To avoid complication in the succeeding equations, replace $\sqrt{zy}$ by m. The solution of eq. (7) is, then,

$$E = D_1e^{ms} + D_2e^{-ms} \tag{15}$$

From eq. (1) $I = (1/z)dE/ds$. Then, from eq. (15)

$$I = 1/z(mD_1e^{ms} - mD_2e^{-ms}) \tag{16}$$

or, since $m = \sqrt{zy}$,

$$I = \sqrt{y/z}(D_1e^{ms} - D_2e^{-ms}) \tag{17}$$

To evaluate D_1 and D_2 let $s = 0$, where I and E have the values of load current and voltage, I_2 and E_2. Then

$$I = I_2 = \sqrt{y/z}(D_1 - D_2) \tag{18}$$

while, from eq. (15), for $s = 0$

$$E = D_1 + D_2 \tag{19}$$

From eqs. (18) and (19)

$$D_1 = 1/2(E_2 + \sqrt{z/y}I_2) \quad . \; . \; . \; . \; . \; . \; . \; . \; . \quad (20)$$

$$D_2 = 1/2(E_2 - \sqrt{z/y}I_2) \quad . \; . \; . \; . \; . \; . \; . \; . \; . \quad (21)$$

Substituting values of D_1 and D_2 into eqs. (15) and (17),

$$E = 1/2(E_2 + \sqrt{z/y}I_2)e^{ms} + 1/2(E_2 - \sqrt{z/y}I_2)e^{-ms} \quad . \; . \quad (22)$$

$$I = 1/2(I_2 + \sqrt{y/z}E_2)e^{ms} + 1/2(I_2 - \sqrt{y/z}E_2)e^{-ms} \quad . \; . \quad (23)$$

Equations (22) and (23) show the potential and current along the line each as the resultant of two exponential quantities, one increasing, the other decreasing, from the receiver to the transmitter. It is as though each consisted of a main (transmitted) wave plus a reflected wave (Fig. 491).

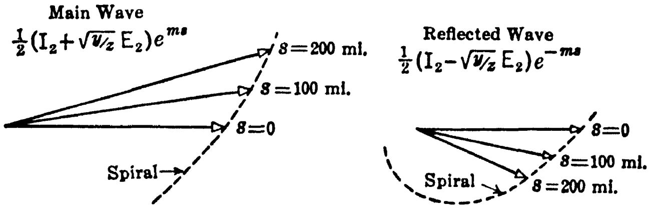

FIG. 491. Graphical representation of main and reflected waves.

The above are the fundamental equations of the transmission line expressed in exponential form. Several other forms are also used. By separating terms in eqs. (22) and (23) and regrouping,

$$E = E_2\frac{e^{ms} + e^{-ms}}{2} + \sqrt{z/y}I_2\frac{e^{ms} - e^{-ms}}{2} \quad . \; . \; . \; . \quad (24)$$

Therefore, since $1/2(e^{\theta} + e^{-\theta}) = \cosh\theta$, and $1/2(e^{\theta} - e^{-\theta}) = \sinh\theta$

$$E = E_2 \cosh ms + \sqrt{z/y}I_2 \sinh ms \quad . \; . \; . \; . \; . \; . \; . \quad (25)$$

Similarly,

$$I = I_2\frac{e^{ms} + e^{-ms}}{2} + \sqrt{y/z}E_2\frac{e^{ms} - e^{-ms}}{2} \quad . \; . \; . \; . \quad (26)$$

$$= I_2 \cosh ms + \sqrt{y/z}E_2 \sinh ms \quad . \; . \; . \; . \; . \; . \; . \quad (27)$$

If $\sqrt{z/y}$ is replaced by Z_0, the so-called " surge impedance " of the line, $\sqrt{y/z}$ by Y_0, and m by $\sqrt{zy}$, called the complex " propagation constant."

per unit length of line (§648), eqs. (25) and (27) become

$$E = E_2 \cosh \sqrt{zy}\, s + Z_0 I_2 \sinh \sqrt{zy}\, s \quad . \; . \; . \; . \; . \; (28)$$

$$I = I_2 \cosh \sqrt{zy}\, s + Y_0 E_2 \sinh \sqrt{zy}\, s \quad . \; . \; . \; . \; . \; (29)$$

The above equations give the values of the current and voltage at any point on the line, a distance s from the receiving end. If s is made equal to l, the total length of the line, the equations give the current and voltage at the sending end. Replacing $\sqrt{zy}\, l$ by $\sqrt{ZY}$, where Z and Y are the total inductive impedance and capacitive admittance of the line, leads to the equations

$$E_1 = E_2 \cosh \sqrt{ZY} + I_2 Z_0 \sinh \sqrt{ZY} \quad . \; . \; . \; . \; . \; (30)$$

$$I_1 = I_2 \cosh \sqrt{ZY} + Y_0 E_2 \sinh \sqrt{ZY} \quad . \; . \; . \; . \; (31)$$

Conversely, if it is desired to express I_2 and E_2 in terms of the current and potential at the sending end of the line, eqs. (30) and (31) may be solved for I_1 and E_1, giving

$$E_2 = E_1 \cosh \sqrt{ZY} - I_1 Z_0 \sinh \sqrt{ZY} \quad . \; . \; . \; . \; . \; (32)$$

$$I_2 = I_1 \cosh \sqrt{ZY} - E_1 Y_0 \sinh \sqrt{ZY} \quad . \; . \; . \; . \; . \; (33)$$

while the potential E and current I at a distance s_g from the sending end of the line (Fig. 440) become

$$E = E_1 \cosh \sqrt{zy}\, s_g - I_1 Z_0 \sinh \sqrt{zy}\, s_g \; . \; . \; . \; . \; . \; (32a)$$

$$I = I_1 \cosh \sqrt{zy}\, s_g - E_1 Y_0 \sinh \sqrt{zy}\, s_g \; . \; . \; . \; . \quad (33a)$$

In §638 the general equations of the transmission line were written in terms of general circuit constants, or

$$E_1 = AE_2 + BI_2 \quad . \; . \; . \; . \; . \; . \; . \; . \; . \; . \; (34)$$

$$I_1 = AI_2 + CE_2 \; . \; . \; . \; . \; . \; . \; . \; : \; . \; . \; . \; (35)$$

In the long line these general circuit constants become (eqs. 30 and 31)

$$A = \cosh \sqrt{ZY} \; . \; . \; . \; . \; . \; . \; . \; . \; . \; . \; . \; . \; . \; . \; . \; (36)$$

$$B = Z_0 \sinh \sqrt{ZY} = Z \frac{\sinh \sqrt{ZY}}{\sqrt{ZY}} \quad . \; . \; . \; . \; . \; (37)$$

$$C = Y_0 \sinh \sqrt{ZY} = Y \frac{\sinh \sqrt{ZY}}{\sqrt{ZY}} \quad . \; . \; . \; . \; . \; (38)$$

The determination of these constants for a given line will be discussed in §§650 and 652.

646. Special Case of the Direct-Current Line. — For the d-c line having distributed leakance, such as the track circuit in railway signaling systems, etc., the equations already developed for the a-c line apply with little change, Z and Y being replaced by $R = rl$ and $G = gl$, respectively. Then $\sqrt{ZY}$ becomes $\sqrt{RG}$, $m = \sqrt{rl} = \alpha$, $Z_0 = R_0 = \sqrt{r/g}$, $Y_0 = G_0 = \sqrt{g/r}$. With these substitutions the various types of equations for the long a-c line are made to apply to the d-c line. For example, eqs. (25) and (27) for the potential and current at a distance s from the receiver become:

$$E = E_2 \cosh \sqrt{rg}\, s + I_2 \sqrt{rg} \sinh \sqrt{rg}\, s \quad . \quad . \quad . \quad (25d)$$

$$I = I_2 \cosh \sqrt{rg}\, s + E_2 \sqrt{rg} \sinh \sqrt{rg}\, s \quad . \quad . \quad . \quad (27d)$$

Similarly, for the values of potential and current at one end of the line in terms of the values at the other end, and of constants for the entire line, there follow the equations:

$$E_1 = E_2 \cosh \sqrt{RG} + I_2R_0 \sinh \sqrt{RG} \quad . \quad . \quad . \quad . \quad (30d)$$

$$I_1 = I_2 \cosh \sqrt{RG} + E_2G_0 \sinh \sqrt{RG} \quad . \quad . \quad . \quad . \quad (31d)$$

or

$$E_2 = E_1 \cosh \sqrt{RG} - I_1R_0 \sinh \sqrt{RG} \quad . \quad . \quad . \quad . \quad (32d)$$

$$I_2 = I_1 \cosh \sqrt{RG} - E_1G_0 \sinh \sqrt{RG} \quad . \quad . \quad . \quad . \quad (33d)$$

647. EXPERIMENT 30-A. — Tests of a Direct-Current Line with Distributed Constants. — A d-c line with uniformly distributed resistance and leakance may be represented in the laboratory in several ways. For instance, two wires of fairly high resistance, such as iron or copper-clad wire, may be strung in the laboratory, say 50 feet long, and incandescent lamps hung at intervals of 6 to 12 inches throughout the length of the line. The lamps should be identical and of high resistance, such as 10-watt lamps. The voltage applied to the line should be low enough so that the lamps will not be heated appreciably, because then their resistances would be unequal. A load of a resistance comparable with that of all the lamps in parallel should be connected at the receiving end. With, say, 6 volts applied to the line, measurements should be taken of potentials and currents at each end and at several points along the wire. The resistance per foot of wire and the resistance of each lamp or " leak " should be known.

Compare experimental values with those obtained by theoretical equations for the d-c wire. Take open-circuit and short-circuit tests of the line for the purpose of determining the line constants from test values (§652). Compare theoretical calculations with measured values and explain discrepancies.

If conditions permit, d-c lines with more nearly uniformly distributed constants may be secured by two parallel wires in an electrolytic bath, or by two cotton-covered wires which have been twisted together and then wet in a conducting solution and allowed partially to dry before measurements are attempted.

648. The Physical Meaning of the Propagation Constant. — The term $m = \sqrt{zy}$ appearing in the fundamental equations of the long line was called the "propagation constant." Writing it in terms of its component parts,

$$m = \sqrt{zy} = \sqrt{(r + j\omega L)(g + j\omega C)} = \alpha + j\beta \quad . \quad . \quad . \quad (39)$$

Thus the propagation constant is seen to be a complex quantity consisting of the terms α and β. The physical significance of these terms can best be seen from a consideration of eqs. (22) and (23). Let a load be chosen with an impedance, $Z_2 = E_2/I_2$, equal in value and phase angle to the surge impedance, $Z_0 = \sqrt{z/y}$. Then from eqs. (22) and (23)

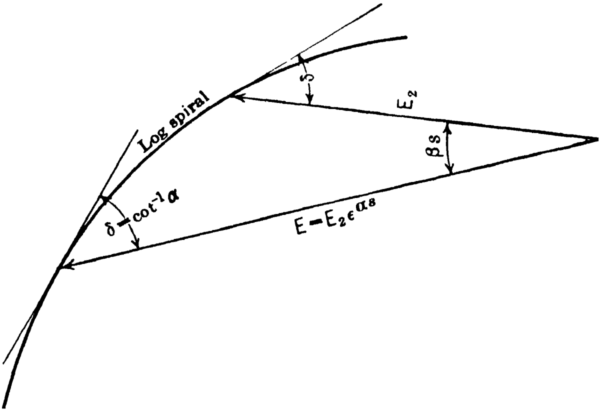

FIG. 492. Geometric interpretation of coefficients α and β.

$$E = E_2 e^{\sqrt{zy}\, s} = E_2 e^{\alpha s} e^{j\beta s} \quad . \quad . \quad . \quad . \quad . \quad . \quad . \quad . \quad (40)$$

$$I = I_2 e^{\sqrt{zy}\, s} = I_2 e^{\alpha s} e^{j\beta s} \quad . \quad . \quad . \quad . \quad . \quad . \quad . \quad . \quad (41)$$

Equation (40) may be written

$$E = E_2 e^{\alpha s} (\cos \beta s + j \sin \beta s) \quad . \quad . \quad . \quad . \quad . \quad . \quad (42)$$

From eq. (42) it is seen that, for the conditions stated, the voltage E at a distance s from the receiver has a numerical value which is $e^{\alpha s}$ times the receiver voltage, and is shifted from it by an angle βs (Fig. 492). Conversely, the line voltage diminishes with distance from the sending end by the factor e^{α} per unit length of line, and shifts in phase (backward) by the angle β. As a result α is called the *attenuation constant* of the line, and β is called the *wavelength constant.* A geometric interpretation of these facts is shown in Fig. 492, where the ends of the vector E lie on a logarithmic spiral.

649. Methods of Computation. — The solution of the equations for the long line involves, first, the determination of the line constants, z and y, for the particular conductor size and spacing. These values are taken from suitable tables (see Chapter XXIX or an electrical handbook). There follows the computation of ZY or $\sqrt{ZY}$ in complex or polar form. Then $\cosh \sqrt{ZY}$ and $\sinh \sqrt{ZY}$ or (see eq. 28*a*) $\sinh \sqrt{ZY}/\sqrt{ZY}$ are best determined from charts of complex hyperbolic functions.[1] If such charts are not available, but one has tables of hyperbolic functions of real values and natural functions of angles, the hyperbolic functions of complex quantities may be altered as follows:

Replacing $\cosh \sqrt{ZY}$ by $\cosh (\alpha_0 + j\beta_0)$ and expanding

$$\cosh (\alpha_0 + j\beta_0) = \cosh \alpha_0 \cos \beta_0 + j \sinh \alpha_0 \sin \beta_0 \quad . \quad . \quad (43)$$

Similarly

$$\sinh (\alpha_0 + j\beta_0) = \sinh \alpha_0 \cos \beta_0 + j \cosh \alpha_0 \sin \beta_0 \quad . \quad . \quad (44)$$

It should be remembered that in these equations α_0 is a real quantity whereas β_0 is an angle (in radians).

In the absence of tables of hyperbolic functions, the equations may be evaluated by expressing them in the form of series with rapidly diminishing terms[2] as follows:

$$\cosh \sqrt{ZY} = 1 + ZY/2 + Z^2Y^2/4\,! + Z^3Y^3/6\,! + \cdots \quad . \quad . \quad (45)$$

$$\sinh \sqrt{ZY} = \sqrt{ZY} + (\sqrt{ZY})^3/3\,! + (\sqrt{ZY})^5/5\,! + \cdots \quad . \quad (46)$$

$$\frac{\sinh \sqrt{ZY}}{\sqrt{ZY}} \quad 1 + ZY/3\,! + Z^2Y^2/5\,! + Z^3Y^3/7\,! + \cdots \quad . \quad (47)$$

The evaluation of α and β. The evaluation of the attenuation constant, α, for unit length of line or of $\alpha l = \alpha_0$ for the total line, and of the wavelength constant β, or $\beta l = \beta_0$, may be easily performed as follows:

---

[1] A. E. Kennelly, "Chart Atlas of Complex Hyperbolic and Circular Functions," Harvard University Press.

L. F. Woodruff, "Complex Hyperbolic Function Charts," *Elec. Eng'g*, May, 1935, p. 550.

[2] J. F. H. Douglas, "Transmission Line Calculations," *Elec. World*, vol. 40, No. 17, p. 1066.

Since $\alpha_0 + j\beta_0 = \sqrt{ZY}$ it follows that, in terms of numerical values,

$$\alpha_0^2 + \beta_0^2 = ZY \quad . \; . \; . \; . \; . \; . \; . \; . \; . \; . \quad (48)$$

Expressing values in complex notation

$$(\alpha_0 + j\beta_0)^2 = \dot{Z}\dot{Y} = (R + jX)(G + jB)$$

or $$\alpha_0^2 - \beta_0^2 + 2j\alpha_0\beta_0 = (RG - BX) + j(GX + RB) \quad . \; . \; . \; . \quad (49)$$

Therefore

$$\alpha_0^2 - \beta_0^2 = RG - BX \quad . \; . \; . \; . \; . \; . \; . \; . \; . \quad (50)$$

Solving eqs. (48) and (50) for α_0 and β_0

$$\alpha_0 = [1/2(ZY + RG - BX)]^{1/2} \quad . \; . \; . \; . \; . \; . \quad (51)$$

$$\beta_0 = [1/2(ZY - RG + BX)]^{1/2} \quad . \; . \; . \; . \; . \; . \quad (52)$$

When the leakance, G, of the line is negligible these equations become

$$\alpha_0 = \sqrt{(B/2)(Z - X)} \quad . \; . \; . \; . \; . \; . \; . \quad (51a)$$

$$\beta_0 = \sqrt{(B/2)(Z + X)} \quad . \; . \; . \; . \; . \; . \; . \quad (52a)$$

In the above, if Z and Y are per mile of line, α_0 and β_0 will be per mile of line also (α and β). In eqs. (51) and (52) the constants are simple numerics.

650. Examples of Transmission-Line Calculations. — The examples which immediately follow and those which will be found in §652 are based upon a three-phase, 60-cycle line, 150 miles long, consisting of 400,000 cir mil hard-drawn copper cables, spaced 12 feet apart between centers, and delivering 40,000 kw at 132,000 volts and at a load power factor of 90 per cent, lagging.

Example I. Determination of line constants. — Applying the methods of §647 to the given transmission line, determine the various constants of the line.

Solution: r = 0.162 ohm per mile (Table I, Chapter XXIX).

x = 0.458 + 0.302 = 0.76 ohm per mile (Tables II and III, Chapter XXIX).

$1/b = (0.104 + 0.0737)10^6 = 0.178 \times 10^6$ ohms per mile (Tables II and III).

therefore, $b = 5.62/10^6$ mho per mile.

$X = 0.76 \times 150 = 114$ ohms per wire,

$R = 0.162 \times 150 = 24.3$ ohms per wire.

$Z = 24.3 + j114 = 116.6\underline{/78°}$.

$Y = 5.62 \times 150/10^6 = 8.43/10^4\underline{/90°}$.

$$Z_0 = \sqrt{Z/Y} = \sqrt{\frac{116.6}{8.43} \times 10^4 \underline{/-12^\circ}} = 372\underline{/-6^\circ}.$$

$$Y_0 = \frac{1}{Z_0} = \frac{2.69}{10^3}\underline{/6^\circ}.$$

$$ZY = 0.0974\underline{/168^\circ}.$$

$$\sqrt{ZY} = ml = 0.312\underline{/84^\circ}.$$

$$\alpha_0 = \sqrt{1/2(8.43)(116.6 - 114)/10^4} = 0.0331 \text{ (eq. 51}a\text{)}.$$

$$\beta_0 = \sqrt{1/2(8.43)(116.6 + 114)/10^4} = 0.3118 \text{ (eq. 52}a\text{)}.$$

$\cosh \sqrt{ZY} = 0.952\underline{/0.6^\circ}$ (Woodruff's charts in *Elec. Eng'g*, May, 1935).

$\dfrac{\sinh \sqrt{ZY}}{\sqrt{ZY}} = 0.9843\underline{/0.2^\circ}$ (Woodruff's charts in *Elec. Eng'g*, May, 1935).

Applying eqs. (43) and (44) to the determination of $\cosh \sqrt{ZY}$,

$$\sqrt{ZY} = 0.0327 + j0.3103$$

$\cosh 0.0327 = 1.0006$ (Table IX of Macmillan's "Log. and Trig. Tables").
$\cos 0.3103$ radian $= 0.952$.
$\cosh \alpha_0 \cos \beta_0 = 0.9526$.
$\sinh 0.0327 = 0.0327$ (*loc. cit.*).
$\sin 0.3103$ radian $= 0.306$.
$\sinh \alpha_0 \sin \beta_0 = 0.01$.
$\cosh \alpha_0 \cos \beta_0 + j \sinh \alpha_0 \sin \beta_0 = 0.953\underline{/0.6^\circ}$.

Expressing $\cosh \sqrt{ZY}$ as a series (eq. 45):

$$\begin{aligned}\cosh \sqrt{ZY} &= 1 + (1/2)0.0974\underline{/168^\circ} + (1/24)(0.0974)^2\underline{/336^\circ} \\ &\quad + (1/720)(0.0974)^3\underline{/504^\circ} \\ &= 1 + j0 - 0.04765 + j0.01013 + 0.000361 - j0.00016 \\ &\quad - 0.000001 + j0.000007 \\ &= 0.9527 + j0.01 = 0.953\underline{/0.6^\circ}\end{aligned}$$

which checks the values by former methods.

651. Summary of Equations for the Long Line. — The various equations which have been developed for the transmission line are here brought together for greater convenience and somewhat amplified.

Type I. Equations of main and reflected waves.

$$E = 0.5(E_2 + \sqrt{z/y}I_2)e^{ms} + 0.5(E_2 - \sqrt{z/y}I_2)e^{-ms} \quad . \ . \ (22)$$

$$I = 0.5(I_2 + \sqrt{y/z}E_2)e^{ms} + 0.5(I_2 - \sqrt{y/z}E_2)e^{-ms} \quad . \ . \ (23)$$

or, *in terms of load admittance*, $Y_2 = I_2/E_2$, or of load impedance, $Z_2 = E_2/I_2$,

$$E = 0.5E_2(1 + Z_0Y_2)e^{ms} + 0.5E_2(1 - Z_0Y_2)e^{-ms} \tag{22a}$$

$$I = 0.5I_2(1 + Y_0Z_2)e^{ms} + 0.5I_2(1 - Y_0Z_2)e^{-ms} \tag{23a}$$

In terms of the *combined line-plus-load impedance and admittance*, Z_1 and Y_1, and of the distance, s_g, from the sending end

$$E = 0.5E_1(1 + Z_0Y_1)e^{-ms_g} + 0.5E_1(1 - Z_0Y_1)e^{ms_g} \tag{22b}$$

$$I = 0.5I_1(1 + Y_0Z_1)e^{-ms_g} + 0.5I_1(1 - Y_0Z_1)e^{ms_g} \tag{23b}$$

In terms of the *potentials and currents at the two ends of the line* and of total line series impedance and shunt admittance

$$E_1 = 0.5E_2[(1 + Z_0Y_2)e^{\sqrt{ZY}} + (1 - Z_0Y_2)e^{-\sqrt{ZY}}] \tag{22c}$$

$$I_1 = 0.5I_2[(1 + Y_0Z_2)e^{\sqrt{ZY}} + (1 - Y_0Z_2)e^{-\sqrt{ZY}}] \tag{23c}$$

Conversely,

$$E_2 = 0.5E_1[(1 + Z_0Y_1)e^{-\sqrt{ZY}} + (1 - Z_0Y_1)e^{\sqrt{ZY}}] \tag{22d}$$

$$I_2 = 0.5I_1[(1 + Y_0Z_1)e^{-\sqrt{ZY}} + (1 - Y_0Z_1)e^{\sqrt{ZY}}] \tag{23d}$$

Type II. Hyperbolic functions of complex values. The fundamental equations for the potential and current at a distance, s, from the receiver in terms of the hyperbolic functions of the complex propagation constant, $m = \sqrt{zy}$, per unit length of line are:

$$E = E_2 \cosh ms + I_2Z_0 \sinh ms \tag{28}$$

or

$$E = E_2 \cosh ms + I_2zs\frac{\sinh ms}{ms} \tag{28a}$$

$$I = I_2 \cosh ms + E_2Y_0 \sinh ms \tag{29}$$

or

$$I = I_2 \cosh ms + E_2ys\frac{\sinh ms}{ms} \tag{29a}$$

In terms of potential and current *at the sending end*, and of the distance, s_g, from that end,

$$E = E_1 \cosh ms_g - I_1Z_0 \sinh ms_g \tag{28b}$$

or

$$E = E_1 \cosh ms_g - I_1zs_g\frac{\sinh ms_g}{ms_g} \tag{28c}$$

$$I = I_1 \cosh ms_g - E_1Y_0 \sinh ms_g \tag{29b}$$

or

$$I = I_1 \cosh ms_g - E_1ys_g\frac{\sinh ms_g}{ms_g} \tag{29c}$$

The potential and current *at one end of the line*, in terms of current and potential at the other end, and of the propagation constant of the whole line are

$$E_1 = E_2 \cosh \sqrt{ZY} + I_2 Z_0 \sinh \sqrt{ZY} \quad \ldots\ldots \quad (30)$$

or

$$E_1 = E_2 \cosh \sqrt{ZY} + I_2 Z \frac{\sinh \sqrt{ZY}}{\sqrt{ZY}} \quad \ldots\ldots \quad (30a)$$

$$I_1 = I_2 \cosh \sqrt{ZY} + E_2 Y_0 \sinh \sqrt{ZY} \quad \ldots\ldots \quad (31)$$

or

$$I_1 = I_2 \cosh \sqrt{ZY} + E_2 Y \frac{\sinh \sqrt{ZY}}{\sqrt{ZY}} \quad \ldots\ldots \quad (31a)$$

$$E_2 = E_1 \cosh \sqrt{ZY} - I_1 Z_0 \sinh \sqrt{ZY} \quad \ldots\ldots \quad (32)$$

or

$$E_2 = E_1 \cosh \sqrt{ZY} - I_1 Z \frac{\sinh \sqrt{ZY}}{\sqrt{ZY}} \quad \ldots\ldots \quad (32a)$$

$$I_2 = I_1 \cosh \sqrt{ZY} - E_1 Y_0 \sinh \sqrt{ZY} \quad \ldots\ldots \quad (33)$$

$$= I_1 \cosh \sqrt{ZY} - E_1 Y \frac{\sinh \sqrt{ZY}}{\sqrt{ZY}} \quad \ldots\ldots \quad (33a)$$

Type III. Hyperbolic functions replaced by series. Closely approximate equations result from the substitution for hyperbolic functions of their values in the series given in eqs. (45) to (47).

For example:

$$\begin{aligned} E_1 = {} & E_2(1 + ZY/2 + Z^2Y^2/24 + Z^3Y^3/720 + \cdots) \\ & + I_2 Z(1 + ZY/6 + Z^2Y^2/120 + Z^3Y^3/5040 + \cdots) \quad . \quad (53) \end{aligned}$$

$$\begin{aligned} I_1 = {} & I_2(1 + ZY/2 + Z^2Y^2/24 + Z^3Y^3/720 + \cdots) \\ & + E_2 Y(1 + ZY/6 + Z^2Y^2/120 + Z^3Y^3/5040 + \cdots) \quad . \quad (54) \end{aligned}$$

Example II. For a load of 40,000 kw at 132,000 volts and at 90 per cent lagging power factor solve for values of current, potential, etc., at the sending end in the system of Example I.

Solution: $I_2 = 40{,}000/(0.9 \times \sqrt{3} \times 132) = 194.5\underline{/-25.9^\circ}$.

Substituting values determined in §648 in eqs. (31*a*) and (30*a*),

$$\begin{aligned} I_1 &= 194.5 \times 0.952\underline{/-25.3^\circ} + 76{,}200\,(8.43/10^4)0.9843\underline{/90.2^\circ} \\ &= 185\underline{/-25.3^\circ} + 63.9\underline{/90.2^\circ} = 167.7\underline{/-5.15^\circ} \\ E_1 &= 76.200 \times 0.952\underline{/0.6^\circ} + 194.5 \times 116.6 \times 0.9843\underline{/-25.9^\circ + 78^\circ + 0.2^\circ} \\ &= 72.540\underline{/0.6^\circ} + 22{,}300\underline{/52.3^\circ} = 88{,}130\underline{/12.1^\circ} \\ \theta_1 &= 12.1^\circ + 5.15^\circ = 17.25^\circ \\ \cos\theta_1 &= 0.955, \text{ lagging} \end{aligned}$$

652. Determination of the Line Constants from No-Load and Short-Circuit Tests. — Let the load be disconnected ($I_2 = 0$), and let the observed no-load voltages at the generator and receiver ends be E_{01} and E_{02}, respectively; let the sending-end current be I_{01}. Then eqs. (25) and (27) become:

$$E_{01} = E_{02} \cosh \sqrt{ZY} \quad . \quad . \quad . \quad (55)$$

$$I_{01} = E_{02} \sinh \sqrt{ZY} \quad . \quad . \quad . \quad (56)$$

Let the receiver end of the line be short-circuited ($E_2 = 0$), and let the generator- and receiver-end currents be I_{s1} and I_{s2}, respectively. Denoting the generator-end voltage by E_{s1}, eqs. (25) and (27) give:

$$E_{s1} = I_{s2} Z_0 \sinh \sqrt{ZY} \quad . \quad . \quad . \quad (57)$$

$$I_{s1} = I_{s2} \cosh \sqrt{ZY} \quad . \quad . \quad . \quad (58)$$

The four equations (55) to (58) are more than sufficient for determining the unknown complex constants, $\sqrt{ZY} = m$, and Z_0 (or Y_0), of the line. Either some of the measurements may be omitted, or else the equations may be so combined as to express the constants as accurately as possible. A convenient method is to eliminate E_{02} and I_{s2}. The foregoing equations then become:

$$\tanh \sqrt{ZY} = E_{s1}/(I_{s1} Z_0) \quad . \quad . \quad . \quad (59)$$

$$\tanh \sqrt{ZY} = I_{01}/(E_{01} Y_0) \quad . \quad . \quad . \quad (60)$$

Multiplying and dividing these equations, term by term, we get:

$$\tanh^2 \sqrt{ZY} = (I_{01} E_{s1})/(E_{01} I_{s1}) \quad . \quad . \quad . \quad (61)$$

$$Z_0^2 = (E_{01} E_{s1})/(I_{01} I_{s1}) \quad . \quad . \quad . \quad (62)$$

or simply:

$$\tanh \sqrt{ZY} = \sqrt{Z_{s1} Y_{01}} \quad . \quad . \quad . \quad (63)$$

$$Z_0 = \sqrt{Z_{01} Z_{s1}} \quad . \quad . \quad . \quad (64)$$

In these expressions

$$Z_{01} = Y_{01}^{-1} = E_{01}/I_{01}$$

is the sending-end impedance at no-load, and

$$Z_{s1} = E_{s1}/I_{s1}$$

is the sending-end impedance on short circuit.

When $\sqrt{ZY}$ and Z_0 are known, the complex values of Z and Y can be determined, as shown below, also r, x, g, and b, if desired.

Example III. (All values are per phase.) It is assumed that the following test data have been taken on a certain three-phase line:

Open-circuit test. $E_{01} = 76{,}200$ volts; $I_{01} = 66.1$ amperes; Input $= 35.2$ kw.
Short-circuit test. $E_{s1} = 11{,}430$ volts; $I_{s1} = 95.2$ amperes; Input $= 234$ kw.
Calculations: $\cos\theta_{01} = 35{,}230/(76.2 \times 66.1) = 0.007$; $\theta_{01} = 89.6^\circ$.

$$Z_{01} = 76{,}200/(66.1\underline{/89.6^\circ}) = 1153\underline{/-89.6^\circ}\text{ ohms}$$
$$Y_{01} = 1/Z_{01} = 8.67/10^4\underline{/89.6^\circ}$$
$$Z_{s1} = 11{,}430/(95.2\underline{/-77.6^\circ}) = 120\underline{/77.6^\circ}$$
$$\cos\theta_{s1} = 234/(11.43 \times 95.2) = 0.215;\ \theta_{s1} = -77.6^\circ$$

Then (eq. 63),

$$\tanh\sqrt{ZY} = \sqrt{(120 \times 8.67/10^4)\underline{/77.6^\circ + 89.6^\circ}} = 0.323\underline{/83.6^\circ}.$$

From chart (for $\tanh\sqrt{ZY}$), $\sqrt{ZY} = 0.312\underline{/84^\circ}$.

From eq. (64)

$$Z_0 = \sqrt{(1153 \times 120)\underline{/-89.6^\circ + 77.6^\circ}} = 372\underline{/-6^\circ}$$

Since $Z_0 = \sqrt{Z/Y} = 372\underline{/-6^\circ}$, and $\sqrt{ZY} = 0.312\underline{/84^\circ}$,

$$Z = Z_0\sqrt{ZY} = 372 \times 0.312\underline{/84^\circ - 6^\circ} = 116.5\underline{/78^\circ}\text{ ohms}$$
$$R = rl = 116.5\cos 78^\circ = 24.3\text{ ohms}$$
$$X = xl = 116.5 \times \sin 78^\circ = 114\text{ ohms}$$
$$Y = \sqrt{ZY}/Z_0 = (0.312\underline{/84^\circ})/(372\underline{/-6^\circ}) = 8.4/10^4\underline{/90^\circ}$$

Thus, the constants of the line have been obtained from the open-circuit and the short-circuit tests.

653. EXPERIMENT 30-B. — Tests of an Experimental Long Line. — The purpose of the experiment is to become familiar with the properties of the long line (transmission line with uniformly distributed constants) and to check the theoretical relations already developed (§§645 and 651). It is assumed that a suitable artificial line is available, with a large number of proper resistors, reactors, and capacitors arranged to simulate a long line.

(1) Using methods described in Chapter XXVIII (A-C Bridges) take measurements of the impedances and admittances and make certain that the artificial line has satisfactory properties.

(2) Test the line for actual performance under assumed conditions of load and power factor, using constant frequency and a sine-form wave of applied potential. To avoid influencing the potentials along the line measure voltages with electrostatic or vacuum-tube voltmeters (Chapter LX).

(3) Determine the line constants from open-circuit and short-circuit tests (§652).

(4) Predict the performance of the line for the same conditions that obtained during the tests, using both calculated and measured line constants, and compare the theoretical and measured values.

(5) Look up methods of constructing circle-diagram charts of the transmission line,[3] and draw such a chart to check calculated values.

(6) Discuss the accuracy and convenience of the methods used.

654. Quarter-Wavelength and Half-Wavelength Lines. — When the length of a line and its linear constants are such that $\beta l = \beta_0 = \pi/2, \pi$, etc., the line possesses somewhat unusual properties which are of considerable practical interest.

(a) *Quarter-wave line.* Consider a line of such length that:

$$\beta l = \pi/2 \quad \dots\dots\dots\dots \quad (65)$$

It is proved in hyperbolic trigonometry (see also eqs. 43 and 44) that:

$$\sinh(a + j\pi/2) = j\cosh a \quad \dots\dots\dots \quad (66)$$

$$\cosh(a + j\pi/2) = j\sinh a \quad \dots\dots\dots \quad (67)$$

Hence eqs. (28) and (29), applied to the sending end, become

$$E_1 = j(E_2 \sinh \alpha l + I_2 Z_0 \cosh \alpha l) \quad \dots\dots \quad (68a)$$

$$I_1 = j(I_2 \sinh \alpha l + E_2 Y_0 \cosh \alpha l) \quad \dots\dots \quad (68b)$$

When the resistance and the leakage are negligible, $\alpha = 0$, and (§648):

$$Z_0 = Y_0^{-1} = \sqrt{x/b} = \sqrt{L/C} \quad \dots\dots\dots \quad (69)$$

Thus, eqs. (68) become[4]

$$E_1 = jI_2\sqrt{L/C} \quad \dots\dots\dots\dots \quad (70a)$$

$$I_1 = jE_2\sqrt{C/L} \quad \dots\dots\dots\dots \quad (70b)$$

On open circuit ($I_2 = 0$), eqs. (68) give

$$E_1 = jE_2 \sinh \alpha l \quad \dots\dots\dots\dots \quad (71a)$$

$$I_1 = jE_2 Y_0 \cosh \alpha l \quad \dots\dots\dots\dots \quad (71b)$$

With a given E_1, as α tends to zero, E_2 increases indefinitely. This shows that with a quarter-wave line a very high receiver voltage may be expected even with a moderate voltage at the sending end. A radio antenna has some properties of a quarter-wave line.

---

[3] L. F. Woodruff, "Principles of Electric Power Transmission," Chapter VI, John Wiley & Sons, 1938.

[4] Equations (70) show that an ideal quarter-wave line converts from constant current to constant voltage, or vice versa.

On short circuit ($E_2 = 0$) eqs. (68) become:

$$E_1 = jI_2Z_0 \cosh \alpha l \qquad (72a)$$

$$I_1 = jI_2 \sinh \alpha l \qquad (72b)$$

With a finite I_2, as α approaches zero, I_1 also becomes very small. This means that a quarter-wave line, when short-circuited, draws only a small current from the generator, and this current may be much smaller than that on open circuit. The receiver-end current on short circuit may be quite large.

For an ideal line, $Z = 2\pi fL$ and $b = 2\pi fC$, so that (eq. 52) becomes:

$$\beta = 2\pi f \sqrt{LC} \qquad (73)$$

Hence, eliminating β from eqs. (65) and (73), we get:

$$4lf\sqrt{LC} = 1 \qquad (74)$$

This equation gives the relationship between the length of an ideal quarter-wave line, its linear constants, and its natural frequency. When r and g are appreciable, eq. (52) should be used in place of eq. (73).

(b) *Half-wave line.* Let the length of the line be such that:

$$l\beta = \pi \qquad (75)$$

It is proved in hyperbolic trigonometry that:

$$\sinh (a + j\pi) = -\sinh a \qquad (76a)$$

$$\cosh (a + j\pi) = -\cosh a \qquad (76b)$$

Therefore, eqs. (28) and (29), applied to the sending end, become:

$$E_1 = -(E_2 \cosh \alpha l + I_2Z_0 \sinh \alpha l) \qquad (77a)$$

$$I_1 = -(I_2 \cosh \alpha l + E_2Y_0 \sinh \alpha l) \qquad (77b)$$

For an ideal line $\alpha = 0$ and these equations become:

$$E_1 = -E_2 \qquad (78a)$$

$$I_1 = -I_2 \qquad (78b)$$

These results could be expected from the very concept of a half-wave line.

On open circuit ($I_2 = 0$), eqs. (77) become:

$$E_1 = -E_2 \cosh \alpha l \qquad (79a)$$

$$I_1 = -E_2Y_0 \sinh \alpha l \qquad (79b)$$

On short circuit ($E_2 = 0$), we have:

$$E_1 = -I_2Z_0 \sinh \alpha l \qquad (80a)$$

$$I_1 = -I_2 \cosh \alpha l \qquad (80b)$$

The length of an ideal half-wave line is twice that determined from eq. (74).

655. EXPERIMENT 30-C. — Study of Quarter-Wave and Half-Wave Lines. — The experimental arrangement is the same as in §653. The necessary theory is given in §654.

(1) Open the receiving end of the line. Start with the generator at the lowest frequency and raise it until the quotient of the supply current by the supply voltage is a maximum; record this frequency. The line has now a *quarter-wave length.* Take readings of voltage and current along the line and plot them against distance; i.e., plot them as ordinates separated by equal horizontal spaces. Note that when the receiving end is short-circuited the supply current falls to a low value.

(2) Short-circuit the receiving end of the line and raise the frequency until the quotient of the supply current by the supply voltage reaches a maximum; record this frequency. The line now has a *quarter-wave length.* Take readings of voltage and current as before, (a) with the receiving end short-circuited, (b) with the receiving end open-circuited, and (*c*) with the receiving end connected to a non-inductive resistance approximately equal to the quotient of the maximum voltage by the maximum current. Plot each set of readings as before, to a new set of axes.

Report. From the readings compute the constants of the line and check the theoretical formulas given in §654.

NOTE. To justify the name of surge impedance for Z_0, consider a pure surge or traveling wave propagated along an ideal line devoid of resistance and of leakage. In such a surge, the amounts of kinetic and potential energy per unit length are equal. Hence, $i^2L = e^2C$, or $e/i = \sqrt{L/C}$. With alternating currents, $Z_0 = \sqrt{L/C} = \sqrt{(2\pi fL)/(2\pi fC)}$, which agrees with the definition in §645.

To prove the equality of the two energies, consider an electrostatic charge, q, in a surge, per unit of its length, moving at a velocity v. The electrostatic energy is $0.5q^2/C$, and the electromagnetic $0.5\,(qv)^2L$, both per unit length. The fundamental differential equation of wave propagation is $d^2e/ds^2 = LCd^2e/dt^2$; this equation is satisfied by any function of $s \pm vt$, where $v^2 = 1/(LC)$. Hence, the foregoing expression for the electromagnetic energy becomes $0.5q^2/C$, and is equal to the electrostatic energy.

REFERENCES

1. L. F. WOODRUFF, Principles of Electric Power Transmission, Second Edition, John Wiley & Sons.

2. F. E. PERNOT, Electrical Phenomena in Parallel Conductors, John Wiley & Sons.

3. A. E. KENNELLY, The Applications of Hyperbolic Functions to Electrical Engineering Problems, McGraw-Hill Book Co.

4. J. A. FLEMING, The Propagation of Electric Currents, Van Nostrand Co.

5. C. P. STEINMETZ, Alternating-Current Phenomena, McGraw-Hill Book Co.

6. O. G. C. DAHL, Electric Circuits — Theory and Applications, Chapters VI, VII, IX, and X, McGraw-Hill Book Co.

7. E. A. Loew, Electric Power Transmission, McGraw-Hill Book Co.

8. CLIFFORD and DAWES, Standard Handbook for Electrical Engineers, sec. 14, McGraw-Hill Book Co.

9. DEL MAR and PHILIP, Electrical Engineers' Handbook, sec. 14, John Wiley & Sons.

10. M. P. WEINBACH, Principles of Transmission in Telephony, Macmillan Co.

11. H. WADDICOR, Principles of Electric Power Transmission, John Wiley & Sons.

12. NORRIS and BINGHAM, Electric Characteristics of Power and Telephone Transmission Lines, International Textbook Co.

13. W. W. LEWIS, Transmission Line Engineering, McGraw-Hill Book Co.

14. S. HAYASHI, *Electrotech. Jour.*, June, 1938, vol. 2, pp. 135–142, New fundamental differential equations of power transmission lines.

15. H. B. DWIGHT, Transmission Line Formulas, Van Nostrand Co.

16. FRANKLIN and TERMAN, Transmission Line Theory, Franklin & Charles Co.

17. J. F. H. DOUGLAS, *Elec. World*, vol. 40, No. 17, p. 1066, Transmission line calculations.

18. WM. NESBIT, Electrical Characteristics of Transmission Circuits, Westinghouse Technical Night School Press, 1926.

19. EDITH CLARKE, *Gen. Elec. Rev.*, May, 1926, Simplified transmission line calculations.

CHAPTER XXXI

GROUND DETECTORS AND INSULATION MEASUREMENTS ON ELECTRIC LINES

656. Two kinds of insulation troubles usually develop in the operation of distribution and transmission lines, viz., faults to the ground and faults between conductors. A breakdown between conductors is more likely to occur in a cable, while a ground connection may develop either in an overhead conductor or in a cable. Three steps are usually necessary before a fault can be remedied, namely:

(1) The existence of the fault must be discovered.
(2) The value of its resistance (or at least its order of magnitude) must be determined, in order to ascertain the seriousness of the damage to insulation.
(3) The fault must be located exactly.

These three steps, together with the most important devices used in practice for each step, are described in this and the following chapter.

GROUND DETECTORS

657. A device which indicates a ground connection, or defective insulation to the ground, is called a ground detector. On high-tension circuits, electrostatic ground detectors, glow lamps, or electronic devices are used; on low-tension circuits, incandescent lamps or a voltmeter may be preferable. An electrostatic instrument requires a considerable voltage for a noticeable deflection.

658. Electrostatic Ground Detectors. — A *single-phase* ground detector is shown in Fig. 493. It consists of two stationary metal vanes, a_1 and a_2, connected to the line, and a movable vane, m, permanently grounded. On lines of moderate voltage the stationary vanes are connected to the line conductors directly. On high-tension lines, tubular or other condensers, k_1 and k_2 are used to reduce the difference of potential across the instrument itself (§§55 and 588). As long as the circuit is perfectly insulated from the ground, the movable vane, for reasons of symmetry, remains in stable equilibrium midway between the stationary vanes. At any instant, one of the line conductors is at a potential which is as much above that of the ground as the other conductor is below the ground potential ($E_1 = -E_2$). Therefore the induced charges and the electrostatic attractions between the stationary vanes and the movable one are balanced when the latter remains in its middle position.

Should one of the line conductors, say No. 2, become completely grounded ($E_2 = 0$), the full line voltage, E, would become impressed between conductor 1 and the movable vane. The instrument then acts as an electrostatic voltmeter in series with the condenser k_1, and the movable vane assumes a position opposite the stationary vane a_1. This is the position in which the total variable capacitance of the instrument is a maximum. It may also be said that the movable vane is attracted to a_1 because of a large difference of potential between them, whereas the attraction between the movable vane and a_2 is zero since both are at the same potential. In other words, *the pivoted vane moves away from the fixed vane connected to the grounded line.* With an imperfect or high-resistance ground, there remains some difference of potential between m and a_2, so that the movable vane is subjected to a differential action and does not move so far to the left as on a " dead " ground. The scale of the instrument may therefore be calibrated in volts, or in some arbitrary divisions, to indicate the seriousness of the ground.

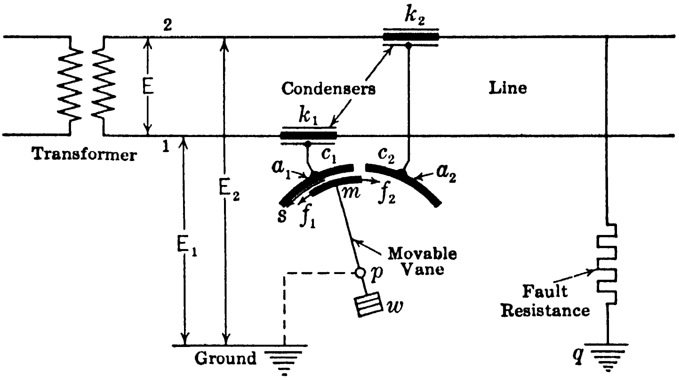

FIG. 493. Single-phase electrostatic ground detector.

The *theoretical relationships* are as follows: With an imperfect ground, the position of the movable vane is determined by the condition:

$$f_1 = f_2 \quad . \ . \ . \ . \ . \ . \ . \ . \ . \ . \ . \ . \quad (1)$$

where f_1 and f_2 are the tangential mechanical forces due to the electrostatic field acting upon the movable vane. According to eq. (1), Chapter XXVI, the charging current, i, of a condenser of capacitance C is

$$i = C\,dE/dt \quad . \ . \ . \ . \ . \ . \ . \ . \ . \ . \quad (2)$$

The energy, W, stored in the condenser is

$$W = \int Ei\,dt = C\int E\,dE = 0.5CE^2 \quad \text{. . . . . . .} \quad (3)$$

Energy may also be written in terms of the force, F, acting in the direction of movement, and of the distance, s, or

$$W = \int F\,ds \quad \text{. . . . .} \quad (4)$$

From eqs. (3) and (4), for constant potential E, but varying capacitance, the mechanical force acting in a direction s, between two electrodes of a condenser of capacitance C, is:

$$f = 0.5E^2(dC/ds) \quad \text{. . . . .} \quad (5)$$

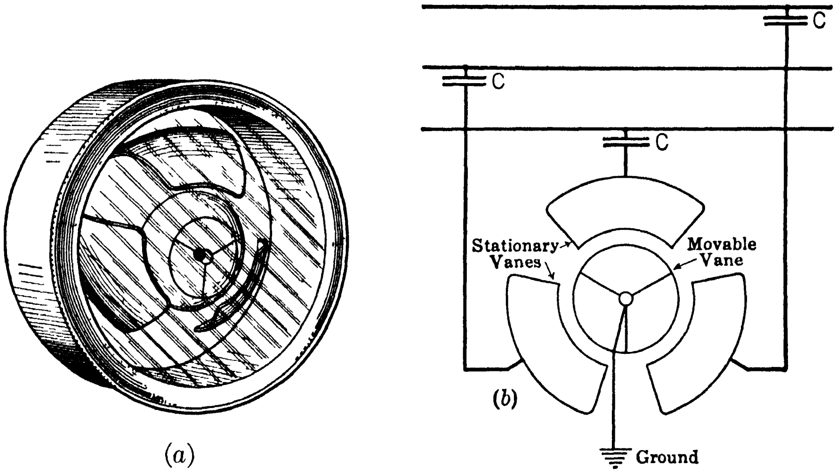

(a) (b)

FIG. 494. A three-phase ground detector. (a) General appearance; (b) circuit diagram.

We thus have in the case under consideration, using the relationship (1):

$$E_1^2(dC_1/ds) = -E_2^2(dC_2/ds) \qquad (6)$$

Here s is measured in the tangential direction, say to the left, and the minus sign is necessary because the capacitance between a_2 and m decreases when the vane moves in the direction of positive s. The capacitance C_1 consists of that of condenser k_1 in series with that of the instrument itself, between a_1 and m. Similarly, C_2 consists of the capacitance of the condenser k_2 in series with that between a_2 and m.

When $E_1 = E_2$, that is, when the insulation is perfect, the movable vane occupies the position for which $dC_1/ds = -dC_2/ds$, which is midway between the stationary vanes. With a large E_1 and small E_2, the absolute value of dC_1/ds must be small and that of dC_2/ds large, in order that eq. (3) may be satisfied. This corresponds to a position of m under a_1, where C_1 itself is comparatively large, but its variations with s are small.

A *three-phase* electrostatic ground detector is shown in Fig. 494*a* and 494*b*. It operates on the same principle as the one described above, but has three stationary vanes, each of which is connected to a line conductor, usually through a condenser (Fig. 494*b*). The movable vane is so pivoted that it can move in all directions about a point. As in the single-phase detector, the movable vane takes a position away from the grounded conductor.

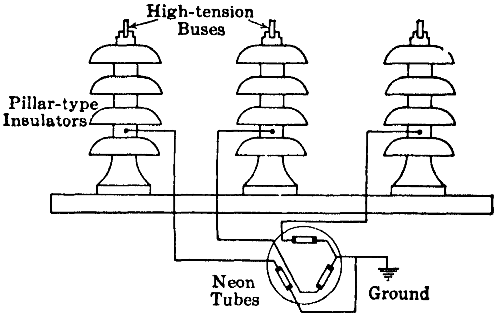

FIG. 495. Glow-type ground detector.

659. Neon-Tube and Vacuum-Tube Ground Detectors. — The use of glow tubes in a three-phase ground detector is shown in Fig. 495.[1] Three neon-gas-filled tubes are connected between taps on strings of insulators and the ground. The taps on the insulators are so placed that a suitable potential above ground is impressed upon the tubes. When the lines are free of ground connections the tubes glow normally and equally. When a ground occurs on one line the tube connected to that line is darkened while the other tubes glow more brightly. Some idea of the resistance from line to ground may be obtained from the relative brightness of the tubes.

Figure 496 illustrates one way in which vacuum tubes[2] may serve as ground detectors and, through relays, operate a warning device. In the installation shown, the grids of three-element vacuum tubes (triodes) receive an a-c potential from taps on strings of insulators connected "star-to-ground" on a 33-kv system. The plates of the tubes are energized from the secondary windings of potential or station transformers with an emf substantially 180 degrees out of phase with the potentials impressed on the respective grids. As long as the grid potentials, which are proportional to the volts to ground of the several lines, retain their normal values, there is little or no plate current and the signal relays do not operate. This is due to the fact that while the plate potentials are positive the grid potentials are sufficiently negative to prevent the flow of plate current. (See Chapter LIX for characteristics of electron tubes.) However, when a ground occurs on one or more lines, the potentials impressed upon the corresponding grids are so reduced that sufficient plate current flows to actuate the relays which in turn operate the alarm signals and call the attention of the station operator to the ground. Such a warning signal may be transmitted from an unattended station to the system operator's office over system telephone or special signal lines. Mr. Hardewyck[3] states that the insertion of a 1-μf condenser at *B* in the detector circuit in series with the 22-megohm resistor *A*, and in parallel with a 14-megohm resistor *C*, provides 5-second delay to prevent unnecessary operation on momentary grounds.

---

[1] Sanderson, "Electric System Handbook," p. 216, McGraw-Hill Book Co.

[2] A. H. Hardewyck, "Locate Phase Grounds with Simple Detector," Operating Guide Book for Central Station Men, 1937, *Elec. World.*

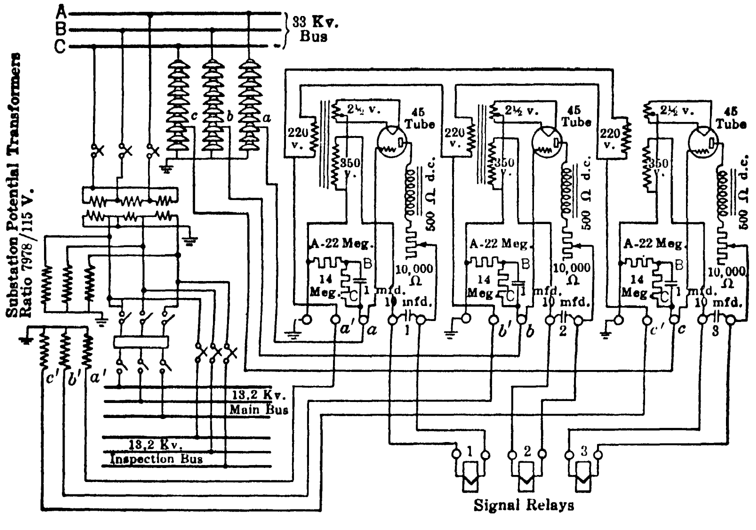

Fig. 496. Hardewyck detector for locating transmission-line grounds.

The ground detectors so far described apply especially to comparatively high-voltage systems, normally ungrounded. With fairly high-resistance grounds on normally grounded three-wire or four-wire systems the fault current may not be sufficient to operate the protective equipment and isolate the faulty section. An ammeter, recording or indicating, in the ground lead of such a system will show any abnormal rise of ground current (the zero phase-sequence component of Chapter XXXIV.) To protect the ammeter against excessive current a relay may be inserted to shunt the ammeter by a low resistance after the current reaches a predetermined maximum for the meter. In some cases the relay operates to insert a resistance to limit the ground current. This, however, has the undesirable effect of increasing the potential to ground of ungrounded lines.

---

[3] *Loc. cit.*

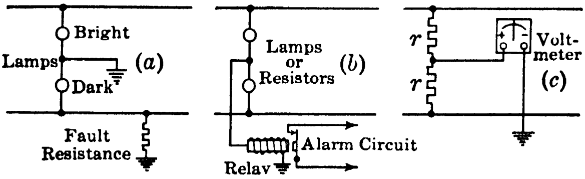

FIG. 497. Ground indicators on a control bus.

660. Ground Detectors in Low-Voltage Systems. — The occurrence of grounds on low-voltage lines should be known at once in order that proper repairs may be made before the fault leads to serious results. In control circuits, for instance, grounds may lead to the improper closing or opening of circuit breakers in the high-voltage system under control.

In Fig. 497 three forms of ground detector for use on a low-voltage (control) bus are shown. At (*a*) an even number of lamps are connected across the line with their central point well grounded. A sufficient number of lamps are used so that they glow dimly when there is no ground on either line. When a low-resistance ground occurs on one line the lamps on that side go out, while the others burn brightly. For a fault of moderately high resistance the difference in brightness of the two sections of lamps shows which line is grounded, and gives some idea of the seriousness of the ground. If desired, an automatic alarm may be caused to operate by the insertion of a relay in the ground lead, as at (*b*). In place of lamps, which are likely to burn out on over-voltage, any suitable resistors may be used with the relay. An accurate estimate of the resistance to ground may be obtained by means of a voltmeter, as at (*c*). On d-c lines a voltmeter with central zero will show which line is grounded, and its reading will give the resistance of the ground connection (see §664). If desired, the scale of the instrument may be calibrated directly in ohms resistance of the ground fault.

661. EXPERIMENT 31-A. — Study and Calibration of Ground Detectors. — The several types of ground detectors described above, and such others as the student can devise, should be studied and applied in the detection of grounds on electric systems. Starting with the low-voltage lines, apply faults of known or measurable value and study each type of ground detector, as follows:

(a) Try to calibrate the lamps of Fig. 497*a* as a function of the fault resistance. Start with a very high-resistance fault and reduce it to a value, say *a* ohms, at which it is just possible to detect the difference in brightness of the lamps in a fairly dark place. Find the value of fault resistance, *b*, at which the difference in brightness is easily detected, and the value *c* at which one set of lamps goes black. Try the effect of varying the type and wattage of lamp, as 10-watt tungsten, 40-watt tungsten, and 50-watt carbon lamp.

(b) Try to apply the color-temperature chart given in Table II, §8, applied to the brighter lamps with a view to plotting a curve of fault resistance against color (or temperature) of lamps.

(c) Arrange a relay with bell and battery, and adjust it for the minimum difference of ground resistance at which reliable operation of the warning signal results. Note the effect of varying the value of the resistance placed across the line.

(d) Using a voltmeter and resistors across the line, calibrate the voltmeter against fault resistance.

Observing all due precautions required by the dangerous voltage involved, investigate the several types of ground detector available for high-voltage systems. For example:

(e) Connect a differential electrostatic voltmeter as in Fig. 493 to detect grounds on a single-phase high-voltage system obtained, say, by stepping up 110 volts a-c by means of an instrument transformer. Calibrate the voltmeter in terms of the fault resistance, using condensers k_1 and k_2 of given value. For a known fault resistance determine the effect of varying condenser capacitance. If a three-phase electrostatic detector is available, follow a procedure similar to the above in studying and calibrating it.

(f) Connect neon lamps in the manner of Fig. 495 and study the effect of varying fault resistance, also position of the taps to insulator strings, attempting to interpret the indications of the lamps in terms of fault resistance, as in (a).

(g) Devise and test a single-phase ground detector using vacuum tubes somewhat as in Fig. 496.

Discuss the results obtained in all the tests made, and state the limitations of the several methods.

INSULATION RESISTANCE MEASUREMENT

662. Insulation Resistance of a Wire, Cable, or Winding. — The safe operation of lines and machines is dependent upon the maintenance of proper insulation between electrical conductors, and between conductors and ground. In the installation of new equipment tests of insulation resistance should be made to insure that the insulation is undamaged and free from excessive moisture. Periodic tests should be made to determine whether there has been any deterioration of the insulation with consequent danger of breakdown and danger of damage to equipment or operators. Such tests are commonly made by means of voltmeters (§§663 and 664), or by special ohmmeters called Meggers (§§667 and 668), and the results are expressed in ohms or megohms for a given conductor or piece of equipment.

For factory tests of cables and other insulated wires the galvanometer method (§665) is ordinarily employed, and insulation resistance is expressed in terms of "megohm-miles," meaning the resistance in megohms of the insulation on 1 mile of wire. If the line being tested is 4 miles in length the insulation resistance in megohm-miles is 4 times that of the total line.

Assuming uniformity of insulation material and thickness, the insulation resistance, in megohms, of 1 mile of metal-sheathed single-conductor cable is

$$R = K \log_{10} D/d \qquad (7)$$

where D = outer diameter of insulation.

d = diameter of conductor.

$K = (2.28/10^6) \times$ resistivity in megohm-centimeters.

TABLE I[4]

Materials	Usual Values of K at 60°C
Vulcanized rubber......	2000–6000
Gutta-percha	2500
Varnished cloth	1000
Impregnated paper	1000

Insulation resistance is normally measured with direct current. If alternating current is used the resistance appears much lower owing to capacitance current (§590).

---

[4] "Electrical Engineers' Handbook," vol. IV, sec. 14, John Wiley & Sons.

663. Measurement of Insulation Resistance on a "Dead" Line — Voltmeter Method. — Insulation resistance measurements may be conveniently performed on a "dead" line or network, i.e., one disconnected from the source of power. Two conditions will be considered: Case I, the combined resistance from lines to ground when there is negligible resistance between lines; Case II, the separate resistances between lines, between line 1 and ground; between line 2 and ground.

Case I. With the lines short-circuited or joined by low-resistance load devices, a voltmeter, *V* (Fig. 498), of known high resistance, *R*, is connected, first across a steady source of test voltage, *Ba*, and then in series with that source but between ground and either line. Let the first reading be *E*, and the second E_1; let the combined resistance between lines and ground be x. Since the deflections of a voltmeter at a given supply voltage are inversely proportional to the total resistance in the voltmeter circuit, it follows that

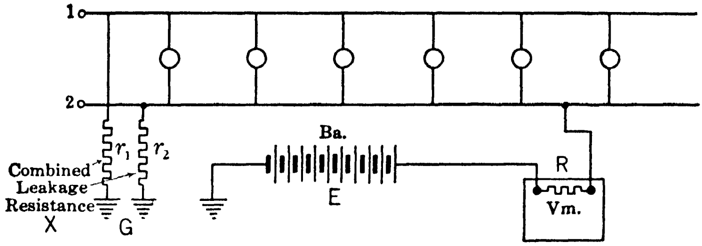

FIG. 498. Insulation measurements on a "dead" line, using battery and voltmeter.

$$E_1/E = R/(R + x)$$

or

$$x = R(E - E_1)/E_1 \quad . \; . \; . \; . \; . \; . \; . \quad (8)$$

Case II. Let r_1, r_2, and r_{12} be, respectively, the resistances line 1 to ground, line 2 to ground, and between lines 1 and 2, with all load devices disconnected. By means of the voltmeter and the source of constant voltage the following readings are taken:

(1) Line 2 dead-grounded, reading between line 1 and ground = E_1.

(2) Line 1 dead-grounded, reading between line 2 and ground = E_2.

(3) Lines 1 and 2 joined, reading lines to ground = E_3.

For condition (1)

$$\frac{E}{E_1} = \frac{R + r_1r_{12}/(r_1 + r_{12})}{R} = 1 + r_1r_{12}/R(r_1 + r_{12}) = A \quad . \; . \quad (9a)$$

For condition (2)

$$\frac{E}{E_2} = \frac{R + r_2r_{12}/(r_2 + r_{12})}{R} = 1 + r_2r_{12}/R(r_2 + r_{12}) = B \quad . \ . \quad (9b)$$

For condition (3)

$$\frac{E}{E_3} = \frac{R + r_1r_2/(r_1 + r_2)}{R} = 1 + r_1r_2/R(r_1 + r_2) = C \quad . \ . \ . \quad (9c)$$

Solving eqs. (9), and letting $1/(A - 1) = k_1$, $1/(B - 1) = k_2$, and $1/(C - 1) = k_3$

$$r_1 = 2R/(k_1 + k_3 - k_2) \quad . \ . \ . \ . \ . \ . \ . \quad (10a)$$

$$r_2 = 2R/(k_2 + k_3 - k_1) \quad . \ . \ . \ . \ . \ . \ . \quad (10b)$$

$$r_{12} = 2R/(k_1 + k_2 - k_3) \quad . \ . \ . \ . \ . \ . \ . \quad (10c)$$

664. Measurement of Insulation Resistance on a "Live" Line — Voltmeter Method. — On a low-voltage line a fairly accurate determination of insulation resistance is possible even when the line is in service. The principle involved is essentially that of the ground-detector voltmeter of Fig. 497*c*. Detailed connections are shown in Fig. 499. A sensitive voltmeter of resistance R gives a reading E_1 when connected from wire 1 to ground, and of E_2 between wire 2 and ground. The unknown resistances to ground are r_1 and r_2 from lines 1 and 2, respectively. Since the voltmeter of resistance R reads E volts when placed across the line, the reading E_1 will be to E as the resistance R is to the total resistance consisting of r_2 in series with the combined resistance of r_1 and R in parallel, or

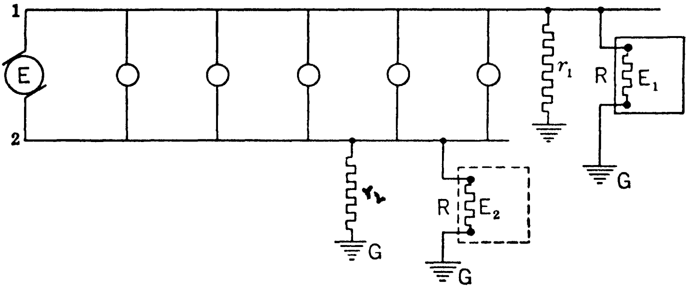

FIG. 499. Tests for insulation resistance on a " live " line.

$$\frac{E}{E_1} = \frac{r_2 + Rr_1/(R + r_1)}{Rr_1/(R + r_1)} = \frac{r_2R + r_2r_1}{r_1R} + 1 \quad . \ . \ . \ . \quad (11)$$

Similarly $$\frac{E}{E_2} = \frac{r_1 + r_2R/(R + r_2)}{r_2R/(R + r_2)} = \frac{r_1R + r_2r_1}{r_2R} + 1 \quad . \; . \; . \; . \quad (12)$$

From (11)

$$r_2R + r_2r_1 = \left(\frac{E}{E_1} - 1\right) r_1R \quad . \; . \; . \; . \; . \; . \; . \quad (13)$$

From (12)

$$r_1R + r_2r_1 = \left(\frac{E}{E_2} - 1\right) r_2R \quad . \; . \; . \; . \; . \; . \; . \quad (14)$$

From eqs. (14) and (15) it follows that

$$r_1 = r_2E_1/E_2 \quad . \; . \; . \; . \; . \; . \; . \; . \; . \; . \quad (15)$$

Substituting in eq. (13) and simplifying

$$r_2 = R(E - E_1 - E_2)/E_1 \quad . \; . \; . \; . \quad (16)$$

Similarly $$r_1 = R(E - E_1 - E_2)/E_2 \quad . \; . \; . \; . \quad (17)$$

665. Insulation Measurements by Means of a Galvanometer. — If the insulation resistance is of such a high value (above 1 megohm[5]) that readings by means of a voltmeter are inadequate, readings may be taken by means of a galvanometer of high sensitivity, say, such that a deflection of 1 mm is produced on a scale at 1-meter distance by a current of the value of 10^{-9} ampere. The galvanometer should be equipped with an Ayrton universal shunt (§14). Readings of the galvanometer are taken first at a reduced and accurately known potential, read, say, by a potentiometer in comparison with a standard cell, and with a standard resistance of 1/10 to 1 megohm in series with the galvanometer, and later with a higher potential in series with galvanometer and insulation resistance. This is the well-known substitution method (see §14, Vol. I). If K_s, D_s, and E_s are, respectively, the shunt multiplying factor, galvanometer deflection, and applied potential during calibration of the instrument, and K_x, D_x, and E_x the corresponding values during the measurement of unknown resistance, while R_s is the standard resistance and R_x the unknown resistance,[6]

$$R_x = R_s(K_sE_xD_s)/(K_xE_sD_x) \quad . \; . \; . \; . \; . \; . \; . \quad (18)$$

Pender and Del Mar (*loc. cit.*) state that with such equipment resistances to 10^5 megohms may be measured, while for higher values the lea age current through the insulation may be used for a given period of time to charge a condenser (§595) which is then discharged through a calibrated ballistic galvanometer (§177). Then, if K = galvanometer constant, D = deflection, t = time of charge, E = impressed volts, and R_x = insulation resistance,

---

[5] "Standard Handbook for Electrical Engineers," Sixth Edition, p. 187, McGraw-Hill Book Co.

[6] "Electrical Engineers' Handbook," Pender and Del Mar, vol. IV, sec. 5, p. 83, John Wiley & Sons.

$$R_x = (Et)/(KD) \quad . \ . \quad . \quad . \ . \ . \ . \ . \quad (19)$$

666. EXPERIMENT 31-B. — Insulation Measurements Using a Voltmeter and a Galvanometer. — The methods to be employed are described in §§663 to 665, for both " dead " and " live " lines. Provide a d-c voltmeter of high sensitivity (ohms per volt) and one of lower sensitivity, each with a full-scale deflection corresponding to the potential to be used in the tests. Determine the resistances of the voltmeters. If these are unknown they may easily be found by taking two readings of the same voltage, one with and one without a known series resistance. Application of eq. (8) will give the voltmeter resistance.

(1) Simulate the conditions of Cases I and II for " dead " lines, connecting known and adjustable high resistances from two lines to a third well-insulated wire to serve in place of the ground, in order to avoid difficulties due to possible leakage from the lines to earth. Take readings with both voltmeters for values of fault resistance varying from a few ohms to the maximum at which dependable readings can be obtained. Use a storage battery, if available, for the source of steady potential.

(2) Secure a commercial power or lighting circuit disconnected from its source of power. Using, preferably, 500 volts d-c supply and employing all due precautions to insure the safety of the observers, connect the wires and test for resistance to earth as in §663, Case I. Open all connections between the wires of the system and test for resistance between wires, and from wires to ground, as in Case II above.

(3) Energize the lines of the system at normal voltage and take measurements as in §664 for the " live " line, using voltmeters of known resistance but of different sensitivity.

(4) Take insulation resistance measurements on the armature and, separately, on the field windings of a generator or motor, with the machine cold, and then after the machine has been carrying a heavy load long enough to reach its operating temperature.

(5) Following the instructions of §665, use a highly sensitive galvanometer in the two ways described to measure high resistances.

Report. (a) Calculate the insulation resistances for the several tests and, where the resistance values are previously known, compare given values with test values.

(b) Discuss values obtained with voltmeters of different sensitivities, also with the galvanometer, and state the limitations found for the different instruments. How are these limiting values affected by the potential employed?

(c) Discuss the values obtained on the commercial line as to reliability and accuracy. Suggest improvements in method or equipment. What are the relative merits of the " live " line and " dead " line methods?

(d) Give results obtained in the measurement of insulation resistance on the machine armature and field windings. Discuss the effect of temperature upon insulation resistance. Compare the values of resistance obtained with the minimum specified in the Standardization Rules of the A.I.E.E., namely,

$$\text{Insulation resistance in megohms} = \text{Rated voltage}\Big/\left(\frac{\text{rated kva}}{100} + 1000\right)$$

667. The Megger Insulation Tester. — The instrument known under this trade name (Figs. 500 to 502) is a direct-reading portable ohmmeter of the permanent-magnet moving-coil type. It has its own hand-operated d-c generator. Motor-driven sets are also available. The instrument is made in ranges up to 20,000 megohms, and by means of supplementary ohm scales readings can be made to as low as 1 ohm. To measure an insulation resistance, the Earth terminal (Fig. 501) is connected to the ground, and the Line terminal to the line or apparatus under test. By turning the crank (Fig. 500) a direct current is generated, part of which flows through the insulation under test. The resistance of the insulation is indicated by the pointer on the scale.

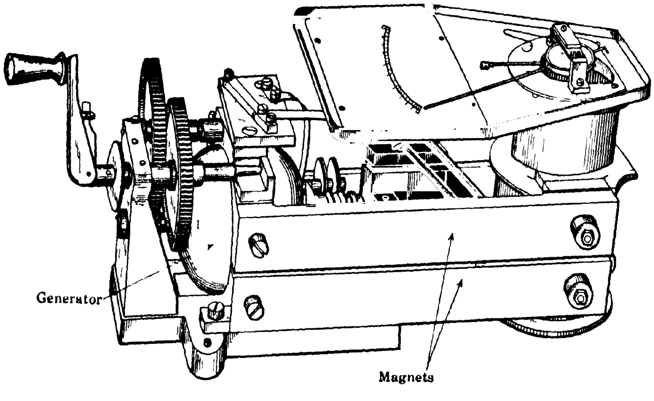

Fig. 500. The Megger insulation tester.

Megger insulation testers are made in both variable- and constant-pressure types. Variable-pressure types have ranges up to 100 megohms, with generators developing (according to the range) a testing potential up to 500 volts direct current. The armature and the crank are directly geared together, and normal potential is produced at about 120 to 160 rpm of the crank; by increasing the speed, the potential becomes proportionately greater. Variable-pressure sets are not recommended for testing circuits having capacitance of more than about $\frac{1}{2}$ μf. It is impossible to turn the generator at a constant speed, and, consequently, the voltage will vary. The resulting charging and discharging currents cause the readings to fluctuate.

Constant-pressure Megger instruments are available in ranges up to 20,000 megohms, the generators developing (according to the range) up to 5000 volts direct current. Constant voltage is maintained by connecting the armature and the crankshaft through a friction clutch. At a crank speed of approximately 120 to 160 rpm, the normal voltage is produced; but if the speed is increased above this limit, the clutch automatically slips so that the armature speed remains constant within less than 1 per cent. When testing a circuit with considerable capacitance, the generator must be operated long enough to charge the circuit, just as with any other method used under similar conditions; otherwise the readings will be too low.

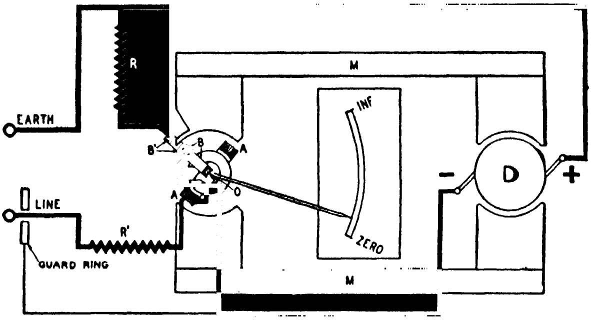

FIG. 501. Circuits of the Megger insulation tester.

668. Details of the Megger Insulation Tester. — The essential magnetic circuit and the electrical connections are shown in Fig. 501. *M*, *M* are permanent bar-magnets. Between the poles at one end is the armature, *D*, of the hand-driven generator; between the poles at the other end is the moving system of the ohmmeter. This is a true ohmmeter capable of measuring resistance independently of the exact voltage supplied for the test;[7] no adjustment or any indication of the voltage of the generator is required.

---

[7] The following notes describing the Megger insulation tester were largely contributed by Mr. T. B. Whitson of the James G. Biddle Company.

Fundamentally the Megger ohmmeter consists of a moving-coil system, with pointer attached, placed in a permanent-magnet field and carrying two coils, *A* and *B* (Fig. 502). The moving system is mounted in spring-supported jeweled bearings and is free to rotate about its axis at *O* (Fig. 501) unaffected by any controlling or restraining springs, current being led to the coils by very flexible conducting strips, *L*, in Fig. 502. As a result the pointer may stand in any position over the scale when the generator is idle.

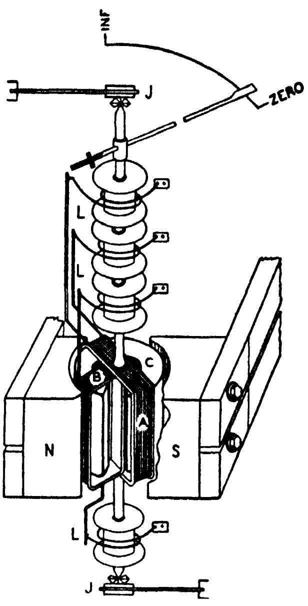

Fig. 502. Moving-coil system of the Megger tester.

Coil *A* (Fig. 501) is connected in series with a resistance *R′*, between one side of the generator and the "Line" terminal, and is called the "current" coil. Coil *B*, in series with a suitable resistance *R*, is connected across the generator terminals and is called the "potential" coil. When currents flow in these two coils they tend to turn the moving system in opposite directions. The pointer then takes a position over the scale where these two forces are equal. Thus potential opposes current and the result is interpreted in ohms.

When the crank of the generator is turned and there happens to be perfect insulation between the line terminals, "Earth" and "Line" (Fig. 501), no current flows in the current coil. The potential coil alone controls the movement, taking a position opposite the gap in the C-shaped iron core, and the pointer indicates "Infinity." When, however, a finite resistance is connected across the terminals, current flows in the current coil and the corresponding torque draws the potential coil away from the Infinity position into a field of gradually increasing strength until a balance is obtained between the opposing forces acting on the two coils. By introducing resistances of different known values across the instrument terminals and marking the corresponding position of the pointer in each case, a scale calibrated in ohms and megohms is obtained. The resistance *R′* protects the current coil in case of low resistance or short circuit in the external circuit, and the pointer merely indicates "Zero."

Effect of varying voltage. Because the two elements of the ohmmeter receive current from the same source, namely, the generator, any change in the generator potential affects both coils to the same degree; therefore the pointer always assumes the same position for a given resistance, and the calibration of the instrument is unaffected by the exact voltage of the generator (or the speed at which the crank is turned). Owing to the higher emf generated at high speeds, the instrument is then more sensitive.

The compensating coil. In order to secure Megger ohmmeter scales as open as possible for both high and low values of resistance a special magnetic circuit is employed, involving the C-shaped core already mentioned. In addition, to improve the scale and to avoid the influence of stray magnetic fields upon the indications of the instrument, a supplementary compensating coil, *B′* (Fig. 501), is attached to the outer side of the potential coil *B*, and is so wound and connected that the two coils form an astatic combination as far as external fields are concerned. The scale is further opened up at low values of resistance by the horn-shaped tip on the main pole onto which *B′* moves.

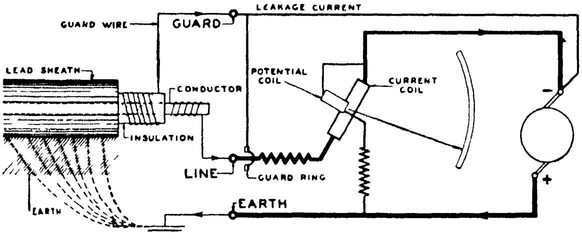

FIG. 503. Guard ring and wire used in the testing of cable insulation.

The guard system. When measuring the resistance of insulating materials, both the specimen and the measuring equipment must be adequately *guarded* to prevent error due to surface leakage. To make the instrument free from error due to internal and surface leakage, the guard system shown in Fig. 503 is used, a precaution that is especially important in high-range instruments. The purpose of the guard system is to by-pass all current that might leak across from the positive to the negative side of the circuit *inside* the Megger instrument, or across external surfaces from Earth to Line terminals. Since this current is led around the ohmmeter circuit it does not affect the indications of the instrument. To accomplish this a metal guard washer is placed behind the hard rubber bushing supporting the Line terminal, and is electrically connected to the negative side of the generator (Fig. 503). The guard washer must be insulated from the case if the case is of metal. In the same manner the various resistances and even the ohmmeter itself are guarded, the guard system offering a low-resistance path to leakage current, so that it does not pass through the current coil and, therefore, does not affect readings.

Figure 503 also shows the use of a guard wire to eliminate errors due to surface leakage in shop tests of insulated wires and cables. With lead-covered cables, and wires pulled into metal conduits, a similar scheme can be used, with the Earth terminal of the Megger connected directly to the lead sheath or to the metal conduit, as the case may be. Any error due to leakage across the surface of the insulation under test is eliminated by wrapping a bare end of a wire around the insulation, between the conductor and the earth as shown, and connecting it to the guard terminal provided for the purpose on high-range Megger instruments.

Effect of capacitance. If the capacitance in apparatus under test exceeds, say, $\frac{1}{2}$ μf it is difficult to turn the crank of the variable-pressure generator at a sufficiently constant speed to prevent variation of voltage and consequent unsteady readings. With the constant-pressure instruments (those having the slip-clutch feature), the voltage remains constant and the readings steady. When the capacitance amounts to several microfarads it takes an appreciable time to charge the apparatus while making an insulation resistance test. Readings should not be taken in cable work until after the reading has become steady; a minute or more of cranking may be necessary.

669. EXPERIMENT 31-C. — Insulation Measurements with a Megger Insulation Tester. — The Megger insulation tester is described above, and detailed instructions for its use in various practical cases are furnished by the makers.[8] The student should measure with it the insulation of some available machine, a transformer, power cable, overhead line, high-tension insulator, a complete low-voltage installation, a condenser, etc. The numerical data should be compared with those specified in the "Standards of the American Institute of Electrical Engineers," in the "Fire Underwriters' Code," or in some other authoritative rules. In performing each measurement, attention should be paid to the following three points: (a) the characteristics of the Megger insulation tester, sources of error, limits of accuracy,[9] the best method of arranging the measurements, leakage prevention, effect of different voltages upon the accuracy of the result, the sensitivity of the instrument, etc.; (b) the characteristics of the insulation resistance under measurement, the influence of the test voltage, moisture, dirt, heat, etc.; (c) the advantages and disadvantages of the "Megger" compared with the other suitable methods of measuring the same insulation resistance, for example, the voltmeter method described above or the direct-deflection galvanometer (§§663 and 665).

---

[8] See "Pocket Manual of 'Megger' Practice," J. G. Biddle Co.

[9] See H. B. Brooks, "Accuracy Tests for 'Meggers,'" *Electrical World*, vol. 85 (1925), p. 973.

670. The "Bridge-Meg" Resistance Tester. — As the name implies, this device combines the functions of the above-described Megger and of a Wheatstone bridge (§17). The purpose of such an arrangement is to extend the range of the device down to a fraction of an ohm, while keeping intact its upper range, extending into hundreds of megohms. The diagram of connections is shown in Fig. 504. A change-over switch may be turned either to establish the regular Megger connections or to convert the ohmmeter proper (Fig. 502) into a galvanometer for the Wheatstone bridge.

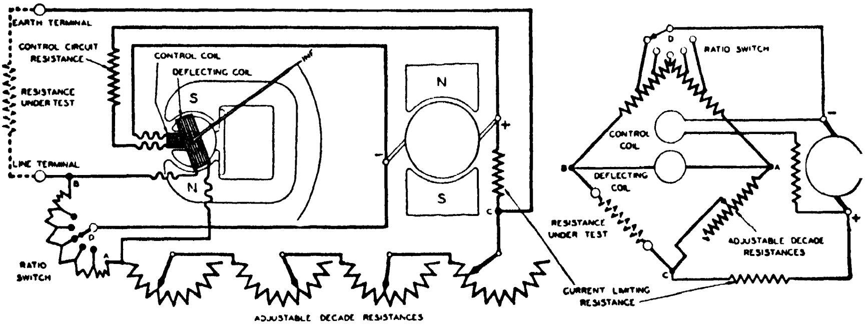

FIG. 504. Circuits of the "Bridge-Meg."

Of the four branches of the bridge, the Megger case contains two, which serve as the ratio coils. By means of the "ratio switch," this ratio may be set at will to equal 0.01, 0.1, 1, 10, or 100. A self-contained adjustable decade resistance with four direct-reading dials constitutes the third branch of the bridge. The resistance under test forms the fourth branch.

The "Bridge-Meg" is intended for the measurement of insulation resistance, and also for the determination of conductor resistances and the location of faults (§679). Directions for using the instrument will be found in the "Pocket Manual for 'Megger' Practice" mentioned above. If the Megger used in Experiment 31-C is the Bridge-Meg type it should be used in the measurement of various resistances from 10,000 ohms to a fraction, say $\frac{1}{10}$, of an ohm.

671. EXPERIMENT 31-D. — Resistance Measurements with a "Bridge-Meg." — The device is described briefly in the preceding section, and the purpose of the experiment is to become familiar with its use. The instructions given in §669, with suitable modifications, will be found useful in planning this experiment.

REFERENCES

1. A. H. HARDEWYCK, *Elec. World*, vol. 107, p. 1096, March 27, 1937, Locate phase grounds with simple detector.

2. *Edison Elec. Inst. Bul.*, vol. 5, pp. 197–8, May, 1937, Characteristics of power system faults to ground.

3. H. L. CURTIS, *Trans. A.I.E.E.*, 1927, p. 1039, The electrical resistivity of insulating materials.

4. C. H. SANDERSON, Electric System Handbook, McGraw-Hill Book Co.

5. James G. Biddle Co., Pocket Manual of " Megger " Practice.

6. Electrical Engineers' Handbook, Third Edition, vol. IV, secs. 5 and 14, John Wiley & Sons.

7. Standard Handbook for Electrical Engineers, Sixth Edition, secs. 3, 4, and 12, McGraw-Hill Book Co.

8. ANON., *Elec. Jour.*, April, 1925, p. 191, Resistance measurements.

9. C. M. SMITH, Electric and Magnetic Measurements, Macmillan Co.

10. F. A. LAWS, Electrical Measurements, McGraw-Hill Book Co.

11. V. H. TODD, *Power Plant Eng'g*, vol. 25, No. 20, Oct. 15, 1921, Ground detecting devices.

CHAPTER XXXII

FAULT LOCATION ON LINES

672. In order that service may be restored to defective lines with the least possible delay it is essential that accurate methods be available for locating these faults with sufficient accuracy to enable the repairman to proceed to the vicinity of the fault and there determine its exact position and make necessary repairs.

A low-resistance fault is usually easier to locate than an open circuit, a high-resistance ground, or a partial short circuit. If the fault is of high resistance an attempt is often made to reduce it to lower resistance by the application of a high voltage to the defective line; special transformers are frequently provided for this purpose. Mercury-arc rectifiers (Chapter LVI) or kenotrons (vacuum-tube rectifiers) (Chapter LIX) are employed to apply high-voltage direct current to underground cables. Burning out a fault sometimes helps to locate it, by causing arcing-over, noise, bubbles (in water), or smoke, and by reducing its resistance by carbonizing the insulation at the point of the fault.

There are various more or less standard methods of fault location.[1] Those described below are typical, and with a clear understanding of these the reader should be able to follow the descriptions of other methods or to devise new ones to suit special conditions.

673. Methods of Fault Location. — The following table gives a summary of the problem of fault location and of the various methods in use, as described in the remainder of this chapter.

1. Single-conductor tests.
   No-load, short-circuit, and load tests in various combinations.
2. Loop tests.
   - *A*. Drop-of-potential method.
     - (*a*) The volt-ammeter test.
     - (*b*) The two-ammeter test.
   - *B*. Bridge loops.
     - (*a*) The Murray loop.
     - (*b*) The Varley loop.

---

[1] See "Electrical Engineers' Handbook," Third Edition, vol. 4, sec. 14, p. 223, John Wiley & Sons.

3. Capacitance method.
   - *A*. The Jamieson-Higgitt loop.
   - *B*. Capacitance measurement.
   - *C*. Comparison of capacitance values.
4. Tracing or signal-current method.
   - *A*. Miscellaneous simple tests.
     - (*a*) The sheath-potential test.
     - (*b*) The magnetic-needle test.
     - (*c*) Metal shoes.
   - *B*. Induction localizers.
     - (*a*) Transverse surface coil.
     - (*b*) Current transformer.
     - (*c*) Longitudinal surface coil.
   - *C*. Bullard's method.
5. Resonance methods.

For various practical methods of fault location on overhead lines and in cables, see numerous short articles in the *Electrical World;* also reports of Overhead and Underground Systems Committees of the National Electric Light Association.[2]

674. Single-Conductor Tests.—Consider a single conductor, AB (Fig. 505), with a fault to the ground at an unknown point, C. Let the unknown resistances, AC and CB, be x and y, respectively, and let that of the fault equal z, in all ohms. Let it be further assumed that no other conductor is available for testing between A and B, so that the ground return is the only means of obtaining a circuit, and that the resistance of the ground return is negligible. The ground connections are denoted by G_1 and G_2. It is presupposed that the observer is able to send his instructions to an assistant at the other end, either over the line or by some other means.

There are different possibilities and combinations of tests that can be performed on a faulty line, such as is shown in Fig. 505. The three types of tests are:

- (a) Open-circuit tests.
- (b) Short-circuit tests.
- (c) Load tests.

These tests may be performed either from one end or from both ends of the line. Three tests are necessary for the determination of x, y, and z. This number is reduced to two when the sum of $x + y = R$ is known from the dimensions of the conductor or from a previous measurement, made when the line was perfect. When x or y has been determined, and the resistance of the conductor per unit length is known, the distance from one of the ends to the fault can be readily computed. The following combinations of tests will show the possibilities of the general method.

---

[2] Among noteworthy foreign contributions, the following two may be mentioned: F. Haas, *Arch. f. Elek.*, vol. 15 (1925), p. 44; R. Fiedler, *ibid.*, vol. 12 (1923), p. 101.

(a) *No-load and short-circuit tests from one end.* First, an open-circuit test is performed from A. With B insulated from the ground, the line resistance between the terminals A and G_1 is measured with a Wheatstone bridge, or by the drop-of-potential method, etc. Let this resistance be R_1. Then B is connected to G_2 and the line resistance between the terminals A and G_1 is measured again. Let the new and lower resistance be R_2. Assuming R to be known, we then have the following three simultaneous equations:

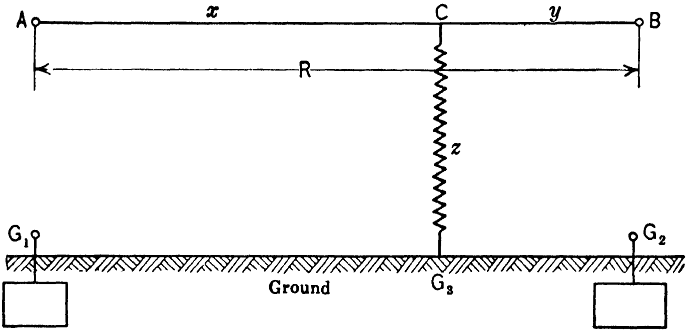

FIG. 505. Test for locating fault on a single conductor.

$$x + y = R \quad (1)$$

$$x + z = R_1 \quad (2)$$

$$x + yz/(y + z) = R_2 \quad (3)$$

Solving these equations, we obtain:

$$x = R_2 - R' \quad (4)$$

$$y = R + R' - R_2 \quad (5)$$

$$z = R_1 + R' - R_2 \quad (6)$$

where:

$$R' = \sqrt{(R_1 - R_2)(R - R_2)} \quad (7)$$

(b) *Open-circuit test from both ends.* The line resistance is measured between the terminals A and G_1, with the terminal B open. Let the value of the resistance be R_1. The resistance is then measured between the terminals B and G_2, with A open. Let its value be R_2. Assuming the total line resistance, R, to be known, we have the following simultaneous equations:

$$\left.\begin{aligned} x + y &= R \\ x + z &= R_1 \\ y + z &= R_2 \end{aligned}\right\} \quad \ldots\ldots\ldots \quad (8)$$

from which:

$$\left.\begin{aligned} x &= 0.5(R + R_1 - R_2) \\ y &= 0.5(R + R_2 - R_1) \\ z &= 0.5(R_1 + R_2 - R) \end{aligned}\right\} \quad \ldots\ldots\ldots \quad (9)$$

(c) *Short-circuit test from both ends.* The resistance is measured between the terminals A and G_1, with the terminals B and G_2 short-circuited. Let this resistance be R_1. The resistance is then measured between the terminals B and G_2, with the terminals A and G_1 short-circuited. Let its value be R_2. Assuming the total resistance, R, to be known, we have:

$$\left.\begin{aligned} x + y &= R \\ x + yz/(y + z) &= R_1 \\ y + xz/(x + z) &= R_2 \end{aligned}\right\} \quad \ldots\ldots\ldots \quad (10)$$

The solution of these equations is:

$$\left.\begin{aligned} x &= a(a - b)/c \\ y &= b(a - b)/c \\ z &= (aR_2 - bR_1)(a - b)/c^2 \end{aligned}\right\} \quad \ldots\ldots\ldots \quad (11)$$

where:

$$\left.\begin{aligned} a &= \sqrt{R_1(R - R_2)} \\ b &= \sqrt{R_2(R - R_1)} \\ c &= R_1 - R_2 \end{aligned}\right\} \quad \ldots\ldots\ldots \quad (12)$$

(d) *Three load tests.* As a more general case, let the terminals B and G_2 be connected by a known resistance, r_2, when measuring the line resistance between A and G_1. Similarly, let a resistance, r_1, be connected between A and G_1 when measuring the resistance between B and G_2. Moreover, let us assume that R is not known, so that altogether three measurements are needed. Let two measurements be performed from the A end and one from the B end. Denoting the actually measured resistances by R_1, R_1', and R_2, respectively, we have

$$\left.\begin{aligned} x + \frac{z(y + r_2)}{z + y + r_2} &= R_1 \\ x + \frac{z(y + r_2')}{z + y + r_2'} &= R_1' \\ y + \frac{z(x + r_1)}{z + x + r_1} &= R_2 \end{aligned}\right\} \quad \ldots\ldots\ldots \quad (13)$$

From these equations the unknown quantities, x, y, and z, can be determined. Although the solution is more complicated, the advantage of the load tests is that the values of the load resistances may be so chosen as to make the measurements more sensitive, or to bring them within the best range of the available apparatus.

675. EXPERIMENT 32-A. — Fault Location on a Single-Conductor Line. — The purpose of the experiment is to enable the student to become familiar with the possibilities and limitations of the methods described in the preceding section. Provide a resistance, AB (Fig. 505), of the order of magnitude of a distributing or transmission line, and arrange a contact, C, which may be attached at will at one of several desired places along AB. Provide a resistance, z, that can be varied between zero and infinity. (a) Set the value of z to represent a ground of comparatively low resistance and determine its location by performing both open-circuit and short-circuit tests. Check the actual location and the magnitude of the fault with the computed values. (b) Investigate the relative accuracy of the open-circuit and short-circuit tests when the fault is near one of the ends of the line and when it is in its middle part. (c) Perform similar measurements with medium- and high-resistance grounds. (d) Investigate the effect of an uncertain ground connection at G_3 and of a ground whose resistance depends upon the magnitude and direction of the measuring current. (e) Perform some load tests, both alone and in combination with no-load and short-circuit tests. Find at least an approximate empirical rule for the best range of load resistances, for different orders of magnitude and different locations of the fault.

Report. On the basis of the tests and computations performed, write definite instructions and recommendations as to the best method of performing the test in various cases. Select a combination of tests not treated in §674 and obtain a final solution of the equations.

LOOP TESTS

676. The principle of the loop tests described below is as follows: The faulty conductor is connected at the distant end to a good conductor, thus forming a loop. This loop is connected at the free near-end terminals to a source of direct current, and certain measurements are performed on it. From the data taken, the unknown resistance of the faulty conductor, from one of its terminals to the fault, is computed. If the resistance of the conductor, per unit length, is known, the distance to the fault can be determined. The loop methods may be broadly divided into those in which the drop of potential is used directly, and those based upon the Wheatstone-bridge principle. Two tests of each kind are described below.

677. Loop Tests Based upon the Drop-of-Potential Method. — The general diagram of connections is shown in Fig. 506. The faulty conductor, *mn*, grounded at *t*, and an unfaulted conductor, *pq*, are connected together at one end by means of clamps C_1 and C_2 and a jumper of negligible resistance. At the other end a source of voltage, *Ba.*, may be applied to either conductor or to both simultaneously, and the current read on the ammeters, A_1 and A_2. A voltmeter, *V*, of resistance *R*, is connected between the points *m* and *p*. If, instead of being

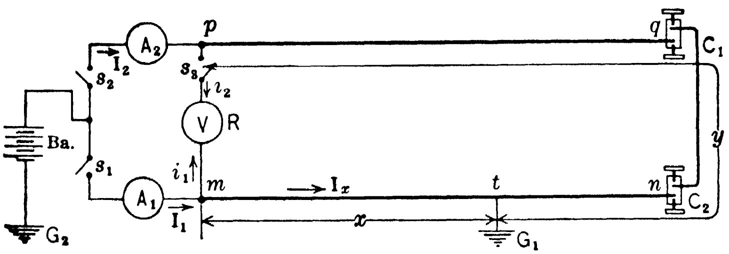

FIG. 506. Location of fault by the drop-of-potential method.

grounded, the conductor has an insulation fault to another conductor, the connections remain the same except that the other faulty conductor takes the place of the ground.

(a) *The volt-ammeter method.* Let the switches s_1 and s_3 (Fig. 506) be closed, and s_2 open. Let the current in *mt* be I_x and the difference of potential between *m* and *t* be E_x. Then the unknown resistance of the conductor to the fault is:

$$x = E_x/I_x \quad . \; . \; . \; . \; . \; . \; . \; . \; . \; . \; . \quad (14)$$

The current I_1, read on the ammeter A_1, is greater than I_x by the amount of voltmeter current, i_1. If the voltmeter current is negligible, then $I_x = I_1$. Furthermore, if the combined resistance, *y*, of the conductors *pq* and *nt* is negligible in comparison with the resistance, *R*, of the voltmeter itself, the reading of the latter, say E_1, is practically equal to E_x. Under these conditions $x = E_1/I_1$.

Should the voltmeter current, i_1, be an appreciable fraction of I_1, as in the case of a high-resistance ground, the correct values of *x* and *y* are determined as follows: First the switches s_1 and s_3 are closed. Let the ammeter and voltmeter readings be I_1 and E_1, respectively. Then the switch s_1 is opened and s_2 is closed. Let the new readings be I_2

and E_2. The voltmeter currents are:

$$i_1 = E_1/R \tag{15}$$

$$i_2 = E_2/R \tag{16}$$

respectively. Eq. (14) becomes, for the first set of readings:

$$x = i_1(R + y)/(I_1 - i_1) \tag{17}$$

and for the second set of readings, by analogy:

$$y = i_2(R + x)/(I_2 - i_2) \tag{18}$$

Solving eqs. (17) and (18) as simultaneous equations for x and y, we obtain:

$$x = E_1[I_1 - i_1 - i_2(I_1/I_2)]^{-1} \tag{19}$$

$$y = E_2[I_2 - i_2 - i_1(I_2/I_1)]^{-1} \tag{20}$$

(b) *The two-ammeter method.* The voltmeter shown in Fig. 506 is not used, and both ammeter switches, s_1 and s_2, are kept closed at the same time. The two currents are then inversely as the resistances of the paths between G_1 and G_2. Neglecting the resistances of the ammeters and of the connections, we have:

$$I_1x = I_2y \tag{21}$$

The total resistance of the loop can be measured by the drop-of-potential method. Let it be equal to r. We then have:

$$x + y = r \tag{22}$$

Solving eqs. (21) and (22) together, we get

$$x = rI_2/(I_1 + I_2) \tag{23}$$

$$y = rI_1/(I_1 + I_2) \tag{24}$$

The two-ammeter method, using high-tension alternating currents, has been applied to the location of broken insulators on long transmission lines.[3]

678. EXPERIMENT 32-B. — Fault Location by the Drop-of-Potential Loop Method. — Two different tests are described in the preceding section, and the student should become familiar with both. Two resistances should be provided, *mn* and *pq*, of the order of magnitude of a power-transmission line, telephone line, or underground cable. The position of the fault, G_1, and its resistance should be adjustable within wide limits. It is desired to investigate the accuracy and the limitations of the two methods under different conditions. Adjust the fault resistance to a rather low value, and place the fault near point *m*. Determine its location by computations according to both methods, and compare with the actual position of the fault. Then shift the ground in steps to point *n*, keeping its resistance constant, and take similar readings at each point. Make similar tests with a medium- and a high-resistance fault. As a result of these tests, state the advantages and the relative accuracy of the two tests, and the best field of application of each.

---

[3] L. C. Nicholson, *Trans. A.I.E.E.*, vol. 26 (1907), p. 1319.

679. Bridge Loop Tests.—The Wheatstone-bridge method of resistance measurement (§17), being a null method, has certain advantages in accuracy and convenience over the drop-of-potential method. For this reason it is widely used for location of faults. The general arrangement is shown in Fig. 507. The faulty conductor, *mn*, and an unfaulted conductor, *pq*, are connected together at one end by means of the jumper *nq*. At the other end they are connected to two resistances, *M* and *N*, a galvanometer, and a battery, *Ba.*, forming a Wheatstone bridge. With this bridge, the resistance *x* can be determined and the point *t* located.

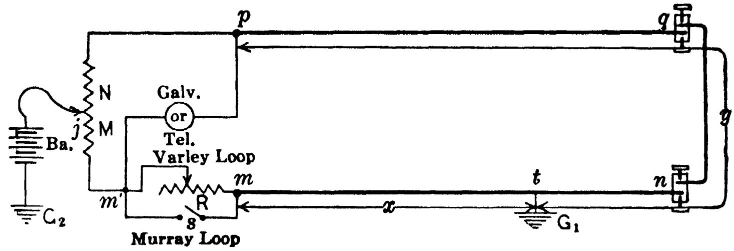

Fig. 507. The bridge method of fault location.

The positions of the battery and of the galvanometer in a Wheatstone bridge are interchangeable, but the particular arrangement shown in Fig. 507 is preferable when there are stray earth currents. The emf of such currents is algebraically added to that of the battery, *Ba.*, and does not affect the balance of the bridge. If G_1 is a short circuit or a fault to another conductor, then G_2, instead of being a ground connection, should also be a connection to that conductor.

(a) *Murray loop.* With this method, the contact point, *j*, is adjustable, and the resistance *R* does not exist, so that the points *m* and *m'* coincide. In other words, the switch *s* is closed. The contact point, *j*, is moved along the resistances *M* and *N* until the galvanometer reads zero. We then have:

$$x/y = M/N, \quad \ldots\ldots\ldots\ldots \quad (25)$$

or:

$$x/(x + y) = M/(M + N) \quad \ldots\ldots\ldots \quad (26)$$

Let, for example, the total length of the loop, *mnqp*, be 3000 meters, and let both conductors be of the same length and cross-section, so that the resistances are proportional to the lengths. Let *MN* be a slide-wire with 1000 divisions, and let the balance be obtained with $M = 210$ divisions. We then have, according to eq. (26), $x/3000 = 210/1000$, or $x = 630$ meters. This means that the fault *t* is located at a distance of 630 meters from point *m*. Should the two conductors be of different cross-section, a proportional correction would be necessary for the length of one of them.

It is also possible to reconnect the bridge and to take a second measurement, considering $(x + y)$ as an unknown resistance to be compared with a standard resistance. When $(x + y)$ is known, the value of x can be computed in ohms from eq. (26), and then the distance to the fault *t* determined from the known resistance of the conductor *mn* per unit length.

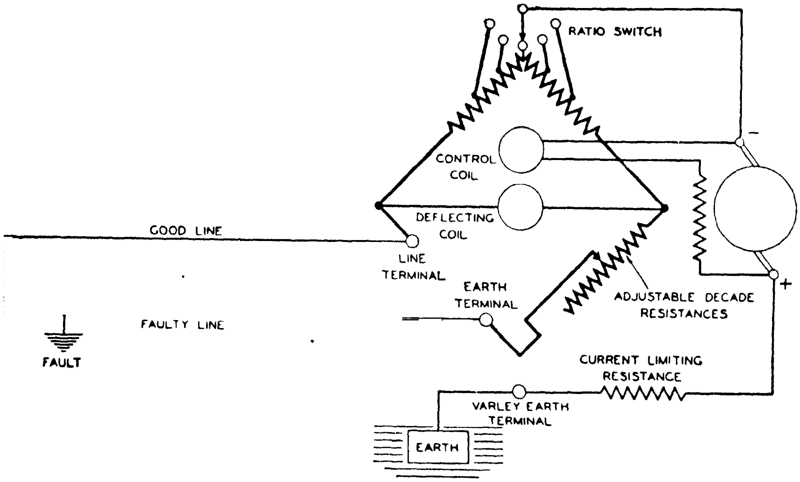

FIG. 508. Use of the "Bridge-Meg" in fault location by the loop method.

(b) *Varley loop.*[4] With this method, the point *j*, and consequently the ratio of *M* to *N*, is fixed. The switch *s* is now assumed to be open. A balance is obtained by means of an adjustable resistance, *R*, in series with x. When the galvanometer current is equal to zero, we have:

---

[4] "Standard Handbook for Electrical Engineers," Sixth Edition, sec. 3, §172.

$$(R + x)/y = M/N \quad \dots\dots\dots\dots (27)$$

The bridge is then reconnected so as to measure the total resistance of the loop. Let this resistance be equal to r; we then have:

$$x + y = r \quad \dots\dots\dots\dots (28)$$

Eliminating y and solving for x, gives:

$$x = [r(M/N) - R]/[1 + (M/N)] \quad \dots\dots (29)$$

A special arrangement of the "Megger" described in §§710 to 713 has been developed for making bridge measurements, including the Varley loop test, in the form called the "Bridge-Meg." Figure 508 shows the schematic diagram of circuits involved. The instrument is recommended for the location of faults on telephone and telegraph circuits or others of similar characteristics, but not for use on power cables since the Wheatstone bridge is not sufficiently accurate when used for the measurement of resistances of very low value, say below 0.1 ohm.

680. EXPERIMENT 32-C. — Exercises with Murray and Varley Loops. — The method is described in the preceding section. For the points to be investigated, see §§675 and 678. If a "Bridge-Meg" is available it should be employed in the location of faults, using the Varley loop on lines of low, medium, and high resistance, and its limitations determined.

CAPACITANCE TESTS

681. The Jamieson-Higgitt Loop for High-Resistance Faults. — As the resistance of a fault increases, the accuracy of the above-described loop methods decreases. Moreover, with a high-resistance fault, the electrostatic capacitance of the cable causes a considerable charging current and thus exerts a disturbing influence upon measurements. With the bridge shown in Fig. 509, the capacitance, instead of disturbing the balance, is made use of in establishing a balance.

The loop *mnqp* consists of a faulty and an unfaulted conductor and corresponds to the loops denoted by the same letters in Figs. 506 and 507. It is drawn as a straight line to serve as a reference line in showing the potential drops *ab* and *cd*. The places of the battery and of the galvanometer are interchanged, as compared with those in the preceding sketches. Let *ab* be the curve of distribution of potential referred to *mp* as the axis of abscissas; let the line potential at g be zero and that at the fault t equal to the height *th* above *mp*. Generally speaking, the slider, j, on the resistance MN is at some other point than that corresponding to g; that is, initially the bridge is not balanced. Therefore, when the galvanometer key, *s*, is closed, a charge or discharge will take place through the galvanometer, its resistance being small compared with that of the fault. The slider, *j*, is then shifted back and forth until there is no throw. A certain time must be allowed for the charge to adjust itself before each trial.

The null point, say j_1, corresponding to *g*, having been found on the resistance *MN*, the battery is reversed. The charge, having adjusted itself through the fault, produces a new potential-distribution curve, such as *cd*, with zero at *f*. The slide is adjusted until the corresponding null point, say j_2, is found on *MN*. The position of the fault is then midway between *f* and *g*, corresponding to a point midway between j_1 and j_2.

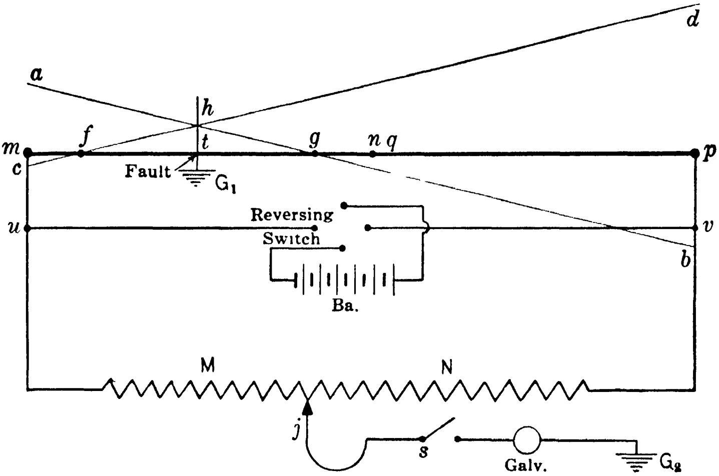

FIG. 509. The Jamieson-Higgitt loop test for high-resistance faults.

It is of interest to note that, though the adjustment depends upon the capacitance of the cable, the distribution of charge does not enter into the test, the result being true to the distribution of the resistance. With faults of very high resistance, such as those occurring in a submarine cable, or an incipient fault in a power cable, this test is far more sensitive than an ordinary loop test (§679). Moreover, it requires a much lower battery voltage and current.[5]

682. Localization of Total Break by Capacitance Measurement.—Let a conductor be disconnected somewhere on the line, owing to a burn-out or some other cause, and, at the same time, let there be no ground or short-circuit connection. The break may be located by measuring the capacitance of the conductor with respect to another parallel conductor, to the ground, or to the sheath. For example, let the capacitance of an unfaulted conductor between two stations, *A* and *B*, be 20 μf, and let a faulty conductor measure 5 μf from the end *A* and 15 μf from the end *B*. Then the fault lies at one-quarter of the distance *AB*, nearer *A*.

---

[5] For further details see *Electrician*, vol. 86 (1921), p. 96.

The methods of capacitance measurement described in §§592 and 619 are particularly suitable for this test. The capacitance method is more satisfactory with telephone cables, on account of the clean break. The capacitance of an unfaulted pair of wires is convenient to use as a standard of comparison.[6]

A bridge method suggested by Professor W. R. Work is illustrated in Fig. 510. C_1 and C_2 are the values of capacitance between the two sections of the broken wire and an unbroken wire in the cable, or to the sheath. C_3 and C_4 are continuously adjustable air capacitors mechanically coupled together so that an increase in C_3 is accompanied by a decrease in C_4, etc. *E* is a source of audio-frequency alternating potential. Head phones are used as the detector. Increasing C_3 and decreasing C_4 (or vice versa) until a minimum signal is heard indicates that the break is at a point *c* such that the distance *ac* is to the distance *cb* as C_3 is to C_4.

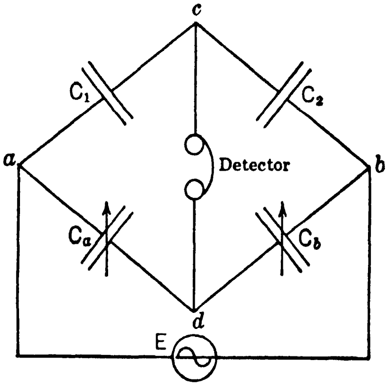

Fig. 510. Bridge circuit for determination of length of a broken wire.

683. EXPERIMENT 32-D. — Fault Location by the Capacitance Method. — The tests are described in §§681 and 682. For the points to be investigated, see §§675 and 678.

TRACING-CURRENT METHODS

684. The methods of fault location thus far described are based on a computation of the distance to the fault from one of the conductor ends. There is another group of methods in which a tracing current (signal current) is applied to the faulty cable at one end, and an observer actually follows the cable and measures the signal current, or listens for it with a telephone receiver tone test. At the fault there is a sudden change either in the intensity or in the direction of the signal current, and thus the fault may be located. The two methods may be conveniently combined; that is, a fault may be approximately located by a loop measurement, and then finally located by a signal current. The following three varieties of the tracing-current method require but simple apparatus and often lead to the location of a fault without much difficulty.

---

[6] For an application of this method to three-phase power cables, see L. Lewin, *Elektrotech. Zeitschrift*, vol. 42 (1921), p. 1132.

(a) *The sheath-potential method.* To locate a ground in a cable, a direct current of about 50 amperes is caused to flow from one of its ends to the fault, and back through the sheath and the earth. Near the fault, the sheath current is large and flows away from (or toward) the fault in both directions. With a millivoltmeter, observations are made on the potential gradient in the sheath. A reversal of polarity in adjacent manholes will indicate the faulty section of the cable.

(b) *The use of a magnetic needle.* This method consists in sending into the faulty cable a direct current, with interruptions of very low frequency, say once every two seconds. Observations are made with a pocket compass along the cable for the point at which the d-c magnetic field undergoes a sudden change, by reason of the escape of current through the fault. The current is interrupted periodically in order that the observer on the line may distinguish its field from that due to stray currents or other sources.

(c) *Metal shoes.* This device consists of a pair of metal-soled sandals worn by the observer and connected to a telephone receiver. An alternating current of audible frequency is applied between the faulty cable and the ground. An observer equipped with these sandals, and walking over the ground in the vicinity of a leak, will notice a noise in the telephone on account of the potential difference in the region near the fault. The device makes it possible to ascertain the direction and intensity of such stray currents, and, by following in the direction of the increasing intensity of sound, the source of the leakage can be found. On energized high-tension lines, ground potential gradients can attain a very considerable intensity, so that the observer must be on his guard lest he subject his body to a dangerous potential difference as he approaches the grounded point of the high-tension line.

685. Induction Localizers. — Three types of induction localizers are shown in Figs. 511 to 513. An alternating current of audible frequency is sent through the faulty conductor from a source whose other terminal is grounded. The current returns through the fault, the sheath, and the ground, to the source. The magnetic field due to this current is essentially in planes perpendicular to the axis of the cable, and the lines of force are linked with the conductor. Secondary currents are induced by this flux in an exploring coil, such as is shown in Fig. 511*a*, and a noise is heard in the telephone receiver. The character of the noise changes suddenly when the coil passes over the fault, since the magnitude of the current also changes.

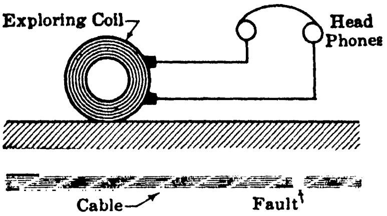

FIG. 511(*a*). Exploring coil used in fault location.

The device shown in Fig. 511*b* is a current transformer (§564) for which the faulty cable serves as a primary; the secondary winding is connected to a telephone receiver or an ammeter. The transformer core consists of two parts hinged together so that the device can be put on the cable at any place. The position of the fault is indicated by a change in the hum produced in the telephone receiver, or by a change in the ammeter current. The same device may be used for measuring alternating current in a cable, without opening its circuit.

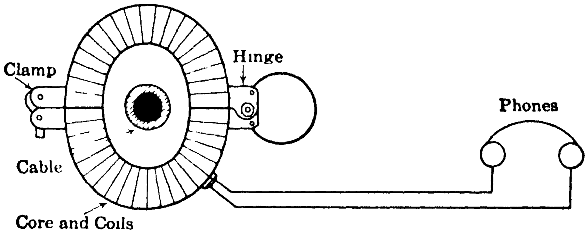

FIG. 511(*b*). Current transformer used for fault location.

Near a fault, the tracing current in a cable core and the return current in the sheath may produce practically equal and opposite mmf's in the surrounding space, so that, with the device shown in Fig. 511*a*, it may not be possible to locate a ground exactly. With three-phase cables, a longitudinal exploring coil (Fig. 512*a*) obviates this drawback. This method is based upon the fact that in a three-phase cable the conductors are given a "lay," that is, they are spiraled about the longitudinal axis of the cable. Therefore, the magnetic intensity due to an element of the conductor has a longitudinal as well as a transverse component. On the other hand, the mmf due to the sheath current lies entirely in transverse planes.

The core of the exploring coil is so placed that secondary currents can be induced in the telephone circuit only by the longitudinal field. Near the fault, on the side on which the signal current is generated, there are distinct regions of maximum and minimum noise, as the exploring coil is moved along the cable. Beyond the fault, the device is silent because the sheath current only is present and it produces no longitudinal field. Near the signaling apparatus the device is also silent because the return current covers a large ground area and its mmf masks the effect of the core "lay."

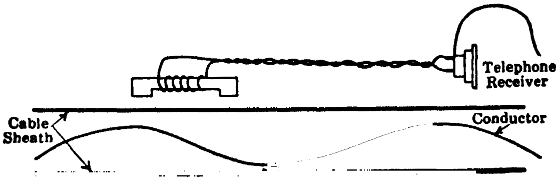

FIG. 512(*a*). A longitudinal exploring coil.

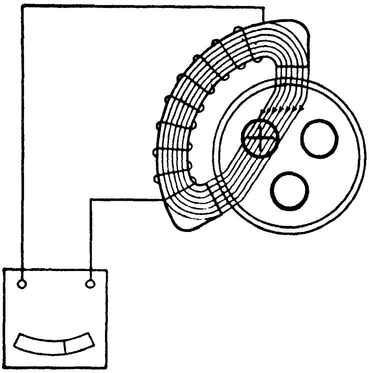

FIG. 512(*b*). Transformer with open magnetic circuit for fault location on a three-phase cable.

In high-voltage cables the insulation introduces a capacitive effect of relatively large magnitude (§§681 and 682). The signal current, being of rather high frequency, is mostly consumed in charging the cable, and only a small portion of it takes the path across the high-resistance fault. Consequently, there may be little or no distinction in the current in the exploring coil on the two sides of the fault, so that it is necessary to resort to some other method of fault location (§673).

The Lundin cable fault locater. Certain power companies[7] make use of the Lundin fault locater shown schematically in Fig. 513. This testing equipment includes, first, a step-up transformer of variable ratio for carbonizing the cable insulation at the fault by forcing a considerable current through it. This sometimes leads to the detection of the fault location (§672) without further testing. Second, the tester makes use of the principle of resonance by inserting a variable inductance in the line supplying the cable-ground circuit. The degree of resonance is revealed by a lamp across the a-c supply, greater resonance showing that the fault is of high resistance, and vice versa. Finally, an interrupter in the supply sends a signal along the cable which is picked up by a search coil and head phones to show the point of the fault. Thus the device serves several purposes and is largely relied upon by certain power companies in maintaining continuity of service on cable distribution lines.

---

[7] *Publication* A12, *Edison Electric Institute*, p. 13.

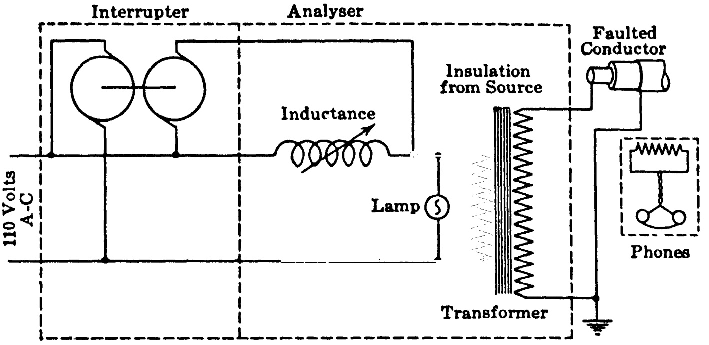

FIG. 513. Schematic diagram of the Lundin set.

686. Bullard's Method of Tracing Faults. — The principle of the method and the apparatus are shown in Fig. 514. A direct current is applied at one end of the cable, between the faulty conductor and the ground. This tracing current is made to magnetize the soft-iron field of a small hand-driven generator. The induced emf of this generator (which may be either d-c or a-c), owing to the ground leak, changes suddenly beyond the fault, thus locating it.

It has been found advisable to interrupt the tracing current periodically, say for one second, and to close the circuit for the next second. These interruptions have nothing to do with the method itself, but they help the observer to distinguish the signal current from the effect of possible stray currents, and from the current due to the residual magnetism of the field pieces. With this low frequency of interruptions, the capacitance effect, even in a large power cable, is negligible. Two separate methods for detecting the induced emf of the hand generator are shown in Fig. 514, namely, telephone receivers and a millivoltmeter.

(a) *Telephone receivers.* The generator itself has a two-segment commutator, and, when driven at a moderate rate by hand, gives a frequency of about thirty pulsations per second. The peaks of this emf are smoothed out by the condenser. Since the frequency of thirty pulsations per second is too low for good audibility, an interrupter, in the form of a buzzer operated by a small battery, Ba. 1, is used, to make and to break the telephone circuit.

The coil placed on the soft-iron core serves to neutralize residual magnetism or stray currents. This coil is excited from a small battery, Ba. 2, and the current is adjusted by means of the rheostat shown in the lower part of the diagram. By means of the coil and the rheostat, a flux passing through the field pieces of the instrument in either direction can be neutralized if constant.

The procedure is first to clamp the instrument around the cable and then to revolve the armature and listen for constant sound in the telephones. The rheostat is then adjusted for minimum constant sound.

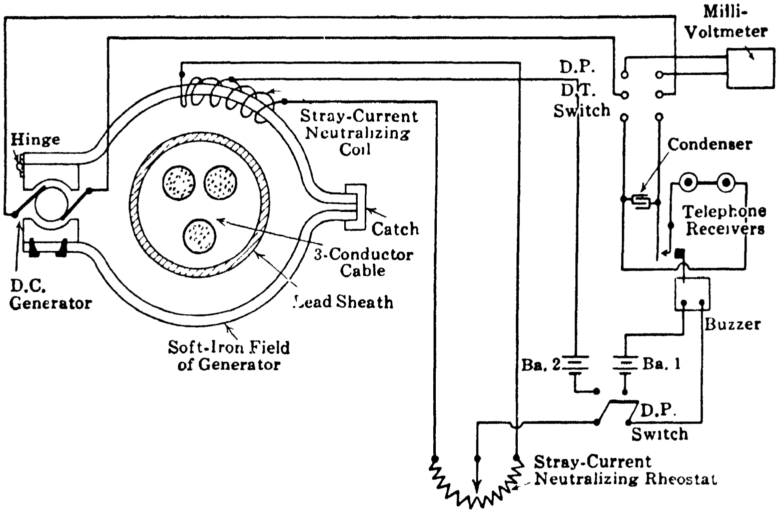

FIG. 514. Bullard's method of fault location.

As soon as this is done, the periodic rise and fall of sound due to the tracing current can be heard. It will be noted that the same switch which is used to open the buzzer circuit also opens the neutralizing coil circuit.

(b) *Millivoltmeter.* For a more accurate quantitative determination of the tracing current, a d-c millivoltmeter is used to give a true indication of the average unidirectional current. Disturbances produced by stray alternating fields, or stray alternating current in the sheath of the cable, are entirely eliminated. Furthermore, the swings of the needle, due to the periodic application of tracing current, give a fairly accurate indication of the amount of tracing current that flows through the cable.

The instrument is clamped around the cable, the armature then being revolved and the neutralizing rheostat adjusted until the minimum indication of the needle is in the neighborhood of zero (the center of the scale). Now, if the observer is between the point of application of tracing current and the fault, the needle of the millivoltmeter will periodically swing forward and back.

When the fault resistance is so high as to limit the tracing current to a small fraction of an ampere at ordinary voltages, and where it is practically impossible to reduce the resistance of the fault by burning it with a source of high potential, the fluctuations due to stray currents tend to drown out those due to the tracing current. However, the effects of stray currents can be considerably reduced by " tuning " the millivoltmeter to correspond with the period of the applied tracing current. The fluctuations caused by the stray currents are thereby minimized, while those caused by the tracing current are multiplied many times.

For this purpose the millivoltmeter must be devoid of all damping so that the moving element will swing freely with a natural period in the neighborhood of one or two seconds. A meter of this type can be readily constructed from an ordinary d'Arsonval type millivoltmeter by rewinding the moving element on a non-metallic frame to eliminate damping, and by adjusting the period of the instrument by changing the length of the spring or by moving adjustable weights toward or from the pivot.[8]

687. EXPERIMENT 32-E. — Fault Location by Tracing Signal Current. — Various tests of this kind are described in §§684 to 686. For points to be investigated see §§675 and 678.

A RESONANCE METHOD OF FAULT LOCATION

688. An ingenious method of locating faults on transmission lines — open circuits, short circuits or grounds — is described by J. E. Allen and G. J. Gross in *Edison Electric Institute Bulletin* for August, 1935.[9] This method consists in applying an essentially constant alternating emf of a frequency which is varied continuously from 1000 to 100,000 cycles, and recording the current input to the line as a function of the applied frequency, by means of a graphic ammeter. Figure 515 shows the circuit used by Allen and Gross. As the impressed frequency passes through certain critical values (points of resonance) the line impedance changes from a minimum to a maximum, repeatedly. The recording ammeter then gives peaks and nodes of input current as shown by the recorded curve in Fig. 516. From the frequency difference between these peaks (or nodes) the distance to the point of fault may be calculated from the general theory of the long line (Chapter XXX) on the basis of incident and reflected waves, since the portion of a transmission line of uniformly distributed constants which is either open-circuited or short-circuited will assume the characteristics of a line whose length is the distance from the sending end to the fault. This is due to the fact that there is reflection of current and voltage waves from a point where the line characteristics suddenly change.

---

[8] For further details see *Electrical World*, vol. 76, p. 1057, and vol. 86, p. 1297.

[9] See "Operating Guide for Central Station Men," *Electrical World*, 1937, pp. 38 and 41.

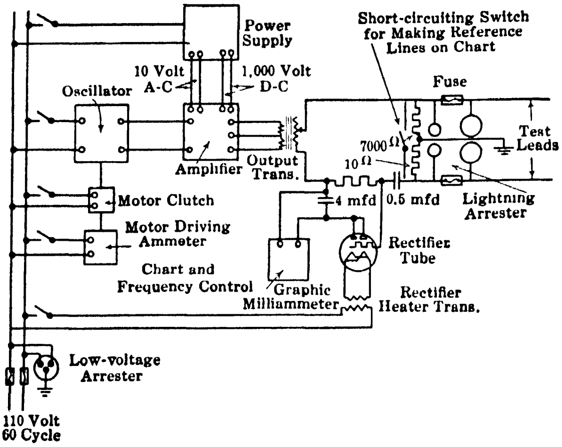

FIG. 515. Circuit diagram of the Allen and Gross fault locater.

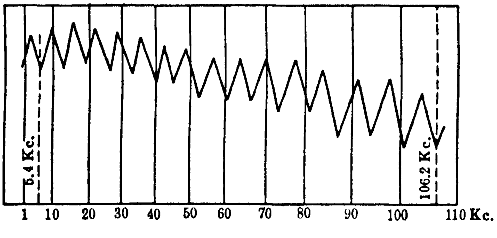

FIG. 516. Typical Allen and Gross chart.

689. Theory of Fault Location by Varying Frequency. — For a line having uniformly distributed constants, eqs. (30) and (31) in Chapter XXX give

$$E_1 = E \cosh l_g\sqrt{zy} + Z_0 I \sinh l_g\sqrt{zy} \quad . \; . \; . \; . \quad (30a)$$

$$I_1 = I \cosh l_g\sqrt{zy} + Y_0 E \sinh l_g\sqrt{zy} \quad . \; . \; . \; . \quad (30b)$$

In these equations E_1 and I_1 are the values of test voltage and current at the sending end, E and I are voltage and current at the point of the fault, l_g is distance in miles from sending end to fault, z and y are the series impedance and parallel admittance per mile of the line. α and β are the attenuation constant and wavelength constant, while Z_0 and Y_0 are the surge impedance and surge admittance, respectively.

If the line is short-circuited at the fault, $E = 0$, so that the sending-end impedance becomes

$$Z_{1s} = Z_0(\sinh l_g\sqrt{zy})/(\cosh l_g\sqrt{zy}) = \sqrt{z/y}\,\frac{\sinh l_g(\alpha + j\beta)}{\cosh l_g(\alpha + j\beta)} \quad . \; . \quad (31a)$$

$$= \sqrt{z/y}\,\frac{\sinh(\alpha l_g)\cos(\beta l_g) + j\cosh(\alpha l_g)\sin(\beta l_g)}{\cosh(\alpha l_g)\cos(\beta l_g) + j\sinh(\alpha l_g)\sin(\beta l_g)} \quad . \; . \; . \; . \quad (31b)$$

From eqs. (51a) and (52a) of Chapter XXX, and neglecting leakance

$$\alpha = \sqrt{b(z - x)/2} \quad . \; . \; . \; . \; . \; . \; . \; . \; . \quad (32)$$

$$\beta = \sqrt{b(z + x)/2} \quad . \; . \; . \; . \; . \; . \; . \; . \; . \quad (33)$$

where $z = \sqrt{r^2 + x^2}, = x + r^2/2x$, approximately,

$$b = \omega C, \quad \text{and} \quad x = \omega L \quad . \; . \; . \; . \; . \; . \; . \; . \; . \; . \; . \quad (34)$$

all values being per unit length of single line.

Making these substitutions in eqs. (32) and (33)

$$\alpha = \sqrt{r^2C/4L} \quad . \; . \; . \; . \; . \; . \; . \; . \; . \; . \; . \quad (35)$$

$$\beta = \sqrt{\omega^2LC + r^2C/4L} \quad . \; . \; . \; . \; . \; . \; . \; . \quad (36)$$

while $Z_0 = \sqrt{z/y} = \sqrt{x/b + r^2/2xb} = \sqrt{L/C + r^2/2\omega^2LC}$

$$= \sqrt{L/C}, \text{ approximately} \quad . \; . \; . \; . \; . \; . \; . \; . \; . \; . \; . \; . \; . \quad (37)$$

Substituting into eq. (31b)

$$Z_{1s} = \sqrt{L/C}\left[\frac{\sinh(l_g\sqrt{r^2C/4L})\cos(l_g\sqrt{\omega^2LC + r^2C/4L})}{\cosh(l_g\sqrt{r^2C/4L})\cos(l_g\sqrt{\omega^2LC + r^2C/4L})}\right.$$

$$\left.\frac{+\,j\cosh(l_g\sqrt{r^2C/4L})\sin(l_g\sqrt{\omega^2LC + r^2C/4L})}{+\,j\sinh(l_g\sqrt{r^2C/4L})\sin(l_g\sqrt{\omega^2LC + r^2C/4L})}\right] \quad . \; . \; . \quad (38)$$

In eq. (38) the quantity $\sqrt{r^2C/4L}$ is independent of frequency (constant). Call $\sinh(l_g\sqrt{r^2C/4L}) = A$, and $\cosh(l_g\sqrt{r^2C/4L}) = B$. In the case of the typical aerial line treated in §650, at the lowest test frequency of the oscillator, namely, at 1000 cycles, ω^2LC proves to be $11.8/10^4$, while $r^2C/4L = 4.86/10^8$, so that the latter can safely be ignored, particularly since at higher frequencies the smaller term becomes still less important. Dropping the term $r^2C/4L$ eq. (38) becomes

$$Z_{1s} = \sqrt{L/C}\,\frac{A\cos(l_g\omega\sqrt{LC}) + jB\sin(l_g\omega\sqrt{LC})}{B\cos(l_g\omega\sqrt{LC}) + jA\sin(l_g\omega\sqrt{LC})} \quad . \; . \; . \; . \; . \quad (39)$$

In the aerial line previously cited and for a length of line of 100 miles A and B have the values, respectively, of 0.022 and 1.00024, so that A is small compared with B. Examination of eq. (39) shows that Z_{1s} will have its maximum for values of $l_g\omega\sqrt{LC} = \pi/2, 3\pi 2$, etc., $= n\pi/2$, where n is any integer. It will have its minimum for values of $l_g\omega\sqrt{LC}$ of $0, \pi, 2\pi$, etc., $= n\pi$, where n is any integer (or zero).

By substitution of these values into eq. (39) it is seen that

$$\text{Min. } Z_{1s} = \sqrt{L/C}\;A/B \quad . \; . \; . \; . \; . \; . \; . \quad (40)$$

at a frequency

$$f_1 = n/4\sqrt{LC}\,l_g \quad . \; . \; . \; . \; . \; . \; . \; . \quad (40a)$$

while

$$\text{Max. } Z_{1s} = \sqrt{L/C}\;B/A \quad . \; . \; . \; . \; . \; . \; . \quad (41)$$

at a frequency

$$f_2 = n/2\sqrt{LC}\,l_g \quad . \; . \; . \; . \; . \; . \quad (41a)$$

Equations (40) and (41) ignore the effect of line resistance in the cos and sin terms which may readily be taken into account by substitutions into eq. (38) instead of the simpler eq. (39).

Line open-circuited. If the line is open-circuited at a distance l_g from the sending end, I will be equal to zero, and the sending-end impedance, as shown by eqs. (30a) and (30b), becomes

$$Z_{10} = E_1/I_1 = \cosh\,[l_g(\alpha + j\beta)\;/Y_0 \sinh l_g(\alpha + j\beta)] \quad . \; . \; . \; . \; . \quad (42)$$

$$= \sqrt{(r + j\omega L)/j\omega C}\left[\frac{\cosh\alpha\cos\beta + j\sinh\alpha\sin\beta}{\sinh\alpha\cos\beta + j\cosh\alpha\sin\beta}\right] \quad . \; . \; . \; . \quad (43)$$

$$= \sqrt{L/C}\left[\frac{B\cos(l_g\omega\sqrt{LC}) + jA\ \sin(l_g\sqrt{LC})}{A\ \cos(l_g\omega\sqrt{LC}) + jB\sin(l_g\omega\sqrt{LC})}\right]\text{(approx.)} \quad . \quad (44)$$

This impedance is a minimum, or the sending current a maximum, when $\cos(l_g\omega\sqrt{LC}) = 1$, or $l_g\omega\sqrt{LC} = n\pi$. Impedance is a maximum when $\sin(l_g\omega\sqrt{LC}) = 1$, or when $l_g\omega\sqrt{LC} = n\pi/2$. Substituting these values in eq. (44)

$$\text{Min. } Z_{10} = \sqrt{L/C}\,(B/A) \quad . \; . \; . \; . \; . \; . \; . \; . \quad (45)$$

at a frequency $f_1 = n/2\sqrt{LC}\,l_g$, or $l_g = n/2f_1\sqrt{LC}$ . . . (45a)

$$\text{Max. } Z_{10} = \sqrt{L/C}\,(A/B) \qquad (46)$$

at a frequency

$$f_2 = n/4\sqrt{LC}\,l_g \qquad (46a)$$

The velocity of propagation of electric current on a line, expressed in miles per second, is

$$V = 2\pi f/\beta = 2\pi f/\sqrt{\omega^2 LC + r^2 C/4L} = 1/\sqrt{LC} \text{ (approx.)} \qquad (47)$$

Substituting the values of L and C, taken from handbook tables, as applying to the line used in the previous examples, V is about 182,000 miles per sec. Substituting the value of V from eq. (47) into eq. (41a) for the short-circuited line, the distance to the fault is

$$l_g = nV/2f_1 = V/(2f_1/n) \qquad (48)$$

where f_1/n is the frequency difference between nodes of current on the recording chart. This frequency difference is best determined, according to Allen and Gross, by taking the difference between the frequencies for the last node and the first node on the chart and dividing by the number of nodes. If these frequencies are f_2'' and f_2'

$$l_g = \frac{V}{2(f_2'' - f_2')/n} \qquad (48a)$$

The same equation results if eq. (47) is substituted into eq. (45a), for the open-circuited line. It is possible to judge, however, whether the line is open-circuited or short-circuited by the values of the current peaks on a line which is free from faults and one which has a fault (Fig. 516).

690. EXPERIMENT 32-F.—Fault Location by the Method of Varying Frequencies.—The purpose of the experiment is to verify the method just described. For this purpose an artificial long line, well insulated, should be available, preferably the same line which was used in Exps. 30-B and 30-C.

(a) With the receiving end of the line open-circuited, make sure that the line is free from open circuit, short circuit, or ground faults (§§663 and 669).

(b) Assemble a suitable equipment, including a beat-frequency or other oscillator and amplifier, etc., somewhat as in Fig. 515 (see Chapter LIX), with a range of frequency of, say, 1000 cycles to 6000 cycles, with suitable control for continuous and fine adjustment.

(c) Open-circuit the line at a given point, say one-third the distance from the receiving end, and apply a constant potential at frequencies varying over as wide a range as the oscillator will permit — at least 4 to 1. Take readings of milliamperes input and of impressed frequency, and plot the curve of current against frequency (Fig. 516), making sure that the successive peaks and nodes of current are determined as accurately as possible.

(d) Take similar curves for the whole line, and for a small fraction of the line.

(e) Repeat the tests with the line grounded, or short-circuited at different points.

Report. Verify the correctness of the equations developed in §689, and determine the accuracy possible with the equipment; suggest changes in the apparatus or circuits to make such measurements commercially satisfactory.

REFERENCES

1. W. R. BULLARD, *Elec. World,* Nov. 27, 1920, p. 1057, Locating faults on underground cables.

2. J. F. BEEDLE, *Elec. World,* Oct. 1, 1921, p. 673, Improved practices make cable fault location more certain.

3. C. G. WATSON, *Elec. World,* June 21, 1924, p. 1286, Locating high-resistance faults in cables.

4. S. ARONOFF, *Elec. World,* Nov. 21, 1925, p. 1041, Locating circuit faults.

5. J. Urmston, *Jour. I.E.E.*, August, 1931, p. 983.

6. *Edison Electric Institute Pub.* A12, 1933, Fault location methods used on underground cable systems.

7. S. MATSUDA, *The Electrical Engineer's Note Book,* 1935, p. 123 (*Electrical World,* Pub.), Detector locates low-resistance open faults.

8. *Elec. Rev.* (London), vol. 119, p. 896, Dec. 25, 1936, Cambridge direct-reading fault localizers.

9. A. H. HARDEWYCK, *Elec. World,* vol. 107, p. 1096, March 27, 1937, Locate phase grounds with simple detector.

10. *Elec. World,* April 10, 1937, p. 1212, Transmission faults located accurately; telemetrograph.

11. R. C. R. SCHULZE, *Operating Guide Book for Central Station Men,* 1937, p. 50 (*Electrical World,* Pub.), Faults by quick graphics in neutral.

12. ALLEN and GROSS, *Operating Guide Book for Central Station Men,* 1937, p. 41 (*Electrical World,* Pub.), Accurate line fault location.

13. GILKESON, JEANNE, and DAVENPORT, *Elec. Eng'g,* vol. 56, p. 421, April, 1937, Characteristics of power system faults to ground.

14. *Leeds and Northrup Company Note Book* E–53–441, 1938, Notes on fault location in cables.

15. PENDER and DEL MAR, Electrical Engineer's Handbook, vol. IV, sec. 14, p. 223, John Wiley & Sons.

16. Standard Handbook for Electrical Engineers, Sixth Edition, sec. 3, art. 172, McGraw-Hill Book Co.

17. James A. Vahey, *Report of the Transmission and Distribution Committee of the Edison Electric Institute*, Feb. 8, 1939, Recent developments in cable fault location.

18. H. S. Hubbard, Mercury vapor tube rectifier for cable fault reduction and localization (Publication of the General Electric Company).

19. Morse and Newhall, *Elec. World*, Aug. 27, 1938, New cable fault locater, fast, convenient, accurate.

CHAPTER XXXIII

CURRENT AND VOLTAGE RELATIONS IN POLYPHASE Y-CONNECTED SYSTEMS

691. A polyphase electric circuit is a circuit energized by two or more alternating emf's of the same frequency, differing in time phase by a definite angle. In practice, the symmetrical three-phase system is used almost exclusively, and will therefore be considered first. In a few cases the two-phase system and the six-phase system are used.

The arrangement of the armature windings in a three-phase alternator, as shown in §440, is such that the three induced voltages differ from each other in phase by one-third of a cycle, or by 120 electrical degrees.

There are four principal ways in which the windings of a generator, motor, or transformer can be connected to form a three-phase system, namely:

(a) The Y-connection (Fig. 518).
(b) The delta (Δ)-connection (Fig. 553*a*).
(c) The V-connection (Fig. 553*b*).
(d) The T-connection (Fig. 553*c*).

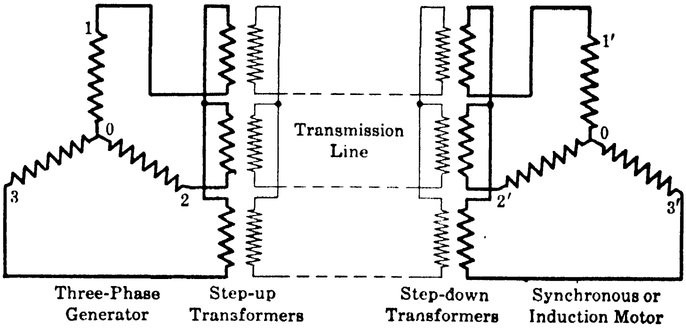

FIG. 517. Three-phase system.

692. Uses and Advantages of the Three-Phase System. — A three-phase power-transmission system is shown schematically in Fig. 517. Electric power is generated in the three-phase alternator shown at the left and driven by a steam turbine, gas engine, or water wheel. This power is stepped up to a higher voltage by means of three single-phase transformers (or a three-phase transformer) and is transmitted, over a line consisting of three conductors, to the receiver end, where it is stepped down to a lower voltage by means of similar transformers and is used for lighting, mechanical power, heating, etc. An a-c three-phase motor is shown, to indicate the conversion of the electrical into mechanical power.

It is of interest to enumerate briefly the advantages of the three-phase over the single-phase method of generation, distribution, and consumption of electrical energy.

Energy-consuming devices. The three-phase system has no advantages for lighting, power for which is distributed over the separate phases of a three-phase system. Three-phase electric motors are greatly superior to single-phase motors, in starting torque, in efficiency, in overload capacity, and in output per unit weight. This is one of the principal reasons for the universal adoption of the three-phase system for power transmission and distribution. For other applications, such as industrial heating and electric furnaces, the three-phase system has no serious disadvantages, except some duplication of apparatus and complication in switching.

Power generation. A three-phase generator is more efficient and weighs less per unit output than a single-phase machine, owing to the fact that in a three-phase armature the winding space is much better utilized. This is of unquestionable advantage, even though there is some additional complication in the switching equipment, transformers, etc.

Transmission. Since three-phase power is essential for motors, it is logical to transmit power in the three-phase form. In a comparison of the relative weights of line conductors, single-phase and three-phase, with the same minimum voltage, and at the same power loss (or with the same voltage drop), it was shown in §635 that the single-phase line requires 33 per cent more copper. This gives the three-phase line a distinct advantage even though the cost of extra insulators, cross-arms, line hardware, installation, maintenance, etc., must also be considered.

The purpose of the treatment in this and succeeding chapters is to acquaint the reader with the principal electric properties of, and measurements in, three-phase and two-phase circuits, with a brief mention of other polyphase systems.

Y-CONNECTED THREE-PHASE SYSTEM

693. Balanced Voltages and Balanced Load (Symmetrical System).— The simplest three-phase system has three equal phase voltages displaced with respect to each other by 120 electrical degrees (Fig. 519).

If the load impedances are also equal, then, for reasons of symmetry, the three currents will be equal to each other and their vectors will form an equilateral triangle. The voltage between the neutral points *O* and *N* (Fig. 518) is then zero, and the phase voltages with respect to either neutral are equal to each other. The voltage induced in the generator (or transformer) windings in each phase is entirely used up in that phase. The phase angle ϕ, between the current and the corresponding Y voltage, is determined by the ratio of the load reactance to the load resistance, as in a single-phase circuit. When the load is non-inductive, the current vectors are in phase with the corresponding Y voltages ($\phi = 0$).

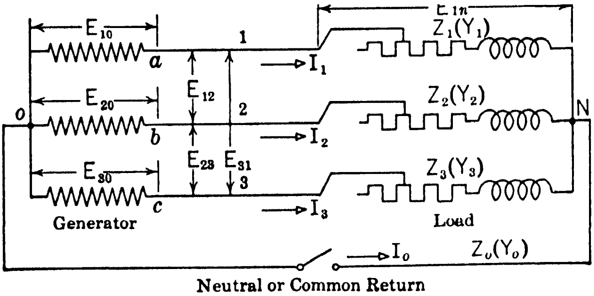

FIG. 518. A Y-connected generator and load (three-wire or four-wire system).

The geometric sum of the three line currents equals zero, so that the current in the neutral conductor and the voltage between its ends should be zero. In practice these conditions are difficult to realize, partly because the phase voltages or loads can hardly ever be perfectly balanced, and partly because the wave form of the actual voltages departs somewhat from the pure sine curve.

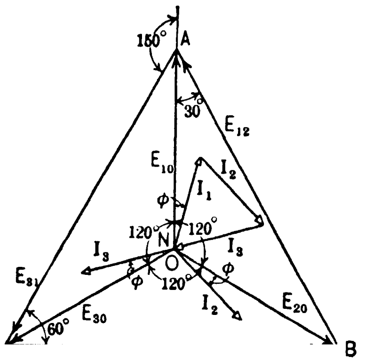

FIG. 519. Vector relations in a symmetrical three-phase system.

From Fig. 519 it will be seen that in a symmetrical three-phase system the ratio between the line voltage and the phase voltage is equal to the square root of three:

$$E_\Delta = E_Y \sqrt{3} \quad \ldots\ldots\ldots\ldots \quad (1)$$

Another important relationship is that, when $\phi = 0$, a current, say I_1, is in phase with its phase voltage, E_{10}, but not in phase with any of the line voltages. It will be seen from the vector diagram that for $\phi = 0$ the angles between I_1 and the line voltages are as follows:

I_1, E_{12}; 30° (current lagging)
I_1, E_{23}; 90° (current leading)
I_1, E_{31}; 150° (current lagging)

When there is a phase displacement, ϕ, between I_1 and E_{10}, the current lagging behind E_{10}, the foregoing three angles become $30° + \phi$, $90° - \phi$, and $150° + \phi$, respectively.

Since the current and voltage relationships in Fig. 519 are identically the same in all the three phases, it is sufficient in practical problems to make calculations in one phase only. In other words, the three branches in a balanced symmetrical three-phase system being identical (Fig. 518), one may deal with one branch only, for instance, *OaN*.

As an example, let a 220-kv three-phase line be designed to transmit 75,000 kw at a power loss of 5 per cent. The Y voltage is $220/\sqrt{3} =$ 127 kv, and the power transmitted per phase is 25,000 kw. Five per cent of this is 1250 kw. Thus, the given problem is identical with that of designing a single-conductor line for a voltage of 127 kv, to transmit 25,000 kw at a loss of 1250 kw.

694. EXPERIMENT 33-A. — Current and Voltage Relations in a Symmetrical and Balanced Y System. — The purpose of the experiment is to check the relations shown in Fig. 519. The general arrangement of apparatus is similar to that in Fig. 518. The induced Y voltages should be nearly sinusoidal.

(1) Show that at no load the ratio of the voltages satisfies eq. (1).

(2) Load the available source of supply on three equal non-inductive resistances, and adjust the three currents to be as nearly equal to each other as possible, making use of one of the polyphase boards described in §60.

(3) Show that the voltage between the neutral points is nearly equal to zero.

(4) Connect the two neutral points through an ammeter, and show that very little current flows through this connection, so that the currents in the three phases are hardly affected by closing and opening the neutral connection.

(5) By means of a wattmeter, check the angles between one of the currents and the three line voltages.

(6) Repeat some of the readings with a partly inductive balanced

load. When adjusting this load, use a wattmeter or a power-factor meter (§109) to facilitate the setting of the resistances and the reactances.

Report. Draw vector diagrams of the currents and voltages read; show how closely the observed data check with the theoretical relationships; explain possible causes of discrepancy, if any.

UNSYMMETRICAL, UNBALANCED Y SYSTEM

695. Current Notation. — The general case of a Y-connected armature winding and a Y-connected load, consisting of impedances, Z_1, Z_2, Z_3, is shown in Fig. 518. The voltages and currents are assumed to be sinusoidal, but for the sake of generality the three load impedances are assumed to be different from each other. In the neutral conductor a switch, S, is provided, which can be either open or closed, thus forming either a three-phase three-wire system, or a three-phase four-wire system. The three induced voltages, E_{10}, E_{20}, E_{30},[1] will be taken as differing from each other in magnitude and displaced in phase by different angles.

The effective values of the currents in the three phases are denoted by I_1, I_2, I_3. The current in the neutral is I_0. The corresponding instantaneous values are i_1, i_2, i_3, and i_0. *The arrowheads indicate the directions in which instantaneous values of currents are assumed to be positive.* This is different from the d-c notation, in which an arrowhead usually indicates the actual direction of current flow. With alternating currents such a notation would be meaningless, since at different instants a current flows in opposite directions. The arrowhead in phase 1, pointing from 0 to N, means that, at the instants at which the current actually flows from 0 to N, it is to be considered as positive in equations, and drawn above the axis of abscissas in graphs and oscillograms. This notation is purely arbitrary, but if strictly and consistently adhered to will avoid confusion and wrong results.

When denoting a current in more complicated diagrams of connections, it is advisable to use double subscripts. For example, the current I_1 should be denoted I_{01}, meaning that the current is considered as positive when it flows from 0 to 1. The subscript 0 is omitted in this chapter, where no ambiguity arises, but is used where it is necessary to distinguish between Y and delta currents (§744).

Let the switch S be open; then according, to the first Kirchhoff law, applied to the effective values of currents either at 0 or at N:

$$I_1 + I_2 + I_3 = 0 \quad . \; . \; . \; . \; . \; . \; . \; . \; . \quad (2)$$

---

[1] Read e-one-o, e-two-o, e-three-o.

In vector notations this means that the vectors of the currents form a closed triangle (Fig. 520).

When the switch S is closed, eq. (2) becomes:

$$I_1 + I_2 + I_3 + I_0 = 0 \quad . \; . \; . \; . \; . \; . \; . \; . \quad (3)$$

The corresponding polygon of vectors is shown in Fig. 520*b*. It will thus be seen that, with the current notation shown in Fig. 518, *the vectors of the Y currents always form a closed polygon.*

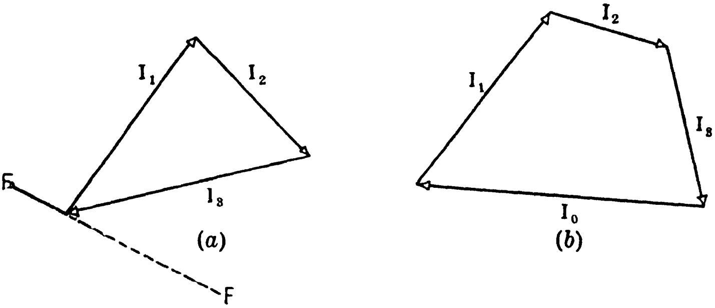

(*a*) (*b*)

FIG. 520. Vectors illustrating the application of the first Kirchhoff law in a three-phase system: (*a*) with the neutral open, (*b*) with the neutral closed.

696. Voltage Notation. — Two kinds of voltages are indicated in Fig. 518, the phase or Y voltages, E_{10}, E_{20}, E_{30}, and the line or delta voltages, E_{12}, E_{23}, E_{31}. The capital letters indicate the effective values (sometimes maximum values); the corresponding small letters denote instantaneous values. The following (arbitrary) convention is used here in regard to the subscripts: *The first subscript refers to the point that is at a higher potential when the instantaneous value is positive.* Thus, at the instants at which conductor 2 is actually positive electrically with respect to conductor 3, the value of e_{23} is considered to be positive. At instants when terminal 3 is at a higher potential than 2, the voltage e_{23} has a negative value. Transposing the subscripts reverses the sign of the voltage; in other words:

$$e_{mk} = -e_{km}, \quad \text{and} \quad E_{mk} = -E_{km} \quad . \; . \; . \; . \; . \quad (4)$$

where m and k are any two phase numbers. The foregoing notation, although arbitrary, is consistent, and, if strictly adhered to, will save many difficulties and mistakes. The double subscripts in currents have a different meaning and should not be confused with the voltage subscripts (§695).

At any instant, the voltage e_{10} indicates the amount by which the potential of point a (Fig. 518) is above that of point O. Similarly, e_{20}

gives the amount by which the potential at b is above that at O. Hence, at any instant:

$$e_{12} = e_{10} - e_{20} \quad \ldots \ldots \quad (5)$$

In terms of effective values and vectors

$$E_{12} = E_{10} - E_{20} \quad \ldots \ldots \quad (6)$$

For the other two phases we may write, by analogy:

$$E_{23} = E_{20} - E_{30} \quad \ldots \ldots \quad (7)$$

$$E_{31} = E_{30} - E_{10} \quad \ldots \ldots \quad (8)$$

Adding the three equations together gives:

$$E_{12} + E_{23} + E_{31} = 0 \quad \ldots \ldots \quad (9)$$

697. The Cyclic Order of Subscripts. — With a consistent notation in a polyphase circuit, a relationship obtained for one phase holds true for any other phase, if the subscripts are properly interchanged in the *cyclic order*. In a three-phase circuit this means a substitution of the subscripts in the order 1, 2, 3. For example, in the table in §693, advancing the subscripts by one, we find that the current I_2 lags behind the voltage E_{23} by 30 degrees. If the first relationship has been derived from a vector diagram and is correct, then the second relationship may be written directly, without any reference to the sketch. Similarly, advancing the subscripts by two places, we can say that the current I_3 lags behind the voltage E_{31} by 30 degrees and leads the voltage E_{12} by 90 degrees, etc.

This rule is convenient in checking relations and in obtaining new ones. Of course, the subscripts must be kept strictly in the original order, and a voltage that is originally written as E_{31} should not later be carelessly changed to E_{13}, unless its sign be also reversed. See eq. (4).

698. Solution for Currents in the Unbalanced Case. — In the unbalanced three-wire system the current in any phase may be calculated as follows: Applying the second Kirchhoff law to the circuit *bOaNb* (Fig. 518), namely, that the sum of the drops around a complete circuit equals the sum of the emf's, one may write

$$E_{12} = I_1Z_1 - I_2Z_2 \quad \ldots \ldots \quad (10)$$

Similarly, for the circuit *cObNc*

$$E_{23} = I_2Z_2 - I_3Z_3 \quad \ldots \ldots \quad (11)$$

Solving eqs. (2), (10), and (11),

$$I_1 = (E_{12}Z_3 - E_{31}Z_2)/(Z_1Z_2 + Z_2Z_3 + Z_3Z_1) \quad . \; . \; . \quad (12a)$$

$$I_2 = (E_{23}Z_1 - E_{12}Z_3)/(Z_1Z_2 + Z_2Z_3 + Z_3Z_1) \quad . \; . \; . \quad (12b)$$

$$I_3 = (E_{31}Z_2 - E_{23}Z_1)/(Z_1Z_2 + Z_2Z_3 + Z_3Z_1) \quad . \; . \; . \quad (12c)$$

In the four-wire case, with negligible resistance in the neutral wire the three currents are found as if there were three independent single-phase circuits.

Y load replaced by an equivalent delta.[2] The case of the unbalanced Y-connected load may be solved by replacing the Y-connected impedances, Z_1, Z_2, and Z_3, by the impedances which, if connected in delta across the same voltage supply, will pass the same total (line) currents at the same power factors. Calling the equivalent delta-connected impedances between lines 1 and 2, Z_{12}, etc., it may be shown that (see §748)

$$Z_{12} = (Z_1Z_2 + Z_2Z_3 + Z_3Z_1)/Z_3 = N/Z_3 \quad . \; . \; . \quad (13a)$$

$$Z_{23} = (Z_1Z_2 + Z_2Z_3 + Z_3Z_1)/Z_1 = N/Z_1 \quad . \; . \; . \quad (13b)$$

$$Z_{31} = (Z_1Z_2 + Z_2Z_3 + Z_3Z_1)/Z_2 = N/Z_2 \quad . \; . \; . \quad (13c)$$

By calculating the delta currents through these equivalent impedances, due to corresponding line voltages, and combining two currents which meet at a given terminal, the line current is found. Thus:

$$I_{12} = E_{12}/Z_{12} \quad . \; . \; . \; . \; . \; . \; . \; . \; . \; . \; . \; . \; . \; . \; . \; . \quad (14a)$$

$$I_{23} = E_{23}/Z_{23} \quad . \; . \; . \; . \; . \; . \; . \; . \; . \; . \; . \; . \; . \; . \; . \; . \; . \quad (14b)$$

$$\begin{aligned} I_2 &= I_{23} - I_{12} = E_{23}/Z_{23} - E_{12}/Z_{12} \\ &= (E_{23}Z_1 - E_{12}Z_3)/(Z_1Z_2 + Z_2Z_3 + Z_3Z_1) \quad . \; . \; . \quad (12b) \end{aligned}$$

Similarly eqs. (12*a*) and (12*c*) are obtained, showing that the " delta " of impedances given by eqs. (13) is truly equivalent to the original " star " load.

699. EXPERIMENT 33-B. — Current and Voltage Relations in an Unsymmetrical Y-Connected Three-Phase System. — The purpose of the experiment is to illustrate the general relations explained in the preceding section. With an arbitrary unsymmetrical system no time is spent in carefully balancing the voltages and the load. The measurements may be performed by connecting some three impedances in Y to an available three-phase power supply, if its neutral point is accessible. Otherwise Y-connected transformers may be used for obtaining a neutral point (Fig. 517). A separate alternator, the windings of which can be connected at will, may also be used. To obtain unsymmetrical induced voltages, connections can be made to different taps on transformer or armature windings. Be sure to have the phase voltages as nearly sinusoidal as possible, because otherwise complicated secondary phenomena, due to higher harmonics, will take place. Instead of connecting an ammeter in each of the four conductors (Fig. 518), a polyphase board may be used (§60) with only one ammeter. One voltmeter with a suitable multipoint switch or voltage board is also sufficient.

---

[2] R. R. Lawrence, " Principles of Alternating Currents," Second Edition, Chapter X, McGraw-Hill Book Co.

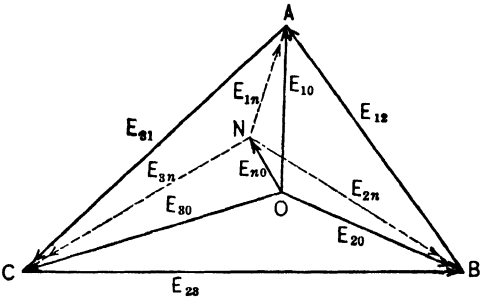

FIG. 521. The Y and delta voltages in an unsymmetrical three-phase system.

(1) Select three different impedances and connect them to the source of power, which should preferably have unsymmetrical voltages. Omit the neutral conductor. Having adjusted the currents and the voltages to the desired values, read the three currents and the ten voltages shown in Fig. 521.

(2) Determine the phase angles of the three currents with respect to some reference voltage, for example by using a wattmeter, an oscillograph, or by some other means. Be sure that there is no ambiguity about the sign of the angle, since $\cos \phi = \cos(-\phi)$.

(3) Connect a neutral conductor of negligible impedance and repeat the readings.

(4) Connect an appreciable impedance in the return conductor and again take readings.

(5) With conditions as in (1) interchange two of the supply leads and repeat (1) and (2).

Report. (1) Draw the triangle *ABC* of line voltages (Fig. 521). With the values of E_{10}, E_{20}, E_{30} as radii, describe arcs of circles from *A*, *B*, and *C*, respectively. The three arcs should intersect in one point, which is point *O*. (2) In a similar manner, find the point *N* and check the measured voltage *ON*. (3) Compute the phase angles between the currents and the reference voltage and draw the vector diagrams shown in Fig. 520. If the magnitudes of the currents and the phase angles were read and plotted correctly, both figures should be closed polygons. (4) Transfer the current vectors to the vector diagram of the voltages, in their proper phase position, so as to get a complete picture of the conditions in the circuit. (5) Calculate the impedances Z_1, etc., from the readings of amperes, volts, and watts in each leg of the load, and substitute in eqs. (12), (13), and (14). Solve for the three currents in the unbalanced three-wire case and compare these values with those actually read. Note the effect of reversed phase sequence.

700. Methods of Determining Phase Sequence or Phase Rotation.— In Fig. 519, the voltage in phase 1 is shown leading that in phase 2, and lagging behind that in phase 3. This is determined by the arrangement of the armature windings. Usually, the armature windings are inaccessible, and if the *phase sequence* of voltages in a given installation is required, it must be deduced from some observed electrical relationship between the line terminals, as by the following means:

(a) The *revolving field* in an induction motor moves from a leading to a lagging phase (§484). Therefore, a small induction motor, with a known arrangement of windings, connected to the three line terminals under test, will determine the phase sequence. Phase-sequence meters built on this principle are available. The direction of rotation of a disk shows the order of phase sequence with reference to the meter terminals, A, B, and C.

(b) *Comparison of wattmeter readings.* If a small, balanced, and partly inductive load, such as that provided by a small three-phase induction motor (Chapter XXII), is measured by the two-wattmeter method (§106), one meter reading will be $EI \cos (\theta + 30°)$, while the other reading will be $EI \cos (\theta - 30°)$. At power factors less than unity (and more than zero) one reading will be larger than the other. The phase current of the larger reading leads that of the smaller.

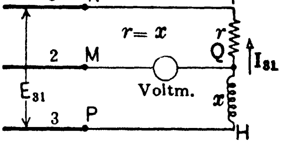

FIG. 522. Test for phase sequence by means of a single-phase load.

(c) *Single-phase load* (Fig. 522). Let 1, 2, 3 be the line terminals at which it is desired to determine the phase sequence. Apply a single-phase load FH, and connect a voltmeter between the points M and Q. The resistance, r, and the reactance, x, are so selected as to satisfy the condition $x = r$ as nearly as possible and should be much lower in value than the voltmeter resistance. Assuming the phase sequence of the voltages to be according to Fig. 519, the load current, I_{31}, has the phase position shown in Fig. 523a. The current then lags by 45 degrees with respect to the voltage E_{31}; the voltage drop in r is represented by AD, and that in x by DC. A voltmeter applied between the points M and Q (Fig. 522) will read the voltage DB (Fig. 523*a*). From the geometry of the figure, for the absolute value of BD, we have:

$$BD = BB' + B'D = 0.5\sqrt{3}E_{31} - 0.5E_{31} = 1.366E_{31} \quad . \quad .(15a)$$

Should the voltmeter actually read somewhere near this value, the assumed phase sequence is correct and E_{31} leads E_{12}. If, however, the actual phase sequence is according to Fig. 523*b*, with the phases 2 and 3 reversed, the vector BD is much smaller, and the voltmeter will read:

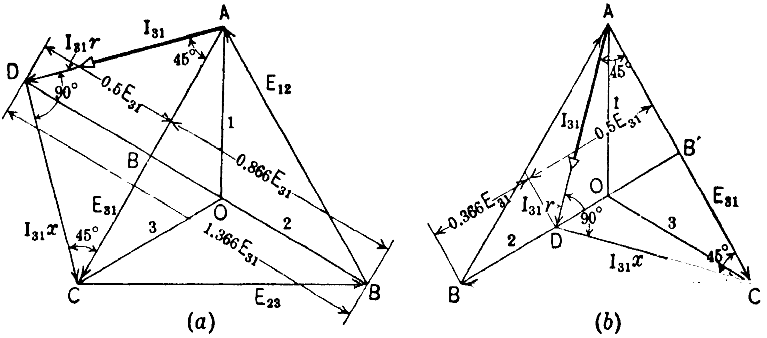

FIG 523. Vector relations in the circuit of Fig. 522.

$$BD = BB' - DB' = 0.5\sqrt{3}E_{31} - 0.5E_{31} = 0.366E_{31} \quad . \quad .(15b)$$

(d) *A semi-balanced three-phase load,* shown in Fig. 524, consists of two equal resistances, r, and a reactance, x. The voltage between terminal 1 and the neutral point N is higher than that between 3 and N, when the phase sequence is as shown in Fig. 523*a*, i.e., when E_{12} leads E_{23} and lags E_{31}. With the phase sequence indicated in Fig. 523*b*, the voltage E_{3N} is higher than E_{1N}. In practice, two equal incandescent lamps of the same rated voltage and wattage are employed for resistances, r, and a highly inductive coil for the reactance, x;. for example, one used in the potential circuit of an induction watthour meter (§126). One lamp then glows brighter than the other. The arrangement can be tried first on a circuit of known phase sequence, and then used on any other circuit. A theoretical deduction of the relative values of the two lamp voltages is given in §706.[3]

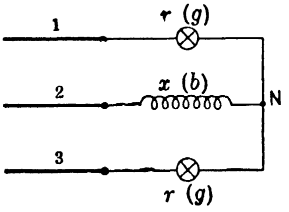

FIG. 524. Test for phase sequence by means of a semi-balanced load.

---

[3] See also J. Auchincloss, *Electrical World*, vol. 86 (1925), p. 420.

(e) *A phase-sequence component voltmeter* (§720) may be used. Since in practice the three line voltages are nearly balanced, the indication for one phase sequence will be much higher than that for the opposite one, and the predominant sequence is thus found.

(f) If an *oscillograph* with three vibrating elements is available (Chapter LVII) the waves of the three voltages (or currents) can be thrown on the tracing table, or photographed, thus showing their time sequence.

701. EXPERIMENT 33-C. — Determination of the Phase Sequence in a Three-Phase System. — Several methods are described in the preceding section. It is desired to determine the order of phase rotation in a given three-phase system. It is advisable to have the alternator windings accessible, or at least the winding diagram given, so as to be able to check the results directly. The methods indicated in §700 may be tried with and without instrument transformers (Chapter XVIII). Then the student should endeavor to devise a method of his own, or find one in the literature of the subject.[4]

UNBALANCED Y SYSTEM; NEUTRAL-VOLTAGE METHOD

702. When the voltages in a three-phase system are unsymmetrical, or the load is unbalanced, a theoretical determination of the line currents offers some difficulties. Although it is always possible to solve the problem by writing down Kirchhoff's laws for the network and solving a number of simultaneous equations (§698), certain practical methods have been developed, based on these equations, which save time and computations. Some of these methods are described below and also in the next chapter.

Let the three-phase voltages, E_{10}, E_{20}, E_{30} (Fig. 518), of a generator or of a bank of transformers be given, and let the magnitude and the phase position of the vectors of these voltages be constant, that is, independent of the load. Let the load be given by means of its three impedances, Z_1, Z_2, Z_3 (or admittances Y_1, Y_2, Y_3), and let it be required to find the vectors of the three currents. We shall first assume at least one of the neutral points to be insulated from the ground, in other words, the switch S open.

Let the three generator voltages be those shown in Fig. 521, and let E_{n0} be the unknown voltage between the two neutral points. Then, according to §696, the vectors of the three load voltages are those radiating from point N in Fig. 521, and may be written

---

[4] See G. Kapp, *Institution of Electrical Engineers* (British) *Journal*, vol. 55 (1917), p. 309.

$$\begin{aligned} E_{1n} &= E_{10} - E_{n0} \\ E_{2n} &= E_{20} - E_{n0} \\ E_{3n} &= E_{30} - E_{n0} \end{aligned} \quad \ldots\ldots\ldots \quad (16)$$

Each of these, multiplied by the corresponding admittance, will give the current in that phase; that is, vectorially,

$$E_{1n}Y_1 = I_1; \quad E_{2n}Y_2 = I_2; \quad E_{3n}Y_3 = I_3 \quad \ldots\ldots \quad (17)$$

To multiply an E by Y means to multiply the vector E by a scalar y and to turn the resultant vector by the angle corresponding to Y. In other words, all the symbols are understood to be expressed as complex quantities.[5] Substituting for the three load voltages their expressions from eqs. (12), we get:

$$(E_{10} - E_{n0})Y_1 = I_1; \quad (E_{20} - E_{n0})Y_2 = I_2; \quad (E_{30} - E_{n0})Y_3 = I_3 \quad (18)$$

But, according to the first Kirchhoff law, $\Sigma I = 0$. Therefore, adding the three eqs. (18), term by term, gives:

$$E_{10}Y_1 + E_{20}Y_2 + E_{30}Y_3 - E_{n0}(Y_1 + Y_2 + Y_3) = 0 \quad \ldots \quad (19)$$

or, solving for E_{n0},

$$E_{n0} = (E_{10}Y_1 + E_{20}Y_2 + E_{30}Y_3)/(Y_1 + Y_2 + Y_3) \quad \ldots \quad (20)$$

This equation may be written more briefly as:

$$E_{n0} = \Sigma EY/\Sigma Y \quad \ldots\ldots\ldots \quad (21)$$

E_{n0} having been determined from eq. (20), the vectors of the three load currents can be computed (or constructed graphically) from eqs. (18).

The preceding theory can be extended to any number of phases, so that eq. (21) holds true quite generally. In particular, if there is a return conductor of admittance Y_0 (switch S closed in Fig. 518), this conductor may be considered as the fourth phase, in which the generator voltage is zero and the load admittance is Y_0. Hence, in this case eq. (20) becomes:

$$E_{n0} = (E_{10}Y_1 + E_{20}Y_2 + E_{30}Y_3)/(Y_1 + Y_2 + Y_3 + Y_0) \quad \ldots \quad (22)$$

In addition to eqs. (18), we have for the return current I_0:

$$-E_{n0}Y_0 = I_0 \quad \ldots\ldots\ldots \quad (23)$$

If both neutrals are well grounded so that the admittance Y_0 is infinitely great, eq. (22) gives $E_{n0} = 0$. Equation (23) in this case becomes indefinite, and the return current has to be computed from the equation:

---

[5] For the theory and use of complex quantities in electrical problems, see, among other sources, V. Karapetoff's "Electric Circuit," Chapters VIII and IX.

$$I_1 + I_2 + I_3 + I_0 = 0 \quad . \quad . \quad . \quad . \quad . \quad . \quad . \quad . \quad (24)$$

where the first three currents are determined from eqs. (18). For some examples of the use of this method, see §§705 and 706.

The voltage E_{n0} in eq. (21) becomes infinitely great when $\Sigma Y = 0$. This is possible when one or two of the Y's are negative, that is, when the corresponding phases contain capacitance. We then have a case of three-phase resonance (§609) with large currents. The condition $\Sigma Y = 0$ may obtain for one of the higher harmonics of voltage so that pronounced resonance currents and voltages may be of a higher frequency.[6]

703. Methods Based on the Principle of Superposition.—An unbalanced Y-system may also be solved for currents by using the principle of superposition, according to which the actual instantaneous current in a conductor is equal to the algebraic sum of the partial currents in the same conductor, due to the individual applied voltages or their combinations. A similar relationship holds true geometrically for the corresponding vectors. For example, in Fig. 518, the current I_1 may be determined as follows: Assume the voltages E_{20} and E_{30} to be equal to zero. This will give a single-phase system in which the impedance Z_1 is in series with the parallel combination of Z_2 and Z_3. The current I_1' in conductor 1, due to the voltage E_{10}, can be readily determined. Then let the voltages E_{10} and E_{30} be equal to zero and determine the current I_1'' in conductor 1 due to the voltage E_{20}. Finally, put $E_{10} = E_{20} = 0$, and determine the current I_1''' in conductor 1 due to the voltage E_{30}. The actual current I_1, when all the three voltages are applied simultaneously, is equal to the geometric sum of the partial currents; that is,

$$I_1 = I_1' + I_1'' + I_1''' \quad . \quad . \quad . \quad . \quad . \quad . \quad . \quad . \quad (25)$$

The principle of superposition holds strictly true only when there are no saturated magnetic cores, and follows directly from the linear form of the equations that express Kirchhoff's laws. For example, the second Kirchhoff law for the instantaneous values in the circuit comprising phases 1 and 2 (Fig. 518) is:

$$r_1 i_1 - r_2 i_2 + L_1\, di_1/dt - L_2\, di_2/dt = E_{10} \sin \omega t - E_{20} \sin (\omega t - \alpha) \quad (26)$$

where $\omega = 2\pi f$, and α is the time-phase angle between E_{10} and E_{20}.

---

[6] The neutral-voltage method, described above, was first given by V. Karapetoff in 1900 in a pamphlet entitled *Ueber Mehrphasige Stromsysteme bei ungleichmaessiger Belastung* (Enke, Stuttgart). See also *Elektrot. Zeitschr.*, vol. 39 (1918), pp. 245 and 256.

Two similar equations may be written for the circuits 1-3 and 2-3. Let $E_{20} = E_{30} = 0$, and determine the sinusoidal functions, i_1', i_2', i_3', which satisfy these equations. Then put $E_{10} = E_{30} = 0$ and again determine sinusoidal functions, i_1'', i_2'', i_3'', which satisfy these equations. It will be seen that the sums, $(i_1' + i_1'')$, $(i_2' + i_2'')$, and $(i_3' + i_3'')$, also satisfy eq. (26), because each term $(ri + L\,di/dt)$ will cancel with the corresponding voltage term on the right-hand side, *there being no products or other combinations of the i's except their sums and derivatives.*

Three different combinations of partial voltages suggest themselves for a solution of an unbalanced Y-connected network on the principle of superposition, namely:

(a) The use of the individual star voltages, as explained above; this method is somewhat tedious.

(b) The superposition of the reverse neutral voltage, E_{n0}, explained in the next section. This method is equivalent to that described in §702.

(c) The resolution of the given system of voltages into two symmetrical components of opposite phase sequence (Chapter XXXIV).

704. Superposition of a Reverse Neutral Voltage. — Let it be required to solve the network given in Fig. 518 by the method of superposition. For the sake of generality, let the switch S be closed, and the impedance of the return conductor not be negligible. Imagine a *fifth conductor* of zero impedance between the points O and N, and let this conductor contain a source of sinusoidal voltage of the same frequency as the three applied voltages, and of such a magnitude and phase position as to be equal and opposite at every instant to the *actual* voltage between the points O and N. In other words, let the new voltage be $-E_{n0}$. Under these conditions no current can flow through the fifth conductor, and the new system is absolutely equivalent to the given network.

Now let us determine (1) the currents I' due to the three applied voltages, with the new voltage equal to zero and the zero impedance conductor present, and (2) the currents I'' due only to the applied emf, $-E_{n0}$, in the new conductor, with $E_{10} = E_{20} = E_{30} = 0$. According to the principle of superposition (§703), the actual current in any conductor is then equal to the geometric sum of the two partial currents, I' and I''. With the assumption (1), the fifth conductor simply acts as a short circuit between the two neutral points, so that the partial current in the fourth conductor is equal to zero ($I_0' = 0$), and the current in phase 1 is:

$$I_1' = E_{10}Y_1 \quad \ldots\ldots\ldots\ldots \quad (27)$$

The current in the fifth conductor is:

$$I_n = \Sigma I' = \Sigma EY \quad \ldots \quad (28)$$

With the assumption (2), the partial current in phase 1 is:

$$I_1'' = -E_{n0}Y_1 \quad \ldots \quad (29)$$

while the neutral current is:

$$I_0'' = -E_{n0}Y_0 \quad \ldots \quad (30)$$

Hence the total or actual current in phase 1 is

$$I_1 = I_1' + I_1'' = (E_{10} - E_{n0})Y_1 \quad \ldots \quad (31)$$

This agrees with eqs. (18), so that E_{n0} is determined by eq. (21). Consequently, eq. (29) may be written in the form:

$$I_1'' = -I_n(Y_1/\Sigma Y) \quad \ldots \quad (32)$$

and eq. (31) becomes:

$$I_1 = I_1' - I_n(Y_1/\Sigma Y) \quad \ldots \quad (33)$$

The last two equations are convenient in applications.

705. A Graphical Example of the Use of the Neutral-Voltage Method. — In order to illustrate the theory given in §§702 to 704, we shall solve two examples: one is solved graphically in this section and another analytically in the next section.

In Fig. 525, E_{10}, E_{20}, E_{30} are three given unsymmetrical generator Y voltages. If the line voltages are given instead, that is, if the triangle connecting the points A_1, A_2, A_3 is given, then we can select an arbitrary neutral point, O (§696), and thus obtain a set of Y voltages. With any position of O, and with the same triangle $A_1A_2A_3$, the final result for the line currents will be the same. The neutral conductor will be supposed to be open or absent, and the three load admittances given graphically as Y_1, Y_2, Y_3 in the polygon $xfgh$. Each admittance is characterized by its numerical value (length) and by the angle ϕ which it makes with the reference axis xx'. The admittance Y_2 is assumed to contain some capacitance, the angle ϕ_2 being of the opposite sign from that of ϕ_1 and ϕ_3.

To find the three currents, we shall use eq. (33), and determine separately the currents I' and I''. The current I_1', eq. (27), is obtained by multiplying the vector E_{10} by the numerical value of the admittance Y_1, and turning the resulting vector back (clockwise) by the angle ϕ_1. With a convenient radius $Oa_1 = r$ we describe a circle, lay off $Od_1 = xf = Y_1$, at an angle ϕ_1 to E_{10} in the lagging direction, and draw A_1D_1

parallel to a_1d_1. From the similar triangles, we have:

$$OD_1/y_1 = E_{10}/r \tag{34}$$

where y_1 is the scalar value of the admittance Y_1. Hence:

$$r \cdot OD_1 = E_{10}y_1 \tag{34a}$$

If this expression is compared with eq. (27), it will be seen that OD_1 is proportional to the current I_1'. The scale depends on the chosen value of r. In this manner the three currents, OD_1, OD_2, and OD_3, are obtained.

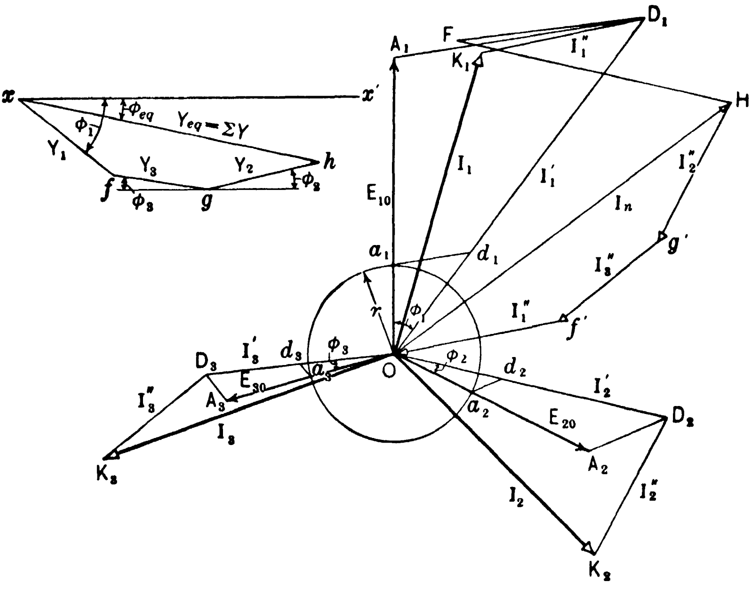

FIG. 525. Graphical determination of currents in an unsymmetrical Y-connected network, by superposition of the neutral voltage.

In order to determine the currents I'', it is first necessary to construct the current vector I_n. According to eq. (28), I_n is equal to the geometric sum of the currents I'. Hence, we draw D_1F equal and parallel to OD_3, and FH equal and parallel to OD_2. The resultant, OH, is then equal to I_n. It remains to subdivide I_n into the three components proportional to the admittances Y, eq. (32). For this purpose, on OH we draw the figure $Of'g'H$, geometrically similar to $xfgh$. This gives the required component currents I'' in their magnitude and phase position. The arrowheads on these components are shown in the opposite direction from that on OH, because of the minus sign in eq. (32). It remains to add the component currents I' and I'' geometrically in each phase. From D_1 we draw a vector D_1K_1, equal and parallel to $f'O$. This gives point K_1, and the total current is $OK_1 = I_1$. The currents OK_2 and OK_3 are obtained in a similar manner. Their geometric sum is equal to zero, and this is a check on the construction.

706. An Analytical Example of the Use of the Neutral-Voltage Method. — As a second example we shall consider the voltage relationships in the phasing-out device shown in Fig. 524 and described in §700d. Let this device constitute the load in Fig. 518, and let it be required to determine (a) whether the lamp in the leading phase or in the lagging phase glows brighter, and (b) the ratio of the lamp resistance, r, to the reactance, x, for which the difference in the brightness of the two lamps is a maximum. The return connection is supposed to be open, and the phase sequence to be according to Fig. 519. We shall first determine the value of the neutral voltage E_{n0}, according to eq. (20).

By vectorial methods, a knowledge of which is here assumed, the solution of the problem is as follows:

Assuming positive phase sequence (see Chapter XXXIV), the symmetrical voltages to the neutral of the generator may be written

$$E_{10} = E/\underline{0^\circ}, \quad E_{20} = E/\underline{-120^\circ}, \quad \text{and} \quad E_{30} = E/\underline{120^\circ} \quad . \; . \quad (35)$$

The admittances in the three lines are

$$Y_1 = g/\underline{0^\circ}, \quad Y_2 = b/\underline{-90^\circ}, \quad \text{and} \quad Y_3 = g/\underline{0^\circ} \quad . \; . \; . \quad (36)$$

where g is the lamp conductance and b is the susceptance of the choke coil (neglecting its resistance).

Substituting the values from eqs. (35) and (36) in eq. (20)

$$\begin{aligned} E_{n0} &= \frac{Eg/\underline{0^\circ} + E/\underline{-120^\circ}\, b/\underline{-90^\circ} + E/\underline{120^\circ}\, g/\underline{0^\circ}}{2g - jb} \\ &= \frac{Eg/\underline{60^\circ} - Eb/\underline{-30^\circ}}{2g - jb} \\ &= E\,\frac{g(0.5 + j0.866) - b(0.866 - j0.5)}{2g - jb} \quad . \; . \; . \quad (37) \end{aligned}$$

Then

$$\begin{aligned} E_{1n} &= E_{10} - E_{n0} \\ &= E\,\frac{2g + b/\underline{-90^\circ} - g/\underline{60^\circ} + b/\underline{-30^\circ}}{2g - jb} \\ &= \sqrt{3}E\,\frac{g/\underline{-30^\circ} + b/\underline{-60^\circ}}{2g - jb} \\ &= \sqrt{3}E\,\frac{/\underline{30^\circ}g + b/\underline{-30^\circ}}{2g - jb} \quad . \; . \; . \; . \; . \; . \; . \; . \; . \quad (38) \end{aligned}$$

Numerically
$$|E_{1n}| = \sqrt{3}E\frac{\sqrt{g^2 + b^2 + 1.73gb}}{\sqrt{4g^2 + b^2}} \quad . \; . \; . \; . \; . \; . \; . \; . \; . \tag{39}$$

Similarly
$$\begin{aligned} E_{3n} &= E_{30} - E_{n0} \\ &= \frac{E\angle 120^\circ(2g + b\angle -90^\circ - g\angle 60^\circ + b\angle -30^\circ}{2g - jb} \qquad (40) \\ &= \sqrt{3}E\frac{g\angle 150^\circ + b\angle 0^\circ}{2g - jb} \end{aligned}$$

Numerically
$$|E_{3n}| = \sqrt{3}E\frac{\sqrt{g^2 + b^2 - 1.73gb}}{\sqrt{4g^2 + b^2}} \quad . \; . \; . \; . \; . \; . \; . \; . \; . \tag{42}$$

A comparison of eqs. (39) and (42) shows that the voltage across the lamp in the *lagging* phase is the higher. This lamp, therefore, will glow more brightly, thus identifying the phase rotation.

Equations (39) and (42) may be written[7]

$$|E_{1n}| = \sqrt{3}E\frac{\sqrt{r^2 + x^2 + 1.73rx}}{\sqrt{r^2 + 4x^2}} \quad . \; . \; . \; . \; . \tag{39a}$$

$$|E_{3n}| = \sqrt{3}E\frac{\sqrt{r^2 + x^2 - 1.73rx}}{\sqrt{r^2 + 4x^2}} \quad . \; . \; . \; . \; . \tag{42a}$$

On the assumption that the greatest difference in brightness of the lamps will occur when the numerical difference between the voltages is greatest, or

$$|E_{1n}| - |E_{3n}| = \sqrt{3}E\frac{\sqrt{g^2 + b^2 + 1.73gb} - \sqrt{g^2 + b^2 - 1.73gb}}{\sqrt{4g^2 + b^2}} \quad . \; . \tag{43}$$

is a maximum. This may be determined either by differentiating eq. (43) or by substituting various values of b(or x) into eqs. (39) and (42) or eqs. (39*a*) and (42*a*), holding g (or r) constant, and plotting curves. Such curves, shown in Fig. 526, indicate that the greatest difference exists between the voltages across the lamps when $x = 0.8r$ (approximately). By differentiation of eq. (43), squared, in order to secure simpler forms with which to work, it is found that $b = \sqrt{8/5}\,g$, or $x = \sqrt{5/8}\,r$ for the greatest difference $E_{1n} - E_{3n}$.

---

[7] A solution of this problem involving similar equations was submitted to the authors by Harry Silk, of Newark University, in 1929.

707. EXPERIMENT 33-D. — Study of an Unbalanced Y System by the Neutral-Voltage Method. — The purpose of the experiment is to make clear the theoretical relations deduced in §§702 to 706. The general diagram of connections is shown in Fig. 518. Measuring instruments and a polyphase board (§60) should be provided for determining all the currents, voltages, and phase angles. The load reactances and resistances should be measured in advance, or else provision should be made for measuring r and x with any desired setting. The experiment consists in applying both symmetrical and unsymmetrical voltages to a load of unbalanced impedances (or adjusting to some chosen percentage of current unbalance) and reading all the quantities necessary for constructing complete vector diagrams. Then these diagrams should be checked with the theory developed above. It is advisable to perform this experiment with several widely different degrees of unbalance, and with both directions of phase rotation, so as to have a more complete check on the theory; see also §708.

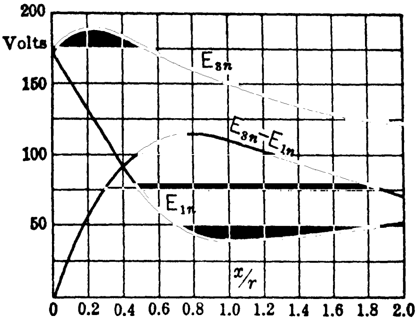

FIG. 526. Curves showing the effect of varying the ratio x/r in the semi-balanced phase-sequence meter.

The problem of the semi-balanced device for determining phase sequence, as discussed in §706, should be studied experimentally: first, for the purpose of obtaining the phase rotation of the voltage supply; and second, to verify the stated relation of x to r for best operation. The theory should be checked by some different method of analysis. Equation (43) should be differentiated to prove the optimum relation between x and r.

708. Effect of Mutual Inductance. — Let an appreciable coefficient of mutual induction, M_{12}, exist between the load phases 1 and 2, and a similar coefficient, M_{31}, between the phases 3 and 1 (§157). The equation for the instantaneous voltages in phase 1 then becomes:

$$e_{10} - e_{n0} = r_1 i_1 + L_1\, di_1/dt + M_{12}\, di_2/dt + M_{31}\, di_3/dt \quad . \quad . \quad (44)$$

Similar equations may be written for the other two phases. For the vectors of the effective values of the voltages and currents, these equations become:

$$\left.\begin{aligned} E_{10} - E_{n0} &= Z_1 I_1 + X_{12} I_2 + X_{31} I_3 \\ E_{20} - E_{n0} &= Z_2 I_2 + X_{23} I_3 + X_{12} I_1 \\ E_{30} - E_{n0} &= Z_3 I_3 + X_{31} I_1 + X_{23} I_2 \end{aligned}\right\} \quad . \quad . \quad . \quad . \quad . \quad (45)$$

where $X_{12} = 2\pi f M_{12}$, $X_{23} = 2\pi f M_{23}$, $X_{31} = 2\pi f M_{31}$ are the mutual reactances between the corresponding phases. Equations (45) take the place of eqs. (18); the two sets of equations become identical when all the X's are equal to zero. Besides eqs. (45), the three currents must satisfy the condition:

$$I_1 + I_2 + I_3 = 0 \quad \dots\dots\dots \quad (46)$$

In order to eliminate the three currents from eqs. (45) and (46), we multiply the first equation by an arbitrary coefficient a_1, the second by a_2, the third by a_3, and add the four equations term by term. The three coefficients a can then be so chosen that the factors by which I_1, I_2, I_3 are multiplied in the resultant equation are all equal to one. In other words, a_1, a_2, a_3 are to have such values that:

$$\left.\begin{aligned} a_1Z_1 + a_2X_{12} + a_3X_{31} &= 1 \\ a_1X_{12} + a_2Z_2 + a_3X_{23} &= 1 \\ a_1X_{31} + a_2X_{23} + a_3Z_3 &= 1 \end{aligned}\right\} \quad \dots\dots\dots \quad (47)$$

Then the result of the addition of the eqs. (45) and (46) simply becomes:

$$E_{10}a_1 + E_{20}a_2 + E_{30}a_3 - E_{n0}(a_1 + a_2 + a_3) = 0 \quad \dots \quad (48)$$

from which,

$$E_{n0} = \Sigma Ea/\Sigma a \quad \dots\dots\dots \quad (49)$$

The form of eq. (44) is similar to that of eq. (21), and the two expressions become identical when all the coefficients of mutual induction are equal to zero so that $a_1 = Z_1^{-1}$, $a_2 = Z_2^{-1}$, and $a_3 = Z_3^{-1}$. In the general case:

$$a_1 = D_1/D; \quad a_2 = D_2/D; \quad a_3 = D_3/D \quad \dots\dots \quad (50)$$

where D, D_1, D_2, D_3 are the familiar determinants made up of the Z's and X's in eqs. (47). It is not necessary at present to follow the problem any further, since the rest of the solution can be deduced from the simpler cases considered in §§702 to 706.

It will thus be seen that the neutral-voltage method is also applicable when mutual induction is present, provided that the coefficients X_{12}, X_{23}, and X_{31} are independent of the currents and voltages. This condition holds true for stationary impedances with a moderate saturation in iron cores, but in revolving machinery the reactances for currents of one phase sequence (§710) may be entirely different from those for the opposite phase sequence, depending upon the direction of rotation of the revolving part. In such cases the method of symmetrical components, treated in the next chapter, is preferable.

REFERENCES

1. R. R. LAWRENCE, Principles of Alternating Currents, McGraw-Hill Book Co.

2. M. P. WEINBACH, Alternating Current Circuits, Macmillan Co.

3. V. KARAPETOFF, The Electric Circuit, McGraw-Hill Book Co.

4. MORECROFT and HEHRE, Alternating Currents, John Wiley & Sons.

5. KERCHNER and CORCORAN, Alternating-Current Circuits, John Wiley & Sons.

6. BRYANT, CORRELL, and JOHNSON, Alternating-Current Circuits, McGraw-Hill Book Co.

7. C. E. MAGNUSSON, Alternating Currents, McGraw-Hill Book Co.

8. M. G. MALTI, Electric Circuit Analysis, John Wiley & Sons.

9. V. KARAPETOFF, *Jour. A.I.E.E.*, vol. 41, January, 1922, p. 11, The use of superposed imaginary emf's, currents, and fluxes in the solution of a-c problems.

CHAPTER XXXIV

SYMMETRICAL COMPONENTS IN THE ANALYSIS OF UNBALANCED POLYPHASE SYSTEMS

709. In the previous chapter certain devices were used in the analysis of unbalanced three-phase circuits: namely, (a) the general application of Kirchhoff's laws (§698); (b) the substitution of an equivalent delta for the given impedances in star (§698); (c) the neutral-voltage principle (§702); and (d) the method of superposed currents (§703). A means of solution preferable to any of the above in the analysis of many problems involving unbalanced conditions is the method of *symmetrical components* proposed by Mr. Fortescue.[1]

Briefly stated, the method of symmetrical components consists in resolving an unsymmetrical system of voltages, currents, or impedances into a number of symmetrical systems. Thus a system of three unequal voltages displaced by unequal angles may be resolved into one set of three equal voltages displaced by 120 degrees and of the same phase order as the original system (positive phase-sequence component); another set of three equal voltages, usually different in value from the first, and of opposite phase order (negative phase-sequence component); and also, in the more general case, a set of three equal voltages in phase with one another (zero phase-sequence or " uniphase " component). These components, added together for the individual phases will, of course, reproduce the original unsymmetrical system. This method has become increasingly useful in the solution of polyphase network problems, particularly when unsymmetrical faults occur on power systems, and in the analysis of the operation of induction motors on unsymmetrical voltage supply, of synchronous machines subjected to unbalanced loading, etc.

In stationary equipment — transformers and transmission lines — impedances of opposite phase sequence are commonly equal, while in rotating machines the impedances of the windings to currents of opposite phase sequence are commonly unequal. Since the impedances of the several phases are usually balanced, when referred to a particular phase-sequence component, the resultant performance of the machine becomes the sum or difference of the performances due to balanced currents of opposite phase sequences.

---

[1] C. L. Fortescue, " Method of Symmetrical Coordinates Applied to the Solution of Polyphase Networks, " *Trans. A.I.E.E.*, vol. 37, p. 1027.

To illustrate the idea of symmetrical components, Fig. 527*a* shows positive, negative, and zero-sequence components of voltage; Fig. 527*b* shows these components combined to produce an unsymmetrical three-phase voltage system.

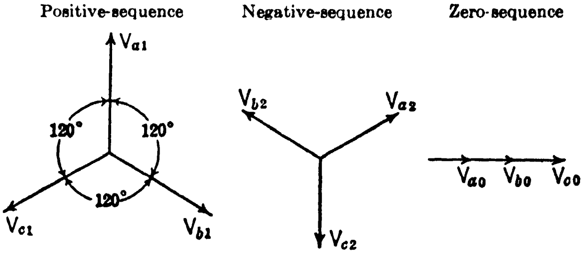

FIG. 527(*a*). Phase-sequence components in a three-phase system.

V_{a1}, V_{b1}, and V_{c1} are three equal voltages displaced by 120 degrees, with V_{a1} leading V_{b1}. These are the positive-sequence components, or sequence components of the first order (note the subscripts). V_{a2}, V_{b2}, and V_{c2} constitute a symmetrical three-phase system of voltages, with V_{b2} leading V_{a2}. These are the negative-sequence components, or components of the second order. V_{a0}, V_{b0}, and V_{c0} are three equal voltages in phase and are the zero-sequence components (zero order, or third order). Adding the component voltages of each phase together (Fig. 527*b*) gives the total voltage of the phase, as V_a, V_b, or V_c.

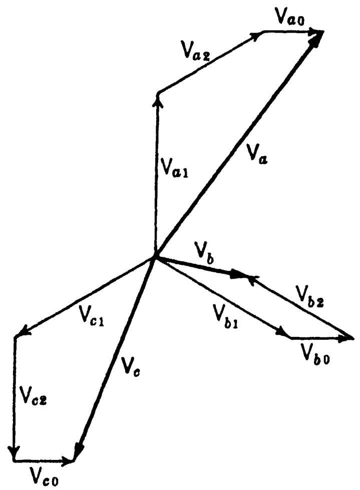

FIG. 527(*b*). Phase components of Fig. 527(*a*) combined to produce an unsymmetrical three-phase voltage system.

710. Principles Underlying the Resolution of an Unsymmetrical Three-Phase System of Vectors into Phase-Sequence Components. — The positive-sequence vectors V_{a1}, V_{b1}, and V_{c1} of Fig. 527 may be written in terms of V_{a1} as follows.

$$\begin{aligned} V_{a1} &= V_{a1}\underline{/0^\circ} \\ V_{b1} &= V_{a1}\underline{/-120^\circ} \qquad \ldots\ldots\ldots\ldots \quad (1) \\ V_{c1} &= V_{a1}/-240^\circ = V_{a1}/120^\circ \end{aligned}$$

Similarly, the negative-sequence vectors V_{a2}, V_{b2}, and V_{c2}, in terms of V_{a2} are:

$$\begin{aligned} V_{a2} &= V_{a2}\underline{/0^\circ} \\ V_{b2} &= V_{a2}\underline{/120^\circ} \\ V_{c2} &= V_{a2}\underline{/240^\circ} = V_{a2}\underline{/-120^\circ} \end{aligned} \qquad (2)$$

Since the zero-sequence vectors are all in phase:

$$V_{a0} = V_{b0} = V_{c0} \qquad (3)$$

As stated in §709:

$$V_a = V_{a1} + V_{a2} + V_{a0} \qquad (4)$$

$$V_b = V_{b1} + V_{b2} + V_{b0} = V_{a1}\underline{/-120^\circ} + V_{a2}\underline{/120^\circ} + V_{a0} \qquad (5)$$

$$V_c = V_{c1} + V_{c2} + V_{c0} = V_{a1}\underline{/120^\circ} + V_{a2}\underline{/-120^\circ} + V_{a0} \qquad (6)$$

Adding, and remembering that the sum of three equal vectors 120 degrees apart is zero:

$$V_a + V_b + V_c = 3V_{a0} \qquad (7)$$

or

$$V_{a0} = (V_a + V_b + V_c)/3 \qquad (8)$$

Turning operator, h. In the complex number method of expressing vectors the symbol j is used to indicate rotation of a vector through 90 degrees in the counterclockwise (positive) direction (§143). In the method of symmetrical components it is essential to have an operator which rotates a vector through 120 degrees. If h is this "turning operator," then:

$$h = -0.5 + j0.866 = e^{j2\pi/3} = \cos 2\pi/3 + j \sin 2\pi/3 \qquad (9)$$

Let **A** be any vector; then h**A** is the same vector turned through 120 degrees in the positive (counterclockwise) direction. Evidently h serves as a unit vector leading the axis of reference by 120 degrees, since the product of two vectors has a value equal to the product of the amplitudes of the vectors at an angle from the reference equal to the sum of the angles of the two vectors.

Evidently, also, h^2 is an operator which rotates a vector by 240 degrees in the positive direction, while h^{-1} rotates a vector *backward* 120 degrees. But turning by 240 degrees in the positive direction is equivalent to turning by 120 degrees in the negative direction, so that:

$$h^2 = h^{-1} = -0.5 - j0.866 \qquad (10)$$

We see also that

$$h^3 = 1 \qquad (11)$$

and in general

$$h^n = h^{(n-3)} \tag{12}$$

while, from eqs. (9) and (10),

$$1 + h + h^2 = 0 \tag{13}$$

Rewriting eqs. (5) and (6):

$$V_b = V_{a0} + h^2V_{a1} + hV_{a2} \tag{14}$$

$$V_c = V_{a0} + hV_{a1} + h^2V_{a2} \tag{15}$$

711. Analytical Determination of Positive-, Negative-, and Zero-Sequence Components. — Let the values and the phase angles of the three vectors V_a, V_b, and V_c be given, for instance, in the form of complex numbers. From eqs. (4), (14), and (15):

$$\begin{aligned} V_a + hV_b + h^2V_c = V_{a0} &+ V_{a1} + V_{a2} \\ &+ hV_{a0} + h^3V_{a1} + h^2V_{a2} \\ &+ h^2V_{a0} + h^3V_{a1} + h^4V_{a2} \end{aligned} \tag{16}$$

Adding like terms

$$\begin{aligned} V_a + hV_b + h^2V_c = V_{a0}(1 + h + h^2) &+ V_{a1}(1 + h^3 + h^3) \\ &+ V_{a2}(1 + h^2 + h^4) \end{aligned} \tag{17}$$

Substituting from eqs. (12), (13), and (15) into eq. (17) and solving for V_{a1}

$$V_{a1} = \tfrac{1}{3}(V_a + hV_b + h^2V_c) \tag{18}$$

Similarly, to determine the negative-sequence component, multiply V_b by h^2, V_c by h, and add to V_a. Thus:

$$\begin{aligned} V_a + h^2V_b + hV_c = V_{a0} &+ V_{a1} + V_{a2} \\ &+ h^2V_{a0} + h^4V_{a1} + h^3V_{a2} \\ &+ hV_{a0} + h^2V_{a1} + h^3V_{a2} \end{aligned} \tag{19}$$

Again adding like terms

$$\begin{aligned} V_a + h^2V_b + hV_c = V_{a0}(1 + h + h^2) &+ V_{a1}(1 + h^2 + h^4) \\ &+ V_{a2}(1 + h^3 + h^3) \end{aligned} \tag{20}$$

Consequently, from eqs. (12), (13), and (15)

$$V_{a2} = \tfrac{1}{3}(V_a + h^2V_b + hV_c) \tag{21}$$

The zero-sequence component was given by eq. (8), §710.

Example. Given that $V_a = 150\underline{/60^\circ}$, $V_b = 120\underline{/-45^\circ}$, and $V_c = 130\underline{/-120^\circ}$, it is required to resolve this unsymmetrical voltage system into its phase-sequence components. In complex numbers

$$V_a = 150\ (\cos 60^\circ + j \sin 60^\circ) = 75 + j130$$

$$V_b = 120\ (\cos -45^\circ + j \sin -45^\circ) = 84.8 - j84.8$$

$$V_c = 130\ (\cos -120^\circ + j \sin -120^\circ) = -65 - j112.6$$

The zero-sequence component, V_{a0} (eq. 8), is:

$$V_{a0} = \tfrac{1}{3}(75 + j130 + 84.8 - j84.8 - 65 - j112.6) = 31.6 - j22.5$$

The positive-sequence component, from eq. (18), becomes:

$$\begin{aligned} V_{a1} &= \tfrac{1}{3}(150\underline{/60^\circ} + 120\underline{/-45^\circ + 120^\circ} + 130\underline{/-120^\circ + 240^\circ}) \\ &= \tfrac{1}{3}(75 + j130 + 31.1 + j116.0 - 65 + j112.6) \\ &= 13.7 + j119.5 = 120.3\underline{/83.5^\circ} \end{aligned}$$

Consequently (eq. 1)

$$\begin{aligned} V_{b1} &= 120.3\underline{/-36.5^\circ} = 96.8 - j71.5 \\ V_{c1} &= 120.3\underline{/203.5^\circ} = -110.5 - j48.0 \end{aligned}$$

From eq. (21), the negative-sequence component of V_a is:

$$\begin{aligned} V_{a2} &= \tfrac{1}{3}(150\underline{/60^\circ} + 120\underline{/-45^\circ + 240^\circ} + 130\underline{/-120^\circ + 120^\circ}) \\ &= \tfrac{1}{3}(75 + j130 - 116.0 - j31.1 + 130) \\ &= 29.7 + j33 = 44.4\underline{/48.1^\circ} \end{aligned}$$

Therefore (eq. 2),

$$\begin{aligned} V_{b2} &= 44.4\underline{/168.1^\circ} = -43.5 + j9.1 \\ V_{c2} &= 44.4\underline{/-71.9^\circ} = 13.8 - j42.2 \end{aligned}$$

Arithmetical checks. Since the sum of three equal vectors 120 degrees apart is zero, $V_{a1} + V_{b1} + V_{c1} = 0$. On substituting the values found above in the following table, the numerical values are found to check.

ADDITION OF POSITIVE AND NEGATIVE PHASE-SEQUENCE COMPONENTS

Vector	+	−	+j	−j
V_{a_1}	13.7		119.5	
V_{b_1}	96.8			71.5
V_{c_1}		110.5		48.0
Sum	110.5	−110.5	+j119.5	−j119.5 = 0

Vector	+	−	+j	−j
V_{a_2}	29.7		33	
V_{b_2}		43.5	9.1	
V_{c_2}	13.8			42.2
Sum	43.5	−43.5	+j42.1	−j42.2 = 0

Also, the sum of the positive-, negative-, and zero-sequence components of any vector, such as V_a, must give the original vector. Thus (eq. 4):

$$\begin{aligned} V_a &= 13.7 + j119.5 + 29.7 + j33 + 31.6 - j22.5 \\ &= 75 + j130 \end{aligned}$$

which checks the values obtained.

712. General Case of the *n*-Phase System. — One may express an unsymmetrical polyphase system of n phases in terms of a zero-sequence component and $n - 1$ symmetrical sequence components.[2] In an n-phase voltage system consisting of the vector voltages, V_a, V_b, V_c, V_d, etc., the several phase voltages, in terms of symmetrical components, are

---

[2] Wagner and Evans, "Symmetrical Components," Chapter XVI, McGraw-Hill Book Co. W. V. Lyon, "Application of Symmetrical Components," Chapter I, McGraw-Hill Book Co.

$$V_a = V_{a0} + V_{a1} + V_{a2} + V_{a3} + \cdots V_{a(n-1)} \quad . \; . \; . \; . \; . \; . \; . \; . \quad (22)$$

$$V_b = V_{a0} + \alpha^{-1}V_{a1} + \alpha^{-2}V_{a2} + \alpha^{-3}V_{a3} + \cdots \alpha^{-(n-1)}V_{a(n-1)} \; . \quad (23)$$

etc.

In these equations $\alpha = e^{j2\pi/n}$.

One may solve for the sequence components by methods described in the previous article (§711). Then

$$V_{a1} = V_a + \alpha V_b + \alpha^2 V_c + \alpha^3 V_d + \cdots \alpha^{n-1} V_k \; . \; . \; . \quad (24)$$

while, in general,

$$V_{a(n-1)} = V_a + \alpha^{n-1}V_b + \alpha^{2(n-1)}V_c + \alpha^{3(n-1)}V_d + \cdots \alpha^{(n-1)(n-1)}V_k \quad (25)$$

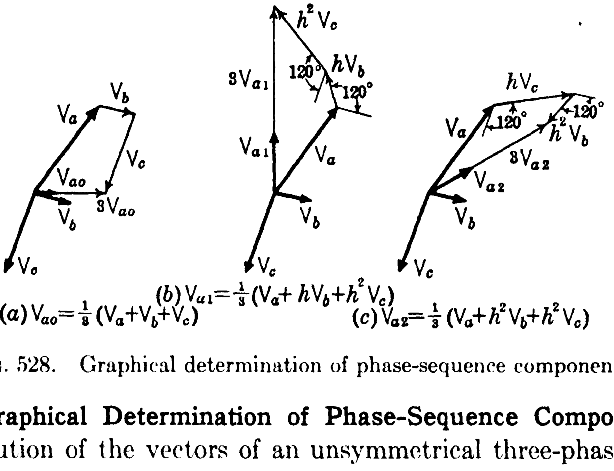

(a) $V_{ao} = \frac{1}{3}(V_a + V_b + V_c)$ (b) $V_{a1} = \frac{1}{3}(V_a + hV_b + h^2V_c)$ (c) $V_{a2} = \frac{1}{3}(V_a + h^2V_b + h^2V_c)$

FIG. 528. Graphical determination of phase-sequence components.

713. Graphical Determination of Phase-Sequence Components.— The resolution of the vectors of an unsymmetrical three-phase system into zero-, positive-, and negative-sequence components by analytical methods was described in the previous article. The same operation may of course be performed graphically, as follows:

(a) *Zero-sequence component.* In Fig. 528*a*, the three vectors V_a, V_b, and V_c are added in accordance with eq. (8) to yield $V_{a0} = \frac{1}{3}(V_a + V_b + V_c)$.

(b) *Positive-sequence component.* To perform the operation indicated by eq. (18), rotate V_b *forward* (counterclockwise) 120 degrees and add to V_a, giving $V_a + hV_b$; then rotate V_c *backward* 120 degrees and add to $V_a + hV_b$ to give $V_a + hV_b + h^2V_c$. Then V_{a1} is $\frac{1}{3}$ the sum. Figure 528*b* illustrates this.

(c) *Negative-sequence component.* In Fig. 528*c*, V_{a2} is found by rotating V_b backward 120 degrees (V_bh^2), and adding to V_a; then rotating V_c forward 120 degrees (V_ch), and adding to $V_a + V_bh^2$. This sum, by eq. (21), gives $3V_{a2}$.

714. Phase-Sequence Components of Line Currents and Voltages in an Unsymmetrical Three-Wire System. — (a) *Zero-sequence component.* In any three-wire system, such as a three-phase delta-connected supply or load, a three-phase star-connected system without a neutral wire, or a three-wire two-phase system, the sum of the line currents as well as the sum of the potential between lines is zero. In each of these cases, therefore, there is no zero-sequence component.

(b) *Positive-sequence component.* Referring to the currents in the system under discussion:

$$I_a + I_b + I_c = 0 \qquad (26)$$

or

$$I_c = -(I_a + I_b) \qquad (26a)$$

From eqs. (4), (14), and (15)

$$\left.\begin{aligned} I_a &= I_{a1} + I_{a2} \\ I_b &= h^2 I_{a1} + h I_{a2} \\ I_c &= h I_{a1} + h^2 I_{a2} \end{aligned}\right\} \qquad (27)$$

From eq. (18), by analogy,

$$\begin{aligned} I_{a1} &= \tfrac{1}{3}(I_a + hI_b + h^2 I_c) \\ &= \tfrac{1}{3}(I_a + hI_b - h^2[I_a + I_b]) \\ &= \tfrac{1}{3}[I_a(1 - h^2) + I_b(h - h^2)] \end{aligned} \qquad (28)$$

But,
$$I_a - I_a h^2 = I_a - I_a\underline{/240^\circ} = \sqrt{3} I_a \underline{/30^\circ}$$

and
$$I_b h - I_b h^2 = I_b\underline{/120^\circ} - I_b\underline{/240^\circ} = \sqrt{3} I_b\underline{/90^\circ}$$

Therefore

$$\begin{aligned} I_{a1} &= \frac{1}{\sqrt{3}}\,(I_a\underline{/30^\circ} + I_b\underline{/90^\circ}) \\ &= \frac{\underline{/30^\circ}}{\sqrt{3}}\,(I_a + I_b\underline{/60^\circ}) \end{aligned} \qquad (29)$$

Figure 529*a* illustrates the operation expressed by eq. (29). The three vectors I_a, I_b, and I_c, whose phase sequence is in the order named, are drawn as a closed triangle. Vector I_b is rotated counterclockwise 60 degrees and added to vector I_a. This sum is the quantity in the parentheses of eq. (29). At the extremities of the vector of summation, construction lines are drawn at 30 degrees. Their intersection shows the length and phase position of I_{a1}, 30 degrees *ahead* of $I_a + I_b/60^\circ$.

(c) *Negative-sequence component.* From eqs. (21) and (26*a*),

$$\begin{aligned} I_{a2} &= \tfrac{1}{3}(I_a + h^2 I_b + h I_c) \\ &= \tfrac{1}{3}[I_a + h^2 I_b - h(I_a + I_b)] \\ &= \tfrac{1}{3}[I_a(1 - h) + I_b(h^2 - h)] \quad \ldots\ldots \quad (30) \end{aligned}$$

But $$I_a - I_a h = I_a - I_a\underline{/120^\circ} = \sqrt{3}I_a\underline{/-30^\circ}$$

Likewise $$I_b h^2 - I_b h = I_b\underline{/240^\circ} - I_b\underline{/120^\circ} = \sqrt{3}I_b\underline{/-90^\circ}$$

Therefore: $$I_{a2} = \frac{1}{\sqrt{3}}\,(I_a\underline{/-30^\circ} + I_b\underline{/-90^\circ})$$

$$= \frac{\underline{/-30^\circ}}{\sqrt{3}}\,(I_a + I_b\underline{/-60^\circ)} \quad \ldots\ldots\ldots \quad (31)$$

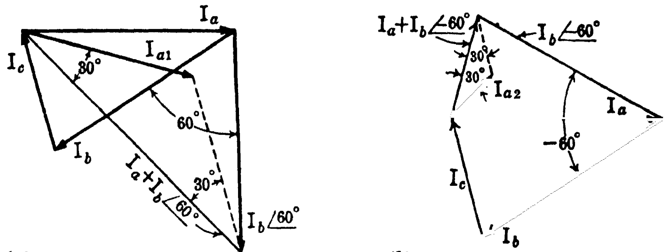

(*a*) **Positive-sequence Component** (*b*) **Negative-sequence Component**

FIG. 529. Graphical determination of phase-sequence currents in a three-wire system.

This is illustrated by Fig. 529*b*, where I_b is rotated *backward* 60 degrees and added to I_a, and lines drawn at 30 degrees with this sum give I_{a2}, 30 degrees *behind* it. This latter construction was unnecessary, since I_{a2} could have been found as $I_a - I_{a1}$. It is evident that the equations which apply to line currents apply also to the positive and negative components of line potentials in a three-wire system. Rewriting eqs. (29) and (31) in terms of potentials between lines:

$$V_{ab1} = \frac{\underline{/30^\circ}}{\sqrt{3}}\,(V_{ab} + V_{bc}\underline{/60^\circ} \quad \ldots\ldots\ldots \quad (29a)$$

$$V_{ab2} = \frac{\underline{/-30^\circ}}{\sqrt{3}}\,(V_{ab} + V_{bc}\underline{/-60^\circ)} \quad \ldots\ldots \quad (31a)$$

715. Line Potential and Phase Potential Sequence Components. — Since the positive- and negative-sequence components of line potentials constitute symmetrical three-phase systems of vectors, each of these may be replaced by three potentials to neutral of $1/\sqrt{3}$ times the line potential. Note (Fig. 530) that the positive-sequence potential to neutral,

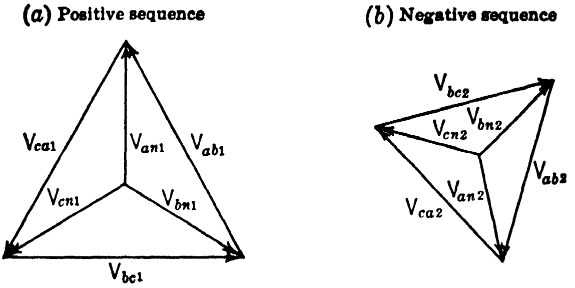
(*a*) Positive sequence (*b*) Negative sequence

FIG. 530. Positive- and negative-sequence components of voltage; between lines, and to neutral.

say V_{an1}, lags its line potential, V_{ab1}, by 30°, while the negative-sequence component of neutral potential, for example V_{an2}, leads its line potential V_{ab2} by 30°. Therefore (see eq. 29*a*),

$$V_{an1} = (1/\sqrt{3})V_{ab1}\underline{/-30^\circ} = \tfrac{1}{3}(V_{ab} + V_{bc}\underline{/60^\circ}) \quad . \; . \; . \quad (32)$$

and (see eq. 31*a*)

$$\begin{aligned} V_{an2} &= (1/\sqrt{3})V_{ab2}\underline{/30^\circ} \\ &= \tfrac{1}{3}(V_{ab} + V_{bc}\underline{/-60^\circ}) \quad . \; . \; . \; . \; . \; . \; . \; . \; . \; . \; . \quad (33) \end{aligned}$$

Note that in a symmetrical three-phase voltage system of positive phase sequence there can be no negative-sequence component, either in the line potentials or in the potentials to neutral. Note also that before analyzing a three-phase potential system it is necessary to know the sequence of the system potentials, since, in the equations which have been developed, phase *a* is assumed to lead phase *b*, which leads phase *c*. In §700 a method is given for determining phase sequence.

716. Symmetrical Components of Impedances. — In solving the circuit problem presented by three dissimilar impedances connected in star to a three-phase supply without a neutral wire, it develops that it is of advantage to resolve the impedances into zero-, positive-, and negative-sequence components, as was done for potentials and currents. Thus, for the system shown in Fig. 531, if V_{an}, V_{bn}, and V_{cn} are the several potential drops across the load impedances, then:

$$\left.\begin{aligned} V_{an} &= I_a Z_a \\ V_{bn} &= I_b Z_b \\ V_{cn} &= I_c Z_c \end{aligned}\right\} \tag{34}$$

Expressing the phase-sequence components in terms of the potential drops to neutral:

$$V_{an0} = \tfrac{1}{3}(I_a Z_a + I_b Z_b + I_c Z_c) \tag{35}$$

$$V_{an1} = \tfrac{1}{3}(I_a Z_a + hI_b Z_b + h^2 I_c Z_c) \tag{36}$$

$$V_{an2} = \tfrac{1}{3}(I_a Z_a + h^2 I_b Z_b + hI_c Z_c) \tag{37}$$

Expressing the load currents in terms of sequence components.

$$I_a = I_{a0} + I_{a1} + I_{a2}, \quad \text{etc.}$$

$$\begin{aligned} V_{an0} = \tfrac{1}{3}[(I_{a0} + I_{a1} + I_{a2})Z_a + (I_{a0} + h^2 I_{a1} + hI_{a2})Z_b \\ + (I_{a0} + hI_{a1} + h^2 I_{a2})Z_c] \end{aligned} \tag{38}$$

$$\begin{aligned} = I_{a0}\frac{(Z_a + Z_b + Z_c)}{3} + I_{a1}\frac{(Z_a + h^2 Z_b + hZ_c)}{3} \\ + I_{a2}\frac{(Z_a + hZ_n + h^2 Z_c)}{3} \end{aligned} \tag{39}$$

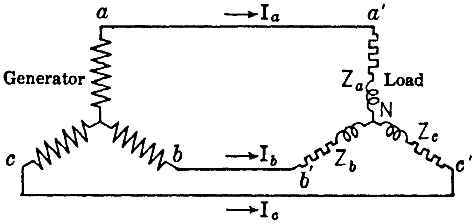

FIG. 531. Three-phase system with load impedances in "star"

The three impedance terms are in the form of zero-, negative-, and positive-sequence components, where:

$$\left.\begin{aligned} Z_{a0} &= \tfrac{1}{3}(Z_a + Z_b + Z_c) \\ Z_{a1} &= \tfrac{1}{3}(Z_a + hZ_b + h^2 Z_c) \\ Z_{a2} &= \tfrac{1}{3}(Z_a + h^2 Z_b + hZ_c) \end{aligned}\right\} \tag{40}$$

or eq. (39) may be written:

$$V_{an0} = I_{a0}Z_{a0} + I_{a1}Z_{a2} + I_{a2}Z_{a1} \tag{41}$$

Note that the sums of the numerical subscripts in the several terms are 0 and 3, which indicate zero-sequence components

By a reasoning similar to that which gave eq. (41), we may write, for the positive-sequence component of load potential to neutral,

$$V_{an1} = I_{a0}Z_{a1} + I_{a1}Z_{a0} + I_{a2}Z_{a2} \quad . \ . \ . \ . \ . \ . \quad (42)$$

Here the sums of numerical subscripts indicate the first-order or positive sequence.

For the negative-sequence component of volts drop to neutral:

$$V_{an2} = I_{a0}Z_{a2} + I_{a1}Z_{a1} + I_{a2}Z_{a0} \quad . \ . \ . \ . \ . \ . \quad (43)$$

Again, note that the sums of the numerical subscripts indicate the second-order or negative-sequence components.

717. Solution of Problems Involving Unbalanced Y-Connected Loads. — The preceding article (§716) outlines the method of symmetrical components in the solution of the problem offered by three unequal impedances connected in star to a three-phase supply, without neutral return (Fig. 531). Assume the following data to be given.

$$V_{ab} = 220; \quad V_{bc} = 220\underline{/-120°}; \quad \text{and} \quad V_{ca} = 220\underline{/120°} \text{ volts}$$

These constitute a symmetrical three-phase supply. Three impedances, $Z_a = 1 + j2$; $Z_b = 2 + j3$, and $Z_c = 3 + j4$ are connected in "star." It is required to calculate the line currents, the volts to neutral, and the power consumed in each load.

(a) *Volts to neutral.* From eq. (32),

$$V_{an1} = \tfrac{1}{3}(220 + 220\underline{/-60°}) = (220/\sqrt{3})\underline{/-30°} = 127\underline{/-30°} = 110 - j63.4$$

From eq. (33),

$$V_{an2} = \tfrac{1}{3}(220 + 220\underline{/-180°}) = 0$$

while V_{an0} is to be determined later.

(b) *Impedance components.* From eqs. (40),

$$Z_{a0} = \tfrac{1}{3}(1 + j2 + 2 + j3 + 3 + j4) = 2 + j3 \text{ ohms}$$

$$Z_{a1} = \tfrac{1}{3}[1 + j2 + (2 + j3)(-0.5 + j0.866) + (3 + j4)(-0.5 - j0.866)]$$
$$= -0.21 - j0.79 = 0.818\underline{/-104.7°} \text{ ohm}$$

$$Z_{a2} = \tfrac{1}{3}[1 + j2 + (2 + j3)(-0.5 - j0.866) + (3 + j4)(-0.5 + j0.866)]$$
$$= -0.79 - j0.21 = 0.818\underline{/-165.2°} \text{ ohm}$$

Checking by the formula $Z_a = Z_{a0} + Z_{a1} + Z_{a2}$

$$Z_a = 2 + j3 - 0.21 - j0.79 - 0.79 - j0.21 = 1 + j2, \quad \text{as given}$$

From eq. (42), remembering that there can be no zero-sequence component of current, since there is no neutral return:

$$V_{an1} = I_{a1}Z_{a0} + I_{a2}Z_{a2} \quad . \ . \ . \ . \ . \ . \ . \ . \ . \quad (42a)$$

From eq. (43)

$$V_{an2} = I_{a1}Z_{a1} + I_{a2}Z_{a0} = 0, \quad \text{or} \quad I_{a1} = -I_{a2}(Z_{a0}/Z_{a1}) \quad . \ . \quad (43a)$$

Substituting known values:

$$
\begin{aligned}
V_{an1} &= 110 - j63.4 = I_{a1}(2 + j3) + I_{a2}(-0.79 - j0.21)\\
V_{an2} &= \quad 0 \quad\;\; = I_{a1}(-0.21 - j0.79) + I_{a2}(2 + j3)
\end{aligned}
$$

Solving:

$$
\begin{aligned}
I_{a2} &= 3.1 - j7.8 = 8.4\underline{/-68.5^\circ} \text{ amp}\\
I_{a1} &= 1.7 - j37.1 = 37.2\underline{/-87.4^\circ} \text{ amp}
\end{aligned}
$$

Therefore:

$$I_a = 4.8 - j44.9 = 45.20\underline{/-83.9^\circ} \text{ amp}$$

and

$$
\begin{aligned}
I_b &= I_{a1}\underline{/-120^\circ} + I_{a2}\underline{/120^\circ}\\
&= 37.2\underline{/-207.4^\circ} + 8.4\underline{/51.5^\circ}\\
&= -27.77 + j23.67 = 36.45\underline{/+139.6^\circ} \text{ amp}\\
I_c &= I_{a1}\underline{/120^\circ} + I_{a2}\underline{/-120^\circ}\\
&= 37.2\underline{/32.6^\circ} + 8.4\underline{/-188.5^\circ}\\
&= 23.0 + j21.3 = 31.3\underline{/41.9^\circ} \text{ amp}
\end{aligned}
$$

CHECK OF CALCULATIONS

Vector	+	−	+j	−j
I_a	4.8			44.9
I_b		−27.77	23.67	
I_c	23.0		21.30	
Sum	27.8	−27.77	+j44.97	−j44.90 ≅ 0

From eq. (41)

$$
\begin{aligned}
V_{an0} &= I_{a1}Z_{a2} + I_{a2}Z_{a1}\\
&= (2 - j37)(-0.79 - j0.21) + (3.1 - j7.9)(-0.21 - j0.79)\\
&= -16.4 + j27.9 \qquad (41a)
\end{aligned}
$$

Then:

$$
\begin{aligned}
V_{an} &= V_{a0} + V_{a1} + 0\\
&= -16.4 + j27.9 + 110 - j63.4 = 93.6 - j35.5 = 100 \text{ volts}\\
V_{bn} &= V_{a0} + V_{a1}\underline{/-120^\circ} + 0 = -126.4 - j35.5 = 131.4 \text{ volts}
\end{aligned}
$$

As a check:

$$V_{ab} = V_{an} - V_{bn} = 93.6 - j35.5 + 126.4 + j35.5 = 220 + j0, \quad \text{as given}$$

Finally, since $V_{bc} = V_{bn} - V_{cn}$, $V_{cn} = V_{bn} - V_{bc}$,
or:

$$V_{cn} = -126.4 - j35.5 - (-110 - j190.5) = -16.4 + j155.0 = 155.9 \text{ volts}$$

Check:

$$V_{ca} = V_{cn} - V_{an} = -16.4 + j155 - 93.6 + j35.5$$
$$= -110 + j190.5 \text{ volts, as given}$$

(c) *Power values.* Watts consumed by each load may be easily determined in this case by I^2R calculation. Thus,

$$W_a = I_a^2R_a = (45.2)^2 \times 1 = 2043 \text{ watts}$$
$$W_b = I_b^2R_b = (36.45)^2 \times 2 = 2660 \text{ watts}$$
$$W_c = I_c^2R_c = (31.3)^2 \times 3 = 2930 \text{ watts}$$

As a check on power in load a take the product of I_a by the conjugate of vector V_{an}:

$$W_a = (4.8 - j44.9)(93.6 + j35.5)$$
$$= (449 + 1598) - j(4200 - 170)$$
$$= 2047 - j4030 \text{ voltamperes or 2047 watts (fair check)}$$

Symmetrical components will be applied later in the solution of problems relating to parallel transformer banks (§756), to polyphase induction motors operating on unbalanced voltage supply (§910), and on single-phase supply (§975), etc.

718. EXPERIMENT 34-A. — Study of Symmetrical Components in an Unbalanced Y-Connected System. — This experiment is for the purpose of illustrating the principles of the method of symmetrical components, and to check the formulas so far developed.

In order to build up a system of zero-, positive-, and negative-sequence voltages, two three-phase alternators of the same number of poles, and rigidly coupled together, should be available. It should be possible to shift the phase relation of the two machines. Connect the alternator armature windings in series and for opposite phase rotation. If two such machines are not available, a three-phase induction regulator may replace one machine. Its primary should be connected across the alternator windings and its secondary in series with them, but with reversed phase rotation. A three-phase wound-rotor induction motor having electrically independent stator windings and blocked rotor may be used as a polyphase induction regulator, the rotor windings serving as primary and the stator as secondary, or vice versa. Insert zero-sequence components into the phase potentials by means of equal-ratio single-phase transformers excited from one of the supply phases. Figure 532 suggests the series connections of the three sequence windings.

(1) With no load on the system, measure all voltages and check phase rotation (§700). Note the effect upon the various potentials of exciting only G_1 (Fig. 532); only G_2; only G_0; G_0 and G_2; G_2 and G_1; then G_0, G_2, and G_1. Vary individual voltages. Note especially the

values which result when the voltages of G_1 and G_2 are numerically equal. Note the effect of shifting the phase of G_2 with respect to G_1. Construct approximate vector diagrams of sample data to verify the relations expected and to show that sufficient information is available.

(2) Connect three identical impedances in Y to the unsymmetrical three-phase supply, with neutral available. Provide a switch and ammeter in the wire joining the neutral points of generator and load. Read all currents, voltages, and the power of each phase of the load, with neutral open and neutral closed. Change the amount of voltage unbalance by definite amounts, and again take readings.

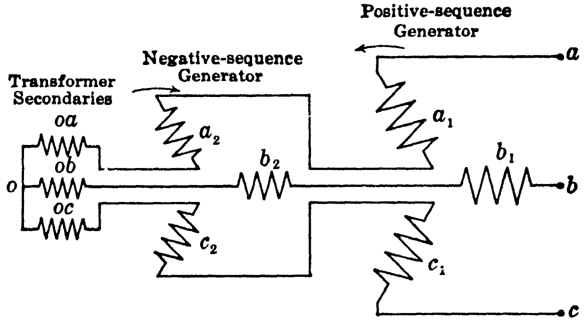

FIG. 532. Schematic arrangement of phase-sequence generators.

(3) Connect three unequal impedances (without mutual induction) in Y to a symmetrical three-phase source and take readings as in (2). Note the effect of reversing phase rotation of the supply.

Report. (a) Using the data taken in (1), build up the voltage system by adding the zero-, negative-, and positive-sequence potentials. Next by means of the principles developed in §§711 to 715, analyze both graphically and analytically the phase and line voltages to find the phase-sequence components, and compare results with the data taken. Discuss the causes of inaccuracy and the relative merits of analytical and graphical methods.

(b) Draw vector diagrams for typical sets of data taken in (2) for neutral open and neutral closed. Resolve line currents into phase-sequence components, and discuss results.

(c) For values of load impedances and line potentials actually used, solve for the line currents and phase voltages for the case of neutral line open, making use of the method of §717. Compare results with experimental values, and discuss.

(d) Calculate power values from the symmetrical components of current and potential and compare with measured values.

References. See end of Chapter XXXV.

CHAPTER XXXV

METHODS OF MEASUREMENT IN SYMMETRICAL COMPONENTS

719. Unbalance Factor. — Although the degree of unbalance in a polyphase system is known, in general, from the usual measurements of potentials and currents in the system, an accurate analysis of the unbalance requires a knowledge of the several symmetrical components. For instance, in a three-phase system, unbalance is expressed as the ratio of negative-sequence to positive-sequence component, which ratio is called the *unbalance factor*. Methods of metering these components are therefore necessary. Three-phase systems devoid of zero-sequence components will first be considered, i.e., line voltages, and line currents of three-phase systems without a neutral wire.

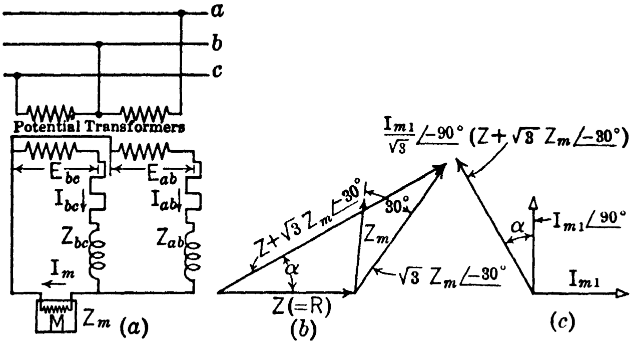

FIG. 533. (*a*) Phase-sequence voltmeter connections. (*b*) Impedance relations in positive-sequence network. (*c*) Voltage and current vectors in positive-sequence network.

720. Phase-Sequence Voltmeters. — (a) *Zero-sequence component absent.* In Fig. 533, the primary windings of two potential transformers of equal ratio are connected, respectively, between lines *c* and *b*, and between *b* and *a*. Secondary circuits are connected in parallel through impedances Z_{cb} and Z_{ba} to a low-resistance voltmeter (or sensitive ammeter) of impedance Z_m. Proper choice of the impedances will cause the meter to read in proportion to either the positive-sequence or negative-sequence component of line potential. This may be shown as follows:

From Kirchhoff's laws come the following:

$$E_{bc} = I_{bc}Z_{bc} + I_mZ_m \quad . \; . \; . \; . \; . \; . \; . \; . \; . \; . \quad (1)$$

$$E_{ab} = I_{ab}Z_{ab} + I_mZ_m \quad . \; . \; . \; . \; . \; . \; . \; . \; . \; . \quad (2)$$

$$I_{ab} + I_{bc} = I_m \quad . \; . \; . \; . \; . \; . \; . \; . \; . \; . \; . \; . \quad (3)$$

Multiplying (1) by Z_{ab} and (2) by Z_{bc}, and adding:

$$\begin{aligned} E_{bc}Z_{ab} + E_{ab}Z_{bc} &= I_{bc}Z_{bc}Z_{ab} + I_{ab}Z_{bc}Z_{ab} + I_mZ_m(Z_{ab} + Z_{bc}) \\ &= I_m[Z_{bc}Z_{ab} + Z_m(Z_{ab} + Z_{bc})] \quad . \; . \; . \; . \; . \; . \; . \quad (4) \end{aligned}$$

or

$$I_m = \frac{E_{bc}Z_{ab} + E_{ab}Z_{bc}}{Z_{bc}Z_{ab} + Z_m(Z_{ab} + Z_{bc})} \quad . \; . \; . \; . \; . \; . \; . \; . \; . \quad (5)$$

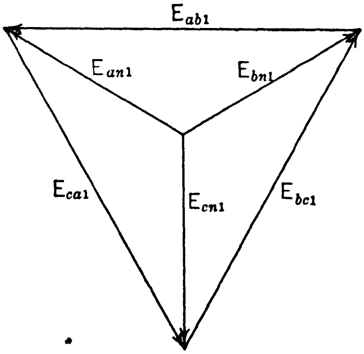

FIG. 534. Positive-sequence line and phase emf vectors.

Now, expressing line potentials in terms of positive- and negative-sequence components, and assuming a phase sequence (see Fig. 534) E_{ca}, E_{ab}, E_{bc}, eq. (5) becomes:

$$I_m = \frac{h^2E_{ab1}Z_{ab} + hE_{ab2}Z_{ab} + E_{ab1}Z_{bc} + E_{ab2}Z_{bc}}{Z_{bc}Z_{ab} + Z_m(Z_{ab} + Z_{bc})} \quad . \; . \; . \quad (6)$$

By proper choice of Z_{bc} and Z_{ab} one may make I_m read either the positive- or negative-sequence component of line potential.

721. Value of the Positive-Sequence Component. — For I_m (Fig. 533) to contain only a positive-sequence component, the negative-sequence component terms in eq. (6) must vanish; i.e.:

$$hE_{ab2}Z_{ab} + E_{ab2}Z_{bc} = 0 \quad . \; . \; . \; . \; . \; . \; . \; . \; . \quad (7)$$

Therefore $-hZ_{ab} = Z_{bc}$, or $Z_{ab}\underline{/-60°} = Z_{bc}$, and $Z_{ab} = Z_{bc}\underline{/60°}$. (8)

That is, if $Z_{bc} = Z\underline{/0°}$ = pure resistance, then $Z_{ab} = Z\underline{/60°}$ = resistance plus inductive reactance in proportion of $X = 0.866Z$, $R = 0.5Z$.

Substituting from Eq. (7) and (8) into Eq. (6):

$$I_{m1} = \frac{h^2E_{ab1}Z\underline{/60^\circ} + E_{ab1}Z}{Z^2\underline{/60^\circ} + Z_m(Z\underline{/60^\circ} + Z)}$$

$$= \frac{E_{ab1}(h^2\underline{/60^\circ} + 1)}{Z\underline{/60^\circ} + Z_m(\underline{/60^\circ} + 1)} = \frac{\sqrt{3}E_{ab1}\underline{/-30^\circ}}{Z\underline{/60^\circ} + \sqrt{3}Z_m\underline{/30^\circ}}$$

$$= \frac{\sqrt{3}E_{ab1}}{Z\underline{/90^\circ} + \sqrt{3}Z_m\underline{/60^\circ}} \quad . \; . \; . \; . \; . \; . \; . \; . \; . \; . \; . \; . \; . \; . \quad (9)$$

Therefore:

$$E_{ab1} = \frac{I_{m1}\underline{/90^\circ}}{\sqrt{3}}(Z + \sqrt{3}Z_m\underline{/-30^\circ}) \quad . \; . \; . \; . \; . \; . \; . \quad (10a)$$

while

$$E_{ca1} = hE_{ab1} = I_{m1}\frac{\underline{/-150^\circ}}{\sqrt{3}}(Z + \sqrt{3}Z_m\underline{/-30^\circ}) \quad . \; . \quad (10b)$$

and

$$E_{bc1} = h^2E_{ab1} = \frac{I_{m1}\underline{/-30^\circ}}{\sqrt{3}}(Z + \sqrt{3}Z_m\underline{/-30^\circ}) \quad . \; . \quad (10c)$$

The relations expressed by eq. (10*a*) are illustrated in Fig. 533(*b*) and (*c*).

722. Value of Negative-Sequence Component. — If I_m is to indicate the negative-sequence component of line potential the condition to be met is (Eq. 6):

$$h^2E_{ab1}Z_{ab} + E_{ab1}Z_{bc} = 0 \quad . \; . \; . \; . \; . \; . \; . \; . \; . \quad (11)$$

or

$$h^2Z_{ab} = Z_{bc} \quad \text{or} \quad Z_{ab}\underline{/60^\circ} = Z_{bc} \quad . \; . \; . \; . \; . \; . \; . \quad (12)$$

Thus, Z_{ab} and Z_{bc} should be equal numerically with Z_{bc} leading Z_{ab} by 60 degrees. If Z_{ab} is pure resistance, or $Z_{ab} = Z\underline{/0^\circ}$, then

$$Z_{bc} = 0.5Z + j0.866Z$$

Substituting from (12) and (11) into (6)

$$I_{m2} = \frac{hE_{ab2}Z + E_{ab2}Z\underline{/60^\circ}}{Z_2\underline{/60^\circ} + Z_m(Z + Z\underline{/60^\circ})}$$

$$= \frac{\sqrt{3}E_{ab2}\underline{/90^\circ}}{Z\underline{/60^\circ} + \sqrt{3}Z_m\underline{/30^\circ}}$$

$$= \frac{\sqrt{3}E_{ab2}}{Z\underline{/-30^\circ} + \sqrt{3}Z_m\underline{/-60^\circ}} \quad . \; . \; . \; . \; . \; . \quad (13)$$

Therefore $E_{ab2} = (1/\sqrt{3})\, I_{m2}\underline{/-30^\circ}(Z + \sqrt{3}Z_m\underline{/-30^\circ})$ . . (14*a*)

and $E_{ca2} = (1/\sqrt{3})\, I_{m2}\underline{/-150^\circ}(Z + \sqrt{3}Z_m\underline{/-30^\circ})$. (14*b*)

also $E_{bc2} = (1/\sqrt{3})\, I_{m2}\underline{/90^\circ}(Z + \sqrt{3}Z_m\underline{/-30^\circ})$ . . . (14*c*)

Rewriting eq. (10*a*) in terms of phase volts (see Fig. 534),

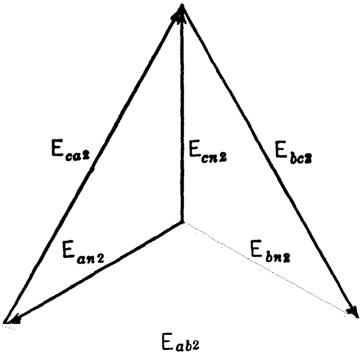

FIG. 535. Negative-sequence line and phase emf vectors.

$$E_{an1} = (E_{ab1}/\sqrt{3})\underline{/-30^\circ} = (I_{m1}/3)\underline{/60^\circ}(Z + \sqrt{3}Z_m\underline{/-30^\circ}), \text{ etc.} \quad (15)$$

Likewise from Fig. 535,

$$E_{an2} = (E_{ab2}/\sqrt{3})\underline{/30^\circ}$$

or

$$E_{an2} = (I_{m2}/3)(Z + \sqrt{3}Z_m\underline{/-30^\circ}), \text{ etc.} \; . \; . \; . \; . \quad (16)$$

723. Simultaneous Readings of Opposite Phase-Sequence Components. — When it is required to read voltages of both sequences simultaneously, the two conditions discussed under §§721 and 722 are combined into one network as in Fig. 536. The circuit of each meter is formed as in Fig. 533, potential transformers of equal ratio being again used. For M_1 to read the positive-sequence component $Z_{bc1} = Z\underline{/0^\circ}$, $Z_{ab1} = Z\underline{/60^\circ}$. For M_2 to read negative-sequence potential $Z_{ab2} = Z\underline{/0^\circ}$, $Z_{bc2} = Z\underline{/60^\circ}$. More generally speaking, it is only necessary for Z_{ab1} to lead Z_{bc1} by 60°, or $Z_{ab1}\underline{/\alpha} = Z_{bc1}\underline{/\alpha + 60^\circ}$ while $Z_{bc2}\underline{/\beta} = Z_{ab2}\underline{/\beta + 60^\circ}$. Obviously capacitive, rather than inductive, impedances may be used if preferred. It should be remembered that inductances give an impedance a leading angle whereas capacitance gives impedance a lagging angle.

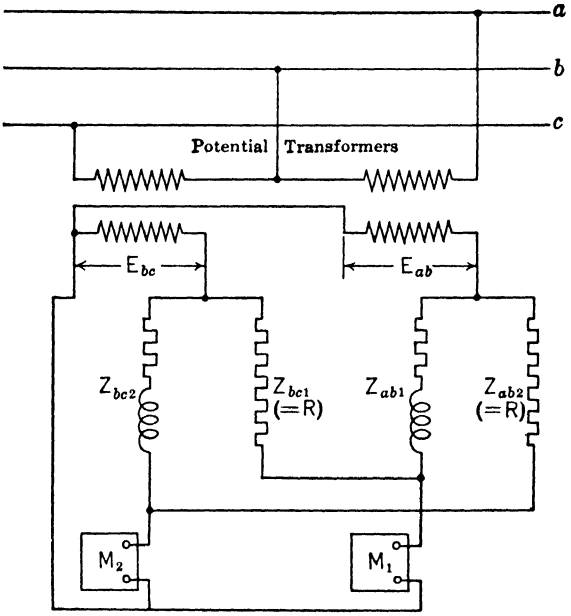

FIG. 536. Sequence network for simultaneous reading of opposite sequence components.

Although the sequence networks so far discussed are not suitable for connection across unbalanced Y voltages because these include a zero-sequence component, yet, as suggested above, the positive- and negative-sequence volts to neutral (phase-volts) may be determined from the readings taken with these networks applied to the line potentials, since, individually, the two sequence components constitute symmetrical systems. Obviously the meters shown in these networks may be replaced by relays when it is desired to operate protective or recording devices in case of system unbalance.

724. Measurement of the Zero-Sequence Component of Voltage.—Since the value of the zero-sequence component in a three-phase system is (§710) one-third the sum of the three-phase voltages, the networks of Figs. 537 and 538 will serve for this measurement. In Fig. 537 a standard voltmeter, M_0, will obviously read the sum of the secondary voltages of the three potential transformers; or, assuming a ratio of *unity* for the transformers,

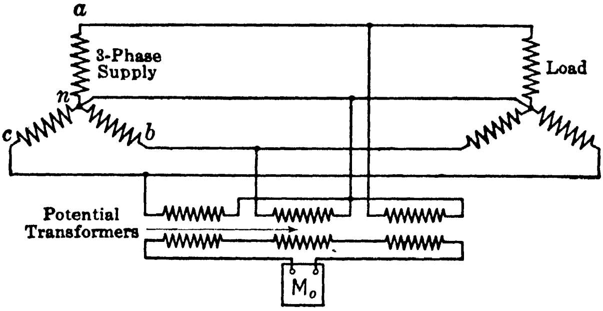

FIG. 537. Zero-sequence component of voltage by means of three identical potential transformers.

$$M_0 = E_{an} + E_{bn} + E_{cn} = 3E_{a0} \quad \ldots\ldots \quad (17)$$

A special scale may be employed to make the reading equal the zero-sequence voltage directly.

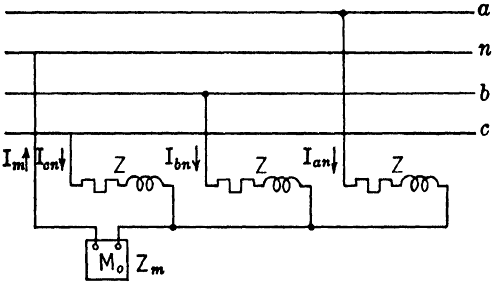

FIG. 538. Zero sequence of voltage by means of three identical impedances.

If the transformers have a ratio of 3 : 1

$$M_0 = E_{an}/3 + E_{bn}/3 + E_{cn}/3 = E_{a0} \quad \ldots\ldots \quad (18)$$

In Fig. 538, three accurately determined and identical impedances are connected in Y to the three lines, with a voltmeter M_0 between the neutrals of the impedances and of the three-phase system. Then:

$$\left.\begin{aligned} E_{an} &= I_{an}Z + I_mZ_m \\ E_{bn} &= I_{bn}Z + I_mZ_m \\ E_{cn} &= I_{cn}Z + I_mZ_m \end{aligned}\right\} \quad \ldots\ldots\ldots \quad (19)$$

Also

$$I_{an} + I_{bn} + I_{cn} = I_m \quad \ldots\ldots\ldots \quad (20)$$

Therefore:

$$E_{an} + E_{bn} + E_{cn} = I_mZ + 3I_mZ_m$$

$$E_{a0} = (E_{an} + E_{bn} + E_{cn})/3 = I_m(Z/3 + Z_m) \quad \ldots \quad (21)$$

This equation should be obvious from observation of the diagram.

725. EXPERIMENT 35-A.—Study of Phase-Sequence Voltmeters.—Methods of measuring phase-sequence voltages, as explained in the previous section, should be applied to measure the phase-sequence components in an unsymmetrical three-phase system built up as described in §718, and with the several components accurately known. The advantages and disadvantages of the several methods should be determined, also limits of accuracy, the best values of R and Z, the merits of inductive reactance and capacitive reactance, the effect of varying frequency and of harmonics in the voltage supply, the best type of meter to use, etc. Apply the networks to the operation of relays and circuit breakers upon the appearance of negative-sequence components in the supply voltage, and to produce records by means of curve-tracing meters and oscillographs. After the several methods have been studied, try to devise new schemes for measuring the symmetrical components.

726. Measurement of Symmetrical Components of Current.—(a) *Three-wire systems—zero-sequence component absent.* Ammeters, connected to measure the current in each of the three wires, will show the extent of the current unbalance in a three-wire system. From these three currents the phase-sequence components may be obtained by analytical or by graphical means. However, it is desirable to be able to measure these components directly. Figure 539 is a network that may be used to measure phase-sequence components.

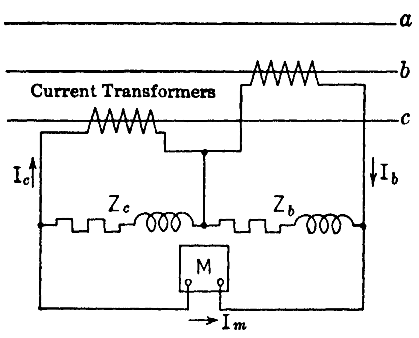

FIG. 539. Network for reading positive- and negative-sequence components of current.

Referring to the figure:

$$(I_m + I_b)Z_b + (I_m + I_c)Z_c + I_mZ_m = 0 \quad . \; . \; . \; . \quad (22)$$

Therefore:

$$I_m = -\frac{I_bZ_b + I_cZ_c}{Z_b + Z_c + Z_m} \quad . \; . \; . \; . \; . \; . \; . \; . \; . \quad (23)$$

In terms of components, remembering that there is no zero-sequence component current in an ungrounded three-wire system:

$$I_m = -\frac{h^2I_{a1}Z_b + hI_{a2}Z_b + hI_{a1}Z_c + h^2I_{a2}Z_c}{Z_b + Z_c + Z_m}$$

$$= -\frac{(h^2Z_b + hZ_c)I_{a1} + (hZ_b + h^2Z_c)I_{a2}}{Z_b + Z_c + Z_m} \quad . \; . \; . \quad (24)$$

For I_m to contain no negative-sequence component (eq. 24):

$$(hZ_b + h^2Z_c)I_{a2} = 0, \quad \text{or} \quad Z_b + hZ_c = 0$$

Then

$$Z_b = -hZ_c = Z_c\underline{/-60^\circ}, \quad \text{and} \quad Z_c = Z_b\underline{/60^\circ} \quad . \; . \; . \quad (25)$$

so that, if $Z_b = Z\underline{/0^\circ}$, $Z_c = Z\underline{/60^\circ}$, then, from (25) and (24),

$$I_{m1} = -\frac{(h^2Z + hZ\underline{/60^\circ})I_{a1}}{Z + Z\underline{/60^\circ} + Z_m} = \frac{(Z\underline{/60^\circ} + Z)I_a}{Z + Z\underline{/60^\circ} + Z_m}$$

$$= \frac{\sqrt{3}ZI_{a1}\underline{/+30^\circ}}{\sqrt{3}Z\underline{/30^\circ} + Z_m} \quad . \; . \; . \; . \; . \; . \; . \; . \; . \; . \; . \; . \; . \; . \; . \quad (26)$$

so that

$$I_{a1} = I_{m1}\frac{(\sqrt{3}Z\underline{/30^\circ} + Z_m)}{\sqrt{3}Z\underline{/+30^\circ}} = I_{m1}\left(1 + \frac{Z_m\underline{/-30^\circ}}{\sqrt{3}Z}\right) \quad . \quad (27)$$

For the positive-sequence component to disappear (eq. 24):

$$(h^2Z_b + hZ_c)I_{a1} = 0$$

Therefore

$$hZ_b + Z_c = 0 \quad . \; . \; . \; . \; . \; . \; . \; . \; . \; . \; . \quad (28)$$

Consequently

$$Z_c = Z_b\underline{/-60^\circ} \quad \text{and} \quad Z_b = Z_c\underline{/60^\circ} \quad . \; . \; . \; . \quad (29)$$

Thus, if

$$Z_c = Z\underline{/0^\circ}, \; Z_b = Z\underline{/60^\circ} \quad . \; . \; . \; . \; . \; . \; . \; . \quad (30)$$

Substituting from (30) and (28) into (24)

$$I_{m2} = -\frac{(hZ\underline{/60^\circ} + h^2Z)I_{a2}}{Z\underline{/60^\circ} + Z + Z_m} = \frac{Z(1 + \underline{/60^\circ})I_{a2}}{Z(1 + \underline{/60^\circ}) + Z_m}$$

$$= \frac{\sqrt{3}Z\underline{/30^\circ}I_{a2}}{\sqrt{3}Z\underline{/30^\circ} + Z_m} \quad \ldots\ldots\ldots\ldots\ldots \quad (31)$$

From eq. (31):

$$I_{a2} = \frac{I_{m2}(\sqrt{3}Z\underline{/30^\circ} + Z_m)}{\sqrt{3}Z\underline{/30^\circ}} = I_{m2}\left(1 + \frac{Z_m\underline{/-30^\circ}}{\sqrt{3}Z}\right) \quad \ldots\ldots \quad (32)$$

727. Bridge-Type Sequence Network.—The network of Fig. 540 suggested by Mr. C. L. Fortescue[1] makes it possible to measure simultaneously the positive- and negative-sequence components of current in a circuit which contains no zero-phase-sequence current. The two ammeters, M' and M'', should have identical impedance, Z_m; R may be a non-inductive resistance, and Z an inductive impedance such that, $Z + Z_m = (R + Z_m)\underline{/60^\circ}$. Two current transformers, T_a and T_b, of equal ratio, are connected in two of the lines, as lines a and b, and to the network as in Fig. 540. The ammeters M' and M'' will read, respectively, the positive-sequence and the negative-sequence com-

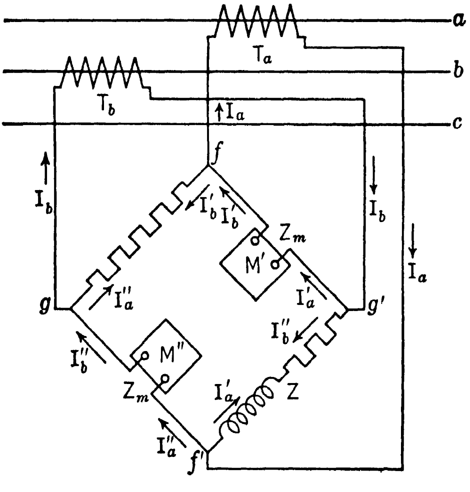

FIG. 540. Bridge-type sequence network.

---

[1] See Wagner and Evans, "Symmetrical Components," p. 286, McGraw-Hill Book Co.

ponents of the current in the third line c, reduced, of course, by the ratio of the current transformers. The impedances should be of a low enough value so that the current transformers will not be overloaded.

728. Proof of the Bridge Network. — The secondary currents I_a and I_b are assumed to divide as indicated in Fig. 540. Current I_a divides into components I_a' and I_a'' in right-hand and left-hand branches, inversely as their impedances: or

$$I_a'/I_a'' = (R + Z_m)/(Z + Z_m) \quad \ldots\ldots \quad (33)$$

But

$$I_a' + I_a'' = I_a \quad \ldots\ldots\ldots\ldots \quad (34)$$

from (33) and (34):

$$I_a''\left(\frac{R + Z_m}{Z + Z_m}\right) + I_a'' = I_a$$

or

$$I_a''(R + Z_m + Z + Z_m) = I_a(Z + Z_m)$$

Therefore:

$$I_a'' = \frac{I_a(Z + Z_m)}{R + Z_m + Z + Z_m} = I_a\frac{Z + Z_m}{D} \quad \ldots\ldots \quad (35)$$

Similarly

$$I_a' = \frac{I_a(R + Z_m)}{R + Z_m + Z + Z_m} = I_a\frac{R + Z_m}{D} \quad \ldots\ldots \quad (36)$$

I_b divides between upper and lower branches of the network as follows:

$$I_b' = I_b\frac{Z + Z_m}{R + Z_m + Z + Z_m} = I_b\frac{Z + Z_m}{D} \quad \ldots\ldots \quad (37)$$

$$I_b'' = I_b\frac{R + Z_m}{R + Z_m + Z + Z_m} = I_b\frac{R + Z_m}{D} \quad \ldots\ldots \quad (38)$$

By the principle of superposition meter M' reads $I_a' + I_b'$ while meter M'' reads $I_a'' + I_b''$.

Therefore

$$M' = I_a' + I_b' = I_a\frac{R + Z_m}{D} + I_b\frac{Z + Z_m}{D} \quad \ldots\ldots \quad (39)$$

$$M'' = I_a'' + I_b'' = I_a\frac{Z + Z_m}{D} + I_b\frac{R + Z_m}{D} \quad \ldots \quad (40)$$

Rewriting M' and M'' in terms of the sequence components of the current I_c

$$M' = (I_{c1}/D)[h^2(R + Z_m) + h(Z + Z_m)] + (I_{c2}/D)[h(R + Z_m) + h^2(Z + Z_m)] \quad . \ . \ . \quad (41)$$

$$M'' = (I_{c1}/D)[h^2(Z + Z_m) + h(R + Z_m)] + (I_{c2}/D)[h(Z + Z_m) + h^2(R + Z_m)] \quad . \ . \ . \quad (42)$$

The negative-sequence component of M'' will disappear if:

$$h(R + Z_m) = h^2(Z + Z_m), \quad \text{or} \quad R + Z_m = -h(Z + Z_m) \quad (43)$$

Then

$$M' = I_{c1}/D[(Z + Z_m)(h - 1)] = I_{c1}\left[\frac{-(R + Z_m + Z + Z_m)}{R + Z_m + Z + Z_m}\right] = -I_{c1} \quad . \ . \ . \ . \quad (44)$$

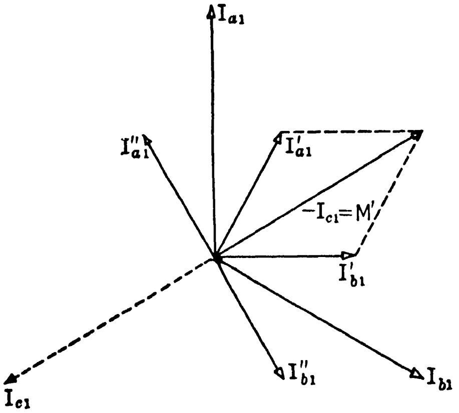

FIG. 541. Vector diagram of relations in the bridge-type sequence network (for positive-sequence values).

or meter M' reads the positive sequence component of I_c. The negative sign of I_{c1} is of significance in power measurements, etc., and is verified by the vector diagram of Fig. 541.

Note that, if

$$R + Z_m = -h(Z + Z_m), \quad Z + Z_m = (R + Z_m)\underline{/60^\circ} \quad . \ . \quad (45)$$

as stated in §727.

Substituting from eq. (43) into eq. (42):

$$M'' = (I_{c1}/D)[h^2(Z + Z_m) - h^2(Z + Z_m)] + (I_{c2}/D)[(Z + Z_m)(h - 1)] = -I_{c2} \quad . \ . \ . \quad (46)$$

Thus, the two ammeters read the two sequence components of I_c, as required.

Referring to Fig. 541, which is drawn for a symmetrical system of positive sequence, it may be seen that: $M' = I_a' + I_b' = -I_{c1}$, while $M'' = I_{a1}'' + I_{b1}'' = 0$ as it should be for this condition.

The network of Fig. 540 can be used with relays replacing the ammeters for the purpose of providing protection to electrical machines against abnormal conditions. A three-phase induction motor so protected would be removed from the circuit in case of a partial short circuit or open circuit which would unbalance the currents in the three phases and cause negative-sequence current to operate the relay which replaces the meter M''. An ordinary overload, or a complete short circuit, would actuate the M' relay.

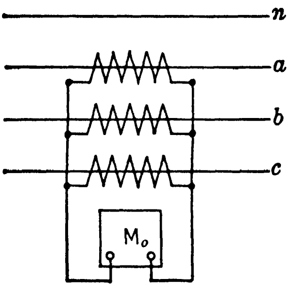

FIG. 542. Zero-sequence current network.

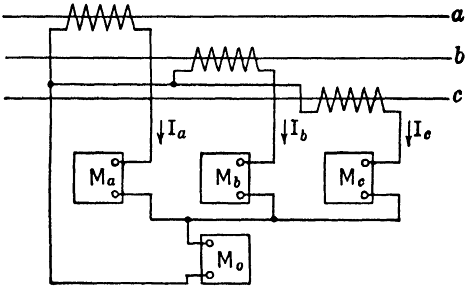

FIG. 543. Network for reading the line currents and zero-sequence component simultaneously.

729. Measurement of Zero-Sequence Current. — An obvious method for metering the zero-sequence component of current in a three-phase four-wire system, or a three-phase system with grounded neutrals, is suggested by eq. (8), §710, when written for currents, namely:

$$I_0 = \tfrac{1}{3}(I_a + I_b + I_c) \quad . \; . \; . \; . \; . \; . \; . \; . \; . \; . \quad (47)$$

Figure 542 shows three current transformers connected in parallel to a single meter M_o. Obviously M_o reads 3 times the zero-sequence current when transformers of 1 : 1 ratio are used, or $3/a \times I_0$ when the transformers have a ratio a : 1. A special scale may be provided to make the ammeter direct-reading. If it is desirable for the current transformers to serve their usual burdens, as M_a, M_b, and M_c, the network may be modified as in Fig. 543.

730. EXPERIMENT 35-B. — Measurement of Phase-Sequence Component Currents. — The methods described in §§726 to 729 should be applied in the measurement of phase-sequence components in three-phase three-wire and four-wire systems with unbalanced loads. Arrange to read the current in each line and phase relation, using wattmeters and voltmeters in the usual way (Chapter IV).

At the same time, measure phase-sequence components by the various methods suggested. Take readings first with balanced loads and with positive sequence of phases. Reverse the phase sequence and again take all readings, making sure that the networks give the expected readings. Now, having restored the positive sequence of phases, apply unbalanced non-inductive loads, then unbalanced inductive loads, and take all readings. Finally reduce the load to single-phase and take readings.

Report. First give the results with balanced loads. Next draw vector diagrams for the several examples of unbalanced load, making use of the usual readings of amperes, volts, and watts. Analyze the unbalanced currents into sequence components and compare these values with those taken by means of the sequence networks. Comment upon the results obtained and suggest other methods of measurement from a study of the literature references at the end of the chapter

POWER MEASUREMENTS

731. Real and Reactive Power due to Currents and Voltages of Positive and Negative Sequence.[2] — Consider a three-phase line with unbalanced voltages and currents. Using the theory given in §§711 to 715, and assuming no residue, we can resolve these voltages and currents into those of positive and negative sequence. But the positive-sequence currents give zero power with the negative-sequence voltages, and vice versa (§732). Consequently, there are only two components of real power, the one due to the positive-sequence currents and voltages, and the one due to the negative-sequence currents and voltages. There are also the two corresponding components of reactive power.

The two component parts of real power can be directly measured on ordinary single-phase wattmeters (or watthour meters, if energy is desired), by using "discriminating networks," such, for example, as those shown in Figs. 533 and 539. The potential circuits of the wattmeters are connected in place of the voltmeters, and the current windings in place of the ammeters. Of course, the line connections must be such as to give the correct phase angle between the current and the voltage. Furthermore, by quadraturing the potential windings, and by using similar connections, the two components of the reactive power can be measured directly (§741). Similar discriminating networks can be used with the current and potential elements of a power-factor meter (§109), and the power factor of the positive-sequence currents indicated separately from that of the negative-sequence currents. The same applies to the reactive-factor meter (§114).[3]

---

[2] For other connections of reactive-component meters see the *Electrical World*, vol. 77 (1921), p. 1491; J. Auchincloss, *General Electric Review*, vol. 27 (1924), p. 263; A. Sengel, *Elek. Zeits.*, vol. 45 (1924), p. 973.

Thus, in the most general case, a three-phase, three-wire, unbalanced load may be characterized by the following quantities:

(a) Positive-sequence voltage.
(b) Negative-sequence voltage.
(c) Positive-sequence current.
(d) Negative-sequence current.
(e) Various phase angles between the currents and the voltages.
(f) True power of positive sequence.
(g) True power of negative sequence.
(h) Reactive power of positive sequence.
(i) Reactive power of negative sequence.

Of course, not all these quantities are usually needed; moreover, not all of them are independent of one another, so that when some of them have been measured the remainder can be computed.

The question of a definite characterization of an unbalanced, three-phase load arises in connection with the problem of rates to be charged, and also in the problem of balancing the currents or the voltages. Although a discussion of these questions is outside the scope of this book, it may not be amiss to point out that a resolution of unbalanced currents, voltages, and power into their symmetrical components offers one way of analyzing charges for electric service.[4] For example, in addition to the total kilowatthours consumed, the customer may have to pay so much for the reactive energy of one or both phase sequences, and he may also be charged on the basis of " unbalance factor " (§719).

On the other hand, the power company may have to guarantee an agreed maximum unbalance factor in phase voltages at the customer's premises. Some power-consuming devices, when unbalanced, *generate* energy of negative sequence; others readily absorb such energy with a comparatively small unbalance of voltages at their terminals, and thus serve as *phase balancers*. For example, a three-phase electric furnace may cause unbalanced currents and thereby unbalance the line voltages. A synchronous or induction motor, running idle near by on the same line, offers a small impedance to currents of negative sequence and thus relieves the generators of furnishing unbalanced currents. Watthour meters of positive and negative sequence will show this difference in the behavior of the two loads, and the customer whose load absorbs negative-sequence power may be entitled to a more favorable rate than the one who causes or generates such power.

---

[3] For a general theory of energy transmission with unbalanced currents and voltages, see L. G. Stokvis, *Revue générale de l'électr.*, vol. 16 (1924), p. 979.

[4] For a different method of analysis, based on the concept of circulating energy, see V. Karapetoff, United States Patent No. 1,566,879, of Dec. 22, 1925.

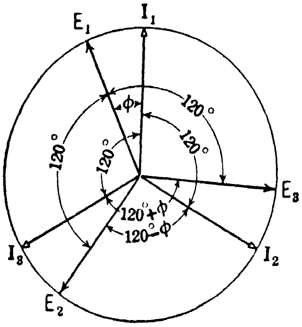

FIG. 544. A set of three-phase currents of positive sequence and voltages of negative sequence.

732. Proof that Positive-Sequence Currents and Negative-Sequence Voltages Give Zero Power. — Let I_1, I_2, I_3 (Fig. 544) be positive-sequence currents, and E_1, E_2, E_3, negative-sequence voltages. Let the phase angle between the two in the first phase be ϕ. It will be seen that the phase angle between E_2 and I_2 is $120° - \phi$, and that between E_3 and I_3 it is $120° + \phi$. Thus, the total power is given in the expression:

$$\cos\phi + \cos(120° - \phi) + \cos(120° + \phi) = \cos\phi + 2\cos 120° \cos\phi = \cos\phi - \cos\phi = 0 \qquad (48)$$

Similarly, it can be proved that positive-sequence voltages give zero power with negative-sequence currents. As a result, we conclude that, in an unbalanced three-phase system, without residue current, two independent flows of energy may be said to exist, one due to the currents and voltages of positive sequence, and the other due to those of negative sequence. These results are used in the preceding section.

733. EXPERIMENT 35-C. — Resolution of Three-Phase Unbalanced Power into Components of Positive and Negative Sequence. — The theory is given in §§731 and 732. An unbalanced three-phase load should be established and the power conditions in it analyzed, both by computation from the measured total currents and voltages, and by connecting wattmeters through discriminating networks. The difference between the behavior of a motor running idle and that of a set of stationary impedances should be investigated, and the direction of flow of negative-sequence power ascertained in both.

REFERENCES TO CHAPTERS XXXIV AND XXXV

1. C. L. Fortescue, *Trans. A.I.E.E.*, vol. 37 (1918), p. 1027, Symmetrical coordinates applied to the solution of polyphase networks.

2. R. D. Evans, *Elec. World*, vol. 85 (1925), p. 761, Finding single-phase short-circuit currents on calculating boards.

3. A. P. Mackerras, *Gen. Elec. Rev.*, vol. 29, April, 1926, July, 1926, Calculation of single-phase short-circuits by the method of symmetrical components.

4. G. W. Stubbins, *Elec. Rev.*, vol. 108, May, 1931, Volt-amperes in a circuit.

5. Edith Clarke, *Trans. A.I.E.E.*, vol. 50, September, 1931, p. 919, Simultaneous faults on three-phase systems.

6. F. M. Denton, *Inst. Elec. Eng'rs*, vol. 71, October, 1932, p. 663, Symmetrical components and their application to the phase converter.

7. A. Garnett, *Metr. Vickers Gaz.*, vol. 13, August, 1932, Phase sequence components.

8. W. C. Sealey, *Elec. Rev.*, June, 1938, Symmetrical components simplified.

9. Edith Clarke, *Gen. Elec. Rev.*, November, 1938, December, 1938, Problems solved by modified symmetrical components.

10. Wagner and Evans, Symmetrical Components, McGraw-Hill Book Co.

11. W. V. Lyon, Applications of Symmetrical Components, McGraw-Hill Book Co.

12. R. R. Lawrence, Principles of Alternating Currents, Chapter XIII, McGraw-Hill Book Co.

CHAPTER XXXVI

POWER MEASUREMENTS IN THREE-PHASE CIRCUITS

734. The general theory of measurement of electric power and energy is given in Chapters IV and V, Vol. I, and the principal types of instruments and connections are also described there. Attention is called in particular to the two-wattmeter method (§§105 and 106), which is of great importance in three-phase measurements. The treatment in this chapter is devoted to the application of the general principles to various special cases.

Balanced load and voltages. Let a three-phase load and voltages be balanced (Fig. 547); the power delivered to each phase of Y is:

$$P_{ph} = E_{10}I_1\cos\phi = E_{20}I_2\cos\phi = E_{30}I_3\cos\phi \quad . \; . \; . \quad (1)$$

Hence, the total power is:

$$P = 3E_{Y}I_{Y}\cos\phi \quad . \; . \; . \; . \; . \; . \; . \; . \; . \; . \quad (2)$$

Since $E_Y = E_\Delta/\sqrt{3}$:

$$P = \sqrt{3}\,E_\Delta I_Y\cos\phi \quad . \; . \; . \; . \; . \; . \; . \; . \; . \quad (3)$$

Equation (3) is convenient for use when the line voltage is known. With a balanced and symmetrical three-phase circuit, this equation is true whether the load is connected in Y or in any other manner, because only the line current, and not the load current, enters into it. In other words, if the load is connected, say, in delta, one can imagine an equivalent load, Y-connected, which will give the same line current and the same phase displacement between the line currents and the line voltages. Equation (3) applies either to the original or to the equivalent circuit.

735. The Three-Wattmeter Method. — With a Y-connected load, either balanced or unbalanced (Fig. 545), it is always possible to measure the total power delivered to the load by using three separate wattmeters, W_1, W_2, W_3. The current coils of the instruments are connected in series with the line conductors, and the potential circuits are connected between each terminal and the common neutral, N. The total average power is equal to the algebraic sum of the three readings. This is true whether there is a return conductor or not, although with an unbalanced load the readings and their sum will be different in the two cases.

It is of importance to observe the proper polarity of the wattmeter terminals. Referring to Fig. 93 (Vol. I), note that the ± current terminal is connected in the line toward the supply, and the unmarked terminal is connected toward the load. The ± potential terminal is connected to the current terminals; the " high range " terminal, usually marked " 150 volts," " 300 volts," etc., is connected to the opposite line. Usually, all the three readings should be positive, but, with an unbalanced load, power may be " pumped back " in one or two phases. This is possible when there is mutual inductance between the phases, or when a single-phase machine, which acts as a generator, is part of the load. For this reason, when measuring a load of unknown nature, it is essential to ascertain the direction of the flow of power in each phase. If the current or the voltage is non-sinusoidal, the accuracy of the power readings depends upon the accuracy of the instruments themselves under such conditions. The same applies to the use of current and potential transformers (Chapter XVIII). A polyphase board (§60) may be used when the load is steady; in this case only one single-phase wattmeter is needed, since then it can be transferred from one line to the other without interrupting the circuit.

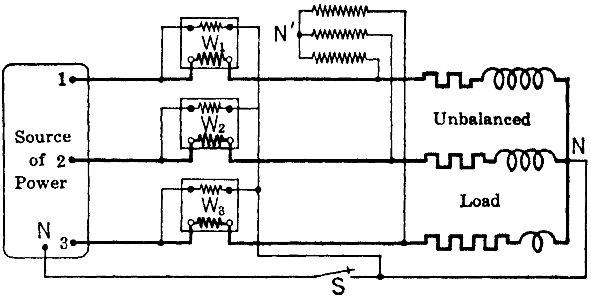

FIG. 545. Connections for measuring power in an unbalanced three-phase system by means of three wattmeters.

When a load is approximately balanced, as in motors, it is sometimes sufficient to measure the power in one phase only and to multiply the result by three. If the load neutral, N, is not accessible, an artificial neutral (point N') may be provided by connecting three equal impedances in Y. The potential terminals of the wattmeters are then connected to N', instead of N. Note that these impedances must be low in value compared with the resistance of the potential circuit of the wattmeter; otherwise the potential of N' will shift when the wattmeter is connected between any line and N'.

736. The Two-Wattmeter Method. — When there is no neutral or return conductor, the two-wattmeter method (§§105 and 106) is largely used. Its advantages over the three-wattmeter method, described above, are: (1) the neutral point is not required; (2) only the line voltages and the line currents are used, so that it is immaterial whether the load is connected in Y, delta, or any other way; (3) only two wattmeter movements are required. The moving parts of polyphase meters are usually mounted on a common shaft so that the pointer (or the dial in a watthour meter) reads the total power or energy.

This method presupposes that the third conductor serves as a common return for the other two; hence, the method should not be used when there is a neutral connection, or a fourth conductor of any kind, which carries an appreciable current, a three-phase four-wire system being equivalent to a four-phase system and therefore requiring three wattmeter movements, the fourth conductor being a common return. It is possible, however, to measure power in a four-wire system by means of two single-phase wattmeters and three current transformers.[1]

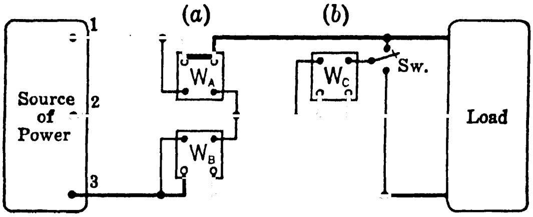

Fig. 546. Connections for measuring power in a three-wire system: (a) two-wattmeter method; (b) single-wattmeter method (for balanced loads only).

Let two wattmeter movements be connected as in Fig. 546(*a*), with vector relations as in Fig. 547. Then both component readings will be positive when the load consists of three nearly non-inductive and fairly well-balanced resistances, or of a three-phase motor running at a high power factor. If now the load should become very much unbalanced or of low power factor, one of the readings may become negative. If the motor should be converted into a generator, both readings may become negative. In such a case, it may be necessary to reverse the current or potential terminals of one or both instruments (unless the zero point of the scale is in the center), and to consider such readings negative. For example, if one wattmeter reads +140, and the other pointer deflects in the negative direction, one pair of terminals of the second movement must be reversed. If then the reading is, say, +90, the total average power of the three-phase system is 140 − 90 = 50. With two movements mounted on the same shaft, it would be wrong to reverse the terminals of one of the component wattmeters as long as the total flow of power remained in the same direction. The instrument itself subtracts a partial negative reading. Should the total deflection become negative, the polarity of both component movements should be reversed.

---

[1] B. C. Dennison, "Measurement of Power in Polyphase Systems," *Southern Electrician*, September, 1912, p. 393.

In a high-tension three-phase circuit, with two current transformers, two potential transformers, and eight meter terminals, the problem of correct connections is a serious one. The polarity markings of the transformers and of the meters must be carefully observed in order to secure correct polarity of the several terminals. For specific instructions the reader is referred to Dr. Kouwenhoven's paper.[2]

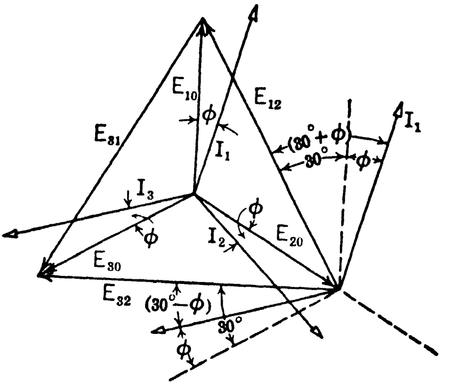

FIG. 547. Vector relations in a symmetrical three-phase system with balanced load.

In calculating the multiplying factor due to instrument transformators it should be remembered that each component wattmeter (or watthour meter) operates exactly as if it were a single-phase instrument. Individual meter readings must be multiplied by the product of the multiplying factor (ratio) due to the current transformer, and that due to the potential transformer.

737. The Watt-Ratio Curve. — With the two-wattmeter method, *on a balanced load,* the two component readings are equal to each other only when the power factor of the load is equal to unity. In this case, each reading is equal to $0.5E_\Delta I_Y\sqrt{3}$, in accordance with eq. (3). When the power factor is different from unity, the sum of the readings is still equal to P in eq. (3), but the two component readings are different from each other, for the reason explained below.

The ratio of the two readings depends on the power factor of the balanced load, and a curve may be plotted (Fig. 548) between this ratio and the power factor. This curve is sometimes useful in estimating the power factor, or as a check on the value of the power factor computed from the ammeter, voltmeter, and wattmeter readings.[8]

---

[2] W. B. Kouwenhoven, "A Method of Determining the Correctness of Polyphase Wattmeter Connections," *Proc. A.I.E.E.*, February, 1916. See also "Handbook for Electrical Metermen," N.E.L.A., New York City.

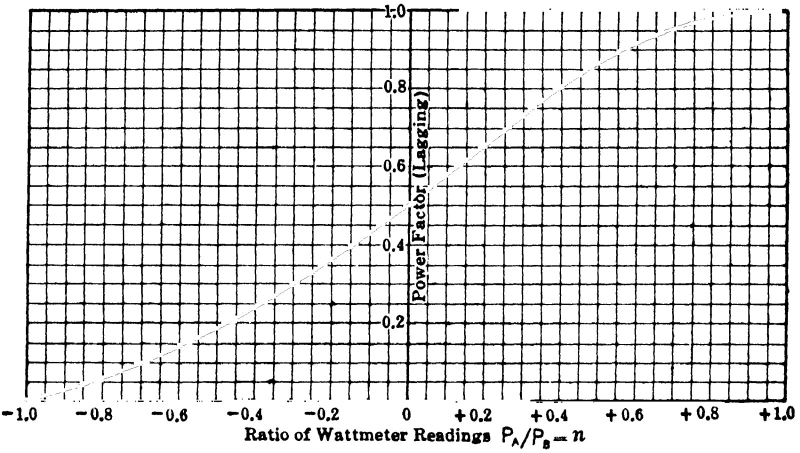

FIG. 548. The watt-ratio curve for the two-wattmeter method.

Let the two component wattmeters be connected as in Fig. 546*a* and let the circuit conditions be as shown in Fig. 547. The wattmeter *A* measures the average power:

$$P_A = E_{12}I_1 \cos (30° + \phi) \quad . \; . \; . \; . \; . \; . \; . \; . \quad (4)$$

The wattmeter *B* registers:

$$P_2 = -E_{23}I_3 \cos (150° + \phi) = E_{23}I_3 \cos (30° - \phi) \quad . \; . \quad (5)$$

the minus sign is used in order to make the expression for P_B positive; the wattmeter is assumed to be so connected that with small values of ϕ the deflection is positive.

Denoting the ratio of the two readings by n, and with balanced voltages $(E_{12} = E_{23})$ and balanced currents $(I_1 = I_3)$, we have:

$$n = P_A/P_B = \cos (30° + \phi)/\cos (30° - \phi) \quad . \; . \; . \; . \quad (6)$$

When the angle ϕ is known, n can be computed from this equation. When n is known, and it is desired to determine ϕ, eq. (6) is transformed as follows:

$$n = (\cos 30° \cos \phi - \sin 30° \sin \phi)/(\cos 30° \cos \phi + \sin 30° \sin \phi) \quad (7)$$

---

[8] For an alignment chart which serves the same purpose, see the *Electrical World*, vol. 75 (1920), p. 1095.

After division by sin 30° cos ϕ, this gives:

$$n = (\sqrt{3} - \tan\phi)/(\sqrt{3} + \tan\phi) \quad . \quad . \quad . \quad . \quad . \quad . \quad (8)$$

from which:

$$\tan\phi = \sqrt{3}(1 - n)/(1 + n) \quad . \quad . \quad . \quad . \quad . \quad . \quad . \quad (9)$$

When n is known, $\tan\phi$ can be computed; the angle ϕ itself and $\cos\phi$ can be readily found from trigonometric tables.

Since:

$$\cos\phi = (1 + \tan^2\phi)^{-0.5} \quad . \quad . \quad . \quad . \quad . \quad . \quad . \quad . \quad (10)$$

we may also write directly from eq. (10) the following expression for the power factor:

$$\cos\phi = \left[1 + 3\left(\frac{1-n}{1+n}\right)^2\right]^{-0.5} \quad . \quad . \quad . \quad . \quad . \quad . \quad . \quad (11)$$

This is the equation of the curve shown in Fig. 548.

For convenience in calculating power factor from the two wattmeter readings, eq. (11) may be changed to the form:

$$\cos\phi = \left[1 + 3\left(\frac{P_B - P_A}{P_B + P_A}\right)^2\right]^{-0.5} = \frac{1}{\sqrt{1 + 3\left(\frac{P_B - P_A}{P_B + P_A}\right)^2}} \quad . \quad . \quad (11a)$$

The following characteristic points on this curve can be obtained from eq. (6):

ϕ	Cos ϕ	$P_A/P_B = n$	
90°	0	−1	Current lagging
60°	0.5	0	Current lagging
0°	1.0	+1	Current in phase
−60°	0.5	∞	Current leading
−90°	0	−1	Current leading

Thus, when the current and the voltage are in phase, both P_A and P_B are positive and equal to each other. When the current is lagging, the reading P_A is smaller than P_B. P_A becomes equal to zero at a power factor of 50 per cent, and then becomes negative. With a leading current, P_A is greater than P_B, and this is one way of discovering when the current becomes leading. At a power factor of 50 per cent, with the current leading, P_B becomes equal to zero, and n becomes infinitely great. The part of the curve for the leading current is not plotted, because the same curve can be used for the inverse ratio, P_B to P_A.

738. Supplementary Proof of the Two-Wattmeter Method. — A proof of the accuracy of the two-wattmeter method, similar to that given in §106, but expressed in vector notation,[4] is as follows: Referring to Fig. 549 for the unsymmetrical, unbalanced case of the general three-wire system, with wattmeters connected as in Fig. 546*a*:

$$P_1 = \mathbf{E}_{12} \cdot \mathbf{I}_1$$

$$P_2 = \mathbf{E}_{32} \cdot \mathbf{I}_3 \qquad (12)$$

Since $\mathbf{E}_{12} = \mathbf{E}_{10} - \mathbf{E}_{20}$, and $\mathbf{E}_{32} = \mathbf{E}_{30} - \mathbf{E}_{20}$

$$P_1 + P_2 = \mathbf{E}_{10} \cdot \mathbf{I}_1 - \mathbf{E}_{20} \cdot \mathbf{I}_1 + \mathbf{E}_{30} \cdot \mathbf{I}_3 - \mathbf{E}_{20} \cdot \mathbf{I}_3 \qquad (13)$$

But $-(\mathbf{I}_1 + \mathbf{I}_3) = \mathbf{I}_2$, and so

$$P_1 + P_2 = \mathbf{E}_{10} \cdot \mathbf{I}_1 + \mathbf{E}_{20} \cdot \mathbf{I}_2 + \mathbf{E}_{30} \cdot \mathbf{I}_3 \qquad (14)$$
$$= \text{total power.}$$

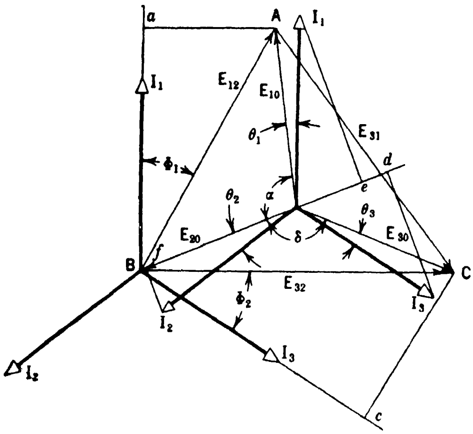

FIG. 549. Vector relations in the measurement of power by the two-wattmeter method.

739. The Single-Wattmeter Method. — In Fig. 546 (*b*) a single wattmeter is shown, with its current coil permanently in line 2, and its potential coil alternately from 2 to 1, and from 2 to 3. The two readings so obtained constitute the single-wattmeter method of measuring power, suitable for symmetrical three-phase systems with balanced load (such as a three-phase motor), but inaccurate for unsymmetrical systems or unbalanced loads. For the balanced case (see Fig. 547), calling the two readings P_c' and P_c'':

---

[4] It is assumed that the reader is familiar with the system of vector notation in which such an expression as $E \cdot I$, called the " dot product " or " scalar product " of the two vectors, is equivalent to $E \times I \times \cos \theta_E{}^I$, i.e., the product of the absolute values of the vectors and of the cosine of the phase angle between (product of in-phase components).

$$P_c' = \mathbf{I}_2 \cdot \mathbf{E}_{21} = \mathbf{I}_2 \cdot \mathbf{E}_{20} - \mathbf{I}_2 \cdot \mathbf{E}_{10} \quad . \quad . \quad . \quad . \quad (15)$$

$$P_c'' = \mathbf{I}_2 \cdot \mathbf{E}_{23} = \mathbf{I}_2 \cdot \mathbf{E}_{20} - \mathbf{I}_2 \cdot \mathbf{E}_{30} \quad . \quad . \quad . \quad . \quad (16)$$

$$P_c' + P_c'' = 2\mathbf{I}_2 \cdot \mathbf{E}_{20} - \mathbf{I}_2 \cdot (\mathbf{E}_{10} + \mathbf{E}_{30})$$

For the symmetrical, balanced case $I_1 = I_2 = I_3 = I$; $E_{10} = E_{20} = E_{30} = E$; and $\mathbf{E}_{10} + \mathbf{E}_{30} = -\mathbf{E}_{30}$. Therefore, for the case in question,

$$P_c' + P_c'' = 3\mathbf{E} \cdot \mathbf{I} = \text{total power}$$

740. EXPERIMENT 36-A. — Exercises with the Two-Wattmeter and Single-Wattmeter Methods. — The methods are described in §§736 and 739. The purpose of the experiment is to obtain experience in measuring three-phase power under various conditions of load, power factor, etc., and to determine the limitations of each method. Two separate single-phase wattmeters should preferably be used for the two-wattmeter method, in order to obtain component readings and to study the effect of reversed connections.

(1) Begin with a balanced non-inductive three-phase load, and, for both instruments, find the polarity with which the component readings are positive. Satisfy yourself as to the minus sign before E_{23} in eq. (5). Check the sum of the readings by the two-wattmeter method with the sum of the three readings, using the three-wattmeter method (§735). Take readings also by the single-wattmeter method.

(2) Unbalance the load, and introduce a neutral connection, with a switch. Measure the power by the three methods with the neutral open. For the two-wattmeter and three-wattmeter methods, the total power should be the same. Now close the neutral connection and repeat the measurements. The results obtained by the three methods will no longer check. To show that in this case both the single-wattmeter and the two-wattmeter methods are incorrect, choose another line conductor for the common return and show that for each case the sum of the two readings is different from the values previously obtained.

(3) Select a balanced partly inductive load. A synchronous motor (Chapter XLIV), driving a generator, is convenient for this purpose because the power consumed can be easily varied by changing the generator output, and the current can be made either lagging or leading at will, by adjusting the field excitation of the motor. Choose a load and a convenient lagging current; measure the total power by the three methods; also read the line volts and the line amperes. Check the value of the power factor obtained from the curve in Fig. 548 with that computed from eq. (3). Note whether this curve applies to the single-

wattmeter readings. Show that the sum and the ratio of the component readings remain the same, no matter which of the three conductors is taken as the return wire. Find out the phase sequence, using one of the methods described in §700. Keep the load approximately the same and cause the current to lead the voltage. Note the change in the relative values of the two component readings.

(4) Take a few readings with an unbalanced, partly inductive load.

(5) Arrange a three-phase line with an unbalanced load, and let it not be known on which side is the generator and on which side the load. Connect the two wattmeters (or a polyphase watthour meter) so as to measure correctly the total power (or energy) and find the direction of flow of the energy. In other words, find by purely electrical means, and without access to any terminal apparatus, the direction in which energy is flowing along the line.

In summarizing the results of this experiment, arrange the readings under the various conditions in tabular form. State the limitations of each method of measuring power. Note that when the larger of the two wattmeter readings, for balanced inductive load, is less than $0.866EI$, the power factor of the load is less than 50 per cent.

741. Reactive-Component Wattmeters. — Sometimes it is required to measure reactive volt-amperes (§107) delivered to a three-phase load. This is done, for example, when it is desired to control the amount of reactive power furnished by each of two or more interconnected stations; when a load is to be adjusted for a desired power factor; when, in the rates charged for energy, there is a penalty for low power factor; etc. The measurement of reactive power in a single-phase circuit is discussed in §§107, 108, and 114. In a three-phase circuit, the reactive power may be defined as the algebraic sum of the readings of two or three wattmeters whose potential circuits have been " quadratured " with respect to the connections for measuring the true power (§§735 and 736). By quadraturing is meant connecting to a source of voltage of the same magnitude but displaced by 90 degrees in phase. This applies specifically to the three-wattmeter connections in Fig. 545 and to the two-wattmeter connections in Fig. 546. It is understood, of course, that if the source of voltage for one of the three wattmeters is turned by 90 degrees, so as to lead the original voltage, the voltages for the other two wattmeters must also be turned in the leading and not in the lagging direction. The proper polarity for the two-wattmeter method is shown in Figs. 550 to 552.

When the load is balanced, the reactive volt-amperes (or reactive power) is:

$$P_r = \sqrt{3}\, E_\Delta I_Y \sin\phi \quad . \; . \; . \; . \; . \; . \; . \; . \; . \quad (17)$$

as may be seen by analogy with eq. (3); sin ϕ is called the reactive factor (§107). For computation of reactive power in an unbalanced system, see §743.

There are various ways of connecting standard polyphase wattmeters (or watthour meters) so as to read reactive volt-amperes, and a few examples are given below to illustrate the principal possibilities.

(a) *Resistance and capacitance in the potential circuit.* In an ordinary single-phase induction-type wattmeter or watthour meter (§§102 and 125) the flux in the potential circuit is made to lag by exactly 90 degrees behind the applied voltage. As a result, the meter torque is proportional to the voltage times the current in phase with it. If, instead, this potential flux is caused to be exactly in phase with the applied voltage, the meter will read the product of the voltage times the current in quadrature with it, in other words, the reactive volt-amperes. This can be accomplished approximately by using a high non-inductive resistance (in place of a choke coil) in series with the potential winding. A small phase angle will be left, owing to unavoidable inductance in the circuit; to reduce the angle to zero, a condenser is connected across the resistance, to compensate for this inductance.

Such a " quadratured " meter will indicate reactive volt-amperes in a single-phase circuit. Consequently, if three of them are connected between each phase and the neutral (§735), the algebraic sum of their readings will represent the total reactive power. Two wattmeter movements can be used in a single instrument, as in Figs. 551 and 552.

When there are appreciable higher harmonics in the voltage wave, the substitution of a resistance for a reactance is only approximately correct. A resistance allows higher harmonics of current in the same proportion in which they are present in the voltage, while a reactance cuts their magnitude down in proportion to their frequency. In the two methods described below, the same inductances are used in measuring the reactive and the real power, and therefore the inaccuracy, if any, is the same in both cases.

(b) *Standard potential transformers, special meter scale.* Let Fig. 550 represent the currents and the voltages in a balanced three-phase system. The real power in phase 1 is $I_1E_{10}\cos\phi$. The reactive power may be obtained by connecting the current winding of a single-phase wattmeter in phase 1, and the potential winding to a source of voltage equal to and in quadrature with E_{10}. It will be seen from Fig. 550 that the voltage E_{23} is in quadrature with E_{10}, and is numerically equal to $E_{10}\sqrt{3}$. Thus, if E_{23} is used as the source of voltage, the wattmeter will register $E_\Delta I_Y \sin\phi$. By comparison with eq. (17), we see that it is only necessary to multiply the reading by $\sqrt{3}$, or to calibrate the scale accordingly.

In practice, a polyphase wattmeter connected on this principle is sometimes used (Fig. 551). The total reading is then $2E_\Delta I_Y \sin \phi$, and to obtain the true reactive volt-amperes, the result must be divided by $2/\sqrt{3} = 1.155$. In Fig. 551 the two inner sets of meter terminals are for the currents, and the two outer ones for the potential connections. The letters R (right) and L (left) refer to the right and left of the observer who is viewing the meter from the front. The current I_1 and the voltage E_{23} are applied to the left-side terminals of the meter, I_3 and E_{12} to the right-side terminals.

The polarity of the terminals must be carefully observed in order to make the readings cumulative. When the vector I_1 (Fig. 550) is resolved into its components, Ob and ba, it will be seen that the reading is proportional to the reactive component, ba. When the current becomes leading, the wattmeter pointer indicates in the opposite direction, so that a scale with zero in the center is preferable. A watthour meter, connected as in Fig. 551, will run in one or the other direction according to whether the current is leading or lagging. If the customer is to be penalized for the lagging current but not given credit for the leading current, the meter should have some kind of ratchet attachment to keep it from running backward. On low voltage, the potential transformers can be omitted, or replaced by auto-transformers.

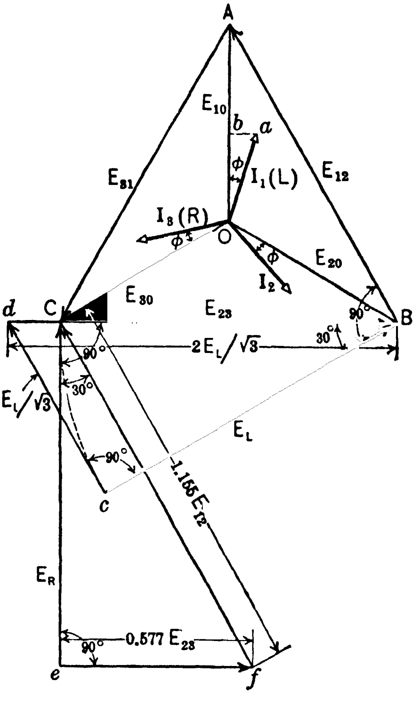

FIG. 550. A vector diagram to explain relations with connections as in Figs. 551 and 552.

(c) *Standard meter scale, special potential transformers.* In measuring reactive power, it is of considerable practical advantage to be able to use wattmeters (and watthour meters) with a standard scale. In Fig. 546, let the potential circuit of the meter A be connected to some source of voltage equal to E_{12} but in time quadrature with it. Similarly, let the potential circuit of the meter B be connected to an emf equal to and in quadrature with E_{23}. Let the polarity of the connections be such that the meter shaft is subjected to the difference of the two torques. Then, by analogy with eqs. (4) and (5), we have:

$$P_{rA} + P_{rB} = E_{\Delta} I_{Y}[\sin\ (30^\circ + \phi) - \sin\ (30^\circ - \phi)]$$
$$= E_{\Delta} I_{Y}\ \sin \phi\sqrt{3} \qquad (18)$$

This agrees with eq. (17), and the meter will register the total reactive power.

In Fig. 550, the voltage $cB = E_L$ of the above mentioned other source is numerically equal to E_{12}, and lags behind it by 90 degrees; therefore, E_L is the correct voltage for the first reactive meter. Resolving E_L into the components, cd and dB, in phase with E_{12} and E_{23} respectively, we have for the absolute values:

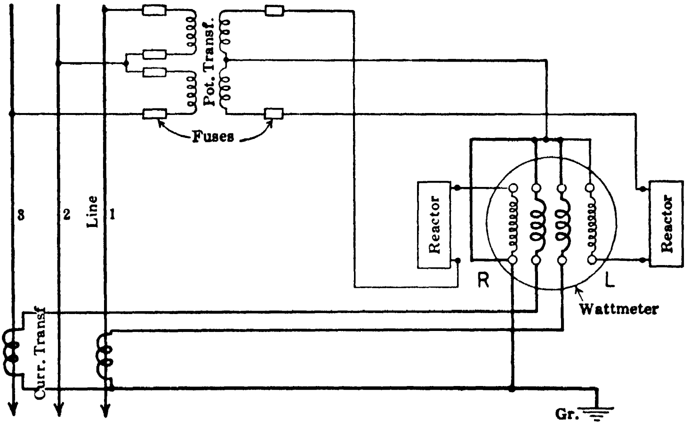

FIG. 551. Connections of a polyphase induction-type wattmeter to read reactive power; standard potential transformers and a special scale.

$$cd = E_L \tan 30^\circ = 0.577E_{23} = 0.577E_{12} \qquad (19)$$

$$dB = E_L/\cos 30^\circ = 1.155E_{23} \qquad (20)$$

Hence, *geometrically,*

$$E_L = cd + dB = 0.577E_{12} + 1.155E_{23}$$

or, factoring out 1.155,

$$E_L = 1.155(0.5E_{12} + E_{23}) \qquad (21)$$

A diagram of connections embodying this principle is shown in Fig. 552. On the L (or left-hand) side of the meter, the series coil carries the current in phase 1, and the potential circuit is connected across a secondary voltage equal to one-half of E_{12} plus E_{23}. The potential transformers are wound for a secondary voltage 15.5 per cent above a standard voltage. For example, instead of the ratio of 6600 to 110 volts, they are wound for 6600 to 110 × 1.155 volts. This takes into account the factor 1.155 in eq. (21).

On the right-hand side of the meter, the voltage E_R (Fig. 550) is in quadrature with E_{23}, and E_R consists of $0.577E_{23}$ plus $1.155E_{12}$, so that the same potential transformers may be used. The meter runs in one or the other direction, depending on whether the current is leading or lagging. If standard potential transformers are used, the meter readings must be multiplied by the factor 1.155. The same factor applies if there are no potential transformers.[5]

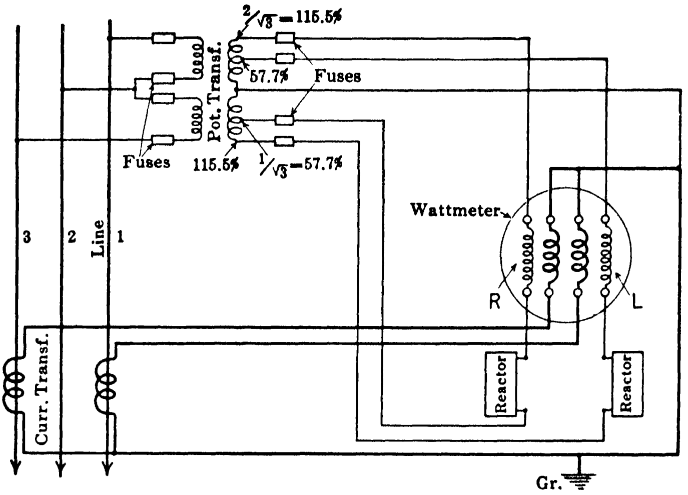

FIG. 552. Connections for a polyphase induction-type wattmeter used to measure reactive power; special potential transformers and a standard scale.

742. EXPERIMENT 36-B. — Measurement of Reactive Power in a Three-Phase System. — The purpose of the experiment is to familiarize the student with the methods described in the previous section. Particular attention should be paid to checking the reactive volt-amperes obtained by either method with those obtained by metering the power in the usual way and calculating power factor and reactive

[5] For other connections of reactive-component meters see the *Electrical World*, vol. 77 (1921), p. 1491; J. Auchincloss, *General Electric Review*, vol. 27 (1924), p. 263; A. Sengel, *Elek. Zeits*, vol. 45 (1924), p. 973. For reactive power in an unbalanced circuit, see §731.

factor from amperes, volts, and watts. Another check is that the total reading on a non-inductive load must be zero. A polyphase meter should indicate in one direction or the other, depending upon whether the load is of leading or lagging power factor.

REFERENCES

1. A. E. KNOWLTON, Electric Power Metering, McGraw-Hill Book Co.
2. NATIONAL ELECTRIC LIGHT ASSOCIATION, Handbook for Electrical Metermen.
3. P. C. JONES, *Trans. A.I.E.E.*, vol. 43, p. 356, Three-phase wattmeter connections.
4. J. AUCHINCLOSS, *Gen. Elec. Rev.*, May and July, 1928, Methods for connecting wattmeters.
5. V. H. TODD, *Elec. Jour.*, 1922, p. 477, Calibration data on polyphase wattmeters.
6. H. K. HUMPHREY, *Jour. A.I.E.E.*, May, 1926, A method for determining the sign of the smaller wattmeter reading in balanced three-phase power measurements.
7. W. B. KOUWENHOVEN, *Proc. A.I.E.E.*, February, 1916, A method of determining the correctness of polyphase wattmeter connections.

CHAPTER XXXVII

THREE-PHASE DELTA-, V-, AND T-CONNECTED SYSTEMS

743. The Y connection described in Chapter XXXIII is more used than any other in three-phase machinery. In a comparatively few cases some other connections have certain advantages, for example, lower first cost, suppression of higher harmonics, possibility of phase transformation, etc. Three kinds of connections, known as delta, V, and T, are shown in Fig. 553 and are described below.

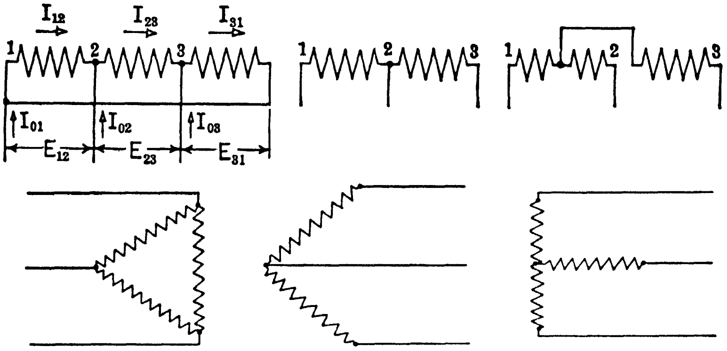

(*a*) Delta (*b*) Vee (*c*) Tee

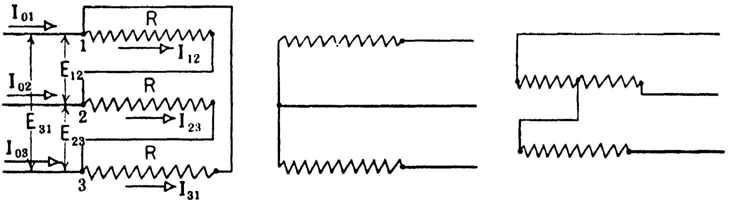

FIG. 553. Delta, V, and T connections represented by straight-line, geometric, and parallel-line diagrams.

The names of these connections are due to a similarity between their conventional representations and the corresponding letters of the alphabet (Fig. 553, top row). However, experience has shown that there is a possibility of confusion between a vector diagram of voltages and a similarly drawn diagram of connections. For this reason, some prefer the " parallel-line " representation of connections, as indicated in the middle row, or " straight-line " arrangement as in the lower row.

DELTA CONNECTION

744. Current and Voltage Notation. — Let three equal non-inductive resistances, R, be connected in delta to a source of symmetrical three-phase voltages, E, as shown in Fig. 553*a*. Let the generator be located below the line and be Y-connected. The six voltages shown in Fig. 554 are the same as those in Fig. 519, and the line currents, I_{01}, I_{02}, I_{03}, are shown in phase with the corresponding phase voltages, E_{10}, E_{20}, E_{30}, since the load is assumed to be non-inductive. As explained in §§695 and 696 double subscripts are used for line currents in order to indicate explicitly that a line current is to be considered positive at the instants when it flows *from* the generator neutral *to* a load terminal. For the load current in the phase 1-2 we have:

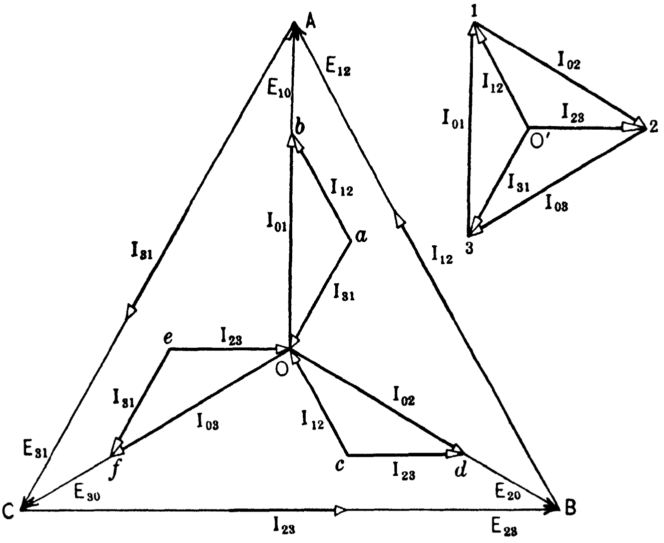

Fig. 554. Voltage and current relations with a delta-connected, non-inductive, balanced load.

$$I_{12} = E_{12}/R \quad . \quad . \quad . \quad . \quad . \quad . \quad . \quad . \quad . \quad . \quad . \qquad (1)$$

and the corresponding formulas for the other two phases. The load being non-inductive, the delta currents are shown in Fig. 554 in phase with the corresponding line voltages.

The subscript 1-2, in application to the voltage, means (§§695 and 696) that instantaneous values of the voltage E_{12} are to be considered positive when point 1 is actually at a higher potential than 2. But at such instants the current flows from 1 to 2, so that the current subscript is identical with the voltage subscript. On the other hand, the voltage notation 1-0 in this case refers to the generator neutral, and when this voltage is positive, the current flows from 0 to 1. Hence, the current subscript is 0-1, that is, the inverse of the voltage subscript 1-0. The difference is due to the fact that in a load the current flows from a point of higher potential to a point of lower potential; in a generator, with the same convention as to signs, the current flows in the opposite direction. This shows that the current vectors must be carefully marked in accordance with the physical interpretation of the diagram of connections, in order to get consistent and correct results.

745. Relation between Delta and Y Currents in a Balanced System. — The first Kirchhoff law applied to the vectors of current at point 1 (Fig. 553*a*) gives:

By analogy:

$$\left.\begin{aligned} I_{01} + I_{31} &= I_{12} \\ I_{02} + I_{12} &= I_{23} \\ I_{03} + I_{23} &= I_{31} \end{aligned}\right\} \quad \ldots\ldots\ldots\ldots \quad (2)$$

Adding the three equations gives:

$$I_{01} + I_{02} + I_{03} = 0 \quad \ldots\ldots\ldots\ldots \quad (3)$$

which expresses the first Kirchhoff law at the generator neutral, and means that the vectors of the three line currents form a closed triangle.

This triangle is shown in Fig. 554, in the upper right-hand corner. Vectors drawn from the center, *O′*, of this triangle to its vertices represent the delta currents, in magnitude and in direction, because they satisfy eqs. (2), and are also in phase with the corresponding line voltages. Equations (12) are also represented graphically by the triangles *Oab*, *Ocd*, *Oef*. It will be seen that, numerically,

$$I_{\Delta} = I_{Y}/\sqrt{3} \quad \ldots\ldots\ldots\ldots \quad (4)$$

The current I_{12} leads I_{01} by 30 degrees and leads I_{02} by 150 degrees; I_{12} lags behind I_{03} by 90 degrees.

These relations can be expressed in the following vectorial notation:

$$I_{12} = (I_{01}/\sqrt{3})e^{j\pi/6} = (I_{02}/\sqrt{3})e^{j5\pi/6} = (I_{03}/\sqrt{3})e^{-j\pi/2} \quad \ldots\ldots \quad (5)$$

or in the form:

$$I_{12} = (I_{01}/\sqrt{3})\underline{/30^\circ} = (I_{02}/\sqrt{3})\underline{/150^\circ} = (I_{03}/\sqrt{3})\underline{/-90^\circ} \quad \ldots \quad (6)$$

Now let the load consist of three balanced impedances, in place of the resistances *R*. The vector diagram is shown in Fig. 555; it differs from Fig. 554 only in that there is a phase angle, ϕ, between the delta currents and the delta voltages. As a result, the Y currents are also displaced with respect to the Y voltages by the same angle, ϕ.

746. Unbalanced Delta System. — A general case of unsymmetrical delta connection, with unbalanced line voltages and an unbalanced load, is shown in Figs. 556 and 557. The load in phase 1–2 consists of a resistance R and a reactance X; for this reason the current I_{12} is shown lagging behind E_{12} by an angle ϕ_{12}. The load in phase 2–3 consists of a resistance R' shunted by a condenser, C, and of a resistance R'' in series with the two. The current is leading, and this is indicated by the angle ϕ_{23}. In the phase 3–1 an emf, E, is assumed to be connected in series with the resistance r, and the current I_{31} is shown lagging behind E_{31} by the angle ϕ_{31}.

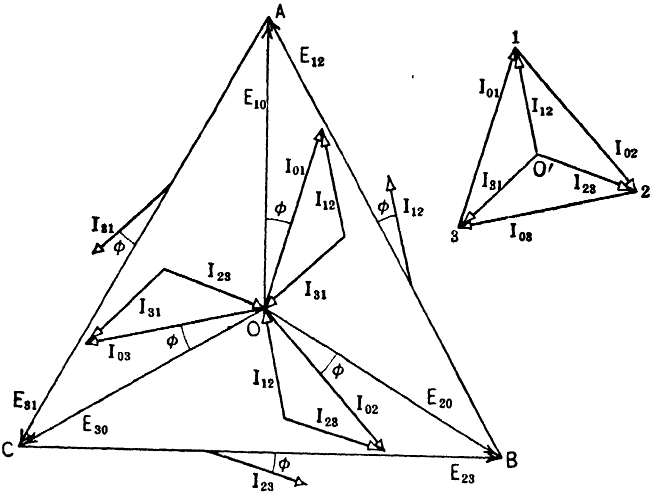

FIG. 555. Voltage and current relations with a delta-connected, partly inductive balanced load.

The same three current vectors are drawn from point O'; by connecting their ends, the triangle of the line currents, 1, 2, 3, is obtained.

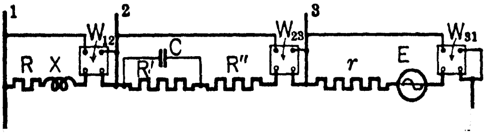

FIG. 556. An unbalanced, delta-connected load measured by means of three wattmeters.

Equations (2) and (3) hold true for either a balanced or an unbalanced load, but the relationship (4) is true only for a balanced delta. A wattmeter, W, is shown connected in each phase of the delta, to indicate that the total power can be measured in this manner, if so desired. The result should check with the power measured in the line by the three-wattmeter or two-wattmeter method (§§735 and 736).

It will be seen from the triangle of the currents that *for a given vector set of delta currents there is only one corresponding set of Y currents,* but the converse is not true. Thus, if the delta currents are known, it is possible to compute the line currents, but not vice versa.

In the triangle of voltages (Fig. 557), the point O is arbitrary, so that the set of Y voltages shown is only one out of an infinite number of possible combinations. Nevertheless, the Y currents are perfectly definite; and if the point O is shifted, say to O'', only the phase angles ϕ_1, ϕ_2, ϕ_3 would thereby be modified, but not the current vectors themselves.

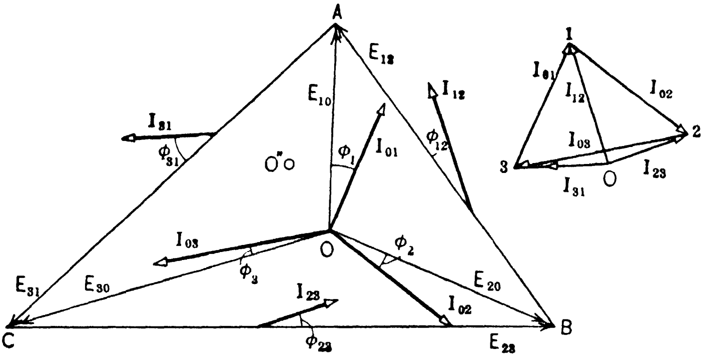

FIG. 557. Vector diagrams showing the relations in Fig 556.

Delta currents can be resolved into symmetrical components by the methods explained in Chapter XXXIV. Since their sum usually is not zero the zero-sequence component must not be overlooked.

Sometimes a load is supplied through three dissimilar transformers, connected in delta. Since they have different percentages of internal ohmic and reactive drop, there is an appreciable unbalance of the secondary voltages and there are circulating currents in the transformer windings.[1] An extreme example of this is treated in §752, where the problem of transformer banks in delta and in V, operating in parallel, is solved by the method of symmetrical components.

747. EXPERIMENT 37-A. — Study of the Delta-Connected Systems. — The electrical relationships in a delta-connected three-phase system are explained in the preceding sections, and the purpose of the experiment is to check them in a specific case. The generator used should preferably be Y-connected; if power is supplied from an inaccessible source, an artificial neutral should be provided.

---

[1] See J. B. Gibbs, *Electric Journal,* 1925, p. 121.

(1) Connect a balanced non-inductive load in delta to the Y-connected voltage supply and check the square-root-of-three ratio between the currents and between the voltages. Show directly by wattmeter readings that the total power measured in the line is equal to that absorbed by the resistances. Check experimentally the phase displacements between the Y currents and the delta currents, according to Fig. 554.

(2) Perform similar measurements with a balanced, partly inductive load.

(3) Unbalance the load in one phase in steps, and at each step take careful readings of all the currents and voltages necessary for constructing a diagram similar to the one shown in Fig. 557. Be sure to measure phase angles, as otherwise the data may be insufficient for a vector diagram. Check the total power absorbed in the load with that measured in the line.

Report. Follow the theory given in §§745 and 746 and confirm the statements made there by means of experimental data. Point out discrepancies and inaccuracies, if any, and indicate possible reasons for them. Draw vector diagrams for each condition studied.

748. Equivalent Unbalanced Delta and Y Combinations. — In §698 one method given for the solution of problems involving unbalanced loads was the substitution of an equivalent delta of impedances for a load of three unequal impedances in Y. It remains to prove the relations there stated.

The delta of impedances or admittances equivalent to a given Y. Consider the general case of three unequal admittances, Y_{12}, Y_{23}, Y_{31}, connected in delta, and another set of unequal admittances, Y_1, Y_2, Y_3, connected in Y. Let it be required to find the conditions which these six quantities must satisfy in order to be called equivalent, in the sense of the definition given in §698. We shall assume the applied phase voltages to be unbalanced, and shall show that they are eliminated from the results, so that two sets of impedances which are equivalent on a given combination of three-phase unsymmetrical voltages will be equivalent on any combination of voltages.

Let some arbitrarily chosen point in the generator winding, or on the line, be permanently grounded, and let the alternating potentials of the three line terminals, 1, 2, 3 (to which the given admittances are to be connected), be A, B, C (Figs. 518 and 556). Let the alternating potential of the load neutral, for the Y-connected admittances, be N. Then the alternating voltage across the admittance Y_1 is $A - N$, and the corresponding current is $Y_1(A - N)$. In the following theory all the voltages and admittances are assumed to be expressed as complex quantities or vectors. The first Kirchhoff law at the load neutral gives:

$$Y_1(A - N) + Y_2(B - N) + Y_3(C - N) = 0 \quad . \; . \; . \quad (7)$$

from which:

$$N = (Y_1A + Y_2B + Y_3C)/\Sigma Y_y \quad . \; . \; . \; . \; . \; . \quad (8)$$

where

$$\Sigma Y_y = Y_1 + Y_2 + Y_3 \quad . \; . \; . \; . \; . \; . \; . \; . \; . \quad (9)$$

Consequently, the current in phase 1 is:

$$\begin{aligned} I_1 &= Y_1(A - N) = Y_1(A\Sigma Y_y - Y_1A - Y_2B - Y_3C)/\Sigma Y_y \\ &= (A - B)Y_1Y_2/\Sigma Y_y - (C - A)Y_3Y_1/\Sigma Y_y \quad . \; . \; . \; . \; . \; . \quad (10) \end{aligned}$$

With the delta-connected load, the current through the admittance Y_{12} is equal to $(A - B)Y_{12}$, and the current through Y_{31} is $(C - A)Y_{31}$.

Applying the first Kirchhoff law at the terminal 1, we get for the line current in phase 1:

$$I_1 = (A - B)Y_{12} - (C - A)Y_{31} \quad . \; . \; . \; . \; . \; . \quad (11)$$

Since the two sets of admittances are by assumption equivalent, this I_1 is equal to that in eq. (10). Combining the two equations, we get:

$$\begin{aligned} (A - B)Y_1Y_2/\Sigma Y_y &- (C - A)Y_3Y_1/\Sigma Y_y \\ &= (A - B)Y_{12} - (C - A)Y_{31} \quad . \; . \; . \; . \quad (12) \end{aligned}$$

This expression must hold true for any arbitrarily chosen values of A, B, C. Consequently, it must be an identity, and by equating the coefficients we get:

$$Y_{12} = Y_1Y_2/\Sigma Y_y \quad . \; . \; . \; . \; . \; . \; . \; . \; . \quad (13a)$$

By analogy,

$$Y_{23} = Y_2Y_3/\Sigma Y_y \quad . \; . \; . \; . \; . \; . \; . \; . \; . \quad (13b)$$

$$Y_{31} = Y_3Y_1/\Sigma Y_y \quad . \; . \; . \; . \; . \; . \; . \; . \; . \quad (13c)$$

If, in eqs. (13), one substitutes for Y_{12} its equivalent, $1/Z_{12}$, for Y_1 the expression $1/Z_1$, etc., eqs. (13) of §698 immediately follow.

For the special case of balanced load, with $Y_1 = Y_2 = Y_3$, substitution into eqs. (13) shows that

$$Y_\Delta = Y_y/3 \quad . \; . \; . \; . \; . \; . \; . \; . \; . \; . \quad (14)$$

and:

$$Z_\Delta = 3Z_y \quad . \; . \; . \; . \; . \; . \; . \; . \; . \; . \; . \quad (15)$$

These relations are often convenient in the solution of problems involving transmission lines and delta-connected transformer banks or loads, etc.[2] Multiplying eq. (13*a*) by Y_3, eq. (13*b*) by Y_1, and eq. (13*c*) by Y_2, we find that:

$$Y_{12}Y_3 = Y_{23}Y_1 = Y_{31}Y_2 \quad . \; . \; . \; . \; . \; . \; . \; . \; . \quad (16)$$

The Y equivalent of a given delta. Equations (13) to (16) are convenient when Y-connected impedances (or admittances) are given, and it is required to compute the equivalent delta-connected admittances. When, however, the latter are given, and the values of the equivalent Y-connected impedances are required, we proceed as follows: By combining eqs. (13), we get:

$$Y_{12}Y_{23} + Y_{23}Y_{31} + Y_{31}Y_{12} = Y_1Y_2Y_3/\Sigma Y_y = Y_1Y_{23} \quad . \; . \quad (17)$$

from which:

$$Y_1 = Y_{12} + Y_{31} + (Y_{12}Y_{31}/Y_{23}) \quad . \; . \; . \; . \; . \; . \quad (18)$$

Similar expressions may be derived for Y_2 and Y_3, by a cyclic substitution of the subscripts. Equation (18) can be further transformed by using the impedances of the six branches, that is, the reciprocals of the six admittances. We then get, after some transformations,

$$Z_1 = Z_{12}Z_{31}/\Sigma Z_\Delta \quad . \; . \; . \; . \; . \; . \; . \; . \; . \quad (19)$$

and similar expressions for Z_2 and Z_3, by a cyclic transformation of the subscripts. In these expressions:

$$\Sigma Z_\Delta = Z_{12} + Z_{23} + Z_{31} \quad . \; . \; . \; . \; . \; . \; . \; . \; . \quad (20)$$

When the impedances are equal, eq. (19) gives $Z_y = Z_\Delta/3$, which agrees with eq. (15).[3]

749. EXPERIMENT 37-B. — Study of Equivalent Y and Delta Impedances. — The theory is explained in §748. First a balanced circuit should be investigated and eqs. (14) and (15) verified. Then a set of unbalanced delta-connected impedances should be tested on a symmetrical three-phase line and checked against a set of equivalent Y-connected impedances as found by eq. (19). Finally the same two sets of impedances should be tested with unsymmetrical applied voltages. Any failure of the experimental results to check the theoretical formulas should always be investigated. The formulas and relations deduced hold true only for vectors or complex quantities, and not merely for the absolute values. This should be kept in mind in checking experimental results.

---

[2] O. G. C. Dahl, "Electric Circuits, Theory and Applications," Chapter 1, McGraw-Hill Book Co.

[3] See also Chapters II and III in the pamphlet mentioned in the footnote at the end of §702.

V CONNECTION

750. In Fig. 475, *aa′* and *cc′* represent two a-c generator windings so placed that the induced voltages, E_{10} and E_{30}, are numerically equal, but are displaced by 60 electrical degrees with respect to each other, as shown in the vector diagram to the right. The two right-hand ends of the windings, *a′* and *c′*, and the common point, *O*, serve as the terminals 1, 2, 3 of the machine. Such an arrangement of windings is known as the V connection. Only generator, motor, or transformer windings can be connected to form a three-phase V.

Let the terminal voltages be denoted, as usual, by E_{12}, E_{23}, E_{31}. Since the points 2 and *O* electrically coincide, we immediately obtain:

$$E_{10} = E_{12}; \quad E_{30} = E_{32} = -E_{23} \quad . \; . \; . \; . \; . \; . \quad (21)$$

The voltage between the points 3 and 1 is the geometric difference of the vectors E_{30} and E_{10}; therefore:

$$E_{31} = E_{30} - E_{10} = -(E_{23} + E_{12}) \quad . \; . \; . \; . \; . \; . \quad (22)$$

It will thus be seen that, ignoring the drops in the windings, the vectors of the three line voltages form an equilateral triangle, as if there were three Y-connected generator windings.

Let the load consist of three equal Y-connected impedances, $Z = r + jx$. In accordance with Fig. 519, we draw the vectors of the Y voltages from the load neutral *N*, and the line currents, I_1, I_2, I_3, at an angle ϕ to these voltages. The currents I_1 and I_3 also flow through the generator windings, and therefore their vectors are drawn from point *O* as well, to show their phase relationship to the generator voltages. It will be seen that the current I_1 lags behind the voltage E_{10} by an angle $30° + \phi$, and the current I_3 leads E_{30} by an angle $30° - \phi$.

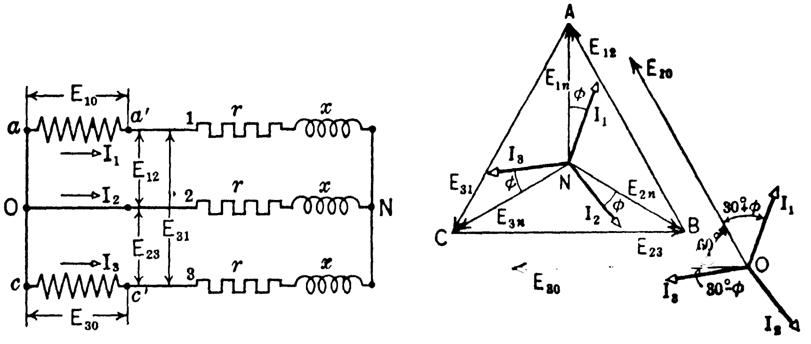

FIG. 558. V connection of generator windings with resultant vector relations.

In the preceding discussion, the internal impedance drop in the generator itself is disregarded. This drop is different in the two phases, because of the different values of the angles between the current and the voltage. Consequently, distorted terminal voltages result even with a balanced load, although the no-load generator voltages may be perfectly balanced. This is considered to be one of the disadvantages of the V connection (see the next section). The generator output, in the ideal case under discussion, is:

$$\begin{aligned} P &= E_\Delta I_Y \cos(30° + \phi) + E_\Delta I_Y \cos(30° - \phi) \\ &= 2E_\Delta I_Y \cos 30° \cos \phi \quad \ldots \ldots \ldots \ldots \quad (23) \end{aligned}$$

This is identically equal to the power:

$$P = 3(E_\Delta/\sqrt{3})I_Y \cos \phi \quad \ldots \ldots \ldots \quad (24)$$

consumed by the load.

The difference of potential between the generator neutral, O, and the load neutral, N, is the same as the load voltage, E_{2n}; therefore:

$$E_{n0} = E_\Delta/\sqrt{3} \quad \ldots \ldots \ldots \ldots \quad (25)$$

Thus, if one of the neutrals is grounded, the other must be carefully insulated from the ground.

A V-connected winding may be obtained by omitting one of the phases of a delta-connected winding. It is for this reason that the V connection is sometimes referred to as the *open delta.*

751. V Connection of Transformers. — Single-phase transformers are frequently connected in V (Fig. 559), for the sake of economy in the first investment, or in order to save on core losses on light loads. In an emergency, two out of the three transformers of a delta connection may be operated in V or " open delta."

The vector diagram in Fig. 559 is intended to show the effect of the *internal drop in the transformers* themselves (§395) upon the unbalancing of the load voltages. The triangle ABC and the three currents are the same as in Fig. 558, and we shall assume that a set of symmetrical voltages is impressed from the generator upon the transformer primaries, and that these voltages are first converted into a symmetrical set of *ideal* secondary voltages, ABC.

Let the equivalent internal resistance of each transformer be r_t and the internal reactance x_t, both reduced to the secondary circuit; let $Z_t = r_t + jx_t$ be the corresponding impedance. Then the voltage drop in the transformer 1 can be represented by the cross-hatched triangle D_1, with its sides equal to $I_1 r_t$ and $I_1 x_t$; the hypotenuse is equal to $I_1 Z_t$. Similarly, the voltage drop in the transformer 3 can be represented by the triangle D_3, congruent with D_1.

Subtracting now the drop I_1Z_t in phase 1 from BA, and the drop I_3Z_t in phase 3 from BC, we obtain an irregular triangle, $BA'C'$, representing the vectors of the *actual* secondary line voltages. This shows the distortion of the voltages due to the V connection. The above construction is only approximately true because the currents are also distorted on account of the voltage unbalance. For a more accurate solution see §752.

The irregular triangle $BA'C'$ can be converted into the equilateral triangle $B'A'C'$ by introducing a vector, BB', which has the same vectorial relationship to the current I_2 as AA' has to I_1, or as CC' has to I_3. This can be done electrically by connecting in the line conductor 2 (Fig. 559) a resistance, r_t, and a reactance, x_t, equal to those of either transformer (triangle D_2). Then the three vectors of voltage drop become numerically equal and displaced in phase by 120 degrees, so that the equilateral triangle ABC, for ideal transformers, is converted into the equilateral triangle $A'B'C'$ for the actual transformers, and the three line voltages remain balanced.

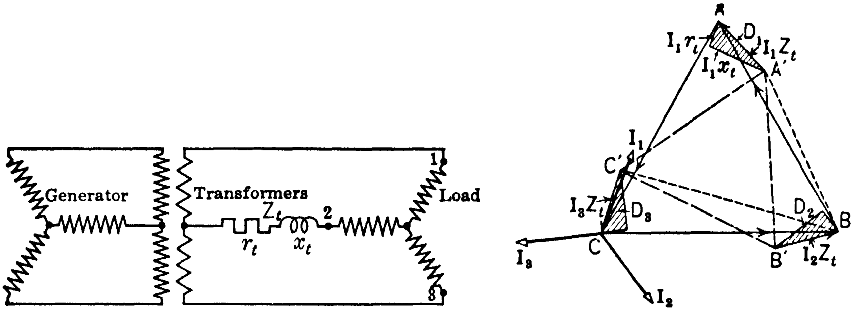

FIG. 559. Circuit diagram and vector relations for a system using V-connected transformers.

752. The General Case of the Unbalanced V Connection. — Let the load of Fig. 559 be unbalanced, and assume that the voltage supply is unsymmetrical. To determine the line currents the neutrăl-voltage method, described in §702, may be used. Two procedures suggest themselves. In one the V connection of the transformer primary windings is considered to be a special case of the unsymmetrical Y connection in which $E_{20} = 0$. All the formulas deduced for the unsymmetrical Y connection can then be used, by putting $E_{20} = 0$. In the other solution, it is necessary first to replace the actual transformers by ideal ones, of one-to-one ratio, and to put all their imperfections in the line conductors (§§404 to 407). After this, the transformers can be eliminated and the load assumed to be connected directly to the generator. We then have a case of an unbalanced load supplied by a Y-connected generator. If the load is also Y-connected, the neutral-voltage method can be used (§702). If the load is delta-connected, it can be first converted into an equivalent Y combination (§748).[4]

Symmetrical-component solution. The above problem may also be solved by the method of symmetrical components, following the procedure outlined in §716. Figure 560 is the schematic diagram of the equivalent circuit which represents the given condition. E_{ab}, E_{bc}, and E_{ca} are the (unequal) voltages impressed upon the line. Z_t' and Z_t'', in lines a and c, are the equivalent impedances of the transformer windings (equal if the transformers are identical). Z_a', Z_b', and Z_c' are the load impedances. Then the combined series impedances are: $Z_a = Z_t' + Z_a'$, $Z_b = Z_b'$, and $Z_c = Z_t'' + Z_c'$.

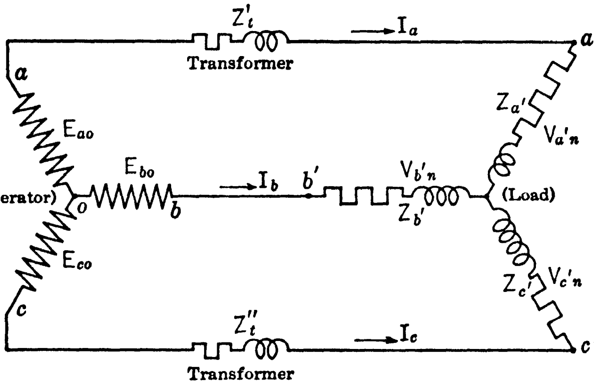

FIG. 560. Schematic diagram of an unbalanced, unysmmetrical three-phase system from V-connected transformers.

Proceed as follows:

1. Resolve the given supply voltages into the positive- and negative-sequence component phase volts, V_{an1}, and V_{an2}, by the use of eqs. (32) and (33), of Chapter XXXIV. There are no zero-sequence components of line voltage or line current in a three-wire line, so that $V_{an0} = 0$.

2. Find the equivalent zero-, positive-, and negative-sequence impedances, Z_{a0}, Z_{a1}, and Z_{a2} (eqs. 40).

3. Substitute into eqs. (41), (42), and (43), and solve for I_{a1}, and I_{a2}, from which will follow I_{b1} and I_{b2}, I_{c1}, and I_{c2}.

---

[4] For further details, computations, and tests on V connection, see Roux, *General Electric Review*, vol. 18 (1915), p. 52; Gibbs, *Electric Journal*, vol. 13 (1916), p. 100; *ibid.*, vol. 21 (1924), p. 36; Curtis, *Electrical World*, vol. 70 (1917), p. 302; De Merit, *ibid.*, vol. 79 (1922), p. 774; A. Boyajian, *ibid.*, vol. 83 (1924), p. 417.

4. Combine components of line currents to find I_a, I_b, and I_c.
5. From the line currents and load impedances solve for the load voltages to neutral and between lines.

753. EXPERIMENT 37-C. — Electrical Relations in a V-Connected Three-Phase Circuit. — The theory is explained in §§751 to 753, and the purpose of the experiment is to make these relationships clear on a specific circuit. Two V-connected emf's can be obtained either by means of transformers, as shown in Fig. 559, or else a modified delta-connected generator may be used. In the latter case, two phases are used as they are, and the third is left out altogether. This will give the connections shown in Fig. 555. A usual load experiment is then performed, first with balanced impedances, then with unbalanced impedances. The readings should be taken with a view to checking the vector diagrams shown in Figs. 555 and 559; therefore, not only the currents and the voltages should be read, but watts and phase angles as well. If transformers are used, their internal impedances should be determined by a short-circuit test (§393) and an equal impedance eventually inserted in the " through phase," to correct for the voltage unbalance. Line voltages should then be read with and without this corrective impedance.

T CONNECTION

754. In Fig. 561, *bc* and *aa′* represent two armature windings of an alternator, which are so placed that the voltages induced in them are displaced by 90 electrical degrees with respect to each other, as shown by the lines *BC* and *OA* of an equilateral triangle in the vector diagram to the right. The left-hand end of the winding *aa′* is connected to the middle point of the winding *cb*. Such an arrangement of two windings is known as the T connection; see §696. From the geometry of the equilateral triangle *ABC*, $OA = BC \cos 30° = 0.866BC$, so that the winding *aa′* should have 86.6 per cent of the number of turns in the winding *bc*.

The three-phase line is connected at points *a*, *b*, *c*. The part *ad* of the winding is idle and electrically need not exist, but it is sometimes preferable to provide two identical windings with taps, so that either winding can be used as the *main phase* or as the *teaser phase*. Only windings in which there are suitable induced emf's can be connected in T. Ordinary stationary impedances cannot be so connected to form a balanced three-phase load, because there would be no externally induced emf, or voltage drop, to keep the neutral point of the load at the proper potential.

Let the terminal voltages be denoted, as before, by E_{12}, E_{23}, E_{31}, and for the present let the internal voltage drop in the windings themselves be disregarded. The emf induced in *bc* serves as the line voltage E_{23}, and is represented by the vector *CB* in the diagram to the right. The voltage induced in *a'a* is in quadrature with *CB* and is numerically equal to 86.6 per cent of it. This voltage is plotted as the vector $OA = E_{10}$ from the middle point of *CB*.

The phase voltage induced in the part *Ob* of the winding (*O* is midway between *c* and *b*) is equal to one-half of *CB* and is represented by $OB = E_{20}$. The voltage induced in the part *Oc* of the winding is also equal to one-half of *CB*; therefore, $E_{03} = 0.5E_{23}$. Interchanging the subscripts so as to measure this voltage from point *O*, we get $E_{30} = -0.5E_{23}$, and for this reason the arrowhead of $E_{30} = OC$ is shown pointing toward *C*; see the voltage notation in §696.

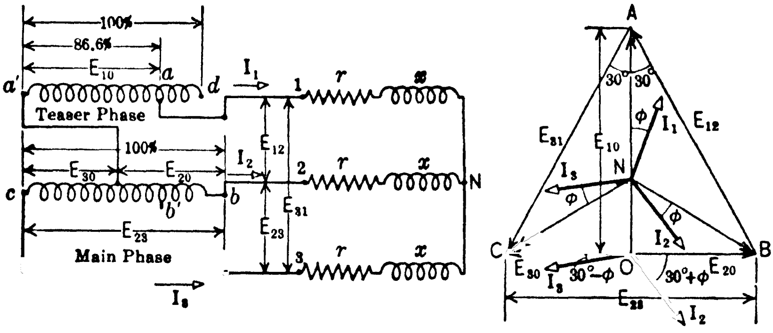

FIG. 561. Connections and vector relations with T-connected generator windings.

It will thus be seen that the vectors of the phase voltages, plotted from *O*, terminate at *A*, *B*, *C*. The triangle *ABC* being equilateral (because *OA* has been chosen equal to *BC* cos 30°), the three line or delta-voltages, *AB*, *AC*, *BC*, are equal. In other words, the above-described combination of generator windings gives a set of ordinary symmetrical three-phase line voltages, just as a set of Y- or delta-connected windings would do.

Let the load consist of three equal Y-connected impedances, $Z = r + jx$. In accordance with Fig. 519, we draw the vectors of the Y voltages to the load neutral *N*, and the line currents, I_1, I_2, I_3, at an angle ϕ to these voltages. The line current I_1 flows through the teaser phase, so that the angle ϕ is also equal to the phase displacement between the current and the voltage in that winding. The line current I_2 flows through the part *Ob* of the main winding, and I_3 flows through the part

Oc. The vectors of these currents are also drawn from point *O* to show that the phase displacement between the current and the voltage in *Ob* is 30° + ϕ, and that in *Oc* it is 30° − ϕ.

In the preceding discussion, the impedance drops in the generator windings themselves have been disregarded. It will be seen from the foregoing vector diagram that these drops, generally speaking, are different in the three phases and that, consequently, somewhat distorted terminal voltages should be expected even with a balanced load, though the generator voltages at no load may be perfectly balanced. This is considered one of the disadvantages of the T connection (see the next section).

The generator output is:

$$P = E_\Delta \cos 30° I_Y \cos\phi + (0.5E_\Delta)I_Y \cos(30° + \phi) + (0.5E_\Delta)I_Y \cos(30 - \phi) \quad . \; . \quad (26)$$

In this expression, the three terms on the right-hand side represent the output in the phases 1, 2, 3, respectively. After simplification, we get:

$$P = 2E_\Delta I_Y \cos 30° \cos\phi \quad . \quad . \; . \; . \; . \; . \quad (27)$$

which is identical with the power consumed in the load and represented by eq. (24).

The difference of potential, *ON*, between the generator neutral and the load neutral is seen from the vector diagram to be equal to one-third of *OA*. Hence:

$$E_{n0} = E_\Delta \cos 30°/3 = 0.289E_\Delta \quad . \; . \; . \; . \; . \; . \quad (28)$$

Thus, if one of the neutrals is grounded, the other must be carefully insulated from the ground. For the use of the T connection in the two-phase to three-phase transformation, see §771.

755. T Connection of Transformers.—Alternators are seldom, if ever, T-wound, but single-phase transformers are sometimes connected in T (Fig. 562). The transformer terminals are marked with the same letters as in Fig. 561, with the addition of the subscripts *p* (primary) and *s* (secondary). The phase unbalancing is somewhat less with the T connection than with the V connection, because the currents in all the three phases pass through the transformer windings.

The vector diagram in Fig. 562 is intended to show the effect of the *internal drop in the transformers* (§395) upon the unbalancing of the load voltages. The triangle *ABC* and the three currents are the same as in Fig. 561. It is assumed that the generator impresses upon the transformer primaries a set of symmetrical voltages.

Let the equivalent internal resistance of the teaser transformer, between the points a_p and a_p' (Fig. 562), be r_1, and the internal reactance x_1, both reduced to secondary terms. Then the voltage drop in the teaser transformer can be represented by the cross-hatched triangle D_1. The vector αA is parallel to I_1 and equal to I_1r_1; the vector $A'\alpha$ leads I_1 by 90 degrees and is equal to I_1x_1. Similarly, the internal voltage drop in the two halves of the main transformer is represented by the triangles D_2 and D_3. The resistances and the reactances used in these triangles are those of one-half of the main transformer, and are generally different from those in the triangle D_1. Owing to the voltage drops, the shape of the triangle of line voltages, $A'B'C'$, may depart from equilateral, and $A'O$ may not be exactly in quadrature with OB' or OC'. The balance can be restored by inserting some impedance in series with the secondary leads.

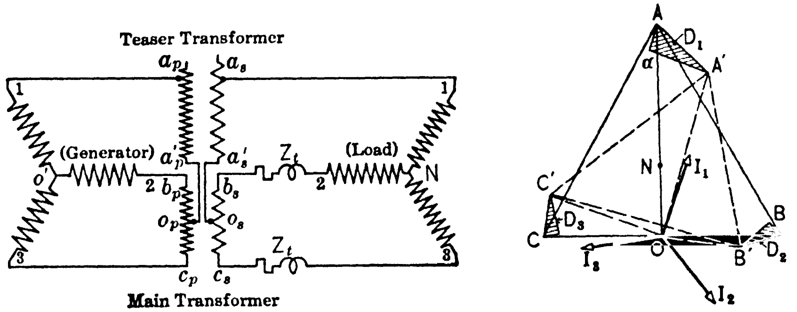

FIG. 562. Connections and vector relations in a system using T-connected transformers.

With an unbalanced load or with an unsymmetrical set of T voltages, the theory is similar to that given in §752 in application to the V connection. Both the V and the T connections are special cases of an unsymmetrical Y connection and can be treated as such.

756. Parallel Delta- and T-Connected Transformer Banks. — *Symmetrical Component Solution.* — Assume that five identical transformers are connected, three in delta and two in T, to a three-phase source, and supply power to a load consisting of three impedances in Y, as in Fig. 563. It is required to find the current in each branch of the load, the voltages between lines at the load, and the current and power output of each transformer.

Let Z_t be the equivalent impedance (§392) of each transformer, and Z_a, Z_b, and Z_c the impedances of the three branches of the load. All impedances are expressed in the same terms (§392).

The two transformer banks being in delta and T, they may be considered as possessing impedances which are connected, three in delta, and three in Y (the two halves of the main transformer of the T combination form two legs of the Y). The delta impedances are each of value Z_t, while the Y impedances are taken as $0.5Z_t$, $0.5Z_t$, and $0.866Z_t$. The following is the suggested method of solution:

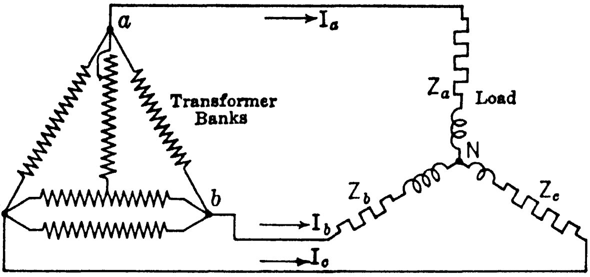

FIG. 563. Delta and T banks of transformer windings serving a common load.

1. Replace the delta of transformer impedances, Z_t, by equivalent Y values (eq. 15) of value $Z_y = Z_t/3$.

2. Combine the parallel Y transformer impedances (Fig. 564*a*) into the equivalent single Y of Fig. 564*b*. Thus, $Z_{0a} = (0.866 \times 0.333)/(0.866 + 0.333)Z_t = 0.25Z_t$; $Z_{0b} = Z_{0c} = Z_t(0.5 \times 0.333)/(0.5 + 0.333) = 0.2Z_t$.

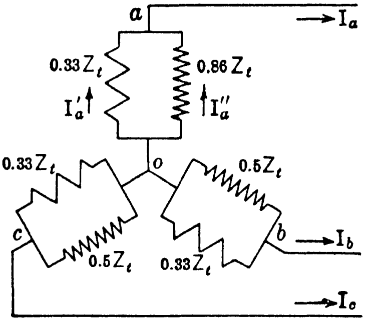

FIG. 564(*a*). Parallel Y impedances.

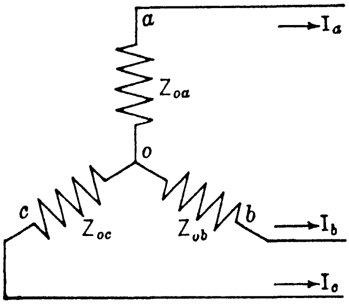

FIG. 564(*b*). Equivalent Y of transformer impedances.

3. The problem may now be solved as in §717, considering a loss-free voltage supply (Fig. 565) of potentials V_{ab}', V_{bc}', and V_{ac}', applied across three unequal impedances, $Z_a' = Z_{0a} + Z_a$, $Z_b' = Z_{0b} + Z_b$, and $Z_c' = Z_{0c} + Z_c$. Calculate the line currents I_a, I_b, and I_c, in terms of their positive-, negative-, and zero-sequence components as in §717. The line currents will divide between the transformer windings in inverse proportion to the impedances of the parallel branches in Fig. 564*a*. For instance, $I_a'/I_a'' = 0.866/0.333 = 2.6$; $I_a' + I_a'' = I_a$; etc.

4. Find the voltage drops across each load impedance and between lines at the load. These latter are the secondary terminal voltages V_{ca}'', etc.

5. From the secondary voltages, found above, and the component currents at their respective phase angles the power output of each transformer may be calculated.

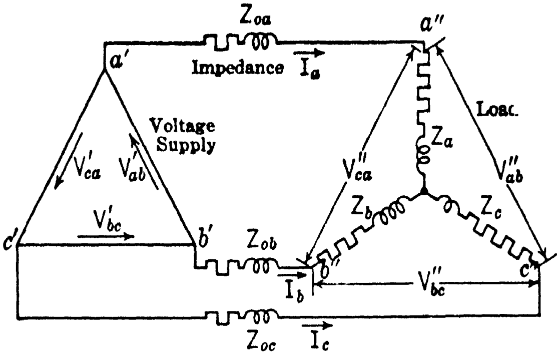

Fig. 565. Final equivalent circuit of transformer banks and load.

757. EXPERIMENT 37-D. — Electrical Relations in a T-Connected Three-Phase Circuit. — The theory of the T connection is given in the preceding two sections; the instructions are similar to those in §753. Using the method of §756, solve the example there given but for three transformers in delta operating in parallel with two transformers in V. Verify these results experimentally.

CHAPTER XXXVIII

TWO-PHASE AND QUARTER-PHASE SYSTEMS

758. The two-phase system and its modification, the quarter-phase system, are used so little in practice that only a brief treatment of their salient features is given here. For transformation of a two-phase system into a three-phase system, or vice versa, see §771.

The connections shown in Fig. 566 constitute what is known as the two-phase four-wire system with independent phases. The lines *ab* and *cd* are windings of an alternator, so placed on the core that the voltages E_1 and E_2 induced in them have a relative displacement of 90 electrical degrees. The angle between the vectors, E_1 and E_2, is shown to be 90 degrees, although it might differ materially from this value in the more general case. The currents and the phase angles are shown as different from each other, to represent an unbalanced load. Each phase is electrically independent of the other, and may be treated as a single-phase circuit, except for the mutual induction between the phases (§157). Such a system has been used in some smaller installations, with lamps connected to either phase and two-phase induction motors connected to both phases. The revolving flux in the alternator and that in the induction motor serve as magnetic links between the phases. The windings *ab* and *cd* might also be the secondary windings of two transformers whose primaries are connected to a suitable polyphase source of power.[1]

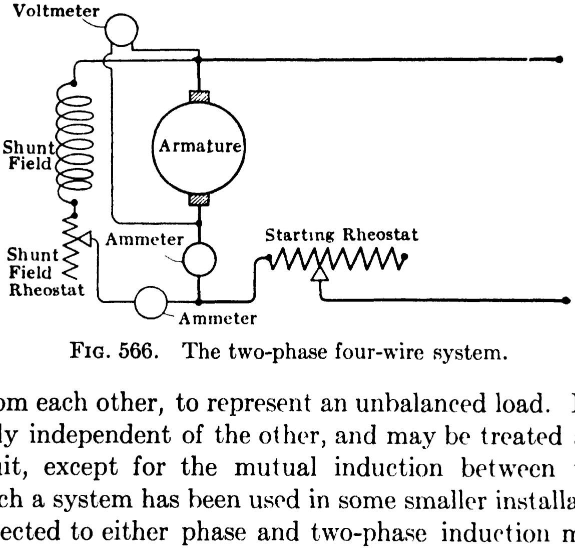

FIG. 566. The two-phase four-wire system.

759. Two-Phase Three-Wire System. — In Fig. 567, *ab* and *cd* are two generator or transformer windings in which two emf's, E_{10} and E_{20}, are induced 90 degrees out of phase with each other. The points *a* and *c* are electrically connected together, and so are the points *a′* and *c′* of the load. Two of the line conductors, *aa′* and *cc′* (Fig. 566), are combined into a common return conductor *ON*. Such an arrangement is known as the two-phase three-wire system. Its advantage over the four-wire system is the saving in the number of the line conductors and in their total weight.

---

[1] For an example of two-phase distribution, see *Electrical World*, vol. 85 (1925), p. 1031.

Besides the phase voltages, E_{10} and E_{20}, we have in this case to consider the "cross-phase" voltage E_{12} between the outside lines (points *b* and *d*). In accordance with the voltage notation explained in §696, we have, geometrically:

$$E_{12} = E_{10} - E_{20} \quad \ldots\ldots\ldots\ldots \quad (1)$$

as shown in Fig. 568(*a*). The currents in the two phases are denoted by I_1 and I_2, and the current in the return conductor by I_0. With the arrows as in the sketch, we have:

$$I_0 + I_1 + I_2 = 0 \quad \ldots\ldots\ldots\ldots \quad (2)$$

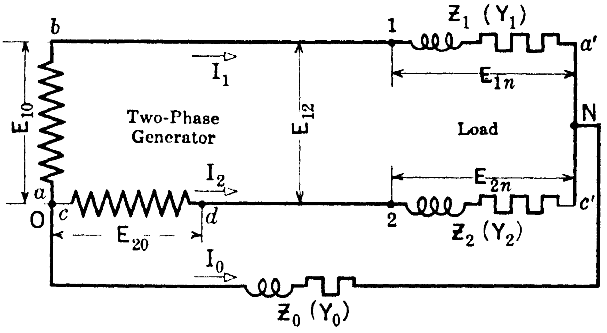

FIG. 567. Two-phase three-wire system.

The simplest case of the two-phase three-wire system is shown in Fig. 568(*a*). The two generator voltages are shown in quadrature with each other, and the impedance of the return conductor is assumed to be equal to zero. Hence, the points *N* and *O* are at the same potential and the generator voltages are equal to the load voltages. The "cross-phase" voltage, E_{12}, is equal to the hypotenuse of a 45-degree triangle; therefore, numerically:

$$E_{12} = E_{10}\sqrt{2} = E_{20}\sqrt{2} \quad \ldots\ldots\ldots \quad (3)$$

In the diagram the load is assumed to be balanced and partly inductive. The current, I_0, in the return conductor, is equal to the sum of the line currents, I_1 and I_2, and consequently is also represented by the hypotenuse of a 45-degree triangle; therefore, numerically:

$$I_0 = I_1\sqrt{2} = I_2\sqrt{2} \quad \ldots\ldots\ldots\ldots \quad (3a)$$

This means that, with the same current density in the three line conductors, the return conductor must have a $\sqrt{2}$ times the cross-section of the other two conductors. Under these conditions, the ratio of the total weights of the conductors in the four-wire and three-wire systems is as $4/(2 + 1.41) = 4/3.41$.

Effect of impedance in the return wire. The conditions shown in Fig. 568(*b*) are as follows: The generator voltages, E_{10} and E_{20}, are in quadrature; the load is non-inductive and balanced; the return conductor has an appreciable resistance, but no inductance. The load voltages, E_{1n} and E_{2n}, are displaced by more than 90 degrees, and the voltage drop in the neutral, $E_{0n} = NO$, is in phase with the return current, I_0. The load currents, I_1 and I_2, are in phase with the corresponding load voltages, E_{1n} and E_{2n}.

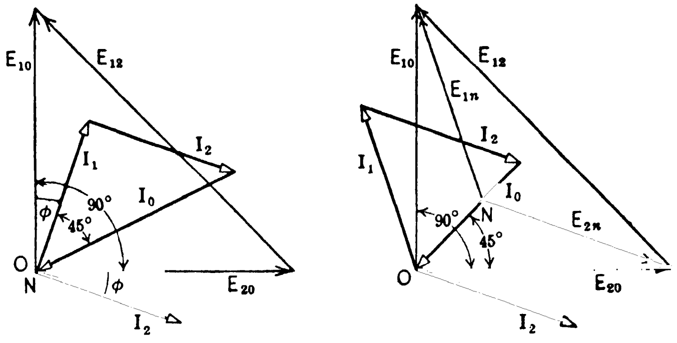

(*a*) (*b*)

FIG. 568. Relations in the two-phase three-wire system with and without impedance in the common wire.

Generally speaking, the return conductor will possess an appreciable impedance, Z_0, so that there will usually be a difference of potential between the generator neutral, O, and the load neutral, N.

Vectorially:

$$E_{0n} = I_0 Z_0 \quad \text{. . . . .} \quad (4)$$

and the phase angle between the current I_0 and the voltage E_{0n} is determined by the ratio of the reactance to the resistance in the return conductor. The voltages across the load phases, E_{1n} and E_{2n}, have the following geometric relationships:

$$E_{12} = E_{1n} - E_{2n} \quad \text{. . . . .} \quad (5)$$

$$E_{1n} = E_{10} + E_{0n} \quad \text{. . . . .} \quad (6)$$

$$E_{2n} = E_{20} + E_{0n} \quad \text{. . . . .} \quad (6a)$$

The load currents and the load voltages satisfy the relations:

$$I_1 = E_{1n}Y_1 \qquad (7)$$

$$I_2 = E_{2n}Y_2 \qquad (8)$$

Thus, the resistance of the neutral (or, more generally, its impedance) causes the load voltages and the load currents to depart from true quadrature. This is a disadvantage of the two-phase three-wire system, in that the operation of polyphase motors is somewhat less efficient. Induction regulators and other means may be used for bringing the load voltages into exact quadrature.

760. EXPERIMENT 38-A. — Electrical Relations in Two-Phase Systems. — Connect and load a two-phase alternator, as in Fig. 566. If a two-phase generator is not available, use the Scott transformation (§771) from a three-phase source of supply. Measure the power in each phase independently, and determine the total power delivered by the machine, with balanced and with unbalanced load. Leaving one phase unloaded, note the effect of varying load in the other phase upon the voltage of the first phase. Test for voltages between the phases. Connect the generator to a two-phase induction motor in order to obtain a revolving magnetic field (Chapter XLVII). Observe the effect upon the motor of reversing one or both phases.

Connect the generator and the load as in Fig. 567 forming a two-phase three-wire system. Provide an ammeter, a voltmeter, and a wattmeter, all of which, by means of a suitable polyphase board (§60), may be connected in any of the phases. With a return conductor of negligible impedance, measure the currents, the voltages, the power, and the phase angles, (a) with a balanced, non-inductive load; (b) with an unbalanced, non-inductive load; (c) with a partly inductive load, balanced and unbalanced. Increase the resistance of the return conductor in steps, repeating some of the foregoing measurements at each step. Similarly, investigate the effect of the reactance in the return conductor and of combinations of resistance and reactance. Where the current or voltage vectors form a closed triangle, be sure to measure the necessary phase angles, so as to have sufficient data to draw a triangle in its correct relative position to another triangle or vector.

Report. Using the observed data, construct vector diagrams and show to what extent they confirm the theory given in the text above.

Indicate any errors between metered values and corresponding combined currents or voltages obtained from the vector diagram. Explain how the load in one phase affects the voltage induced in the other phase.

Analyze at least one set of data by the method described in the next article.

761. The Neutral-Voltage Method of Solution of Unbalanced Two-Phase Systems. — In Fig. 567, let the generator voltages and all the impedances (or admittances) be given, and let it be required to find the currents. The voltage E_{n0} between the two neutrals may be taken as the auxiliary unknown quantity. We then have, from eq. (20) in §702:

$$E_{n0} = (E_{10}Y_1 + E_{20}Y_2)/(Y_1 + Y_2 + Y_0) \quad . \; . \; . \; . \quad (9)$$

This is because the electrical connections in Fig. 567 are identical with those in Fig. 518 (with the switch S open), except that E_{30} is equal to zero and Y_3 is called Y_0. If E_{n0} $(= -E_{0n})$ is known, the load voltages can be computed from eqs. (6) and (6*a*), and the currents from eqs. (7), (8), and (4). Equation (2) constitutes a check on the values obtained.

As an example of the application of eq. (9), consider the case shown in Fig. 568(*b*). Let: $E_{20} = E$; $E_{10} = jE$; $Y_1 = Y_2 = R^{-1}$; $Y_0 = r^{-1}$. Then $E_{n0} = E(1 + j)R^{-1}/(2R^{-1} + r^{-1}) = E\alpha(1 + j)$, where $\alpha = r/(2r + R)$. The sum $1 + j$, interpreted geometrically, means a unit vector along the axis of abscissas plus a unit vector along the axis of ordinates. The sum is equal to a vector of magnitude $\sqrt{2}$, at an angle of 45 degrees to both axes. Thus, E_{n0} is in the direction of the positive bisector of the axes, as shown in Fig. 568(*b*).

From eqs. (6), (6*a*), (7), (8), and (4), we get the following values of the three currents:

$$I_1 = E(j - \alpha - j\alpha)/R; \quad I_2 = E(1 - \alpha - j\alpha)/R; \quad I_0 = -E\alpha(1 + j)/r$$

By actually adding these three expressions together, their sum will be found to be equal to zero. For more complicated examples of unbalanced polyphase load, see §§705, 706, and 717.

762. Quarter-Phase Star-Connected System. — The arrangement of windings shown in Fig. 569 may be thought of as obtained from that in Fig. 566 by connecting together the two middle points of the generator windings. *Oa* and *Ob* are the two halves of the winding *ab*, and *Oc* and *Od* are the two halves of the winding *cd*. Let the voltage induced in *ab* be E_{ab}; then $E_{a0} = 0.5E_{ab}$ (Fig. 569), and $E_{b0} = -0.5E_{ab}$, as shown in the vector diagram to the right (see voltage notation in §696). Similarly, $E_{c0} = 0.5E_{cd}$; $E_{d0} = -0.5E_{cd}$.

Such a system is known as the quarter-phase (or four-phase) star connection. It corresponds to the three-phase Y connection, except that the phase angle between the consecutive induced emf's is 90 instead of 120 electrical degrees. The load can be similarly connected in star, and if the induced voltages and the load impedances are all equal, the difference of potential between the neutral points O and N is zero. With unsymmetrical voltages, or with an unbalanced load, the problem can be solved as indicated in §§702 to 706 and in §761. The method of symmetrical components (Chapter XXXIV) can also be used, by applying the general equations (§712) for an n-phase system (see bibliography).

With the connections shown in Fig. 569, there are voltages of three different magnitudes. For example, let the phase voltage, such as E_{a0}, be 100 volts. Then the line voltage between adjacent phases, such as E_{ac}, is equal to $100\sqrt{2} = 141$ volts. The voltage between " diagonal " phases, e.g., E_{ab}, is twice the phase voltage, or 200 volts.

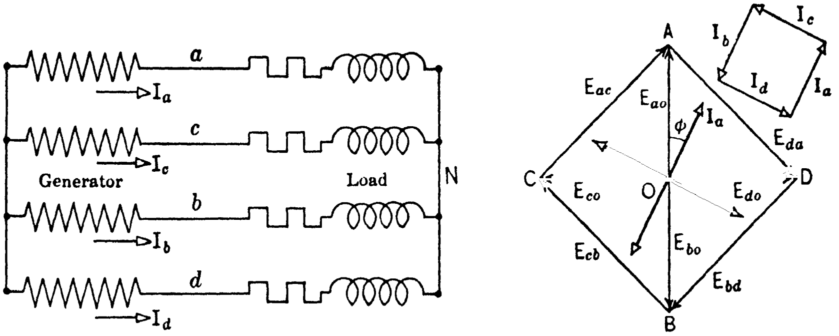

FIG. 569. Circuit diagram and vector relations in a quarter-phase, star-connected system.

The load in Fig. 569 being assumed to be partly inductive, each current vector is shown lagging by an angle ϕ behind the corresponding phase voltage. The geometric sum of the current vectors is equal to zero, to satisfy the first Kirchhoff law at points O and N. To indicate this fact, the current vectors are also shown separately as forming a square. With an unbalanced load, this square becomes an irregular quadrangle.

763. EXPERIMENT 38-B. — Electrical Relations in Quarter-Phase Star-Connected Systems. — The connections and the vector diagram are explained in the preceding section. The purpose of the experiment is to check these relations on an actual circuit. If a quarter-phase-connected alternator or rotary converter (Chapter XLV) is not available, obtain quarter-phase power by transformation from an available three-phase supply (§771). Measure at no load the three kinds of voltages mentioned in the preceding section. Arrange a non-inductive balanced load and check the current and voltage relations. Measure the total power first by connecting the current coil in each line and the potential circuit of the wattmeter between that conductor and the neutral, and then the current coil in each of three lines, with the potential coil between that line and a common return line. These correspond to the three-wattmeter and two-wattmeter methods in the three-phase system (Chapter XXXIII). Find the corresponding relations on a partly inductive balanced load, and then with a few combinations of unbalanced load. Be sure to read all the currents, voltages, power, and phase angles, in order to be able to construct the necessary vector diagrams and to check the results by computation.

Report. Construct vector diagrams, compare the results with the theoretical relationships, and explain discrepancies, if any.

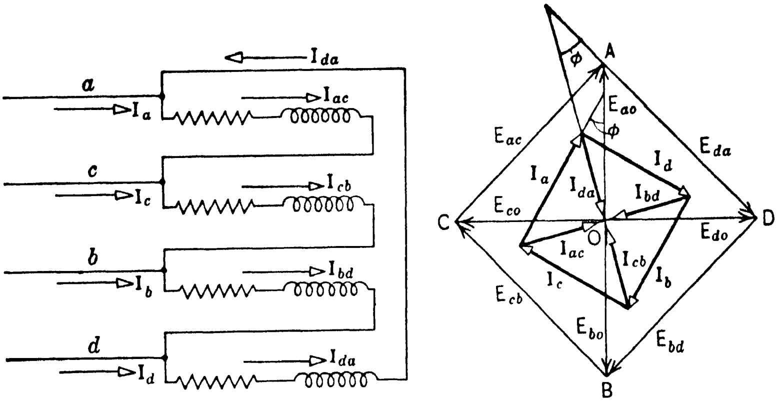

FIG 570. Diagram and relations in a quarter-phase mesh-connected system

764. Quarter-Phase Mesh-Connected Systems. — The essential characteristics of the mesh-connected quarter-phase system are shown in Fig. 570. The vector diagram of voltages and the four line conductors are the same as in Fig. 569, but the individual load impedances are connected between the adjacent phase conductors, forming a *closed mesh.* The connections in Fig. 569 correspond to a Y in a three-phase system, while those in Fig. 570 correspond to a delta. Not only the load, but the armature windings of a generator as well, may be connected in mesh. For example, in a four-ring rotary converter (Chapter XLV), the armature is quarter-phase mesh-connected.

Applying the first Kirchhoff law to any of the four points at which the mesh is connected to the line conductors, we see that the line current is equal to the difference between the two consecutive mesh currents. Consequently, in the vector diagram it is convenient to represent the line (or star) currents by a square and the mesh currents by radial lines between the center and the vertices of the square. Then each line current, such as I_a, is equal to the difference between two mesh currents, I_{ac} and I_{da}. The direction of the arrowheads on the vectors is made to agree with those in the diagram of connections.

The load being partly inductive, the load currents (those with the double subscripts) are drawn at an angle ϕ lagging behind the corresponding voltages. As a result, the line currents lag by the same angle behind their phase voltages. This relation is similar to the one that obtains in a delta-connected three-phase system (Fig. 555).

765. EXPERIMENT 38-C. — Electrical Relations in Quarter-Phase Mesh-Connected Systems. — The connections and the vector diagram are explained in the preceding section. The instructions for performing the experiment are similar to those in §763.

REFERENCES

1. C. P. Steinmetz, Alternating-Current Phenomena, McGraw-Hill Book Co.
2. Bryant and Johnson, A-C Machinery, Chapters X, XI, McGraw-Hill Book Co.
3. Puchstein and Lloyd, A-C Machines, Chapter XIX, John Wiley & Sons.
4. C. E. Magnusson, Alternating Currents, Chapter XXVI, McGraw-Hill Book Co.
5. R. R. Lawrence, Principles of Alternating Currents, Chapter XII, McGraw-Hill Book. Co.
6. V. Karapetoff, The Electric Circuit, McGraw-Hill Book Co.

CHAPTER XXXIX

POLYPHASE TRANSFORMATIONS

766. The use of transformers in various combinations makes it possible to convert one polyphase system into another, with the same or with a different number of phases. Thus electric power is sometimes generated by means of two-phase alternators and then transmitted and distributed by means of three-phase lines. Also it is often necessary to connect two-phase energy-consuming devices to an existing three-phase source. Frequently a two- or three-phase supply is converted into a six-phase system, for example, for rotary converters (Chapter XLV), or for mercury-vapor rectifiers (Chapter LVI). In some electric traction systems, single-phase power from the trolley is converted into three-phase power on the locomotive itself and supplied to the motors. (This requires more than static transformers, §787.)

Questions similar to those of phase transformation also arise in the following two cases: (1) when a three-phase voltage has to be raised or lowered by means of transformers of which the primaries are connected, say, in delta, and the secondaries in Y, or vice versa; (2) when three-phase transformers of different types or makes have to be connected in parallel on both the primary and the secondary sides, and the correct polarity must be preserved.

THREE-PHASE TO THREE-PHASE TRANSFORMATION

767. When it is necessary to raise or to lower the voltage of a three-phase power supply, by means of three transformers, any one of the following four combinations of connections may be used:

Low-tension side	*High-tension side*
Y	Y
Δ	Δ
Δ	Y
Y	Δ

Theoretically, all four combinations may be made to give correct results; but in practice, in a given case, one particular combination usually has some advantages.[1] For example, a Y-connected high-tension winding is less expensive because it is designed for only $1/\sqrt{3} = 0.577$ of the voltage involved in a delta connection, and thus a considerable amount of insulation space is saved. Moreover, the neutral point of a Y connection can be grounded, if so desired; this limits the potential above earth of any conductor, when grounds occur on the system. It is of advantage in the application of relays and protective devices.[2] On the other hand, a delta connection of windings is of advantage in that it provides a ready path for the third, ninth, etc. harmonics of the current (§790). When both the primary and the secondary windings of a three-phase transformer are Y-connected, it is sometimes of advantage to provide a so-called *tertiary delta winding* short-circuited upon itself. Its effect in suppressing the third harmonic in the Y voltage is discussed in §790. Such a delta winding is also useful in lessening the severity of a single-phase short circuit between the secondary terminals, and in permitting enough current to flow to operate the protective apparatus. An unbalanced condition in the secondary winding causes currents to flow through the tertiary delta, and consequently also through the primary circuit, thus distributing the current demand among the three phases; besides, the additional impedance of this winding helps to limit the short-circuit current.[3]

That three-phase power can be transformed into three-phase power of a different voltage by using only two transformers, V-connected or T-connected, has been discussed (§§750 and 754).

When transformer primaries are connected in Y and the secondaries in delta, or vice versa, the line voltages in the two circuits become displaced by 30 electrical degrees, and this method may be used for shifting the phase of the voltage, with or without changing its magnitude.

In Fig. 571, two more general methods are shown for shifting the phase of the secondary voltage by a desired angle with respect to the primary voltage. In the diagram to the left, each secondary winding consists of two separate sections. For example, in phase 2, the voltage induced in the larger section is OB, and in the smaller section it is

---

[1] For a further discussion of the merits of the several groupings of transformers, see A. S. Langsdorf, "Theory of A-C Machinery," Chapter IV, McGraw-Hill Book Co.; also O. G. C. Dahl, "Electric Circuits, Theory, and Applications," Chapter IV, McGraw-Hill Book Co.

[2] Robinson and Monseth, "Theory and Application of Relay Systems," *Elec. Jour.*, 1931, p. 299.

[3] "Standard Handbook for Electrical Engineers," Index under Transformer, tertiary winding; *Electrical World*, vol. 82 (1923), p. 863; O. G. C. Dahl, "Electric Circuits, Theory and Applications," Chapter IV, McGraw-Hill Book Co.

$AA' = b$. The smaller section of phase 2 is connected in series with the larger section of phase 1, so that the total secondary voltage of phase 1 becomes OA', instead of OA. In this manner the large and the small sections are interconnected, to shift the line voltages by a desired angle, α.

In the diagram to the right, the secondary windings are provided with taps. For example, the winding 1–3′ is provided with the tap 3. The three taps and the three ends of the windings, farthest from the taps, are connected to form the delta 1–2–3; the remaining ends, 1′, 2′, 3′, form the line terminals. It will be seen from the sketch that in this manner the voltage phase can be shifted by a desired angle.[4]

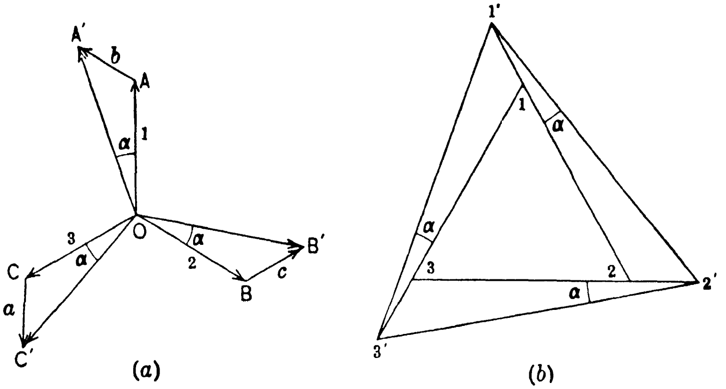

FIG. 571. Two methods of shifting the phase of three-phase voltages: (a) in Y connection, (b) in mesh connection.

768. EXPERIMENT 39-A. — Three-Phase to Three-Phase Transformation. — The purpose of the experiment is to study the principal characteristics of the four combinations of transformer windings discussed in the preceding section. For the polarity test, see §390; for the phase-sequence tests, see §700. If the Y and delta relations have been previously studied (Chapters XXXIII and XXXVII) and load tests already performed, this experiment may be limited to no-load measurements, merely to ascertain the voltage relations and to get some practice in connecting transformers three-phase. (a) Connect three single-phase transformers (or a three-phase transformer) in succession in the four possible ways (YY, ΔΔ, YΔ, ΔY) and measure all the voltages; also determine the phase angle between the primary and the secondary emf's, and the phase sequence. (b) Using the references given in the preceding article, set up experimentally some of the abnormal conditions mentioned there and check the statements as to the relative advantages of delta and Y connections. (c) Provide a tertiary winding; investigate the third harmonic current in it; also the generator currents due to a single-phase short circuit and to other abnormal conditions on the secondary side. Measure the currents in the tertiary winding under such abnormal conditions, so as to check the theory, to get an idea of the necessary size of conductors, and to see how this winding can be used for operating protective devices. (d) Try the phase-shifting arrangements shown in Fig. 571.

---

[4] See also under polyphase induction regulators, §954.

769. Paralleling Three-Phase Transformers. — The conditions which must be fulfilled for a satisfactory operation of single-phase transformers in parallel (§414) must be fundamentally fulfilled when paralleling three-phase transformers; only in this case the polarity test is more involved, because the secondary voltages of the two polyphase transformers must agree with each other in all the three respective phases.

Consider first two identical three-phase transformers, with the same arrangement of the windings and the terminals. Let the primaries of each transformer be connected, for example, in delta, and the secondaries in Y, and let the corresponding terminals on the primary side be connected together to a source of supply. Then the corresponding secondary terminals can also be connected together, after having been joined at one point and checked with a voltmeter to make sure that there is no voltage between them, owing to an error in the internal connections. If the transformers are of different makes, and have the terminals differently arranged, several different combinations of phases. and polarities will have to be tried before the transformers can be properly paralleled on the secondary side.

If one of the transformers (or transformer banks) is connected delta-delta, or Y-Y, it cannot be connected in parallel with a delta-Y- or a Y-delta-connected transformer, because the secondary line voltages of the two transformers are 30 electrical degrees out of phase with each other.

Mr. James Dixon, after investigating the possible combinations of connections and polarities, has given rules for checking transformer connections according to a definite plan.[5] With the aid of his table and diagrams, the problem of locating the proper terminals or of indicating the necessary changes in the connections can be solved systematically and without guessing.

---

[5] *Electrical World*, vol 80 (1922), p 667. For the recommended lead markings, see the *Standards of the A.I.E.E.*, under Transformer Construction.

770. EXPERIMENT 39-B. — Exercises in Paralleling Three-Phase Transformers. — The purpose of the experiment is to familiarize the student with the various voltage combinations possible with two three-phase transformers, or transformer banks, as discussed in the preceding section. The available transformers should be such that the student could change the internal connections and the number of turns, and thus obtain combinations that will parallel satisfactorily and others that will not. He can then try different combinations and deduce his own method of procedure, or use Mr. Dixon's instructions and satisfy himself as to their correctness and completeness.

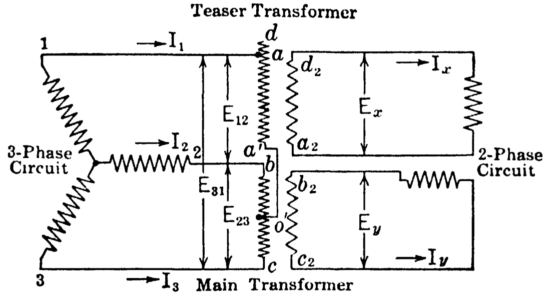

FIG. 572. The Scott system of transformation from three phase to two phase or vice versa.

TWO-PHASE TO THREE-PHASE TRANSFORMATION

771. The T or Scott Connection. — The usual method of transforming power from three-phase to two-phase, or vice versa, is shown in Figs. 572 and 573. Two single-phase transformers, T-connected on the three-phase side (§755), are used. On the two-phase side, the windings may form two independent quadrature phases or be interconnected to form any of the other two-phase or quarter-phase systems described in Chapter XXXVIII.

In Fig. 573, *ABC* is the triangle of the line voltages on the three-phase side, *CB* being the voltage across the main transformer winding, *cb*, and *OA* that across the " teaser " phase, between *a'* and the 86.6 per cent tap, *a*. *OD* = *BC* is the voltage induced in the whole winding, *a'd*, of the teaser transformer. Let the total number of turns on the two-phase side of each transformer be N_2 and on the three-phase side N_3. Then, if we distinguish the currents and the voltages on the two-phase side by the subscripts *x* and *y*, as indicated in Fig. 572, we have:

$$E_x = (N_2/N_3)OD, \quad \text{and} \quad E_y = (N_2/N_3)CB \quad . \quad . \quad . \quad . \quad (1)$$

The ratio of the currents in the windings of the teaser transformer is found from the relation, $I_1 n_1 = I_2 n_2$, eq. (1) of §391. The actual number of turns through which the current I_1 flows is $N_3 \cos 30°$ (§754); therefore:

$$I_1 N_3 \cos 30° = I_x N_2 \quad . \; . \; . \; . \; . \; . \; . \; . \; . \; . \quad (2)$$

or:

$$I_x = 0.866(N_3/N_2)I_1 \quad . \; . \; . \; . \; . \; . \; . \; . \; . \; . \quad (3)$$

With a balanced load,

$$I_1 = I_2 = I_3, \quad \text{and} \quad I_y = I_x$$

As a check on the foregoing relations, we shall write the expression for the power transmitted through the transformers:

$$E_x I_x \cos \phi + E_y I_y \cos \phi = OA \cdot I_1 \cos \phi + OB \cdot I_2 \cos (30° + \phi)$$
$$+ OC \cdot I_3 \cos (30° - \phi) \quad . \; . \; . \; . \; . \; . \; . \; . \; . \; . \; . \; . \quad (4)$$

When E_x, E_y, I_x, I_y are substituted for the values given above, this equation will be found to be an identity.

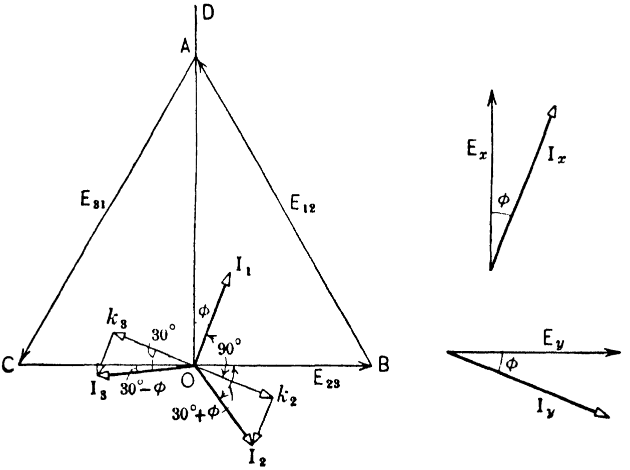

FIG. 573. Vectors of currents and voltages in the Scott system.

Power-distribution companies that change from two-phase to three-phase usually face a transition period during which both kinds of service must be furnished. Schemes have been devised by means of which this can be done with a Scott connection, and the final change-over is made with the least possible inconvenience to the customers.[6]

772. Unbalancing of Voltages with the Scott Connection.—The magnetic relations in the main transformer deserve special attention.

---

[6] See, for example, Pritchard, *Electrical World*, vol. 80 (1922), p. 1045; Hussey and Paine, *Electric Journal*, vol. 20 (1923), p. 214.

In the main transformer between the terminal b and the middle point, the current I_2 may be considered to consist of two components (Fig. 573), viz., $Ok_2 = I_2 \cos 30°$, in phase with I_y, and k_2I_2 in quadrature with Ok_2. With the arrowheads shown in Fig. 572, the mmf's due to Ok_2 and I_y are opposed to each other, and their resultant mmf is:

$$M = 0.5N_3I_2 \cos 30° - 0.5N_2I_y \quad . \quad . \quad . \quad . \quad . \quad . \quad (5)$$

Substituting for I_y its value from eq. (3), we find that $M = 0$. Strictly speaking, M has a small value, sufficient to excite one-half of the main magnetic path. Similarly, in the other half of the main transformer, corresponding to the terminal c, the mmf's due to Ok_3 and I_y practically cancel each other. Thus, only the mmf's due to the component currents k_2I_2 and k_3I_3 remain. With the positive directions of the currents I_2 and I_3 shown in Fig. 572, i.e., toward the middle tap, the mmf's due to the above components oppose each other.

We thus have a magnetic condition leading to a considerable leakage flux and consequently a comparatively large reactive drop in the transformer. In order to reduce this magnetic leakage, the coils of the main transformer are often "interlaced."[7] For the best balancing of the voltages a certain relation must exist between the internal impedances of the two transformers. If this condition is not fulfilled, a corrective impedance can be inserted in series with one of the leads on the two-phase side.[8]

773. EXPERIMENT 39-C. — Study of the Scott Two-Phase to Three-Phase Transformation. — The connections and the theory will be found in the preceding two sections. The purpose of the experiment is to familiarize the student with the characteristics of the transformers so connected and with their voltage regulation on balanced and unbalanced loads, with leading and lagging currents. Transformers preferably of 1 to 1 ratio and with a rather high internal drop should be selected in order to bring out more clearly the changes in the terminal voltages and phase angles.

Connect a', a_2, and b_2 together (Fig. 572) in order that voltages between primary and secondary circuits may be read, as well as the "cross-voltage" of the two-phase side. First check voltage relations under no-load conditions to prove that two-phase, three-phase transformation exists. Read all primary and all secondary voltages; also such voltages as those between points a and d_2, b and b_2, and c and c_2 as well as the two wattmeter readings on the two-phase side, and three wattmeter readings on the three-phase side, using voltages to a'.

---

[7] For detailed diagrams, see E. G. Reed, *Electric Journal*, vol. 7 (1910), p. 407.

[8] "Standard Handbook for Electrical Engineers," Index under "Transformations, two-phase to three-phase." See also *La lumière élect.*, vol. 24 (1913), p. 267; *Soc. franc. élect. bull.*, vol. 3 (1923), p. 729.

Take complete sets of voltage, current, and power readings for balanced and unbalanced, inductive and non-inductive loads. For one load condition, the behavior of the system should be studied when it is transmitting the same amount of power, and at the same power factor, both ways, that is, from three-phase to two-phase, and vice versa. Determine empirically the best value of corrective impedance to be inserted in one of the phases on the two-phase side and find out whether it corrects equally well under different load conditions.

Report. From the readings, construct vector diagrams and compare the experimental results with the theory; give reasons for discrepancies, if any.

Note that in the diagrams the vectors I_x and I_1 must be parallel, I_y must be parallel to the vector difference, $I_2 - I_3$, but that E_x need not be exactly parallel to OA, nor E_y to CB. Explain these facts in detail.

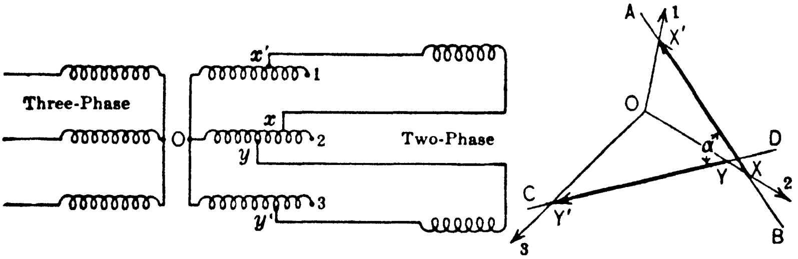

Fig. 574. Three-phase to two-phase transformation with Y-connected transformer or generator windings

774. Various Methods of Two-Phase to Three-Phase Transformations. — The above-described T connection, though it is the one mostly used in practice, is not the only one possible for transforming from two-phase to three-phase. By using three transformers, instead of two, three-phase power can be converted into two-phase, or vice versa, in several other ways, some of which are shown in Figs. 574 and 575.

In Fig. 574, to the right, let the vectors 01, 02, 03 represent some unbalanced phase voltages induced in the unsymmetrical Y-connected windings shown to the left and similarly marked. These may be transformer or alternator windings; in the latter case the other set of windings, to the extreme left, should be omitted. Draw two arbitrary lines, AB and CD, at an angle α to each other, where α is equal to the desired phase displacement between the voltages on the two-phase side. Let these lines intersect the three-phase vectors at points X, X'; Y, Y'. The vectors XX' and YY' may be taken as the voltages on the two-phase side. By locating the corresponding tap points x, y, x', y' on the windings themselves, connections can be obtained for the two-phase line. At the same time, the terminals 1, 2, 3 can be used for a three-phase load, or for a three-phase source of power. In the latter case, the transformers act as auto-transformers and the three windings shown to the extreme left can be omitted.

In the three sketches in Fig. 575, ABC is the triangle of voltage vectors, corresponding to three delta-connected windings of a three-phase transformer, auto-transformer, or alternator. Within each triangle, two straight lines are drawn, equal and perpendicular to each other, and terminating on the sides or vertices of the triangle. The points so located correspond to definite points on the windings themselves. From these latter points, leads can be taken to a two-phase line.

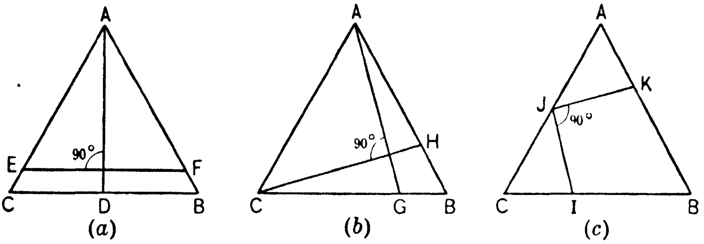

FIG. 575. Three-phase to two-phase transformation with delta-connected generator or transformer windings.

The wiring diagram corresponding to Fig. 575(*a*) is known as the Taylor connection. It has the advantage of symmetry, but requires three taps, D, E, F. The advantage of the (*b*) connection is that it requires only two taps, G and H, the terminals A and C being also used for the two-phase connection. Moreover, the transformer corresponding to AC may be omitted altogether, the other two transformers being V-connected (§750). The (*c*) scheme is of advantage when one desires to use the three-wire two-phase system (§759); the tap J then serves as the common-return terminal.[9]

775. EXPERIMENT 39-D. — Study of Various Two-Phase to Three-Phase Transformations.

— The general principle of such transformations is described in the preceding section. In addition to the arrangements shown there, the student should devise some of his own, particularly one in which a single auto-transformer, and the wires of a three-phase supply, accomplish the desired results. First, the voltages and their phase angles should be studied at no load, and then on a balanced load, at least up to the full capacity of the transformers, so as to bring out the distortion of the voltages. The load should be tried on the two-phase side as well as on the three-phase side. Instead of two-winding transformers, auto-transformers with taps may be used. A more advanced problem is to find unsymmetrical loads of such character that the unbalancing of voltages is a minimum.

---

[9] For a discussion of these connections, see *La lumière électrique*, vol. 20 (1912), p. 242; vol. 24 (1913), pp. 267 and 294; *Electrical World*, vol. 62 (1913), p. 907.

Report. Construct vector diagrams from the readings, and compare the experimental results with the theory. State the advantages and the disadvantages of the various connections tried. Draw the vectors and solve for the resultant currents in each section of three auto-transformers used in the Taylor connection, when the load is balanced, inductive.

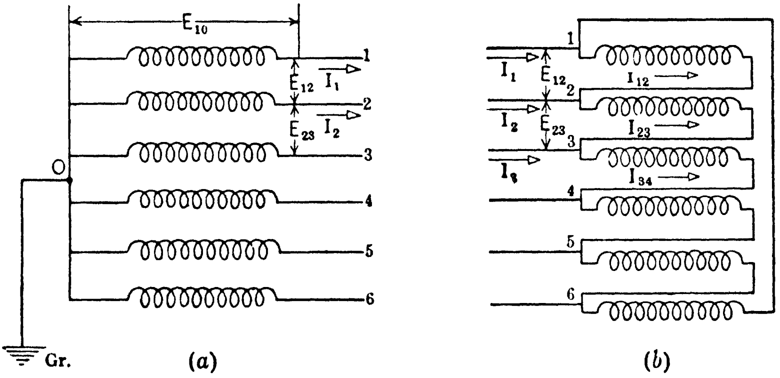

(a) (b)

FIG. 576. Star-connected and mesh-connected six-phase systems.

SIX-PHASE SYSTEM

776. By analogy with Figs. 518 and 569, imagine six windings connected in star, that is, with one end connected to a common neutral and the other to a line conductor (Fig. 576*a*). Such a combination of windings, in which all the emf's are displaced in time phase with respect to each other by 60 electrical degrees, is called the *star-connected six-phase system.* The same six windings can also be connected *in mesh* (Fig. 576*b*) forming a closed circuit, like the delta connection in Fig. 563 or the quarter-phase mesh in Fig. 570. The six-phase system is used with some large rotary converters and mercury-vapor rectifiers, for the reasons explained in §§882 (2) and 1095.

The voltage relations in a balanced six-phase system are shown in Fig. 577, to the left. The six star voltages, 01, 02, etc., are displaced by 60 electrical degrees. The corresponding mesh voltages between adjacent phases are 1-2, 2-3, etc. Each mesh voltage is a geometric difference between the two corresponding phase voltages, as in the three-phase and the quarter-phase systems. The voltage between the conductors 1 and 3 is represented by the vector 1-3. The vectors 1-3, 3-5, 5-1 form a delta, and may be called *delta voltages.* There is also an identical delta between the points 2, 4, and 6. The voltage between the conductors 1 and 4 is equal to the vector 1-4, and the voltages 1-4, 2-5, and 3-6 are called *diametrical voltages.*

The current vectors are shown to the right. With a partly inductive load, the current I_1 in conductor 1 lags behind the phase voltage, E_1, by an angle ϕ. Since the positive directions of all the six line currents are shown in Fig. 576(*a*) away from the neutral point, the current vectors form a closed regular hexagon. At each junction point between a line conductor and the mesh (Fig. 576*b*), according to the first Kirchhoff law, the line current is equal to the difference between the two mesh currents. Hence, the vectors of the mesh currents can be represented by radii from the center of the hexagon. The mesh currents thus lag behind the mesh voltages by the same angle, ϕ, by which the line currents lag behind the star voltages.

From the geometry of the figure it will be seen that numerically the star voltages and the mesh voltages are equal to each other, and so are the two kinds of currents. Each delta voltage is equal to the square root of three times the mesh voltage, and the diametrical voltages are twice as large as the star voltages.

777. EXPERIMENT 39-E. — Electrical Relations in a Balanced Six-Phase System. — The purpose of the experiment is to check the relations discussed in the preceding section, and the order of the experiment is similar to that used in the previous study of the three-phase and quarter-phase relations. If a six-phase alternator or rotary converter (Chapter XLV) is not available, six-phase voltages can be obtained by a transformation from an available two-phase or three-phase source, as is explained below.

778. Transformation for Three-Phase (or Two-Phase) to Six- and Twelve-Phase. — It will be seen from the vector diagram of the voltages in Fig. 577 that only three of the star voltages, for example, 0-1, 0-3, 0-5, are of different time phase. The voltage 0-4 is the same as 0-1, only reversed in phase. Consequently, the voltages 0-1 and 0-4 can be induced in the two halves of the same winding, and so can the voltages 0-2 and 0-5, and 0-3 and 0-6, respectively. We shall now show several ways in which this principle is utilized in practice.

(a) *Star connection.* In Fig. 578, a three-phase transformer is shown, with each of the three secondary windings divided into two sections. The terminals of each section are marked *s* (start) and *f* (finish). The voltages induced in sections 1 and 4 are the same, when considered, say, from *s* to *f*. But the voltage induced in section 4 is opposite to that induced in section 1, if we consider it as *s–f* in one of the sections and *f–s* in the other (§696). Thus, to obtain a six-pointed star of voltages as in Fig. 577, we connect the *s* points of the sections 1, 3, 5 and the *f* points of the sections 2, 4, 6, to a common neutral. Then the remaining terminals, in the order 1, 2, 3, 4, 5, 6, will form the line terminals of a star-connected six-phase system.

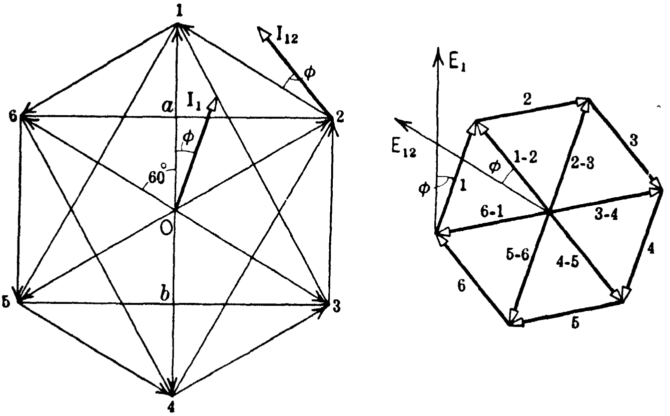

FIG. 577. Voltage and current relations in a balanced six-phase system.

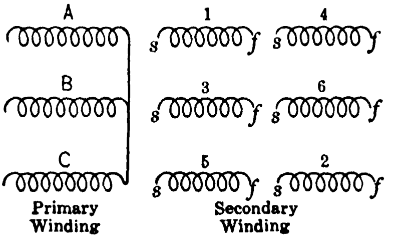

FIG. 578. Three-phase to six-phase transformation by star connection.

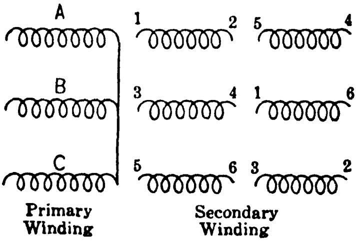

FIG. 579. Three-phase to six-phase transformation using mesh connections.

(b) *Mesh connection.* The six secondary sections of the winding (Fig. 579) can also be connected in mesh. In Fig. 577, the mesh voltage 1–2 is equal and opposite to the voltage 4–5, and for this reason the two sections of the secondary winding, corresponding to the primary phase A (Fig. 579), are marked accordingly. The marking of the remaining sections corresponds to the other four sides of the hexagon. It remains to connect together each two terminals marked by the same numeral, thus forming a closed mesh. Each junction point serves as a terminal for a line conductor.

When actually connecting six such windings into a mesh, it is advisable to apply a voltmeter between the last two points, before joining them, to make sure that no mistake has been made and that the potential difference between these points is practically zero. On the other hand, the mere fact that this potential difference is zero is no conclusive proof that the six windings have been connected in the right order, because the sum of the induced voltages is zero in any order. It is necessary to check the delta voltages and the diametrical voltages as well.

The two above-described methods of converting a three-phase system into a six-phase system are not the only possible ones. There are as many methods of transformation as there are different ways of connecting the six vertices of the voltage hexagon (Fig. 577) by lines of not more than three directions. The latter limitation is necessary, because there are only three primary voltages to begin with (or only two with the T connection), and in forming a six-phase system the phase voltages are supposed to be only reversed but not shifted by an angle. The first of the above-described transformations (Fig. 578) corresponds to connecting the six vertices to the center O; the second method (Fig. 579) corresponds to connecting the adjacent vertices directly. When all the phases are interconnected at one end of the circuit, as for example in the armature winding of a rotary converter, it is not necessary to interconnect them at the other end (the transformer end), as long as the voltages and the load are balanced. We then obtain the following four combinations:

(c) *Diametrical connection.* In Fig. 580(a), the three transformer secondaries are marked to correspond to the vertices of the voltage hexagon in Fig. 577. The three diameters, 1–4, 3–6, 5–2, are displaced with respect to each other by 120 degrees and thus correspond to the three voltages induced in the secondary windings (Fig. 580a). The proper interconnection potentials must be obtained through a mesh or star connection at the other end of the circuit. An advantage of this method is that each secondary winding of the transformer consists of one section only.

(d) *Double-delta connection.* The voltage hexagon in Fig. 577 may be considered to consist of two independent deltas, 1–3–5 and 2–4–6. The vectors 1–3 and 4–6 are equal and opposite; the corresponding windings are represented in Fig. 580(*b*) by the two secondary sections of phase *A*, with the properly marked terminals. Similar double sections are shown for phases *B* and *C*. The sections 1–3, 3–5 5–1 are connected into a delta, and the junction points constitute three of the terminals of the six-phase system. Similarly, the sections 4–6, 6–2, 2–4 are connected into a delta and furnish the remaining three terminals. The proper voltages between the two deltas must be maintained through a mesh or star connection at the other end of the circuit.

(e) *Double-V connection.* By omitting one of the three single-phase transformers in Fig. 580(*b*), and connecting the remaining two in V on the primary side (§750), a double V can be realized on the secondary side. One V is connected to the points 1, 3, 5; the other to 2, 4, 6 (Fig. 577). The disadvantage of such connections is that the voltages become unbalanced under load.

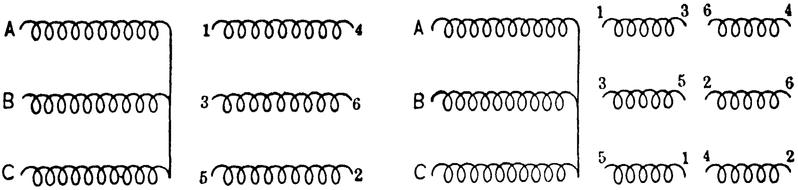

(*a*) (*b*)

Fig. 580. Three-phase to six-phase transformation using (*a*) the diametrical connection, and (*b*) a double delta.

(f) *Double-T connection.* Two transformers are used, with the primaries connected in T (§755). Let these transformers be called *A* and *B*. Each transformer has two secondary windings, say A', A'', and B', B''. The windings A' and B' are T-connected and serve to maintain the voltages 3–5 and *b*–1 (Fig. 577). The windings A'' and B'' are also T-connected and maintain the voltages 2–6 and *a*–4.[10] The arrangement is similar to the double delta described above, except that the delta voltages are produced by means of T-connected windings.

Theoretically, a somewhat different T connection is also possible. One transformer secondary serves to maintain the voltage 1–4 (Fig. 577) and is provided with taps corresponding to the points *a* and *b*. The other transformer has two separate secondary windings in which the voltages 2–6 and 3–5 are induced. A midway tap is provided in each of these windings for connection to the points *a* and *b*.

(g) *Two-phase to six-phase transformation.* This transformation is accomplished by means of two transformers, whose primaries are connected to the two-phase system. On the secondary side the windings are connected in double T, as described under (f) above.[11]

---

[10] For details see the "Standard Handbook for Electrical Engineers," sec. 6, 131–168, McGraw-Hill Book Co.

(h) *Three-phase to twelve-phase transformation.* A transformation from a three-phase star to a six-phase star is shown in Fig. 578. To complete a twelve-phase secondary system, it is only necessary to provide six more voltages displaced by 30 electrical degrees from the secondary voltages so obtained. In a three-phase system, delta voltages are displaced by 30 degrees with respect to the Y voltages (Fig. 577). Imagine, therefore, a second transformer, similar to that shown in Fig. 578, but with the primaries delta-connected, and let this second transformer be connected, in parallel with the first transformer, to the same supply. Then, the voltages induced in the six star-connected secondaries of the second transformer will furnish the required six additional phases for a star-connected twelve-phase system. In other words, this transformation may be schematically represented by the following table:

	Transformer 1	*Transformer* 2
Primaries	Y-connected	Delta-connected
Secondaries	Six-phase star	Six-phase star
Furnish phases	1, 3, 5, 7, 9, 11	2, 4, 6, 8, 10, 12

Such a twelve-phase secondary system is sometimes used with large mercury-vapor rectifiers,[12] polyphase commutator motors, rotary converters, etc., where increasing the number of phases is of advantage.

779. EXPERIMENT 39-F. — Study of Transformations from Three-Phase and Two-Phase to Six-Phase. — The theory and the connections are explained in the preceding section; for the properties of the six-phase system, see §§776 and 777. The voltage relations should first be studied at no load, and a sufficient number of readings taken to draw vectors in their proper phase position with respect to each other. Then a balanced six-phase load, consisting either of stationary impedances or of a rotary converter (Chapter XLV), should be provided. Current and power readings should be taken and checked with the theoretical values. A special study should be made of various methods of measuring power in six-phase systems.

Report. Draw vector diagrams of observed currents and voltages and compare them with the theoretical values to be expected. For a given load, compute the theoretical current, voltage, and kva rating of the individual transformers, and state the advantages and the disadvantages of the different connections given in the text above. Discuss the problem of power measurement in six-phase systems with balanced and with unbalanced loads.

---

[11] See also A. Boyajian, *A.I.E.E.*, *Journal*, vol. 44 (1925), p. 591.

[12] Marti and Winograd, " Mercury Arc Power Rectifiers," Chapter VI, McGraw-Hill Book Co.

GENERAL TRANSFORMATION OF POLYPHASE SYSTEMS

780. With two or more available sources of a-c voltage of the same frequency, but out of phase with each other, it is possible to obtain by combination and transformation an emf of any desired magnitude and phase position, and of the same frequency. In Fig. 581, two transformers are shown connected to a source of two-phase power to the left. For the sake of generality, one of the transformers, *FG*, is shown as an auto-transformer with taps *m* and *n*. *H* and *K* are the primary terminals of a two-winding transformer, whose secondary terminals are *p* and *q*. By connecting *mn* and *pq* in series, a voltage is obtained between the terminals *C* and *D*, which is out of phase with both *A* and *B*. In the vector diagram to the right, *MN* is the voltage between the taps *m* and *n*, and *NQ* is that across the winding *pq*. The sum of the two, *MQ*, is the voltage across *CD*. Thus, with the two available voltages, *OA* and *OB*, a voltage, *MQ*, of any desired magnitude and phase position may be obtained.

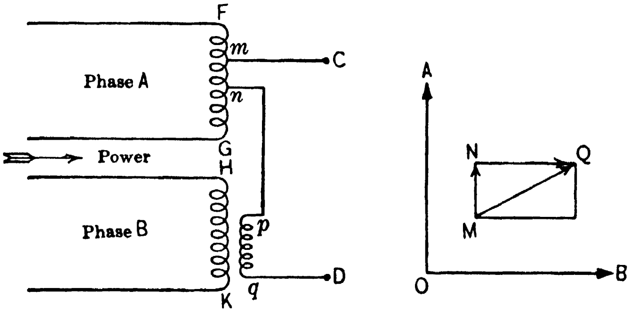

FIG. 581. A combination of two out-of-phase voltages into a third voltage.

An auto-transformer can also be used in phase *B*, in place of the two-winding transformer, provided that the phases *A* and *B* are not electrically interconnected at some other point, say in the generator (§132). If their neutrals are connected in the generator, as in Fig. 569, then connecting the taps on the load side would cause a partial short circuit. For this reason, a two-winding transformer is shown in one of the phases.

By using several taps and several secondary windings, various secondary voltages can be produced, all out of phase with each other and forming a polyphase system. Thus, an *n*-phase system can be obtained out of a two-phase system. Similarly, from a given three-phase system, voltages of any desired magnitude and phase can be obtained by combining parts of the given emf's through transformers and auto-transformers, for example, as in Fig. 575. It can be generally stated that *any desired symmetrical or unsymmetrical n-phase system can be obtained out of any other given symmetrical or unsymmetrical m-phase system, by means of stationary transformers only.* The integers m and n may be equal or different from each other, but m must be not less than 2.

781. Energy Relations in Polyphase Transformations. — In a single-phase circuit with sinusoidal currents and voltages, power as a function of time consists of a constant average value, and of sinusoidal variations of double frequency. Using expressions (4) and (5), §94, we get for the instantaneous power, p:

$$p = ei = E_m I_m \sin 2\pi ft \sin (2\pi ft + \phi) \quad . \; . \; . \; . \; . \quad (6)$$

By a familiar trigonometric transformation this becomes:

$$p = 0.5E_m I_m [\cos \phi - \cos (4\pi ft + \phi)] \quad . \; . \; . \; . \; . \quad (7)$$

Here $0.5E_m I_m \cos \phi$ represents the average power, in accordance with eq. (6), §94, while $0.5E_m I_m \cos [2\pi (2f)t + \phi]$ is the part which fluctuates at the frequency $2f$.

In a general unbalanced n-phase system, the power delivered to the load consists of n such constant terms and of n double-frequency terms, so that, generally speaking, the power is fluctuating. Consequently, the mechanical inertia of the revolving parts of the machines connected to the network is called upon periodically to store and to deliver energy into the line, since the amount of energy stored in the magnetic and electrostatic fluxes of the network itself is usually insufficient for the purpose. Only in a balanced symmetrical n-phase system is the sum total of the power fluctuations in the individual phases identically equal to zero. The currents in the individual phases can be represented as:

$$I_m \sin 2\pi ft,\ I_m \sin (2\pi ft + \alpha),\ I_m \sin (2\pi ft + 2\alpha) \cdots$$
$$I_m \sin [2\pi ft + (n - 1)\alpha]$$

and the voltages as:

$$E_m \sin (2\pi ft + \phi),\ E_m \sin (2\pi ft + \phi + \alpha),\ E_m \sin (2\pi ft + \phi + 2\alpha) \cdots$$
$$E_m \sin [2\pi ft + \phi + (n - 1)\alpha] \quad . \; . \; . \; . \; . \; . \; . \quad (8)$$

where $\alpha = 2\pi/n$. Consequently, forming expressions similar to eq. (7) for all the phases and adding the first terms on the right-hand side of those equations, we find that the total average power is:

$$np = 0.5nE_m I_m \cos \phi \quad . \; . \; . \; . \; . \; . \; . \; . \; . \quad (9)$$

The sum of the second terms is equal to zero, because:

$$\cos\beta + \cos(\beta + 2\alpha) + \cos(\beta + 4\alpha) + \dots + \cos[\beta + 2(n-1)\alpha] = 0 \quad . \; (10)$$

where

$$\beta = 4\pi f t + \phi \quad . \; . \; . \; . \; . \; . \; . \; . \; . \; . \; . \; (11)$$

To see the truth of eq. (10), imagine a "twice-around" regular polygon with n sides, each side being equal to unit length (Fig. 582). In this particular case, $n = 11$, and the polygon is formed by omitting on a circle every second point of division corresponding to $\alpha = 2\pi/11$. Thus, from point A the first side extends to B, instead of h. It is necessary to go around the circle twice before the polygon is closed at A. Such a polygon may be called a "4π polygon," as distinct from an ordinary or 2π polygon. The external angle between any two consecutive sides is $4\pi/n = 2\alpha$, and eq. (10) simply expresses the fact that the sum of the projections of the sides of such a closed polygon on any arbitrary axis is equal to zero.

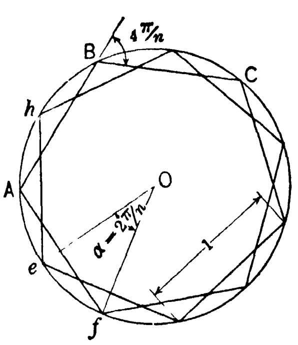

FIG. 582. A "twice-around" or 4π polygon with 11 equal sides.

Thus, the total instantaneous power in a balanced polyphase system remains constant throughout a cycle, and equal to the average power. This fact is of importance in reaching the conclusions stated in the next article.[13]

782. Transformation from Balanced Polyphase to Single-Phase System or Vice Versa. — A single-phase load unbalances a three-phase system, and therefore is undesirable from the operating point of view. Much ill-advised effort has been spent in devising combinations of *stationary* transformers, etc., for obtaining a single-phase load current with balanced three-phase currents in the distributing line. From the theory given in the preceding section it should be clear that a balanced three-phase output takes a constant power from the generator at all instants of a cycle, while a single-phase load requires a fluctuating power with a double-frequency component. Hence, a periodic energy storage between the two, for fractions of a cycle, is indispensable. At the present writing, the only feasible storage of energy of this kind is afforded by the moment of inertia of a *revolving machine.* This means a motor-generator or converter of some sort, connected both to the three-phase line and to the single-phase load.

---

[13] For a mathematical theory of the general unsymmetrical phase transformation see *Archiv für Elektrot.*, vol. 7 (1919), p. 426. Some general properties of polyphase systems will also be found in the last chapter of the pamphlet mentioned in the footnote at the end of §702.

Of course, a single-phase load can be so connected as to draw some current from all the three phases, and thus to cause a minimum of unbalance. For example, let the three-phase terminals be A, B, C, and let an auto-transformer be connected between B and C, with a center tap at D. Then, a single-phase load connected between A and D will cause less unbalance than one directly connected between A and B, or A and C.

The inverse problem, namely, a conversion of single-phase into polyphase power, without revolving machinery, has also occupied the attention of inventors. From the preceding theory it should be clear that such a conversion into a balanced polyphase system also requires energy storage during some parts of the cycle, since the energy flow from a single-phase source is fluctuating. Hence, a revolving converter seems indispensable[14] (§518). Imperfect two- and three-phase combinations may be obtained from a single-phase supply, by using inductance and capacitance (§§508, and 511).[15]

REFERENCES

1. BRYANT and JOHNSON, Alternating-Current Machinery, Chapter XI, McGraw-Hill Book Co.

2. O. G. C. DAHL, Electric Circuits, Theory and Applications, Chapter IV, McGraw-Hill Book Co.

3. C. P. STEINMETZ, Alternating-Current Phenomena, Chapter XXXVI, McGraw-Hill Book. Co.

4. PUCHSTEIN and LLOYD, Alternating-Current Machines, Chapter XIX, John Wiley & Sons.

5. BLUME and BOYAJIAN, Transformer Connections, General Electric Co.

6. Standard handbook for Electrical Engineers, Sec. VI, McGraw-Hill Book Co.

7. E. G. REED, Transformer Practice, Chapters XXV–XXVIII, Van Nostrand Co.

8. BLUME et al., Transformer Engineering, Chapters VII and VIII, John Wiley & Sons.

9. MARTI and WINOGRAD, Mercury Arc Rectifiers, Chapter VI, Rectifier transformers, McGraw-Hill Book Co.

---

[14] For phase balancing and phase transformation, see *General Electric Review*, vol. 16, pp. 87 and 962; vol. 20, pp. 352 and 479; vol. 21, p. 196; *Revue générale de l'électr.*, vol. 2 (1917), pp. 403 and 443.

[15] It is becoming commercially practicable to employ thyratron rectifiers (Chapter LVIII) or mercury-arc rectifiers (Chapter LVI), to change polyphase a-c power to d-c power, and then by means of the same devices to convert the direct current to single-phase alternating current. The system is reversible.

CHAPTER XL

HARMONICS IN POLYPHASE SYSTEMS

783. In the preceding chapters on polyphase relations, the currents and the voltages have been assumed to vary with the time according to the sine law. Although this simplifying assumption gives sufficiently accurate results in most practical cases, yet there are other cases in which higher harmonics (§1132) in the currents or in the voltages are of sufficient magnitude to cause relations appreciably different from those deduced above. Higher harmonics sometimes cause operating troubles, such as voltages of audible frequencies induced by a power line in a paralleling telephone line; oscillating neutral; wrong operation of relays in the ground connection; excessive dielectric stresses in transformers; resonance conditions; circulating currents in delta-connected windings; distorted field and current in induction machines (§963), with consequent modification of operating characteristics, etc. For these reasons, a treatment of the three-phase system is not complete without at least a brief outline of the principal properties of its higher harmonics.

Sources of higher harmonics in a-c systems. Among the more usual causes for the existence of harmonics in electric circuits are:

(a) The non-linear relation between the flux in a transformer core and the exciting current. This is discussed below with reference to Fig. 586.

(b) A non-sinusoidal flux distribution in the air-gaps of alternators, leading to non-sine form emf's in the individual conductors and, to a lesser degree, at the terminals of the machine (§810).

(c) Supplementing (b) above, ripples in the air-gap flux distribution due to periodic variation in the air-gap permeance as the number of stator teeth beneath a pole changes, or stator teeth come opposite, first rotor teeth, and then rotor slots.

(d) Cyclical changes in the resistance or impedance of such attached apparatus as mercury-arc rectifiers (Chapter LVI), electric arcs, or gaseous conductors (Chapter LIX), etc.

784. Harmonics That Are Multiples of Three, or Triplen Harmonics. — Let the Y voltages induced in a three-phase alternator depart from the sine wave owing to the imperfect distribution in space of the magnetic field and of the armature winding. Furthermore, let it be assumed, for the sake of simplicity, that the irregular wave of the induced emf can be represented with sufficient accuracy by its fundamental and a third harmonic only.

In Fig. 583, A_1, B_1, C_1 are the fundamental sine waves of three voltages, displaced by 120 electrical degrees, while A_3, B_3, C_3 represent the sine waves of the third harmonics. These harmonics coincide, because an interval of time corresponding to 120 electrical degrees for the fundamental represents 360 degrees for the third harmonic. The zero point of the third harmonic is assumed to be displaced by an angle δ_3 with respect to that of the fundamental, and the harmonic is drawn from point *a*. Similarly, the harmonic B_3 is drawn from point *b*, and C_3 from point *c*. By extending these third harmonics, in time, indefinitely both ways, it will be seen that they are graphically represented by the same sine curve. The same relationship is shown by vectors to the right. The reader can satisfy himself of the fact that the same is true of all higher harmonics that are multiples of three, that is, the ninth, fifteenth, twenty-first, etc.

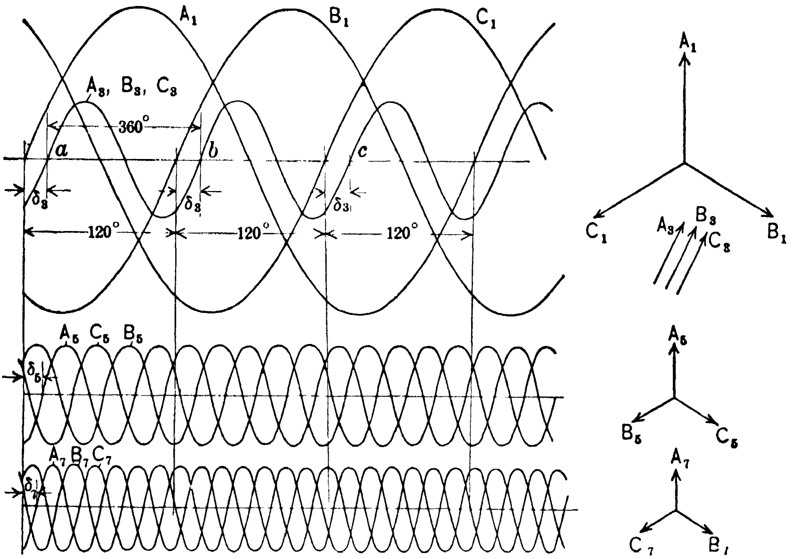

FIG. 583. Sine waves of the first, third, fifth, and seventh harmonics in a three-phase system.

Electrically, this means that, *when three voltages or currents are displaced with respect to each other by 120 electrical degrees, their corresponding higher harmonics of any order that is a multiple of three are in time phase with one another.* It is shown below that this property of harmonics multiple of three leads to important secondary phenomena in power plants and transmission systems.

The term "triplen," meaning "of the order $3n$," has been adopted by the authors as an abbreviation of the expression "multiple of three."[1] It may be further simplified to "$3n$," used as an adjective. Harmonics of the order 5, 7, 11, 13, etc., may be called "non-triplen" harmonics.

785. Oscillating Neutral. — In Fig. 584, the Y voltages induced in the alternator $OABC$ are assumed to be strictly sinusoidal, and an additional fictitious single-phase alternator, H, is supposed to be connected in series with each lead. The voltages induced in the three H windings are of the triple frequency and in phase with one another. Then, in accordance with Fig. 583, the total star voltages impressed upon the primary terminals, 1, 2, 3, of the transformer are the same as if the generator voltages were non-sinusoidal and consisted of the fundamental and a third harmonic.

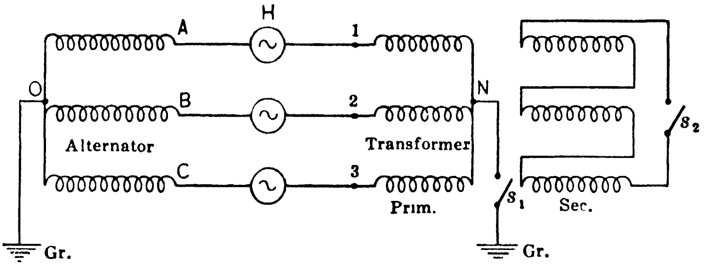

FIG. 584 Circuits for the explanation of the oscillating neutral and of ground currents due to triplen harmonics

Assume the following conditions to exist in the circuit: The secondary circuit of the transformer is open; the magnetic saturation in the transformer cores is negligible; the generator neutral, O, is grounded, and the transformer neutral, N, is disconnected from the ground. The potential of the point N is equal to the sum of those due to the first and the third harmonics. With balanced voltages and equal line impedances, the potentials of O and N are the same so far as the first harmonic (or fundamental) is concerned. For the third harmonic, the three-phase circuit is an open single-phase circuit with three parallel branches $A1$, $B2$, $C3$. Hence, if the maximum value of the voltage of the generator H is E_3, the potential of N varies with respect to the ground at O as a sine wave, between the limits $\pm E_3$. For this reason, when such a condition actually obtains, N is called an *oscillating neutral.*

Let the amplitude of the fundamental of the alternator Y voltage be

---

[1] V. Karapetoff, *Electrical World*, vol. 83 (1924), p 237.

E, and let the third harmonic be a fraction, α, of E. Then the instantaneous potentials of N with respect to the ground reach values $E_3 = \alpha E$, which under some circumstances may lead to considerable electrostatic disturbances and other complications in the operation of the system.

A third harmonic in a Y voltage does not appear in the delta voltage, because a delta voltage, say E_{12}, is a difference between the two Y voltages, E_1 and E_2. Since the third harmonic is the same in both (Fig. 583), it disappears in subtraction. In other words, the voltage between the terminals A and B (Fig. 584) is the same as between the terminals 1 and 2, and is a pure sine wave in both cases. Moreover, an appreciable third harmonic cannot be produced in the line voltage by connecting the three alternator windings in delta, because the circulating third harmonic current in the delta in part consumes the third harmonic emf by the IR and IX drops which it causes in each unit length of circuit; in part it reacts upon the field flux of the machine and so modifies it as practically to wipe out the triple harmonic. The same is true of the ninth, fifteenth, twenty-first, and other triplen harmonics. Thus *triplen harmonics do not appear in the line or delta voltages, and their absence is no indication of the extent of such harmonics in the Y voltages. It is the triplen harmonics in the Y voltages that give rise to an oscillating neutral.*

786. Harmonics Other Than Multiples of Three, or Non-Triplen Harmonics. — Let us assume now that each of the three voltages, A, B, C (Fig. 584), has a fifth harmonic. The phase angle between the fifth harmonics belonging to the phases A and B is 5 × 120° = 600°, or, which is the same, 600 − 2 × 360 = −120°. Thus, while the fundamental, B_1, *lags behind* A_1 by 120°, the fifth harmonic, B_5, *leads* A_5 by 120°. This is shown in the middle part of Fig. 583 by sine waves and by vectors. Similarly, for the seventh harmonic the phase angle between A_7 and B_7 is 7 × 120 = 840°, or +120°. We thus arrive at the following table:

Non-triplen harmonics of positive phase sequence, $6n + 1$	1			7			13		
Triplen harmonics, $6n + 3$		3			9			15	
Non-triplen harmonics of negative phase sequence, $6n - 1$			5			11			17

In this table, the expressions positive and negative phase sequence, and the terms triplen and non-triplen, are used in the sense explained in §§710 and 784. In the harmonics of the orders 1, 7, 13, etc., the wave in phase B lags behind that in phase A by 120 electrical degrees. The orders of these harmonics are obtained from the formula $6n + 1$, by putting $n = 0, 1, 2, 3$, etc. For the triplen harmonics, of the orders 3, 9, 15, etc., the amplitudes of the waves in all the three phases are reached at the same time. In the remaining non-triplen harmonics (the third line of the table) the clockwise order of the phases is A, C, B, instead of A, B, C.

It has been shown above that the triplen harmonics modify the characteristics of a Y-connected three-phase system, by adding to it some properties of a single-phase system. The harmonics of the orders 7, 13, 19, etc., constitute a three-phase system of the same phase sequence as the three fundamental waves, and therefore modify the properties of the system only quantitatively. Thus, if the star voltages contain α per cent of the seventh harmonic, the delta voltages will also contain α per cent of the seventh harmonic. If, in a machine, the revolving field due to the armature currents rotates clockwise for the fundamental waves, it will also rotate clockwise for the seventh harmonics, at seven times the synchronous angular velocity.[2] The harmonics of the negative phase sequence also form a three-phase system, and are present to the same extent in the Y and line voltages, but the magnetic and electrostatic fields due to these harmonics revolve in the opposite direction from those due to the fundamental waves.

787. Higher Harmonics Caused by Saturation in Transformer Core.— In §785 it was assumed that the third harmonic in the voltage is due to an externally applied emf, such as H in Fig. 585. Often, such an harmonic is due to saturation in the magnetic circuit of the transformers.

In Fig. 585 a typical hysteresis loop (flux-current curve) for a transformer core is shown, together with the flux-time curve, and curve of applied emf, the last two being shown as sine waves. The counter emf is assumed to be equal and opposite to the applied voltage at every instant. Strictly speaking, a sine wave of impressed voltage will not lead to a pure sine wave of counter emf and of flux, owing to the non-sinusoidal iR drop in the primary winding, which is of the same form as the exciting current. This small effect is here neglected.

The construction by which the wave of exciting (magnetizing plus hysteresis) current may be derived is shown in Fig. 585. At the flux ϕ_0 the current is zero as shown by the hysteresis loop. This occurs, according to the flux-time curve, at time t_0. Similarly ϕ_1 requires a current i_1 which, by the flux-time curve, comes at time t_1. Proceeding in this way the complete loop of exciting current is constructed. In addition the current curve ought to contain a small component, in phase with the impressed voltage wave, to supply the eddy-current loss (§217). This is here neglected, and it affects the form of the exciting current but little.

---

[2] See Note on p. 262.

An inspection of the exciting current curve shows that it has a prominent third harmonic. Analysis of the wave forms of transformer exciting currents[3] shows the relative values of components varying with

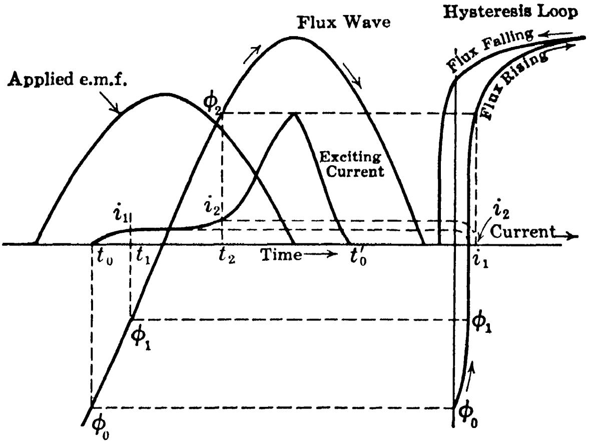

FIG. 585. Graphical construction to show the effect of hysteresis upon the exciting current wave shape.

maximum flux density somewhat as follows: the fundamental is from 95 to 90 per cent of the equivalent sine wave of current; the third harmonic from 30 to 40 per cent, and the fifth harmonic from 7½ to 15 per cent, with the flux density varying from 7.5 to 15 kilogausses.

Thus, in order to produce a sinusoidal counter emf, the transformer magnetizing current must have a pronounced third harmonic. But, according to Fig. 583, which shows three transformers connected in Y, without a neutral return, the triple harmonics in the three line leads are in phase with each other, and since the ground connection at N is broken, such harmonic currents cannot flow. The same is true of other triplen harmonics. Consequently, the actual conditions with the switch s_1 open are those shown in Fig. 586. The magnetizing current, I, is nearly sinusoidal (or at least devoid of the third harmonic). Hence, in a saturated magnetic circuit, the flux, Φ, varies with the time as a flat-top wave.

---

[3] For values of higher harmonics in the magnetizing current for silicon steel, see *Electric Journal*, vol. 21 (1924), p. 17.

The induced voltage, E, at any instant is proportional to $d\Phi/dt$, and consequently is a peaked wave. This wave can be resolved into a fundamental, E_1, and a third harmonic, E_3 (there are also other higher harmonics). This harmonic, as well as other triplen harmonic voltages, causes an oscillating neutral. Thus, *because with an isolated neutral point triple-frequency exciting currents cannot flow, the flux wave in a saturated transformer is flat and the induced-voltage wave is peaked and has a considerable triple harmonic.* With highly saturated cores, the third harmonic of the voltage may reach as high as 50 per cent of the fundamental and thus cause a serious additional strain on the insulation.

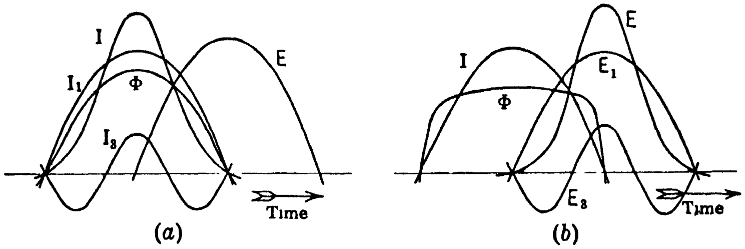

FIG. 586. Curves showing a third harmonic, (a) in the current, (b) in the voltage, due to magnetic saturation.

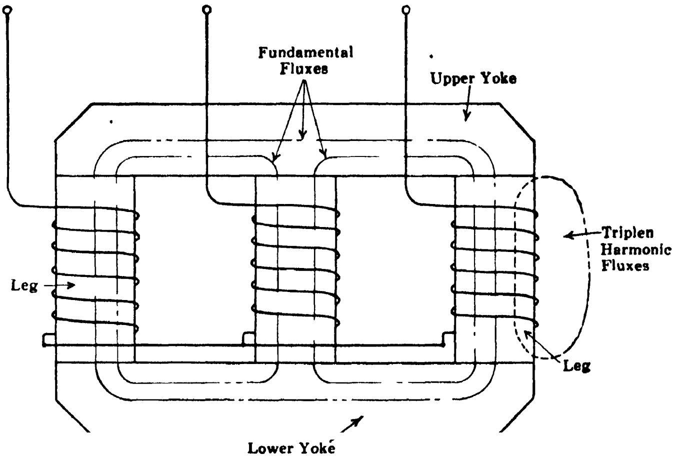

FIG. 587. Magnetic and electric circuits of the three-phase core-type transformer.

The foregoing explanation applies to a bank of three single-phase transformers or to a shell-type three-phase transformer. The latter consists of three sections, each built somewhat like that shown in Fig. 272, with practically independent magnetic circuits. In a three-phase core-type transformer (Fig. 587), each core has to serve as the common return for the fluxes of the other two. Thus, the three legs are magnetically Y-connected by the upper and lower yokes. Hence, the triplen harmonics of the fluxes, being in phase with one another, cannot exist in such a core, for the same reason that triplen harmonics of current cannot exist when one of the neutrals is open. Consequently, with sinusoidal exciting currents (Fig. 586) and flat-top fluxes, only the fundamental sinusoidal components of these fluxes and their non-triplen harmonics can exist in the end yokes. The triplen harmonics must follow leakage magnetic paths through the air. These paths are of high reluctance, so that only comparatively small fluxes of triplen frequencies are found, and the corresponding triplen harmonic voltages are also comparatively small.[4] Some three-phase core-type transformers are made with five legs, the two outside legs, without windings, being intended to provide low-reluctance paths for triplen fluxes.

788. Triplen Harmonic Currents in the Neutral Return. — We have so far assumed the switch s_1 (Fig. 584) to be open. Now let this switch be closed, while the secondary circuit is still open at s_2. The triplen harmonic voltages can actually produce currents which are in phase with each other in all the three line conductors; a current equal to their sum flows through the ground and the two neutral connections.[5] The conditions in the transformers become those shown in Fig. 585. The flux and the induced emf can vary according to the sine law because the magnetizing current can have the required triplen harmonics. Therefore, even with highly saturated magnetic cores, only comparatively small third harmonics of voltage, just sufficient for the flow of the triplen currents, are produced.

---

[4] Several papers and valuable discussion on transformer connections and their effect upon higher harmonics will be found in the *Trans. A.I.E.E.*, vol. 33 (1914), part 1, pp. 685 to 817; *ibid.*, vol. 34, p. 2157; vol. 36, p. 1081; *Jour. A.I.E.E.*, vol. 41 (1922), p. 351. See also *Electrical World*, vol. 65 (1915), p. 157; vol. 75 (1920), p. 780; vol. 80 (1922), p. 1276. *Electrical Journal*, vol. 16 (1919), p. 477. *Revue générale de l'élect.*, vol. 2 (1917), p. 363; vol. 8, pp. 299 and 363; vol. 9, p. 557. *Elektrot. und Maschinenbau*, vol. 36 (1918), pp. 185 and 197; vol. 41 (1923), pp. 333 and 349. O. G. C. Dahl, *National El. Light Assn.*, in the 1923 "Report of the Inductive Coördination Committee"; S. A. Stigant, *El. Times*, vol. 65 (1924), p. 239, and vol. 66, p. 657; P. Kemp and H. P. Young, *Inst. El. Engrs.* (British), *Journal*, vol. 63 (1925), p. 877.

[5] For an actual case of a large triplen ground current, see *Engineering*, vol. 116 (1923), p. 40.

The triplen currents may be objectionable because of their inductive effect upon paralleling telephone lines, and there may be other objections to grounding both neutrals solidly. For example, triplen currents in the neutral connection may cause faulty operation of some relays which are supposed to respond only on an unbalanced load, that is, to a current of fundamental frequency in the neutral. Since triple-frequency currents may exist with a perfectly balanced load, such relays must be designed to discriminate between, say, a 60-cycle and a 180-cycle current.

789. EXPERIMENT 40-A. — Harmonics in Y-Connected System. — The purpose of the experiment is to investigate the presence and the extent of the voltage and current harmonics described in §§783 to 788. For a thorough study it is convenient to have a set of harmonic alternators (§1141), by means of which a multiple-frequency voltage of any desired magnitude and phase position may be added to the fundamental voltage. In the absence of such a set, harmonics can be produced by using saturated iron cores, arcs, resonating circuits, etc.

An oscillograph (Chapter LVII) offers the natural means of ascertaining the presence or absence and the extent of various harmonics. For the purposes of this experiment it is desirable to produce harmonics sufficiently large in comparison with the fundamental to be directly discernible on the oscillograms, without the tedious process of analyzing each curve (Chapter LVII).

Wherever possible, a qualitative result should also be obtained without the oscillograph. For example, with an oscillating neutral, a high-impedance telephone receiver, connected between the insulated neutral and the ground, will respond at a frequency of 180 cycles. This tone is readily distinguishable by the ear from the 60-cycle hum and can be checked with an organ pipe, etc. A current or voltage of a higher frequency can also be made to cause resonance in a properly tuned test circuit. In this manner, an ingenious and thoughtful student will find various ways of demonstrating the existence of certain harmonics, with comparatively simple means.

As to the points to be investigated, any of the statements made in the foregoing sections of the chapter can be made a subject of test or study, by properly choosing the circuit conditions.

790. Triplen Harmonic Currents in Delta-Connected Windings.[6] — In Fig. 584, let the switch s_1 be open and the switch s_2 closed. The delta-connected secondary winding (§744) may be the one to which the outgoing circuit is connected, or it may be a special *tertiary* winding not connected to any circuit and provided for the express purpose of wiping out the triplen harmonics in the transformer fluxes.

---

[6] See O. G. C. Dahl, "Electric Circuits, Theory and Application," Chapter VIII, McGraw-Hill Book Co.

The fundamental waves (first harmonics) of the induced emf's sum up, around the delta, to a total voltage equal to zero, being a sum of three voltages displaced in time phase by 120 electrical degrees. But the three third harmonics of the flux and induced emf are all in time phase with each other (§784). Consequently, a third harmonic current will flow in the closed delta, in such a direction as to oppose the inducing triplen fluxes and to weaken them. The conditions are similar to those in a short-circuited single-phase transformer; with a proper design, a very small triplen flux can be made to circulate large triplen delta currents.

We thus see that, in a three-phase transformer with a low-impedance delta-connected secondary winding, only very small fluxes and voltages of triplen frequencies can exist. Therefore, one of the neutral points can be kept insulated from the ground without producing an objectionable oscillating neutral (§785). Even with both neutrals grounded, the triplen currents can be made to flow mainly in the secondary (or tertiary) winding, rather than through the ground.

It is sometimes stated that the tertiary delta-connected winding furnishes the required triple-frequency currents to keep the flux sinusoidal (Fig. 586). Perhaps theoretically it is more correct to say that the secondary delta provides a low-impedance electric circuit linked with the triple harmonics of the flux, and thus prevents them from reaching an appreciable magnitude. The tertiary winding has no effect upon the non-triplen harmonics, because at such frequencies the sum of the emf's induced in a closed delta is equal to zero (§786).

Sometimes transformers are connected in delta both on the primary and on the secondary side. With saturated cores, triplen harmonic currents will circulate in both the primary and the secondary delta, in a concurrent direction, and not against each other as do the fundamental currents. The relative magnitude of the triplen harmonic currents in the two deltas will depend upon the relative impedances of the two windings.

It will be understood from the preceding theory that large circulating currents of triplen frequencies may exist in the delta-connected windings of a transformer or in a delta-connected load, without any trace of them in the line currents. Thus, in delta-connected windings of a generator or motor there is always a possibility of such currents due to non-sinusoidal fluxes. These currents cause additional copper loss, and for this and other reasons have to be guarded against. A delta-connected three-phase generator or motor is the exception rather than the rule.

791. EXPERIMENT 40-B. — Triplen Harmonic Currents in a Delta-Connected Winding. — The purpose of the experiment is to investigate the relations described in §790. For general instructions, see §789. It is not absolutely necessary to have the transformer primaries connected in Y and the secondaries in delta. The primaries may be delta-connected and the secondary winding may be absent altogether. Then, with saturated cores, triple harmonics of current will be found in the delta-connected windings, although absent in the line conductors. This will explain the fact that the ratio of the Y currents to the delta currents will be found to be different from the square root of three. If the primaries are Y-connected and the secondaries are in delta, then by opening one of the " corners " of the delta, a triple-frequency voltage can be measured.

Notice that the effective value of the exciting current is *smaller* with the secondary delta open, while the corresponding effective value of the voltage is then *larger*. This is because the triplen components in the distorted voltage wave increase its effective value, but have such a phase that they decrease its *average* value, on which the exciting current depends

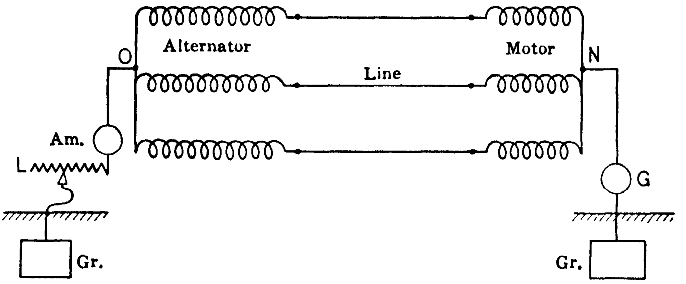

FIG. 588. Superposed three-phase and single-phase power transmission.

792. Superposed Transmission over a Three-Phase Line. — Consider a three-phase system (Fig. 588) consisting of an alternator, a line, and a load, say a motor. Assuming the load in the three phases to be nearly balanced, and no appreciable triplen harmonic voltages to exist, the current in the ground connections will be very small. Now let a source of electric energy, *G*, be connected in one of the neutrals, say *N*, and a single-phase load, *L*, be placed in the other neutral connection. In this way, it is possible to transmit this superimposed single-phase energy (or signals) between points many miles apart, by using an existing three-phase line. The source, *G*, may be an alternator of a frequency entirely different from that of the three-phase source, or it may be a d-c generator or battery. The currents due to this source are transmitted over the three line conductors in parallel, and are recombined at the load end. The output can be regulated at will.

Let i be the current in one of the line conductors, due to the three-phase source, and let i' be that due to the single-phase source. Then, if r is the resistance of the conductor, the instantaneous power loss is $(i + i')^2r$, and the integrated energy loss is:

$$W = \int_0^T (i + i')^2 r \, dt \quad . \; . \quad . \quad . \; . \; . \quad (1)$$

where T is an interval of time sufficiently long for the conditions to become identical with those at $t = 0$. For example, if the frequency of one source is 60 cycles and that of the other 25 cycles, then T may be equal to one-fifth of a second or to any of its multiples. Expanding the right-hand side of eq. (1) and omitting the factor, we get:

$$\int_0^T (i + i')^2 \, dt = \int_0^T i^2 \, dt + \int_0^T i'^2 \, dt + 2 \int_0^T ii' \, dt \quad . \; . \quad (2)$$

With regular current curves, the third integral on the right-hand side is usually equal to zero, because there are as many positive as negative products of the same magnitude. Hence,

$$I^2_{eq} = I^2 + I'^2 \quad . \; . \; . \; . \; . \; . \; . \; . \; . \; . \quad (3)$$

where the capital letters denote the effective values of the currents $(i + i')$, i, and i', respectively. In other words, the total heating corresponds to the sum of the losses due to each effective current as if it were acting alone.

Although the superposition of two sources of energy has not been used in practice to any extent, except in telegraph and telephone work, the theoretical features of the combination are of sufficient interest to warrant an experimental investigation.

793. EXPERIMENT 40-C. — Superposition of Uniphase Transmission between Three-Phase Neutrals. — The arrangement is explained in the preceding section, and it is desired to investigate its possibilities, limitations, and practical difficulties. The three-phase system may consist of an alternator and an induction motor, or of an alternator and a set of balanced stationary impedances. The superimposed source may be direct or alternating current of any desired frequency. First, the three-phase system should be set for some desired conditions, without the single-phase power, and then left without further adjustment. The single-phase voltage and load should then be increased in steps, and their effect upon the three-phase voltages, currents, power, etc., studied at each step. A few oscillograms should be taken, and the observed phenomena interpreted theoretically.

794. Harmonics in a Symmetrical *M*-Phase System. — The treatment given above for the three-phase system can be extended to any number of phases. The general problem may be stated thus: "What are the properties of the *n*th harmonic in an *m*-phase system?" A solution of this problem is outside the scope of the present work.[7]

795. Inductive Coordination between Power and Communication Circuits. — A loaded high-tension power-transmission line creates strong alternating magnetic and electrostatic fields in the surrounding space. These fields may induce, in a paralleling telephone, telegraph, or signal circuit, voltages and currents that may either interfere with the transmission of intelligence or be dangerous to life or property.[8] The problems of the theoretical amount of mutual induction, measurement of interference, and means for reducing it, are too large and too special to be treated here. The preceding theory, especially the treatment of unbalanced currents and voltages, phase sequence, residue currents, triplen and non-triplen harmonics, etc., should prepare the reader to deal intelligently with practical problems of inductive interference and adjustment, or *coordination,* as it is called.

A considerable amount of experimental and theoretical work on the subject has been done jointly by the American Telephone & Telegraph Co. and the National Electric Light Association. As a result, practical rules and recommendations have been worked out for a proper coordination of the two kinds of circuits and for a cooperative adjustment of a possible interference.[9]

796. EXPERIMENT 40-D. — Study of Inductive Interference between Power and Communication Circuits. — The underlying principles will be found in the preceding section and in §§156 to 159, Vol. I. Some of the reports in the above-mentioned "California Book" may be taken as a guide, and the laboratory conditions approximated to those observed on actual lines. Coils of wire can be used to produce the required mutual magnetic induction and static condensers interposed to represent the mutual electrostatic fluxes.

---

[7] See Hague, *Electrician,* vol. 78 (1916–17), pp. 710, 740, 765; V. Karapetoff, *Electrical World,* vol. 71 (1918), p. 660.

[8] See various reports of the Joint General Committee of National Electric Light Association and Bell Telephone System, on Physical Relations between Electrical Supply and Signal Systems; also a large volume entitled "Inductive Interference between Electric Power and Communication Circuits," published by the Railroad Commission of the State of California in 1919. This volume contains a large amount of experimental data, methods of measurement, a valuable bibliography, etc.

[9] See R. R. Lawrence, "Principles of Alternating Currents," Second Edition, Chapter XIV, McGraw-Hill Book Co. "Electrical Engineers' Handbook," Vol. V, Sec. 8, John Wiley & Sons. Marti and Winograd, "Mercury Arc Power Rectifiers," Chapter XIII, McGraw-Hill Book Co.

NOTE *to p. 253. In* V. *Karapetoff's* "Magnetic Circuit," on pp. 136 and 137, *statements are made to the effect that the linear velocity of higher harmonics of mmf is lower than that of the fundamental.* This in no way contradicts the statement on p. 253 above, because in this case harmonics *in time* are meant, whereas in the "Magnetic Circuit" the *space* harmonics of the mmf are understood, due to the fundamental component of the current. See also R. R. Lawrence, "Principles of A-C Machinery," Third Edition, p. 505, McGraw-Hill Book Co.

CHAPTER XLI

PERFORMANCE DIAGRAMS OF NON-SALIENT-POLE SYNCHRONOUS MACHINES

797. Chapters XIX to XXI treated the synchronous generator in the more usual aspects of performance, regulation, and parallel operation. It is proposed now to develop the general vector and locus diagrams for both the salient-pole and the non-salient-pole machines in order that by their means the performance of a machine of given constants can be predicted, or the observed performance interpreted.

Figures 318 and 319 illustrate, somewhat schematically, the salient-pole alternator. The field structure consists of a spider and rim to which are fastened definite poles, each pole carrying a concentrated field winding, and each pole shoe covering about $\frac{2}{3}$ to $\frac{3}{4}$ of a pole pitch. The air-gap of such machines varies from a fraction of an inch under the center of the pole to several inches between poles.

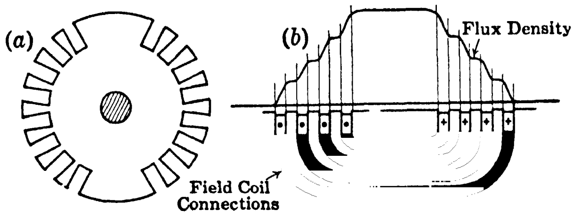

Fig. 589. (*a*) Section through rotor core of a non-salient pole alternator, (*b*) Developed field winding and resultant flux distribution.

In the non-salient-pole machine the field structure (rotor) consists of a cylinder of steel in which slots have been milled for the reception of a distributed field winding (Fig. 589*a*). Except for the influence of stator and rotor slots the air-gap is uniform in length throughout the circumference of the machine. This accounts for much of the difference in performance of the two types. The distributed field winding, giving a form of field mmf and flux which is nearly sinusoidal (Fig. 589*b*), leads to further difference between the machines.

As a result of this nearly sine-form distribution it is quite accurate to represent the field mmf by a vector, so that vector diagrams involving the combined effects of armature mmf (essentially sine form) and field mmf lead to more truthful results than in the non-salient-pole machine.

All the diagrams developed below apply to both the synchronous generator and the synchronous motor. The same synchronous machine is capable of being operated either in the "generator range" or in the "motor range," and with the current either lagging or leading, so that, with a proper choice of the phase angle between the current and the voltage, the same vector diagram can be made to represent four different operating conditions (Fig. 590).

798. Phase-Angle Notation. — The agreement regarding the phase angle is shown in Fig. 590. Whether the machine is operating as a generator or as a motor, two equal and opposite terminal voltages may be distinguished. One, the *generator voltage*, E_g, is that part of the voltage induced in the machine which appears at the terminals, after accounting for the impedance drop in the armature. It may be called the "voltage rise" through the machine. The other, E_l, is the *line voltage* imposed, say, by the other machines connected to the same bus-bars and is the voltage drop across the alternator. When the vector of the armature current is within 90 degrees of the voltage rise through the alternator, or has a position such as I_1, the machine is operating as a generator, with a lagging current. In this case, the phase angle ϕ_1 is less than 90 degrees, and we shall arbitrarily assume it to be positive. This assumption is convenient in practical applications because the current is usually lagging and it is not necessary to introduce a negative angle. Thus, when the phase angle is 30 degrees we shall understand that the voltage *leads* the current by 30 degrees. When the current is leading, as I_2, the phase angle ϕ_2 will be considered negative.

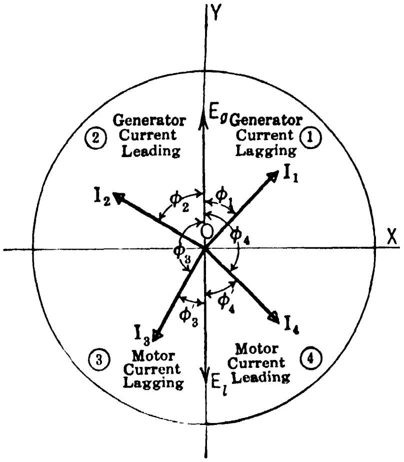

Fig. 590. Quadrants of generator range and motor range in a synchronous machine.

In motor operation, it is customary to refer the phase of the armature current not to E_g but to E_l. Consequently, in the position I_3 the armature current is said to be lagging by the angle ϕ_3', while the current I_4 is said to be leading by ϕ_4'. However, in order to be able to use the same vector diagrams and equations in the motor range as in the generator range, it is convenient to refer the position of the current vector to E_g in all cases. The current I_3 then leads E_g by the angle ϕ_3, and I_4 slag behind E_g by the angle ϕ_4.

When a current has a positive component along the Y axis, the machine is operating as a generator; when this component is negative, the machine is working as a motor. When the current vector has a positive component along the X axis, the current is lagging with respect to the generated voltage, E_g, or leading with respect to the line voltage, E_l. In other words, referring either to the current I_1 or I_4, it is proper to say that the machine is *delivering* a lagging component of the current to the line or *taking* a leading component from the line. Similarly, for the operating conditions I_2 and I_3, the machine may be said to be generating a leading current or absorbing a lagging component of a line current.

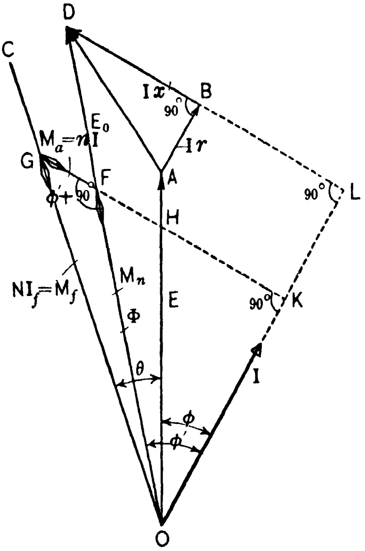

FIG. 591. The Potier diagram of the synchronous machine with non-salient poles.

799. The Potier Diagram. — The Potier method was illustrated in Fig. 340, Vol. I, in conjunction with the no-load saturation curve. It is shown in a slightly different form in Fig. 591. Let $OA = E$ be the terminal voltage of a generator, corresponding to E_g in Fig. 590, and let I be the vector of the current generated by the machine, the current lagging by an angle ϕ. Adding the ohmic drop, $AB = Ir$, in phase with the current, and the reactive drop, $BD = Ix$, in a leading quadrature therewith, we obtain the vector OD, which represents the induced voltage, E_g, of the machine, in magnitude and in phase position (compare Figs. 591 and 340).

This voltage, E_g, is induced by the air-gap flux Φ, the vector of which we shall draw in phase with E_g. For our purposes, the position of Φ with respect to E_g is immaterial because Φ is used in a *space* diagram, while E_g belongs to the *time* diagram. The flux Φ is due to the resultant action of two mmf's, that of the field winding and that of the armature reaction. As stated (§797), the two mmf's can be added or subtracted geometrically. The vector OG represents the field mmf, M_f, and $FG = M_a$ is the more or less opposing mmf of the armature ampere-turns. The resultant or *net* mmf, M_n, is in phase with the resulting flux, and is represented by the vector OF.[1]

---

[1] See V. Karapetoff, "Magnetic Circuit," Chapters VII and VIII, McGraw-Hill Book Co.

The space, or vector, relation between field and armature mmf's is illustrated in Fig. 592, which is drawn for a three-phase salient-pole alternator. For simplicity, or as a first approximation, it is assumed that the flux is symmetrical about the axis of the poles. At unity (internal) power factor (Fig. 592*a*) maximum current occurs in the phase which is in the most dense field, shown here at the center of the poles, with lesser currents (half the maximum) in the phase groups to right and left. The axis of armature mmf, M_a, is then displaced 90 electrical degrees from the axis of the field. In this position it is called "transverse armature reaction."

At zero power factor, lagging, maximum current exists in a phase after the field has moved 90 degrees. This brings the axis of the armature mmf, M_a, into direct opposition to the field (Fig. 592*b*), and it is now called "direct armature reaction."

Figure 592*c* illustrates conditions at a lagging internal power factor, between zero and 100 per cent (cos ϕ'). The axis of armature reaction, M_a, is now at the angle ($90 - \phi'$) from the axis of the field.

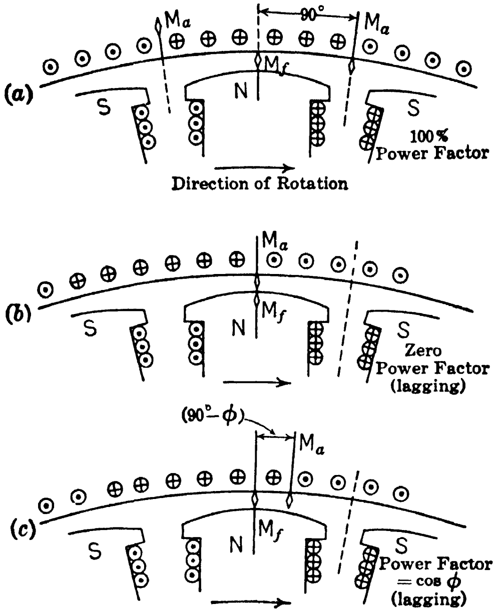

FIG. 592. Relative positions of the axes of field and armature mmf's at various power factors (zero field distortion assumed).

Strictly speaking, for any power factor except zero, the axis of the resultant field does not coincide with the center line of the poles so that, at unity power factor, for instance, M_a is at 90 degrees from the resultant field, or mmf, M_n. This is in accordance with Fig. 591 and the other diagrams which appear in the text.

The relationship between Φ (or E_g) and M_n is given approximately by the no-load saturation curve of the machine. More accurately, the relationship is a curve that lies somewhat below the no-load saturation curve, because with a loaded machine the magnetic leakage factor is somewhat higher than at no load (Karapetoff, "Magnetic Circuit," p. 113).

In the simplest case, let E, I, and ϕ be given, and let it be required to find the necessary field current, or the mmf M_f, all the constants of the machine being known. The figure $OABD$ can then be constructed and E_g found. From the no-load saturation curve of the machine (Fig. 340) the field ampere-turns, $M_n = OF$, corresponding to E_g, are then read off, and the ampere-turns of the armature reaction, $M_a = FG$, are computed from the known number of turns and the arrangement of the armature winding (§810). A triangle constructed on OF and FG will give the field ampere-turns, OG, required for the given load. The relations shown in Fig. 591 can be expressed analytically[2] as follows:

$$\dot{E}_g = (E + Ir\cos\phi + Ix\sin\phi) + j(Ix\cos\phi - Ir\sin\phi)$$
$$= A + jB \quad \ldots\ldots \quad (1)$$

Numerically

$$E_g = \sqrt{A^2 + B^2} \cong A + B^2/2A \quad \ldots\ldots \quad (2)$$

Similarly

$$M_f = \sqrt{M_n{}^2 + M_a{}^2 + 2M_nM_a\cos(90^\circ - \phi')} \quad \ldots \quad (3)$$

If the data are so given that a straightforward solution seems too involved, the problem can usually be solved by successive approxima-

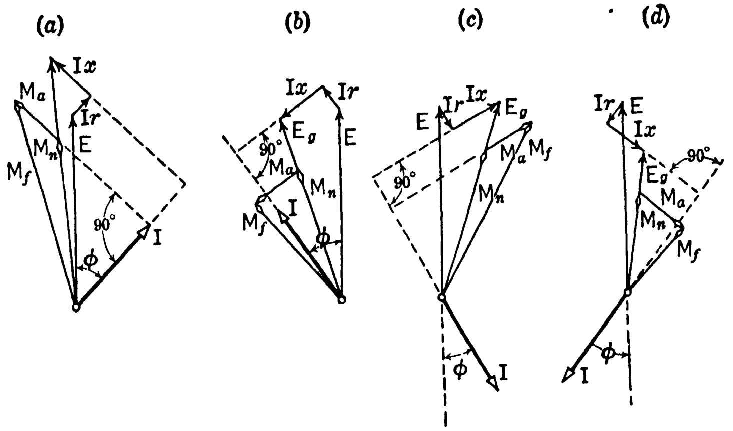

FIG. 593. Potier diagrams for the four conditions of Fig. 590: (a) generator, I lagging; (b) generator, I leading; (c) motor, I leading; (d) motor, I lagging.

tions, or by assuming reasonable values of the unknown quantities and checking them backward. Some special cases are treated in more detail below.

The Potier diagram shown in Fig. 591 is drawn for a generator and a lagging current. In Fig. 593 similar diagrams are drawn for the four cases shown in Fig. 590. This should make clear several important points in the theory and operation of synchronous machines, particularly the effect of the phase angle of the current upon the required field excitation. It is also useful to draw such diagrams for unity power factor and for zero power factor, since under these conditions the influence of the armature reaction is brought out more prominently.

---

[2] For a more accurate diagram, see A. Blondel, *Comptes Rendus*, vol. 159 (1914), p. 604.

The Potier diagram is commonly used also for machines with salient poles. In this case the geometric addition of the mmf's, represented by the triangle *OFG*, is theoretically incorrect, but gives results sufficiently accurate for many practical purposes.

800. Torque Angle and Synchronizing Power.—The angle *AOC* (Fig. 591) is known as the torque or displacement angle; its practical importance in synchronous-motor operation is explained in §§851 and 852. In the generator, the field structure is shifted in an opposite direction from that in a motor, so as to create, along the magnetic lines of force, a tension which the prime mover has to overcome. This means that, in a machine with a revolving field and stationary armature, the field-frame structure is shifted forward, in the direction of rotation, by an electrical angle θ.

This angle is made up of two parts: first, the angle between M_f and M_n, by which the resultant flux (and mmf) is shifted with respect to the axis of the field; second, the angle between terminal and generated voltages, which is necessary in order that the current, *I*, of stated power factor, be made to flow from the machine. This may best be seen if one considers the loaded machine to be operating in parallel with an "infinite bus" whose voltage, *OA*, is not affected (either in magnitude or in phase position) by changes in the load of the machine under consideration. If the induced emf, *OD*, of the machine were equal to and in phase with the terminal voltage, *OA*, no current would flow from the machine. When the generated emf is made of the value and shifted forward to the position of *OD* current *I* flows (Fig. 591). If the machine were loaded as a motor *OG* would be shifted to the right of *OA*, i.e., the field structure would become lagging with respect to the terminal voltage (see Figs. 593*b* and 593*c*).

If the constants of the machine are known, the diagram shown in Fig. 591 can be constructed for any desired operating conditions. From this diagram, the angle θ and the electric power, $P = \sqrt{3}\, EI \cos \phi$, can be determined. When *P* is known, the i^2r loss in the armature, the core loss, and the mechanical power, P_m, transmitted from the field to the armature (or vice versa in a motor) can be computed. When the values of θ and P_m have been obtained for several values of the load, say, first at a constant excitation and second at a constant *E*, the values of P_m can be plotted against θ as abscissas. From the curve so obtained, values of $dP_m/d\theta$, known as *synchronizing power*,[3] can be measured at any desired operating point. The quantity $dP_m/d\theta$ is proportional to the restoring torque which plays a part in the mechanical oscillations of the machine under unbalanced conditions. Together with the moment of inertia of the revolving part, this restoring torque, or synchronizing power, determines the frequency of oscillation, or hunting, about a position of average load (see the references given in §§854 and 855).

801. EXPERIMENT 41-A. — Experimental Study of Potier Diagram. — The diagram is shown in Fig. 591; strictly speaking, it applies only to polyphase machines with non-salient poles. However, for practice in its use, it can be applied to a machine with salient poles, if no other is available. The purpose of the experiment is to compare the performance characteristics obtained experimentally with those predicted by means of the diagram.

(a) Unless this has already been done for the machine in question, measure the armature resistance and determine its reactance and the value of armature reaction at rated current as in Experiment 20-B; also the excitation characteristics as in Experiment 19-D.

(b) Endeavor to set up some device (§852) for the measurement of torque angle (§800), and determine it for several values of load, at various power factors and field currents, and with the machine acting first as a generator and then as a motor.

(c) Apply the data obtained in (a) to the construction of Potier diagrams similar to Figs. 591 and 593, for several of the values of load and power factor studied in (b). Compare the results of the diagrams with the experimental curves and measured torque angle.

If desired this experiment may well be extended to include a comparison of results by the synchronous impedance (§468) and Potier diagrams. If the machine tested is a salient-pole alternator the influence of this factor should be appreciated (§§814 and 815).

802. Unsaturated Machine. — The diagram shown in Fig. 591 presents no difficulties in practical applications when OF can be determined, or, in other words, when the point of the saturation curve at which the machine is working can be ascertained. In other cases, the use of the diagram may be somewhat cumbersome since the no-load saturation curve is a necessary part of the diagram in determining the relationship between E_g and M_n. If, however, in a particular case, it is permissible to assume that the machine is operating on the lower straight part of the no-load saturation curve, the diagram is much simplified, and a locus diagram can be devised (Fig. 595) which gives at a glance all the operating conditions of the machine. Although in practice it is seldom that a synchronous machine should operate on the lower straight portion of the saturation curve, a study of the machine under such conditions is instructive in that it gives a general qualitative idea of the performance characteristics of a machine.

---

[3] See A. S. Langsdorf, "Theory of Alternating-Current Machinery," Chapter VII, McGraw-Hill Book Co.

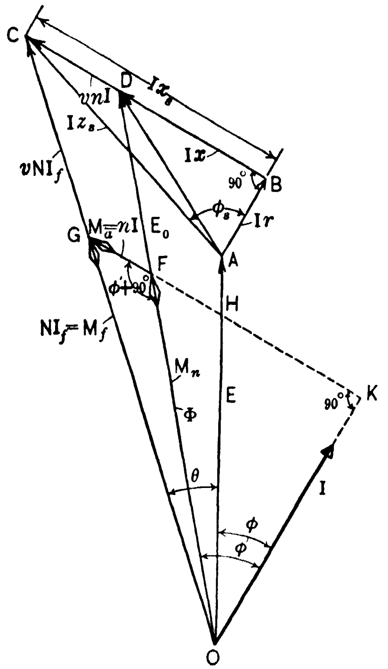

FIG. 594. A transformation of the Potier diagram for the machine without saturation.

Let the lower part of the no-load saturation curve be such that v volts are induced per field ampere-turn. Then the relationship between the induced voltage and the net mmf, M_n, is:

$$E_g = vM_n \quad . \quad . \quad . \quad . \quad (4)$$

We may also write:

$$M_a = nI \quad . \quad . \quad . \quad . \quad . \quad (5)$$

where n is the effective number of armature turns per pole, as it enters into the expression for the polyphase armature reaction (§460).

When the three sides of the triangle OFG are multiplied by v, it is converted into a similar triangle ODC (Fig. 594) in which $DC = vnI$ and $OC = vNI_f$. Here I_f is the field current and N is the corresponding number of field turns per pole. We thus obtain the closed polygon $OABDCO$, from which the troublesome quantity M_n has been eliminated. The vector BC may be considered as a new reactive drop due to a fictitious reactance,

$$x_s = x + vn \quad . \quad . \quad . \quad . \quad . \quad . \quad . \quad . \quad . \quad . \quad . \quad (6)$$

The quantity x_s, which combines the armature reaction and the true leakage reactance, is called the *synchronous reactance* of §463. The geometric sum of the ohmic drop Ir and of the fictitious drop $BC = Ix_s$ due to the synchronous reactance of the machine gives the impedance drop $AC = Iz_s$, where

$$z_s = \sqrt{x_s^2 + r^2} \quad . \quad . \quad . \quad . \quad . \quad . \quad . \quad . \quad . \quad . \quad (7)$$

The quantity z_s is called the *synchronous impedance* of the machine, and the angle $CAB = \phi_s$ is the corresponding internal phase angle on short circuit.

It will be seen that, in a machine with non-salient poles, x_s and z_s remain constant as long as v is constant, i.e., on the lower straight part of the saturation curve.[4] Since, by assumption, the machine operates on this part of the saturation curve, a constant x_s can be used. Knowing x_s, one can construct the figure $OABC$ and measure (or compute) the length OC. Dividing OC by vN will give the required value of the field current, I_f.

803. Locus Diagram of Unsaturated Machine. — To construct a locus diagram, turn the triangle OAC, shown in Fig. 594, clockwise by the angle ϕ_s and divide all its sides by z_s (Fig. 595). This converts the side AC into the current vector I in its true phase position with respect to the voltage E_0 drawn vertically (compare with Fig. 590). The direction AO remains the same under all operating conditions, and the remainder of the triangle can be constructed if sufficient data are given. Of the four quantities, E, I, I_f, ϕ, three must be given to determine the fourth. Of particular practical interest is the case of a given constant terminal voltage E, since this condition usually obtains with synchronous motors and with generators controlled by a voltage regulator. Then the point O is fixed, and of the three quantities, I, I_f, ϕ, any given two determine the third. In order to obtain a clear picture of various operating conditions, it is convenient to draw auxiliary lines for which one of the important quantities remains constant. These lines are as follows:

(a) *Constant field current.* Concentric circles are drawn with O as a center; for each circle the value of I_f is constant. Thus, if the machine is operating at a constant terminal voltage and with a constant field current, the end C of the vector of armature current must remain on one of these circles, because when I_f is constant, $vNI_f/z_s = OC$ is also constant. It will be seen at once that, when overexcited (quadrants 1 and 4, Fig. 590), the machine furnishes a lagging current to the line, or takes a leading current from the line (which amounts to the same thing).

(b) *Constant armature current.* The loci are concentric circles with A as a center; one of these circles, CDB, is shown in Fig. 595.

---

[4] In a machine with salient poles, x_s does not remain constant even under these conditions, but depends upon the power factor of the load (§839).

(c) *Constant power factor.* For any straight line passing through A, such as AC, the power factor, $\cos \phi$, of the electrical input or output remains constant, and AC represents the locus of point C.

(d) *Constant electric power.* Let the end C of the current vector AC move on a horizontal line, that is, one parallel to HM. Then the vertical projection of the vector, or the energy component of the current, remains constant. Hence, at a constant terminal voltage, horizontal lines above HM correspond to constant values of generator output, and those below HM to constant values of motor input.

(e) *Constant mechanical power.* With a large machine, the stator losses are so small that the foregoing curves of electric power may also be taken to represent approximately the mechanical power transmitted from the stator to the rotor, or vice versa. With smaller machines, in which the losses may be considerable, loci of armature current for constant mechanical power are more nearly represented by arcs of large concentric circles, such as CK. To deduce the equation of such circles, write the following expression for the power:

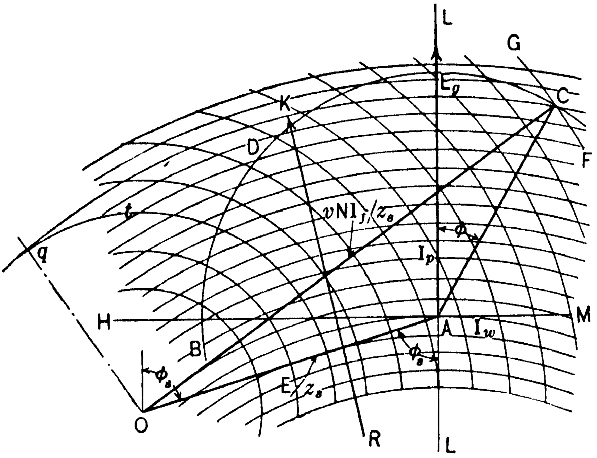

FIG. 595. A complete performance diagram of the synchronous machine with cylindrical rotor and no saturation.

$$P = IE\cos\phi + I^2r + P_o \tag{8}$$

In the case of a generator, $IE \cos \phi$ is the electrical output, I^2r is the armature copper loss, P_o is the sum of the core loss and mechanical losses (or the core loss alone, as the case may be), and P is the mechanical input, all the quantities being *per phase.* Let the armature current be resolved into the power component, $I_p = I \cos \phi$, along AL, and the reactive (wattless) component, $I_w = I \sin \phi$, along AM. Dividing both sides of eq. (8) by r, and rearranging the terms, $I_w^2 + I_p^2 + I_pEr^{-1} = (P - P_o)r^{-1}$. Adding to both sides of the equation the quantity $0.25E^2r^{-2}$, to complete the square, gives:

$$I_w^2 + (I_p + 0.5Er^{-1})^2 = (P - P_o)r^{-1} + 0.25E^2r^{-2} \quad . \quad . \quad (9)$$

Considering I_w and I_p as the coordinates x and y, respectively, eq. (9) represents a circle, provided that P, P_o, and E are constant. The radius of the circle is:

$$R = \sqrt{(P - P_o)r^{-1} + 0.25E^2r^{-2}} \quad . \quad . \quad . \quad . \quad . \quad . \quad (10)$$

The center lies on the negative part of AL, at the distance I_o from A, where

$$I_o = -0.5Er^{-1} \quad . \quad . \quad . \quad . \quad . \quad . \quad . \quad . \quad . \quad . \quad (11)$$

Equation (8) also holds true for the synchronous motor, but in this case ϕ is greater than 90 degrees (Fig. 590), $\cos \phi$ is less than 0, and the term $IE \cos \phi$ is negative. The mechanical power, P, must also be considered negative. Equations (10) and (11) can then be used, and concentric circles drawn below as well as above HM.

With the aid of Fig. 595, complete performance curves of the machine can be plotted, x_s being known from a short-circuit test and v (volts per ampere-turn) from a no-load test. When plotting "V curves" (§847), the stability limit is determined by the point of tangency of a power circle and a circle corresponding to a constant I_f. For example, the power circle KC is tangent to the excitation circle qt, and at that value of power the machine cannot operate at a field current lower than that corresponding to Oq.

It is understood, of course, that Fig. 595 applies only within the range of exciting current for which the saturation curve is sensibly a straight line passing through the origin.

804. EXPERIMENT 41-B. — Performance Characteristics of an Unsaturated Synchronous Machine. — The purpose of the experiment is to check, on an actual machine, the locus diagram shown in Fig. 595 with some performance characteristics obtained experimentally. Any polyphase alternator may be used, but the performance curves (both as generator and as motor) should be taken at a voltage sufficiently low to lie on the lower straight part of the no-load saturation curve. Of course, the diagram applies rigorously only to a machine with non-salient poles, but it should give fairly close results for a machine with salient poles as well. Various sets of readings should be so planned as to make a check with the diagram as simple as possible. For example, when operating at a constant terminal voltage, E, and at a constant field current, I_f, the locus of the point C should be a circle (such as FCG); the quantities I and ϕ are varied by changing the load (§803).

805. Saturated Machine. — The performance of a machine with non-salient poles and operating on the curved part of the saturation curve is represented vectorially in Fig. 591. The length OF is the abscissa and OD the corresponding ordinate of a point on the no-load saturation curve, and herein lies the difficulty in obtaining a locus diagram that would show at a glance the performance of the machine under different operating conditions.

A Potier diagram and the no-load saturation curve of a machine are shown combined in Fig. 596. The voltage polygon $OABD$ is denoted by the same letters in both figures, and the mmf triangle OFG (Fig. 591) is denoted by $O'FG$ in Fig. 596. By drawing the line HO which bisects the axes of coordinates, it becomes possible to place the triangle OAD in such a position that the induced voltage, $OF = E_0$, and the corresponding net excitation, $O'F = M_n$, lie on the same horizontal line. This, in turn, makes it possible to use a separate strip of paper, *mnpq*, with two scales as shown. The edge Fp is calibrated in values of armature reaction nI, for various values of I, to the same scale as the abscissas of the saturation curve. The edge Fq is calibrated in values of the armature impedance drop, to the same scale as the ordinates of the saturation curve. The angle pFq on the paper scale strip may be determined from the relations in the triangle FBA. Thus, by laying this strip on the curve-sheet in a desired position, one can obtain the terminal voltage $E = AO$, the field excitation $NI_f = O'G$, and the phase angle ϕ at A.

The problem usually has to be solved by trials, which, however, are not tedious, since no computations are necessary, but merely the judgment of the eye. Let, for example, the armature current, the terminal voltage, and the power factor be given, and the field excitation be unknown. Then the point A on the paper strip is fixed, as well as the length AO and the angle ϕ at A. An arbitrary line, such as FO, is selected, and an attempt is made to realize the triangle FAO on it. If the extremity O of AO does not lie on the 45-degree line, other horizontal lines are chosen, above and below FO, until the triangle FAO has been properly located. Since the point G is known, it remains only to measure the length $O'G$. The torque angle θ can be measured at L. When the armature current is not given, but the field current is given instead, more trials are required, because it is then necessary to assume several values of armature current.

Four quantities enter into the problem of electrical characteristics, viz., the terminal voltage (E), the armature current (I), the phase angle (ϕ), and the field current (I_f). If three out of four are given, the remaining one can be found by trials, as shown in Fig. 596. If only two are given, a curve can be plotted between the remaining two. The strip of paper is shown in a position corresponding to operation as a generator with a lagging current. To obtain the three other typical positions (Fig. 590), the reader should simply redraw Fig. 591 for such conditions and place the figure *mnpq* accordingly.

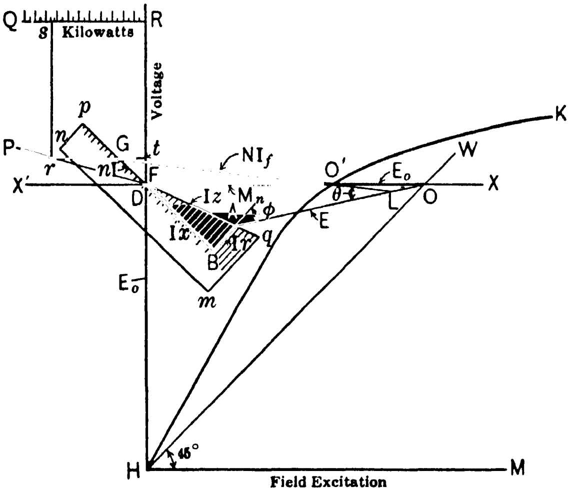

FIG. 596. A Potier diagram combined with the saturation curve of the machine.

When the voltage, the current, and the angle ϕ are known, the power can be readily computed. With a generator, the output per phase is proportional to $AF \cdot AO \cos \phi$ (Fig. 596). The input into the armature (not counting the core loss, but only the i^2r heat loss) is proportional to $FO \cdot Ft$, where Ft is the component of the armature current FG in phase with the induced voltage $HF = E_0$. By means of the scale QR, shown in the upper left-hand corner, the electric power $FO \cdot Ft$, corresponding to a given setting, can be read off directly. For this purpose, a line FP is drawn, as explained below, and the point G is first projected as r and then as s. The length Rs then will give the power in kilowatts. The direction FP is determined by finding a point on it, such as r. For example, if HF is 10 kv and $Ft = 100$ amperes, the power is $10 \times 100 \times \sqrt{3} = 1732$ kw. The scale RQ being arbitrary, lay off $Rs = 1732$ kw and draw the direction line sr. Then lay off $Ft = 100$ amperes and draw tr. The intersection will give the point r, and consequently the direction *FP*. The same line, *FP*, will then give correct readings for any setting of the device at point *F*. For each point *F* on the axis *HR*, the direction *FP* is different (Fig. 597).

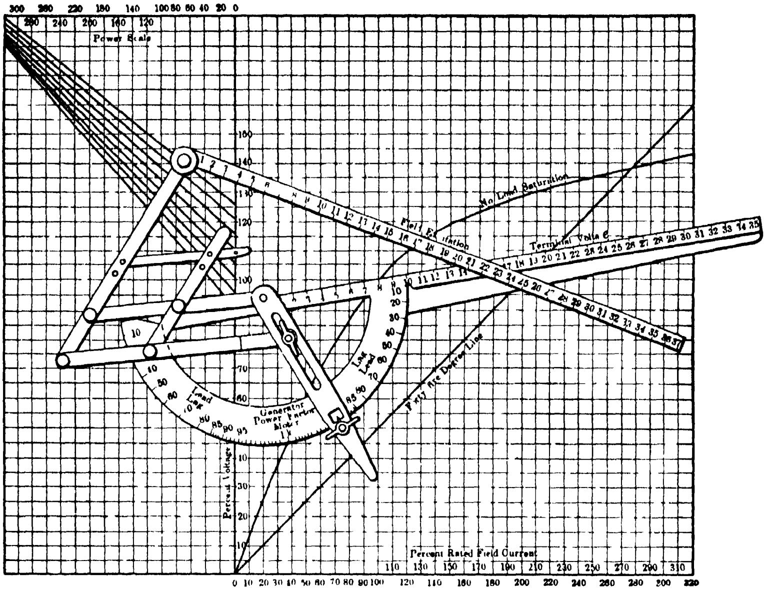

FIG. 597. The Potierion — a device for computing electrical characteristics of the synchronous machine with non-salient poles.

806. The Potierion. — The principles stated in the preceding section have been incorporated by V. Karapetoff in a kinematic computing device (Fig. 597) which he has named the Potierion. In this device the ohmic drop is neglected, and therefore the directions *pF* and *Fq* coincide. In place of a strip of paper, proportional dividers are used, so that, when once set for the constants of the machine, the values of the reactive drop and the armature reaction remain correct for any opening of the dividers. The protractor is calibrated directly in values of power factor. The scales of terminal voltage and field excitation are preferably calibrated in centimeters, so as to be usable with any saturation curve, and the readings are multiplied by proper factors. This device has been found useful in checking experimental data, in predicting the performance of new machines, and in some other general studies of the properties of synchronous generators and motors.[5]

---

[5] For details see *Sibley Journal of Engineering*, vol. 40 (1926), pp. 54 and 73; also reprinted as *Bulletin* 6 of the Engineering Experiment Station, Cornell University.

807. Synchronous-Machinery Charts Involving Circular Loci. — For the purpose of determining complete performance characteristics of synchronous machines it is of advantage to construct charts[6] from which may be read the ratios of generated to terminal voltage (E_g/E), and of total to net field currents (M_f/M_n), together with their respective angular displacements (Figs. 598 and 599). Once such charts are drawn the performance items for all possible conditions of operation as to load and power factor may be read off and corresponding curves drawn.

(a) *Chart of induced and terminal voltage.* Referring to Fig. 591 of the Potier method for non-salient pole machines, one may write:

$$\dot{E}_g = \dot{E} + \dot{I}Z_a = (E + I_p r + I_w x_a) + j(I_p x_a \mp I_w r) \quad . \; . \; . \; . \quad (12)$$

where I_p and I_w (§803) are the power and reactive components of the armature current, referred to the terminal voltage, E. Upper signs are for lagging and lower signs for leading currents.

Multiplying eq. (12) by E/x_a

$$\dot{E}_g E/x_a = (E^2/x_a + EI_p r/x_a \pm I_w E) + j(I_p E \mp EI_w r/x_a) \quad . \quad (13)$$

Numerically, writing $EI_p = P$, and $EI_w = Q$ (the real and reactive powers),

$$(E_g E/x_a)^2 = (P \mp Qr/x_a)^2 + (\mp Q - E^2/x_a - Pr/x_a)^2 \quad . \; . \quad (14)$$

Dividing by $(E^2/x_a)^2$

$$(E_g/E)^2 = \left(\frac{P}{E^2/x_a} \mp \frac{Q}{E^2/x_a} r/x_a\right)^2$$

$$+ \left[\left(\mp \frac{Q}{E^2/x_a} - \frac{P}{E^2/x_a} r/x_a\right) - 1\right]^2 \quad . \; . \quad (15)$$

$$= A^2 + (B - 1)^2 \quad . \; . \; . \; . \; . \; . \; . \; . \; . \quad (15a)$$

Equation (15) gives E_g in proportional (per-unit) values, referred to E.

If the resistance is neglected, as is usually permissible in large machines, eq. (15) becomes

$$(E_g/E)^2 = \left(\frac{P}{E^2/x_a}\right)^2 + \left(\mp \frac{Q}{E^2/x_a} - 1\right)^2 \quad . \; . \; . \; . \quad (16)$$

Equations (15) and (16) are equations of circles, for a constant value of E, the center of the circles being located on the axis of ordinates a distance of 1 above the origin. The chart of Fig. 598 is drawn for eq. (15) and therefore includes the effect of armature resistance. Circular loci are drawn for various ratios E_g/E, and radial lines to give the angle between E_g and E. Applying this chart to the data for the alternator of §§464 to 470, $r = 0.064\omega$, $x_a = 0.16\omega$, $E = 240/\sqrt{3}$ volts per phase, $E^2/x_a = 120{,}000$ watts per phase. The rating of the three-phase alternator is 37.5 kva. It is desired to find the total field current and torque angle of the machine at 2 × rated kva, 80 per cent lagging power factor. Then $P/(E^2/x_a) = (12.5 \times 0.8 \times 2)/120 = 0.1667$; $Q/(E^2/x_a) = -(12.5 \times 0.6 \times 2)/120 = -0.125$, $\frac{P}{E^2/x_a} r/x_a = 0.066$, $\frac{Q}{E^2/x_r} r/x_a = -0.05$. Then (eq. 15*a*) $A = 0.1167$, $B = -0.125 - 0.066 = -0.191$. Entering the chart with these values, as shown by the dotted lines it is found that $E_g/E = 1.195$, while $\angle\frac{E_g}{E} = 6°$.

---

[6] O. G. C. Dahl, "Electric Circuits, Theory and Applications," Chapter XI, McGraw-Hill Book Co.

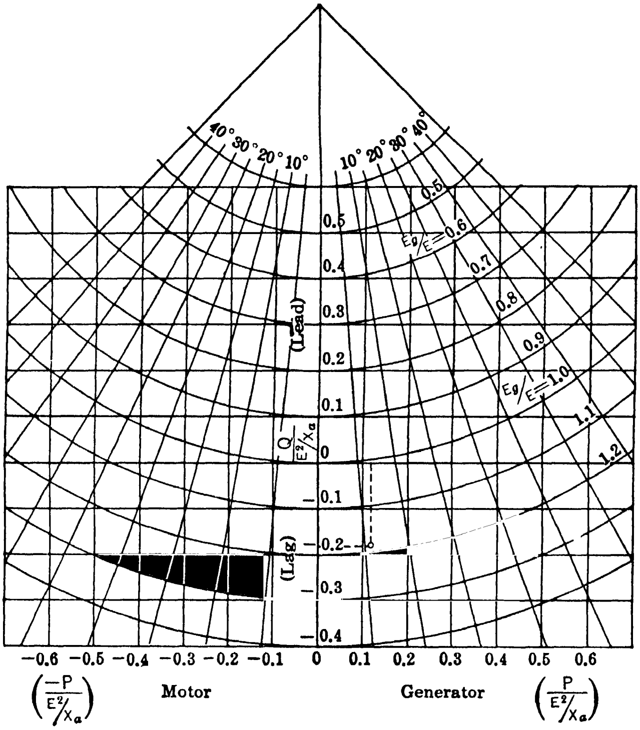

FIG. 598. General chart for determining E_g in terms of E and $\angle\frac{E_g}{E}$, including effects of resistance.

(b) *Chart of total and net exciting current.* Again refer to Fig. 591.

$$M_f = M_n + jnI = M_n + jn(I_p' + jI_w') \quad . \; . \; . \; . \quad (17)$$

where I_p' and I_w' are the power and reactive components of the armature current, I, referred to E_g.

From eq. (17) after dividing by n and squaring components,

$$(M_f/n)^2 = (I_w' - M_n/n)^2 + (I_p')^2 \quad . \; . \; . \; . \; . \quad (18)$$

Calling the internal power and reactive power P' and Q', respectively,

$$P' = E_g I_p', \quad \text{and} \quad Q' = E_g I_w'$$

so that

$$I_p' = P'/E_g, I_w' = Q'/I_w' \quad . \; . \; . \; . \; . \; . \; . \; . \quad (19)$$

Substituting from eqs. (19) into eq. (18)

$$(M_f/n)^2 = (Q'/E_g - M_n/n)^2 + (P'/E_g)^2 \quad . \; . \; . \quad (20)$$

or

$$(M_f/M_n)^2 = (nP'/M_nE_g)^2 + (nQ'/M_nE_g - 1)^2 \; . \; . \; . \quad (21)$$

Q' is negative for lagging currents.

If M_o is the field current for normal voltage at no load, from the saturation curve, in per-unit values (when $I = 1$), $nI = M_a/M_o$. Similarly M_n is referred to M_o so that n/M_n becomes M_a/M_n. Therefore eq. (21) may be written

$$(M_f/M_n)^2 = \left(\frac{M_aP'}{M_nE_g}\right)^2 + \left(\frac{M_aQ'}{M_nE_g} - 1\right)^2 \; . \; . \; . \; . \quad (21a)$$

Equation (21) or (21*a*) represents a series of circles, each for a particular ratio of M_f/M_n, with the centers of the circles on the axis of ordinates at a distance of unity above the origin. Figure 599 is a chart so drawn. It is called the "auxiliary chart." The radial lines give the angles between M_f and M_n, and the quantities are again in proportional, or per-unit, values. From Fig. 591 it may be seen that for the same terminal voltage and for the value of load and power factor for which the voltage chart (Fig. 598) was drawn

$$\left.\begin{aligned} P' &= P + I^2r = IE\cos\phi + I^2r \\ Q' &= Q + I^2x_a = IE\sin\phi + I^2x_a \end{aligned}\right| \quad . \; . \; . \; . \; . \quad (22)$$

These values are in watts. They should be expressed in per-unit values by referring them to rated watts. Again referring to the machine of §§465 to 470:

$I = 90.3$ at rated kva. $nI = M_a = 3.2$ field amperes (Fig. 336). For $E_g = 1.195 \times$ normal (Fig. 598) it is found that $M_n = 8.1$ (Fig. 335).

$P' = 180.6 \times 138.6 \times 0.8 + \overline{180.6}^2 \times 0.064 = 22{,}080$ watts, equivalent to $22{,}080/12{,}500 = 1.77$ in per-unit value.

Likewise $Q' = 180.6 \times 138.6 \times 0.6 + \overline{180.6}^2 \times 0.16 = 20{,}200$ watts, equivalent to $20{,}200/12{,}500 = 1.62$ per unit. Therefore $M_aP'/M_nE_g =$ 0.586, and $M_aQ'/M_nE_g = 0.535$. Entering the chart (Fig. 599) with these values it is seen that $M_f/M_n = 1.65$, $\angle\frac{M_f}{M_n} = 21.5°$. These values check those found by the more usual method of Fig. 340 or Fig. 591.

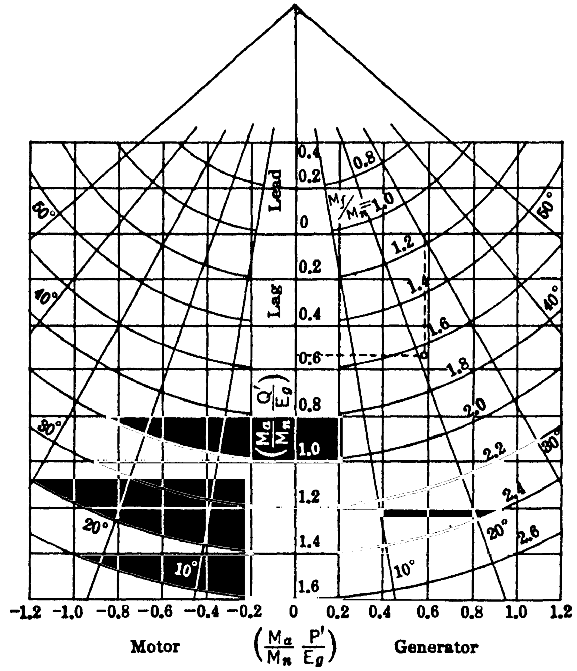

FIG. 599. Auxiliary chart for the non-salient-pole alternator, ratio M_f/M_n and $\angle\frac{M_f}{M_n}$.

Combining results by the two charts, the total torque angle is 27.5°; the total excitation, $M_f = 1.65 \times M_n$; $M_n = 8.1$ amperes; the open-circuit voltage (Fig. 340) is 335 volts between lines; and regulation is $(335 - 240)/240 = 39$ per cent.

It is convenient to arrange values in the form of a table as follows:

Table of Calculated and Derived Quantities for Charts, Figs. 598 and 599
(per-unit values)

E	P	Q	$\frac{P}{E^2/x_a}$	$\frac{Q}{E^2/x_a}$	E_g	$\angle\frac{E_g}{E}$ (degrees)	M_n	P'	Q'	$\frac{M_aP'}{M_nE_g}$	$\frac{M_aQ'}{M_nE_g}$	$\frac{M_f}{M_n}$	$\angle\frac{M_f}{M_n}$ deg	ϕ (deg.)	Regul.

It should be noted that Fig. 598 is a chart which is applicable at any value of terminal voltage, E, and for any load and power factor, for motor (§845) and for generator. It may be used with equal facility for short transmission lines and transformers. Figure 599 is also a general chart and, except for range of values and significance of coordinates, is identical with Fig. 598. It is used in connection with Fig. 598 and the no-load saturation curve of the machine in question.

808. EXPERIMENT 41-C. — Performance Characteristics of a Saturated Non-Salient Pole Alternator. — This experiment is a continuation of the preceding two experiments, with the addition of an analysis of the results, as described in §§805, 806, and 807. It is suggested that charts of Figs. 598 and 599 be applied to the data of Experiments 41-A and 41-B and values obtained to fill out tables such as that in §807 at, say, three terminal voltages, for a range of power from 0 to 2 × normal, and at power factors from 0 lag to 0 lead. Groups of curves should be plötted such as: (a) active power vs. field current for various values of reactive power (all in per-unit values; (b) torque angle vs. active power for various values of reactive power and at a given terminal voltage; and (c) regulation against kva output for several values of constant power factor, rated voltage. Cross curves should be taken from these groups of curves and the performance of the machine thoroughly discussed.

REFERENCES

1. V. Karapetoff, The Magnetic Circuit, Chapters VII and VIII, McGraw-Hill Book Co.
2. A. Blondel, *Comptes rendus*, vol. 159 (1914), p. 604.
3. A. S. Langsdorf, Theory of Alternating-Current Machinery, Chapter V, McGraw-Hill Book Co.
4. V. Karapetoff, *Sibley Jour. Eng'g*, vol. 40, pp. 54 and 73, Some kinematic devices for predetermination of characteristics of synchronous machinery.
5. O. G. C. Dahl, Electric Circuits, Theory and Applications, Chapter XI, McGraw-Hill Book Co.
6. R. R. Lawrence, Principles of A-C Machinery, Chapters IV and V, McGraw-Hill Book Co.

CHAPTER XLII

DIRECT AND TRANSVERSE ARMATURE REACTION IN SALIENT-POLE SYNCHRONOUS MACHINES

809. The purpose of this study is to establish the principles necessary in order to understand and to construct the performance diagrams of the salient-pole synchronous machine, treated in the next chapter. A review of the theory of armature reaction in d-c machines (§§366 to 368) should prove of value, and the reader should go over §§797 and 798 again, looking up the references given there.[1]

Since a thorough understanding of the magnetomotive force of a polyphase winding is necessary before its effects upon the performance of a machine can be considered, the following discussion of the mmf of polyphase windings is given.

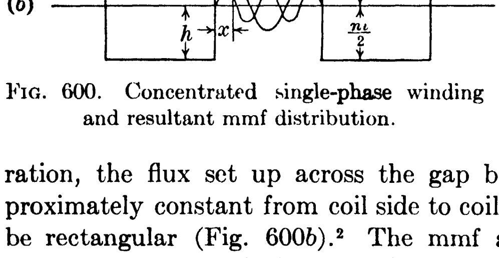

FIG. 600. Concentrated single-phase winding and resultant mmf distribution.

810. The Magnetomotive Force of Alternating-Current Windings. — (a) *Concentrated single-phase winding.* Figure 600(*a*) represents a concentrated single-phase winding of one slot per pole, on one side of an air-gap of uniform length. Neglecting saturation, the flux set up across the gap by such a winding will be approximately constant from coil side to coil side, i.e., its distribution will be rectangular (Fig. 600*b*).[2] The mmf acting across each gap, and having this form, will have the instantaneous value

$$h = ni/2 \quad . \; . \; . \; . \; . \; . \; . \; . \; . \; . \; . \quad (1)$$

where n = turns per coil (or conductors per pole) and i = current at the instant. This is the height of the rectangle of mmf at the given time. Under alternate poles this mmf is of alternate sign and symmetrical, giving a periodic alternating wave in space.

---

[1] See also V. Karapetoff, "The Magnetic Circuit," Chapter VIII, McGraw-Hill Book Co.

[2] See W. V. Lyon, "The Application of Harmonic Analysis to the Theory of Synchronous Machines," *Trans. A.I.E.E.*, vol. 37 (1918), p. 1487.

Such a periodic quantity can be resolved (Chapter LVIII) into a fundamental and higher (space) harmonics. The amplitude of the fundamental sine wave is given by the expression:

$$h_1 = 2/\pi \int_0^\pi f(x) \sin x \, dx \quad . \quad . \quad . \quad . \quad . \quad . \quad . \quad . \quad (2)$$

Since $f(x)$ has the value $ni/2$ between the limits stated

$$h_1 = (4/\pi)ni/2 = (4/\pi)h \quad . \quad . \quad . \quad . \quad . \quad . \quad . \quad (3)$$

Similarly, the amplitude of the third harmonic of the mmf will be

$$h_3 = 2/\pi \int_0^\pi (ni/2) \sin 3x \, dx$$

$$= (4/3\pi)ni/2 = (4/3\pi)h \quad . \quad . \quad . \quad . \quad . \quad . \quad (4)$$

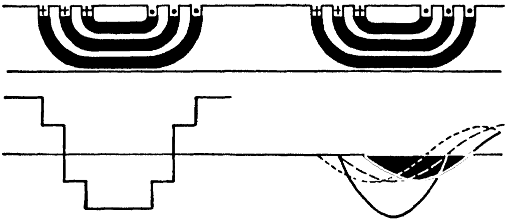

FIG. 601. Mmf of a single-phase distributed winding — stepped curve and fundamental components.

Proceeding in this way for the several harmonics the rectangular wave form may be replaced by the Fourier's series

$$h = (4/\pi)(ni/2) [\sin x + (1/3) \sin 3x + (1/5) \sin 5x + \cdots] \quad . \quad . \quad (5)$$

It must be remembered that these components are harmonics in space, not in time, and all harmonics are of fundamental frequency as to time. Therefore, all harmonics will reach their maximum values when $i = \sqrt{2}I$, so that the maximum values of the several harmonics are

$$H_1 = (4/\pi) \times 0.707nI = 0.9nI$$

$$H_3 = (4/3\pi) \times 0.707nI = 0.3nI, \text{etc.} \quad . \quad . \quad . \quad . \quad . \quad (6)$$

(b) *The distributed winding.* The mmf of a distributed single-phase winding having three slots per pole is shown in Fig. 601. At (*b*) the three rectangles of mmf, each identical with that of Fig. 600, are shown added, point by point, to give the stepped curve shown for the resultant mmf. In Fig. 601 only the fundamental sine components, due to each coil, are shown, together with their sum (also a sine wave). For most purposes the higher harmonics in space distribution of mmf may be neglected. This is particularly true with three-phase windings since there the triplen harmonics (§784) are 120 degrees apart in terms of the fundamental, or 360 degrees apart in terms of the harmonic. These triplen harmonics in space distribution, being of fundamental frequency in time, are out of time phase by 120 degrees. Thus there occurs the addition of sine waves of equal amplitude, coincident in space but 120 degrees out of phase, so that the sum is zero at all points. This eliminates the triplen harmonics of flux distribution in three-phase machines with balanced conditions. The remaining harmonics, the fifth, seventh, eleventh, etc., diminish, first of all, with the order of the harmonic (eq. 5), and they are further reduced by the increasing angle at which the harmonics of higher order add, as will be seen below.

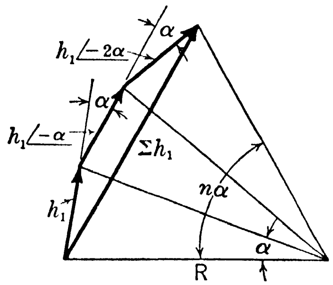

FIG. 602. Vector addition of mmf's or emf's in adjacent coils, leading to breadth factor.

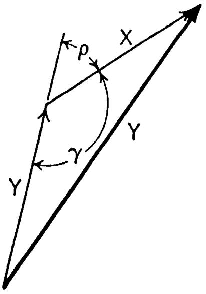

FIG. 603. Vector addition of mmf's or emf's due to fractional-pitch coils, leading to pitch factor.

811. Breadth and Pitch Factors.[3] — (a) *Breadth factor.* In Fig. 601 the fundamental mmf's produced by three coils, the angle α apart, are shown added to give a fundamental sine wave. Such additions are commonly represented graphically by vectors, as in Fig. 602. It is evident from the geometry of the figure that, if there are n vectors, each of value h_1, and α degrees (angle between adjacent slots) apart,

$$\Sigma h_1 = 2R \sin n\alpha/2 \qquad (7)$$

If they had been added directly their sum would have been nh_1. Now (Fig. 602)

$$h_1 = 2R \sin \alpha/2 \quad . \; . \; . \; . \; . \; . \; . \; . \; . \quad (8)$$

[3] V. Karapetoff, "The Magnetic Circuit," Chapter IV, McGraw-Hill Book Co.

Therefore, the ratio, k_{b1}, of the geometric sum of the (fundamental) vectors to the arithmetic sum is

$$k_{b1} = (\sin n\alpha/2)/(n \sin \alpha/2) \quad . \ . \ . \ . \ . \ . \ . \quad (9)$$

This ratio is called the *breadth factor* of the distributed winding. It applies both to the emf's generated in the winding, and to the mmf's which are set up by the winding.

For any harmonic, say the pth, the emf's set up in adjacent slots, or the mmf's produced by coils in adjacent slots, will differ in phase by $p\alpha$ degrees. Therefore, the breadth factor for the pth harmonic in a distributed winding will have the value

$$k_b = (\sin pn\alpha/2)/(n \sin p\alpha/2) \quad . \ . \ . \ . \ . \ . \quad (10)$$

In the usual form of a-c windings (open-circuit type) if m = number of phases and S = slots per pole, then $n = S/m$, $n\alpha = 180°/m$, and $\alpha = 180°/S$ so that

$$k_b = (m \sin p\ 90°/m)/(S \sin p\ 90°/S) \quad . \ . \ . \ . \ . \quad (11)$$

(b) *Pitch factor.* Most a-c windings are arranged in a double layer and the throw of the coils is generally less than 180 degrees (a pole pitch). This has the effect of shifting the phase groups in the upper layer of coil sides with respect to the phase groups in the lower layer by the angle $\rho = 180° - \gamma$, where γ is the angle of coil throw. The effect of this shifting of the upper and lower layers of coil sides upon the combined mmf of the two layers is obvious. The fundamental mmf's of the two layers add at the angle ρ and those of the pth harmonic at the angle $p\rho$. In Fig. 603 two vectors, each of value X, are added at an angle ρ. The vector sum, Y, then has the value

$$Y = 2X \cos \rho/2 \quad . \ . \ . \ . \ . \ . \ . \ . \ . \quad (12)$$

Direct addition, giving a result $2X$, would have resulted with a full-pitch coil. The ratio $Y/2X$ is called the *pitch factor*, k_p. Thus,

$$k_p = \cos \rho/2 \quad . \ . \ . \ . \ . \ . \ . \ . \ . \ . \quad (13)$$

for the fundamental or, more generally,

$$k_p = \cos p\rho/2 \quad . \ . \ . \ . \ . \ . \ . \ . \ . \quad (13a)$$

The product of pitch factor by breadth factor is called *distribution factor*, or

$$k_d = k_b k_p \quad . \ . \ . \ . \ . \ . \ . \ . \ . \ . \ . \quad (14)$$

812. Example of the Effect of Distribution of the Winding upon MMF Wave Form.—As previously stated, the effect of distributing the winding, both by the use of several slots per phase per pole and by the use of a coil throw less than a pole pitch, is to reduce the higher harmonics of mmf (and emf) to a greater degree than it does the fundamental. As an example, consider a three-phase alternator with 9 slots per pole, and a coil throw of 7 slots (140 degrees). Consider the fundamental and higher harmonics to be of the relative values occurring in the rectangular wave, eq. (5). Then, if $h_1 = 100$, $h_3 = 33.3$, $h_5 = 20$, $h_7 = 14.3$, $h_{11} = 9.09$, etc. Their relative numerical values, as affected by the distribution of any one phase, are as shown in the following table.

Effect of Winding Distribution upon Harmonic MMF's in One Phase
($\alpha = 20°$, $\gamma = 140°$)

Harmonic	MMF per coil (h)	k_b	k_p	k_d	$k_d h$	Harmonic mmf / Fundamental mmf
1	h_1	0.958	0.94	0.90	$0.9h_1$	1.0
3	$h_1/3$	0.667	0.50	0.33	$0.11h_1$	0.12
5	$h_1/5$	0.218	0.174	0.038	$0.007h_1$	0.008
7	$h_1/7$	0.177	0.766	0.136	$0.019h_1$	0.021
9	$h_1/9$	0.333	1.0	0.33	$0.039h_1$	0.043
11	$h_1/11$	0.177	0.766	0.136	$0.012h_1$	0.074

In the above table the third and ninth harmonics have been included, although they disappear in a balanced three-phase machine. Of the remaining fifth, seventh, and eleventh harmonics the maximum is only 2 per cent of the fundamental.

It is seen from the above discussion that the usual assumption of a sine form of mmf produced by a distributed winding is, in general, justified.

813. Combined MMF of Distributed Polyphase Windings.—*Rotating magnetic field.* Assuming, in line with the above argument, that each phase of a distributed three-phase winding produces a sine-form mmf, and that the currents are balanced, each of these will have a maximum value, when modified by the distribution factor, of

$$H_1 = 0.9k_d nI \qquad (15)$$

ampere-turns per pole, where n is the number of turns per coil × coil sides per phase group, and I is the rms value of current per phase.

If N = turns per phase per pole

$$H_1 = 1.8k_d NI \quad . \; . \; . \; . \; . \; . \; . \; . \; . \; . \quad (16)$$

At any instant of time, t, after the current in phase 1 has passed through zero, becoming positive, assuming that the phase sequence is 1, 2, 3, the maximum mmf's of the three phases at that moment will be (Fig. 604)

$$\left.\begin{aligned} M_1 &= H_1 \sin \omega t \\ M_2 &= H_1 \sin (\omega t - 120°) \\ M_3 &= H_1 \sin (\omega t + 120°) \end{aligned}\right\} \quad \ldots\ldots \quad (17)$$

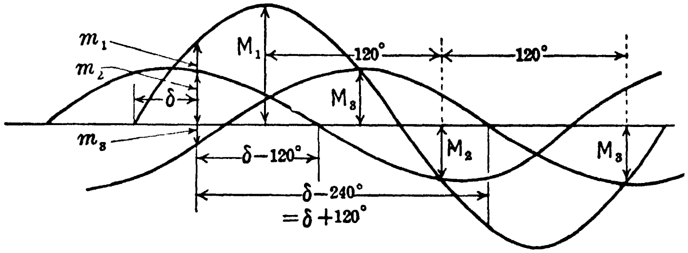

FIG. 604. Mmf's of three phases at $\omega t = 90°$. $M_1 = H_1 \sin \omega t = H_1$; $M_2 = H_1 \sin (\omega t - 120°) = -0.5H_1$; $M_3 = H_1 \sin (\omega t + 120°) = -0.5H_1$.

Since these windings are displaced in space by 120 degrees the mmf's at a point in the air-gap an angle δ from the center of the conductor group of phase 1 (Fig. 604) will be:

$$\left.\begin{aligned} m_1 &= M_1 \sin \delta \\ m_2 &= M_2 \sin (\delta - 120°) \\ m_3 &= M_3 \sin (\delta + 120°) \end{aligned}\right\} \quad \ldots\ldots \quad (18)$$

From eqs. (17) and (18) the resultant mmf due to the three phases, at the designated point in the air-gap and at instant t, is:

$$m_a = m_1 + m_2 + m_3 = H_1 [\sin \omega t \sin \delta + \sin (\omega t - 120°) \sin (\delta - 120°) + \sin (\omega t + 120°) \sin (\delta + 120°)] \quad .\ . \quad (19)$$

Making use of the relation, $\sin \alpha \sin \theta = (1/2) \cos (\alpha - \theta) - (1/2) \cos (\alpha + \theta)$ eq. (19) may be reduced to the form:

$$m_a = H_1[(3/2) \cos (\omega t - \delta) - (1/2) \cos (\omega t + \delta) - (1/2) \cos (\omega t + \delta - 240°) - (1/2) \cos (\omega t + \delta + 240°)] \quad (20)$$

Since the sum of the last three terms is zero eq. (20) reduces to

$$m_a = (3/2)H_1 \cos (\omega t - \delta) \quad \ldots\ldots \quad (21)$$

or, substituting from eq. (16) into eq. (21),

$$m_a = 0.9 \times k_d \times 3NI \cos (\omega t - \delta) \quad \ldots\ldots \quad (22)$$

This is seen to be the equation of a rotating mmf of constant amplitude, moving at synchronous speed, for, if the space angle δ, which indicates the distance along the air-gap from a fixed point, is made to increase synchronously ($\delta = \omega t$), m_a is seen to be at its maximum continuously. For a winding of any number of phases, m (greater than one), eq. (22) may be written

$$m_a = 0.9k_d mNI \cos(\omega t - \delta) \quad . \; . \; . \; . \; . \; . \; . \quad (23)$$

The maximum value of the fundamental rotating mmf due to a polyphase winding carrying balanced currents is then

$$M_a = 0.9k_d mNI \quad . \; . \; . \; . \; . \; . \; . \; . \; . \quad (24)$$

It should be noted that a polyphase winding carrying unbalanced currents may be treated by the method of symmetrical components, each sequence component (Chapter XXXIV) being considered to produce its own uniform rotating mmf in accordance with the above equations. Even the single-phase winding may be handled in the same manner. The single-phase current being equivalent to two systems of three-phase currents of opposite sequence, the mmf of the single-phase winding becomes two oppositely rotating mmf's of one-half the amplitude of the single-phase mmf (§976).

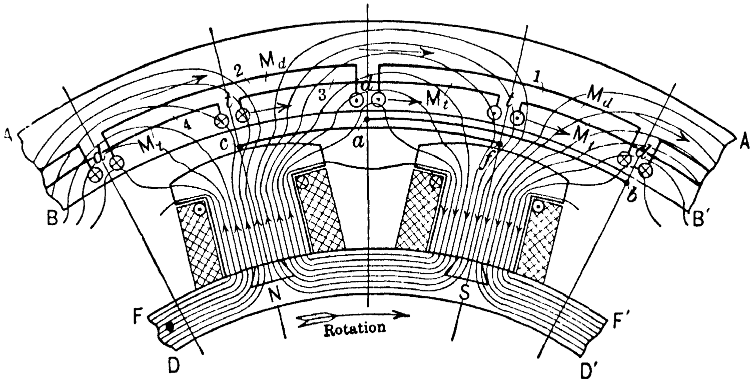

FIG. 605. The mmf's of direct and transverse reaction represented by fictitious revolving coils.

814. Transverse Armature Reaction. — Part of a synchronous machine with salient poles is represented in Fig. 605. The armature coils shown are not the actual stationary coils of the armature winding but are fictitious revolving coils equivalent in their effect to the armature reaction of the machine. These fictitious coils will be referred to from time to time in explanation of the effects of armature reaction.

Consider a three-phase armature winding (Figs. 318 and 319), and assume the machine to operate first as a generator at no load. The induced voltage reaches its maximum in each armature conductor when it is opposite the center of a field pole (Fig. 592*a*). Now let the machine be loaded at such a power factor that the armature current reaches its maximum at the same instant as the above-mentioned emf. The armature currents of the three phases produce a combined mmf which glides synchronously with the field poles (§§484 and 813). As was shown in §799 for the condition of unity internal power factor (referred to no-load emf), the crest of the resultant mmf is midway between the center lines of the field poles, i.e., is displaced 90 electrical degrees with respect to the pole centers, and *lags* in space by that angle. This result holds true for every instant, the rotating mmf of the polyphase armature maintaining a fixed position with respect to the poles. In a synchronous motor the current in phase with the induced emf is in the opposite direction from that considered above and its mmf *leads* that of the poles by 90 space degrees, represented in Fig. 605 by coils 3 and 4 whose axes are midway between the poles. This armature mmf which acts midway between the poles is called the *transverse armature reaction.* Its existence at power factors other than unity and its effect upon the machine characteristics will be considered later.

815. Direct Armature Reaction. — Assume that the power factor of the load is such that the armature current in any phase group of conductors reaches its maximum 90 electrical degrees after the corresponding group of conductors has passed the center of a pole (Fig. 592*b*). The resultant gliding mmf of the armature has its maximum value over the center of the poles and, with *lagging current,* is in such a direction as to *oppose directly* the field mmf. On the other hand, when the *current leads* the induced emf by 90 degrees the polarity of the armature reaction is reversed so that it *adds to* the field mmf. The direct reaction of the armature is represented in Fig. 605 by the fictitious revolving coils 1 and 2, whose axes coincide with the center line of the poles.

Direct armature reaction is thus an mmf acting around the same magnetic circuit as the field poles and is usually considered (see §817) to subtract directly from or add directly to the ampere-turns of the field. This is not quite correct numerically because an opposing mmf increases the leakage flux (§169), but with moderate values of the leakage factor the error introduced in the result is inconsiderable, although there may be an appreciable change in the leakage factor (§821). This is sometimes taken into consideration by replotting the no-load saturation curve with an increased leakage factor to correspond to the assumed load conditions. The influence of direct armature reaction upon machine characteristics is treated in some detail in §817 below.

816. Direct and Transverse Components of Armature Current.—Consider the alternator under discussion to be carrying a load of lagging power factor, between unity and zero. The current in each phase of the armature may be resolved into two components (in time), one of which is a maximum when the corresponding group of conductors is under the center of the pole, and the other a quarter cycle later. Each of these component currents may be considered to produce its own gliding mmf, the former, which may be said to be of unity "polar" power factor (designating angle between pole center and maximum current), producing the transverse armature reaction and being called the *transverse component* of current, I_t. The latter component, zero (polar) power factor current, sets up the direct armature reaction and is called the *direct component*, I_d.

Let I_1 be an armature current which reaches its maximum at angle ψ_1 after the conductors of its phase group have passed the center of the poles. Transverse and direct components of current are then:

$$I_t = I_1 \cos \psi_1 \quad \dots\dots\dots\dots \quad (25)$$

$$I_d = I_1 \sin \psi_1 \quad \dots\dots\dots\dots \quad (26)$$

From an inspection of Fig. 592(a), in which the currents in the three phases, being of unity "polar" power factor, are all in the same direction over a pole of given polarity, it will be seen that the mechanical force acting between every armature conductor and the field flux is such as to exert a drag upon the poles. In a synchronous motor at unity internal power factor ($\psi_1 = 0$) the currents would have the reverse direction from that shown in Fig. 592(a) and the force would be a pull or forward torque upon the poles. The component I_d, which is the reactive component of the current, since it reverses at the center of the poles and has equal but opposite values in corresponding conductors either side of the center line of a pole (Fig. 592b), can exert neither retarding nor advancing torque on the poles.

When the field excitation of a synchronous machine is fixed in value, and the machine is connected to a source of constant a-c voltage (infinite bus), the armature current will have a reactive component of such magnitude and direction as to bring the total excitation ampere-turns to a value consistent with the impressed terminal voltage. This results in an overexcited alternator delivering current with a lagging component, while an overexcited synchronous motor draws a current of leading power factor. In both cases the reactive component, I_d, acts to correct the generated voltage to a value differing from the impressed voltage only by the internal Ir and Ix_a drops of the armature.

817. Direct and Transverse Reaction Coefficients. — In the Blondel two-reaction method of analyzing the performance of salient-pole synchronous machines, the influence of direct armature reaction upon the flux from the poles may be evaluated in either of two ways. In the first of these the field ampere-turns are reduced directly (for lagging currents) by the amount of the effective direct armature reaction. Then from the no-load saturation curve the emf due to this resultant mmf is read.[4] In the second method (§819), determinations are made, first of the fundamental component of flux which the sine-form direct armature reaction would set up across the particular air-gap, together with the reactive emf which such a flux would produce; and second, the fundamental component of flux which the field would set up across the air-gap, with the emf which this flux would generate in the armature.[5] The former method, because of its greater simplicity, will be treated here.

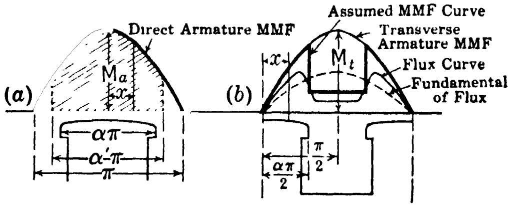

Fig. 606. (a) Determination of average direct armature reaction; (b) calculating fundamental of flux due to transverse reaction.

(a) *Direct reaction coefficient.* In Fig. 606(a) the average value of direct armature reaction mmf, $M_{d(\text{av})}$ over the pole arc is

$$M_{d(\text{av})} = (2/\alpha\pi)\int_0^{\alpha\pi/2} M_d \cos x \, dx = (2/\alpha\pi)M_d \sin \alpha\pi/2 \quad . \ . \ . \quad (27)$$

where α is the ratio (pole arc) (pole pitch).

But M_d, the maximum value of the direct armature reaction, is (see eqs. 24 and 26)

$$M_d = M_a \sin \psi = 0.9k_d mNI_d \quad . \ . \ . \quad . \quad (28)$$

where ψ is the angle of internal (polar) power factor (§798).

Designating by K_D the direct reaction coefficient

$$K_D = (2/\alpha\pi) \sin \alpha\pi/2 \quad . \ . \ . \ . \ . \ . \ . \ . \quad (29)$$

it is seen that the direct reaction coefficient is defined as the factor by which the maximum value of direct armature reaction must be multiplied to obtain the average direct reaction over the pole arc.

---

[4] E Arnold, " Die Wechselstromtechnik," vol. IV, Chapter II, Julius Springer.

[5] Doherty and Nickle, " Synchronous Machines, I, An Extension of the Blondel Two-Reaction Theory," *Trans. A.I.E.E.*, vol. 45 (1926), p. 912.

Substituting from eq. (29) into eq. (28)

$$M_{d(\text{av})} = 0.9K_D k_d mNI_d \quad . \; . \; . \; . \; . \; . \; . \; . \; . \quad (30)$$

In the calculation of this factor it is preferable to use, instead of the actual ratio, α, of pole arc to pole pitch, a slightly greater value α' = (effective pole arc)/(pole pitch), the effective pole arc being somewhat greater than the actual pole arc to allow for the fringing of flux at the pole tips. Adding two to three times the maximum air-gap length to the pole arc should be sufficient. The two factors, direct reaction coefficient, K_D, and winding distribution factor, k_d, should not be confused. They are often combined into one factor.

(b) *Transverse reaction coefficient.* The transverse armature reaction has a maximum value of

$$M_t = M_a \cos \psi = 0.9k_d mNI_t \quad . \; . \; . \; . \; . \; . \; . \; . \quad (31)$$

This sine-form armature mmf, with its axis midway between the poles of the machine, would produce a flux in the air-gap which, neglecting saturation, would be somewhat as shown in Fig. 606(*b*). It has been customary, in the application of the Blondel method, to consider that such a flux would be produced by an mmf of essentially the same shape but acting across the normal air-gap of the machine and therefore applying to the normal no-load saturation curve. In Fig. 606(*b*) the curve "assumed mmf" is a sine wave following the curve of "transverse armature reaction" from $x = 0$ at the center of the pole, to $x = \alpha\pi/2$. It then drops to about $0.2 \times M_t$ from $x = \alpha\pi/2$ to $x = \pi - \alpha\pi/2$, there rising to the original sine wave.

The fundamental sine component of the sawtooth wave which results from this assumption will have, as its maximum value,

$$M_{t1} = 2 \times \pi/2 \left[\int_0^{\alpha\pi/2} M_t \sin x \cdot \sin x \, dx + \int_{\alpha\pi/2}^{\pi/2} 0.2M_t \sin x \, dx \right] \quad (32)$$

which reduces to the form

$$M_{t1} = M_t[\alpha - (1/\pi) \sin \alpha\pi + (0.8/\pi) \cos \alpha\pi/2] \quad . \; . \; . \; . \quad (33)$$

Since this is the maximum value of the fundamental wave, its average value will be obtained by multiplying by $2/\pi$. Thus, the expression for the transverse reaction coefficient, defined as the ratio of the average mmf corresponding to the fundamental of transverse flux to the maximum of transverse reaction, is

$$K_T = \frac{2}{\pi}[\alpha - (1/\pi)\sin\alpha\pi + (0.8/\pi)\cos\alpha\pi/2] \quad . \; . \; . \quad (34)$$

and

$$M_{t1(\text{av})} = 0.9 K_T k_d m N I_t \quad . \; . \; . \; . \; . \; . \; . \; . \quad (35)$$

Examples. The following is an example of the calculation of K_D from the dimensions, or proportions, of a given machine. Let τ and $\delta_{\min}$ be the pole pitch and minimum air-gap clearance of a machine in which $\alpha = 0.65$ and $\delta_{\min} = 0.025\tau$, with $\delta_{\max}/\delta_{\min} = 2.0$, or $\delta_{\max} = 0.05\tau$. Then, approximately, $\alpha' = 0.65 + 2 \times 0.05 = 0.75$, so that (eq. 29)

$$K_D = (2/0.75\pi)\sin 0.75\pi/2 = 0.78$$

As an example of the calculation of K_T the values of the example above are substituted in eq. (34) as follows:

$$K_T = 2/\pi[0.75 - (1/\pi)\sin 0.75\pi + (0.8/\pi)\cos 0.75\pi/2] = 0.35$$

For a check upon this value, and upon eq. (34), Fig. 607 is reproduced through the courtesy of Mr. R. W. Wieseman and the editor of *Electrical Engineering.*[6] Figure 607 gives curves derived from a great number of flux plots made on certain salient-pole alternators in which the fundamental transverse armature reaction was the only mmf present, and for various values of α, of $\delta_{\max}/\delta_{\min}$, and of $\delta_{\min}/\tau$. Applying the values used in the previous example (K_D) to Fig. 607, and calculating K_T as the product of $A \times B$ from the curves, it is seen that for $\delta_{\min}/\tau = 0.025$, and $\delta_{\max}/\delta_{\min} = 2$, $B = 0.24$. Also, for $\alpha = 0.65$, and $\delta_{\min}/\tau = 0.025$, $A = 1.47$. Therefore, $K_T = 0.24 \times 1.47 = 0.35$, which checks eq. (34) more closely than would usually be expected.

818. Experimental Study of Armature Reaction — Machine Stationary.

— Although direct armature reaction, in terms of corresponding field amperes, was evaluated by means of the Potier triangle (§465), using the no-load and zero power factor load saturation curves, so far no method has been given for the measurement of transverse reaction. Any further consideration of indirect methods of evaluating the two reactions should be postponed until after the presentation of the complete performance diagrams of salient-pole machines in the next chapter. For the present it is preferable to keep the machine stationary and to excite the armature by means of direct currents of proper magnitude and direction.[7] In a three-phase machine on a balanced load, let the instantaneous current in one phase be represented as

---

[6] R. W. Wieseman, "Graphical Determination of Magnetic Fields," *Trans. A.I.E.E.*, vol. 46 (1927), p. 141.

[7] For a detailed experimental analysis of various factors which enter into the performance of a synchronous machine, see Blondel and Carbenay, *Revue générale de l'électr.*, vol. 5 (1919), pp. 811 and 843. Attention is called in particular to the method of measuring the flux ballistically without a test coil; p. 812.

$$i_1 = I_m \sin (2\pi ft + \alpha) \quad \ldots\ldots\ldots\ldots \quad (36)$$

Then the currents in the other two phases may be written as

$$i_2 = I_m \sin (2\pi ft + \alpha - 2\pi/3) \quad \ldots\ldots \quad (37)$$

$$i_3 = I_m \sin (2\pi ft + \alpha + 2\pi/3) \quad \ldots\ldots \quad (38)$$

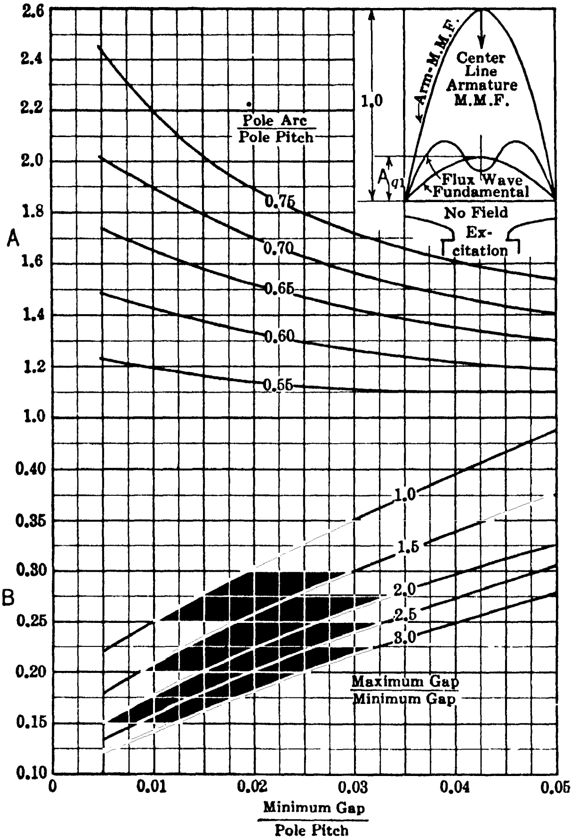

FIG. 607. Curves for calculation of transverse reaction coefficient, $K_T = A \times B$ (Wieseman).

where I_m is the amplitude, f the frequency in cycles per second, t the time in seconds, and α an arbitrary angle (in radians) which depends on the desired phase of current and the selected origin of time.

From eqs. (36), (37), (38), it is possible to compute a set of instantaneous values of the three currents corresponding to any instant and actually to realize them in the armature windings by means of direct currents, as shown in Fig. 608(*a*). W_1, W_2, W_3 are the three armature windings connected to a source of direct current through double-throw switches, S_1, S_2, S_3, and regulating resistances, R_1, R_2, R_3. This will give the total armature reaction at the chosen instant of a cycle, and the field structure can be blocked in a desired position with respect to the armature mmf. The resulting conditions in the magnetic circuit may then be studied with the aid of a ballistic galvanometer or other known means (Chapter XV).

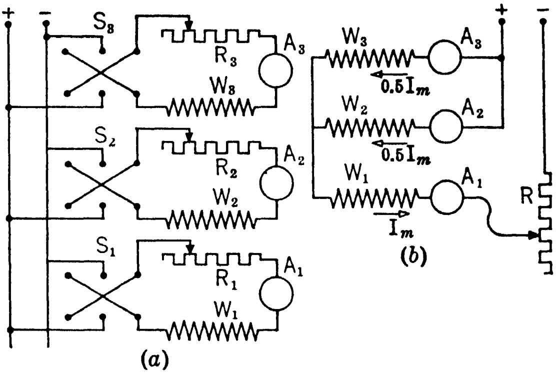

FIG. 608 Measurement of armature reaction using direct current.

At an instant when $2\pi ft + \alpha = \pi/2 + 2\pi n$, where n is an integer, $i_1 = I_m$, that is, the current in phase 1 reaches a maximum. At the same instant,

$$i_2 = I_m \sin(\pi/2 + 2\pi n - 2\pi/3) = -0.5I_m \quad . \quad . \quad . \quad . \quad (39)$$

$$i_3 = I_m \sin(\pi/2 + 2\pi n + 2\pi/3) = -0.5I_m \quad . \quad . \quad . \quad . \quad (40)$$

This condition is represented in Fig. 608(*b*), the currents in phases 2 and 3 flowing *towards* the neutral and each being equal to one-half of the current in phase 1, the latter flowing *away* from the neutral. Since the gliding mmf produced by distributed polyphase windings is practically constant in form (sinusoidal) at all instants, it is sufficient for some purposes to investigate the armature reaction for this particular instant. It presents two advantages: (a) The center of the resultant mmf is opposite the center of the coil in phase 1, so that the desired relative position of the field and the armature is readily found; (b) the adjustment of direct currents is easier, and fewer switches and rheostats are required.

In determining the values of direct current to correspond to a desired alternating current, the factor $\sqrt{2}$ must not be forgotten: Thus, if the
]]>

rated current of the alternator is, say, 100 effective amperes, the actual direct current through phase 1 must be 141.4 amperes, with one-half of it flowing through each of phases 2 and 3.

819. EXPERIMENT 42-A. — Measurement of Direct Reaction. — Provide a test coil, *ab* (Fig. 605), which will embrace the whole air-gap flux, Φ_g, that enters the armature. Connect this coil to a ballistic galvanometer (§177) or a fluxmeter (§180). Excite the field and also excite the stator with direct current, as explained above. Place the poles in such a position that the field mmf directly opposes that of the armature (fictitious coils 1 and 2 in Fig. 605). The field excitation should be stronger than that of the armature, but the resultant flux, Φ_g, must lie on the lower straight portion of the no-load saturation curve. Let the field ampere-turns per pole be $n_f i_f$ and the resultant armature ampere-turns per pole, in the combination in which they affect the main magnetic path, be $K_D'mNI$ (§460), where m is the number of phases, I is the effective value of the a-c armature current per phase, N is the number of turns per pole per phase, and $K_D' = 0.9K_D k_d$ combines the direct reaction coefficient (§817) and the distribution factor (§811). Then the air-gap flux, Φ_g, is excited by $n_f i_f - K_D'mNI$ ampere-turns. Measure this flux, by simultaneously reversing the field and the armature excitation, or by some other equivalent operation. Then open the armature circuit and decrease the field current to such a value, i_{f0}, that the air-gap flux, Φ_g, is the same as before. Then, approximately,

$$n_f i_{f0} = n_f i_f - K_D'mNI \quad . \; . \; . \; . \; . \; . \; . \; . \quad (41)$$

so that:

$$K_D'N = n_f(i_f - i_{f0})/(mI) \quad . \; . \; . \; . \; . \; . \; . \quad (42)$$

From eq. (42), the product $K_D'N$ can be computed, and then the direct armature reaction,

$$M_d = K_D'mNI_d \quad . \; . \; . \; . \; . \; . \; . \; . \; . \; . \quad (43)$$

determined for any desired value of direct component, I_d, of the actual a-c current. If the number of field turns, n_f, is not known, the preceding test may be used to determine the ratio $(i_f - i_{f0})/I$, that is, the number of field amperes equivalent to the armature reaction produced by one effective ampere per phase in the armature winding.

In practice, it will be found convenient to plot curves of Φ_g against values of $n_f i_{f0}$ and also against values of $n_f i_f$ as abscissas, at a constant I. This should give two parallel slanted straight lines which intercept any horizontal straight line at a distance $K_D'mNI$ from each other. When it is inconvenient to mount a test coil in the air-gap, the flux can be measured by a bridge connection (Chapter XXVIII), the armature winding in phase 1 (Fig. 608*b*) being used as the flux branch of the bridge. Of course, the measured flux in this case includes also that of the leakage inductance of the armature, which has to be eliminated from the result. From the data taken in the experiment calculate the direct reaction coefficient K_D, and composite factor K_D', and compare with values calculated from the winding data and physical dimensions.

820. EXPERIMENT 42-B. — Measurement of Transverse Reaction. — This test is also performed with direct current and with the machine stationary. A test coil, *cf* (Fig. 605), connected to a ballistic galvanometer or a fluxmeter, is placed on the center lines of two adjacent poles. The armature is excited as shown in Fig. 608*b*, and phase 1 is placed in the position of the fictitious coils 3 and 4 (Fig. 605), so that its maximum mmf is midway between the poles. The flux of transverse reaction is measured ballistically, by reversing the armature current. With a given I_m, this flux is somewhat affected by the field excitation, because the latter determines the reluctance of the iron parts of the circuit. Therefore, this test should be performed at different values of armature current and of field current. Of course, the latter current should *not* be reversed when the armature current is reversed for measuring the flux. The flux can also be measured by a bridge connection, as mentioned for the direct reaction above.

The flux of the transverse reaction (Fig. 606) has a complicated space distribution, and it is sufficient for practical purposes to take into consideration only its fundamental sinusoidal distribution, because it is this component which induces the fundamental emf in the armature winding.[8] A set of fictitious poles, of the same shape as the real poles, and placed midway between them, is assumed. This makes it possible to use the no-load saturation curve of the real poles for expressing the transverse reaction. In other words, after the flux, Φ_t, has been found, the corresponding number of ampere-turns is found from the no-load saturation curve of the machine. This gives the relationship:

$$n_f i_f = K_T' mNI_t \quad \ldots \ldots \ldots \quad (44)$$

where $K_T' = 0.9K_T k_d$ is a coefficient combining the transverse reaction coefficient (§817) and the distribution factor (§811) of the machine. From eq. (44) the product $K_T'N$ can be computed if the other quantities are known. If the number of the field turns is not known, the preceding test will make it possible at least to compute the ratio of i_f/I_t, that is, the transverse reaction per ampere of armature current, expressed in field amperes. Here I_t is expressed in effective a-c amperes, so that the d-c value, I_m, used in the text, must be divided by $\sqrt{2}$.

---

[8] "The Magnetic Circuit," p. 161.

In practice, the effect of the transverse reaction is sometimes expressed as a fictitious reactance, in ohms; that is, the fictitious poles mentioned above may be assumed to be unsaturated, and their flux characterized by the value of

$$v = E_{tr}/n_f i_f \quad \ldots\ldots\ldots\ldots \quad (45)$$

where v is the induced no-load voltage per field ampere-turn. This quantity, v, can be obtained from an ordinary no-load saturation curve of the machine, since by assumption the fictitious poles are identical with the real ones. Thus, eq. (44), after being multiplied on both sides by v, becomes:

$$E_{tr} = vK_T'mNI_t \quad \ldots\ldots\ldots\ldots \quad (46)$$

This may also be written as

$$E_{tr} = x_t I_t \quad \ldots\ldots\ldots\ldots \quad (47)$$

where

$$x_t = vK_T'mN \quad \ldots\ldots\ldots\ldots \quad (48)$$

The quantity x_t is called the reactance corresponding to the transverse armature reaction, or simply the transverse armature reactance. As such it enters into performance diagrams and equations of the machine.[9]

Since the value of Φ_t, corresponding to a given I_t, is known from test, the corresponding values of i_f and E_{tr} are found from the no-load saturation curve, and the ratio of E_{tr} to I_t gives the value of x_t. The transverse reactance can also be computed indirectly from a load test (§824).

Compare the values of K_T' and K_T determined from experimental data with values obtained by calculation from the winding data and physical dimensions of the machine.

821. Magnetic Leakage between Field Poles. — Because of the demagnetizing direct armature reaction, described above, a machine requires more field ampere-turns when loaded for the same useful air-gap flux as at no load. Hence, the difference of magnetic potential between the pole tips, and consequently the leakage flux, is greater than at no load. Conversely, when the direct armature reaction strengthens the field, the pole leakage is reduced. Since the leakage path is mostly in the air (except for the saturated pole tips), its reluctance is nearly constant. When this reluctance has been determined, the leakage flux itself can be obtained for any desired load by dividing the free ampere-turns between the pole tips by this reluctance.

---

[9] This quantity, x_t, does not include the armature slot leakage or the end-connection leakage. The corresponding transverse inductance, L_t, used by Blondel (*Comptes rendus*, vol. 159 (1914), p. 574), includes the slot leakage. This difference in the assumptions must be kept in mind, and it is for this reason that the test coil, *cf*, is shown as near as possible to the pole shoes, so as to exclude the tooth-leakage fluxes.

As an example, let the reluctance of the leakage paths between a pole and the plane of symmetry between it and one of the adjacent poles be 0.05 rel;[10] let the ampere-turns per pole be 9000. Assume that 1000 ampere-turns are used in the pole itself, leaving 8000 between the pole tip and the plane of symmetry. Then the total leakage flux, to both adjacent poles, is $2(8000/0.05) \times 10^{-6} = 0.32$ megaline.

The pole leakage reluctance may be conveniently measured by applying a direct armature reaction by means of d-c excitation in the armature (§§818 and 819). Let the subscripts p, g, l refer to the pole, air-gap, and leakage paths, respectively, and the subscripts 0 and 1 to the conditions existing when the field alone is excited and when both the field and the armature are excited. Then we may write the following two equations:

$$ni_0 = R_{p0}\Phi_{p0} + R_l\Phi_{l0} \quad . \quad . \quad . \quad . \quad . \quad . \quad . \quad . \quad (49)$$

$$ni_1 = R_{p1}\Phi_{p1} + R_l\Phi_{l1} \quad . \quad . \quad . \quad . \quad . \quad . \quad . \quad . \quad . \quad (50)$$

Equation (49) means that the total field excitation, ni_0, is partly used up in the reluctance, R_{p0}, of the poles, and the rest is consumed as the drop of mmf in the leakage reluctance, R_l. Equation (50) has a similar meaning when the armature excitation is also present, although the armature mmf does not enter explicitly into the equation. If all the fluxes and mmf's are per pole, then R_l is the combined reluctance of the two leakage fluxes in parallel, between the pole under consideration and the planes of symmetry between it and the two adjacent poles.

In an actual experiment, the field poles are first excited with a certain current, i_0, and the fluxes, Φ_{p0} and Φ_{g0}, are measured ballistically. Then a direct armature reaction is applied and the field current is increased to a value, i_1, for which

$$\Phi_{p0} = \Phi_{p1} \quad . \quad . \quad . \quad . \quad . \quad . \quad . \quad . \quad . \quad . \quad . \quad (51)$$

Let the air-gap leakage flux, under these conditions, be Φ_{l1}. Since the total flux in the pole waists is the same in both cases, the reluctances

---

[10] For magnetic units see "The Magnetic Circuit," p. 10.

R_{p0} and R_{p1} are also equal. Thus, subtracting eq. (49) from eq. (50), we get

$$ni_1 - ni_0 = R_l(\Phi_{l1} - \Phi_{l0}) \quad \dots\dots\dots\dots \quad (52)$$

But

$$\Phi_{l1} = \Phi_{p1} - \Phi_{g1} \quad \dots\dots\dots\dots \quad (53)$$

and

$$\Phi_{l0} = \Phi_{p0} - \Phi_{g0} \quad \dots\dots\dots\dots \quad (54)$$

so that:

$$ni_1 - ni_0 = R_l(\Phi_{g0} - \Phi_{g1}) \quad \dots\dots\dots\dots \quad (55)$$

From this expression:

$$R_l = (ni_1 - ni_0)/(\Phi_{g0} - \Phi_{g1}) \quad \dots\dots \quad (56)$$

If n is not known, this equation may be solved for R_l/n. The experiment should be performed with different values of i_0, so as to investigate the influence of the saturation of the pole tips upon the value of R_l.

822. EXPERIMENT 42-C. — Measurement of Pole Leakage in a Synchronous Machine. — The theory and the method are explained in the preceding section. The results should contain not only values of R_l, but also the values of the leakage coefficient, Φ_p/Φ_g, for various values of field excitation and armature reaction. In some of the tests, this reaction should be applied in such a direction as to assist the field mmf, instead of opposing it.

CHAPTER XLIII

PERFORMANCE DIAGRAMS OF SALIENT-POLE SYNCHRONOUS MACHINES

823. The Blondel Diagram.—After the armature reaction has been resolved into its direct and transverse components, as shown in the preceding chapter, the performance of a synchronous machine with salient poles may be analyzed as suggested in Fig. 609. $OA = E$ is the terminal voltage in one phase, and $OP = I$ is the corresponding current, which is assumed to lag behind the voltage by an angle ϕ. $AB = Ir$ is the ohmic drop in the armature, drawn in phase with OP. The effective resistance, r, is that obtained from the actual I^2r loss in

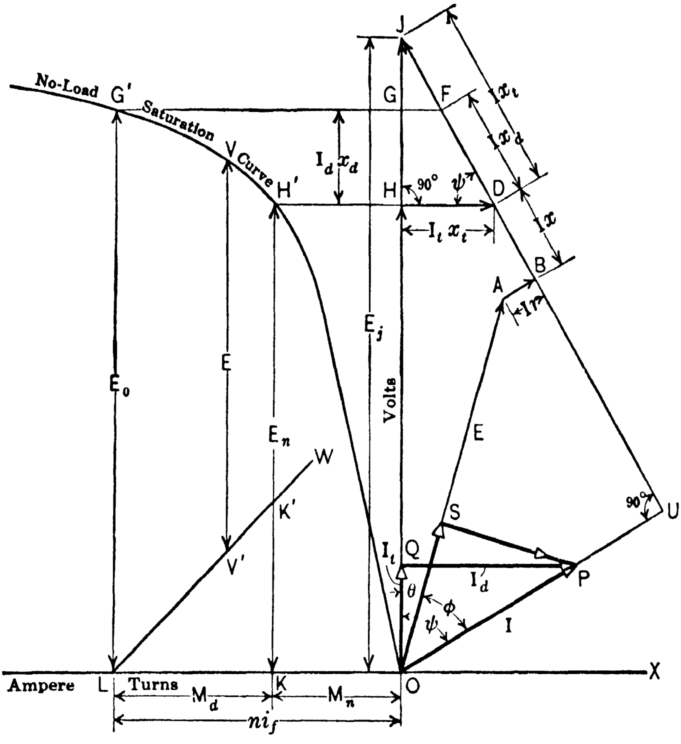

FIG. 609. Performance diagram of the synchronous generator with salient poles at a lagging power factor (Blondel).

the armature (§154), say on short circuit (§445), and not a lower value measured with direct current. $BD = Ix$ is the leakage reactance drop in the armature,[1] in quadrature with I (§460). Therefore, OD is the resultant voltage induced by the real and the " fictitious " poles (§820). Let OH be the voltage, E_n, induced by the real poles, where the subscript n stands for " net." Then $HD = I_t x_t$ is the voltage induced by the fictitious poles, where x_t is the reactance corresponding to the transverse armature reaction (§820). The two emf's, OH and HD, are in quadrature with each other because the flux due to transverse armature reaction is midway between the poles. In a generator, the transverse reaction lags behind the real poles, and for this reason HD is shown lagging behind OH.

The net emf, E_n, induced in the armature winding by the real poles, corresponds to the net excitation,

$$M_n = ni_f - M_d \quad . \; . \; . \; . \; . \; . \; . \; . \; . \; . \quad (1)$$

where ni_f is the field excitation and M_d is the (average) direct armature reaction (§815). Let $OH'G'$ be the no-load saturation curve of the machine, and let $M_n = OK$. Adding to it $KL = M_d$ gives the field excitation $OL = ni_f$. This excitation corresponds to the voltage $E_0 = LG' = OG$. This means that when the machine operates at the field current i_f, under the load conditions shown in Fig. 609, its terminal voltage is $OA = E$, while if the load were thrown off the terminal voltage would rise to $OG = E_0$.

The voltage OH is in phase with the centers of the poles; consequently, the angle $AOH = \theta$ is the torque angle (§800) by which the pole structure is shifted forward with respect to an identical machine operating in parallel at no load. It will be seen that:

$$\theta = \psi - \phi \quad . \; . \; . \; . \; . \; . \; . \; . \; . \; . \; . \quad (2)$$

where ψ is the internal phase angle and ϕ is the external or load phase angle.

Let OH and BD be extended to their intersection at J. Since $HD = I_t x_t$ and the angle at D is equal to ψ, we see, from the similarity of the triangles OPQ and DJH, that:

$$DJ = Ix_t \quad . \; . \; . \; . \; . \; . \; . \; . \; . \; . \; . \; . \quad (3)$$

This shows that point H may be obtained without computing the vector DH. It is sufficient to lay off $BJ = I(x + x_t)$ at right angles to the current vector and to connect J to O. A perpendicular from D on OJ will give point H. In view of the importance of point J in the construction of the diagram and of certain loci, A. Blondel proposed to name the fictitious voltage OJ the *Joubertian* voltage or emf, in honor of the pioneer French electrical engineer and physicist, Joubert. The point J may be called the Joubertian point.

---

[1] In the discussion below, the reactance, x, is assumed to be constant. For a more accurate diagram, see §839.

It will be seen from Fig. 609 that the use of the no-load saturation curve is indispensable, since one and the same value of the direct armature reaction, M_d, will give a different value of $E_0 - E_n = HG$, depending upon the average slope of the saturation curve. Thus, while it is possible to represent the effect of the direct armature reaction by a fictitious reactance, x_d, this reactance is a variable quantity. It has a large constant value on the lower part of the saturation curve and then gradually decreases on the knee, to a small constant value on the upper part of the curve. If the machine is supposed to work only on the upper or only on the lower part of the saturation curve, a constant value of x_d can be determined for that particular range, and the value $Ix_d = DF$ used to determine point G. In this case it is not necessary to use the saturation curve. For operating points on the lower part of the saturation curve, x_d is greater than x_t, and point F lies beyond J. By replacing the curved part of the saturation curve by two or more straight lines, a different constant value of x_d may be used for each, and will be approximately correct within that range (§831).

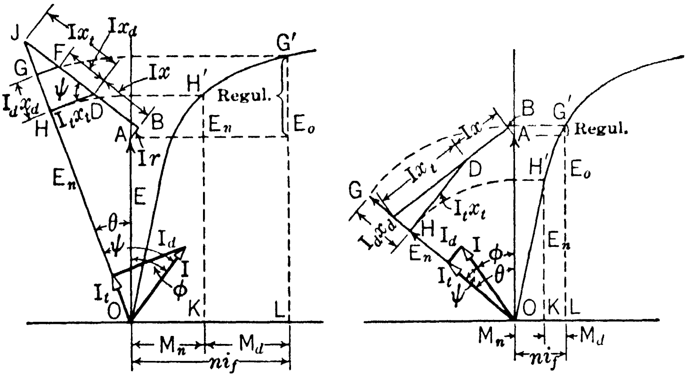

(*a*) Generator, Current Lagging (*b*) Generator, Current Leading

FIG. 610. Comparative Blondel diagrams for the synchronous generator.

Figure 609 corresponds to the operating conditions in the first quadrant of Fig. 590. Figures 610 and 611 are comparative diagrams drawn for the operating conditions in the four quadrants A study of these will give an insight into the influence of the field current and of the two reactions upon the operation of the synchronous generator and motor. In particular, the magnitudes and the signs of the angles ψ, θ, and ϕ should be carefully examined in order to keep the equations deduced below valid for both the generator and the motor, at both a lagging and a leading current (§798). For this study it was thought best to keep the vector of the terminal voltage, E, constant both in magnitude and in direction, and the current vector, I, constant in magnitude but with the phase angle, ϕ, representing the same power factor (80 per cent), leading and lagging, for generator and for motor action. The loci of the points B, D, and J lie on concentric circles with their common center at A. The position of the line FG has to be determined from the no-load saturation curve separately for each value of ϕ.

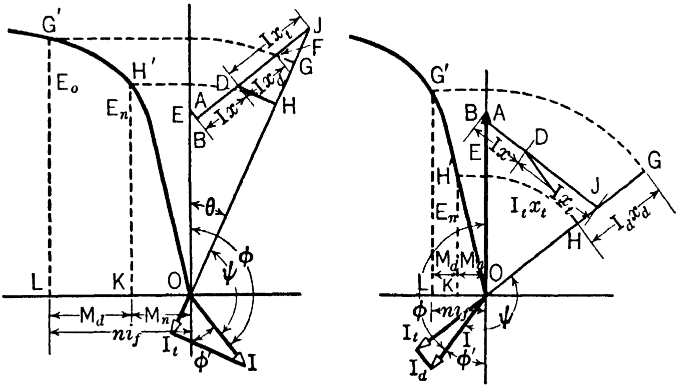

(c) Motor, current leading

(d) Motor, current lagging

FIG. 611 Blondel diagrams for the synchronous machine during motor action.

Another case of interest is that of constant power input or output, at a constant terminal voltage. Neglecting the ohmic drop, AB, the locus of the point J is a straight line parallel to OA. This is because JB is proportional and perpendicular to the current vector, and, since the projection of I upon OA must remain constant, the projection of BJ upon a direction perpendicular to OA must also be constant. For the same reason, the locus of the point D is a straight line parallel to OA. The point F has to be determined separately for each value of ϕ, by means of the no-load saturation curve.

If the coefficient of direct reaction, K_D (§817), were put equal to that of transverse reaction, K_T (§817), the theory outlined above would become identical with that for the machine with non-salient poles (Chapter XLII), since there would be no need of resolving the total armature reaction into its two components.

824. Special Cases of $\phi = 0$ and $\phi = -\theta$. — The conditions which obtain when the current and the terminal voltage are in phase ($\phi = 0$) are shown in Fig. 612. The diagram (*a*) refers to a generator; (*b*) refers to a motor. It will be seen that the torque angle, θ, in this case is equal to the internal phase angle, ψ, and this fact is sometimes used to determine experimentally the value of $(x + x_t)$, by measuring θ (§852). We then have, from the triangle *OBJ*:

$$I(x_t + x) = (E \pm Ir) \tan \theta \quad . \quad . \quad . \quad (4)$$

The plus sign refers to the generator, the minus sign to the motor. From this equation, $x_t + x$ may be computed. Additional data are necessary to separate the two. For example, x may be determined separately (§465) or x_t may be found with direct current (§820). Again, if the direct reaction of the machine is known (§819), point *H* may be found from the no-load saturation curve and point *D* located by erecting the perpendicular *HD*.

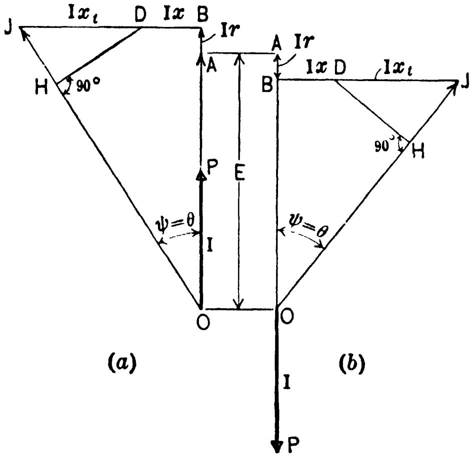

FIG. 612. Blondel diagram for $\cos \phi = 1$.

Blondel has suggested the term *torsance* for the quantity $x_t + x$, because it is this quantity that determines the torque angle, θ, and consequently the electric power of the machine with a given terminal voltage and current.[2] Thus, from the triangle *OUJ* (Fig. 609) we have, for a generator,

$$\tan \psi = [E \sin \phi + I(x_t + x)]/(E \cos \phi + Ir) \quad . \quad . \quad . \quad . \quad . \quad (5)$$

The value of ψ having been computed from this expression, the angle θ is found from eq. (2). With a proper interpretation of the angles and of the sign of the Ir drop, similar relations hold true for a motor (§798). When $\phi = 0$, eq. (5) is simplified to eq. (4).

Another interesting operating condition of the machine is that of $\psi = 0$ for the generator (Fig. 613*a*) or of $\psi = 180°$ for the motor (Fig. 613*b*). The direction of the current vector coincides with that of the Joubertian emf, *OJ*, and $\theta = -\phi$. Since there is no interpole component of the armature current ($I_d = 0$), the direct armature reaction is equal to zero and $E_0 = E_n$. In Fig. 613*a*, $VA = -BJ$, or

---

[2] *Comptes rendus*, vol. 165 (1917), p. 1092.

$$-E \sin \phi = I(x + x_t) \quad . \; . \; . \; . \; . \; . \; . \; . \; . \quad (6)$$

This agrees with eq. (5), because, when the left-hand side is equal to zero, the numerator on the right-hand side must be equal to zero.

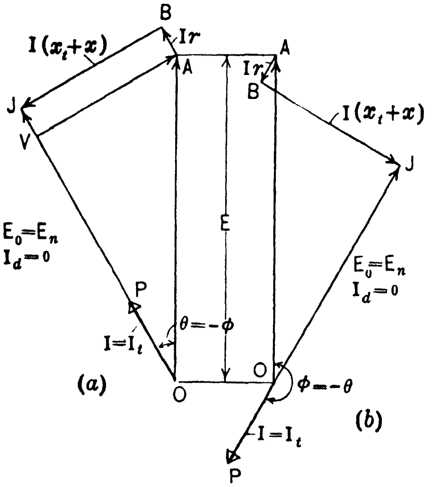

FIG. 613. Blondel diagrams for cases of $\psi = 0$ and $\psi = 180°$.

The diagram shown in Fig. 613*a* suggests the following experiment: The machine is loaded as a generator, at a partly leading current, and the torque angle, θ, is measured by suitable means (§852), as well as the phase angle, ϕ. When the two angles are equal (and of opposite sign), the following readings are taken: E, I, ϕ $(= -\theta)$, and i_f. From the reading of i_f, the corresponding value of $E_0 = E_n$ is obtained. From eq. (6) the value of $x + x_t$ may then be computed. From Fig. 613*a* we also have:

$$E \cos \phi + Ir = E_0 \quad . \quad (7)$$

Since all the quantities in this equation are known from the experiment, the equation itself is a check on the accuracy of the measurements or on the degree of accuracy with which the theory applies to that particular machine. Equation (7) may also be used to eliminate the necessity of a direct measurement of θ. With given E and I, the angle ϕ is varied by adjusting the field current until eq. (7) is satisfied. Then Fig. 613*a* holds true and $x_t + x$ may be computed from eq. (6). A similar experiment may be performed with the machine running as a motor, according to Fig. 613*b*.

825. EXPERIMENT 43-A. — Comparison of Actual Performance with the Graphical Solution of the Blondel Diagram. — The purpose of the experiment is to familiarize the student with the diagrams explained in the preceding sections. Load characteristics of the machine, operating both as a generator and as a motor, and also the no-load saturation curve, should be obtained by experiment as accurately as possible, and a few typical points checked with the Blondel diagram. This diagram requires the numerical values of the armature resistance, r, leakage reactance, x, and the two components of the armature reaction, M_d and x_t. These may be determined from separate experiments, as outlined above. It is also possible to estimate the leakage reactance and the direct reaction from a test at zero power factor (see §465) and to choose by trials such a value of x_t that the diagram will check satisfactorily with the results of load tests at high values of power factor.

The problem is considerably simplified if an experimental arrangement is available for measuring the torque angle, θ (§852). When ϕ, θ, E, and I (Fig. 609) are known, the polygon $OABJO$ can be constructed, and it remains only to locate the lines GF and HG. See also §830.

826. Analytical Solution.—Instead of constructing a diagram, such as Fig. 609, the field excitation necessary for a given load and terminal voltage may be determined analytically. We shall consider only the most important practical case of negligible armature resistance drop, and shall put, for the sake of brevity,

$$x + x_t = c \quad . \; . \; . \; . \; . \; . \; . \; . \; . \; . \; . \quad (8)$$

Let E, I, and ϕ be given. The direct component of the armature current is:

$$I_d = I \sin(\phi + \theta) \quad . \; . \; . \; . \; . \; . \; . \; . \; . \quad (9)$$

so that the direct armature reaction is:

$$M_d = aI_d = aI \sin(\phi + \theta) \quad . \; . \; . \; . \; . \quad (10)$$

where:

$$a = K_D' mN. \quad . \; . \; . \; . \; . \; . \; . \; . \; . \; . \; . \quad (11)$$

See §819, eq. (8). Projecting $OABD$ upon OH, and remembering that by assumption $AB = 0$, we get:

$$E_n = E \cos\theta + Ix \sin(\phi + \theta) \quad . \; . \; . \; . \; . \; . \; . \quad (12)$$

When $AB = 0$, the projections of OA and BJ upon the direction HD are numerically equal, so that:

$$E \sin\theta = Ic \cos(\phi + \theta) \quad . \; . \; . \; . \; . \; . \; . \quad (13)$$

from which

$$\tan\theta = \cos\phi / [(E/Ic) + \sin\phi] \quad . \; . \; . \; . \quad (14)$$

The order of computations is as follows: The angle θ is determined from eq. (14), and then M_d and E_n are found from eqs. (10) and (12). By means of the no-load saturation curve, the value $OK = M_n$ is found next, and then the field excitation, OL, is computed from the formula:

$$ni_f = M_n + M_d \quad . \; . \; . \; . \; . \; . \; . \; . \; . \; . \quad (15)$$

This will also give the no-load emf $LG' = E_0$.

For the conditions shown in Fig. 609, viz., a generator with a lagging current, the angles ϕ and θ are both positive and less than 90 degrees. For the values of these angles in the three other cases, see §§798 and 814, and Figs. 610 and 611. The problem is not always stated in the form assumed above. Sometimes the terminal voltage may not be known and the field excitation may be given instead, or the power may be given in place of the current, etc. With the aid of the above equations, such problems can usually be solved either directly or by a few successive approximations

827. Power as a Function of the Torque Angle. — In a study of the stability of a machine, hunting, synchronizing power, etc. (§800), it is necessary to know the relationship between the electromagnetic power passing from the a-c line through the armature into the field structure, or vice versa, and the torque angle, θ. The terminal voltage and the field excitation are assumed to remain constant. Physically, this means that, while the machine is operating (either as a generator or as a motor) at a constant terminal voltage and constant field current, the load P is being varied, and it is required to find the relationship between P and θ.

This problem may be conveniently solved analytically, by means of some of the expressions deduced in the preceding section. The direct armature reaction, M_d, is taken as the independent variable. Eliminating $I \sin (\phi + \theta)$ from eq. (12) by substitution from eq. (10), we get:

$$E_n = E \cos \theta + (x/a)M_d \quad . \; . \; . \; . \; . \; . \; . \; . \quad (16)$$

from which

$$\cos \theta = [E_n - (x/a)M_d]/E \quad . \; . \; . \; . \; . \; . \; . \; . \quad (17)$$

In Fig. 609, let OL be the constant field excitation at which the machine is operating. Then, for any assumed value of M_d, such as LK, the corresponding net emf is $E_n = KH'$. The corresponding value of θ can be computed from eq. (17). Instead of computing the expression in the brackets, its value can be determined graphically by drawing the line LW at such a slope that for any value of $LK = M_d$, the ordinate $KK' = (x/a)M_d$. Then the expression in the brackets is represented by the length $K'H'$, and it remains only to divide it by E. It is convenient first to locate the position of the ordinate $VV' = E$, because for it, $\cos \theta = 1$ and $\theta = 0$; see eq. (17). This corresponds to the minimum value of M_d possible with the assumed values of E and ni_f. Other operating points correspond to larger values of M_d.

Solving eqs. (10) and (13) for I and ϕ, we find:

$$I = [(E/c)^2 \sin^2 \theta + (M_d/a)^2]^{0.5} \quad . \; . \; . \; . \quad (18)$$

$$\tan (\theta + \phi) = \frac{M_d/a}{(E/c) \sin \theta} \quad . \; . \; . \; . \; . \; . \; . \; . \; . \; . \; . \quad (19)$$

For any assumed value of M_d, if the corresponding θ is known, the values of I and ϕ may be computed from these equations. Then the power, per phase, is:

$$P = IE \cos \phi \quad . \; . \; . \; . \; . \; . \; . \; . \; . \; . \quad (20)$$

By plotting values of P against θ as abscissas, the synchronizing power, $dP/d\theta$, may be determined graphically for any desired operating condition. By continuing the P curve to a point for which $dP/d\theta = 0$, the pull-out torque of the machine can be found.

828. EXPERIMENT 43-B. — Comparison of Actual Performance with Analytical Solution of the Blondel Diagram. — The experiment is similar to that outlined in §825, except that the checking of the performance is to be done analytically, as explained in the preceding two sections.

829. The Blondelion. — It is shown in §805 that the no-load saturation curve and some scales may be so combined as to facilitate the determination of performance characteristics by trials. As a further development of this idea, there is described, in §806, a kinematic device in which the reactive drop and the armature reaction are made to vary automatically by means of proportional dividers. An analogous device (the Blondelion) has been developed by V. Karapetoff to represent the diagram shown in Fig. 609. In its simplest form, it is similar to the device shown in Fig. 597, except that the proportional dividers have an additional member, since the two components of armature reaction must be represented separately. In a more elaborate form of the Blondelion, the saturation curve itself is represented by an adjustable cam, and the kinematic linkages are such that for a given set of operating conditions, for example, for given E, I, ϕ, the device can be set without trials and the required field excitation obtained directly.[3]

830. Performance at a Constant Field Current. — The diagram shown in Fig. 614 is similar to that in Fig. 609, and the corresponding points are lettered accordingly. The ohmic drop in the armature is neglected. Let the field excitation, OL, be kept constant, and let the armature current vary in such a manner that its direct or interpole component, I_d, remains constant. This means that the direct armature reaction, KL, also remains constant. Therefore, the points G and H are fixed for all the operating conditions subject to the above two limitations (I_f = constant and I_d = constant). As a result, the Joubertian point, J, is fixed, and the locus of the extremity A of the voltage vector OA is the straight line $A'C$ parallel to OX. The length $JA = I(x + x_t)$, being proportional to the armature current, may be taken to represent its magnitude, and the angle yAz is the phase angle, ϕ, since Az is in phase with I and Ay with E. The fact that the point A must remain on $A'C$ can be seen by drawing two current vectors, such as JA and JA''. By assumption, H, D'', and D lie on the same horizontal line. The ratio of AD to DJ is equal to x/x_t, and is constant. These conditions can be satisfied only when the point J is fixed and A moves on a horizontal line.

---

[3] *Trans. A.I.E.E.*, vol. 42 (1923), p. 144; *Sibley Journal of Engineering*, vol. 40 (1926), pp. 54, 73, 84; also reprinted as *Bulletin* 6 of the Engineering Experiment Station, Cornell University.

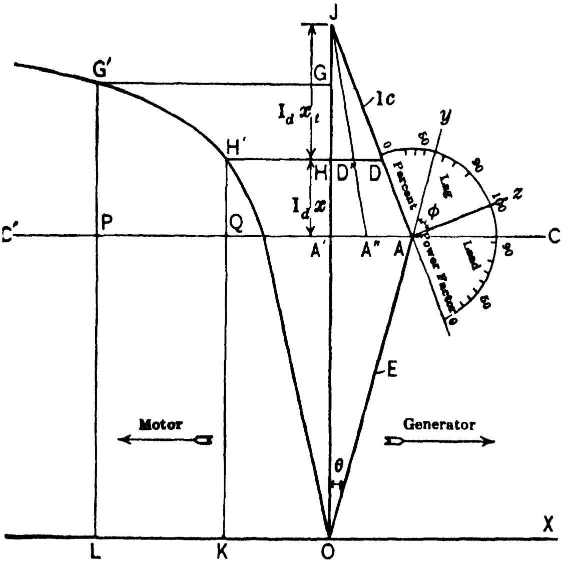

FIG. 614. Locus diagram at constant field current and constant direct armature reaction.

To obtain the position of the points J and A', knowing OL, consider the operation when the whole armature current is equal to the interpole component, I_d. This component being given (or assumed), the direct armature reaction, LK, can be computed from eq. (43), §819. This will determine the points H' and H. The length HA' is equal to $I_d x$, and $HJ = I_d x_t$.

Having located J and CC', take any point on CC', such as A, and connect it to O and J. Then OA will represent the terminal voltage, and AJ, being equal to $I(x + x_t)$, will be proportional to the current. The actual direction of the current vector is 90 degrees lagging behind AJ. It is convenient, therefore, to use a protractor, as shown in the figure, to measure the power factor, $\cos \phi$, or the angle ϕ, directly. The torque angle, θ, can be measured at O, and the power computed as the product $IE \cos \phi$. Since this product is proportional to the area of the triangle OJA, considered as a triangle of base $OA = E$, and of altitude $= AJ \sin (90 - \phi) = I(x + x_t) \cos \phi$, the power is also proportional to the product of OJ and $A'A$. OJ being constant, the power is simply proportional to the length $A'A$. For positions of A to the right of OJ, the machine is operating as a generator, and in the region $A'C'$ it operates as a motor.

Keeping OL constant, assume other values of I_d, corresponding to different positions of point K. For each value of I_d, a new point J and another line $C'C$ can be found, as explained above, and thus a new set of operating conditions found for the given field current. By a judicious selection of values of I_d, a complete operating picture of the machine at that particular value of field current may be obtained. A few positions of K should be also tried to the left of L, when the direct armature reaction strengthens the field. Of all the operating combinations thus found, sometimes only those need be considered which are limited by an additional condition, for example, a constant armature current, a constant terminal voltage, etc.

LOCUS DIAGRAMS WITH SECTIONALIZED SATURATION CURVE

831. The diagram shown in Fig. 609 represents the performance of a synchronous machine under certain specific conditions of voltage, current, power factor, and excitation. It is of considerable interest to construct various *locus diagrams* of the machine, that is, diagrams which indicate the performance when one or more factors are kept constant, or are varied in a prescribed manner. Two such locus diagrams are suggested at the end of §823, and one more is described in §830. The difficulty with all such diagrams lies in the necessity of using the no-load saturation curve, which makes the use of the diagram quite cumbersome.

On the other hand, locus diagrams based on the assumption of a straight-line saturation curve passing through the origin are easily constructed (§803), but are mainly suitable for qualitative study, unless the machine is actually operating at very low flux densities.

A partial solution of the difficulty lies in replacing the actual saturation curve by a number of straight lines (Fig. 615). The lower and upper sections are practically straight lines anyway, and two or three intermediate straight lines can be made to represent the knee with an accuracy sufficient for ordinary practical purposes. The saturation curve affects only the value of the reactance x_d, corresponding to the direct armature reaction (Fig. 609). For each straight line in Fig. 615, x_d has a constant value which can be computed from the slope of that particular line (see below). Hence, it is not necessary to use the saturation curve itself.

With this method, the machine is first assumed to have the straight line *GH* (Fig. 615) for its saturation curve, and in the construction of the corresponding locus diagram the value of x_d for this line is used. Then the diagram is modified, the values of x_d for the straight lines *DF*, *BC*, and *OA* being used in turn. Thus, four sets of performance characteristics of the machine are obtained, among these characteristics being the values of E_n. Then, of the characteristic curves obtained with the line *GH*, only that part is used which corresponds to the values of E_n greater than *P'P*. Of the characteristics obtained with the line *DF*, only that part is used for which E_n lies between the values *L'L* and *P'P*, etc.

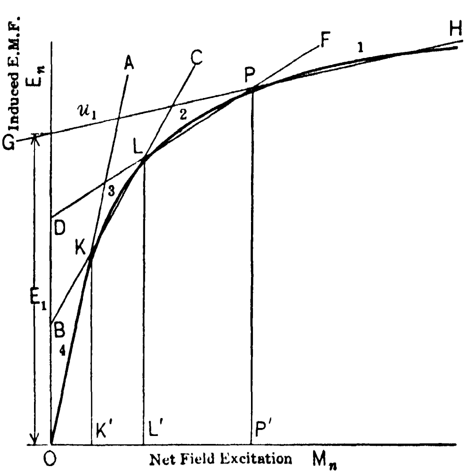

FIG. 615. A saturation curve sectionalized into four straight parts.

A few examples of such locus diagrams with a sectionalized saturation curve are shown below, and the reader can devise more, to meet a particular problem on hand. Of course, such diagrams have an evident drawback in necessitating a check on the limits of E_n. On the other hand, locus diagrams in which an actual saturation curve is used are also quite tedious in actual application. A kinematic device (§829) which permits the use of the actual saturation curve may often be found more convenient than either kind of diagram.

Still another possible solution would be to express the saturation curve analytically, and to include its equation among those deduced in §§826 and 827. So far, all efforts in this direction have led to a set of simultaneous equations too involved for a solution or for an analysis of the influence of the principal factors.

832. The Value of the Direct Reactance from a Straight-Line Saturation Curve. — Let the actual no-load saturation curve of the machine be replaced by a straight line, such as *GH* (Fig. 615), and let this line be characterized by its intercept $OG = E_1$ and the slope u_1, the equation of the line being:

$$E_n = E_1 + u_1 M_n \quad . \; . \; . \; . \; . \; . \; . \; . \; . \; . \quad (21)$$

At no load,

$$E_0 = E_1 + u_1 M_f \quad . \; . \; . \; . \; . \; . \; . \; . \; . \; . \quad (22)$$

so that:

$$M_f = (E_0 - E_1)/u_1 \quad . \; . \; . \; . \; . \; . \quad . \quad (23)$$

Subtracting eq. (21) from eq. (22) gives, with reference to Fig. 609,

$$E_0 - E_n = u_1(M_f - M_n) = I_d x_{d1} \quad . \; . \; . \; . \; . \quad (24)$$

But $M_f - M_n$ is the direct armature reaction, M_d, so that, using eqs. (10) and (11), we get:

$$x_{d1} = u_1 a = u_1 K_D' mN \quad . \; . \; . \; . \; . \; . \; . \; . \quad (25)$$

For the remaining three straight lines the slopes are u_2, u_3, u_4, and the corresponding intercepts are E_2, E_3, $(E_4 = 0)$. On the highly saturated part, *PH*, of the actual curve, u_1 is small, and hence x_{d1} is also comparatively small. For the portion *OK*, the slope u_4 is large, and consequently x_{d4} is also large, being in fact greater than x_t. On the portions 2 and 3 of the curve, u has intermediate values between u_1 and u_4. It will be noted that x_d depends only upon the slope u and not upon the magnitude of the intercepts, E_1, E_2, etc. The values of the intercepts enter only in eqs. (21), (22), and (23).

833. The Circle Diagram for Constant Terminal Voltage and Constant Armature Current (Sectionalized Saturation Curve). — In Fig. 616, the points that have the same significance as in Fig. 609 are denoted by the same letters. The ohmic drop is neglected, as it is usually of the order of one per cent of the terminal voltage; if necessary, the *ir* drop could be taken into consideration in Fig. 616 by an additional circle. The terminal voltage, $OA = E$, is assumed to be constant, and the armature current is assumed to be constant in magnitude but varying in phase (see Figs. 610 and 611). Consequently, the loci of the points *D*, *F*, *J* are concentric circles. Since *AJ* is perpendicular to the current vector, the phase angle, ϕ, is measured between *AJ* and the horizontal diameter C_1C_3. For a non-inductive load, *AJ* coincides with AC_1. The two left-hand quadrants refer to operation as a generator; those to the right correspond to operation as a motor.

For any position of AJ, corresponding to a desired value of ϕ, the torque angle is $\theta = JOA$ and the no-load voltage is $OG = E_0$. The arc pq is drawn from O as center with a radius equal to E_1, obtained from section GH (Fig. 615) of the sectionalized no-load saturation curve. Thus OY is equal to E_1. According to eq. (23), GY is proportional to the field excitation, M_f, which may thus be read off directly from the diagram. The arc mn is drawn from O with a radius equal to the minimum value of E_n (such as $P'P$ in Fig. 615) for which the particular value of x_d, or section GN, Fig. 615, applies. It is not necessary to determine the length OH for each operating point, except to see that OH is greater than OY'. After the limit $OH = OY'$ has been reached, a larger middle circle must be drawn, to correspond to the value of x_d for the straight line DF (Fig. 615), and a new arc pq drawn for the value of $E_2 = OD$.

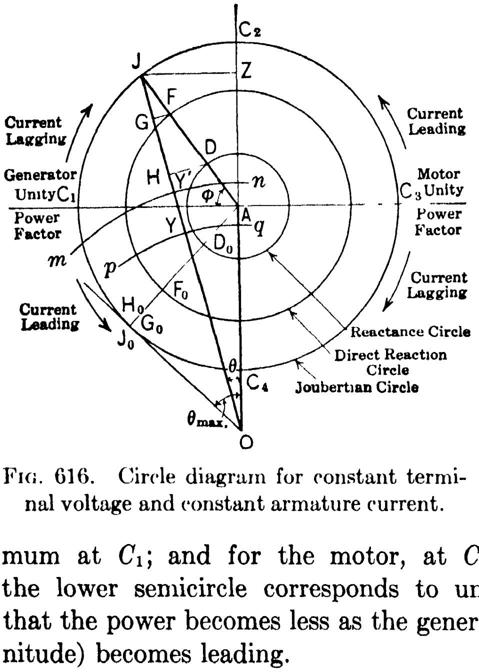

FIG. 616. Circle diagram for constant terminal voltage and constant armature current.

Power, being proportional to the component of the current in phase with E, is represented by JZ, since AJ is proportional to the current vector and leads it by 90 degrees. For the generator, the power reaches a maximum at C_1; and for the motor, at C_3. This does not mean that the lower semicircle corresponds to unstable operation, but simply that the power becomes less as the generator current (of constant magnitude) becomes leading.

At J_0 the torque angle reaches a maximum. This point is of particular interest in that the points G and H then coincide. The direct reaction, HG (Fig. 615), is therefore equal to zero. Thus, by determining maximum θ experimentally, the transverse reaction of the machine may be conveniently computed (§820) and the Joubertian circle drawn.

At zero power factor ($\phi = 90°$), OJ assumes the position OC_2, and the transverse reaction, HD (Fig. 609), is equal to zero; the direct reaction reaches its maximum, so that the middle circle can be drawn. In each case, the proper straight line, representing the saturation curve at that particular E_n, must be used.

834. Locus Diagrams for Constant Armature Current and Constant Excitation. — The diagram shown in Fig. 616 may be adapted to the case in which the armature current and the field excitation remain constant, while the terminal voltage varies with the power factor. As long as the operation is limited to one of the straight lines on the saturation curve (Fig. 615), a constant field excitation means a constant value of E_0; eq. (22). After AJ has been drawn at a desired angle, ϕ, a semicircle is described on JF as the diameter, and a straight edge is laid through the point J in such a position that GO is equal to the desired value of E_0. The length AO gives the corresponding magnitude of the terminal voltage. For each value of ϕ, the position of O is different; and for each point it is necessary to check the value of E_n in order to be sure that the proper straight-line section on the saturation curve has been used.

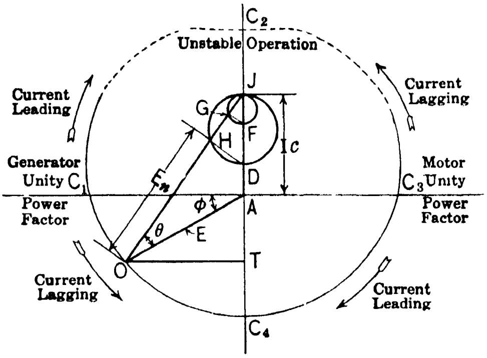

FIG. 617. Locus diagram of terminal voltage when field current and armature current are constant.

A drawback to the foregoing diagram is that it gives no visual locus of E as a function of ϕ. For some purposes it may be preferable to keep the vector AJ stationary and to rotate OA (Fig. 617). The point O then describes a curve known as *Pascal's limaçon.*[4] The corresponding points in Figs. 616 and 617 are denoted by the same letters. The loci of points G and H are circles with JF and JD as diameters. To construct the locus of O, take an arbitrary direction, JO, and draw $GO = E_0$. Do the same for a number of other directions, and connect all the points so obtained by a smooth curve, $C_1C_2C_3C_4$. The power is proportional to $E \cos \phi$, that is, to the distance OT of point O from C_2C_4. This power reaches a maximum where the point O is farthest from C_2C_4. The torque angle, θ, can also be read off directly at O. As in the case of Fig. 616, it is necessary to watch the value of $OH = E_n$, since the diagram is valid on only a part of the saturation curve. After this limit has been reached, it is necessary to change the values of x_d and E_1, and also to use a different E_0 for the same M_f.

---

[4] For the use of the limacon in locus diagrams of synchronous machinery, see Léauté, *Soc. intern. des électr., Bulletin*, vol. 8 (1918), p. 155; Blondel, *Revue générale de l'électr.*, vol. 12 (1922), pp. 203 and 235.

835. The Locus at a Constant Terminal Voltage and Constant Field Current. — In Fig. 609, let the vector OA be constant in magnitude and direction, and let $r = 0$, so that $AB = 0$. If the field current is kept constant, then E_0 will also be constant for any straight part of the saturation curve (Fig. 615). In Fig. 618, an arc of a circle, st, drawn with O as a center, represents the locus of the vector E_0. Let OG be one of the possible positions of the vector E_0, characterized by the torque angle θ, and let C be the foot of the perpendicular from A on OG. We then have (the point F does *not* lie on the arc st):

$$CG/GJ = (x + x_d)/(x_t - x_d) \quad . \quad . \quad (26)$$

Thus, for any CG, the position of the Joubertian point J can be readily found with a pair of proportional dividers. The locus of J is a limaçon (§834). The corresponding armature current is proportional to AJ, and the power is proportional to its projection, JJ'. As in the preceding locus diagrams, it is necessary to check the magnitude of E_n, and to change the values of E_0 and x_d accordingly, for the different straight parts of the saturation curve.

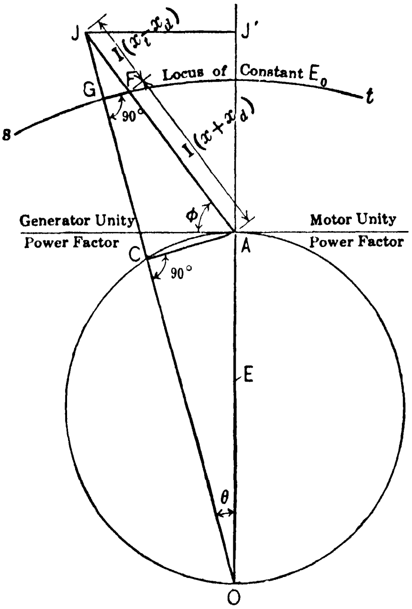

FIG. 618. Locus of armature current when the terminal voltage and the field current are constant.

836. Locus Diagram for Constant Power. — In Fig. 619, the triangle OAJ corresponds to the vector polygon $OABJ$ in Fig. 609, with the ohmic drop neglected, and the current drawn for operation as a motor. Let the machine be operating at a constant terminal voltage and at a constant value of power, the field excitation being variable (V curve, Fig. 624). Then the projection of AJ upon AC, perpendicular to E, remains constant, and the loci of the points J, F, D are straight lines 11′, 22′, 33′, parallel to E.

For any position of J, the armature current (proportional to AJ) and the angles ϕ and θ may be read off directly. Projecting F on OJ gives the no-load voltage, $OG = E_0$. Let a circle of radius E_1 be drawn with O as the center. Then, according to eq. (23), YG is proportional to the field current, and it is therefore possible to plot directly values of armature current against field excitation as abscissas, for a V curve (§844). OH is the net voltage, E_n, and it is necessary to check its values in order to know when to change the values of x_d and E_1 for the next straight section of the saturation curve.

The pull-out point on a V curve corresponds to the minimum excitation possible with the given value of power. This condition is shown in Fig. 619 by the vector AJ''; the excitation $Y''G''$ is a minimum. The stable region lies above J''. Of course, this is not a true minimum unless proper values of x_d and E_1 have been used. The pull-out point often lies on the lower leg of the saturation curve, for which a much larger value of x_d must be used than that assumed in the figure. It is possible to express the length OG analytically, as a function of ϕ or θ, and to find the position of J'' by equating to zero the derivative of the expression for OG. However, it is thought that the same result can be accomplished more readily, after a few trials, by the judgment of the eye.

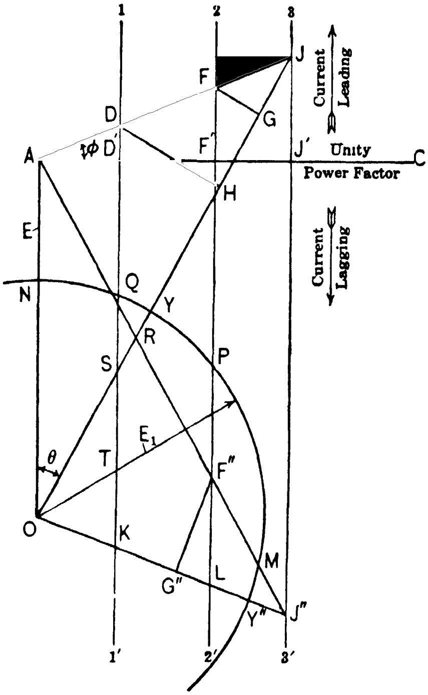

FIG. 619. Locus diagram for a motor operating at a constant terminal voltage and at constant output (V curve).

837. EXPERIMENT 43-C. — Locus Diagrams of a Salient-Pole Synchronous Machine Studied in Connection with Sectionalized Saturation Curve.

— The diagrams are described in §§831 to 836. The purpose of the experiment is to learn their practical use and also to determine how closely they represent the actual behavior of a machine. The experimental determination of the constants of the armature reaction is explained in Chapter XLII. Very accurate load tests should be performed, those quantities being kept constant, in each case, which are assumed to be constant in the corresponding locus diagram. Draw the locus diagram of Figs. 616 to 619. Then compare the experimental results with those derived from the diagram, and discuss the results.

838. Influence of the Armature Resistance. — In the foregoing locus diagrams, the armature resistance has been neglected, because in large and medium-sized machines its effect on voltage relations is too small to warrant the complication of taking it into consideration. Should it be necessary to consider the armature resistance in a special machine, the vector *AB* (Fig. 609) may be retained and the locus diagrams modified accordingly. Thus, in Fig. 616 another concentric circle of radius Ir must be added, and the position of the axis of unity power factor changed accordingly.

In Fig. 619, each of the straight lines 11′, 22′, 33′ becomes an arc of a circle of a rather large radius, with the center on the extension of *AC* to the right. This may be seen from the following simple considerations: Let *AJ* be a current vector, I; its energy component along *AC* is $AJ' = I_e$, and its reactive component is $JJ' = I_r$. Then, for a constant armature output, we have:

$$EI_e - r(I_e^2 + I_r^2) = P = \text{const.} \quad \ldots\ldots \quad (27)$$

or, after a transformation,

$$[(E/2r) - I_e]^2 + I_r^2 = (E^2/4r^2) - (P/r) \quad \ldots \quad (28)$$

This is the equation of a circle whose center is at a distance $E/2r$ to the right of A, and whose radius is equal to $[(E^2/4r^2) - (P/r)]^{0.5}$.

These two examples show how the ohmic resistance of the armature may be taken into account.

839. Correction for Variable Leakage Reactance. — In the foregoing theory and diagrams, the leakage reactance, x, is considered to be constant and independent of the power factor of the load. A little consideration will show, however, that the reactance of a group of armature conductors is smaller when situated midway between the poles than when opposite the center of a pole. In the first case, the leakage lines of force between the tooth tips are entirely in the air; in the second, part of the path is in the pole shoe. Thus, when the whole armature current consists of an interpole component, I_d, only, the leakage flux is smaller than with a current of equal magnitude which consists only of a pole-center component, I_t. Since an actual current can be resolved into these two components, it may be said that the effective leakage reactance, x, is a function of the phase angle of the current, being in general higher at higher values of power factor. In particular, the value of x obtained on short circuit, or at zero power factor, represents a minimum value which is usually exceeded under actual operating conditions.

Let the position of a group of armature conductors with reference to a pole center be determined by an electrical angle, α. Then the variable inductance of this group may be expressed as[5]

$$L_\alpha = L + \Delta L \cos 2\alpha \quad \ldots\ldots\ldots \quad (29)$$

where L is the average value of the leakage inductance and ΔL is the maximum deviation from the average, either way. Under each pole, that is for $\alpha = 0, \pi, 2\pi$, etc., L_α reaches its maximum value of $L + \Delta L$, while its minimum value, $L - \Delta L$, is midway between the poles. For the sake of simplicity, a harmonic variation is assumed between these two limits.

The instantaneous value of the armature current in the same group of conductors is:

$$i_\alpha = I_m \cos(\alpha - \psi) \quad \ldots\ldots\ldots \quad (30)$$

where I_m is the amplitude of the current, and ψ is the internal phase angle, marked in Fig. 609. Multiplying eqs. (29) and (30) term by term, in order to obtain the instantaneous magnetic linkages, we get:

$$L_\alpha i_\alpha = LI_m \cos(\alpha - \psi) + \Delta LI_m \cos 2\alpha \cos(\alpha - \psi) \quad \ldots \quad (31)$$

Using in the last term the familiar trigonometric transformation,

$$\cos a \cos b = 0.5 \cos(a - b) + 0.5 \cos(a + b) \quad \ldots \quad (32)$$

the foregoing expression becomes:

$$L_\alpha i_\alpha = LI_m \cos(\alpha - \psi) + 0.5\Delta LI_m \cos(\alpha + \psi)$$
$$+ 0.5\Delta LI_m \cos(3\alpha - \psi) \quad \ldots \quad (33)$$

The reactive voltage drop in the armature, e_x, is equal to the rate of change of these magnetic linkages with time. The first two terms on the right-hand side give voltages of the fundamental frequency, while the last term, containing 3α, gives a triple harmonic voltage which we shall disregard. Remembering that $\alpha = 2\pi ft$, we may write:

$$d/dt = 2\pi f\, d/d\alpha \quad \ldots\ldots\ldots \quad (34)$$

---

[5] V. Karapetoff, "Variable Armature Leakage Reactance," *Jour. A.I.E.E.*, July, 1926, p. 665.

that is, the derivative of any function with respect to t is equal to $2\pi f$ times the derivative of the same function with respect to α. Therefore,

$$e_x = -2\pi f L I_m \sin(\alpha - \psi) - 0.5 \times 2\pi f \Delta L I_m \sin(\alpha + \psi) \qquad (35)$$

The wave $-\sin(\alpha - \psi)$ leads the current wave (30) by 90 electrical degrees, so that the first term on the right-hand side of eq. (35) represents the ordinary reactive drop corresponding to the *average reactance*,

$$x = 2\pi f L \quad . \quad . \quad . \quad . \quad (36)$$

The wave $-\sin(\alpha + \psi)$ leads the wave $-\sin(\alpha - \psi)$ by an angle 2ψ. Therefore, the last term may be said to represent *the voltage drop due to a supplementary reactance,*

$$\Delta x = 2\pi f \cdot \Delta L \quad . \quad . \quad . \quad (37)$$

This voltage drop leads that due to the average reactance x by the electrical angle 2ψ.

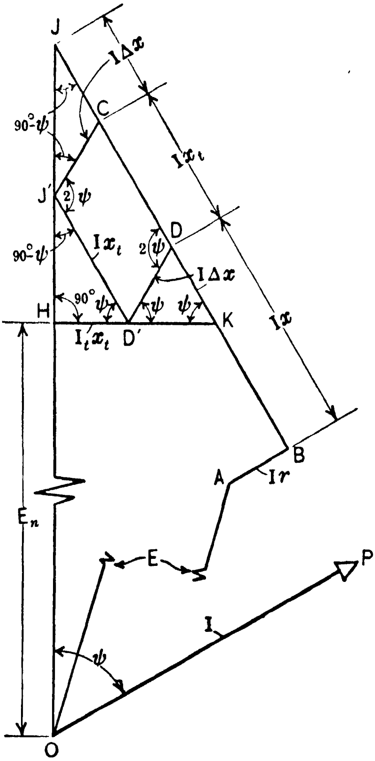

FIG. 620. Generalized Blondel diagram, with variable leakage reactance in the armature.

These relations are shown in Fig. 620 which is an elaboration of Fig. 609. BD represents the drop due to the average reactance x, and DD' is that due to the supplementary reactance Δx, drawn at an angle 2ψ to BD. The new Joubertian point is J', where $D'J'$ is equal to Ix_t, as before. By extending the lines OJ' and BD to their intersection at J, it will be seen that $DJ = Ix_t + I\Delta x$. This follows from the fact that the triangles KDD' and $J'CJ$ are isosceles. Therefore, it is not necessary to locate the point J'; the three vectors, Ix, Ix_t, $I\Delta x$, can be laid off directly from the point B, thus locating the Joubertian point, J. The point K is at a distance $I\Delta x$ from D, and a perpendicular from K on OJ will give the net voltage, $OH = E_n$. The direct armature reaction is taken into consideration in the same manner as before.

On the basis of Fig. 620, the treatment in the whole chapter and the locus diagrams may be corrected accordingly. It is left to the reader to make such changes and to devise experiments from which the minimum and the maximum values of the leakage reactance can be computed.[6]

Circular locus charts similar to those of §807, but adapted to the salient-pole machine, may of course be drawn. The reader is referred to O. G. C. Dahl, "Electric Circuits, Theory and Applications," Chapter XI, McGraw-Hill Book Co.

REFERENCES TO CHAPTERS XLII AND XLIII

1. HOBART and PUNGA, *Trans. A.I.E.E.*, vol. 23 (1904), p. 291, A contribution to the theory of the regulation of alternators.
2. A BLONDEL, *Trans. Int. Elec. Congress*, 1904, Sec. B., p. 635, Methods of calculation of armature reactions (direct and transverse) of alternators.
3. E. ARNOLD, Die Wechselstromtechnik, vol. IV, Chapter II, Julius Springer.
4. V. KARAPETOFF, The Magnetic Circuit, Chapter VIII, McGraw-Hill Book Co.
5. DOHERTY and NICKLE, Synchronous Machines: Parts I and II, *Trans. A.I.E.E.*, vol. 45 (1926), p. 912; III, vol. 46 (1927), p. 1; IV, vol. 47 (1928), p. 457; V, vol. 49 (1930), p. 700.
6. R. W. WIESEMAN, *Trans. A.I.E.E.*, vol. 46 (1927), p. 141, Graphical determination of magnetic fields.
7. W. V. LYON, *Trans. A.I.E.E.*, vol. 37 (1918), p. 1487, The application of harmonic analysis to the theory of synchronous machines.
8. J. F. H. DOUGLAS, *Jour. A.I.E.E.*, February, 1927, p. 109, Transverse reaction in synchronous machines.
9. PARK and ROBERTSON, *Jour. A.I.E.E.*, May, 1928, p. 345, The reactances of synchronous machines.
10. P. L. ALGER, *Trans. A.I.E.E.*, vol. 47 (1928), p. 493, The calculation of armature reaction of synchronous machines.
11. L. A. KILGORE, *Trans. A.I.E.E.*, vol. 50 (1931), p. 1201, Calculation of synchronous machine constants.
12. V. KARAPETOFF, *Trans. A.I.E.E.*, vol. 45 (1926), p. 729, Variable leakage reactance in salient-pole synchronous machines.
13. R. A. SCHAEFER, *Jour. A.I.E.E.*, August, 1927, p. 811, A study of transverse reaction in synchronous machines.
14. L. P. SHILDNECK, *Gen. Elec. Rev.*, November, 1932, p. 560, Synchronous machine reactances.
15. S. H. WRIGHT, *Trans. A.I.E.E.*, vol. 50 (1931), p. 1331, Determination of synchronous machine constants from tests.
16. R. E. DOHERTY, *Trans. A.I.E.E.*, vol. 42 (1923), p. 841, A simplified method of analyzing short-circuit problems.

---

[6] For some special and advanced investigations on the armature reaction and reactance of alternators, see E. Roth, *Revue générale de l'électr.*, vol. 17 (1925), p. 217; A. Blondel, *ibid.*, p. 129; J. Fallou, *ibid.*, vol. 16, p. 491; A. Blondel and F. Carbenay, *ibid.*, vol. 5 (1919), pp. 811 and 843. The last-named article is particularly recommended for a thorough study.

17. B. H. Caldwell, Jr., *Trans. A.I.E.E.*, vol. 56 (1937), pp. 455 and 474, End-winding induction of a synchronous machine.

18. S. B. Crary, *Trans. A.I.E.E.*, vol. 56 (1937), p. 27, The two-reaction theory of synchronous machines.

19. Crary, March, and Shildneck, *Elec. Eng'g*, January, 1934, p. 124, Equivalent reactance of synchronous machines.

CHAPTER XLIV

THE SYNCHRONOUS MOTOR — OPERATING FEATURES

840. In the previous discussion of the synchronous machine (Chapters XIX to XXI and XLI to XLIII) the assumption has been made repeatedly that the armature current might lead or lag the terminal voltage by more than 90 degrees, and that under such circumstances the machine would be operating as a motor. Thus, Fig. 590 shows the generator and motor ranges of armature current; Fig. 611(*a*) and (*b*) is drawn for the motor range, currents leading and lagging; the charts of Figs. 598 and 599 cover the motor operation of the non-salient-pole synchronous machine. To a certain extent the operation of the synchronous motor has been covered by these diagrams. It remains to discuss the performance characteristics and to develop such additional diagrams as may assist in an understanding of these characteristics.

When a machine of the type shown in Figs. 318 and 319 is brought up to synchronous speed, properly excited and connected to a source of a-c power, and when the driving motor (or the prime mover) is disconnected from its source of energy, the machine will operate as a *synchronous motor* and will run at a speed, n, corresponding to the supply frequency, f, and the number of poles, p, or

$$n = \frac{120f}{p} \quad \dots\dots\dots\dots \quad (1)$$

The synchronous machine can now be loaded mechanically, by applying a resisting torque to its shaft, and it will carry load up to a certain limit. When the critical load (which, for a given machine, depends upon the excitation and the terminal voltage) has been exceeded, the motor will " pull out of step " and become stalled.

841. Elementary Explanation of the Action of the Synchronous Motor. — The following explanations are intended to enable the student to understand, in a qualitative way, why a synchronous machine can operate as a motor.

(a) Transformations of electrical into mechanical energy, and vice versa, by means of electromagnetic linkages and motion, are usually reversible. In other words, let a certain mechanical motion, causing a deformation of a magnetic circuit and an induced emf, generate some electrical energy. Then, by applying electrical energy in a similar form to the same machine from an external source, a similar mechanical motion is produced. It is for this reason that all the known types of electromagnetic machines can operate either as generators or as motors.

(b) Consider the action of the armature phase 1 alone (Fig. 319). Let the machine be brought up to synchronous speed by some external means, and let the direction of the armature current, at the instant shown in the figure, be such as to attract the north poles, thus causing the field structure to continue to rotate to the right. Let the attraction predominate during one alternation of the armature current. During the next alternation, the south poles will occupy the same space positions as the north poles did before, but the armature current will also be reversed, so that the predominant mechanical action again will be to the right. By actually drawing the currents in the three phases from instant to instant, it can be shown that the predominant resultant average action consists of a torque to the right.

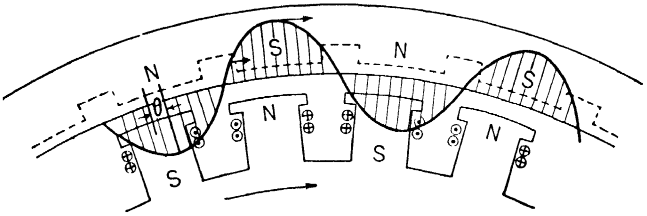

FIG. 621. Schematic representation of rotating armature mmf and revolving field poles of a synchronous motor.

(c) With a two-phase or three-phase winding (Fig. 621), the armature currents produce a revolving magnetic flux represented in Fig. 621 by the sine waves of flux and by the fictitious poles shown by broken lines (see also §813 and Chapter XLVI). With the field poles at a standstill, owing to the inertia of the rotor, such a revolving flux cannot start the machine, because repulsions and attractions follow each other in too rapid succession. However, if the field poles are already revolving synchronously, in the same direction as the rotating flux, a permanently double-excited magnetic circuit will be formed. The field excitation will be lagging in space behind the armature mmf (angle θ in Fig. 621), so as to create a tangential component of the flux, necessary for producing the mechanical torque. As the load increases more and more, the rotor is shifted back farther and farther, until eventually the magnetic flux cannot balance the applied torque, and the machine falls out of step.

With a single-phase stator, the pulsating mmf due to its winding can be replaced by two fictitious component mmf's revolving synchronously in opposite directions (§969). The direct mmf, that is, the one revolving in the same direction as the field poles, gives a constant positive torque as in a polyphase machine. The inverse field produces alternate attractions and repulsions, and its average torque is zero. Thus, the revolving-field explanation is applicable to a single-phase synchronous motor as well.

PERFORMANCE CHARACTERISTICS

842. Consider a polyphase synchronous motor to be brought up to speed and synchronized, and let it be running at no load. During the process of synchronization field current and speed have been so adjusted that the induced emf of the motor is approximately equal and opposite to the line voltage. Figures 622 and 623(*a*) show the vector relations of the applied voltage, V, the excitation voltage,[1] E_v, and the current, I, after the motor has attained equilibrium. The motor has drawn back until (Fig. 622*a*) there is a sufficient phase angle, α, between the motor voltage, E_v, and its initial (180-degree) position along $-V$, so that the machine takes only the small current, I, necessary for overcoming the losses. Now let the field current be somewhat decreased (Fig. 623*b*). The motor adjusts itself to the new conditions by drawing a lagging current from the line, or delivering a leading reactive component to the line (§844), which amounts to the same thing. Such a reactive current causes an armature mmf which strengthens the field, although not quite to the value corresponding to the line voltage. The relations are the same as described in §478 and shown in Fig. 348*a*. The vector sum of the bus-bar voltage, V, and the motor excitation voltage, E_v, gives a resultant, E_z, the synchronous impedance drop in the armature. E_z may be thought of as consisting of an actual voltage drop $(Ir + jIx)$ in the armature, plus the equivalent of an emf, E_a, due to the armature reaction (Figs. 622 and 623*c*). In reality the field mmf and the armature mmf are combined into one mmf which produces the flux, which in turn induces an emf, E_g.

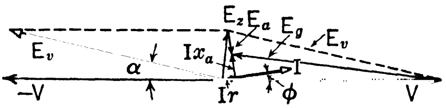

Fig. 622 Synchronous impedance diagram of the synchronous motor at a light load

From Fig. 622 or 623 one may write for the synchronous motor:

$$\dot{V} + \dot{E}_g = \dot{I}z, \quad \text{or} \quad \dot{E}_g = -\dot{V} + \dot{I}z \qquad \ldots \ldots \quad (2)$$

---

[1] Open-circuit or virtual voltage produced by a given field current.

Likewise, in terms of the synchronous impedance, Z_s, and virtual or excitation voltage, $\dot{E}_v$:

$$\dot{V} + E_v = \dot{I}Z_s, \quad \text{or} \quad \dot{E}_v = -\dot{V} + \dot{I}Z_s \quad . \; . \; . \; . \; . \quad (3)$$

At no load, and in a machine with salient poles, the field can be reduced almost or entirely to zero without the motor falling out of step, since the torque required to overcome the losses is very small. The motor remains in synchronism without excitation, when it runs as a "reaction machine," all the flux being due to armature mmf.

If the excitation is increased above normal, the machine will draw a leading reactive current from the line (Fig. 623c). The induced emf corresponding to the field current is E_v. The demagnetizing armature reaction reduces it to the value E_g. Subtracting the impedance drops, Ir and Ix, gives the bus-bar voltage, V. The more the machine is overexcited, the larger leading current it will draw from the line (within the limits of stability).

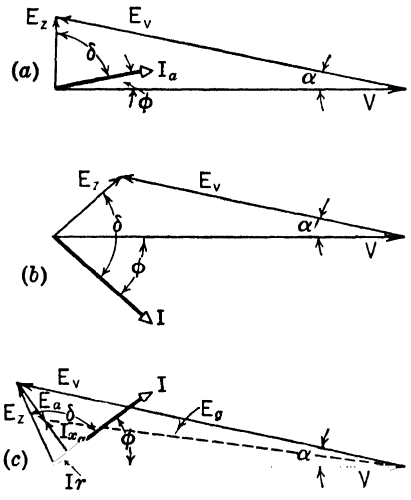

FIG. 623. Simplified vector diagrams of the synchronous motor: (a) normal excitation; (b) motor underexcited; (c) motor overexcited.

Figures 623a, b, and c, all drawn for the same supply voltage, V, and for constant power input to the motor (constant projection of I upon V) show the effect of excitation upon the value and power factor of the armature current (§847).

The lower curve in Fig. 624 represents the relationship between the field current and the armature current at no load. At a, the field excitation is normal and the machine takes only a small in-phase current. As the excitation is increased, the armature current becomes largely leading and increases as indicated by the portion ab of the curve. When the excitation is reduced, the current becomes lagging and follows the branch ac of the curve. Because of their shape, the performance curves shown in Fig. 624 are known as *V curves*. The particular curve just considered is called the no-load V curve.

843. Operation as a Synchronous Condenser. — That property of the synchronous machine which enables it to draw either a leading or a lagging current from the line, at no load, is utilized when it is desired for some purpose to draw such a current, for example, for voltage regulation, for power-factor correction, etc. To accomplish this purpose, a synchronous motor is connected across the line at the desired place and is run idle at the proper excitation. The field current can be controlled either by hand or by an automatic regulator, for a desired performance. For example, if it is desired to keep the line voltage constant, with varying load, the excitation is controlled by a field regulator, such as is described in §452. When the load is light and the voltage tends to increase, the regulator causes the synchronous motor to draw a lagging current, and vice versa.

A synchronous machine used at no load for purposes of regulation is called a *synchronous condenser*. A better name is phase-adjuster, since at times the machine may draw a lagging instead of a leading current.

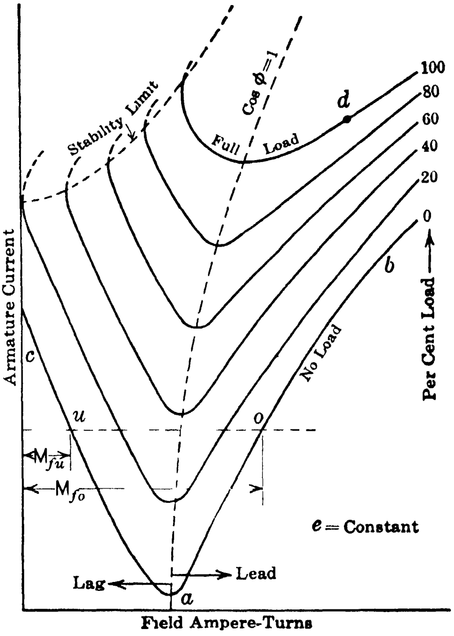

Fig. 624. V curves of the synchronous motor.

844. Theory of the Synchronous Motor V Curve. — The fundamental properties of the V curve may be derived from vector diagrams. Figures 625*a*, *b*, and *c* are Potier diagrams (§799) similar to Figs. 593*c* and 593*d* except that they include the no-load saturation curve and are drawn for a small and constant input which is approximately the condition for a motor running light or at a small but fixed load. Figure 625*a* corresponds to point *a* in Fig. 624, and is for an excitation such that the power factor of the input is fairly high, and leading. Figure 625*b* is for a power factor of about 25 per cent, leading, and is intended to apply at a point on the no-load V curve such as *o*. Figure 625*c* applies at the point *u* where the motor is underexcited and drawing a fairly large current of lagging power factor.

As previously stated, the actual emf, E_g, induced in the motor armature, and expressed by eq. (2), is due to the resultant of the field mmf, M_f, and the armature mmf, M_a, combined vectorially. Although these diagrams apply more strictly to the non-salient-pole machine they are frequently used also for the salient-pole motor. Note that in Figs. 625*b* and 625*c*, with power factors of 25 per cent or below, the armature reaction, M_a, almost directly subtracts from or adds to the field mmf, M_f. It is evident that approximate V curves (for constant input rather than constant output) may be obtained from a series of diagrams such as these. Considerable labor would be required, however, and the curves would not be the true V curves for the reason stated. Consequently, some form of locus diagram or chart is to be preferred, and one of these will be discussed in §§845 to 847.

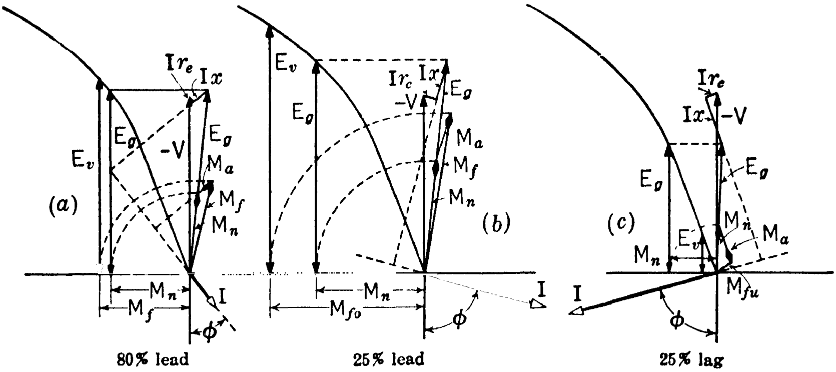

80% lead 25% lead 25% lag

FIG. 625. Potier diagrams of the synchronous motor at light load and varying excitation.

The values of the leakage reactance x, of synchronous impedance Z_s, and of armature reaction M_a, may well be determined by means of the Potier triangle explained in §465.

THE CIRCLE DIAGRAM

845. Proof that the Locus of the Current Vector Is a Circle.[2] — In Fig. 626 the vector diagram of the synchronous motor similar to Fig. 623*b* is drawn, but, for convenience, the vector V is made vertical. It is assumed that the impressed voltage V, the synchronous impedance Z_s, and the excitation voltage E_v are constant in value, but that the angle α varies over a wide range. The locus of the vector E_v is therefore a circle, as shown. In Fig. 626 a line OC is drawn at the angle δ behind OV and of a length such that $OC = V/Z_s$, where δ is the angle by which I lags behind the voltage vector E_z, where $E_z = IZ_s$. Joining the extremity of the vector I with the point C, a triangle, OCI, is formed, which is seen to be similar to the triangle OVP since the angles β are equal, and adjacent sides are respectively proportional. As a result the angle OCI equals α. The side CI must equal E_v/Z_s, being in that proportion to the side VP of the similar triangle. Therefore, for constant E_v, variable α, the point I travels along a circular arc of radius E_v/Z_s, called the excitation circle. For each new value of E_v, obtained by changing the field current, a new circular locus of I results. These excitation circles are identified by either the per cent excitation (E_v/V) which they represent, or by the corresponding value of the field current.

---

[2] A. S. McAllister, *Elec. World*, Aug. 24, 1907.

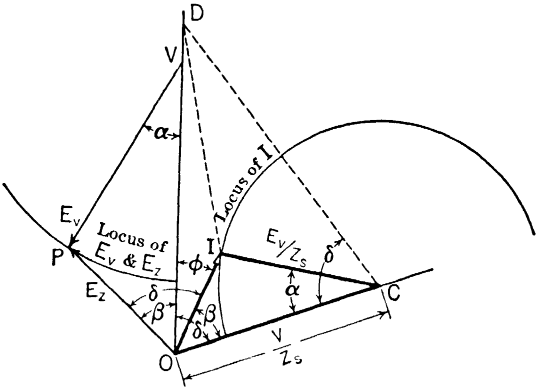

FIG. 626. Constructions showing that the current locus is a circle.

846. Circular Loci for Constant Mechanical Power. — If from the point C (Fig. 626) a line is drawn at the angle δ with OC it will intersect the line OV, extended, at D. Then OCD is an isosceles triangle, and one may write:

$$OD = CD = OC/2\cos\delta = (V/2Z_s)/(r_e/Z_s) = V/2r_e \quad . \quad . \quad (4)$$

Draw a line from D to the extremity of I. Then $OI = I$ at an angle ϕ with V. From the triangle OID

$$\overline{DI}^2 = \overline{OI}^2 + \overline{OD}^2 - 2OI\,OD\cos\phi \quad . \quad . \quad . \quad . \quad (5)$$

Since $OI = I$ and $OD = V/2r_e$, eq. (5) becomes

$$\overline{DI}^2 = I^2 + (V/2r_e)^2 - 2IV\cos\phi/2r_e$$

or

$$DI = \left\{(V/2r_e)^2 - (VI\cos\phi - I^2r_e)/r_e\right\}^{1/2} \quad . \quad . \quad . \quad (6)$$

But $VI \cos \phi - I^2 r_e$ = power input − armature I^2r loss = motor power, P_m, developed by the rotor. Consequently, one may write:

$$DI = \left\{(V/2r_e)^2 - P_m/r_e\right\}^{1/2} \quad . \; . \; . \; . \; . \; . \; . \; . \quad (7)$$

For constant motor power the length DI is constant, and, in consequence, the locus of the extremity of the current vector is a circle with the center at D.

The circle for zero mechanical power ($P_m = 0$) has a radius (eq. 7) $DI = V/2r_e$, and passes through points O and C (Fig. 627a).

Maximum theoretical motor power corresponds to $P_m/r_e = V^2/4r_e$ (eq. 7), or P_m (max) $= V^2/4r_e$, and for this circle the radius is zero.

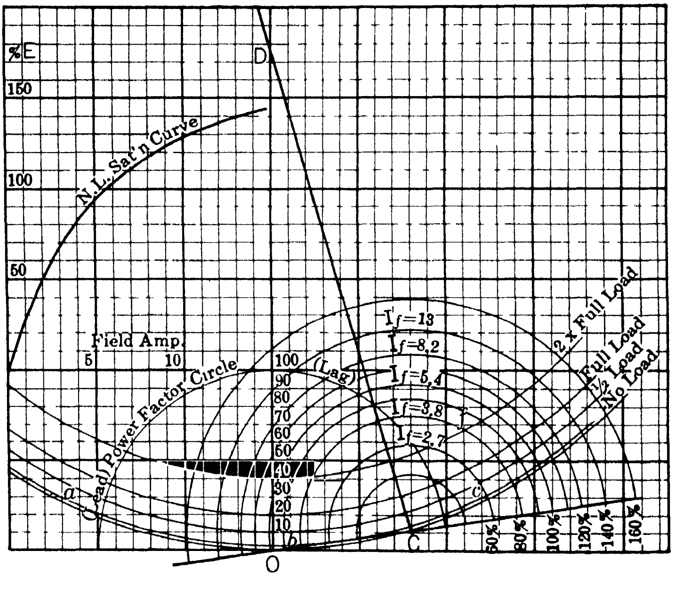

FIG. 627a. The circle diagram of a 40-hp, 240-volt synchronous motor.

Figure 627a is a complete circle diagram drawn for the synchronous machine to which Figs. 325 and 336 apply. The power circle abc is for P_m = rotational loss and so is for the condition of no load. Other power circles are drawn for loads up to 200 per cent of normal, while excitation circles are included for excitations to 160 per cent of normal. By referring to the no-load saturation curve of the machine these values of per cent excitation have been expressed in terms of the field current. A power-factor circle has been included for convenience in taking data from the diagram.

Limits of stability. Inspection of Fig. 627a will show that points on the circle of constant mechanical power beyond the line CD represent unstable operation. If the motor could operate, for example, at the point *f*, any increase in load would cause the motor to increase its torque angle, i.e., pull back in phase. As a result the current vector would travel along the excitation circle towards the right. This would cause it to encounter power circles of greater radius, therefore of less power, and, since the increased load has been met by a decrease in power developed, this process would continue until the motor became stalled.

847. V Curves from the Circle Diagram.—From the points of intersection of a circle of constant power with the several excitation circles the corresponding values and power factors of armature current may be read and the V curve plotted for the load in question. Such values have been taken from Fig. 627*a* and drawn as V curves in Fig. 627*b*. The results must be considered as approximate since the assumptions have been made that Z_s and the rotational loss are constant, neither of which is exact. However, the circle diagram serves to explain in a general way the performance characteristics of the synchronous motor.

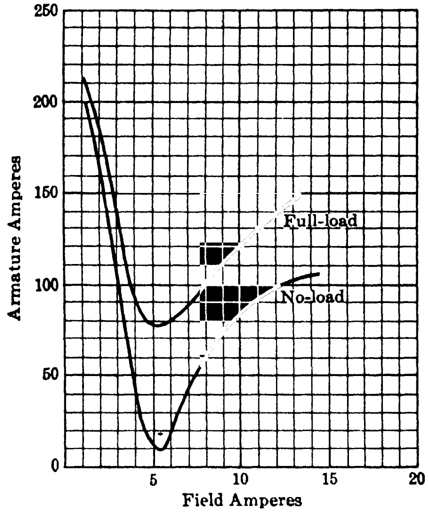

FIG. 627*b*. V curves from the circle diagram of Fig. 627*a*.

More exact results may be obtained from the charts of Figs. 598 and 599, based upon the Potier diagram, and in which the effects of armature reaction are taken into account more accurately than is the case where Z_s is assumed to be constant.

Cross-curves. From V curves and inverted V curves (power factor vs. field current at constant load) certain "cross-curves" may be derived. For instance, a vertical line through the curves of Fig. 624 will give the variation of armature current with load, at constant field current. A similar line through the inverted V curves will give the variation of power factor with load, at constant field. Horizontal lines across Fig. 624 give the adjustment of field current needed to maintain constant kva input at varying load and power factor.

848. EXPERIMENT 44-A.—V Curves of a Synchronous Motor.—The machine should be wired and connected to a source of supply in such a manner as to make it possible to measure the current, the voltage, and the power input. Provision should be made for starting it by one of the methods described in §§857 to 864, and for synchronizing (§§472 to 476). A calibrated d-c generator is a convenient load for the purpose of this experiment. It may be loaded on resistances, or else allowed to " pump " the energy back into a d-c source of supply. Some provision may also be made for measuring the displacement angle (§§851 and 852).

To obtain a V curve (Fig. 624), set the load at a desired value, vary the field current in steps from the highest feasible value to the lowest at which the motor threatens to fall out of step,[3] and at each point read the armature current, the field current, and the kilowatt input. The line voltage and the frequency must be kept constant. Change the load and take a similar set of readings, etc. The displacement angle should be noted at each point, if an arrangement is available for measuring it.

In order to be able to analyze the results obtained, a no-load saturation curve and a zero-power-factor load saturation curve (§466) should be taken. The armature resistance and the no-load losses should also be measured (§§444 to 448). If the efficiency or the losses of the d-c generator are not known, they should be determined by a separate test (Chapter XIII).

Report. (1) Plot the V curves as shown in Fig. 624. (2) On the same curve-sheet, plot curves of power factor (inverted V curves). (3) Plot at least one " cross-curve " of each kind, that is, the relationship between power and armature current at a constant field excitation, and the relationship between power and field current at a constant armature current. (4) Plot values of displacement angle, as a function of the power output and of the field current, and compute the corresponding values of synchronizing torque. (5) Check some of the power readings by adding the motor losses to the output. (6) Check a few points on the V curves, and the displacement angle, using either the Potier diagram (Fig. 625), the circle diagram, or a more accurate theory given in Chapter XLIII.

849. Example of the Synchronous Motor as a Synchronous Condenser. — One of the most important fields of application of the synchronous motor is its use as a synchronous condenser, or phase control device. The no-load V curve shows (Fig. 624) that the synchronous motor, running light and overexcited, as at point *b*, may draw full-load current or more at a very low power factor, leading. This leading current is used to offset the effects of inductive devices such as induction motors and electric furnaces. As a result of this improvement in power factor the total kva load upon the generating station is reduced, generator and line operate at improved efficiency, and the voltage regulation of the transmission line is improved.[4] The following example will illustrate these statements.

---

[3] J. F. H. Douglas, *Trans. A.I.E.E.*, vol. 44 (1925), p. 164.

Case I. A load, consisting of induction motors operating at various fractions of full load, totals 1000 kva at a power factor of 75 per cent (reactive factor of 0.66), lagging. Power is received over a power line which, on the basis of 1000 kva, has a resistance of 4 per cent and an inductive reactance of 8 per cent. The given load over this line will cause a voltage regulation (see §408 on transformer regulation) of

$$\begin{aligned}\%\text{ Reg.} &= 0.75 \times 4 + 0.66 \times 8 + (1/200)(0.75 \times 8 - 0.66 \times 4)^2 \\ &= 8.35 \text{ per cent}\end{aligned}$$

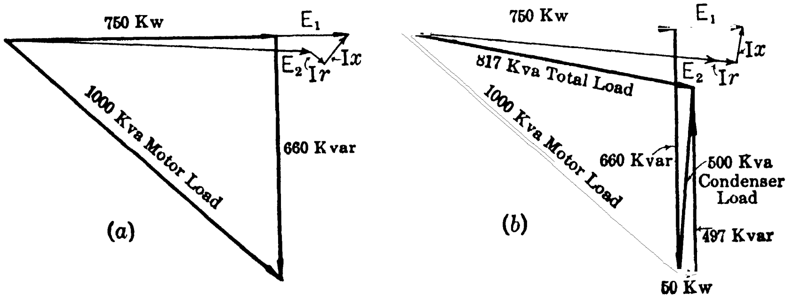

FIG. 628. Examples of synchronous condenser application: (*a*) motor load only, (*b*) motor load plus synchronous condenser.

The power loss in resistance of the line is, of course, 4 per cent of 1000 kw, or 40 kw (5.3 per cent of the 750 kw delivered). The power and voltage conditions are illustrated by Fig. 628*a*.

Case II. To the load of Case I a synchronous motor, rated 500 kva, is added and operated at rated kva, and at a leading power factor of 10 per cent (reactive factor of 0.994). The volt-ampere load due to the synchronous condenser is therefore $500(0.1 + j0.994) = 50 + j497$. The total load is now

$$\text{Load} = 750 + 50 - j(660 - 497) = 800 - j163 = 817 \text{ kva}$$

The new regulation of the transmission line is

$$\begin{aligned}\%\text{ Reg.} &= 0.8 \times 4 + 0.163 \times 8 + (1/200)(0.8 \times 8 - 0.163 \times 4)^2 \\ &= 4.66 \text{ per cent}\end{aligned}$$

The transmission loss is now $(0.817)^2 \times 4 = 2.67$ per cent of 1000 kw or 26.7 kw. The load imposed upon the generating station is now 817 kva, instead of 1000 kva as before. The regulation of the line is improved and the line power loss has been reduced from 40 kw to 26.7 kw, a reduction of 33 per cent. Figure 628*b* shows the vector relations of Case II.

---

[4] J. A. Koontz, Jr., "Voltage Control of Long Lines by Use of Synchronous Condensers," *Trans. A.I.E.E.*, vol. 42 (1923), p. 1054.

850. EXPERIMENT 44-B.—Improved Power Factor and Voltage Regulation by Means of a Synchronous Condenser.—The purpose of the experiment is to study the influence of a synchronous motor, running idle, upon the voltage and power factor of a given load (§849) and upon the voltage characteristics of a given transmission line. The equipment should comprise a source of three-phase power of constant voltage, a transmission line of considerable and known impedance, an adjustable partly inductive load, and a synchronous condenser (motor). Ammeters, voltmeters, and wattmeters (possibly, also, power-factor meters) should be provided. First investigate the influence of the synchronous condenser on power-factor regulation, by using a line of negligible impedance, or by connecting the synchronous condenser directly across the inductive load and the source of power. Read (a) the power input and the power factor of the load; (b) the reactive kva of the condenser, and (c) the power output and the power factor of the generator. Vary the load and the condenser excitation in some systematic way. In view of the presence of both lagging and leading currents, make sure that the sign of the phase angle of the generator load is determined correctly.

Place the synchronous condenser at the receiver end of a line of considerable impedance, in parallel with a load of lagging power factor. Vary the load in some systematic way, and adjust the field current of the condenser for each load, to keep the receiver voltage constant. Take readings with the condenser on and off. If conditions permit connect a voltage regulator in the condenser field (§452) in order to provide an automatic means of keeping the voltage constant.

Report. (1) Plot the data of and draw vector diagrams (§849) for the first part of the experiment in such a way as to bring out clearly the effect of the synchronous condenser upon the power-factor control. Suggest some automatic means of controlling the field current so as to keep the power factor either constant or above an agreed minimum. (2) Plot the data of the second part of the experiment to show the beneficial effect of the synchronous condenser on voltage regulation. (3) On the basis of the data obtained, assume an actual industrial load, estimate the required size of synchronous condenser, and predict what the effect would be in improving the power factor and voltage regulation of the load.

851. The Displacement or Torque Angle.—Consider a synchronous motor running at no load, with the field current adjusted for a minimum of armature current (Fig. 624, point *a*). Neglecting a small impedance drop in the armature, the motor counter emf at each instant is equal and opposite to the line voltage, on the supposition that the wave-form of both voltages is nearly the same (see Fig. 625*a*). Let the armature be Y-connected. Then the voltage between the neutral point and one of the machine terminals reaches its maximum at the instant when the corresponding group of armature conductors is opposite the center of a pole, because at this instant the induced emf is at a maximum. Now let an identical synchronous motor be run from the same source of supply, but heavily loaded (say, at point *d* in Fig. 624). It will be found by experiment that the poles of the second machine, while revolving at the same speed, *lag in space* behind those of the first machine, by an angle known as the *displacement angle*, or the *torque angle*. With a constant field current, the heavier the load the greater the torque angle. When the load is increased beyond a certain limit, the machine falls out of step and stops. The higher the field current, the smaller is the displacement angle for the same load.

The existence of the torque angle is due to the elastic nature of the electromagnetic coupling between the stator and the rotor (Fig. 629) This figure represents schematically an electromagnetic coupling (not a motor). The driving member, AA', is excited with direct current and is being rotated at a certain speed by a prime mover. The driven member, BB', is also excited with direct current and follows AA' at the same speed because of magnetic attraction between the opposite poles. When there is no mechanical load acting on BB', its N' poles are practically opposite the S poles of the driving part, and no tangential force is exerted between the two. When BB' is loaded, its poles lag in space (*not* in time) behind those of AA', and the electrical angle θ, between the centers of the two nearest poles of opposite polarity, is called the torque angle or displacement angle. The flux is crowded between the adjacent edges of the two poles and its tangential component gives rise to an electromagnetic torque. To put it in another way, a distorted magnetic circuit tends to change the relative position of its parts in such a way as to shorten the lines of force, to increase their cross-section, and to bring the permeance of the circuit to a maximum.[5] Thus, the tendency of the poles is to come into opposition, but the applied torque prevents this. The driven member lags behind by an angle θ (in electrical degrees or radians) at which the applied torque is equal and opposite to the torque due to the tangential component of the magnetic flux.

As the load increases, the driven member is shifted farther and farther back until a position is reached (at about 90 electrical degrees) beyond which the electromagnetic torque reaches a maximum and begins to decrease, owing to a much increased reluctance of the magnetic circuit. At this point the coupling is disengaged and the driven part stops. Increasing the current in either member causes the coupling to become stiffer; that is, because of a greater flux, a given angle θ corresponds to a greater torque. Also, pull-out takes place at a higher load.

---

[5] More generally, the inductance tends to a maximum; V. Karapetoff, "The Magnetic Circuit," p. 251, eq. (182). The force F disappears when $dL/ds = 0$.

The conditions in a synchronous motor are more complicated than those described above, partly because of the armature impedance, which affects the value of θ, and partly because of the reactive component of the armature current, which affects the magnitude of the flux itself. Nevertheless, fundamentally and qualitatively, the phenomenon is as described above: The field structure is shifted back with respect to its no-load position, the magnitude of the angle increasing with the load and with decreasing excitation. Vector diagrams which enable one to determine the angle θ from the constants of the machine will be found in §§800 and 827.

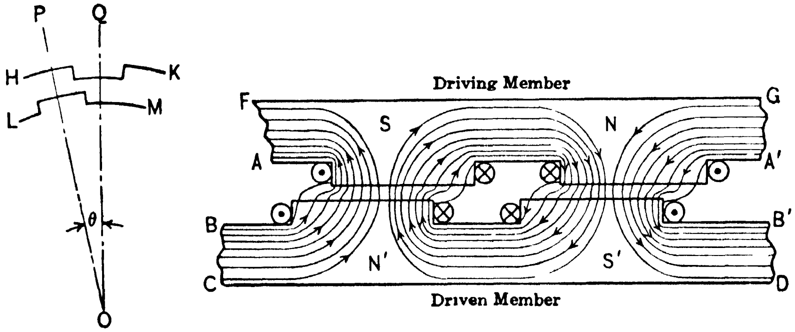

FIG. 629. Torque production and displacement angle in a synchronous machine.

852. Experimental Determination of the Torque Angle. — The torque angle can be measured by means of an arrangement similar to that described in §312. One of the disks is mounted on the shaft of the motor under test, the other on the shaft of a motor running idle. When the motor under test is running idle, the two brushes are set in a position at which the contacts are closed simultaneously, so that there is a noise in the telephone receiver. As the motor under test is loaded, the noise ceases, and it is necessary to shift one of the brushes by a certain angle to cause the noise to be heard again. This angle, reduced to electrical degrees, is equal to the torque (or displacement) angle, θ.

Another method is to observe a point on the revolving part through some stroboscopic arrangement, for example, through a hole or holes near the periphery of a rotating disk driven by an unloaded synchronous motor operating from the same voltage supply, or by viewing a sectored disk (§493) driven by the loaded motor and viewed in the light of a neon tube or arc lamp on the same a-c supply (Fig. 367). At no load, the sectors appear in one position, and, as the load is increased, their apparent position shifts. The value of the torque angle may be read by means of a stationary angular scale.[6]

853. EXPERIMENT 44-C. — Measurement of the Torque Angle in a Synchronous Machine. — Various methods are briefly mentioned in the preceding section, and at least one of them should prove practicable under the given conditions. If not, another and perhaps less accurate, though simpler method, may be devised and tried.

854. Hunting of Synchronous Machines. — The above-described torque angle is of great importance in the study of the so-called hunting of synchronous motors or generators. The electromagnetic coupling shown in Fig. 629 is of the nature of a spring between the revolving field and the revolving mmf of the armature. The rotor with its connected parts possesses a certain moment of inertia, and this inertia, in combination with the electromagnetic spring action, causes the rotor to have a certain definite natural frequency of oscillation. Such oscillations, when they take place, occur during the rotation of the machine, and are manifested in a fluctuating angular velocity and in surges of the line current. As with any mechanical or electrical system possessing a definite natural frequency of oscillation, a comparatively small external cause which happens to be of nearly the same frequency (or of one of its submultiples), is likely to result in quite violent oscillations. Knowing the so-called *synchronizing torque* (that is, the electromagnetic spring action per degree of rotor displacement) and the moment of inertia of the revolving part, one can predict the natural frequency of oscillation of a given machine with sufficient accuracy, using the ordinary pendulum equations of mechanics.[7]

Hunting may also take place at a forced frequency, for example, when a synchronous motor drives a pump or a compressor with a small number of cylinders and insufficient flywheel effect. Knowing the unbalanced periodic torque of the load and the constants of the machine, one can predict periodic variations in the angle θ, and the corresponding pulsations of the line current. If these should prove to be beyond a permissible limit, one or more factors in the whole aggregate can usually be so modified as to obtain a satisfactory operation. The non-uniformity of rotation can be measured with a sensitive recording tachometer, such as a tuning fork tracing a wavy line on a smoked cylinder driven by the motor. Current fluctuations are usually determined with an oscillograph.

---

[6] Other methods for measuring this angle are described in E. Arnold, *Wechselstromtechnik*, vol. 4, p. 642. See also Tolwinski, *Elektrot. und Maschinenbau*, vol. 31 (1913), p. 1004; A. Blondel, *Comptes rendus*, vol. 165 (1917), p. 1092; *ibid.*, vol. 171, p. 329.

[7] For detailed information, see E. Arnold, *Wechselstromtechnik*, vol. 4, Chapters XIV to XVII; V. Karapetoff, "Hunting and Parallel Operation of Synchronous Machines," *Sibley Journal of Engineering*, March, 1920, vol. 34, No. 3, p. 3. See also the references at the end of the next section.

855. Damper Winding. — To reduce the amplitude of hunting, a low-resistance squirrel-cage winding is sometimes placed on the field poles (Fig. 630). As long as the rotor revolves at exactly the same speed as the armature mmf, no currents are induced in this winding. As soon as the rotor begins to lag behind, the armature flux begins to cut it, as in an induction motor (Chapter XXII), tending to pull the rotor back into synchronism. Should the rotor accelerate ahead of the armature mmf, the damper winding makes the machine act as an induction generator, delivering electric power to the line (§899). The torque so developed slows the rotor down to synchronism. The damping winding is also known as the *amortisseur* winding. Any solid metal parts on the poles, such as solid pole shoes or bronze wedges, also act to a smaller degree as a damper winding. Eddy currents induced in these parts act as a load which damps out oscillations of the field structure.

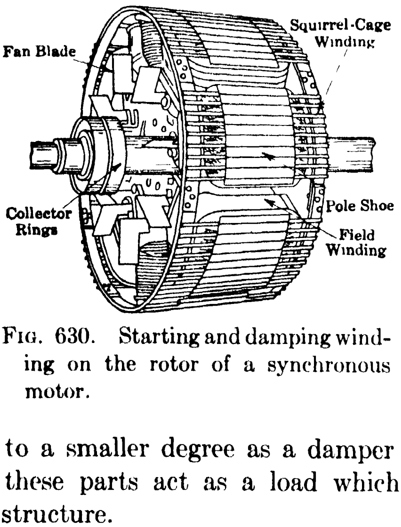

FIG. 630. Starting and damping winding on the rotor of a synchronous motor.

In most modern motors the damper winding is also used for starting (§859). In this case it has to have a higher resistance in order to produce a sufficient starting torque (end of §485). This makes it less effective as an amortisseur winding. When a high starting torque is required, a phase-wound rotor is sometimes used (§861).

The following references to articles on damper windings and on hunting of synchronous machines may be of interest:

Feldman, *Archiv für Elektrot.*, vol. 1 (1912), p. 291.
Boucherot, *La lumière électrique*, vol. 24 (1913), pp. 166, 199, and 230.
Smith, *General Electric Review*, vol. 16 (1913), p. 232.
Rogowski, *Archiv für Elektrot.*, vol. 3 (1914–15), p. 150.
Schmidt, *Elek. Zeits.*, vol. 36 (1915), p. 187.
Knight, *Electrical World*, vol. 70 (1917), p. 517.

Blondel, *Comptes rendus*, vol. 168 (1919), pp. 376, 439, 532, and 587.
de Marchena, *Soc. franç. élect., Bull.*, vol. 9 (1919), p. 17.
Dreyfus, *Archiv fur Elektrot*, vol. 8 (1919–20), p. 132.
Doherty, *General Electric Review*, vol. 23 (1920), p. 125.
Liwschitz, *Archiv fur Elektrot.*, vol. 10 (1921–22), p. 96.
Nishi, *General Electric Review*, vol. 25 (1922), pp. 146–150.
Fischer-Hinnen, *Electrician*, vol. 89 (1922), pp. 185–187.
Bethenod, *Soc. franç. élect., Bull.*, vol. 3 (1923), pp. 29–39.

856. EXPERIMENT 44-D.—Study of Hunting of a Synchronous Motor.—This experiment requires considerable advanced knowledge and special equipment, and is of the nature of a prolonged investigation. The main purposes are as follows: (a) To make clear the physical factors involved; (b) to devise means for a simple and practical measurement of non-uniformity of rotation, current fluctuations, torque angle, synchronizing force, etc.; (c) to apply suitable remedies whereby the performance, which is initially intolerable, may become satisfactory; (d) to connect the observed values with the constants of the machine, and to show that the actual intensity and frequency of hunting could have been predicted from the drawings and specifications of the motor and the load.

STARTING OF SYNCHRONOUS MOTORS

857. A motor, of which one member (say the stator) is excited with alternating current and the other member (the rotor) with direct current, possesses no starting torque because the direction of attraction between the two members is reversed with each alternation of the supply voltage. For a similar reason, the machine has no torque at speeds other than synchronous. It is only when the poles alternate under a given armature coil at the same rate at which the current in the coil itself changes its direction, that a unidirectional tangential effort can exist. For this reason, a synchronous motor has to be brought up to speed either by means of another machine or by being temporarily converted into an induction motor. The following methods of starting are among those mostly used:

(1) When a synchronous motor is a part of a motor-generator set, the other machine being a d-c or induction generator, the generator sometimes can be converted into a motor for starting and synchronizing the synchronous motor. For details see §§476 and 481.

(2) A small induction motor (or an a-c commutator motor) can be used to bring a synchronous motor up to speed, provided that the latter can be synchronized before the load is put on. When direct-connected, the starting induction motor should have a smaller number of poles

than the main motor, in order to be able to bring the latter through synchronous speed (§858).

(3) The field structure of the synchronous motor is provided with a squirrel-cage winding (Fig. 630) of sufficient resistance to give the required starting torque (§855). This is the usual method of starting and it is described in detail in §§859 and 860.

(4) A cylindrical three-phase wound rotor, like that of an induction motor, is used. This winding is closed on resistances for starting, and is excited with direct current in regular operation (§§863 to 865).

In special cases, other methods of starting are possible. For example, if a synchronous motor is supplied with power from a separate generator to which no other load is connected, the generator and motor, with field fully excited, can be started simultaneously. As the generator runs faster and faster the motor also gains in speed, until the normal running speed of both has been attained.

A friction clutch is sometimes interposed between the synchronous motor and its load, to reduce the starting current and the size of the machine. The stator itself may be used as such a clutch.[8] It is then mounted on auxiliary bearings, which are used only during the starting period. A brake is provided, of such proportions as to bring the stator quickly from synchronous speed to rest and to be clamped securely in place. This constitutes the so-called "super-synchronous motor." A high starting torque is obtained by virtue of the fact that no torque whatever is exerted on the load until the stator has come to synchronous speed and full excitation has been applied, thus establishing between the stator and the rotor the same condition electrically and the same relative peripheral speed, that exist when the motor is operating under load. Therefore, the torque that is available as the rotor speeds up and the stator retards, is the maximum load torque, or what is known as the "pull-out" torque.

858. EXPERIMENT 44-E. — Starting a Synchronous Motor by Means of an Auxiliary Induction Motor. — If the auxiliary motor is direct-connected to the synchronous motor, its number of poles should preferably be less than that of the main motor, by at least two, in order that the main motor may be brought to exact synchronism. The auxiliary motor can also be belted or geared to the main motor. The following three ways of synchronizing by this method should be tried:

(1) As in §476, that is, closing the main a-c switch only after the main motor has been brought exactly into synchronism.

(2) The main motor is brought up to a speed above synchronous,

---

[8] *Trans. A.I.E.E.*, vol. 43 (1924), p. 1308.

the field is excited, and then the armature is connected to the a-c line through protective reactances (or resistances) to limit a rush of current. As the field structure slows down, it automatically locks itself in synchronism, and then the protective reactances are short-circuited.

(3) The main motor is brought to a speed a few per cent below synchronism, is excited, and is connected to the a-c line. It will then pull itself into synchronism, provided that its rotor has suitable solid metal parts or a squirrel-cage winding in which secondary currents, sufficient to produce a pull-in torque, may be induced. It may be necessary to use protective reactances or resistances, as in the preceding case; or else, auto-transformers can be used and the motor first connected to a lower voltage (Fig. 359).

Report. Describe in detail the three ways of bringing the motor into synchronism, give the exact connections used, and the advantages and disadvantages of each method. Consider theoretically a large industrial motor, say of the order of 2000 kw, 6600 volts, and lay out a diagram of connections in detail, for starting and for running, with all the required measuring instruments and transformers, protective apparatus, etc.

859. Starting with a Squirrel-Cage Winding. — A squirrel-cage winding (Fig. 630) placed on the pole pieces can be so designed as to give a high starting torque. In fact, motors are built which will start at several times full-load torque, although, of course, with a rather large starting kva. Berkshire and Winne[9] show curves of torque and kva demand during a-c starting of a large synchronous motor, in which the initial torque is nearly 3.4 × full-load torque, produced at 5.8 × normal kva input. The torque at 95 per cent of synchronous speed, called the " pull-in " torque, is 1.1× full-load torque, at a demand of 1.75 × normal kva. One of the usual diagrams of connections, suitable for a large motor, is shown in Fig. 631. The field winding is usually short-circuited or closed through a low resistance when the motor is started. This prevents a high alternating voltage from being induced in it by the armature flux. Moreover, this winding then also contributes somewhat to the starting torque. If there should be a tendency for the rotor to " stick " at half speed, the field winding should be left open, and provision made to take care of the dangerous high voltage which in this case will be induced when the rotor is starting.

Assuming the field to be short-circuited and all the switches open, the procedure in starting is as follows: (a) Close the transformer switch, *A*, thus energizing the auto-transformers. (b) Close the starting switch,

---

[9] Berkshire and Winne, " Synchronous Motors for Driving Steel Rolling Mills," *Trans. A.I.E.E.*, vol 47 (1928), p. 237.

B, thus allowing the motor to start at a reduced voltage. (c) When a nearly synchronous speed has been reached, excite the field with direct current. (d) Open the switch *B*, and immediately close the switch *C*, applying the full voltage to the armature. (e) Adjust the field current to a desired value.

It is of importance to wait until the motor has reached its maximum speed as an induction motor, before exciting the field. If the excitation is applied too soon, the machine will usually fail to pull into step. The field ammeter gives a good indication of the speed and should be watched by the operator. When the machine approaches full speed the needle oscillates slowly owing, when the field is short-circuited or closed through a resistance, to currents of "slip frequency" induced in the field winding. Its rate of oscillation decreases as the speed rises, and falls to zero when the motor reaches synchronous speed. Should it be found impossible to pull into step by following the foregoing procedure, the motor should be transferred to full voltage by closing the running switch, before the field is excited.

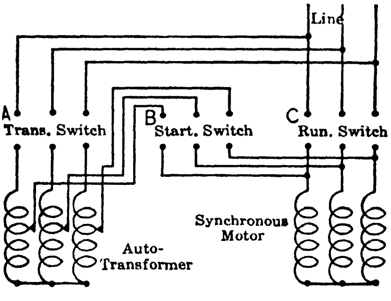

Fig. 631. Connections of switches and auto-transformers for a self-starting synchronous motor.

The switches, *A*, *B*, *C*, are shown as separate switches; with a large high-tension motor this would be the usual procedure. With a small motor, the switch *B* may be omitted altogether, and the switches *A* and *C* combined into a double-throw switch. The auto-transformers can be used in a V connection, instead of Y (Fig. 359). In place of auto-transformers, protective reactances or resistances may be used for starting. Even large motors can be directly connected to the line if the power supply is adequate so that the rush of current is not objectionable. A clutch is sometimes used between the motor and the load, to facilitate starting.

860. EXPERIMENT 44-F.—Exercises in Starting a Squirrel-Cage Synchronous Motor.—The procedure is described in the preceding section; the purpose of the experiment is to acquire facility in starting, and to investigate the influence of the various factors. Among these factors the following may be mentioned: The characteristics of the squirrel-cage winding; the maximum value of the torque at which the motor will start; the magnitude of the starting voltage; the value of the field current at the first instant; the moment at which it should be applied; etc. The influence of each factor should be investigated and analyzed separately, and definite conclusions reached wherever possible. For references to the theory see §862.

861. Additional Methods of Starting Large Synchronous Motors.—In the Korndorfer method of starting, as the motor picks up in speed, the three auto-transformers of Fig. 631 are separated at the common neutral, thereafter constituting three reactors in series with the stator of the synchronous motor. Later the running switch, *C*, short-circuits these reactors and impresses full voltage on the synchronous motor windings. In a modification of this method[10] additional reactors are placed in parallel with the auto-transformer reactors to furnish an intermediate step in the starting of very large motors.

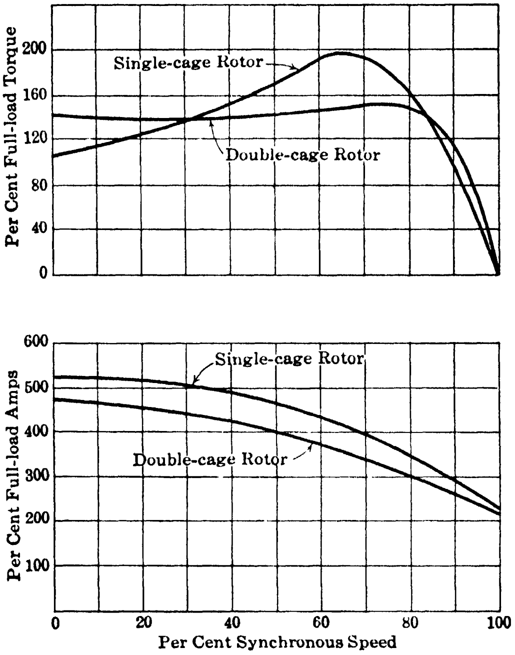

FIG. 632. Starting curves of a 600-hp synchronous motor (C. E. Buchan).

In the so-called "simplex" synchronous motor[11] the starting winding, instead of being a squirrel-cage winding as in Fig. 630, is a three-phase winding placed in slots in the pole faces and brought out, through slip-rings, to an adjustable resistance. By this means the starting torque and power factor may be materially increased, and the current demand reduced, as in wound-rotor the induction motor (§487).

In a third method used for starting large synchronous motors two three-phase windings are placed on the stator. To limit the current in starting only one winding is used; to improve efficiency and pull-out torque, the two sets of windings are placed in parallel after the motor reaches speed.[12] To improve starting conditions with a squirrel-cage starting winding (Fig. 630) double squirrel-cage windings (Fig. 361) of suitable design are used. Figure 632 shows the starting torque and current curves of a synchronous motor for the conditions of single-cage and double-cage starting windings.[13]

---

[10] Berkshire and Winne, "Synchronous Motors for Driving Steel Rolling Mills," *Trans. A.I.E.E.*, vol. 47 (1928), p. 237.

[11] M. A. Hyde, "Simplex Synchronous Motor Has Wound-Rotor Starting Characteristics," *Elec. Jour.*, February, 1931, p. 77.

[12] McLenegan and Ferriss, "Multiple-Winding Starting Method for Synchronous Motors," *Gen. Elec. Rev.*, October, 1930, p. 574.

862. Theory of Starting and Pulling into Step. — In a synchronous motor with salient poles and a squirrel-cage winding, a quantitative theory of the phenomena which occur during the starting period, and especially during the period of pulling into synchronism, is rather complex. The following literature references may help the reader who is interested in the subject:

Dreyfus, *Archiv für Elektrot.*, vol. 9 (1920), p. 35.
Shirley, *General Electric Review*, vol. 24 (1921), p. 873.
Böhm, *Elek. Zeits.*, vol. 43 (1922), p. 426.
Weiss, *Elektrot. und Maschinenbau*, vol. 40 (1922), p. 497.
Fraenkel, *BBC Mitteil.*, February, 1923, vol. 10.
Shirley, *General Electric Review*, vol. 26 (1923), p. 412.
Fraenkel, *Elektrot. und Maschinenbau*, vol. 41 (1923), pp. 377 and 393.
Smith, *Journal A.I.E.E.*, vol. 42 (1923), p. 901.
Doswald, *BBC Mitteil.*, vol. 10 (1923), pp. 139 and 167.
Cotton, *Electrician*, Feb. 22, 1924, vol. 92.
James and Graybill, *Electric Journal*, vol. 21 (1924), p. 335.
Verbèke, *Révue générale de l'électr.*, vol. 17 (1925), p. 190.
Putnam, *Trans. A.I.E.E.*, vol. 46 (1927), p. 39.
Edgerton and Fourmarier, *Elec. Eng'g*, June, 1931.
Edgerton *et al.*, *Elec. Eng'g*, October, 1933.

863. Induction-Start Synchronous Motor. — The method of starting described in §859 gives a sufficient starting torque for many applications. However, the advantages of the synchronous motor, such as a constant speed and a favorable power factor, make its application desirable also where an extremely high starting torque is indispensable and is beyond the possibilities of a squirrel-cage winding. As is explained in §485, a high-resistance rotor is required for a high starting torque, and this resistance must be gradually reduced, to keep the torque at a maximum up to a nearly synchronous speed. Thus, a three-phase winding on a cylindrical rotor with non-salient poles (Fig. 633) offers the desired solution for a high starting torque. Moreover, the same winding can later be excited with direct current and used as a regular field winding in synchronous operation. Such a motor is variously called induction-start synchronous motor, synchronous induction motor, synchronized asynchronous motor, etc.

---

[13] C. E. Buchan, " Selection of Motors for Difficult Starting," *Elec. World*, July 19, 1930.

A suitable diagram of connections is shown in Fig. 633. At the start, the short-circuiting bar, *S*, is in its extreme right position, all the starting resistance being " in." The field circuit of the exciter is broken at *f*, the resistance *R* is cut out, and the low-resistance armature of the exciter is in series with phase 1 of the rotor. When the main circuit breaker, *C.B.*, is closed, the motor starts at a high torque; the starting bar, *S*, is then moved to the left until all the resistance has been cut out and the motor runs at a speed a little below synchronous. In the running position of *S*, it closes the circuit between *f* and *a*, thus causing the exciter to generate direct current. This current, *I*, flows through phase 1, and then is divided into two equal parts which return to the point *a* through phases 2 and 3 in parallel. The motor pulls itself into synchronism and continues to operate as an ordinary synchronous machine.

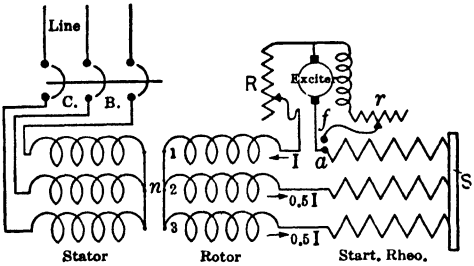

Fig. 633. Starting connections for a synchronous motor having a three-phase field winding.

The starting control is shown in the form of the bar *S* for the sake of simplicity. In reality, it may be of any of the types shown in Chapters XXV, LIV, and LV, depending upon the size of the motor and the automatic features desired. The field winding has to be of low resistance in order to bring the machine almost to the synchronous speed during the starting period. Consequently, it is necessary to have a low-voltage exciter, much lower than the standard d-c voltage of 125 v. This requirement introduces some difficulties, such as high currents and extra-low-resistance brushes.

SELF-EXCITED SYNCHRONOUS INDUCTION MOTOR (FYNN-WEICHSEL)

864. In small sizes, an objection to the usual synchronous motor is that it requires a d-c source of excitation. In the Fynn-Weichsel motor[14] (Figs. 634 to 636), a commutator and brushes are an integral part of the machine itself, and direct current is furnished to the field automatically the instant the machine is in synchronism. In starting, the machine has essentially the characteristics of a slip-ring induction motor (§485) and can be started with a considerable load. The machine also automatically becomes an induction motor and continues to operate at a moderate slip when the pull-out torque value for synchronous operation has been exceeded. The two operating ranges are shown in Fig. 636.

---

[14] For a detailed description and theory of the motor, see Val. A. Fynn, *Trans. A.I.E.E.*, vol. 43 (1924), p. 660; also *Journal A.I.E.E.*, vol. 44 (1925), p. 164; H. Weichsel, *ibid.*, p. 356.

The rotor of the machine is provided with two windings (Fig. 634): A three-phase winding, 2′, 2″, 2‴, connected to the slip-rings 16, 17, 18; and a winding 11, similar to that of a d-c armature and provided with a commutator (not shown) and the brushes 7, 8. The stator, which in this motor is the secondary member, carries two windings, 23, 24, displaced by 90 electrical degrees, and forming a two-phase secondary. The winding 23 is connected to the brushes 7, 8, through the adjustable resistance 26; the winding 24 is closed over the adjustable resistance 27. The winding 23 usually covers two-thirds and the winding 24 one-third of the available space. The brush axis is displaced from the axis of the winding 23 by less than 90 electrical degrees, usually by some 20 to 30 degrees.

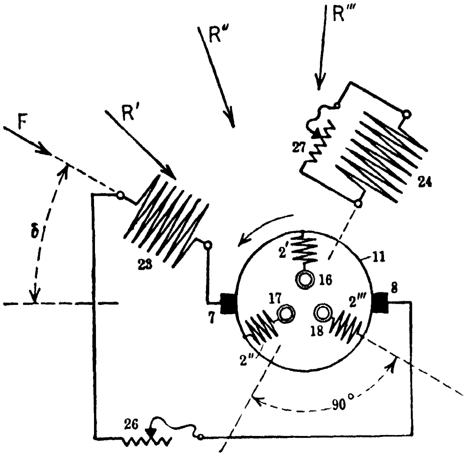

FIG. 634. Internal connections of the Fynn-Weichsel motor.

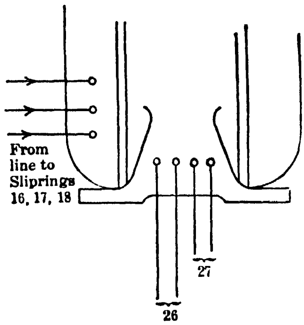

FIG. 635. External connections of the Fynn-Weichsel motor.

In order to start the motor, the resistances 26, 27 are set to a value corresponding to the torque required, and the primary is connected to the supply by way of the slip-rings 16, 17, 18. Either the full line voltage or a fraction thereof is used for starting, according to the size of the machine. As the motor speeds up, the resistances 26, 27 are diminished in one or more steps. The machine synchronizes automatically, provided that the torque required when near synchronism is not in excess of the maximum synchronous torque. When running synchronously, the power factor of the motor can be adjusted by changing the value of the resistance 26. The overload capacity, however, also changes when 26 is changed. Both the power factor and the overload capacity can also be changed by displacing the brushes 7, 8. The value of the synchronizing torque also depends on the value of 26 and on the magnitude of the angle δ.

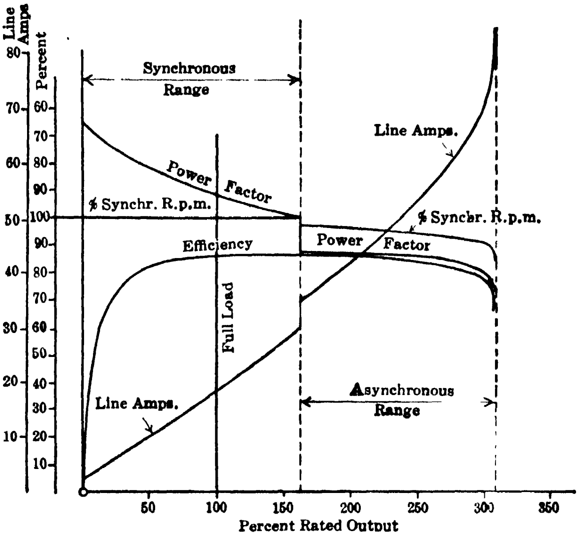

Fig. 636. Performance curves of a Fynn-Weichsel motor.

For a further description of the motor and explanation of its theory the attention of the reader is directed to the literature references cited above or those at the end of the chapter.

865. EXPERIMENT 44-G. — Study of the Fynn-Weichsel Self-Excited Synchronous Induction Motor. — The purpose of the following tests is to make clear to the student the various points in the theory of the machine and also to show how its operating characteristics can be obtained. The connections of the machine are shown in Figs. 634 and 635, and sample performance curves are given in Fig. 636.

A. Starting Torque.

1. A speed-torque curve with windings 23 and 24 closed over starting resistances 26, 27, but with the exclusion of the commuted winding 11 from the circuit of 23.
2. A speed-torque curve with the motor connected as shown in Fig. 634. The last part of this curve will be very difficult if not impossible

to take, because near synchronism the rapidly changing synchronizing torque is superimposed on the rapidly dropping induction-motor torque. The first part, when compared with the first part of the curve of test 1, will show to what extent the connections used in the machine interfere with the starting characteristics of a standard induction motor.

B. Synchronizing Torque.

3. For different values of the angle δ which determines the position of the brushes, and for the same maximum ampere-turns in 23, ascertain the maximum load which the motor can bring to synchronism.

4. For a given value of δ and for different maximum ampere-turns in 23, ascertain the maximum load which the motor can bring to synchronism. The load may be a suitably calibrated d-c generator.

C. Compounding or Power-Factor Regulation (Normal Operation).

5. Run the machine connected as shown in Fig. 634, with various values of δ and with the same ampere-turns in 23 as, say, at no load. Note variations in the exciting voltage, exciting current, primary current, and watts, with varying load.

6. Repeat for a constant value of δ and changing values of the resistance 26.

D. Asynchronous Overload.

7. Determine the asynchronous overload capacity for varying values of δ, and for several values of the resistance 26 for each value of δ. It will be found that the asynchronous overload capacity increases as the negative wave of the synchronizing torque decreases. The smaller δ the smaller this negative wave for otherwise equal conditions. For a given value of δ, the asynchronous overload capacity increases with decreasing ampere-turns in F.

It will be found that the angular velocity of the rotor is not constant when operating asynchronously under overload conditions; the motor does not run smoothly and appears to hunt. This phenomenon is the more pronounced the greater the negative wave of the synchronizing torque, and is not absent when the synchronizing torque is unidirectional. It may be clearly shown, and perhaps even measured, by a stroboscopic method.

REFERENCES

1. A. S. MCALLISTER, *Elec. World*, Aug. 24, 1907, Circular current loci of the synchronous motor.

2. W. T. BERKSHIRE, *Gen. Elec. Rev.*, February, 1920, Synchronous motors.

3. J. K. KOSTKO, *Trans. A.I.E.E.*, vol. 42 (1923), p. 1138, Polyphase reaction synchronous motors.

4. Douglas, Engeset and Jones, *Trans. A.I.E.E.*, vol. 44 (1925), p. 164, Complete synchronous motor excitation characteristics.

5. H. Weichsel, *Trans. A.I.E.E.*, vol. 44 (1925), p. 7, A new alternating-current general-purpose motor.

6. V. A. Fynn, *Trans. A.I.E.E.*, vol. 44 (1925), p. 64, Another new self-excited synchronous induction motor.

7. R. W. Wieseman, *Trans. A.I.E.E.*, vol. 44 (1925), p. 436, A two-speed salient-pole synchronous motor.

8. J. K. Kostko, *Trans. A.I.E.E.*, vol. 44 (1925), p. 447, Self-excited synchronous motors.

9. P. C. Jones, *Elec. Jour.*, March, 1926, Correction of power factor by the use of synchronous motors.

10. H. V. Putnam, *Trans. A.I.E.E.*, vol. 46 (1927), p. 39, Starting performance of synchronous motors.

11. C. E. Buchan, *Elec. World*, July 19, 1930, Selection of motors for difficult starting, heavy duty, fluctuating load.

12. McLenegan and Ferriss, *Gen. Elec. Rev.*, October, 1930, Multiple-winding starting method for synchronous motors.

13. M. A. Hyde, *Elec. Jour.*, February, 1931, Simplex synchronous motor has wound-rotor starting characteristics.

14. Edgerton and Fourmarier, *Elec. Eng'g*, June, 1931, Synchronizing salient-pole motors.

15. McLenegan and Ferriss, *Elec. Eng'g*, October, 1931, Synchronous motors for special loads.

16. C. C. Shutt, *Elec. Jour.*, August, 1932, High-torque synchronous motors.

17. Bordeau and Early, *Elec. Eng'g*, December, 1932, Synchronous motors in rolling mill service.

18. P. H. Trickey, *Elec. Jour.*, April, 1933, Small synchronous motors without exciters.

19. M. N. Halberg, *Gen. Elec. Rev.*, May, 1933, New developments in synchronous motor control.

20. C. C. Shutt, *Elec. Jour.*, August, 1933, Starting synchronous motors.

21. Edgerton, Germehausen, Brown, and Hamilton, *Elec. Eng'g*, October, 1933, Pulling-into-step equations solved.

22. R. H. Wright, *Elec. Jour.*, September, 1938, p. 336, Synchronous motors for main roll drives.

23. F. K. Brainard, *Elec. Rev.*, June, 1938, p. 5, Flywheels for synchronous motors.

CHAPTER XLV

THE SYNCHRONOUS CONVERTER — OPERATING FEATURES

866. Most modern installations of rectifying equipment are in the form of the Rectox, or copper-oxide rectifier, the Ignitron (Chapter LIX), the mercury-arc rectifier (Chapter LVI), or some form of vacuum-tube rectifier (Chapter LIX). However, the synchronous converter is still in service in a great many installations, and new units are being manufactured for use in railway substations or in electrochemical plants. It seems desirable, therefore, to treat the important features of the synchronous converter in this text, and to suggest experiments designed to emphasize its principal characteristics.

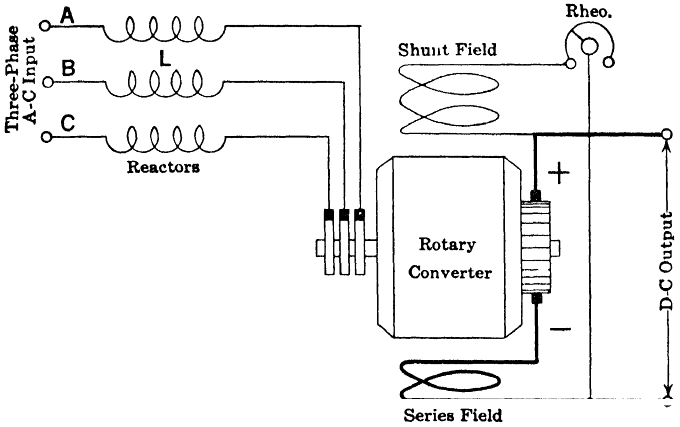

FIG. 637. Circuit diagram of a compound-wound three-phase synchronous converter.

867. General Description. — A two-pole three-phase synchronous converter is shown schematically in Figs. 637 and 639; a single-phase armature is shown schematically in Fig. 638. In its general construction, the synchronous converter resembles a d-c machine (Chapter X), except that the armature winding is connected not only to a commutator on the d-c side, but also to slip-rings on the a-c side. Self-excitation is furnished by the shunt field winding, and there may also be an additional series winding. Commutating poles are often provided to improve commutation. The inductance coils, *L* (Fig. 637), shown between the a-c terminals and the slip-rings, are not an indispensable part of the machine, but are sometimes used in connection with the series winding for voltage regulation (§878).

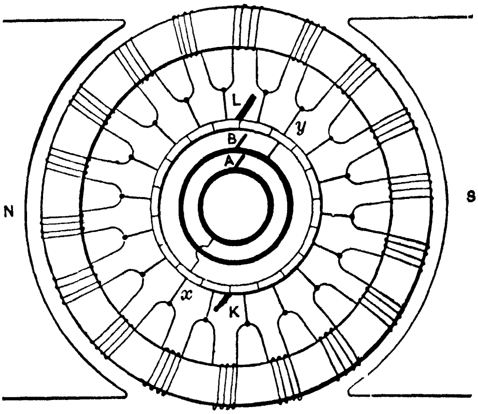

Fig. 638. Armature connections in a single-phase converter.

A three-ring (three-phase) synchronous converter is obtained by mounting three slip-rings on the shaft and connecting them to three points on the armature, 120 electrical degrees apart (Fig. 639).

The armature may be tapped at four equidistant places and connected to four slip-rings, giving a four-ring converter, but in commercial work six-ring converters are most commonly used in order to increase the capacity of the machine by reducing armature heating (§882). For special or experimental purposes, other combinations of taps and slip-rings are also employed.

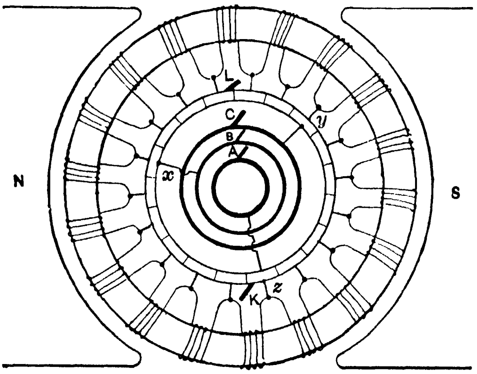

Fig. 639. Armature connections in a three-phase (three-ring) converter.

A completely equipped synchronous converter, in addition to the above parts, may also have some or all of the following:

(a) Starting motor.
(b) Speed-limit device.
(c) Brush-lifting device.
(d) Voltage booster.

A rotary converter may be operated in different ways, such as:

(a) Running as a synchronous motor and delivering direct current (§876) to a load (*synchronous converter*).

(b) Running as a d-c motor and delivering single-phase or polyphase currents (§871) to a load (*inverted converter*).

(c) Driven by a prime mover, and delivering simultaneously direct and alternating currents to two different load circuits (*double-current generator*).

(d) Taking in direct and alternating currents simultaneously and delivering mechanical power on the shaft (*double-current motor*).

868. Induced Voltages. — Since both the d-c and the a-c voltages of a rotary converter are produced in the same armature winding, rotating through the same field, it follows that the ratio of the a-c to the d-c voltages induced in the armature is independent of variations in speed or field current provided that the wave-form of the flux distribution remains unchanged.

In order to determine the numerical value of this ratio, consider the armature of a single-phase (two-ring) converter (Fig. 638) at an instant when the a-c brushes, A and B, are electrically in coincidence with the d-c brushes, K and L (taps x and y along the d-c brush axis). At such instants, the induced a-c voltage is equal to the d-c voltage. If the d-c brushes are midway between the poles, the induced a-c voltage is now a maximum, so that with a-c taps at 180 electrical degrees the (maximum) amplitude of the induced a-c voltage is equal to the induced d-c voltage.

As the armature revolves, the d-c voltage remains the same, but the voltage between the taps x and y is alternating. Its effective value depends upon the wave-form, which is determined by the flux distribution and the character of the winding. If the induced emf is nearly sinusoidal, as it usually is, the ratio between the amplitude and the effective value is practically equal to $\sqrt{2}$, so that the ratio of the d-c voltage to the effective value of a-c voltage is also nearly equal to $\sqrt{2} = 1.414$.

Now let two a-c taps be taken at an electrical angle of α degrees, instead of 180 degrees. It can be then shown that:

$$E_\alpha = (E_{dc}/\sqrt{2}) \sin 0.5\alpha \quad . \quad . \quad . \quad . \quad . \quad . \quad . \quad . \qquad (1)$$

where E_α is the effective value of the a-c voltage (assumed to be sinusoidal) and E_{dc} is the magnitude of the d-c voltage. For a three-phase converter, $\alpha = 120°$, and $E_{120} = (E_{dc}/\sqrt{2}) \sin 60° = 0.612E_{dc}$. For a two-phase converter,[1] $\alpha = 90°$ and $E_{90} = 0.5E_{dc}$. In general, for an n-ring converter $\alpha = 2\pi/n$ and (see Fig. 640)

$$E_n = (E_{dc}/\sqrt{2}) \sin \pi/n \quad . \quad . \quad . \quad . \quad . \quad . \quad . \qquad (1a)$$

A more rigid derivation of eq. (1*a*) may be made by writing the fundamental equations for induced emf in the rotary converter considered, first, as a d-c generator, and then as an a-c machine, since it is both.

---

[1] See E. Arnold, *Wechselstromtechnik*, vol. 4, p. 704; R. R. Lawrence, "Principles of A-C Machinery," p. 421; V. Karapetoff, "The Magnetic Circuit," p. 78.

From eq. (1), Chapter X, the equation of d-c emf is

$$E_{dc} = (p/a)(\text{rpm}/60)Z\phi \times 10^{-2} \text{ volt} \quad . \; . \; . \; . \quad (2)$$

where p = number of poles.
a = number of parallel paths to direct current.
Z = total conductors on the armature.
ϕ = flux per pole entering the armature, in megalines.

Similarly the equation for the alternating emf induced between adjacent taps is (eq. 9, Chapter XIX):

$$E_{ac} = 4.44k_b k_p N f \phi \times 10^{-2} \quad . \; . \; . \; . \; . \; . \; . \; . \quad (2a)$$

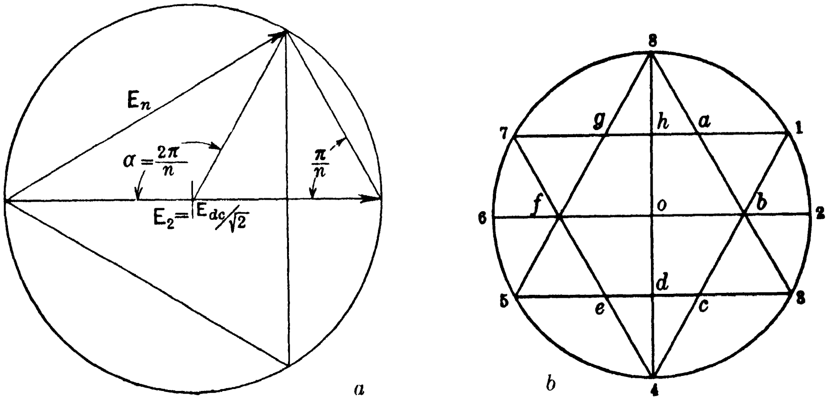

FIG. 640. (a) Voltage vectors in an n-ring converter; (b) vectors of no-load voltage in a special 8-ring converter.

where N = turns in series between adjacent taps = Z/pn.
n = number of rings.
f = $p \times \text{rpm}/120$.
k_p = pitch factor = 1 for a winding suitable for d-c current, since the coil throw must be practically equal to the pole pitch (§811).
k_b = breadth factor which, for the closed circuit winding, is the ratio of the chord, E_n in Fig. 640a, to the included arc, or

$$k_b = (n/\pi) \sin \pi/n \quad . \; . \; . \; . \; . \; . \; . \; . \; . \quad (3)$$

Substituting these values in eq. (2a), it becomes:

$$E_{ac} = (2.22/\pi) \sin \pi/nZ \, (\text{rpm}/60)\phi \times 10^{-2} \quad . \; . \; . \; . \quad (4)$$

so that from eqs. (2) and (4) the ratio of induced a-c voltage to d-c voltage is:

$$E_{ac}/E_{dc} = (1/\sqrt{2}) \sin \pi/n$$

which verifies eq. (1a).

869. EXPERIMENT 45-A. — Ratio of No-Load Voltages in a Synchronous Converter. — The purpose of the experiment is to verify the relations explained in the preceding section. A converter with six or eight slip-rings is particularly suitable for this purpose. The machine is run as a shunt motor, from the d-c side, at various speeds, corresponding to different values of the applied d-c voltage, and with different values of field current. The runs should be arranged according to some system; for example, the d-c voltage, the speed, or the field current should be kept constant for a set of runs. All the possible a-c voltages are read at each setting. It is desirable to trace the tap connections to the armature so as to check the electrical angles between them. If an oscillograph is available, a few curves of induced a-c voltages should be taken.

Report. Give the observed ratios of a-c to d-c voltages, and compare them with the theoretical values on the sine-wave assumption (eq. 1*a*). Explain possible discrepancies, using the oscillograms, and computing one or two non-sinusoidal ratios, from the known shape of the flux distribution curve. Draw vectors of all measured a-c voltages as in Fig. 640*b* which shows the voltages in a special converter built for experimental purposes.

870. Ratios of Direct and Alternating Currents. — (a) *Coil currents.* Consider a synchronous converter with a multiple (lap) winding, having p poles and n collector rings. There will then be $pn/2$ a-c circuits through the armature, each carrying a current of I_a, and p d-c circuits each carrying a d-c coil current of I_d. Let E_n = a-c volts between adjacent rings (taps), $\cos\theta$ = the a-c power factor, and η = the efficiency (ratio of d-c output to a-c input) of the converter. Then we may write

$$\text{Output} = pI_dE_{dc} = \eta\cos\theta np/2I_aE_n$$

Therefore

$$I_a/I_d = 2E_{dc}/(nE_n\,\eta\cos\theta)$$

But, from eq. (1*a*), $E_n = (E_{dc}/\sqrt{2})\sin\pi/n$, so that the ratio of a-c to d-c coil currents is

$$I_a/I_d = 2\sqrt{2}/(\eta\cos\theta n\sin\pi/n)\quad\ldots\ldots\quad(5)$$

Example. If $n = 2$, $I_a/I_d = \sqrt{2}/(\cos\theta\eta)$, so that in a two-ring converter at unity power factor and efficiency (approximately) the effective value of the a-c coil current = 1.41 × the direct current in the coils.

(b) *Line currents.* The d-c line current = p × d-c coil current, or $I_{dc} = pI_d$. Each tap from the winding to a slip-ring carries the vector difference of the alternating coil currents in the adjacent sections of the winding, as shown in Fig. 641(*a*). The tap current (Fig. 641*b*) is therefore

$$I_t = 2I_a \sin \pi/n \quad . \; . \; . \; . \; . \; . \; . \; . \; . \; . \qquad (6)$$

and since there are as many taps from each ring to the winding as there are pairs of poles on the machine the a-c line current

$$I_{ac} = I_t \times p/2 = pI_a \sin \pi/n \quad . \; . \; . \; . \; . \; . \; . \qquad (7)$$

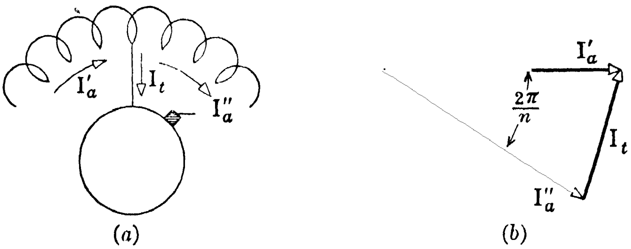

FIG. 641. Coil and tap currents in a rotary converter.

From eq. (5) the value of I_a is substituted in eq. (7), giving as the ratio of line currents

$$I_{ac}/I_{dc} = 2\sqrt{2}/(n \cos \theta\eta) \quad . \; . \; . \; . \; . \; . \; . \; . \qquad (8)$$

TABLE I

RATIOS OF CONVERTER ALTERNATING AND DIRECT CURRENTS

No. of Rings n	Ratio of Coil Currents[2] I_a/I_d	Ratio of Line Currents I_{ac}/I_{dc}
2	1.41/(cos $\theta\eta$)	1.41/(cos $\theta\eta$)
3	1.09/ "	0.943/ "
4	1.00/ "	0.707/ "
6	0.943/ "	0.472/ "
12	0.91/ "	0.236/ "

871. EXPERIMENT 45-B. — Operation of the Rotary Converter from the D-C Side (Inverted Converter). — The purpose of the experiment is to study the current relations discussed in the preceding section, and to determine the operating characteristics of the inverted converter. The machine is started and brought up to speed as a shunt d-c motor, after which the following runs should be made.

---

[2] When the converter is operated from the d-c side the efficiency, η, enters the above values in the reciprocal sense.

(a) Holding impressed volts constant and keeping the field current at the value which gives normal speed at no load, connect the machine as a single-phase (two-ring) alternator and proceed as follows:

(1) Apply non-inductive load and vary load amperes from zero to 25 per cent above normal (about 8 steps). At each point read d-c volts, armature amperes and field amperes, a-c volts, amperes and watts, and speed.

(2) Keep a-c amperes constant at about 3/4 normal (full-load) value, and vary the power factor from 100 per cent to the lowest value, lagging, which is obtainable, or at which the speed is within safe limits. Also take one or more points at the same value of load current but at low power factor, leading (using condensers or a synchronous condenser as load). *Note:* Lagging current in the inverted converter, as in any alternator, exerts an armature reaction (§815) tending to weaken the field flux. Since the inverted converter is operating as a shunt d-c motor this reduced flux causes an increase in speed.

(b) Operating as before from the d-c side, load as a three-ring or four-ring converter, applying a balanced non-inductive load. Take several points from no load to rated load, reading as in (a-1).

(c) Synchronize the converter (Chapter XXI) with an available a-c source, preferably polyphase, using transformers if necessary to make the voltages of the inverted converter and a-c source nearly equal.

(1) Hold the d-c supply voltage constant and vary the field current in small steps, taking all readings.

(2) Keeping the setting of the field rheostat fixed vary the impressed d-c volts in small steps and take readings.

Report. (a) 1. Plot a-c amperes, volts and watts, d-c amperes, volts and watts, machine efficiency and speed, against a-c watts output.

2. Against power factor of the load plot a-c and d-c amperes, volts and watts, machine efficiency and speed. Plot also change in speed (referred to the no-load value) against reactive component of a-c amperes ($= I_{ac} \times \sqrt{1 - (\text{p.f.})^2}$). (b) Compare the efficiency of the polyphase converter with that of the two-ring converter at the same value of watts output. Calculate the ratios of a-c line amperes to d-c line amperes at several loads, using metered values. Compare with Table I. Do the same for coil currents, determined from the line currents through eq. (4). (c) Give the results of test (c), stating any difficulties encountered and means of reducing them.

Discuss the operation of the inverted converter as revealed by the curves plotted.

872. Armature Reaction in the Rotary Converter. — In the experiment with the inverted converter it was found that when the a-c load was partly inductive the converter speed rose, owing to the effects of armature reaction. Since the armature of the converter carries the resultant of motor and generator currents, the armature reaction becomes the sum of the reactions due to direct current (§366) and to alternating current (§810). In Fig. 642 the armature reaction due to the direct current in the armature, with brushes on the neutral, has a triangular distribution, passing through zero at the pole center, and rising to a value of $(1/2)(Z/p)I_d$ at the brushes, or

$$M_{dc} = (1/2)(Z/p)I_d \quad . \; . \quad (9)$$

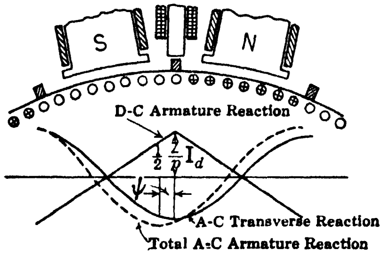

FIG. 642. Superposed mmf's due to direct and alternating currents in a polyphase converter.

The reaction due to the alternating current is sine form in distribution in a polyphase converter, and its position with respect to the poles depends upon the internal (pole-center) power factor of the alternating current. The mmf due to the transverse component (§814) of armature current, or $I_a \cos \psi$, passes through zero at the pole centers and is maximum midway between the poles. It is opposite in sign to the d-c reaction. Its maximum value (§814) is

$$M_t = 0.9k_d mNI_a \cos \psi \quad . \; . \; . \; . \; . \; . \; . \; . \quad (10)$$

where mN = turns per pole, I_a = a-c coil current, and $k_d = (n/\pi)\sin \pi/n$ (eq. 3). In terms of the total conductors, Z, and the number of poles, p, $nN = Z/2p$, so that

$$M_t = 0.9(n/\pi)\sin \pi/n(Z/2p)I_a \cos \psi \quad . \; . \; . \; . \; . \quad (11)$$

But, neglecting losses and calling $I_a \cos \psi = I_a \cos \theta$, from eq. (5) $I_a \cos \psi = (2\sqrt{2})/(n \sin \pi/n)I_d$. Substituting in eq. (11)

$$M_t = 0.405(Z/p)I_d \quad . \; . \; . \; . \; . \; . \; . \; . \; . \; . \quad (12)$$

Fundamental sine component of d-c reaction. The triangular distribution of d-c armature reaction (Fig. 642) may be analyzed to determine its fundamental sine component (Chapter LVIII) which may then be compared with the sine-form a-c reaction. Calling the amplitude of this curve M_{dc}'

$$M_{dc}' = 2/(\pi/2)\int_0^{\pi/2} f(x)\sin x\,dx$$

$$= 4/\pi \int_0^{\pi/2} (1/2)(Z/p)I_d x/(\pi/2)\sin x\,dx$$

$$= 4/\pi[ZI_d/(p\pi)(\sin x - x\cos x]_0^{\pi/2} = 0.405(Z/p)I_d \quad . \; . \quad (13)$$

From eqs. (12) and (13) it follows that the space fundamental of the reaction due to the d-c component current, and the transverse reaction due to the alternating current (neglecting losses), are equal. They are opposite in sign and so cancel. Actually the transverse component of a-c input to the synchronous converter must exceed the value used above by enough to supply the armature losses. This component, however, is small compared with the load current. Therefore, there is little resultant armature reaction along the brush, or interpole, axis so that the ampere-turns required on the interpoles of the converter are very low.

Effect of reactive component of alternating current. The direct component (§815) of alternating coil current is $I_{ad} = I_a \sin \psi$. The reaction due to this current is not compensated for by any corresponding and opposing d-c reaction and so is free to modify the useful flux of the machine. In the synchronous converter, since it runs as a synchronous motor, a leading component of alternating current weakens, and a lagging component strengthens, the field. Conversely, in the inverted converter, which runs as a d-c motor and delivers current as an a-c generator, lagging current weakens (§815), and leading current strengthens, the main field. This explains the action of lagging power factor of load upon the speed of the inverted converter in Experiment 45-B.

873. Methods of Starting. — For starting a synchronous converter, the following three general methods are in use:

(a) Starting from the d-c side as a shunt-wound motor (Chapter XXV).

(b) Self-starting from the a-c side, using the converter itself as an induction motor (§859).

(c) Starting by means of a mechanically direct-connected induction motor or a-c commutator motor (§858).

Most modern converters are started from the a-c supply using method (b).

(a) *Starting from the d-c side.* The machine is wired on the d-c side as shown in Fig. 228; on the a-c side, synchronizing connections are provided (Chapter XXI). The series-field winding, if any, is cut out during the starting period, because the reversed current would weaken the field instead of strengthening it. The interpole winding may be left in the circuit.

After the machine has reached approximately its rated speed, synchronizing is done by adjusting the starting and the field rheostats, and then the line switch on the a-c side is closed.

(b) *Self-starting of a synchronous converter from the a-c side.* Just as a synchronous motor may be made self-starting by temporarily converting it into an induction motor (§859), so a synchronous converter can be made to start from the a-c side by utilizing secondary currents induced in the damper winding (Fig. 643). When the armature is connected to an a-c source and the field circuit is open, the machine is equivalent to an induction motor, the armature constituting the primary member, and the damper winding the squirrel-cage secondary (§482). Consequently, the armature starts and rotates against the revolving flux, coming up almost (or quite) to synchronous speed. As the machine approaches synchronism the field circuit may be closed at a moment when the polarity of the machine is correct, and it will lock into step.

When the armature is just starting, the velocity of the revolving flux relative to the field poles is high. As a result, a-c voltages of considerable magnitude are induced in the field coils. One method of absorbing this voltage is to leave the field winding closed in its regular connection across the d-c brushes through its rheostat. The machine then runs up to speed, excites itself, and locks in synchronism without any other attention on the part of the operator, except for the possibility of the wrong polarity.

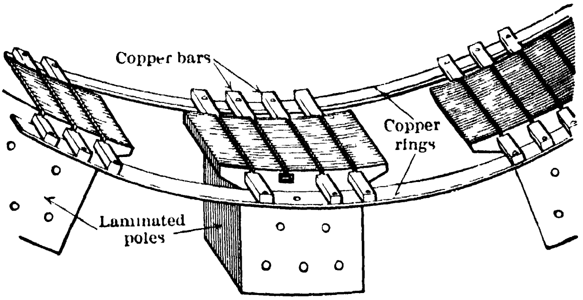

FIG. 643 Copper dampers (amortisseur winding) on the poles of a self-starting rotary converter.

874. Special Features of A-C Starting. — (a) *Polarity.* In order to obtain correct polarity, various means may be used, some of which are as follows:

(1) If the d-c voltmeter indicates a reversed polarity, interchange the leads of the shunt-field winding by means of a double-throw switch provided for this purpose, thus reversing the shunt current and connecting the field winding directly across the armature (without any resistance). This operation will unlock the armature and it will fall out of step. When the voltmeter pointer returns to zero, indicating a probable slippage of over 90 electrical degrees, quickly move the switch to its original position. By this time, the armature has slipped by about 180 electrical degrees, and therefore is building up a voltage between

the brushes in the correct direction. If this operation does not succeed the first time, it may be repeated.

(2) Connect a zero-center d-c voltmeter between the d-c brushes. As the machine approaches synchronism, the voltmeter needle will swing back and forth. Just as it begins to move in the right direction past zero, the field switch may be closed.

(3) The field may be temporarily excited from an external source of direct current, having a fixed polarity.

(4) The starting switch on the a-c side may be opened for an instant, thus permitting the converter to slow down somewhat.

(b) *Sparking during starting.* The same revolving magnetic field which includes a high emf in the field coils induces a considerable voltage in the armature coils short-circuited by the d-c brushes. Therefore, during the early stages of starting, considerable sparking may ensue. This phenomenon is particularly pronounced in converters provided with interpoles because the magnetic field density in the commutating zone can then reach a much higher magnitude, the air-gap reluctance being much lower. It is therefore customary to provide a brush-lifting device for raising the brushes during the starting period. One brush on each stud is made narrow and is left on the commutator, for field excitation and for the determination of polarity.

(c) *Automatic starting.* In automatic railway substations, in which converters are started from the a-c side as induction motors, the first relay comes into action when the trolley voltage has remained below a certain value for a few seconds, indicating that more power is needed. The control bus is then energized, the brushes are automatically lifted from the commutator, the a-c circuit-breaker is closed, and the starting contactors (partial voltage) are also closed, allowing the armature to start. If the d-c polarity is incorrect, a certain relay causes the field circuit to be reversed and then again restored in its original position. Should the polarity be now correct, the converter is automatically disconnected from the starting taps, and the contactors to the running taps are closed. The brushes are then automatically lowered and the machine connected to the trolley circuit, first through a protective resistance and then directly. The machine continues to operate as long as it can deliver sufficient load current. When this current falls below a predetermined value for several seconds, a relay disconnects the machine both on the d-c side and on the a-c side, and all the devices are returned to their initial positions ready for another start.

875. EXPERIMENT 45-C. — Practice in Starting Rotary Converters. — The purpose of the experiment is to obtain practice in the several methods discussed above for starting and synchronizing rotary converters. Therefore a polyphase converter is required, also a corresponding source of alternating current with means of obtaining various values of reduced voltage, an induction motor having two less poles than the converter and arranged for direct connection to it, also meters and control equipment.

(a) *Starting from the d-c side.* The method is explained in the preceding section. Having arranged the connections and tried synchronizing a few times, the student should proceed with the problem of reducing the necessary time to a minimum, from the instant when an order is given to start the machine to the instant when the converter is delivering its share of the load on the d-c side. The time can be reduced by a proper selection of the steps in the line and field rheostats, and by switching in on the a-c side an instant before perfect synchronism has been reached. Numerical values should be taken for the report. Synchronizing should also be tried with the d-c voltage fluctuating irregularly within definite limits, the difficulties noted, and remedies tried.

If *automatic equipment,* such as contactors operated by relays, is available, it should be operated under normal conditions. Then it should be tried for automatic starting and synchronizing of the converter when the d-c voltage drops below a predetermined value.

(b) *Starting by means of an induction motor.* Assuming that a wound-rotor induction motor having two poles less than the converter is available, proceed as follows:

Direct-connect the motor to the converter. Provide synchronizing devices and meters (§475). Driving by means of the motor, bring the converter to speed, self-exciting its field, and proceed to synchronize as though it were a synchronous alternator. Endeavor to develop a procedure which will result in a minimum of time to bring the machine from rest and put it into service, carrying load.

(c) *Starting from the a-c side.* Try various voltages, bringing the machine up in speed and synchronizing from the a-c side, first with the field circuit short-circuited, then with a low value of field provided from a separate source, and finally with the field circuit connected across the pilot brushes (§874*b*). Try starting with the brushes down and with them raised, determining in each case the minimum voltage at which the machine will start and come to approximately synchronous speed. Read the armature current at the moment of start and every few seconds until full speed is reached. Note the effect of the value of the field current upon the final value of armature amperes. Indicate the degree of sparking in each case. Determine the best conditions for starting, and practice this method with a view to reducing the time required.

Each time the machine is synchronized allow it to run for a few minutes with the value of field current resulting in a minimum armature current in order that the machine shall not overheat.

Report. Discuss each method of starting the converter, and give such numerical data as are available. Where possible, plot curves of armature current against time. Discuss sparking, polarity, and ease of operation.

876. EXPERIMENT 45-D. — Operation of the Synchronous Converter from the A-C Side. — The purpose of this experiment is to determine the operating characteristics of a synchronous converter and to suggest some of its possibilities for voltage regulation.

Start and synchronize the machine by any of the methods described above. Arrange to measure all a-c and d-c quantities and to vary the d-c load in convenient steps. Unless otherwise instructed, hold supply volts and frequency constant. Take the following runs.

(a) Hold the d-c load current constant and vary the field excitation from the maximum obtainable to the minimum at which the machine will operate. Take curves at no load, half load, and normal load, with the points closer together near 100 per cent power factor (minimum a-c amperes) since the curves change more rapidly at this point. Read a-c amperes, frequency, volts, and watts. A power-factor meter or reactive-factor meter is desirable. Read d-c amperes, volts, exciting current, also speed. Take notes regarding hunting and commutation, and be sure you know when the a-c current is leading and when lagging.

(b) Insert reactances in series with the a-c leads. These should be equal in value and such as to cause a voltage drop of 10 to 20 per cent of rated volts at rated current (10 to 20 per cent reactance). Hold supply a-c volts and frequency constant and take readings of all values while holding d-c amperes constant and varying the field current. Note in particular a-c supply volts, drop across reactances, ring voltage, and d-c voltage.

(c) Decrease the d-c load to zero and separately excite the field, keeping the field current constant at the value found to give 100 per cent power factor in (a). Vary the a-c supply volts from 20 per cent below to 20 per cent above normal. Read amperes, watts, and volts of supply, also drop across reactors and at the slip-rings.

Report. (a) 1. Plot curves of a-c armature amperes against field current for each constant d-c load (V curves).

2. Plot power factor against field current for each load (inverted

V curves). Note whether the same power factor occurs at the same field current for each load. Compare the range of power-factor regulation, leading and lagging, at full load and at no load.

(b) Plot a-c ring volts and d-c volts against power factor. Suggest how the synchronous converter may be made self-compounding.

(c) Compare the variation in a-c supply volts with those in slip-ring volts, and on the basis of these figures explain how a synchronous motor, running light at the end of a line possessing reactance, tends to hold the line voltage constant.

CHAPTER XLVI

THE SYNCHRONOUS CONVERTER
(Continued)

REGULATION, HEATING, AND COMPOUNDING

877. Methods of Controlling D-C Voltage. — In a constant-speed d-c generator, the terminal voltage is usually controlled by one of the following four means: (a) manually, by the shunt-field rheostat (Fig. 204); (b) by an automatic voltage regulator (§§252 to 254); (c) by the addition of a series-field winding (§248); or (d) by a series booster (§§284 and 556).

The first two methods are not applicable to the ordinary synchronous converter because the ratio of the voltages induced in the armature (alternating to direct current) is constant (§868). Varying the field excitation will merely mean a corresponding reactive current from the a-c source, to compensate the wrong excitation by the direct reaction, as in the synchronous motor (Chapter XLIV). However, this method may be used by so modifying the construction of the machine that the field flux (and consequently the d-c voltage) can be changed without materially changing the a-c counter emf. One solution is the split-pole converter, which was used for some time but at the present writing is not being built.[1]

A field winding in series with the d-c leads is not effective in itself, for the same reason that shunt-field regulation is not effective, that is, because it would merely mean a reactive current from the a-c line. However, if these lagging or leading currents pass through inductance coils placed between the a-c source of constant voltage and the slip-rings of the converter (Fig. 637), the voltage drop in these coils can be made to cause increase or decrease of the a-c voltage at the slip-rings, and thus bring about corresponding variations in the d-c voltage. This method of voltage regulation is described in §878.

A booster can be used on either the d-c or the a-c side. In practice, one on the a-c side is preferred, because of its lower cost and easier regulation. An a-c booster may be either stationary, consisting of transformers with several taps, induction regulators, or an additional rotating part (§880). Summing up, there are available the following methods of voltage control:

---

[1] Those interested will find a description and literature references in the "Standard Handbook for Electrical Engineers," Sixth Edition, indexed under Converter, synchronous, split-pole.

(1) By varying the a-c voltage at the slip-rings by means of transformer taps, a booster transformer, an induction regulator, or a combination of these.

(2) By a combination of a series reactance and compound field winding or voltage regulator operating to change the shunt field.

(3) By means of an a-c booster, with a revolving field or armature, between the transformer and the slip-rings.

(4) By using split poles.

(5) By means of a d-c booster, between the d-c brushes and the bus.

Methods (2) and (3) are described in more detail below. Method (1) has nothing to do with the converter itself, and its efficacy depends on the available means of automatically and promptly varying the voltage in small steps and without arcing contacts.[2] Method (4) is now practically obsolete. In method (5), if the booster is driven by a separate motor, its performance is independent of that of the converter. If it is direct-connected to the converter shaft, the converter at times acts also as its driving motor, so that part of the alternating current is not rectified into direct current. This fact must be considered in using eqs. (5) and (8) in §870. A d-c booster is seldom used because of its expense and the necessity of using a second large commutator.

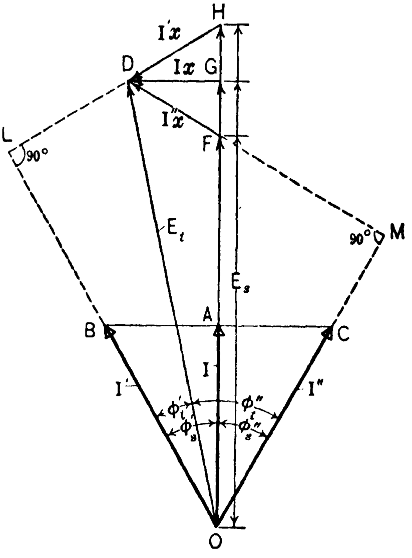

FIG. 644. Vectors illustrating the effect of series reactance on the slip-ring voltage, with leading and with lagging current.

878. Combination of Series Field and Series Reactance. — The connections are shown in Fig. 637. A series winding is provided on the poles, and an inductance is placed between the source of a-c voltage and the slip-rings. Often it is possible to increase the leakage reactance of the transformers (§406) sufficiently to make external reactances unnecessary.

---

[2] For variations in the power factor of a converter working with an induction regulator, see B. Schwarz, *Elektrot. und Maschinenbau*, vol. 43 (1925), p. 417.

The principle of automatic voltage control by this method is shown in Fig. 644. Let *OA* be a vector of the alternating current taken by the converter, in phase with the corresponding star voltage at the slip-rings, $OG = E_s$. In other words, let the converter excitation be so adjusted that the armature operates at unity power factor. Let the external reactance, including that of the transformer, be x. Adding $GD = Ix$, in leading quadrature to *OG*, and neglecting a small ohmic drop, the vector of the primary voltage, $OD = E_t$, is obtained, reduced to the secondary circuit.

Now let the converter field be overexcited; as a consequence, the converter will take a leading current, $OB = I'$ (§870). Assume the d-c load to be so readjusted that the in-phase component of the new a-c current remains equal to *OA*. The new reactive drop is equal to *HD*, in leading quadrature with *OB*. Assuming the primary transformer voltage, $E_t = OD$, to remain constant, the voltage at the slip-rings must now be equal to *OH*, in order that its geometric sum with *HD* be equal to *OD*.

Thus a leading a-c current, flowing through a reactance, causes a voltage rise at the a-c terminals of the converter. But, the ratio of the d-c voltage to the a-c voltage being practically constant, the d-c voltage is raised accordingly. In reality, the voltage drop in the converter itself must be subtracted, but this is usually small.

If the field excitation is reduced below its normal value (corresponding to the current *OA*), a lagging reactive current will flow into the converter, to supplement the lacking excitation. Assuming again the power component of the current to be the same as before, the current itself may be represented by a vector such as $OC = I''$. Subtracting from *OD* the reactive drop *FD*, in leading quadrature with *OC*, we find that the voltage, $E_s = OF$, at the slip-rings is lower than *OG*.

Thus, with a proper magnitude of the series reactance and a corresponding number of turns in the series-field winding, a synchronous converter may be automatically overexcited in proportion to its output, and hence its a-c voltage may be raised as the load increases. This will allow the d-c voltage to remain nearly constant, giving a "flat compounding." (See, however, the "hump" at *c'* in Fig. 215.) Or, the machine may be over-compounded to compensate for the voltage drop in the d-c feeders, if so desired. It must be remembered, however, that this automatic voltage regulation, by its change in the power factor of the input, requires considerably larger a-c armature currents in the machine, so that the armature I^2r loss is greatly increased and the d-c rating is accordingly reduced; §882(4).[3]

879. EXPERIMENT 46-A. — Compounding a Synchronous Converter by Means of a Series Reactance. — The purpose of the experiment is to obtain voltage characteristics of a synchronous converter with a compound field winding and a series reactance, as explained in the preceding section, and to study the influence of the various factors on the performance of the machine. It is preferable not to include the transformers in this study, but to keep the a-c voltage constant at the low-tension terminals. Having selected a reasonable value of reactance, start the machine and bring it into synchronism (§§473 to 476). No series field is used in this preliminary experiment. Apply a moderate load on the d-c side, vary the shunt-field current within wide limits, and take complete readings for each field current. Also vary the load resistance, and adjust the shunt field so as to maintain d-c volts constant. From the increase in the shunt current necessary for keeping the voltage constant, figure out the required number of turns in the series winding, in order to produce the same effect automatically. If the number of turns of the shunt winding is not known, it can be determined as is explained in §250. Put the calculated number of series turns on the machine and verify the predetermined performance. Then increase the number of series turns so as to get a certain specified amount of over-compounding; and if the machine is over-compounded too much, place a shunt across the series winding, as is done in compound-wound generators (Figs. 213 and 214).

After this, begin a more detailed load test, varying the main current on the d-c side from zero to a permissible maximum, and keeping the setting of the shunt-field rheostat the same throughout. The voltages and the currents should be read on both sides of the converter armature, as well as the voltage across the reactances and at the transformer terminals. The power input, the field current, etc., should also be measured. The value of the reactance and the number of series turns may then be modified by steps, to get some other degrees of compounding or over-compounding, and the load test may be repeated, until the characteristics of the machine have been thoroughly explored. Approximately the same degree of compounding may be obtained with a comparatively small reactance and a large number of series turns, or with a large reactance and a smaller number of series turns. It is desirable to investigate the difference in the performance characteristics of the machine on the a-c side in these two extreme cases Since the saturation in the magnetic circuit of the converter exerts considerable influence upon its compounding characteristics, a set of curves should also be taken at a much lower d-c voltage, when the machine is not saturated. Load characteristics of the machine should also be obtained when only the shunt-field winding and no reactances are used. A no-load characteristic (saturation curve) of the converter should be taken, and the resistances and the no-load losses measured, as in a d-c machine.

---

[3] For further details, mathematical theory, and limitations of this method of voltage control, see E. Arnold, "Wechselstromtechnik," vol. 4, Chapter XXIX; Alex. Russell, "Alternating Currents," vol. 2, p. 476; Juhlin, *Institution of Electrical Engineers* (British), *Journal*, vol. 55 (1917), p. 241; *BBC Mitteil.*, vol. 11 (1924), p. 220. For the general mathematical theory of the armature resistance, reactance and reaction in a converter, see Guilbert, *La lumière électrique*, vol. 35 (1916), p. 141; Neville, *Electrician*, vol. 80 (1917), pp. 267 and 304.

Report. Against d-c load amperes as abscissas, plot all the voltages, the a-c amperes, the power input and output, the power factor at the slip-rings and at the line terminals, the efficiency (excluding and including the reactance coils), the field current, etc. These curves, for different values of reactance and series turns, should be so arranged as to make clear the influence of these factors. Construct a few vector diagrams, showing the measured currents and voltages in their true phase position, and explain discrepancies or inconsistencies, if any. Check the measured efficiencies with those computed from the losses; be sure to use the correct I^2r loss in the armature (§882).

Draw diagrams of connections showing how the d-c voltage could be controlled automatically, without the series winding and without series reactances, by varying the a-c voltage by means of transformer taps, a booster transformer, an induction regulator, etc Discuss the advantages and the disadvantages of the two methods.

880. Synchronous Booster Converter. — A synchronous booster (Fig. 645) is a machine (usually direct-connected to the converter shaft) in which an additional adjustable voltage is induced between the a-c source and the converter armature. In this manner, the a-c voltage impressed on the armature winding, and consequently the d-c voltage, may be varied at will. The booster shown in Fig. 645 has a revolving armature and stationary field poles. Sometimes the booster is of the revolving-field type, like an ordinary alternator (Figs. 318 and 319); it is then located outside the collector rings. The booster armature is provided with the usual polyphase a-c winding, of the same number of phases and poles as the converter itself. This winding is connected in series with the a-c leads which constitute taps on the converter armature winding. The booster field winding, *w*, may be excited at will with direct current of either polarity, to " boost " or to " buck " the a-c bus-bar voltage.

The converter shown in Fig. 645 is provided with a shunt winding, *Sh*, on the main poles, and has two windings on the commutating poles. The main winding, *M*, is the usual commutating series winding, while the auxiliary winding, *Au*, is necessary because of a changing armature reaction due to the booster (§884). The windings *Au* and *w* are of the nature of shunt windings, but there must be a definite relationship between the currents in these windings and the main direct current in order to obtain the correct commutating field. It would be unwise to describe here the various electrical and electromechanical arrangements of rheostats used for such control.[4] The necessity for such a correlation of the currents is indicated in the sketch by a control box, *C*, to which the various leads are taken.

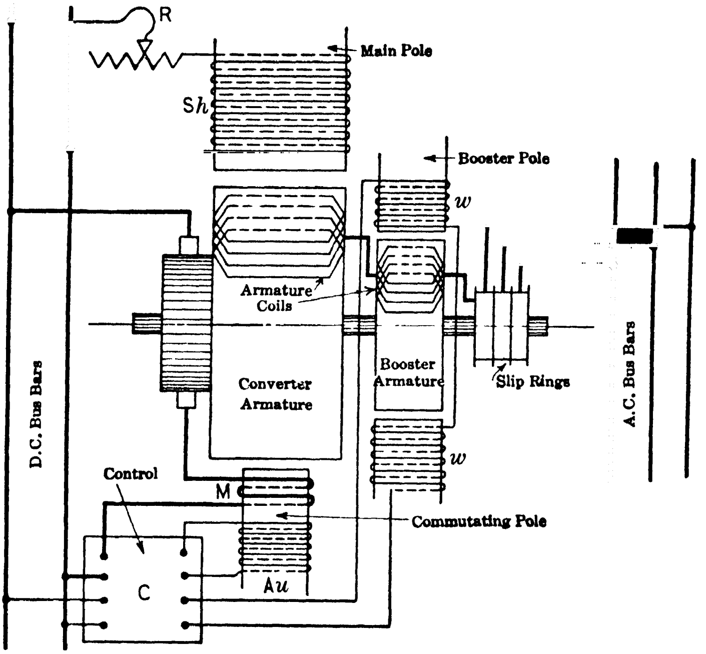

Fig. 645. Circuits of a booster converter having commutating poles.

The two advantages of booster control over series reactances (§878) are: (a) The voltage may be varied, both up and down, within wider limits; and (b) the power factor may be controlled by the field rheostat, *R*, independently of the voltage control, by means of the booster field current. For a critical comparison of the two methods, see Juhlin,

---

[4] See, for example, an article by M. W. Smith in *Electric Journal*, December, 1917.

Institution of Electrical Engineers (British), *Journal*, vol. 55 (1917), pp. 248 to 251, and a lengthy discussion following it.

When the voltage induced in the booster armature is additive with respect to that at the a-c bus-bars, the booster acts as a generator, driven by the converter as a motor. Consequently, not all of the alternating current is converted into direct current; part of it is used for driving the booster. This fact must be considered when using eqs. (5) and (8) in §870. Contrariwise, when the booster is " bucking " the bus-bar voltage so that the current flows through the booster armature against the induced emf, it is acting as a synchronous motor which drives the converter. Consequently, the converter not only rectifies all the alternating current supplied to it, but may also generate additional direct current by the conversion of the power furnished through the shaft, unless that power is only sufficient to cover the losses in the machine itself.

881. EXPERIMENT 46-B. — Study of a Booster Converter. — The machine is described in the preceding section. If a regular booster converter is not available, one may be improvised by using an ordinary converter and direct-connecting to it a synchronous alternator with the same number of poles and phases. The principal points to be studied are as follows: (a) limits of voltage control both ways from zero boost; (b) variations in power factor, simultaneous with voltage regulation and independent of it; (c) efficiency by the input-output method and from the losses; (d) automatic voltage regulation with the load; (e) simultaneous control of the booster field and of the auxiliary field on the commutating poles; (f) critical comparison of voltage control by means of a booster and by other methods (§877).

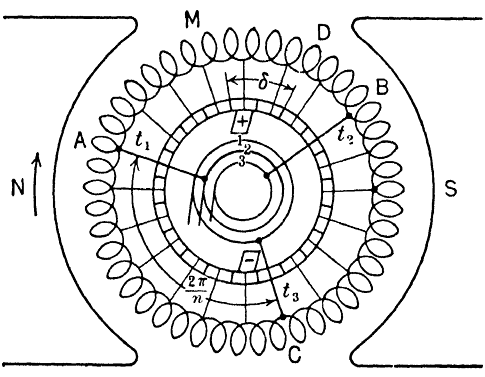

FIG. 646. Armature circuits of a three-phase converter showing mid-coil and tap coils.

882. The I^2R Loss in a Converter Armature. — (a) *The resultant current.* At unity power factor the coil, M, midway between adjacent a-c taps (Fig. 646), and called the " mid-coil," will have its alternating current and its direct current reverse at the same instant, independently of the number of rings. This reversal of the two currents happens when the mid-coil, M, is halfway between the poles of the converter, at which time the emf induced in the section of winding between taps t_1 and t_2 is zero. Assuming a sine wave of alternating current, and a rectangular wave of direct current, these current waves are, as shown in Fig. 647(a), opposite in phase and of the relative values given in Table I (§870). The resultant wave of current is expressed by the equation (mid-coil at unity power factor)

$$i = I_d - I_{a(\max)} \sin \omega t \quad . \quad (1)$$

where t is the time counted from the instant the two currents reverse.

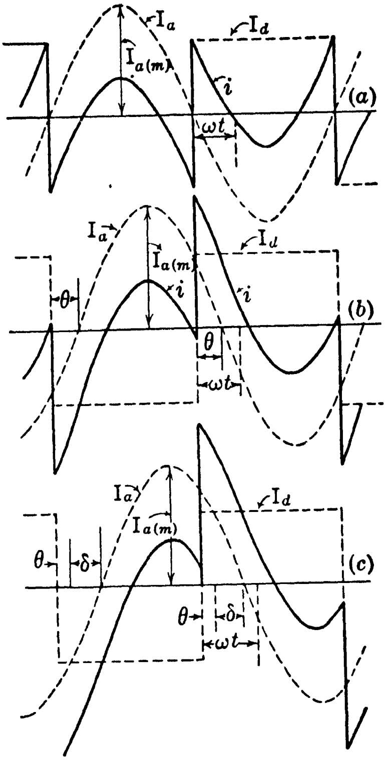

FIG. 647. Combined a-c and d-c currents in a rotary converter.

If the alternating current lags an angle θ behind the emf of the phase eq. (1) becomes (see Fig. 647b)

$$i = I_d - I_{a(\max)} \sin (\omega t - \theta) \quad (2)$$

For a coil D, an angle δ ahead of the mid-coil, the direct current reverses the angle δ *ahead* of the alternating emf which, as far as the relative phase of the currents is concerned, is equivalent to the alternating emf reversing an angle δ *behind* the direct current, or the alternating current reversing an angle $(\theta + \delta)$ behind the direct current. As a result, the combined current in a coil the angle δ ahead of the mid-coil and carrying a current lagging behind the a-c emf by the angle θ is

$$i = I_d - I_{a(\max)} \sin [\omega t - (\theta + \delta)] \quad . \; . \; . \; . \; . \; . \quad (3)$$

These currents are shown in Fig. 647(c).

(b) *The I^2r loss in the individual coil.* From eq. (3) the expression for the average i^2 of any coil is easily derived, as follows:

$$i^2 = I_d^2 + I_{a(m)}^2 \sin^2 [\omega t - (\theta + \delta)] - 2I_dI_a \sin [\omega t - (\theta + \delta)] \quad . \quad (4)$$

Average $i^2 = (1/\pi)\int_0^\pi i^2\, d\omega t$ which, from eq. (4), after integration, becomes:

$$\text{av. } i^2 = I_d^2 + I_{a(m)}^2/2 - (4/\pi) I_d I_{a(m)} \cos (\theta + \delta) \quad . \; . \quad (5)$$

or, in terms of rms current, I_a,

$$\text{av. } i^2 = I_d^2 + I_a^2 - 1.8I_dI_a \cos(\theta + \delta) \quad . \quad . \quad . \quad . \quad (6)$$

From the values of I_a/I_d given in Table I (§870), substitution may be made for a machine having any number of rings and operating at any power factor and efficiency, also for a coil anywhere between the taps of a phase. It should be noted that for coils an angle δ *behind* the mid-coil δ becomes *negative*, while for *leading* power factors θ is *negative* in the above equations. From eq. (6) the relative I^2r losses in the several coils may be calculated.

As an example assume a three-ring converter operating at a power factor of 90 per cent, lagging, and at an efficiency of 95 per cent. The greatest loss (i^2_{av}) will occur in the leading tap coil since the subtractive term in eq. (6) is least for this coil. The least loss will occur in a coil the angle θ behind the mid-coil. In terms of the direct current, I_d, $I_a = 1.09I_d/0.9 \times 0.95 = 1.275I_d$. The values of av. i^2 for the two coils are:

$$\begin{aligned} \text{Highest av. } i^2 &= I_d^2 + (1.275I_d)^2 - 1.8 \times 1.275I_d^2 \cos\ (25.9^\circ + 60^\circ) \\ &= 2.46I_d^2 \\ \text{Lowest av. } i^2 &= I_d^2 + (1.275I_d)^2 - 1.8 \times 1.275I_d^2 \cos\ 0^\circ = 0.33I_d^2 \end{aligned}$$

The ratio (max. coil I^2r)/(min. coil I^2r) = 7.4. Although the losses are in this high ratio the temperature-rise values for the two coils will differ by much less owing to the flow of heat from one part of the winding to another.

(c) *Average coil I^2r loss and converter rating.* To get the mean loss, or heating, of a converter armature one should find the mean value of av. i^2 (eq. 6) from $\delta = \pi/n$ to $\delta = -\pi/n$ (from tap t_1 to tap t_2).

Let

$$\begin{aligned} h = \text{mean } i^2_{\text{av}} &= (n/2\pi) \int_{-\pi/n}^{+\pi/n} i^2_{\text{av}}\, d\delta \\ &= (n/2\pi) \int_{-\pi/n}^{+\pi/n} [I_d^2 + I_a^2 - 1.8I_dI_a \cos(\theta + \delta)]\, d\delta \quad . \quad (7) \\ &= I_d^2 + I_a^2 - 0.572nI_dI_a \cos\theta \sin(\pi/n) \quad . \quad . \quad . \quad . \quad . \quad . \quad (8) \end{aligned}$$

or, substituting from eq. (5), §870, in the subtractive term:

$$h = I_d^2 + I_a^2 - 1.62I_d^2/\eta \quad . \quad . \quad . \quad . \quad . \quad . \quad . \quad (9)$$

As an example of the relative loss occurring in the same machine when operating first as a two-ring converter, and next as a six-ring converter, carrying the same direct-current load and operating at unity power factor, with an efficiency of 95 per cent in each case, the following values are given (see Table I, §870):

Two-ring converter:

$$I_a = (1.41/0.95)I_d = 1.485I_d$$
$$I_d^2 + I_a^2 = 3.21I_d^2$$
$$1.62I_d^2/\eta = 1.7I_d^2$$
$$h' = 1.5I_d^2$$

Six-ring converter:

$$I_a = (0.943I_d/0.95) = 0.994I_d$$
$$I_d^2 + I_a^2 = 1.99I_d^2$$
$$1.62I_d^2/\eta = 1.7I_d^2$$
$$h'' = 0.29I_d^2$$

$$\text{Ratio: (two-ring loss)}/\text{(six-ring loss)} = 1.5/0.29 = 5.15$$

Since the loss, h, varies as I_d^2, the rating or allowable current I_d, will vary as $\sqrt{(1/h)}$, and the rating of the six-ring machine may be $\sqrt{5.15} \times$ rating of two-ring machine, or the six-ring machine may carry about 2.2 times the load of the machine as a two-ring converter, with the same heating.

883. EXPERIMENT 46-C. — Oscillographic Study of Armature Currents in a Synchronous Converter. — The purpose of the experiment is to verify the general theoretical relations discussed in §882. For this purpose, the end connections of two or three armature coils are cut open, and small strips of high-resistivity material (such as manganin) are inserted to serve as ammeter shunts. Care must be taken to place these strips so that they do not cut the main field. Potential leads are to be provided, connected to two small, carefully made slip-rings with low-resistance brushes. These slip-rings can be connected at will to any desired shunt, while the brushes are connected to an oscillograph (Chapter LVII). The whole arrangement is identical with that mentioned in §379(g). If desired, a similar shunt can be provided in one of the commutator leads. The wave-form of the incoming alternating current should also be determined oscillographically, and it is well to check the outgoing direct current for ripples and fluctuations.

Since this experiment is of the nature of an advanced and extended investigation, it is hardly feasible to give detailed instructions. The literature references at the end of this chapter will suggest the principal topics of interest, and any of these may be made the subject of an experimental study. In most mathematical investigations, certain simplifying assumptions are made, while in a real machine there are unavoidable secondary phenomena, such as field and current harmonics, imperfect commutation, complicated mmf reactions, etc., which modify the theoretical results and suggest supplementary studies.

884. High-Reluctance Commutating Poles. — Modern converters are provided with commutating poles of high magnetic reluctance. This result is obtained by interposing a layer of non-magnetic material between the field frame and the root of the pole (Fig. 232). The purpose of this construction is to preserve at least the polarity (if not the magnitude) of the commutating flux under abnormal conditions, such as starting, hunting, short circuits, etc., as is explained below. As stated in §872, the armature mmf along the center line of a commutating pole is the difference between the transverse armature reactions of a d-c generator and of a synchronous motor. In normal operation of the converter, the difference between these two is quite small, the peak value (Fig. 642) of the d-c reaction being usually the larger of the two and creating a flux in the wrong direction (§374). If the reluctance of the commutating pole is low, a comparatively small number of exciting ampere-turns on the pole is sufficient to compensate for this differential mmf and to create a flux of proper direction and magnitude for current reversal in a coil undergoing commutation.

During a sudden short circuit, the direct current at first increases faster than the a-c input, the necessary energy being supplied by the stored mechanical energy of the revolving part (the armature swings back). Consequently, the transient d-c armature reaction greatly predominates and might reverse the commutating flux maintained by a comparatively small mmf, with a resulting flash-over between the brushes of opposite polarity. If the pole has a high reluctance, a large number of ampere-turns is required on it under normal conditions to produce the required flux. Consequently, an abnormal increase in the armature mmf would only weaken the field, not reverse it. A converter with high-reluctance interpoles is more immune from flash-overs on short circuits.

After the circuit-breaker has cleared the short circuit, and there is no more direct current, an inrush of alternating current takes place to swing the armature forward unless the d-c and a-c circuit-breakers are interlocked so that they open together. With low-reluctance commutating poles, the resulting a-c armature reaction would produce an excessive flux along the interpole axis, causing sparking and heating under the d-c brushes. With high-reluctance interpoles, only a moderate flux builds up before the current relations again become normal. Somewhat similar conditions obtain in starting and during hunting.

When the converter is carrying a d-c or a-c booster, the latter acts at times either as a generator or as a motor (§880), there being an excess of either direct current or alternating current as compared with the operation as a plain converter. Hence, there may be an excess of either d-c or a-c armature reaction along the axis of a commutating pole. Even with a high-reluctance pole, it is not always possible to preserve the required field strength for sparkless commutation at all values of d-c and a-c voltages. It is for this reason that an auxiliary winding is placed on the commutating poles (Fig. 645), its current being made a function of the direct current and of the amount of "boost" or "buck." When the booster is raising the transformer voltage, thus operating as a generator, the converter has an excess of motor action, and its armature reaction helps the mmf of the main winding on the interpoles. Hence, under these conditions, fewer ampere-turns are needed on the interpoles, and the current in the *Au* winding should oppose that in the *M* winding. The opposite is true when the booster is bucking the transformer voltage and is operating as a motor.

885. Other Means of Preventing Flashing. — As is explained above, a synchronous converter easily develops large mmf's and fluxes in the commutating zone and is therefore likely to flash over the commutator under sudden abnormal conditions. While high-reluctance poles have proved to be quite effective in reducing the frequency and the severity of such flash-overs and in improving commutation, two more devices have been found necessary under extremely severe railway service, viz., flash barriers and high-speed circuit-breakers. All three or any one or two of these means may be used in combination.

Flash barriers are stationary insulating boxes and transverse partitions placed around the brushes and along the commutator, to prevent the formation of an arc from brush to brush and to make its spread more difficult. A high-speed breaker in the d-c leads or in a d-c feeder is a special circuit-breaker which opens in a small fraction of a second after a short circuit occurs. In this way, the direct current is interrupted before it reaches a dangerous magnitude.[5]

886. Hunting. — Under certain conditions, the revolving armature of a synchronous converter oscillates about its true synchronous position, the torque angle (§850) being periodically greater and less than the correct angle imposed by the load. This so-called hunting is similar to that described in §854 for synchronous machines; the frequency of oscillations is determined by the synchronizing torque and by the moment of inertia of the revolving part.

Hunting is the more objectionable in a synchronous converter in that it causes sparking at the d-c brushes and may even result in a flash-over. The reason can be readily seen from the theory of transverse armature reaction, given in §884. During hunting, a periodic inrush of alternating currents is not balanced by the corresponding d-c output, but partly goes to accelerate the armature itself. Consequently, the commutating flux varies within wide limits without corresponding changes in the direct current, so that current reversals in the coils undergoing commutation take place in a wrong field. Moreover, the flux oscillates to and fro along the armature periphery, making the conditions still worse.

---

[5] The problem of flashing and its remedies will be found discussed in detail in the *Trans. A.I.E.E.*, vol. 41 (1922), pp. 108 to 121. In the light of the foregoing theory of differential armature reaction, the reader should have no difficulty in following the arguments advanced. See also *General Electric Review*, vol. 25 (1922), p. 348, and vol. 31 (1928), p. 635.

The most effective remedy against hunting is a damper or amortisseur winding (Fig. 643) on the pole faces. Secondary currents induced in this winding by the swinging flux impede departures of the armature from its synchronous speed. Hunting usually occurs because of resonance with some source of periodic non-uniformity in the system (for example, a reciprocating compressor or pump driven by an electric motor). A remedy is therefore sought in a change of the natural frequency of the converter's armature. In a finished machine, the only factor that can be changed conveniently is the moment of inertia of the revolving part. This can be done by providing a flywheel on the converter shaft or by belting it to one. The natural frequency is thus lowered and may be brought below that of the disturbing factor in the system.

The characteristics of the connecting line between the power plant and the converter are also an important factor in hunting. A converter may run satisfactorily when connected directly at the power station, and yet may be easily set to hunting when connected by a line of considerable impedance. The line impedance causes a phase angle between the voltages at its ends, so that the vector of the receiver voltage may oscillate back and forth by a small angle without disturbing the rest of the system. A connection by means of a line of low impedance is analogous to a mechanical coupling by means of a stiff shaft, while a line of high impedance corresponds to a " twistable " shaft. A driven machine at the end of such a shaft is likely to hunt. Thus, the impedance of an a-c line feeding synchronous converters should be kept as low as possible.

886a. EXPERIMENT 46-D. — Hunting of a Synchronous Converter and Remedies Therefor. — The purpose of the experiment is to apply the theory given in the preceding section. Using some stroboscopic device, such as a sectored disk and neon lamp (§493) operating from the a-c supply, observe the stability and tendency of the machine to hunt under the following conditions:

(a) Suddenly applied load.
(b) Operation at light and at heavy loads.
(c) Under- and overexcitation.
(d) Operation at less than normal voltage.
(e) With and without added flywheel effect, as when belted to an unloaded machine.
(f) With various values of reactance in the supply lines.

REFERENCES

1. E. **Arnold**, Wechselstromtechnik, vol. 4, Chapter XXVII, J. Springer Co.

2. A. **Russell**, Alternating Currents, vol. 2, Chapter XVII.

3. R. R. Lawrence, Principles of A-C Machinery, Chapters XXX to XXXVII, McGraw-Hill Book Co.

4. **Puchstein** and **Lloyd**, A-C Machines, Chapters XLVIII–LI, John Wiley & Sons.

5. A. S. **Langsdorf**, Theory of A-C Machinery, Chapter VIII, McGraw-Hill Book Co.

6. Standard Handbook for Electrical Engineers, Sec. 9, McGraw-Hill Book Co.

7. B. G. **Lamme**, *Elec. Jour.*, February, 1920, The technical story of the synchronous converter.

8. **Hambleton** and **Bewley**, *Jour. A.I.E.E.*, May, 1927, p. 479, The synchronous converter, theory and calculations.

9. B. L. **Robertson**, *Gen. Elec. Rev.*, August, 1928, p. 436, Synchronous converter armature windings.

10. W. B. **Snyder**, *Gen. Elec. Rev.*, February, 1926, p. 115, Synchronous converters and synchronous motor-generator sets compared for industrial service.

11. **Newton** and **Marthens**, *Elec. Jour.*, April, 1930, p. 195, Synchronous converters now are arc-welded.

12. E. B. **Shand**, *Elec. Jour.*, December, 1924, p. 545, Operation at reduced voltages.

13. N. **Stahl**, *Elec. World*, October, 1911, p. 1060, The heating of synchronous converters.

14. **Lee** and **Hildenbrand**, *Elec. Jour.*, March, 1926, p. 108, Synchronous converter copper loss.

15. S. **Neville**, *World Power*, vol. 4 (1925), p. 158, Armature heating of a rotary converter.

16. **Dreyfus**, *Archiv für Elektrot.*, vol. 4 (1915), p. 42, Supplementary copper losses.

17. **Hambleton** and **Robertson**, *Gen. Elec. Rev.*, December, 1928, p. 635, Flashing of synchronous converters.

18. E. B. **Shand**, *Trans. A.I.E.E.*, vol. 41 (1922), p. 109, Causes of flashing of synchronous converters.

19. **Linke**, *Archiv für Elektrot.*, vol. 2 (1914), p. 395, Pulsations in d-c voltage due to a-c harmonics.

20. J. H. **Morecroft**, *Elec. World*, vol. 59 (1912), p. 1437, Oscillograph tests of wave-form of current.

CHAPTER XLVII

THE APPROXIMATE CIRCLE DIAGRAM OF THE POLYPHASE INDUCTION MOTOR

887. In Chapter XXII, §504, the approximate equivalent diagram (Fig. 374) for one phase of the polyphase induction motor was given, together with formulas for, and an example of calculations of, motor performance, based upon this equivalent circuit. In §505 it was stated that the locus of the currents in the equivalent circuit was a circle. The determination of motor performance from the circle diagram was explained. It remains to be proved, however, that for both the approximate and the exact equivalent circuits of the motor the loci of stator and rotor currents are circles, and to discuss the use of these circular loci in the analysis of motor operation under various conditions.

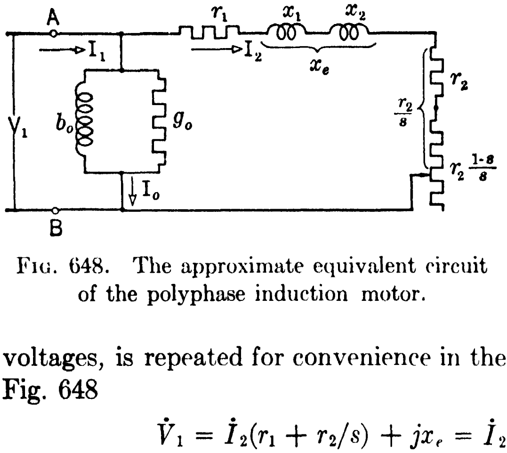

FIG. 648. The approximate equivalent circuit of the polyphase induction motor.

888. Proof of the Circular Locus of Currents in the Approximate Equivalent Circuit. — In Fig. 648 the approximate equivalent circuit for the polyphase induction motor, operating on a symmetrical system of voltages, is repeated for convenience in the following discussion. From Fig. 648

$$\dot{V}_1 = \dot{I}_2(r_1 + r_2/s) + jx_e = \dot{I}_2R_e + j\dot{I}_2x_e \quad . \; . \; . \; . \; . \quad (1)$$

or

$$V_1^2 = \overline{I_2R_e}^2 + \overline{I_2x_e}^2 \quad . \; . \; . \; . \; . \; . \; . \; . \; . \; . \; . \; . \; . \; . \; . \quad (2)$$

V_1 being constant and R_e variable in eq. (2), it is evidently the equation of a circle, which is the locus of the intersection of the vectors I_2R_2 and I_2x_e (Fig. 649). Evidently $I_2x_e/I_2R_e = x_e/R_e = \tan\alpha$. Then $I_2x_e/V_1 = \sin\alpha$, or

$$I_2 = (V_1/x_e)\sin\alpha \quad . \; . \; . \; . \; . \; . \; . \; . \; . \; . \quad (3)$$

Equation 3 is the equation of a circle, the locus of the current vector, $\dot{I}_2$.

But the total current input to the equivalent circuit, $\dot{I}_1 = \dot{I}_2 + \dot{I}_n$. Since $\dot{I}_n$ is constant in magnitude and direction the current vectors $\dot{I}_1$ and $\dot{I}_2$ terminate on the common circular locus (Fig. 649). The center of the circle is on a horizontal line drawn from the extremity of $\dot{I}_n$. The diameter of the circle has a value V_1/x_e, all quantities being per phase.

889. EXPERIMENT 47-A. — Experimental Determination of the Current Locus in a Polyphase Induction Motor. — The purpose of this experiment is to obtain data from which the value and power factor of the stator current will be known at various loads, in order that the vectors of this current may be drawn and the shape of the locus studied. The motor may be of either the squirrel-cage or wound-rotor type. While it is necessary to apply various loads to the motor it is not necessary for the purpose of this study to know the value of the load.

Maintaining rated voltage and frequency on the motor, vary the load in steps from no load to the breakdown point. Measure stator amperes, watts, and (constant) volts for each load. Take one point with the rotor blocked, reducing the applied voltage if necessary to avoid overheating the motor. These data may be corrected to rated voltage by multiplying the current by the ratio of rated volts to applied volts. The power factor may be assumed to be independent of the voltage.

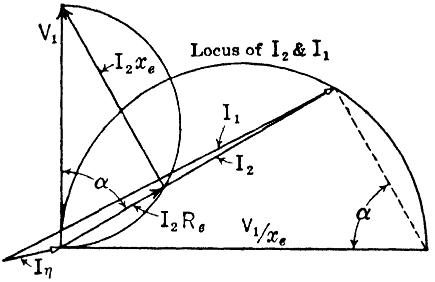

Fig. 649 Circular loci of voltage drops and of currents in the circuit of Fig 648

Calculate the power factor for each point taken, and draw the vector of each current with reference to the applied voltage vector and from a common origin, using a power-factor quadrant and scale to simplify the laying out of the vectors (Fig. 375). Draw a smooth curve through the extremities of these vectors and attempt to fit a circular arc to this curve, locating the center of the circle by drawing perpendicular bisectors to two chords of the experimental curve. Draw the diameter of the semicircle from the end of the no-load current vector. Note whether this diameter is at right angles with V_1. State conclusions as to the shape of the current locus and the apparent accuracy of the equivalent circuit of Fig. 648.

890. Performance Items from the Circle Diagram. — In §505 directions were given for the determination of various items of performance from the circle diagram (Fig. 650), but without the proof. While values of primary current, I_1, of power factor, $\cos \theta_1$, and the input, $V_1 I_1 \cos \theta_1$, are obvious from an inspection of the diagram, such quantities as output, slip, and torque require proof.

I^2r loss and slip. The current input with the rotor blocked, or OP_s, has a component P_sh in phase with V_1, so that the power input under this condition is proportional to P_sh. This input is made up of the fixed losses, represented by fh, plus the sum of the stator I^2r loss due to I_2 and the rotor I^2r loss, which sum must be represented by the height P_sf. The point g is so chosen that $P_sg/gf = r_2/r_1$. Assuming that rotor resistance, r_2, is constant, the straight lines AP_s and Ag still give the rotor copper loss and added stator copper loss when the motor is running and operating at any point, P, on the circle, these losses being given by the lengths ab and bc, as will now be shown.

Proof.[1] Draw construction lines Pk and P_sk. They are perpendicular, respectively, to AP and AP_s. A vertical line from P intersects AP_s at a, Ag at b, and AK at c. It is required to prove that ab and bc are proportional to the rotor copper loss and added stator copper loss, respectively, of the running motor. From similar triangles

$$ac/P_sf = Ac/Af = AP \cos \angle caP / AP_s \cos \angle fAP_s \quad . \quad (4)$$

But

$$\cos \angle caP = AP/AK, \quad \text{and} \quad \cos \angle fAP_s = AP_s/AK$$

Therefore

$$ac/P_sf = \overline{AP}^2/\overline{AP_s}^2 = I_2^2/I_{2b}^2 = \frac{\text{Copper loss due to } I_2}{\text{Copper loss due to } I_{2b}} \quad . \ . \quad (5)$$

which proves that ac is proportional to the rotor copper loss plus the added stator copper loss for any point P.

Moreover, from similar triangles, $ab/ac = P_sg/P_sf = r_2/(r_1 + r_2)$, so that ab and bc are seen to represent, individually, the rotor copper loss and the added stator copper loss. ad then represents the total loss, and, since Pd represents total input, Pa must give the output (power developed) by the motor.

Slip. That slip is given by the expression

$$s = ab/Pb \quad . \ . \ . \ . \ . \ . \ . \ . \ . \ . \ . \quad (6)$$

is shown as follows:

It has been seen that ab and Pb give the values of rotor copper loss and output plus rotor copper loss (which equals the rotor input or power transferred across the air-gap). Therefore, to prove eq. (6) it is necessary to show that

---

[1] R. R. Lawrence, "Principles of A-C Machinery," Chapter 43, McGraw-Hill Book Co.

$$\text{Slip/Syn. speed} = (\text{Rotor } I^2R \text{ loss})/(\text{Rotor input}) \quad . \ . \quad (7)$$

If E_2 = emf induced in the rotor (in stator terms), the rotor current, I_2, may be written

$$I_2 = E_2/\sqrt{(r_2/s)^2 + x_2^2} \quad . \ . \ . \ . \ . \ . \quad (8)$$

$$\text{Rotor input} = E_2I_2 \cos \theta_2 \quad . \ . \ . \ . \ . \ . \ . \ . \ . \ . \quad (9)$$

But

$$\cos \theta_2 = (r_2/s)/\sqrt{(r_2/s)^2 + x_2^2} \quad . \ . \ . \ . \ . \quad (10)$$

Therefore

$$\text{Rotor input} = E_2I_2(r_2/s)/\sqrt{(r_2/s)^2 + x_2^2} = I_2^2r_2/s \quad . \ . \quad (11)$$

or

$$s = I_2^2r_2/(\text{Rotor input})$$

But, from Fig. 650,

$$I_2^2r_2/(\text{Rotor input}) = ab/Pb$$

so that

$$\text{Slip} = ab/Pb$$

Torque. That torque is proportional to Pb may be seen as follows:

Power developed $= P_2 = 2\pi \times \text{rpm} \times \text{Torque} \times 746/33{,}000 = (1 - s)\ \text{Syn. rpm} \times T/7.04N_s$ where power is in watts (total); torque, T, is in pound-feet; N_s = synchronous rpm. Then

$$T(\text{lb-ft}) = 7.04P_2/(1 - s)N_s \quad . \ . \ . \ . \ . \ . \ . \ . \ . \quad (12)$$

or

$$T = 7.04 \times kmV_1Pa/(1 - s)N_s \quad . \ . \ . \ . \ . \quad (13)$$

where (§505) k = amperes per inch of diagram, V_1 = volts per phase, m = number of phases.

At start the torque becomes

$$T_s = 7.04 \times kmV_1P_sg/N_s \quad . \ . \ . \ . \ . \ . \ . \quad (13a)$$

Since

$$ab/Pb = s$$

one may write:

$$(Pb/Pb) - (ab/Pb) = 1 - s = Pa/Pb$$

Therefore

$$T = 7.04kV_1mPb/N_s = K\,Pb \tag{14}$$

which makes the line *Abg* the torque line.

Torque may also be expressed in terms of the circuit constants. The rotor power developed is the power dissipated in the fictitious load resistance, $r_2(1 - s)/s$ (Fig. 648), or

$$P_2 = mI_2^2r_2(1 - s)/s \tag{15}$$

But (Fig. 648)

$$I_2 = V_1/\sqrt{(r_1 + r_2/s)^2 + x_e^2} \tag{16}$$

so that

$$\begin{aligned} P_2 &= mV_1^2r_2(1 - s)/\left[(s(r_1 + r_2/s)^2 + x_e^2\right] \\ &= mV_1^2r_2s(1 - s)/\left[(r_1s + r_2)^2 + s^2x_e^2\right] \end{aligned} \tag{17}$$

Therefore (eq. 12)

$$T = (7.04mV_1^2r_2s)/\left[(r_1s + r_2)^2 + s^2x_e^2\right]N_s \tag{18}$$

Starting torque. Substituting the condition that $s = 1$, for the rotor at standstill, gives the starting torque, which, from eq. (18), becomes:

$$T_s = (7.04mV_1^2r_2)/\left[(r_1 + r_2)^2 + x_e^2\right]N_s \tag{19}$$

NOTE: In the above calculations, and in others in which the approximate equivalent circuit is the basis for the equations used, greater accuracy of results will follow if the voltage, V_1, is replaced by $V_1' = \dot{V}_1 - \dot{I}_nz_1$, or, approximately, by $V_1' = V_1 - I_nx_e/2$.

891. EXPERIMENT 47-B. — A Check upon the Relation between Slip and Rotor I^2r Loss. — To verify the relation derived in the previous article a polyphase induction motor should be run at various loads and careful readings taken of slip, input, and output, with such other data as are necessary to calculate the losses of the motor. If a d-c generator is used as the load device it must be calibrated as to losses (§326).

Run the motor at rated voltage and frequency and vary the load from zero to the maximum at which accurate readings of slip are possible. Read stator amperes, volts and watts, rotor amperes (if a wound-rotor machine), frequency, slip, rpm, and output of the d-c generator, or torque by a prony brake (§311) or electrodynamometer (§313). Take careful readings of stator and (if a wound rotor) of rotor resistances. Disconnect the motor from its load and take readings to permit the separation of core loss from friction and windage (Experiment 22-E).

From the data so taken calculate the input to the rotor for each load, either as stator input minus stator losses, or as rotor output plus rotor I^2r loss, friction, and windage.

Plot a curve of (slip/syn. rpm) against (rotor I^2r/rotor input). Note whether this gives a 45-degree line, indicating that the two are equal, and attempt to explain any discrepancies. Discuss the effect of neglecting friction and windage, or of including it among the stator losses as is done in the approximate equivalent circuit.

892. Rotor Ohmic and Effective Resistances. — At start, or with the rotor blocked, the current in the rotor has full stator frequency with the result that in the bars of the rotor there are appreciable eddy-current losses which have the effect of increasing the rotor resistance to what is called its "effective value." This value of resistance is greater than that measured (in wound rotors) with direct current. With the motor running at a slip of, say, 3 to 5 per cent, the frequency of the rotor current becomes 3 to 5 per cent of stator frequency so that, under ordinary operating conditions, the rotor resistance approaches the *ohmic*, or d-c, value. To calculate performance from the circle diagram at ordinary loads the output line should be lowered from the position AP_s to position of AP_s' (Fig. 650) to correspond to ohmic, rather than effective, resistance. AeP_s' is drawn so that (Fig. 650) $eg/P_sg = r_2$ (ohmic)/r_2 (effective). Ohmic resistance may easily be from 20 to 40 per cent less than effective resistance in single-squirrel-cage motors of ordinary design. In motors designed for high starting torque the difference may be much greater.

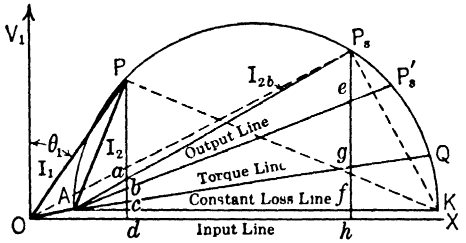

FIG 650. Approximate circle diagram of the polyphase induction motor

893. Special Scales for Use with the Circle Diagram. — (a) *Slip scale.* In Fig. 651 a construction line is drawn from Q through P_s' and of indefinite length. A line is then drawn perpendicular to the radial line QM, intersecting the line AQ at 0 (zero) and QP_s' at $S = 100$. This is the slip scale. Its exact location is immaterial, it being only necessary that its length between AQ and QS be easily divisible into 100 parts. To read on this scale the slip corresponding to the operation of the motor at some point P on the circle, lay a straight-edge from Q to P and read the slip Oa'. To prove that Oa' is slip to the chosen scale it is necessary to show that $Oa'/OS = ab/Pb$.

Proof. Angles cAb and MQO are equal (isosceles triangle), and of value α. Then

$$\angle Aba = \angle QOa' = (90^\circ + \alpha) \quad .$$

Angles APa and $a'QO$ are equal, since they are interior angles subtending equal chords (chords AP and AP'). Therefore triangles AbP and $a'OQ$ are similar. As a result

$$Ab/Pb = Oa'/OQ \quad . \; . \; . \; . \; . \; . \; . \; . \; . \; . \quad (20)$$

Also, triangles aAb and OSQ are similar since, as shown above, angles Aba and QOa' are equal. Likewise angles bAa and QSO are equal, as may be seen as follows: Extend QM to L and draw $P_s'L$. Then $\angle P_s'LQ = \angle aAb$ (subtend the same chord). But LP_s' and SQ are perpendicular; also LQ and Sa' are perpendicular (by construction). Therefore,

$$\angle P_s'LQ = \angle OSQ = \angle aAb.$$

This makes triangles bAa and OSQ similar, so that

$$ab/Ab = OQ/OS, \quad \text{or}$$
$$OQ = ab \times OS/Ab \quad . \; . \; . \quad (21)$$

Substituting from eq. (21) into eq. (20) gives

$$Oa'/OS = ab/Pb = \text{slip}$$

which proves the slip scale.

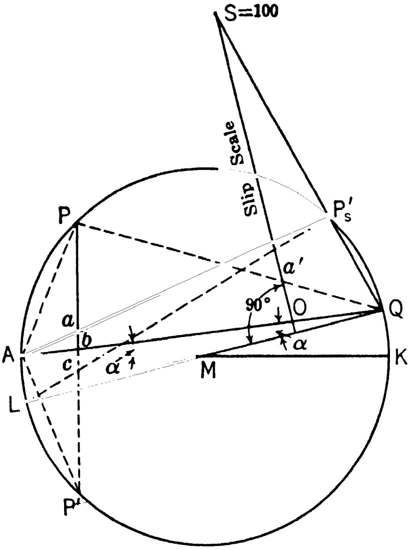

FIG. 651. Constructions to prove the slip scale.

It is usually preferable to show only the lower part of the slip scale, say to 10 per cent, much enlarged and located near the points of operation on the circle, in order to increase the accuracy of slip readings (see Fig. 652). This is done by first locating the point P on the circle at which the slip is 10 per cent and drawing the local slip scale accordingly.

(b) *Efficiency scale.* The efficiency scale is drawn parallel to the input line, OX (Fig. 652), with the zero of the scale at N on the line AP_s' extended, and 100 per cent at N_1 vertically above the intersection, l, of $P_s'A$ with OX. Then (Fig. 652) triangles ldP and N_1nl are similar (parallel sides); also triangles adl and N_1lN, for the same reason.

Therefore $ad/ld = N_1l/N_1N$, also $ld/Pd = nN_1/N_1l$ or $N_1l = nN_1 \times Pd/ld$.

Substituting and solving

$$ad/Pd = nN_1/NN_1 = \text{per cent loss}$$

Since nN_1 gives the per cent loss, Nn gives the per cent efficiency. Figure 652 is the complete (approximate) circle diagram for the polyphase induction motor with scales of slip, efficiency, power factor, and kilowatt input. The complete circle is shown with scales denoting both motor and generator performance (§901). It should be noted that

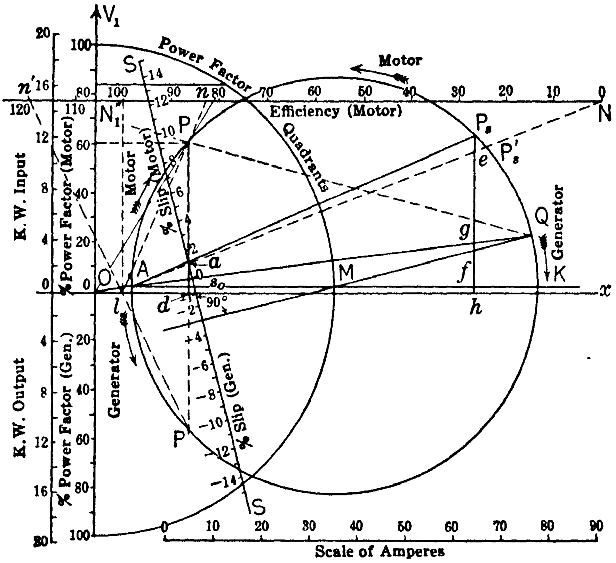

FIG. 652. Complete circle diagram (approximate) for the induction motor and generator, including various convenient scales.

efficiency of the generator is expressed as the ratio of N_1N to $n'N$, or per cent loss by the ratio $n'N_1/n'N$, so that the scale is no longer uniform, as it was for the motor, and the zero of the scale is at an infinite distance to the left. However, the uniform scale could be extended to the left to values greater than 100 per cent, it being understood that such values express the input, in terms of output, or the reciprocal of efficiency.

The upper part of the circle represents motor operation, from running light at A to rotor blocked at P_s and being driven backward by some external force from P_s to Q, where the slip would be minus infinity. Generator action is from A downward on the circle, with slip negative and infinite when the current vector has come again to the point Q. Thus the complete circle is utilized, although part of it represents impractical operation.

To illustrate the readings obtained from the circle diagram, values are taken from the several scales for the point *P*. At *P* the line *OP* represents a stator current of 36 amperes, according to the current scale. *OP*, extended to the power-factor circle and horizontally to the power-factor scale, gives a reading of 83 per cent power factor. A line to the left from *P* to the input scale shows 11.3 kw input. This being a 240-volt, three-phase motor, $3V_1I_1 \cos\theta_1 = \sqrt{3} \times 240 \times 36 \times 0.83 =$ 11,400 watts, which is a fair check. The line *CP* extended to slip scale shows 10 per cent slip. Line *lP*, extended, cuts efficiency scale at about 82 per cent. *Pa*, interpreted in terms of watts output, gives about 9.3 kw, which, for an input of 11.4 kw, gives an efficiency of 81.5 per cent — again a fair check. The data used in drawing this diagram were obtained from tests of a 10-horsepower, 240-volt, three-phase motor with wound rotor.

From the circle diagram it is easy to determine points of maximum efficiency, maximum power factor, maximum input, pull-out torque, starting torque, etc., and to read off these values. Unless the performance of the induction motor was read from the complete circle diagram and compared with the characteristic curves obtained from load test, in Experiment 22-F, this should be done here, making use of the special scales described above. The degree of agreement of results by the two methods should be fully discussed.

The application of the circle diagram to the induction motor operating as a generator will be further explained after the general theory of the induction (asynchronous) generator has been taken up (§899).

894. Some Other Methods of Predicting Induction Motor Characteristics. — The circle diagram is the standard graphical method of predicting induction motor characteristics; the equations resulting from the equivalent diagram constitute the standard analytical method of treatment. Some modifications of the graphical method may be of interest.

(a) *The method of tangents.* Let an induction motor be started at its full rated voltage and allowed to run up to speed, without any load. Its current vector then describes the locus P_sPA (Fig. 650), the inertia of the revolving part acting as a load. Let a polyphase wattmeter arrangement (§105) and a power-factor meter (§109) be included in the circuit. The indications of these instruments vary too rapidly to allow of any readings during the acceleration period, but the maximum deflection can be estimated quite accurately, for example, by following the pointers with a sharp pencil as long as the deflection increases. The maximum reading of the wattmeter, or the maximum input, gives the vertical distance between *Ox* and the horizontal tangent to the circle at its highest point. The maximum reading of the power-factor meter gives the cosine of the angle between OV_1 and the tangent to the circle from O.

Thus, the circle is determined not only by the vectors OA and OP_s, but by two tangents as well, and can therefore be drawn much more accurately. There is always some uncertainty about the point P_s because of the large currents involved in the short-circuit test. Even should it be necessary to start the machine at a fractional voltage, it can be switched over to the full voltage before the maximum indications of the two instruments have been reached. This is especially true of the maximum power factor. With a small machine, a flywheel can be attached to reduce the acceleration and to make it possible to observe the points of maxima with more certainty.

(b) *The photographic method.* This is a further development of method (a). In addition to the wattmeter and the power-factor meter, an ammeter and an electrical tachometer are used, the four instruments being mounted close to each other. As the motor accelerates from standstill to full speed, a series of instantaneous photographs of the foregoing instruments are taken with a high-speed camera under strong illumination. The indications of the instruments are later read from the photographs, the data are plotted in the form of current vectors, and the most probable circle is drawn through the points so obtained. This circle checks satisfactorily with one drawn from the no-load and short-circuit readings.[2]

(c) *Alignment chart or nomogram.* Professor R. G. Warner has constructed an ingenious computing device, consisting of movable and stationary scales, by means of which the principal performance characteristics of a motor may be read off directly, without constructing a circle diagram. The data required to use this nomogram are the same as those necessary to construct a circle diagram, namely, the voltage, the current, and the power at no load and with the rotor locked, and the primary resistance.[3]

(d) *The indumor.* A kinematic computing device has been constructed, with linkages which represent the various vectors shown in Fig. 660. Proper mechanical constraints are provided to satisfy the electrical conditions. To vary the load, certain linkages are moved, and the constraints cause the relationships to be correct with any possible setting. An original setting is made for the given motor constants, and the principal performance characteristics can be determined by simply reading certain lengths and angles, as on any vector diagram.[4]

---

[2] See a thesis by S. Y. Lung and M. M. Morisuye, Cornell University, February, 1923.

[3] R. G. Warner, *Journal A.I.E.E.*, vol. 40 (1921), p. 808.

STARTING AND SPEED CONTROL ANALYZED BY MEANS OF CIRCLE DIAGRAMS

895. Effect of Rotor Resistance upon Motor Performance. — (a) *Starting torque.* Circle diagrams such as Fig. 650 may be used to analyze quickly the effects of changing supply voltage, changing frequency, or added resistance in the rotor, upon such items as starting torque, speed, power factor, etc., in the performance of the motor. Several such analyses follow. In Fig. 653 the circle diagram is drawn for a certain motor, at a fixed voltage, V_1, and frequency, f, but with rotor resistance progressively increased. This gives rotor-blocked or starting points P_s, P_{s1}, P_{s2}, etc. With only the resistance r_2 of the rotor windings, the starting torque $= K\,P_s g$. Starting current is OP_s, power factor is shown by the point t. Adding resistance r_x to the rotor increases starting torque to a value shown by $P_{s1}g_1$, starting current diminishes to OP_{s1}, at power factor t_1, etc. Calling angle $P_sAK = \beta$,

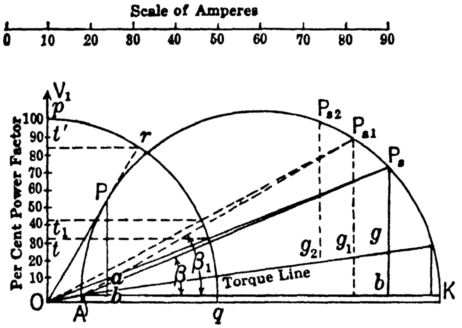

FIG. 653. Diagram showing influence of rotor resistance upon starting torque, speed, etc

$$\tan\beta = (r_1 + r_2)/x_e \quad . \; . \; . \; . \; . \; . \; . \; . \; . \quad (22)$$

For any added resistance, r_x,

$$\tan\beta_1 = (r_1 + r_2 + r_x)/x_e \quad . \; . \; . \; . \; . \; . \; . \; . \quad (23)$$

and

$$r_x = x_e \tan\beta_1 - (r_1 + r_2) \quad . \; . \; . \; . \; . \; . \quad (24)$$

By calculating values of $\tan\beta$ for various values of added resistance, r_x, points P_{s1}, P_{s2}, etc., are located for each value of r_x, and the items listed above may be read from the diagram. Figure 365, Vol. I, gives curves so obtained on a 10-horsepower motor for which Fig. 652 also was drawn. Although the circle diagram has been used to derive the curves of Fig. 365, it is obvious that the same values might have been calculated from eqs. (16) and (19) for $s = 1$, replacing r_2 by $(r_2 + r_x)$.

---

[4] V. Karapetoff, *Trans. A.I.E.E.*, vol. 41 (1922), p. 177.

(b) *Speed as a function of rotor resistance.* The same diagram which was used to study starting conditions in the motor may be used to find the values of slip, speed, efficiency, etc., which result from the insertion of various values of r_x, when the motor is running and delivering a fixed torque, with V_1 and f constant. Assuming that for each value of rotor resistance the motor speeds up until the point P is reached on the diagram, the torque will be shown by the height Pb. For the several values of rotor resistance, $(r_2 + r_x)$, current input and power factor will remain the same, but slip will be measured by successively greater values of the ratio ab/Pb, as point a moves up onto each new output line, AP_{s1}, AP_{s2}, etc. Values from Fig. 653 are plotted in Fig. 654 to show the variation of speed and efficiency with added rotor resistance.

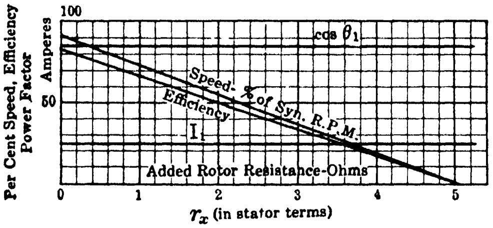

FIG. 654. Curves of speed, etc., against rotor added resistance at constant torque (from the circle diagram).

896. Effects of Varying Applied Voltage. — Circle diagrams to show the influence of varied voltage at constant frequency upon the starting torque or speed might be drawn in either of two ways: (a) Several circles of changing diameter $(I_d = V_1/x_e)$ might be drawn, all to the same scale of amperes. Then, from eq. (13a), starting torque being proportional to V_1, to P_sg, and to k (amperes per inch of diagram), since k is constant and P_sg is proportional to V_1, the starting torque will be proportional to V_1^2. This follows also from eq. (19). Assuming that exciting current is proportional to V_1 it is seen that starting current will be proportional to V_1, and $\cos \theta_1$ will be constant.

(b) A single circle diagram may be used for the several values of V_1, it being necessary only to change the scale factor k in proportion to the voltage. Then a single height P_sg would represent a different value of current, proportional to k (or V_1). Starting torque would again be seen to vary as V_1^2 (eq. 13a), since both V_1 and k vary.

Speed control by varying applied voltage may be studied by the diagrams of Fig. 655, drawn for normal V_1, $0.8V_1$, and $1.2V_1$. Points P_2, P, and P_1 represent the same torque at these several voltages. Note that the lengths Pb are inversely as the voltages (eq. 14). Speed being given by Pa/Pb, it is seen that for voltages near normal and above there is little change in speed, but the point P_2 being near the maximum torque point for $0.8V_1$ the motor has slowed down materially and, at any further reduction of voltage, will stall. Curves of speed, efficiency, and current obtained from the circle diagrams of Fig. 655 are drawn in Fig. 656.

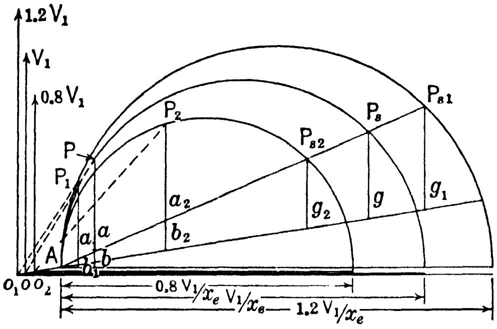

FIG. 655. Circle diagrams for applied voltages of $0.8V_1$, V_1, and $1.2V_1$ to study the effect of voltage upon starting torque, etc.

As stated above the same results might be read from a single circle, the scale factor, k, being changed in direct proportion to V_1. This would mean that the height Pb, representing a constant torque, would vary inversely as the voltage, V_1 (eq. 14), thus locating a series of points P, all corresponding to the same torque.

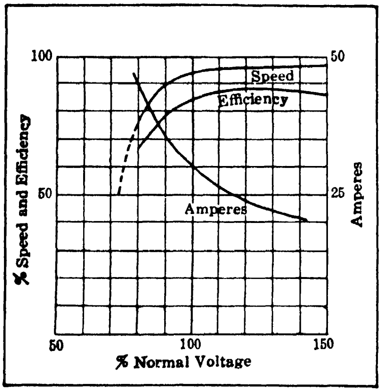

FIG. 656. Motor performance as a function of voltage (frequency and torque constant).

897. Effects of Changing Frequency. — It is evident from the foregoing discussion that, although a wide range of speed is possible in the induction motor by varying rotor resistance, this speed reduction (Fig. 654) is accompanied by a corresponding reduction in efficiency. Speed control by varying the applied voltage was seen to be very limited in extent, although with a satisfactory efficiency (Fig. 656). A wider range of speed control at good efficiency may be expected from operation at varying frequency. This problem may also be analyzed by means of the circle diagram.

Since I_d has the value

$$I_d = V_1/x_e = V_1/2\pi f L_e \quad . \ . \ . \ . \ . \ . \ . \ . \quad (25)$$

for constant applied voltage, variable frequency, $I_d = K/f$. Therefore, to make it possible to use the same circle at various frequencies, the scale factor, k, would need to vary inversely as f. From the emf equation of a-c machines (eq. 3, Chapter XX), or

$$E = 4.44k_d f n p \phi \, 10^{-8} \quad \ldots\ldots\ldots \quad (26)$$

it is evident that if E remains constant while f varies, the flux per pole, ϕ, must vary inversely as f. This means that with lowered f, or increased ϕ, the magnetic circuit of the motor will approach saturation, and the no-load current will increase more rapidly than ϕ so that it will be quite in error to represent the exciting current by a constant length OA, even though k is varied inversely with f.

A more logical method of speed control would result if f and V_1 were to vary in direct proportion. Then (eq. 26) ϕ would remain constant, as would the exciting current OA (Fig. 657a), except for the change in its power component due to changing no-load losses. This change may be ignored in a study of general effects, such as are being investigated by means of the circle diagram.

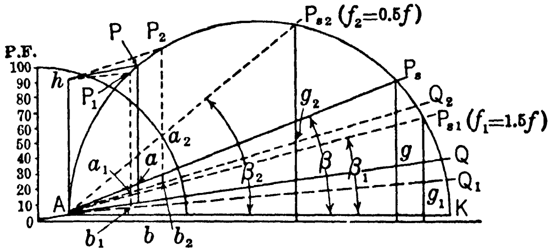

Fig. 657(a). Circle diagram for constant torque, variable frequency (V_1/f constant).

Now, if f and V_1 are kept in direct proportion, I_d will remain constant (eq. 25), and k, the scale factor, need not change. Thus, a single circle will serve to give motor performance with changing f and V_1. But x_e varies directly with frequency and (eq. 22) $\tan \beta = (r_1 + r_2)/x_e$ (Fig. 657a) so that, since r_1 and r_2 are constant, $\tan \beta$ will change inversely with f, or

$$\tan \beta_1 / \tan \beta = f/f_1 \quad \ldots\ldots\ldots \quad (27)$$

where $\tan \beta$ gives the slope of AP_s at normal voltage and frequency. This is illustrated in Fig. 657a, in which it is seen that the positions of both the output line and the torque line vary as f is changed. In eq. (14) torque is seen to vary directly with k, V_1, and Pb, but inversely with N_s, the synchronous speed. Since $N_s = 120f/p$, where f is in cycles per second and p is the number of poles on the motor, eq. (14) may be written

$$T = (7.04mkV_1Pb)/(120f/p) \quad \ldots\ldots \quad (28)$$

or

$$T = CkV_1Pb/f \quad \ldots\ldots\ldots\ldots \quad (29)$$

In the conditions stated above k and V_1/f are assumed to be constant; therefore Pb will be of constant length for constant torque. However, the point P must change its position on the circle since the torque line Ab changes its slope with frequency (eq. 27). Consider that with normal V_1 and f the motor operates at the point P on the circle, torque being shown by Pb. A vertical line Ah is then erected of length Pb. To locate points on the circle at which the motor will operate for frequencies of f_1 and f_2 lines are drawn from h parallel to Ag_1 and Ag_2 to intersect the circle at P_1 and P_2. By dropping vertical lines from these points to the respective torque lines and noting their intersections with the output lines the various items of performance may be read. These are shown in Fig. 657b.

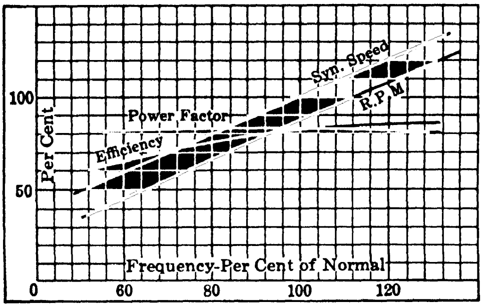

FIG. 657(b). Motor performance as a function of frequency.

898. EXPERIMENT 47-C. — Speed Control of the Induction Motor by Tests and as Predicted by the Circle Diagram. — Connect a wound-rotor induction motor to an a-c source of adjustable frequency and voltage. Insert variable (balanced) resistances in the rotor circuits. Couple the motor to an electrodynamometer, a Prony brake, or a separately excited shunt d-c generator connected to a variable load. In the tests which follow, if a generator is used for loading the motor, hold the armature and field currents constant in order to insure an essentially constant torque of a value approaching one-half normal load torque of the motor. Arrange to read stator amperes, volts, watts and frequency, rotor amperes (a very low-impedance meter is required), rpm and volts; also the d-c armature and field currents.

(a) *Speed control by rotor resistance.* Keep the output torque of the motor constant and maintain constant supply frequency and voltage. Having started the motor, hold the rotor resistances respectively equal and vary their value from zero to the maximum at which the motor can deliver the required torque. At each point take all the readings provided for above.

(b) *Control by varying voltage.* Again holding output torque constant, and with no added resistance in the rotor circuits, vary the applied voltage of the motor while keeping frequency constant. Hold torque constant as before, and vary applied voltage from an upper value at which the exciting current of the motor becomes excessive, to the lowest at which the motor can drive the load. Take all electrical readings, the rpm, and the slip.

(c) *Control by varying voltage and frequency.* Repeat (b) but with the ratio of voltage to frequency held constant at the normal value, and both varied from the minimum V and f at which the motor can carry the load, to values at which the motor reaches its maximum safe speed. Take all readings, including slip.

(d) Repeat (c), varying the frequency but keeping applied voltage constant at normal value.

(e) Unless complete data are available on the motor for drawing circle diagrams, take running light, rotor-blocked, and resistance data. Be sure to measure rotor resistance with currents covering the range of values read in the tests, since brush-contact resistance makes this resistance variable. Measure the ratio of transformation of the motor by applying rated stator volts with the rotor circuit open and reading rotor volts. Repeat, applying a similar rotor voltage, and read open-circuit stator volts. Letting V represent applied voltages and E the induced values, the ratio of transformation is

$$a = \sqrt{\frac{V_1E_1}{E_2V_2}} \quad . \; . \; . \; . \; . \; . \; . \; . \; . \; . \; . \quad (30)$$

Report. Plot observed data in the form of curves of dependent variables against independent variables (see Figs. 654, 656, and 657). Construct the necessary circle diagrams (Figs. 653, 655, and 657), and from them plot curves corresponding to those obtained by direct test. Compare the curves by the two methods and comment upon the two ways of obtaining the necessary values. In particular discuss the value of the circle diagram as a means of analyzing the performance of the motor under a wide variety of conditions.

THE INDUCTION GENERATOR

899. Assume that a polyphase induction machine, of the type described in the preceding chapters, is connected to an a-c network supplied with power from synchronous generators. Assume these alternators to be quite large as compared with the rating of the induction machine, so that in effect the induction machine is connected to an "infinite bus." Let the induction machine be driven by a prime mover at a speed a few per cent above its synchronous speed, in the direction of rotation of its magnetic field. Wattmeters in the line will then show that the induction machine delivers power to the line, operating as a generator. The same conclusion will be reached by noting that the prime mover becomes loaded and delivers power to its shaft.

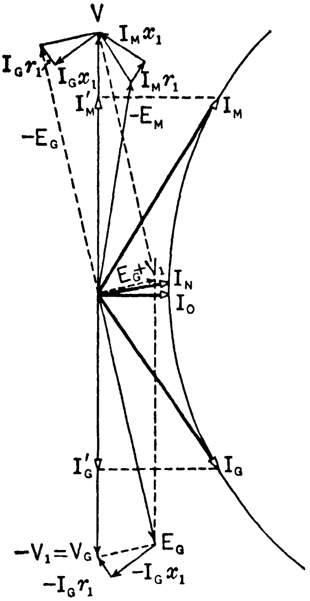

FIG. 658. Vector relations in the induction machine as a motor and as a generator.

By measuring the reactive power or the power factor at the terminals of the induction machine operating at positive slips (as a motor) and at negative slips (as a generator) (Fig. 658), it will be found: (a) that the power component of the line current, I_G', is reversed in phase, compared with that (I_M') when operating as a motor, and (b) that the reactive component of the current, I_0, is in the same direction whether the machine operates as a generator or as a motor. These conditions may be expressed in two equivalent ways, viz., (1) an induction generator always operates at a leading power factor, or (2) an induction generator always draws a lagging current from the line. In the first statement we have in mind the phase position of I_G relative to the *generator voltage*, $V_G = -V_1$; in the second statement, the phase of I_0 relative to the *line, or supply, voltage*, V_1.

900. Theory of the Induction Generator. — When the rotor conductors of an induction motor are being revolved at a velocity higher than that of the magnetic field, the emf induced in these conductors, and consequently the current, is opposite to that in motor operation (positive and negative slip). The total primary flux must remain of essentially the same value and in the same phase relation to the terminal voltage, whether the machine is operating below or above synchronism, since this flux has to balance the same applied voltage (less a small ohmic drop). The secondary mmf being reversed, the primary mmf must also be changed accordingly, in order to give approximately the same magnetizing current as in motor operation.

The induction generator, not being provided with d-c excitation, has to have its magnetic field excited from the a-c line, and therefore must operate in parallel with at least one synchronous machine or another device which is able to furnish the required reactive current. The frequency of the power current, furnished by the induction generator, is equal to and determined by the frequency of the synchronous exciter. Just as the lagging reactive component of current taken by an induction motor is not all magnetizing current, but is due in part to the leakage reactances of the windings, so the lagging reactive current taken by an induction generator (or the leading current delivered by it, which is the same) is larger than the magnetizing current, for the same reason.

One way of studying the characteristics of the induction generator is by means of the equivalent diagram (Fig. 648). When the machine runs at synchronous speed ($s = 0$), the load resistance $R = \infty$. When the slip becomes negative, the resistance also becomes negative, and at $s = 0$ jumps from $+\infty$ to $-\infty$. Then, as the speed increases, R decreases indefinitely in its absolute value. A negative resistance furnishes energy to the circuit, instead of absorbing it. Therefore, in this range, the machine operates as a generator, and its performance may be computed according to the same formulas as those of the motor (§504). A second method is by means of the circle diagram, as described in the next section.

The field of application of the induction generator is quite limited, mainly because it can furnish only the power component of the total load current. Synchronous generators in parallel with induction generators have to supply all the reactive current of the load and of the induction machines. Where these conditions are not disadvantageous, induction machines have been found both economical and convenient in operation. See bibliography below.

An interesting phenomenon, which occurs when an induction machine passes through synchronism, is a sudden change in the total wattmeter reading. Let the machine be driven at a speed just *below* synchronism and differing from it by an infinitesimal amount. The driving motor supplies the friction and windage losses, while the a-c line furnishes the core loss and the I^2r loss of the magnetizing current. Now let the speed be raised to an infinitesimal amount *above* synchronism. The machine then operates as a generator and the driving motor has to furnish all its losses. The wattmeter reading therefore suddenly drops to zero (unless there are secondary effects of higher harmonics, etc.). This is a sensitive indication of the passage through true synchronism.[5]

[5] G. Benischke, *Elek. Zeits.*, vol. 31 (1910), p. 238.

901. The Circle Diagram of the Induction Generator. — The approximate circle diagram shown in Figs. 651 and 652, as well as the exact diagrams described in Chapter XLVIII, hold true for the induction generator. The generator range is indicated in Fig. 652 with reference to the slip line AQ. At A and for a short portion of the circle below it, the slip is practically equal to zero, corresponding to a change from the motor to the generator action. For a point on the lower semicircle, such as P', a straight-edge laid between P' and Q meets the slip scale s_0S below s_0, that is, in the range of negative slip. Moving from P' to Q, the negative slip increases, indicating a higher and higher speed of the machine, until at Q the line QP' is parallel to Ss_0 and the slip is equal to $-\infty$, the speed of the machine being infinitely great.

All the characteristics enumerated in §§890 and 893 for the motor range may be obtained in a similar manner in the generator range, except that the meaning of the words "input" and "output" is reversed. $P'a$ represents the mechanical input and $P'd$ the electrical output. The power-factor quadrant is simply extended downward; the slip scale is extended downward, and the divisions assumed to be negative. The efficiency scale is extended to the left of N_1, the divisions being 110, 120, 130, etc. Let, for example, a straight-edge laid between P' and l read 120 on the efficiency scale. The efficiency then is $100/1.20 = 83.3$ per cent, in accordance with the changed meaning of the input and output.

902. EXPERIMENT 47-D. — Load Characteristics of a Polyphase Induction Generator. — The theory of the machine is given in the preceding sections. Electrically, the induction machine is connected to an a-c source supplied by synchronous generators of a rating large in comparison with that of the machine under test. Mechanically, it is connected to a d-c shunt-wound machine, so that power may be interchanged between a-c and d-c sources in either direction, depending upon the field strength of the d-c machine. The sign of the total wattmeter reading in the a-c circuit and of the ammeter in the armature circuit of the d-c machine will indicate which machine is operating as a generator. The load test is made in the usual manner, and then data are obtained for the circle diagram (Fig. 652). It is also of interest to observe the sudden change in the wattmeter indication at the passage through synchronism (end of §900).

Report. Plot the performance characteristics and compare them with those predicted from the circle diagram. Note that each power and current output is at a definite value of power factor, while with a synchronous machine the power factor may be varied without changing the current or the power output.

903. EXPERIMENT 47-E. — Parallel Operation of Induction and Synchronous Generators. — The purpose of the experiment is to study various conditions which may arise when synchronous generators operate in parallel with induction generators, in the same plant or in a distant interconnected power plant. Provide a synchronous generator and an induction machine, each driven by a separate adjustable-speed d-c motor. Connect the two a-c machines in parallel, and provide the necessary measuring instruments and a balanced non-inductive load of a value comparable to the rated kva of the asynchronous generator.

(a) Keeping the speed and excitation of the synchronous machine constant, vary the field current of the d-c prime mover for the asynchronous machine, from values at which this machine is well loaded as a motor, to those at which it is well loaded as a generator. Take all electrical readings and slip (including the sign of same) for the asynchronous machine, also the electrical readings of the synchronous machine, being sure in every case of the direction of total power reading of each machine. Plot a-c watts of both machines and power factor of the asynchronous machine against slip.

(b) Having operated the asynchronous machine as both a motor and a generator in (a) connect a synchronous motor in parallel with the balanced non-inductive load across the buses supplied by the synchronous and the asynchronous machines. Now disconnect the synchronous generator and note that the asynchronous machine is able to supply power for the non-inductive load and for the synchronous motor. Determine how the excitation of the latter affects the a-c voltage, and how the mechanical input to the asynchronous machine affects the system frequency. Attempt to replace the synchronous motor by a static capacitor capable, at rated voltage and frequency, of absorbing a current equal to the magnetizing current of the asynchronous machine. Try the effects of increasing or decreasing this capacitance and of varying the power input to the asynchronous machine. Take sufficient data to permit the drawing of curves. Discuss the results obtained in (a) and (b) and draw conclusions as to the advantages, the disadvantages, and the best field of application of induction generators.

BRAKING OF INDUCTION MOTORS

904. Consider an induction motor operating a hoist, a locomotive, or some such machine, which, among other duties, has to lower heavy unbalanced loads. Four methods of braking may be used:

(a) Mechanical brakes.
(b) Regenerative braking.
(c) Dynamic braking.
(d) Motor counter torque.

Regenerative braking consists in allowing the load to accelerate by gravity to a speed slightly above synchronism, with the motor connected to the line. It then operates as an induction generator (§899) on the part AP' (Fig. 652) of the circle diagram, returning electric power to the line. This prevents the load from accelerating to a dangerous speed. To stop the hoist or the train, it is necessary to use mechanical brakes or to throw the motor into the first or second point of the "reverse." The regenerative method of braking is economical, but is practicable only for fairly long cycles in which there is sufficient time for the manipulation of the control.[6] It is used in a-c railway service when the train is running down a long grade.

Dynamic braking consists in supplying d-c excitation to the stator windings of the induction motor and obtaining speed control by a secondary rheostat. This method requires a phase-wound rotor and a source of d-c power, but allows a considerable range of lowering speeds and is economical in power consumption.[7]

Motor counter torque is developed by connecting the induction motor to the line so that it tends to lift the load while the load in reality is being lowered. This method is sometimes referred to as "plugging" the motor. It is simple and effective, but is very wasteful of energy and requires a heavy-duty rheostat. Moreover, it causes practically a double voltage and frequency to be induced in the rotor at the instant of reversal. While the motor is being rotated against its magnetic field, it absorbs mechanical power from the shaft and also some electric power from the line. All this power is converted into heat in the machine itself. On the circle diagram (Fig. 652) the "brake" range lies between the points P_s and Q. At P_s the slip is 100 per cent and at Q it is infinitely great. For any point on the circle in this range, the electrical input, i.e., the distance Pd, is positive, indicating that the machine is taking power from the line. At the same time the mechanical output, or the distance Pa, is negative, showing that mechanical power is being delivered from the lowered load.

905. EXPERIMENT 47-F. — Study of Various Methods of Braking the Induction Motor. — Three available methods are described in the preceding section. The purpose of the experiment is to try these methods under adequate laboratory conditions, with a view to becoming familiar with the details and limitations of the methods. Conclusions should be drawn as to the advantages, disadvantages, and particular fields of application of each method. An asynchronous motor with a phase-wound rotor should be available.

---

[6] K. L. Hansen, *Electrical World*, vol. 84 (1924), p. 846; H. G. Jungk, *Electric Journal*, vol. 13 (1916), p. 371.

[7] For details see T. P. Kirkpatrick, *Electric Journal*, vol. 20 (1923), p. 131; H. C. Specht, *Trans. A.I.E.E.*, vol. 31 (1912), p. 627.

906. The Performance of Polyphase Induction Motors on an Unsymmetrical Voltage Supply. — As another example of the use of the equivalent circuit (Fig. 648) and of the approximate circle diagram, consider the application of the method of symmetrical components (Chapter XXXIV) to the calculation of the performance of induction motors operating on unbalanced voltage systems.

The method of symmetrical components makes it possible to analyze cases in which the resistance and reactance of the windings in revolving machines are different for currents of opposite phase sequences. In Chapter XXII and in the earlier part of this chapter the performance of the induction motor operating on a symmetrical voltage supply has been determined, both by analytical and by graphical methods. The equations of the analytical method will apply in the method of symmetrical components for unbalanced voltages. The procedure is as follows:

(a) Resolve the unsymmetrical voltage supply into positive- and negative-sequence components (§§711 and 713).

(b) Calculate the motor impedance for each sequence, remembering that for a slip of s to the field produced by the positive-sequence currents, the slip is $2 - s$ to the field caused by those of negative sequence, and the rotor resistance, which has essentially the ohmic (d-c) value for ordinary slips, will be materially greater at a slip of $2 - s$, to negative-sequence components.

(c) Find the performance items, such as horsepower and torque, separately for the positive- and negative-sequence voltages, and subtract to obtain the resultant performance.

(d) Combine currents of opposite sequence to obtain total current in each phase, and the total volt-amperes. Find total watts input, motor power factor, total torque, total output, and efficiency.

907. Notation for Solution by Symmetrical Components. — Since the subscripts 1 and 2 were used in the method of symmetrical components to denote positive and negative sequences, respectively, it will be necessary to change the notation used in the earlier treatment of the motor, as follows:

V_{ab}, V_{bc}, and V_{ca} constitute the unsymmetrical three-phase voltage supply.

V_{n1} = positive-sequence volts to neutral.

V_{n2} = negative-sequence volts to neutral.

s = per-unit slip to positive-sequence field.

R_s = stator effective resistance, at supply frequency.

X_e = equivalent reactance, stator plus rotor, from blocked-rotor test.
X_s = stator reactance, assumed $X_e/2$.
$Z_s = \sqrt{R_s^2 + X_s^2}$ = stator impedance.
R_r = rotor ohmic resistance.
R_{r2} = rotor effective resistance, at slip near 200 per cent.
I_{r1} = positive-sequence rotor current per phase.
I_{r2} = negative-sequence rotor current per phase.
I_s = total stator current.
I_{n1} = positive-sequence exciting current. NOTE: Negative-sequence exciting current is negligible both because of the small value of negative-sequence potential with any ordinary degree of voltage unbalance, and because of the low impedance to negative-sequence current — see eq. (32).
T_1 = torque due to positive-sequence current.
T_2 = torque due to negative-sequence current.
P_1 = power developed due to positive-sequence current.
P_2 = power developed due to negative-sequence current.
P_0 = total power developed.
m = number of phases.
N_s = synchronous speed, rpm.
T_0 = total torque developed.
W_0 = power input.
η = efficiency.
$\cos\theta$ = power factor.
VA = vector volt-amperes input.
VAR = reactive volt-amperes.

Analytical solution of performance[8] (see §504, Vol. I)

$$\dot{I}_{r1} = \frac{\dot{V}_{n1} - \dot{I}_{n1}Z_s}{R_s + R_r/s + jX_e} \qquad (31)$$

$$\dot{I}_{r2} = \frac{\dot{V}_{n2}}{R_s + (R_{r2})/(2 - s) + jX_e} \qquad (32)$$

$$I_s = I_{r1} + I_{r2} + I_{n1} \text{ (vectorial)} \qquad (33)$$

$$P_1 = m \times I_{r1}^2R_r(1 - s)/s, \text{ watts} \qquad (34)$$

$$P_2 = mI_{r2}^2R_{r2}(1 - s)/(2 - s), \text{ watts} \qquad (35)$$

$$T_1 = 7.04/N_s \times mI_{r1}^2R_r/s, \text{ lb-ft} \qquad (36)$$

$$T_2 = 7.04/N_s \times mI_2^2R_{r2}/(2 - s), \text{ lb-ft} \qquad (37)$$

$$T_0 = T_1 - T_2 \qquad (38)$$

---

[8] See Wagner and Evans, "Symmetrical Components," Chapter 15, McGraw-Hill Book Co.

$$P_0 = P_1 - P_2 \quad \ldots\ldots \quad (39)$$

$$\begin{aligned} VA &= \sum \hat{E} I_s \\ &= (W_a + W_b + W_c) - j(VAR_a + VAR_b + VAR_c) \quad . \quad (40) \end{aligned}$$

$$\cos\theta = \frac{W_a + W_b + W_c}{[(W_a + W_b + W_c)^2 + (VAR_a + VAR_b + VAR_c)^2]} \quad (41)$$

$$\eta = P_0/W_0 \quad \ldots\ldots \quad (42)$$

908. Analytical Solution of the Unbalanced Case. — These equations will be illustrated by calculating the performance of the motor for which the circle diagrams of §§893 to 897 were drawn.

Given:

$$V_{ab} = 270\underline{/0^\circ}, \quad V_{bc} = 240\underline{/-132^\circ}, \quad V_{ca} = 210\underline{/121.6^\circ}$$

or

$$V_{ab} = 270 + j0, \quad V_{bc} = -160 - j179, \quad V_{ca} = -110 + j179$$

$R_s = 0.23\omega$, $R_r = 0.387\omega$, $R_{r2} = 0.52\omega$, $X_e = 1.65\omega$, $I_{n1} = 1.02 - j7.94$ amperes at 240 volts, balanced, between lines, or 138.6 volts per phase.

(a) *Sequence components of line voltages*

From eq. (18), Chapter XXXIV

$$\begin{aligned} V_{ab1} &= \tfrac{1}{3}(V_{ab} + V_{bc} + V_{ca}) = \tfrac{1}{3}[V_{ab} - 0.5(V_{bc} + V_{ca}) + j0.866(V_{bc} - V_{ca})] \\ &= [270 - 0.5(-270) + j0.866(-50 - j358)] \times 1/3 \\ &= 238.3 - j14.4 = 238.7\underline{/-3^\circ 28'} \end{aligned}$$

From eq. (21), Chapter XXXIV

$$V_{ab2} = V_{ab} - V_{ab1} = 31.7 + j14.4 = 34.8\underline{/24.5^\circ}$$

(b) *Phase voltages* (eqs. 32 and 33, Chapter XXXIV)

$$V_{an1} = (1/\sqrt{3})V_{ab1}\underline{/-30^\circ} = 137.7\underline{/-33.5^\circ} = 114.7 - j76.1$$

$$V_{an2} = (1/\sqrt{3})V_{ab2}\underline{/30^\circ} = 20\underline{/54.5^\circ} = 11.6 + j16.3$$

$$I_{n1}Z_s = (1.02 - j7.94)(137.7/138.6)(0.23 + j0.825) = 6.75 - j0.99$$

$V_{an1} - I_{n1}Z_s = 108 - j75.1 = 131.8\underline{/-34.9^\circ}$ volts per phase

At a slip of 10 per cent:

$R_r/s = 3.87$ ohm, $R_r/s - R_r = 3.49$ ohm, $R_s + R_r/s = 4.1$ ohms, $X_e = 1.65$ ohms

$$(R_s + R_r/s)^2 + X_e^2 = 19.54$$

$G_{r1} = 4.1/19.54 = 0.21$ mho; $B_{r1} = 1.65/19.54 = 0.0843$ mho

$$Y_{r1} = 0.21 - j0.0843 = 0.2265\underline{/-21.9^\circ}$$

$I_{ar1} = V_{an1}Y_{r1} = 131.8\underline{/-34.9^\circ} \times 0.2265\underline{/-21.9^\circ} = 29.85\underline{/-58.8^\circ} = 16.37 - j25.0$ amperes

$R_{r2}/(2 - s) = 0.52/1.9 = 0.2735$ ohm; $R_s + R_{r2}/(2 - s) = 0.5035$ ohm; $[R_s + R_{r2}/(2 - s)]^2 + X_e^2 = 2.973$

$G_{r2} = 0.5035/2.973 = 0.1693$ mho; $B_{r2} = 1.65/2.973 = 0.556$ mho

$$Y_{r2} = 0.58/-73.3^\circ$$

$I_{ar2} = 20\underline{/54.5^\circ} \times 0.58\underline{/-73.3^\circ} = 11.6\underline{/-18.8^\circ} = 10.96 - j3.74$ amperes

$I_{an1} = -3.51 - j7.15$ (referred to V_{ab}) $= 7.96\underline{/-116.2^\circ}$

(c) *Line currents*

$I_a = I_{ar1} + I_{ar2} + I_{an1} = 29.85\underline{/-58.8^\circ} + 11.6\underline{/-18.8^\circ} + 7.96\underline{/-116.2^\circ} =$ $23.82 - j35.89 = 43.1\underline{/-56.4^\circ}$ amperes

$I_b = 29.85\underline{/-176.8^\circ} + 11.6\underline{/101.2^\circ} + 7.96\underline{/123.8^\circ} = -36.47 + j16.32 =$ $40\underline{/156^\circ}$ amperes

$I_c = 29.85\underline{/63.2^\circ} + 11.6\underline{/-138.8^\circ} + 7.96\underline{/3.8^\circ} = 12.69 + j19.6 = 22.35\underline{/57.2^\circ}$ amperes

(d) *Output*

$P_0 = 3[I_{r1}^2R_r(1 - s)/s - I_{r2}^2R_{r2}(1 - s)/(2 - s)]$

$3[29.85^2 \times 3.49 - 11.6^2 \times 0.9 \times 0.2735] = 9230$ watts, inclusive of friction plus windage of 250 watts

or the net output is

$$P_0' = 9230 - 250 = 8980 \text{ watts} = 12.05 \text{ horsepower}$$

(e) *Input*

The vector volt-ampere input is calculated as the sum of the products of line currents by the conjugates of the phase voltages.

Since

$$\begin{aligned} V_{an} &= 137.7\underline{/-33.5^\circ} + 20\underline{/54.5^\circ} = 126.3 - j59.8 \text{ volts} \\ V_{bn} &= 137.7\underline{/-153.5^\circ} + 20\underline{/174.5^\circ} = -143.2 - j58.1 \text{ volts} \\ V_{cn} &= 137.7\underline{/86.5^\circ} + 20\underline{/-66.5^\circ} = 16.4 + j119.2 \text{ volts} \end{aligned}$$

The conjugate voltages are

$\check{V}_{an} = 126.3 + j59.8$; $\check{V}_{bn} = -143.2 + j58.1$; $\check{V}_{cn} = 16.4 - j119.2$ volts

Vector volt-ampere input is

$$\begin{array}{rccccc} VA = & 126.3 + j59.8 & + & -143.2 + j58.1 & + & 16.4 - j119.2 \\ & \underline{23.82 - j35.89} & & \underline{-36.47 + j16.32} & & \underline{12.69 + j19.6} \\ & 5160 + j3110 & + & 4275 - j4445 & + & 2543 - j1190 \end{array}$$

$$= 11{,}980 - j8755 = 14{,}850 \text{ volt-amperes}$$

Input (real component of VA) $= 11{,}980$ watts

Power factor $= 11{,}980/14{,}850 = 0.807$

Efficiency $= P_0'/W = 8980/11{,}980 = 0.75$

(f) *Torque* $= 7.04P_0'/N_s(1 - s) = 7.04 \times 8980/(1200 \times 0.9) = 58.6$ lb-ft

909. The Circle Diagram Applied to Unbalanced Voltages. — From the equations used in the analytical solution (§908) it should be possible to adapt the circle diagram to the case of unsymmetrical voltage supply.

The voltage system having been resolved into two systems of opposite rotation, two circles may be drawn to the same scale and for the particular values of positive- and negative-sequence voltages which have been found; or a single circle may be drawn, corresponding to normal voltage, and the scale changed to correspond to the component voltages. Owing to the different resistances, R_r and R_{r2}, to positive- and negative-sequence currents in the rotor, different output lines must be used in the diagram, as shown in Fig. 659, which is drawn for the same motor for which analytical calculations were made. Then, for the example of §908, the positive-sequence values are read at p_1 where the slip is 10 per cent, and values worked out for the voltage $V_{n1} - I_{n1}z_s = 131.8$ volts. For the negative-sequence-component values the point p_2 is found such that slip $= (2 - s) = 1.90$, in the case cited. These values are worked out for a voltage $V_{n2} = 20$ volts. The values as read from the circle diagram of Fig. 659 will be found to check the calculations with reasonable accuracy.

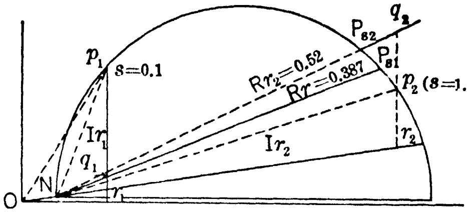

Fig. 659. The circle diagram applied to the case of unsymmetrical voltage supply.

910. EXPERIMENT 47-G. Operation of a Polyphase Induction Motor on an Unsymmetrical Voltage Supply. — This experiment should preferably be performed on the same polyphase motor upon which load tests have already been run with balanced voltage supply (Experiments 22-F and 47-B). An unsymmetrical voltage supply should be secured, say by connecting three transformers, which have a series of secondary taps, in star or delta. The motor should be operated with different degrees of unbalance ("unbalance factors") in the voltage supply, each time loading the motor to the same degree, preferably normal load. All voltages and currents should be read, also watts by the three-wattmeter method, using the neutral of the generator or an artificial neutral if that of the motor is not available. In each case note the no-load voltages as well as the voltages across the loaded motor, and explain the balancing effect of the motor.[9]

Unless already available, the constants of the equivalent circuit of the motor should be taken, by no-load and rotor-blocked tests at rated (balanced) voltages; also the resistances should be taken.

In the report the unsymmetrical voltage supply should be analyzed for positive- and negative-sequence components (§711), and the motor performance should be calculated from the analytical equations (§908) or the circle diagram (§909). Estimate the effect of a given unbalance in the voltage supply upon the heating and, consequently, the proper rating of the motor.

---

[9] O. G. C. Dahl, "Electric Circuits, Theory and Applications," Chapter V, McGraw-Hill Book Co.

APPENDIX

A Proof of the Circle Diagram Based upon Fluxes and Mmf's. — The following proof is based directly upon a consideration of the magnetic fluxes, currents, and voltages in the motor. Let OE_1 (Fig. 660) be the vector of applied voltage and OA_1 the direction of the vector of primary current. Assume at first the primary current to be acting alone and let $OB_1 = \Phi_1$ represent the flux which the primary mmf would produce in the air-gap, that is, the flux which will link with the secondary winding. The total primary flux is greater than OB_1, because of the primary magnetic leakage. Let $OA_1 = v_1\Phi_1$ be the total flux, where v_1 (the primary leakage coefficient) is greater than 1. The portion $B_1A_1 = (v_1 - 1)\Phi_1$ represents the primary leakage flux. We disregard a possible slight saturation in the magnetic circuit and assume the fluxes to be proportional to the mmf's which produce them. Let OA_2 be the direction of the vector of secondary current, as it reacts upon the stator. Let OB_2 be that portion of the flux produced by the secondary currents (acting alone) which links with the primary winding, and let B_2A_2 be the secondary leakage flux. We may write, as for the primary circuit, $OB_2 = \Phi_2$, $OA_2 = v_2\Phi_2$, and $B_2A_2 = (v_2 - 1)\Phi_2$, the factor $v_2(>1)$ being the secondary leakage coefficient.

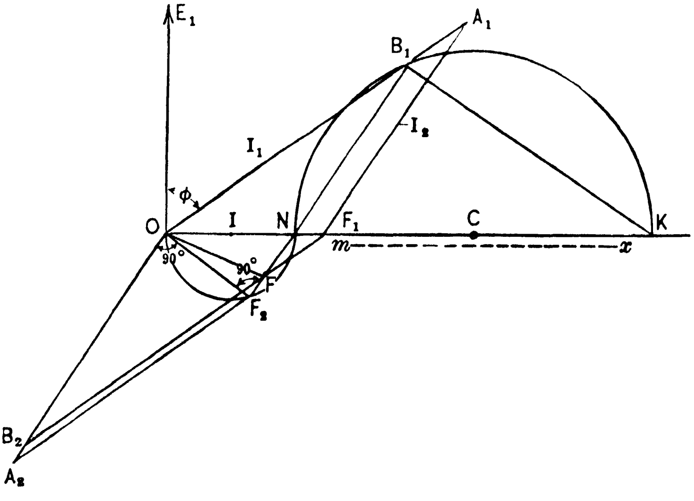

FIG. 660. Development of the circle diagram based on the relations of fluxes and mmf's.

In reality, the primary and the secondary currents act simultaneously, and the actual fluxes in a machine without saturation may be obtained by superposition of the fictitious fluxes considered above. In this manner we obtain the three real fluxes, OF, OF_1, and OF_2. The flux OF_1 is a geometric sum of OA_1 and OB_2, and is therefore the total real flux linking with the primary winding. Similarly, OF_2 is the total real flux linking with the secondary winding. The flux OF is the resultant of the two " transmitted " fluxes, that is, those that cross the air-gap, and therefore is the actual air-gap flux.

The total secondary flux, OF_2, induces in the secondary winding an emf in lagging quadrature with itself, and this emf is spent solely in overcoming the ohmic resistance of the secondary winding. The effect of the secondary leakage inductance is already comprised in OF_2 and need not be considered in the induced emf. To put it in another way, the air-gap flux, OF, induces a secondary emf, part of which is used up in overcoming the secondary resistance and the remainder in overcoming the secondary reactance. But the flux of the secondary leakage reactance is B_2A_2. Hence, resolving OF into two components, of which one, FF_2, is equal to B_2A_2, the other component, OF_2, will give that flux whose induced emf is used up in the secondary ohmic drop. This emf is in phase with the secondary current, OA_2; consequently, OF_2 is perpendicular to both OA_2 and F_2B_1.

Neglecting the primary ohmic drop, OF_1 is constant and lags behind E_1 by 90 degrees. This is because OF_1 must induce in the primary winding an emf equal and opposite to E_1 under all load conditions. But, from the similar triangles OA_1F_1 and OB_1N, if OF_1 is constant, ON must also be constant and equal to OF_1/v_1.

Combining the conditions that OF_2 is perpendicular to F_2B_1 and that ON is constant, it will be seen that the locus of point F_2 is a semicircle with ON as diameter. To prove that the locus of B_1 is also a semicircle, we note that F_2N is always a definite fraction of NB_1. That is, $FB_1 = F_2B_1/v_2$; so that

$$NB_1 = F_1A_1/v_1 = F_2B_1/(v_1v_2) \quad \text{. . . . . . .} \quad (43)$$

and

$$F_2N = F_2B_1[1 - (v_1v_2)^{-1}] \quad \text{. . . . .} \quad (44)$$

Hence,

$$F_2N/NB_1 = v_1v_2 - 1 \quad \text{. . . . .} \quad (45)$$

Since the extremity F_2 of the vector NF_2 moves on a semicircle, point B_1 also moves on a semicircle, NB_1K, turned through 180 degrees. The diameter of this semicircle is determined by the relationship:

$$ON/NK = F_2N/NB_1 = v_1v_2 - 1 \quad \text{. . . . .} \quad (46)$$

The expression:

$$\sigma = v_1v_2 - 1 \quad \text{. . . . .} \quad (47)$$

is of considerable interest in the theory of the induction machine and is known as the leakage factor or *dispersion coefficient*.

Equation (46) becomes

$$NK = ON/\sigma \quad \text{. . . . .} \quad (48)$$

Since OB_1 may be taken as a measure of the primary current, the length *ON*, to the same scale, is the ideal no-load or magnetizing current, without the core-loss component. *OK* is the ideal short-circuit current, that is, the current which the machine would take with the rotor blocked if it had no resistances but only the leakage inductances. To take the core loss and friction into consideration, the origin, *O*, should be shifted down to the line *mx*, as in Fig. 650.[10]

The semicircle obtained in Fig. 660 is somewhat different from that in Fig. 650, for the following reasons: (a) the primary ohmic drop has been disregarded altogether; (b) the primary reactive drop is correctly assumed to be due to the primary current I_1 and not to its part I_2, as in Fig. 648, from which Fig. 650 is derived. Thus, Fig. 660 corresponds to an equivalent diagram in which: (1) b_0 is placed as in Fig. 661; (2) g_0 is connected as in Fig. 648; (3) r_1 is assumed to be equal to zero. A correction can be made for the voltage drop in r_1, as shown in §§918 and 919 below.[11]

REFERENCES

NOTE: *For a more complete bibliography of the circle diagram see end of Chapter XLVIII.*

1. B. G. LAMME, *Elec. Jour.*, January and March, 1927, The circle diagram of the induction motor.

2. B. G. LAMME, *Elec. Jour.*, May, 1927, p. 213, Induction motor characteristics.

3. H. M. NORMAN, *Trans. A.I.E.E.*, vol. 45 (1926), p. 369, Starting characteristics and control of induction motors.

4. V. KARAPETOFF, *Jour. A.I.E.E.*, February, 1922, The "indumor."

5. A. M. DUDLEY, *Elec. Jour.*, July, 1924, p. 339, The induction motor on unbalanced circuits.

6. D. F. ALEXANDER, *Elec. Jour.*, August, 1928, p. 376, The polyphase induction generator.

7. J. SLEPIAN, *Elec. World*, 1920, p. 313, Induction motors on unbalanced voltages.

8. SCHOENFELD, *Elec. Jour.*, 1925, p. 30, Effect of unbalanced voltages on the operation of induction motors.

9. E. ARNOLD, Die Wechselstromtechnik, vol. V, pt. 1, J. Springer.

10. B. A. BEHREND, The Induction Motor and other A-C Motors, McGraw-Hill Book Co.

11. B. F. BAILEY, Induction Motor, McGraw-Hill Book Co.

12. A. HEYLAND, Graphical Treatment of the Induction Motor, McGraw-Hill Book Co.

[10] For a theory of the induction motor based on fluxes and stray fields, see B. A. Behrend, "The Induction Motor," Chapter II, McGraw-Hill Book Co.

[11] See also B. A. Behrend, *ibid.*, Chapter III; V. Karapetoff, *Sibley Journal of Engineering*, vol. 35 (1921), p. 42.

CHAPTER XLVIII

EXACT CIRCLE DIAGRAM OF POLYPHASE INDUCTION MOTOR

911. It is proved in the preceding chapter that when a constant a-c voltage is applied to the terminals (Fig. 648) of the simplified equivalent diagram and the resistance R is varied from zero to infinity, the locus of the primary current is part of a semicircle (Fig. 649). A similar conclusion can be reached with regard to the exact diagram shown in Fig. 661, except that the diameter of the semicircle is somewhat different, and the base line, AK (Fig. 665), is inclined at an angle to the axis of abscissas, Ox. For motors with a high primary impedance drop (especially in small sizes) the approximate diagram is not accurate enough, and we shall deduce a circle diagram corresponding to the exact equivalent diagram shown in Fig. 661.

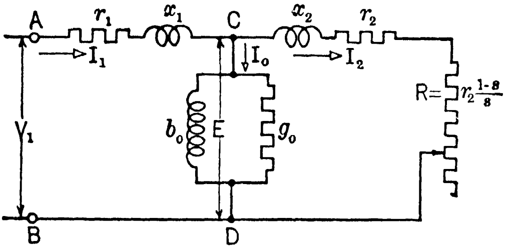

FIG. 661. The exact equivalent circuit of the polyphase induction motor.

There are various methods, analytical and graphical, of proving that the diagram shown in Fig. 661 leads to a circle (see bibliography in §923). Of these methods, two have been chosen: One due to a Japanese engineer, Mr. H. Ho, because of its didactic and practical advantages; and another, derived by V. Karapetoff and based on vector algebra, to show the advantages of vectorial notation.

HO'S CIRCLE DIAGRAM

912. Ho's Theorem. — The following theorem greatly facilitates the proof and construction of the exact circle diagram, as well as an analytical computation of currents.[1] *Each actual current in the exact*

---

[1] H. Ho, "Circle Diagram of Polyphase Induction Motor," *Institute of Electrical Engineers of Japan, Journal,* No. 424, November, 1923. An English translation was kindly made for one of the authors of this book by a former student.

equivalent diagram of a polyphase induction motor (Fig. 661) may be obtained by a superposition of the currents in the two fictitious circuits, (a) and (b), shown in Fig. 662.

We shall call these component circuits a and b, respectively. The a circuit consists of the primary impedance, $Z_1 = r_1 + jx_1$, and the exciting impedance, $Z_0 = (g_0 - jb_0)^{-1}$, in series; in other words, it is identical with Fig. 661 when $R = \infty$, and represents the conditions at no load, without friction and windage. The applied voltage, E_1, is taken equal to the actual line voltage under operating conditions. The b circuit is obtained from Fig. 661 by short-circuiting the points A and B and inserting in the secondary circuit an emf, E, equal to and in phase with the voltage between the points C and D in the a circuit.

Two proofs of the foregoing theorem are given in the following sections. It is desired here to point out the practical significance of this transformation. The impedances Z_1 and Z_0 being known, the a circuit is a simple series combination, so that the voltage, E, and the current, I_{1a}, can be readily determined from the relationships:

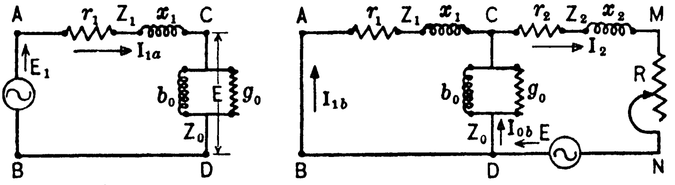

(a) (b)

FIG. 662. Ho's resolution of the exact equivalent circuit into two circuits.

$$E = E_1Z_0/(Z_0 + Z_1) \quad \ldots\ldots\ldots \quad (1)$$

and

$$I_{1a} = E_1/(Z_0 + Z_1) \quad \ldots\ldots\ldots \quad (2)$$

In these equations, vectors and complex quantities are understood.

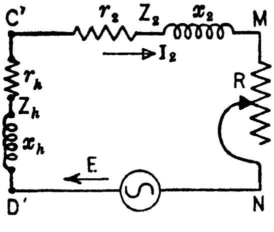

FIG. 663. A simplification of the circuit shown in Fig. 662(b).

The b circuit can be simplified to that shown in Fig. 663, by combining the parallel impedances Z_0 and Z_1 into Z_h, where

$$Z_h^{-1} = Z_0^{-1} + Z_1^{-1} \quad \ldots\ldots \quad (3)$$

or

$$Z_h = Z_0Z_1/(Z_0 + Z_1) \quad \ldots\ldots \quad (4)$$

Therefore,

$$I_2 = E/(Z_h + Z_2)$$

where

$$Z_2 = r_2 + R + jx_2 \quad \ldots\ldots \quad (5)$$

The component currents I_{0b} and I_{1b} (Fig. 662b) can be determined from the Kirchhoff equations:

$$I_{1b} Z_1 = I_{0b} Z_0 \text{ and } I_{0b} + I_{1b} = I_2 \quad . \quad . \quad . \quad . \quad (6)$$

which give:

$$I_{0b} = I_2 Z_1/(Z_0 + Z_1) \quad . \quad . \quad . \quad . \quad . \quad . \quad . \quad . \quad . \quad . \quad (7)$$

$$I_{1b} = I_2 Z_0/(Z_0 + Z_1) \quad . \quad . \quad . \quad . \quad . \quad . \quad . \quad . \quad . \quad . \quad (8)$$

Thus, using Ho's theorem, we immediately find the currents in Fig. 661 to be as follows:

$$I_0 = I_{1a} - I_{0b} \quad . \quad . \quad . \quad . \quad . \quad . \quad . \quad . \quad . \quad (9)$$

$$I_1 = I_{1a} + I_{1b} \quad . \quad . \quad . \quad . \quad . \quad . \quad . \quad . \quad . \quad . \quad (10)$$

$$I_2 = 0 + I_2 \quad . \quad . \quad . \quad . \quad . \quad . \quad . \quad . \quad . \quad . \quad (11)$$

The last equation merely shows that I_2, determined from Fig. 662(*b*), is the total or actual secondary current, because it exists only in the *b* circuit, its component in the *a* circuit being equal to zero. The foregoing results can be used either in analytical computations of motor characteristics or in the construction of a circle diagram.

913. First Proof of Ho's Theorem. — The theorem stated in the preceding section can be proved either by using the principle of superposition or by actually comparing the sums of the values of the currents obtained from Figs. 662(*a*) and (*b*) with those deduced directly from Fig. 661. In view of the importance of the theorem, both proofs are given below.

According to the principle of superposition, the actual currents in a network with two or more separate emf's are additive, so that the currents due to each emf may be computed separately and added together. In so doing, the omitted emf's are replaced by "jumpers," or connections of negligible impedance. This principle follows from the fact that all Kirchhoff's equations are linear. In fact, the validity of the principle is limited to networks whose current-voltage relations can be expressed by linear equations with constant coefficients, either algebraic or differential. For example, the principle of superposition, strictly speaking, does not hold true for an a-c network containing windings with saturated iron cores.

Consider the network shown in Fig. 664, which is identical with that shown in Fig. 661, except for an additional arbitrary emf, E_2, in the secondary circuit. The actual currents in such a network can be computed as follows: First replace E_2 by a short circuit and determine the currents in all the branches, due to E_1. Then short-circuit E_1 and evaluate the currents due to E_2. Finally add the two component currents in each branch, taking into consideration their signs and phase angles. Let the currents that flow when both emf's are acting be designated by (1, 2), those due to E_1 alone by (1), and those due to E_2 alone by (2). Then, symbolically, for the current in any branch, according to the principle of superposition,

$$(1, 2) = (1) + (2) \quad . \quad . \quad . \quad . \quad . \quad . \quad . \quad . \quad . \quad (12)$$

Select E_2 of such a magnitude and phase as to reduce to zero the current in the branch *CMND* when the emf E_1 is acting. In other words, open the branch *CMND*, measure the voltage E between the points C and D, and choose E_2 equal and opposite to that voltage. Then, when the circuit *CMND* is again closed, no current will flow through it. Referring to Fig. 662(a), this means that we should choose $E_2 = -E$. The principle of superposition still holds true under these conditions, and eq. (12) may be rewritten as:

$$(1, -a) = (1) + (-a) \quad . \quad . \qquad . \quad . \quad . \quad (13)$$

where the symbol a stands for the action of the emf E. From this equation:

$$(1) = (1, -a) + (a) \qquad . \quad . \quad . \quad (13a)$$

In Fig. 664 the combined action of the emf's E_1 and $E_2(= -E)$ gives Fig. 662(a), because the emf $-E$ prevents a current from flowing through the branch *CMND*. When the emf $-E_2 = E$ is applied alone, we obtain Fig. 662(b). Hence, eq. (13a) states in effect that each current in Fig. 661 is equal to the sum of the corresponding currents in Figs. 662(a) and (b).

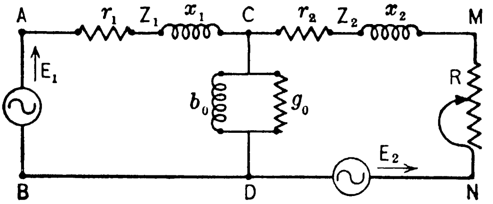

FIG. 664. Diagram for the proof of Ho's theorem.

To put the same reasoning in other words: In Fig. 664, let two equal and opposite emf's, each equal to E, be inserted in the branch *DN*. The actual currents are not affected thereby, but they may be considered as a result of superposition of the currents due (a) to a combination of the voltages E_1 and $-E$, and (b) to the voltage $+E$. The first combination gives Fig. 662(a); the second gives Fig. 662(b).

914. Second Proof of Ho's Theorem. — If Ho's theorem holds true, then the value of I_1 determined from eq. (10) must agree with that obtained directly from the equivalent impedance of the circuit shown in

Fig. 661. The latter impedance is $Z_1 + (Z_0^{-1} + Z_2^{-1})^{-1}$, so that·

$$I_1 = E_1/[Z_1 + (Z_0^{-1} + Z_2^{-1})^{-1}] \quad . \quad . \quad . \quad . \quad . \quad (14)$$

On the other hand, using in eq. (10) the values of I_{1a} and I_{1b} from eqs. (2) and (8), we get:

$$I_1 = (E_1 + I_2Z_0)/(Z_0 + Z_1) \quad . \quad . \quad (15)$$

Substituting for I_2 its value from eq. (5) and using expressions (1) and (4) for E and Z_h, eq. (15) becomes:

$$I_1 = [E_1/(Z_0 + Z_1)]\,[1 + Z_0^2/(Z_0Z_1 + Z_0Z_2 + Z_1Z_2)] \qquad (16)$$

From eq. (14)

$$\begin{aligned} I_1 &= E_1/[Z_1 + Z_2Z_0/(Z_2 + Z_0)] \\ &= E_1(Z_2 + Z_0)/(Z_0Z_1 + Z_0Z_2 + Z_1Z_2) \quad . \quad . \quad . \quad (16a) \end{aligned}$$

Multiplying and dividing eq. (16*a*) by $(Z_0 + Z_1)$ and collecting terms again gives eq. (16). By this algebraic transformation, expressions (14) and (16) are shown to be identical. Similarly, the expression for I_0 derived from eq. (9) may be proved to agree with that derived directly by Kirchhoff's laws from Fig. 661.

915. Circle Diagram Derived from Ho's Theorem. — The circle diagram (Fig. 665) is primarily intended to give the locus of the primary current, I_1, when the load varies. According to eq. (10), the current vector I_1 is a geometric sum of the vectors I_{1a} and I_{1b} (Figs. 662*a* and *b*). Figure 662(*a*) gives a no-load current, I_{1a}, whose vector, *OA*, is drawn in Fig. 665 at an angle ϕ_0 to the line voltage E_1. To determine ϕ_0, consider the exciting impedance, g_0, b_0, to be replaced by an equivalent series combination,[2] r_0, x_0. Then,

$$\tan \phi_0 = (x_0 + x_1)/(r_0 + r_1) \quad . \quad . \quad . \quad (17)$$

To determine the locus of I_{1b}, we shall first determine the locus of I_2 (Fig. 663), since I_{1b} is a definite fraction of I_2. Let g_1 and b_1 be the conductance and the susceptance of a parallel combination equivalent to Z_1. Then,

$$Z_h^{-1} = (g_0 + g_1) - j(b_0 + b_1) \quad . \quad . \quad . \quad (18)$$

and consequently the components r_h and x_h of Z_h may be computed in the usual manner.

Figure 663 represents a series combination of a constant reactance and a variable resistance. As is shown in §888, the current locus in this case is a semicircle. Its diameter, lagging 90 degrees behind E, is equal to $E/(x_h + x_2)$. Equation (8) shows that the ratio of I_2 to I_{1b} is constant and equal to $(Z_0 + Z_1)/Z_0$. The numerical value of this ratio (Fig. 666) is:

---

[2] V. Karapetoff, "The Electric Circuit," p. 78.

$$I_2/I_{1b} = m = \sqrt{(r_0 + r_1)^2 + (x_0 + x_1)^2}/\sqrt{r_0^2 + x_0^2} \quad . \; . \; (19)$$

I_{1b} leads I_2 by an angle

$$\alpha = \tan^{-1}(x_0/r_0) - \tan^{-1}(x_0 + x_1)/(r_0 + r_1) \quad . \; . \; . \; (20)$$

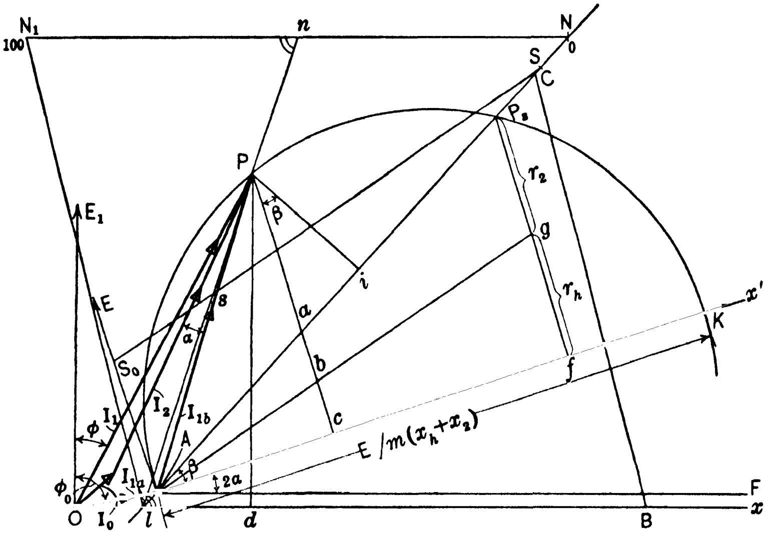

FIG. 665. An exact circle diagram of the polyphase induction motor.

A comparison of eqs. (1) and (8) shows that E is obtained from E_1 in the same manner in which I_{1b} is obtained from I_2. Consequently, eqs. (19) and (20) apply also to E and E_1, so that, numerically,

$$E = E_1/m \quad . \; . \; . \; . \; . \; . \; . \; . \; . \; . \; . \; (21)$$

and E leads E_1 by an angle α determined by eq. (20). Thus, in Fig. 665, if we wanted the circle diagram to give the current I_2, the direction Ax' of the diameter of the semicircle should be inclined at an angle α to Ox. The diameter of the circle of the locus of I_2 (not shown in the sketch) is equal to $E/(x_h + x_2)$. However, we are interested in the locus of I_{1b}; therefore, the diameter AK is taken equal to $E/m(x_h + x_2) = E_1/m^2(x_h + x_2)$, and tipped further by another angle α, making the angle $x'AF$ equal to 2α. The vector E is also shown in Fig. 665, turned by a second angle α, and not in its true position.

OP, being equal to $I_{1a} + I_{1b}$, represents the primary current, and the semicircle is its locus. *OA* is equal to the magnetizing current *at no* *load only.* To find the magnetizing current at any other load, it is first necessary to construct the corresponding I_2. According to eqs. (19) and (20), the vector I_2 is obtained by multiplying I_{1b} by m and retarding its phase by the angle α, as shown in Fig. 666. The geometric difference between I_1 and I_2 is the magnetizing current at that load. In most problems, only OP and AP (Fig. 665) are required, so that the foregoing construction is not needed.

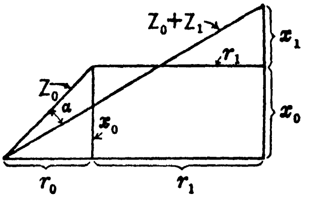

FIG. 666. Derivation of I_{1b} from I_2 and of E from E_1.

916. Other Characteristic Quantities Derived from Ho's Diagram. — As in Figs. 652 to 658, so in Fig. 665, other motor characteristics, besides the currents, may be obtained from the circle diagram. To the reader familiar with §§890 and 894, it is sufficient to indicate these quantities briefly.

Input. The component Pd of the current, multiplied by the terminal voltage, E_1, gives the power input per phase. The circle may be drawn to such a scale that Pd will give directly the total power in any desired units. The length OP represents the apparent input to the same scale. The real input reaches its maximum at that point on the circle at which the tangent is parallel to Ox.

Power factor. A power-factor quadrant, with center at O (Figs. 652 and 653) may be used. The power factor reaches its maximum at that point on the circle at which the tangent passes through O.

Primary copper loss. There is no length in the diagram which represents the primary copper loss directly. It has to be computed from the formula $I_1^2r_1$ for each value of I_1. However, it is not necessary to know this quantity in order to predetermine the operating characteristics of the motor.

Secondary copper loss. The semicircle with the origin at A correctly represents the secondary circuit of the actual motor, except that the current I_{1b} must be multiplied by m to obtain I_2; see eq. (19). Therefore, the secondary copper loss, by analogy with Fig. 650, is equal to $m \times ab \times E$. But $mE = E_1$, so that the secondary copper loss is equal to $ab \times E_1$. In other words, ab represents the secondary copper loss to the same scale to which Pd represents the input.

Output. From the foregoing statement regarding the secondary copper loss, it follows that Pa represents the power delivered to the resistance R; in other words, Pa represents the motor output to the same scale to which Pd represents the input. The energy component of the no-load current, I_{1a}, should include only the core loss, and not the mechanical losses (friction and windage). The mechanical losses should be subtracted from the output, Pa, their magnitude being a function of the motor speed at that particular load. The output reaches its maximum at that point on the circle at which the tangent is parallel to AP_s.

Torque. Since the torque (in synchronous watts or kilowatts) is equal to the input into the secondary circuit, it is represented in the diagram by the length Pb, to the same scale to which Pd represents the input into the primary. The torque is a maximum for the point on the semicircle at which the tangent is parallel to Ag.

Efficiency scale. The efficiency of the machine is equal to the ratio of Pa (less mechanical losses) to Pd. If the mechanical losses are disregarded, or included in the energy component of I_{1a}, the efficiency is equal to Pa/Pd. It is then possible to construct an efficiency scale similar to that shown in Fig. 652. For this purpose, produce P_sA to its intersection with Ox at l and lay off $lC = AK$ and $lB = AP_s$. Draw the direction line lN_1 parallel to BC, and a horizontal line, such as NN_1. Divide the latter into 100 equal parts, with zero at N and 100 at N_1. By placing a straight-edge through points l and P, the efficiency can be read off directly at n. The proof is based on similar triangles and is analogous to that given in §893.

Slip scale. A second form of slip scale (see Fig. 652) is shown in Fig. 665. It is somewhat simpler to construct than that of Fig. 652, but it is probably less accurate at low values of slip. The slip scale, S_0S, is drawn parallel to the line Ag (Fig. 665), with zero of the scale on the line AE, perpendicular to line Ax, and 100 per cent of the scale on the line AP_s (or continued). The line AP intersects the slip scale at s. Slip is then S_0s/S_0S.

Proof. Triangles Aab, and AS_0S are similar, the sides being parallel, so that

$$ab/Ab = AS_0/S_0S \quad \ldots\ldots\ldots\ldots \quad (22)$$

Triangles AbP and AS_0s are similar for the same reason. Therefore,

$$S_0s/AS_0 = Ab/Pb \quad \ldots\ldots\ldots\ldots \quad (23)$$

Multiplying (22) by (23)

$$ab/Pb = S_0s/S_0S$$

which proves the slip scale.

917. EXPERIMENT 48-A. — Derivation of Induction-Motor Characteristics from an Exact Circle Diagram. — The motor selected for this experiment should possess a considerable primary impedance drop. Its primary resistance, no-load current, short-circuit current, and mechanical losses can be measured as explained in preceding chapters. For a check, a brake test may be performed. The total equivalent reactance obtained from the short-circuit test is assumed to be nearly equally divided between the primary and the secondary circuits. From these data, a circle diagram may be constructed, as explained above, and the results compared with those derived from the brake test. For another comparison, an approximate circle diagram should also be constructed (§893), and the motor characteristics derived from it. This will give an idea as to the magnitude of the error committed in assuming a constant magnetizing current. Should even the "exact" diagram give results at variance with the brake test, the error may lie in an improper division of the equivalent impedance between the two branches. One or two other modes of division may be tried, or a circle constructed from the brake test and the value of x_1 determined from x_h corresponding to that circle. In place of a brake test, either method (a) or method (b), described in §494, may be used as a check.

EXACT CIRCLE DIAGRAM DERIVED BY VECTOR ALGEBRA

918. Equation of a Circle in Vector Notation. — A deduction of the exact circle diagram, based on vector analysis, is given below. In order to understand this proof it is necessary to know the equation of a circle in vector notation.

Definition. The scalar (or dot) product of two vectors (§738) is a scalar quantity equal to the product of their lengths multiplied by the cosine of the angle between them; that is,

$$\mathbf{A} \cdot \mathbf{B} = AB \cos (A, B) \quad . \; . \; . \; . \; . \; . \; . \; . \; . \quad (24)$$

Bold-face letters denote vectors in magnitude and phase position; the same letters in italics mean the scalar lengths of the corresponding vectors. The dot in the scalar product should never be omitted, because a combination of two vectors with a cross (×) or no sign between them means something entirely different. From eq. (24) it will be seen that the condition:

$$\mathbf{A} \cdot \mathbf{B} = 0 \quad . \; . \; . \; . \; . \; . \; . \; . \; . \; . \; . \; . \quad (25)$$

means that the vectors **A** and **B** are perpendicular to each other.

In a circle (Fig. 667*a*), two chords, such as *AP* and *KP*, which end on the same diameter, are perpendicular to each other, and therefore the equation of the circle may be derived from eq. (25). Let *O* be the origin, and let a circle of diameter *AK* be defined by the vectors

$\mathbf{D}_1 = OA$ and $\mathbf{D}_2 = OK$. The vectors $\mathbf{D}_1$ and $\mathbf{D}_2$ are understood to be given by their magnitude and direction. Let P be a point on the circle, determined by the vector $\mathbf{r}$. We then have:

$$PA = \mathbf{D}_1 - \mathbf{r} \quad . \; . \; . \; . \; . \; . \; . \; . \; . \; . \quad (26)$$

$$PK = \mathbf{D}_2 - \mathbf{r} \quad . \; . \; . \; . \; . \; . \; . \; . \; . \; . \quad (27)$$

geometric subtraction being understood. Hence, according to eq. (25),

$$(\mathbf{D}_1 - \mathbf{r}) \cdot (\mathbf{D}_2 - \mathbf{r}) = 0 \quad . \; . \; . \; . \; . \; . \; . \; . \quad (28)$$

This is the equation of the circle referred to O as origin. The independent variable is the vector $\mathbf{r}$, and for any point on the circle it must satisfy eq. (28).[3]

In a more general case (Fig. 667*b*), let a circle be defined by a chord AB and by the angle, δ, which this chord makes with the diameter AK. AB and δ being known, the right triangle ABK may be completed and thus the diameter AK and the center of the circle determined. Let AB be given by means of the vectors $\mathbf{F}_1$ and $\mathbf{F}_2$ from the origin O, and let P be a variable point on the circle, determined by the vector $\mathbf{r}$. The vectors $PA = \mathbf{F}_1 - \mathbf{r}$ and $PB = \mathbf{F}_2 - \mathbf{r}$ are not perpendicular to each other, but the vectors PA and PK are. To obtain the direction PK, the vector PB has to be turned clockwise by an angle δ. The turning operator may be written in the form $\epsilon^{-j\delta}$. Thus, eq. (25) gives:

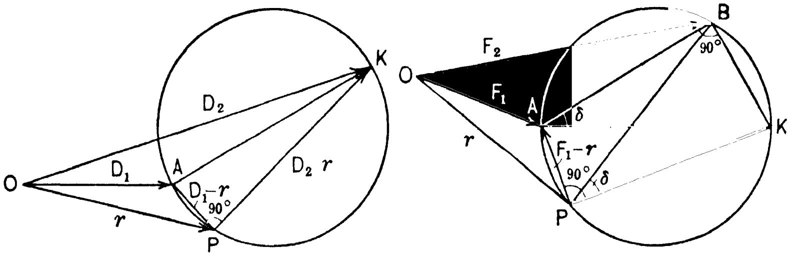

(*a*) (*b*)

FIG. 667. A circle defined by a diameter, or by a chord and an angle.

$$(\mathbf{F}_1 - \mathbf{r}) \cdot [(\mathbf{F}_2 - \mathbf{r})\epsilon^{-j\delta}] = 0 \quad . \; . \; . \; . \; . \; . \; . \quad (29)$$

Both vectors, PA and PB, may be turned by the same arbitrary angle, say γ, and will still remain normal to each other. Hence, the foregoing equation may be generalized to

---

[3] For some applications of this equation in deriving various circle diagrams, see V. Karapetoff, "The Use of the Scalar Product of Vectors in Locus Diagrams of Electrical Machinery," *Journal A.I.E.E.*, vol. 42 (1923), p. 1181; also *Proc. National Acad. of Sciences*, vol. 11 (1925), p. 683.

$$(\mathbf{F}_1 - \mathbf{r})\epsilon^{j\gamma}\cdot [(\mathbf{F}_2 - \mathbf{r})\epsilon^{j(\gamma-\delta)}] = 0 \quad . \ . \ . \ . \ . \ . \ (30)$$

Either of these equations represents the circle given by $\mathbf{F}_1$, $\mathbf{F}_2$, and δ; these equations are used in §920 below.

919. Diagram of Currents and Fluxes, with Correction for the Primary Ohmic Drop. — In Fig. 668, E_1, is the terminal voltage, and $OB_1 = I_1$ is the primary current. OB_1 also represents a certain flux, as will be explained later. If there were no primary Ir drop a flux, which may be represented by OF_1, would be required to induce an emf equal and opposite to E_1. A magnetizing current, ON, would be needed to produce such a flux. However, there is a primary ohmic drop which must be corrected for. Subtracting from E_1 the drop I_1r_1, in phase with I_1, gives the " corrected " terminal voltage E_c which must be balanced by the total counter emf which must be induced in the primary winding by a flux OF_{1c}. The voltage E_c is variable because of the variable ohmic drop, I_1r_1, which varies with the load. Consequently OF_{1c} is also variable.

In Fig. 668, OA_1 represents the fictitious total flux which the primary current, acting alone, and assuming no saturation, would cause to link the primary winding. OB_1 represents the portion of this total primary flux which would link with the secondary, so that B_1A_1 indicates the primary leakage flux. If v_1 is the primary leakage coefficient, $OA_1 = OB_1v_1$. Similarly, A_1F_{1c} represents the flux which the secondary current, acting alone, would cause to link with the primary winding, so that OF_{1c}, corresponding to the net flux linking the primary, $= OA_1 + A_1F_{1c}$. B_1F_2 represents the total flux which the secondary, acting alone, would cause to link the secondary, or $B_1F_2 = v_2A_1F_{1c}$. Since the flux B_1F_2 is in phase with I_2, and includes the flux which causes the reactance of the rotor, the net rotor flux, OF_2, must induce an emf equal to the Ir drop of the rotor. Therefore, B_1F_2 and OF_2 must be at right angles.

Also in Fig. 668 the triangle OA_1F_{1c} represents the superposition of the fictitious fluxes in the primary winding, and the triangle OB_1F_2 of those in the secondary winding. The point N moves to N_c and F_1 to F_{1c}. Since the voltages E_1 and E_c are proportional to the fluxes that balance them, the two cross-hatched triangles are similar, and the vectors $F_{1c}F_1$ and N_cN are perpendicular and proportional to I_1. We may therefore write:

$$NN_c = kI_1 \quad . \ . \ . \ . \ . \ . \ . \ . \ . \ . \ (31)$$

where k is the *primary resistance factor.* Neglecting saturation, the vectors ON and ON_c have been considered, to a certain scale, the resultant mmf's which produce the fluxes OF_1 and OF_{1c}. These mmf's may be further expressed as currents in terms of the primary circuit. The equivalent magnetizing current, ON, without the correction for the primary drop, is denoted by I, while the actual or corrected magnetizing current is $ON_c = I_m$. From similar triangles,

$$kI_1/I = r_1I_1/E_1 \quad \ldots\ldots\ldots\ldots \quad (32)$$

so that:

$$k = r_1I/E_1 \quad \ldots\ldots\ldots\ldots \quad (33)$$

Multiplying and dividing the right-hand side by I_1, this equation becomes:

$$k = (r_1I_1/E_1)(I/I_1) \quad \ldots\ldots\ldots \quad (34)$$

Thus, k, in per cent, is equal to per cent primary ohmic drop at the rated current times the ideal magnetizing current expressed as a fraction of the rated current. For example, if the drop I_1r_1 at the rated current is 3 per cent and the magnetizing current is 30 per cent, $k = 3 \times 0.30 = 0.9$ per cent. We have, from Fig. 668,

$$\mathbf{I} = \mathbf{I}_m - jk\mathbf{I}_1 = \text{Const.} \quad \ldots\ldots \quad (35)$$

This expression is used in the next section in the proof of the circle diagram.

920. A Proof of the Circle Diagram Based on Vector Algebra.—With the notation in Fig. 668, we may write the following vectorial relations:

$$v_1\mathbf{I}_1 + \mathbf{I}_2 = v_1\mathbf{I}_m \quad \ldots\ldots\ldots \quad (36)$$

$$\mathbf{I}_1 + v_2\mathbf{I}_2 = \mathbf{I}_s \quad \ldots\ldots\ldots\ldots \quad (37)$$

$$\mathbf{I}_2 \cdot \mathbf{I}_s = 0 \quad \ldots\ldots\ldots\ldots \quad (38)$$

The leakage coefficients, v_1 and v_2, are defined in §919. Equation (38) expresses the condition that $\mathbf{I}_s$ is perpendicular to $\mathbf{I}_2$, OF_2 having been shown to be perpendicular to B_1F_2 in §919.

In order to obtain the locus of $\mathbf{I}_1$, the vector $\mathbf{I}_m$ must be eliminated from eqs. (35) and (36) and the resulting equation solved for $\mathbf{I}_2$. This gives:

$$\mathbf{I}_2 = v_1\mathbf{I} - v_1\mathbf{I}_1(1 - jk) \quad \ldots\ldots\ldots \quad (39)$$

Substituting this value in eq. (37), we obtain:

$$\mathbf{I}_s = v_1v_2\mathbf{I} - \mathbf{I}_1(v_1v_2 - 1 - jv_1v_2k) \quad \ldots\ldots \quad (40)$$

Using the values of $\mathbf{I}_2$ and $\mathbf{I}_s$ from eqs. (39) and (40) in eq. (38), and dividing $\mathbf{I}_2$ and $\mathbf{I}_s$ by v_1 and by v_1v_2, respectively, we get:[4]

$$[\mathbf{I} - \mathbf{I}_1(1 - jk)] \cdot [\mathbf{I} - \mathbf{I}_1\{1 - (v_1v_2)^{-1} - jk\}] = 0 \quad . \; . \; . \quad (41)$$

It is desired to reduce eq. (41) to the form of eq. (29), in order to show that it represents a circle. We may write

$$1 - jk = h\epsilon^{j\eta}; \quad 1 - (v_1v_2)^{-1} - jk = t\epsilon^{j\theta} \quad . \; . \; . \; . \; . \quad (42)$$

where η and θ are negative angles. Factoring out the above quantities in eq. (41), we obtain:

$$[(\mathbf{I}/h)\epsilon^{-j\eta} - \mathbf{I}_1]h\epsilon^{j\eta} \cdot [(\mathbf{I}/t)\epsilon^{-j\theta} - \mathbf{I}_1]t\epsilon^{j\theta} = 0 \quad . \; . \; . \; . \; . \quad (43)$$

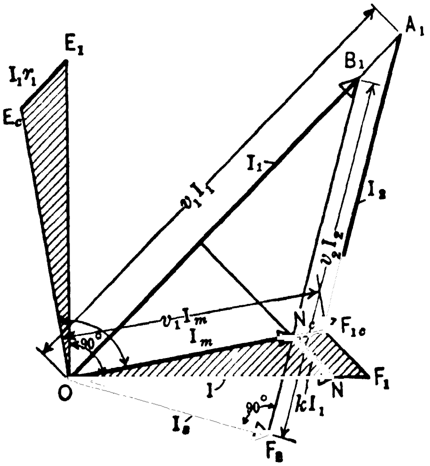

FIG. 668. A correction for Fig. 660 to account for the primary ohmic drop.

Omitting the scalar factors, h and t, and turning both expressions in the brackets by an angle $-\eta$, we finally obtain:

$$[(\mathbf{I}/h)\epsilon^{-j\eta} - \mathbf{I}_1] \cdot [(\mathbf{I}/t)\epsilon^{-j\theta} - \mathbf{I}_1]\epsilon^{-j(\eta-\theta)} = 0 \quad . \; . \; . \; . \quad (44)$$

This expression is of the same form as eq. (29), so that the locus of $\mathbf{I}_1$ is a circle. This circle is determined by a chord whose extremities are defined by the vectors

$$\mathbf{F}_1 = (\mathbf{I}/h)\epsilon^{-j\eta}; \quad \mathbf{F}_2 = (\mathbf{I}/t)\epsilon^{-j\theta} \quad . \; . \; . \; . \; . \; . \quad (45)$$

and by the inscribed angle:

$$\delta = \eta - \theta \quad . \; . \; . \; . \; . \; . \; . \; . \; . \; . \; . \quad (46)$$

---

[4] It is permissible to divide either vector in eq. (38) by a scalar quantity because this does not change the direction of the vector. It would be wrong, however, to divide one of the vectors by a complex quantity, because this would change the direction of the vector, and the turned vector would not be normal to the other.

After these three parameters have been computed from the known electrical constants of the machine, the circle itself can be drawn.

As a specific case of eqs. (44), (45), (46), let us apply them to an approximate diagram, that is, when $k = 0$. We then have:

$$\eta = \theta = \delta = 0; \quad h = 1; \quad t = 1 - (v_1 v_2)^{-1} \quad . \ . \ . \ . \ (47)$$

In this particular case we shall denote $\mathbf{F}_1$ (eq. 45) by $\mathbf{F}_{01}$ and $\mathbf{F}_2$ by $\mathbf{F}_{02}$. Both $\mathbf{F}_{01}$ and $\mathbf{F}_{02}$ are in the direction of $\mathbf{I}$, and, since $\delta = 0$, $\mathbf{F}_{01}$ and $\mathbf{F}_{02}$ define a diameter of the circle. Numerically,

$$\mathbf{F}_{01} = \mathbf{I} \quad \text{and} \quad \mathbf{F}_{02} = \mathbf{I}v_1 v_2/(v_1 v_2 - 1) \quad . \ . \ . \ . \ . \ (48)$$

The ratio of the diameter of the circle, $\mathbf{F}_{20} - \mathbf{F}_{10}$, to the distance $\mathbf{F}_{10}$ is:

$$(F_{02} - F_{01})/F_{01} = (v_1 v_2 - 1)^{-1} = \sigma^{-1} \quad . \ . \ . \ . \ . \ (49)$$

921. Change from an Approximate to an Exact Circle Diagram.— Although the position of the exact circle may be determined by means of eqs. (45) and (46), in practice it will be found more convenient first to determine the approximate values, $\mathbf{F}_{01}$ and $\mathbf{F}_{02}$, from eq. (48) and then apply to these values the necessary corrections. We shall put

$$\mathbf{F}_1 = (\mathbf{F}_{01}/a)\epsilon^{j\alpha} \quad . \ . \ . \ . \ . \ . \ . \ . \ . \ . \ (50)$$

$$\mathbf{F}_2 = (\mathbf{F}_{02}/b)\epsilon^{j\beta} \quad . \ . \ . \ . \ . \ . \ . \ . \ . \ . \ (51)$$

Equation (50) means that the exact value of $\mathbf{F}_1$ is to be derived from the approximate value, $\mathbf{F}_{01}$, by dividing it by a factor a and turning by an angle α counterclockwise. The quantities b and β are similar corrections for $\mathbf{F}_{02}$. Substituting in eq. (50) the values of $\mathbf{F}_1$ and $\mathbf{F}_{01}$ from eqs. (45) and (48), and using eq. (42), we find:

$$1 - jk = a\epsilon^{-j\alpha} \quad . \ . \ . \ . \ . \ . \ . \ . \ . \ (52)$$

from which, equating the real and the imaginary parts,

$$\tan \alpha = k \quad . \ . \ . \ . \ . \ . \ . \ . \ . \ . \ . \ (53)$$

$$a = \sec \alpha \quad . \ . \ . \ . \ . \ . \ . \ . \ (54)$$

After α has been determined from eq. (53), a may be computed from eq. (54). Usually α is so small that a is only slightly greater than unity. By analogy, from eq. (51),

$$\tan \beta = v_1 v_2 k/\sigma \quad . \ . \ . \ . \ . \ . \ . \ . \ . \ . \ (55)$$

$$b = \sec \beta \quad . \ . \ . \ . \ . \ . \ . \ . \ . \ . \ (56)$$

The angle β is considerably greater than α, and b will be found to be much greater than a. In other words, the ohmic resistance hardly affects the current locus near the no-load point, but reduces the diameter of the circle and tilts its horizontal diameter. This causes an appreciable difference in the region near the full-load point and on short circuit.

When a motor operates at the end of a line of considerable resistance and reactance, and the voltage is kept constant at the generator end of the line, the line reactance and resistance may be added to those of the primary winding of the motor. This may give such an appreciable primary resistance that one of the two exact circle diagrams described above may have to be used.

922. EXPERIMENT 48-B. — Effect of the Primary Resistance upon the Circle Diagram of the Polyphase Induction Motor. — The theory is given in §§918 to 921 above, and the experiment is of the nature of an extended investigation of both the motor characteristics and the properties of the circle diagram. Among other things, it is desired to ascertain the amount of correction and the error committed with different values of ohmic resistance, as related to the other motor constants. It is also of importance to find a convenient way of measuring graphically the principal motor characteristics; or else it should be shown that the practical usefulness of the exact circle diagram is limited to finding the current and the power factor corresponding to a given input, and that the remaining quantities, such as the torque and the slip, can be more conveniently computed analytically. See also §917.

923. Bibliography on the Circle Diagram and Analytical Theory.[5]

CIRCLE-DIAGRAM TREATMENT

G. KRON, *Trans. A.I.E.E.*, vol. 49 (1930), p. 666, The generalized theory of electrical machinery.

TERMAN, LENZEN, FREEDMAN, and ROGERS, *Trans. A.I.E.E.*, vol. 49 (1930), p. 374, The general circle diagram of electrical machinery.

W. J. BRANSON, *Trans. A.I.E.E.*, vol. 49 (1930), p. 319, Polyphase induction motors — a method of calculation.

H. PFLIEGER-HAERTEL, *Archiv fur Elektrot.*, vol. 12 (1924), p. 486.

V. GENKIN, *Revue générale de l'électr.*, vol. 14 (1923), p. 653.

H. HO, *Inst. Elec. Engrs. Japan, Journal*, 1923, p. 870.

H. KAFKA, *Elek. Zeits.*, vol. 44 (1923), p. 686.

V. KARAPETOFF, *Journal A.I.E.E.*, vol. 42 (1923), p. 1181.

R. MOSER, *Schweiz. Elekt. Ver., Bulletin*, vol. 14 (1923), p. 642.

T. SCHMITZ, *Elektrot. und Maschinenbau*, vol. 41 (1923), p. 745.

J. K. KOSTKO, *Journal A.I.E.E.*, vol. 41 (1922), p. 30.

K. KUHLMANN, *Schweiz. Elekt. Ver., Bulletin*, vol. 13 (1922), p. 129.

---

[5] The authors are indebted to the staff of the Main Library of the General Electric Company for this list of references.

W. O. Schumann, *Archiv für Elektrot.*, vol. 11 (1922), p. 140.
J. T. Takeuchi, *Inst. Elec. Engrs. Japan, Journal,* 408 (1922), p. 491.
L. E. Widmark, *Journal A.I.E.E.*, vol. 41 (1922), p. 687.
A. Blondel, *Revue générale de l'électr.*, vol. 9 (1921), p. 385; vol. 10, p. 5.
V. Genkin, *Revue générale de l'électr.*, vol. 9 (1921), pp. 419 and 755; vol. 8, p. 579; vol. 3, p. 931.
H. Kafka, *Archiv für Elektrot.*, vol. 9 (1921), p. 405.
J. K. Kostko, *Journal A.I.E.E.*, vol. 40 (1921), p. 326.
R. Le Cocq, *Revue générale de l'électr.*, vol. 9 (1921), pp. 5 and 483; vol. 8, p. 891.
J. Le Monnier and F. Decotte, *Revue générale de l'électr.*, vol. 9 (1921), p. 463.
R. G. Warner, *Journal A.I.E.E.*, vol. 40 (1921), p. 808.
R. G. Warner, *Electrical World,* vol. 77 (1921), p. 980.
H. K. Whitehorn, *Electrician* (London), vol. 87 (1921), p. 346.
J. Goldstein, *Schweiz. Elekt. Ver., Bulletin,* vol. 11 (1920), p. 1.
F. Margand, *Revue générale de l'électr.*, vol. 8 (1920), p. 3.
L. Lagron, *Revue générale de l'électr.*, vol. 5 (1919), p. 507; vol. 4, p. 861.
M. J. Bethenod, *Revue générale de l'électr.*, vol. 4 (1918), p. 941.
Otto Bloch, *Elek. Zeits.*, vol. 39 (1918), p. 34.
H. Kafka, *Elektrot. und Maschinenbau,* vol. 33 (1915), pp. 301 and 316; vol. 32, p. 589.
J. S. Nicholson, *Inst. El. Engrs.* (British), *Journal,* vol. 51 (1913), p. 778.
L. Dreyfus, *Archiv für Elektrot.*, vol. 1 (1912), p. 124.
C. R. Moore, *Gen. Elec. Rev.*, vol. 15 (1912), pp. 484, 564, and 646.
T. F. Wall, *Inst. El. Engrs.* (British), *Journal,* vol. 48 (1911), p. 499.
K. Krug, *Elektrot. und Maschinenbau,* vol. 28 (1910), p. 1047.
L. Solomon, *Electrician* (London), vol. 62 (1909), p. 530.
H. J. Laurell, *Electrical World,* vol. 52 (1908), p. 78.
C. F. Smith, *Mech. Engr.*, Dec. 21, 1907.
A. M. Gray, *Electrical World,* vol. 48 (1906), p. 284.
A. S. McAllister, *Electrical World,* vol. 47 (1906), p. 1077.
H. C. Specht, *Electric Journal,* vol. 2 (1905), p. 749.
F. Besig, *Zeits. für Elekt.*, vol. 22 (1904), p. 405.
H. Grob, *Elek. Zeits.*, vol. 25 (1904), pp. 447 and 474.
A. Heyland, *Elek. Zeits.*, vol. 25 (1904), p. 60.
P. Müller, *Elek. Zeits.*, vol. 25 (1904), p. 173.
H. Görges, *Elek. Zeits.*, vol. 25 (1904), p. 271.
J. K. Sumec, *Zeits. für Elekt.*, Jan. 4, 1903.
R. Goldschmidt, *Elek. Zeits.*, vol. 21 (1900), p. 693.
C. C. Hawkins, *Electrician* (London), vol. 42 (1899), p. 467.

ANALYTICAL TREATMENT

D. B. Hoseason, *Inst. El. Engrs.* (British), *Journal,* vol. 63 (1925), p. 280.
A. della Riccia, *Revue générale de l'électr.*, vol. 16 (1924), p. 933.
L. Binder, *Arch. für Elektrot.*, vol. 12 (1923), p. 230.
Mathieu, *Arts et métiers,* vol. 76 (1923), p. 785.
Cesare della Salda, *Elettrotecnica,* vol. 10 (1923), p. 770.
L. Ots-Chevalier, *Revue générale de l'électr.*, vol. 11 (1922), p. 771.
E. Siegel, *Elektrot. und Maschinenbau,* vol. 40 (1922), p. 217.
G. T. Smith, *Electric Journal,* vol. 19 (1922), p. 485.

C. M. LAFFOON, *Electrical World*, vol. 73 (1919), p. 1258.

A. NORMIER, *Ind. Elect.*, vol. 27 (1918), pp. 43 and 69.

WALDO V. LYON, *Electrical World*, vol. 65 (1915), p. 1240.

S. M. ROBINSON, *Jour. Am. Soc. Nav. Engrs.*, vol. 24 (1912), p. 1194.

G. BENISCHKE, *Elek. Kraft. und Bahnen*, vol. 8 (1910), p. 61.

C. J. SPENCER, *Elec. Age*, May, 1907.

W. ROGERS, *Elec. Engr.* (London), vol. 35 (1905), p. 662.

G. L. HOXIE, *Jour. Franklin Inst.*, September, 1903.

A. LINDSTRÖM, *Elek. Zeits.*, vol. 23 (1902), p. 521.

A. E. WIENER, *Elec. Age*, January, 1902.

H. C. TROW, *Engr.*, U.S.A., Sept. 1, 1901.

B. A. BEHREND, *Elec. World and Engr.*, vol. 36 (1900), pp. 676, 725, 767, 802, 843, 884, 920, and 998.

J. HEUBACH, *Elek. Zeits.*, vol. 21 (1900), p. 73; vol. 20, pp. 301 and 314.

B. A. BEHREND, *Elek. Zeits.*, vol. 18 (1897), p. 165.

A. HEYLAND, *Electrician* (London), vol. 36 (1896), pp. 505, 579, 650, and 719.

B. A. BEHREND, *Elek. Zeits.*, vol. 17 (1896), p. 63.

A. HEYLAND, *Elek. Zeits*, vol. 16 (1895), p. 649.

A. HEYLAND, *Elek. Zeits.*, vol. 15 (1894), p. 561.

CHAPTER XLIX

REGENERATIVE SPEED AND POWER-FACTOR CONTROL OF POLYPHASE INDUCTION MOTORS

924. A general introduction to the subject of speed control of polyphase induction motors was given in §488, and certain of these methods are discussed with reference to the circle diagram in §§894 to 897. The regenerative control mentioned in §488 under (d) is discussed in more detail below, because of the importance of its use in steel mills. Another method of speed control is possible when two induction motors drive the same load, for example in an electric locomotive. They can then be connected " in cascade " (§925), and in this manner two or more operating speeds can be obtained. For various controllers used in speed regulation of induction motors, see Chapter LV.

The subject of this chapter is treated in a more comprehensive manner in the book by Miles Walker entitled " The Control of the Speed and Power Factor of Induction Motors " (London, 1924). The following elementary explanations are intended mainly to facilitate the reading of that and other original sources.

CASCADE OR CONCATENATION

925. When two induction motors drive the same load, and so operate at the same speed (Fig. 669), the slip-rings of the first machine may be connected to the stator (or rotor) of the second machine, while the rotor (or stator) of the second machine is either short-circuited or connected to suitable resistors. Figure 670 illustrates the electrical connections of the two machines. It is seen that the secondary of the first motor serves as the source of power for the primary of the second motor. The machines are then said to be concatenated or connected in cascade. The second machine then furnishes an emf in series with the rotor winding of the first machine. If this emf opposes the flow of current, then the first machine slows down to such a speed that the slip emf is sufficient to overcome this counter emf and to circulate a secondary current, I_2, through the impedance of the two windings. At the same time, the speed of the set must be a little below that of the revolving flux caused by I_2 in the stator of the second machine, to have the proper slip in that machine. It will be shown below that these two conditions are satisfied simultaneously when the synchronous speed of the set is equal to that of an induction motor whose number of poles is equal to the *sum* of the numbers of poles of machines *A* and *B*. This connection is known as the *cumulative cascade* (§926).

If the emf of machine *B* is in the same direction as I_2, the current the synchronous speed of the set is equal to that of an induction motor whose number of poles is equal to the *difference* between the numbers of poles of the two machines. Such a connection is called the *differential cascade* (§927).

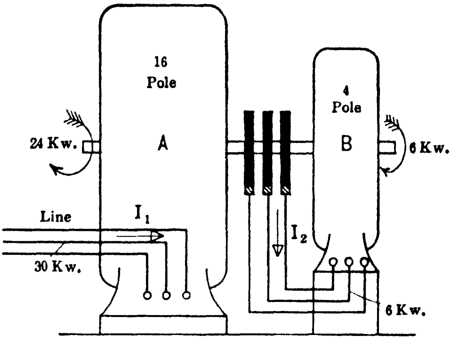

FIG. 669. Two induction motors in cumulative concatenation, or cascade.

926. Cumulative and Differential Cascade.— (a) *Cumulative connection.* Let the connections of the two motors be such that they both tend to run in the same direction. The no-load speed of the set will be below that of machine *A* when running alone with its rotor short-circuited. It may be shown that the running-light speed of the set is equal to that of a motor having a number of poles equal to the sum of the poles on the two motors.

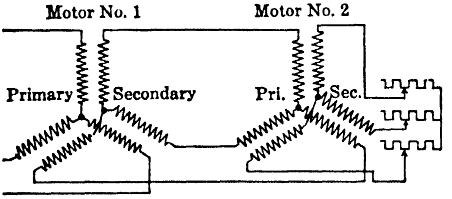

FIG. 670. Cascade connection of induction motor windings.

In the cascade connection of Fig. 670 the frequency impressed upon the primary of motor *B* is the slip frequency induced in the rotor of machine *A*, or

$$f_2 = f_1 s_1 \quad \quad (1)$$

The speed of machine *A*, having p_1 poles and operating on a supply frequency f_1, is

$$\text{rpm}_1 = 120 f_1 (1 - s)/p_1 \quad \quad (2)$$

The speed of machine *B*, having p_2 poles and operating on the frequency coming from the secondary of machine *A* (eq. 1), will be:

$$\text{rpm}_2 = 120 f_1 s_1 (1 - s_2) p_2 \quad \quad (3)$$

But, since the machines are assumed to be running light with the rotor of machine B short-circuited, s_2 may be neglected. Also, since the machines are coupled together, $\text{rpm}_1 = \text{rpm}_2 = \text{rpm}$, so that (eqs. 2 and 3)

$$f_1(1 - s_1)/p_1 = f_1 s_1/p_2$$

or

$$s_1 = p_2/(p_1 + p_2) \tag{4}$$

Therefore, in per-unit value, the speed of the set is

$$\text{Speed} = 1 - s_1 = p_1/(p_1 + p_2) \tag{5}$$

The speed in revolutions per minute is

$$\text{rpm} = 120f_1(p_1 + p_2) \tag{6}$$

Equation (6) shows that the two machines, connected in cumulative cascade, have a synchronous speed equal to that of a motor having $p_1 + p_2$ poles.

As an example, consider machine A to have 16 poles, and machine B to have 4 poles, the supply being at 60 cycles per second. At light loads the set will approach the speed (eq. 6):

$$N_s = 120 \times 60/(16 + 4) = 360 \text{ rpm}$$

The synchronous speed of motor A is 450 rpm; it is running, therefore, at a speed of 80 per cent of synchronous speed, or with a slip of 20 per cent, while the frequency, f_2, from its rotor is $0.2 \times 60 = 12$ cycles.

When the set is loaded, it slows down by a few per cent, on account of the I^2r loss in the two rotors. Neglecting this slight reduction in speed, we may say that the first motor still runs at a slip of 20 per cent; therefore, 80 per cent of the input into its secondary is delivered directly to the shaft. The remaining 20 per cent is transmitted to the second motor and there converted into mechanical power. In Fig. 669 the losses in the machines are neglected; therefore, if the primary input is 30 kw, 24 kw is delivered to the shaft through rotor A and 6 kw through rotor B.

It is also possible to connect the stator of the 4-pole machine to the line, and its rotor to the stator of the 16-pole machine. It is left to the reader to figure out the speed of the set and the relative amounts of output of both machines. The two rotors may also be connected together electrically and the stator of machine B used as its own secondary. The advantage of such an arrangement is that no slip-rings are necessary. With two identical motors (having equal numbers of poles) in cumulative cascade, the synchronous speed is reduced to one-half of that of each motor. This arrangement has been sometimes used in electric locomotives equipped with induction motors.[1]

The disadvantage of having two separate motors has led several inventors to devise induction machines in which two or more speeds could be obtained by recombining the windings of a single machine. The simplest solution is so to arrange the stator coils that they can be connected to produce either p poles or $2p$ poles at will (§488a). Of the more special motors, the following may be mentioned: the Oerlikon spinner motor,[2] Hunt's cascade induction motor,[3] and Creedy's multi-speed motor.[4] All these machines are also described in the above-mentioned book by Miles Walker.

(b) *Differential cascade.* Let the 4-pole machine (Fig. 669) be connected to the line and the 16-pole one in cascade with it, but let the connections and the direction of rotation be such that the set runs *against* the normal direction of rotation of the 4-pole machine and in the normal direction for the 16-pole machine. Then the 4-pole machine operates as a frequency changer, while the 16-pole machine runs as a motor, supplying useful mechanical power and also driving the frequency changer as a generator.[5] This connection is seldom used because the set is not self-starting, and the power factor and the output are rather low. It may now be shown that the synchronous speed of the set is equal to that of a motor with 16 − 4 poles, or

$$\text{Synchronous speed} = 7200/12 = 600 \text{ rpm}$$

The frequency induced in the rotor of the first machine, which is connected to the line but driven against the direction of its rotating magnetic field, is

$$f_2 = f_1 + (\text{rpm}/60) \times p_1/2 \quad \dots\dots\dots \quad (7)$$

The speed of the second machine, neglecting its slip, is

$$\text{rpm}_2 = 120f_2/p_2 = 120f_1/p_2 + \text{rpm}_1 p_1/p_2$$

---

[1] A large number of articles and papers have been written on the cascade connection, but its use in practice is too limited to warrant going into further details. Considerable information on the subject will be found in the books quoted in §935. See also H. Cotton, *Inst. El. Engrs.* (British), *Journal*, vol. 61 (1923), p. 284; J. Tscherdanzev, *Elek. Zeits.*, vol. 46 (1925), p. 1219.

[2] *Electrical World*, vol. 63 (1914), p. 1247.

[3] *Inst. El. Engrs.* (British), *Journal*, vol. 52 (1914), p. 406.

[4] *Ibid.*, vol. 61 (1923), p. 309.

[5] C. della Salda, *Elettrotecnica*, vol. 9 (1922), p. 266; summarized in the *Science Abstracts*, vol. 25B (1922), Abstract No. 930.

Since the two values of rpm are equal,

$$\text{rpm} = 120f_1/(p_2 - p_1) \quad . \; . \; . \; . \; . \; . \; . \; . \quad (8)$$

which shows that the speed of the set approaches that of a single motor with a number of poles equal to the difference of the poles of the two motors.

Assuming that the two machines shown in Fig. 669 may be operated either singly or in cascade, the following four synchronous speeds may be had: 360, 450, 600, and 1800 rpm.

927. EXPERIMENT 49-A. — Speed Control of Induction Motors by Concatenation. — Belt or couple together two wound-rotor polyphase induction motors. Those having different numbers of poles are to be preferred. If the motors have the same ratio of transformation connect the rotor of motor *A* to the rotor of motor *B* with suitable starting resistors across the stator of motor *B*. With maximum resistance in the secondary of motor *B* connect the primary of motor *A* to an a-c source of rated voltage and frequency; then proceed as follows:

1. Make certain that the motors are connected in cumulative cascade. Gradually reduce the starting resistances to zero, meantime watching the input current and the speed of the set. Hold impressed frequency and voltage constant and gradually load the set, taking all electrical readings, also speed and secondary frequency. Increase the load until the pull-out torque of the set is reached. Determine this torque, at least approximately.

2. If the motors have unequal numbers of poles connect them in differential cascade and proceed as in 1.

3. Run each motor separately from the a-c source and determine their synchronous speeds, also approximate values of pull-out torque.

Verify eqs. (6) and (8). Compare the maximum torque of motors in cascade with the maximum torques of each motor, also the approximate horsepower of the set with the combined horsepower of the two motors running independently. Estimate approximate efficiencies of two motors in cascade and of individual motors run at the same speeds by means of resistance in their rotor circuits. State conclusions regarding this method of speed control.

SPEED CONTROL BY EXTERNAL EMF APPLIED TO THE SECONDARY

928. Let the rotor of a polyphase induction machine be provided with a three-phase winding connected to slip-rings. Let the stator be connected in the usual manner to a source of power, and let the rotor be revolved by a prime mover, the secondary circuit being open at the slip-rings. Let the speed of rotation be, say, about 20 per cent below synchronous speed, and let the magnitude, the frequency, and the phase of the slip-ring voltage be measured by suitable instruments. If an equal and opposite voltage is applied to the slip-rings from an external source, no current will flow through the rotor windings. However, let the external voltage be slightly lowered and its phase shifted, to allow a secondary current to flow, just sufficient to produce a torque for overcoming the rotor losses. Then the prime mover may be disconnected, and the motor will continue to run at about 20 per cent slip at no load. Should the slip-rings be short-circuited and the external secondary emf removed, the rotor would speed up practically to synchronism. Thus, by applying to the rotor circuit a proper external voltage, the machine may be made to run at no load at any desired speed, either below or above synchronism.

Now let the induction motor under test be loaded mechanically in the usual manner, and let it be running at, say, 5 per cent slip, with the slip-rings short-circuited. By inserting an external resistance in series with the rings, the slip may be increased, for example, to 20 per cent, the same load torque being kept. The machine then operates as a general a-c transformer (§944), delivering some output in a mechanical form and the rest in the form of an electrical I^2r loss in the resistances. These resistances can now be replaced by a revolving auxiliary a-c machine (§938) whose emf is equal and opposite to the actual voltage drop in the resistances. The same currents will continue to flow through the rotor windings, and the main motor will continue to function exactly as heretofore. However, the energy delivered to the auxiliary machine need not be lost; it may be converted into either mechanical work, electrical energy of the primary frequency, or d-c energy, and thus regained.

This is the principle of speed regulation used with very large induction motors, rated at thousands of kilovolt-amperes, where it would be very wasteful to absorb the power in resistances. Furthermore, by reversing the phase of the applied external secondary voltage, the main motor is caused to reverse the phase of its internal induced emf. This it can do only by running above synchronism, because then the conductors cut the air-gap flux in the opposite direction. The conditions are the same as if the rotor were running in series with *negative* external resistances. Thus, by using an external source of secondary a-c voltage of adjustable frequency, phase, and magnitude, the speed of an induction motor with a phase-wound rotor may be controlled economically within wide limits, both below and above synchronism.

Sometimes an auxiliary winding with a commutator, for speed control and for power-factor correction, is incorporated in the induction motor itself. Such " compensated machines " are considered with other types of commutator motors, in Chapter LIII, §1033.

929. Explanation by Means of Equivalent Diagrams. — The numerical relationships which obtain in an induction machine with a secondary external emf may be better understood with reference to the equivalent diagram of the induction motor (Fig. 661). Figure 671*a* corresponds to the right-hand end of Fig. 661, with the rotor resistance $r_2 = 0.1$ ohm per phase and the equivalent load resistance $R = 1.9$ ohm. The secondary current is assumed to be 100 amperes. All the quantities are reduced to the primary circuit, and the resistance R absorbs an electrical output equal to the useful mechanical output (in other words, R is *not* a speed-regulating resistance). According to eq. (7) in §889, the slip of the machine is $0.1/(1.9 + 0.1) = 0.05$, or 5 per cent. The useful output is 19 kw, and the secondary copper loss is 1 kw. In Fig. 671*b*, the resistance R is split into $R = 1.6$ ohm and $r_3 = 0.3$ ohm, the latter representing an actual resistance in series with the slip-rings, for speed reduction. The machine now operates at a slip $s = 0.4/(1.6 + 0.4) = 0.20$. Assuming the conditions to be so adjusted that the secondary current is still equal to 100 amperes, the useful power output is 16 kw, the rotor loss is 1 kw, and the loss in the external resistance is 3 kw.

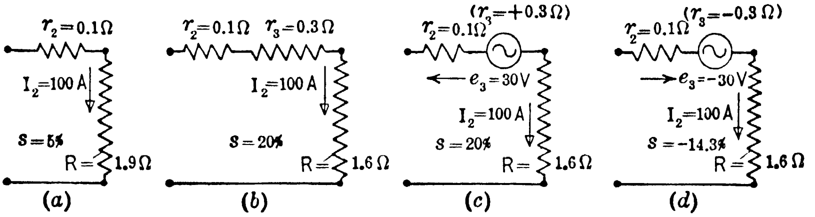

Fig. 671. Theory of speed regulation of an induction motor below and above synchronism by means of an external secondary emf.

In Fig. 671*c*, the resistance r_3 is replaced by an auxiliary motor with a counter emf $e_3 = 30$ volts, in phase opposition with the current I_2. In all other respects the conditions are the same as in the diagram (*b*), and consequently the slip is also equal to 20 per cent. The 3 kw delivered to the auxiliary machine may be recovered either in mechanical or in electrical form; the theoretical efficiency is therefore the same as in (*a*), in spite of a much higher slip. In Fig. 671*d*, the phase of the auxiliary machine is shown reversed, so that it operates as a generator and boosts the emf induced in the rotor of the main motor. This is equivalent to a fictitious negative resistance of 0.3 ohm, as indicated in the parentheses, so that the total resistance of the secondary circuit is $r_2 + r_3 = -0.2$ ohm. Hence, the slip $s = -0.2/(1.6 - 0.2) = -0.143$; in other words, the rotor speed is 14.3 per cent above synchronism.

Power-factor control. So far we have considered only the cases of e_3 in phase agreement and in phase opposition with I_2. A natural question arises: What would occur if e_3 had a component in quadrature with I_2? The answer is that such a component of e_3 would modify both the phase and the magnitude of I_2 and consequently would also change the power factor of the primary current. This subject is treated in §§932 to 942. The auxiliary machines described below for speed control are usually adjusted to improve the power factor of the main motor at the same time. In order to simplify the treatment, we shall first assume that e_3 produced by one of these auxiliary machines is either in phase or in phase opposition with I_2 and consequently affects only the speed of the main motor, without changing the power factor of its primary current. In other words, we shall assume that the motor has the same circle diagram as it would have without e_3. Later we shall consider the effect of shifting the phase of e_3.

930. Classification of Methods of Dynamic Speed Control.—The fundamental principle associated with methods of dynamic speed control is that an external emf, when introduced into the rotor circuit, in opposition to the emf due to rotor slip, at once reduces the rotor current. This, because of the resultant reduction in motor torque, lowers the speed of the motor to a point where the slip voltage again exceeds the external emf by sufficient to circulate the rotor current required by the load. Conversely, an external emf in phase with the slip voltage increases the rotor current above the value required by the load, and the rotor speeds up. This increase in speed continues until the new resultant of slip and external emf's leads to the required rotor current, even if this means that the motor must run above synchronous speed.

Various combinations and types of machines have been used to control the speed of large induction motors by this introduction of external emf's, these machines absorbing energy from the rotor of the main motor and returning it either to the supply or to the shaft of the motor. Though it is not feasible to explain the various systems in detail it should be possible for the reader, making use of the principles laid down in this chapter, to follow the literature on the subject. Characteristic methods by which the power corresponding to e_3, for speeds below synchronism, is regained electrically and those in which this power is regained mechanically will be illustrated.

A. Slip Power Regained Electrically:

(1) Through a polyphase commutator motor (§937) which drives an induction generator (§899) connected to an a-c line capable of absorbing this power (Fig. 672). Usually it is the same line to which the main induction motor is connected (the Scherbius system). Considerable auxiliary equipment not shown in Fig. 672 is required, and the control is rather complicated. The speed of the main motor is adjusted by changing the taps on the control transformer (Fig. 672), the motor slowing down as the polyphase commutator motor is made to speed up and return more power to the a-c line. This power, obviously, is drawn from the rotor of the main motor.

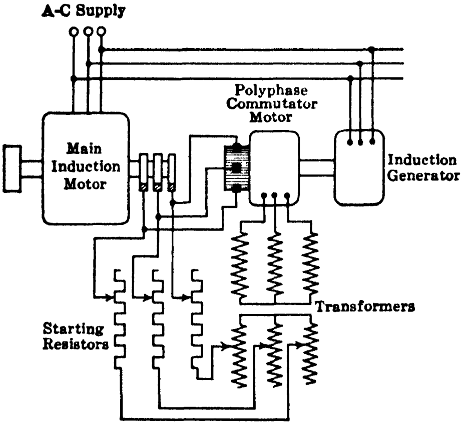

FIG. 672. Schematic diagram of the Scherbius system of speed control.

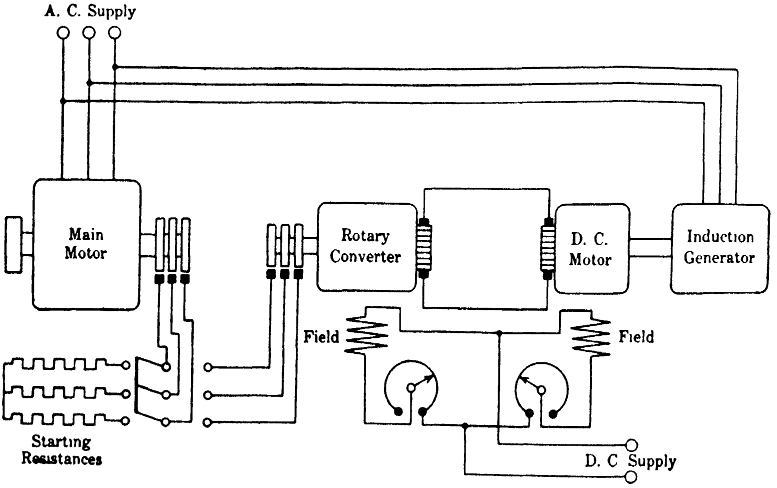

FIG. 673. One form of the Kraemer system of speed control of a large induction motor.

(2) Through a rotary converter (Chapter XLIV) which supplies direct current to a motor which drives a generator of any desired kind and furnishes power where it may be used to advantage; for example, the

motor may drive an induction generator connected to the same line as the main motor (Fig. 673). The speed of the rotary converter (see Vol. I, p. 650) is determined by the slip frequency of the main motor. Likewise, the voltage impressed upon the rotary converter slip-rings is proportional to the main motor slip. This voltage, rectified by the rotary converter, is applied to the d-c motor which, in turn, drives the induction generator and sends power back to the a-c supply. Control is by the field of the d-c motor which is separately excited, from an auxiliary d-c supply, as is the field of the converter.

(3) Through a frequency converter[6] (§938) which, when mounted on the main motor shaft, changes currents of the slip frequency into currents of the frequency of the line to which the main motor is connected. Excess power is returned to the a-c supply line.

B. Slip Power Regained Mechanically:

(1) Through a polyphase commutator motor (§937) mounted on the shaft of the main motor or mechanically connected thereto (the original Kraemer system) (Fig. 674).

(2) Through a rotary converter and a d-c motor direct connected to the main induction motor (Kraemer).

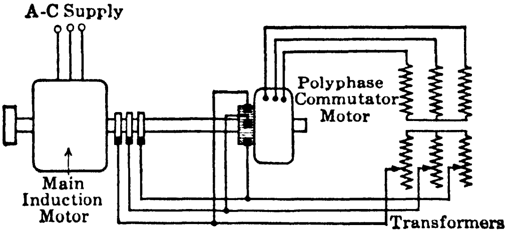

FIG. 674. Speed control by means of a polyphase commutator motor on the shaft of the main motor (Kraemer).

(3) Through a frequency converter (§938) and a synchronous motor (generator) direct connected to the main induction motor. The frequency converter has to be driven by a small synchronous motor at the proper speed (Fig. 675). When the frequency converter (§938) is mounted on the shaft of the main motor, it must be designed for low speed and will be expensive for its rating. A better design results if the frequency converter is driven by a small synchronous motor running at high speed (Fig. 675) and fed from a synchronous generator on the shaft of the main motor. In Fig. 675 the synchronous generator on the main shaft supplies an adjustable emf of $(1 - s)$ times supply fre-

---

[6] For a general theory of frequency transformations, see A. Scherbius, " Die magnetische Induktion in geschlossenen Spulen," Oldenbourg, 1919.

quency to the frequency converter which is driven at synchronous speed by its synchronous motor. It therefore generates emf of slip frequency which it impresses upon the rotor circuit of the main motor. Speed control is by means of the field of the synchronous generator. Power factor may be adjusted by the synchronous motor field.

In the foregoing classification, the expressions " motor " and " generator," in application to the auxiliary machines, are used on the supposition that the main induction motor operates below synchronism. In the range above synchronism, electric power has to be delivered to the rotor, and the functions of the auxiliary generators and motors are reversed.

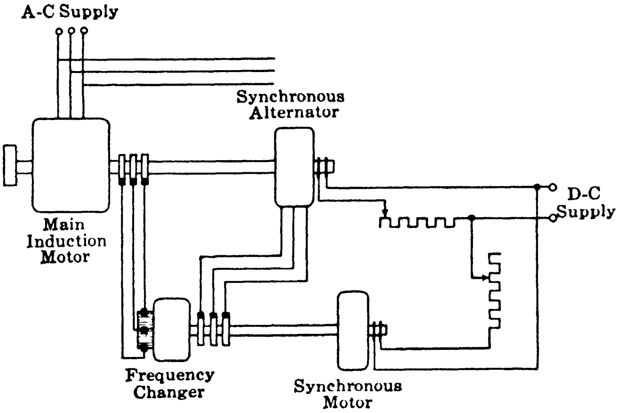

FIG. 675. Induction motor speed control by means of a frequency-changer set.

931. Electronic Speed Control.[7] — Various means have been devised to utilize electronic methods in the speed control of a-c motors. Figure 676 shows a three-phase electronic rectifier (Chapter LIX) receiving power at slip frequency from the rotor of an induction motor and converting it into direct current. This current is then supplied to the armature of a d-c motor mounted on the shaft of the induction motor. The field of the d-c motor is separately excited and capable of control by means of a rheostat. Adjustment of this field determines what counter emf the d-c motor generates when driven at a certain speed by the induction motor. When the counter emf is such as to just permit a required rotor current to flow in the induction motor the speed of the set does not change. However, if the load increases, or if the field of the d-c machine is increased so that its counter emf increases, the rotor current of the induction motor (and its torque) falls below the value required by the load and the set starts to slow down. This reduction in speed continues until the value of the rectified rotor emf again exceeds the counter emf of the d-c machine by enough to circulate the required rotor current. Meanwhile, the d-c machine acts as a motor and helps drive the set, thus converting the output of the rotor of the induction motor into useful work, instead of wasting it in heat as happens when speed control is obtained by resistance in the rotor circuit of an induction motor.

---

[7] Alexanderson, Edwards, and Willis, *Elec. Eng'g*, June, 1938, p. 343, "Electronic Speed Control of Motors."

If desired, the d-c motor may be used to drive an induction generator and so return power to the supply. The method is thus seen to be similar to the Kraemer system of speed control (§930).

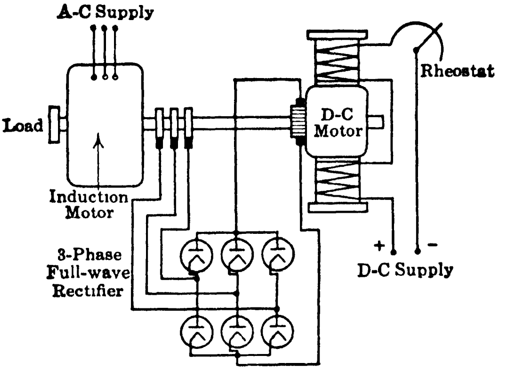

FIG 676 Electronic device for the control of induction motor speed.

POWER-FACTOR CONTROL

932. The polyphase induction motor has many advantages in its favor, but it also has two disadvantages, namely: (a) it is inherently a constant-speed machine, and (b) it takes a considerable lagging reactive current from the line. We have considered above various means whereby the speed of an induction motor may be regulated at will, by introducing an external emf into the secondary circuit. Similar means may be used for improving the power factor of the primary current. To avoid repetition, it will be assumed that the reader is familiar with the contents of §§928 to 930, so that only additional features will be considered below.

Besides the power-factor control by means of a secondary inserted emf, another self-evident solution is to compensate for the lagging reactive component of the primary current consumed by an induction motor, by connecting to the same line, in parallel with the stator, a device which takes a leading current. As such, static condensers (Chapter XXVII) offer the simplest solution, and are being used to an increasing extent. An overexcited synchronous motor or a synchronous condenser (Chapter XLIV) is another solution, where it can be used economically. In considering power-factor control by means of an external secondary emf, we shall limit ourselves to separate auxiliary machines. Induction motors in which such an additional emf is provided by means of a commutated winding in the machine itself are described with the commutator machines in Chapter LII.

933. An External EMF Leading the Secondary Voltage. — Let an external emf from a suitable source be introduced into the rotor circuit, and let this emf be of the same frequency as the emf induced in the secondary conductors by the common air-gap flux of the machine, and leading it by a considerable angle. The phase of the secondary current is advanced thereby, and since an induction motor is essentially a transformer, the phase of the primary current will be also advanced.

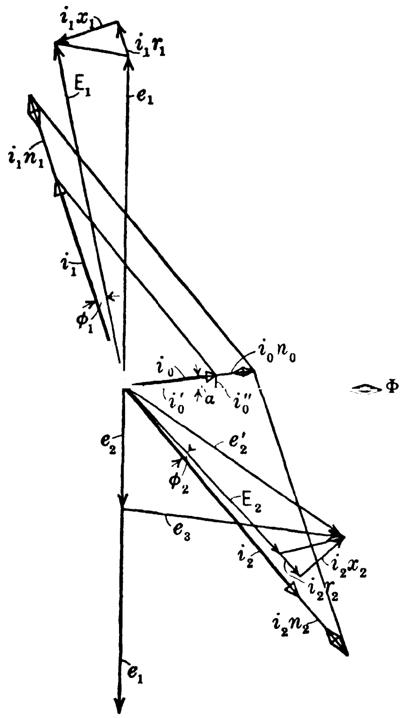

FIG. 677. A vector diagram of a transformer with leading primary current.

Figure 677 is similar to Fig. 283 and represents the relationships in a transformer in which an external emf, e_3, has been applied in the secondary circuit, leading the secondary induced emf, e_2, by nearly 90 degrees. The total applied voltage in the secondary circuit is therefore $e_2' = e_2 + e_3$. Subtracting from it the secondary impedance drop, $i_2r_2 + ji_2x_2$, gives the secondary terminal voltage, E_2. Assuming the external load to be unchanged, the current i_2 lags behind E_2 by the same angle ϕ_2 as before. Let the useful flux, Φ, also be the same as before, requiring the same magnetizing ampere-turns, i_0n_0. Adding the secondary ampere-turns, i_2n_2, gives the required primary mmf, i_1n_1, and consequently the primary current, i_1. It will be seen that, by sufficiently advancing the phase of i_2, the current i_1 may be made to lead the primary terminal voltage, E_1. A similar conclusion may be drawn for an induction motor, except that for it i_2 is always in phase with E_2.

Neglecting the primary impedance drop, an induction motor or a transformer (connected to a source of constant voltage) operates at a constant useful flux which requires a definite magnetizing current, and consequently a definite number of primary reactive volt-amperes. It may be argued that there is no economy in furnishing the same reactive volt-amperes from the secondary circuit since ultimately they have to come from the same primary line. However, in the case of an induction motor, the excitation supplied from the secondary circuit, by means of an additional emf, e_3, is at the slip frequency, which is only a few per cent of the primary frequency. Therefore, the required reactive voltage is much lower; and if the necessary lagging volt-amperes are taken from the primary line through a frequency converter, their amount is much smaller than the leading volt-amperes which the primary winding has to take in as a consequence.

934. Explanation by Means of an Equivalent Diagram. — In Fig. 671, the external emf, e_3, is assumed in §929 to be in phase agreement (or in phase opposition) with the secondary current. Now assume e_3 to be out of phase with I_2. Then e_3 may be resolved into a component in phase with I_2 and one in quadrature with it. The first component will cause an increase or decrease in the speed of the machine; the second component will shift the phase of the secondary current. If the quadrature component of e_3 lags behind I_2, the result will be the same as if the secondary leakage reactance of the machine were increased. If, however, the quadrature component of e_3 leads I_2, then its effect is to counterbalance the reactive drop in the machine. By making this component of e_3 sufficiently large, the reactive drop can be made negative. This is equivalent to substituting a capacitance for the secondary leakage inductance; the modified equivalent diagram is shown in Fig. 678 (compare with Fig. 661).

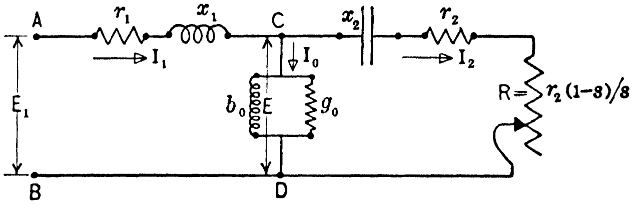

FIG. 678. An equivalent diagram of the induction motor, with a capacitance in the secondary circuit.

The secondary circuit, *CRD*, contains only capacitance and resistance; hence I_2 leads E. The exciting current, I_0, is lagging behind E, but the sum of I_0 and I_2 (equal to I_1) may be made to lead E. The primary impedance being comparatively small, I_1 can also be made to lead E_1. This is another explanation of the reason why a leading e_3 causes the phase of I_1 to be advanced.

SPECIAL COMMUTATING MACHINES USED IN THE CONTROL OF SPEED AND POWER FACTOR OF INDUCTION MOTORS

935. Various Types of Commutating Machines. — In the several methods described in §§930 and 931 for the control of speed and power factor of large wound-rotor induction motors, it was necessary to make use of commutator machines, some of which have not previously been described in this book. In order that the simpler aspects of their performance may be understood the remainder of this chapter is devoted to a brief description of these machines, including:

a. The generalized rotary converter (§936).
b. Polyphase commutator machines (§937).
c. Commutator-type frequency converters (§938).
d. The Leblanc-Scherbius phase advancer (§939).
e. The Kapp vibrator (§942).

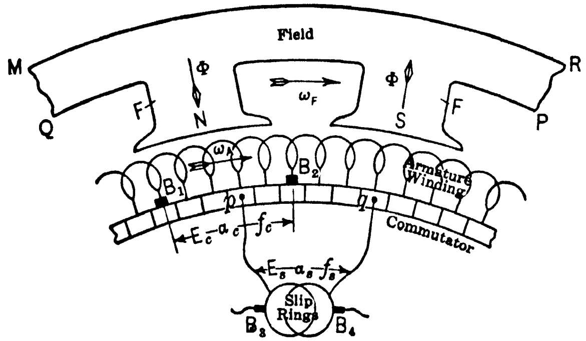

FIG. 679. A generalized rotary converter.

936. Generalized Rotary Converter. — Consider a rotary converter (Fig. 679), such as is described in Chapter XLIV, and let the two sets of brushes of opposite polarity, B_1 and B_2, be displaced by an angle, α_c, different from 180 electrical degrees. With the stationary field poles excited with direct current, no matter what the magnitude of this angle, a direct voltage, E_c, will be induced between the brushes, at any velocity of rotation of the armature. The position of the brushes and the speed of rotation affect merely the value of the voltage E_c. Let the two slip-rings shown in the sketch be connected to the armature winding at two arbitrarily chosen points, p and q, an electrical angle α_s apart.[8] The magnitude, E_s, and the frequency, f_s, of the alternating voltage between the slip-rings depend, in the usual manner, upon the speed of rotation of the armature.

---

[8] The subscripts c and s are used to indicate "commutator" and "slip-rings," respectively.

Let the field structure, FF (excited with direct current), instead of being stationary, be rotated at a certain constant angular velocity ω_F, while the armature velocity is ω_A in the same direction. To make our conclusions independent of the number of poles, let ω_F and ω_A be expressed in electrical radians per second; that is, let them refer to the actual angular velocities of a bipolar machine. The voltage E_c between the brushes B_1 and B_2 is then no longer continuous, but alternating, of a frequency, say, f_c; the voltage E_s is also alternating, of a different frequency, f_s. As is explained below, we may write the following relationships:

$$E_c = m\Phi(\omega_F - \omega_A) \quad \text{. . . . .} \quad (9)$$

$$E_s = n\Phi(\omega_F - \omega_A) \quad \text{. . . . .} \quad (10)$$

$$f_c = \pm\omega_F/2\pi \quad \text{. . . . .} \quad (11)$$

$$f_s = \pm(\omega_F - \omega_A)/2\pi \quad \text{. . . . .} \quad (12)$$

where Φ is the useful flux per pole and m and n are certain constants or proportionality factors which include the number of armature turns per pole. The plus-or-minus sign in eqs. (11) and (12) is necessary because a frequency is always positive, while ω_F and ω_A may be either positive or negative.

To see the truth of eq. (11), consider again the field structure to be stationary, and let the brush gear be shifted by 180 electrical degrees. The polarity of the brushes will be reversed thereby. Now let the brushes be rotated continuously; their polarity will be changed as many times as the number of poles which they pass. The velocity of rotation of the armature winding will in no way affect the frequency of these reversals. The result will be the same if the brushes are kept stationary and the field structure revolved. *The frequency, f_c, of the alternating emf, E_c, between brushes resting on a commutator is equal to the frequency of the relative motion of the brushes and the inducing field.* For an ordinary rotary converter, $\omega_F = 0$ and consequently $f_c = 0$, which means direct voltage.

The armature conductors cut the flux Φ at a velocity $\omega_F - \omega_A$; consequently, the two induced voltages, E_c and E_s, are proportional to $\omega_F - \omega_A$ and to the inducing flux, Φ. This proves eqs. (9) and (10). As to eq. (12), *the frequency of the voltage between the slip-rings is independent of the existence or non-existence of the commutator and its brushes; it is determined solely by the relative motion of the armature conductors with respect to the field flux.*

We thus see that a combination of a revolving commutated winding and a moving field flux may be used as a basis for a source of emf of adjustable frequency, independent of the velocity of rotation of the armature. The addition of slip-rings permits combining two different frequencies in the same machine. The flux Φ need not be rotated by bodily revolving the field structure. This flux may be produced by a combination of polyphase currents (§810) which will cause it to revolve with respect to a stationary exciting winding and iron core. With these principles in mind, the reader should have no difficulty in understanding the action of the following two machines.

937. The Polyphase Commutator Machine. — One of the types of auxiliary machines used for speed control of large induction motors is shown in Fig. 680. It has a stator similar to that of an induction motor and is provided with the usual three-phase winding (Fig. 350). The revolving part is similar to a d-c armature (Fig. 198), that is, it has a winding closed upon itself, the junctions of the individual coils being connected to commutator segments. The brushes are spaced 120 instead of 180 electrical degrees apart. The connections between the stator and the brushes may be of the series, shunt, or compound type, as in d-c machines (§273). A compensating winding (not shown in the sketch) may also be provided. It is placed on the stator, coaxially with the brushes (§377), and serves to cut down the armature flux and its inductance.[9]

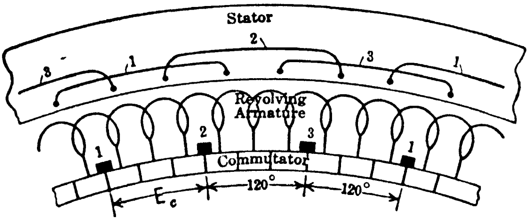

FIG. 680. A three-phase commutator motor or generator.

At the brushes of such a machine, there is produced an emf whose frequency is entirely determined by the frequency of the stator currents and is independent of the velocity of rotation of the armature; see eq. (11). In other words, this machine can be used in series with the rotor winding of an induction motor, and it will adjust itself automatically to the frequency of the rotor currents. The velocity of rotation of the auxiliary machine will depend upon the value of the emf which it is called upon to furnish, and upon the magnitude of its flux; see eq. (8). When operated as a motor, it can either furnish mechanical power, directly, on the same shaft as the main motor, or drive a generator through which power is recovered electrically.

---

[9] Polyphase commutator motors are considered in more detail in Chapter LIII. It is desired here to give only enough information for a clear understanding of the production of the auxiliary emf, e_3, for speed control of an induction motor.

The Scherbius machine. A modification of the polyphase commutator machine in Fig. 680 is shown in Fig. 681. The stator is provided with salient poles, and the armature winding has a pitch of 120, instead of 180, electrical degrees. With these features, it is possible to use commutating poles, connected as in a d-c machine (§274), and thus to improve the commutation considerably. The winding on the main poles may be of the series, shunt, or compound type, depending upon the characteristics desired. Two emf's are induced in the armature by the main poles: one due to the rotation of the armature (generator emf), the other due to pulsations of the flux itself (transformer emf). The latter is usually undesirable, and its effect can be neutralized by a distributed compensating winding (not shown in the sketch) placed on the stator and, as nearly as possible, identical with the armature winding. The transformer emf's induced in the two windings are then equal, and by connecting the windings in opposition these emf's are canceled.

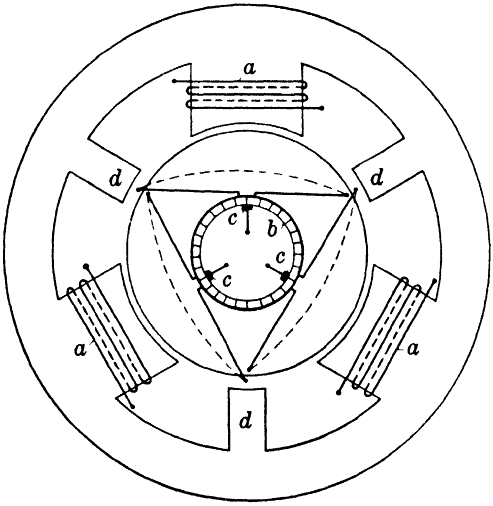

Fig. 681. The Scherbius polyphase commutator machine.

938. Commutator-Type Frequency Converter. — The auxiliary machine of the type shown in Fig. 682 is sometimes used for converting currents of the slip frequency into those of the line frequency, or vice versa. Its rotating part, or the armature, is similar to that of a three-phase rotary converter, except that there are three sets of brushes on the commutator for every 360 electrical degrees. With the bipolar construction shown in the sketch, there are three sets of brushes, set 120 mechanical degrees apart. In the simplest case, the stator consists of a laminated iron ring without any winding, and serves only to provide a high-permeance path for the armature flux. Consequently, the machine can develop no electromagnetic torque and must be driven by a motor.[10]

---

[10] This machine is to be distinguished from the induction-type frequency converter described in §§944 to 949.

When the commutator brushes are connected to a source of three-phase currents, a revolving magnetic flux is produced in the air-gap. *This flux rotates in space at a speed that depends upon the frequency of the currents flowing through the commutator brushes and is independent of the speed of rotation of the armature itself.* The rotation of the armature merely substitutes one individual coil for another in the group between two brushes, but the instantaneous value of the current in that group (and consequently its mmf) is determined by the current at the brushes. Hence, so far as the mmf is concerned, the armature may be considered to be stationary.

We thus have a machine which, on the commutator side, can oppose an applied emf of any frequency, independent of the velocity of rotation of the armature; see eq. (11). On the other hand, the frequency of the currents delivered through the slip-ring brushes depends upon the frequencies of rotation of both the field and the armature. Hence, the machine acts as a frequency converter.

Let currents of a definite frequency, f_s, be sent into the armature through the slip-rings; the frequency of the currents delivered through the commutator is then determined by the magnitude and direction of the velocity of rotation of the armature. The flux rotates at an angular velocity determined by the frequency f_s, with respect to the armature conductors. Adding to this frequency, algebraically, the frequency of rotation of the conductors themselves gives the frequency, f_c, of rotation of the flux in space, and hence the frequency of the currents delivered through the commutator; see eq. (11).

In the machine shown in Fig. 682, the air-gap flux is produced by the combined action of the mmf's of the currents of both frequencies. For some purposes it is desirable to regulate this flux by varying the voltage applied at the slip-rings. The armature reaction of the currents delivered through the commutator is then removed by providing a compensating winding on the stator (§377). This winding is connected in series with the leads to the commutator brushes. Sometimes a short-circuited winding is also placed on the stator for the purpose of improving commutation. High-frequency fluxes concomitant with current reversals are wiped out by secondary currents in this winding.[11]

As an example of application of a frequency converter, let the machine be operating under the following simultaneous conditions (see Fig. 675):

(a) The stator winding of the main induction motor is connected to a primary source of power of frequency f_1.

(b) The rotor of the main induction motor revolves at such a speed that the frequency of the secondary currents is f_2.

---

[11] J. Kozisek, *Elek. Zeits.*, vol. 46 (1925), p. 142.

(c) The armature of the frequency converter is driven by a small synchronous motor connected to the same primary line of frequency f_1.

(d) The commutator brushes of the frequency converter are connected to the slip-rings of the main motor.

(e) The slip-rings of the frequency converter are connected to the armature terminals of an auxiliary synchronous motor.

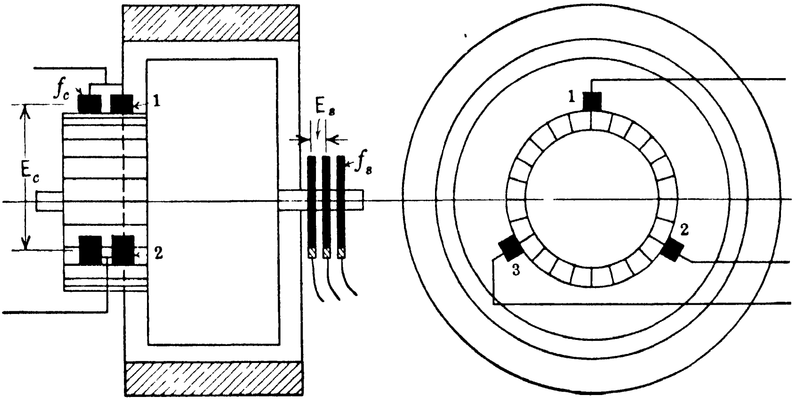

FIG. 682. A commutator-type frequency converter.

Let it be required to compute the frequency of the currents delivered to the latter motor, in order to ascertain its speed and thus to determine how the mechanical power regained in this motor may be utilized. We have: $\omega_A = 2\pi f_1$; $\omega_F = 2\pi f_2$. Hence, eq. (12) gives: $f_s = f_1 - f_2$. This means that the auxiliary synchronous motor receives currents at a frequency corresponding to the actual speed of the main induction motor. Consequently, this synchronous motor may be mounted directly on the same shaft with it and made to drive the same load.

939. The Commutator-Type Phase Advancer. — In its simplest form, this phase advancer (Fig. 682) consists of a revolving armature of the d-c type, with a commutator and three sets of brushes per pair of poles, and a laminated iron ring outside. The slip-rings should, for the present, be disregarded. The external iron core serves merely to provide a high-permeance path for the flux, and may either be stationary or revolve with the armature. The machine can exert no electromagnetic torque and has to be driven by a small motor, just capable of overcoming the losses in the phase advancer itself.

Let the machine be rotated at a certain speed, and let three-phase currents of a known frequency be conducted into the armature through the brushes. Since the brushes are stationary they connect always to conductors in the same position in space, so that the velocity of rotation of the magnetic flux produced by such currents is independent of the speed of rotation of the armature, and is determined solely by the frequency of the currents themselves. The magnitude of the flux depends upon the magnitude of the current and upon the permeance of the magnetic path. We shall now determine the magnitude and the phase of the emf induced in the armature winding by this flux.

Since the rotation of the armature conductors does not affect the magnitude, phase, or speed of rotation of the flux, we shall first assume the conductors to be stationary. Then the device becomes simply a three-phase reactive coil, and (neglecting the ohmic drop) the emf applied at the brushes *leads* the current by 90 degrees. Hence, the flux revolves in such a phase position, with respect to the groups of conductors, that in each phase the induced emf *lags* behind the current by 90 degrees. Let the armature be rotated at a speed less than that of the flux. The foregoing conditions will still exist, but the induced counter emf will be reduced because the relative speed between the flux and the conductors is now lower; eq. (9), §930. Consequently, with the same current, the applied voltage is less, but is still leading the current.

At synchronous speed, the counter emf becomes equal to zero, and the applied voltage is reduced to a small value necessary for overcoming the ohmic resistance of the machine. If now the speed of the armature is increased beyond synchronism, the sign of the induced emf is reversed because $\omega_F - \omega_A$ becomes negative. Therefore, with the same current, the applied voltage also has to be reversed so as to lag behind the current. *In a commutated polyphase armature, driven at a supersynchronous speed, the current leads the voltage applied at the brushes by nearly* 90 *electrical degrees.* Hence, such an armature may be used for the purpose of advancing the phase of the secondary current.

940. The Self-Excited or Series-Excited Phase Advancer. — The phase advancer described in the preceding section may be called a series-excited or self-excited machine, since its magnetic flux is produced by the same current whose phase it is sought to advance. Such a machine is usually driven at a high speed by a separate small motor and is electrically connected in series with the slip-rings of the main induction motor. By a proper choice of conditions, it is possible to increase the power factor of the primary current to unity and even to make the current slightly leading, between, say, half load and full load. At small loads, when the secondary current is small, the flux of the phase advancer is also reduced and is not sufficient to bring the power factor to unity.

In Fig. 683, the circle $APQN$, with its center at C, represents the locus of the primary current when the motor is operating without any phase advancer (Chapters XLVII and XLVIII). OA is the no-load current, and OP is a current somewhere near the rating of the machine. It can be shown theoretically that with a self-excited phase advancer, without saturation in its magnetic circuit, the locus of the primary current is still a circle (see References). This circle, AP_1QN_1, with its center at C_1, is of larger radius and lies higher above the axis of abscissas. The line gh is drawn parallel to Ox, so that the power input at P_1 is the same as at P. The current vector OP_1 leads the terminal voltage E_1, and a satisfactory power-factor compensation is obtained within the working range of the machine. However, at small loads the compensation is imperfect, and at no load it is zero.

It is also of interest to note that the overload capacity of the motor is greatly increased, the highest point, M_1, on the new circle being much above the point M on the original circle. On the other hand, the performance characteristics as a generator (below Ox) are much inferior, the influence of the phase advancer being to reduce the maximum output and to lower the power factor. This, of course, can be remedied by reversing the sign of the emf of the phase advancer. When the magnetic circuit of the phase advancer is saturated, its emf does not increase as rapidly as the current. In this case, the current locus has the general shape indicated by the curve AP_3B.

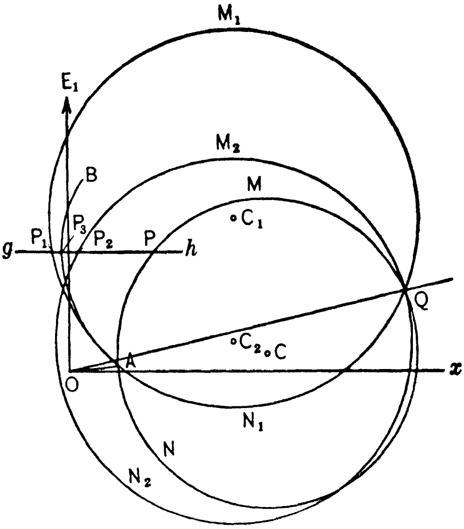

Fig. 683. Circle diagrams of an induction motor with and without a phase advancer.

941. Separately Excited Phase Advancer. — The drawbacks of a self-excited phase advancer are (a) its ineffectiveness at light loads and (b) absence of provision for improving the commutation. Its good features are its simplicity and the possibility of being driven at a high speed by a separate motor. In order to enable a phase advancer to develop a sufficiently high leading emf at small values of the main rotor current, it may be separately excited from a source of voltage which does not become small at light loads. The most natural source of such excitation is the primary line, and the simplest way of introducing this excitation is through the slip-rings connected to the armature winding of the phase advancer (Fig. 682). With such an addition, the phase advancer simply becomes a frequency converter; for further details the reader is referred to §938.

In order to cause the external secondary emf to lead with respect to the internal one, the phase of the voltage, either at the slip-rings or at the commutator brushes of the phase advancer, must be suitably shifted forward. The line voltage is usually applied to the slip-rings of the phase advancer through transformers, and its phase can be adjusted by a proper polyphase interconnection or by using an induction regulator (§954). The slip-frequency emf may be advanced by simply shifting the commutator brushes against the direction of rotation of the flux.

As is explained in §938, such a frequency converter must be driven at the same angular electrical velocity as the main induction motor, in order to have a secondary voltage induced in it at the correct slip frequency. If made with the same number of poles as the main machine, it is directly connected to it; otherwise it has to be driven through gears or some equivalent rigid mechanical or electrical coupling. The phase advancer may be provided with a compensating winding on the stator, and may also have suitable means for improving its commutation.

Assuming the emf, e_3, delivered by such a separately excited phase advancer to be constant in magnitude and in phase, and independent of the secondary current, the primary current locus of the main motor is still a circle (see the reference to Dreyfus' article in §943). Such a circle, $QM_2P_2N_2$, is shown in Fig. 683; its center is at C_2. It will be seen that the power factor remains high throughout the useful motor range, say between half load and overload, while at light loads the current is leading instead of lagging. Both the generator and the motor ranges are satisfactory, and the overload capacity is greater than without the phase advancer.

With this fundamental information, and with the references in §943, the reader should be prepared to make a more thorough study of the subject and to follow future advances of the art.

942. The Kapp Vibrator. — This device for improving the power factor of an induction motor consists of three separately excited d-c machines; each armature is connected in series with a corresponding slip-ring of the rotor of the main motor. Low-frequency alternating currents, flowing through these armatures, make them oscillate to and fro, and the counter emf developed by this motion leads the current wave. Consequently, such a set is a source of a leading emf, e_3, and may be used for power-factor correction. The subject is of considerable theoretical interest but has not been sufficiently developed in practice to warrant more space here. We give below some references to the literature on Kapp vibrators.

943. EXPERIMENT 49-B. — An Experiment in Dynamic Speed Control. — As an example of the principles of dynamic speed control of polyphase induction motors it is suggested that the student set up one of the systems described in §930, and determine the limits within which it is possible to control both speed and power factor of an induction motor.

For this experiment a polyphase wound-rotor induction motor of fair size is needed, also a small rotary converter, and a d-c motor coupled to a small induction motor of the same voltage and frequency as the main motor. A separate source of direct current for excitation is also required.

Assuming a 110-volt, three-phase, 60-cycle source, the following is an example of equipment which should prove suitable: A 25-horsepower, three-phase, 60-cycle wound-rotor induction motor, having an open-circuit voltage ratio of 110/250 volts, and coupled to a d-c generator or other suitable load device; a 10-kw, three-phase, 25-cycle, 110-volt rotary converter; a 15-horsepower, 220-volt d-c motor driving a 15-horsepower, three-phase, 110-volt, 60-cycle induction motor.

Connect the machines as in Fig. 673 except that for the equipment assumed it may be necessary to connect the rotor of the main motor to the a-c supply and the stator to the rotary converter and starting resistors. Then, at a slip of 40 per cent, and neglecting losses, the emf impressed on the rotary converter would be $0.4 \times 250 = 100$ volts, at 24 cycles. The output voltage impressed by the rotary converter upon the d-c motor would be (Chapter XLV) $100/0.612 = 163$ volts.

Start the main motor without load, using resistance in the secondary circuit. After this resistance is all out and the motor running near synchronous speed connect the rotary converter to the secondary of the main motor, having opened the leads from the converter to the d-c motor, and having opened the starting resistances. Apply normal field to the rotary converter and gradually load the main motor, thus bringing up the voltage and frequency impressed upon the converter, which should start and run at a speed determined by the slip frequency of the main motor. Start the small induction motor and apply a weak field to the d-c machine; then parallel it with the d-c terminals of the converter, first making sure that polarity and voltage are correct (§257). In case the converter has failed to start it may be brought up in speed by first closing the line between the converter and the d-c motor, and then applying weak field to the d-c machine.

Having the set running in a normal manner, load the main motor and hold this load constant, meantime varying speed by adjusting the field of the d-c motor while keeping the field of the converter constant. Take all electrical and speed readings.

Now, with a given setting of the fields, vary the load on the motor and again take readings. Finally, for a given load and speed adjustment vary the field current of the rotary converter and note, especially, the variation in power factor of the main motor.

Plot curves of main motor speed against regulating (d-c motor) field current, at constant load; also of main motor power factor against converter field, at constant load. The data may be analyzed further as the student may desire.

As a part of the discussion of results specify the equipment needed to control properly the speed and power factor of a rolling-mill motor of several thousand horsepower. Comment upon the effectiveness and ease of power factor and speed control by this method.

REFERENCES

ARTICLES

1. JOHN I. HULL, *Trans. A.I.E.E.*, vol. 39 (1920), p. 1135, Theory of speed and power factor control of large induction motors by neutralized polyphase alternating-current commutator machines.

2. W. O. OSCHMANN, *Trans. A.I.E.E.*, vol. 33 (1914), p. 899, Concatenated induction motors for rolling mill drive.

3. G. A. MAIER, *Trans. A.I.E.E.*, vol. 30 (1911), p. 2455, Methods of varying the speeds of alternating-current motors.

4. F. W. MEYER and W. SYKES, *Trans. A.I.E.E.*, vol. 31 (1912), p. 2067, The economical speed control of alternating-current rolling motors.

5. K. L. HANSEN, *Jour. A.I.E.E.*, December, 1923, Modification of polyphase induction motor performance by the introduction of emf in the secondary.

6. H. M. NORMAN, *Trans. A.I.E.E.*, vol. 45 (1926), p. 369, Starting characteristics and control of polyphase squirrel-cage induction motors.

7. ALEXANDERSON, EDWARDS, and WILLIS, *Elec. Eng'g*, June, 1938, p. 343, Electronic speed control of motors.

8. A. K. BUSHMAN, *Gen. Elec. Rev.*, October, 1923, Adjustable-speed main roll drives.

9. G. FOX, *Blast Furnace and Steel Plant Magazine*, March, April, 1923, Speed control of polyphase motors.

10. M. H. MORGAN, *Iron and Steel Engineer*, October, November, 1928, Adjustable speed main roll drives.

11. J. D. WRIGHT, *Gen. Elec. Rev.*, vol. 20 (1917), p. 104, Speed control of induction motors for steel mill drive.

12. L. A. UMANSKY, *Iron and Steel Engineer*, May, 1927, p. 3, Speed regulation of main roll drives.

13. W. NÜRNBERG, *E.T.Z.*, Sept. 8, 1938, Asynchronmotoren mit Drehzahlregelung.

14. G. E. STOLTZ, *Elec. Jour.*, vol. 11 (1914), p. 277.

15. L. DREYFUS, *Archiv für Elektrot.*, vol. 15 (1925), p. 1; vol. 13 (1924), p. 507.

16. A RAUTH, *Revue générale de l'électr.*, vol. 17 (1925), p. 999.

17. W. SEIZ, *BBC Mitteil.*, vol. 11 (1924), p. 139; vol. 12 (1925), p. 29.

18. A. HARTMAN, *ibid.*, vol. 11, pp. 31 and 127; vol. 12, p. 17.

19. S. A. PRESS, *ibid.*, vol. 12, p. 434; vol. 13, pp. 214 and 403.

20. H. COTTON, *Beama* (now *World Power*), vol. 12 (1923), pp. 158 and 226.

21. M. GUIDÉE, *Revue générale de l'électr.*, vol. 13 (1923), p. 969.

22. A. SCHERBIUS, *Elek. Zeits.*, vol. 42 (1921), p. 969.

23. M. OSNOS, *Elek. Zeits.*, vol. 40 (1919), p. 127.

24. M. LATOUR, *Electrical World*, vol. 72 (1918), p. 484.

BOOKS

MILES WALKER, The Control of the Speed and Power Factor of Induction Motors, Van Nostrand.

HERBERT VICKERS, The Induction Motor, Pitman & Sons.

M. SCHENKEL, Die Kommutatormaschinen, Berlin, 1924.

Standard Handbook for Electrical Engineers, Sixth Edition, sec. 7.

B. A. BEHREND, The Induction Motor.

C. P. STEINMETZ, Theory and Calculation of Electrical Apparatus.

C. P. STEINMETZ, Alternating-Current Phenomena, Chapter XIX.

E. ARNOLD, Die Wechselstromtechnik, Vol. V, part 2, Chapters VIII and X, Springer.

A. S. LANGSDORF, Theory of Alternating-Current Machinery, Chapter XIII, McGraw-Hill Book Co.

P. B. HARWOOD, Control of Electric Motors, Chapter XI, John Wiley & Sons.

CHAPTER L

DIVERSE TOPICS ON INDUCTION MACHINES

944. The Induction Machine as a Frequency Converter. — In most applications the polyphase induction machine (asynchronous machine) operates as a motor, at a minimum of slip in order to reduce the secondary copper loss. In certain cases resistances are inserted in the secondary circuit in order to obtain speed control (§§894 and 895), the energy consumed in these resistances usually being wasted as an unavoidable loss. Occasionally the asynchronous machine is operated above synchronous speed, whereupon it becomes a generator, either as a primary source of power or, by regeneration, as a means of returning power to the supply lines (§§899 to 903). When the machine is driven against its normal direction, i.e., against the direction of the rotating field, with the secondary circuit closed, the machine acts as a brake (§904).

The possibility of using this machine in connection with an a-c source for the production of a frequency either higher or lower than that of the source, in other words, as a frequency changer, was utilized in the cascade method of speed control (§§925 and 926). Thus it is seen to be a machine of many uses, some of which will be described in this chapter.

Generally speaking, an induction machine with a phase-wound secondary may be said to possess three points of application of power, namely, the primary terminals, the secondary terminals, and the shaft. At each of these three places, power may be either absorbed or delivered by the machine. This is shown in the following table, which gives the various possibilities and combinations:

Primary Terminals		*Secondary Terminals*		*Shaft*	
Electric power		Electric power		Mechanical power	
absorbed	delivered	absorbed	delivered	absorbed	delivered

Some combinations are evidently impossible for steady conditions; for example, power cannot be delivered at all the three places simultaneously, except momentarily, as this would be contrary to the law of conservation of energy. Various combinations are possible, and when an induction machine is being operated in this generalized manner it is known as a *general alternating-current transformer*, and sometimes, more specifically, as a *frequency converter* or *frequency changer*.[1] An induction motor, operating with an external resistance in the secondary circuit, is an example of such a general transformer, in that it converts the primary electric-power input partly into mechanical power on the shaft and partly into low-frequency currents in the resistances; the latter power under some circumstances could be utilized for a useful purpose, for example, for heating. Resistances can also be replaced by a commutator motor or by a rotary converter, and that part of the power input regained (§996).

Another case of operation as a general transformer is for the purpose of obtaining electric power at a higher frequency than that of an available supply (§944). For example, let the rotation of the magnetic field in the air-gap be clockwise, and let the field be produced by 60-cycle currents. This field rotates at synchronous speed. If the rotor is driven by external mechanical power at the same speed, counterclockwise, the frequency of the induced voltage at the slip-rings will be 120 cycles per second, or, if it is driven at one-half synchronous speed in the clockwise direction the frequency of the rotor emf is 30 cycles. The secondary terminals may be connected to a circuit where power of this frequency is needed, and the machine thus made to operate as a frequency changer. When the frequency changer is used to raise the frequency, electric power is delivered to the machine at the primary terminals and mechanical power to the shaft. The sum of these two power inputs, less the losses, will be available as the electrical output at 120 cycles. When used to reduce the frequency, electric power is taken in at the stator, while both electric power and mechanical power are delivered by the rotor.

At a constant primary voltage and frequency, and with the secondary terminals open but the rotor driven at various speeds, the air-gap flux of an induction machine is practically constant. It would be absolutely constant if it were not for the changes in primary resistance drop, the primary leakage reactance drop, and the reaction of the secondary core loss. With a constant air-gap flux, the secondary induced emf depends only upon the relative velocity between the revolving flux and the rotor conductors, both the magnitude of this emf and its frequency being proportional to the slip. Thus, plotted against either speed or slip as abscissas, the curves of secondary induced emf and frequency are approximately straight lines passing through zero at synchronous speed.

---

[1] The induction-type frequency converter is to be distinguished from the commutator type described in §938.

In general, the secondary frequency is given by the expression:

$$f_2 = f_1(1 \pm \text{rpm}/N_s) \quad \ldots \ldots \quad (1)$$

$$= f_1 \pm (\text{rpm}/60)(p/2) \quad \ldots \ldots \quad (2)$$

The plus sign applies when the rotor is driven *against* the direction of rotation of the stator field.

945. EXPERIMENT 50-A. — Induction-Type Frequency Converter; Secondary Voltage and Frequency at No Load. — The purpose of the experiment is to check the relationship discussed at the end of the preceding section. The voltmeter used across the slip-rings must give indications independent of frequency, or be properly calibrated (Chapters II and III). For frequency measurements, see §§455 to 457. As a check, the secondary frequency should also be computed from the primary frequency and the rotor speed. The machine under test should be driven by an adjustable-speed motor (Fig. 684), and the rotor circuits should be open, except for a voltmeter and possibly a frequency meter.

Begin with the rotor stationary and the primary connected to a proper source of a-c supply. Read the primary volts, amperes, watts, and frequency, and the secondary volts and frequency. Start the set in the direction of rotation of the stator field and increase its speed in steps, taking similar readings and measuring the speed at each step. The primary voltage and frequency are to be kept constant throughout the run. Go as far beyond synchronism as is mechanically safe. Stop the set and repeat the test, running the rotor against the revolving flux.

It is also of interest to find the law of increase in the secondary core loss with the frequency. To this end, the driving motor should be calibrated in the usual manner (Chapter XIII) and the mechanical losses of the induction machine determined separately. At synchronous speed, the secondary core loss is zero, and the primary power input covers the primary core loss and the primary copper loss. At other speeds, the secondary core loss may be supplied either electrically or mechanically (§900).

946. General A-C Transformer under Load. — Let the rotor of an induction machine be running in a stable manner at any speed whatever, other than synchronous, and let its slip-rings be connected to a circuit which either absorbs electric power or supplies power to the rotor. In other words, let the machine be operating at one of the possible combinations indicated in the table in §943. The following mechanical and electrical conditions are then satisfied:

(a) The total power input is equal to the total output plus the losses in the machine itself.

(b) The air-gap flux is of such a magnitude that the counter emf in the primary circuit, plus or minus the primary impedance drop, balances the applied voltage.

(c) The primary and the secondary currents are such that their combined mmf produces an air-gap flux which satisfies condition (b).

(d) The emf induced in the rotor circuit is such that the generalized Ohm's law is satisfied for this circuit, including the drop in the internal and external impedances, an external emf, if any, etc.

(e) The secondary emf is of the slip frequency.

By expressing these conditions analytically or graphically, the fundamental properties of the general transformer are obtained.[2] In general, the method of attack is the same as that developed in Chapters XLVII and XLVIII for the induction motor, and the reader is referred to Dr. Steinmetz's works for details.

In the operation as a frequency changer, when the useful output is obtained electrically from the secondary circuit, the machine is usually run at a constant speed, so as to keep the frequency of the output constant. If the load varies, while the primary voltage is kept constant, the secondary voltage also varies. To keep the secondary voltage constant, it is necessary to vary the primary voltage with the load. We have here two different conditions, somewhat analogous to the operation of a synchronous generator at a constant field current and at a constant terminal voltage (§449).

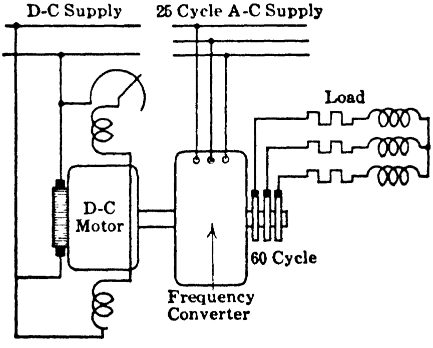

FIG. 684. Connections for load test of a frequency converter.

947. EXPERIMENT 50-B. — Induction-Type Frequency Converter Load Test: Characteristics at Constant Primary Voltage. — The machine is to be studied at a constant secondary frequency, say 60 cycles, the primary supply consisting of a 25-cycle source. The rotor is driven by a suitable motor against the revolving field. Figure 684 shows suitable connections for frequency converter tests. Make the usual provisions for measuring volts, amperes, watts, and the frequency in the primary and secondary circuits. Obtain load characteristics with varying, balanced, non-inductive resistances in the secondary, and also at constant secondary current and varying power factors (see Fig. 685 for typical performance curves). Keep the primary voltage and frequency constant. If a synchronous generator of suitable frequency is available, try feeding power from it into the secondary circuit of the frequency changer, at different values of current and power factor (§949). Should efficiency computations be contemplated, the driving motor should be properly calibrated, and the internal resistances of the windings and the no-load losses of both machines carefully measured. A short-circuit test (§503) will give an idea of the primary and secondary leakage reactance, for theoretical computations.

---

[2] C. P. Steinmetz, "Theory and Calculation of Electrical Apparatus," Chapter XII; same, "A-C. Phenomena," Chapters XVIII and XIX; Pichelmayer, *Elektrot. und Maschinenbau*, vol. 32 (1914), p. 203.

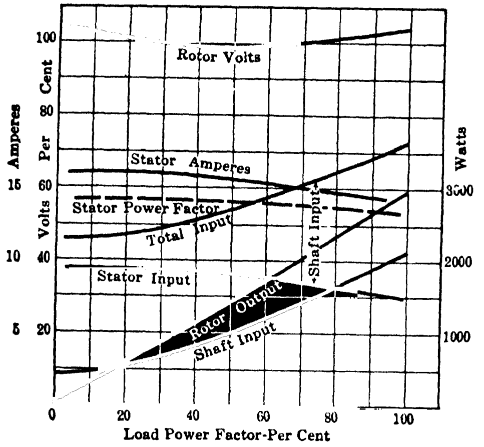

FIG. 685. Performance of a small frequency converter at constant load current, variable power factor (stator frequency = 25 cycles, rotor frequency = 60 cycles).

Report. Plot the readings to secondary output watts as abscissas. Show by a few examples that the observed results agree (at least approximately) with those computed from the analytical or graphical theory of the machine.

948. EXPERIMENT 50-C. — Induction-Type Frequency Converter; Load Characteristics at Constant Secondary Voltage (Compounding Curve). — The experiment is performed as in §947, except that the secondary terminal voltage is kept constant, while the primary voltage is increased with the load, by some suitable regulating arrangement, such as field control of the supply alternator, or a bank of transformers with a series of secondary taps. Load curves should be taken at two or three widely differing secondary frequencies.

949. EXPERIMENT 50-D. — The Operating Ranges of a General A-C Transformer. — On p. 185 of Steinmetz's " Theory and Calculation of Electrical Apparatus," four ranges of energy transformation are indicated, depending upon the limits of the slip. These ranges correspond to some of the combinations in the table given in §943 above. By "pumping" power into the secondary circuit, instead of receiving it, other combinations become possible, and some of these combinations were seen to be of practical importance in the concatenation of one induction machine with another, or with a commutator machine (Chapter XLIX). It is desired to investigate the performance characteristics of an induction machine, at least qualitatively, in all these ranges. In at least one of the ranges, the driving motor will be working as a generator, sending power back into its circuit.

INDUCTION REGULATORS

950. In many practical applications it is desired to keep a terminal a-c voltage constant, independent of the load, or to vary it gradually and continuously in a desired manner. One of the several ways of accomplishing this result is by means of a so-called induction regulator. Single-phase and polyphase regulators operate on somewhat different principles and therefore will be described separately.

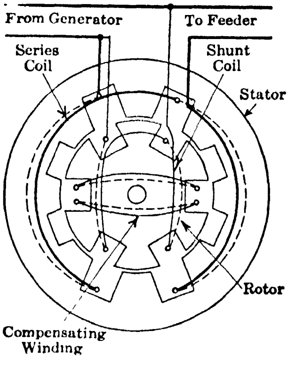

FIG. 686(*a*). A single-phase induction regulator.

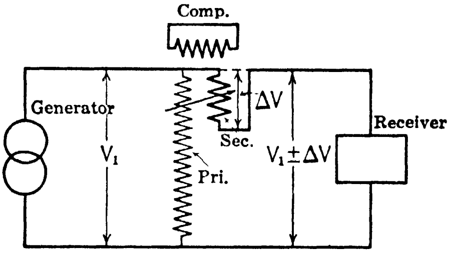

FIG. 686(*b*). Schematic connection diagram for a single-phase induction regulator.

951. Single-Phase Induction Regulator. — The electrical connections and arrangements of parts in a single-phase induction regulator are shown diagrammatically in Fig. 686(*a*) and (*b*). If the generator voltage varies the feeder voltage may be kept constant by means of the regulator, or the regulator may be used to raise the voltage at the sending end of the feeder to compensate for line drop at various loads (§952). The regulator has a laminated stator similar to that of a single-phase induction motor or a single-phase alternator. The stator coils consist of a few turns of rather large conductor, placed in slots. This winding is connected in series with the circuit to be regulated. The rotor also has a laminated and slotted iron core with a single-phase winding. This winding consists of many turns of small-sized conductor and is connected across the line. A compensating winding, short-circuited upon itself, is placed on the rotor, at 90 electrical degrees to the shunt winding. By means of a worm gear, or any other suitable mechanical transmission, the rotor may be slowly rotated through any angle up to 180 electrical degrees, or kept stationary in any position indefinitely. This motion can be produced either by hand or by a small electric motor. The motor may be started and stopped by hand, or automatically through a contact voltmeter and relays. Figure 687(*a*) is the cross-section of a single-phase induction regulator, equipped with a small motor geared to the rotor. Figure 687(*b*) shows the rotor and stator separately. Oil under pressure has also been used for turning the rotor.

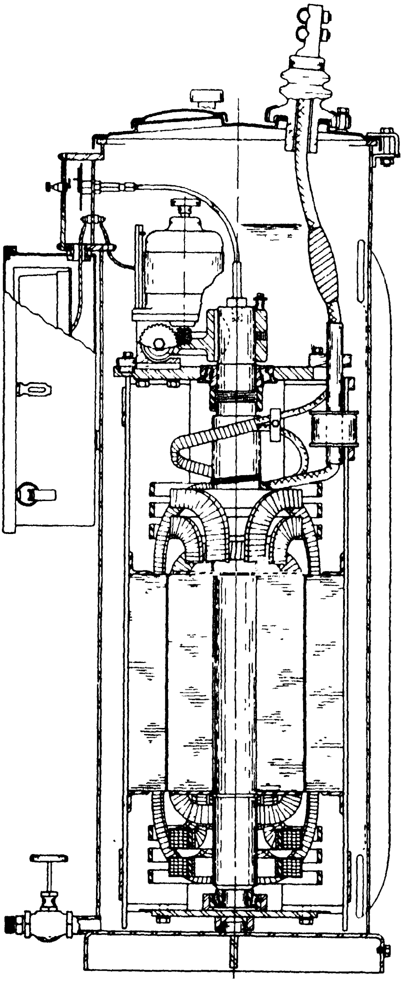

FIG. 687(*a*). Cross-section of a single-phase induction regulator (courtesy of the General Electric Co.)

When the rotor is in the position of maximum inductive relation (closest coupling) between the primary and the secondary, or series, windings, with the emf induced in the series winding adding directly to the generator voltage, it is in the " maximum boost " or " maximum raise " position. By turning the rotor 180 degrees, the " maximum buck " or " maximum lower " position is obtained, in which the feeder voltage is reduced instead of being increased. In the position midway between the two, the rotor flux induces no voltage in the series winding, the two being in space quadrature. Between the two extreme positions the voltage induced in the series coil varies gradually, approximately as the cosine of the angle between the axes of the two windings.

In the quadrature position of the two windings, the shunt winding is inactive, but the self-inductance of the series coil would cause a considerable voltage drop in the main circuit and would lower the power factor of the generator load, if it were not for the compensating winding. In the quadrature position of the two main windings, the compensating winding is coaxial with the series winding and forms a short-circuited secondary with respect to it. The flux of the series coil, and consequently its inductive action, is thereby reduced to a small amount. In the two extreme positions of the main coils, the compensating winding is inactive, and gradually comes into action as the quadrature or " zero " position is reached.

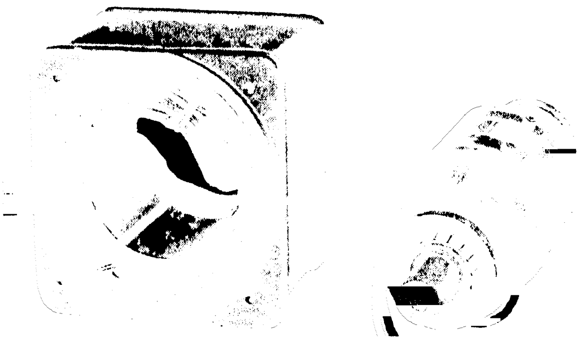

FIG. 687(*b*). Parts of the single-phase induction regulator (General Electric Co.).

952. Automatic Operation — The Line Drop Compensator and Contact-Making Voltmeter. — Figure 688 shows an arrangement of circuits for making the induction regulator automatic in action, in order that it may hold the voltage at the receiving end of a line constant in value, regardless of the value or power factor of the load. Two special devices are required: the *line drop compensator*, and the *contact-making voltmeter*. The contact-making voltmeter (Fig. 689) is connected across the feeder on the load side of the induction regulator, through a potential transformer. It acts as a relay in the circuit of the motor which turns the rotor of the regulator. If the voltage drops below the value for which it is set, the contact-making voltmeter closes an auxiliary switch and starts the regulating motor turning in the direction to boost the voltage to the desired value. If the feeder voltage becomes too high the contact-making voltmeter reverses the motor and causes the regulator to reduce the feeder voltage. Thus, it acts to hold feeder voltage constant within narrow limits.

In order that the regulator may hold the voltage constant at the receiver end of the feeder a voltage corresponding to the line drop in the feeder is introduced into the circuit of the contact-making voltmeter, making it act as if it were connected across the far end of the feeder. This is accomplished by means of the "line drop compensator," which consists of an adjustable inductance, L, and resistance, R (Fig. 688), which are set to correspond to the line characteristics. A current proportional to the line current, and of like phase, is supplied by a current transformer in the feeder circuit, and is sent through the line drop compensator. This being in the secondary circuit of the potential transformer also, the voltage drops in L and R modify the voltage across the contact-making voltmeter so that the resultant voltage corresponds to that at the receiver end of the line. It is therefore possible for the contact-making voltmeter to operate the regulator in such a way as to hold receiver voltage constant, or even to raise it with load, the effect depending upon the setting.

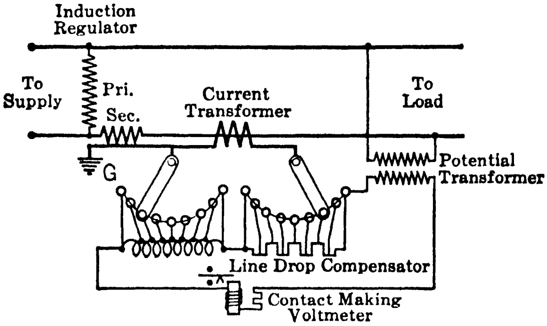

FIG. 688. Line drop compensator used with an induction regulator for automatic control of voltage at the load.

953. EXPERIMENT 50-E. — Study of a Single-Phase Induction Regulator and Auxiliary Devices. — The regulator and auxiliary devices are described in the preceding sections. One problem is to investigate the electromotive relations of the regulator at no load, the rotor being turned through progressively greater angles, first in the direction of boost and then of buck, with readings taken of angle, of secondary voltage ΔV, supply volts V_1, receiver volts $V_1 + \Delta V$, also primary or shunt current, and primary watts. Similar readings should be taken with various fixed values of load current and power factor. Another problem is to study the action of the driving motor, contact-making voltmeter, relays, etc., and the promptness of voltage recovery with sudden load changes. A study should be made of a commercial line drop compensator, or of one built up of available equipment. After an artificial short line has been set up in which the values of resistance and inductance are known, the line drop compensator should be connected as in Fig. 688, properly adjusted, and the readings of a voltmeter, replacing the contact-making voltmeter of Fig. 688, should be compared with actual volts as read at the receiver, for various values of load and power factor. In the absence of an induction regulator an induction motor with wound rotor may be used for part of this study.

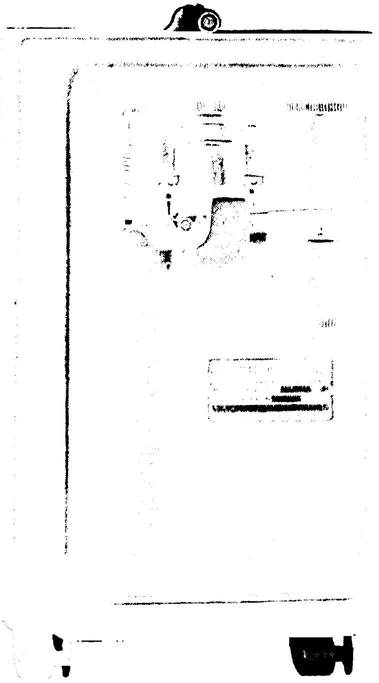

Fig. 689. Contact-making voltmeter of the General Electric Co.

954. Polyphase Induction Regulator. — The connections of the series and shunt windings in a three-phase induction regulator are shown in Fig. 690. The arrangement of the windings on the two cores can be imagined by replacing the two single-phase windings, shown in Fig. 686, by three-phase windings. See also the stator parts in Figs. 318, 319, and 350. No compensating coil is used, because here we have revolving and not pulsating fluxes and the resultant mmf of the rotor is always in a position to oppose that of the stator. The theory of the regulator can be understood from the vector diagram in Fig. 690. Let the generator voltage, *EO*, be practically constant in magnitude and in phase position, and let it be required to vary the receiver voltage at will. Since the air-gap flux produces in the rotor winding a counter emf, approximately equal and opposite to *EO*, this flux is nearly constant in all positions of the rotor and has the same phase position with respect to the rotor conductors. The emf induced by this flux in the stator winding is also nearly constant in magnitude, but varies in phase, depending upon the position of the rotor. The vectors *OA*, *OB*, *OC*, *OD* represent this voltage, which is geometrically added to *EO*. The corresponding voltages on the receiver side of the regulator are *EA*, *EB*, *EC*, *ED*.

It will be seen that the voltage may be raised or lowered at will within the limits of the voltage induced in the stator of the regulator. Of course, the actual relationships are more complicated because of the leakage reactances, resistances, and other secondary factors in the regulator itself. Since the gliding mmf of the stator is properly compensated for by that of the rotor in all positions of the rotor, no separate compensating coils are needed and the reactive drop in the regulator can be kept low. The magnetizing current is also small because the air-gap can be reduced almost to zero. The actual movement of the rotor can be produced either by hand or by a small electric motor through a worm gear (§951).

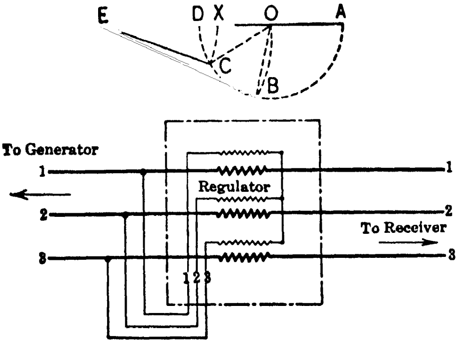

FIG. 690. The three-phase induction regulator and locus diagram of its voltage.

The phase shifter. Sometimes a polyphase induction regulator is used for shifting the phase of a secondary circuit with respect to the primary. The regulator is then connected like a three-phase transformer (Fig. 517). By turning the rotor, the phase of the secondary induced voltages is shifted with respect to that of the primary. The voltages themselves can at the same time be transformed in a desired ratio, approximately equal to that of the numbers of turns in the two windings. Such a regulator is sometimes called a *phase-shifter* or *phase-modifier*.[3]

955. EXPERIMENT 50-F. — Study of a Polyphase Induction Regulator and Phase-Shifter. — See §§953 and 954.

OPERATION UNDER ABNORMAL CONDITIONS

956. In the foregoing discussion, an inductance machine is supposed to be operating on a balanced two- or three-phase circuit, with sinusoidal voltages, the load varying slowly, if at all, and all the windings within the machine being electrically balanced and in perfect condition. In actual operation, one or more of these conditions may not be fulfilled, and as a consequence the performance characteristics of the machine may differ to some degree from those obtained under ideal assumptions.

---

[3] Literature references: E. F. Gehrkens, "The Induction Voltage Regulator," published by the General Electric Co., 1923; A. Brunn, *Association suisse des électriciens, Bull.*, November, 1925; L. H. A. Carr, *Inst. El. Engrs.* (British), *Journal*, vol. 63 (1925), p. 864.

It would be impracticable to foresee all possible abnormal conditions and their combinations; moreover, such a discussion would be far beyond the scope of this treatise. Only the most important cases are indicated below, with literature references. No specific experiments are included, it being understood that each abnormal condition may be made the subject of an extended experimental or theoretical investigation.

THREE-PHASE INDUCTION MOTOR WITH SINGLE-PHASE ROTOR

957. Analysis by the Method of Symmetrical Components. — The method of symmetrical components has been used (Chapter XXXIV) to determine the performance of a three-phase induction motor operating on a system of unbalanced voltages.[4] The extreme case of this, namely, the operation of the three-phase motor on a single-phase supply, will be treated in Chapter LI in connection with the single-phase induction motor. When, in a three-phase Y-connected rotor, one of the phases becomes open for any cause, the remaining two phases operating in series carry the same current and so constitute a single-phase rotor. This is again a case in which the method of symmetrical components is effective in analyzing the performance of the motor and will be used in the treatment to follow.

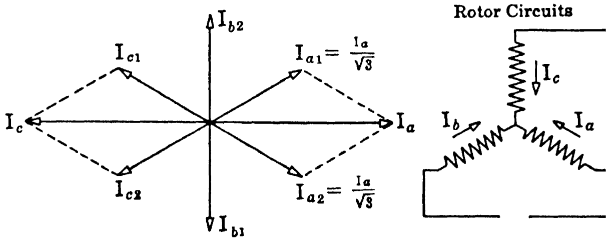

FIG. 691. Single-phase rotor current resolved into opposite-sequence components (phase *b* open).

An open phase in the rotor is a special case of unbalanced rotor impedances. It is assumed that normal positive-sequence voltages have been applied to the stator. The unbalanced currents in the rotor are resolved into positive- and negative-sequence components (Chapter XXXIV). For the special case of single-phase current in the rotor with, say, phase

---

[4] See also M. Rosenbaum, *Electrician*, vol. 76 (1916), p. 701.

b open, currents I_a and I_c are equal and opposite in phase when considered both toward the junction of the two windings. Figure 691 shows the positive- and negative-sequence components, the subscript 1 indicating positive sequence while the subscript 2 denotes negative sequence. The subscript r will denote rotor, and s stator quantities.

The rotor currents are of slip frequency, the positive-sequence components reacting upon the positive-sequence stator field in the normal manner, while the negative-sequence currents in the rotor set up a field rotating negatively with respect to the rotor at slip speed and inducing in the stator currents of fundamental frequency minus 2 × slip frequency. The reactions in the machine are analyzed into these two groups.[5]

958. The Equivalent Circuit for Positive-Sequence Quantities.—For the first group of relations (positive-sequence) one may write, for the stator:

$$\dot{V}_{s1} = \dot{E}_{g1} + (R_s + jX_s)\dot{I}_{s1} \quad . \quad . \quad . \quad . \quad . \quad . \quad . \quad (3)$$

In the rotor:

$$s\dot{E}_{g1} = \dot{I}_{r1}(R_r + jsX_r) + \dot{E}_{r1} \quad . \quad . \quad . \quad . \quad . \quad . \quad . \quad (4)$$

where E_{r1} is the positive-sequence component terminal voltage in the rotor, of slip frequency, and E_{g1} is the emf induced by the mutual positive-sequence flux. Dividing eq. (4) by s:

$$\dot{E}_{g1} = \dot{I}_{r1}(R_r/s + jX_r) + \dot{E}_{r1}/s \quad . \quad . \quad . \quad . \quad . \quad . \quad (5)$$

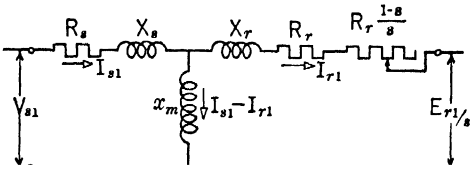

FIG. 692. Equivalent circuit for positive-sequence quantities.

E_{g1}, which is due to the air-gap flux, may be written:

$$\dot{E}_{g1} = jX_m(\dot{I}_{s1} - \dot{I}_{r1}) \quad . \quad . \quad . \quad . \quad . \quad . \quad . \quad . \quad . \quad (6)$$

The usual form of equivalent circuit, shown in Fig. 692, applies to these equations.

From eqs. (5) and (3), neglecting the voltage drop due to exciting current:

$$\dot{E}_{r1}/s = \dot{V}_{s1} - [(R_s + R_r/s) + j(X_s + X_r)]\dot{I}_{r1} \quad . \quad . \quad . \quad (7)$$

The approximate equivalent circuit of Fig. 693 applies to eq. (7).

---

[5] Wagner and Evans, "Symmetrical Components," Chapter V, McGraw-Hill Book Co.

Wagner and Evans[5] suggest that to evaluate the effects of the negative-sequence components one should consider the rotor stationary and the stator rotating at a relative speed of $(1 - s)N_s$ in the negative direction.

Assume that the negative-sequence rotor current is due to an applied voltage, E_{r2}, of slip frequency sf. This negative-sequence voltage sets up a flux rotating at a speed $-sN_s$, and, since the assumed speed of the stator is $-(1 - s)N_s$, the result is that when $s = 0.5$ these speeds are equal. Consequently, at $\frac{1}{2}$ synchronous speed, no voltage is induced in the stator by the flux due to the negative-sequence rotor current, which condition corresponds to synchronous speed as far as the negative-sequence current is concerned. For speeds above $N_s/2$, ($s < 0.5$), the assumed negative velocity of the stator is greater than the negative velocity due to negative-sequence current, and generator action results, with a torque opposing that due to positive-sequence current. For speeds below $N_s/2$, i.e., $s > 0.5$, the assumed negative velocity of the stator is less than the speed of the field set up by the negative-sequence rotor current, and useful torque is produced.

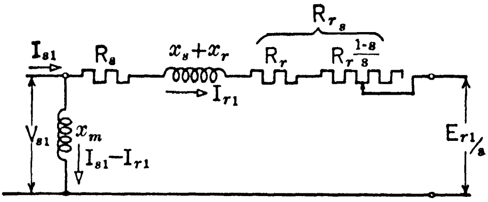

FIG. 693. Approximate equivalent circuit for the positive-sequence quantities.

959. The Equivalent Circuit for Negative-Sequence Values. — The voltage relations in the rotor, due to negative-sequence current, are:

$$\dot{E}_{r2} = \dot{E}_{g2} - \dot{I}_{r2}(R_r + jsX_r) \quad . \quad . \quad . \quad . \quad . \quad . \quad . \quad (8)$$

or

$$\dot{E}_{r2}/s = \dot{E}_{g2}/s - \dot{I}_{r2}(R_r/s + jX_r) \quad . \quad . \quad . \quad . \quad . \quad (8a)$$

where I_{r2} = the negative-sequence rotor current.

E_{g2} = negative-sequence voltage induced in the rotor, due to negative-sequence reactions within the machine, and may be written:

$$\dot{E}_{g2} = jX_m s(\dot{I}_{s2} - \dot{I}_{r2}) \quad . \quad . \quad . \quad . \quad . \quad . \quad . \quad . \quad (9)$$

The emf E_{g2} is produced by a flux having a speed of $-sN_s$ with respect to the rotor, and of $(1 - 2s)N_s$ with respect to the stator. It induces in the stator the emf $-(1 - 2s)E_{g2}/s$. Assuming that the impedance of the supply may be neglected, as compared with the impedances of the motor (supply large compared with the motor), the negative-sequence emf induced in the stator is all consumed in the stator impedance, or

$$-(1 - 2s)\dot{E}_{g2}/s = -\dot{I}_{s2}[R_s - j(1 - 2s)X_s] \quad . \quad . \quad . \quad (10)$$

The negative sign used with the stator reactance is consistent with the generator action due to negative-sequence field at low values of slip.

Dividing eq. (10) by $-(1 - 2s/s)$

$$\dot{E}_{g2} = \dot{I}_{s2}[R_s s/(1 - 2s) - jsX_s] \quad \ldots\ldots\ldots \quad (11)$$

$$= \dot{I}_{s2}[R_s(1 - s)/(1 - 2s) - R_s - jsX_s] \quad \ldots \quad (12)$$

or

$$\dot{E}_{g2}/s = \dot{I}_{s2}[R_s(1 - s)/s(1 - 2s) - R_s/s - jX_s] \quad . \quad (13)$$

From eqs. (8*a*) and (13) the approximate equivalent circuit may be drawn for the negative-sequence quantities as in Fig. 694. The shaft power, P_2, due to negative-sequence current is represented by the power absorbed in the resistance $-R_s(1-s)/(1-2s)$,

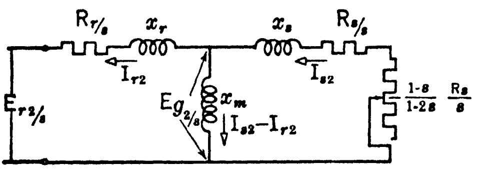

FIG. 694. Negative-sequence equivalent circuit.

or

$$P_2 = -3I_{s2}^2R_s(1 - s)/(1 - 2s) \quad \ldots\ldots \quad (14)$$

For slips less than 0.5 the shaft power is negative and subtracts from that due to the positive-sequence current. At slips greater than 0.5, P_2 becomes positive and adds to torque due to positive-sequence current.

960. The Combined Equivalent Circuit. — Figures 693 and 694 may be combined into one equivalent circuit as in Fig. 695, in which E_{r1}/s

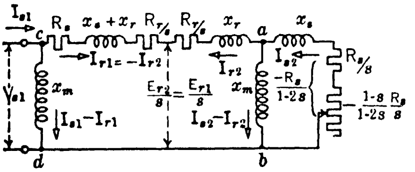

FIG. 695(*a*). Composite equivalent circuit of the induction motor with single-phase rotor.

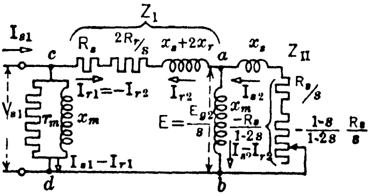

FIG. 695(*b*). Simplified composite diagram of a polyphase induction motor with single-phase rotor.

and E_{r2}/s are equal, while $-I_{r2}$ and I_{r1} are equal (see Fig. 691). The power input to the circuit, or the sum of the I^2r values in all the resistances shown in Fig. 695, is

$$P_i = 3I_{r1}^2R_s + 6I_{r1}^2R_r/s - 3I_{s2}^2R_s/(1 - 2s)$$

Subtracting the loss terms, $3I_{r1}^2R_s$, $6I_{r1}^2R_r$ and $3I_{s2}^2R_s$ leaves the total shaft power

$$P_0 = 6I_{r1}^2R_r(1 - s)/s - 6I_{s2}^2R_s(1 - s)/(1 - 2s) \quad . \quad . \quad (15)$$

The corresponding torque is:

$$T_0 = 7.04P_0/N_s(1 - s) \quad . \; . \; . \; . \; . \; . \; . \; . \; . \quad (16)$$

where N_s = synchronous rpm.

961. Analytical Solution of the Equivalent Circuit. — Referring to the simplified equivalent circuit of Fig. 695(*b*), the following analytical solution is suggested for the calculation of motor performance when a three-phase induction motor is operating with one rotor phase open.[6]

For the extreme right-hand branch of the circuit:

$$Z_{II} = -R_s/(1 - 2s) + jX_s \quad . \; . \; . \; . \; . \; . \; . \; . \; . \; . \; . \; . \; . \quad (17)$$

$$Y_{II} = \frac{-R_s/(1 - 2s)}{R_s^2/(1 - 2s)^2 + X_s^2} - j\frac{X_s}{R_s^2/(1 - 2s)^2 + X_s^2} \quad . \; . \quad (18)$$

$$= G_{II} - jB_{II} \quad . \; . \; . \; . \; . \; . \; . \; . \; . \; . \; . \; . \; . \; . \; . \; . \; . \quad (19)$$

Vectorially:

$$-\dot{I}_{s2} = \dot{E}(G_{II} - jB_{II}) \quad . \; . \; . \; . \; . \; . \; . \; . \; . \; . \; . \; . \; . \; . \; . \quad (20)$$

Numerically:

$$I_{s2} = E\sqrt{G_{II}^2 + B_{II}^2} \quad . \; . \; . \; . \; . \; . \; . \; . \; . \; . \; . \; . \; . \; . \quad (21)$$

For the extreme right-hand branch, plus the exciting branch:

$$Z_{ab} = \frac{jX_m[(-R_s)/(1 - 2s) + jX_s]}{j(X_m + X_s) + [-R_s/(1 - 2s)]} \quad . \; . \; . \; . \quad (22)$$

$$\frac{-X_m^2R_s/(1 - 2s)}{R_s^2/(1 - 2s)^2 + (X_m + X_s)^2}$$

$$+ j\frac{X_m[R_s^2/(1 - 2s)^2 + X_mX_s + X_s]}{R_s^2/(1 - 2s)^2 + (X_m + X_s)^2} \quad . \; . \; . \quad (23)$$

$$= R_{ab} + jX_{ab} \quad . \; . \; . \; . \; . \; . \; . \; . \; . \; . \; . \; . \; . \quad (24)$$

Vectorially:

$$\dot{I}_{r1} = \dot{E}(G_{ab} - jB_{ab}) \quad . \; . \; . \; . \; . \; . \; . \; . \; . \; . \; . \; . \quad (25)$$

Numerically:

$$I_{r1} = E\sqrt{G_{ab}^2 + B_{ab}^2} \quad . \; . \; . \; . \; . \; . \; . \; . \; . \; . \; . \; . \quad (26)$$

$$\dot{V}_{s1} = \dot{E} + \dot{I}_{r1}(R_I + jX_I) \quad . \; . \; . \; . \; . \; . \; . \; . \; . \; . \quad (27)$$

where R_I and X_I are the constants of the branch between *c* and *a*, with

$$R_I = R_s + 2R_r/s, \quad \text{and} \quad X_I = X_s + 2X_r$$

---

[6] See also W. V. Lyon, "Application of the Method of Symmetrical Components," §§110 to 112, McGraw-Hill Book Co.

From eqs. (26) and (27)

$$\dot{V}_{s1} = \dot{E}(1 + G_{ab}R_I + B_{ab}X_I) - j(B_{ab}R_I - G_{ab}X_I) \quad . \; . \; (28)$$

$$= \dot{E}(M + jN) \quad . \; . \; . \; . \; . \; . \; . \; . \; . \; . \; . \; . \; . \; . \; . \; . \; (29)$$

Numerically:

$$E = V_{s1}/\sqrt{M^2 + N^2} \quad . \; . \; . \; . \; . \; . \; . \; . \; . \; . \; . \; . \; . \; . \; . \; (30)$$

From the above equations one may solve for E, I_{r1}, and I_{s2} for the known constants of the motor, and at any assumed value of slip.

Power developed (see eq. 15):

$$P_0 = 6[I_{r1}^2R_r/s - I_{s2}^2R_s/(1 - 2s)](1 - s) \quad . \; . \; . \; . \; (31)$$

Internal torque (§889, see also eq. 16):

$$T_0 = \frac{6 \times 7.04}{\text{Syn. rpm}} [I_{r1}^2R_r/s - I_{s2}^2R_s/(1 - 2s)] \quad . \; . \; . \; (32)$$

Line current:

$$\dot{I}_{s1} = \dot{I}_{r1} + \dot{V}_{s1}(1/r_m - j1/X_m)$$
$$= I_{s1} \cos \theta_1 - jI_{s1} \sin \theta_1 \quad . \; (33)$$

Input:

$$W_1 = 3V_{s1}I_{s1} \cos \theta_1 \quad . \; . \; . \; . \; . \; (34)$$

Efficiency:

$$\text{Eff.} = [P_0 - (\text{Friction} + \text{Windage})]/W_1 \quad . \; . \; . \; . \; (35)$$

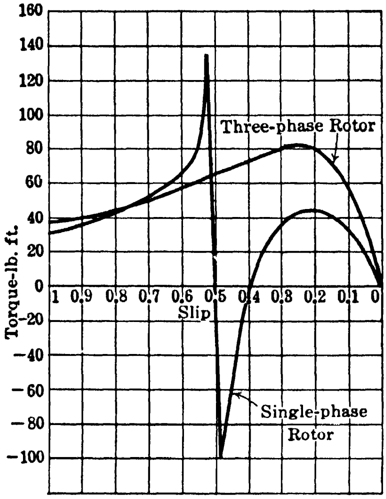

FIG. 696. Torque-slip curve of a three-phase motor with single-phase rotor.

Figure 696 is the slip-torque curve of a 10-horsepower three-phase motor, as obtained from the equations above. For purposes of comparison the slip-torque curve with three-phase short-circuited rotor is shown on the same sheet. It will be noticed that, while the starting torque of the motor in question is nearly the same with single-phase and with three-phase rotors, the torque rises to a materially greater pull-out value with single-phase rotor just below half-speed, then becomes negative, then positive, but at ordinary slips is materially less than that with the three-phase rotor.

The motor will not, in many cases, pass the $\frac{1}{2}$ synchronous point but "sticks" just below that figure (see Fig. 696).[7]

962. Operation at Voltages below and above the Rated Value. — With a line voltage below that for which a motor has been designed, the current necessary for the same output is greater, while the air-gap flux is less, and also the magnetizing current. As a result, the power factor and the slip are higher, while the efficiency is generally lower. The overload capacity decreases approximately as the square of the voltage. With a terminal voltage above the rated value, the opposite is true. Moreover, at a higher voltage the total flux is greater, and the increased saturation causes a rapid increase in the magnetizing current and in the core loss.[8] The effect of varying voltage upon the performance of the motor was discussed with reference to the approximate circle diagram in §896.

963. Effect of Voltage and Flux Harmonics. — An induction motor is sometimes operated on a line whose voltage has pronounced higher harmonics, due, for example, to arc furnaces on the same line. Assuming that the principle of superposition applies to the individual harmonics, the performance of the machine may be estimated by considering its equivalent diagram (§503) separately for each harmonic of the applied voltage, in its proper magnitude, frequency, and phase position.[9] Or else a circle diagram (Chapters XLVII and XLVIII) may be constructed for each harmonic.[10]

Higher harmonics in the revolving flux may be present even when the applied voltage is strictly sinusoidal. They are then caused by a non-sinusoidal distribution of phase mmf's in space, mainly due to a limited number of slots per pole per phase. As a result, the counter emf of the machine is non-sinusoidal, and so is the primary current. When the magnetic circuit is saturated, the magnetizing current is also non-sinusoidal.[11]

964. Fluctuating Load and Short Circuit. — When the load delivered by an induction machine is rapidly fluctuating, the performance is affected by a periodic storage of kinetic energy in the revolving masses.

---

[7] The theory of this phenomenon has been discussed in detail by E. Arnold, in his "Wechselstromtechnik," Vol. V, pt. 1, pp. 186 to 193. See also Dreyfus, *Elek. Zeits.*, vol. 33 (1912), p. 91; Mittag, *Gen. Elec. Rev.*, vol. 19 (1916), p. 234; A. A. Gazda, *Trans. A.I.E.E.*, vol. 36 (1917), p. 339; B. G. Lammé, *Elec. Jour.*, September, 1915; and W. V. Lyon, *op. cit.*

[8] T. F. Wall, "World Power," vol. 2 (1924), p. 164.

[9] A. S. Langsdorf, "Theory of Alternating-Current Machinery," Chapter X, Art. 38, McGraw-Hill Book Co.

[10] V. Paschkis, *Archiv fur Elektrot.*, vol. 14 (1925), p. 606.

[11] V. Karapetoff, "The Magnetic Circuit," p. 136.

For theory and computations, see various articles on application of electrical machinery to elevators, steel mills, railway traction, etc.

When the line to which an induction machine is connected becomes suddenly short-circuited, the stored mechanical and magnetic energy in the machine causes a sudden rise in current and a gradual readjustment to the permanent short-circuit condition, that is, zero current in the machine.[12]

965. Unsymmetrical Terminal Voltages. — Owing to the presence of a single-phase load connected to the same line, or to other causes outside the machine, the individual phase voltages at the terminals of an induction machine may not be equal to each other, or may not be displaced by the proper angles. Under these conditions, the machine takes in excessive currents, its efficiency and overload capacity are lowered, and the temperature is increased. Moreover, because of the mutual inductance of the phases and a common revolving flux, an induction machine tends to balance the line load and the voltages by causing large circulating currents.[13] The same is true of a synchronous machine connected to a line with unbalanced voltages.

Experience shows that a comparatively small unbalance in voltages causes quite large idle currents, and the better an induction motor the more sensitive it is to unbalanced conditions. In fact, three-phase synchronous or induction machines, running at no load, have been proposed in conjunction with large single-phase loads, to improve the line voltages and partly to relieve the main generators of unbalanced loads. It has also been pointed out that a double injustice is done to a customer who has three-phase revolving machinery on the same line with another customer who has large single-phase loads. In the first place, his machinery runs hotter and its rating and efficiency are lowered, through no fault of his. In the second place, he is charged for the extra energy which is absorbed by his machines and which really serves to improve the line conditions due to a single-phase customer.

A theoretical investigation of operation with unsymmetrical terminal voltages was made by resolving these into balanced systems of positive, negative, and zero sequence (§§906–910, Chapter XLVII). An extensive literature exists on this problem, and the references below will assist the reader interested in the subject.

966. EXPERIMENT 50-G. — Characteristics of an Induction Machine under Abnormal Conditions. — The principal abnormal conditions are enumerated in §§956 to 965. Each of these may be made the subject of a brief experiment or of an extended investigation.

---

[12] R. E. Doherty, *Jour. A.I.E.E.*, vol. 40 (1921), p. 1.

[13] O. G. C. Dahl, " Electric Circuits," Vol. I, p. 144, McGraw-Hill Book Co.

967. References.

ARTICLES

1. H. C. STANLEY, *Trans. A.I.E.E.*, vol. 57 (1938), p. 571, An analysis of the induction machine.
2. G. HOMMEL, *Elek. Zeits.*, vol. 33 (1912), p. 69.
3. L. G. STOKVIS, *Electrical World*, vol. 65 (1915), p. 1111.
4. C. L. FORTESCUE, *Trans. A.I.E.E.*, vol. 37 (1918), pt. 2, p. 1119.
5. VON P. MUELLER, *Elek. Zeits.*, vol. 39 (1918), p. 343.
6. J. SLEPIAN, *Electrical World*, vol. 75 (1920), p. 313.
7. C. J. FECHHEIMER, *Trans. A.I.E.E.*, vol. 39 (1920), p. 1469.
8. L. G. STOKVIS, *Comptes rendus*, vol. 174 (1922), p. 1418.
9. C. L. FORTESCUE, *Trans. A.I.E.E.*, vol. 42 (1923), p. 358.
10. E. ZACHRISSON, *Elek. Zeits.*, vol. 44 (1923), p. 897.
11. A. M. DUDLEY, *Electric Journal*, vol. 21 (1924), p. 339.
12. O. C. SCHOENFELD, *Electric Journal*, vol. 22 (1925), p. 30.
13. A. F. KENYON, *ibid.*, p. 435.

BOOKS

1. C. P. STEINMETZ, Theory and Calculations of Electrical Apparatus, Chapter XII, McGraw-Hill Book Co.
2. A. S. LANGSDORF, Theory of Alternating-Current Machinery, Chapters IX, X, and XII, McGraw-Hill Book Co.
3. E. F. GEHRKENS, The Induction Voltage Regulator, General Electric Co.
4. E. ARNOLD, Wechselstromtechnik, Vol. V, Pt. 1.
5. WAGNER and EVANS, Symmetrical Components, Chapter V, McGraw-Hill Book Co.
6. W. V. LYON, Applications of Symmetrical Components, McGraw-Hill Book Co.
7. R. LUNDHOLM, A Generalized Vector Theory, pp. 31–37, Stockholm (in English).

CHAPTER LI

THE SINGLE-PHASE INDUCTION MOTOR

968. This chapter is a continuation of Chapter XXIII, and the reader is supposed to be familiar with the contents of that chapter. The purpose of the treatment here is to provide the elements of the underlying theory of the machine, so as to make it possible to interpret and to predict experimental data and to study more advanced and special works on the subject.

There are two theories of the single-phase induction motor, or rather ways of looking at the interaction between the stator and the rotor: (a) the theory of oppositely rotating fields, best solved by means of the method of symmetrical components; and (b) the cross-field or quadrature-flux theory. Certain operating features are clearer from one point of view; others are better understood in the light of the other theory. The elements of both theories are given below, although it has been shown that they are equivalent and lead to the same results.[1]

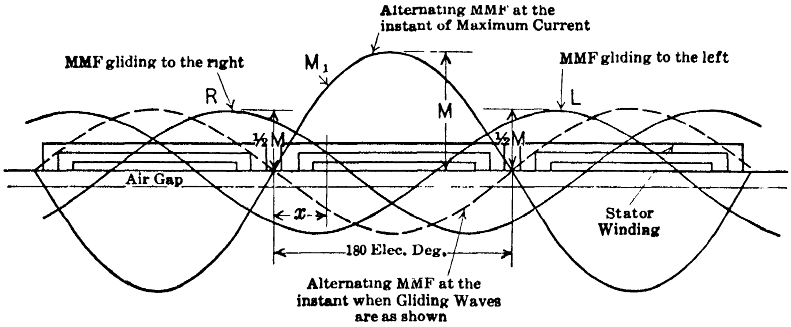
Alternating MMF at the instant of Maximum Current
MMF gliding to the right
M_1
R
M
MMF gliding to the left
L
½M
½M
Air Gap
x
180 Elec. Deg.
Stator Winding
Alternating MMF at the instant when Gliding Waves are as shown

FIG. 697. Resolution of pulsating mmf into two oppositely gliding mmf's.

THE THEORY OF TWO OPPOSITELY ROTATING MMF'S

969. The primary current in the main stator winding of a single-phase motor produces an mmf which varies approximately according to the sine law both in space and in time. In Fig. 697, M_1 represents the space distribution of this mmf at the instant when the current reaches its maximum. A pole pitch of the machine is marked " 180 electrical degrees." For purposes of analysis, this mmf, of amplitude M, may be resolved into two fictitious component mmf's, R and L, each of amplitude $0.5M$, gliding synchronously in opposite directions.[2] At an instant when the primary current and the actual primary mmf, M_1, reach their maxima, the gliding components completely overlap, thus giving a wave of amplitude M. A quarter of a cycle later, when the actual mmf is zero, the two gliding components, having each moved by 90 electrical degrees, are in phase opposition and give a sum equal to zero. One way of satisfying oneself as to the correctness of the resolution of an alternating sinusoidal wave into two oppositely gliding waves of half the amplitude is to cut two such waves out of celluloid, place them in the proper relative positions for different instants of time, and add ordinates point by point. The analytical proof follows from the identity:

---

[1] V. Karapetoff, *Journal A.I.E.E.*, vol. 40 (1921), p. 640.

$$M \sin x \cos 2\pi ft = 0.5M \sin (x - 2\pi ft) + 0.5M \sin (x + 2\pi ft) \quad . \quad . \quad (1)$$

where x is an angle measured from the zero point of the resultant alternating wave. The left-hand side of this equation represents a pulsating wave of amplitude M which varies according to the sine law, both in time and in space. The right-hand side represents two oppositely gliding waves, each of amplitude $0.5M$.

970. Two Stators Acting on the Same Rotor.—When the primary pulsating mmf has been resolved into two gliding mmf's, the single-phase stator is thereby replaced by two polyphase stators of opposite phase rotation, acting upon the same rotor. The action of each fictitious polyphase stator upon the rotor may be considered separately, it being kept in mind that at low values of slip the rotor of a polyphase induction motor behaves as though it possessed a high resistance, and produces a high value of torque per ampere, while at high values of slip the rotor impedance and power factor are low, as is the torque per ampere which is produced. While the two primary gliding mmf's are equal, the corresponding fictitious air-gap fluxes are not equal to each other, except at standstill. At any other speed, the reaction of the rotor affects the field gliding in the direction of its rotation (or the direct field) less than the other or inverse field. This is more easily understood in terms of the frequency of the rotor currents. At low values of slip, the frequency of the secondary induced emf is low, and consequently the resistance of the rotor conductors is relatively of greater influence than their inductance. The rotor currents are therefore practically in phase with the induced emf. This is the situation near synchronism and corresponds to a transformer operating on a non-inductive load. The reverse is true at higher values of slip, and the secondary currents produce an mmf approximately 90 degrees in lagging time phase with the secondary induced emf.

---

[2] V. Karapetoff, "The Magnetic Circuit," p. 126. The letters R and L in Fig. 697 stand for "right" and "left," respectively.

In the operating range of the machine, that is, at small values of slip, the inverse field is gliding at nearly 200 per cent slip with respect to the rotor conductors and is therefore reduced to a comparatively small value by the reaction of its secondary currents, while the direct field remains of considerable magnitude. Figure 698 shows the torque-slip curves due to oppositely rotating fields of equal value. The two oppositely gliding field fluxes are actually of such values and of such relative phase position that the sum of the emf's induced by them in the single-phase primary winding is equal to the real counter emf of the motor. This counter emf is equal and opposite to the applied voltage, less a small primary impedance drop.

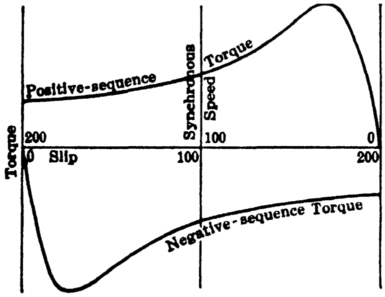

FIG. 698. Torque-slip curves due to oppositely rotating fields, on the basis of 100 per cent normal voltage.

The assumptions made in this theory may be actually realized by replacing the given single-phase motor by two identical polyphase induction motors, with the stator windings connected in series, and the rotors mounted on the same shaft. The stator phases must be so interconnected as to produce rotating mmf's in the opposite directions; when one rotor revolves in the direction of the revolving flux of its stator, the other rotor runs against its stator field. With the proper design constants, the performance of such a set is practically equivalent to that of the given single-phase machine. The stator currents in the two machines being equal, the two primary gliding mmf's are also equal and opposite at all loads. Because the two stator windings are connected in series, the total applied voltage, less the primary impedance drop, is balanced by the sum of the emf's induced in these windings by the actual revolving fluxes in the air-gaps of the two machines.

971. Operating Characteristics. — At standstill, for reasons of symmetry, the two fictitious revolving fluxes and the torques which they exert upon the respective fictitious rotors are equal and opposite. However, after the set has been brought up to a certain speed by some external means, the direct flux becomes greater than the inverse, and, moreover, the low-frequency secondary currents which the direct flux induces are more nearly in space phase with the flux itself and hence produce a greater torque. There being an excess torque in one direction, the set runs up to almost synchronous speed. The exact no-load speed is slightly below synchronous, not only because of the no-load losses, but also because the driving torque has to overcome a small torque due to the inverse flux. These characteristics of the equivalent set of polyphase machines agree with those of a single-phase motor.

With reference to Fig. 698, it will be seen that when the motor runs within the operating range, i.e., at a slip of a few per cent for the direct flux and at a slip of about 200 per cent for the inverse flux, the torque due to the inverse flux is not only small but varies only a little with the slip. Therefore, in this particular range, the operating characteristics of a single-phase machine are essentially similar to those of a polyphase machine, except for a small counter torque due to the inverse field and a larger voltage drop due to the primary leakage impedance. The latter is due to the inverse leakage field, which is proportional to the primary current and acts like a choke coil in series with the primary winding.

The direct and the inverse torques of a single-phase motor cannot be taken from Fig. 698 in their correct proportion, because this figure represents the operating characteristics of two polyphase machines at the same applied voltage. In the two fictitious polyphase machines, together equivalent to the single-phase motor, the total applied voltage is constant, but only a small part of it is used up in the "inverse" machine. Hence, the inverse torque near synchronism is relatively much smaller than the extreme ordinate to the left in Fig. 698, which corresponds to a slip of about 200 per cent at full voltage.

The magnetizing current of a single-phase motor, driven at synchronous speed, is twice as large when the secondary circuit is closed as when it is open. This can be explained on the revolving-mmf theory as follows: The inverse flux being practically wiped out, the direct flux must be large enough to induce in the primary winding an emf almost equal to the applied voltage. With the rotor winding open, both fluxes are present, so that each needs to be only one-half as large. As an example, in a single-phase motor, let an alternating mmf of 5000 ampere-turns (maximum value) produce an alternating flux of 0.2 megaline maximum value. With the secondary circuit open, this alternating flux may be thought of as being replaced by two oppositely gliding fluxes of 0.1 megaline each. With the secondary closed and running at or near synchronous speed, the inverse flux is wiped out by the secondary currents, and the direct flux alone must equal 0.2 megaline, to balance the applied voltage. Hence, the magnetizing current must be large enough to produce 10,000 alternating ampere-turns, in order that the direct gliding component may be equal to 5000 ampere-turns.

972. The Secondary Copper Loss. — In a polyphase induction motor, the percentage of secondary copper loss is equal to per cent slip, the input into the secondary being taken as 100 per cent (§889). In a single-phase motor, at small values of slip, the percentage of copper loss is equal to twice the per cent slip (§517). An exact proof of this proposition would require more analytical theory than can be given here, but this relationship can be readily shown to be at least approximately true. The two gliding stator mmf's (§969) are equal to each other under all load conditions. At small values of slip, the inverse flux being wiped out, the inverse secondary mmf is practically equal to either of the primary gliding mmf's. The direct secondary mmf is smaller than the primary gliding mmf, the geometric difference between the two being equal to the exciting mmf, as in a transformer (Fig. 283). However, at a considerable load, the magnetizing ampere-turns are small as compared with the secondary ampere-turns, so that the direct secondary mmf is also approximately equal to the direct primary mmf (i_1n_1 and i_2n_2 in Fig. 283). Thus, the two rotor mmf's are approximately equal to each other, and the secondary copper loss must be twice that due to the direct mmf alone. But the latter loss, in per cent, is equal to per cent slip, as in a polyphase induction motor. Hence, the total percentage of copper loss in the rotor is equal to twice per cent slip.

973. — EXPERIMENT 51-A. — Resolution of the Air-Gap Field in a Single-Phase Induction Motor into Two Revolving Components. — For this test use a single-phase motor having a second, or starting, winding displaced 90 degrees from the main winding, and with both ends brought out to a voltmeter. In the absence of such a motor a three-phase motor may be used with the ends of one phase brought out. Operate the motor at various values of load, beginning with the no-load condition, and measure the voltages across the open phase and across the working phase, both in value and in phase. Read also motor speed. If the air-gap clearance is sufficient a fine wire may be stretched tightly against the inner bore of the stator and the ends taken to an oscillographic element. Oscillograms of the emf induced in this wire will indicate the flux distribution in the gap. From these measurements, the component fluxes and the actual flux-density distribution, as a function of both space and time, can be ascertained. Using the theory given in the References, or by trials, this "elliptical" field can be resolved into two oppositely rotating fields of different magnitudes.

The performance characteristics of the motor can then be coordinated and checked in terms of these components. A method of doing this may be evolved after a study of some of the references in §992.

974. EXPERIMENT 51-B. — Performance Characteristics of a Twin Polyphase Induction Motor Equivalent to a Single-Phase Machine. — The purpose of the experiment is to verify the method of representation of a single-phase motor, used in §970. Two identical polyphase motors are connected electrically and mechanically as indicated there. The set is then started and loaded as if it were a single-phase machine (§515), and its performance characteristics are determined in the usual way. These characteristics are then compared with those of the individual polyphase machines and of the equivalent single-phase motor. It is of particular importance to measure the vectorial division of the total voltage between the two machines. The number of turns in the stators of the polyphase machines must be properly correlated with those of the equivalent single-phase motor. For details see Hansen's article referred to below.

975. The Calculation of the Performance of Single-Phase Induction Motors by the Method of Symmetrical Components. — In Chapters XLVII and L the method of symmetrical components has been used to calculate the performance of the polyphase induction motor, first, on a system of unbalanced voltages, and then when one phase of the rotor winding is open-circuited. The method is effective also in calculating the performance of the single-phase induction motor, or the operation of the three-phase motor on single-phase supply. The latter case will be considered first.

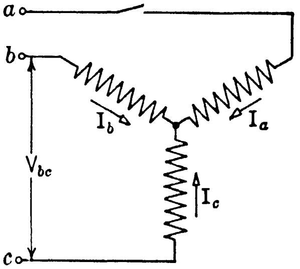

FIG. 699 Three-phase motor operating on a single-phase supply.

976. Operation of Three-Phase Induction Motor on Single-Phase Supply.[3] — This is, of course, an extreme example of unsymmetrical voltage supply. Assume that after a three-phase induction motor has been started on a three-phase supply, one line, say *a* (Fig. 699), is opened and the motor then operates on the single-phase voltage V_{bc}.

Neglecting exciting current, and remembering that zero-sequence current is absent in a Y-connection without neutral (§714):

---

[3] O. G. C. Dahl, "Electric Circuits, Theory and Application," Chapter V, McGraw-Hill Book Co.; Wagner and Evans, "Symmetrical Components," §159, Chapter XVII, McGraw-Hill Book Co.

$$I_a = I_{a1} + I_{a2} = 0 \quad \ldots \quad (2)$$

$$I_b = -I_c = I \quad \ldots \quad (3)$$

From §714, eq. (28):

$$\begin{aligned} I_{a1} &= (1/3)(I_a + hI_b + h^2I_c) = (1/3)(0 + hI - h^2I) \\ &= (I/3)[-0.5 + j0.866 - (-0.5 - j0.866)] = jI/\sqrt{3} \quad (4) \end{aligned}$$

Therefore:

$$I_{b1} = \frac{jI\angle -120^\circ}{\sqrt{3}} = (I/\sqrt{3})\angle -30^\circ \quad \ldots \quad (5)$$

and

$$I_{c1} = (jI/\sqrt{3})\angle 120^\circ = -(I/\sqrt{3})\angle 30^\circ$$

From eqs. (2) and (4)

$$I_{a2} = -jI/\sqrt{3}$$

Therefore

$$\left.\begin{aligned} I_{b2} &= (-jI/\sqrt{3})\angle 120^\circ = (I/\sqrt{3})\angle 30^\circ \\ \text{and} \quad I_{c2} &= (-jI/\sqrt{3})\angle -120^\circ = (-I/\sqrt{3})\angle -30^\circ \end{aligned}\right\} \quad \ldots \quad (6)$$

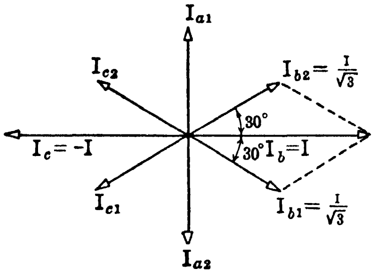

FIG. 700. Positive- and negative-sequence components of a single-phase current.

Figure 700 shows these component currents in their relative phase positions.

Neglecting the exciting components, $I = I_b$, the current drawn by the motor, is determined by the voltage across phase b and the impedance per phase of the motor at a given value of slip, s. Let Z_{m1} be the impedance per phase to positive-sequence and Z_{m2} the impedance to negative-sequence current, where

$$\left.\begin{aligned} Z_{m1} &= R_s + R_r/s + jX_e \\ \text{and}\qquad & \\ Z_{m2} &= R_s + R_{r2}/(2 - s) + jX_e \end{aligned}\right\} \quad \dots\dots \quad (7)$$

R_r is the rotor resistance per phase at low frequencies, and R_{r2} at double the supply frequency. Since

$$\left.\begin{aligned} V_{bn} &= V_{bn1} + V_{bn2} = I_{b1}Z_{m1} + I_{b2}Z_{m2} \\ \text{and}\qquad & \\ V_{cn} &= V_{cn1} + V_{cn2} = I_{c1}Z_{m1} + I_{c2}Z_{m2} \end{aligned}\right\} \quad \dots\dots\dots \quad (8)$$

therefore

$$V_{bc} = V_{bn} - V_{cn} = (I_{b1} - I_{c1})Z_{m1} + (I_{b2} - I_{c2})Z_{m2} \quad \dots \quad (9)$$

But (see Fig. 700) $I_{b1} - I_{c1} = I_b$, and $I_{b2} - I_{c2} = I_b$, so that

$$V_{bc} = I_b(Z_{m1} + Z_{m2}) \quad \dots\dots\dots\dots\dots\dots \quad (10)$$

and

$$I_b = V_{bc}/(Z_{m1} + Z_{m2}) \quad \dots\dots\dots\dots\dots\dots \quad (11)$$

Writing eq. (11) in terms of motor constants (eqs. 7) and slip:

$$\begin{aligned} \dot{I}_b &= \frac{\dot{V}_{bc}}{[R_s + R_r/s + jX_e] + [R_s + R_{r2}/(2 - s) + jX_e]} \\ &= \frac{\dot{V}_{bc}}{2R_s + R_r/s + R_{r2}/(2 - s) + 2jX_e} \quad \dots\dots\dots \quad (12) \end{aligned}$$

Numerically:

$$I_b = \frac{V_{bc}}{\sqrt{[2R_s + R_r/s + R_{r2}/(2 - s)]^2 + 4X_e^2}} \quad \dots \quad (12a)$$

From eq. (5), numerically,

$$I_{b1} = I_{c1} = I_b/\sqrt{3} \quad \dots\dots\dots\dots \quad (13)$$

The power developed by phase b is (see eq. 15, Chapter XLVII):

$$\begin{aligned} P_b &= I_{b1}^2 R_r \frac{1 - s}{s} - I_{b2}^2 \frac{R_{r2}(1 - s)}{2 - s} \\ &= I_b^2/3[R_r(1 - s)/s - R_{r2}(1 - s)/(2 - s)] \quad \dots \quad (14) \end{aligned}$$

Hence the total internal power developed by the hypothetical three phases of the motor is:

$$P_i = I^2(1 - s)[R_r/s - R_{r2}/(2 - s)] \text{ watts} \quad \dots\dots \quad (15)$$

The net output is less than P_i by the amount of the friction and windage loss.

The total internal torque is:

$$T = (7.04/N_s)I^2[R_r/s - R_{r2}/(2 - s)] \text{ lb-ft} \quad . \; . \; . \qquad (16)$$

Power input is determined by adding to the power developed (eq. 15) the core loss, P_{h+e}; the copper loss, $P_c = I^2(2R_s + R_r + R_{r2})$; plus the added I^2r loss due to the exciting current, I_n.

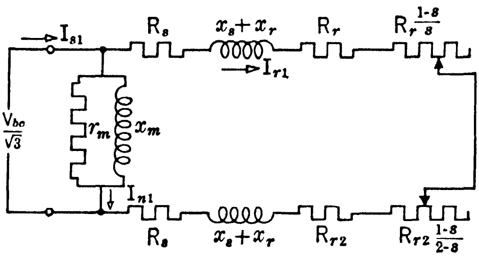

FIG. 701. The approximate equivalent circuit for one phase of a three-phase motor operating on single-phase supply.

977. Numerical Example.[4] — From the running-light, the rotor-blocked, and the resistance measurements made on a three-phase motor the following data are known (Fig. 701):

$$R_s = 0.23\omega, R_r = 0.387\omega, R_{r2} = 0.052\omega \text{ (assumed } R_r \times 1.35)$$

$$X_1 + X_2 = 1.65\omega, \quad I_{n1} = 8 \text{ amperes; friction + windage loss} = 250 \text{ watts;}$$
$$\text{core loss} = 130 \text{ watts;} \quad N_s = 1200$$

It is required to calculate the approximate performance of this motor when operating on a single-phase circuit of 240 volts, and at a slip of 5 per cent.

For the slip in question:

$$R_r/s = 0.387/0.05 = 7.74\omega, \quad R_{r2}/(2 - s) = 0.52/1.95 = 0.27\omega$$

$$Z_{m1} = 0.23 + 7.74 + j1.65 = 7.97 + j1.65$$

$$Z_{m2} = 0.23 + 0.27 + j1.65 = 0.5 + j1.65$$

$$Z_{m1} + Z_{m2} = 8.47 + j3.3$$

The exciting current will be neglected except as it is considered to affect the available line voltage, V_{bc}' where $V_{bc}' = V_{bc} - I_nZ_s = 240 - \sqrt{3} \times 8.0 \times 0.825 = 228.6$ volts, approximately.

---

[4] For a more accurate method of calculating the performance of the induction motor on single-phase supply the reader is referred to the work of O. G. C. Dahl in "Electric Circuits, Theory and Applications," pp. 149–168, McGraw-Hill Book Co.

Then (eq. 12*a*):

$$I = 228.6/(\sqrt{8.47^2 + 3.3^2}) = 25.1 \text{ amperes}$$

From eq. (15) the internal power developed is

$$P_i = (25.1)^2 \times (1 - 0.05)(7.74 - 0.27) = 4480 \text{ watts}$$

Allowing for friction plus windage loss the net power is

$$P = 4480 - 250 = 4230 \text{ watts} = 5.67 \text{ horsepower}$$

Net torque $= 7.04 \times P/N_s = 7.04 \times 4230/1200 = 24.8$ lb-ft.

Losses. Friction plus windage = 250 watts, core loss = 130 watts.

I^2r loss $= I^2(2R_s + R_r + R_{r2}) = (25.1)^2(0.46 + 0.387 + 0.52) = 935$ watts.

Total loss $= 935 + 250 + 130 = 1315$ watts.

Input $= 4230 + 1315 = 5545$ watts.

Efficiency $= 4230/5545 = 0.765$.

Stator current, including exciting current, $= \sqrt{25.1^2 + 3 \times 8^2} = 28.6$ amperes.

Apparent input $= 28.6 \times 240 = 6530$ volt-amperes.

Power factor $= 5545/6530 = 0.85$.

The above treatment applies specifically to the operation of a three-phase motor on single-phase power supply. The same method applies equally to the single-phase induction motor with squirrel-cage rotor, the single stator phase being understood to represent the two phases *b* and *c* of Fig. 699. In the determination of the constants of the equivalent circuit, the resistance R_s is one-half the resistance of the entire stator; $X_1 + X_2$ is one-half the total leakage reactance; etc.

978. EXPERIMENT 51-C. — Performance of the Induction Motor Operating on Single Phase, by Test and by Calculation. — This experiment is intended to check the theory of the preceding sections. The tests should be performed on a three-phase motor. First determine the constants of the equivalent circuit (§503) by tests on a balanced three-phase supply, then on a single-phase supply.

Operate the motor on single phase, and take several points of a load run, reading stator amperes, volts and watts, slip, rpm, and rotor output by means of a calibrated d-c generator (§313), an electrodynamometer (§313), or a Prony brake (§311).

Calculate the constants of the motor and check the performance of the motor by calculations similar to those in §977, and at certain slips actually measured during the load run. Look up the references previously cited and calculate the performance by the more exact methods there described. Compare the calculated and test results, explaining any failure of agreement. Discuss the performance characteristics of the motor on single-phase supply and compare with those of the same, or a similar, motor on three-phase supply.

THE QUADRATURE-FLUX OR CROSS-FIELD THEORY

979. The fundamental assumptions of this theory are shown in Fig. 702. The stator coils are denoted by A_1, and the consecutive axes of these coils are marked $+A$ and $-A$. Whether the rotor is stationary or moving, the current in the primary coils exerts a transformer action upon the rotor winding, so that there is an alternating flux ϕ_a along the $\pm A$ axes, and we can imagine fictitious stationary rotor coils, A_2, in which the currents act in opposition to the primary currents. While the real rotor conductors revolve, the fictitious coils, A_2, may be assumed to be stationary in space, since new conductors are continually replacing the outgoing ones. The magnitude and the phase of the flux ϕ_a are such that it induces in the stator coils a counter emf which, together with the primary impedance drop, balances the applied voltage.

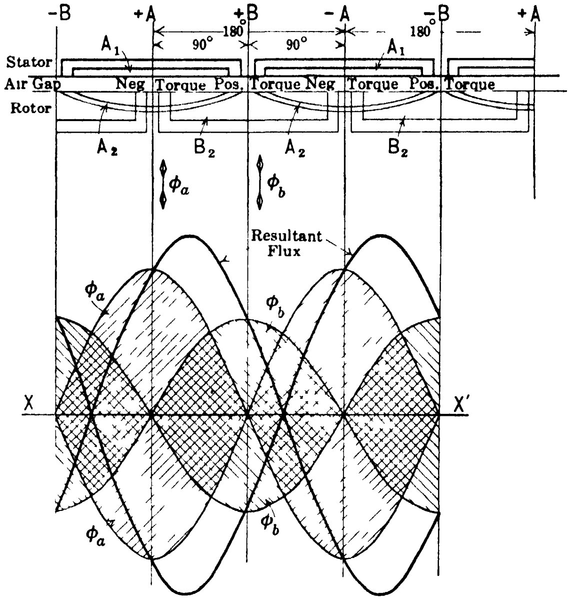

FIG 702. The quadrature flux and two sets of fictitious coils.

When the rotor is revolving, another air-gap flux, ϕ_b, comes into existence, in space quadrature with ϕ_a. The axes of this flux are denoted by $+B$ and $-B$. At and near synchronism, the magnitude of this flux is found to be nearly equal to ϕ_a, and the two fluxes are approximately in time quadrature. But two fluxes in time and in space quadrature produce together a circular revolving flux (§813). This agrees with the statement made in §971 regarding the wiping out of the inverse rotating flux.

Since the primary winding cannot excite a flux, such as ϕ_b, in space quadrature with itself, we conclude that there are alternating rotor currents, stationary in space, which furnish the exciting ampere-turns for ϕ_b. The corresponding fictitious coils are denoted by B_2. Even though the actual rotor conductors are revolving, these fictitious coils are stationary in space, new conductors continually replacing the preceding ones.

The actual rotor currents having been replaced by two sets of currents in the fictitious coils A_2 and B_2, the rest of the problem consists of finding the magnitudes and the phase positions of the various currents, voltages, and fluxes involved.

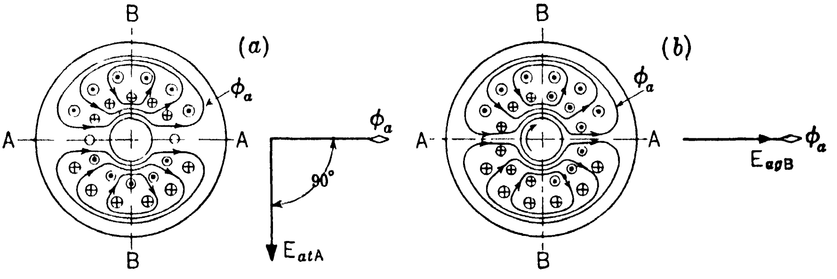

FIG. 703. Stator pulsating field inducing emf's in the rotor: (*a*) by transformer action along *A–A*; (*b*) by generator action along *B–B*.

980. Transformer and Rotational EMF's Induced in the Rotor. — A system of triple subscripts will be used to characterize the emf's induced in the rotor. The first subscript, *a* or *b*, denotes the flux ϕ_a or ϕ_b inducing the emf; the second subscript shows the action, generator *g*, or transformer *t*, which induces the emf; while the third subscript, *A* or *B*, indicates the axis along which the emf divides in the rotor. Referring to Fig. 703(*a*), the main flux, $\boldsymbol{\phi}_a$, is shown along the axis *A–A* of a single-phase induction motor with squirrel-cage rotor. Pulsations of the flux, $\boldsymbol{\phi}_a$, induce in the rotor a transformer emf along the *A–A* axis, and shown in the vector diagram of Fig. 703(*a*) as $\mathbf{E}_{atA}$, 90 degrees behind $\boldsymbol{\phi}_a$ in time phase but acting along the *A–A* axis.

In Fig. 703(*b*) it is assumed that the rotor is turning in a clockwise direction. As the rotor bars move through the flux, ϕ_a, a speed or generator voltage is induced, dividing along the *B–B* axis, and shown in the vector diagram as $\mathbf{E}_{agB}$. While this emf acts along the *B–B* axis it is in time phase with the flux ϕ_a, as shown in the vector diagram.

The quadrature flux. Due to the generator (speed) voltage $\mathbf{E}_{agB}$, induced in the rotor, currents of like distribution will flow, dividing along the *B–B* axis, i.e., at right angles in space with regard to ϕ_a. This flux is shown in Fig. 704(*a*). Since the axis of the stator winding is *A–A*, no current in the stator can react directly along the *B–B* axis. As a result, the inductance of the rotor along the *B–B* axis is very high, and the current I_b, producing ϕ_b, lags nearly 90 degrees in time behind the emf $\mathbf{E}_{agB}$ which produces it. Also, owing to the presence of an air-gap in the magnetic circuit, the flux ϕ_b will be nearly in phase with the current I_b. With the passage of the rotor bars through ϕ_b there will be a speed (generator) voltage $\mathbf{E}_{bgA}$, induced in the rotor along the axis *A–A*. While this emf is a maximum when ϕ_b is a maximum its direction is such that the current which it produces exerts an mmf opposing ϕ_a. This emf, therefore, will be in substantial opposition to $\mathbf{E}_{atA}$.

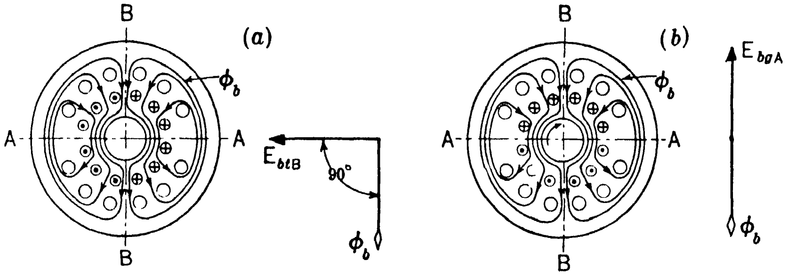

FIG. 704. Stator pulsating field inducing emf's in the rotor: (*a*) by transformer action along *B–B*; (*b*) by generator action along *A–A*.

981. The Vector Diagram of the Single-Phase Induction Motor.—In Fig. 705 the vector diagrams of Figs. 703 and 704 are combined, the following assumptions being made:

a. The motor is running at synchronous speed.
b. Fluxes ϕ_a and ϕ_b are equal and 90 degrees apart, both in space and in time.
c. All transformer and rotational voltages are equal.
d. The windings are practically devoid of resistance and leakage reactance.

In Fig. 705 the ratio between effective stator and rotor turns is taken as slightly greater than unity. Thus $E_1 = -E_s$, which is the voltage drop in the stator due to the inductive effect of the flux ϕ_a, is shown somewhat greater than E_{atA}.

A more accurate vector diagram is drawn in Fig. 706, for a speed below synchronism, and including the effect of rotor resistance, R_2, and leakage reactance, X_2. For simplicity the ratio of the motor is taken as unity. At a speed $N = N_s(1 - s)$, below synchronism, the rotational voltage E_{agB} is less than the transformer voltage $\mathbf{E}_{atA}$, and ϕ_b is less than ϕ_a, owing both to the reduction in speed and to the impedance of the rotor, which requires that the counter emf E_{btB} shall be less than the rotational emf E_{agB}. Moreover, the flux ϕ_a is less in the loaded motor than in the motor at synchronous speed, owing to the leakage impedance drop in the stator.

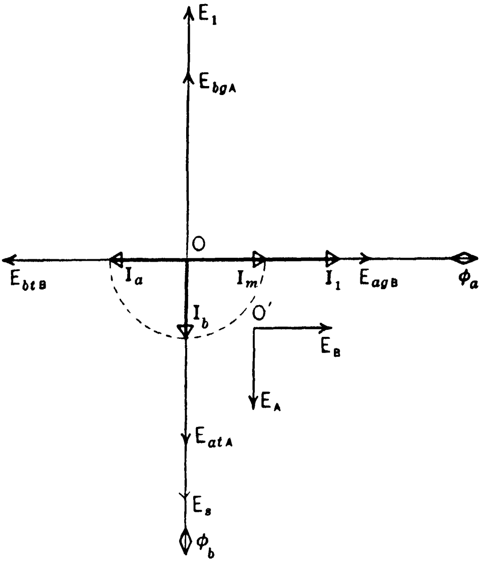

FIG. 705. A vector diagram of an ideal single-phase induction motor at synchronism.

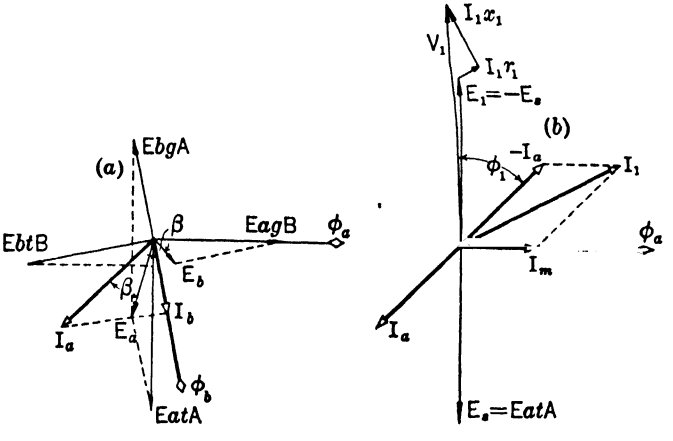

FIG. 706. Vector diagrams of the motor below synchronism: (a) rotor vectors; (b) stator vectors.

The speed voltage E_{bgA} varies as (speed)^2 owing to the reduction in ϕ_b and to the reduced speed of the rotor conductors through $\mathbf{\Phi}_b$. This results in E_A and I_a increasing in value and moving toward $\mathbf{E}_{atA}$ in phase.

982. Fundamental EMF Equations.—The relative values of the several induced emf's (rms values) are:

Transformer voltage:

$$E_{atA} = \sqrt{2}\pi n_2 f \phi_a k_b \, 10^{-8} \tag{17}$$

$$= K\phi_a \tag{17a}$$

where n_2 = number of rotor turns, expressed in stator terms.
k_b = breadth factor of the distributed rotor winding.

Speed voltage, assuming N_s = syn. rpm, f = supply frequency, and p = number of poles:

$$E_{agB} = \sqrt{2}\pi n_2 N_s (1 - s) p \phi_a k_b \times 10^{-8} \tag{18}$$

$$= \sqrt{2}\pi n_2 f (1 - s) \phi_a k_b \times 10^{-8} = K\phi_a(1 - s) \tag{18a}$$

Transformer voltage:

$$E_{btB} = \sqrt{2}\pi n_2 f \phi_b k_b \times 10^{-8} \tag{19}$$

$$= K\phi_b \tag{19a}$$

Speed voltage:

$$E_{bgA} = \sqrt{2}\pi n_2 N_s (1 - s) p \phi_b k_b \times 10^{-8} \tag{20}$$

$$= K(1 - s)\phi_b \tag{21}$$

The current, $\mathbf{I}_b$, in the rotor is expressed in terms of $\mathbf{E}_{agB} + \mathbf{E}_{btB}$, and the rotor impedance, Z_2, or

$$\mathbf{I}_b Z_2 = \mathbf{E}_{agB} + \mathbf{E}_{btB} \tag{22}$$

$$\tan \beta = x_2 r_2 \tag{22a}$$

Since $\mathbf{I}_b$ is a small magnetizing current, required to produce $\mathbf{\Phi}_b$, $\mathbf{I}_b Z_2$ is small, and is at a large angle with respect to either $\mathbf{E}_{agB}$ or $\mathbf{E}_{btB}$. As a result E_{agB} and E_{btB} are nearly equal in value, so that (eqs. 18*a* and 19*a*)

$$\phi_a(1 - s) = \phi_b$$

nearly, or

$$\phi_b/\phi_a = (1 - s) \tag{23}$$

At synchronous speed $(s = 0)\phi_b = \phi_a$, nearly, while at standstill

$(s = 1)\phi_b = 0$. Substituting from eq. (23) into eq. (21):

$$E_{bgA} = K(1 - s)^2\phi_a \quad \text{. . . . .} \quad (24)$$

or E_{bgA} varies as the square of the rpm, assuming ϕ_a constant.

The torque current, $\mathbf{I}_a$, in the rotor is due to the resultant of the two emf's acting along the A-A axis, divided by the rotor leakage impedance, or

$$\mathbf{I}_a = (\mathbf{E}_{atA} + \mathbf{E}_{bgA})/Z_2 \quad \text{. . . . .} \quad (25)$$

983. Motor and Generator Action. — In Fig. 706 the current vector $\mathbf{I}_b$ has a positive projection upon the speed voltage, $\mathbf{E}_{agB}$, indicating generator action and causing a torque which opposes the rotation of the motor. Current $\mathbf{I}_a$ has a negative projection upon its speed voltage $\mathbf{E}_{bgA}$, which accounts for the useful (motor) torque of the machine. At synchronous speed $\mathbf{E}_{agB}$ and $\mathbf{E}_{atA}$ are equal and displaced 90 degrees; likewise $\mathbf{E}_{btB}$ and $\mathbf{E}_{bgA}$ are equal and 90 degrees apart. As a result the net voltage acting along the B-B axis, or $\mathbf{E}_B$ $(= \mathbf{E}_{agB} + \mathbf{E}_{btB})$, and the voltage acting along the A-A axis, $\mathbf{E}_A$ $(= \mathbf{E}_{atA} + \mathbf{E}_{bgA})$, are equal and 90 degrees out of phase, so that $\mathbf{I}_a$ and $\mathbf{I}_b$ are also equal and at 90 degrees. The stator current $\mathbf{I}_1$ consists of a magnetizing current $\mathbf{I}_m$ required to produce the flux Φ_a plus a current to balance $\mathbf{I}_a$ (equal to $-\mathbf{I}_a$ in stator terms). Therefore, the cross-magnetizing current $\mathbf{I}_b$, which cannot react directly upon the stator, does react indirectly upon the stator through its equal, $\mathbf{I}_a$. At speeds below or above synchronism the total rotor torque current $\mathbf{I}_a$ may be thought of as the $\mathbf{I}_a$ at synchronous speed, plus a varying component required to produce the motor torque at the speed in question. The stator current I_1 then always contains the equivalent of the exciting currents required to produce the two fluxes, Φ_a and Φ_b.

984. The Rotating Magnetic Field. — The resultant field of the rotating single-phase motor, being the sum of Φ_a and Φ_b, will rotate as does the field of the polyphase motor (§484), since it is the resultant of component fields displaced in space 90 electrical degrees, and nearly 90 degrees apart in time phase. The trace of the rotating field vector will, in general, be an ellipse, with the major axis along Φ_a for speeds below synchronism, and along Φ_b for speeds above synchronism. At synchronous speed it is substantially a circle. Figure 707 illustrates this.

985. Performance Calculations. — The performance of the motor might be determined from vector diagrams such as Fig. 706(a) and (b) by assuming various speeds, i.e., values of E_{agB}, in terms of E_{atA}, each time starting with E_{atA} equal to the applied voltage, V_1. By working through the diagram to determine the value and phase position of $\mathbf{I}_a$, and then drawing the diagram of stator vectors it would be found that the required V_1 would not agree with the known supply voltage.

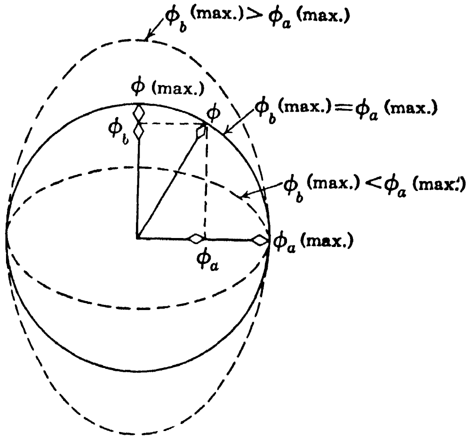
ϕ_b (max.)> ϕ_a (max.)
ϕ (max.)
ϕ
ϕ_b (max.)=ϕ_a (max.)
ϕ_b
ϕ_b (max.) <ϕ_a (max.)
ϕ_a (max.)
ϕ_a

FIG. 707. Ellipses representing the trace of resultant field vector in a single-phase motor.

Now by reducing all rotor vectors in the ratio of (V_1 actual)/(V_1 required) a revised diagram (or scale of the diagram) would result, and from this diagram values of $\mathbf{I}_a$, $\mathbf{I}_a \cdot \mathbf{E}_{bgA}$ = power developed, $\mathbf{I}_1$, θ_1, power input, etc., might be determined.

More rigid graphical and analytical solutions are discussed below, and the reader is directed to the references at the close of this chapter, particularly to the textbooks of Puchstein and Lloyd,[5] and of A. S. Langsdorf.[6]

986. EXPERIMENT 51-D. — A Study of Vector Relations Involved in the Quadrature-Flux Theory of the Single-Phase Induction Motor. — A single-phase commutator motor of the type shown in Fig. 720, having two sets of brushes displaced by 90 degrees, should be used for this test.

1. With the circuits of both sets of brushes open, apply rated voltage and frequency to the stator winding. Move the two sets of brushes until the emf induced between the *a* brushes is a maximum and that between the *b* brushes is zero. The *a* brushes are then along the axis of the stator field, while the *b* brushes are along the axis of the quadrature field.

Read the voltage E_a between the *a* brushes, which corresponds to E_{atA} of §980. Read also the stator volts, amperes, and watts.

2. By means of an adjustable-speed d-c motor direct connected or belted to the induction-type machine drive it at various speeds, from a fraction of synchronous speed to synchronous speed and above. Again read E_a and note whether it has changed. Read $E_b = E_{agB}$, and note

---

[5] Puchstein and Lloyd, "Alternating Current Machines," Chapters XXXVI and XXXVII, John Wiley & Sons.

[6] A. S. Langsdorf, "Theory of A-C Machinery," Chapter XI, McGraw-Hill Book Co.

whether it has the value $E_a(1 - s)$. Reverse the direction of rotation of the machines and again take readings.

3. With the motor at rest close the circuit of the *b* brushes through an ammeter and the current coil of a wattmeter or power-factor meter. With the stator excitation at the same value as before drive the motor at various speeds and read the rotor amperes, I_b. Determine its phase relation with respect to stator applied volts. Note the effect upon the input to the driving motor of opening and closing the circuit of the *b* brushes. Read the voltage between the *a* brushes.

4. Open the stator circuit but send a current through the rotor by means of the *b* brushes and adjust this current when driving the motor at various speeds to the same values and phase positions as were found in 3 at the same speeds. Read the emf between the *a* brushes (E_{bgA}), also the drop across the rotor between the *b* brushes, both in value and in phase position. This is nearly the equal and opposite of E_{btB}.

5. Finally close the circuits of both the *a* and *b* brushes through ammeters and wattmeters and, after bringing the motor up somewhat in speed, note that it will now operate as an induction motor and carry a load. Vary the load by means of the coupled d-c machine and take readings to determine the operating characteristics of the motor. Take readings also of I_a and I_b in value and phase.

From the data taken attempt to draw vector diagrams similar to Fig. 706 for operation at various loads and speeds. State conclusions and explain how this commutator motor is equivalent to a single-phase induction motor with a squirrel-cage rotor.

THE CIRCLE DIAGRAM THEORY

987. The Five Fundamental Relations. — The reader is supposed to be familiar with the circle diagram of a polyphase induction motor (Chapters XXII, XLVII, and XLVIII). The locus of the primary current of a single-phase induction machine, operating at a constant terminal voltage, is also nearly a circle. Each of the two theories described above leads to a different equivalent diagram, but both diagrams result in the same circle. The equivalence of the two diagrams having been demonstrated,[7] we shall deduce the equation of the circle on the basis of the quadrature flux theory. Under steady operating conditions, a single-phase induction machine must satisfy five electromagnetic relations, each of which leads to a corresponding *vectorial equation*. These relations are as follows:

1. The geometric sum of the voltages $\mathbf{E}_{atA}$ and $\mathbf{E}_{bgA}$ (Fig. 705),

---

[7] V. Karapetoff, *Journal A.I.E.E.*, vol. 40 (1921), p. 640.

induced in the rotor, is equal to the leakage impedance drop (self and mutual) in these coils due to the currents $\mathbf{I}_a$ and $\mathbf{I}_b$. This impedance is due to the ohmic resistance of the rotor circuit, its leakage reactance, and the mutual leakage reactance on the part of the current $\mathbf{I}_b$.

2. Similarly, the geometric sum of the voltages $\mathbf{E}_{btB}$ and $\mathbf{E}_{agB}$, induced in the rotor along the B–B axis, is equal to the leakage impedance drop due to the current $\mathbf{I}_b$ and the mutual reactance drop due to $\mathbf{I}_a$.

3. The flux $\mathbf{\Phi}_b$ lags slightly behind the mmf due to the current $\mathbf{I}_b$ (because of the core loss; angle α in Fig. 283), and is numerically equal to the magnetizing component of this mmf multiplied by the permeance of the useful path.

4. The flux $\mathbf{\Phi}_a$ lags slightly behind the geometric sum of the mmf's due to the currents $\mathbf{I}_1$ and $\mathbf{I}_a$, and is numerically equal to the in-phase component of this resultant mmf multiplied by the permeance of the path.

5. The geometric sum of the primary applied voltage and of that induced in the stator winding by the transformer action of the flux $\mathbf{\Phi}_a$ is equal to the primary impedance drop.

With a clear understanding of these principles, the reader should have no difficulty in following the mathematical treatment given below or that found in special works on the subject (§992).

988. The Five Fundamental Equations. — From the five relations which were stated in the previous article the fundamental equations of the single-phase motor are:

$$-j\sqrt{2}\pi f n_2 \mathbf{\Phi}_a\, 10^{-8} - v\sqrt{2}\pi f n_2 \mathbf{\Phi}_b\, 10^{-8} = Z_2\mathbf{I}_a + v x_2 \mathbf{I}_b \quad . \; . \; (26)$$

$$-j\sqrt{2}\pi f n_2 \mathbf{\Phi}_b\, 10^{-8} + v\sqrt{2}\pi f n_2 \mathbf{\Phi}_a\, 10^{-8} = Z_2\mathbf{I}_b - v x_2 \mathbf{I}_a \; . \; . \; . \; (27)$$

$$\mathbf{\Phi}_b = n_2 \mathbf{I}_b \mathcal{P} \; . \; . \; . \; . \; . \; . \; (28)$$

$$\mathbf{\Phi}_a = (n_2 \mathbf{I}_1 + n_2 \mathbf{I}_a)\mathcal{P} \qquad (29)$$

$$\mathbf{E}_1 - j\sqrt{2}\pi f n_2 \mathbf{\Phi}_a\, 10^{-8} = \mathbf{I}_1 Z_1 \quad . \; . \; . \; . \; . \; (30)$$

The notation is shown in part in Fig. 705; the symbols for both the currents and the fluxes refer to the effective values; bold-face type is used to denote vectors. The meaning of the other symbols is as follows: f is the primary frequency; n_2 is the number of effective secondary turns expressed in primary terms, and with the breadth factor taken into consideration; $\mathcal{P} = (\mathcal{P}_r \cos\alpha) \cdot \epsilon^{-j\alpha}$ is the complex permeance of the useful path; $\mathcal{P}_r$ is the real permeance; α is the angle of flux lag due to the core loss; r_2 is the effective secondary resistance per circuit; $v = (1 - s)$ is the rotor speed, expressed as a fraction of the synchronous speed; x_2 is the leakage reactance of the rotor winding, per circuit, at the primary frequency; Z_1 is the complex leakage impedance of the primary winding; $Z_2 = r_2 + jx_2$ is the leakage impedance of the secondary winding, per circuit. All quantities are understood to be per pole where such an interpretation is possible.

Equation (26) may be interpreted as follows: The effective value of emf induced along the A-A axis by the transformer action of the flux Φ_a is $\sqrt{2}\pi f n_2 \phi_a \, 10^{-8}$. This emf lags 90 degrees behind the flux Φ_a; hence, the foregoing expression is multiplied by $-j$. The effective value of the emf induced along the same axis by rotation through the flux Φ_b, at synchronous speed, is $\sqrt{2}\pi f n_2 \phi_b \, 10^{-8}$; at a speed which is a fraction v of the synchronous speed, this emf is less, in the ratio of v to 1 (§980). The minus sign shows that the vector of this emf is in a direction opposite to Φ_b (Fig. 705).

On the right-hand side of eq. (26), the term $Z_2\mathbf{I}_a$ represents the leakage impedance drop along the A-A axis, due to the current $\mathbf{I}_a$. The same conductors are linked with the leakage flux due to the current $\mathbf{I}_b$, and are rotating in this leakage flux; hence, the expression for the voltage drop due to the mutual inductance is $vx_2\mathbf{I}_b$.

Another way of deriving the term $vx_2\mathbf{I}_b$ is as follows: Let the permeance of the leakage paths along the B-B axis be $\mathcal{P}_l$; then the leakage flux itself is $\mathbf{I}_b n_2 \mathcal{P}_l$. Hence, the total flux produced by the current $\mathbf{I}_b$ is $\Phi_b + \mathbf{I}_b n_2 \mathcal{P}_l$. The rotor bars revolve in this flux, so that the total speed emf induced in them is:

$$v\sqrt{2}\pi f n_2(\Phi_b + \mathbf{I}_b n_2 \mathcal{P}_l) \, 10^{-8} = v\sqrt{2}\pi f n_2 \Phi_b \, 10^{-8} + v 2\pi f n_2^2 \mathcal{P}_l \mathbf{I}_b \, 10^{-8} \quad (31)$$

But $n_2^2\mathcal{P}_l$ is the leakage inductance and $\sqrt{2}\pi f(n_2^2\mathcal{P}_l) \times 10^{-8} = x_2$ is the leakage reactance along the B-B axis. Consequently, the last term in eq. (31) is equal to $vx_2\mathbf{I}_b$. It could be entered with the minus sign on the left-hand side of eq. (26), together with the term $v\sqrt{2}\pi f n_2 \Phi_b \, 10^{-8}$. Instead, it is placed on the right-hand side with the plus sign.

Equation (27) may be interpreted similarly. Where the subscript a is replaced by b, the sign of the term is kept the same; where b is replaced by a, the sign is reversed. Equations (28) and (29) follow directly from the corresponding statements in §987. The necessary reduction in the value of the permeance and a lag of the vectors Φ_a and Φ_b with respect to their mmf's are obtained by assuming the permeance $\mathcal{P}$ to be a complex quantity, characterized by an angle α. In many cases α may be assumed to be equal to zero and a real $\mathcal{P}$ used. In eq. (30), the second term on the left-hand side is identical with the first term in eq. (26).

989. Solution for the Primary Current. — Equations (26) to (30) may be considered as five simultaneous equations, with five unknown quantities, $\boldsymbol{\phi}_a$, $\boldsymbol{\phi}_b$, $\mathbf{I}_a$, $\mathbf{I}_b$, $\mathbf{I}_1$. Since our purpose is to find the locus of $\mathbf{I}_1$, the other four unknown quantities should be eliminated. The expressions for the quantities $\boldsymbol{\phi}_a$ and $\boldsymbol{\phi}_b$ from eqs. (29) and (28) may be substituted in the remaining three equations, and then $\mathbf{I}_a$ and $\mathbf{I}_b$ eliminated by subtraction or by any other well-known method. The final result is:

$$\mathbf{E}_1 = \mathbf{I}_1[Z_1 + (Z_2M - v^2jx_2N)/(M^2 - v^2N^2)] \tag{32}$$

where

$$M = 1 + Z_2Y \tag{33}$$

$$N = 1 + jx_2Y \tag{34}$$

Y is the exciting admittance reduced to the secondary circuit and determined by the expression:

$$Z = Y^{-1} = j2\pi f\mathcal{P}n_2^2 \tag{35}$$

Z is the reciprocal of Y, or the exciting impedance. From eq. (32), for an assumed speed v, the vector of the primary current $\mathbf{I}_1$ may be determined in magnitude and in phase position, if the constants of the machine are known.

Equation (32) is more suitable for small values of v, that is, near standstill. For values of v near synchronism it is more convenient to introduce the factor $1 - v^2$. Equation (32) then becomes:

$$\mathbf{E}_1 = \mathbf{I}_1\left[Z_1 + \frac{(Z_2M - jx_2N) + (1 - v^2)jx_2N}{(M^2 - N^2) + (1 - v^2)N^2}\right] \tag{36}$$

or:

$$\mathbf{E}_1 = \mathbf{I}_1[Z_1 + (Q + \sigma jx_2N)/(YR + \sigma N^2)] \tag{37}$$

In this expression,

$$\sigma = 1 - v^2 = 1 - (1 - s)^2 = s\,(2 - s) \tag{38}$$

where the slip

$$s = 1 - v \tag{39}$$

s is expressed as a fraction of the synchronous speed.

$$Q = Z_2M - jx_2N \tag{40}$$

or, substituting for M and N their expressions from eqs. (33) and (34),

$$Q = r_2[1 + Y(2jx_2 + r_2)] \tag{41}$$

Similarly,

$$R = (M^2 - N^2)/Y = (Q + r_2) \tag{42}$$

The complex ratio of $\mathbf{E}_1/\mathbf{I}_1$ from either eq. (32) or eq. (37) represents the total equivalent impedance of the motor at that particular speed. This ratio agrees with the common equivalent impedance of the three diagrams shown in the article referred to at the end of §986 above.

990. An Equation of the Circular Locus. — Equation (37) may be shown to represent a circular locus of the current vector I_1, when the terminal voltage E_1 is constant and the speed function σ varies. Eliminating the denominator, and factoring out σ, gives

$$[\mathbf{E}_1 YR - \mathbf{I}_1(Z_1 YR + Q)] + \sigma[\mathbf{E}_1 N^2 - \mathbf{I}_1(Z_1 N^2 + jx_2 N)] = 0 \quad . \quad (43)$$

To obtain the locus, the variable σ must be eliminated from this equation. According to §918, we take a "dot" product of eq. (43) with a vector normal to that by which σ is multiplied. Then the term with σ vanishes, and we obtain

$$[j\mathbf{E}_1 N^2 - \mathbf{I}_1(jZ_1 N^2 + j^2 x_2 N)] \cdot [\mathbf{E}_1 YR - \mathbf{I}_1(Z_1 YR + Q)] = 0 \quad . \quad (44)$$

Let

$$jZ_1 N^2 - x_2 N = C\epsilon^{j\gamma} \quad . \; . \; . \; . \; . \; . \; . \; . \; . \quad (45)$$

and

$$Z_1 YR + Q = D\epsilon^{j(\gamma-\delta)} \quad . \; . \; . \; . \; . \; . \; . \; . \quad (46)$$

Factoring out these quantities in eq. (44), we get:

$$C\epsilon^{j\gamma}[\mathbf{E}_1/(Z_1 + jx_2 N^{-1}) - \mathbf{I}_1] \cdot D\epsilon^{j(\gamma-\delta)}\{\mathbf{E}_1/[Z_1 + Z(Q/R)] - \mathbf{I}_1\} = 0 \quad (47)$$

C and D, being scalars, can be dropped without impairing the validity of the equation. Comparing eq. (47) with eq. (30) in §918, we see that it represents a circle defined by the angle δ and by the vectors:

$$\mathbf{F}_1 = \mathbf{E}_1/(Z_1 + jx_2 N^{-1}) \quad . \; . \; . \; . \; . \; . \; . \; . \quad (48)$$

and

$$\mathbf{F}_2 = \mathbf{E}_1/[Z_1 + Z(Q/R)] \quad . \; . \; . \; . \; . \; . \; . \quad (49)$$

It will be seen that $\mathbf{F}_1$ and $\mathbf{F}_2$ are completely determined by the motor constants and by the magnitude of the applied voltage. The angle δ depends only upon the motor constants.

991. EXPERIMENT 51-E. — The Circle Diagram of a Single-Phase Induction Motor. — The purpose of the experiment is to familiarize the student with the theory of the machine in a form in which it leads to a circular locus of the primary current. Either the derivation of the circle given in §§986 to 989 may be used, or any other method of approach indicated in the references in §992. See also the references at the end of Chapter XLVIII. A very accurate load test should be performed and the actual locus of the primary current obtained; see also the method of tangents and the photographic method in §894. Tests should then be devised from which those constants of the machine which determine the circular locus may be computed. The aim of the study should be to obtain a theoretical circular locus and to compare it with that obtained from the load test.

992. References.

BOOKS

1. V. KARAPETOFF, The Magnetic Circuit, McGraw-Hill Book Co.
2. O. G. C. DAHL, Electric Circuits — Theory and Applications, Vol. I, McGraw-Hill Book Co.
3. WAGNER and EVANS, Symmetrical Components, Chapter XVII, McGraw-Hill Book Co.
4. PUCHSTEIN and LLOYD, Alternating-Current Machines, Chapters XXXVI and XXXVII, John Wiley & Sons.
5. A. S. LANGSDORF, Theory of A-C Machines, Chapter XI, McGraw-Hill Book Co.
6. W. V. LYON, Applications of Symmetrical Components, McGraw-Hill Book Co.
7. R. R. LAWRENCE, Alternating Current Machinery, Chapters LV to LVII.
8. HERBERT VICKERS, The Induction Motor, Pitman & Sons.
9. B. A. BEHREND, The Induction Motor, Chapters XVII and XVIII.
10. C. P. STEINMETZ, Theory and Calculations of Electrical Apparatus, Chapter V.
11. E. ARNOLD, Die Wechselstromtechnik, Vol. 5, part 1, Chapters VII and VIII.

ARTICLES

1. H. R. WEST, *Jour. A.I.E.E.*, vol. 45 (1926), p. 160.
2. K. L. HANSEN, *ibid.*, vol. 44 (1925), p. 170.
3. L. M. PERKINS, *ibid.*, p. 499.
4. J. K. KOSTKO, *Trans. A.I.E.E.*, vol. 41 (1922), p. 215.
5. K. KUHLMANN, *Schweiz. Elekt. Ver.*, *Bull.*, vol. 13 (1922), p. 129.
6. V. KARAPETOFF, *Jour. A.I.E.E.*, vol. 40 (1921), p. 640.
7. HELLMUND, LAMME, and others, *Trans. A.I.E.E.*, vol. 37 (1918), pp. 539–702.
8. G. BENISCHKE, *Elek. Kraftb. u. Bahnen*, Heft 4 (1910).

CHAPTER LII

SINGLE-PHASE COMMUTATOR-TYPE MOTORS

993. Single-phase a-c commutator motors of satisfactory performance have long been available in small sizes for use on branch lines which do not warrant three-phase distribution. With improvements in commutation, brought about by better design, such motors are of great advantage in electric railway service because the single-phase supply requires only one trolley wire. The single-phase induction motor, discussed in the preceding chapter, has a field of application of its own, especially where a nearly constant speed between no load and full load (shunt-motor characteristics) is required and a comparatively low power factor is not objectionable. On the other hand, for traction, crane, or hoisting service, an a-c motor with series characteristics is required (§295), and so far the only kinds of single-phase motors which possess such characteristics are those provided with a commutator similar to that of a d-c machine.

Consider the d-c motor shown in Fig. 229, and let its armature be running, say, clockwise. Should the polarity of the line terminals be reversed, the armature would continue to run in the same direction, even though the current would be flowing through the machine in the opposite direction. The reason for this is that both the armature current and the field flux are reversed, and therefore the torque between the two is still in the same direction. To reverse the direction of rotation, it is necessary to reverse either the armature or the field, but not both.

Because the armature of a series-connected d-c motor runs in a given direction, irrespective of the direction of the current through it, such a machine can be operated with alternating current. This is the fundamental idea underlying the series a-c motor described below. Of course, a motor designed for a-c operation has to have a laminated field structure, and its best proportions are different from those of a d-c motor. However, these are details as compared to the fundamental principle of torque formation between the field and the armature current, this torque and its variations with speed being of the same general nature as in a series-connected d-c motor. Because of the possibility of conveying alternating currents by induction as well as by conduction, and also because of the possibility of using an external transformer for part of the machine, various modifications of the plain a-c series motor are possible. Some of these are described below, up to §1012.

Some types of single-phase a-c commutator motors with so-called "shunt characteristics" (§274), that is, machines whose speed varies but little with the load, have also been developed. While such machines are more expensive and complicated than the plain induction motor, they can be made to start with a considerable torque, and also have a higher power factor. In some types, speed adjustment is also possible. A general introduction to the theory of such machines will be found in §§1013 to 1022.

The field of application of a-c commutator motors so far has been rather limited, partly because considerable difficulty is experienced in obtaining sparkless commutation, especially in starting, and partly because these motors are heavier and more costly per unit of rating. For this reason, only a brief sketch of their principal general properties is given below. For further details the reader is referred to the bibliography in §1046.

THE SERIES MOTOR

994. The electrical connections in a single-phase a-c series motor[1] are shown schematically in Fig. 708. *A* is the armature, similar to that of a d-c machine (Figs. 198 and 199) and provided with a commutator and brushes, *bb*. The field winding, *F*, produces an alternating flux, Φ, in space quadrature with the theoretical brush line, *bb*. By the brush line is meant the line along which the armature is magnetized by a current flowing in the usual manner through the brushes. The brushes them-

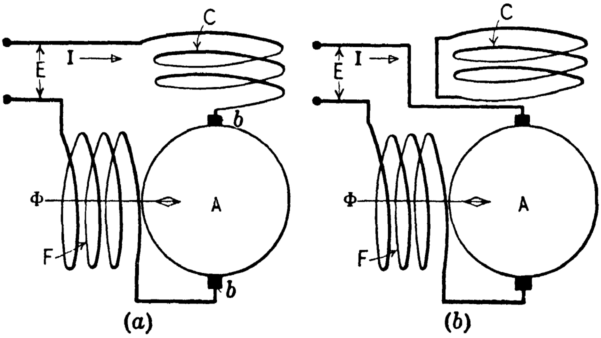

FIG. 708. Single-phase series commutator motor compensated (*a*) conductively, (*b*) inductively.

---

[1] For an excellent treatment of the series a-c motor see Felix Konn, "The Single-Phase Commutator-Type Traction Motor," *Gen. Elec. Rev.*, April, May, and June, 1932.

selves bear on the commutator and, depending upon the shape of the end-connections of the coils, are placed on the theoretical brush line or are shifted with respect thereto. For theoretical purposes, the commutator may be omitted and the brushes assumed to bear directly upon the armature conductors, as shown, for example, in Figs. 264 and 265.

Since the flux Φ is excited by the same current which flows through the armature, both reach their maxima at nearly the same instant and are also reversed almost simultaneously, thus giving the maximum possible torque. The equivalent vector of the flux lags slightly behind that of the exciting current, partly because of the core loss (Fig. 194) and partly because of the reaction of the currents in the armature coils short-circuited by the brushes; the theoretical torque is therefore somewhat reduced. The actual arrangement of the field winding on the poles is shown in Fig. 709 which represents a multipolar motor with salient poles. The notation is the same as in Fig. 708.

995. Compensation of Armature Reaction. — With the brushes in the geometric neutral (Fig. 709), the armature mmf tends to produce a flux along the center lines *xx* and *yy* (§366). As in a d-c machine, this armature mmf distorts the main flux and makes commutation more difficult. Moreover, in an a-c machine, any flux produced by the armature mmf results in a leakage reactance. This reactance does not appreciably affect the useful torque, but consumes part of the applied voltage in overcoming it, thus needlessly lowering the power factor of the machine.

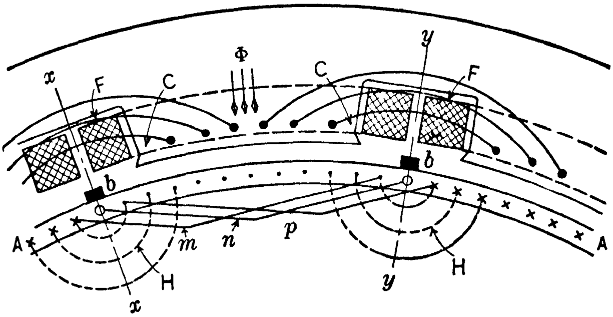

FIG. 709. The arrangement of the field and compensating windings in a single-phase commutator motor with salient poles.

Some of the actual armature coils are denoted in Fig. 709 by *m, n, p*. For the purpose of visualizing the armature reaction, these coils may be replaced by fictitious concentric coils, *HH*, shown by dotted lines. To neutralize the armature reaction, similar concentric coils, *CC*, are placed on the field poles, with their center lines along the axes *xx* and *yy*. This *compensating winding, CC*, may be connected to the armature either conductively (Fig. 708*a*) or inductively (Fig. 708*b*).

With conductive compensation, in order to wipe out the armature flux, the number of turns in the winding *C* must be such as to produce an mmf essentially equal and opposite to that in the armature winding. If desired, the armature reaction may be under-compensated or over-compensated, to obtain some other favorable characteristics of the machine. With inductive compensation, the winding *C* is closed upon itself, like the secondary winding of a transformer on short circuit. The closer the winding *C* is to the armature winding, and the lower its resistance and leakage reactance, the more nearly is the armature flux wiped out. The number of turns is not essential, since the current in *C* adjusts itself automatically to a value and phase position in which the secondary mmf is nearly equal and opposite to the primary mmf, as in a transformer (§391).

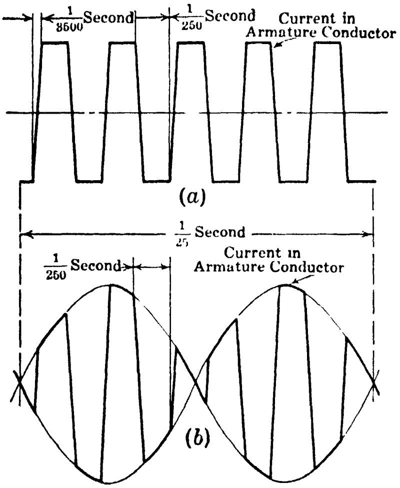

Fig. 710. Curves showing current reversal; (*a*) in a d-c motor; (*b*) in an a-c commutator motor (F. Konn).

996. Difficulties in Commutation. — In an a-c commutator motor, sparking at the brushes may be considered as due to two distinct causes, one being the emf of self and mutual induction (reactance voltage), as in a d-c machine, the other the transformer action of the alternating flux. We shall consider these two causes separately.

Emf of self and mutual induction, due to current reversal. The interval of time for current reversal in a coil undergoing commutation (Figs. 266 and 710), being of the order of 1/3000 second, is quite short as compared with that of one alternation of the line current, say 1/50 second. Therefore, the main armature current may be considered as remaining practically constant during each local reversal. The general theory of d-c commutation given in §§371 to 381 thus applies to a-c motors, with the main current slowly varying in magnitude. Commutating poles (Figs. 266 and 232) are used in larger a-c series motors for facilitating current reversal. Since a compensating winding is nearly always employed for improving the power factor (§995), interpoles of moderate size are sufficient for creating the necessary commutating flux.

Transformer emf. This emf, the nature of which is explained below, causes additional commutation difficulties for which no completely satisfactory remedy at all speeds is available. This is probably the main reason for the comparatively small number of a-c commutator motors in use. This transformer emf makes it necessary to use large commutators, with many segments per pole and a small number of turns per coil. As a result, such motors are heavier, more expensive, and less satisfactory in operation than d-c motors. When the problem of compensation of this transformer emf has been fully solved, there should be a marked improvement in the operating characteristics and especially in the quality of commutation of a-c motors. In anticipation of a solution of this difficulty, considerable effort has been made to improve and diversify the speed-torque and power-factor characteristics of this class of machine (see bibliography in §1041).

The reason for the transformer emf in the coils undergoing commutation may be seen in Fig. 709. Consider the armature to be stationary, with an alternating current flowing through the field winding *F* only. With respect to the winding *F*, the armature coil *n*, short-circuited by the brushes, acts as the secondary of a transformer closed upon itself. The circulating currents so produced are harmful in three respects:

(a) When the armature is turned even by a small angle, sufficient to remove the short circuit, a spark occurs under the brush. When the armature is revolving, sparking is continuous.

(b) The circulating currents produce no useful torque and cause additional heating.

(c) The reaction of the secondary currents reduces the useful flux, Φ, of the machine.

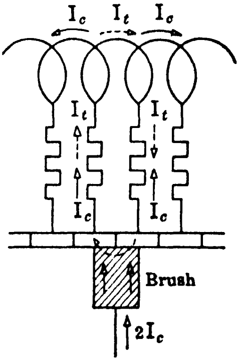

FIG. 711. Resistance leads used to limit the transformer current, I_t, in the coils undergoing commutation.

Transformer action takes place at any armature speed, its severity being determined mainly by the magnitude of the inducing field. The lower the speed of the machine the higher the armature current (Fig. 241); for this reason the most destructive sparking takes place at start.

Remedies for transformer emf. Two remedies suggest themselves: One is to provide resistances in the leads between the armature coils and the commutator segments (Fig. 711). This device has been used to some extent, but the resistance leads occupy considerable space, are expensive and sometimes burn out. They would lower the efficiency of the machine if it were not for the fact that they reduce the circulating current so that their net effect is a lowering of the I^2r loss.

The other remedy is to induce in the short-circuited coils an emf substantially equal and opposite to that due to the alternating flux, Φ. The only practical way, so far proposed, of inducing such an emf is by means of interpoles. But the action of an interpole is due to the cutting of its flux by the armature conductors. At start the cutting action and the effect of the interpoles are practically nil, while the sparking due to the transformer action is a maximum. Within a certain range of operating speeds and values of current, it is possible to compensate for the combined emf due to the current reversal (as in a d-c machine) and to the transformer action by a careful design of interpoles and by exciting them with a current of proper magnitude and phase. At start, and beyond the above-mentioned range, commutation remains unsatisfactory, although the use of narrow brushes of high contact resistance is of material advantage.

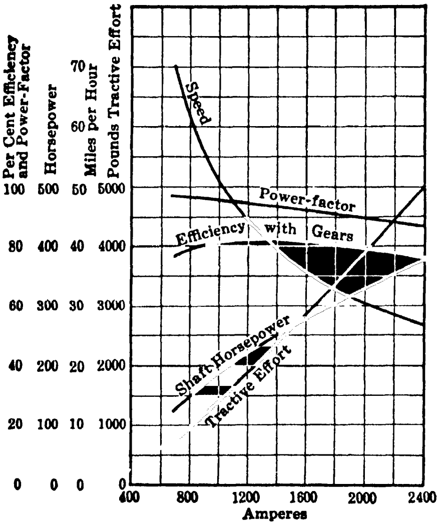

FIG. 712. Performance characteristics of an a-c traction motor.

Much ingenuity and skill have been displayed in developing various connections for exciting interpoles in order to produce the proper commutating flux, at least under running conditions. For information on this subject the reader is referred to §1041. At this writing, complete neutralization of the transformer emf should be considered an unsolved problem.

997. Performance Characteristics and the Vector Diagram. — The general characteristic curves, as shown by Fig. 712,[2] are essentially the same as for the series d-c motor (Fig. 241). Power factor is lowest at start and increases with the speed.

The current and voltage relations at a particular speed are shown vectorially in Fig. 713. E is the terminal voltage, I the current, and Φ the useful torque-producing flux. The generated emf, $-E_g$, between the brushes, is induced by the rotation of the armature in the flux Φ and hence is in time phase with it, as is evident from the general relation:

[2] *Loc. cit.*

$e = Blv$. In other words, *a voltage induced in a commutated armature by rotation follows variations in the inducing flux.* Since the flux is alternating, so also is the voltage, $-E_g$, induced between the brushes. The frequency of the exciting current is equal to the line frequency, and is independent of the speed of rotation of the armature. Hence, *in a commutated armature, the frequency of the induced voltage (between brushes) is always equal to that of the exciting current. The magnitude of the induced voltage is proportional to the number of revolutions per unit time.* Part of the terminal voltage E is used in opposing this generated emf, and is denoted in the sketch by E_g.

The current, I, is shown slightly leading Φ, because of the core loss and because of the reaction of the currents in the short-circuited armature coils. With these factors disregarded, the flux can be drawn in phase with its exciting current, I.

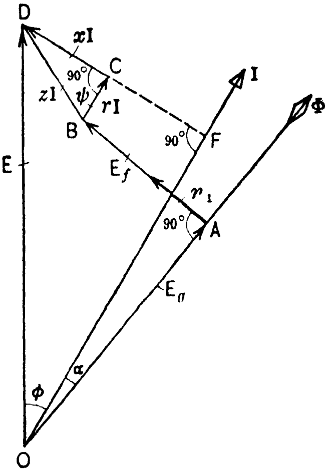

Fig. 713. A vector diagram of a single-phase series commutator motor.

The applied voltage, E, is used up in four parts: (1) the part E_g balances the counter emf produced by the rotation of the armature; (2) the part E_f, in leading quadrature with Φ, balances the reactive emf induced in the field winding by the useful flux Φ; (3) the voltage rI, in phase with I, is the ohmic drop in the armature and in the field; also in the compensating winding if it is conductively connected; (4) the voltage xI, in leading quadrature with I, is the reactive drop due to all the leakage fluxes in the machine. As the load changes, the magnitude and the phase position of the current I also change, and with them all the other vectors and the speed of the machine vary accordingly. Because of saturation in the iron core, there is no simple relationship between I and Φ, and the performance curves have to be predicted point by point. Disregarding saturation, the current locus is a circle (§999).

998. Analytical Theory.—The polygon $OABCD$ may be represented analytically by the vector equation:

$$\mathbf{E} = va\mathbf{\Phi} + jb\mathbf{\Phi} + Z\mathbf{I} \quad . \; . \; . \; . \; . \; . \; . \; . \quad (1)$$

where

$$va\mathbf{\Phi} = \mathbf{E}_g \quad . \; . \; . \; . \; . \; . \; . \; . \; . \; . \; . \; . \; . \; . \quad (2)$$

In this expression, v is the speed of the machine in rpm and a is an armature constant (§234). The term $jb\mathbf{\Phi}$ represents $\mathbf{E}_f$, and b is a constant of the field winding. For a concentrated winding, $b = 4.44 \times$ number of poles $\times$ turns per pole $\times$ frequency (§441). The term $Z\mathbf{I} = (r + jx)\mathbf{I}$ represents the leakage impedance drop in the machine. The relationship between the flux Φ and the exciting current may be written in the form:

$$\mathbf{\Phi} = k\mathbf{I} \quad \ldots\ldots\ldots\ldots \quad (3)$$

where k is proportional to the permeance of the main path at that particular value of the flux. The relationship between Φ and I is expressed by the saturation curve of the machine, and k is simply the ratio of Φ to I for a particular point on that curve. In order to take the core loss and the angle α into consideration, k may be generalized to K, which may be thought of as a complex quantity of the form:

$$K = (k \cos \alpha)\epsilon^{-j\alpha} \quad \ldots\ldots\ldots \quad (4)$$

where k is the quotient Φ/I obtained from the saturation curve.

Equation (1) contains three unknown quantities, $\mathbf{\Phi}$, $\mathbf{I}$, and v. To eliminate v, take a dot product (§918) of both sides of the equation with a unit vector[3] $\mathbf{n}_1$ in the direction AB normal to $\mathbf{\Phi}$. The term $va\mathbf{\Phi}$ vanishes; $jb\mathbf{\Phi}$, being in the direction of $\mathbf{n}_1$, becomes a scalar quantity $b\mathbf{\Phi}$ (without any direction), and we get the following scalar equation:

$$\mathbf{E} \cdot \mathbf{n}_1 = b\mathbf{\Phi} + Z\mathbf{I} \cdot \mathbf{n}_1 \quad \ldots. \quad (5)$$

The angle between $\mathbf{E}$ and $\mathbf{n}_1$ is $90 - (\phi + \alpha)$; the angle between $Z\mathbf{I}$ and $\mathbf{n}_1$ is $90 - (\psi + \alpha)$, where

$$\tan \psi = x/r \quad \ldots\ldots\ldots\ldots \quad (6)$$

Hence, eq. (5) becomes:

$$E \sin (\phi + \alpha) = b\Phi + ZI \sin (\psi + \alpha) \quad \ldots\ldots \quad (7a)$$

To eliminate the term $jb\mathbf{\Phi}$ from eq. (1), take a scalar product of both sides with $\mathbf{p}_1$, where $\mathbf{p}_1$ is a unit vector in the direction of $\mathbf{\Phi}$. The result is

$$E \cos (\phi + \alpha) = va\Phi + ZI \cos (\psi + \alpha) \quad . \quad . \quad (7b)$$

Equations (7) could also be obtained by projecting the polygon $OABD$ on the directions of E_f and E_0, respectively. The method of scalar products is used above in order to show that it is entirely automatic in its application and does not require visualizing a geometric figure.

In actual computations, it is convenient to assume a reasonable value of I, to find the corresponding Φ on the saturation curve, and to estimate

---

[3] A unit vector is a vector of unit length which has a definite direction in space.

α from the core loss and commutation currents (or simply, put $\alpha = 0$). From eq. (7*a*), the phase angle ϕ may then be computed and the corresponding v found from eq. (7*b*). The electrical input is then calculated, and the losses being known the output may be computed. The output, P, and the speed, v, being known, the torque becomes:

$$T = 7.04P/v \quad . \; . \; . \; . \; . \; . \; . \; . \; . \; . \quad (8)$$

In this manner, all the important characteristics of the motor may be determined for several assumed values of current, and plotted as curves.

999. The Circle Diagram. — Neglecting saturation and assuming the angle α to be constant, the locus of the end of the vector **I** may be shown to be a circle. Substituting the value of Φ from eq. (3) in eq. (1) gives:

$$\mathbf{E} = va K\mathbf{I} + \mathbf{I}(jbK + Z) \quad . \; . \; . \; . \; . \; . \; . \; . \quad (9)$$

To eliminate v, we take a scalar product of both sides with $-jK\mathbf{I}$, the result being

$$-jK\mathbf{I} \cdot [\mathbf{E} - \mathbf{I}(jbK + Z)] = 0 \quad . \; . \; . \; . \; . \quad (10)$$

Let:

$$jbK + Z = z_1\epsilon^{j(0.5\pi-\theta)} \quad . \; . \; . \; . \; . \; . \; . \; . \; . \; . \quad (11)$$

Moreover, from eq. (4),

$$jK = k\cos\alpha\epsilon^{j(0.5\pi-\alpha)} \quad . \; . \; . \; . \; . \; . \; . \; . \; . \quad (12)$$

Substituting these values in eq. (10) and omitting the scalar factors, z_1 and $k \cos \alpha$, we get:

$$(0 - \mathbf{I})\epsilon^{j(0.5\pi-\alpha)} \cdot [\mathbf{E}/(jbK + Z) - \mathbf{I}]\epsilon^{j(0.5\pi-\theta)} = 0 \quad . \; . \quad (13)$$

Comparing this expression with eq. (30) in §918, we see that the locus of the end of **I** is a circle for which $\mathbf{F}_1 = 0$,

$$\mathbf{F}_2 = \mathbf{E}/(jbK + Z) = (\mathbf{E}/z_1)\epsilon^{-j(0.5\pi-\theta)} \quad . \; . \; . \; . \; . \quad (14)$$

and

$$\delta = \theta - \alpha \quad . \; . \; . \; . \; . \; . \; . \; . \; . \; . \; . \; . \; . \; . \; . \; . \quad (15)$$

It must be clearly understood, of course, that eq. (13) gives a circle only when K is independent of I. This means operation on the lower leg of the saturation curve, at comparatively small values of current and at high speeds. It would be a mistake to use such a circle for finding the starting current. Or else, if the vector of the starting current is assumed to lie on the circle, this circle will be wrong for operating points at high speeds.

1000. EXPERIMENT 52-A. — Study of the Single-Phase Series Commutator Motor. — The theory and the characteristics of the motor are explained above. Tests similar to those usually made on a d-c series motor (§§295 to 304) should be performed in order to determine the general performance characteristics (Fig. 712) of the motor. Certain modifications are necessary: (a) a wattmeter must be used; (b) the voltages across the armature, the field, and the compensating winding should be measured separately in their magnitudes and relative phase; (c) the machine may be started by using taps on an auto-transformer (Fig. 282). Of the special tests that apply to an a-c motor only, the following may be mentioned:

1. A comparison of the characteristics when operated with direct and alternating currents.
2. Starting characteristics on fractional voltages.
3. Study of the compensating winding, connected conductively and inductively (§378), also of over- and under-compensation.
4. Study of commutation and brush behavior (§§379 to 384).
5. Commutating poles and methods of excitation to neutralize the transformer emf and reactance voltage.
6. Regenerative action.[4]

THE REPULSION MOTOR

1001. This type of single-phase commutator motor is shown schematically in Figs. 380 and 381 and is also discussed briefly in §§513 and 514. Much of the general theory given above in the treatment of the series motor applies here, and to avoid repetition it will be assumed that the reader is familiar with the contents of §§994 to 1000. The name " repulsion " is mainly of historical interest, but is retained here in view of its universal use.

1002. The Principle of Action with Two Separate Field Windings. — The motor shown in Fig. 714(*a*) may be considered a modification of that in Fig. 708(*b*). In the latter machine, the armature winding is connected conductively and acts as the primary of a transformer, while the compensating winding *C* acts as a short-circuited secondary. In the motor shown in Fig. 714(*a*), the compensating winding *C* is connected into the main circuit conductively, while the armature brushes are short-circuited and the armature winding therefore acts as a transformer secondary. Sometimes the machines shown in Fig. 708 are referred to as " conductively fed," and those in Fig. 714 as " inductively fed."

Whereas the change in the connections from Fig. 708(*a*) to 708(*b*) causes only a slight difference in the operating characteristics, the change from Fig. 708(*b*) to 714(*a*) considerably modifies the properties of the machine, because a short-circuited armature is subjected not only to a transformer action, but to a generator action as well, so that the flux along the *bb* axis is not wiped out as in the former case.

---

[4] L. J. Hubbard, *Trans. A.I.E.E.*, vol. 42 (1923), p. 133.

The action of the machine shown in Fig. 714(*a*) may be explained as follows: The line current I and the armature current I' together create a flux Φ_t along the brush line *bb*. The line current I alone excites the flux Φ, in space quadrature with Φ_t. The flux Φ, in conjunction with the component of the armature current I' in time phase with it, produces the useful torque of the motor. At a given load torque, the armature speed is such that the values of Φ and I' for the required electromagnetic torque are compatible with the electric and magnetic conditions within the machine itself. These conditions are as follows:

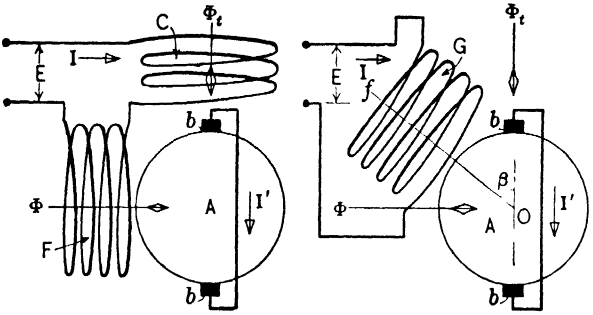

(*a*) (*b*)

FIG. 714. Connections in a repulsion motor: (*a*) with separate field windings; (*b*) with a single field winding.

1. The sum of the voltages at the terminals of the windings F and C is equal to the applied voltage E.

2. The sum of the voltages induced in the armature by the generator action of the flux Φ and by the transformer action of the flux Φ_t is just sufficient for maintaining the current I' through the leakage impedance of the armature winding.

3. The mmf of the current I in the winding F is of the proper magnitude for exciting the useful flux Φ.

4. The sum of the mmf's of the currents I and I' in the windings C and A, respectively, is just sufficient to produce the flux Φ_t.

At standstill, the flux Φ_t is comparatively small and the flux Φ predominates. As the armature gains speed, the flux Φ_t increases and Φ decreases. At synchronism, the two fluxes are nearly equal in magnitude and are approximately in time quadrature with each other. Together they then form a resultant revolving air-gap flux, and for this reason the machine is usually made with non-salient poles. At any speed, v, let the frequency of rotation be f_r and the line frequency f. The emf of rotation induced in the armature is (see eq. 10, Chapter LI):

$$E_r = \sqrt{2}\pi\Phi N f_r \qquad (16)$$

and that due to the transformer action is:

$$E_t = -j\sqrt{2}\pi\Phi_t N f \qquad (17)$$

Neglecting the small impedance drop in the armature circuit, the two induced emf's must be equal and opposite, since the armature is short-circuited. Hence,

$$\Phi f_r = j\Phi_t f \qquad (18)$$

At synchronism, $f_r = f$, and consequently $\Phi = j\Phi_t$. Thus, at synchronous speed, the two fluxes are approximately equal and in time quadrature with each other. Below synchronism, $\Phi > \Phi_t$; above synchronism, $\Phi < \Phi_t$, the two fluxes remaining approximately in time quadrature with each other.

1003. Repulsion Motor with One Field Winding. — The motor shown in Fig. 714(a) is preferably provided with a stator with non-salient poles (Fig. 352), in order to obtain a maximum permeance of the air-gap for both fluxes. Moreover, each of the windings would usually be placed in several slots per pole, giving an approximately sinusoidal distribution of flux density in space. In so far as their mmf's are concerned, the two windings, F and C, may be combined into one, marked G in Fig. 714(b). Let the letters F, C, G signify also the number of turns in the respective windings. Then, in order that the winding G be equivalent to a combination of F and C its number of turns and the angle of shift β with respect to the brushes must satisfy the conditions:

$$C = G\cos\beta \qquad (19)$$

$$F = G\sin\beta \qquad (20)$$

from which,

$$\tan\beta = F/C \qquad (21)$$

and

$$G^2 = F^2 + C^2 \qquad (22)$$

A repulsion motor is often built as shown in Fig. 714(b), with one field winding and with brushes that may be shifted by a desired angle, β. For theoretical purposes, such a motor may be replaced by one of the type shown in Fig. 714(a), using eqs. (19) and (20).

For each value of brush shift, β, there is a separate set of performance curves. At $\beta = 0$, $F = 0$; large currents are induced in the armature but there is no field flux Φ to form a torque with these. At $\beta = 90°$,

$C = 0$; there is a large flux Φ, but no armature current to react with it. Between $\beta = 0$ and $\beta = 90°$ there is a value of β for which the starting torque is a maximum. This is the best starting position but usually not the best running position of the brushes. In investigating a new motor, and before closing the line switch, the brushes should be shifted to the position of $\beta = 90°$. After power is applied they may be brought back, thus gradually increasing the armature current.

The F winding, being singly excited, is a source of a large reactive voltage drop in the machine, and lowers its power factor. Therefore, in order to keep the power factor as high as possible, the number of turns of the F winding, and the flux Φ, must be kept as low as possible. Equation (20) shows that this means as small an angle β as is compatible with the other requirements. When β is too small, the torque becomes low and the current I' is too large for satisfactory commutation.

In the machine of the type shown in Fig. 714(*b*), the direction of rotation is reversed by shifting the brushes from the position $+\beta$ to $-\beta$, the axis Of being the neutral. If shifting the brushes is not convenient, for example on account of a remote position of the motor, two separate stator windings are used, as in Fig. 714(*a*). Reversing the terminals of the F winding causes the direction of rotation to be reversed, and is equivalent to a brush shift from $+\beta$ to $-\beta$.

1004. Conditions at Start. — Some a-c motors are started as repulsion motors and are then changed to some other type, after a considerable speed has been reached.[5] Therefore, the starting conditions of a repulsion motor are of particular interest and are shown in more detail in Fig. 715. In order to show the possibility of a point of view different from the one adopted above, the total flux due to the winding G is not resolved into its component fluxes, but the armature winding is sectionalized into fictitious belts in which transformer action and motor action, respectively, take place.

The sketch represents a machine of the type shown in Fig. 714(*b*), with the stator and rotor surfaces developed into planes. Instantaneous directions of the currents in the stator conductors are indicated in the usual manner by dots and crosses, and the corresponding instantaneous flux, produced by the winding G, is shown by the sine wave, $MPQRN$. The armature is assumed to be stationary, or moving at a low speed, so that the only emf induced in the rotor conductors is that due to the transformer action of the stator flux. The instantaneous directions of the induced emf's are shown by dots and crosses, the directions being opposite to those in the primary winding. The armature conductors between the brushes b_1 and b_2 are electrically connected in series, and the conductors in which the induced voltage is towards the reader are more numerous than those in which the induced emf is away from him. The lines d_1 and d_2 are so drawn that $b_1f_1 = f_1d_1$ and $b_2f_2 = f_2d_2$. The voltage induced in the part b_2C of the winding is balanced by that induced in Cd_1. The resultant voltage is that induced in the part b_1d_1, and it causes a current to flow towards the reader in the whole belt b_1b_2 of the winding, as shown in the lower row by dots and crosses.

---

[5] A shunt-type combination repulsion and induction motor, in which the commutated armature with its short-circuited brushes remains in the circuit in regular operation, is described in §1013 below.

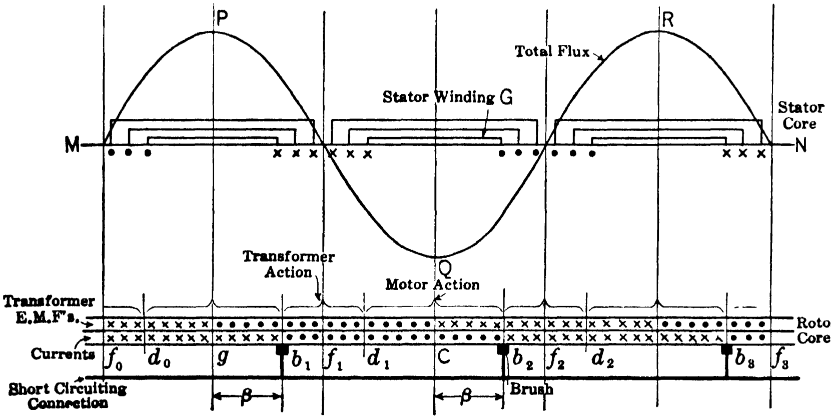

FIG. 715. Torque formation in a repulsion motor at start.

The starting torque is due to an interaction between these currents and the air-gap flux. The tangential forces due to the portions b_1f_1 and f_1d_1 of the armature winding are equal and opposite, the flux changing its sign at f_1. Hence, the net motor action is due to the portion d_1d_2 of the winding, and the motor starts with a considerable torque. The parts of the winding, such as b_1d_1 and b_2d_2, act as the secondaries of a transformer; and the remainders, d_1b_2 and d_2b_3, act as a motor armature. The relative electromagnetic strength of these two parts depends upon the brush shift, β.

1005. Analytical Theory and the Circle Diagram. — The four conditions stated in §1002 for the motor shown in Fig. 714(*a*) may be expressed analytically by the following four equations:

$$jb\mathbf{\Phi} + jc\mathbf{\Phi}_t + Z\mathbf{I} = \mathbf{E} \quad \text{. . . . .} \quad (23)$$

$$va\mathbf{\Phi} - ja\mathbf{\Phi}_t = Z'\mathbf{I}' \quad \text{. . . . .} \quad (24)$$

$$\mathbf{\Phi} = K\mathbf{I} \quad \text{. . . . .} \quad (25)$$

$$\mathbf{\Phi}_t = K'(\mathbf{I} + \mathbf{I}') \quad \text{. . . . . .} \quad (26)$$

These equations will become clear by comparison with eqs. (1) to (4), and with eqs. (16) and (17). The factors b and c convert the fluxes Φ and Φ_t into induced voltages (in magnitude only); the factor a accomplishes the same for the armature. Z and Z' are the leakage impedances of the stator and the rotor, respectively. Equation (24) is written in terms of the armature circuit; the other equations are in terms of the stator circuit. The quantity K is explained in §998; K' has a similar meaning for the magnetic circuit of the flux Φ_t.

For the machine shown in Fig. 714(b), the same equations apply, except that there is a definite relationship between the coefficients b and c. Let g be the factor, similar to b and c, applying to the winding G. Then, according to eqs. (19) and (20),

$$b = g \sin \beta \qquad \text{. . . . .} \qquad (27)$$

$$c = g \cos \beta \qquad \text{. . . . .} \qquad (28)$$

In this manner, the number of turns of the winding G and the brush shift β are introduced into the equations explicitly; at the same time the point of view of the two separate windings, F and C, is preserved.

From eqs. (23) to (26), the variables $\mathbf{\Phi}$, $\mathbf{\Phi}_t$, $\mathbf{I}'$ can be eliminated. The resulting equation for $\mathbf{I}$ is of the form

$$\mathbf{E} = \mathbf{I}(A + vB) \qquad \text{. . . . .} \qquad (29)$$

where A and B are complex quantities containing the constants of the machine and the variable factors K and K'. To eliminate v from eq. (29), we take a dot product of both sides with $j\mathbf{I}B$. The result is:

$$\mathbf{E} \cdot (j\mathbf{I}B) = (\mathbf{I}A) \cdot (j\mathbf{I}B) \qquad \text{. . . . .} \qquad (30)$$

In predicting the performance of a motor with given constants, it is convenient to assume some value of I (magnitude only) and to determine K from eq. (25), using the no-load saturation curve. Since I' is unknown, the value of K' can be only estimated. In the first approximation, it may be taken equal to K. The values of A and B may then be computed, and eq. (30) solved for the angle ϕ between E and I. The corresponding velocity, v, is found from eq. (29). Equations (24) and (26) may then be solved as simultaneous equations for Φ_t and I'. A few trials for K' may be necessary to bring it into accord with the final value of I'.

With saturated iron, the principle of superposition does not hold true, and the fluxes $\mathbf{\Phi}$ and $\mathbf{\Phi}_t$ cannot be combined in any simple manner. Therefore, at large values of I, the foregoing computations may be expected to give only approximate results.

The circle diagram. Multiplying eq. (29) by $-jIB$, dot product, to eliminate v, we get:

$$-jIB \cdot [\mathbf{E} - \mathbf{I}A] = 0 \quad \ldots\ldots \quad (31)$$

This equation is of the same form as eq. (10). Disregarding saturation, the quantities K and K', which enter into A and B, are constant. With this limitation, eq. (31) represents a circle. It can be transformed into the standard form of eq. (30) in §918, and its coordinates, $\mathbf{F}_1$, $\mathbf{F}_2$, and δ, computed.

1006. EXPERIMENT 52-B. — Study of the Single-Phase Repulsion Motor. — The theory and the general characteristics are explained above. In addition to the tests specified in §§1000 and 514, the influence of the position of the brushes upon the starting and running characteristics should be studied in detail, the experimental results being checked, at least approximately, with the theory.

COMPENSATED REPULSION MOTOR

1007. This type of motor, also known as the Latour motor, or as the Winter-Eichberg motor, is shown diagrammatically in Fig. 716. It differs from the motors shown in Figs. 708 and 714 in that it has four brush arms per pair of poles, instead of two, and no stationary winding F to excite the flux Φ. In its place are the extra or exciting brushes, ff, in space quadrature with the main or energy brushes, bb. Since the magnetic axis of a commutated armature is along the line of the brushes, a flux, Φ, is produced along the axis ff by the line current flowing through the armature. The rest of the action is the same as in the plain repulsion motor (Fig. 714a); that is, a motor torque is produced by the inter-

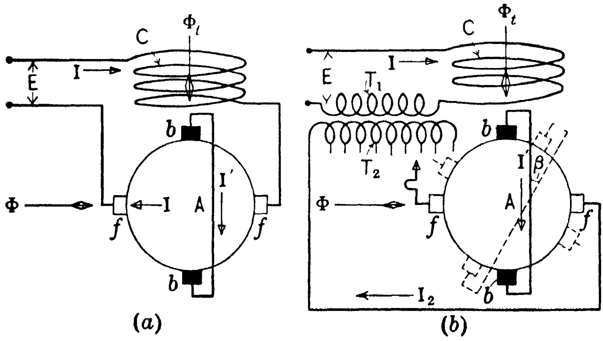

(a) (b)

FIG. 716. Connections in a compensated repulsion motor with the exciting brushes fed (a) directly, (b) through a transformer.

action of the flux Φ with the current I' induced in the armature by a combined action of the compensating winding C and the flux Φ.

At first sight, it may seem that exciting the main flux Φ by means of the brushes *ff*, in place of the field winding F, would entail merely a saving in copper and no change in the operating characteristics of the machine. In reality, the characteristics are changed to a considerable extent, owing to two kinds of action of the flux Φ_t upon the armature circuit in the direction of the brushes *ff*. These new factors are as follows: (1) an emf, E_{fr}, in phase with Φ_t, is induced between the brushes *ff*, due to the rotation of the armature in that flux; and (2) a small torque is introduced between the flux Φ_t and the current I in the armature. These two actions are considered in more detail in the next section.

The motor shown in Fig. 716(*b*) differs from that in Fig. 716(*a*) only by the addition of a current transformer, T_1T_2, between the primary line and the circuit of the exciting brushes, *ff*. This enables the designer to choose a value of the current most suitable with respect to the commutation and to the magnitude of the superimposed current, I'. The general characteristics of the machine are not affected by the transformer to any considerable degree, except as explained in §1011.

1008. Properties of Armature Excitation. — The machines shown in Fig. 716 are excited from the armature, by means of the brushes *ff*, and it is necessary to understand the difference between this kind of excitation and that produced by a stationary winding F. It is explained in §1002 that the short-circuited brushes *bb* cause the fluxes Φ and Φ_t to be essentially in time quadrature, with the flux Φ leading in phase. The emf, E_{ft}, induced between the brushes *ff* by the transformer action of the flux Φ, lags behind this flux by 90 degrees and is therefore nearly in phase with the flux Φ_t. The emf, E_{fr}, induced between the same brushes by the rotation in the flux Φ_t is in time phase with the flux Φ_t. By carefully considering the polarities of the two emf's, it will be found that they oppose each other, so that the rotational emf, E_{fr}, reduces the transformer emf, E_{ft}.

This means that, as the motor speed increases, the voltage drop per unit current between the brushes *ff* decreases. But it is precisely the reactive drop across the stationary field winding that lowers the power factor of the machines shown in Figs. 708 and 714, because the counter emf of the flux Φ is in quadrature with the current. In the machines shown in Fig. 716, the field drop at synchronism ($\Phi_t = \Phi$) is reduced almost to zero, so that the machine can be made to operate at nearly unity power factor. Beyond synchronism, E_{fr} is greater than E_{ft}, and the motor can operate with a leading current. Hence the name *compensated* repulsion motor.

The current I and the flux Φ are nearly in phase with each other; hence, the current I and the flux Φ_t are nearly in time quadrature with each other. Were they displaced in time phase by exactly 90 degrees, the torque between them would be zero. In reality, there is a small component of I in phase with Φ_t which causes a torque between the two. By considering the instantaneous actions, it will be found that this torque is in the direction of rotation of the armature and is added to that between I' and Φ.

1009. Analytical Theory. — The general equations of the motor under consideration are identical with those given in §1005, except that part of the applied voltage goes to balance E_{fr}, the emf of rotation in the field circuit. Therefore eq. (23) becomes:

$$jb\mathbf{\Phi} + jc\mathbf{\Phi}_t + va\mathbf{\Phi}_t + Z\mathbf{I} = \mathbf{E} \quad \ldots\ldots \quad (32)$$

Proceeding as before, and eliminating $\mathbf{\Phi}$, $\mathbf{\Phi}_t$, $\mathbf{I}'$, from eqs. (32), (24), (25), (26), we obtain a vectorial equation of the form:

$$\mathbf{E} = \mathbf{I}(A + Hv + Nv^2) \quad \ldots\ldots\ldots \quad (33)$$

where A, H, N are complex quantities. To eliminate v from this equation, we first form a scalar product with $j\mathbf{I}H$ and obtain:

$$(\mathbf{E} - \mathbf{I}A) \cdot j\mathbf{I}H = v^2(\mathbf{I}N \cdot j\mathbf{I}H) \quad \ldots\ldots \quad (34)$$

Next we multiply eq. (33) by $j\mathbf{I}N$, and get:

$$(\mathbf{E} - \mathbf{I}A) \cdot j\mathbf{I}N = v(\mathbf{I}H \cdot j\mathbf{I}N) \quad \ldots\ldots\ldots \quad (35)$$

Substituting the value of v from eq. (35) in eq. (34), we obtain:

$$[(\mathbf{E} - \mathbf{I}A) \cdot j\mathbf{I}H](\mathbf{I}H \cdot j\mathbf{I}N)^2 = [(\mathbf{E} - \mathbf{I}A) \cdot j\mathbf{I}N]^2(\mathbf{I}N \cdot j\mathbf{I}H) \quad (36)$$

which contains only the vector of the unknown current I.

For numerical computations, a value of I should be assumed, and the phase angle ϕ between it and the voltage E computed from eq. (36). Then v can be determined from eq. (33), and the other quantities from eqs. (24), (25), (26); for details see §1005.

For this motor, the locus of the current I is *not* a circle. This follows from the form of eq. (33) which contains two terms with v. The elimination of v gives eq. (36), which is much more involved than that of a circle.[6] Equation (36) represents the locus of the current vector in the language of vector analysis. If desired, this expression may be transformed to polar coordinates so as to represent a relationship between the magnitude of I and its phase angle ϕ. Or else, it may be rewritten in terms of the projections of I on two chosen axes of coordinates.

---

[6] V. Karapetoff, "General Criterion for the Circular Locus of the Current Vector in *A-C* Circuits and Machinery," *Proc. Nat. Acad. of Sci.*, vol. 11 (1925), p. 683.

1010. EXPERIMENT 52-C. — Study of the Compensated Repulsion Motor. — General operating characteristics should first be determined, and then special studies made. For general suggestions see §§1000 and 1006. Of particular interest is an investigation of the voltage between the brushes *ff*. For this purpose, the short circuit between the brushes *bb* should be removed, the winding *C* excited from the quadrature phase of a two-phase supply, or through an induction regulator, and the machine driven by another motor at different speeds. The magnitude of the current *I* should be kept constant for each set of speeds. The relative phase of the two currents should be so adjusted as to have the two fluxes approximately in time quadrature with each other. With the proper direction of rotation, it will be found that as the speed increases the voltage between the brushes *ff* decreases, passes through zero, and increases again with the phase reversed. This experiment should make clear the purpose and the advantage of providing excitation from the revolving armature, rather than by means of a stator winding.

1011. Compensated Repulsion Motor with Brush Shift. — The motor shown in Fig. 716(*b*) is provided with a transformer (or auto-transformer), and all the brushes may be shifted simultaneously by a desired angle, as shown by the dotted lines. The purpose of the brush shift is to vary the torque-speed characteristics of the machine. As the *bb* brushes are moved from the neutral position, the transformer action of the *C* winding, and consequently the current I', is reduced; the useful torque of the machine also becomes smaller.

Brush shift affords a ready means of starting and speed control. To start the motor, all the brushes are shifted simultaneously by nearly 90 electrical degrees and the main switch is closed. The machine develops only a small torque and takes a comparatively small current. Then the brushes are gradually shifted and the machine starts under load. To develop the rated torque at the rated speed, the brushes must be finally shifted to the positions *bb*, *ff*, so as to have a maximum secondary current and the largest possible field flux. By keeping the brushes partly shifted, the same torque is developed at a lower speed. The efficiency and the power factor are reduced by shifting the brushes, and this method is feasible mainly with small motors.

The transformer has the same effect as an increase of the magnetic reluctance of the path of the motor field flux at low speed. This means that, owing to the reduction in the field drop with a certain brush shift and line voltage, the motor can draw more current from the line, and the torque will be increased as long as the reduction of the motor field flux is not carried too far. The reduction of the motor field flux will further result in improved commutation at low speeds. As soon as the motor runs above synchronous speed, the voltage appearing at the compensating brushes reverses its direction. Hence, the flux in the transformer will be opposite to the line current, and the secondary ampere-turns of the transformer will have to be larger than the primary ampere-turns. The larger the magnetizing current of the transformer the sooner the motor field flux will increase with increasing speed, in spite of the reduction of line current, and thus the speed can be limited. The increase of the secondary current flowing in the energy circuit, *bb*, with increasing speed, helps in limiting the speed. The transformer can be readily designed so that the no-load speed is not over 150 per cent of the synchronous speed.

The current required for exciting the flux of the transformer can be larger than the line current. In that case, when running below synchronous speed, part of the excitation will be furnished by the secondary turns of the transformer and the current in the armature compensating circuit will be reversed so that the ampere-turns yielded by it are opposite to the ampere-turns of the stator field turns. Part of the excitation required by the flux of the transformer is transmitted by transformation from the stator field turns to the armature compensating circuit and flows from there to the secondary of the transformer. Since the primary of this transformer is connected in series with the line, a part or all of the torque-producing flux is excited by the armature, depending on the brush shift, thus making it possible to operate this motor at nearly unity power factor at full load and full speed.

If it is desired to run the motor counterclockwise, in a brush position in which the motor has the same characteristics as in the brush position β in which the motor runs clockwise, the brushes should be shifted clockwise over $180 - 2\beta$ degrees. In the plain repulsion motor (§1001) it would only have been necessary to shift the brushes over 2β degrees counterclockwise to obtain the same result. But in the compensated repulsion motor this cannot be done, as the armature compensating circuit and stator field winding buck one another. Nevertheless, it is possible to obtain counterclockwise operation by shifting the brushes far enough counterclockwise, but the power factor and commutation will be inferior. If the compensating circuit is open, the no-load speed will be excessively high.

Dynamic braking (§293) may be used with this motor, if so desired. For this purpose, the machine is converted into a stator-excited generator. The circuit of the brushes *bb* is opened and the excitation is furnished by the winding *C*. An adjustable resistance is inserted in series with the brushes *ff*, and the kinetic energy of rotation is dissipated in this resistance.

1012. EXPERIMENT 52-D. — Study of the Brush-Shifting Compensated Repulsion Motor. — The machine is described in the preceding section. Assuming that the Experiment 52-C has been performed, there are four additional points to be studied with this machine, viz.: (a) speed-torque characteristics, efficiency, and power factor, with different brush positions; (b) the effect of saturation and of the ratio of turns in the transformer upon the performance of the motor; (c) reversal of the direction of rotation; (d) dynamic braking.

THE REPULSION-INDUCTION MOTOR

1013. The repulsion-start single-phase induction motor, described in §513, satisfies the requirements of a high starting torque and nearly constant speed under varying load, but it has the following drawbacks: (a) a centrifugal device is necessary to short-circuit the commutator, with a resulting sudden change in the characteristics; (b) the power factor under running conditions is rather low. An improvement in both respects is brought about by using two separate rotor windings (Fig. 717), one connected to the commutator, as in Fig. 380, and the other short-circuited on itself.[7] The latter winding is usually of the squirrel-cage type (Fig. 351).

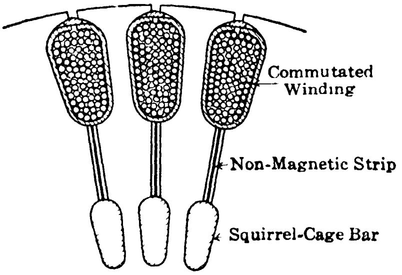

FIG. 717. Part of the rotor of a repulsion-induction motor with two separate windings.

The squirrel-cage winding should not interfere with the commutated winding at start, and for this reason is placed in deep and nearly closed slots. With this arrangement, the leakage inductance of the squirrel-cage winding is quite high, and, moreover, space is provided between the upper and the lower slots in order that a useful flux may link with the commutated winding only. In starting, a voltage of the line frequency is induced in the squirrel-cage bars, and, because of their high inductance, only comparatively small and out-of-phase currents flow through the winding. Such currents can have but little effect upon the starting of the machine as a repulsion motor.

Near synchronism, the commutated winding short-circuited by the brushes requires the existence of two fluxes, Φ and Φ_t (Fig. 714), which are nearly equal in magnitude, and are in space and time quadrature with each other (§1002). But the squirrel-cage winding of a single-phase induction motor also maintains two such fluxes (§981). Thus, near synchronism, the combination machine under discussion possesses a nearly uniform revolving field, and the two rotor windings act in agreement, dividing the load between them. Voltages of slip frequency are induced in the squirrel-cage bars, so that their high inductance has but little effect on the magnitude and phase of the currents, which are determined mainly by the resistance of the winding.

---

[7] S. R. Bergman, *Trans. A.I.E.E.*, vol. 43 (1924), p. 1039.

At no load, the machine operates at a speed slightly above synchronous, for the following reason: the repulsion part of the motor has series characteristics and tends to cause the armature to run away. The induction part has no torque at synchronism and operates as a generator at speeds above synchronous. Therefore, at some speed, a few per cent beyond synchronous, the motor torque of the commutated winding just balances the generator torque of the squirrel-cage winding plus the losses in the machine itself. At loads near the rating of the machine, the rotor speed is a few per cent below synchronous, so that both windings develop a motor torque. In the interest of good commutation, a larger portion of the load should be carried by the squirrel-cage winding. The characteristic curves of such a motor are given in Fig. 718.

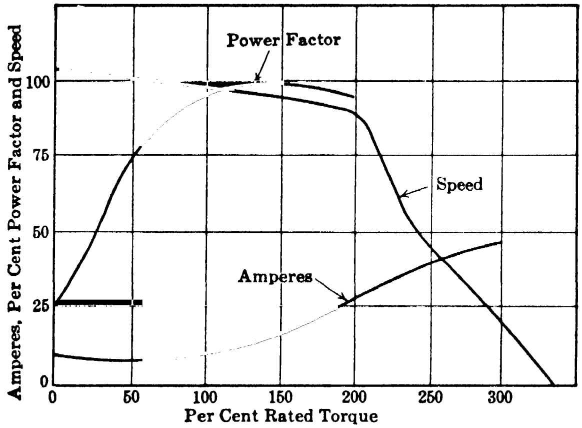

FIG. 718. Typical performance curves of the squirrel-cage repulsion motor (H. R. West).

In the above-described motor, a plain repulsion-type armature (Fig. 714) is used. It is also possible to combine a compensated repulsion motor (Fig. 716) with a squirrel-cage winding,[8] and in this manner to obtain a constant-speed machine with a high starting torque. In the motor of this type developed by Mr. Fynn, an additional compensating winding is provided on the stator, and the power factor within the operating range is raised to unity (§1020).

---

[8] Val A. Fynn, *Trans. A.I.E.E.*, vol. 34 (1915), p. 2483.

1014. Commutation Strips. — As explained in §996, the difficulties in commutation with a pulsating field flux are partly due to its transformer action and partly to the reversal voltage in the coil itself. In the motor under consideration, within its operating range, the fluxes Φ and Φ_t are combined into a more or less regular synchronously revolving flux, so that only comparatively small voltages are induced by the resultant air-gap flux in the coils undergoing commutation. On the other hand, the reactance voltage, due to the leakage flux of the coil itself, is present to its full value, as in a d-c machine. Because the motor should have uniform air-gap reluctance, to accommodate a revolving flux, it is not convenient to provide interpoles, and another remedy is used to insure satisfactory commutation, namely, so-called commutation strips (Fig. 717).

These strips, made of some non-magnetic metal of fairly high resistivity, are placed in the slits between the two rotor windings, and act as short-circuited transformer secondaries with respect to the individual coils of the commutated winding. When the current in one of the coils begins to be reversed under a brush, the leakage field surrounding the conductors in that slot changes rapidly, and secondary currents are induced in the corresponding strip threaded by this flux. The magnitude of the flux is therefore reduced, and a lower spark emf results when the circuit is broken. The conditions with and without a commutation strip are somewhat similar to those in a current transformer with the secondary closed and open (§429). In place of sparking at the brushes, a certain I^2r loss takes place in the commutation strips themselves, but this loss is not serious in view of a favorable location of these strips for heat conduction.

Commutation strips have to have a fairly high resistance, in order not to be much affected by fluxes of the line frequency. Otherwise, currents induced in them would interfere with the starting of the machine as a repulsion motor. Commutation currents are of much higher frequencies, so that even a small flux can produce an appreciable current. Of course, the transformer emf at start remains uncompensated for, as in all other a-c commutator machines, but in this particular machine some sparking during the start is not so harmful, since the motor is primarily intended for constant-speed drives with infrequent starting.

1015. Vector Diagram and Improvement in the Power Factor. — In spite of a highly inductive squirrel-cage winding, the motor described above operates at a higher power factor than either a plain repulsion motor or a plain induction motor of similar constants. The reason for this may be seen from Fig. 719, which represents a simplified vector diagram of the machine near synchronous speed.[9] At and near this speed, the field flux Φ and the transformer flux Φ_t (Fig. 714) are approximately equal and nearly in time quadrature with each other, both for the plain repulsion motor (§1002) and for the plain induction motor (§979). The same is true for the combination motor under discussion.

First, disregard the effect of the secondary currents in the squirrel-cage winding upon the primary winding F (or upon that part of the winding G which represents F). Then, with the primary line current equal to I_0, the field flux is in time phase with it and Φ_t lags behind it by 90 degrees. E_f and E_t are the parts of the applied voltage which balance the emf's induced by the fluxes Φ and Φ_t in the stator windings F and C, respectively. Neglecting the resistances and the leakage reactances of the two windings, the sum of E_f and E_t gives the applied voltage, E. The current I_0 lags behind the voltage by the angle ϕ_0.

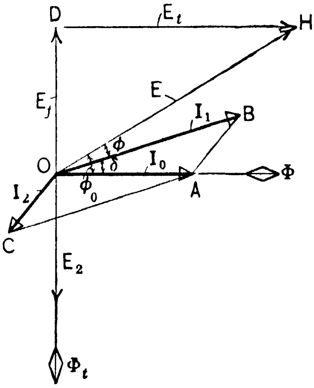

FIG. 719. A vector diagram of the repulsion-induction motor, showing an improvement in the power factor.

In reality, the flux Φ by transformer action induces a secondary voltage, E_2, in the squirrel-cage winding, and this voltage causes a current, I_2, to flow in the winding. The current I_2 lags by a considerable angle behind E_2 because of the high inductance of the winding. As in a transformer, the fictitious magnetizing current, I_0, which excites the flux Φ, is a sum of the primary current, I_1, and the secondary current, I_2 (Fig. 283). Thus, because of the reaction of the secondary squirrel-cage winding, the primary current in the windings F and C leads the field flux Φ by an angle δ. Assuming the load on the shaft to be adjusted to give the same values of Φ and Φ_t as without I_2, the voltages E_f and E_t remain unchanged in phase and in magnitude, and their sum is still equal to the same terminal voltage, E. However, the primary current is now I_1 instead of I_0, and the phase displacement angle has been reduced from ϕ_0 to ϕ.

Besides the reaction of the secondary currents in the squirrel-cage winding, the angle δ is in part also due to the core loss and to the mmf of the coils undergoing commutation, that is, short-circuited by the brushes. In fact, the case considered above is but a specific example of the improvement of the power factor by "lagging the flux" with respect to the current. As another example, let the field winding, F, of a series motor (Fig. 708) be shunted by a non-inductive resistance. This will increase the angle α in Fig. 713. By redrawing the diagram it will be found that the angle ϕ has been reduced. This desirable result is accomplished in this particular case at the expense of the I^2r loss in the non-inductive resistance (see also §1020).

---

[9] For a complete analytical theory see H. R. West, *Trans. A.I.E.E.*, vol. 43 (1924), p. 1048.

In a plain single-phase induction motor, the quadrature field Φ is excited by the rotor currents only (§981), so that I_2 is in phase with Φ. This requires a double magnetizing current in the stator winding. In the motor under consideration, the flux Φ is excited from the stator, and the component of I_2 in phase with Φ is negative. Thus, another way of looking upon the effect on the power factor of the addition of the commutated winding is that the rotor does not have to act in part as its own exciter for the cross field.

1016. EXPERIMENT 52-E. — Study of the Single-Phase Repulsion-Induction Motor. — The machine is described in §§1013 to 1015. The actual performance characteristics should first be determined by means of a brake test or its equivalent. Then a few readings should be taken with different positions of the brushes. For a more thorough investigation, a complete analytical or graphical theory should be developed, and the observed characteristics of the machine made to agree with curves predicted from its measured constants. See also the instructions for performing the other experiments in this chapter.

SHUNT-TYPE MOTORS WITH TWO SETS OF BRUSHES

1017. A series-connected d-c motor with laminated field can be operated with alternating current (§993), but a shunt-connected motor (Fig. 228) would hardly develop any torque. The reason for this is that the shunt-field circuit is highly inductive and the field flux would be almost in quadrature with the armature current, giving an average integrated torque over a cycle almost equal to zero. There are at least two ways out of this difficulty, namely, (a) to supply the field excitation from the second phase of a two-phase supply, and (b) to use the armature of the motor itself as an exciter. The first solution is hardly rational since a polyphase motor can be used if a two-phase supply is available. The second solution, described below, leads to several useful varieties of shunt-type motors with speed and power-factor control. As with most types of a-c commutator motors, their practical application has been so far limited because of the difficulties in commutation. Once these have been overcome, these motors should find a useful place among other types of a-c motors.

1018. Commutator-Type Induction Motor. — The motor shown in Fig. 720(*a*) has a single-phase stator and a revolving armature with a d-c winding and a commutator. Two sets of brushes per pole are provided: one set, *bb*, on the center line of the stator winding; the other, *ff*, displaced by 90 electrical degrees with respect thereto. The brush terminals are denoted by *yy* and *xx*, respectively. These terminals may be either short-circuited or connected to some other windings so as to obtain more desirable characteristics.

Consider first the terminals *yy* and *xx* to be short-circuited, and the stator winding *C* connected to a source of a-c voltage. The armature will not start by itself, being electrically symmetrical. Let it therefore be brought up nearly to synchronous speed by some external means, as with the squirrel-cage type single-phase induction motor. It will then continue to run and may be loaded mechanically as a motor. Its performance characteristics will be similar to those of an ordinary single-phase induction motor (Chapter LI). This can be shown from the point of view of either theory of the latter motor (§§969 and 979). Because of the two sets of brushes, the rotor is capable of developing two mmf's, in time and space quadrature, and these mmf's may be combined into one synchronously revolving mmf. Thus, the theory based upon the resolution of the stator mmf into two oppositely gliding mmf's applies directly to this machine. The cross-flux theory also applies, since the brushes *ff* fix in space an mmf which produces the field flux Φ. It is left to the reader to follow in detail, in application to the motor shown in Fig. 720(*a*), both theories given in Chapter LI.

Both sets of brushes may be shifted by a desired angle β (Fig. 720*b*), and the machine will continue to operate as a single-phase induction motor, because the rotor is still capable of reacting with a revolving mmf, while the field flux Φ can be produced as a resultant of the fluxes along the axes *bb* and *cc*.

With the connections *xx* and *yy* short-circuited, the machines shown in Fig. 720 are of no particular advantage because their characteristics are practically the same as those of an ordinary single-phase induction motor, and a squirrel-cage rotor is incomparably better in operation than a commutated armature with two sets of brushes. We shall therefore indicate in the following sections the advantages which accrue from the introduction of certain additional external emf's between the terminals *xx* and *yy*. Such emf's cannot be introduced into a squirrel-cage winding, and herein lies the justification for the use of a commutator and brushes.

Because of difficulties in commutation, it is of advantage to use a double winding on the armature, viz., a squirrel-cage winding carrying as much working current as possible, and a comparatively small commutated winding for power-factor correction and speed control. It was this idea which led to the development of the induction-repulsion motor described in §1013 and of the Fynn motor mentioned in the footnote at the end of that section. Nevertheless, machines without the squirrel-cage winding, shown in Fig. 720, are of sufficient interest to become familiar with their possibilities.

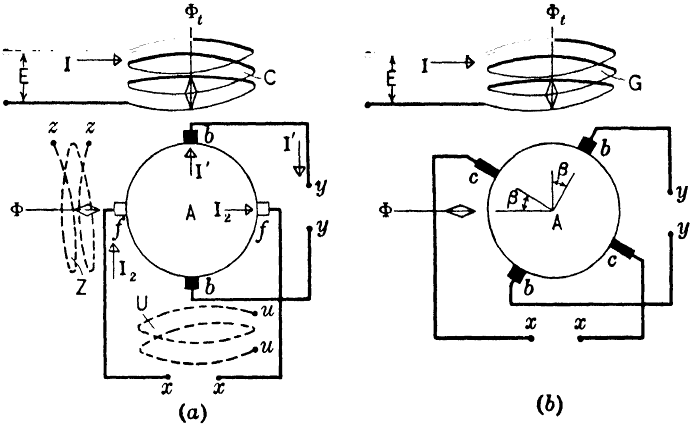

FIG. 720. Commutator-type induction motor with shunt characteristics and with the brushes (*a*) in the neutral position, (*b*) shifted.

1019. Speed Control. — As in a d-c shunt motor, the speed of the machine shown in Fig. 720(*a*) may be adjusted by varying either the armature voltage or the field flux, Φ. Some speed variation can also be obtained by shifting the brushes.

(a) *Changing the armature voltage.* In an ideal motor, the working current, I', through the *bb* brushes is in phase with the line voltage, E, and with the field flux, Φ. The same is approximately true in an actual machine. Therefore, to change the speed of the armature, a voltage in phase with E should be introduced between the terminals *yy*. Such a voltage may be readily obtained by means of an adjustable-ratio transformer whose primary is connected across the line terminals. The *xx* terminals remain short-circuited. A similar result is accomplished by inserting an adjustable resistance between the terminals *yy*, but the efficiency is thereby lowered and the motor acquires a drooping speed-torque characteristic.

(b) *Changing the field strength.* With the terminals *yy* short-circuited, the flux Φ may be changed in different ways, the easiest methods being as follows: (1) An auxiliary winding, *Z*, is placed on the stator, with its axis on the line of the brushes *ff*; its terminals, *zz*, are connected to *xx*. The number of turns in the *Z* winding is thus added to or subtracted from the rotor turns which produce the flux Φ. The number of the supplementary turns may be varied by means of taps on the *Z* coils. (2) An adjustable inductance or capacitance is connected between the terminals *xx*. With the terminals *xx* short-circuited, the emf induced between the brushes *ff* by pulsation of the flux Φ is nearly equal and opposite to that induced by rotation in the flux Φ_t. With an inductance or capacitance between the terminals *xx*, the two emf's are no longer equal. An external inductance acts as an increased leakage flux of the armature winding itself, necessitating a greater excess of the emf of rotation over that of pulsation, and also causing a reduction in the values of I_2 and Φ. Thus, an inductance increases the speed of the machine, and speeds above synchronous may be obtained. A capacitance acts in the opposite sense.

1020. Phase Compensation. — With the terminals *xx* and *yy* short-circuited, the magnetizing current for both fluxes, Φ_t and Φ, is supplied from the line (§981), causing a rather low power factor under operating conditions. To improve the power factor, the required magnetizing current must be generated within the machine itself. A reference to Figs. 283 and 677 will show that, with the secondary current i_2 leading the voltage e_2 by a considerable angle, the magnetizing current i_0 can be supplied from the secondary circuit, and the primary current i_1 may be caused to be in phase with E_1, or even lead it.

In application to Fig. 720(*a*), this means that, in order to relieve the winding *C* of the magnetizing current, the phase of the armature current through the brushes *bb* must be advanced. With the terminals *xx* and *yy* short-circuited, the voltage between the *bb* brushes, induced by rotation in the flux Φ, is equal and opposite to that induced by the transformer action of the flux Φ_t, and both emf's are approximately in phase with the line voltage *E*. It is thus necessary to introduce between the terminals *yy* an emf in leading phase quadrature with the line voltage, or thereabouts.

One way of accomplishing this result is to utilize an auxiliary winding *Z*, since the emf induced in this winding is in quadrature with the flux Φ and consequently is approximately in quadrature with the voltage induced between the brushes *bb*. By connecting the terminals *zz* to *yy*, the desired phase correction is obtained. Of course, the current flowing through *Z* somewhat modifies the original mmf acting along *ff*, but the current I_2 through the brushes *ff* adjusts itself to such a value as to give, together with the current through Z, the proper flux Φ. The relationship between the fluxes Φ and Φ_t is fixed by the short circuit at *xx*.

Another method of advancing the phase of the current I', with the terminals *yy* short-circuited, consists in advancing the phase of the flux Φ. The phase of the flux Φ_t is essentially fixed by that of the applied voltage, E. This determines the phase of the transformer emf between the brushes *bb*. When the time phase of Φ has been advanced from the true quadrature, the rotational emf induced between the brushes *bb* can no longer be balanced by the above transformer emf, and the residual voltage gives rise to a leading current.

The phase of the magnetizing current, I_2, may be advanced by inserting between the terminals *xx* a voltage substantially in leading quadrature with the rotational emf induced between the brushes *ff* by the flux Φ_t. In other words, the required voltage should be approximately in phase with the applied voltage, E. This can be accomplished in at least three different ways, viz.:

(a) By connecting the primary terminals of a transformer across the line and the secondary terminals to the terminals *xx*.

(b) By using on the stator an auxiliary winding, U, coaxial with C, and with its terminals, *uu*, connected to *xx*.

(c) By providing taps on the main stator winding, C, and connecting them to *xx*.

1021. Starting and Reversing. — The motors shown in Fig. 720 are intended for infrequent starting only, and may be temporarily converted into one of the series-type motors described in §§994 to 1011, by changing the connections. The machine shown in Fig. 720(*b*) is particularly well adapted for being converted into a plain repulsion motor, by keeping the connection *yy* short-circuited and the connection *xx* open. The *xx* connection may also be closed through a fairly high impedance, to cut down the effect of the brushes *cc*. This impedance may be so chosen as to give a sufficiently high starting torque and yet not to interfere adversely with the running conditions. It can then be left in the circuit permanently. An increased starting torque may also be obtained by temporarily changing the shift angle, β, of the brushes.

If a motor of the type shown in Fig. 720(*b*) is intended for operation in either direction, two separate field windings, F and C (Fig. 714*a*), are preferably used in place of the winding G. Reversing the terminals of the F winding in Fig. 720(*b*) is equivalent to shifting the brushes from the $+\beta$ to the $-\beta$ position, and this causes the machine to run in the opposite direction. If an auxiliary winding, such as Z or U, is present, its polarity with the reversal of rotation must be carefully considered. The direction of rotation can also be reversed by shifting the brushes.

1022. EXPERIMENT 52-F. — Study of the Single-Phase Commutator Motor of the Shunt Type with Two Sets of Brushes. — The principle of the machine and its various modifications are explained in §§1017 to 1021. The purpose of the experiment is to learn the performance characteristics of such a motor in its simplest form, and to investigate the effect of additional windings, an external reactance or resistance, brush shift, starting, reversal of the direction of rotation, etc. The limitations in commutation and means for improving it should also be studied.

1023. References

1. C. P. STEINMETZ, *Trans. Int. Elec. Congress*, 1904, Sec. F, p. 76, Theory of the single-phase motor.
2. M. M. LATOUR, *ibid.*, p. 144, A-c machines with Gramme commutators.
3. O. S. BRAGSTAD, *ibid.*, Sec. F, p. 155, Theory and method of operation of repulsion motors.
4. E. DANIELSON, *ibid.*, Sec. F, p. 174, Theory of the compensated repulsion motor.
5. FELIX KONN, *Gen. Elec. Rev.*, April, May, and June, 1932, The single-phase commutator-type traction motor.
6. L. J. HIBBARD, *Trans. A.I.E.E.*, vol. 42 (1923), p. 133, Systems of regeneration for use with series-type commutator motors.
7. V. KARAPETOFF, *Proc. Nat. Acad. of Sci.*, vol. 11 (1925), p. 683, General criterion for the circular locus of the current vector in a-c circuits and machinery.
8. S. R. BERGMAN, *Trans. A.I.E.E.*, vol. 43 (1924), p. 1039, A new type of single-phase motor.
9. VAL A. FYNN, *Trans. A.I.E.E.*, vol. 34 (1915), p. 2483, Single-phase squirrel-cage motor with large starting torque and phase compensation.
10. H. R. WEST, *Trans. A.I.E.E.*, vol. 43 (1924), p. 1048, Theory and calculation of the squirrel-cage repulsion motor.
11. B. G. LAMME, *Trans. A.I.E.E.*, vol. 27 (1908), p. 137, The single-phase commutator-type railway motor.
12. A. S. MCALLISTER, Alternating-Current Motors, McGraw-Hill Book Co.
13. BRYANT and JOHNSON, Alternating-Current Machinery, McGraw-Hill Book Co.
14. A. S. LANGSDORF, Theory of A-C Machinery, McGraw-Hill Book Co.
15. E. ARNOLD, Wechselstromtechnik, Vol. V, pt. 2, J. Springer.

CHAPTER LIII

POLYPHASE COMMUTATOR MOTORS

1024. The polyphase induction motor (Chapters XXII, and XLVII to L) is an ideal machine in its simplicity and freedom from operating troubles, but it has two inherent characteristics which, under certain conditions, may be classed as disadvantages, namely, (a) a practically constant speed with varying load, and (b) a lagging current. True, the speed may be varied by several means (§488 and Chapter L), but none of these is as simple or economical as, for example, the speed regulation of a d-c motor (§277). The power factor may be raised by means of static condensers across the primary terminals, or by using a phase advancer (§939). Both methods are expensive and have other limitations.

For these reasons, there has been a steady endeavor to develop a polyphase motor which (a) would have adjustable-speed characteristics similar to those of a d-c shunt motor, or, as another alternative, drooping characteristics of a d-c series motor; and (b) would permit of an inherent power-factor compensation. So far, all polyphase motors which satisfy at least one of these requirements in an economical way have had to be provided with a commutator and at least three sets of brushes per pair of poles. Thus, though theoretically the problem has been solved, and one could obtain a polyphase commutator motor with almost any desired speed-torque and power-factor characteristics, in practice such motors have so far found only a limited field of application, for the following reasons:

1. It is difficult to obtain satisfactory commutation at all speeds, mainly because of the transformer emf (§996).
2. The machines are more expensive than other kinds of electrical machinery of the same rating.
3. The commutator and several sets of brushes are a potential source of trouble and expense; the machines are also likely to be magnetically noisy.

Nevertheless, because of the advantages of variable speed and of unity power factor, such motors are meeting an ever-increasing demand, and their performance is being gradually improved. When a remedy against transformer emf has been found, the field of application of polyphase commutator machines should increase rapidly. For this reason, and also because of interesting electromagnetic relationships involved, a brief outline of the fundamental properties of such machines is given below. For further details the reader is referred to the works listed in §1046.

1025. Arrangement of Parts and Electrical Connections. — A three-phase commutator motor (Fig. 721) consists of a laminated stator with non-salient poles (Figs. 350 and 352), provided with the usual distributed polyphase winding (Figs. 318 and 319); the core and the winding are in all respects similar to those of an induction motor. The rotor is similar to a d-c armature (Figs. 198 and 199), and its winding is connected to a commutator. In a three-phase machine, the minimum number of sets of brushes per pair of poles is three, the studs being spaced at 120 electrical degrees. Some machines have six or more sets of brushes per pair of poles, either for purposes of speed and power-factor control, or in order to provide more phases and consequently more paths in the armature, and thus to facilitate commutation.

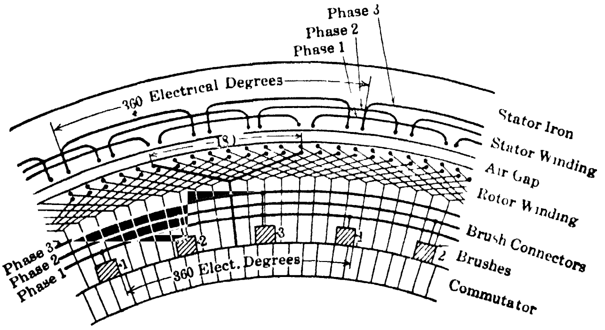

FIG. 721. Arrangement of parts in a three-phase commutator motor.

Various types of connections between the stator winding and the brushes are possible, the two fundamental kinds being series and shunt connections (Fig. 722). The corresponding performance characteristics are in general similar to those shown in Figs. 231 and 241.

The possibility of a unidirectional torque in a single-phase commutator machine is explained in §993. A similar explanation may be given for the action of a polyphase commutator machine. For example, the motor shown in Fig. 722(a) may be looked upon as a combination of three single-phase series commutator motors in a common magnetic circuit. A better explanation is on the basis of a revolving magnetic flux produced by the mmf's of both windings and forming a torque with the armature mmf. This is the principle used in the treatment below.

In view of a rather small number of commutator segments between adjacent sets of brushes, it is essential to reduce the total armature voltage as much as possible. For this reason, the armature is usually connected through a three-phase transformer (Fig. 723), which allows the use of a comparatively high voltage for the stator and a low voltage for the armature. In a series-connected machine, by saturating the transformer, the no-load speed can be reduced to a reasonable value (§1029).

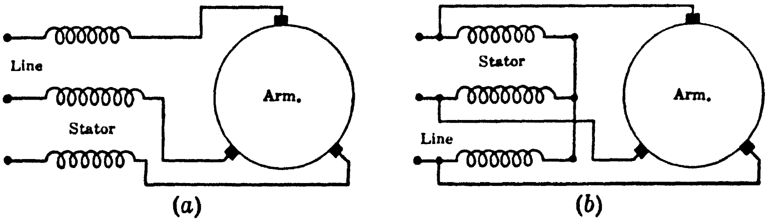

FIG. 722. Series- and shunt-connected commutator motors.

Because of the general flexibility of polyphase connections, the use of transformers, and the possibility of an unlimited brush shift with nonsalient poles, a large number of variations in the connections shown in Figs. 722 and 723 have been proposed and the corresponding motors actually built, at least for experimental purposes. With a clear understanding of the typical connections shown above and of the general theory given below, the reader should have no difficulty in analyzing such more special cases.

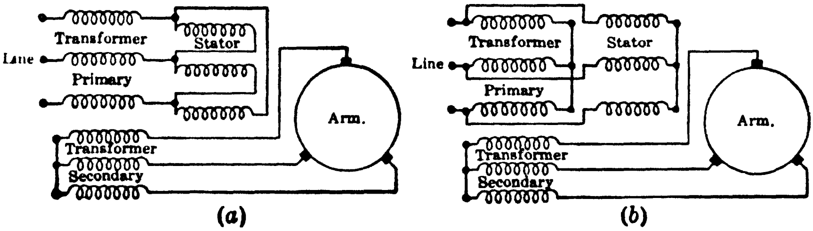

FIG. 723. The armature (a) of a series machine and (b) of a shunt machine, connected through transformers.

1026. The Diagram of MMF's. — In Fig. 721, let the phase sequence in the stator winding be such that the flux produced by three-phase currents is revolving clockwise. Let the armature be stationary, and let the armature currents be in phase with the stator currents (Fig.

722*a*).[1] Let the brushes be so placed that the armature currents produce an mmf also revolving clockwise, but in phase opposition with that of the stator. This position of the brushes we shall call the zero position.[2] The resultant mmf is equal to the algebraic sum of the two mmf's, and the air-gap flux is in phase with this resultant.

Shifting the brushes by an angle β in the direction of rotation of the field, without changing the time phase of the armature currents, will advance the rotor mmf by the same angle in space. Advancing the time phase of the armature currents by an angle θ, without brush shift, will also advance the space position of the rotor mmf by angle θ. The two changes are thus equivalent and interchangeable in their electrical effect.

Let the brushes be shifted by an electrical angle β with respect to the zero position, in the direction of rotation of the magnetic field, and at the same time let the time phase of the armature currents be advanced by an angle θ. This is equivalent to shifting the *space phase* of the secondary mmf by an angle $\beta + \theta$ with respect to its zero position. In Fig. 724(*a*), let $OA = M_1$ represent the clockwise revolving mmf of the stator, and $AB = M_2$ that of the rotor. Originally, M_2 was in opposition to M_1; now it is turned by an angle $\theta + \beta$ in the direction of rotation. The resultant mmf is $M_r = OB$, and the air-gap flux, Φ, is in phase with it. Note that Fig. 724(*a*) is a space-phase diagram.

So far, we have assumed the armature to be stationary. Now let it revolve at any desired speed. Because of a fixed position of the brushes, the groups of conductors between the adjacent sets of brushes act as if they were stationary. As the armature revolves, some coils leave the group, while others come in from the opposite side; however, the magnetic action of each group remains practically the same. The only new factor is the mmf of the coils undergoing commutation, which in a well-designed machine should not be large. Thus, *the mmf of a commutated rotor is determined by the position of the brushes and by the magnitude and phase of the currents fed through the brushes; it is independent of the speed of rotation of the conductors.* Hence, Fig. 724(*a*) holds true at any armature speed, provided that the rotor and stator mmf's remain unchanged.

---

[1] The field winding carries Y currents while the armature winding carries delta currents. Therefore, there is a time-phase displacement of 30 electrical degrees between the currents in the two windings (Fig. 555). This difference is taken into consideration in the zero position of the brushes, and in this sense the mmf's of the currents in the two windings may be said to be in space phase with each other. This interpretation should be kept in mind everywhere when one of the windings is star-connected and the other mesh-connected.

[2] Some authors understand by the zero position that position of the brushes in which the stator and rotor mmf's are in phase agreement with each other. With such a convention, the brush shift in regular operation is more than 120 degrees.

As in any electrical machine, the torque is due to interaction between the groups of armature conductors and the air-gap flux. The rotor mmf reaches its space maximum at points displaced by 90 electrical degrees from the corresponding groups of conductors (§813). Hence, to obtain a maximum torque, the rotor mmf must be in space quadrature with the resultant flux. This condition is approximately fulfilled in Fig. 724(*a*), *AB* being nearly normal to *OB*. With the resultant flux revolving in space clockwise, and the brushes shifted in the same direction, a clockwise torque is exerted upon the armature; this determines the direction of rotation of the machine operating as a motor.

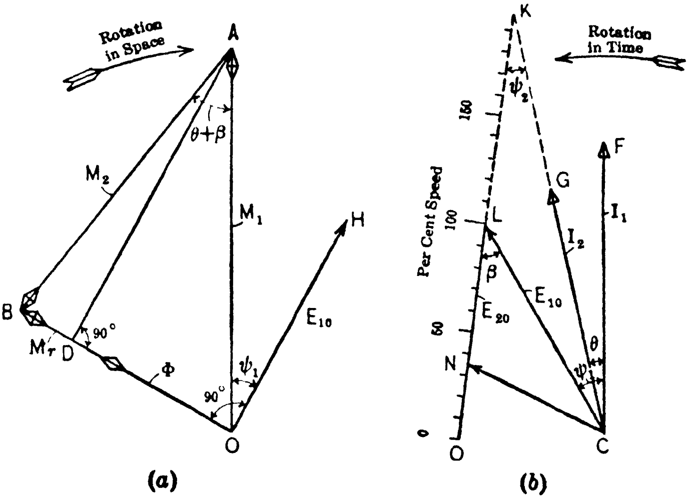

FIG. 724. The mmf's and emf's in a polyphase commutator motor.

In the preceding discussion, the sources of the stator and rotor currents have been assumed to be entirely independent of each other, except for their being strictly of the same frequency. For example, the stator may be fed from the line directly, and the rotor through an induction regulator (§954) and a step-down transformer, by means of which the magnitude and the phase of the rotor currents may be adjusted at will.

1027. The Diagram of EMF's. — With the brushes in the zero position, the emf's induced in the two windings by the common flux, Φ, are in phase opposition with each other. When the brushes are shifted by an angle β in the direction of rotation of the flux, the crest of the flux wave reaches the corresponding stationary groups of armature conductors later than in the zero position. Hence, the rotor emf is retarded with respect to the stator emf by 180° + β. This is represented graphically in Fig. 724(b). $CL = E_{10}$ is that part of the applied voltage which balances the emf induced by the flux Φ in the stator winding. With the brushes in the zero position, the corresponding part of the voltage at the brushes would be in the direction LC. Because of a brush shift, β, this latter voltage is retarded to the position LQ.

The flux, Φ, always revolves synchronously, so that the magnitude of the emf induced in the armature, with a given Φ, is a function of the armature speed. Let LQ be the armature voltage at standstill. When the armature is rotating synchronously, the induced voltage is zero. At any other speed, E_{20} is to LQ as the slip rpm to synchronous rpm. Therefore, with a given LQ, the value of E_{20} may be obtained by dividing LQ, say, into one hundred parts, beginning with Q, and taking that portion of LQ corresponding to per cent actual speed. For example, LN is the value of E_{20} at a speed equal to 35 per cent of synchronous speed.

The position of the vector of the stator current, I_1, in the time diagram may be obtained from its position in the space diagram to the left. Namely, M_1 also represents the position of the belt of stator current I_1 with respect to Φ, while E_{10} leads Φ in space by 90 degrees. Hence, the angle $AOH = \psi_1$ represents either the space angle or the time angle between the stator current and the voltage, the voltage being in this case leading. Transferring ψ_1 to the time diagram gives the vector of the stator current, $I_1 = CF$.

In order to understand clearly the relationship between the various quantities in the space diagram and in the time diagram, the reader should visualize in detail the individual phase mmf's, the positions of the windings, the revolving flux, and the corresponding simultaneous positions of the coils in which the current and the voltage reach their maxima. This may require considerable mental effort and concentration, but only in this way can he satisfy himself of the correctness of the diagrams in Fig. 724.

By assumption, the armature current I_2 leads I_1 in time by an angle θ. This gives directly the vector CG. By extending QL and CG to their intersection at K, the phase angle between the armature voltage and current is found to be equal to ψ_2. From the triangle CLK,

$$\psi_2 = \beta - (\psi_1 - \theta) \quad . \; . \; . \; . \; . \; . \; . \; . \; . \; . \quad (1)$$

Both β and ψ_2 are acute angles; remembering, however, that β is the angle of brush shift, it will be understood that the real phase angles between LQ and the vectors E_{10} and I_2 are obtuse and are supplementary to β and ψ_2.

The diagrams shown in Fig. 724 apply with any kind of connections between the stator windings and the brushes. In order to obtain the terminal voltage and thus to represent the motor characteristics, it is necessary to know the actual connections. Some such specific cases are carried out on the basis of the analytical theory developed below.

1028. Analytical Theory. — We shall assume a general case, namely, the stator connected to a source of voltage, E_1, and the rotor to a different source, E_2, through a saturated transformer. This will lead to general equations from which more specific cases of series or shunt connections, with or without the transformer (Figs. 722 and 723), can be readily derived. For the stator we may write:

$$\mathbf{E}_1 = jk_1\mathbf{\Phi} + \mathbf{I}_1Z_1 \quad . \; . \; . \; . \; . \; . \; . \; . \; . \; . \quad (2)$$

where k_1 is the factor which converts the flux into the induced emf, $-E_{10}$; Z_1 is the leakage impedance of the stator winding.[3] For the rotor circuit we may write:

$$(\mathbf{E}_2 - \mathbf{I}_2'Z_{t1})(n_{t2}/n_{t1}) = -jk_2s\mathbf{\Phi}\epsilon^{-j\beta} + \mathbf{I}_2(Z_2 + Z_{t2}) \quad . \; . \quad (3)$$

Here $\mathbf{I}_2$ is the current in the leads to the brushes, $\mathbf{I}_2'$ is the corresponding current in the transformer primary, Z_{t1} and Z_{t2} are the leakage impedances of the two transformer windings, and Z_2 is the leakage impedance of the armature winding, all the quantities being consistently understood per phase of star or mesh (Chapter XXXIX). The factor (n_{t2}/n_{t1}) represents the ratio of the numbers of turns in the transformer windings and changes the primary transformer voltage into the secondary. The factor k_2 changes the flux Φ into the induced emf in the armature at standstill; s is the slip expressed as a fraction. Just as the proper phase of the stator voltage, E_{10}, has been obtained by multiplying the flux Φ by j, so here Φ is multiplied by $-j$ for the zero position of the brushes. This emf is further retarded by the angle β of brush shift.

The mmf triangle (Fig. 724a) is expressed analytically by the equation:

$$\mathbf{I}_1N_1 - \mathbf{I}_2N_2\epsilon^{j\beta} = \mathbf{\Phi}/\mathcal{P} \quad . \; . \; . \; . \; . \; . \; . \; . \; . \quad (4)$$

Here N_1 and N_2 are the effective numbers of turns per pole in the stator and in the armature, and $\mathcal{P}$ is the corresponding permeance of the useful flux, Φ; $\mathcal{P}$ may be a complex quantity (§987). The angle θ is omitted in the exponent because of the vector $\mathbf{I}_2$. The minus sign before $\mathbf{I}_2$ is due to the fact that in the zero position of the brushes ($\beta = 0$), and, with $\mathbf{I}_1$ in time phase with $\mathbf{I}_2$, the resultant flux is due to the difference and not to the sum of the two mmf's.

---

[3] Because of the form of the right-hand side of eq. (4) below, the effective value (and not the amplitude) of the flux is understood, so that the usual expression for k_1 should be multiplied by $\sqrt{2}$. Or else the right-hand side of eq. (4) should be divided by $\sqrt{2}$, if Φ is the amplitude of the flux.

The conditions in the magnetic circuit of the transformer may be expressed as

$$\mathbf{I}_2'n_{t1} + \mathbf{I}_2n_{t2} = \mathbf{\Phi}_t/\mathcal{P}_t \qquad \ldots\ldots \quad (5)$$

where n_{t1} and n_{t2} are the numbers of turns in the transformer windings, and Φ_t and $\mathcal{P}_t$ are the transformer flux and the permeance of its useful path, respectively. With saturation, $\mathcal{P}_t$ is a function of Φ_t. To take the core loss into consideration, $\mathcal{P}_t$ is considered to be a complex quantity. The relationship between the transformer flux and the primary voltage applied to the transformer is expressed by the familiar emf formula:

$$\mathbf{E}_2 - \mathbf{I}_2'Z_{t1} = j2\pi fn_{t1}\mathbf{\Phi}_t\, 10^{-p} \qquad . \quad . \quad (6)$$

where f is the primary frequency and p is an integer which depends upon the units used.

Equations (2) to (6) represent all the electromagnetic relationships which may be written for the quantities involved. The procedure in the solution of these equations depends upon the problem at hand and upon the actual connections in the machine under consideration, as is shown for two typical cases below.

1029. The Series-Connected Motor.—This type of machine is shown in Figs. 722(*a*) and 723(*a*), and is used to some extent for drives, such as industrial fans and pumps, in which series characteristics are not objectionable. Suitable speed-torque characteristics can be obtained by a proper setting of the brushes. Brushes may be shifted by hand or automatically, for starting and for speed control. The zero position of the brushes corresponds to the greatest inrush of current at start, because the mutual flux is practically wiped out. Therefore, when starting for the first time, the brushes should be shifted in the direction of rotation by 180 electrical degrees, so as to have the greatest possible flux. In this position the current is a minimum and the torque is zero. After the main switch has been closed, the brushes are shifted back until the motor starts. This position is marked and used later in starting. For speed control, the brushes may be shifted farther back. Within certain limits, the nearer the brushes are to the zero position the higher will be the speed for the same torque.

For drives in which the load torque decreases rapidly with the speed (for example, in a blower), the position of the brushes at low speeds is such that the power factor and the efficiency are rather low. The performance may be improved by using a lower terminal voltage. One way of accomplishing this result is to operate the stator delta-connected at higher speeds and to change to the Y connection for lower speeds.

At synchronism, the voltage induced in the armature is zero; beyond synchronism, it is reversed in phase. Above synchronism, the power factor of the machine reaches values near unity. This may be seen from Fig. 724(*b*). Neglecting the leakage impedance drop, the applied voltage is equal to the sum of E_{10} and E_{20}. At a low speed, we have $CL + LN = CN$, and the current I_1 lags the applied voltage by the angle FCN. At a high speed, $CL + LK = CK$, and the phase angle, FCK, is much smaller.

The fact that beyond synchronism the armature voltage begins to increase again is used to limit the no-load speed of the machine. To this end, the transformer core is so designed as to become saturated at a comparatively low applied voltage. With the secondary voltage of the transformer so limited, and with the primary transformer ampere-turns greatly exceeding the secondary, the motor speed at no load is limited to a reasonable figure. A comparatively large primary current keeps up the useful flux of the machine and also causes an additional voltage drop in the primary circuit, which drop further limits the voltage at the transformer terminals.

At low speeds, the transformer also becomes saturated, and, as a result, a given torque is obtained with a smaller flux and a higher current than without saturation. This is of advantage in starting, as it reduces sparking at the brushes due to the transformer emf (§996).[4]

The equations given in §1028 can be applied to this case by supplementing them with the following conditions:

$$\mathbf{E} = \mathbf{E}_1 + \mathbf{E}_2 \qquad . \quad . \quad . \quad . \quad (7)$$

$$\mathbf{I}_2' = \mathbf{I}_1 \quad . \quad . \quad . \qquad . \quad . \quad . \quad . \quad . \quad (8)$$

Equation (7) states that the primary of the transformer is connected in series with the stator circuit, across the line voltage E. Equation (8) expresses the fact that the same current flows through the transformer primary and through the stator winding.

1030. EXPERIMENT 53-A.—Study of a Polyphase Series Commutator Motor.—The machine is described in the preceding section; for the general theory of polyphase commutator machines, see §§1024 to 1028. The experiment may be divided into the following parts: (1) a study of the starting current and torque with different positions of the brushes; (2) performance curves (Figs. 231 and 366) with a fixed position of the brushes; (3) speed characteristics with a constant torque and different brush settings; (4) influence of the saturation in the transformer core upon the characteristics at low speed and at high speed; (5) quality of commutation under different operating conditions; (6) measurement of the actual stator and rotor mmf's and of the resultant flux at standstill (Fig. 724*a*); (7) representation of the currents and the voltages at a certain speed in the form of a vector diagram (Fig. 724*b*). After this elementary study, a more advanced investigation may be attempted on the basis of the equations given in §1028; the sources of information quoted in §§1029 and 1046 will be found useful for this purpose. The ultimate aim should be to check the observed performance characteristics with those predicted from the constants of the machine. Some simple tests should be developed from which these constants could be computed.

---

[4] For further information on series polyphase commutator motors see W. C. K. Altes, *Gen Elec. Rev*, vol. 19 (1916), pp. 115 and 199; R. A. Jones, *ibid.*, vol 24 (1921), p. 921; V. Karapetoff, *Proc. A I E.E.*, vol. 37 (1918), p. 65.

1031. The Shunt-Connected Motor. — This motor is shown in Figs. 722(*b*) and 723(*b*). Since the stator is connected across a source of constant voltage, the total flux linked with it is also approximately constant, that is, independent of the motor speed or load. With moderate leakage, the useful flux is also nearly constant. Hence, the armature, being also connected to a source of constant voltage, runs at a nearly constant speed. In other words, the machine exhibits the so-called shunt characteristics, its speed being nearly independent of the load. An ordinary induction motor has similar characteristics, so that the complication of a commutator would not be warranted if it were not for the fact that speed control or power-factor correction, or both, are possible because of the commutator.

Speed control may be obtained as in a d-c shunt motor, by varying either the field strength (i.e., the voltage across the stator winding) or the armature voltage. Various means for either method of regulation are possible, one being by the use of transformers with numerous taps to change the impressed voltage. Such tap-changing transformers are becoming more and more common. In place of transformers with taps, induction regulators (§1042) may be used. Another method is to connect the field winding to an extra set of brushes, and to regulate the field current by shifting the brushes on the commutator. The power factor may also be raised by suitably shifting the brushes. We shall go into further details of this question in connection with the Crocker-Wheeler shunt motor (§1042) and the Schrage motor (§1033) both of which are compensated induction motors. Those further interested will find considerable information in the books by Arnold and Schenkel (§1046).[5]

In order to apply the equations deduced in §1028 to the motor shown in Fig. 723(*b*), it is only necessary to put

$$\mathbf{E}_1 = \mathbf{E}_2 = \mathbf{E} \quad . \; . \; . \; . \quad . \; . \; . \; . \; . \quad (9)$$

where **E** is the line voltage.

1032. — EXPERIMENT 53-B. — Study of a Polyphase Shunt-Connected Motor. — See §§1030 and 1031.

THE SCHRAGE MACHINE

1033. It is shown in §§928 and 929 that by adding a suitable external emf in series with the secondary circuit of a polyphase induction motor, its speed may be adjusted to a desired value either above or below synchronism, without power loss in resistances. It is also shown in §§933 and 934 that a similar external emf (of a different phase with respect to the current) may be used to supply all or part of the magnetizing current of the machine at the slip frequency, thus causing it to operate at unity power factor or even with a leading current.

In Chapter L, only external secondary emf's, furnished by means of separate auxiliary machines, are considered. Such sources are preferable with large low-speed motors, but with a small high-speed machine an auxiliary emf may be more economically produced in the machine itself, by providing it with an additional commutated winding. A machine of this type, invented by K. H. Schrage of Sweden, has found a considerable field of application in small and medium sizes, where shunt characteristics and adjustable speed are required.

1034. Arrangement of the Windings and Effect of Brush Shift. — The Schrage motor belongs to the class of adjustable-speed compensated polyphase induction motors, and is shown diagrammatically in Fig. 725. The stator core, S, and the stator winding, $S_1S_2S_3$, resemble those of an ordinary induction motor, except that the phases are not connected either in Y or in delta, but the ends of each winding are connected to two sets of brushes resting on the commutator, C. The stator winding takes the place of the secondary winding of an ordinary induction motor, *the functions of the stator and the rotor being interchanged.* In larger sizes of motors, with three-phase power supply for the primary, it is frequently desirable to use a different and larger number of phases in the secondary, and a corresponding spacing of the brushes on the commutator. This is possible since there is no electrical connection between the primary and the secondary. Better commutation and better operating characteristics are thereby obtained.

---

[5] See also W. C. K. Altes, *Gen. Elec. Rev.*, vol. 21 (1918), p. 317.

The rotor core, *R*, is similar to that of a d-c armature and carries two windings: a three-phase primary winding, *P*, connected to the source of power through the collector rings, *N*, and a d-c-type winding, *A*, connected to the commutator, *C*. The commutated winding is known as the regulating or adjusting winding because its purpose is to adjust the speed and the power factor of the machine. It is placed nearest the air-gap to obtain the benefit of lower inductance and thereby give better commutation.

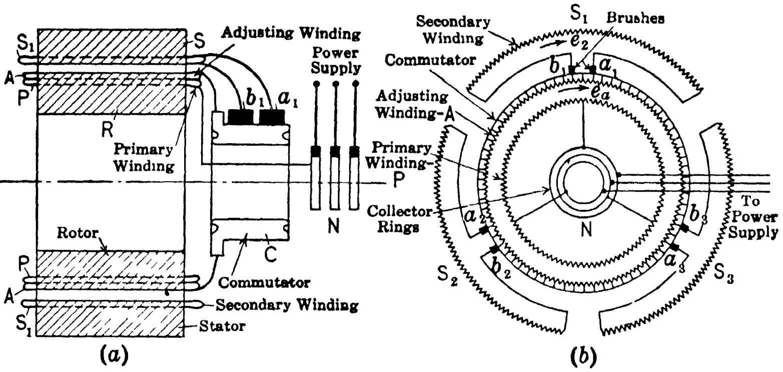

FIG. 725. The Schrage machine.

The function of the commutator and the brushes is to provide an additional emf, e_3 (Figs. 671 and 677), in series with the secondary winding, and in this way to regulate the speed or the power factor of the machine. Spreading two sets of brushes, such as a_1 and b_1, farther apart, increases the magnitude of e_3; crossing them changes the sign of e_3. Shifting both sets of brushes in the same direction changes the phase of e_3. Thus, for a complete regulation of both speed and power factor, the brushes a_1, a_2, a_3 should be fastened to one yoke, and the remaining brushes, b_1, b_2, b_3, to another yoke, both yokes to be shifted independently, either by hand or automatically.

In practice, with a varying load, an operator would hardly be able to regulate the speed and also to adjust the power factor continually. Therefore, both brush yokes are usually so geared to a control shaft as to move simultaneously in the opposite directions (preferably by a different amount). For manual operation, the shaft is provided with a hand wheel, and for automatic or distant control it is driven by a small pilot motor. In this manner, speed regulation is provided for.

The setting of the brushes is so chosen as to give a high power factor at an important speed and load. At other speeds and loads, the power factor then varies considerably. Of course, the brush control could be supplemented, if so desired, by an automatic device which would shift both yokes in the same direction, so as to keep the power factor at a high value over a wider range of load conditions.

1035. The Magnitude and Phase of the Commutator EMF Impressed upon the Stator Winding at No Load. — Let the brushes a_1 and b_1 be so shifted as to bear on the same commutator segment. Let the same be true of a_2 and b_2, and of a_3 and b_3. Each stator phase is then individually short-circuited, the commutated winding furnishes no current, and the machine is converted into a plain induction motor. Let the machine be running at no load. Since the rotor is used as the primary, the direction of rotation will be such that the air-gap flux (which revolves synchronously with respect to the rotor conductors) is almost stationary in space. This will give a small slip, s_0, relative to the stator winding, as it should be in an induction motor running at no load. To make the conditions definite, let the rotor revolve clockwise, looking from the commutator side; the flux then revolves counterclockwise with respect to the rotor conductors. Since the flux revolves synchronously with respect to the rotor, while the rotor itself has a small slip, s_0 (because of the losses), the flux revolves in space at a low speed, s_0, counterclockwise relative to the stator.

Now let the brushes be shifted apart by a certain angle and, as a result, let the rotor slow down somewhat and run at a no-load slip, s, greater than s_0. The frequency of the emf induced between the brushes is determined entirely by the velocity of rotation of the air-gap flux with respect to the brushes (§936). The flux now rotates in space at a velocity s, counterclockwise, and the frequency of the emf between the brushes is the same fraction, s, of the line frequency. But this is also the frequency of the secondary emf induced in the stator winding, as in any induction motor. Consequently, the two emf's can be properly combined into one of the same frequency, and the resulting stator current, together with the air-gap flux, will produce the torque necessary for overcoming the losses. The rotor, therefore, will slow down to a speed at which the geometric sum of the emf's induced in the stator winding and between the brushes gives rise to a current just sufficient for overcoming the losses at that speed.

This balance of the two emf's takes place at a definite speed only, because, with a constant supply voltage at the slip-rings, the air-gap flux is nearly constant under all load and speed conditions within the rating of the machine, as in an induction motor. Hence, the magnitude of the voltage induced by this flux per conductor of the commutated winding is also constant, and independent of the rotor speed, because the flux always revolves synchronously with respect to the rotor conductors. The commutator and the brushes merely change the frequency, but not the magnitude of this voltage. However, setting the brushes a certain distance apart determines the magnitude of the external emf, e_3, applied to the stator winding. The rotor slows down to a speed at which the flux revolves rapidly enough counterclockwise to induce in the stator conductors an emf slightly higher than e_3.

Let the brushes a_1 and b_1 be brought again on the same commutator segment and then shifted past each other in the opposite directions. This will reverse the phase of the emf applied to the stator winding, causing large currents which will accelerate the rotor past synchronism. An equilibrium is reached at a supersynchronous speed, because the flux then rotates clockwise relative to the stator winding, and the phase of the emf induced in it is also reversed. The commutator voltage now exceeds the emf induced in the stator winding. Thus, the machine can operate as a motor either below or above synchronism.

Let the machine be operating at no load and at a *supersynchronous speed*, as described above, and let all the brushes be shifted by an angle *clockwise*, that is, *in the direction of rotation*. Assume the machine to be kept rotating after the brush shift at the same speed as before, by some external means. The magnitude of the emf induced in the group of the rotor conductors determined by the brushes a_1 and b_1 remains the same as before, because the main flux is constant and it revolves synchronously (counterclockwise) with respect to the rotor conductors. However, in the new position of the brushes, the flux reaches the corresponding conductors earlier, so that the phase of the induced emf is advanced.

At speeds above synchronous, the emf induced in the adjusting winding is higher than that induced in the stator, and determines the secondary current. Hence, if previously this emf was of the right phase for speed control, and did not effect any phase compensation, the new adjusting emf will cause the phase of the secondary current to be advanced, thus partly relieving the primary source of supply of its magnetizing current. The machine becomes partly self-exciting and operates at a higher power factor. The speed of the machine is also affected, being brought nearer synchronous, because the total emf, e_3, is the same as before, but the component of it that modifies the speed is smaller.

At speeds below synchronous, the stator emf is higher than that induced in the adjusting winding. Hence, retarding the latter emf causes the vector of the difference between the two (the net emf) to be advanced in phase. Since the secondary current lags behind this net emf by a definite angle, the current phase is also advanced. This causes the phase of the line current also to advance, as will be seen from the transformer diagram (Fig. 283). Thus, for phase compensation below synchronism, the brushes should be shifted *counterclockwise*, that is, *against the direction of rotation.*

1036. Operating Characteristics. — For the sake of simplicity, we have so far assumed the motor to be running at no load. Let it now be overcoming a certain constant applied torque, and therefore carrying heavier currents. The leakage impedance drop in the three windings is then greater, the main flux and the commutator voltage are also affected by changes in the currents, and the explanation given above should be supplemented by taking the effect of the impedance drops into consideration. However, as long as the load does not greatly exceed the rating of the machine, the main flux is reduced by only a few per cent, and the impedance drop does not exceed a moderate percentage of the applied voltage. Hence, the relationships explained at no load hold true approximately under various load conditions. In fact, with a constant brush setting, the drop in speed between no load and full load is only a few per cent.

Usually, a speed range of 3 to 1 is provided, by enabling the machine to run up to 50 per cent above synchronous speed and the same amount below it. Since the commutated winding carries only the " slip energy," its rating can be made smaller than that of either the primary or the secondary winding. Thus, in the foregoing example, the maximum slip is 50 per cent and the regulating winding needs to have only one-half the capacity of either of the other two windings.

The direction of rotation may be reversed by interchanging two line leads, as in a plain induction motor. However, only with a setting of the brushes symmetrical with respect to the stator winding will the operating characteristics be identical with either direction of rotation. Usually, the brushes are shifted to one side for power-factor correction. Consequently, the reverse operation should be permitted only for short periods, since the torque, the power factor, the efficiency, and the heating characteristics will be inferior. When a motor is intended for operation in both directions, either the brushes must be set symmetrically, or an additional provision must be made for shifting them properly every time the direction of rotation of the machine is reversed.

When driven by a prime mover at a speed above the no-load speed corresponding to a given setting of the brushes, the Schrage motor becomes a generator (§899) and returns power to the line.

A comparison of the Schrage motor with the straight shunt-connected commutator motor (§1031) shows that the former possesses an advantage in that the commutated winding is used for the slip energy only. Moreover, the currents collected by the brushes are of slip frequency and not of the full line frequency. The machine is primarily an induction motor and could be operated as such should anything go wrong with the regulating winding or the commutator. In other words, the difficulties in commutation and the size of the commutator are reduced by utilizing the machine as much as possible in the form of an induction motor.

1037. The Starting Torque and Current. — With the brushes in the low-speed position, the motor may be thrown directly on the line, because of a high counter emf, e_3, in the secondary circuit. Under these conditions, a starting torque of nearly twice the full-load torque may be obtained with less than twice the rated current. With the brushes in the high-speed position, the starting torque is considerably lower, and the line current is excessive. The machine should therefore be started with the brushes in the low-speed position. On the other hand, with the brushes in the high-speed position, the pull-out torque is considerably higher than in the low-speed position.

In special applications, starting resistances are used in the secondary, as with a plain induction motor. The stator phases being entirely independent of each other, separate (not interconnected) resistances should be employed. With such resistances, it is not necessary to bring the brushes into the low-speed position for starting. Within narrow limits, auxiliary resistances may be used for speed control below the minimum running speed; also for " creeping speed " in preliminary adjustment of the driven machine, etc.

The Schrage motor is only one of several types of so-called compensated polyphase induction motors, that is, motors in which the necessary magnetizing current is generated in the machine itself and which, therefore, can be operated at unity power factor or thereabout. Such machines require a commutator and brushes, and whether phase compensation pays or not is a question to be decided in each particular case.[6]

1038. The Vector Diagram of MMF's. — The mmf and emf relationships in the Schrage motor, at a speed below synchronous, are shown[7] combined graphically in Fig. 726. The armature is assumed to be revolving clockwise, and the same positive direction of rotation is assumed in the space diagram. For the time diagram (shown in heavier lines), the usual counterclockwise rotation is used. Φ is the useful air-gap flux of the machine, and $I_m n_1$, in phase with it, is the mmf necessary for producing it, n_1 being the effective number of turns in the primary winding and I_m the magnetizing current.

---

[6] For a review of various types of such motors and their characteristics, see Dr. Kade, *Elek. Zeits.*, vol. 45 (1924), p. 456.

[7] H. K. Schrage, *Elek. Zeits.*, vol. 35 (1914), p. 90.

All three windings participate in producing the resultant mmf, $I_m n_1$, namely, the primary winding, with its current, I_1; the stator winding, with the current I_2 and the number of turns n_2; and the adjusting winding whose effective number of turns, n_a, depends upon the spread of the brushes. The current I_2 in the adjusting winding is the same as in the stator winding, but because of the physical connections between the two windings their mmf's (below synchronism and with a symmetrical position of the brushes) are in direct opposition. This is shown in Fig. 725(*b*) by the arrowheads of e_2 and e_a. The mmf of the adjusting winding, $SV = -I_2 n_a$, is indicated in Fig. 726 in phase opposition with $OS = I_2 n_2$. When the brushes are shifted by an angle β against the direction of rotation, to improve the power factor, the space phase of the mmf $I_2 n_a$ is also retarded by the same angle. The actual mmf of the adjusting winding is therefore represented by the vector SC_2. It will be seen that, geometrically,

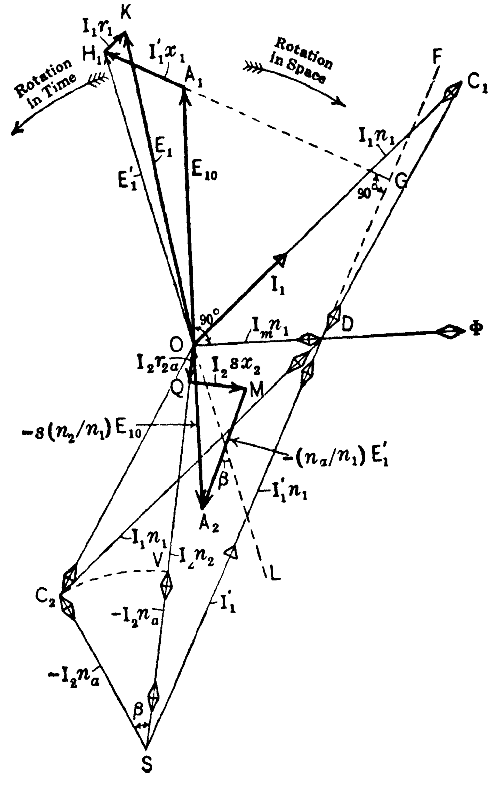

FIG. 726. Vector relationships in the Schrage machine at a speed below synchronism.

$$OD = OS + SC_2 + C_2 D \quad . \quad . \quad . \quad . \quad . \quad . \quad . \quad . \quad (10)$$

In other words, $I_m n_1$ is a geometric sum of the mmf's $I_2 n_2$, $-I_2 n_a$, and $I_1 n_1$.

The combined mmf of the two rotor windings is $SC_2 + C_2 D = SD$, and this mmf may be thought of as due to a fictitious rotor current,

I_1', acting in the primary winding with the number of turns equal to n_1. The current I_1' determines the primary leakage reactance drop, as will be seen below.

1039. The Vector Diagram of EMF's. — The second Kirchhoff law must be satisfied separately for the primary and the secondary circuits. Let $OA_1 = E_{10}$ be a voltage equal and opposite to that induced in the primary winding by the useful flux, Φ; E_{10} leads Φ in time by 90 degrees. The adjusting winding being placed in the same slots with the primary winding, a common leakage flux is produced by the two. Therefore, the leakage reactance is due to the fictitious current I_1', mentioned in the preceding section. The vector of the voltage necessary for overcoming this reactive emf is $A_1H_1 = I_1'x_1$, where x_1 is the primary leakage reactance; A_1H_1 leads I_1' by 90 degrees in time phase. The ohmic drop, $H_1K = I_1r_1$, is in phase with I_1, and the current in the adjusting winding has nothing to do with it, as far as the primary circuit is concerned. The geometric sum of E_{10}, $I_1'x$, and I_1r_1 is equal to the applied voltage $E_1 = OK$.

In the secondary circuit, we have to consider the emf's induced in both the stator winding and the adjusting winding. As in an ordinary induction motor, if an emf $A_1O = -E_{10}$ is induced by the air-gap flux in the primary winding, that induced in the secondary winding, at a slip s, is $OA_2 = -s(n_2/n_1)E_{10}$.

The total emf induced in the adjusting winding consists of two parts, induced by the useful flux and by the leakage flux, respectively. Because the adjusting winding is placed in the same slots with the primary winding, its own leakage flux may be neglected in comparison with that due to the combined action of the two. The total emf induced in the primary winding is equal and opposite to the sum of $OA_1 + A_1H_1 = OH_1 = E_1'$. Consequently, the corresponding emf induced in the adjusting winding is $-(n_a/n_1)E_1' = MA_2$. This vector is shown lagging behind the direction H_1O by the angle β of brush shift, because the revolving flux reaches the corresponding groups of conductors later than if they were located symmetrically with respect to the secondary winding.

While the instantaneous emf's induced by the common flux in the stator winding and in the adjusting winding are in the same direction (arrowheads of e_2 and e_a in Fig. 725), the electrical connections are such that the two emf's are in opposition with each other. This is indicated by the arrowheads in the figure $OQMA_2$, where the secondary induced voltage, OA_2, is shown to balance the sum of the secondary impedance drop OQM and the emf, MA_2, induced in the adjusting winding.

The secondary impedance drop consists of the ohmic drop I_2r_{2a} and of the reactive drop sI_2x_2. The resistance r_{2a} comprises those of the stator winding, adjusting winding, and the brushes. The reactance x_2 is that of the stator winding only (at the line frequency), the leakage reactance drop in the adjusting winding having already been taken into consideration in the vector MA_2.

The time diagram, $OQMA_2$, is drawn for speeds below synchronous. Above synchronous speed, the direction of the stator emf is reversed since the flux then revolves in space clockwise. The direction of the emf induced in the adjusting winding, between the brushes, is also reversed, because of the interchange in the position of the brushes. However, the phase of the current I_2 is not reversed, because the machine continues to operate as a motor. These conditions are fulfilled graphically by placing the point A_2 above O. The emf induced in the adjusting winding is then higher than that in the stator winding and is used partly to balance the latter and partly to overcome the impedance drop. For power-factor correction, the brushes must be shifted in the direction of rotation of the armature.

1040. Analytical Theory and the Circle Diagram.—The relationships shown in Fig. 726 may be expressed analytically by the following five equations:

$$\mathbf{I}_m n_1 = \mathbf{I}_2 n_2 - \mathbf{I}_2 n_a \epsilon^{-j\beta} + \mathbf{I}_1 n_1 \quad \ldots \ldots \ldots \quad (11)$$

$$\mathbf{I}_1' n_1 = -\mathbf{I}_2 n_a \epsilon^{-j\beta} + \mathbf{I}_1 n_1 \quad \ldots \ldots \ldots \quad (12)$$

$$\mathbf{\Phi} = \mathbf{I}_m n_1 \mathcal{P} \quad \ldots \ldots \ldots \quad (13)$$

$$\mathbf{E}_1 = jk_1\mathbf{\Phi} + \mathbf{I}_1' x_1 + \mathbf{I}_1 r_1 \quad \ldots \ldots \ldots \quad (14)$$

$$-sjk_2\mathbf{\Phi} = \mathbf{I}_2(r_{2a} + jsx_2) - (n_a/n_1)(\mathbf{E}_1 - \mathbf{I}_1 r_1)\epsilon^{-j\beta} \quad \ldots \quad (15)$$

Equation (11) is the same as eq. (10); eq. (12) expresses the triangle SC_2D. In eq. (13), $\mathcal{P}$ is the permeance of the useful path; if I_m is an effective value, then Φ is also the effective value (and not the amplitude) of the flux. Equation (14) represents the polygon OA_1H_1KO, and the term $jk_1\mathbf{\Phi} = \mathbf{E}_{10}$. Here k_1 is the factor which converts a flux into an emf induced by it in the primary winding; since $\mathbf{\Phi}$ is an effective value, an additional factor $\sqrt{2}$ must be introduced into the usual expression for k_1. Equation (15) corresponds to the polygon $OQMA_2O$, and k_2 is a factor for the secondary winding similar to k_1 for the primary winding.

Depending upon the problem on hand, the foregoing five equations may be solved for a desired quantity, the others having been eliminated. No general rule can be given; the equations are linear with respect to the vectors, so that an elimination of a desired vector should present no difficulty. The resistance r_1 may often be neglected and the relationships somewhat simplified.

In order to obtain the defining vectors of the circular locus of the primary current (§918), the vectors $\mathbf{I}_2$, $\mathbf{I}_1'$, $\mathbf{I}_m$, $\mathbf{\Phi}$, are eliminated, leaving a single equation between $\mathbf{I}_1$ and the slip, s. In this equation, the terms with s may be separated and s eliminated by taking a scalar product. The operations are the same as in §990, and therefore are not given here in detail. The resulting equation will be found to represent a circle.[8]

1041. EXPERIMENT 53-C. — Study of the Schrage Machine. — The machine is described in §§1033 to 1040. For a general program of study, see §1030.

THE CROCKER-WHEELER ADJUSTABLE-SPEED INDUCTION MOTOR

1042. In a manner analogous to the use of three windings in the Schrage motor (§1034) the Crocker-Wheeler Company[9] builds a three-phase commutator-type induction motor in which speed is adjusted, both above and below synchronism, by applying various values of a-c voltage to the brushes which lead to the rotor windings. The stator of this motor is identical with that of the usual three-phase induction motor (Chapter XXII), and is connected to the three-phase power source. The rotor is similar to the armature of a d-c machine, except that there are three brush arms per pair of poles. If these brushes are short-circuited the motor operates like any wound-rotor induction motor with rotor short-circuited, i.e., like a squirrel-cage motor. However, for speed adjustment there is added a control device in the form of two single-phase induction regulators (§950), V-connected, and with the primary windings connected to the power lines. The secondary terminals connect to the brushes of the motor. The rotor windings are mounted on a common shaft and are turned with respect

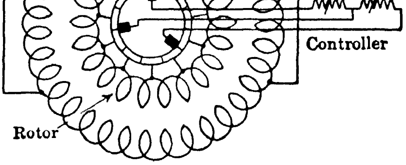

FIG. 727. Schematic diagram of the Crocker-Wheeler motor.

---

[8] For the circle diagram of the Schrage motor, see *A.E.G. Mitteilungen*, 1924, p. 232.

[9] H. M. Edmunds, "Adjusted-Speed A-C Motors," a paper presented before the Middle Eastern District meeting of the A.I.E.E., October, 1939.

to the stator windings by means of a worm gear and hand wheel. Figure 727 is a schematic diagram of the motor and control circuits.

1043. Operating Characteristics. — By means of the control device any desired voltage may be applied to the brushes of the motor. When this emf adds to the emf induced in the rotor of the motor its speed is raised. When this emf opposes that of the rotor the motor slows down. For any given setting of the controller the motor has a speed-torque curve similar to that of a d-c shunt motor with fixed field excitation, as shown in Fig. 728, where several such operating characteristics are given for a 3-horsepower, 1200 (synchronous) rpm motor. Theoretically there is no limit to the number of such curves obtainable on a given motor, since the control voltage may be varied by infinitesimal steps. Practically, however, the motor and control are designed for a motor speed range, at normal load, from $\frac{1}{2}$ synchronous speed to $1\frac{1}{2}$ synchronous speed (3 to 1 ratio), the upper limit being imposed by considerations of cost and safety, the lower limit by heating and the slope of the speed-load curve. Figure 729 gives speed, power factor, and efficiency vs. output curves for a $7\frac{1}{2}$-horsepower motor. It is to be noted that the power factor is more nearly constant over a wide range of load than it is with the ordinary induction motor. Power factor may be controlled to a considerable extent by shifting the brushes, this having the effect of shifting the phase relation between the regulating voltage and the controller-induced emf. Direction of rotation of the motor is reversed by interchanging any two leads of the stator, as in any three-phase motor. Normally the brushes are set to an average "best" position for one direction of rotation. For reversed rotation the brushes should be set to a new position. For frequent reversals the brushes are left in an intermediate position.

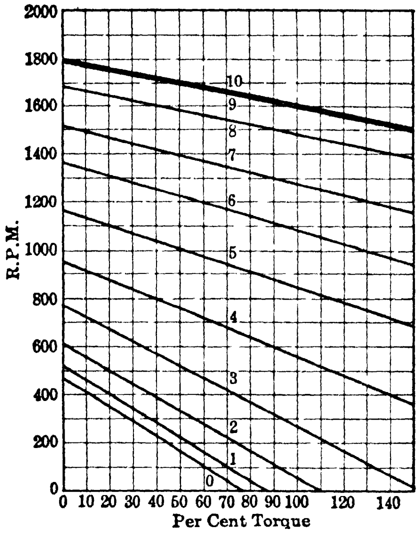

Fig. 728. Curves, speed versus torque, in a 3-hp, 60-cycle Crocker-Wheeler motor.

1044. Rotor Induced EMF. — The presence of a commutator and brushes, instead of the usual slip-rings and fixed taps to the rotor windings, requires that the value and the frequency of emf induced between brushes be considered in some detail. Although it was of advantage in dealing with the single-phase induction motor (Chapter LI) to resolve the pulsating magnetic field of the motor into two oppositely rotating components, it seems to be desirable here to consider the rotating field of the polyphase motor to be resolved into two equal pulsating components, of supply frequency, displaced 90 degrees in both space and time phase. Consider the rotating flux of value ϕ resolved into the pulsating components ϕ_a, symmetrical about a line midway between the brushes; and the component ϕ_b at 90 degrees from ϕ_a. The maximum values of these component fluxes are identical and equal to ϕ.

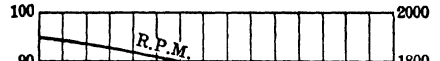

FIG. 729. Performance curves of a 7½-hp Crocker-Wheeler motor.

(a) *Emf induced by the motion of conductors through* ϕ_a. Referring to Fig. 730(a), let B_a equal the instantaneous maximum flux density along the axis of ϕ_a. This value varies between $+B_m$ and $-B_m$ and may be written $B_a = B_m \sin \omega t$. At a point in the air-gap the angle x from the axis of ϕ_a the flux density is

$$B_x = B_m \sin \omega t \cos x \quad . . . . (16)$$

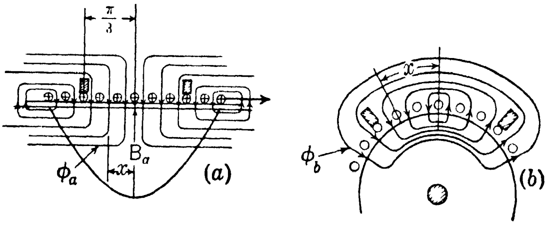

FIG. 730. A study of emf's induced in the rotor of the Crocker-Wheeler motor.

The instantaneous emf induced in a conductor of length l, and moving at a velocity v, through B_x, is

$$e_x = Blv\, 10^{-8} = B_m \sin \omega t \cos xlv\, 10^{-8} \quad . . . . . (17)$$

The average emf per conductor, from brush 1 to brush 2, is

$$e_{av} = (3/\pi)\int_{x=0}^{x=\pi/3} B_m l v \sin \omega t \cos x \, dx$$

$$= 0.826 B_m l v \sin \omega t \, 10^{-8} \quad . \; . \; . \; . \; . \; . \; . \; . \; . \; . \; . \; . \quad (18)$$

The instantaneous emf per phase (between brushes) with T_2 turns is

$$e/\text{phase} = 2T_2 \times 0.826 B_m l v \sin \omega t \, 10^{-8} \text{ volt} \quad . \; . \; . \quad (19)$$

Note that this emf is of supply frequency. The effective emf per phase is

$$E = 2T_2 \times 0.826 \times 0.707 B_m l v \, 10^{-8} \; . \; . \; . \; . \; . \; . \quad (20)$$

$$= 1.17 T_2 B_m l v \, 10^{-8} \quad . \; . \; . \; . \; . \; . \; . \; . \; . \; . \; . \; . \quad (20a)$$

For a machine of diameter D, of synchronous speed N_s, and running at a slip s,

$$B_m l v = B_m l \pi D N_s (1 - s)/60 = (\pi/2) p \phi N_s (1 - s)/60 = \pi f \phi \, (1 - s)$$

Therefore, the instantaneous e per phase may be written (eq. 19)

$$e/\text{phase} = 5.19 T_2 f \phi \, (1 - s) \sin \omega t \, 10^{-8} \quad . \; . \; . \; . \quad (21)$$

Effective emf per phase is

$$E = 3.67 T_2 f \phi \, (1 - s) \, 10^{-8} \quad . \; . \; . \; . \; . \; . \; . \; . \quad (22)$$

(b) *Transformer emf due to pulsating flux.* For rotation in a given direction the second pulsating component of the rotating magnetic field, ϕ_b, must be 90 degrees ahead of ϕ_a in space and must lag 90 degrees behind ϕ_a in time phase. Thus, if $\phi_a = \phi \sin \omega t$, it follows that $\phi_b = \phi \sin (\omega t - \pi/2) = -\phi \cos \omega t$. This total flux links any conductor at b in Fig. 730(b). At an angle x from b the flux linking a conductor will be

$$\phi_x = -\phi \cos \omega t \cos x$$

Instantaneous emf, from the fundamental relation $e = -N \, d\phi/dt$, is

$$e_x = (1/2) \omega \phi \cos x \sin \omega t \quad . \; . \quad . \; . \; . \quad (23)$$

The average e per conductor, between brushes 1 and 2, is

$$e_{av} = (3/\pi) \int_{x=0}^{x=\pi/3} e_x \, dx = -(3/2\pi) \omega \phi \sin \omega t \sin \pi/3 \; 10^{-8} \text{ volt}$$

Total emf between brushes is

$$\sum e = -5.19 T_2 f \phi \sin \omega t \, 10^{-8} \text{ volt} \quad . \; . \; . \; . \; . \; . \quad (24)$$

Note that this emf is of supply frequency.

(c) *Resultant voltage.* From eqs. (21) and (24) it is seen that the emf's induced in the rotor by the two components of the field are of the same frequency but in phase opposition. They therefore subtract, with the result that the total emf induced in the rotor between brushes 1 and 2 is

$$E_0 = 3.67 T_2 f \phi s \, 10^{-8} \text{ volt} \quad \ldots \ldots \quad (25)$$

$$= E_2 s$$

where E_2 is emf induced in the rotor at standstill.

This emf is proportional to slip but is of supply frequency. It differs, therefore, from the emf induced between rings of the slip-ring motor in that the latter is of slip frequency, although the two would be numerically equal. The addition of a commutator and brushes means that the taps to points 120 degrees apart in the winding are moved around the winding at a speed $(1 - s)N_s$ or, in terms of stator frequency, f_1, at a frequency $(1 - s)f_1$. This, added to the slip frequency induced in individual conductors, gives an effect of frequency, f_1, between brushes and makes it possible to apply emf's of supply frequency to the rotor brushes for speed control. The commutator and brushes act as a frequency converter (§944), changing current which is of slip frequency in the rotor to supply frequency in the controller. Therefore, the rotor-plus-controller impedance will be (see Fig. 731)

$$Z_{2a} = r_2 + r_t + j(x_2 s + x_t) \quad \ldots \ldots \quad (26)$$

where r_2 is the ohmic resistance of the rotor windings, x_2 the rotor reactance at stator frequency, r_t and x_t are the resistance and leakage reactance of the regulator circuit at supply frequency.

1045. Performance from the Equivalent Circuits (Method of Superposition). — Figure 731(*a*) is the equivalent electric circuit of the motor and control regulator, assuming the regulator to be turned to the position of zero induced emf. This is identical with the exact circuit of the motor as shown in Fig. 661, except that the impedance of the regulator is included. Figure 731(*b*) assumes the supply voltage, $\mathbf{V}_1$, to be zero but with a controller voltage, $\mathbf{E}_t$, applied in the rotor circuit, the impedance of the supply circuit being neglected. This causes a current, $\mathbf{I}_b$, to flow. By superposing the currents of circuits (*a*) and (*b*) it is proposed to determine the performance of the motor. That these circuits are reasonable is evident from the equations below. For the significance of subscripts see Fig. 731.

(a) *Current,* $\mathbf{I}_a$, *due to motor slip.* From the general theory of the polyphase induction motor (Chapter XXII) the rotor current in circuit (*a*) is

$$\mathbf{I}_{2a} = \frac{\mathbf{E}_{2a}s}{(r_2 + r_t) + j(x_2s + x_t)} = \frac{\mathbf{E}_{2a}}{(r_2 + r_t)/s + j(x_2 + x_t/s)} \tag{27}$$

where $\mathbf{E}_{2a}$ is the emf induced in the rotor at standstill.

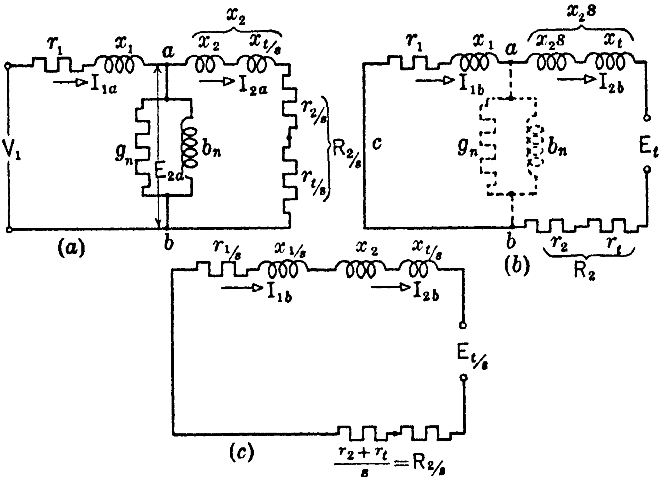

FIG. 731. Equivalent circuits of the Crocker-Wheeler motor.

Continuing the solution of circuit (*a*)

$$\left.\begin{aligned} G_2 &= \frac{(r_2 + r_t)/s}{(r_2 + r_t)^2/s^2 + (x_2 + x_t/s)^2} \\ B_2 &= \frac{x_2 + x_t/s}{(r_2 + r_t)^2/s^2 + (x_2 + x_t/s)^2} \end{aligned}\right\} \quad \dots\dots\dots\dots \tag{28}$$

$$\mathbf{I}_{2a} = \mathbf{E}_{2a}\mathbf{Y}_2 = \mathbf{E}_{2a}(G_2 - jB_2) \quad \dots\dots\dots\dots \tag{29}$$

$$\mathbf{I}_{1a} = \mathbf{E}_{2a}\mathbf{Y}_{ab} = \mathbf{E}_{2a}[(G_2 + G_n) - j(B_2 + B_n)] = \mathbf{E}_{2a}(G_{ab} - jB_{ab}) \tag{30}$$

But

$$\begin{aligned} \mathbf{E}_{2a} &= \mathbf{V}_1 - \mathbf{I}_{1a}z_1 = \mathbf{V}_1 - \mathbf{E}_{2a}\mathbf{Y}_{ab}z_1 \quad \dots\dots\dots\dots \qquad (31) \\ &= \mathbf{V}_1 - \mathbf{E}_{2a}(G_{ab}r_1 + B_{ab}x_1) - j\mathbf{E}_{2a}(G_{ab}x_1 - B_{ab}r_1) \end{aligned}$$

Solving

$$\begin{aligned} \mathbf{V}_1 &= \mathbf{E}_{2a}[(1 + G_{ab}r_1 + B_{ab}x_1) + j(G_{ab}x_1 - B_{ab}r_1)] \\ &= \mathbf{E}_{2a}(M + jN) \end{aligned}$$

Therefore

$$\mathbf{E}_{2a} = \mathbf{V}_1/(M + jN) = \mathbf{V}_1(A - jB) = E_{2a}' - jE_{2a}'' \quad \ldots\ldots \quad (32)$$

If the active and reactive components of $\mathbf{I}_{1a}$ and $\mathbf{I}_{2a}$ are indicated by primes and double primes:

$$\mathbf{I}_{1a} = I_{1a}' - jI_{1a}'' = E_{2a}'G_{ab} - E_{ab}''B_{ab} - j(E_{2a}'B_{ab} + E_{2a}''G_{ab}) \quad . \quad (33)$$

$$\mathbf{I}_{2a} = I_{2a}' - jI_{2a}'' = E_{2a}'G_2 - E_{2a}''B_2 - j(E_{2a}'B_2 + E_{2a}''G_2) \quad . \; . \quad (34)$$

(b) *Component current,* $\mathbf{I}_b$, *caused by the emf,* $\mathbf{E}_t$, *induced in the controller.* Neglecting the impedance of the source, the current $\mathbf{I}_b$, due to $\mathbf{E}_t$, is limited by r_t, x_t, r_2, x_2s, r_1, and x_1. Because of the low voltage involved the exciting admittance of the motor may be neglected. Then, from the circuit of Fig. 731(*b*):

$$X_b = x_1 + x_t + x_2s$$

$$R_b = r_1 + r_2 + r_t$$

$$Z_b^2 = R_b^2 + X_b^2$$

$$G_b = R_b/Z_b^2, \quad B_b = X_b/Z_b^2$$

$$\mathbf{E}_t\underline{/\theta} = E_t \cos\theta + jE_t \sin\theta = E_t' + jE_t''$$

$$\mathbf{I}_{2b} = \mathbf{E}_t\mathbf{Y}_b = I_{2b}' - jI_{2b}'' = \mathbf{I}_{1b} \quad \text{(neglecting excitation admittance)}$$

$$\left.\begin{aligned} I_{2b}' &= E_t'G_b + E_t''B_b \\ I_{2b}'' &= E_t'B_b - E_t''G_b \end{aligned}\right\} \quad \ldots\ldots\ldots\ldots\ldots \quad (35a)$$

(c) *Motor performance by superposition of* $\mathbf{I}_a$ *and* $\mathbf{I}_b$. Designating by $\mathbf{I}_1$ the total stator current, of which the active and reactive components are I_1' and I_1'', it follows that:

$$I_1' = I_{1a}' + I_{1b}' \quad \text{and} \quad I_1'' = I_{1a}'' + I_{1b}'' \quad \ldots\ldots \quad (35b)$$

$$\mathbf{E}_1 = \mathbf{V}_1 - I_1z_1 = V_1 - (I_1'r_1 + I_1''x_1) - j(I_1'x_1 - I_1''r_1) \quad . \; . \; . \quad (36)$$

$$\mathbf{I}_2 = I_{2a}' + I_{2b}' - j(I_{2a}'' + I_{2b}'') \quad \ldots\ldots\ldots\ldots \quad (37)$$

Internal power developed, per phase is

$$P_2 = \mathbf{E}_1 \cdot \mathbf{I}_2 = E_1'I_2' \pm E_1''I_1'' \quad \ldots\ldots\ldots\ldots \quad (38)$$

$$T = \text{torque} = 7.04P_2/N_s \text{ lb-ft per phase} \quad \ldots\ldots\ldots \quad (39)$$

where N_s is synchronous speed in rpm.

Stator current is $I_1 = \sqrt{I_1'^2 + I_1''^2}$ . . . . (40)

Power factor $= \cos\theta_1 = I_1'/I_1$ . . . . (41)

$$\text{Input} = W_1 = I_1'V_1 \pm \mathbf{E}_t \cdot \mathbf{I}_b - I_2^2 r_t, \text{ watts per phase} \quad (42)$$

$$\text{Output} = W_2 = (1 - s)N_s T/7.04 - (\text{friction plus windage}), \text{ watts per phase} \quad (43)$$

Figure 731*a* is drawn from the results of calculations involving these equations.

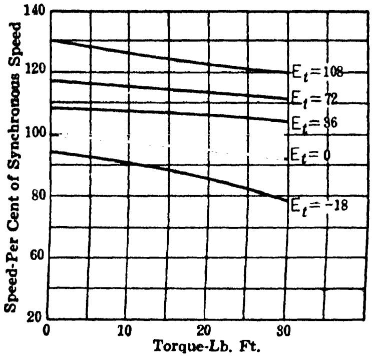

FIG. 731(*a*). Performance curves on a Crocker-Wheeler motor obtained by calculation, following the method of §1045.

1046. Bibliography on A-C Commutator Motors. — Articles and papers on single-phase and polyphase commutator motors are so numerous that it would be futile to give a bibliography here.[10] The reader should consult the latest available information, as the theory and the actual types of machines are being constantly improved. Most first-class periodicals in this country and abroad devote a certain amount of space to these machines, and indexes to the latest volumes should be consulted. *Science Abstracts*, Part B, contains references to practically all noteworthy articles on the subject. As to books, the two special works on the subject are:

E. Arnold, " Wechselstromtechnik," vol. 5, part 2.
M. Schenkel, " Die Kommutatormaschinen."

Considerable theoretical information will be found in C. P. Steinmetz's works, entitled respectively, " Alternating-Current Phenomena " and " Theory and Calculation of Electrical Apparatus." See also the " Standard Handbook for Electrical Engineers," Section 7, and B. A. Behrend, " The Induction Motor." All the above-mentioned books treat of both single-phase and polyphase machines. For single-phase motors only, the following books may also be consulted:

---

[10] Classified references to older articles will be found at the end of Schenkel's "Die Kommutatormaschinen."

A. S. McAllister, " Alternating-Current Motors."
R. R. Lawrence, " Principles of A-C Machinery."
F. Creedy, " Single-Phase Commutator Motors."
L. Barbillon, " Les machines électriques alternatives à collecteur."

The following are among noteworthy articles on the compensated induction motor:

T. Torda, *Electrical World*, vol. 86 (1925), p. 1205.
L. Dreyfus, *Elektrot. und Maschinenbau*, vol. 43 (1925), p. 673.
G. Belfils, *Revue générale de l'électr.*, vol. 18 (1925), p. 409.
A. Heyland, *ibid.*, vol. 17, p. 397; translated into English in *Electrician*, vol. 95, p. 4.

CHAPTER LIV

MAGNETIC CONTACTOR CONTROL FOR D-C MOTORS

1047. With the increasing uses of electric motors in various industries and with the ever-increasing size of the motors themselves, new problems in automatic and semi-automatic control have arisen which cannot be satisfactorily solved by means of the face-plate and drum-type controllers described in Chapter XXV.[1] It has become preferable and even necessary to resort to the unit-switch construction (Figs. 416, 732, and 733), each switch being operated by its own electromagnet. Such an electrically operated switch is known as a *magnetic contactor.* The principal advantages of the magnetic-contactor control are as follows:

(a) Opening and closing of contacts is positive, since the operator cannot retard their motion once a contactor has started to open or to close. This is of particular importance with large currents and high voltages, and insures a long life of the contacts. Moreover, contact pieces are readily renewable and all parts are easy to inspect and repair.

(b) The unit-switch construction gives flexibility in adapting a controller to various problems.

(c) Automatic control and protection are easily obtained by means of relays and properly interconnected contactors. This makes such a controller more " fool-proof " than other types.

(d) Remote control can be obtained by push-buttons or by a small master-controller. The contactor panel with its heavy wiring can therefore be placed near the motor and only small control wires installed between the primary controller and the place where the operator is located.

In view of these advantages, automatic magnetic control is becoming more and more widely used, notwithstanding its higher first cost and the larger space required.

1048. The Principal Functions of Magnetic Switches. — Controllers may be made to operate automatically upon the closing of a switch or the pressing of a button, bringing the motor up to speed in a desired time, or as a function of the (limited) current of the motor or of its speed. Various elements of protection against overload, under-voltage operation, or excessive temperature rise may be incorporated in the control, as well as other special features, such as dynamic braking, operation by limit switches, float switches, photoelectric cells, etc. A typical non-reversing magnetic controller is shown in Fig. 732. To start the motor, it is necessary only to close the line switch and the starting switch. The magnetic switches then close in the proper order and at the proper instants until the motor is running at full speed. Opening the starting switch stops the motor. The line switch may remain closed as long as the motor is periodically started and stopped. The starting switch may be located at a distance from the controller, and the wires leading to it carry only the small current necessary for energizing the holding coil of the line contactor, shown on the extreme left of the panel.

---

[1] For a detailed description of various controllers see H. D. James, " Controllers for Electric Motors," Van Nostrand; also a series of articles by W. Wilson, *World Power* vol. 4 (1925); and P. B. Harwood, " Control of Electric Motors," John Wiley & Sons.

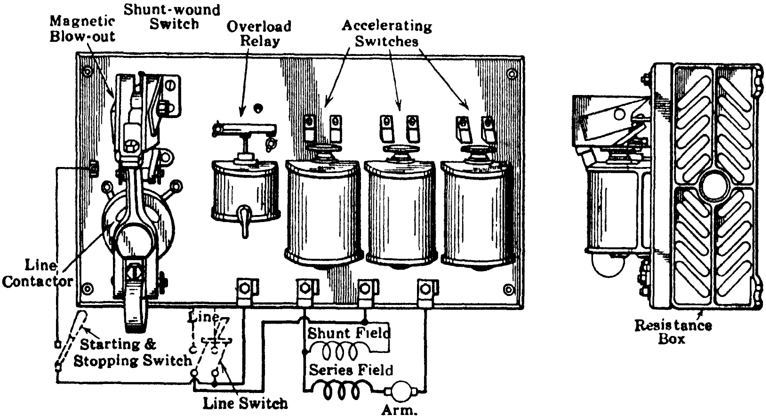

FIG. 732. Contactor panel for starting a d-c motor.

The simplest form of starting switch consists of two push-buttons, one of which is pressed to start the motor, and the other to stop it. With this arrangement three small wires to the switch are necessary (Figs. 740 and 742). If the motor is to be run in either direction, three push-buttons are used, marked "forward," "off," and "reverse." For more complicated operations a secondary master-controller is employed, by means of which individual contactors of the main controller are made to close and to open the circuit as desired.

As soon as the operating coil of the line contactor has been energized by the starting switch (Fig. 732), the contactor is closed, and the main circuit is established through the motor armature, with all the starting resistance in series. As the motor speeds up and the current drops, the three contactors on the right-hand side of the panel close automatically, one after another, short-circuiting the sections of the starting rheostat. The automatic features which cause these switches to operate are described in §§1052 to 1057. The overload and under-voltage protection of magnetic controllers is treated in §1057.

The controller shown in Fig. 732 performs only the functions (a) and (d) indicated in §563. By adding more contactors the remaining functions can be performed also. Diagrams of connections of such controllers are shown in Figs. 735 and 736.

It will be noted that in Fig. 732 only the line contactor (of the so-called clapper type) is provided with a magnetic blowout (§578), the connections being such that the circuit is always finally broken by this contactor. The details of a magnetic blowout can be seen more clearly on the contactor shown in Fig. 734.

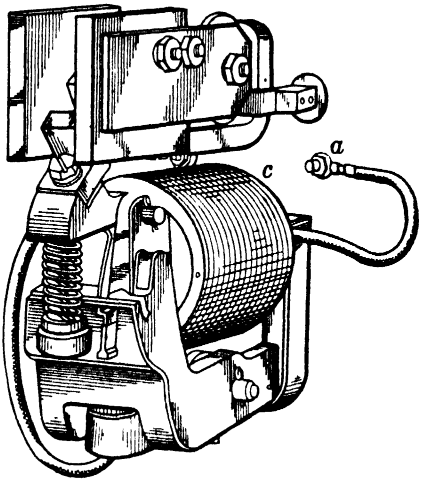

FIG. 733. Clapper-type shunt magnetic contactor.

1049. The Electromagnetic Contactor. — Details of a typical contactor are shown in Figs. 733 and 734.

The two heavy butt contacts (Figs. 733 and 734) which open and close the power circuit are of copper, the upper being fixed in position, while the lower is carried on a hinged armature and is itself attached to a hinged piece which is forced forward by the compression spring. The operating (shunt) coil surrounds an iron core which, with the frame and armature of the contactor, constitute the main magnetic circuit, an air-gap separating armature and core while the contactor is open. When the operating coil is energized the armature is drawn sharply to the core, causing the moving contact to be driven hard against the fixed contact, with a combined sliding and rolling motion which insures clean contact surfaces. The compression spring is thereby further shortened and exerts a continuous pressure between the contacts. The main electric circuit is now completed through the blow-out (series) coil, the main contacts, and leads. A magnetic field is set up by the blow-out coil through its core, into the iron pole-pieces on the outer sides of the arc shields and across the space around and above the main contacts.

When the operating coil is de-energized the compression spring throws the contacts sharply apart, the last points to separate being the upper tips, owing to the rolling action mentioned above. The arc which forms is blown upward by the blow-out field and along the arcing horns or guides which protect the blow-out coil, until it lengthens and breaks, thus opening the main circuit.

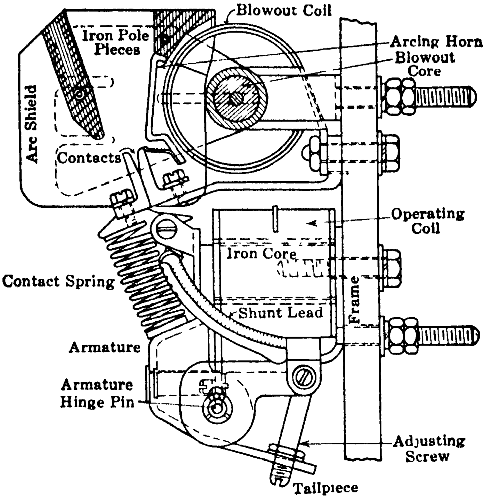

Fig. 734 Details of a magnetic contactor (Westinghouse Electric and Mfg Co.)

Adjustment of the main air-gap between the armature and operating core is made by an adjusting screw which passes through the tail piece of the contactor. This setting determines the voltage at which the contactor closes, also that at which it drops out. Much work has been done by designers to improve magnetic contactors, to simplify construction, to make the blow-out more prompt and effective, etc. The shape and the kind of refractory material used for the arc shield (or arc box) are of great importance for securing a long life of the contacts and of the box itself. The reader is referred to the bulletins of the manufacturers for details. Small additional contacts, interlocks, are frequently carried by the contactor for the purpose of closing or opening auxiliary control circuits, as will be shown in later descriptions of certain contactor assemblies (§§1054 and 1055).

1050. How to Read Contactor Diagrams. — Two typical diagrams of connections of magnetic controllers are shown in Figs. 735 and 736. The auxiliary and control wiring is omitted for the sake of clearness. The diagram of Fig. 735 is of a non-reversing controller for starting duty only. The sequence in which the switches are closed is indicated in the accompanying table. Switch numbers are given in the first column, to correspond to the numbers given in the schematic wiring diagram. The remaining columns represent the various starting connections. A circle within a square indicates that that particular switch is closed.

With the assistance of this table, the diagram reads as follows: First, switch 1 is closed. This connects the shunt field of the motor across the line and at the same time establishes a circuit through the armature, with the entire starting resistance in series. Next, switch 2 is also closed, short-circuiting the section R_1R_2 of the rheostat. Later, switch 3 is likewise closed, short-circuiting the resistance R_3R_4. Finally, switch 4 is closed and the whole resistor is bridged over. At this stage, switches 2 and 3 open, and only switches 1 and 4 remain closed during the normal operation of the motor. Arrows show which coils operate certain contactors.

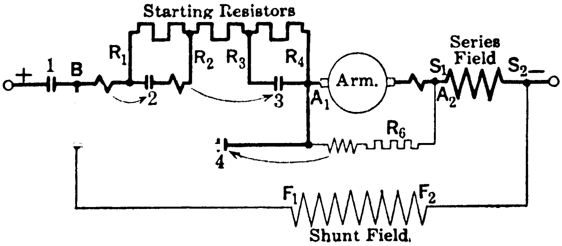

Sequence of Switches

Sw	Run			
1	O	O	O	O
2		O	O	
3			O	
4				O

FIG. 735. Typical example of a contactor control diagram with sequence table (H. D. James).

Figure 736 shows a reversing controller with dynamic braking, i.e., in stopping the motor. The stored energy of the rotating armature is absorbed in a loading resistor shunted across the brushes (§§293 and 294). When switches 2 and 4 are closed, the line current enters the armature through the terminal A_2. When switches 1 and 3 are closed, the current flows from A_1 to A_2 and the armature rotates in the opposite direction. When switches 1, 2, 3, and 4 are open, switches $1A$ and $2A$ are closed and the armature circuit is completed through the brake resistance. In full automatic controllers these two groups of switches are so interlocked that the brake circuit cannot be closed when the motor is connected to the line, and vice versa. Number 5 is the line

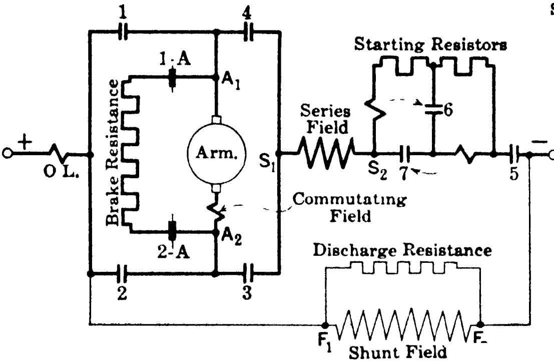

Sequence of Switches

Sw	Forward			Off	Reverse		
1					O	O	O
2	O	O	O				
3					O	O	O
4	O	O	O				
5	O	O	O		O	O	O
6		O				O	
7	O						O
1-A	O	O	O	O			
2-A				O	O	O	O

FIG. 736. A second example of contactor control, showing dynamic braking.

contactor, and the two accelerating switches are marked 6 and 7. The table shows the sequence in which these switches are closed for both directions of rotation. The vertical columns should be read beginning with the one marked " off."

It is particularly desired that the student familiarize himself with these fundamental connections and with their mode of representation by means of a table. A clear understanding of Figs. 735 and 736 will enable him to read considerably more complicated diagrams of industrial and railway controllers.

1051. EXPERIMENT 54-A. — Elementary Exercises with Non-Automatic Magnetic Contactors. — The purpose of the experiment is to familiarize the student with typical contactors and with the simpler connections of unit switches, such, for example, as shown in Fig. 735, with no automatic features. A few contactors should be provided (Figs. 733 and 734), some with blow-out coils, some without. The operating coils should be of the shunt type, so that each can be connected independently across the line. A shunt- or compound-wound motor, a few sections of starting resistance, and a master-switch should be available. The master-switch can be in the form of a small drum controller (§576), or it may consist of small individual knife switches.

1. Study the construction and principles of operation of such contactors as are available. Note what adjustments are possible. Study the manner in which the contacts close, noting whether contacts " wipe " as they close. Examine the arcing tips and guides, blow-out coils and arcing chamber, etc. Study the magnetic and electric circuits of the contactor. Determine by tests the minimum voltage at which the contacts close firmly and promptly.

2. Wire up the motor for plain starting through the contactor switches, as shown in Fig. 733, and connect the operating coils to the master-switch. Consider carefully which contactors should have a blow-out coil and which do not need it. Operate the equipment several times to satisfy yourself that it works properly and take a few readings of volts and amperes.

3. Add unit switches for reversing the motor (Fig. 734) and again operate the equipment.

4. Add the dynamic braking feature.

5. Add speed control by field rheostat.

Report. State the results of observations made in 1. Draw the diagrams of connections to the master-switch and give the instrument readings, with comments. Explain: (a) the disadvantages of having provided no protective or automatic features; (b) the dangers of placing such an equipment in the hands of an inexperienced or careless operator; (c) which automatic features, among those described in the following sections, should be added to make the equipment satisfactory for an assumed concrete practical case.

METHODS OF AUTOMATIC ACCELERATION

1052. Counter-EMF Method of Acceleration. — The three principal methods of automatically controlling the acceleration of a motor by means of magnetic contactors are: (a) the counter-emf, (b) the current-limit, and (c) the time-limit methods. In the counter-emf method the operating coils of the accelerating switches are connected across the armature terminals of the motor, or between one of the terminals and part of the starting resistance in series with the other terminal. Figure 737 illustrates this method. The shunt coil of contactor 1 is connected across the line through a push-button station and closes 1 when the "start" button is pressed. This places the shunt field of the motor directly across the line and the armature of the motor across the line in series with the total starting resistance R_1R_3. The closing coil of contactor 2 is across the motor armature plus the resistance R_1R_2. As the motor speeds up, the counter emf of the armature plus the drop in R_1R_2 reaches the voltage for which contactor 2 is set and it closes, short-circuiting the section R_2R_3 of the starting resistance. The closing coil of contactor 3 is connected across the motor armature. When the motor speed has reached such a value that the counter emf of the motor equals the setting of contactor 3 the latter closes and short-circuits the remainder, R_1R_2, of the starting resistance, and the motor continues to operate at full line voltage. This method is quite simple, and is par-

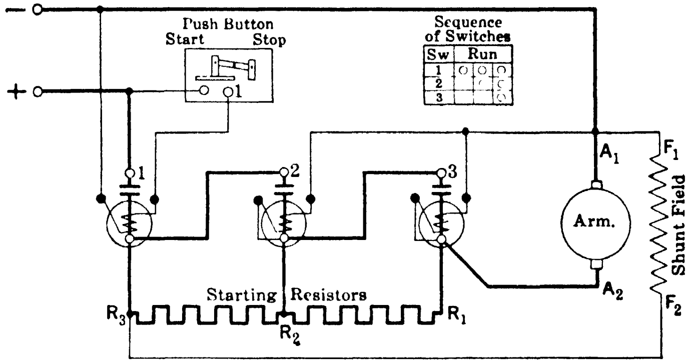

FIG. 737. Diagram of control for starting a shunt motor by the counter-emf method.

ticularly suitable when the line voltage is steady and the motor always starts at approximately the same load. Otherwise there is a possibility of the contactors closing too soon or too late.

The method is generally used only with rather small motors (under 10 horsepower) and with only two or, at most, three accelerating points, since it is not possible to set the switches to operate positively and forcefully on small voltage differences. There is danger that the switches will close hesitantly, with burning and sticking of the contacts, or that they will fail to close.[2]

1053. Current-Limit Methods of Acceleration. — *Series lockout.* There are a number of devices for cutting starting resistance out of the motor circuit after the current has dropped to a predetermined value. Among these are the series-lockout contactor[3] the series relay method (§1054),[4] and the drop-across-resistance method (§1055).

Accelerating switches which lock open until the motor current drops to a desired value, and then close to cut out part of the starting resistance, are called "series lock-out" switches. Figure 738 is an example of this type.

In the clapper-type contactor shown in Fig. 738, the flux produced by the operating coil passes through the steel magnet core and the air-gap to the armature. Part of this flux passes from the armature through the armature bracket to the magnet yoke, and thence to the magnet core, tending to close the contactor. Another part of the flux passes from the armature through the tailpiece to the magnet yoke, exerting a pull which tends to prevent the contactor from closing. The magnetic path through the armature bracket has a small cross-section, so that when the current flowing through the operating coil exceeds a certain value this path becomes saturated, and forces the balance of the flux through the tailpiece, holding the contactor open. As the current decreases, the flux in the saturated armature bracket remains constant, but the flux through the tailpiece decreases until it is not sufficient to hold the contactor open. By changing the hold-out air-gap between the tailpiece and the magnet yoke, the contactor can be adjusted to close at a predetermined current value. The gap is adjusted by means of a calibrating screw; the greater its length, the higher the current value at which the switch will close. When the circuit is first completed through the operating coil, there is danger of the switch closing before the flux in the tailpiece is sufficient to lock it open. This tendency is overcome by placing a heavy copper damping coil around a portion of the armature bracket. When the operating coil is energized, the damping coil forces the flux to build up in the tailpiece sooner than in the armature bracket.

---

[2] R. T. Kintzing, "Control for D-C Industrial Motors," *Elec. Jour.*, January, 1927, p. 23.

[3] H. D. James, "Controllers for Electric Motors," Chapter VIII, D. Van Nostrand Co.

[4] *Ibid.*, Chapter VII.

Some series lock-out switches are provided with two separate coils in series, a lower holding coil and an upper operating coil. The plunger also consists of two parts connected by a spring. With a large current, the lower holding coil keeps its part of the plunger down while the upper operating coil raises its plunger against the tension of the spring. When the current is reduced, the spring overcomes the magnetic force on the lower plunger and raises it also. The contact part is connected to the lower plunger and the switch is thus closed.

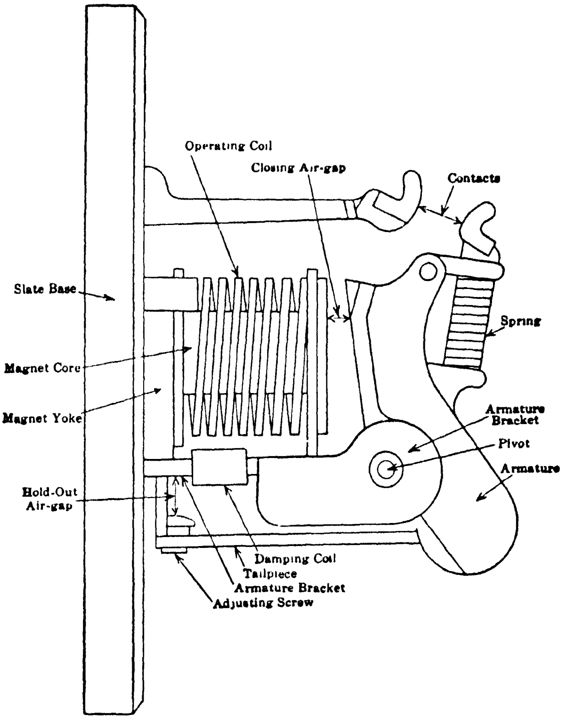

FIG. 738. A series-lockout type contactor.

In spite of the simplicity of the controller the series lock-out switch is now seldom used, since it has the disadvantage that it may fail to operate on light loads and is not suitable for use on adjustable-speed motors. Figure 739 illustrates the control when these switches are used. Upon the closing of the main switch, *S*, which may be a shunt contactor operated by a push-button, the motor starts with all resistance in series. When the current drops sufficiently contactor 1 closes. When the current again drops contactor 2 closes, and finally 3, which short-circuits the last of the starting resistance as well as the series contactor coils. Contactor 3 is now held in by a shunt holding coil.

1054. Current Limit by Series Relay. — Another method of preventing the closing of accelerating switches until the starting current of the motor has fallen to a desired value involves the use of series current-limit relays.[5] These relays carry the starting current, each in its turn, and each holds open the shunt circuit of the next accelerating contactor as long as the current is above a desired value. As one series relay drops and closes the relay of its accelerating contactor this cuts the series coil of the relay out of circuit and inserts that of the next relay. This may be seen best in a circuit diagram. In Fig. 740, pressing the start button energizes the shunt coil 1 of contactor $C1$ and causes it to close. Auxiliary contacts on contactor 1 now bridge around the start button. The motor starts with all the starting resistance in series. Series relay, $SR1$, now carries the starting current and holds open the relay contacts in series with the closing coil of contactor $C2$. When the starting current has fallen sufficiently relay contacts $SR1$ close and energize the shunt coil of contactor $C2$, which closes. Series relay $SR2$ in the same manner closes contactor $C3$ after the current has again fallen. Both series relays are now bridged across and carry no current.

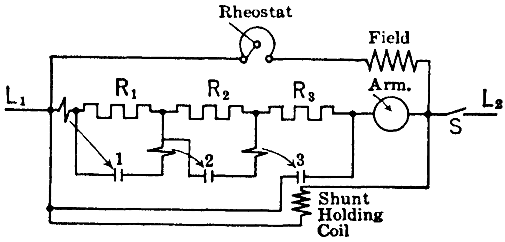

FIG. 739. Control diagram for starting a motor by means of series-lockout contactors.

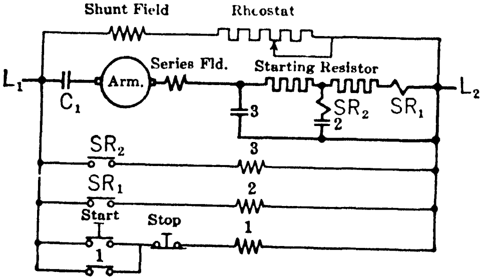

FIG. 740. Starting controller in which starting current is limited by means of series relays.

The current-limit method of starting motors may fail to start the motor when the load is excessive. However, it is possible by this method to use as many accelerating contactors as desired, which makes it superior to the counter-emf method, for large motors. It causes the motor to start quickly on light loads and slowly on heavy loads. To some extent it has been superseded by the "time" and "current-time" methods of acceleration.

---

[5] R. Lee, "College Laboratory Controllers," *Elec. Jour.*, June, 1927.

Figure 741 shows a series relay in section. The plunger is normally held up by the spring on the operating rod so that the carbon disk does not bridge the contact screws. When the line contactor closes it presses down on the fiber knob of the relay so that the plunger would fall and close the relay contacts, except that now the starting current flows in the relay coil and holds the plunger up until the current has fallen to the correct value.

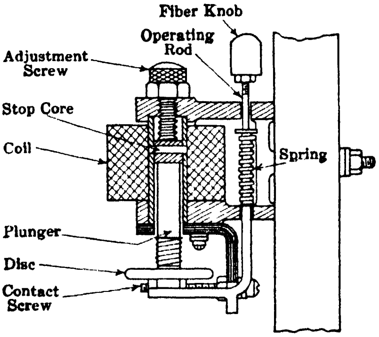

FIG. 741. Section of a typical series relay (Westinghouse Electric and Mfg. Co.).

1055. Drop-across-Resistance Method. — In this method (Fig. 742) a relay with two to four contact fingers is actuated by the voltage drop across the starting resistance. As the starting current decreases this voltage diminishes, with the result that one after another the contact

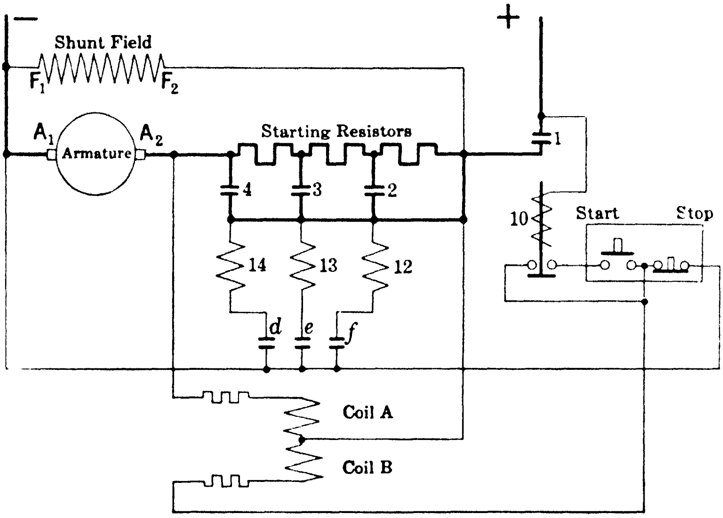

FIG. 742. Automatic starter using the current-limit relay of Fig. 743.

fingers of the relay are released and close, thereby energizing the closing coils of the accelerating contactors which close and short-circuit the several sections of the starting resistance. This accelerating relay (Fig. 743) has two coils, *A* and *B*. Coil *A* is connected across the resistor and, with the decrease in the resistor drop, releases the three finger contacts *d*, *e*, and *f*, thus closing contacts 2, 3, and 4. After the resistor is cut out coil *A* loses its excitation, but coil *B*, being directly across the line, holds the armature of relay 10 (Fig. 742) in the closed position.

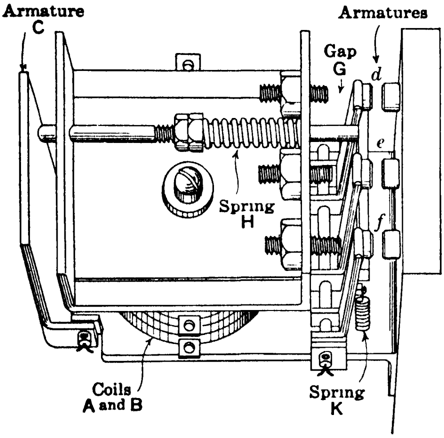

FIG. 743. Three-pole current-limit relay operated by a shunt coil across the starting resistor.

1056. Time-Limit Acceleration. — *Pendulum-timed switches.* In this method the accelerating contactors close after definite intervals of time so that, whether lightly or heavily loaded, the motor is brought to speed in the same length of time. A small starter in which the time element was governed by a pendulum device was illustrated in Fig. 420, which is repeated, together with the schematic diagram of the controller in Fig. 744. This starter operates in a manner similar to that of the unit-switch starter of Fig. 416, except that it closes the individual switches automatically, at definite time intervals, thus cutting out the starting resistance in steps and bringing the motor up to speed, usually in 2 to 8 seconds, the time being governed by a pendulum device. Figure 744(*b*) is a schematic diagram of such a starter connected to a shunt motor.

Overload protection in this starter is provided by a hand-reset temperature overload relay.

Undervoltage protection is provided by the contactor and accelerating fingers dropping open when the line voltage drops below a certain value.

Such a starter as the one just described is suitable for motors of $\frac{3}{4}$- to 20-horsepower rating and, like the solenoid type, may be actuated from a distance by a push-button, etc.

Magnetically timed contactors. In the solenoid-operated starter of Fig. 417 time was determined by the setting of the ports in the dash-pot and by the viscosity of the oil. In recent types of contactors a time delay has been obtained by slowing up the decay of the magnetic field when the circuit of the closing coil is interrupted.

Figure 745 is the schematic diagram of such a magnetically timed

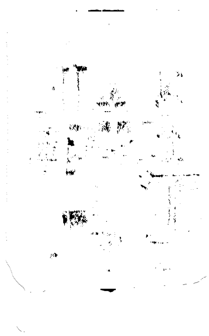

Fig. 744(a). A three-point automatic motor (General Electric Co.).

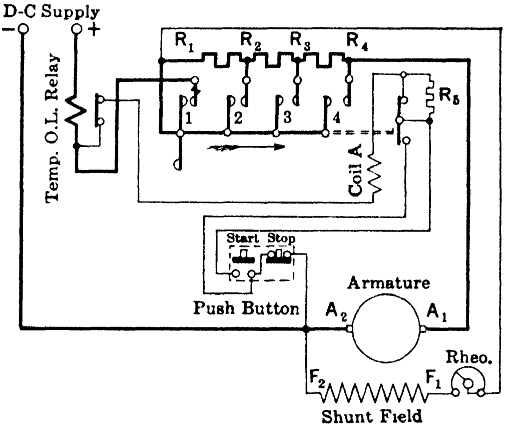

Fig. 744(b). Schematic diagram of the starter of Fig. 744(a).

starting controller. Acceleration is governed by delayed-action contactors, spring-closed but opened by a main shunt coil which saturates

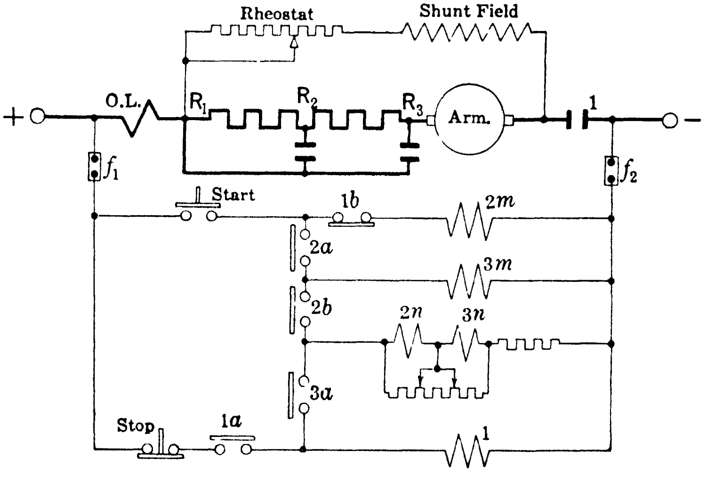

Fig. 745. Diagram of a magnetically timed motor starter.

the magnetic circuit. A copper tube around the iron core acts to slow up the dying out of the flux when the circuit of the main coil is opened, due to current induced in the tube by the flux change. The time within which the contactor will act is adjusted by varying the resistance in series with a second and smaller shunt coil which opposes the main coil. The starter operates as follows:

Pushing the start button energizes the main coil (2*m*) of the time-delay contactor 2 causing it to open contact 2 (at R_2), and to close interlock contacts 2_a and 2_b which close the circuits containing the control coils 2*n* and 3*n*. These interlocks energize 3*m*, the main coil of time-delay contactor 3 which opens contact 3 (at R_3) and closes interlock 3_a, energizing the shunt coil of the main line contactor 1. Contacts 1 close, and the motor is connected across the line with the starting resistance $R_1R_2R_3$ in series with the armature. Closing of 1 also closes interlock 1_a so that the shunt coil of the line contactor is across the line in series with the stop button (closed), but opens interlock 1_b which breaks the circuit of the main coil 2*m* of contactor 2. Consequently, after a definite time (2 to 6 seconds) during which the motor is gaining speed, the flux in accelerating contactor 2 dies down, allowing the spring to close contactor 2, short-circuiting the resistance R_1R_2, and opening interlocks 2_a and 2_b. Contactor 3 is now de-energized and is spring closed after a definite time interval. This short-circuits the remainder of the starting resistor and opens interlock 3_a which disconnects the control coils 2*n* and 3*n*. The motor now operates normally, being protected from overload by the overload relay *OL* which trips the main contactor in case of excessive current. If the line voltage fails, or the stop button is pressed, contactor 1 opens and disconnects the motor from the line.

Instead of double-coil contactors of the type described above, series relays, magnetically timed, may be used with ordinary shunt contactors Figure 746(*a*) illustrates such a relay of the Electric Controller and Manufacturing Company. This "time-current" acceleration relay proportions the time per step to the load to be accelerated as follows: A rush of current in the series coil, *A*, causes a sudden rise of flux through the adjustable steel core, *C*. This changing flux causes an induced current in the aluminum sleeve, *E*. Repulsion between this induced current and the main flux causes the aluminum sleeve to jump up and break contacts between *G* and *H*, which are in the shunt coil circuit of an accelerating contactor. The contactor then opens and inserts resistance in the armature circuit of the motor. Sleeve *E* now starts to drop through the field which *A* has established across the gap at *F*, but, owing to the currents induced in the sleeve by this motion, the sleeve drops more slowly if the motor current, and field at *F*, are high, or more rapidly if the motor current is low. When the sleeve has dropped sufficiently, the relay contacts *GH* again close, energizing the accelerating contactor which closes and cuts resistance from the armature circuit of the motor, thus causing the motor to accelerate at an increased rate. Adjusting the position of core, *C*, changes the reluctance of the path for flux at *F* and so changes the time in which the relay will act.

Figure 746(*b*) shows the *RD* relay of the Electric Controller and Manufacturing Company. The time element of this relay consists of a vacuum cup placed in a dash-pot containing mercury. The plunger is held down by an arm on the accelerating contactor while the contactor is open. When the contactor closes, a spring beneath the vacuum cup forces the cup upward. This movement is delayed until mercury can flow through an orifice and relieve the vacuum. When the plunger does move upward, it closes one set of relay contacts and opens another, thus closing the next accelerating contactor

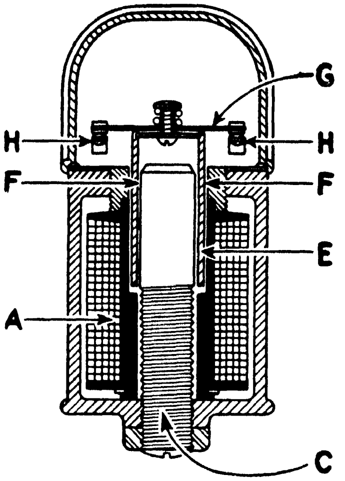

FIG 746(*a*) Magnetically timed series relay of the Electric Controller and Mfg Co

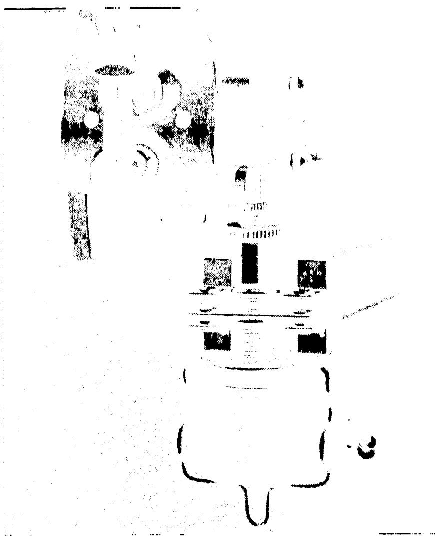

FIG 746(*b*) The *RD* relay of the Electric Controller and Mfg Co.

The magnetically timed (MT) accelerating relay of the General Electric Company (Fig. 747) operates as follows.[6]

The coil of the relay is connected across a section of the starting resistance of the motor, in parallel with an accelerating contactor. The contacts of the relay are in the circuit of the shunt coil of a contactor which is across the next section of the resistance. As long as the relay coil is energized its armature is closed and the relay contacts are open. Closing of the first contactor short-circuits the relay coil. Current in the relay winding then dies down slowly, and at a value determined by the setting of the relay its armature is pulled open by the adjusting spring (see Fig. 747). The relay contacts now being closed complete the shunt circuit for the next accelerating contactor, which closes, short-circuiting the next section of starting resistance. Similar operation of succeeding relays and contactors brings the motor up to speed by a combination of current demand and time.

---

[6] See *General Electric Bulletin* GEA 451-A.

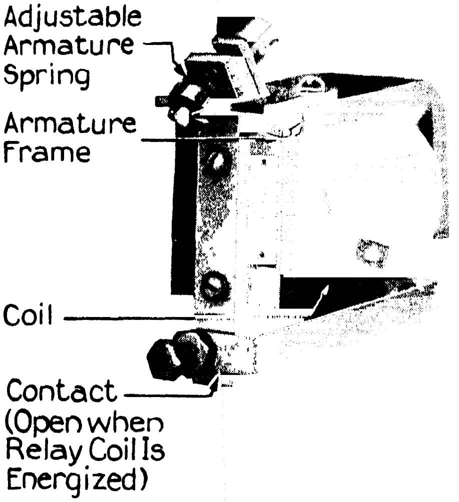
Adjustable Armature Spring
Armature Frame
Coil
Contact (Open when Relay Coil Is Energized)

FIG. 747. The *MT* relay of the General Electric Co.

1057. Overload and Under-Voltage Protection. — A motor operated by a magnetic controller may be protected by fuses or by a circuit-breaker, as is common in other types of control. However, in order to avoid costly fuse replacements, and to shorten the time that the motor is out of service, overload protection is more commonly provided by an overload relay (Fig. 746). The coil of the relay is in the motor circuit, and its contacts are in series with the operating coil of the line contactor (Fig. 744*b*). When the current exceeds that for which the relay is set its contacts open, whereupon the line contactor releases and breaks the motor supply circuit. Such a relay may be reset either by hand or by a push-button at a distance. It can also be made to restore itself to the normal condition after the overload is removed. It is advisable to provide the overload relay with a dash-pot or other time-delay device

(§1056) of quite a long time setting because reasonable overloads are not injurious to the motor and opening the circuit on short overloads only causes unnecessary interruptions. Such a relay should be set for a lower current than fuses, if such are also provided, so that the fuses will operate only in the event of failure of the relay. The relay may be set to operate at a desired (steady) current and will operate on the so-called "inverse-time-element" principle, i.e., it trips more quickly on an excessive overload than on a current which is but slightly above the setting. The time element can also be changed, either by adjusting the ports in the dash-pot or by changing the consistency of the oil. Since the effect of temperature is different with different kinds of oil only special dash-pot oil should be used.

With speed adjustment by field regulation it is desirable to have an additional relay which automatically short-circuits the field rheostat when the armature current exceeds a certain value and again inserts the resistance when the line current drops. This device is known as the "field-fluttering" relay.

Low-voltage protection and low-voltage release. It is necessary to protect the motor after interruptions in power supply, and from operation on too low a line voltage. Since the holding coil of the line contactor is connected across the line this contactor will automatically open the circuit on under-voltage and reinsert the starting resistances.

In some cases, as with motors driving pumps, blowers, compressors, etc., it is usually desired to have the operation resumed automatically as soon as the line voltage is back to normal. The connections are then arranged in such a way that all the accelerating contactors will open as soon as the line contactor is tripped, and will close the circuit again in the proper sequence after the line contactor is "in." Such operation of the controller is called "low-voltage release." In certain motor applications there may be danger either to the operator or to the equipment should the motor start again as soon as normal power is restored, and without any action on the part of the operator. In such cases the automatic control devices should return to the "off" position as soon as power fails and remain there until the starting button or switch is actuated. Such operation is called "low-voltage protection." The face-plate starter of Figs. 412 and 422 were examples of this, while the solenoid starter of Fig. 417 typified low-voltage release. Figures 742 and 743 are also examples of low-voltage protection.

1058. EXPERIMENT 54-B.—Automatic Acceleration of a D-C Motor by Means of Magnetic Contactors.—This experiment should involve, first, a study of available magnetic contactors and other control equipment; second, the drawing of suitable control diagrams involving each of the methods of automatic acceleration described above; third, connecting of a motor and control equipment in accordance with the diagrams; and, finally, the test of the controller under various conditions. Each of the methods should be tried out with the motor (a) unloaded, (b) lightly loaded, (c) at normal load or a reasonable overload. Overload protection and under-voltage release or protection should be included.

For each control equipment records should be made (using a high-speed graphic ammeter or oscillograph) of current peaks, time upon each accelerating point, total time of acceleration, and general behavior of motor and control under each condition of load, with voltage normal, below normal, and above.

Limitations of overload or under-voltage protection should be studied and suggestions made for their improvement.

Finally the different methods of automatic acceleration should be carefully compared in respect to their relative advantages under different conditions of operation, and their limitations should be stated. These conclusions should be based upon a careful tabulation of data and observations, as well as upon a study of suggested literature on the subject of control. This experiment may well be broken up into three tests, each of which is a study of a particular system of automatic acceleration (§1052).

1059. Electronic Control Devices. — With the recent rapid development of electron tubes of various types and ratings (Chapters LIX and LX) it is inevitable that they should have found use in the control of electric motors and generators.[7] It is essential that the student have some conception of the possibilities of these tubes for control purposes. For the theory of electronic devices and most of their applications he is referred to Chapters LIX and LX. Since this is an art which is changing with great rapidity only one or two typical examples will be described here. High sensitivity, quick response, and low power consumption are the principal advantages of electronic devices over electromagnetic types. High-vacuum tubes are suitable to applications where the currents involved are small; thyratron tubes (also called grid-glow tubes) are of use where the currents to be handled are large. Thyratrons may be used to convert constant-voltage a-c power to variable-voltage d-c power for variable-speed d-c motors and similar power applications.

1060. A Time-Delay Relay. — Gulliksen[7] describes a relay with electronic time-delay feature, as illustrated in Fig. 748. The plate circuit of a high-vacuum tube is in series with the operating coil of a relay.

---

[7] G. W. Gulliksen, "Electronic Devices for Industrial Control," *Elec. Eng'g*, February, 1933, p. 106.

Unidirectional power is applied to the tube and relay by means of a copper oxide rectifier and transformer, from an a-c circuit. When the circuit is closed at S, current from the + terminal of the oxide rectifier starts to rise. This current is at first small since the potential of the grid, with respect to the filament, is immediately negative. This is evident if one considers the circuit oR_1C_1 (Fig. 748) to be in parallel with the potentiometer resistance R_2, since the current flow through R_2 is from o to a. Since R_1 is a high resistance (grid-leak), b is at first at the potential of a, there being as yet no charge in the condenser C_1. But gradually, as the charge in C_1 builds up, the grid (point b) approaches the potential of the filament (point o) and the plate current rises so that the relay operates. The time delay obtained by this means depends upon the values of R_1 and C_1 and upon the variable resistance R_2. Gulliksen suggests a range from 3 minutes to 0.05 second. Harwood[8] shows a similar " electronic timer " operating from batteries or other d-c sources.

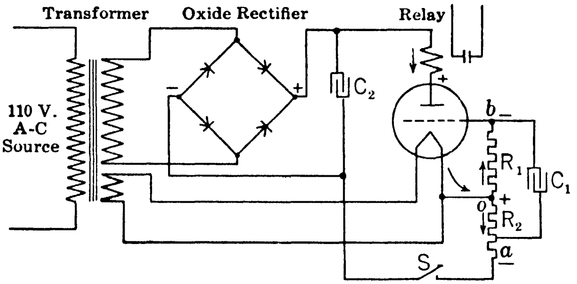

FIG. 748. Electronic-delay feature applied to a relay (Gulliksen).

The Electric Controller and Manufacturing Company (E. C. and M. Co.) has recently developed time-delay and time-current delay acceleration systems which it refers to as " Neo-Time " and " Neo-Time Current " acceleration. In these systems accelerating contactors cut out steps of starting resistance as in the starter of Fig. 735, for example, the timing of the contactors being controlled by a relay which operates when the potential across a neon tube reaches the breakdown value for the tube. The potential across the tube builds up gradually as a 20- to 40-microfarad condenser charges up through an adjustable high resistance. The method is applicable to either d-c or a-c systems (Chapter LV), it being necessary in the latter to rectify the charging current of the condenser, for which a rectifying vacuum tube (Chapter LIX) is used. By varying the resistance through which the condenser charges from 100,000 to 500,000 ohms the time delay of the relay is varied from 3 or 5 seconds to 14 or 27 seconds, depending upon whether the condenser is of 20 or 40 microfarads capacitance. For detailed description of these devices the reader is referred to the bulletins of the company.

---

[8] P. B. Harwood, " Control of Electric Motors," p. 356, John Wiley & Sons.

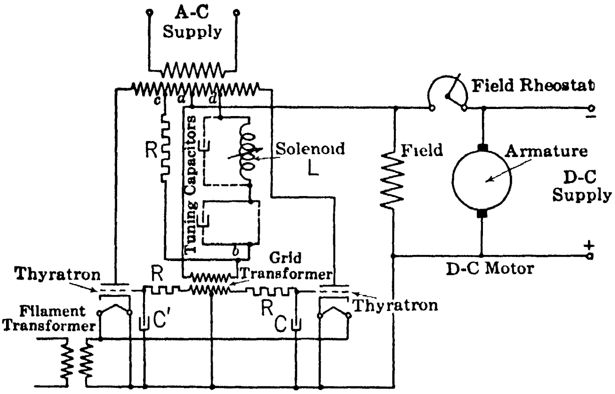

FIG. 749(*a*). Schematic diagram of a thyratron motor speed controller (Garman).

1061. A Thyratron Motor Speed Controller. — In an article by G. W. Garman, cited above, several circuits are given showing electronic devices for controlling the speed of d-c motors. One of these circuits is shown in Fig. 749(*a*). Two thyratrons are connected across the field

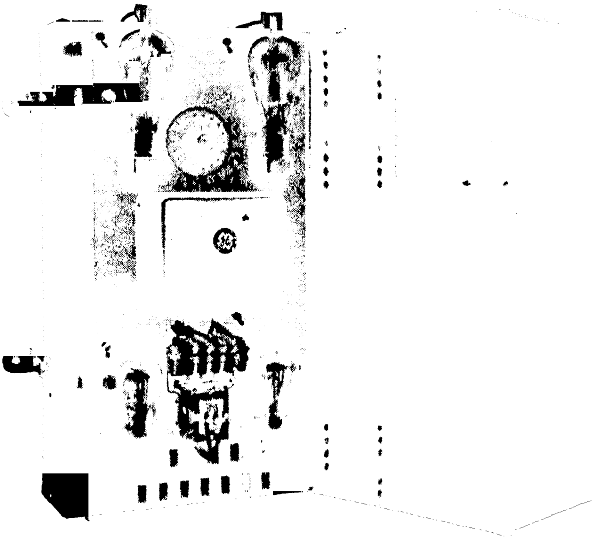

FIG. 749(*b*). Thyratron control panel of the General Electric Co.

of a d-c motor in such a way as to supplement the current from the d-c supply. The motor field rheostat is set for the highest speed desired. The thyratrons add to the field current and bring the motor speed down to a desired value. Control is by means of a bridge circuit in which there is a variable reactor (solenoid), in series with a fixed resistance R, across a constant a-c voltage. By means of a grid transformer connected from the mid-point of the transformer secondary to the junction of R and L (Fig. 749*a*), a constant potential, of which the phase angle may be varied through nearly 180 degrees, may be impressed upon the grids of the thyratrons, thus controlling their outputs (Chapter LIX). Figure 749(*b*) shows a thyratron control panel manufactured by the General Electric Company for a 1-horsepower d-c motor.

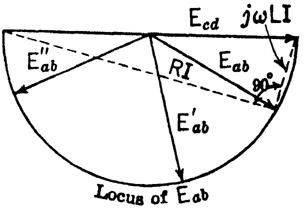

FIG. 750. Diagram showing the varying phase of control voltage with R and L in series.

Figure 750 illustrates the varying phase of the voltage E_{ab} of Fig. 749(*a*). Since the voltage drops across R and L are at 90 degrees, and their sum is constant, the locus of their intersection is a semicircle. Therefore the voltage from *a*, the center of the voltage E_{cd}, to this intersection is constant in value and variable in phase. Further control may be obtained by inserting the condensers which are shown in parallel and in series with the solenoid. Should one or both of the thyratron tubes burn out, the speed of the motor would rise only to the value for which its field rheostat is set.

1062. EXPERIMENT 54-C. — Control by Electronic Devices. — The circuits discussed in §§1060 and 1061 should be set up and the values of the control devices changed until desired results are obtained. Readings should be taken of energy values involved, quickness of response, flexibility, influence of voltage variations in the supply, etc. From the literature references other circuits should be set up and investigated. Special circuits should be devised and tested.

1063. References.

1. W. C. Yates, *Gen. Elec. Rev.*, September, 1926, Trends in industrial control. (See also other articles on this subject in the same issue.)

2. R. T. KINTZING, *Elec. Jour.*, January, 1927, p. 23, Control for d-c motors.

3. B. W. JONES, *Gen. Elec. Rev.*, June, 1928, p. 315, Some recent developments in motor control.

4. Reuben Lee, *Elec. Jour.*, April to October, 1927, College laboratory controllers.

5. JOHN AUCHINCLOSS, *Gen. Elec. Rev.*, July, 1932, p. 389; September, 1932, p. 486, Power station control.

6. E. H. STIVENDER, *Power Plant Eng'g*, May to June, 1931, inclusive, Control of electrical equipment in industrial plants.

7. G. W. HALL, *Elec. World*, August 25, 1934, p. 234.

8. G. W. HALL, *Elec. World*, July 28, 1934, p. 118, Which motor? Which control?

9. K. H. RAPSEY, *Elec. News*, Jan. 1, 1936, p. 23, Motor control equipment . . . for every purpose.

10. G. O. WILMS, *Factory Mgt. and Main.*, July, 1937, p. 91; August, 1937, p. 80, Applying motor controls.

11. F. H. GULLIKSEN, *Elec. Eng'g*, February, 1933, p. 106, Electronic devices for industrial control.

12. L. E. MARKLE, *Elec. Jour.*, September, 1938, p. 359, Control for industrial motors.

13. W. SCHAELCHLIN, *Elec. Jour.*, October, 1935, p. 416, D-c motor starters.

14. B. W. JONES and O. R. SCHURIG, *Gen. Elec. Rev.*, February, 1936, p. 78, The Performance of contactors as circuit interrupting devices.

15. A. J. WILLIAMS, JR., *Elec. Eng'g*, October, 1938, Combined thyratron and tachometer speed control.

16. G. W. GARMAN, *Gen. Elec. Rev.*, April, 1938, p. 202, Thyratron control of d-c motors.

17. GULLIKSEN and STODDARD, *Elec. Eng'g*, January, 1935, p. 40, Industrial electronic control applications.

18. H. D. JAMES, Controllers for Electric Motors, D. Van Nostrand Co.

19. GORDON FOX, Principles of Electric Motors and Control, McGraw-Hill Book Co.

20. P. B. HARWOOD, Control of Electric Motors, John Wiley & Sons.

CHAPTER LV

CONTROLLERS FOR ALTERNATING-CURRENT MOTORS

PART I. POLYPHASE INDUCTION MOTOR CONTROL

1064. The general methods and principles underlying the starting and speed control of polyphase induction motors are treated in §§486 to 490, and in Chapters XLIX and L, so that only the actual controllers, embodying the four principal methods of starting, are described below, viz.:

(1) Across-the-line starters.
(2) Primary-resistance starters.
(3) Auto-transformer (reduced-voltage) starters.
(4) Resistance starters and speed regulators in the rotor circuit.

The first three methods apply to squirrel-cage motors; the last, to wound-rotor motors. The mechanical features of these controllers are similar to those described in Chapters XXV and LIV for d-c motors, and will not be repeated here. Controllers used for induction motors may be of the face-plate, drum, lever, or contactor type, or may be liquid rheostats, etc. The selection of a particular type depends upon the size and voltage of the motor, the service required, the protection desired, etc.

1065. Across-the-Line Starters. — Moderate-sized polyphase motors, when started on light load, can be switched directly on full voltage from standstill, provided that the resulting inrush of current and the line voltage drop are not objectionable from the point of view of other devices connected to the same line. As power systems increase in size larger and larger motors are being built, with suitable rotor resistance and properly reinforced stator windings, so that they can be started upon full voltage without damage to the motors and without objectionable drop of line potential. It is not uncommon to start 50-horsepower 220-volt motors, or 100-horsepower 440-volt motors, in this way. For such starting, special remote-controlled magnetic switches have been developed. A switch of this kind, with overload relays and push-button control, is shown in Figs. 751 and 753. Any number of push-buttons located at different places can be used. All the "start" push-buttons are in parallel and are normally open. All the "stop" push-buttons are in series and are normally closed. When one of the start buttons is pressed down, the circuit of the operating coil of the switch is closed between the line wires *L*1 and *L*3 (Fig. 752) through the control wires *C*1 and *C*3. This causes the main switch to close, and it automatically closes the auxiliary contact *a* between *C*1 and *C*2. The push-button can be released and the coil will continue to hold the switch "in." To open the switch, it is sufficient to break the circuit of the operating coil by pressing one of the "stop" buttons for an instant.

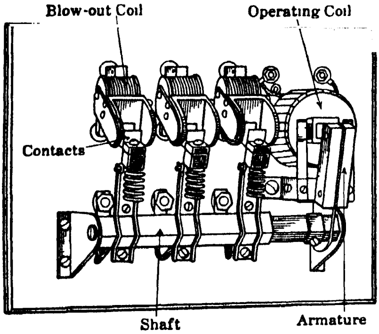

FIG 751 An electrically operated three-pole starting switch.

An important feature of an a-c electromagnet is that it must have some arrangement for preventing or reducing the so-called "chattering" due to a periodic fluctuation of the holding force between zero and a maximum. The usual method is a shading coil (§508) which prevents the total flux in the air-gap from passing through zero at any instant, so that the retaining force is never reduced to zero Another method of accomplishing the same result is to supply the shunt coil of the contactor with direct current, obtained from the a-c circuit by means of a copper oxide rectifier.[1]

In the starter of Fig. 752, when an overload occurs, one of the relay contacts, b_1 or b_2, or both, will break the circuit of the operating coil and stop the motor. These relays may be of the electromagnetic type, but they are usually based upon the thermal principle. In one thermal relay, two current transformers (§428) are inserted in the motor leads, in place of the relay coils. The secondary winding of each transformer is closed through a wire similar to that used in a hot-wire ammeter (§52). A small auxiliary circuit-breaker, in series with the operating coil of the main switch, is kept closed by the tension of these wires. On an overload, the current heats these wires sufficiently to expand them and to trip the circuit-breaker, which in turn opens the main switch. This overload device can be made either self-restoring or to be reset by hand, depending upon the service requirements of the motor.

The overload relays which may be seen in series with the two outer leads in Fig. 753 contain a thermostatic strip which is heated by the passage of the motor current through a heater unit. This heater unit

---

[1] A. L. Sweet, "A-C Contactors with D-C Magnets," *Gen Elec Rev.*, September, 1936, p. 456.

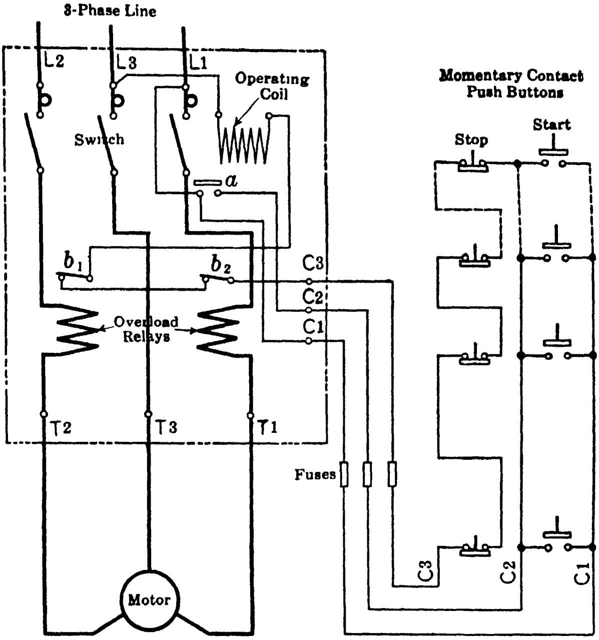

FIG. 752. Push-button connections to the switch shown in Fig. 751.

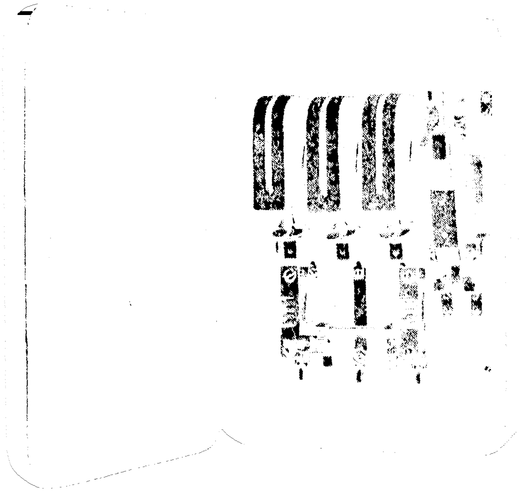

FIG. 753. A commercial across-the-line starter with thermal overload relays.

is selected with regard to the normal current of the motor for which the switch is to be used. When the bimetallic strip reaches a certain temperature it deflects enough to trip the contactor (equivalent to opening relay contacts b_1 and b_2 in Fig. 752). If these heater coils are properly selected they will heat at about the same rate as the motor windings and so trip the switch as the motor approaches an unsafe temperature.

In case of a low line voltage or an interruption of the supply, the starting switch opens automatically, and requires that one of the start buttons be pushed to start the motor. By the use of a "hold-in" start button, the switch can be made to close again automatically as soon as the line voltage is restored. This may be desirable or not, depending upon the nature of the drive.

1066. EXPERIMENT 55-A. — Study of Across-the-Line Starters. — Make a study of available magnetic switches which have been designed, or which may be made suitable, for starting polyphase induction motors at line voltage. Note in particular the means for remote control, provision for under-voltage release or protection, details of overload protection, limitations as to voltage and current for which they are adapted (motor ratings), etc. Examine the blow-out coils, arc chutes, and means of protection to operators and against fire hazard.

Connect the starters to suitable motors and note their behavior under different conditions of supply voltage and motor load. Take readings of starting current peaks and momentary voltage reduction of the supply.

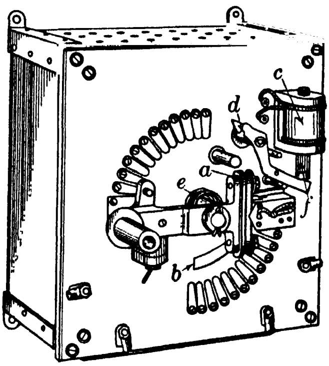

FIG. 754. Manually operated primary resistance starter for a three-phase motor.

Calibrate one or more starters to determine the voltage at which they release, also that at which they again close. Determine the time required for the overload relay to trip at several values of overload current, and to reset after tripping.

1067. Primary-Resistance Starters (Manual). — With a small motor starting on light loads, the inexpensive starter shown in Fig. 754 can be used. It has two resistances, each connected in series with a primary phase. This limits the current in all the three phases, because the current in the third phase returns through the other two line conductors. With a small motor, the resulting unbalance of the line currents is of no consequence. The starter is similar to that shown in Fig. 413, except that there are two rows of contacts, one for each resistance, and the starting arm extends both ways from the center. The two parts of the arm are insulated from each other at *a*. The current connection to the upper phase is through the center piece, and to the lower phase through the copper segment, *b*.

The coil *c* is connected across one of the phases and protects the motor against under-voltage. The starting arm is held in the running position by the latch, *d*, against the spring, *e*. The heavy laminated plunger, *f*, is normally in its upper position within the coil. Should the line voltage drop to a value unsafe for the motor, the plunger falls and trips the switch arm, which returns to the " off " position.

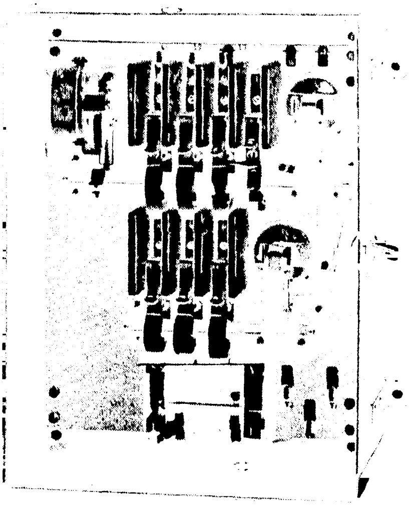

FIG. 755(*a*). Magnetically operated primary resistance starter.

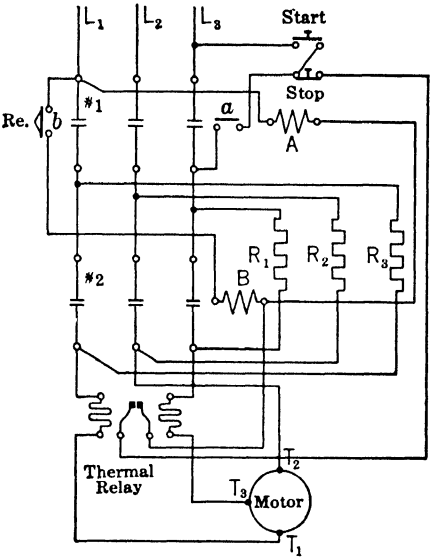

FIG. 755(*b*). Circuit diagram for the starter of Fig 755(*a*) having thermal relay and definite-time acceleration.

1068. Primary-Resistance Starters (Magnetic). — Instead of a manually operated starter such as Fig. 754, in which resistances in series with the motor are cut out, step by step, a magnetic controller may be used to perform a similar function automatically, upon the pressing of a button. Figure 755*a* shows a commercial primary-resistance starter consisting of one triple-pole line contactor with auxiliary relay contacts, one triple-pole accelerating contactor, one definite-time accelerating relay, one temperature overload relay, three starting resistors, and a " start, stop " push-button station. Figure 755*b* is the schematic diagram of such a starter and motor.

Pushing the start button of Fig. 755*b* energizes the closing coil, *A*, of contactor 1, through the thermal relay contacts. The contactor closes and applies power to the motor through the resistors, R_1, R_2, and R_3. An auxiliary contact, *a*, which closes with the contactor, now bridges the contacts of the start button so that it may be released. Also, when contactor 1 closes, the definite-time acceleration relay, *RE*, pendulum-operated, starts its cycle and, at the end of a certain time, closes contacts *b*. This energizes coil *B* of contactor 2, also through the contacts of the thermal relay. Contactor 2 closes and short-circuits the starting resistances. The motor now operates at full voltage, protected by the thermal overload relay against prolonged or excessive overloads and against under-voltage by the shunt coils of the two contactors.

This type of starter is, of course, designed for the starting of squirrel-cage motors. Though it is possible to add to the starter in order to secure more than the one accelerating point this is not necessary in motors of moderate size, and for larger motors it is better to start upon reduced voltage (§1070).

1069. EXPERIMENT 55-B. — Study of Induction-Motor Starters of the Primary-Resistance Type. — Typical devices are described in the preceding sections. The general order of the experiment is the same as in §§569 and 1066. When using the manual starter, for a few positions of the starter arm measure the three line currents; also the voltage across the line, across the motor terminals, and across the resistances, so as to be able to construct vector diagrams of these quantities. Make clear to yourself whether or not the undervoltage coil will protect the motor in all cases against phase failure (§1073), and if not, suggest a simple additional feature that will do so. Follow the suggestions of §1066 in studying the magnetic starter. Try, especially, the effects of various settings of the accelerating relay upon current peaks.

1070. Reduced-Voltage Starters. — The main objection to across-the-line starters is that when the motor is thrown upon full voltage it may draw from 5 to 10 times full-load current at a low power factor. This tends to cause a serious reduction of the line voltage. It also subjects the motor windings to considerable shock and to rapid heating. Even at this large current the starting torque of the squirrel-cage motor unless it is especially designed for high torque, is but little in excess of full-load value. Starting the motor by the insertion of series resistors (§§1067 and 1068), though it has the effect of reducing the motor current to perhaps one-half the value drawn in across-the-line starting, still makes a heavy demand upon the line. Furthermore, since motor torque is proportional to the square of impressed voltage, and this method reduces motor voltage to about half the line value, the starting torque is only about one-quarter that obtained by starting across the line. This is suitable for only those motor applications in which the starting torque is low, as in the driving of fans, in motor-generator sets, etc.

A method of securing the same reduction in motor current without the energy loss attendant upon the use of resistors, and with a current demand from the line only about one-half the motor current, is that in which auto-transformers are used to secure the required reduction in starting voltage. Figure 756 shows three auto-transformers in " star " used in the starting of a motor. When contacts S close, the auto-transformers are connected to the three-phase supply and the motor is connected to some point, p, of each auto-transformer where the voltage is, say, 50 to 70 per cent of line volts. The motor is started at this reduced voltage, and as it approaches synchronous speed the starting contacts, S, are opened, and the running contacts, R, are closed, after which the motor operates at full line voltage, while the auto-transformers are disconnected from the line and from the motor. The same effect is obtained with two less contacts if two auto-transformers are used in V connection.

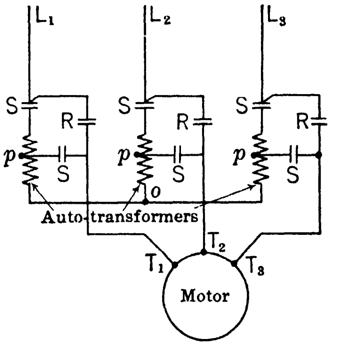

Fig. 756. Simplified diagram of a motor starter using auto-transformers and contactors.

Protective resistances or reactances. In the operation of starting the induction motor by the method just described the motor is disconnected from the starting (reduced-voltage) points, and then connected to the running or full-voltage points of the starter. Since the motor is running at close to synchronous speed when this change is made it may be thought that there will be no current rush when the motor is thrown upon full voltage. This is not the case for two reasons; the values of flux and motor counter emf established when the motor is running at the reduced voltage, and persisting for some seconds after the motor is disconnected, correspond to the starting voltage. Applying double that voltage to the motor will cause a current rush similar to that which occurred when the motor was first started. Moreover, the motor counter emf may happen to be more nearly in phase with, than in opposition to, the applied voltage when the running contacts are made. This may cause an objectionable current rush in large motors. To remedy this, certain "protective" resistances or reactances are sometimes used. It may be desirable to start a large motor on several accelerating points, the motor being started from rest at the minimum voltage at which adequate torque is obtained, and then connected to successively higher voltage taps until full voltage is reached. To avoid short-circuiting sections of the auto-transformers while switching from one voltage tap to the next, and to avoid opening the leads to the motor, "protective" or "transition" resistances may be employed. In Fig. 757, motor leads T_1 and T_3 connect to the center points of two protective resistances, R_t. If points b are connected, for example, to the 60 per cent taps the motor starts with a voltage slightly less than 60 per cent of rated value, owing to the drops in one-half the protective resistances. If points a are now connected to the 80 per cent points the motor has a voltage slightly below 70 per cent, while a moderate circulating current flows through R_t. If points b are now disconnected the motor runs at slightly less than 80 per cent of full voltage, and so on until full voltage is reached.

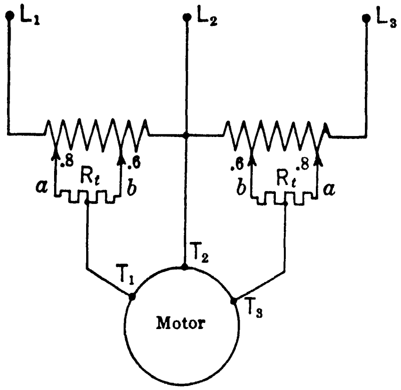

FIG. 757. Protective resistances used on transition points in starting.

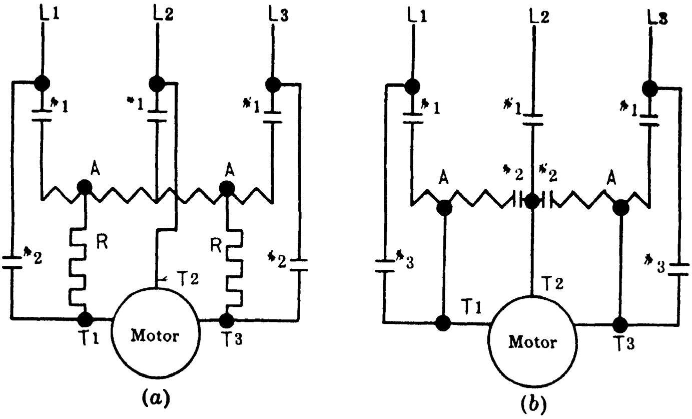

FIG. 758. Types of connection for auto-transformer starters.

A method in which protective resistances are used on one starting point only is shown in Fig. 758. To start the motor, the three-pole switch, 1, is closed. This connects the auto-transformers across the line, and the motor to the transformer taps through the protective resistances *RR*. Switch 2 may now be closed, connecting the motor to full voltage and short-circuiting a portion of each auto-transformer through the protective resistances which limit the circulating current. Switch 1 may now be opened. If desired an additional switch may be inserted in the leads from *A* to *R* to disconnect entirely the auto-transformers from the motor. Instead of resistances *RR*, reactances may be used.

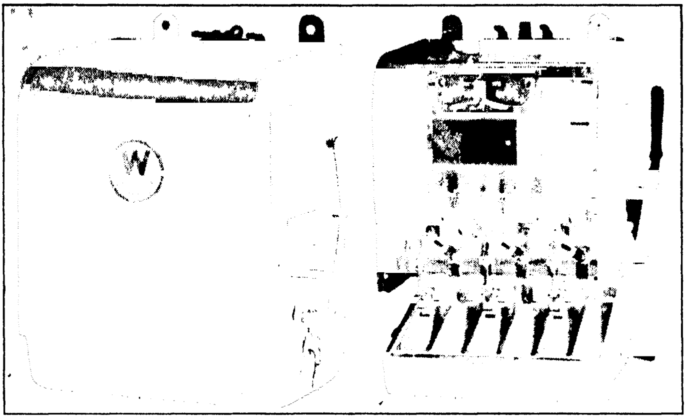

FIG 759 An auto-starter of the oil-switch type (Westinghouse Electric and Mfg Co)

1071. Manually Operated Auto-Starter. — The most common form of starter for squirrel-cage motors employing auto-transformers for reduced-voltage starting is the so-called "auto-starter" or "starting compensator," shown in Fig. 759. The switches are combined into one drum-type switch immersed in oil to limit arcing and burning of the contacts. In the upper part of the case two or three auto-transformers are mounted and several taps are provided so that suitable values of starting voltage may be selected. The starting handle is so limited by means of a mechanical interlock that it is possible to throw the switch only from the "off" position to the "start" position. After the motor gains speed the handle is thrown quickly from the "start" to the "run" position. If the movement is slow the handle stops in the "off" position. Overload and no-voltage protection are usually provided in the starter.

The corresponding diagram of connections is shown in Fig. 760, including the under-voltage and the overload protection. The contacts are shown mounted in three rows, marked *a*, *b*, and *c*. For starting the motor, contacts *b* are connected to *c*. The auto-transformers are then connected to the line, and the motor to the transformer taps. In the running position, the motor contacts of the *b* row are connected to *a*, thereby connecting the motor to the line through the overload relays. In the running position, the operating lever is held by a latch actuated by the low-voltage protective coil. In case of under-voltage, this coil releases the latch and causes the switch to be opened. The circuit of the protective coil is in series with the contacts of the overload relays, so that the same latch releases the switch on an overload. It will be noted that the overload relays are not in the circuit in the starting position of the switch. This allows a larger current to be drawn from the line for starting than would be permissible in regular operation. This elimination of overload protection in starting is also often incorporated when a circuit-breaker or fuses are used in place of overload relays.

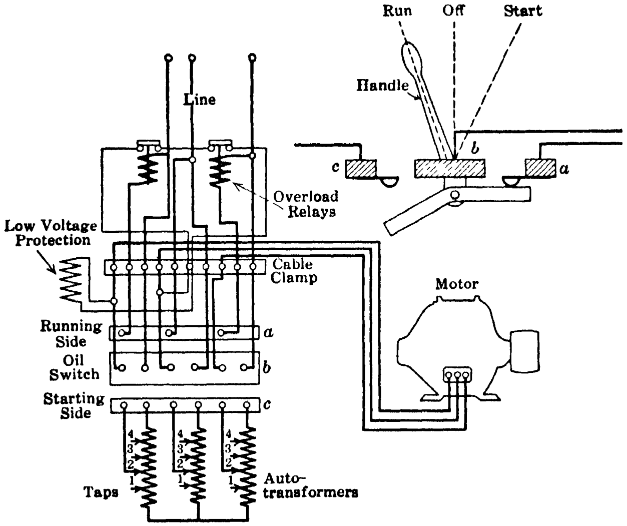

FIG. 760. Manually operated auto-starter with Y-connected auto-transformers.

1072. Reduced-Voltage Starters of the Magnetic-Contactor Type. — The contactor starter shown in Fig. 761 operates on essentially the same principle as that shown in Fig. 760, except that it is electrically operated from a distance by a push-button or master-switch. The six-pole starting contactor makes connections corresponding to those between rows *b* and *c*, and the three-pole running contactor connects *b* to *a*. The change from the starting to the running connections is controlled automatically by the current-limit relay.

The diagram of connections in Fig. 762 refers to a magnetic controller of the same general type as that shown in Figs. 760 and 761, differing from it mainly in the following two particulars:

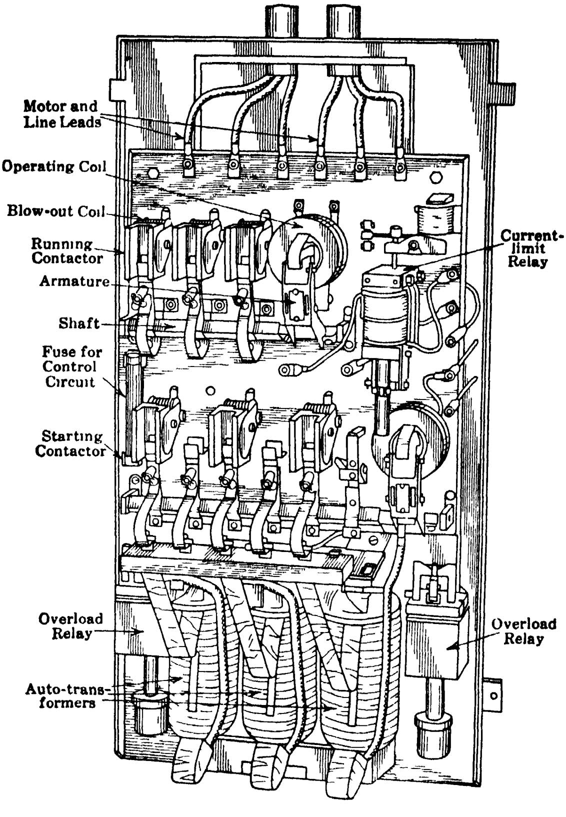

FIG. 761. An auto-transformer starter using magnetic contactors.

(a) The overload relays are of thermal rather than of current type. The starting point on the third auto-transformer goes directly to the motor without being interrupted by the starting contactor. Consequently, the starting switch is five-pole instead of six-pole; the running switch is still three-pole.

(b) Instead of a current-limiting device, the change from the starting to the running connections is controlled by a telechron motor mechanism. The operator simply pushes a lever and lets it go. The correct time interval between the starting and running connections can be adjusted to suit each particular application.

The operation of the automatic reduced-voltage starter for which the circuit diagram is given in Fig. 762 may be explained as follows: Pressing the " start " button causes control current from line $L2$ to flow through the " start " and " stop " buttons to the definite time accelerating relay at point 2, through closed contacts 2–6 in the relay to the closing coil of the accelerating contactor, then through the thermal relay contacts to line $L1$. This causes the starting contacts, S, to close and to start the motor on reduced voltage. At the same time control current passes from 2 through the coil of the under-voltage relay, C, closing the contacts 1–2 around the " start " button. Simultaneously the telechron motor M in the accelerating relay starts up, and at the end of a predetermined time this closes contacts 2–4 and opens 2–6. Opening 2–6 de-energizes the "start" contactor so that it opens and, in doing so, closes contacts 2–5. This allows control current to pass through the closed contacts 2–4, and through the operating coil of the "running" contactor (which closes), and back to the line through contacts 2–5 and the thermal relay. At the same time contacts d open and stop the telechron motor. The induction motor is now running on full line voltage, protected from overload by the thermal relay, and from operating on greatly reduced voltage by the potential relay, C, which gives under-voltage protection (§1057).

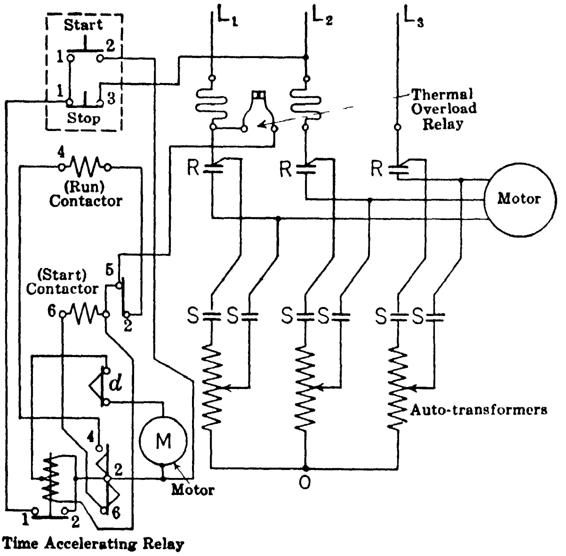

FIG. 762. Schematic diagram of an automatic reduced-voltage starter (General Electric Co).

1073. Protection against Phase Failure and Phase Reversal. — In addition to the overload and under-voltage protection (or release) described above, a polyphase induction motor may be protected, if so desired, against phase failure and phase reversal. Both features may be combined in the same relay.

If one line wire out of three is open, the motor will not start and may become overheated while the operator is looking for the cause of the trouble. To prevent this possibility, two under-voltage relays can be used, one connected across the line terminals 1 and 2, and the other across 2 and 3. The main switch can be connected to these relays, either mechanically or electrically, in such a way that it will not close unless both relays are closed. Such an arrangement will not protect the motor when it is already running, because the revolving magnetic flux induces in the dead phase an emf practically equal to the line voltage. In such an emergency, one has to rely on the overload relays, which must not be set too high If the motor is only partly loaded, it may run single-phase for a considerable time, without tripping the relays, and no particular harm will be done.

A wrong phase sequence may occur after repair men have disconnected the line and connected it again to different generator phases. If two conductors happen to be reversed, the motor will start in the wrong direction (§484). In some applications this may cause damage to machinery, or an accident. Some public-service companies require reverse-phase relays on all elevator motors, to protect themselves against liability in case of an accident.

One type of such relay is similar to a polyphase wattmeter (§126) or motor. With the correct phase sequence, the moving element rotates by a certain angle against a spring or gravity, and keeps the control circuit closed, thus enabling the main switch to be closed and the motor started. Should the phases be reversed, the relay turns in the opposite direction and keeps the control circuit open. One who is familiar with polyphase relations can devise other ways of achieving the same result by different electromagnetic means, based either on a reversal or on a weakening of a mechanical pull with the phases reversed. Such a device could be so made as to develop no mechanical force when one of the phases is open, and could thus serve simultaneously as a protection against phase failure.

1074. EXPERIMENT 55-C. — Study of Induction-Motor Starters of the Auto-Transformer Type. — Various devices of this kind are described in §§1069 and 1073. The purpose of the experiment is to familiarize the student with their connections, electrical and mechanical features, voltage adjustment, and limitations in use. The starting characteristics of the motor itself are covered in §487 and need not be studied here. For each feature of the starter studied, the following points should be ascertained:

1. The basic principle, details of construction, and circuit diagram.
2. Possibilities of adjustment and their effects upon the device itself and upon the motor.
3. Behavior under abnormal conditions, degree to which the device is " fool-proof," and the protective features.
4. Necessary care, replaceable parts, sparking contacts, etc.

Wherever possible, numerical data, and not merely a qualitative judgment, should be obtained.

The report should be partly descriptive of the devices and of the tests, and partly a critical analysis of the starters, discussing their commendable features and the weak points which may cause trouble under severe service conditions. Each adverse criticism should be followed by a constructive suggestion.

RHEOSTATIC CONTROL IN THE SECONDARY CIRCUIT

1075. The principle of rheostatic control in the secondary circuit of wound-rotor motors is illustrated in Fig. 360. This method is used for starting as well as for speed control on intermittent operation, as on cranes, elevators, switching locomotives, etc. The controller itself may be of any of the types described above.

For small motors a *face-plate controller*, similar to the one shown in Fig. 754, is used. Resistance may be introduced either into two or into all of the three phases of the secondary winding. Two resistances are sufficient where a considerable unbalancing of the phases is permissible. An under-voltage and overload release may be provided, with the coils connected in the primary circuit, as in Figs. 760 and 762. On an overload or a failure of the power supply, the starting arm automatically flies to the " off " position, stopping the motor.

The other important types of starters of the secondary-resistance type are described in the remaining sections of this chapter.

1076. A Drum Controller. — Connections to a reversible drum controller[2] for regulating the secondary resistances are shown in Fig. 763. The three lower rows of segments are for the primary connections; the upper three rows serve to short-circuit the secondary resistances in steps. To follow the " forward " connections, the drum segments must be considered as moving to the left, the right-hand segments making contacts with the fingers marked with the subscript 1, and the left-hand

---

[2] For general information on drum-type controllers see §§576 to 582.

segments coming in contact with the fingers marked with the subscript 2. On the "forward" motion of the controller, the line terminal L_1 is connected to the terminal A of the motor, and L_2 to B. On the reverse, L_1 is connected to B and L_2 to A.

The secondary connections are shown for the so-called "single-phase starting." On the first notch, the branch D, D_2 of the secondary rheostat is open, and the starting current can follow only the path F_2, F, E, E_2. On the second notch, D is connected to E_1, thus establishing a new neutral point. On the third notch, D, E_1, and F_1 are connected together. On the remaining three notches, the points D_2, E_2, and F_2

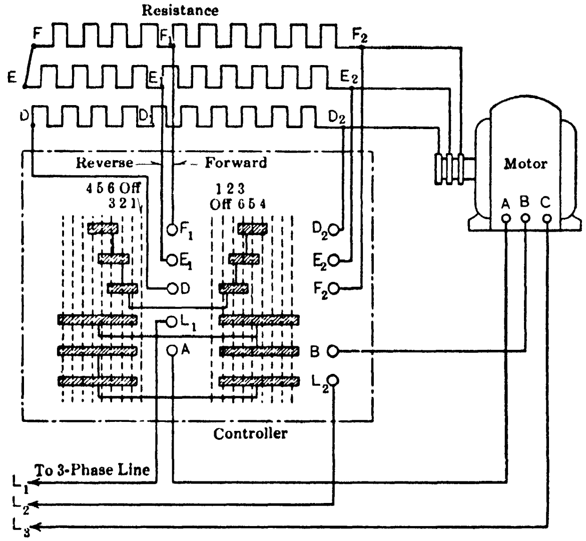

FIG. 763. Drum-type controller for secondary starting and regulating resistances.

of the rheostat are brought in succession to the same neutral point formed by the interconnected drum segments.

Thus, while the three secondary resistances remain unbalanced, the combined resistance is reduced on each successive step. Actual experience shows that under ordinary operating conditions there is no objection to this method of starting. At the same time the number of steps is greatly increased and the number of leads and controller fingers is considerably reduced. Should it be desired to start with the whole Y-connected resistance on the first notch, the connections should be changed as follows: the points D and E on the resistor should be connected together, and the point D on the controller connected to D_1 on the resistor. Reference to Fig. 582, Chapter L, will show, however, that the torque of the motor between zero and one-half synchronous speed is greater with single-phase rotor than with balanced three-phase connection.

1077. Contactor-Type Controllers for Wound-Rotor Motors. — These controllers are of the general type shown in Fig. 761, and are used with comparatively large motors, or where the operating conditions are severe and the service of an exacting nature. Such a controller can be connected to perform automatically all or part of the following operations: It will start, stop, reverse, control the speed of the motor, and provide automatic acceleration, as well as low-voltage and overload protection. In addition, when used with limit switches and other safety devices, it will provide slow-down and emergency stop, and will protect against over-travel. Complete control of the motor is obtained by the operation of a small master-switch placed in the position most convenient for the operator, irrespective of the location of the control panel. The master-switch handles only the small control current for the magnetic contactors.

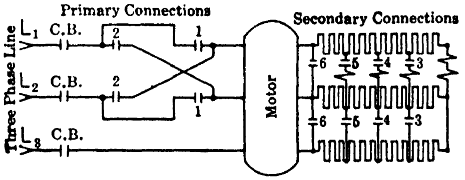

Sequence of Contactors

	Hoist					Off	Lower				
1	○	○	○	○	○						
2							○	○	○	○	○
3	○	○	○	○				○	○	○	○
4	○	○	○						○	○	○
5	○	○								○	○
6	○										○

FIG. 764. A contactor-type controller employing secondary resistances.

A general idea of the standard connections may be obtained from Fig. 764. The motor is protected by the circuit-breaker, *C.B.* On the first notch of the master-switch (not shown in the sketch), one of the two-pole contactors, 1 or 2, is closed, depending on the desired direction of rotation of the motor armature. On the following notches, the two-pole contactors, 3, 4, 5, and 6, are closed in succession, cutting out the secondary resistances in steps. Each contactor is provided with a current-limit coil or relay which prevents the next contactor from being closed as long as the current exceeds a certain value, even though the operator should quickly move the master-switch to the last notch.

1078. Details of an Automatic Contactor-Type Controller. — Figure 765 shows the circuit diagrams of an automatic starter for a wound-rotor induction motor, consisting of two three-pole primary contactors, 1-*F* and 1-*R*, so interlocked that only one can close at a time; two two-pole accelerating contactors (2-*A* and 2-*B*) in the rotor circuit; two series current-limiting relays, *SR*; two overload relays, *OL*; and suitable rotor resistors.

Pressing the forward push-button, *Fwd PB*, completes a control circuit from line L_1 through the reverse push-button (*Rev PB*), the shunt coil of the forward contactor (1 *Fwd Sh Coil*), through the closed " stop " button contacts and overload relay contacts to line L_3.

The forward contactor 1-*F* now closes and the motor starts with all rotor resistance in circuit. The closing of 1-*F* also releases series relay 1 *Fwd SR* which has been held open mechanically (§1056). It also closes the normally open interlock contact 1 *Fwd Int* paralleling the *Fwd PB* contacts. Rotor current now passes through the series relay coils (1 *Fwd SR* and 1 *Rev SR*) which hold the control contacts (*SR Cont*) (Fig. 765*b*) open until the current in the series relay drops to a predetermined value when contacts 1 *Fwd SR Cont* close. This energizes the shunt coil of contactor 2-*A*, which closes and short-circuits one section of the rotor resistance. The series coil of the current-limiting relay, 2-*A SR*, holds open the relay contacts 2 *SR Cont* until the current again drops to the predetermined value when these contacts close and cause the shunt coil of the contactor 2-*B* to close that contactor. This short-circuits the remainder of the rotor resistance and allows the motor to attain full speed.

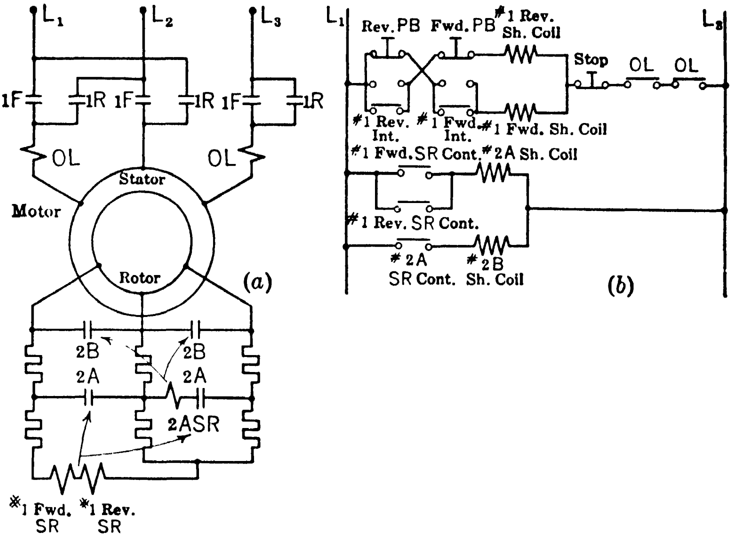

FIG. 765. Circuits of an automatic starter for wound-rotor induction motor: (*a*) motor circuits; (*b*) control circuits.

The motor now operates with overload protection furnished by the overload relays (*OL*) in series with the primary leads, and with low-voltage protection due to the fact that the shunt coil of contactor 1-*F* will release the contactor below a certain voltage. The pressing of the " stop " button causes opening of contactor 1-*F*, which opens the relay contacts in series with the shunt coil of contactor 2-*A*. This opens and, by opening contacts 2-*A SR Cont*, opens contactor 2-*B*. The motor is now ready to start again. If the reverse push-button, *Rev PB*, had been pressed originally the motor would have started up in the opposite direction, but otherwise the functioning of the starter would have been the same. The mechanical interlock between contactors 1-*F* and 1-*R* makes it impossible for one contactor to close in case the other has welded shut.

Frequency relay. The operation of the accelerating contactors in Fig. 765 is controlled by current-limit relays, i.e., by the current in the rotor circuit, which is influenced, in turn, by the load on the motor. It is possible that, if the load on the motor is excessive, the contactors will not operate and the motor will continue to run with high resistance in the rotor circuit and at low speed. One method of preventing this is to have the accelerating contactors operate as a function of rotor frequency, i.e., of motor speed. For this purpose the E.C. and M. Co. has developed a frequency relay which is connected across the rotor in series with a given condenser. By the use of several such relays, each in series with a different capacitance, the relays can be made to drop out at desired motor speeds and so cut out rotor resistance as a function of speed rather than of rotor current.

1079. Liquid Rheostats and Slip Regulators. — For speed control of large wound-rotor induction motors operating on heavy intermittent loads a liquid rheostat in the rotor circuit is sometimes used, being more flexible, less expensive, and smoother in operation than grid resistors controlled by contactors. Liquid rheostats are of two general types: in one, shown in Fig. 766, resistance is varied by changing the height of liquid about fixed electrodes;[3] in the other (Fig. 767) a " torque motor " automatically adjusts the rotor resistance in accordance with changes in the current demand, as described below. In the former type each of the three secondary phases of the motor is connected to a set of electrodes suspended in the upper tank. The operating lever is attached to an arm just above the master-switch. The lever is shown in the "off" position, and the electrolyte, usually a solution of sodium carbonate (commonly known as sal soda or soda ash), is at its lowest level. When the operating lever is moved from the " off " position, the contactors in the primary circuit are operated by the master-switch and the weir is raised. The electrolyte, which is circulated continuously by the pump, rises as the weir is raised. This immerses the electrodes more deeply, decreases the resistance in the rotor circuit, and speeds up the motor. By adjusting the position of the weir, the resistance in the rotor circuit is changed and the speed of the motor regulated. Moving the lever in one direction closes the proper contactors in the primary circuit for starting the motor forward, and raises the weir. Moving the lever in the opposite direction reverses the motor and again raises the weir. The contactors in the primary circuit do not open until the lever has been placed in the " off " position.

---

[3] T. C. Wurts, " Operation of the N. and W. Electric Locomotives," *Elec. Jour.*, October, 1915, p. 473; W. E. Thau, " Liquid Rheostats," *Elec. Jour.*, December, 1914, p. 684.

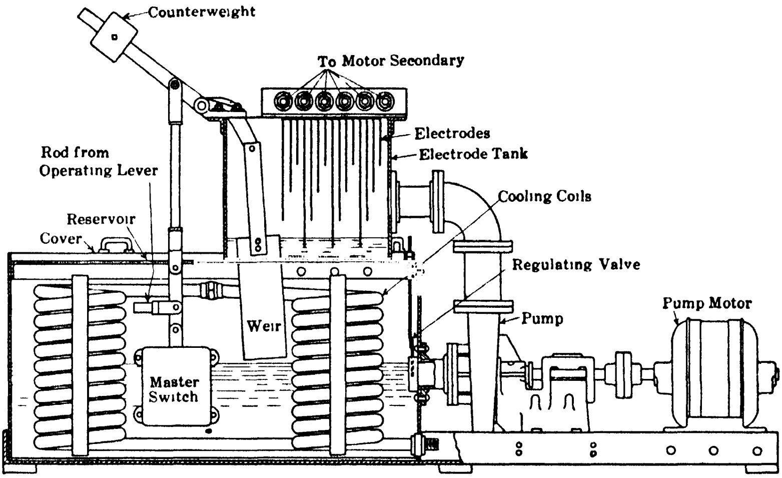

FIG. 766. A controller of the liquid-rheostat type.

A regulating valve in the pump discharge or intake pipe prevents the liquid from rising in the electrode tank at a greater rate than that for which the valve is adjusted. The liquid will therefore rise at the rate determined by the valve setting, even if the lever is moved directly to the " full on " position. The weir, however, is of such a size and design that the electrolyte will flow through to the lower compartment speedily enough to take care of " plugging " when that is practiced.

The liquid " slip regulator " employing the torque motor is found in applications in which flywheels are used in conjunction with induction motors to limit the peaks of power demand. Examples of this are the following:

1. Motor-generator sets in which a wound-rotor induction motor drives one or more d-c generators to supply power to d-c reversing steel mill motors. Here the great peaks of power required as the d-c motors

reverse and carry the steel back and forth through the rolls are reduced by the flywheel which gives up a portion of its stored energy as the induction motor slows down. To make this effect more pronounced the liquid slip regulator is controlled by a torque motor (Fig. 767) through which, by means of series transformers, a fraction of the current to the main motor passes.[4] This current causes the torque motor to assist the counterweight in raising the electrodes and so increasing the rotor resistance and the motor slip. This allows the flywheel to act and also reduces current peaks. As soon as the current demand is reduced the electrodes settle again and allow the motor to speed up and restore the energy lost by the flywheel.

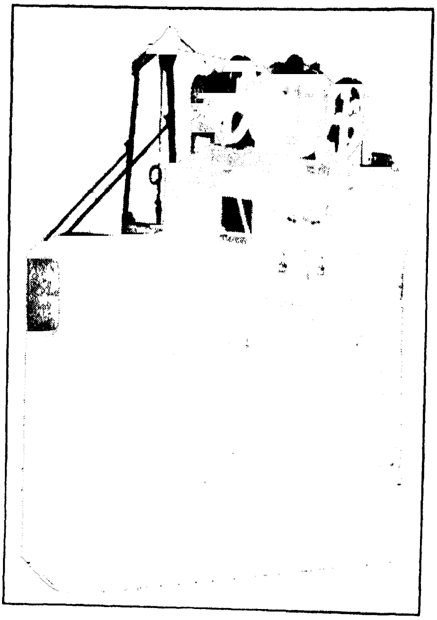

FIG. 767. A liquid slip regulator used in the control of a 3000-hp steel mill motor (General Electric Co.).

2. Induction motors used in roll drive where the flywheel helps carry the load when the ingot passes through the rolls, thus reducing the peak of required power. Here also the liquid regulator, together with the torque motor, operates to limit current demand by inserting resistance and allowing the motor to slow down.

---

[4] W. Sykes and G. E. Stoltz, "The Control of Induction Motors for Rolling Mill Drive," *Elec. Jour.*, 1914, p. 709.

1080. EXPERIMENT 55-D. — Study of Induction Motor Controllers of the Secondary-Resistance Type. — This study should be made in three parts:

a. Drum-type controller (§1076).
b. Push-button starter of contactor type (§1078).
c. Liquid rheostat controllers (§1079).

(a) *Drum-type starter.* Connect a wound-rotor induction motor for starting and speed control, using a drum controller and resistors, as in Fig. 763. Arrange to read stator amperes, volts, and watts, rotor amperes and volts (each phase), and starting torque or mechanical load and speed. Select rotor resistors such that with all resistance in the rotor the currents are limited to, say, $1\frac{1}{2}$ times full-load value on the starting point, with resistances on the succeeding points determined according to some definite plan. For instance, on the second point the resistances might be one-half that on the first point, on the third point half that on the second, etc. With the rotor blocked take all readings, first with the resistances balanced and then with one rotor line open. If desired these readings may be taken at a reduced voltage and converted to rated-voltage values by multiplying currents by the direct ratio of voltages, and torques by ratio of voltages squared (§896).

With the motor coupled or belted to a d-c generator or similar load (§898) maintain the generator field current and armature circuit resistance constant and take readings on each point of the controller, moving the starter handle ahead one point each time the currents drop to a particular value, for instance, to normal amperes. To make the starting period cover a sufficiently long time either the supply voltage may be held at a reduced value or the opposing torque may be made high.

A run should also be made using the controller to adjust the speed while load torque is held approximately constant.

(b) *Contactor-type starter.* Collect the necessary contactors, current-limit series relays, resistors, overload relays, push-button station, etc., to wire up a wound-rotor motor as in Fig. 765. Mount the contactors on a suitable panel, meantime studying details of construction and methods of adjustment. Make a detailed wiring diagram of connections, and after this has been checked and approved wire up the motor and controller. Include a recording ammeter and tachometer, if available.

Provide a d-c generator as load, with its field separately excited and its armature connected to an adjustable resistance load. Try out the starter in forward and reverse operation and including "plugging," i.e., from forward to reverse without first stopping the motor. See that all contactors and relays are in proper adjustment. Take readings of current, time, and speed for different types of loads on the motor, for example: (1) approximately constant torque obtained by holding generator field and armature currents constant; (2) with torque proportional to the speed as with constant generator field and fixed load resistance; (3) torque increasing nearly as the square of the speed, which may be obtained by belting an exciter to the generator, holding the field of the exciter constant so that it will supply a generator field current proportion to speed, while maintaining the generator load resistance constant. (Of course the inertia of the motor and generator will account for a large part of the opposing torque during acceleration.)

Take readings of motor currents and speed against time for each type of load, and at several values of supply volts, to the minimum at which the contactors will operate.

(c) *Liquid rheostat.* Investigate the advantages of using liquid resistors for the starting and speed control of wound-rotor induction motors.

PART II. SYNCHRONOUS MOTOR CONTROL

1081. Automatic Starters for Synchronous Motors.—In Chapter XLIV methods of starting synchronous motors were discussed and simple diagrams given to illustrate the starting of the motor at reduced voltage, using auto-transformers. It is proposed to show in slightly more detail the automatic control circuits required for starting three-phase synchronous motors, both on full line voltage and on reduced voltage.

In manual-control starting of synchronous motors (§859) the d-c field circuit of the motor is closed when, in the judgment of the operator, the motor has nearly enough attained synchronous speed. Any automatic starter must exercise a similar judgment, i.e., it must not energize the field too soon, since then the motor cannot pull into step, and it should not wait unduly, as then too much time is wasted and the motor may overheat. The usual ways of accomplishing this selection are: (a) by the use of a definite-time relay so set that the motor, carrying a certain load, will have had time to reach about 95 per cent of synchronous speed before the relay operates, or (b) by the use of a frequency-sensitive relay which will act when the frequency induced in the field winding by the motor slip has fallen to, say, 5 per cent of supply frequency. In the control circuits of §§1082 and 1083 these two methods are illustrated.

1082. Typical Full-Voltage Starter.—Because of its greater simplicity, lower cost, and higher starting torque full-voltage starting is generally preferred for modern motors designed with that service in mind, and for systems in which the high initial current is admissible.

Figure 768 is the panel of a modern semi-magnetic synchronous motor starter for full-voltage service. The schematic diagram of circuits is given in Fig. 769. The significance of the several symbols is as follows:

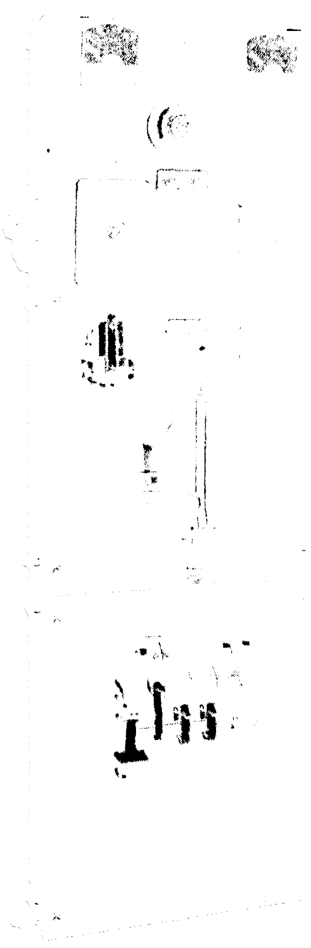

Fig. 768. Panel of a semi-automatic synchronous motor starter for full-voltage service (Westinghouse Electric and Mfg. Co.).

LE = line contactor — contacts or closing coil.
OLR = thermal overload relay.
PFR = power-factor field removal relay, the function of which is to open the d-c field whenever the current drawn by the motor is of low lagging power factor, either at start or as the result of the motor's falling out of step.
FC = field contactor.
TRI = auxiliary time-sequence or time-delay relay (§1056).
FR = field application relay, telechron-motor driven.

The action of the full-voltage starter of Figs. 768 and 769 may be explained as follows:

A-c power being available, pressing the "start" button energizes the coil *LE* which closes the line contactor *LE* and throws the motor across line voltage. At this the motor, with its field short-circuited through the discharge resistance, starts up and, in a time which depends upon its torque and also upon the load conditions, approaches synchronous speed. The closing of contactor *LE* bridges around the start button and thereafter energizes the control circuits, control energy coming from the supply lines either directly or through a step-down transformer. Two relays now act: the power-factor removal relay, *PFR*, due to the low power factor of the starting current, opens the normally closed contacts *PFR* in series with contacts *FC*; also, the auxiliary time sequence relay, *TRI*, operating by direct current through the full-wave copper oxide rectifier, picks up after a brief delay and closes relay contacts *TRI* to complete the circuits through the coil and telechron motor of the field application relay, *FR*, set to close after a definite time. When *FR* operates it closes the field contactor *FC* and applies the d-c field to the motor which then pulls into step.

With the field of the motor excited its power factor rises or even becomes leading and the power-factor field removal relay *PFR* again closes. Meantime the closing of *FC* broke the circuit of the relay *TRI*, which opened, and the starting cycle was complete.

If for any reason the synchronous motor falls out of step it cannot resynchronize until after the d-c field is removed. The power-factor field removal relay acts during the first slip cycle after pull-out to disconnect the field. This permits the motor to speed up and again synchronize as before, with the advantage that now the motor starts, not from rest, but from a speed near synchronism.

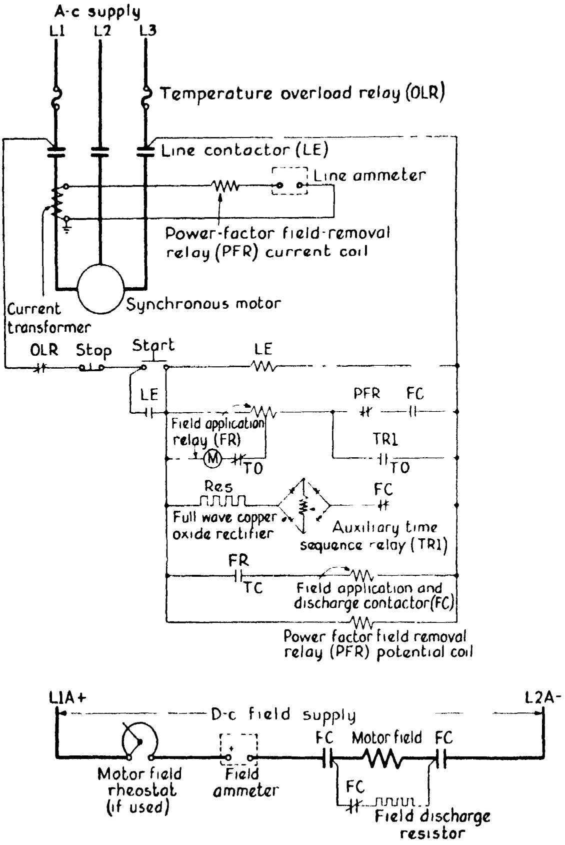
A-c supply
L1 L2 L3
Temperature overload relay (OLR)
Line contactor (LE)
Line ammeter
Power-factor field-removal relay (PFR) current coil
Current transformer
Synchronous motor
OLR Stop Start LE
LE
PFR FC
Field application relay (FR)
M
TO
TR1
TO
Res
FC
Full wave copper oxide rectifier
Auxiliary time sequence relay (TR1)
FR
TC
Field application and discharge contactor (FC)
Power factor field removal relay (PFR) potential coil
L1A+
D-c field supply
L2A-
FC Motor field FC
Motor field rheostat (if used)
Field ammeter
FC
Field discharge resistor

FIG. 769. Circuits of the full-voltage synchronous motor starter of Fig. 768.

1083. Reduced-Voltage Starter for Synchronous Motors.[5] — Figure 770 gives in schematic form the circuits of a reduced-voltage starter, using certain of the contactors which were employed in Experiment 55-D for the wound-rotor induction motor. The meaning of the several symbols will be evident as the action of the starter is explained.

As soon as the exciter bus is energized coil E acts to close control contacts E and complete the circuit to the start button.

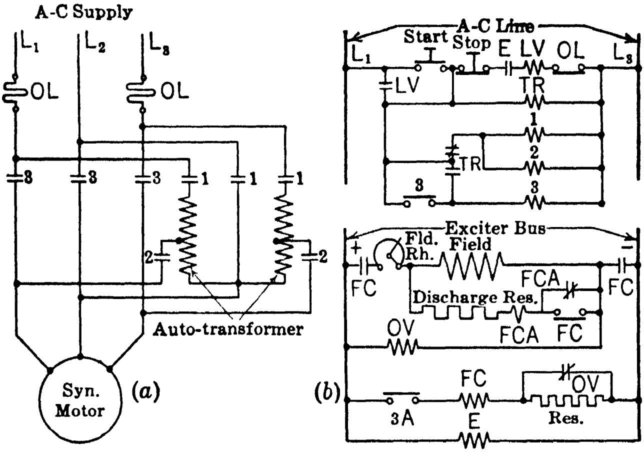

Fig. 770. Typical control circuits for reduced-voltage starting of synchronous motors.

Pressing the start button actuates the low-voltage relay, LV, and closes the control contacts LV around the start button so that it may be released, causes the transfer relay TR to begin its cycle, taking current through the normally closed contacts TR, and also energizes the shunt coils of contactors 1 and 2 which close and start the motor on reduced voltage.

Meantime the field of the motor is closed through the discharge resistance, the hold-open coil FCA, and normally closed contacts FCA of a double-coil field contactor. Through this circuit there flows an induced current which at first is of supply frequency and which remains nearly constant as the motor speeds up, until synchronism is approached when both value and frequency of this current decrease. When the transfer relay, TR, acts it de-energizes the shunt coils of contactors 1 and 2 but energizes the coil of running contactor 3, which closes and completes circuit through interlock contacts 3 and $3A$.

---

[5] R. Lee, "College Laboratory Controllers," Part VI, *Elec. Jour.*, October, 1927, p. 513.

Now the closing coil of the field contactor, *FC*, is across the exciter voltage so that it exerts a pull tending to close the field contactor. At first it is prevented by the opposing coil *FCA*. As the frequency and value of the current induced in the field diminish, the holding power of coil *FCA* also decreases until the closing coil of contactor *FC* shuts that contact and applies direct current to the field, thus completing synchronization.

In case the exciter voltage rises abnormally, so that there is danger of the coil *FC* overheating, the overvoltage relay, *OV*, operates and opens the normally closed contacts which shunt the resistance in series with coil *FC*, thus reducing the current in the coil to a safe value.

In the event of low line voltage or prolonged overload either relay *LV* or *OL* will stop the motor.

1084. EXPERIMENT 55-E. — Study of Synchronous-Motor Starters. — Either the full-voltage or the reduced-voltage automatic starter should be studied somewhat in the manner indicated in §1080 for the wound-rotor induction motor. After a study of available equipment, circuit diagrams should be made and checked, and the motor wired up to start. Suitable adjustments should be made and data taken of starting currents, time required for synchronization, and effects of a-c supply voltage, exciter voltage, etc. If possible oscillograms (Chapter LVII) should be taken of armature and field currents during the starting period.

1085. References.

1. P. B. HARWOOD, Control of Electric Motors, John Wiley & Sons.
2. H. D. JAMES, Controllers for Electric Motors, D. Van Nostrand Co.
3. GORDON FOX, Principles of Electric Motors and Control, McGraw-Hill Book Co.
4. G. H. HALL, Motor and Control Applications, McGraw-Hill Book Co., 1937.
5. H. D. JAMES and J. H. GRAYBILL, *Elec. Jour.*, July, 1924, p. 335, The control of synchronous motors.
6. R. M. MATSON and R. E. R. PARRY, *Gen. Elec. Rev.*, October, 1925, p. 703, Automatic starting of synchronous motors.
7. C. C. LEVY, *Elec. Jour.*, April, 1926, p. 150, Automatic control for synchronous condensers.
8. R. M. MATSON and D. W. McLenegan, *Gen. Elec. Rev.*, September, 1926, p. 707, Choice of control for synchronous motors in industrial plants.
9. REUBEN LEE, *Elec. Jour.*, September, October, 1927, College laboratory controllers.
10. N. L. HADLEY, *Elec. World*, April 29, 1933, p. 550, Synchronous motor excitation control.
11. M. N. HALBERG, *Gen. Elec. Rev.*, May, 1933, p. 244, New developments in synchronous motor control.

12. J. D. Ryder, *Electronics*, April, 1936, p. 31, Tube control of a-c motors.

13. A. L. Sweet, *Gen. Elec. Rev.*, September, 1936, p. 456, A-c contactors with d-c magnets.

14. W. I. Bendz, *Elec. Jour.*, April, 1937, p. 155, Selecting industrial control for a-c motors.

15. L. E. Markle, *Elec. Jour.*, October, 1938, p. 403, Control for squirrel-cage induction motors.

16. T. B. Montgomery, *Elec. Rev.*, September, 1938, p. 9, Low initial-current starters for synchronous and induction motors.

CHAPTER LVI

MERCURY-ARC RECTIFIER

1086. A rectifier is a device for converting alternating currents (single-phase or polyphase) into unidirectional current. This unidirectional current may either have pronounced undulations, or may be practically steady, i.e., continuous. A classification of various types of rectifiers will be found in §866.

Hot-cathode rectifiers may be divided into those containing appreciable amounts of some easily ionizable gas or vapor, and those in which current is due to practically pure electronic emission from the cathode. The former may again be subdivided into those in which the vapor is that of the substance of the hot cathode itself, and those in which a neutral gas is used. We thus have the following three kinds of hot-cathode rectifiers in practical use:

(a) Mercury-arc rectifier, the cathode being a pool of mercury; such rectifiers are the subject of this chapter. Closely similar to this are the " ignitron " and " thyratron " (see Chapter LIX).

(b) Tungsten-argon rectifier (known in the trade under the names of tungar, rectigon, etc.), in which an incandescent tungsten filament is used as cathode, the bulb being filled with an inert gas, argon (§1196).

(c) Pure-electron rectifier, also known as the kenotron (§1176).

1087. Fundamental Connections. — A small single-phase mercury-arc rectifier, used for charging low-voltage storage batteries, is shown in Fig. 771(*a*). It consists of a glass bulb, K, into which are sealed two main positive terminals or anodes, A, A', usually made of graphite, a starting anode, C, and a negative terminal or cathode, B, which is a pool of mercury. The upper part of the bulb serves as a condensing chamber for mercury vapor. As far as possible, all gases other than mercury vapor are exhausted from the tube, and the bulb is then sealed.

The anodes are connected to the secondary winding of a transformer whose primary is connected to a source of a-c supply. The d-c load, in this case the storage battery, J, to be charged, is connected between the cathode and the middle point, O, of the transformer secondary. A steadying inductance, L, is connected in series with the load, to smooth down current fluctuations and to prevent the arc from going out when the applied a-c voltage passes through zero. A current-limiting resistance, *R*, is shown in series with the starting anode. For further details of connections, see §§1092 and 1094.

When the transformer winding is inaccessible, or has no mid-point tap, the diagram of connections shown in Fig. 771(*b*) may be used. Two balancing inductive coils, *E*, *F*, are connected across the transformer secondary, *HG*, and their junction point, *D*, takes the place of the middle point of the transformer winding. With iron cores, the magnetizing current of these choke coils can be kept quite low.

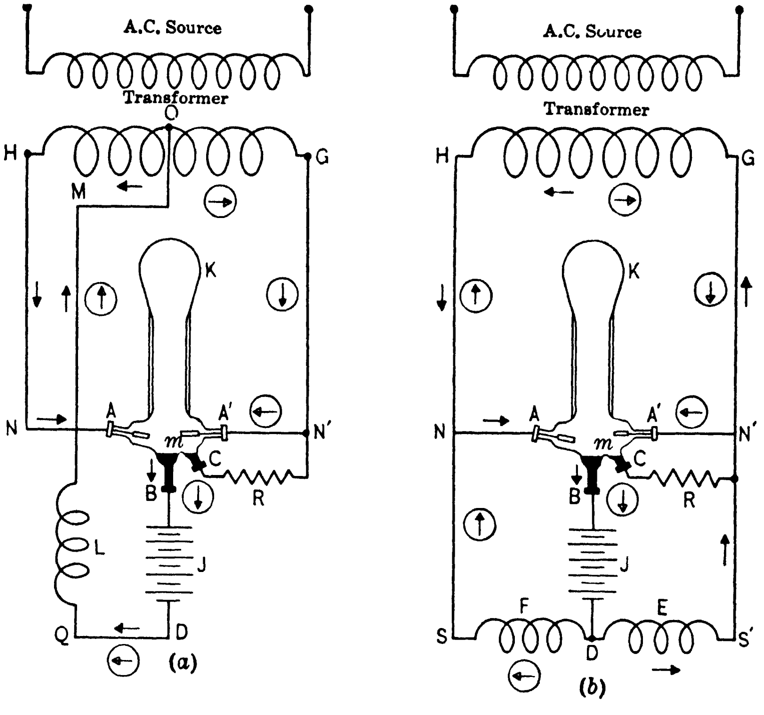

FIG. 771. A single-phase glass-bulb mercury-arc rectifier, showing two ways of obtaining the neutral point.

Mercury rectifiers are used for charging storage batteries, operating special arc lamps, X-ray coils, electrolytic baths, d-c motors, etc. Large-capacity, steel-enclosed, mercury-arc rectifiers, operating on the same principle as the glass-bulb rectifiers, are gradually replacing synchronous converters in d-c light and power distributing systems, in railway substations, etc.[1] Such rectifiers are built in capacities up to

---

[1] For a more detailed treatment see L. B. W. Jolley, "Alternating-Current Rectification," Wiley; K. W. Müller, "Der Quecksilberdampf-Gleichrichter," Springer; J. A. Fleming, "Mercury Arc Rectifiers and Mercury Vapor Lamps," Pitman; A. Güntherschulze, "Elektrische Gleichrichter und Ventile," Kösel & Pustet.

3000 kw at 600 volts, and 6000 kw at 3000 volts. They are made in smaller ratings to 30,000 volts for radio work.

Operation of the rectifier is started by tilting the tube (Fig. 771) until the mercury in the small pool of the starting anode, *C*, bridges from *C* to *B*, allowing current to flow in through the limiting resistance, *R*. As the tube is tilted back again, an arc is produced when the mercury bridge is ruptured. This spark at the surface of the cathode pool, *B*, creates a momentary hot spot on the surface of the pool and is followed, if the applied voltage is sufficiently high, by an arc which strikes between that electrode which is momentarily positive (*A* or *A'*) and the mercury pool *B*; thus a current flows through the tube from anode to cathode.

When the terminal *H* of the transformer is at a higher potential than *G*, the current follows the path *HNABDQMO*, as shown by the plain arrows. The anode *A'* is then inactive. When the potential of *G* is higher than that of *H*, the path of the current is *GN'A'BDQMO*, as shown by the encircled arrows. The direction of the current through the battery, *J*, remains the same, and thus both alternations of each cycle are utilized for charging the battery.

1088. Unidirectional Conduction. — During operation of the rectifier a luminous crater is formed on the surface of the mercury and is maintained at a high temperature (around 2000°C), while the anode remains comparatively cool.

This phenomenon of conduction in one direction is explained on the basis of copious liberation of electrons by a hot body, in this case by the mercury crater. A large number of free electrons are present in mercury which, at high temperatures, pass out through the surface. Being negatively charged, these electrons move against electrostatic lines of force, that is, from a lower to a higher potential. Therefore, with a sufficiently high applied voltage, they are projected at a considerable velocity into the space occupied by the mercury vapor.

Atoms of mercury vapor, like those of other bodies, consist of central nuclei, positively charged, and of negatively charged surrounding electrons. A free electron, accelerated from the hot cathode, finally collides with a mercury atom, causes a bound electron to be detached from it, and in turn is accelerated towards the anode, leaving the atom positively charged. This is known as ionization by collision; as a result, many billion times more free electrons are produced than have been emitted by the crater. The detached electrons in turn ionize other neutral atoms and produce additional positive ions. These move in the direction of the lines of force, that is, toward the cathode, so that under established conditions there is a stream of positively charged particles toward the cathode. They bombard the crater, which is of small area, keeping it heated to a white heat, and in this manner permit a continuous liberation of electrons. Recombination of electrons with positive ions into neutral atoms goes hand in hand with ionization, so that the total number of ions, at a given current and voltage, remains constant.

From the foregoing description it is evident that the mercury-vapor tube can conduct current only in at the momentarily positive electrode (A or A' of Fig. 771) and out at the cathode, B. Thus the hot-cathode mercury-vapor tube may be used as a rectifier of a-c power.

Measurements with an exploring electrode show a nearly constant voltage drop of 5 to 9 volts near the cathode, and a drop of about 5 volts at the anode, so that the mercury rectifier possesses what might be called an electrode counter emf of about 12 volts. The voltage drop in the arc itself is from 0.05 to 0.2 volt per centimeters of its length.[2] Thus, in a large high-tension rectifier of the steel-enclosed type, with an arc 1 meter long, the total drop is about $12 + 0.1 \times 100 = 22$ volts. In a small low-voltage glass bulb for charging batteries, the total internal drop is about 15 volts. This drop is fairly independent of the magnitude of the current passing through the device. It will be seen that in a high-tension rectifier (say for 3000 volts a-c) this drop constitutes but an insignificant percentage of the total voltage, while in a low-voltage circuit the drop in voltage and the percentage of energy loss are quite appreciable.

From the above it is evident that the potential of the (positive) cathode is but little, say 12 to 22 volts, below that of the most positive anode and that, as soon as any anode becomes negative with respect to the cathode, or even, while positive, less than 12 volts above the cathode, its current flow is cut off.

For further details on ionization of mercury vapor, the reader is referred to special books on conduction of electricity through gases, to Chapter LIX, and to numerous articles in physics periodicals.[3]

The actual pressure of mercury vapor may be determined by various means, such as the use of the McLeod gauge, hot-wire gauge,[4] or of the optical-lever manometer, by connecting a high-voltage lead from an induction coil to a terminal of the tube (glow test), and by observing the condensation temperature. For details see special treatises on vacuum tubes and on measurement of low pressures.[5] A simple yet sensitive test for vacuum is as follows: Assuming the tube, such as shown in Fig. 771, to be initially upside down; turn the tube very slowly and observe whether any gas can be trapped under the cathode baffle plate. If no gas can be trapped, the tube is as it should be. The rectifier may still be operative with small bubbles trapped. If the tube does not leak, small amounts of gas may be absorbed by running the tube at a low current, say 10 amperes.

---

[2] Marti and Winograd, "Mercury-Arc Rectifiers," Chapter II, McGraw-Hill Book Co., 1930.

[3] See also Dr. I. Langmuir's articles on the nature of the mercury arc, in the *General Electric Review*, vol. 26 (1923), p. 731; vol. 27 (1924), pp. 449, 538, 616, 762, 810.

[4] A direct-reading hot-wire vacuum gauge, consisting of four resistances arranged in the form of a Wheatstone bridge and based on the principle of heat conductivity of gases at low pressures, has come into use. See O. K. Marti, "Rectification of Alternating Currents," *Journal A.I.E.E.*, vol. 45 (1926), p. 840.

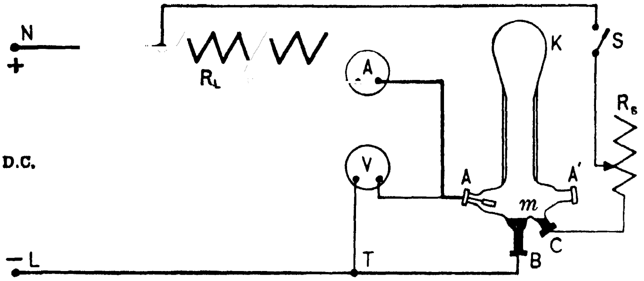

FIG. 772. Diagram of connections for obtaining voltage-current characteristics of the mercury-vapor arc.

1089. EXPERIMENT 56-A.[6] — Internal Voltage Drop in a Mercury-Vapor Arc. — The physics of the arc is explained in §1088; the purpose of the experiment is to measure the internal drop with various values of direct current (Fig. 772) supplied from an independent source. The tube should be securely supported by means of ring stands in its normal operating position, care being taken to heat-insulate all supporting contacts of the tube by asbestos tape or asbestos wool. The starting resistance, R_s, should be able to withstand direct connection across the voltage used to start the arc. For a 20-ampere tube this will be approximately 40 ohms. The voltmeter should have a range to accommodate the line voltage even though the voltage drop will be quickly reduced to about 15 volts after the current once starts to flow through the main anode to the cathode. A meter of this range will not be damaged if the arc should go out. Strike an arc by tilting the tube until the mercury pools make contact at *m*, and then right the tube. See whether this is possible with reversed polarity of the d-c supply. With the arc established proceed to:

---

[5] Saul Dushman, " Production and Measurement of High Vacuum," Schenectady, 1922; Newman, " The Production and Measurement of Low Pressures," London, 1925.

[6] Some of the instructions in the following experiments were furnished by Mr. D. C. Prince, to whom the authors wish to express their sincere appreciation.

1. Vary the current in steps up to 1½ times the rating of the tube, and at each step read the arc voltage drop.
2. Repeat test 1 with both anodes in parallel, to determine the effect of anode area.
3. Repeat test 1 while cooling the tube with an ordinary desk fan or by more effectual means.

Report. Plot curves of voltage drop against amperes as abscissas and give theoretical reasons for their general shape.

1090. Means for Increasing Arc Stability. — Should the load on the rectifier drop below 5 amperes, the main arc is likely to go out. In applications for which it is essential to keep the arc going continuously, even at no load, two or more auxiliary (or holding) anodes are provided near the cathode (Fig. 775). These anodes are supplied with current from the same a-c source, through a small low-voltage transformer, and as they pass a current of about 5 amperes they maintain a hot crater at the cathode at all times. It is also possible to place an artificial load of somewhat over 5 amperes in parallel with the actual d-c load, and in this manner to maintain the arc, at the expense of a constant power loss.

Even with both half-waves of the a-c voltage utilized, the arc would go out (without auxiliary anodes) at the end of each alternation, because there would be no voltage to overcome the internal emf drop in the tube itself. To prevent this, the inductance L (Fig. 771) is used. Its effect is to induce an emf sufficient to carry the arc over the small parts of each half-cycle when the applied voltage passes through zero. Consider the conditions near the end of the half-cycle marked by the plain (non-encircled) arrows. As the voltage between A and B approaches zero, the current in L also decreases, and this decreasing current, according to the law of electromagnetic induction, causes an induced emf in the direction of the current. This helps the available voltage between A and B and also anticipates a potential difference in the proper direction between the inactive anode A' and the cathode. As a result, both anodes are active for a short fraction of a cycle and the arc is transferred without interruption. In Fig. 771(*b*), the coils E and F function in a similar manner at the ends of alternate half-cycles.

Figure 773 shows the effect of the smoothing inductance, L. If no inductance were present the current to the resistance load would tend to follow the sine-form curve of I_1, thus dropping to zero twice per cycle of the supply. The inductance holds the current over for the fraction of a cycle, π/k, after the a-c voltage has dropped to zero, giving the current the curve shown as I_2. Thus, for an instant current flows from both anodes to the cathode, with the result that the attenuated currents,

I_2, of successive alternations overlap, giving the current I_t. In I_t the fluctuations are less than those for a rectified pure sine wave. With a very high inductance, L, or with a large number of phases and corresponding number of anodes, the rectified current is only slightly rippled and for most purposes may be considered to be constant in value (Fig. 783).

Degree of rectification. DR is arbitrarily defined as the ratio

$$DR = \frac{\text{Average value of rectified current}}{\text{Effective value of rectified current}} \quad . \quad . \quad . \quad . \quad (1)$$

This is evidently the same as the ratio of the readings of a d-c ammeter of the moving-coil, permanent-magnet type, and of an a-c ammeter, each in the output lead of the rectifier.

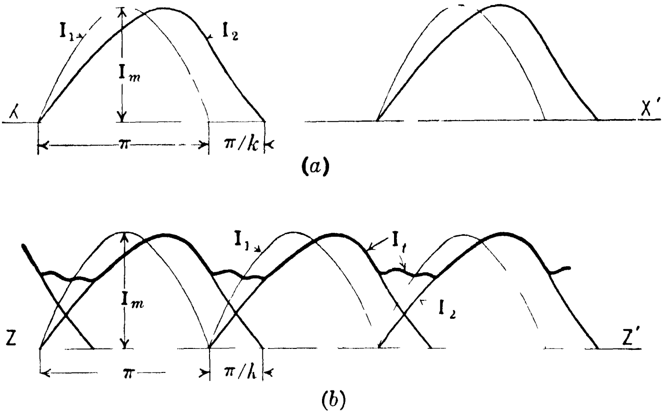

FIG. 773. The effect of an inductance upon the load current wave (a) with half-wave circuit; (b) with full-wave circuit.

1091. EXPERIMENT 56-B.—External Current and Voltage Relations in the Single-Phase Mercury-Vapor Arc Rectifier.—The purpose of the experiment is to investigate the relationship between the a-c and d-c currents and voltages and to determine experimentally their wave form (Chapter LVII) by means of an oscillograph. In order to be independent of inductance for maintaining the arc, it is preferable to provide an auxiliary anode A'' (Fig. 774) excited from a separate d-c circuit. For a 20-ampere tube, R_s should approximate 35 or 40 ohms and R_A about 25 ohms, for a d-c source of 110 volts. The source of a-c voltage must be adjustable from zero to normal in small steps. In the runs below, only the ammeter and voltmeter readings are specified, it being understood that the wave shapes of these quantities should also be obtained if an oscillograph is available.

1. Insert a resistance load that draws a normal d-c current at the normal applied voltage. Reduce the a-c voltage to zero in several small steps and read all the meters.

2. Insert an inductance in the load circuit, with the resistance of run 1 left in the circuit. Repeat the preceding test, and in addition read the separate voltages (with both d-c and a-c voltmeters) across the load resistance and inductance.

3. Replace the load resistance by a storage battery, and then by a d-c motor, and repeat the preceding runs, with and without an inductance.

Report. Plot the observed data in the form of curves. Bring out the effect of inductance and compute values of the degree of rectification (§1090). Calculate the ratio of the average d-c voltage and effective a-c voltage (between the neutral point *D* and anode *A* or *A'*). Knowing the battery counter emf, explain the differences in the behavior of the rectifier with a battery, with a motor and with a plain resistance. Look up some of the references given at the end of the chapter, and compare your results and conclusions with statements made in those articles.

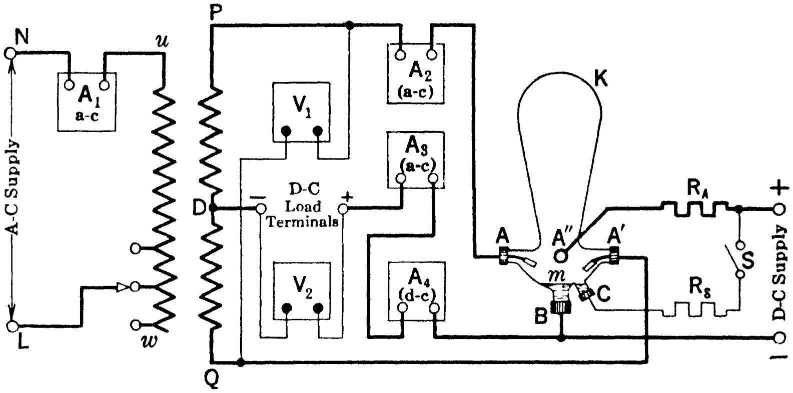

Fig. 774. Diagram of connections for obtaining external current and voltage relations in a mercury-arc rectifier.

1092. Commercial Battery-Charging Rectifiers. — Figure 775[7] shows the schematic wiring diagram of a battery-charging rectifier having certain automatic features and employing two auxiliary electrodes connected through reactances to a special exciting (transformer) winding. The battery to be charged by the rectifier is connected between the mid-point of the main compensator winding and the mercury-pool cathode of the rectifier. Current is passed through the battery only during that part of each half-cycle that the rectifier voltage is higher than the battery emf. During the remainder of the cycle the cathode spot is sustained by the current through the auxiliary electrodes.

---

[7] See "Mercury-Arc Rectifiers," by D. C. Prince, *Jour. A.I.E.E.*, November, 1926, p. 1087.

The rectifier employs a starter-cutout relay, normally closed, which has its holding coils in the leads to the auxiliary electrodes. When the a-c line is energized the current through the contacts of this relay passes through a tilting solenoid and tilter mercury switch so that the tube begins to rock. Current flowing through the starting resistance and starting anode causes the arc to strike, and, as the tube picks up, the current to the auxiliary electrodes opens the starter-cutout contacts and the tube operates in the normal manner.

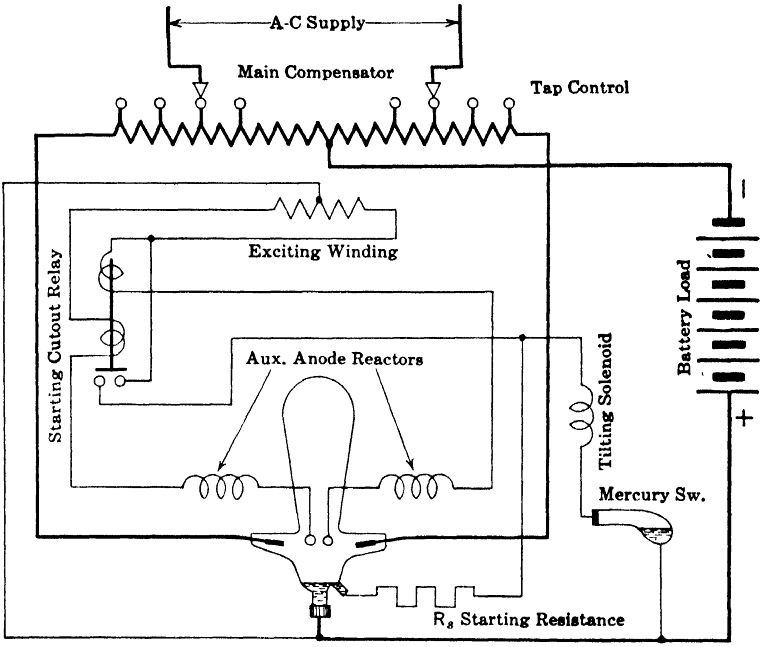

FIG. 775. Schematic diagram of an automatic battery-charging rectifier.

Another commercial rectifier outfit is shown in Fig. 776 (*a*) and (*b*), for charging storage batteries where a wide range of voltages is required. With an a-c voltage of 110 volts, d-c voltages between 5 and 100 volts may be obtained; with a 220-volt a-c supply, the range of d-c voltages is from 30 to 175 volts. Besides the rectifier tube itself, the outfit comprises the following apparatus: the circuit-breaker, *CB*, with its tripping coil, *TC*; a voltmeter and an ammeter; the a-c line switch, S_2;

the single-pole switches, S and S_1, with removable blades; the spring starting switch, S_3; the starting-anode switch, S_4; the double regulating switch, S_5, with contact buttons, segments, and limiting resistors; a starting-load resistance; a starting-anode resistance; a regulating auto-transformer; an a-c series reactance, and a main reactance.

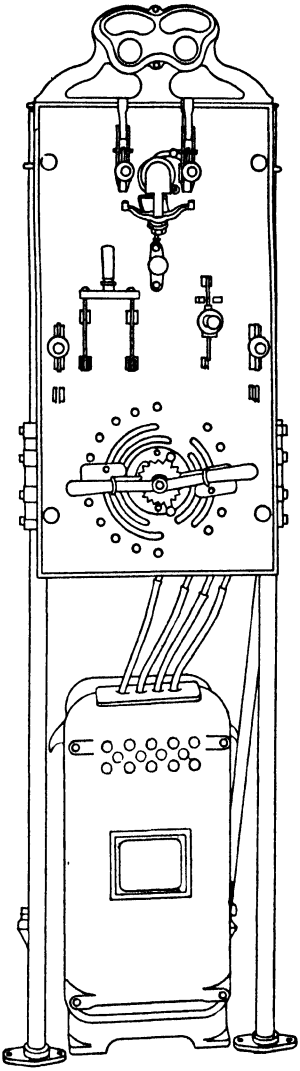

FIG. 776(*a*). Mercury-arc rectifier outfit for charging batteries; front view.

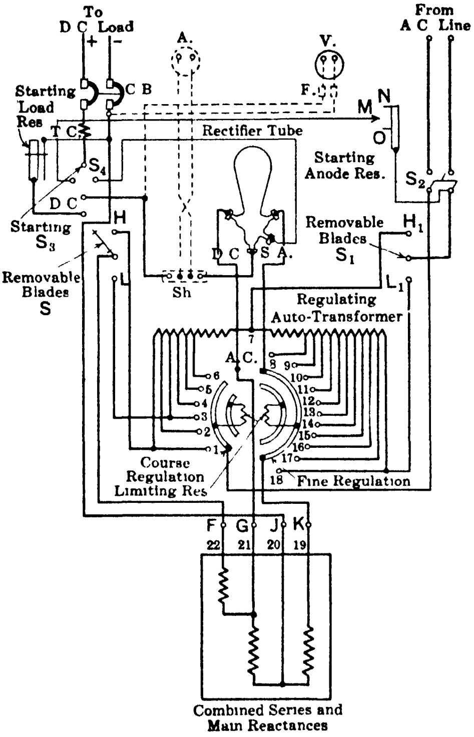

FIG. 776(*b*) Connections in the rectifier outfit of Fig. 776(*a*).

The general principle of the connections in Fig. 776(*b*) is the same as in Fig. 771. The function of the added reactance coil in the a-c circuit is to obtain a drooping d-c voltage characteristic so that the voltage at full load will be considerably lower than at, say, one-third load. This is of great advantage in battery charging as an increase in battery voltage has a tendency to lower the charging current, resulting in a higher rectifier voltage as the battery voltage rises.

Without this feature, the rectifier would require frequent attention during a charge, to raise the charging voltage and thus keep the rectifier arc from going out.

The auto-transformer (§402), with numerous taps and the two dial switches, permits adjustment of the a-c voltage at the beginning of the charge in accordance with the battery voltage. One of the switch arms, that on the right, viewed from the front of the panel, is for rough regulation and the other for fine regulation of the voltage. There are two contact segments for each switch arm, to which connect plunger contacts from the arm. Between these two segments is connected a resistor unit of 1-ohm resistance which serves to prevent a short circuit when two of the contact buttons are connected together through the regulating switch.

The function of the starting switch is to transfer the rectified current from the starting-load resistance on which the rectifier tube starts, to the load. By means of a spring, the switch is normally held in the load position, that is, in the lower clip, and must be transferred and held in the starting position by hand when starting the rectifier. When the starting switch is in the load position, the anode switch is open, and it closes only when the starting switch is thrown into the starting position. The anode switch is connected in series with the starting-anode circuit, as shown in the diagram of connections. The function of the starting-anode resistance is to limit the current flowing through the starting anode of the rectifier tube to about 2 amperes, when the mercury bridge is formed between the starting anode and the cathode during the starting of the tube. The removable-blade switches mounted on the front of the panel are used for changing the connections of the rectifier from the "high-voltage" to the "low-voltage" connections, or vice versa (points *H* and H_1, and *L* and L_1, respectively). Each blade is supplied with three clips arranged vertically, so that the spacing between the upper or lower clips and the center clip will accommodate the blades.

The following steps are necessary in starting the rectifier for the first time:

1. See that the blades are set in the proper clips.
2. Turn the regulating-switch blades to the lowest position.
3. Close the a-c line switch.
4. Close the circuit-breaker.
5. Move the starting switch to the starting position.
6. Rock the tube gently until the arc starts, then release the starting switch.
7. Adjust the current by means of the fine-regulating switch.

In case the tube " goes out " when the starting switch is released, the above operation should be repeated from the third step on, the voltage being raised by the fine-regulating switch until the arc is maintained and the desired current is going into the batteries. If sufficient voltage and current cannot be obtained with the rough-regulating switch set on the lowest step, it should be raised until the desired current is obtained. After the rough-regulating switch has once been adjusted for a given current, it will not be necessary to set it again, provided that the same alternating voltage and d-c load are always used.

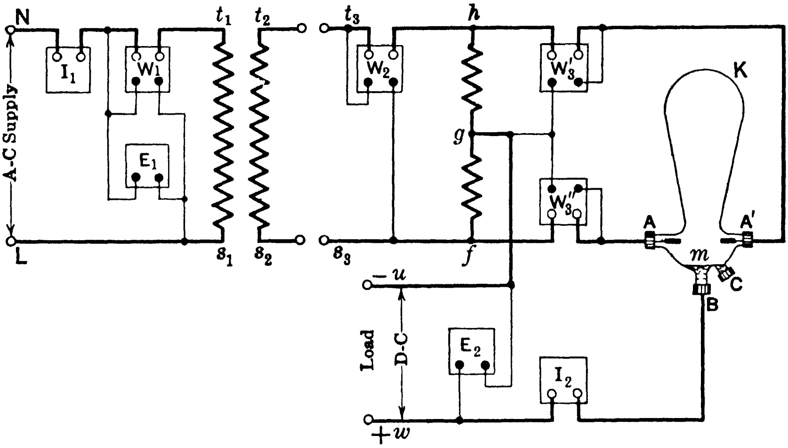

Fig. 777. Connections for obtaining external current and voltage relations in a mercury-arc rectifier.

1093. EXPERIMENT 56-C.—Load Test on a Single-Phase Mercury-Arc Rectifier.

—The purpose of the experiment is to learn to start and handle an actual rectifier outfit, such as is described in §1092, and to become familiar with its operating characteristics. Directions accompanying the unit to be tested should be carefully read before the experiment is begun. The method of computing the efficiency of the unit depends upon the type of load supplied. Electrolytic loads (battery charging, electroplating, etc.) require d-c ammeters in the load circuit. For other loads, an a-c ammeter is used (effective amperes). A convenient arrangement of measuring instruments is shown in Fig. 777. It may be readily extended to polyphase conditions. Each type of unit will have separate problems in connection with auxiliaries and their losses.. The following symbols are used below:

I_1 = effective current input. W_3 = valve-tube input ($W_3' + W_3''$).
E_1 = effective applied voltage. I_2 = load current.
W_1 = total power input. E_2 = load voltage.
W_2 = rectifier-unit input.

In general, the following relations hold:

Power factor = W_1/E_1I_1.
Transformer losses = $W_1 - W_2$.
Power absorbed by the reactor = $W_2 - W_3$.
Transformer efficiency = W_2/W_1.
Valve-tube efficiency = E_2I_2/W_3.
Over-all efficiency = E_2I_2/W_1.
Rectifier-unit efficiency = E_2I_2/W_2.

These ratios assume no auxiliaries except a main reactance. In case there is a separate regulating transformer, the wattmeters should be arranged to measure its losses. Losses in the starting devices which do not remain in the circuit during operation are not taken into account in determining efficiencies. In case there are separate circuit auxiliaries, their power consumption, W_a, should be included. Thus,

Rectifier-unit efficiency = $E_2I_2/(W_2 + W_a)$
Over-all efficiency = $E_2I_2/(W_1 + W_a)$

After some practice with starting (§1092), the unit should be operated at its rated load until steady conditions have been obtained. Reduce the load in several convenient steps to the lowest possible value. Read the meters for each load. If the unit has adjustable elements, such as transformer taps, variable inductance, etc., repeat the test for a few typical settings. If possible, take some oscillograms of the various component currents and voltages

It is of interest to observe the rectifier bulb through a stroboscopic disk. Such a disk is mounted on the shaft of a small synchronous motor and is provided with as many radial slots as the motor has pairs of poles. The motor is connected to the same a-c circuit as the rectifier, and the arc is viewed through the slots. Make careful notes on the phenomena observed.

Report. To a convenient quantity as abscissas (for example, d-c amperes, or d-c power), plot the other observed quantities and also the computed values of power factor, efficiency, losses, degree of rectification, and the ratio of d-c to a-c voltage. Explain the shape of the oscillograms and compare your results with those found in the literature of the subject. Describe and explain the phenomena observed through the stroboscopic disk.

1094. Steel-Tank Rectifiers. — In the mercury-arc rectifiers so far described an evacuated glass bulb was used. The possible output of such a rectifier may be increased, first, by cooling the bulb by forced draft or by immersing it in oil, or second, by increasing the number of anodes to three or more.

Two three-phase rectifiers may be connected as shown schematically in Fig. 778[8] where corresponding secondary transformer windings are shown connected 180 degrees out of phase, giving the effect of a six-phase system. The d-c load is connected between the junction of the two cathodes (+) and the middle point of an "interphase transformer" (−). It will be seen later (§1098) that this arrangement increases the overlap of the d-c current loops and makes for a steadier output current. However, for outputs of several hundred kilowatts and beyond, a glass bulb is inadequate, and is replaced by a steel tank (Fig. 779*a*) which is generally water cooled. The cooling water circulates through a jacket surrounding the tank or through pipes welded to the outer surface of the tank, and through ring-shaped coolers within the anode chamber.

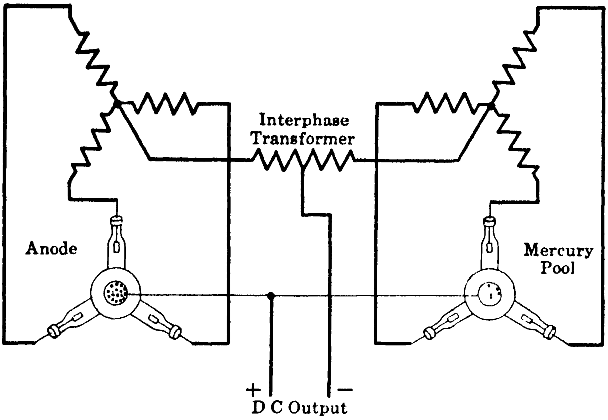

FIG 778. Double three-phase rectifier

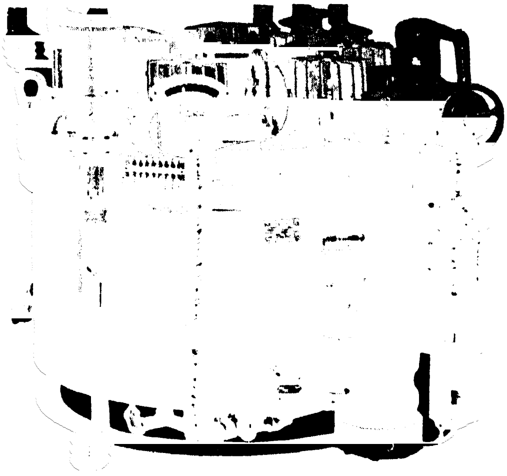

FIG. 779(*a*). Steel-clad rectifier of the Westinghouse Electric and Mfg Co.

---

[8] D. C. Prince, *Jour. A.I.E.E.*, November, 1926, p 1087.

The anodes are made of steel or graphite, and on account of the difficulty of maintaining perfectly tight joints, vacuum pumps are permanently connected to the tank. The pumps may be automatically started and stopped by some sensitive vacuum gauge. *"Arc-back" or "back-firing" (a reverse arc), loss of rectifying effect, and overheating of the anodes occur if the gas pressure is too high, i.e., more than a few "microns" (a micron is the pressure corresponding to that produced by a column of mercury 1/1000 of a millimeter high).* Anodes often have to be cooled artificially, either by air blast or by circulating water.

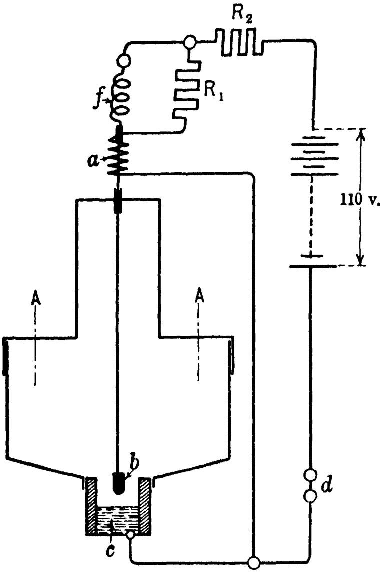

FIG. 779(*b*). Section of a steel-tank rectifier showing means for striking the arc.

The negative electrode should be carefully insulated from the metallic vessel, because otherwise the vessel participates in the discharge. This will cause a gradual loss of the vacuum, a pitting of the metallic walls, "back-firing," and short circuits. It is recommended not only that the vessel be completely insulated but also that all metallic guides for the arc be kept far away from the arc itself. Rectifiers built according to these rules show marked safety against internal short circuits.

In order to increase the output per tank and to reduce fluctuations in the rectified current, the number of anodes is usually increased to six (Fig. 782) or even to twelve or eighteen. Figure 782(*a*) shows a horizontal cross-section of a steel tank with six iron anodes and a mercury cathode in the center. The high-tension side of the transformer is delta-connected, to provide a path for higher harmonics of current (§790). The secondary is six-phase star-connected (§776). The six terminals are connected to the corresponding anodes, the conductors not being shown in order not to obscure the sketch. The d-c load is connected between the transformer neutral and the cathode, as in Fig. 774.

An arrangement for striking the arc in a high-voltage steel-tank rectifier is shown in Fig. 779*b*, *c* being the mercury cathode and *b* the auxiliary anode on a steel rod. This rod is supported by the spring *f* and passes inside the solenoid *a*. A separate source of d-c voltage, in this case a 110-volt storage battery, is shown for starting; *d* is a switch and a fuse, or a circuit-breaker, and R_1 and R_2 are current-limiting resistors. Ordinarily, *b* is at some distance from the surface of the mercury, but when *d* is closed the solenoid overcomes the tension of the spring and brings *b* in touch with the cathode. As *b* is withdrawn an arc is struck, which quickly transfers to the main anodes at *AA*, when potential is applied to them. When *d* is opened, the arc to *b* is extinguished. The arc can also be started with alternating current by using a single-phase transformer and relays; this arrangement is of advantage as it eliminates the need of an independent d-c supply.[9]

1095. Effect of Number of Anodes. — From what has been said above concerning the mercury-arc rectifier it is evident that in a single-phase rectifier with but one anode only one-half of each voltage wave will be rectified, with the result that during alternate half waves of the supply the voltage across the load is zero, as shown in Fig. 773(*a*). This constitutes the " half-wave " rectifier. Such a mercury-arc rectifier would cease to act after the first half wave unless suitable auxiliary, or holding, anodes were included (§1090). With two anodes full-wave rectification is obtained, but, unless there is smoothing inductance in the load circuit, or sufficient leakage reactance in the transformer, the load voltage would drop to zero twice each cycle, as would the load current. By means of a smoothing inductance (§1090) the current from either anode is made to hold over until the second anode is carrying current. Thus the current and voltage of the load assume the form shown by I_t in Fig. 773(*b*). Each anode " fires " for approximately 180 degrees.

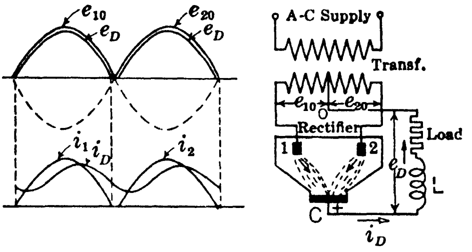

Fig. 780. Voltage and current wave forms in a single-phase rectifier.

In Fig. 780,[10] e_{10} and e_{20} are the waves of emf applied between the anodes 1 and 2 and the mid-point, *O*, of the transformer secondary winding. Curve e_D represents the voltage across the load after allowing for the nearly constant drop across the rectifier. Curves i_1 and i_2 show the currents which would flow through a non-inductive load, assuming no leakage reactance in the transformers. When a smooth-

---

[9] See O. K. Marti, *op. cit.*, p. 842.

[10] See Marti and Winograd, " Mercury-Arc Power Rectifiers," Chapter IV, McGraw-Hill Book Co.

ing inductance, L, is connected in series with the load the rectified current assumes the form of i_D. For greater values of smoothing inductances i_D becomes almost constant.

When three anodes are used on a three-phase supply (Fig. 781) the load voltage, e_D, becomes more nearly continuous but still contains an objectionable ripple, each anode now firing for 120 degrees. Without a smoothing inductance the currents are similar in form to e_D, as shown by i_{d1}, i_{d2}, and i_{d3} in Fig. 781. With a smoothing inductance in circuit the load current has the form shown by i_D, the ripple becoming less prominent as L is made greater, until the current is almost constant. Note in Fig. 781 that the secondary windings of the transformers are in interconnected star which reduces the saturating effect of the unidirectional load current in the transformers.

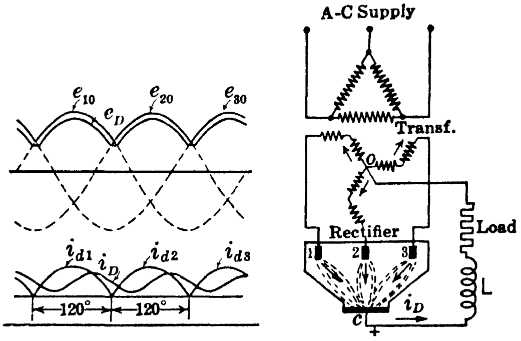

FIG. 781. Wave forms in a three-phase rectifier.

1096. Rectifiers in Parallel. — Two three-phase rectifiers in parallel were shown in Fig. 778. Two six-phase rectifiers in parallel are shown in Fig. 782 (*b*). In order to cut down higher harmonics and to improve voltage regulation, as well as to permit each anode to fire for approximately 120 degrees and so increase the utilization of the secondary windings of the transformers, so-called *interphase auto-transformers* are used in the neutral connections. Current harmonics, flowing between the phases connected to *ab* and those connected to *cd*, meet a high impedance of the interphase transformer and can therefore be of small magnitude only. Moreover, the d-c load voltage is the average of the instantaneous voltages in the four three-phase groups. In the output voltage, all even multiples of the fundamental frequency are displaced by 180 electrical degrees in the two three-phase units. The average of all these frequencies between the two units is therefore zero, and they are eliminated. The same is true in the input current. The rectified currents flow through the two halves of the interphase transformer in opposite directions, as shown by the arrowheads, so that there is no d-c saturation in the auto-transformer core.

The mercury-vapor arc shows characteristics of a negative resistance, that is, between certain values of load current the potential drop across the arc decreases with increase of current. Therefore, for parallel operation, in addition to having the voltage drop in each rectifier approximately the same, the volt-ampere characteristic must be changed to the opposite sense. This is done by inserting a suitable inductance between the cathode of each rectifier and the positive side of the load bus, that is, between *B* and *J* in Fig. 771. Better operation is obtained by shunting each reactance with a resistance, to provide a path for higher harmonics of current.

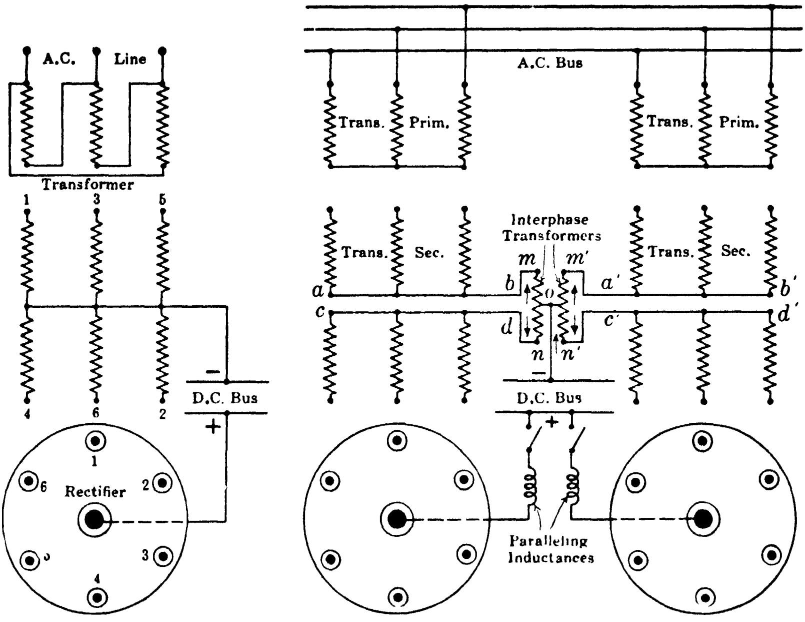

(*a*) (*b*)

Fig. 782. A single six-phase rectifier, and two such rectifiers in parallel.

Two rectifiers may also be paralleled on the a-c side by means of an iron-core choke coil or auto-transformer whose middle point is connected to the corresponding transformer terminal. As long as each rectifier takes its equal share of the total current, the inductive drop in the choke coil is negligible. Should one of the rectifiers take a larger current, the flux so produced in the core would boost the voltage in the other half of the winding, thus helping the other rectifier.

In order further to increase the number of phases and thus to obtain a steadier direct current, the three-phase supply is sometimes converted into twelve phases (§778h). Two six-phase rectifiers are connected to the alternate phases and are operated in parallel on the d-c side, through an interphase transformer, thus forming one unit.

1097. Elementary Voltage and Current Relations.— (a) *Voltage ratio.* Consider an ideal n-phase rectifier[11] with no internal resistance or counter emf, connected between a source of sinusoidal voltage of amplitude E_m, and delivering a practically constant current, I, to the load. With such an n-phase rectifier one may assume that at any instant only that anode is active whose potential with respect to the cathode is highest. Then the load voltage may be represented by the wavy line (Fig. 782) consisting of the tops of the successive sine waves of the n secondary voltages of the transformers. In reality the phenomenon is more complicated because for a fraction of a cycle two anodes are acting simultaneously while the load is being transferred from one to the other (§1090).

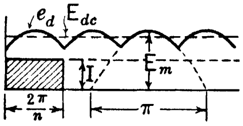

FIG. 783. Current and voltage relations in an n-phase rectifier.

It is of interest to determine the relationship between the effective value, E, of the phase voltage (that is, the voltage applied from the neutral, O, of the transformer secondaries [Fig. 781] to the active anode), and the average d-c voltage, E_{dc}, between the point O and the cathode C. The voltage E is assumed to be measured by means of an a-c instrument, while E_{dc} is measured with a moving-coil, permanent-magnet-type meter (Chapters II and III).

Referring to Fig. 783, the effective a-c voltage, $E = E_m/\sqrt{2}$, where E_m is the amplitude of the a-c voltage.

Average d-c voltage is evidently expressed by the relation:

$$E_{dc} = \frac{1}{2\pi/n}\int_{-\pi/n}^{\pi/n} E_m \cos x \, dx$$

$$= (n/\pi)\sqrt{2}E \sin(\pi/n) \quad . \; . \; . \; . \; . \; . \; . \quad (2)$$

Table I gives the ratio E_{dc}/E for various numbers of phases (anodes).

TABLE I

n	2	3	4	6	12	Inf.
E_{dc}/E	0.9	1.17	1.27	1.35	1.4	1.41

In reality the voltage drop, e, within the rectifier (§1088) reduces the voltage available for the load, so that it is more correct to write:

---

[11] Marti and Winograd, *loc. cit.*

$$E_{dc} = (n/\pi)\sqrt{2}E\sin(\pi/n) - e \quad \ldots\ldots \quad (3a)$$

$$= KE - e \quad \ldots\ldots\ldots\ldots \quad (3b)$$

(b) *Current relations.* Assuming that each anode delivers a constant current, I, during $1/n$th of a cycle, the average current of any anode is I/n. The effective value of this anode current is then:

$$I_A = \sqrt{I^2/n} = I/\sqrt{n} \quad \ldots\ldots\ldots \quad (4)$$

From eqs. (2) and (4) the average d-c power for each anode (product of average voltage by average current) is

$$P_{dc} = E_{dc}I = EI\sqrt{2}(n/\pi)\sin(\pi/n) \quad \ldots\ldots \quad (5)$$

(c) *Ratings of transformer windings.* The combined rating of the secondary windings of the transformers connected to a rectifier is the product of the rms secondary (anode) current, I_A, by the rms a-c voltage per winding, E, times the number of windings. Then:

$$P_2 = nI_AE = EI_A\sqrt{n} = P_{dc}\frac{\pi}{\sqrt{2n}\sin(\pi/n)} \quad \ldots \quad (6)$$

For example, in a full-wave, single-phase rectifier (two anodes)

$$P_{dc} = EI\sqrt{2}(2/\pi)\sin\pi/2 = 0.9EI$$

$$P_2 = EI\sqrt{2} = 1.41EI$$

$$P_{dc}/P_2 = 0.9/1.41 = 0.636$$

This factor is called the *utility factor* (sometimes "power factor") of the secondary windings.

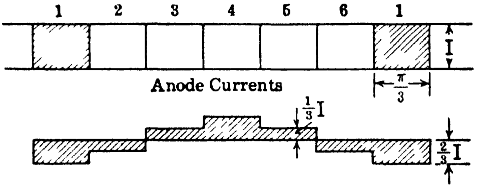

Primary Current-phase 1

Fig. 784 Primary and secondary current wave forms in a six-phase rectifier.

The rating of the primary windings is somewhat more difficult to determine, owing to the complicated wave form of the primary current, occasioned by the fact that the primary mmf must balance the sum of the mmf's of the corresponding secondary windings. In a transformer which has six-phase star-connected secondaries and Y-connected three-phase primary windings, and in which the anode currents are assumed to be constant in value, of $\pi/3$ duration, solution for the primary currents reveals wave forms as in

Fig. 784.[12] It may be shown that the rms value of the current here has the value: $I_p = (\sqrt{2}/3)\ I$. The voltampere rating of the primary windings is then:

$$P_1 = 3\,EI_p = \sqrt{2}EI$$

From eq. (5), $P_{dc} = EI\sqrt{2}(6/\pi)\sin(\pi/6) = (3\sqrt{2}/\pi)EI$.

The utility factor of the primary windings, or ratio of the d-c power to the volt-ampere rating of the primary windings, is then:

$$\text{U.F.} = P_{dc}/P_1 = \frac{3\sqrt{2}EI}{\pi\sqrt{2}EI} = 3/\pi = 0.955$$

These values, with other significant quantities, wave forms, etc., are shown for several rectifier conditions in Table II, which is reproduced with the kind permission of the authors, Prince and Vogdes, from their "Principles of Mercury Arc Rectifiers and Their Circuits," McGraw-Hill Book Co.

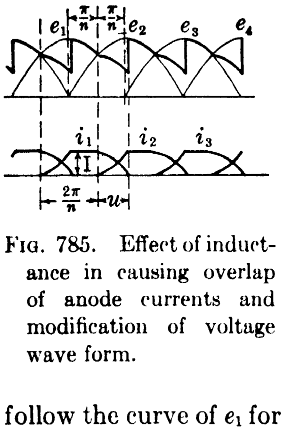

FIG. 785. Effect of inductance in causing overlap of anode currents and modification of voltage wave form.

1098. Effect of Inductance in the Anode Circuits. — Owing to the inductance in the windings of transformers and supply lines it is impossible for the anode currents to rise or drop instantly, as was assumed in Fig. 784, but they have more the wave form shown by i_1 and i_2 in Fig. 785 (§1090). This means that there is an angle of overlap, u, during which two anodes fire simultaneously. During this angle of overlap the resulting d-c voltage lies between the voltages of the active phases. In Fig. 785 the d-c voltage is shown to follow the curve of e_1 for the angle $(2\pi/n) - u$, while i_1 is the only anode current, but to lie between e_1 and e_2 for the angle of overlap, u. It then rises to the curve of e_2, when i_1 reaches zero, and so on. The theoretical relations[13] are as follows:

The angle of overlap, due to a reactance X (at supply frequency) per secondary phase is expressed by the equation:

$$\cos u = 1 - \frac{IX}{E\sqrt{2}\sin(\pi/n)} \quad \ldots\ldots \quad (7)$$

---

[12] H. D. Brown and J. J. Smith, "Current and Voltage Wave Shape of Mercury-Arc Rectifiers," *Trans. A.I.E.E.*, vol. 52 (1933), p. 973.

[13] Marti and Winograd, *op. cit.*, Chapter IV.

TABLE II

Circuit	Connections	Sec. current		Sec. volts to neut.	Sec. V a. & Util. Factor	Prim. current wave	Eff. prim. current & volts	Prim. V.a. & U.F.	Total transf. U.F.	Wave form of line current	Eff. line curr. & volts	Line V.a. & U.F.
		Wave shape	R.M.S.									
Single phase	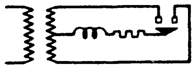	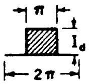	$\frac{I_{dc}}{\sqrt{2}}$ $.707I_{dc}$	$\frac{\pi E_{d.c.}}{2\sqrt{2}}$ $1.11E_{d.c.}$	1.57 x $E_{dc}I_{d.c.}$ U.F. = .637	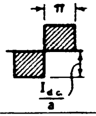	$\frac{I_{dc}}{a}$ $1.11aE_{dc}$	1.11 x $E_{d.c.}I_{d.c.}$ U.F.= .90	.746	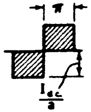	$\frac{I_{dc}}{a}$ $1.11aE_{d.c.}$	U.F.= .90
Three phase	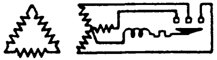	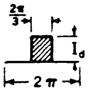	$\frac{I_{d.c.}}{\sqrt{3}}$ $.577I_{dc}$	$\frac{\sqrt{2}\,\pi E_{d.c.}}{3\sqrt{3}}$ $.855E_{dc}$	1.481 x $E_{dc}I_{dc}$ U.F.= .675	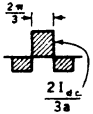	$\frac{\sqrt{2}\ \ I_{dc}}{3a}$ $.855aE_{dc}$	1 209 x $E_{dc}I_{dc}$ U.F.= .827	.743	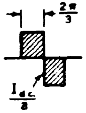	$\frac{\sqrt{2}\,I_{d.c.}}{\sqrt{3}a}$ $.855aE_{dc}$	1.209 x $E_{dc}I_{d.c.}$ U.F.= .827
Six phase star	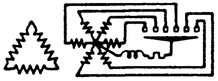	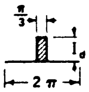	$\frac{I_{d.c.}}{\sqrt{6}}$ $.408I_{dc}$	$\frac{\pi E_{dc}}{3\sqrt{2}}$ $.741E_{dc}$	1.814 x $E_{dc}I_{dc}$ U.F.= .552	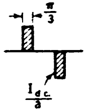	$\frac{I_{dc}}{\sqrt{3}a}$ $.741aE_{dc}$	1.283 x $E_{dc}I_{dc}$ U.F.= .780	.646	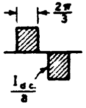	$\frac{\sqrt{2}\,I_{d.c.}}{\sqrt{3}a}$ $.741aE_{dc}$	1.047 x $E_{dc}I_{dc}$ U.F.= .955
Double Y	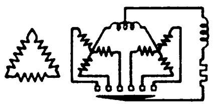	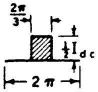	$\frac{I_{dc}}{2\sqrt{3}}$ $.289I_{dc}$	$\frac{\sqrt{2}\,\pi E_{dc}}{3\sqrt{3}}$ $.855E_{dc}$	1.481 x $E_{dc}I_{dc}$ U F.= .675	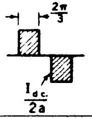	$\frac{I_{dc}}{\sqrt{6}a}$ $.855aE_{dc}$	1 047 x $E_{dc}I_{dc}$ U.F.= .955	.792	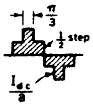	$\frac{I_{dc}}{\sqrt{2}a}$ $.855aE_{dc}$	1.047 x $E_{dc}I_{d.c.}$ U.F.= .955
Y Prim. Six phase star	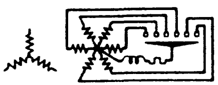	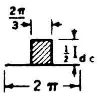	$\frac{I_{dc}}{2\sqrt{3}}$ $.289I_{dc}$	$\frac{\sqrt{2}\,\pi E_{d.c.}}{3\sqrt{3}}$ $.855E_{d.c.}$	1 481 x $E_{dc}I_{d.c.}$ U F.= .675	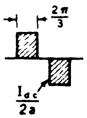	$\frac{I_{dc}}{\sqrt{6}a}$ $.855aE_{d.c.}$	1.047 x $E_{dc}I_{dc}$ U F.= .955	.792	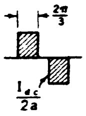	$\frac{I_{dc}}{\sqrt{6}a}$ $1.482aE_{d.c.}$	1.047 x $E_{dc}I_{dc}$ U F = .955

$I_{d.c.}$ = load current E_{dc} = average d c. voltage output. $a = \frac{\text{Primary line potential,}}{\text{Secondary leg potential}}$

* From "Principles of Mercury Arc Rectifiers and Their Circuits," Prince and Vogdes, as modified by Puchstein and Lloyd. Reproduced by permission of the publishers, McGraw-Hill Book Co.

The average value of the d-c voltage is:

$$E_{dc} = \frac{E\sqrt{2}\sin(\pi/n)}{\pi/n}\cos^2(u/2) \quad \ldots\ldots \quad (8)$$

Multiplying eq. (8) by the d-c current, I, gives the d-c power output as:

$$P_{dc} = \frac{EI\sqrt{2}\sin(\pi/n)}{\pi/n}\cos^2(u/2) \quad \ldots\ldots \quad (9)$$

1099. Voltage Control of Rectifiers. — The d-c voltage delivered by the mercury-arc rectifier may be regulated by taps on the transformer windings, by induction regulators in the a-c lines, by d-c boosters, by saturable reactors, by special starting anodes upon which a variable voltage is impressed,[14] etc. More recently starting electrodes dipping into the mercury as in the ignitron (§1100), and electrostatic grids placed before the anodes and in the electron stream, have been developed for voltage control.

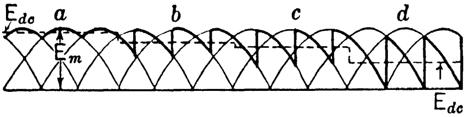

FIG. 786. Effect upon rectifier voltage of delayed ignition of anodes, due to action of energizing control grids.

Such control grids have no effect upon the current from an anode while it is " firing," but if given a suitable negative potential with respect to the cathode they prevent the anodes acting. If given a positive potential the grid allows the anode to " fire " when it becomes positive with respect to the cathode. By delaying the application of positive bias to the grid beyond the normal time for the anode to act the average value of the d-c voltage produced by the rectifier is reduced. Figure 786 illustrates this effect in a simplified manner as applied to a six-anode rectifier. At (*a*) the grid bias is zero and each anode fires as soon as it becomes positive with respect to the cathode, no overlap being assumed. Application of eq. (2) gives the average d-c voltage for this case as $0.955E_m$. At (*b*) the grids delay anode action by about 27 degrees, giving an average d-c voltage, E_{dc}, of about $0.8E_m$. Part (*c*) represents a lag of some 40 degrees, with E_{dc} of about $0.73E_m$, while (*d*), with a lag of 60 degrees, gives E_{dc} of $0.48E_m$, etc. For a more comprehensive treatment of this method of voltage control the reader is referred to the technical literature (§1106).[15] Figure 787 is a schematic diagram[16] of a six-anode rectifier with voltage control by means of energized anode grids.

---

[14] P. H. Thomas, System of electrical distribution, U. S. Patent 783,482.

Special shields and grids serve to de-ionize the region about the anode following firing, and so to prevent arc-back between anodes.

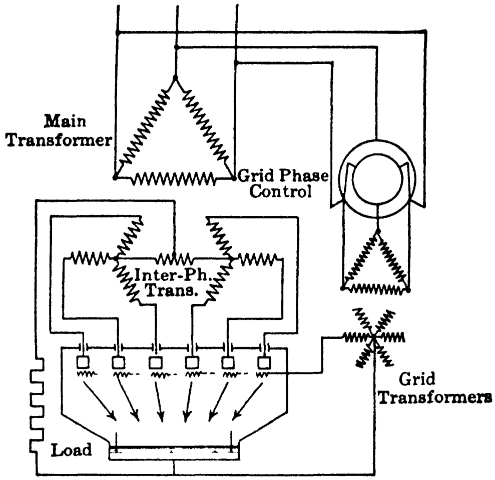

Fig. 787. Mercury-arc rectifier with energized grids for voltage control.

1100. Ignitron-Type Mercury-Arc Rectifier.—The ignitron tube discussed in Chapter LIX has been developed in a form in which metal tubes are used when the rectification of large amounts of power is required. Figure 788 shows such a metal tube ignitron (Westinghouse Electric and Manufacturing Company). A graphite anode, carried on a copper rod, is held by a sealed porcelain bushing in the top of the tube. A mercury pool cathode is at the bottom of the tube, while a third electrode, or ignitor, in the form of a high-resistance crystal (such as Carborundum), is mounted on a metal conducting rod and dips into the mercury pool. The function of this ignitor is to establish, on the surface of the mercury cathode, the hot spot without which (§1088) current cannot be established (at ordinary voltages) from anode to cathode.

To prevent current flowing from the cathode through the ignitor during periods of reversed voltage a small rectifying vacuum tube (Chapter LIX) is connected in series with the ignitor. By controlling the value and phase (timing) of the emf impressed upon the grid of this vacuum tube, the instant when the cathode spot is established may be controlled and the voltage of the rectifier regulated (§1099).

One rectifier of this type, designed for a rating of 400 kw, employs six ignitron tubes connected to a common vacuum pumping system, with such other auxiliary equipment as is required to maintain and measure the conditions of vacuum and temperature in the rectifier (§1095). The mercury cathodes of the six tubes are connected to the common positive terminal of the rectifier, while the anodes are fed from the secondary windings of the rectifier transformer. The neutral point of the transformer windings is the negative terminal of the rectifier. Thus, except for the ignitor circuits, the connections are essentially those of the six-anode rectifier using a single steel tank (Fig. 782).

---

[15] In particular see: D. Journeaux, "Voltage Control of Vapor Rectifiers," *Elec. Eng'g*, June, 1934, p. 974; H. D. Brown, "Grid-Controlled Mercury-Arc Rectifiers," *Gen. Elec. Rev.*, August, 1932, p. 439.

[16] Westinghouse Electric and Manufacturing Company *Bulletin* B-2096, Ed. 2, p. 3.

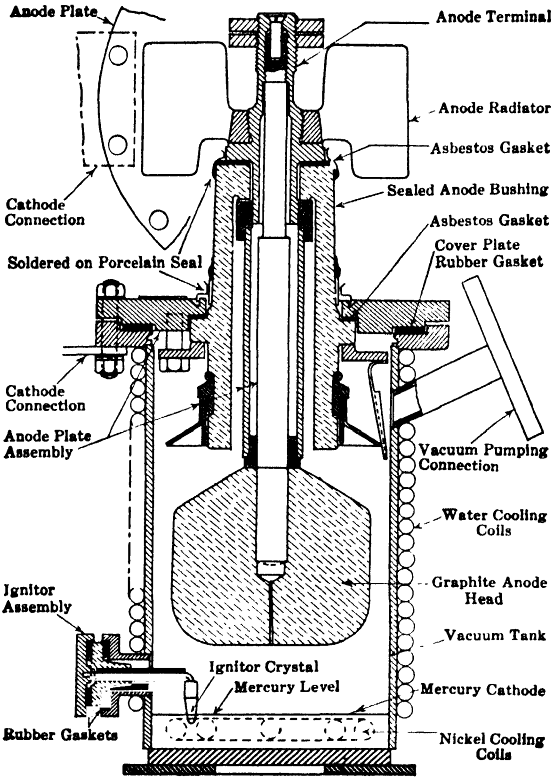

FIG. 788. Section of a steel-tank ignitron rectifier rated 300 amperes at 275 volts (courtesy of the Westinghouse Electric and Mfg. Co.).

1101. Harmonics in the Rectified Wave Forms. — (a) *Voltage wave.* The rectified voltage wave, including the effect of overlap due to inductance in the circuit, so that two anodes are operating simultaneously, may be written[17]

$$e_d = E\sqrt{2}\cos\left(x - \frac{\pi}{n}\right)_0^{2\pi/n} - E\sqrt{2}\sin\left(\frac{\pi}{n}\sin x\right)_0^{u} \quad . \quad (10)$$

---

[17] Marti and Winograd, *op. cit.*, Chapter V.

Such a periodic wave may be represented by a series of sine and cosine components of the several harmonics, or, for an n-phase rectifier

$$\begin{aligned} e_d = E_{dc} &+ A_{n1} \sin nx + A_{n2} \sin 2nx + A_{n3} \sin 3nx + \cdots \\ &+ B_{n1} \cos nx + B_{n2} \cos 2nx + B_{n3} \cos 3nx + \cdots \qquad (11) \end{aligned}$$

One may determine the sine and cosine components, A_{nh} and B_{nh}, respectively, of the hth harmonic (Chapter LVIII) by multiplying the periodic wave first by sin hnx and then by cos hnx. The average product of e_d by these analyzing waves will give the values A_{nh} and B_{nh} as follows:

$$A_{nh} = (E_{d0}/2)\left[\frac{\sin (hn+1)u}{hn+1} - \frac{\sin (hn-1)u}{hn-1}\right] \quad . \; . \; (12)$$

where $E_{d0} = (E\sqrt{2} \sin \pi/n)/(\pi/n)$ is the average d-c voltage at no load. Let $hn + 1 = \alpha$ and $hn - 1 = \delta$. Then

$$A_{nh} = (E_{d0}/2)\left[\frac{\sin \alpha u}{\alpha} - \frac{\sin \delta u}{\delta}\right] \quad . \; . \; . \; . \; . \; . \; (12a)$$

Similarly:

$$B_{nh} = \frac{E_{d0}}{2}\left[\frac{\cos (hn+1)u}{hn+1} - \frac{\cos (hn-1)u}{hn-1}\right] - \frac{E_{d0}}{h^2n^2-1} \qquad (13)$$

$$= \frac{E_{d0}}{2}\left[\frac{\cos \alpha u}{\alpha} - \frac{\cos \delta u}{\delta} - \frac{1}{\alpha\delta}\right] \quad . \; . \; . \; . \; . \; . \; . \; . \; . \; . \; . \; (13a)$$

The rms value of the hth harmonic is

$$C_{hn} = \sqrt{A_{hn}^2 + B_{hn}^2} \quad . \; . \; . \; . \; . \; . \; . \; . \; . \; . \; (14)$$

Table III shows the voltage harmonics in the output of a six-phase rectifier as a function of the angle of overlap, u (Marti and Winograd).

TABLE III

Angle of overlap u	Ratio of $\frac{\text{rms value of harmonic}}{\text{average d-c voltage}}$			
	$h = 1$	$h = 2$	$h = 3$	$h = 4$
0	0.04	0.01	0.0045	0.0025
10	.046	.015	.007	.004
20	.06	.0165	.014	.0125
30	.061	.031	.02	.016

The order of the harmonic = hn, i.e., in a six-phase rectifier on 60-cycle supply, the first harmonic ($h = 1$) is of a frequency 6 × 60 = 360 cycles per second, the third harmonic is of 1080 cycles, etc.

(b) *Current waves.* When rectified voltage waves of the form described above are connected across a load circuit the harmonics in the current wave are those natural to the voltage wave and to the characteristics of the load circuit. In load circuits consisting solely of non-inductive resistance the wave form of the current is identical with that of the voltage wave.

When the load consists of a resistance plus a source of counter emf, for instance, a battery being charged, the current is due to the difference between rectifier voltage and battery voltage. Fluctuations in the voltage wave (§1100) are a greater part of this difference than of the d-c voltage itself, with the result that harmonics in the voltage wave are correspondingly accentuated.

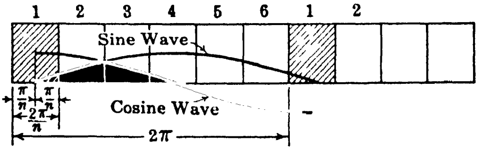

FIG. 789. Process of analyzing waves for the determination of harmonics in the rectified current wave form.

1102. Harmonic Components of the Anode Currents. — Considering the wave form of the anode current to be rectangular (Fig. 789) and of $2\pi/n$ duration, its harmonics may be found by the conventional method (§1101), i.e., by multiplying by sine and cosine analyzing waves. Figure 789 shows the anode current waves of phase 1 in a six-phase rectifier, together with sine and cosine waves, as referred to the center line of the current wave.

The amplitude of the sine component of the hth harmonic is

$$A_h = (1/\pi) \int_{-\pi/n}^{\pi/n} I_{dc} \sin hx \, dx = 0$$

The amplitude of the cosine component is

$$B_h = (1/\pi) \int_{-\pi/n}^{\pi/n} I_{dc} \cos hx \, dx = (2/h\pi) I_{dc} \sin h\pi/n \quad . \quad . \quad (15)$$

In Table IV values of the several harmonics are given for rectifiers of different numbers of phases, in terms of the direct current, I_{dc}.

TABLE IV

Harmonics in Rectifier Input Current

Phases (number of anodes)	2	3	4	6
Fundamental	0 637	0 552	0 450	0 318
Second harmonic	0 0	0 276	0 318	0 276
Third harmonic	0 212	0 00	0 150	0 212
Fourth harmonic	0 0	0 138	0 0	0 138
Fifth harmonic	0 127	0 110	0 090	0 064
Sixth harmonic	0 0	0 0	0 106	0 0
Seventh harmonic	0 091	0 079	0 064	0 045

1103. EXPERIMENT 56-D.—Study of Rectifier Wave Forms.—Oscillograms should be taken of voltage and current waves on single-phase and polyphase rectifiers under different known conditions as to inductance in the transformer and load circuits, and with different degrees of overlap. If a rectifier with grid control is available a further study should be made of voltage control and resulting effect upon wave forms. The question of telephone interference should be studied after an analysis of various rectifier current waves. (See references.)

1104. The Vreeland Oscillator.—The purpose of the Vreeland oscillator is to produce pure sinusoidal oscillations of constant frequency, adjustable within the range of 250 to 2500 cycles per second. The maximum output is only a few watts. The oscillator is particularly convenient as a source of alternating currents for various a-c bridges (Chapter XXVIII), because an a-c galvanometer or a telephone receiver is much more sensitive to changes in current of one frequency only than when harmonics are present. The Vreeland oscillator (Fig. 790) is described in this section because of its similarity to the mercury-arc rectifier treated above.

The lettering in Fig. 790 is the same as in Fig. 771(*a*), *K* being a glass bulb, *A*, *A′* the two anodes, *B* the mercury cathode, and C_s the starting anode. Current is supplied from a d-c source through a pair of ballast resistances, R_1, R_2, and a pair of choke coils, *E*, *F*. These coils and resistances are included in the symmetrical branches of a split circuit, each branch being connected to one of the anodes, *A*, *A′*. The mercury arc thus has two symmetrical paths from the cathode to the two anodes. Shunted across the anodes is the primary oscillating circuit comprising a capacitance, *C*, and a pair of inductance or field coils, L_1, L_1. The two coils encircle the tube so that their magnetic field will traverse it in a direction perpendicular to the plane of the anodes and cathode. Any current in the field coils will thus tend to deflect the arc toward one or the other of the anodes, according to the direction of the magnetic flux.

After the arc has been started, the current is carried between the two anodes and the cathode in two symmetrical streams. The ballast resistances and choke coils serve to maintain equal and constant currents in the two supply branches. Under these conditions, the two anodes, *A* and *A'*, will be at exactly the same potential and no current will flow through the circuit L_1CL_1 shunting them. Suppose, however, that through some means, such as a slight unbalance or a residual charge on the condenser, a current is caused to flow through the field coils.

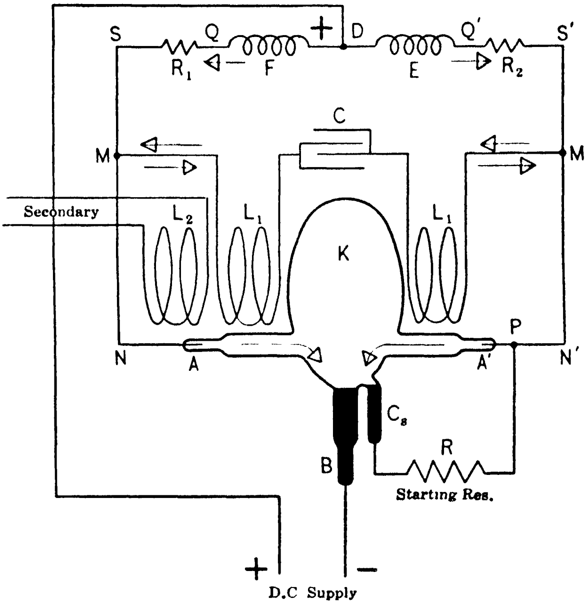

FIG. 790. Circuits of the Vreeland oscillator.

This tends to deflect the arc toward one of the anodes, say *A*, and the path from *A* to *B* is shortened, while that from *A'* to *B* is lengthened. This increases the resistance of the arm of the bridge *M'B* (§1088) and consequently reduces the current in the branch *DM'B*. This decreases the *IR* drop across *DM'*, and there then exists a difference of potential between *M* and *M'*, with *M'* higher than *M*. A current will therefore flow through the oscillating circuit L_1CL_1 from *M'* to *M*, so that still more unequal currents will flow from the two anodes to *B*. The connections of the field coils are such that their currents tend still further to deflect the arc toward the anode *A*, and thus an unstable condition is established. This deflection cannot continue indefinitely because of the physical constants of the tube, and as the steady condition is approached the charging current tends to become zero. But owing to the characteristic of any oscillatory circuit, the condenser in charging oversteps the stable condition because of the inductances L_1, and must subsequently lose part of its charge. The physical constants of the tube and the inductances L_1 largely determine the amplitude of the oscillating voltage. In discharging, the conditions are reversed, M is raised to a potential above M' and the condenser is charged in the opposite sense. There is no complete oscillatory circuit in the ordinary sense, but an equivalent current, equal to the alternating current in the circuit ML_1CL_1M', may be thought of as flowing between the anodes A, A'.

With constant secondary load, the supply of energy from the d-c source remains nearly constant. The current in each of the two branches of the bridge circuit may be represented by an alternating wave with a relatively large d-c component. However, the troughs and crests of the waves are in opposite time phase in the two branches. The d-c component is so large that the current is never zero in either branch; i.e., the arc is never out or non-conducting. The energy absorbed by the load is represented by a change in the magnitude of this d-c component of the two waves.

The natural frequency of oscillation of the branched circuit, in cycles per second, is practically (Chapter XXXII):

$$f = (2\pi\sqrt{LC})^{-1} \quad . \; . \; . \; . \; . \; . \; . \; . \; . \; . \quad (16)$$

where C is the capacitance of the condenser, in farads; and L is the combined inductance of the two coils, L_1, L_1, in henries. The inductance is usually kept constant, and a desired frequency is obtained by a proper setting of the condenser. For a further adjustment, a switch is provided to change the field coils from a series to a parallel connection. Since in the latter case their inductance is one-quarter of its value with the series connection, the frequency will be doubled by changing the coils from series to parallel.

The working current is taken off by means of two secondary coils, L_2, of which one is shown in the sketch, and which may be joined in series or in multiple depending upon whether a high or a low voltage is desired. The coefficient of coupling between the primary and secondary is quite small, so that variations in the working circuit will not materially affect the frequency of oscillation. For all ordinary purposes this effect may be neglected, as at most it amounts to a small fraction of 1 per cent change in the frequency.

1105. EXPERIMENT 56-E. — Study of the Vreeland Oscillator. — The oscillator is described in the preceding section. The properties of the arc itself may be studied as explained in §§1089 to 1093. The purity of the alternating voltage should be determined oscillographically, at different frequencies and with different secondary loads. To determine the operating characteristics, secondary volts and watts are read on suitable sensitive instruments for various values of secondary resistance or impedance, the frequency being kept constant for each run. The power consumption in the instruments themselves must be carefully considered, since the whole output amounts to only a few watts.

1106. References.

1. D. C. PRINCE, *Jour. A.I.E.E.*, November, 1926, p. 1087, Mercury-arc rectifiers.
2. O. K. MARTI, *Trans. A.I.E.E.*, vol. 45 (1926), p. 668, The Rectification of alternating currents.
3. D. C. PRINCE, *Trans. A.I.E.E.*, vol. 45 (1926), p. 688, Rectifier voltage control.
4. A. W. HULL and H. D. BROWN, *Elec. Eng'g*, October, 1931, p. 788, Solving the mystery of mercury-arc rectifiers.
5. E. B. SHAND, *Jour. A.I.E.E.*, June, 1927, p. 597, Steel-tank mercury-arc rectifiers.
6. J. H. COX, *Elec. Eng'g*, June, 1933, p. 462, Improvements in mercury-arc rectifiers.
7. W. E. GUTZWILLER and R. W. DAVIS, *Iron and Steel Eng'r*, November, 1932, p. 475, Mercury-arc rectifiers for steel mill and general industrial applications.
8. J. SLEPIAN and L. R. LUDWIG, *Elec. Eng'g*, October, 1931, p. 793, Backfires in mercury rectifiers.
9. H. D. BROWN, *Gen. Elec. Rev.*, August, 1932, p. 439, Grid-controlled mercury-arc rectifiers.
10. D. JOURNEAUX, *Elec. Eng'g*, June, 1934, p. 974, Voltage control of vapor rectifiers.
11. D. JOURNEAUX, *A-C Elec. Rev.*, December, 1938, p. 9, What goes on in the mercury-arc rectifier.
12. F. A. LAUPER, *A-C Elec. Rev.*, September, 1938, p. 14, Parallel operation of mercury-arc rectifiers and rotating machinery.
13. S. R. DURAND, *A-C Elec. Rev.*, March, 1937. Electronic switching in mercury-arc rectifiers.
14. E. J. REMSCHIED, *Elec. Eng'g*, December, 1938, p. 550, Mercury vapor pressure control for mercury-arc rectifiers.
15. G. R. MCDONALD, *Elec. Eng'g*, November, 1939, p. 563, Voltage control of mercury-arc rectifiers.
16. MARTI and WINOGRAD, Mercury-Arc Power Rectifiers, McGraw-Hill Book Co.
17. PRINCE and VOGDES, Principles of Mercury-Arc Rectifiers and their Circuits, McGraw-Hill Book Co.

CHAPTER LVII

THE OSCILLOGRAPH

1107. An oscillograph is an instrument for recording the wave form of a variable voltage current or power; such a record (voltage wave) is shown in Fig. 791. Abscissas are proportional to time, and ordinates represent instantaneous values of voltage. It will be seen that in this case the wave consists of a fundamental sine wave and of quite a pronounced eleventh harmonic.[1]

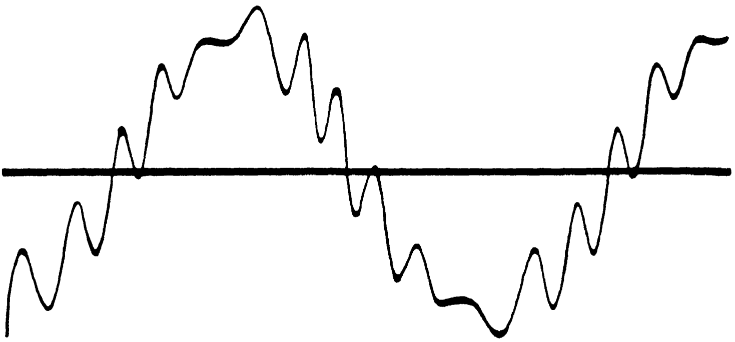

FIG. 791. Oscillogram of a voltage curve having a prominent eleventh harmonic.

1108. Applications. — In many practical problems in design, testing, and operation of electrical apparatus, as well as in research, it is of importance to know the actual wave shape of a variable current or voltage, and for this reason the oscillograph, in its different forms, has acquired an important place among electrical measuring instruments. Some of the applications are as follows:

1. Study of commutation in d-c and a-c machinery (§379).
2. Investigations of electric disturbances and transient phenomena taking place in cables, high-tension lines, oscillating circuits, etc.[2]

---

[1] For a more detailed treatment of oscillographs, see A. E. Kennelly, "Electrical Vibration Instruments," Macmillan, Chapters XIX to XXI; J. T. Irwin, "Oscillographs," Pitman; C. E. Magnusson, "Electric Transients," McGraw-Hill, Chapter II.

[2] V. Bush, "Transmission-Line Transients," *Trans. A.I.E.E.*, vol. 42 (1923), p. 878; C. E. Magnusson, "Electric Transients," Chapters III, IV and V; R. Rüdenberg, "Elektrische Schaltvorgänge," Springer.

3. Research of phenomena taking place in the electric arc, rectifiers, etc. (Chapters LVI and LX).

4. Telephonic studies; voice currents, modulation of high-frequency carrier currents, etc. In the "phonoscope" it is used in teaching the deaf to speak.

5. Current-voltage relations in two- and three-electrode vacuum tubes (Chapter LX).

6. Study of electrical or mechanical systems involving many variables, where an analytical solution becomes exceedingly complex.[3]

7. Magnetic problems involving iron undergoing rapid cyclic changes.[4]

8. High-tension dielectric phenomena, corona, dielectric loss, breakdown, etc.[5]

9. Study of wave forms in a-c generators, motors, transformers, etc.[6]

10. Disturbances during switching of transformers, generators, etc., and during accidental faults on lines.

11. Harmonics in polyphase systems (Chapter XL).

12. Current and voltage in an air-break or oil switch, and in a fuse, on opening the circuit.

13. Various mechanical measurements,[7] especially of phenomena taking place in a very short time, such as the travel of projectiles, etc.

In fact, by going over the experiments in the various chapters in this text, the reader will readily find many measurements in which an oscillographic determination of wave form and phase relations is either useful as supplementary information and a check, or absolutely indispensable for complete knowledge of a phenomenon.

1109. Classification. — There are two principal types of oscillographs, each of which has several variants:

1. The electromechanical (or electromagnetic) oscillograph:
   (a) The bifilar oscillograph.
   (b) The unifilar or string-galvanometer type oscillograph.

Each type may be provided either with electromagnets or with permanent magnets. With the great advances which have been made in permanent magnet materials (cobalt magnet steel, alnico alloy, etc.), most oscillographs are now constructed with permanent magnets.

---

[3] C. A. Nickle, *Trans. A.I.E.E.*, vol. 44 (1925), p. 844; E. M. Terry, "Advanced Laboratory Practice in Electricity and Magnetism," McGraw-Hill Book Co., Chapter X, which contains a theory of some simple transient phenomena.

[4] E. L. Bowles, *Trans. A.I.E.E.*, vol. 42 (1923), p. 346; Charlton and Jackson, *ibid.*, vol 44 (1925), p. 824.

[5] F. W. Peek, "High-Voltage Phenomena," McGraw-Hill Book Co.

[6] C. E. Magnusson, "Electric Transients," McGraw-Hill Book Co.

[7] H. L. Curtis, *Trans. A.I.E.E.*, vol. 44 (1925), p. 264; Miner and Batten, *ibid.*, 1929, p. 742.

2. The cathode-ray oscillograph:
   (a) Cold-cathode.
   (b) Hot-cathode.

The permanently sealed (Braun) tube cathode-ray oscillograph is provided with a fluorescent screen for viewing rapidly recurring waves. The image of these waves on the screen may, of course, be photographed. In the temporarily sealed (Dufour) tube a fluorescent screen and a photographic film are mounted in the vacuum tube itself.

Several other types of oscillographs have been proposed and used to a limited extent, such as electrostatic, piezoelectric, soft-iron, etc.

THE ELECTROMAGNETIC OSCILLOGRAPH

1110. This type of oscillograph consists of three parts: (a) the galvanometer which gives deflections proportional to instantaneous values of currents (ordinates in Fig. 791); (b) the optical system; and (c) the recording device. Provision is made, either in the optical system or in the recording device, for producing deflections proportional to time (abscissas in Fig. 791).

1111. The Galvanometer. — The principle of construction and operation of a bifilar oscillograph (Duddell's type) is shown in Fig. 792. In the narrow air-gap between the poles, *N*, *S*, of a powerful magnet are stretched the parallel sides of a loop, *a*, formed, for example, of silver alloy ribbon some 0.0007 in. thick and 0.007 in. wide. This loop passes over an equalizing pulley, *l*, from terminal posts, *d*. It is further supported by ivory bridges, *b*, about 0.5 in. apart, and carries a small mirror, *m*, which, in a given case, is 0.075 in. high, 0.017 in. wide, and 0.003 in. thick. The spring, *t*, puts the filaments into a tension of, perhaps, 40,000 lb. per sq. in.[8] When a direct current is passing through the loop *a*, it causes one of the legs to advance and the other one to recede in the magnetic field; the mirror is thus turned about a vertical axis. In a properly constructed instrument, this deflection is proportional to the current, so that the instrument is simply a sensitive moving-coil galvanometer (§44).

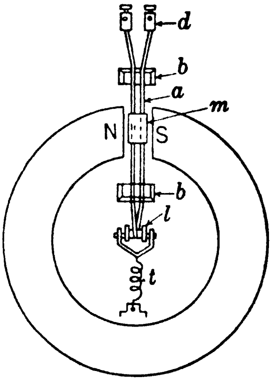

Fig. 792. Vibrator of an electromagnetic oscillograph.

---

[8] J. W. Legg, "Oscillography," *Elec. Jour.*, June, 1927.

If the current is variable, instantaneous deflections of the mirror are proportional to instantaneous values of the current through the strip. This is indicated by a beam of light reflected from the mirror on to a suitable screen or photographic film. The only difference between this instrument and an ordinary galvanometer is that the moving system of the oscillograph is very light, and that, because the strips are stretched tightly, it has a very short period of natural vibration. Therefore, the mirror easily follows rapid variations of the current, which an ordinary galvanometer could not follow because of its inertia. In the most accurate high-frequency oscillographs of this type the natural period of vibration of the loop is in the neighborhood of one ten-thousandth of a second. The moving system is immersed in a transparent viscous oil, which has a damping effect and prevents free oscillations of the vibrator from acquiring an appreciable magnitude and showing on the curve.

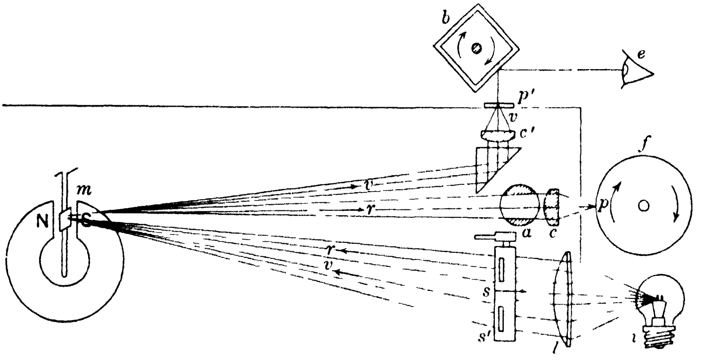

Fig. 793. Optical system for simultaneously viewing and photographing.

When variable currents traverse the loop *a*, the beam of light, reflected from the mirror, oscillates to and fro in a horizontal plane, and thus traces a straight line (ordinates). To obtain an image of the wave on the screen or on a photographic film, it is necessary to superimpose a vertical motion or time element (abscissas), as is explained below.

In many problems, it is necessary to record more than one current or voltage simultaneous, and for this reason many oscillographs are provided with three, six, and sometimes even nine elements, similar to the one shown in Fig. 792. They are known as the three-vibrator oscillograph, the six-vibrator oscillograph, etc.

1112. The Optical System. — The optical system of an oscillograph for simultaneously viewing and photographing electric waves is shown schematically in Fig. 793.[9] The light from an incandescent lamp *i* passes through a condensing lens l and through two adjustable slots s and s' as two beams, v and r (viewing and recording), to the vibrator mirror m. From m the two light beams diverge, one (r) passing through the shuttered opening a and cylindrical lens c which focuses it upon a rotating film f, carried by the drum p in a light-tight box. The other beam, v, is reflected by a prism through the cylindrical lens c' to the ground glass p', and the image of the moving spot on this screen is viewed in the rotating mirror, b, as a wave having rectangular coordinates.

---

[9] J. W. Legg, *Elec. Jour.*, February, 1932, p. 72.

The actual optical system of an oscillograph manufactured by the Westinghouse Company and embodying these features is shown in Fig. 794, also the control panel, rotating mirror within the cabinet, viewing or tracing screen above the mirror, and motor-driven film-holder.

1113. Recording Apparatus. — Currents which flow through the oscillograph vibrators may be recorded by one of several methods: (a) The beam of light falls upon a uniformly rotating photographic film, f, Fig. 793. (b) The beam falls upon a photographic plate which is allowed to drop by force of gravity down a slide; this method should not be used when absolutely uniform abscissas are required. (c) The beam falls upon a photographic plate rotated about an axis perpendicular to its own plane, thus giving a polar oscillogram.[10] (d) A piece of tracing paper is stretched over the viewing screen (Fig. 794) and the wave is traced by hand. The latter method cannot be used unless the phenomenon recurs in synchronism with the revolving mirror. Some transient phenomena may also be traced if they can be made to recur periodically by some such device as that described in §1116. When it is desired to produce waves to a larger scale, for demonstration purposes, a large stationary mirror is substituted for the tracing screen, and the vibrating beam of light is thrown on the projection screen, or directly on the wall.

When method (a) is employed the film may consist of a single turn about a drum, in which case the shutter must be automatically closed after one revolution of the drum, or it may be a long film or sensitized paper moved past the slot by a motor-driven long-film holder.

If transient phenomena are being taken, the exposure must be *timed*, that is, the shutter must be opened just before the transient begins and closed again before the film has completed one revolution (in the case of the revolving film).

The zero line or the axis of abscissas (Fig. 791) may be recorded before or after the oscillogram is taken, by making an exposure with no current passing through the vibrator. The field current should be on, however, in the types using electromagnetic fields. Different zero lines are sometimes used for the different vibrators, in order to keep distinct the several waves on one film.

---

[10] A. G. Beliavsky, *Electrician*, vol. 92 (1924), p. 38.

When the frequency or the duration of a phenomenon is not known, a voltage of known frequency is impressed upon one of the vibrators, and this " timing wave " is reproduced on the film, above or below the other records. Time intervals can then be marked on the axis of abscissas if the duration of one cycle of the timing wave is known.[11]

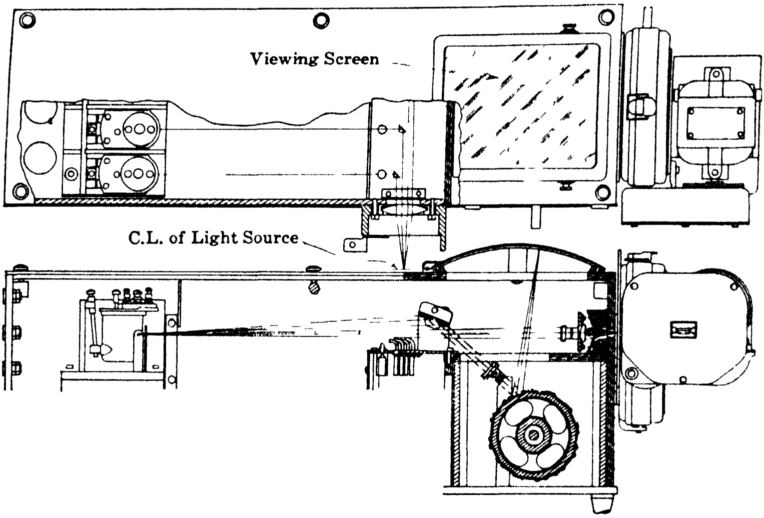

FIG. 794. Optical system for simultaneously viewing and recording (Westinghouse Electric and Mfg. Co.).

1114. The Electrical Circuits. — Figure 795[12] shows the connections of a two-element portable oscillograph of the General Electric Company. There are two vibrators, c and v, for taking a current wave and a voltage wave at the same time. The vibrator v is connected across the line, in series with an adjustable high resistance, marked " volts per millimeter," to trace the voltage wave. The other vibrator, c, is connected as a millivoltmeter in series with a protective resistance, R_1, across a variable shunt resistor controlled by a second dial-type switch marked " amperes per millimeter." It indicates the current wave. The vibrators are protected by fuses f_1, f_2, and are connected to suitable binding posts. The motor shown in the diagram is for driving a vibrating mirror which performs the function of the rotating mirror of Fig. 794.

---

[11] E. A. Eckhardt, *Journal of the Franklin Institute*, vol. 194 (1922), p. 49.

[12] M. A. Rusher, *Gen. Elec. Rev*, September, 1932, p. 494.

This motor is primarily a variable-speed motor, but a synchronizing device, *SM*, makes it possible to hold the motor in synchronism with the a-c supply at a speed resulting in about $1\frac{1}{4}$ cycles of a 60-cycle wave appearing on the screen. Motor and lamps are intended to operate from a 60-cycle, 110-volt a-c source.

The current galvanometer with its shunts is suitable for currents from about 0.01 ampere to 7 amperes, while the potential galvanometer and multiplier may be used for voltages from about 0.03 volt to 250 volts

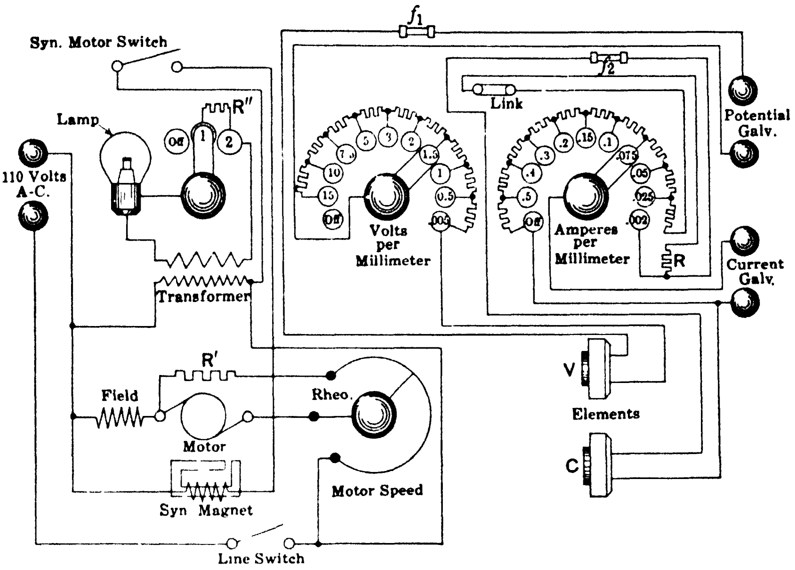

FIG. 795. Diagram of circuits in a two-element portable oscillograph (General Electric Co.).

(rms values). By the use of current and potential transformers the upper limits of these values may be extended indefinitely, and the oscillograph be insulated thereby from the high-voltage line. As a rule, a transformer introduces an error into the wave form, especially with transient phenomena, and it is necessary to determine in each case by separate experiments whether or not the use of an instrument transformer is permissible (Chapter XVIII).

1115. The String-Galvanometer Oscillograph. — The galvanometer of the unifilar or string-galvanometer oscillograph consists of a powerful electromagnet and one or two fine metallic filaments in a vertical plane at right angles to the direction of the magnetic field. A beam of light passes through holes in the pole-pieces and is focused by a lens in one of the pole-pieces to illuminate the metallic filaments strongly. A lens in the other pole-piece focuses a real image of the shadows of the metallic filaments in the plane in which the photographic film or paper moves. If a current is sent through either filament, it moves at right angles to its own direction and that of the magnetic field, so that the shadow of the filament moves at right angles to the direction of motion of the recording film. A cylindrical lens with its axis horizontal converts the long shadow of the filament to a point shadow. If both the film and the filament are moving, a curve will be traced by the point shadow on the film.

Waves are recorded on photographic paper which is fed through rollers and is developed before leaving the apparatus. This makes the possible length of the oscillogram almost unlimited and minimizes the time involved in securing the finished oscillogram. A timing device is used which consists of a spoked wheel driven by an induction motor, which in turn is controlled by a tuning fork. Shadows of the spokes are thrown on the recording paper and, since their frequency is known, give a record of time on the oscillogram.[13]

1116. The Transient Visualizer. — As long as the electrical phenomenon being studied with the oscillograph is periodic and steady, it may be observed on the viewing screen, because the frequent repetition makes the curve of light appear continuous. With a transient phenomenon, the spot of light makes only one sweep across the screen, and the eye cannot see it as a curve. If, however, the transient curve can be made to repeat itself rapidly, the light may be made to traverse the same path each time on the screen; a continuous curve will be seen and may be studied visually.

A device which accomplishes this result has been developed by H. M. Turner and named by him the transient visualizer.[14] This device (Fig. 796) consists of a number of circular disks, *s*, *s*, mounted on a common shaft. The shaft is driven through gears, *g*, *g*, by a synchronous motor, *M*. The circumference of all but one of the drum sections is divided into two segments, one a conductor and the other an insulator. The conducting segments are of various lengths, for use with transients of different durations. The remaining section is one continuous conductor and is electrically connected to the others. Brushes mounted on a common arm, *A*, make contact with these sections. These brushes may be rotated by an angle and locked in any desired position. Connections are made from these brushes to the circuits under test. The small geared shaft, *n*, at the right drives the photographic film drum, *f*, of the oscillograph (Fig. 793). The gears are interchangeable to permit different drum speeds. There is thus a definite relation between the speed of the drum and that of the oscillograph mirror, because both are driven by synchronous motors from the same a-c source. Consequently, the test circuit is opened and closed at definite intervals and the transient is repeated. The curve of the transient is similarly repeated in the oscillograph, and the result is a visible stationary curve.[15]

---

[13] A. Trowbridge, *Journal of the Optical Soc. of Amer.*, vol. 9 (1924), p. 557.

[14] H. M. Turner, *Trans. A.I.E.E.*, vol. 43 (1924), p. 805. See also H. J. Reich, "Electronic Transient Visualizer," *Elec. Eng'g*, December, 1936, p. 1314.

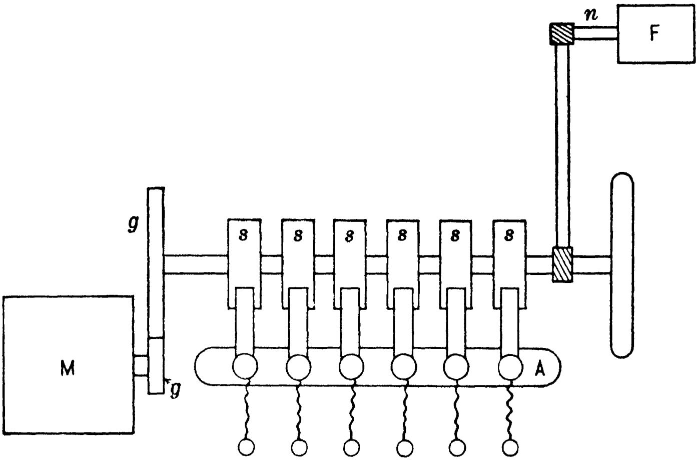

Fig. 796. Arrangement of parts in the transient visualizer.

The device may be put to various other uses, such as (a) to start oscillograms of transients at predetermined points on the film; (b) to make multiple exposures on a film where it is desired to start successive curves from the same point on the film; (c) to obtain a constant cycle length, independent of frequency variations of the power source, for convenience in comparing curves; (d) to close the circuit at a predetermined point of the emf wave; (e) to control the amount and direction of the residual magnetism left in a transformer so that the initial magnetic condition will be known the next time the starting transient is repeated.

1117. Demonstration Oscillograph. — It is possible to construct oscillographs that may be mounted in a lecture room and made to throw waves 1 to 2 ft high upon a projecting screen. An interesting instrument of this type, as described by H. Lloyd,[16] makes use of the mechanism of a radio loud-speaker unit to actuate a fairly large mirror and project waves upon a screen. These instruments, though less accurate, are more rugged than those previously described, and are usually air-damped. They will not show high harmonics accurately and may even introduce harmonics of their own, due to natural vibration; but when accurate quantitative results are not required, they are useful because of their ruggedness and greater ease of adjustment, and because they permit an image to be viewed simultaneously by a group of persons.

---

[15] For a different attachment, which permits records of transients to be made upon a stationary photographic plate, see P. Charpentier, *Revue générale de l'électr.*, vol. 17 (1925), p. 677.

[16] H. Lloyd, "Demonstration Oscillograph Outfit," *Jour. Sci. Instr.*, April, 1935, p. 119.

Such an oscillograph usually consists of a set of galvanometers each carrying a fair-sized mirror, a revolving mirror with numerous faces, and a source of light. An enclosing box is not necessary as the oscillograph is used in a darkened room. The light is focused by suitable lenses upon the galvanometer mirrors, reflected to the revolving mirror, and then thrown upon the screen. In addition to the spots of light produced by the galvanometer mirrors, a spot is thrown onto the screen by a stationary mirror. When the revolving mirror rotates, this spot traces a horizontal luminous line representing the axis of abscissas. The speed of the mirror should be a multiple of the frequency of the supply to be investigated. Then the waves appear stationary on the screen.

At the beginning of the experiment all the spots must be made to coincide on the screen, with the current off. This is done by varying the relative positions of the galvanometers on the stand, and also the position of the stationary mirror which traces the axis of abscissas. When alternating current is passed through the galvanometers, the vertical lines produced on the screen (with the revolving mirror at rest) must be perpendicular to the axis of abscissas. After being thus adjusted, the apparatus is ready for use. It is capable of many interesting demonstrations in the lecture room.[17]

1118. The Use of a Vacuum-Tube Amplifier with an Oscillograph. — It is sometimes undesirable to have the oscillograph (used as a voltmeter) draw any current from the line, for instance, when transients on an artificial transmission line (§§653 to 655) are being recorded. The energy consumed in the oscillograph may be a large portion of the total energy of a surge. In such cases the voltage under observation may be impressed between the grid and the filament of a thermionic vacuum tube (Fig. 797), the grid being given a negative bias with respect to the filament. Under proper conditions (§1183), variations in the impressed voltage will be repeated as current variations in the plate circuit; therefore, oscillograms of plate currents will also represent those of the impressed voltage. The only current drawn by the grid will be its charging current, which is negligible compared with that drawn by an oscillograph.[18]

---

[17] Sutton and Hopkins, "The Oscillograph as a Lecture Demonstration Instrument," *World Power*, vol. 6, August, 1926, p. 77.

The grid potential is adjusted by means of the potentiometer, *RG*, supplied by the battery, *C*. This potential may be read on the voltmeter, *VG*. Since the inductance of the circuit must be kept as low as possible, the voltage to the vibrator is taken from the resistance, *RO*, and not through a transformer. A battery, *E*, is inserted to keep the vibrator current zero when no voltage is impressed at the input terminals, *m*, *n*. The filament current must be accurately controlled. Since an ammeter is not sufficiently accurate, a potentiometer consisting of resistance *r*, battery *D*, and galvanometer *G* is used and is so adjusted that the galvanometer reads zero when the current is correct. *A* and *B* are the usual filament and plate batteries. The system should be so adjusted that the operation over the range of the transient to be investigated will be on the straight part of the characteristic curve of the tube. If the resistance of the circuit connected to *m*, *n* is extremely high, it may also be necessary to connect a very high resistance across *m*, *n*, in order to keep the *C* battery effective.

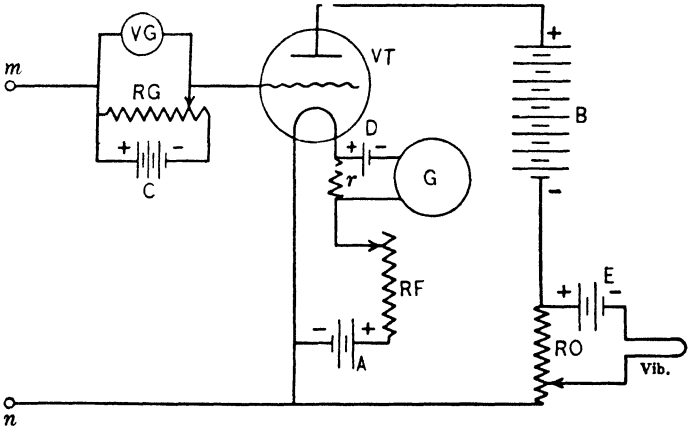

FIG. 797. A thermionic amplifier used in connection with an oscillograph.

1119. Experimental Comparison of Vibrator Constants. — The constants of an oscillograph vibrator are usually determined by comparison with another vibrator of known constants.[19] This latter vibrator is placed in the field of a permanent magnet and has air damping to secure sharpness of resonance. Such a standard vibrator is especially useful for determining the resonant frequency of another vibrator. A vibrating system at resonance possesses the characteristic that its phase of displacement is in lagging quadrature to that of the applied torque, whereas, when not at resonance, the displacement is nearly in phase with the applied torque. Since the torque in an oscillograph vibrator is proportional to the current, the frequency of vibration is known. If, then, the vibrator being tested is compared with one whose natural frequency is different, a difference in phase of deflection will result when the impressed frequency is the natural frequency of either vibrator.

---

[18] F. S. Dellenbaugh, Jr., *Trans. A I.E.E.*, vol. 42 (1923), p. 818.

[19] For a comprehensive theory of and tests on oscillographs see A. E. Kennelly, " Electrical Vibration Instruments," Chapters XVII to XXI; a very detailed theory will also be found in an article by S. Numakura, in the *Researches of the Electrotechnical Laboratory of the Ministry of Communications*, Tokyo, Japan, April, 1924, No. 135.

The method of comparison is shown in Fig. 798. The two vibrators are electrically connected in series to a source of alternating current of adjustable frequency. A beam of light strikes the mirror, m_1, of the vibrator being tested, is reflected to the mirror, m_2, of the standard vibrator, and from there to a screen, S. The two mirrors have their axes of rotation at right angles; therefore, if their vibrations are in phase with each other, the beam of light will trace a straight line on the screen; if their vibrations are in quadrature, the light will trace an ellipse. With exact phase quadrature, the principal axis of the ellipse will coincide with the line traced by one vibrator acting alone; otherwise both axes of the ellipse will be inclined to this line. The two vibrators must be placed in close proximity in order that the light reflected from the first may remain on the mirror of the second, but they must not be so close that the field of the second is affected by that of the first.

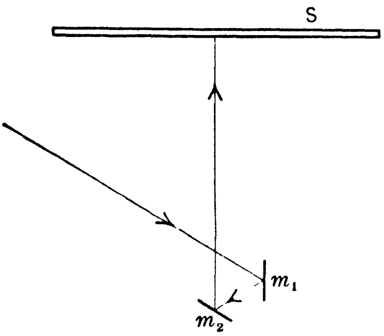

FIG. 798. Method of comparison of two vibrators.

1120. EXPERIMENT 57-A. — Study and Use of the Electromagnetic Oscillograph. — Set up and adjust the oscillograph according to the instructions furnished by the manufacturer of the instrument. Impress a nearly sinusoidal voltage on a resistor and observe the waves of voltage and current simultaneously on the screen. Repeat with a reactor, then with a condenser. Repeat these tests using a voltage of poor wave form. Now connect the three load devices in series, and, using the nearly sine-form voltage supply, trace the waves of the line voltage and current; also the voltage across each component part of the circuit. Before impressing a voltage on the oscillograph, be sure that the component voltages are not too high, since this is a resonant circuit and component voltages may be many times the line voltage (§609). Repeat the above test with the impressed voltage of very poor wave form. Explain the results, especially the suppression and accentuation of harmonics. Load the film drum and make photographs of some of the foregoing curves.

Switch a reactor or a condenser on to an a-c source and observe the results obtained by throwing the waves of voltage and current on the viewing screen. Record the same waves on a film and compare the results. The phenomenon must be timed; that is, the exposure must be made at just the right time. This is done by a tripping device, usually furnished with the instrument. Repeat the test and obtain the transient on the viewing screen by means of the transient visualizer (§1116). Calibrate the oscillograph elements by applying suitable known values of d-c voltage and determine the volts per inch or per centimeter of deflection.

The foregoing tests cover the manipulation of the oscillograph. Having acquired the necessary skill, the student may try any of the problems enumerated in §1108, or some other problem in which he is particularly interested, for instance, the wave form of transformer exciting currents at various values of impressed voltage or the flux distribution in the air-gap of a revolving-field alternator, obtained by stretching a single conductor tightly in the air-gap and applying its emf to the oscillograph. This distribution should be taken with the machine at no load, at rated load non-inductive, and at rated load zero power factor lagging. Another series of waves of interest is that of the no-load emf in an alternator (1) of the single conductor, (2) of one phase group or phase, (3) of two phases in star, and (4) of three phases in opened delta. The wave forms of a mercury-arc or other rectifier are also of interest.

THE CATHODE-RAY OSCILLOGRAPH

1121. When a current or a voltage is of extremely high frequency, the electromagnetic oscillograph described above cannot respond because of its inertia. Since very high frequencies, or phenomena of exceedingly short duration, are met in telephone and radio circuits, and in some instances in power circuits (in transients), the need arose for an oscillograph possessing little or no inertia. Such an instrument is the cathode-ray or Braun-tube oscillograph, or oscilloscope.

In this instrument, instead of the wave being shown by the movements of a light beam reflected from the vibrating mirror of the electromagnetic galvanometer, a stream of electrons inside a highly evacuated tube is deflected from its normal position by a magnetic or an electrostatic field produced by the varying current or potential to be studied.

As the moving electron beam impinges upon a screen of fluorescent material at the end of the tube (Fig. 799) a luminous moving spot is produced which, through persistence of vision, appears as a line. If another component of periodic motion can be imparted to the ray at right angles with the vibrations due to the quantity under observation, and synchronized with it, a stationary wave will appear on the screen. If this " sweep " motion can be made linear, i.e., of uniform velocity, the wave will appear in rectangular coordinates. The ray may also be used to produce a permanent record upon a photographic film. The electron stream, or cathode ray, has such a low value of inertia that it will respond to frequencies even of millions of cycles per second.

1122. The Braun Tube (Cold-Cathode Oscillograph). — In Fig. 799, *T* is a glass tube, *C* is the cold cathode or the negative terminal, and *A* the anode or the positive terminal. At *S* is a shield pierced in the center by a small hole about half a millimeter in diameter. The tube is evacuated to a low pressure. When the cathode stream strikes the shield, most of the electrons are absorbed, but some pass through the hole and impinge upon the viewing screen, *V*. This screen is covered with calcium tungstate, zinc silicate, or some such material, which becomes fluorescent under electronic bombardment, so that a small luminous spot may be distinctly seen on the screen. After passing through the shield, *S*, the ray may be deflected by either an electrostatic or a magnetic field, or both, in directions normal to the motion of electrons. The force acting upon the electrons is proportional to the strength of either field. Consequently, by making the two fields proportional to the current (or to the voltage) to be measured, and to time, the stream of electrons can be suitably deflected and the luminous spot made to describe a figure from which the wave shape of the unknown current or voltage can be determined. As an example, a magnetic field directed toward the reader is shown by dots at *H*. The electron stream is deflected by it and the spot shifted from *k* to *k'*. If the field H varies

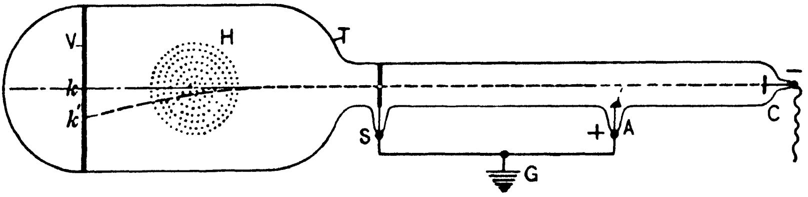

FIG. 799. The Braun tube or cathode-ray oscillograph with cold cathode.

periodically the electron spot will move periodically on the screen. The details of recording are described below, in connection with the hot-cathode oscillograph.

In the Braun tube, the shield, *S*, is connected to the anode, *A*, and the two are grounded. A high d-c voltage is impressed between the cathode and the anode. Such voltage may be obtained, for example, from a condenser charged by a transformer in series with a vacuum-tube rectifier (§1171).

The Braun tube has two major limitations: (a) the slight trace of air left in it becomes gradually exhausted and has to be renewed; and (b) the d-c voltage required to operate it is quite high (from 10 to 50 kv). Besides, the tube is not always stable. Its electrical characteristics vary with the amount of gas in the tube, and the electron stream is falsely deflected by negative charges collected on the glass walls of the tube. These charges collect on the walls of the tube because the pressure of the gas is not high enough to dispose of them. For these reasons the Braun tube has never been used as much as might be expected when its advantages are considered. It has been largely replaced by the Dufour oscillograph and modifications of the same described in §§1127 to 1130.

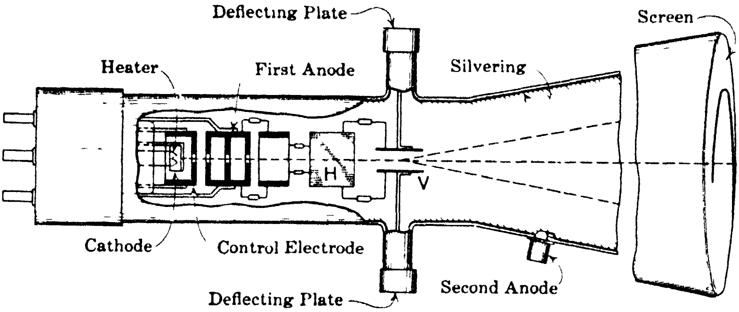

FIG. 800. Section showing the construction of the cathode-ray oscillograph.

1123. Hot-Cathode Oscillograph. — A stream of electrons may be obtained much more easily from a cathode heated to incandescence (§1088) than from a cold cathode. Such an oscillograph is shown in Fig. 800.[20]

---

[20] Warner and Kunz, *Univ. of Illinois Bulletin*, 1919, No. 114, p. 110. J. B. Johnson, *Journal of the Optical Soc. of Amer.*, vol. 6 (1922), p. 701; Jones and Tasker, *ibid.*, vol. 9 (1924), p. 471; J. W. Buchta, *ibid.*, vol. 10 (1925), p. 581; D. A. Keys, *Journal of the Franklin Institute*, vol. 196 (1923), p. 577. Three important articles on the cathode-ray oscillograph will be found in the *Journal of the Inst. Elec. Engrs.* (British), November, 1925. An important publication on this subject is issued by the RCA Mfg. Co., Radiotron Division, under the heading "Cathode-Ray Tubes and Allied Types."

The beam of cathode rays is produced by an oxide-coated cathode heated indirectly by a small internal heater coil (Fig. 800) carrying either direct or alternating current, usually the latter. The cathode is surrounded by a cylindrical " control electrode," or grid, closed, except for a small hole through which a slender ray of electrons can shoot toward the distant screen. This movement of electrons is accelerated by two anodes, the first of which has a (positive) potential of, say, 200 to 400 volts, and is in the form of a cylinder with nearly closed ends (Fig. 800). The other anode is formed by a silver coating on the inside of the flaring glass tube and is connected by a sealed-in lead to a source of higher (positive) potential of the order of 2000 volts.

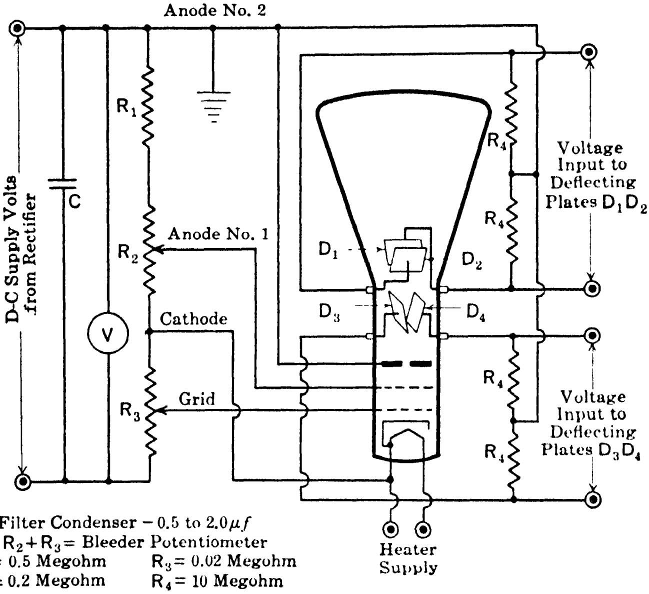
Anode No. 2
D-C Supply Volts from Rectifier
C
V
R₁
R₂
R₃
Anode No. 1
Cathode
Grid
D₁
D₂
D₃
D₄
R₄
R₄
R₄
R₄
Voltage Input to Deflecting Plates D₁D₂
Voltage Input to Deflecting Plates D₃D₄
Heater Supply

C = Filter Condenser – 0.5 to 2.0μf
$R_1+R_2+R_3$ = Bleeder Potentiometer
R_1 = 0.5 Megohm R_3 = 0.02 Megohm
R_2 = 0.2 Megohm R_4 = 10 Megohm
V = Voltmeter

FIG. 801. Typical circuit diagram of a General Radio cathode-ray oscillograph.

The electron beam is focused upon the screen by properly adjusting the ratio of potentials on the two anodes, while the intensity of the image is controlled by the grid voltage. Where the cathode ray is deflected by a magnetic field a wave 1 in. high is produced by a periodic mmf of perhaps 25 rms ampere-turns (1.5 milliamperes and 7.5 volts drop in the coils).[21]

Magnetic controlled tubes are applicable in frequencies of only a few kilocycles per second. The electrostatic-controlled tube may be used to some millions of cycles, and has a sensitivity of perhaps 100 to 150 volts (d-c) per inch of deflection.[22]

---

[21] W. O. Osbon, " A New Cathode-Ray Oscilloscope," *Elec. Jour.*, May, 1931, p. 322.

The general-purpose cathode-ray oscillograph is arranged for operation from a 110-volt, 60-cycle source. Transformers, rectifying electron tubes, and potentiometer resistors provide the several voltages required for the grid (control electrode), and two anodes. Figure 801[23] shows schematically the method of voltage control. In the plate circuit of the rectifier tube, not shown, the " bleeder potentiometer " resistance $R_1 + R_2 + R_3$ totals some 720,000 ohms. Taps to this potentiometer resistance apply the required potentials.

1124. Sweep-Frequency Control. — Sweep or timing-wave frequencies up to 3000 or more cycles per second may be set by the sweep-frequency control and may be synchronized with the wave under investigation by connecting a voltage of that frequency across the control terminals. If the sweep frequency is identical with that of test wave one cycle of the wave will appear upon the screen; if it is one-fifth that of the test wave five cycles of the latter will appear. In both cases the image on the screen is stationary.

This sweep or timing wave is produced in various ways. In one make of oscillograph[24] a condenser is very rapidly charged from the rectified d-c source through a thyratron tube. When the potential across the condenser reaches a certain value the grid of the tube acts to prevent any further plate current so that the condenser discharges gradually and almost linearly through an inductance and high resistance in series, the condenser voltage therefore dropping uniformly. This process is repeated periodically.

In another system a neon lamp is connected in parallel with a condenser to a source of d-c potential (Fig. 802). This method depends upon the property of the neon-filled lamp (or a similar device) or " striking " only when a certain voltage is reached, the discharge " failing " again at a second potential lower than the striking value. In Fig. 802, this time-deflection circuit is shown applied to a pair of the oscillograph plates. The potential difference across the lamp gradually builds up to the critical striking voltage of the lamp and then, as the lamp lights, the condenser discharges through it. The lamp then goes out, the battery again charges the condenser, etc.

The potentials at which the lamp strikes and fails being known, the frequency of the blink may be readily determined. This method may be further improved by substituting a saturated electron-tube rectifier for the resistance *R*. The condenser is charged linearly with time through the constant-current saturated electron-tube rectifier and then discharged very quickly through the neon tube. By connecting one pair of deflecting plates of the cathode-ray tube between the filament and plate of the electron-tube rectifier, a deflection of the cathode-ray spot occurs linearly with time and returns very rapidly to its initial position, from which point the cycle is repeated at a constant frequency.[25]

---

[22] Sutherlin and Harcher, " Cathode-Ray Tubes," *Elec. Jour.*, August, 1932, p. 388.

[23] RCA Radiotron Company.

[24] H. P. Kuehni, " A Low-Voltage Cathode-Ray Oscillograph with Fluorescent Viewing Screen," *Gen Elec Rev.*, September, 1934, p. 429

Additional methods of producing the timing wave will be considered with reference to the Dufour-type oscillograph (§1129).

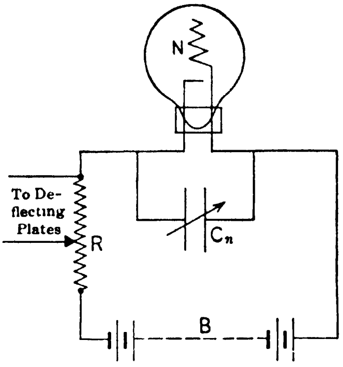

FIG. 802. Method of producing deflections proportional to time (sweep circuit) in a cathode-ray oscillograph.

1125. EXPERIMENT 57-B. — Study and Use of the Hot-Filament Cathode-Ray Oscillograph. — First make a careful study of the specific instructions applying to the cathode-ray oscillograph available. Be certain that you understand the controls and the permissible limits of the voltage and current to be used. Connect the instrument to the specified power supply — usually 110 volts at 60 cycles. Establish the cathode beam and immediately start the sweep motion to keep the spot moving, as otherwise the spot may burn the screen or even overheat and puncture the tube. Focus the beam by adjusting the two anode voltages, and secure satisfactory intensity of the beam by varying the control electrode potential.

Now use the tube to study a variety of wave shapes over a wide range of frequencies. The following are suggested:

(a) The commercial 60-cycle lighting circuit — current and voltage in inductive and capacitive circuits.

(b) Currents produced by speech and musical tones before a telephone microphone, using a suitable electron-tube amplifier to secure currents and potentials of the proper magnitude.

(c) Output waves of an electron-tube oscillator, set for various frequencies.

(d) The output of the power tube of a radio set receiving broadcast programs.

---

[25] Austin Bailey, *Physical Review*, vol. 25 (1925), p. 585.

Other problems should be suggested by the student for study.

Permanent records of the waves should be made by tracing upon thin paper, or by taking photographs of the viewing screen using an ordinary camera.

In the report give the circuit diagrams of the oscillograph. Explain how the several control voltages and sweep frequencies are obtained. Discuss the studies made with this oscillograph and compare its potentialities with those of the electromagnetic oscillograph.

1126. The Dufour-Type Cathode-Ray Oscillograph.[26] — For the recording of transients of very short duration (microseconds) and of high-frequency phenomena over considerable periods of time the Dufour oscillograph with certain modifications is generally used. This instrument consists of a glass tube about 1 in. in diameter and 10 in. long sealed into the end of a seamless steel tube, several inches in diameter, connected to a vacuum pump. Inside the glass tubing are located the cathode, usually of the cold type, and an anode having a pinhole to allow a slender pencil of electrons (cathode rays) to pass through into the enlarged metal tube. Inside the metal tube are the deflecting plates or coils (Fig. 803*a*) which impart the two components of motion (§1111) to the electron beam, and, near the bottom of the tube, a film holder and a fluorescent screen, both of which may be controlled from outside the

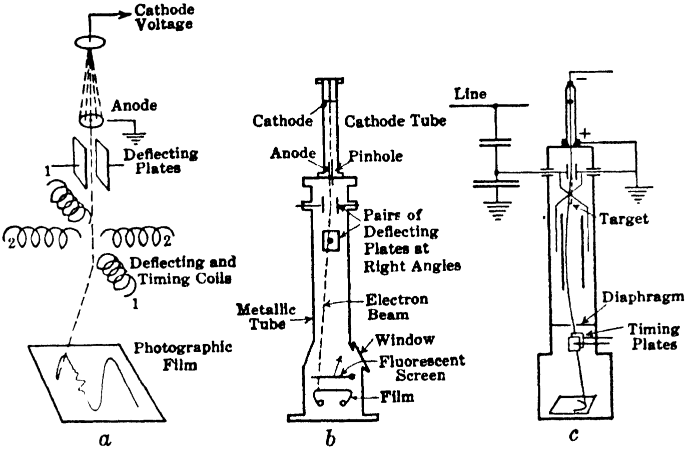

Fig. 803. Schematic diagrams of cathode-ray oscillographs: (*a*) beam deflection by either electric or magnetic field; (*b*) modified Dufour oscillograph; (*c*) oscillograph with Norinder relay.

---

[26] Two excellent articles descriptive of the Dufour-type oscillograph and its operation, by F. D. Fielder, appear in the *Electric Journal* for February and March, 1931.

tube. The screen may be made to cover the film or turned to leave it exposed to the electron ray. A sealed window is built in for viewing the screen. A drum is provided with a film magazine which allows several films to be taken in succession. When a phenomenon is being viewed, the fluorescent screen is turned up into position covering the opening into the interior of the drum so that the films are not exposed. After the films have been put in the drum, it is placed inside the chamber and locked in position. The opening is closed by a door having a very carefully ground joint or rubber gasket so that the tube may be made airtight. Three cocks, turning in ground joints placed in the door, serve to operate the mechanism for changing films and moving the fluorescent screen.

For low-speed work, a moving drum, to take the place of the magazine drum, may be used. This drum is driven by means of an external motor and magnetic clutch. Such a method is limited in its usefulness to comparatively low frequencies or long transients. These details are shown schematically in Fig. 803(*b*). Means are provided for more or less automatically maintaining the vacuum within the tube by nearly continuous pumping, a vacuum of about 5 microns being required. In some forms of the oscillograph non-magnetic sections interrupt the steel tube and permit the use of magnetizing coils both to produce beam deflections and to focus the beam.[27]

A high negative potential applied to the cathode causes it to emit electrons which, owing to the electric field, are hurled at high velocity toward the anode and through it into the recording chamber.

For the recording of occasional phenomena of short duration two systems of operation of the oscillograph are used:

(a) The electron beam is produced continuously but is prevented from falling on the film except during the disturbance to be recorded (Norinder relay).

(b) The electron beam is not started until the disturbance begins (modified Dufour).

1127. Modified Dufour-Type Oscillograph.—This type is especially suited to the recording of surges, etc., which are under the control of the experimenter. The cathode voltage, the timing wave, and the occurrence of the test wave being under the control of the operator a single sweep of the electron beam across the film serves to record the phenomenon. F. D. Fielder (*loc. cit.*) describes the operation of this oscillograph in connection with a surge generator for high-voltage tests of insulation, cables, transformers, bushings, etc. With this equipment the condensers of the surge generator (Fig. 804) are first charged to the desired high voltage. The operator then, by remote control, institutes the unidirectional cathode supply which is applied as soon as its voltage builds up to the value for which a three-electrode gap is set. Breakdown of this gap applies high voltage to the cathode and starts the cathode beam; it also sends a surge to the master gap of the surge generator, causing it break down and apply high voltage to the test piece, at the same time starting the single-sweep timing wave which moves the electron beam across the film along the time axis. Meantime a fraction of the test voltage is transmitted from a voltage divider, say a tapped high resistance across the test specimen, to the deflecting plates of the oscillograph, thus causing the electron beam to deflect along the voltage axis. Since the cathode beam is maintained for only a few microseconds and then goes out the beam does not return across the film to confuse the record. A study of Fig. 804 will make these details clear.

---

[27] O. Ackermann, "A Cathode-Ray Oscillograph with Norinder Relay," *Trans. A.I.E.E.*, vol. 49 (1930).

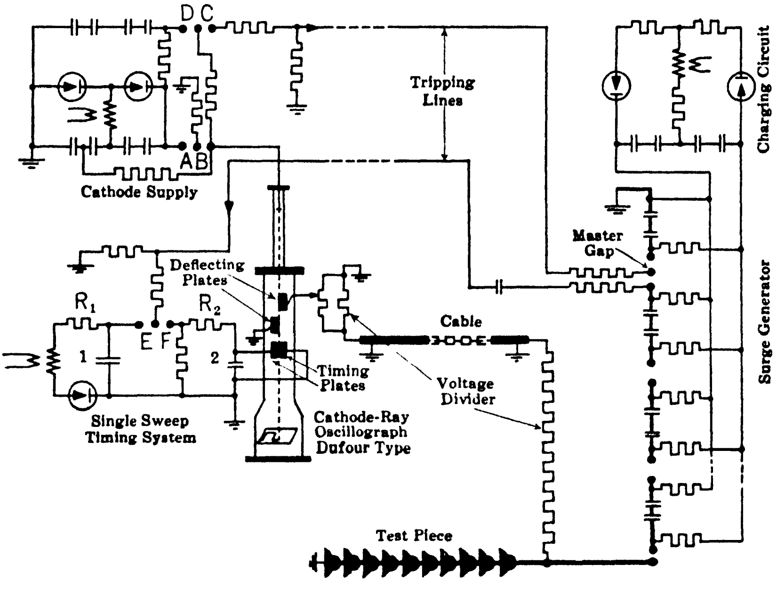

FIG. 804. Circuits of surge generator and cathode-ray oscillograph with automatic timing features (F. D. Fielder).

1128. Norinder Relay Oscillograph. — The Norinder relay is an ingenious device which permits the electron beam to be established in advance of the recording of a surge — say when a lightning stroke is expected — but, by means of a small target placed in the path of the electron beam, prevents the beam from falling too soon upon the film and blurring it. However, when the anticipated surge occurs, its voltage, or some fraction of it, is applied to two sets of deflecting plates (Fig. 803*c*) in the oscillograph tube which constitute the Norinder relay. The first set of plates bends the ray to one side of the target; the second set bends it back toward the axis of the tube and causes it to fall upon the film. The usual deflecting and timing plates of the oscillograph cause the beam to describe the wave to be recorded.

1129. Timing Systems. — (a) *Single-sweep timing.* In §1127 the single-sweep timing system was employed. This single-sweep motion was accomplished by applying to the timing plates the voltage across a condenser which was being charged through a high resistance. Thus, in Fig. 804, condenser 1 is first charged through a rectifying vacuum tube (Chapter LIX) and the resistance R_1. When a high voltage is applied to the test piece by means of the surge generator an impulse comes from the surge generator along the lower tripping wire and causes gaps E and F to break down. The voltage of condenser 1 is then applied to condenser 2 through the calibrating high resistance, R_2, with the result that the emf across condenser 2 builds up at a rate controllable by R_2. This voltage is applied to the timing plates.

The timing wave may be calibrated by applying an alternating emf of known frequency to the deflection plates, then impressing the sweep-circuit voltage to the timing plates and recording the resultant wave. The extent to which the timing wave is linear is shown by the uniformity of spacing of the alternating wave, while the sweep per microsecond is shown by the spacing and the known frequency of the wave.

(b) *Oscillatory timing system.* If an alternating emf of known high frequency, say 100,000 pps, is applied to the timing plates and the record made of a voltage surge the resulting figure consists of a series of near-sine waves of varying base and constant width. The height of the chart gives the maximum value of the surge being recorded, while the value of the surge at any instant may be determined by height of the wave above the base, the time being interpreted from the number of cycles of the known frequency of the timing wave. Such a record may then be redrawn if desired to a linear timing scale. The constant of the oscillograph, i.e., the volts per centimeter of deflection, may be found by applying known d-c voltages to the deflection plates and applying the sweep voltage to the timing plates. The height of the nearly horizontal line which results above that for zero applied voltage gives the constant in question.

1130. EXPERIMENT 57-C. — Study and Use of the Dufour-Type Cathode-Ray Oscillograph. — *This is a high-voltage device; therefore take extreme care at all times.* Make a thorough study, first of the manufacturer's instructions and then of the oscillograph and attendant circuits. Also look up the literature of the Dufour-type oscillograph (§1131).

When completely familiar with the equipment make a calibration of the instrument. Use the oscillograph to record certain transient phenomena of short duration, such as the application of high voltage from a surge generator to a lightning arrester, a bushing, etc. Use both the single-sweep and oscillatory timing system.

Describe in detail the form of instrument used and the results obtained, and discuss the operation and possible applications of the oscillograph.

1131. References.

1. J. W. Legg, *Elec. Jour.*, June, 1927, to February, 1928, Oscillography.

2. C. M. Hathaway, *Jour. A.I.E.E.*, August, 1930, p. 646, A new portable oscillograph.

3. M. A. Rusher, *Gen. Elec. Rev.*, September, 1932, p. 493, The portable two-element oscillograph improved.

4. V. S. Thomander, *Elec. Jour.*, October, 1935, p. 429, An oscillograph for universal application.

5. C. M. Hathaway, *Gen. Elec. Rev.*, November, 1934, p. 517, The Oscillograph in education.

6. J. T. Johnson, Jr., *Elec. Jour.*, August, 1931, p. 406, Automatic recording of system disturbances.

7. H. L. Curtis, *Jour. A.I.E.E.*, January, 1925, p. 45, Use of an oscillograph in mechanical measurements.

8. Miner and Batten, *Trans. A.I.E.E.*, vol. 48 (1929), p. 742, The oscillograph for measuring non-electrical quantities.

9. S. C. Leyland, *Elec. Jour.*, February, 1932, p. 71, Viewing and recording simultaneously.

10. G. W. Sutton and D. W. Hopkin, *World Power*, vol. 6, August, 1926, p. 77, The oscillograph as a lecture demonstration instrument.

11. C. Anderson and S. C. Leyland, *Elec. Jour.*, May, 1931, p. 281, A new automatic power oscillograph.

12. Pennoyer and Evans, *Gen. Elec. Rev.*, September, 1933, p. 389, A control panel for an oscillograph laboratory.

13. S. K. Waldorf, *Jour. Franklin Inst.*, June, 1932, p. 605, Amplifiers for precise oscillographic measurements.

14. H. Lloyd, *Jour. Sci. Inst.*, April, 1935, p. 119, Demonstration oscillograph outfit.

15. F. Hauffe and W. Philepoff, *Zeit. f. Instrumentenkunde*, p. 145, April, 1933, High-tension oscillograph for projection and photography.

16. A. D. MacAffer, *Gen. Elec. Rev.*, March, 1935, p. 146, The automatic oscillograph and its utility.

17. F. Bedell and H. J. Reich, *Jour. A.I.E.E.*, June, 1927, p. 563, The oscilloscope; a stabilized cathode-ray oscillograph with linear time axis.

18. H. P. KUEHNI, *Gen. Elec. Rev.*, September, 1934, p. 429, A low-voltage cathode-ray oscillograph with fluorescent viewing screen.

19. F. D. FIELDER, *Elec. Jour.*, February, 1931, p. 106, and March, 1931, p. 161, High-voltage surge testing with the cathode-ray oscillograph.

20. E. R. WHITEHEAD and W. G. ROMAN, *Elec. Jour.*, April, 1934, p. 156, The cathode-ray oscillograph.

21. O. ACKERMANN, *Jour. A.I.E.E.*, April, 1930, p. 285, A cathode-ray oscillograph with Norinder relay.

22. G. F. HARRINGTON and A. M. OPSAHL, *Elec. Jour.*, August, 1927, p. 384, Technique of Dufour cathode-ray oscillograph.

23. R. H. GEORGE, *Jour. A.I.E.E.*, July, 1929, p. 534, A new type of hot cathode-ray oscillograph.

24. J. T. MACGREGOR-MORRIS and R. MINES, *Jour. I.E.E.*, November, 1925, p. 1056, Measurements in electrical engineering by means of cathode rays.

25. GEORGE, MEYER, HEIM, and ROYS, *Trans. A.I.E.E.*, 1935, p. 1095, A cathode-ray oscillograph for observing two waves.

26. L. F. WOODRUFF, *Elec. Eng'g*, October, 1935, p. 1045, Multielement operation of the cathode-ray oscillograph.

27. BORDEN and BEHAR, *Instruments*, November and December, 1936, January and February, 1937, Oscillography.

28. H. J. REICH, *Elec. Eng'g*, December, 1936, Electronic transient visualizer.

29. R. R. BATCHER, *Instruments*, December, 1936, January–June, 1937, Cathode-ray oscillograph applications; August, 1937, High-voltage oscillographs.

30. H. F. MOYER, *Gen. Elec. Rev.*, April, 1937, p. 203, New applications of cathode-ray oscillographs.

31. W. E. PAKALA, *Elec. Eng'g*, December, 1938, p. 682, A memory attachment for oscilloscopes.

CHAPTER LVIII

HARMONIC ANALYSIS OF PERIODIC WAVES

1132. An irregular periodic wave, such as is shown in Figs. 791 and 805, may be resolved into a sine wave of fundamental frequency and those of double, triple, etc., frequencies. In Fig. 805, the amplitude of the fundamental sine wave is denoted by C_1, that of the sine wave of triple frequency by C_3, etc. Such component waves of higher frequencies are known as the third harmonic, the fifth harmonic, etc. The sine wave of the lowest frequency is called the fundamental or the first harmonic.

In some problems in electrical engineering it is required to resolve a given irregular wave into its harmonic sine waves, or at least to separate one or more harmonics. Such a wave may represent a current, a voltage, a flux, or any other quantity that may be plotted as a periodic curve. The available methods of wave analysis may be broadly divided into two groups:

(A) Wave analysis by measurement on the actual circuit in which the irregular current or voltage takes place.

(B) Wave analysis of a record of the irregular wave obtained with an oscillograph (Chapter LVII) by a contact maker[1] or in some other way.

The various methods of group (B) may be subdivided into:

1. Mechanical (machine analyzers).
2. Analytical.
3. Graphical.

It is desired here to give merely an outline of the underlying mathematical theory, together with a brief sketch of one or two fundamental methods, so that the student will be able to analyze a given wave when necessary. Literature references are given for those who wish to follow the matter in more detail.[2]

---

[1] See Arnold and Bragstadt, "Die Wechselstromtechnik," Vol I, Chapter XVII.

[2] For an extensive bibliography of various methods under (A) and (B), with their advantages and disadvantages given, see F. S. Dellenbaugh, Jr., *Trans. A.I.E.E.*, vol. 40 (1921), p. 471. A list of references will also be found in an Appendix to the paper by Cockcroft, Coe, Tyacke, and Walker, *Inst. El. Engrs.* (British), *Journal*, vol. 63 (1925), p. 69, and at the end of Chapter III in Russell's book referred to in the next section.

THEORY OF THE FOURIER SERIES

1133. If y is a periodic function of x (Fig. 805), then y generally may be expressed as an infinite series of the form:

$$y = C_0 + C_1 \sin(x - \alpha_1) + C_2 \sin 2(x - \alpha_2) + C_3 \sin 3(x - \alpha_3) + \text{etc.} \quad (1)$$

which is known as Fourier's theorem, series, or expansion.[3] In this expression, y is an ordinate of the given irregular curve; C_0, its average value over a cycle; C_1, C_2, C_3, etc., the amplitudes of the harmonics (component sine waves); and α_1, α_2, α_3, etc., the phase angles of these harmonics.

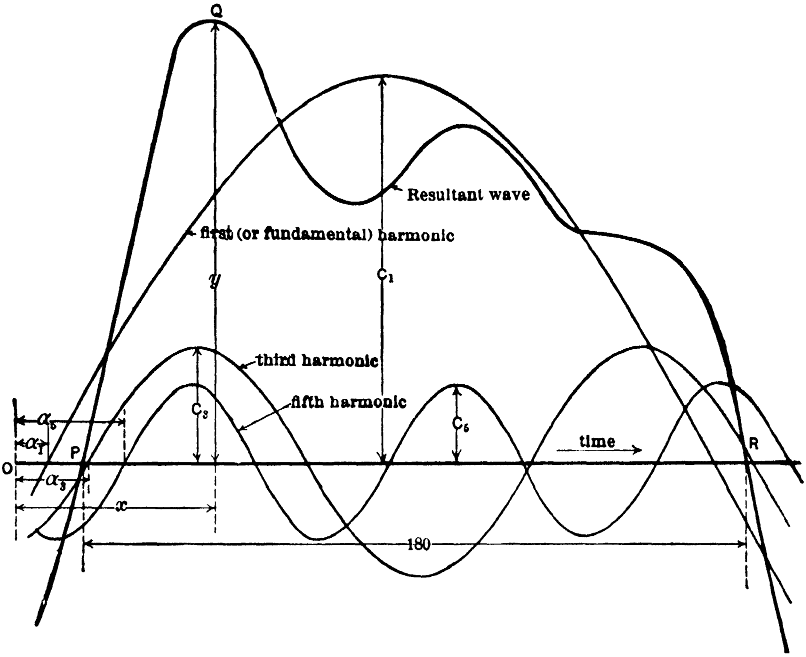

FIG. 805. An irregular periodic wave resolved into its fundamental and higher harmonics.

Let O be an arbitrary origin from which abscissas x and angles α are measured.[4] These abscissas are angles, considering the total period of the wave to be equal to 2π radians or 360 degrees. In Fig. 805, the given curve is assumed to repeat itself for the negative ordinates on the next half-cycle, and for this reason its base, *PR*, is taken as 180 degrees. The angle α_1 denotes the angular distance between O and the point at which the fundamental sine wave crosses the axis of abscissas in the positive direction. Ordinates of the first harmonic are therefore proportional to $\sin (x - \alpha_1)$. Similarly, α_3 denotes the distance between O and the point at which the third harmonic crosses the axis of abscissas in the positive direction; α_3 is measured to the same scale as α_1. But the base of the third harmonic is only one-third of that of the fundamental, so that the angles x and α_3, measured on the scale $PR = 180$ degrees, represent only one-third of these quantities measured on the scale of the base of the third harmonic taken as 180 degrees. It is more convenient to measure all the angles on the scale $PR = 180$ degrees, and to multiply the results by the order of the harmonic. Thus, ordinates of the third harmonic are proportional to $\sin 3(x - \alpha_3)$, those of the fifth harmonic to $\sin 5(x - \alpha_5)$, etc.

---

[3] For a detailed discussion of the validity of this theorem and for its proof, see Albert Eagle, "Fourier's Theorem and Harmonic Analysis," Longmans, Green; Alex. Russell, "Alternating Currents," Cambridge Univ. Press, Vol. II, Chapter III; L. B. W. Jolley, "Alternating Current Rectification, Wiley, Part I, Chapter I; W. E. Byerly, "Fourier's Series and Spherical, Cylindrical, and Ellipsoidal Harmonics," Ginn & Co.

Equation (1) expresses the condition that any ordinate, y, of the given curve is equal to the sum of C_0 and the corresponding ordinates of all the harmonics, for the same value of x.

1134. Waves with Odd Harmonics Only.— (a) *D-c component.* In order to determine C_0, the d-c component, in eq. (1), find the average value of the wave, i.e., multiply both sides by dx and integrate over a complete cycle, that is, between some value x_0 and $x_0 + 2\pi$, and divide by 2π. The integral of each sine wave is zero, because such an integral stands for the area of that particular harmonic, and there are equal numbers of identical positive and negative areas. Thus, the result of integration is:

$$\int_{x_0}^{x_0+2\pi} y\,dx = C_0 \int_{x_0}^{x_0+2\pi} dx = 2\pi C_0 \quad . \quad . \quad . \quad . \quad (2)$$

The average is

$$C_0 = (2\pi)^{-1} \int_{x_0}^{x_0+2\pi} y\,dx \quad . \quad . \quad . \quad . \quad . \quad . \quad (3)$$

We shall assume in the rest of the chapter that this average value has been determined by some well-known method.

In a great majority of practical curves, especially those of voltages and currents obtained by electromagnetic induction, without a commutator, there is no d-c component, and the areas above and below the axis of abscissas are equal. In all such cases $C_0 = 0$. Sometimes a d-c component is present in an a-c circuit, due to rectification (Fig. 783), unilateral conduction, electrolytic action, etc., in which case it is necessary to determine the value of C_0 from eq. (3), or by some equivalent method.

---

[4] Point O may be chosen to coincide with P, if so desired, and if there is an advantage of simplification in so doing.

(b) *Even harmonics.* By drawing a fundamental sine wave and a second harmonic, and adding the ordinates point by point, it will be found that the resultant ordinates above and below the axis of abscissas do not follow in the same order. In other words, every two consecutive alternations are dissimilar. On the other hand, by drawing a fundamental and a third harmonic, it will be found that the ordinates above and below the axis of abscissas follow in the same order.

Many practical waves to be analyzed consist of similar consecutive alternations, and therefore contain no even harmonics. Omitting these harmonics and C_0 in eq. (1), we get, for curves with identical positive and negative half-waves and without the unidirectional component C_0:

$$y = C_1 \sin (x - \alpha_1) + C_3 \sin 3(x - \alpha_3) + C_5 \sin 5(x - \alpha_5) + \text{etc.} \quad (4)$$

The limitations of this equation should be kept well in mind and the more general eq. (1) used, should a particular problem require it.

1135. Sine and Cosine Components of Harmonics. — An nth harmonic in eq. (1) or (4) may be rewritten in the following form:

$$C_n \sin n(x - \alpha_n) = C_n \cos n\alpha_n \sin nx - C_n \sin n\alpha_n \cos nx \quad . \quad (5)$$

We shall introduce the following notations:

$$A_n = C_n \cos n\alpha_n \quad . \; . \; . \; . \; . \; . \; . \; . \; . \; . \quad (6)$$

$$B_n = -C_n \sin n\alpha_n \quad . \; . \; . \; . \; . \; . \; . \; . \; . \quad (7)$$

so that eq. (5) becomes:

$$C_n \sin n(x - \alpha_n) = A_n \sin nx + B_n \cos nx \quad . \; . \; . \quad (8)$$

Equation (1) may therefore be rewritten in the form:

$$\begin{aligned} y = C_0 &+ A_1 \sin x + A_2 \sin 2x + A_3 \sin 3x + \text{etc.} \\ &+ B_1 \cos x + B_2 \cos 2x + B_3 \cos 3x + \text{etc.} \quad . \; . \quad (9) \end{aligned}$$

In other words, each harmonic may be split into its sine and cosine components with respect to the origin, O. This is shown in Fig. 806 for the fifth harmonic. The sine component passes through O; the cosine component has its maximum value at O. A_n is positive when the sine curve passes through O in the positive direction (that is, opposite to that shown in Fig. 806), the ordinates of the first half-wave to the right of O being positive. B_n is positive if the cosine curve reaches its positive maximum at O. Thus, in Fig. 806, B_n is negative. Adding the curves A_5 and B_5 point by point, the original curve C_5 (Fig. 805) is obtained. The position and magnitude of C_5 with respect to the given irregular curve are independent of the chosen position of O, but the magnitudes of the components A_5 and B_5 are determined by the position of O.

From a mathematical point of view, eqs. (1) and (9) are equivalent, in that in both expressions each harmonic is characterized by two parameters. In eq. (1) these parameters are C_n and α_n; in eq. (9) they are A_n and B_n. When C_n and α_n are known, A_n and B_n may be computed from eqs. (6) and (7). In Fig. 805, the angle α_5 happens to be such that $5\alpha_5$ is greater than 90 degrees. Consequently, A_5 in eq. (6) comes out negative, and for this reason the curve A_5 starts at O in the negative direction. Sin $5\alpha_5$ happens to be positive, so that B_5 is also negative, and the curve B_5 has its negative maximum at O.

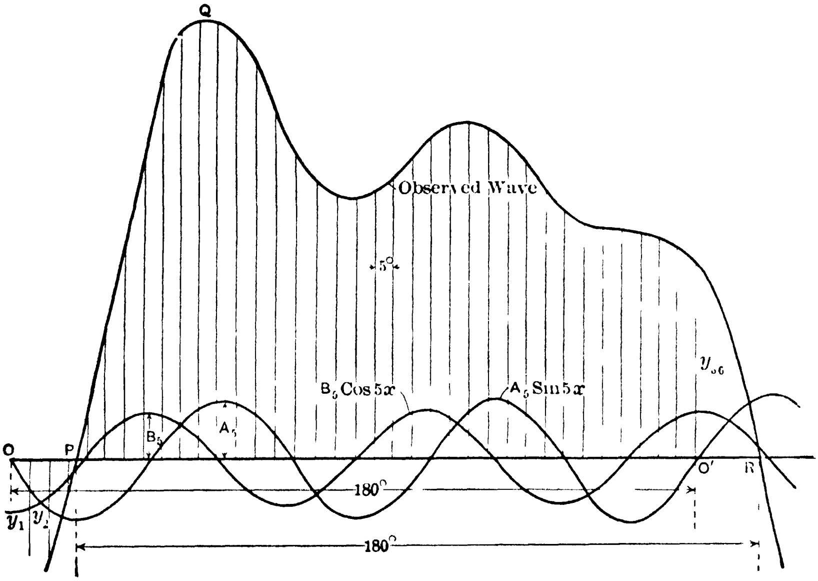

FIG. 806. The sine and cosine components of the fifth harmonic in an observed periodic wave.

Usually A_n and B_n are determined first and it is sometimes required to find C_n and α_n. From eqs. (6) or (7) we have:

$$\tan n\alpha_n = -B_n/A_n \qquad (10)$$

$$C_n^2 = A_n^2 + B_n^2 \qquad (11)$$

In practical applications, it is convenient to compute $n\alpha_n$ from eq. (10) and then compute C_n from either eq. (6) or (7), avoiding the use of eq. (11), unless a table of squares is available.

Equation (10) is satisfied by two values of $n\alpha_n$, differing from each other by 180 degrees, because $\tan n\alpha_n = \tan (n\alpha_n \pm \pi)$. The question is decided by reference to eqs. (6) and (7), since C_n *is always positive.* Of the two values of $n\alpha_n$, that is chosen in which the signs in both eqs. (6) and (7) are satisfied.

1136. Fundamental Rules Applying to Wave Analysis. — Three rules regarding the products of sine waves of varying frequency and phase relation furnish the fundamental basis of the analysis of periodic waves. These rules[5] are as follows:

1. The average product of two sine waves *of the same frequency and in phase equals one-half the product of their amplitudes.* Ex.: Av. power = $E_mI_m/2$, when E and I are in phase.

2. The average product of two sine waves *of the same frequency but displaced 90 degrees is zero.*

3. The average product of two sine waves *of different frequencies,* when taken over 2π radians for the wave of lower frequency *is zero.*

Proofs. (1) Consider two sine waves, $E_m \sin x$, and $I_m \sin x$ *of the same frequency and in phase* (see Chapter VI). The average product over 2π radians is then:

$$\text{Av. prod.} = \frac{E_mI_m}{2\pi}\int_0^{2\pi} \sin^2 x\, dx = \frac{(E_mI_m)}{2\pi}\int_0^{2\pi} \frac{(1 - \cos 2x)}{2}\, dx$$

$$= E_mI_m\ 2 \qquad . \ . \ (12)$$

Hence, if the amplitude of one wave is known to be unity, it follows that the amplitude of the second wave is twice the average product of the two.

(2) *The product of two sine waves of the same frequency but displaced 90 degrees:*

$$\text{Av. prod. of } E_m \sin x \text{ by } I_m \cos x = \frac{E_mI_m}{2\pi}\int_0^{2\pi} \sin x \cos x\, dx$$

$$= \frac{E_mI_m}{2\pi}\int_0^{2\pi} (1/2) \sin 2x\, dx = 0 \quad . \ . \ . \ . \ . \ . \ . \ . \quad . \ . \ (13)$$

---

[5] Ryan, Norris, and Hoxie, "Textbook of Electrical Machinery," Chapter IV, John Wiley & Sons.

(3) *Average product of sine waves of different frequencies:*

$$\text{Av. prod. of } E_m \sin mx \text{ by } I_m \sin nx = \frac{E_m I_m}{2\pi}\int_0^{2\pi} \sin mx \sin nx\, dx$$

But

$$\sin mx \sin nx = (1/2)\,[\cos(m-n)x - \cos(m+n)x]$$

and

$$\int_0^{2\pi} [(\cos m - n)x - \cos(m+n)x] = 0 \quad . \; . \; . \quad (14)$$

when m and n are integers. Therefore, the average product of sine waves of different (multiple) frequencies is zero.

1137. Determination of the Coefficients A_n and B_n. — From §1136 it is evident that to determine the coefficient A_n of the term $A_n \sin nx$ in eq. (9), one should multiply both sides of the equation by $\sin nx\, dx$ and integrate between the limits $x = 0$ and $x = 2\pi$. In accordance with eqs. (12) to (14), all the terms on the right-hand side are equal to zero, except that containing $\sin^2 nx$. We therefore have:

$$\int_0^{2\pi} y \sin nx\, dx = \pi A_n \quad . \; . \; . \; . \; . \; . \; . \; . \; . \quad (15)$$

from which,[6]

$$A_n = (1/\pi)\int_0^{2\pi} y \sin nx\, dx \quad . \; . \; . \; . \; . \; . \; . \; . \quad (16)$$

Similarly, to determine B_n, multiply both sides of eq. (9) by $\cos nx\, dx$ and integrate between the limits $x = 0$ and $x = 2\pi$. The result is:

$$B_n = (1/\pi)\int_0^{2\pi} y \cos nx\, dx \quad . \; . \; . \; . \; . \; . \quad (17)$$

When even harmonics are absent, the limits of integration can be narrowed down to $x = 0$ and $x = \pi$, so that formulas (16) and (17) become:

$$A_n = (2/\pi)\int_0^{\pi} y \sin nx\, dx \quad . \; . \; . \; . \; . \; . \; . \; . \quad (18)$$

$$B_n = (2/\pi)\int_0^{\pi} y \cos nx\, dx \quad . \; . \; . \; . \; . \; . \; . \; . \quad (19)$$

---

[6] In §§817 and 872 this equation was used in the form

$$A_n = (1/\pi)\int_0^{2\pi} F(x) \sin nx\, dx$$

Since y is given as a function of x, the integrals (16) and (17), or (18) and (19), may be evaluated to a required degree of accuracy by one of the methods indicated in §1132, and in this manner the values of A_n and B_n may be obtained for any desired harmonic. Then, if necessary, C_n and α_n may be computed as shown in §1135, and thus the total nth harmonic found. By performing this process for a sufficient number of harmonics, beginning with the fundamental and continuing until values of C_n become negligibly small, the given curve may be resolved into its harmonics to any desired degree of accuracy.

1138. A Property of Equidistant Ordinates. — Let the given curve be ruled with equidistant ordinates, as shown in Fig. 806, beginning with the origin O. Let $2p$ be the total number of divisions per cycle; in this particular case $2p = 72$, there being 36 divisions per half-cycle. Let the ordinate at O be denoted by y_0, the next ordinate y_1, etc. Let the angular distance between adjacent ordinates be β, where

$$\beta = 2\pi/2p = \pi/p \quad . \; . \; . \; . \; . \; . \; . \; . \; . \quad (20)$$

Then, using eq. (9), we may write the following $2p$ equations:[7]

$$y_0 = C_0 + B_1 + B_2 + \text{etc.} + B_p + \text{etc.} \quad . \; . \; . \; . \; . \quad (21)$$

$$\begin{aligned} y_1 = C_0 &+ A_1 \sin \beta + A_2 \sin 2\beta + \text{etc.} + A_p \sin p\beta + \text{etc.} \\ &+ B_1 \cos \beta + B_2 \cos 2\beta + \text{etc.} + B_p \cos p\beta + \text{etc.} \quad . \; . \quad (22) \end{aligned}$$

. . . .

$$\begin{aligned} y_{2p-1} = C_0 &+ A_1 \sin (2p-1)\beta + A_2 \sin 2(2p-1)\beta \\ &+ \text{etc.} + A_p \sin p(2p-1)\beta + \text{etc.} + B_1 \cos (2p-1)\beta \\ &+ B_2 \cos 2(2p-1)\beta + \text{etc.} + B_p \cos p(2p-1)\beta + \text{etc.} \quad . \quad (23) \end{aligned}$$

From these expressions, it is possible to eliminate all the harmonics, except B_p, B_{3p}, B_{5p}, etc., and in this manner to obtain a useful relationship among these latter quantities. For this purpose, add the $2p$ eqs. (21) to (23) term by term, reversing the sign of every second equation; in other words, form the expression $y_0 - y_1 + y_2 - \text{etc.} - y_{2p-1}$. There being an even number of equations, all the C_0's will cancel each other. Collecting together the terms with A_1, we shall find that they satisfy eq. (27), which is proved in the next section, so that the result does not contain A_1. The same is true for all the other A's. Factoring out B_1, B_2, etc., we shall find that the expressions in the parentheses are of the form (26), so that these B's also drop out of the result.

When we come, however, to B_p, we find that it is multiplied by the expression $1 - \cos p\beta + \cos 2p\beta - \text{etc.} - \cos p(2p - 1)\beta$. But, according to eq. (20), $p\beta = \pi$, so that the foregoing series simply becomes $1 + 1 + 1 + \text{etc.} + 1 = 2p$. The same is true of the terms containing B_{3p}, B_{5p}, etc. Thus, the final result is:

---

[7] Since p is an integer, the numbers p, $2p$, $3p$, etc., occur in the subscripts of A and B, in the course of expressing an irregular wave by means of a Fourier series.

$$y_0 - y_1 + y_2 - y_3 + \text{etc.} - y_{2p-1} = 2p(B_p + B_{3p} + B_{5p} + \text{etc.}) \quad . \quad (24)$$

As an example, let $p = 7$; let B_7, the amplitude of the cosine component of the seventh harmonic, be of an appreciable magnitude, and let $B_{3p} = B_{21}$, $B_{5p} = B_{35}$, etc., all be negligible. Then, from eq. (24), *approximately:*

$$B_7 = (y_0 - y_1 + y_2 - y_3 + \text{etc.} - y_{13})/14 \quad . \quad . \quad . \quad (24a)$$

so that B_7 can be determined by measuring 14 equidistant ordinates per cycle. The limitation of the method is the fact that the higher harmonics that are odd multiples of the one under consideration are neglected. Equation (24) is given here because of its theoretical interest and also because some authors recommend it, without always making clear the inaccuracy involved in neglecting B_{3p}, B_{5p}, etc.

In order to deduce a similar relationship for the A coefficients, shift the origin O to the right by an angle $\pi/(2p)$, to a point O', and again rule the curve with $2p$ equidistant ordinates. These ordinates will be situated midway between the former ones; let them be denoted y_0', y_1', y_2', etc. The new cosine component of the pth harmonic will be the same as the sine component for the old origin. Therefore, we may write directly, by analogy with eq. (24):

$$y_0' - y_1' + y_2' - y_3' + \text{etc.} - y_{2p-1}' = 2p(A_p + A_{3p} + A_{5p} + \text{etc.}) \quad (25)$$

1139. Sums of Sines and Cosines of Angles Differing by Equal Increments. — Consider a regular closed polygon with k sides, the length of each side being equal to unity. Let the first side form an angle ϕ with an axis of reference, and let the angles which the consecutive sides form with the same axis be $\phi + \beta$, $\phi + 2\beta$, etc., where $\beta = 2\pi/k$. The sum of the projections of the sides of a closed polygon on any axis is equal to zero. Consequently, we may write:

$$\cos\phi + \cos(\phi + \beta) + \cos(\phi + 2\beta) + \text{etc.} + \cos[\phi + (k-1)\beta] = 0 \quad (26)$$

This expression need not be limited to its foregoing geometric interpretation; it is a general trigonometric relationship which holds true for any value of ϕ and for $\beta = 2\pi/k$, where k is an integer.

In an ordinary regular pentagon the angle between the consecutive sides is $360/5 = 72$ degrees. Instead of turning by 72 degrees when following from one side to the next, one may turn by the double amount, that is, by 144 degrees. The result will also be a closed pentagon, but of a different shape. The sum of its projections on any axis is also equal to zero, so that eq. (26) also holds true for $\beta = 4\pi/k$. Generalizing this reasoning, it will be found that eq. (26) holds true for $\beta = N(2\pi/k)$, where N and k are positive integers. The only evident exception is when N is a multiple of k, because then all the terms in eq. (26) are equal to each other and their sum cannot be equal to zero. In this case there is no closed polygon either, but only a straight line.

Take now a reference axis perpendicular to the former one, and express again analytically the fact that the sum of the projections of the sides of the polygon is equal to zero. This will give:

$$\sin\phi + \sin(\phi + \beta) + \sin(\phi + 2\beta) + \text{etc.} + \sin[\phi + (k - 1)\beta] = 0 \quad (27)$$

where $\beta = N(2\pi/k)$, with the limitation mentioned above.

Equations (26) and (27) are useful in some problems in connection with the Fourier series, and also in the theory of polyphase systems.

PRACTICAL METHODS OF HARMONIC ANALYSIS

1140. There exists a vast literature describing various specific methods of application of Fourier's expansion, represented by eq. (1) or (9), to the analysis of a-c waves. Anyone who has to analyze numerous curves into harmonics regularly will find it necessary to make a study of various methods and decide on the one best suited for his purposes. Lists of references to important articles will be found in the sources mentioned in §1132 and at the end of §1145; contributions are mentioned below, in a brief outline of the principal methods.

1141. Experimental Separation of Harmonics. — Let it be required to measure directly the value of a certain harmonic in an alternating current flowing through a given circuit, or of an a-c potential between two points. Connect one of the coils of an electrodynamometer (§50) in the circuit to be investigated, and the other coil to a source of strictly sinusoidal voltage of exactly the frequency of the desired mth harmonic. Consider the unknown current as resolved into its various harmonics. Then the dynamometer torque is equal to the algebraic sum of the component torques between the individual harmonics and the external analyzing current. The average torque between the nth harmonic of the unknown current and the analyzing current is represented by expressions such as (14), and therefore is equal to zero, if the frequency of the nth harmonic is different from that of the analyzing current (§1136). When $m = n$, these expressions become of the form (12), and are no longer equal to zero. In other words, the dynamometer torque is due only to the mth harmonic in the unknown current, and more particularly to that component of this harmonic which is in phase with the analyzing current. If the dynamometer constant is known, the value of this component may be readily computed from the dynamometer reading. By shifting the phase of the analyzing current by 90 electrical degrees, the other component of the same harmonic may be similarly measured.

The harmonic set. For obtaining various harmonic currents, a set of alternators may be used, mounted on the same shaft and driven by a suitable motor. One of the alternators may have 2 poles, the next 6 poles, the next 10 poles, etc., the frequencies being in the ratios of 1 : 3 : 5 : etc. If the alternators are so designed as to give practically pure sine waves, such a set can be used for measuring at least the lower harmonics in an unknown current or voltage. Another use of such a set is to obtain irregular waves by synthesis. Pure sinusoidal oscillations of higher frequencies may be produced by means of the Vreeland oscillator (§1104) or vacuum-tube oscillators, in preference to revolving machines.

The foregoing dynamometer method is only one of several possible methods for experimental determination of harmonics. The following sources should be consulted for details:

Alex. Russell, "Alternating Currents," vol. 2, Chapter IV.

Cockcroft, Coe, Tyacke, and Walker, *Inst. El Engrs.* (British), *Journal*, vol. 63 (1925), p. 69.

A. Blondel, *Revue générale de l'électr.*, vol. 17 (1925), p. 363; also *Comptes rendus*, vol. 180 (1925), p. 785.

R Schimpf, *Elek. Zeits.*, vol. 46 (1925), p. 75.

R. L. Wegel and C. R. Moore, *Trans. A.I.E.E.*, vol. 43 (1924), p 457.

1142. Instrumental and Mechanical Methods of Wave Analysis.— The ultimate solution of the problem of analyzing a given wave (drawn on a sheet of paper) into its harmonics should be purely mechanical, or electromechanical. One should merely follow the outline of the wave with a stylus of a calculating machine, and, as a result, read somewhere on the machine the amplitudes of the harmonics. Since the amplitudes of harmonics are expressed by eqs. (26) and (27), the function of the machine is to multiply the ordinates of a given curve by the proper values of sin nx and cos nx, and to integrate the results over a cycle. Of the devices mentioned by Dellenbaugh (*loc. cit.*), the Henrici harmonic analyzer is probably the most accurate and speedy; its only disadvantages are its cost and size.[8]

---

[8] K. Noguchi has simplified the construction of the machine and reduced its size, apparently without impairing its accuracy; *Engineering*, vol. 118 (1924), p. 876.

In this country, the Michelson analyzer and the Chubb machine have been used to some extent. Of the more recent developments, the Woodbury analyzer[9] and Dellenbaugh's device,[10] both involving electric features, deserve to be mentioned.

1143. Analytical Methods. — Fundamentally, any accurate analytical computation of amplitudes of harmonics must be based upon eqs. (26) and (27). When a curve to be analyzed is a regular function, which can be expressed as $y = f(x)$, the actual integrations can be performed by one of the methods given in the integral calculus. Examples of such integrations appear in §§817 and 872, and for the cases of a rectangle, a triangle, a rectified sine wave, etc., as well as for some continuous functions, will be found in Eagle (Chapters III and IV), Russell, and Jolley (*loc. cit.*, §1133).

When a curve to be analyzed is an irregular empirical curve, for example, an oscillogram (Figs. 791 and 805), the first step is to measure and to tabulate a sufficient number of equidistant ordinates. After this, the curve itself does not exist, and all the computations are performed with these ordinates. Therefore, the accuracy of the result depends upon a judicious choice of the origin and number of these ordinates and upon the accuracy with which they have been measured.[11] After this, two ways are open:

(a) One method is to multiply each ordinate y by the value of sin nx for the desired harmonic, to plot the products as a new curve and to measure its area with a planimeter. Dividing the area by π will give A_n. If the curve contains odd harmonics only, eq. (18) may be used instead. A similar process is then employed to determine B_n from eq. (17) or (19). Tables or *schedules* are included in the appendix to this chapter,[12] which give values of sin nx and cos nx for the fundamental, the third, the fifth, and the seventh harmonic, for ordinates spaced 5 degrees apart, as shown in Fig. 806. These tables save time in looking up values in trigonometric tables and reduce the probability of an error in the magnitude or in the sign of a trigonometric function.

---

[9] F. S. Dellenbaugh, Jr., *Jour. A.I.E.E.*, vol. 42 (1923), p. 58.

[10] F. S. Dellenbaugh, Jr., *Trans. A.I.E.E.*, vol. 40 (1921), p. 451.

[11] Eagle (*op. cit.*, p. 102) has proposed to increase the accuracy of the analytical method by assuming the ordinates to be connected by parabolas of different degrees; this, of course, makes the computations more laborious.

[12] Prepared by the authors and published by John Wiley & Sons. For more extensive tables and schedules, see L. W. Pollok, "Rechentafeln zur harmonischen Analyse"; F. W. Grover's "Analysis of Alternating Current Waves by the Method of Fourier, with Special Reference to Methods of Facilitating the Computations," *Bureau of Standards Bulletin*, vol. 9 (1913), p. 567; J. Kopeliowitch, *Schweiz. Elekt. Ver., Bull.*, vol. 16 (1925), p. 409.

(b) Another method is to do the work analytically throughout. The integrals are then replaced approximately by sums of a finite number of terms equal to the chosen number, $2p$, of ordinates per cycle. In this case, dx becomes a finite increment Δx, where

$$\Delta x = 2\pi/2p = \pi/p \qquad (28)$$

Equations (30) to (33) are transformed into

$$\bar{A}_n = (1/p) \sum_0^{2\pi} y \sin nx \qquad (29)$$

$$\bar{B}_n = (1/p) \sum_0^{2\pi} y \cos nx \qquad (30)$$

or

$$\bar{A}_n = (2/p) \sum_0^{\pi} y \sin nx \qquad (31)$$

$$\bar{B}_n = (2/p) \sum_0^{\pi} y \cos nx \qquad (32)$$

A bar is placed over the A's and B's to remind the reader that the values obtained from eqs. (29) to (32) are only approximate and that their accuracy depends upon the number of measured ordinates. The first two formulas are used when even harmonics are present, the summation being extended over the whole cycle. The latter two formulas are used when the two half-waves are identical, odd harmonics only being present. The summation is then extended over 180 electrical degrees only. The above-mentioned schedules may be used for analytical computations as well, separate blank columns being provided for positive and negative values, to avoid confusion.

In view of the considerable amount of numerical computation involved in harmonic analysis, many investigators have suggested possible simplifications, usually at the expense of accuracy. For example, in eq. (30) the ordinates correspond to the following values of x:

$$x = 0, \pi/p, 2\pi/p, 3\pi/p, \text{etc.} \qquad (33)$$

Take the number of divisions, p, per half-cycle equal to the order, n, of the harmonic to be separated. Then, according to eq. (28), the values of nx for the points of division will be:

$$nx = 0, \pi, 2\pi, 3\pi, \text{etc.} \qquad (34)$$

and the corresponding values of cosines will be $+1, -1, +1, -1$, etc. In other words, in this case:

$$\bar{B}_n = (1/n)(y_0 - y_1 + y_2 - y_3 + \cdots - y_{2n-1}) \qquad (35)$$

the summation being extended over the whole cycle. Equation 32 becomes:

$$\bar{B}_n = (2/n)(y_0 - y_1 + y_2 - y_3 + \cdots \pm y_{n-1}) \quad . \; . \; . \quad (36)$$

the summation extending over half a cycle only. To obtain $\bar{A}_n$, the origin O is shifted to the right by an angle $\pi/(2p)$, and the computations repeated with the new ordinates in the expression for $\bar{B}_n$. The new value of $\bar{B}_n$ is equal to $\bar{A}_n$ for the first position of O.

At first sight, eq. (35) may be thought to be in contradiction to eq. (24), and more especially to eq. (24*a*). However, eq. (24) is an exact relationship deduced from Fourier's series, while eq. (35) is only approximate, being deduced from the approximate formula (30). Therefore, the two could not be expected to agree.

While various "short cuts," such as eq. (35), reduce the amount of time spent in analyzing a given wave, the question of the resulting error must be carefully considered in an important problem. Equations (29) to (32) are only approximate, and the accuracy of the result increases with the number of ordinates. By taking $p = n$, the number of ordinates is considerably reduced, especially for lower harmonics. For accurate results it is preferable to use eqs. (29) to (32) in their original form, taking a sufficiently large number of ordinates, p.

Ample references to various approximate analytical methods will be found in the sources referred to throughout this chapter.[13] One of the author's purposes in giving the rigorous theory of the Fourier series has been to enable the reader to take an intelligent critical attitude toward such approximate methods, using in a given case one that possesses sufficient accuracy with a minimum of numerical work.

1144. Graphical Analysis. — Considerable ingenuity has been displayed in devising various purely graphical ways[14] of using eqs. (29) to (32). Projection on a cylinder has been employed; coordinate paper has been used with abscissas varying as cos nx or sin nx, instead of x; ordinates have been measured with special scales for each harmonic; charts have been constructed, etc. Those who prefer graphical methods and who require only moderate accuracy will find some of these methods[15] useful in particular problems.

1145. Chaffee Simplified Method of Harmonic Analysis. — In *Review of Scientific Instruments* for October, 1936, Dr. E. L. Chaffee describes a method which he has developed particularly for the analysis of vacuum-tube output waves when sinusoidal emf's are impressed upon the grid of the tube (Chapter LIX). The following is a digest of this method.

---

[13] See also W. F Dunton, *Beama* (later *World Power*), vol. 13 (1923), p. 45.

[14] For literature references to such methods, see Dellenbaugh, *loc. cit.*, §1132.

[15] J. B. Hutcheson, "Graphical Harmonic Analysis," *Electronics*, January, 1936, p. 16.

Values of ordinates of the periodic curve are taken corresponding to certain carefully chosen points along the voltage axis, and not necessarily at evenly spaced points along the time axis.

For brevity in the expressions cos ωt is replaced by C in terms such as $e = E_m \cos \omega t$, or

$$e = E_m C \quad . \; . \; . \; . \; . \; . \; . \; . \; . \; . \; . \; . \quad (37)$$

This emf is usually superimposed upon a d-c voltage, E_s, which would cause a " quiescent " (d-c) current, I_s.

The plate current due to a sinusoidal emf is then

$$i = I_s + \bar{\imath} = F(E_s + e) \quad . \; . \; . \; . \; . \; . \; . \; . \quad (38)$$

Taking the " quiescent " point, Q (Fig. 807), as the origin and considering the current $\bar{\imath}$, measured above or below I_s, as a function of e, it may be written, including both odd and even harmonics, as:

$$\bar{\imath} = (I_{\text{av}} - I_s) + I_{m1} \cos \omega t + I_{m2} \cos 2\omega t + I_{m3} \cos 3\omega t + \cdot \cdot \cdot \; . \quad (39)$$

The change in average current, $I_{\text{av}} - I_s$, is due to the application of the varying emf, e.

Rewriting eq. (39) in terms of eq. (37) and expanding the cosines of multiple angles

$$\begin{aligned} \bar{\imath} = (I_{\text{av}} - I_s) &+ I_{m1}C + I_{m2}(2C^2 - 1) + I_{m3}C(4C^2 - 3) \\ &+ I_{m4}(8C^4 - 8C^2 + 1) + I_{m5}C(16C^4 - 20C^2 + 5) \\ &+ I_{m6}(32C^6 - 48C^4 + 18C^2 - 1) \\ &+ I_{m7}C(64C^6 - 112C^4 + 54C^2 - 7) + \cdot \cdot \cdot \cdot \cdot \; . \; . \quad (40) \end{aligned}$$

For $C = 0$

$$I_{av} - I_s = I_{m2} - I_{m4} + I_{m6} - I_{m8} + \cdot \cdot \cdot \cdot \; . \; . \; . \quad (41)$$

Let $\bar{\imath}'$ and $\bar{\imath}''$ represent the values of $\imath$ corresponding to equal values of C of opposite sign (Fig. 807). It becomes of advantage to take the sum, S, and difference, D, of expressions such as eq. (40) for various values of C. Then

$$S = \bar{\imath}' + \bar{\imath}''$$

$$D = \bar{\imath}' - \bar{\imath}'' \quad . \; . \; . \; . \; . \; . \; . \; . \; . \; . \; . \quad (42)$$

In general

$$\begin{aligned}S = 2C\,[I_{m1} + I_{m3}(4C^2 - 3) + I_{m5}(16C^4 - 20C^2 + 5)\\ + I_{m7}(64C^6 - 112C^4 + 56C^2 - 7)\\ + I_{m9}(256C^8 - 576C^6 + 432C^4\\ - 120C^2 + 9) + \cdots] \quad . \; . \; . \; . \; . \quad (43)\end{aligned}$$

$$\begin{aligned}D = 4C^2\,[I_{m2} + I_{m4}(4C^2 - 4) + I_{m6}\,(16C^4 - 24C^2 + 9)\\ + I_{m8}(64C^6 - 128C^4 + 80C^2 - 16)\\ + \cdots] \quad . \; . \; . \; . \; . \; . \; . \; . \; . \; . \; . \; . \quad (44)\end{aligned}$$

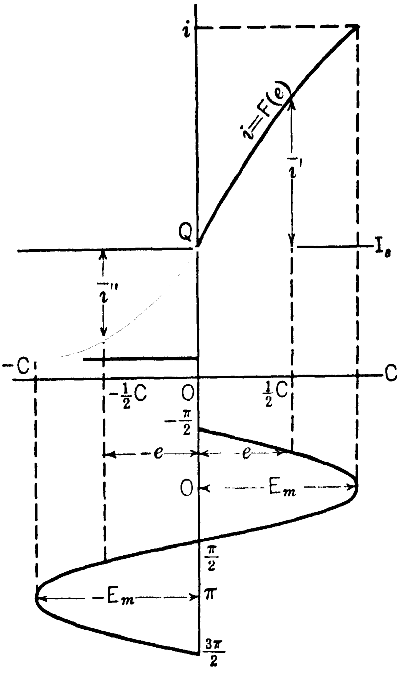

FIG. 807. Curves of vacuum-tube plate current and sine-form impressed emf (E. L. Chaffee).

Notice that the sum S contains the odd harmonics, and the difference D, the even.

For properly selected values of C the coefficients in eqs. (43) and (44) reduce to zero or to simple integral values. For a five-point analysis (nine points in the complete cycle), when the values $C_1 = \pm 1$, and $C_2 = \pm\frac{1}{2}$, that is, $\omega t = 0$ and π, $\pi/3$, and $-\pi/3$. Equations (43) and (44) give:

$$\left.\begin{aligned} S_1/2 &= I_{m1} + I_{m3} \\ S_2 &= I_{m1} - 2I_{m3} \\ D_1/4 &= I_{m2} \\ D_2 &= I_{m2} - 3I_{m4} \end{aligned}\right\} \quad \ldots\ldots\ldots \quad (45)$$

Equations (41) and (45) yield the following:

$$\left.\begin{aligned} I_{m0} &= I_{av} - I_s = D_1/6 + D_2/3 \\ I_{m1} &= S_1/3 + S_2/3 \\ I_{m2} &= D_1/4 \\ I_{m3} &= S_1/6 - S_2/3 \\ I_{m4} &= D_1/12 - D_2/3 \end{aligned}\right\} \quad \ldots\ldots \quad (46)$$

Only five points on the curve were taken, and the amplitudes of only five harmonics were determined. Dr. Chaffee (*loc. cit.*) carries the method further to determine as many as thirteen harmonics. For waves in which the even harmonics (§1133) are absent such terms as $I_{av} - I_s$, I_{m2}, etc., drop out.

In the analysis of a symmetrical wave through the eleventh harmonic values of C taken were $C = 0$, $C_1 = \pm 1$, $C_2 = \pm 0.966$, $C_3 = \pm 0.866$, $C_4 = \pm 0.707$, $C_5 = \pm 0.5$, $C_6 = \pm 0.259$. It will be seen that these values of C correspond to $\omega t = \pi/2$, 0, and π, $\pm\pi/12$, $\pm\pi/6$, $\pm\pi/4$, $\pm\pi/3$, and $\pm\pi 5/12$. These points give, for the several odd harmonics,

$$\left.\begin{aligned} I_{m1} &= 1/12(S_1 + 1.93S_2 + \sqrt{3}S_3 + \sqrt{2}S_4 + S_5 + 0.518S_6) \\ I_{m3} &= 1/12(S_1 + \sqrt{2}S_2 - \sqrt{2}S_4 - 2S_5 - \sqrt{2}S_6) \\ I_{m5} &= 1/12(S_1 + 0.518S_2 - \sqrt{3}S_3 - \sqrt{2}S_4 + S_5 + 1.93S_6) \\ I_{m7} &= 1/12(S_1 - 0.518S_2 - \sqrt{3}S_3 + \sqrt{2}S_4 + S_5 - 1.93S_6) \\ I_{m9} &= 1/12(S_1 - \sqrt{2}S_2 + \sqrt{2}S_4 - 2S_5 + \sqrt{2}S_6) \\ I_{m11} &= 1/12(S_1 - 1.93S_2 + \sqrt{3}S_3 - \sqrt{2}S_4 + S_5 - 0.518S_6) \end{aligned}\right\} \quad . \quad (47)$$

For the expressions which give the even harmonics see Dr. Chaffee's article, in which the following references are also given:

D. C. ESPLEY, *Proc. I.R.E.*, vol. 21 (1933), p. 1439, The calculation of harmonic production in thermionic valves with resistive loads.

L. G. A. SIMS, *Wireless Eng'r and Exp. Wireless*, vol. 11 (1934), p. 419, Analysis of wave forms.

D. C. ESPLEY and L. I. FARREN, *ibid.*, vol. 11 (1934), p. 183, Direct reading harmonic scales.

I. E. MOUROMTSEFF and H. N. KOZANOWSKI, *Proc. I.R.E.*, vol. 22 (1934), p. 1090, A short-cut method for calculation of harmonic distortion in wave modulation.

1146. EXPERIMENT 58-A.—Practice in Analysis of Periodic Waves. —For the purpose of practice and of emphasis the methods of wave analysis described in this chapter should be employed to determine the harmonic components of one or more wave shapes. As an example, the wave form of the exciting current in an overexcited transformer (§787) might be taken by means of an oscillograph (Chapter LVII) and then analyzed, as follows:

(a) Using the method of §§1137 and 1143, carefully measure the ordinates of the curve at 5-degree intervals, and multiply these ordinates by the values of sin nx and cos nx, for $n = 1, 3, 5$, etc. (see appendix of this chapter).

Determine the average products of the irregular wave with the analyzing waves, either by plotting the products, drawing smooth curves, and measuring the areas under the curves for 2π radians (or until the product curve repeats) by means of a planimeter, or average the products, preferably by Simpson's rule.

Compare the magnitudes of the harmonics so determined with the usual values for transformer exciting currents (§787) as given by O. G. C. Dahl, " Electric Circuits, Theory and Applications," Chapter VIII.

Finally plot the harmonic waves and add, point by point, comparing the resultant curve with the original. Explain discrepancies.

(b) Check at least one of the harmonics, say the third, by the method of electrodynamometer measurement (§1141). A wattmeter may be used for this purpose, passing the current in question through the current coil and applying third-harmonic voltage to the potential coil. By using the emf's from each phase of a two-phase alternator the sine and cosine components may be determined.

(c) Apply the method of Dr. Chaffee (§1145), eqs. (47), to ordinates of the curve taken every 15 degrees, and determine the several harmonics.

Compare the various methods employed as to ease and accuracy. If time permits, analyze a different type of wave, such as the plate current of a three-element vacuum tube with sine-form emf plus d-c bias applied to the grid.

APPENDIX TO CHAPTER LVIII

The following tables, which include sine and cosine functions of angles for each 5 degrees of the fundamental wave, are intended to facilitate the analysis of periodic waves by the analytical methods described in §1143.

FUNDAMENTAL WAVE.*

1	2	3	4	5	6	7	8
Sin x	Products y sin x		No.	Measured Ordinates y	Cos x	Products y cos x	
	(positive)	(negative)				(positive)	(negative)
.0872			1		.9962		
.1736			2		.9848		
.2588			3		.9659		
.3420			4		.9397		
.4226			5		.9063		
.5000			6		.8660		
.5736			7		.8192		
.6428			8		.7660		
.7071			9		.7071		
.7660			10		.6428		
.8192			11		.5736		
.8660			12		.5000		
.9063			13		.4226		
.9397			14		.3420		
.9659			15		.2588		
.9848			16		.1736		
.9962			17		.0872		
1.0000			18		.0000		
.9962			19		−.0872		
.9848			20		−.1736		
.9659			21		−.2588		
.9397			22		−.3420		
.9063			23		−.4226		
.8660			24		−.5000		
.8192			25		−.5736		
.7660			26		−.6428		
.7071			27		−.7071		
.6428			28		−.7660		
.5736			29		−.8192		
.5000			30		−.8660		
.4226			31		−.9063		
.3420			32		−.9397		
.2588			33		−.9659		
.1736			34		−.9848		
.0872			35		−.9962		
.0000			36		−1.0000		
	$\Sigma'_{pos}=$	$\Sigma'_{neg}=$				$\Sigma''_{pos}=$	$\Sigma''_{neg}=$

---

* Measured ordinates of the periodic wave to be analyzed should be read each 5 degrees, beginning at ordinate zero.

THIRD HARMONIC.

	2	3	4	5	6	7	8
Sin $3x$	Products y sin $3x$		No.	Measured Ordinates y	Cos $3x$	Products y cos $3x$	
	(positive)	(negative)				(positive)	(negative)
.2588			1		.9659		
.5000			2		.8660		
.7071			3		.7071		
.8660			4		.5000		
.9659			5		.2588		
1.0000			6		.0000		
.9659			7		−.2588		
.8660			8		−.5000		
.7071			9		−.7071		
.5000			10		−.8660		
.2588			11		−.9659		
.0000			12		−1.0000		
−.2588			13		−.9659		
−.5000			14		−.8660		
−.7071			15		−.7071		
−.8660			16		−.5000		
−.9659			17		−.2588		
−1.0000			18		.0000		
−.9659			19		.2588		
−.8660			20		.5000		
−.7071			21		.7071		
−.5000			22		.8660		
−.2588			23		.9659		
.0000			24		1.0000		
.2588			25		.9659		
.5000			26		.8660		
.7071			27		.7071		
.8660			28		.5000		
.9659			29		.2588		
1.0000			30		.0000		
.9659			31		−.2588		
.8660			32		−.5000		
.7071			33		−.7071		
.5000			34		−.8660		
.2588			35		−.9659		
.0000			36		−1.0000		
	$\Sigma'_{pos}=$	$\Sigma'_{neg}=$				$\Sigma''_{pos}=$	$\Sigma''_{neg}\pm$

FIFTH HARMONIC.

1	2	3	4	5	6	7	8
Sin $5x$	Products	y sin $5x$	No.	Measured Ordinates y	Cos $5x$	Products	y cos $5x$
	(positive)	(negative)				(positive)	(negative)
.4226			1		.9063		
.7660			2		.6428		
.9659			3		.2588		
.9848			4		−.1736		
.8192			5		−.5736		
.5000			6		−.8660		
.0872			7		−.9962		
−.3420			8		−.9397		
−.7071			9		−.7071		
−.9397			10		−.3420		
−.9962			11		.0872		
−.8660			12		.5000		
−.5736			13		.8192		
−.1736			14		.9848		
.2588			15		.9659		
.6428			16		.7660		
.9063			17		.4226		
1.0000			18		.0000		
.9063			19		−.4226		
.6428			20		−.7660		
.2588			21		−.9659		
−.1736			22		−.9848		
−.5736			23		−.8192		
−.8660			24		−.5000		
−.9962			25		−.0872		
−.9397			26		.3420		
−.7071			27		.7071		
−.3420			28		.9397		
.0872			29		.9962		
.5000			30		.8660		
.8192			31		.5736		
.9848			32		.1736		
.9659			33		−.2588		
.7660			34		−.6428		
.4226			35		−.9063		
.0000			36		−1.0000		
	$\Sigma'_{pos}=$	$\Sigma'_{neg}=$				$\Sigma''_{pos}=$	$\Sigma''_{neg}=$

SEVENTH HARMONIC.

1	2	3	4	5	6	7	8
Sin 7 x	Products y sin 7 x		No.	Measured Ordinates y	Cos 7 x	Products y cos 7 x	
	(positive)	(negative)				(positive)	(negative)
.5736			1		.8192		
.9397			2		.3420		
.9659			3		-.2588		
.6428			4		-.7660		
.0872			5		-.9962		
-.5000			6		-.8660		
-.9063			7		-.4226		
-.9848			8		.1736		
-.7071			9		.7071		
-.1736			10		.9848		
.4226			11		.9063		
.8660			12		.5000		
.9962			13		-.0872		
.7660			14		-.6428		
.2588			15		-.9659		
-.3420			16		-.9397		
-.8192			17		-.5736		
-1.0000			18		.0000		
-.8192			19		.5736		
-.3420			20		.9397		
.2588			21		.9659		
.7660			22		.6428		
.9962			23		.0872		
.8660			24		-.5000		
.4226			25		-.9063		
-.1736			26		-.9848		
-.7071			27		-.7071		
-.9848			28		-.1736		
-.9063			29		.4226		
-.5000			30		.8660		
.0872			31		.9962		
.6428			32		.7660		
.9659			33		.2588		
.9397			34		-.3420		
.5736			35		-.8192		
.0000			36		-1.0000		
	$\Sigma'_{pos}=$	$\Sigma'_{neg}=$				$\Sigma''_{pos}=$	$\Sigma''_{neg}=$

CHAPTER LIX

FUNDAMENTALS OF ELECTRONIC DEVICES

BY

PROFESSOR R. T. GABLER
Carnegie Institute of Technology

1147. This chapter deals with principles[1] underlying the operation of electron tubes and allied devices. Certain simpler applications are considered and references given which will provide good starting points in a library search for more detailed information.

1148. Electrons in Metals. — The operation of all vacuum tubes depends primarily upon the emission of electrons from metals. Emission may be accomplished by heating (thermionic emission), exposure to light (photoelectric emission), application of an intense electric field (field emission), and bombardment with electrons, ions, or excited atoms (secondary emission). The phenomena of thermionic emission, photoelectric emission, and secondary emission are of fundamental importance in the engineering application of electronics.

The Bohr atom. According to the Bohr concept the atom may be considered as a miniature solar system with a very concentrated nucleus containing nearly all the mass of the atom and all the excess positive electrical charge. About this positively charged nucleus negative electrons are constrained to move in more or less fixed orbits. Each electron has a charge of 1.591×10^{-19} coulomb and a mass of 9.035×10^{-28} gram. In a given atom there are just enough electrons to neutralize the positive charge in the nucleus. For the hydrogen atom this requires one electron; for helium, two electrons; for lithium, three electrons; etc., to uranium with 92 extranuclear electrons. Many phenomena including spectra are explained by considering the electrons to be arranged on shells representing stable energy states. The first or inner shell when completely filled has two electrons with 8, 18, 32, etc., or $2n^2$ electrons in succeeding shells when completely filled. Atoms such as helium, argon, krypton, xenon, and neon, in which the outer shells are entirely filled, are very stable (inactive) chemically. Atoms lacking one or two electrons necessary to fill one of the outer shells completely are very active chemically. This is also true for atoms which have only one or two electrons in the outer shell.

---

[1] E. L Chaffee, "Theory of Thermionic Vacuum Tubes," McGraw-Hill Book Co.; H. J. Reich, "Theory and Applications of Electron Tubes," McGraw-Hill Book Co., 1939.

Current flow in metals. In the heavy metals in particular, the outer electrons are very loosely attached to the atomic centers and are consequently called " free electrons." It is the gradual drift of these " free electrons " under the influence of an electrostatic field which constitutes the current in metallic conduction. The accepted picture is thus one of an electron gas (atmosphere) permeating the body of the metallic conductor, with the individual electrons encountering little opposition to movement. The forces binding these outer electrons to the atoms, although finite, must be very small, since Ohm's law has been found to hold for extremely minute currents, and large binding forces would result in a minimum field below which there would be no current flow. The complete analysis of current flow in metals should consider many factors, including the wave nature of electrons. However, it seems plausible that " collisions " between electrons and atomic centers might constitute ohmic resistance and that one might by applying kinetic theory account for the increase in temperature of a conductor carrying current. The thermal motions of electrons in metals at ordinary temperatures involve speeds of the order of 3×10^6 feet per second. For conduction of currents in copper conductors with current densities of 1000 amperes per square inch, the average drift velocity of the electrons constituting the current is only about 0.0026 foot per second.

1149. Thermionic Emission. — At ordinary temperatures practically none of the electrons in metals have sufficient energy to overcome the forces which hold them within the boundaries. At elevated temperatures increasing numbers of electrons attain kinetic energies greater than that necessary to overcome the potential barrier at the metal surface. The escape of electrons from metals due to high temperatures is known as *thermionic emission.* The first quantitative relation between the temperature of a metal and the electronic emission was derived by Richardson.[2] Applying kinetic theory to the " electron gas " in the metallic structure, he arrived at the relation:

$$J = aT^{1/2}\epsilon^{-b/T} \quad \ldots\ldots\ldots\ldots \quad (1)$$

where J is the current density in amperes per square centimeter, a is a constant for the particular metal surface, T is the temperature in degrees Kelvin, ϵ is the base of natural logarithms, $b = \phi/k$, where ϕ is the work function in ergs, and k is Boltzmann's constant in ergs per degree Kelvin (1.372×10^{-16}). Richardson suggested that an alternative form for the equation might be:

---

[2] Richardson, "Emission of Electricity from Hot Bodies," Longmans, Green, 1916.

$$J = AT^2\epsilon^{-b_0/T} \quad . \; . \; . \; . \; . \; . \; . \; . \; . \; . \qquad (2)$$

This form was later derived by Dushman,[3] who assumed the Fermi-Dirac distribution of momentum or energy for the "free electrons" in a metal.[4] This distribution for tungsten is shown in Fig. 808. Increased temperature results in higher energy for the few electrons that previously possessed the highest energy. The forces at the boundary are represented by a potential wall. The difference between the energy just necessary to overcome the potential barrier and so escape

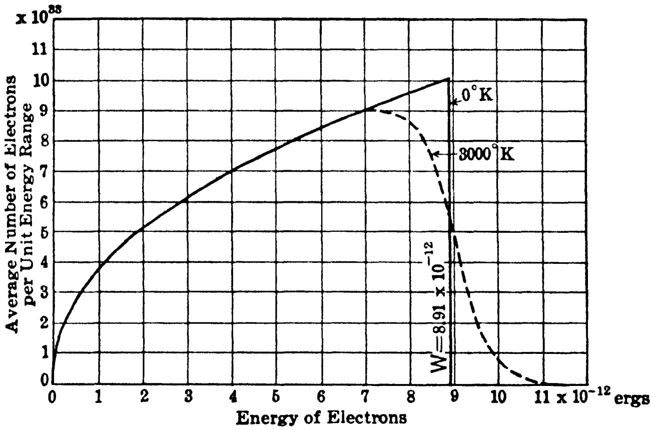

Fig. 808. Fermi-Dirac distribution of free electrons in tungsten, on an energy basis.

and that possessed by the highest-energy electrons at 0°K, is known as the "work function" of the metal surface, which may be measured in ergs, but is usually expressed in "electron volts," sometimes abbreviated to volts. The conversion from electron volts to ergs is made by the equation

$$W = Ve \times 10^7 \quad . \; . \; . \; . \; . \; . \; . \; . \; . \; . \qquad (3)$$

where W is the energy in ergs, V is the energy in volts, and e is the electronic charge in coulombs (1.591×10^{-19}).

Experimental verification. The exponential form of the Richardson-Dushman equation is easily verified experimentally (§1152), and the constants for a particular metal surface may also be determined. Metals with the lowest work functions will not withstand the necessary high temperatures when used by themselves. Of the pure metals, tungsten is the most satisfactory material, since it will withstand temperatures of 2800°K with a reasonable life and has a work function of 4.53 volts. The work functions of other metals range from 1 to 10 volts. Table I lists experimentally determined values for A and b_0 for different cathode materials.

---

[3] Dushman, "Thermionic Emission," *Rev. Mod. Phys.*, vol. 2 (1930), p. 381.

[4] Sommerfeld, *Zeits. Physik*, vol. 47 (1928), p. 1.

TABLE I

CONSTANTS FOR THERMIONIC CATHODE MATERIALS

Substance	ϕ_0 volts	A amp/cm²/deg²	b_0	J amp/cm²
Tungsten (W)	4.52	60.2	52,400	1×10^{-3} at 2000°K
Thoriated tungsten (Th-W)	2.63	3	30,500	1.2 at 1900°K
Oxide coating (BaO,SrO) typical	1.04	10^{-2}	12,000	0.06 at 1000°K
Platinum (Pt)	6.26	17,000.	72,500	3×10^{-9} at 1600°K
Tantalum (Ta)	4.07	60.2	47,200	4×10^{-6} at 2000°K
Calcium (Ca)	2.24	60.2	26,000	4×10^{-3} at 1100°K

1150. Thermionic Cathodes. — Practical cathodes are of the filament type and the indirectly heated types. These are illustrated in Figs. 809 and 810. The majority of small tubes with a-c heater supply for the cathode are of the indirectly heated types. The cathodes most commonly used are tungsten, thoriated tungsten, and oxide-coated.

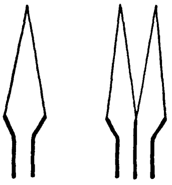

FIG. 809. Directly heated cathodes (filament type).

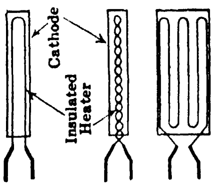

FIG. 810. Indirectly heated cathodes (heater type).

In high-voltage tubes, it is necessary to employ the tungsten cathode, although it is less efficient than other types, as the thoriated tungsten and oxide-coated types will not withstand bombardment by high-speed positive ions. For medium-voltage tubes, thoriated tungsten may be satisfactory, but the most efficient oxide-coated type is used in comparatively low-voltage tubes. In order to secure reasonable life and efficiency, tungsten filaments are operated at a temperature of about 2500°K.

Thoriated filaments are made by dissolving thorium oxide and carbon in a tungsten filament. By an activation process[5] wherein the filament is heated in vacuo for a short period at 2800°K and then held at a temperature of about 2100°K, the thoria in the filament is reduced to metallic thorium, which diffuses to the surface, forming a layer one atom deep. The operating temperature of the thoriated filament is from 1800°K to 2000°K. A thoriated filament which loses its emitting power can usually be reactivated by a process similar to the original activation. This may be repeated until all the thorium has been removed from the filament and evaporated.

In 1904 Wehnelt discovered that the oxides of barium, strontium, and calcium, coated upon platinum, provided good emission. The oxide-coated cathode was later developed in various forms, and several manufacturing processes were employed. Oxide-coated cathodes operate at a temperature of 900°K to 1100°K with much greater emission efficiency than either thoriated or pure tungsten filaments, which operate at much higher temperatures.

1151. Cathode Efficiencies. — The efficiency of a thermionic cathode is measured in milliamperes per watt of heating power. Tungsten filaments operating at about 2500°K have an efficiency of the order of 3 milliamperes per watt, and thoriated tungsten filaments operating at 2000°K have an efficiency near 100 milliamperes per watt. The oxide-coated cathode can be expected to have an efficiency of over 100 milliamperes per watt to nearly 1 ampere per watt. The higher efficiencies are obtained only in the heat-shielded cathodes used in gaseous rectifiers and thyratrons.

In order to facilitate comparison of cathodes, Dr. C. J. Davisson of the Bell Telephone Laboratories devised a form of cross-section paper (Fig. 811) which enables the plot between emission current and cathode power to be almost a straight line. It uses a system of curvilinear coordinates based upon Richardson's law for thermionic emission and the Stefan-Boltzmann law for cooling by radiation. The radiation law in this case is:

$$P_A = BT^4 \qquad . \; . \quad (\text{[illegible]})$$

Combining this with Richardson's equation, (1), we are able to obtain the relation between J and P_A and consequently between I, the total emission current, and P_A, the cathode power, as

---

[5] Koller, "The Physics of Electron Tubes," p 20, McGraw-Hill Book Co., 1934.

$$\log_e I = C_1\left(\frac{1}{P_A{}^{1/4}}\right) + C_2 \log_e (P_A)^{1/4} + \log_e C_3 \tag{5}$$

C_1, C_2, and C_3 are constants.

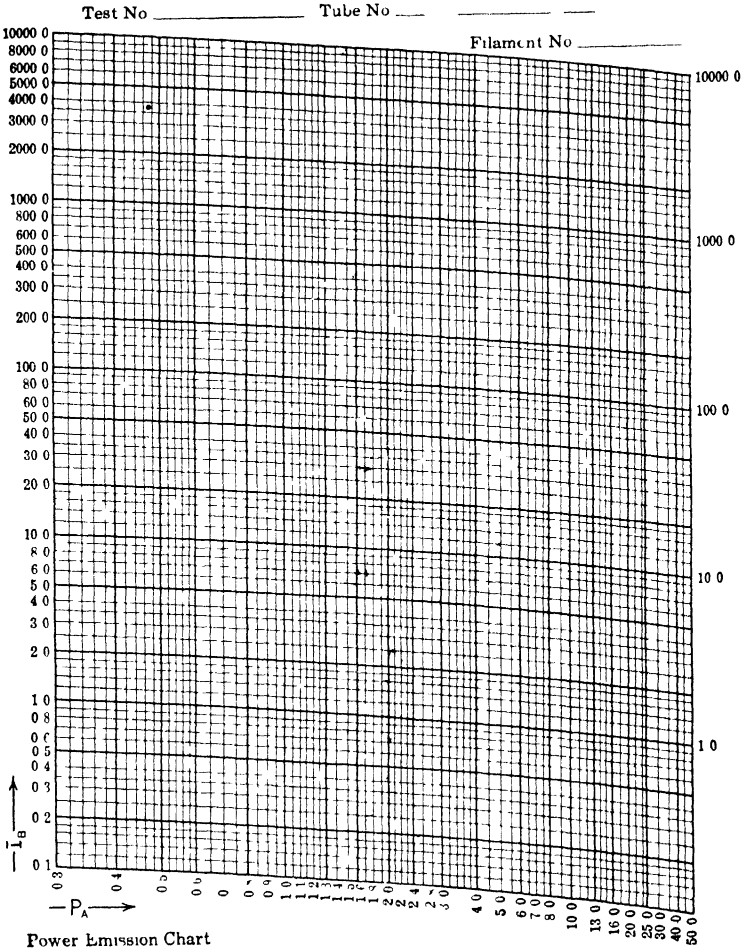

Fig. 811 Davisson power-emission chart (reproduced by permission of Keuffel and Esser Co , graph sheet No 359–98)

On the power emission paper with Davisson coordinates as illustrated by Fig 811,[6] the vertical lines are spaced according to an inverse fourth power law and the horizontal lines are spaced logarithmically. The horizontal lines are given a downward curvature so that each represents a constant value of emission current. One great advantage of power emission paper is the possibility of more accurate extrapolation to rated filament power. When testing thoriated and oxide-coated cathodes the emission current at rated cathode power may permanently damage the tube if permitted to flow longer than a fraction of a second. Extrapolation of the curve avoids the necessity of a special test method to limit the time of current flow.

---

[6] This paper (Sheet No 359–98) may be obtained from Keuffel & Esser Co , New York City

1152. EXPERIMENT 59-A. — Measurement of Emission Characteristics of Hot Cathodes. — In order to determine the characteristics of a particular cathode, the tube may be considered as a diode and operated as such by connecting all electrodes (except the cathode), to form one anode or plate. In this test it is important that the plate voltage should be high enough to permit the plate current to be controlled entirely by cathode temperature. A test for this condition is to increase the plate voltage until no appreciable change in plate current results from a further increase in plate voltage. This should be done for a maximum plate current not exceeding 120 per cent of the rated operating plate current of the tube, which will occur with a filament voltage considerably below rated filament voltage for oxide-coated cathodes and thoriated filaments. The circuit diagram with indicated meter ranges for testing a type-81 diode is shown in Fig. 812.

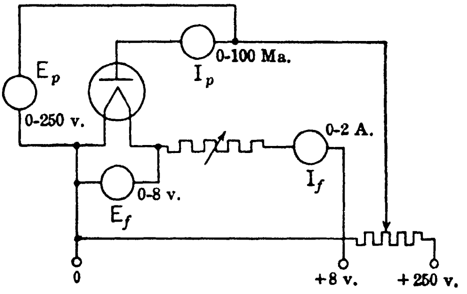

FIG. 812. Circuits for determining emission characteristics of a diode.

After the required plate voltage has been determined (about 200 volts for the 81 tube), vary the filament voltage slowly and carefully from 0 to the value which gives about 20 per cent more than the rated plate current. Record values of filament volts, filament amperes, plate volts, and plate current.

To afford a comparison, the above test should be repeated for tubes having tungsten and thoriated tungsten filaments. It is also possible to measure temperatures with an optical pyrometer (see also §8) during the run and in this way determine the constants for the Richardson-Dushman emission equation. When temperature measurements on filaments are made with an optical pyrometer, it is necessary to correct for the spectral emissivity of the filament surface, which is different from that of a black body.[7]

Report. Plot a curve of emission current *vs.* cathode power. If power emission paper (Fig. 811) is used, extrapolation may be made to rated filament power. A curve of T^4 *vs.* cathode power will show whether the filament cooling follows the Stefan-Boltzmann law assumed. With large tungsten filaments, it may be necessary to consider the cooling effect of the electron evaporation. This amounts to ϕI_B watts, where ϕ is the work function in volts and I_B is the emission current in amperes. From Dushman's equation it follows that if one plots $[\log_\epsilon J - \log_\epsilon(1/T)]$ *vs.* $(1/T)$, a straight line should result. The slope of this line is b_0, and the infinite temperature intercept $(1/T = 0)$ is $\log_\epsilon (A)$.

1153. Photoelectric Emission.—Photoelectric emission was first discovered by Hertz in 1887.[8] He observed that a discharge across a gap occurred more readily when the negative electrode was illuminated with ultra-violet light. Elster and Geitel[9] investigated further and found that the cause of the observed effects was the emission of electrons from the illuminated electrode. They also made the important discovery that certain of the alkali metals would emit electrons with visible light and some with infra-red light.

The important points to be noted in connection with the ordinary surface photoelectric effect are:

1. For a given surface there is a maximum wavelength or a minimum frequency for the light which ejects photoelectrons from the surface.
2. With light of a frequency greater than the threshold or minimum frequency the rate of electronic emission is directly proportional to the light intensity.
3. The kinetic energy of emitted electrons increases linearly with the frequency of the light ejecting the electrons and is independent of intensity.
4. The surface photoelectric effect is almost instantaneous. The elapsed time between the illumination of the surface and the start of the photoelectric current is less than 3×10^{-9} second.

---

[7] The optical pyrometer measures the apparent black-body temperature. The relation between apparent black-body temperature and the true temperature of a tungsten filament, from the measurements of Forsythe and Worthing (*Astrophys. J.*, 1925, p. 61), is given in Table II. Since the operating temperatures of oxide-coated cathodes are normally much lower than those for tungsten, and since the spectral emissivity varies with the surface condition, it is difficult to make accurate temperature measurements on oxide-coated cathodes by means of an optical pyrometer.

[8] H. Hertz, *Ann. Physik*, vol. 31 (1887), p. 983.

[9] J. Elster and H. Geitel, *ibid.*, vol. 38 (1889), pp. 40, 497.

It is almost impossible to reconcile experimental facts about the photoelectric effect with the classical electromagnetic theory of light. A more satisfactory explanation can be made on the basis of the quantum principle that light energy is delivered in bundles or photons. The size of the photon is $h\nu$ ergs where h is Planck's constant (6.55×10^{-27} erg second) and ν is the light frequency in cycles per second. Einstein first proposed[10] that the mechanism of photoelectric emission could be represented by

$$\tfrac{1}{2}mv^2 = h\nu - p \quad . \quad . \quad (6)$$

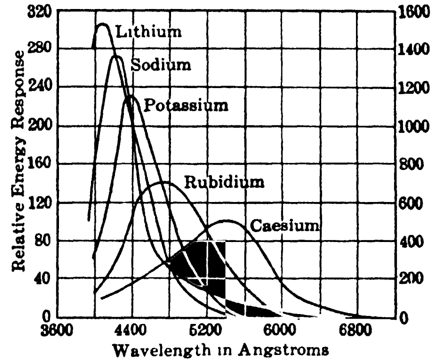

FIG. 813. Color sensitivity curves; data from *Astrophys. Jour.*, vol 52 (1920).

An electron which receives the photon of light energy is emitted with a maximum velocity determined by the above equation. For a given maximum frequency of incident light no electrons would be emitted with a velocity greater than that given by the Einstein equation. p is the photoelectric work function for the particular surface. It appears that, if surface conditions can be duplicated, the photoelectric work function and the thermionic work function would be identical. It is obvious from the above equation that electrons could not be emitted photoelectrically when $p \geqq h\nu$. The frequency given by $\nu = p/h$ is known as the "threshold frequency" for the surface. Einstein's equation is readily verified by experiment, and such studies form a very reliable method of evaluating Planck's constant.

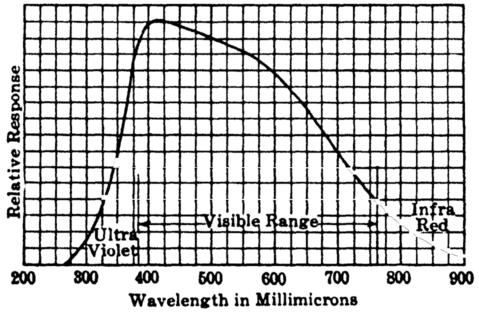

FIG. 814. Spectral sensitivity curve of high-vacuum photo tube (Westinghouse).

1154. Color Response and Selective Effects. — The spectral sensitivity for certain metals is shown in Fig. 813. Ives[11] discovered that for thin films of sodium on platinum the photoelectric current and the spectral sensitivity were both functions of the film thickness. Composite film cathodes are used extensively in present-day phototubes. The cesium-oxygen-silver type is commonly employed because of its high sensitivity over the visual and infra-red range. A spectral sensitivity curve for a high-vacuum phototube with a cesium-oxygen-silver cathode is shown in Fig. 814.

---

[10] Einstein, *Ann. Physik*, vol. 17 (1905), p. 132; vol. 20 (1906), p. 199.

[11] H. E. Ives, *Astrophys. Jour.*, vol. 60 (1924), p. 219.

1155. EXPERIMENT 59-B. — Determination of the Characteristics of a Photoemissive Cell. — The linear relation between light intensity and phototube current can be readily demonstrated with comparatively simple apparatus. Figure 815 shows the schematic circuit and arrangement of apparatus. A convenient light source is a 200-watt, 115-volt projection-type lamp with pre-focus base. The filament is sufficiently concentrated to permit the use of the inverse square law in calculating the light flux on the photocell cathode. The lamp is housed in a light-tight container provided with sufficient ventilation. A similar housing may be used for the photocell, except that it is not necessary to provide ventilation. It is important to have low leakage insulation for the photocell terminals.

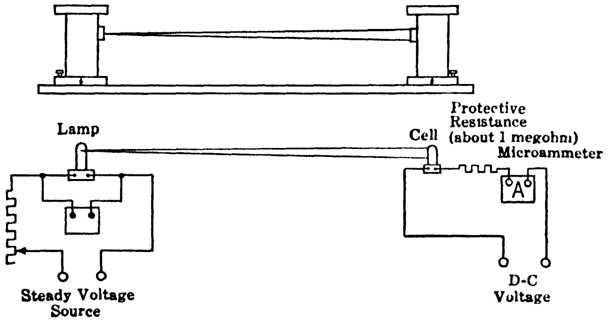

FIG. 815. Arrangement of apparatus for determining the characteristics of a photoemissive cell.

The d-c power supply for the lamp should be from a steady source, such as a storage battery, since a 1 per cent change in voltage causes about a 6 per cent change in illumination. The voltage source for the phototube may be a battery, although a rectified a-c supply with good filtering and automatic regulation is quite satisfactory. For measurements of the current in a PJ-22 or similar high-vacuum phototube, a 0–15 microampere moving-coil meter may be used. A wall galvanometer equipped with an Ayrton shunt may also be used, but is less convenient.

The phototube housing and lamp housing should be arranged to move in guides (Fig. 815) with provision for measuring the distance between the photocell cathode and the lamp filament. The entire apparatus should be painted a dull black and oriented so as to minimize the amount of stray room light or indirectly reflected light reaching the photocell. With 100 volts applied to the 200-watt, 115-volt projection lamp, the luminous intensity is about 300 candles. This value, or a better value obtained from a calibration, may be used to calculate the distance between light source and phototube to give an illumination of 1.5 lumens. The formula is $L = C \cdot A/d^2$, where L is the luminous flux in lumens, C is the luminous intensity of the source in candles, A is the projected area of the cathode surface, and d is the distance between light source and phototube. The anode supply voltage is first adjusted to about 25 volts. With 1.5 lumens, full deflection of the 15-microampere meter is secured for the ordinary high-vacuum cell similar to the PJ-22; although individual tubes may be expected to vary somewhat. Readings of the photocell current should be taken for increasing distance between the light source and phototube until the tube current is less than 1 microampere. Readings should be made for at least one other anode voltage, about 180 volts.

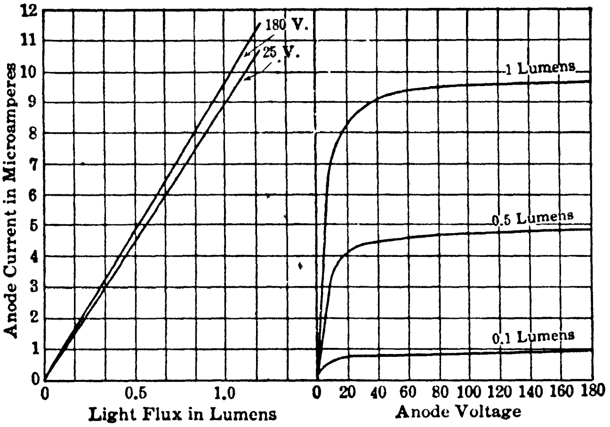

FIG. 816. Typical high-vacuum photocell characteristics.

In order to show the effect of space charge at low anode voltages and the saturation at high anode voltages, sets of readings for fixed illuminations, such as 0.1, 0.5, and 1.0 lumen, should be taken.

Report. From the data obtained, curves of photocell current *vs.* light flux in lumens may be plotted. Also curves of photocell current *vs.* applied voltage for constant illumination will show space charge effects and saturation. Typical results are shown in Fig. 816. Owing to the selective effect with regard to light frequency for a particular type of photocell, the temperature of the light source will influence the values obtained. Curves for commercial photocells are ordinarily made with a Mazda lamp source at 2870°K.

MOTIONS OF IONS AND ELECTRONS IN ELECTRIC AND MAGNETIC FIELDS

1156. Outline of Treatment.—We shall consider the forces and resulting motion of charged particles in uniform electric and magnetic fields separately and then in combined fields. The equations of motion will be obtained on the assumption that the vacuum is sufficiently high to make unnecessary a consideration of the collisions with other particles and the forces between electrons and ions. This condition exists for a variety of apparatus from the cathode-ray oscillograph to the many new devices developed principally for television and other special applications.

1157. Motion in a Uniform Electric Field.—An electron between plane parallel electrodes will, because of its negative charge, have a force tending to cause it to move towards the electrode of higher potential. The force will be given by $F = eE$ dynes, where e is the electronic charge in esu (electrostatic units), and E is the electric field intensity or potential gradient in esu. An electron starting from rest and passing through a potential difference V will attain a velocity given by:

$$v = \sqrt{2V\frac{e}{m}} \quad \ldots\ldots\ldots\ldots \quad (7)$$

when all quantities are expressed in cgs esu or cgs emu. The equation becomes:

$$v = 5.95 \times 10^7 \sqrt{V} \text{ cm per sec} \quad \ldots\ldots \quad (7a)$$

when V is expressed in volts. Equation (7) above is correct for ions as well as electrons when e and m respectively are replaced by the charge and mass of the ion. If the charged particle possesses an initial velocity, this must be added vectorially to the result obtained by eq. (7) to give the final velocity.

1158. Motion in a Uniform Magnetic Field.—The force on a moving electron or ion in a magnetic field can be derived from the familiar expression $F = Bli$ and by the further consideration that the current due to moving electrons is given by $i = Anev$, where A is the cross-sectional area of the assumed conductor, n is the number of electrons per unit volume, and v is their velocity. As usual, e is the charge on the electron. Since we are considering only one particle, $Anl = 1$, and the force is given by:

$$F = Bev \text{ dynes} \quad \ldots\ldots\ldots\ldots \quad (8)$$

when B is in lines per square centimeter, e is 1.591×10^{-20} abcoulomb, and v is in centimeters per second. An electron or ion entering a magnetic field will have a force acting on it which is mutually at right angles to the velocity and to the magnetic field. The path of a particle acted on by a force always at right angles to the velocity must be a circle, and the magnitude of the original velocity must remain unchanged. Equating centrifugal and centripetal forces, i.e., $mv^2/r = Bev$, the radius of the circle is:

$$r = mv/Be \quad \ldots\ldots\ldots\ldots \quad (9)$$

where v is the component of initial velocity perpendicular to B. The component of initial velocity parallel to B remains unchanged. The resulting path is thus a helix with its axis parallel to the direction of B. The radius for the rotating particle is smaller for larger values of B, which suggests the use of a magnetic field for focusing a stream of electrons. An application of this principle is found in the cathode-ray oscillograph (Chapter LVII).

1159. Generalized Equations of Motion. — In cartesian coordinates, the equations which govern the motion of an electron or ion in an assumed space-charge-free region are as follows:

$$\left.\begin{aligned} m\frac{dv_x}{dt} &= eE_x + e(B_z v_y - B_y v_z) \\ m\frac{dv_y}{dt} &= eE_y + e(B_x v_z - B_z v_x) \\ m\frac{dv_z}{dt} &= eE_z + (B_y v_x - B_x v_y) \end{aligned}\right\} \quad \ldots\ldots \quad (10)$$

These are the component equations which are contained in the general vector expression:[12]

$$m\frac{d\bar{v}}{dt} = e\bar{E} + e\bar{v} \times \bar{B}$$

The equations follow immediately from the consideration that force is equal to the rate of change of momentum, and that the force in any component direction is the sum of the forces due to both the electric and magnetic fields.

---

[12] Page and Adams, "Principles of Electricity," p. 279, D. Van Nostrand Co., 1932.

1160. Motion in Combined Electric and Magnetic Fields. — In uniform fields, it is usually convenient to choose the orientation of the axes so that B is in the direction of x, y, or z, since the motion parallel to B is uniformly accelerated motion due to the component of E in this direction only. For instance, if B_z has a value with $B_x = B_y = 0$, the only force on the ion in the z direction is that due to E_z, and consequently:

$$\left.\begin{aligned} m\frac{dv_z}{dt} &= eE_z \\ m\frac{dv_y}{dt} &= eE_y - eB_zv_x \\ m\frac{dv_x}{dt} &= eE_x + eB_zv_y \end{aligned}\right\} \quad \cdots\cdots\cdots\cdots \quad (11)$$

For uniform electric and magnetic fields at right angles to each other, the equations may be conveniently written:

$$\left.\begin{aligned} m\frac{dv_y}{dt} &= eE_y - eB_zv_x \\ m\frac{dv_x}{dt} &= eB_zv_y \end{aligned}\right\} \quad \cdots\cdots\cdots\cdots \quad (12)$$

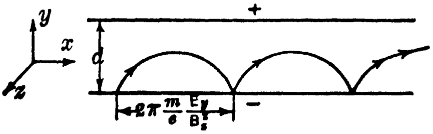

FIG. 817. Path of electron through crossed electric and magnetic fields, initial velocity zero (starting at rest from cathode).

The general solution of these simultaneous differential equations gives the motion of the particle in the xy plane. With zero initial velocity, the path of the particle is that of the common cycloid as illustrated by Fig. 817. Assuming the origin of coordinates where the electron starts from the cathode, the equations of motion are:

$$\left.\begin{aligned} x &= \frac{m}{e}\frac{E_y}{B_z^2}\left[\frac{e}{m}B_zt - \sin\left(\frac{e}{m}B_zt\right)\right] \\ y &= \frac{m}{e}\frac{E_y}{B_z^2}\left[1 - \cos\left(\frac{e}{m}B_zt\right)\right] \end{aligned}\right\} \quad \cdots\cdots \quad (13)$$

The uniform electric field is supplied by the plane parallel plates with a potential difference, V, between them. Since E_y is negative and the charge e of the electron is negative, the flux density B_z must be negative or away from the reader in the illustration. The equations are algebraic and automatically take care of any situation when the proper signs are given to the different components for a right-handed system of axes. It should be noted that x and y are in centimeters when E_y is in absolute electromagnetic units (sometimes designated abvolts per centimeter). B_z is in lines per square centimeter, t is in seconds, e is the charge in absolute electromagnetic units (abcoulombs), and m is the mass of the ion in grams.

When the ion possesses an initial velocity, the solution is much more complicated, and the path of the ion or electron is a trochoid.

The resultant equations are:

$$\left.\begin{aligned} x &= x_0 + \frac{m}{e}\frac{E_y}{B_z^2}\left(\frac{e}{m}B_z t + \phi_0\right) - b\sin\left(\frac{e}{m}B_z t + \phi_0\right) \\ y &= y_0 + \frac{m}{e}\frac{E_y}{B_z^2} - b\cos\left(\frac{e}{m}B_z t + \phi_0\right) \\ \phi_0 &= \tan^{-1}\left(\frac{-v_{0y}}{v_{0x} - \dfrac{E_y}{B_z}}\right) \quad b = \frac{\sqrt{\left(v_{0x} - \dfrac{E_y}{B_z}\right)^2 + v_{0y}^2}}{\dfrac{e}{m}B_z} \end{aligned}\right\} \qquad (14)$$

v_{0x} and v_{0y} are the components of initial velocity as the ion enters the crossed fields. The values for x_0 and y_0 depend upon the choice of the origin for the coordinate system. They may be determined by giving x and y their chosen values when the ion just enters the field between the parallel plates. It is assumed possible to terminate abruptly the electric and magnetic fields at the edges of the parallel plates and to maintain them uniform throughout the region between the plates. A typical path for an electron possessing an initial velocity is shown in Fig. 818.

In this illustration, an electron is projected, possibly by an electron gun, into the crossed electric and magnetic fields at an angle of 45 degrees with the horizontal and with the velocity components given. The path may be determined by substitution in equations (14) or may be constructed graphically. The trochoidal path is traced out by the terminus of a line lying along the radius of a circle which rolls along a horizontal line. In this case the path is traced by the extended spoke of a wheel rolling along a line parallel to the X axis. The radius of the wheel, $a = (m/e) \cdot (E_y/B_z^2)$; b and ϕ_0 are given by equations (14). From the values given on the figure, $E_y = -40 \times 10^9$ abvolts per centimeter;

$B_z = -50$ lines per square centimeter; $a = 0.91$ centimeter; $b = 3.44$ centimeters; and $\phi_0 = 124° 13' = 2.167$ radians. If $x = 0$, $y = 0$, $t = 0$ when the electron just enters the crossed fields, in the parametric equations (14), $x_0 = 0.871$ and $y_0 = -2.82$. It should be noted that these results depend upon the assumption of sharp cut-off of the electric and magnetic fields at the edges of the plates.

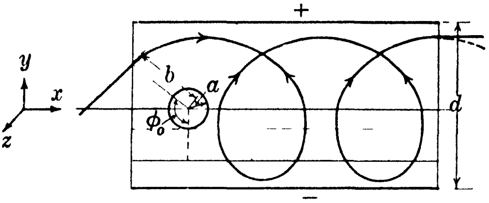

FIG. 818. Path of electron through crossed electric and magnetic fields, initial velocity of electron, $v_{0x} = v_{0y} = 2.5 \times 10^9$ cm per sec. Flux density = 50 lines per sq. cm, into the paper; potential difference between plates = 3200 volts; $d = 8$ cm.

1161. Change of Electron Mass with Velocity. — Because there is a direct relation between the energy of an electron and its mass, the mass of an electron increases with velocity. This is due to the energy storage in the magnetic field generated by a moving electron. The relation between the " rest mass " (m_0) of an electron and the mass when moving with a velocity v is given by:

$$m = \frac{m_0}{\sqrt{1 - (v/c)^2}} \qquad (15)$$

where c is the velocity of light.[13]

1162. Electron Optics. — The solution of equations (10) gives the path of an electron through electric and magnetic fields of any configuration. The solution for uniform fields has been given in §1160. In certain problems, especially when the electric and magnetic fields possess axial symmetry, the analogy between the path of a ray of light through refracting media and the path of a particle through conservative fields of force simplifies the solution. In electron optics the path of an electron is analogous to a ray of light. Instead of abrupt changes in the index of refraction that occur in a lens system for light, the quantity which corresponds to the index of refraction in an electron optical system is a continuous function of position and direction. For pure electrostatic systems, the index of refraction is a function of position only. For a treatment of the electron optical method, the student is referred to special treatises.[14]

[13] Harnwell and Livingood, " Experimental Atomic Physics," McGraw-Hill Book Co., p. 121, 1933.

[14] Myers, " Electron Optics, Theoretical and Practical," D. Van Nostrand Co., Maloff and Epstein, "Electron Optics in Television," McGraw-Hill Book Co., 1938.

1163. Applications of the Equations of Motion.—The electron or cathode-ray oscillograph described in Chapter LVII illustrates the motion of electrons under conditions which permit the application of the equations developed. Figure 819 shows the principle of the cathode-ray oscillograph employing electrostatic deflection. The electron gun, *A* (see also Fig. 800), provides a stream of electrons (cathode ray) more or less concentrated along the axis. The plates *B* have the voltage under investigation applied to them, and the screen *C* fluoresces as the result of the energy received from the electron impacts. In a practical case we might wish to calculate the voltage sensitivity of the oscillograph, i.e., the ratio of the displacement of the beam on the fluorescent screen to the voltage applied to the deflecting plates, usually expressed in millimeters per volt. This could be done in the following manner:

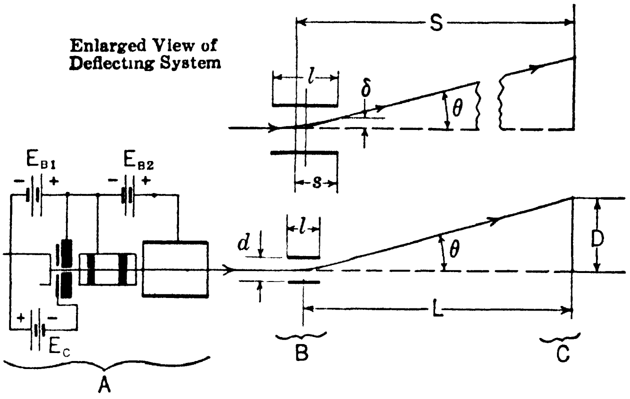

FIG. 819. Principle of the cathode-ray oscillograph employing electrostatic deflection; $E_{B1} + E_{B2} = 2000$ volts, $l = 3$ cm, $L = 25$ cm, $d = 2$ cm.

The speed of an electron starting with zero velocity at the cathode is proportional to the square root of the total accelerating voltage in the electron gun, or $v_{0x} = \sqrt{2e/m}\,\sqrt{E_{B1} + E_{B2}}$. This is the electron velocity as it enters the space between deflecting plates. At this point the electric field produced by the voltage V between the deflecting plates exerts an upward force on the electron. This is given by $F_y = eE_y$. Since there are no other components of force, there will be no acceleration in any except the y direction. The total deflection of the electrons while passing between the plates will depend on the time of transit. This is given by $t = l/v_{0x}$. The acceleration in the y direction,

$dv_y/dt = (eE_y)/m = e/m(-V/d)$. ($e$ is negative.) Therefore

$$\delta = \tfrac{1}{2}(e/m)\,(V/d)\,(l^2/v_{0x}^2)$$

The angle θ which the final electron velocity makes with the horizontal axis is given by: $\theta = \tan^{-1} v_y/v_{0x}$. Then $S = L - (l/2) + s$ and $s = \delta/\tan\theta$. Since $\tan\theta = D/S$, $D = (L - l/2)\tan\theta + \delta$.

$$\frac{D}{V} = \frac{Ll}{2d(E_{B1} + E_{B2})} \quad \text{cm per volt}$$

For the values given in Fig. 819, the sensitivity is 0.125 millimeter per volt.

Dempster mass spectrograph. An arrangement used for measuring the ratio of charge to mass of positive ions is shown in Fig. 820. Ions, after falling through a potential difference V, enter slit S_1. A strong magnetic field is maintained in the region $ABCD$, and shielding is provided to eliminate effectively the magnetic field in the space above AB. After passing through S_1, the ions are forced into a circular path. The radius of the circle is given by $r = \sqrt{2V}/B\,\sqrt{m/q}$ from equations (7) and (9). From this relation the ratio of charge to mass, q/m, may be calculated. Practically, B is sometimes difficult to measure accurately, and the instrument is used to compare the mass of an unknown ion with that of another, such as oxygen, the mass of which is 16 by definition. An important feature of this type of mass spectrograph due to Dempster[15] is the focusing action on ions that enter at different angles. Ions entering perpendicularly arrive at S_2 farthest away from S_1. Detection at S_2 is accomplished either electrically or photographically. The width of the trace, $S = 2r(1 - \cos\alpha) = r\alpha^2$ for small α's. It is thus seen to be very narrow with a sharp edge farthest away from S_1.

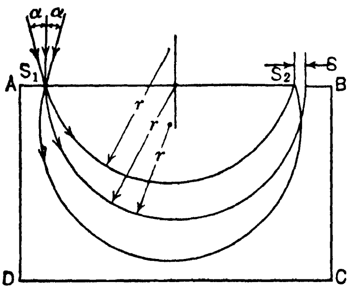

FIG. 820. Elements of Dempster's mass spectrograph.

1164. The Magnetron. — A vacuum tube consisting of a cylindrical anode surrounding concentrically a long straight filament with a magnetic field parallel to the filament is known as a magnetron. The important characteristics of this tube are independent of space-charge effects, and may be considered conveniently at this time as an illustration of some of the preceding theoretical relations. A cross-sectional view of the magnetron is shown in Fig. 821. Electrons traveling from filament to anode follow a curved path, due to the presence of the magnetic field. Radial symmetry prompts the use of cylindrical coordinates in setting up the equations of motion. For an electron at the point r, θ, the torque due to the magnetic field B parallel to the filament, is $Be\, dr/dt \cdot r$. Equating this to the rate of change of angular momentum, we have:

---

[15] Dempster, *Phys. Rev.*, vol. 11 (1918), p. 316; vol. 18 (1921), p 415; vol. 21 (1923), p. 209.

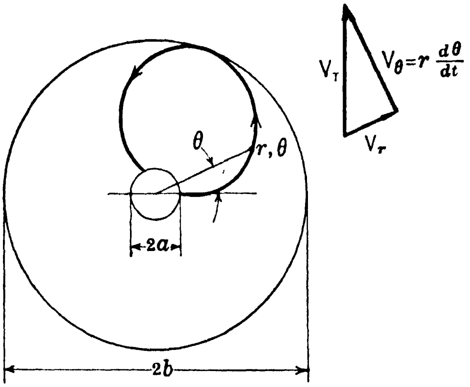

FIG. 821. Typical electron path in the magnetron.

$$d/dt\,(mr^2\, d\theta/dt) = Be\, dr/dt\, r$$

or

$$(r^2\, d\theta/dt) = \int_a^r (Be/m) r\, dr$$

where a is the radius of the filament.

This yields: $d\theta/dt = (Be/2m)(1 - a^2/r^2)$.

Assuming that the electron starts with zero velocity at the filament, the total kinetic energy, $(1/2)mV_T{}^2 = e\int_a^r E\, dr$, where E is the potential gradient or electric field strength, since the magnetic field contributes no energy. Now

$$V_T{}^2 = (dr/dt)^2 + r^2(d\theta/dt)^2$$

Therefore,

$$(1/2)m[(dr/dt)^2 + r^2(d\theta/dt)^2] = e\int_a^r E\, dr$$

This relation enables one to determine the conditions for plate current cut-off. The electron paths are approximately circular. For a sufficiently large value of B the radius of the circle will be so small that the electrons will not enter the plate. The condition for " grazing incidence " is obtained by substituting $dr/dt = 0$, $r = b$. Now:

$$\int_a^b E\,dr = V_b, \text{ plate potential}$$

assuming that the filament is at zero potential, regardless of the manner in which E varies. Therefore,

$$B = \sqrt{8m/e}\,\frac{1}{(1 - a^2/b^2)}\,\frac{\sqrt{V_b}}{b} \quad \ldots\ldots \quad (16)$$

when all quantities are expressed in cgs electromagnetic units. In practical units:

$$B = \frac{6.72V_b}{[1 - (a/b)^2]b} \quad \ldots\ldots \quad (17)$$

Equation (16) shows that the magnetron could be used to determine the value of e/m when B is known, or, conversely, assuming a value for e/m the magnetron may be used to explore and measure the strength of a magnetic field. Complete solutions for the electron path have been developed by Hull.[16] It is shown that, for very small values of a/b which hold in practical cases, the relation

$$B = \frac{6.72V_b}{b} \quad \ldots\ldots \quad (18)$$

is a good approximation whether space charge is considered or neglected.

1165. EXPERIMENT 59-C. — Use of the Magnetron to Determine *e/m* or *B*. — Commercial tubes such as the FP-85 may be used to determine approximately the value of e/m. The known value of B is obtained by placing the tube inside of a long solenoid whose dimensions are known. The arrangement is shown in Fig. 822. Curves of plate current *vs.* current in the solenoid for different plate voltages should be plotted to determine the point at which the plate current is cut off. For a specially designed magnetron with a fine wire filament accurately located at the center of the cylindrical anode, the plate current drops very abruptly when the critical value of B is reached. Commercial tubes are likely to have some dissymmetry preventing extremely sharp cut-off and lowering the accuracy of the determination. Spacing of the elements in a commercial tube may be measured with a cathetometer. For a relatively long solenoid the value of B is given by

---

[16] Hull, A. W., " The Effect of a Uniform Magnetic Field on the Motion of Electrons between Coaxial Cylinders," *Phys. Rev.*, vol. 18 (1921), p. 31; " The Path of Electrons in the Magnetron," *ibid.*, vol. 23 (1924), p. 112.

$$B = 0.4\pi N I_s / l \qquad (19)$$

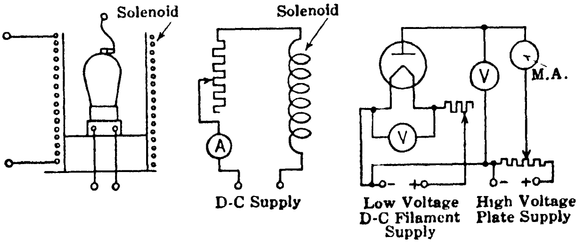

Fig. 822. Arrangement for calibration of magnetron for measurement of flux densities or for measurement of e/m.

N = the number of turns in the solenoid, I_s = solenoid current in amperes for plate current cut-off, and l = length of solenoid in centimeters. From the data obtained in these runs and eq. (16), e/m may be calculated.

It is obvious that the critical relation between B and V_b for the abrupt change in plate current may be used in exploring a magnetic field. In order to show sensitiveness to the direction of B, the axis of the tube should be set at a small angle with respect to the axis of the solenoid and readings of plate current and solenoid current taken. Typical curves for an FP-85 are shown in Fig. 823. A newer tube, the FP-400, gives a more abrupt cut-off than the FP-85.

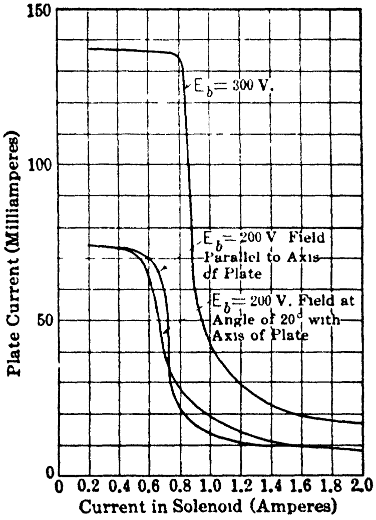

Fig 823. Typical magnetron characteristics (General Electric Co).

1166. High-Vacuum Diodes. Definition. — The simplest type of high-vacuum tube is the diode, which consists essentially of a filament or cathode as an electron-emitting source and the conducting plate as a collector, all placed in an evacuated container. High-vacuum diodes are used as rectifiers, modulators, and demodulators where the currents are not too large.

Tubes containing gas are employed for heavier currents. The name kenotron has been applied to the high-vacuum thermionic diode.

1167. Plate Current-Voltage Relation. — Electrons pass from the hot cathode to the plate in a diode under the influence of the electrostatic field set up by the potential difference between the plate and filament. Figure 812 shows a schematic circuit suitable for obtaining the curves of Fig. 824(*a*). A different curve is obtained for each value of filament current. For the lower values of filament current there is a definite tendency for the plate current to reach a saturation value. This is due to the condition that all the electrons emitted at that particular filament temperature are being drawn away. The curves do not have a flat top because of secondary effects such as non-uniform temperature of the emitter surface, surface irregularities, and the effect of field emission. Curves of plate current *vs.* filament current for different values of plate voltage are shown by Fig. 824(*b*). Here another type of saturation is noted for the lower plate voltages. This is caused by the space charge near the cathode due to the presence of an electron cloud. The potential distribution in the diode is thereby altered so that an increased emission no longer results in a corresponding increase in plate current. Figure 825 shows typical cases of potential distribution with different values of filament power and with constant plate

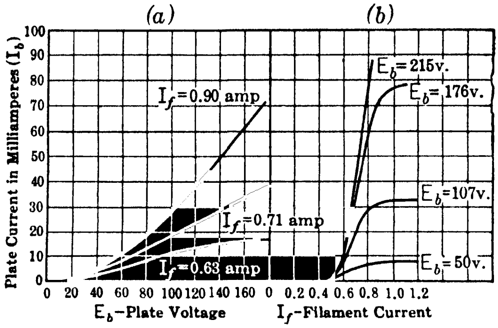

FIG. 824. Typical characteristics of the diode.

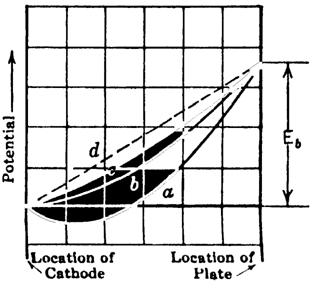

FIG. 825. Potential distribution in a diode: (*a*) maximum filament power; (*d*) filament cold.

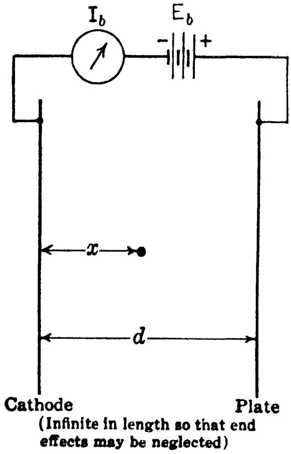

FIG. 826. Theoretical diode with plain parallel electrodes.

voltage. The potential distribution in a diode would be a straight line if space charge were not present. It should be noted that the potential distribution curve approaches a straight line for lower filament powers.

1168. Child's Law. — When certain tenable assumptions are made, it is possible to derive the relation between plate current and plate voltage in a diode. This relation, $I_b = KE_b^{3/2}$, was first derived by Child.[17] If we first consider a diode (Fig. 826) with plane parallel electrodes infinite in extent, the most general relation

$$\partial V/\partial x^2 + \partial^2 V/\partial y^2 + \partial^2 V/\partial z^2 = -4\pi\rho \qquad (20)$$

known as Poisson's law[18] describes the potential at points between the parallel plates. For the symmetry assumed this reduces to $\partial^2 V/\partial x^2 = -4\pi\rho$, where ρ is the space-charge density. The current density, $J = \rho v$, where v is given by eq. (7), therefore,

$$\rho = J\sqrt{m/2Ve}$$

and $\partial^2 V/\partial x^2 = 4\pi J\sqrt{m/2e}\sqrt{1/V}$, since ρ is negative. Let

$$4\pi\sqrt{m/2e} = b$$

Then $\partial^2 V/\partial x^2 = bV^{-1/2}J$, or, in this case, $d^2V/dx^2 = bV^{-1/2}J$. Making the left-hand side a perfect differential by multiplying in $2dV/dx$ we have:

$$2dV/dx\, d^2V/dx^2 = 2bJV^{-1/2}\, dV/dx$$

Integrating:

$$(dV/dx)^2 = 4bJV^{1/2} + C$$

If it is assumed that $dV/dx = 0$ at the cathode where $V = 0$, then $C = 0$. (This corresponds to a potential distribution like curve b of Fig. 825.)

Separating the variables and performing a definite integration:

$$\int_0^{E_b} dV/V^{1/4} = \int_0^d 2b^{1/2}J^{1/2}\, dx$$

$$(16/9)E_b^{3/2} = 4bJd^2$$

$$J = (4E_b^{3/2})/(9bd^2)$$

or, substituting the value of b:

$$J = (\sqrt{2}/9\pi)\sqrt{e/m}E_b^{3/2}/d^2, \text{ in cgs electromagnetic units} \qquad (21)$$

---

[17] Child, *Phys. Rev.*, vol. 32 (1911), p. 498.

[18] Page and Adams, "Principles of Electricity," D. Van Nostrand Co.

$J = 2.33 \times 10^{-6} E_b^{3/2}/d^2$ amperes per square centimeter when E_b is expressed in volts and d in centimeters.

For the case where the cathode and anode are coaxial cylinders, it has been shown[19] that

$$J = 14.65 \times 10^{-6} \frac{E_b^{3/2}}{r\beta^2} \text{ ampere per sq cm} \quad . \; . \; . \quad (22)$$

where r is the radius of the anode or plate in centimeters and β^2 is a function of the ratio of the cathode and anode radii. Values of β^2 are given in Table II.

TABLE II

VALUES OF β^2 AS A FUNCTION OF THE RADII

r_0 = radius of cathode
r = radius at any point P
β^2 applies to case where $r > r_0$
$-\beta^2$ applies to case where $r_0 > r$

r/r_0 or r_0/r	β^2	$-\beta^2$
1.00	0.0000	0.0000
1.50	0.11934	0.2282
2.00	0.2793	0.8454
4.00	0.6671	6.0601
8.0	0.9253	24.805
20.0	1.0715	115.64
40.0	1.0946	327.01
100.0	1.0782	1174.9
200.0	1.0562	2946.1
500.0	1.0307	9502.2

$u = \log r/r_0$
$\beta = u - 2/5u^2 + 11/120u^3 - 47/3300u^4 + \cdots$

1169. Types of High-Vacuum Diodes. — The size and other design features of high-vacuum diodes depend upon the use for which particular types are intended. Figure 827 shows a range of styles from the smaller 6H6 Twin Diode (two diodes in one envelope with a common cathode) to the relatively large 100,000-volt, 0.5-ampere tube designed for X-ray power supply and other high-voltage applications.

The maximum plate current rating of high-vacuum diodes is usually determined by the size and type of cathode, the voltage rating by the spacing of the elements, the cathode design, and the degree of vacuum possible to maintain. In any tube, no matter how complete the evacuation, there are always some gas atoms present. Under the impact of moving electrons, these atoms may become positive ions which are impelled to bombard the negative cathode, sometimes with destructive effects. This phenomenon prevents the use of oxide-coated cathodes in high-voltage tubes and at still higher voltages prevents the use of thoriated tungsten filaments. In a few types, careful design has extended the upper voltage limit for the composite cathode, but tungsten filaments are still used exclusively for the highest voltages.

---

[19] I. Langmuir and Katherine Blodgett, "Currents Limited by Space Charge between Co-axial Cylinders," *Phys. Rev.*, October, 1923.

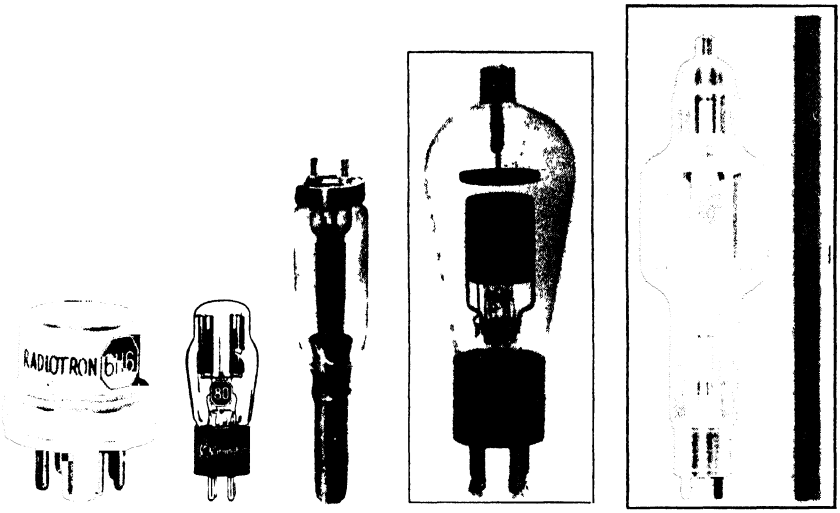

FIG. 827. Typical diodes from the small 6H6 twin diode with common cathode to the 100,000-volt, 0.5-ampere tube for X-ray power supply.

1170. EXPERIMENT 59-D. — Measurement of Diode Parameters. — Although the conditions under which Child's law was derived are not completely satisfied,[20] the relation between plate current and plate voltage in a high-vacuum diode can be represented reasonably well by $I_b = KE_b^\eta$. It has been shown by van der Bijl[21] that, when the potential drop along the filament in a diode with filamentary cathode is considered, the value of η should be 5/2 for $E_f > E_b$. The experimentally determined value of η is usually somewhere between 1.4 and 2.0.

---

[20] In particular the effect of initial velocity of emission and contact potential between cathode and plate are significant at very low plate voltages, and saturation must be considered at high plate voltages. The student is referred to E. L. Chaffee, "Theory of Thermionic Vacuum Tubes," McGraw-Hill Book Co., for a summary of this theory treated by Schottky, Langmuir, and others.

[21] H. J. van der Bijl, "Thermionic Vacuum Tubes," McGraw-Hill Book Co., 1920.

The same apparatus and circuit diagram (Fig. 812) used in Experiment 59-A may be used to measure diode parameters. If a type-81 tube is used, the meter ranges indicated on this diagram will be satisfactory. With a constant plate voltage of about 20 volts, the filament current should be varied from a value sufficiently low to give a minimum of 1 milliampere of plate current to the point where the maximum allowable filament voltage is reached. Readings of E_b, I_b, E_f, and I_f should be taken. This run should be repeated for a constant plate voltage of about 180 volts. It will be necessary to adjust the filament current very carefully, making sure that the maximum plate current rating is not greatly exceeded. The above runs will illustrate the condition of temperature saturation.

In order to study voltage saturation phenomena, runs should be made at the rated filament voltage (7.5 volts for the 81 tube), and variable plate voltages should be adjusted in convenient steps from 0 to a value sufficiently high to give maximum rated plate current. The same quantities are recorded as in previous runs. Using a new filament voltage of about half the rated value, readings should be taken as before.

Report. If curves of plate current *vs.* filament voltage are plotted from the data in the first two runs, the saturation at low plate voltages will be observed. The data for the last two runs plotted as plate current *vs.* plate voltage will illustrate the tendency toward a saturation condition for the low filament voltage.

From the data obtained at the rated filament voltage, the student should plot log of I_b *vs.* log of E_b, or the values of these quantities should be plotted on log log paper. A straight-line plot should be obtained. This may necessitate neglecting certain points at the high voltages where saturation prevents the typical Child's law relation. The constants for the equation $I_b = KE_b^\eta$ are obtained from the straight-line curve. The slope of the line is proportional to eta (η), and the value of K is determined by the intercept on the Y axis.

1171. Rectification with the Diode. — (a) *The circuit.* One of the primary characteristics of the high-vacuum diode is unidirectional current flow. A typical rectifier circuit consists of a diode in series with the secondary of a transformer and the load, as shown in Fig. 828(*a*). The applied voltage and the resulting current wave are given in Fig. 828(*b*). The current for the ideal rectifier is also shown, following the pattern of the wave of voltage from the transformer secondary and neglecting the non-linear characteristic of the diode. A Fourier series analysis of the ideal wave form will give:

$$i = I_m/\pi(1 + \pi/2 \sin \omega t - \tfrac{2}{3} \cos 2\omega t - \tfrac{2}{15} \cos 4\omega t \cdots) \quad . \; . \; (23)$$

Another typical arrangement for the use of the diode as a rectifier is shown in Fig. 829(a). This is the full-wave rectifier circuit using two

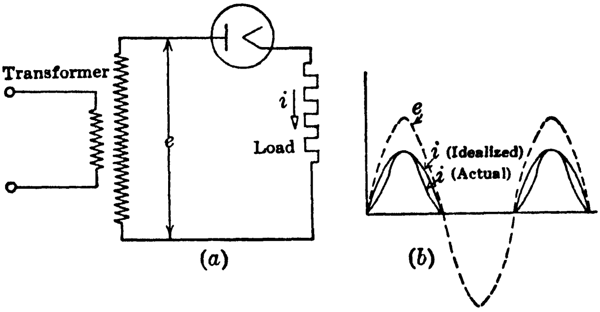

FIG. 828. Half-wave rectifier circuit.

separate diodes or two diodes in one envelope. The resulting idealized current wave form is also shown for which the Fourier series is

$$i = 2I_m/\pi(1 - \tfrac{2}{3} \cos 2\omega t - \tfrac{2}{15} \cos 4\omega t - \tfrac{2}{35} \cos 6\omega t - \cdots) \quad . \; . \; (24)$$

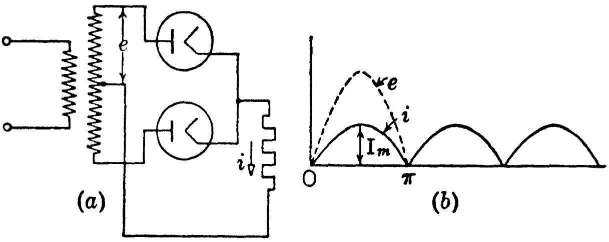

FIG. 829. Full-wave rectifier circuit.

The full-wave circuit requires a split secondary on the transformer, but gives a better transformer load factor and twice the output current. This scheme also eliminates residual flux in the transformer core.

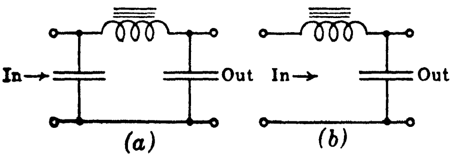

FIG. 830. Filters for rectifiers.

(b) *Filters.* For many requirements it is desirable to have the d-c output reasonably free from ripple. To accomplish this a filter is used. Figure 830 shows two common types of filter circuits, the pi-section or condenser-input filter and the L-section or choke-input type. These and other sections are sometimes combined.

1172. EXPERIMENT 59-E. — Determination of Rectifier Regulation and Hum Percentage. — The schematic circuit diagram for a full-wave rectifier connected to a pi-section filter and load is shown in Fig. 831. A convenient tube for this test is the type-80 full-wave rectifier. The maximum output rating of this type is about 135 milliamperes, so the filter choke, load, and milliammeter should be chosen accordingly. A suitable load device consists of five or six 10,000-ohm, 20-watt resistors suitably mounted and connected to switches so as to give series-parallel combinations. The transformer secondary should be designed to give a rectifier output voltage of not more than 500 volts d-c (see Table III) at no load. The d-c voltages should be measured with a high-resistance voltmeter. Ripple voltages may be determined by a vacuum-tube voltmeter having a condenser in series with one terminal to prevent the d-c component of the voltage from affecting the reading. A suitable voltmeter circuit is shown in Fig. 894.

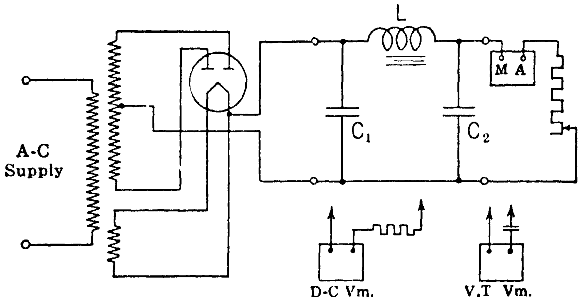

FIG. 831. Circuit for testing single-phase full-wave rectifier.

After all connections have been made and checked, the load current should be varied from zero to the maximum rated value in convenient steps. For each load, the value of the d-c input and output voltages to the filter should be measured, as well as a-c ripple (or hum) voltage at the terminals. Similar runs should be made with increased filter capacitance connected to the input and again at the output end, in order to compare the voltage regulation and hum percentage for different arrangements. It is also desirable to make a run with the pi-section filter replaced by a choke-input filter.

The capacitance values of the filter condensers used should be measured if they are not already known, and complete data on the inductance of the filter choke as a function of the d-c current should be obtained. (See §1174.)

Report. Curves of d-c input and output voltages to the filter *vs.* d-c load current will enable the comparison of the regulation for different types of filter to be made. Ripple voltages plotted on the same curve sheet will permit the comparison of the effect of each type of filter in this respect. Some analysis should be made of the effect of the size of the filter condensers upon the d-c output voltage.

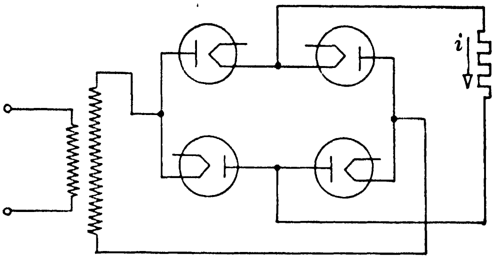

Fig. 832. Full-wave bridge circuit — wave form same as in Fig. 829(*b*).

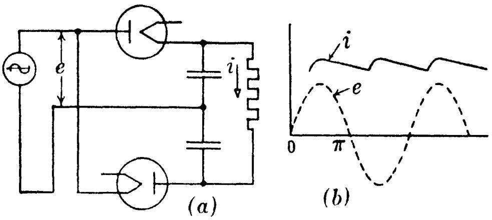

Fig. 833. Voltage-doubling rectifier circuit.

1173. Rectifier Circuits. — Aside from the simple half-wave and full-wave circuits previously described, two other schemes are used for single-phase rectifiers. The one is the full-wave bridge rectifier employing four diodes connected as shown in Fig. 832, and the other the voltage-doubling circuit of Fig. 833.

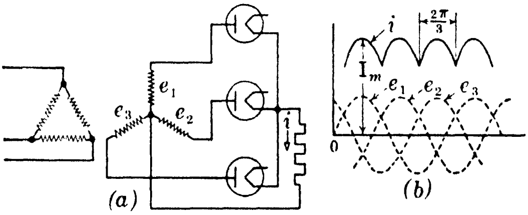

Fig. 834. Three-phase half-wave rectifier.

High-voltage rectifiers with high power output usually employ three-phase power supply. The three-phase half-wave rectifier circuit is shown in Fig. 834. Lower ripple voltage and higher ripple frequency permit more economical filter design for three-phase rectifiers. Other types of three-phase rectifier circuits are shown in Figs. 835 and 836.

1174. Rectifier-Filter Design. — Table III lists the important constants and ratios used in the design of rectifiers with choke input (L section). Certain ideal conditions have been assumed which represent approximations leading to a good practical design. Item *a* in the table is obtained by taking the ratio $\frac{\text{rms}}{\text{average}}$ for the idealized output wave form. Item *b* is the ratio of the peak voltage applied to any tube in the non-conducting direction, to the d-c output voltage. The voltage drop across tubes in the conducting direction is assumed to be zero. This factor (*b*) dictates the inverse peak voltage rating of the tube used. Item *c* is obtained by applying Fourier series analysis to the idealized output wave form. The series for half-wave and full-wave single-phase rectifiers are given by eqs. (23) and (24). The general relation for a polyphase rectifier is[22]

$$i = \frac{pI_m}{\pi} \sin \frac{\pi}{p} \left[1 + 2 \sum_{m=1}^{m=\infty} \frac{\cos mp\omega t}{1 - (mp)^2} \right] \quad . \quad . \quad . \quad . \quad . \quad (25)$$

where m = order of harmonic ($m = 1$ for fundamental ripple frequency).
p = number of phases ($p = 6$ for three-phase, full-wave).

Items *d*, *e*, and *f* in the table are obvious. Items *g* and *h*, the transformer utilization factors[23] represent the ratio between the d-c power output and the normal a-c rating of transformer winding for the same I^2r losses that occur in rectifier service. In calculating this ratio and other factors, the filter inductance is assumed to be large enough to maintain constant current. This means rectangular wave shapes for the transformer currents.

Using the factors in Table III, it is possible to design rectifier filter combinations with choke-input filters. The specifications for a rectifier usually include the output voltage and current, the permissible ripple in the output expressed as a percentage of output voltage, and the maximum impedance represented by the output terminals of the rectifier filter to the load circuit at some relatively low frequency. This latter specification determines the ability of the rectifier to maintain steady voltage to a fluctuating load and puts a lower limit on the size of the filter condenser. Table III gives the rms value of the lowest-frequency component of ripple voltage, obtained by multiplying the

---

[22] B. Liebowitz, *Proc. I.R.E.*, vol. 5 (1917), p. 33.

[23] Prince and Vogdes, "Principles of Mercury Arc Rectifiers and Their Circuits," McGraw-Hill Book Co., 1927.

TABLE III

Type of Circuit	Single-Phase Half-Wave (Fig. 828)	Single-Phase Full-Wave (Fig. 829)	Single-Phase Bridge (Fig. 832)	Three-Phase Half-Wave (Fig. 834)	Three-Phase Full-Wave (Fig. 836)	Three-Phase Double Y (Fig. 835)
Ratio of a-c voltages to d-c output voltage. (Assuming no drop in choke, tubes, and transformer)						
a. Transformer secondary (rms per leg)	2.22	1.11	1.11	0.855	0.428	0.855
b. Inverse peak voltage	3.14	3.14	1.57	2.09	1.05	2.09
c. Ripple components (rms)						
1. Fundamental (E_1)	1.11	0.472	0.472	0.177	0.040	0.040
2. 2nd harmonic	0.472	0.095	0.095	0.040	0.010	0.010
3. 3rd harmonic	0.095	0.040	0.040	0.018	0.004	0.004
d. Ripple frequency (fund.) (f = supply frequency)	f	$2f$	$2f$	$3f$	$6f$	$6f$
Ratio of tube currents to d-c output current. (Assuming steady output current)						
e. Peak anode current	1.00	1.00	1.00	1.00	1.00	0.5
f. Average anode current	1.00	0.5	0.5	0.33	0.33	0.167
Transformer utilization factors						
g. Primary	0.637	0.900	0.900	0.827	0.955	0.955
h. Secondary	0.637	0.637	0.900	0.675	0.955	0.675

factor under item *c* by the d-c output voltage of the rectifier. This result is the ripple voltage at the input of the filter, and is designated by E_1. The value of current of ripple frequency through the filter choke is given by $I_1 = E_1/\omega L$, since the impedance of the condenser may be considered negligible in comparison. The ripple voltage E_2 appearing at the output terminals of the filter is given by:

$$E_2 = I_1/\omega C = E_1/\omega^2 LC,$$

$$\text{or} \quad LC = E_1/\omega^2 E_2 \quad . \; . \; . \quad (26)$$

The requirement of maximum output impedance at a specified minimum frequency sets a lower limit for C, and this value substituted in eq. (26) permits L to be determined. Another criterion fixing a minimum value for L is the requirement that the current through L should not be discontinuous. This is a function of the minimum d-c load current (I_{0m}). To maintain continuous current through L, the peak value of the ripple current through L, ($\sqrt{2}I_1$), should be less than I_{0m}, or as a limit:

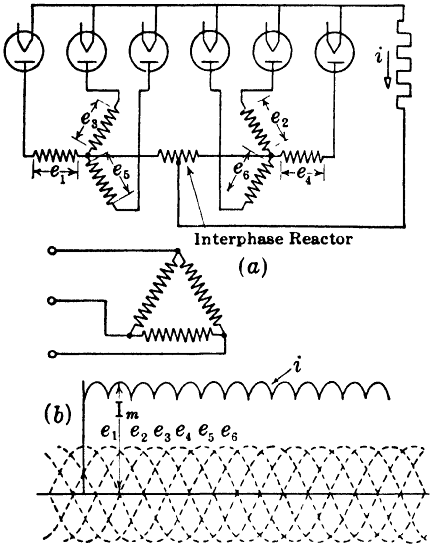

FIG. 835. Three-phase half-wave double-Y rectifier with interphase transformer — six-phase wave form.

$$I_{0m} = \sqrt{2}I_1 = \sqrt{2}E_1/\omega L \quad . \; . \; . \; . \; . \; . \; . \; . \quad (27)$$

from which the minimum L is obtained. The product of the minimum L and the minimum C may in some cases be greater than that given by eq. (26), in which event the ripple percentage will be less than the specified limit. It should be noted that the inductance L is the incremental inductance and is a function of the direct current flowing through the choke. The choice of a tube type is governed by the peak and average currents (items *e* and *f* in Table III) and the inverse peak voltage (item *b* in Table III). The d-c voltage drop through the tubes and choke is added to the output d-c voltage to determine a new d-c voltage. This multiplied by the factor under item *a* gives the secondary voltage rating of the transformer. The kva ratings are determined by the d-c load and the utilization factors (items *g* and *h* in Table III). With only slight modifications, the above method will serve as a basis of design for any rectifier filter having sufficiently large choke input. A mathematical analysis of a rectifier employing condenser input filter due to R. L. Freeman and F. E. Terman is given by Terman.[24]

1175. EXPERIMENT 59-F. — Test of a Three-Phase Rectifier Filter. — The characteristics of a rectifier filter designed according to the preceding methods may be checked experimentally. The apparatus is connected according to the diagrams of Figs. 834, 835, or 836, depending upon the type. Great care must be exercised to prevent bodily contact with the circuit when voltages may be dangerously high. Provision should be made for showing the tube current, current input, and voltage input to the filter and the load voltage on an oscillograph (Chapter LVII). It is also interesting to observe the wave form of current in the primary and secondary windings of the transformer. If measurements are to be made by the oscillograph, the electromagnetic type is preferred, although the cathode-ray oscillograph will give excellent qualitative results for the voltages. Usually, a potentiometer is required to adjust the voltage on the deflecting plates of the cathode-ray oscillograph. The output current and voltage are measured by means of a vacuum-tube voltmeter as explained in Experiment 59-E. A load run should be made in which the load current is varied from zero to the maximum rated value, or slightly higher. Readings of load current, load voltage, and ripple voltage should be taken, and the various wave forms should be observed on the oscillograph for several different load values. It is important to note the value of load current at which the current flow to the filter becomes discontinuous.

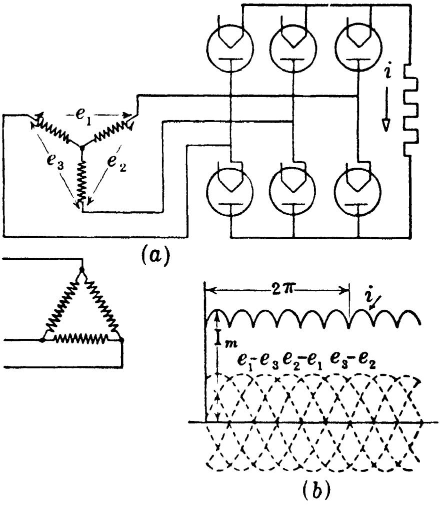

FIG. 836. Three-phase full-wave rectifier circuit — six-phase wave form.

Report. If sufficient data are secured on the constants of the component parts of the rectifier filter, the characteristics determined experimentally may be compared with the results calculated by the methods described in §1174. The ripple voltage and voltage regulations should be exhibited as a function of the load current.

---

[24] F. E. Terman, "Radio Engineering," McGraw-Hill Book Co., 1937.

1176. High-Vacuum Triodes. — In the usual three-element tube the control grid is placed between the cathode and anode and consists of a wire mesh or grid whose potential affects the distribution of potential through the tube, but otherwise imposes the least mechanical hindrance to the flow of electrons from cathode to plate. Figure 837 shows a cutaway view of a commercial receiving-type tube. This is a pentode (five electrodes, three grids), but illustrates the general arrangement. High-vacuum tubes with control grids are sometimes called "pliotrons."

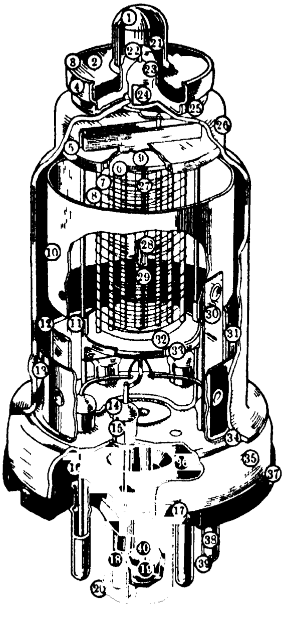

Fig. 837. Structure of an all-metal radio tube. Courtesy of RCA Mfg. Co.

1 = solder
2 = cap insulator
3 = rolled lock
4 = cap support
5 = grid lead shield
6 = control grid
7 = screen
8 = suppressor
9 = insulating spacer.
10 = plate
11 = mount support.
12 = support collar.
13 = getter tab
14 = glass bead seal

15 = eyelet
16 = lead wire
17 = crimped lock
18 = aligning key
19 = pinched seal
20 = aligning plug
21 = grid cap
22 = grid lead wire
23 = glass bead seal
24 = eyelet
25 = brazed weld
26 = vacuum-tight steel shell
27 = cathode
28 = helical heater

29 = cathode coating
30 = plate insulating support
31 = plate lead connection.
32 = insulating spacer
33 = spacer shield
34 = shell-to-header seal weld
35 = header
36 = shell connection
37 = octal base
38 = base pin
39 = solder
40 = exhaust tube

1177. Potential Distribution in a Triode. — From the purely electrostatic viewpoint, Maxwell[25] first calculated the effect of a grid placed between plane parallel electrodes infinite in extent. Dow[26] has given a method of calculating the electrostatic field of a triode through the use of conformal transformation, and Chaffee[27] has exhibited plots of equipotential lines and lines of force in a triode obtained by setting up a model in a shallow tray containing acidulated water, with a probe to trace the equipotential lines. Figure 838 shows typical potential distribution curves for different values of grid potential or "grid bias." Owing to the position of the grid, it is much more effective in controlling the potential gradient near the cathode than is the plate. The effectiveness of the grid is determined not only by position but by size and spacing of grid wires. By making the grid sufficiently negative, the plate current may be cut off entirely. When the grid is positive,[28] the effect is to increase the plate current enormously, although this is modified by the fact that the grid itself will have an electron current.

---

[25] J. C. Maxwell, "Electricity and Magnetism," Third Edition, Vol. I, page 203, Oxford, 1904.

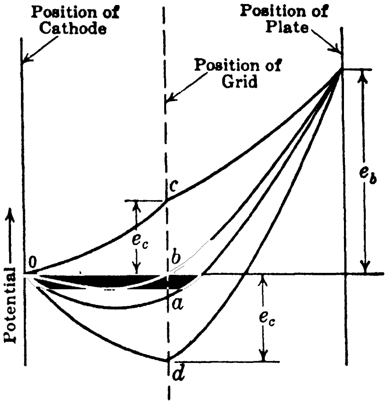

Fig. 838. Potential distribution in a triode: *a*, free grid; *b*, grid at zero (cathode) potential; *c*, grid at positive potential; *d*, grid at negative potential.

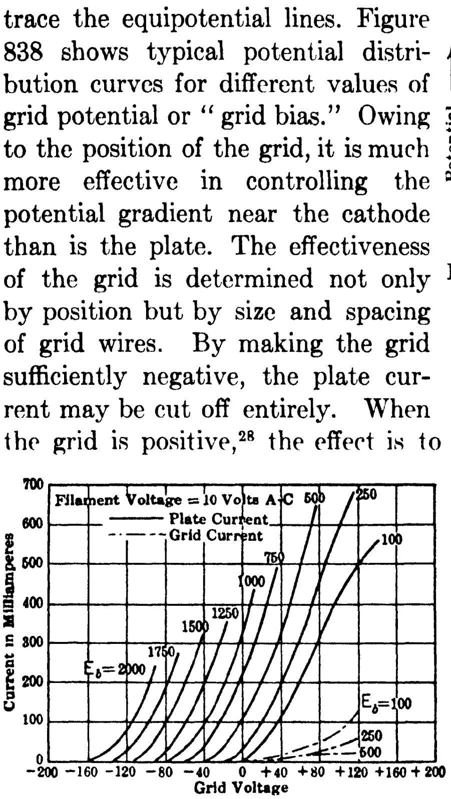

Fig. 839. Triode characteristics (Western Electric Co. catalog).

1178. Static Characteristic Curves. — Figure 839 shows the plate current and grid current in a triode as a function of plate and grid voltages, with the filament voltage constant. The same characteristics are shown in a different way by Fig. 840. These are the usual methods of representing triode characteristics, although other methods have been used when advantageous.[29] Figure 841*a* illustrates a suitable circuit for obtaining static characteristic curves. If data far into the positive grid region are desired, some special method of testing is necessary[30] to avoid damage to the tube.

---

[26] J. B. Dow, "Fundamentals of Engineering Electronics," Chapter II, John Wiley & Sons.

[27] E. L. Chaffee, "Theory of Thermionic Vacuum Tubes," pp. 175–177, McGraw-Hill Book Co.

[28] Potentials of both grid and plate are measured from the cathode in equipotential cathode tubes and from the negative filament terminal in filamentary cathode tubes.

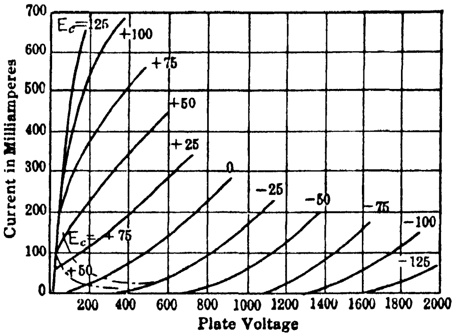

FIG. 840. Triode characteristics (from Western Electric Co. catalog).

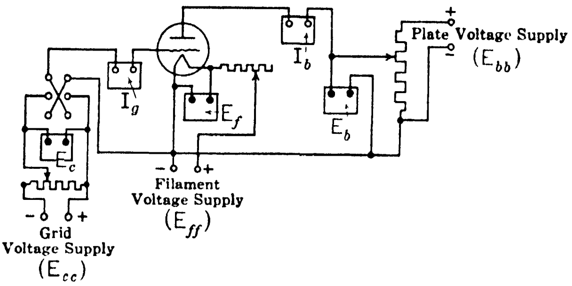

FIG. 841(*a*). Typical circuit for obtaining static triode characteristics.

1179. Symbols. — At this point some definite set of symbols must be adopted. Letter symbols given in the I.R.E. publication, "Standards on Electronics for 1938," will be used. A partial list, sufficient for use in this chapter, is given below.

e_c	Instantaneous total grid voltage.
e_b	Instantaneous total plate voltage.
i_c	Instantaneous total grid current.
i_b	Instantaneous total plate current.
E_c	Average or quiescent value of grid voltage.
E_b	Average or quiescent value of plate voltage.

---

[29] E. L. Chaffee, *op. cit.*, Chapter VII.

[30] Kozanowski and Mouromtseff, "Vacuum Tube Characteristics in the Positive Grid Region by an Oscillographic Method," *Proc. I.R.E.*, August, 1933, p. 1082.

I_c	Average or quiescent value of grid current.
I_b	Average or quiescent value of plate current.
e_g	Instantaneous value of varying component of grid voltage.
e_p	Instantaneous value of varying component of plate voltage.
i_g	Instantaneous value of varying component of grid current.
i_p	Instantaneous value of varying component of plate current.
E_g	Effective value of varying component of grid voltage.
E_p	Effective value of varying component of plate voltage.
I_g	Effective value of varying component of grid current.
I_p	Effective value of varying component of plate current.
E_f	Filament or heater terminal voltage.
I_f	Filament or heater current.
I_s	Total electron emission.
g_j	Conductance of electrode j.
r_j	Resistance of electrode j.
g_p	Plate conductance.
r_p	Plate resistance.
g_g	Grid conductance.
r_g	Grid resistance.
g_{jk}	Transconductance from electrode k to electrode j.
g_m	($\equiv g_{gp}$) Grid-plate transconductance (mutual conductance).
g_n	($\equiv g_{pg}$) Plate-grid transconductance (inverse mutual conductance).
μ_{jkl}	μ factor, electrodes j and k with respect to the current of electrode l.
μ	Amplification factor.

1180. Plate-Current Equation. — The most general relation for a triode is given by:

$$i_b = f(e_c, e_b) \qquad \text{. . . . .} \quad (28)$$

There is no simple mathematical expression to define accurately the characteristics of Figs. 839 and 840 over a wide range. For some purposes approximate representation over a fairly wide but limited range is desirable, and for other purposes fairly accurate representation over a limited range will suffice, so that working equations for plate current have been developed. For symmetrical structures, it has been shown[31, 32, 33] that the electrostatic field near the cathode of a three-electrode tube is a function of $(e_c + e_b/\mu)$. In terms of the equivalent diode:

$$i_b + i_c = K(e_b/\mu + e_c)^\eta \quad \text{where} \quad \eta \cong 3/2 \qquad \text{. . . . . .} \quad (29)$$

With the grid sufficiently negative as it is in a large number of applications,

$$i_c = 0; \quad \text{and} \quad i_b = K(e_c + e_b/\mu)^\eta \qquad \text{. . . .} \quad (30a)$$

---

[31] King, *Phys. Rev.*, vol. 15 (1920), p. 526.

[32] Vogdes and Elder, *ibid.*, vol. 24 (1924), p. 683.

[33] Dow, "Fundamentals of Engineering Electronics," John Wiley & Sons.

The amplification factor, μ, may be considered constant over a fairly wide range of values. Equation (30) may be converted to:

$$i_b = K'(\mu e_c + e_b)^\eta \quad \ldots\ldots\ldots \quad (30b)$$

In putting eqs. (29), (30*a*), or (30*b*) to practical use, the three assumed constants are evaluated for the middle of the desired range and should represent mean values. K and η may be determined in a manner similar to that used for the diode (§1170); i.e., from the straight-line plot of log i_b *vs.* log $(e_c + e_b/\mu)$ after a value has been assigned to μ. This value may be determined from the relation between e_b and e_c for constant plate current:

$$\mu = -\partial e_b/\partial e_c \quad \ldots\ldots\ldots\ldots \quad (31)$$

This may be shown as follows:[34]

$$i_b = \mathbf{f}(e_c, e_b) = K(e_c + e_b/\mu)^\eta$$

$$di_b = \partial f/\partial e_c \, de_c + \partial f/\partial e_b \, de_b$$

Considering i_b = constant:

$$\partial e_b/\partial e_c = -\frac{\partial f/\partial e_c}{\partial f/\partial e_b} = -\frac{K\eta(e_c + e_b/\mu)^{\eta-1}}{K\eta(e_c + e_b/\mu)^{\eta-1}(1/\mu)} = -\mu$$

The negative sign in eq. (31) is significant and means that a positive increment in grid voltage may be compensated by a negative increment in the plate voltage, μ times as large, to keep the plate current constant. Where the variations in plate current are relatively small, eq. (28) may be expanded in a Taylor series. This method is particularly well suited to the analysis of distortion in class A amplifiers and is accordingly considered in §1190.

1181. Triode Parameters. — Just as μ, the amplification factor, may be defined by

$$\mu = -\left.de_b/de_c\right]_{i_b=\text{Constant}} = -\partial e_b/\partial e_c \quad \ldots\ldots \quad (32)$$

it has been found desirable to define other factors useful in vacuum-tube analysis.

Mutual conductance or grid-plate transconductance:

$$g_m = \left.di_b/de_c\right]_{e_b=\text{Constant}} = \partial i_b/\partial e_c \quad \ldots\ldots \quad (33)$$

---

[34] See any standard textbook on the calculus for these differentiation formulas, for instance, Woods and Bailey, "Analytic Geometry and Calculus," Chapter XV, Ginn & Co., 1917.

expresses the ratio between a change in plate current and the corresponding infinitesimal change in grid voltage when the plate voltage is maintained constant. The units for g_m are generally micromhos.

Differential plate resistance or a-c plate resistance,

$$r_p = de_b/di_b\Big]_{e_c=\text{Constant}} = \partial e_b/\partial i_b \quad . \; . \; . \; . \; . \; . \; . \quad (34)$$

is the resistance offered by the plate circuit to infinitesimal changes in plate current, when the grid voltage is maintained constant. This is to be distinguished from the d-c plate resistance:

$$R_{0p} = E_b/I_b \quad . \; . \; . \; . \; . \quad (35)$$

Only two of the above parameters are independent, for at any one point (i.e., for any one set of values for e_c and e_b) it is apparent that:

$$\mu = \frac{(\partial i_b/\partial e_c)}{(\partial i_b/\partial e_b)} = g_m r_p \quad . \; . \; . \; . \quad (36)$$

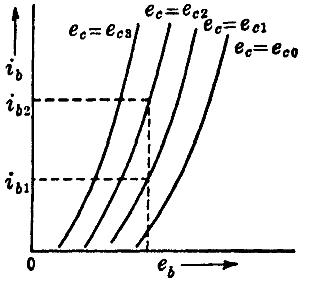

FIG. 841(*b*). Method of evaluating g_m from the static characteristics of a triode.

In a similar manner, starting with the relation $i_c = \phi(e_c, e_b)$, parameters referring primarily to the grid may be defined.

Grid amplification factor $\mu_g = -\partial e_c/\partial e_b$ . . . (37)

Grid resistance $r_g = \partial e_c/\partial i_c$ . . . . . (38)

Plate-grid transconductance $g_n = \partial i_c/\partial e_b$ . . . . . (39)

The above definitions all involve infinitesimal changes, but these factors may be determined from the static characteristic curves by considering small but finite changes in the currents and voltages. For instance, referring to Fig. 841*b*, the mutual conductance may be determined from the static characteristics if we take:

$$g_m \cong \Delta i_b/\Delta e_c\Big]_{e_b=\text{Constant}} = (i_{b1} - i_{b2})/(e_{c1} - e_{c2}) \quad . \; . \; . \quad (40)$$

It is probably better to consider this to be the value of g_m halfway between the i_{b1} and i_{b2} values. Other parameters may be obtained in a similar way.

1182. EXPERIMENT 59-G. — Determination of Static Characteristics and Evaluation of Parameters of Triodes. — Figure 841*a* shows the schematic circuit for obtaining the static characteristics of a triode.

The meter sizes are determined from the manufacturer's ratings, if a commercial tube is being tested. If the tube is an experimental type, the procedure must be slower until the operating limits are established. First make a test of the cathode similar to that described in Experiment 59-A. This gives some idea of the emission capabilities and serves to establish approximately the maximum plate current rating. Unless the type of cathode is definitely known, it is best to assume first that it is oxide coated and designed to operate at about 1000°K or less. The measured cathode efficiency tests the correctness of this assumption. Regardless of the type of tube tested, it is always advisable to apply the proper filament voltage and to check this circuit before applying plate or grid voltages.

First obtain data with the grid at the maximum negative potential and the plate voltage varied from zero to about 50 per cent above the maximum rated value. In no event should the plate voltage exceed the insulation value of the tube or circuit, and it should be kept below the point where there is excessive plate or grid heating for the type of tube being used. Take similar runs for negative grid voltages, decreasing in absolute value for each succeeding run. In the negative grid region the grid current is essentially zero.[35] As the grid voltage is changed over to the positive region a small grid current will be observed. As a rule, runs should not be made with the grid more than a few volts positive, on account of the danger of excessive grid or plate heating. The allowable limit will again depend on the type of triode being tested. If an adjustable and automatically regulated plate power supply is available, a convenient method in the positive grid region is to dispense with the potentiometer in the plate circuit, set the plate voltage at successive values, and vary the grid voltage over the desired range.

Report. The data should be plotted according to the method of Fig. 839 or Fig. 840. From these curves, calculate the values of μ, r_p, and g_m at two or three assumed operating points. The expected accuracy is not high, but the values obtained serve to emphasize the definition of these quantities. A check on the accuracy is obtained by substituting the values in equation (36). A check on μ can be readily obtained by setting up the circuit of Fig. 842. E_{cc} and E_{bb} are chosen to give the desired operating point. With the switch thrown to point 1, R is set at a convenient value, R_1, usually of 1000 ohms, and the plate current noted. The switch is then thrown to position 2, and

---

[35] Sensitive indicators will show extremely small currents due mainly to positive ions in the tube. Also the exact point at which electrons start to flow to the grid is influenced by initial velocity of emission and contact potential, but is within 1 or 2 volts of zero potential.

R adjusted to a new value R_2 until the plate current is the same as before. A more sensitive method of setting the plate current is given in Fig. 842(b). By this scheme a low-range meter may be substituted for that of Fig. 842(a), but careful manipulation is necessary to avoid damage to the sensitive meter. Starting with the definition:

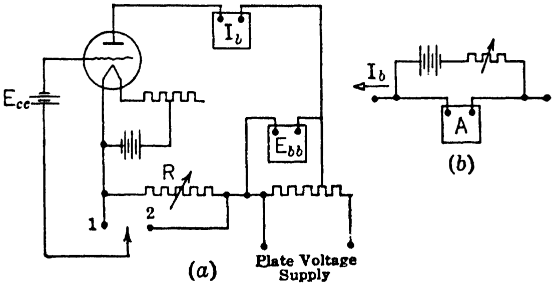

FIG. 842. Scheme for determination of amplification factor μ.

$$\mu \cong -\Delta E_b/\Delta E_c\Big]_{i_b = \text{Constant}} \quad . \quad . \quad . \quad . \quad . \quad . \quad . \quad (41)$$

the student can readily derive the relation:

$$\mu = (R_1 - R_2)/R_2 \quad . \quad . \quad . \quad . \quad . \quad . \quad . \quad . \quad . \quad (42)$$

1183. Dynamic Characteristics of Triodes. — Dynamic characteristics usually mean the characteristics of a tube under actual operating conditions.

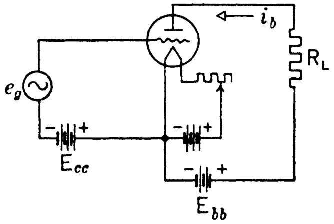

FIG. 843. Elementary circuit of a triode amplifier.

Certain operating characteristics of triodes as amplifiers will now be considered. Figure 843 shows the conditions of operation. A grid-bias voltage E_{cc} supplies the proper average or quiescent value of grid potential, and the applied e_g represents the variation from this value, considered to be a sine wave. The plate voltage supply E_{bb} is connected through a load resistance R_L. It follows that, with no external grid resistance, $E_c = E_{cc}$ and

$$e_b = E_{bb} - i_b R_L \quad . \quad . \quad . \quad . \quad . \quad . \quad . \quad . \quad . \quad (43)$$

Equation (43) may be plotted in the plane of the mutual characteristics or the plane of the plate characteristics of the particular triode shown in Fig. 844. In the former case, the curve known as a dynamic transfer characteristic is obtained by assuming values of e_b which coincide with the static curves and from the equation calculating the corresponding value of i_b. On the plate characteristic plane, eq. (43) is a straight line with an intercept at $e_b = E_{bb}$ on the X axis and a slope determined by R_L. It is usually more convenient to work with the plate characteristic diagram, where this straight line is called the "load line."

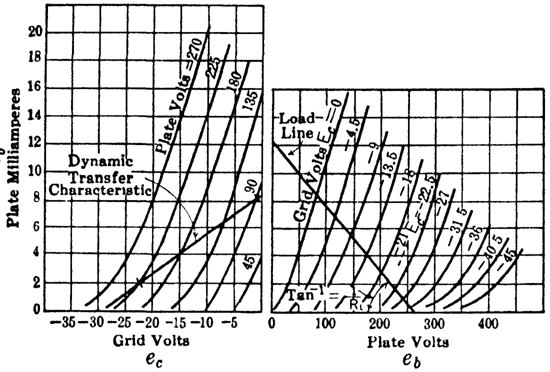

FIG. 844. Construction for dynamic transfer characteristic and load line.

With a given applied sine-wave voltage, e_g, at the grid it is possible to determine graphically the plate current, by using the construction of Fig. 845 working with either mutual characteristics or plate charac-

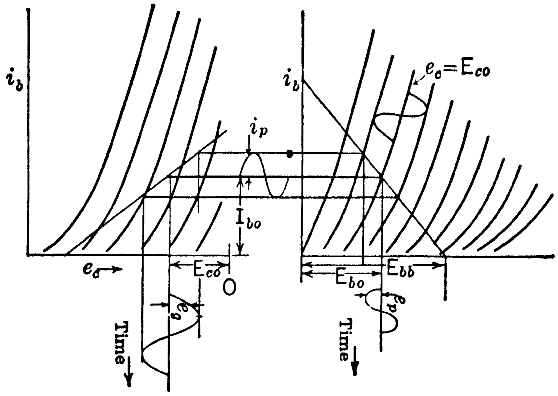

FIG. 845. Plate-current curve determined graphically.

teristics. The operating point E_{c0}, E_{b0}, is determined by the intersection of the dynamic transfer characteristics with vertical line $e_c = E_{c0}$, or by the intersection of the load line with the curves for $e_c = E_{c0}$. For Fig. 843, $E_{c0} = E_{cc}$. It should be noted that while the sine wave of e_g is shown along the e_c axis of the mutual characteristics and also along the load line in the plate characteristic plane, the instantaneous values of e_g are not linearly displaced along the load line, and projections from the sine wave to the load line cannot be employed:

The foregoing analysis has been based upon a value of load resistance R_L, which is the same for a-c and d-c currents. A typical circuit in which the a-c and d-c resistances are not the same is shown in Fig. 846. To determine the alternating plate current and voltage by the graphical method requires a construction shown by Fig. 847. The d-c load line whose slope is determined by the d-c value of load resistance fixes the operating point P_1 where it intersects the curve for $e_c = E_{c0}$. Since the non-linear characteristics of the triode cause the plate current to contain an added d-c component, this component through the d-c load resistance establishes a new d-c plate voltage, at point P_2 on the d-c load line. The a-c load line passes through P_2, since it represents the point where the a-c component of the plate current is zero. The slope of the a-c load line is determined by the a-c load resistance (r_l). The point P_3 about which the applied grid voltage e_g operates is the intersection of the a-c load line with the curve $e_c = E_{c0}$. It is evident that this construction cannot be carried through until the change in the d-c component (ΔI_b) of the varying plate current is assumed. This means a cut-and-try solution. Fortunately the effect is small enough so that methods of harmonic analysis applied to the resulting plate-current curve (see §1145) resolve the situation rapidly.[36]

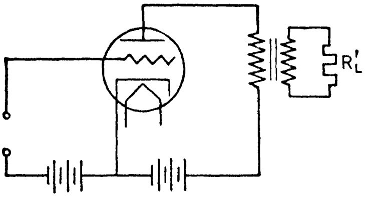

FIG. 846. Amplifier circuit having different a-c and d-c load resistances.

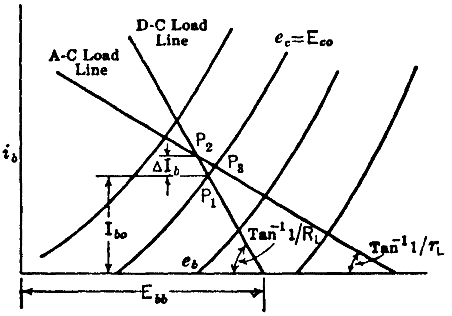

FIG. 847. Construction of a-c and d-c load lines.

1184. Triode Characteristics with an Impedance Load. — When the load impedance (Z_L) is not pure resistance, the dynamic operating path in the plate characteristic plane is approximately an ellipse instead of a straight line (Fig. 848). The elliptical path can be determined by assuming grid voltage (e_g), plate current (i_p), and plate voltage (e_p) to be sine waves. The circuit and vector diagrams are shown in Fig. 849. The above assumption means that there is a linear variation of plate current with plate and grid voltage near the operating point. This assumption may be written as:

---

[36] L. H. Bedford, *Wireless Eng'g*, vol. 8 (1931), p. 599.

$$i_p = ae_g + be_p = b\left(\frac{a}{b}e_g + e_p\right)$$

Therefore at this operating point, $r_p = \partial e_p/\partial i_p = 1/b$, and $\mu = -\partial e_p/\partial e_g = a/b$.

$$i_p = 1/r_p\,(\mu e_g + e_p)$$

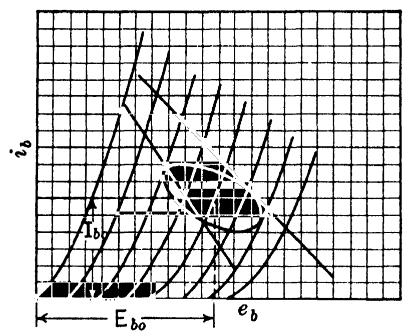

FIG. 848. Dynamic operating path in plate characteristic plane for impedance load.

since

$$e_p = -i_pZ_L$$

$$i_p = \mu e_g/(r_p + Z_L) \quad . \quad . \qquad . \quad . \quad . \quad . \quad (44)$$

For inductive loads the ellipse of Fig. 848 is traced in the counterclockwise direction. With capacitive loads an ellipse is traced in the clockwise direction.

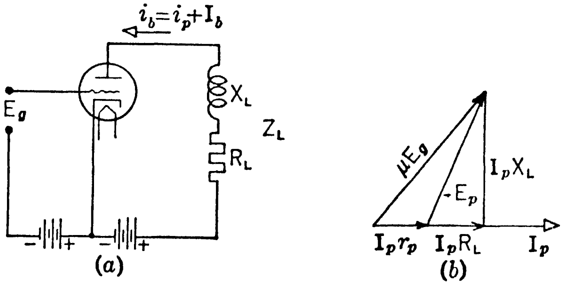

FIG. 849. (a) Circuit diagram for amplifier with inductive load; (b) vector diagram for same.

1185. EXPERIMENT 59-H. — Measurement of Triode Parameters by A-C Bridge Methods. — Many circuits have been devised for the practical measurement of tube parameters or coefficients, employing a bridge principle.[37,38,39] A voltage-ratio method of measuring tube

---

[37] J. M. Miller, *Proc. I.R.E.*, vol. 6, pp. 141-148, June, 1918.

[38] E. L. Chaffee, " Theory of Thermionic Vacuum Tubes," Chapter IX.

[39] R. W. Hickman and F. V. Hunt, *Rev. Sci. Inst.*, vol. 6, p. 268, September, 1935.

parameters has been described by W. N. Tuttle,[40] and a commercial instrument built on this principle is available.[41, 42] Figure 850 illustrates a circuit for the measurement of μ. For the condition of no current in the telephones:

$$\mu = R_2/R_1 \qquad (45)$$

and

$$C_1/C_2 = R_2/R_1 \qquad (46)$$

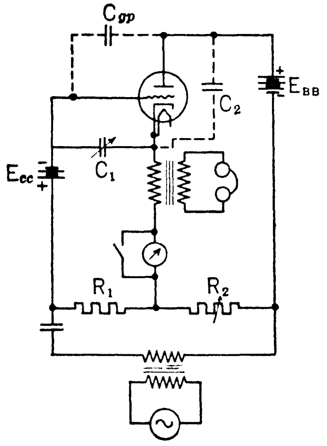

FIG. 850. Schematic bridge circuit for measurement of amplification factor μ of a triode.

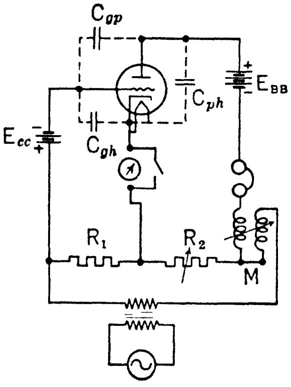

FIG. 851. Alternative bridge method for measurement of μ.

C_1 is composed of the grid-cathode capacitance of the tube and a small variable air condenser in the circuit, and C_2 is the plate-cathode capacitance. R_1 is a resistance of about 10 ohms. R_2 is a decade resistor which is adjusted alternately with C_1 to obtain a balance. In some arrangements for the measurement of μ, the quadrature component of voltage causing current through telephones is balanced out by a variometer connected as shown by Fig. 851. The variometer accomplishes a purpose similar to that of the small air condenser in the circuit of Fig. 850. It should be noted that the grid current is assumed to be zero, necessitating that the grid " bias " shall always be negative. The plate-current meter enables the d-c plate voltage to be corrected for the IR drop in the bridge circuit. In order to secure close adjustment of plate and grid potentials, potentiometers may be used in connection with plate and grid batteries, but should be by-passed by relatively large fixed condensers. Greater sensitivity to balance is obtained by connecting an amplifier between the output transformer and the telephones. This permits the use of smaller a-c input, which should be as low as possible to prevent excessive harmonic production.

---

[40] W. N. Tuttle, *Proc. I.R.E.*, vol. 21, p. 844, June, 1933.

[41] *General Radio Experimenter.*

[42] F. E. Terman, " Measurements in Radio Engineering," p. 168, McGraw-Hill Book Co., 1935.

A bridge circuit for measuring r_p is shown in Fig. 852. The manipulation is similar to that of the bridge for measuring μ, the balance condition being approached by alternate adjustment of C and R_2. The equations for balance are:

$$r_p = \frac{R_1 R_3}{R_2} \quad . \; . \; . \; . \; . \; . \; . \; . \; . \; . \; . \; . \quad (47)$$

and

$$C = (C_{ph} + C_{pg}) \frac{R_3}{R_2} \quad . \; . \; . \; . \; . \; . \; . \; . \; . \; . \quad (48)$$

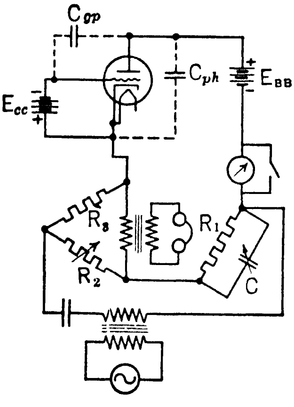

FIG. 852. Schematic circuit for measurement of r_p.

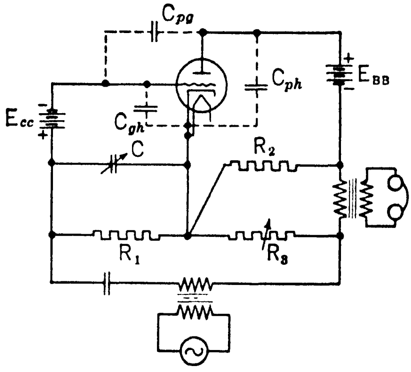

FIG. 853. Schematic circuit for measurement of g_m.

When r_p is very large, C may be undesirably large, and it is better to connect C across R_3, in which event:

$$C = (C_{ph} + C_{pg}) \frac{R_1}{R_2} \quad . \; . \; . \; . \; . \; . \; . \; . \; . \; . \quad (49)$$

R_3 is usually of the order of magnitude of the plate resistance, and R_1 is about 1/10 of this value, unless the plate resistance is very low, when R_1 may be made larger. R_2 is a decade resistor.

The circuit diagram shown in Fig. 853 is used to measure the grid-plate transconductance or mutual conductance (g_m). R_1 and R_2 are fixed resistors, and R_3 is varied with C to obtain a balance. When R_2 is small compared with r_p, the equation for balance gives:

$$\frac{\mu}{r_p} = g_m \cong \frac{R_3}{R_1R_2} \qquad \dots\dots\dots\dots \qquad (50)$$

To make a direct-reading bridge, R_1 may be set to 1000 ohms and R_2 to 100 ohms.

Report. Values of μ, r_p, and g_m should be plotted as functions of the plate voltage for constant grid voltage, or in some other manner chosen to exhibit a certain trend. It should be noted that g_m may be calculated from the values of μ and r_p as a check. The actual operating d-c plate voltage of the tube is the plate supply voltage minus the *IR* drop through the bridge.

1186. Multielectrode Vacuum Tubes. — As classified by Pidgeon,[43] tubes with more than three electrodes are of two general types: those designed to perform some function better than a triode, and those designed to perform more than one function simultaneously. It should be noted that the cathode and heater are considered as one electrode.

The screen-grid tetrode is an improvement over the triode for certain applications such as radio-frequency amplification. The fourth electrode consists of a screen or grid structure almost completely enclosing the plate. The principal advantage is the shielding effect of the screen grid, which reduces the capacitance between control grid and plate. In triode radio-frequency amplifiers, it is necessary to employ special balancing circuits to overcome the effects of grid-plate capacitance. The arrangement of electrodes in a screen-grid tube is shown in Fig. 854. The screen grid is operated at a fixed d-c potential with respect to ground and in radio-frequency circuits operates essentially at ground potential to the high-frequency currents. The total space current in a tetrode is de-

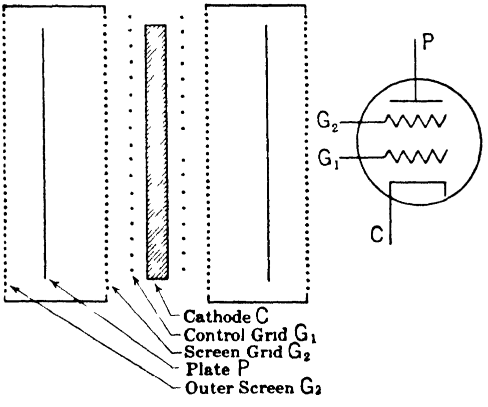

FIG. 854. Arrangement of parts in a screen-grid tetrode. (H. A. Pidgeon, *Elec. Eng'g,* November, 1934, p. 1487.)

---

[43] H. A. Pidgeon, " Theory of Multi-Electrode Vacuum Tubes," *Bell System Tech Jour.*, vol. 14, No. 1, p. 44, January, 1935.

termined by the voltage gradient produced at the cathode by the various electrode potentials. This may be written as:

$$i_s = F(e_b, e_{c1}, e_{c2}) \quad . \ . \ . \ . \ . \ . \ . \ . \ . \quad (51)$$

e_{c1} and e_{c2} are, respectively, control-grid and screen-grid voltages. Grids are usually numbered consecutively, starting with the grid nearest the cathode. The plate voltage e_b has a very slight effect on the total current, and indeed a change of plate voltage does not produce much change in plate current at high plate voltages. This is to be expected as a result of the shielding action of the screen grid. The plate current may be expressed by:

$$i_b = f\ (e_b, e_{c1}, e_{c2}) \quad . \ . \ . \ . \ . \ . \ . \ . \ . \quad (52)$$

The a-c plate resistance, $r_p = \partial e_b/\partial i_b$, is very high at normal plate voltages, owing to the dependence of the plate current upon the available electrons which pass through the interstices of the screen grid. At zero plate voltage, the plate current is zero and a negative space charge exists in the region between plate and screen due to electrons passing through the screen and eventually coming back. As the potential of the plate is increased from zero, electrons are attracted to the plate and the plate current increases up to a certain point. At this value of plate

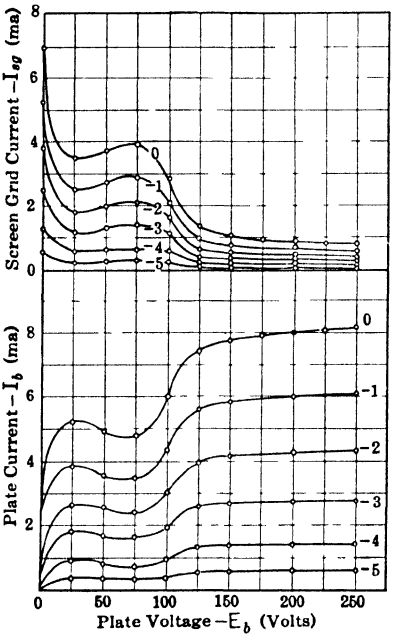

FIG. 855. Static characteristics of 6C6 tube connected as a screen-grid tetrode (suppressor grid connected to screen grid) — curves by R. L. Smithley.

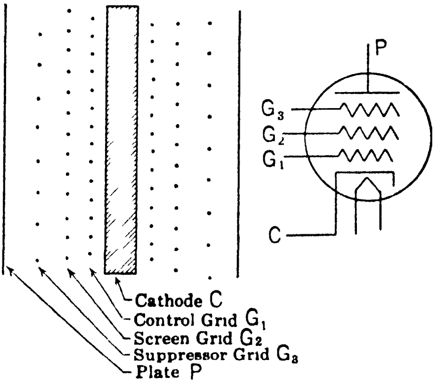

FIG. 856. Arrangement of parts in a power pentode (H. A. Pidgeon).

voltage, electrons are striking the plate with velocities which produce appreciable secondary emission. This ejection of electrons from the plate surface due to bombardment of primary electrons causes an important change in the plate-current, plate-voltage curve. The secondary electrons are collected by the screen which is at a higher potential than the plate. The result is eventually a decrease in the plate current as the plate voltage is raised. In some cases, the primary electron current reaching the plate is less than the secondary electron current passing from plate to screen, and the net plate current is negative. The number of secondary electrons per primary electron depends upon the nature of the surface. Carbonization of the surface tends to reduce the effect materially. In any case, the phenomenon usually causes the plate-current, plate-voltage curve to have a region with a negative slope. As the plate voltage increases beyond this critical region, more of the secondary electrons are recaptured by the plate, and the plate current begins to rise again. This continues until a saturation condition, due to the limited supply of electrons from the screen, flattens out the plate-current curve. Typical curves are given in Fig. 855. The complementary character of the plate-current and the screen-current curves should be observed.

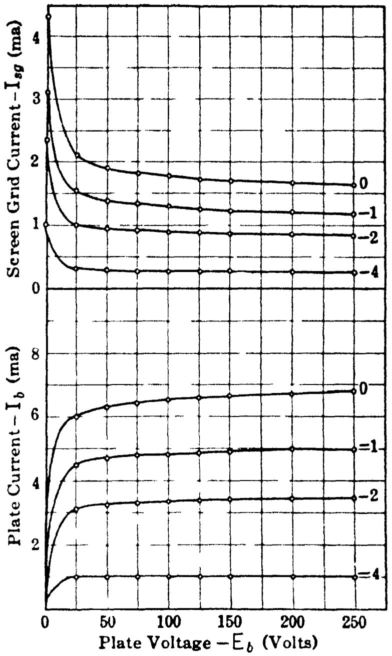

FIG 857 Static characteristics of 6C6 tube as a radio-frequency pentode (curves by R. L. Smithley).

In order to prevent the effects of secondary emission on the plate current, a fifth electrode known as the suppressor grid was placed between screen and plate. This grid, operated at cathode potential, provides a potential minimum which turns back the relatively slow-moving secondary electrons from either plate or screen. The tube thus created is the power pentode, with an electrode arrangement shown in Fig. 856. Greater power output is obtainable, owing to the greater permissible swing in plate current and voltage. Pentode construction is also used for tubes intended for radio-frequency amplification. Plate and screen current curves for a radio-frequency pentode are shown in

Fig. 857, and for a power pentode by Fig. 858. The coarser grid structure of the power pentode permits a greater slope for the plate-current curves and is not so completely effective in eliminating the secondary emission effects.

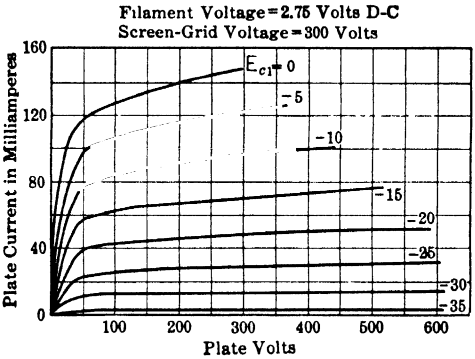

FIG. 858. Plate-current characteristics of a 306-A tube (Western Electric Co.).

In the four- and five-electrode tubes mentioned thus far, the grid nearest the cathode serves as the control grid. Another pentode with limited application is the space-charge grid pentode in which the innermost grid is operated at a fixed positive potential. This has the effect of eliminating the negative space charge near the cathode and creating a virtual cathode of larger radius outside this first grid. The remaining electrodes are operated as a screen-grid tetrode having a very high grid-plate transconductance. The applications of tubes employing space-charge grids is limited to cases where low plate voltages must be used and large swings in grid potential are not necessary.

1187. EXPERIMENT 59-I. — Determination of Static Characteristics of a Tetrode and a Pentode by Measurements on a Single Tube. — Some pentode tubes have the suppressor grid connected internally to the cathode, while others have the suppressor grid lead brought outside the tube for greater flexibility in application. Using a tube of the latter type, it is possible to connect the suppressor grid to the screen grid or connect it with the plate and determine the static characteristics of the resulting screen-grid tetrode. The connections for making this test are shown in the diagram (Fig. 859). If a 6C6-type tube is used, the screen voltage may be maintained at 100 volts and the plate voltage varied from 0 to about 250 volts. Plate current and screen current may be read on milliammeters with a maximum range of 10 ma. Readings

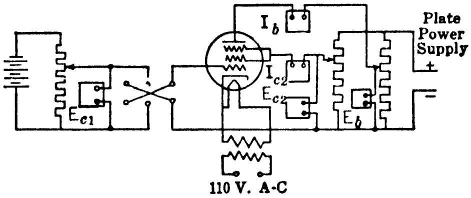

FIG. 859. Circuit for determining the static characteristics of a multielectrode high-vacuum tube.

should be taken for several fixed values of control grid voltage (E_{c1}) between 0 and -6. Similar runs should also be made for a lower screen-grid voltage (about 70 volts).

If the connections are now changed for normal pentode operation, with the suppressor grid connected to the cathode, readings may be taken as before to determine screen-current and plate-current variation.

Report. A plot of the plate current *vs.* plate voltage and screen current *vs.* plate voltage for the different fixed control-grid voltages will show typical screen-grid tetrode characteristics, when the suppressor grid is connected to the screen (or connected to the plate), although the tube is actually a pentode design. The $\mu = -\partial e_b/\partial e_{c1}$, $r_p = \partial e_b/\partial i_b$, and $g_m = \partial i_b/\partial e_{c1}$ should be calculated at some chosen operating point after the manner used for triodes (see §§1181 and 1179). The minimum value of negative plate resistance should also be calculated. This value is important in the operation of the tube as a dynatron oscillator.[44]

The parameters obtained for the tube operated as a screen-grid tetrode should be compared with those obtained for the tube operated as a pentode.

1188. Beam Power Tubes. — While the suppressor grid apparently performed thoroughly the job of stopping secondary electrons, the resulting pentode characteristics were not ideal from the standpoint of high efficiency and low distortion. A tetrode which accomplishes suppressor grid action without a suppressor grid structure and possesses other important advantages, especially for power-amplifier applications, has been developed.[45] The beam power tube is designed to decrease substantially the non-uniformity in the electron stream passing from cathode to plate, by a pair of beam-forming plates operated at cathode potential and by careful alignment of grid wires (Fig. 860). The beam-forming plates prevent passage of electrons through the grid wires near the supports, thus confining the current to the uniform part of the grid structure. Alignment of the control grid with the screen-

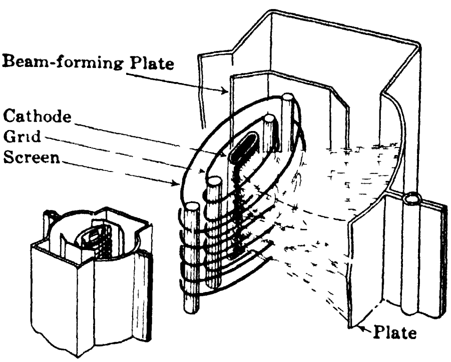

Fig. 860. Internal structure of a beam power tube.

---

[44] Totuo Hayasi, *Proc. I.R.E.*, vol. 22 (1934), p. 751.

[45] O. H. Schode, " Beam Power Tubes," *Proc. I.R.E.*, vol. 26 (1938), No. 2, p. 137.

grid wires effectively reduces the screen current and helps to secure increased electron density in the region between screen and plate, which is necessary to secure a potential minimum for suppressor action. The relatively uniform potential distribution at this potential minimum or virtual cathode results in more closely ideal variation of plate current with plate voltage for low plate voltages than is obtained in the power pentode with suppressor grid. The characteristic curves (Fig. 861) for the beam power tubes should be compared with those for the power pentodes.

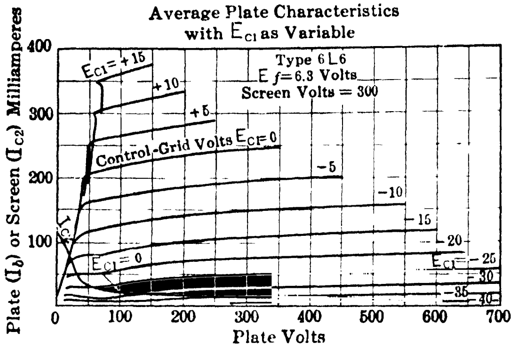

FIG. 861. Static characteristics of a beam power tube.

1189. EXPERIMENT 59-J. — Measurement of Multielectrode Tube Parameters by A-C Methods. — Modifications of the bridge circuits used in Experiment 59-H are necessary for multielectrode tubes having a wider range of values.

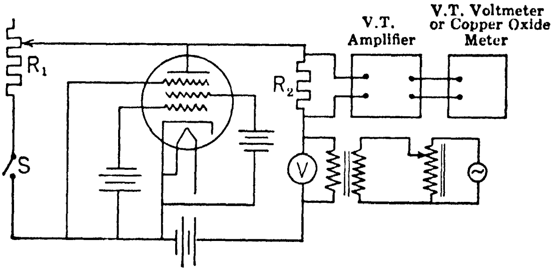

FIG. 862. Circuit for measuring plate resistance.

A scheme for measuring plate resistance or other electrode resistance of high value is given in Fig. 862. R_2 is a resistor low in value compared to the plate resistance. In operation, with switch S open, a small a-c voltage is applied in the plate circuit. The value is adjusted to give a convenient reading on the vacuum-tube voltmeter. A 60-cycle power source may be used and the adjustment accomplished by means of a "variac." The tube is then removed from the circuit, switch S closed, and R_1 adjusted to give the same deflection on the voltmeter as before. R_1 is now equal to the plate resistance.

The $\mu_{jkl} = -\frac{\partial e_j}{\partial e_k}$, i_l constant (see §1179), may be determined by an arrangement shown in Fig. 863. When balance is secured by alternate adjustment of R_2 and M, $\mu_{jkl} = R_2/R_1$. The variable mutual inductance M is necessary to secure minimum sound in the telephones, since tube capacitances introduce a quadrature component in the electrode current i_l.

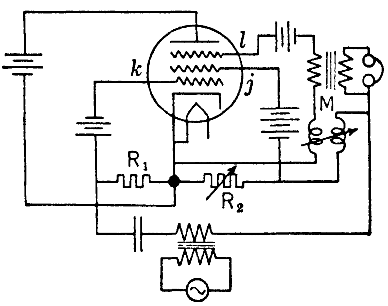

FIG. 863. Circuit for measuring μ_{jkl}.

An obvious modification of the circuit given in Fig. 853 will serve to measure g_m for a multielectrode tube. Other methods and further information will be found in "Standards on Electronics for 1938," published by the Institute of Radio Engineers. The references given for Experiment 59-H should also be consulted.

1190. Class A Amplifiers. — A review of §§1183 and 1184 will give a picture of the way a triode operates with an impedance in the plate circuit. The input voltage is applied to the grid circuit, and the output voltage appears across the plate load impedance. Amplifiers are considered to be in one of three general classes, depending upon the region of the operating point and the magnitude of the input grid voltage. In a class A amplifier, the operating point is in the negative grid region, so located that plate current flows at all times. The result is an alternating component of plate current that is more closely a reproduction of the alternating grid voltage, but at the expense of efficiency and output.

Equation (44) is the fundamental amplifier equation. Applying this to the circuit of Fig. 843 the voltage amplification is found to be:

$$\alpha = E_{\text{out}}/E_g = -\mu R_L/(r_p + R_L) \quad . \; . \; . \; . \; . \; . \quad (53)$$

The minus sign indicates that the output voltage across the plate load resistor is 180 degrees out of phase with the input voltage in the grid circuit. For the more general case, R_L is replaced by Z_L, when α

will be in general a complex quantity or vector operator. Amplifiers may be operated in cascade so that the overall amplification of two stages would be $\alpha_1\alpha_2$, where α_1 and α_2 are respectively the amplifications of the first and second stages. The plate load impedance of stage 1 would, of course, be modified by the coupling circuit employed between the output of stage 1 and the input to stage 2. Three common methods of coupling employed in class A amplifiers are shown in Fig. 864. In applying eq. (53) to the first stage of the resistance-capacitance coupled amplifier, note that Z_L is in this case the combination of R_1, R_2, and C_1,

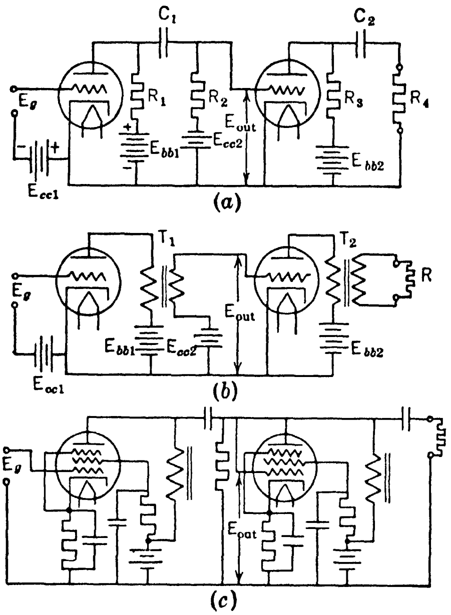

FIG. 864. Types of coupling for class A amplifiers: (a) resistance-capacitance coupling; (b) transformer coupling; (c) impedance coupling.

or $$Z_L = \frac{R_1(R_2 - j/\omega C_1)}{R_1 + R_2 - j/\omega C_1}$$

It is also shown by the equivalent circuit, Fig. 865, that eq. (53) must be multiplied by $R_2/(R_2 - j/\omega C_1)$ to give the voltage amplification, since E_{out} now appears across R_2. This is the situation at low frequencies. At higher frequencies the reactance of C_1 becomes negligible, and the amplification is given by:

$$\alpha = -\mu R_L/(r_p + R_L)$$

where

$$R_L = R_1R_2/(R_1 + R_2)$$

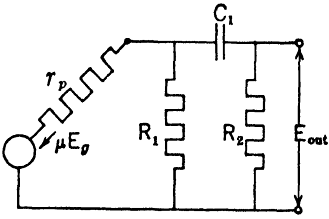

FIG. 865. Equivalent circuit of resistance-capacitance coupled amplifier.

For still higher frequencies, the equivalent circuit must include the interelectrode capacitances of both tube and wiring. In effect, the resistances R_1 and R_2 are shunted by the output capacitance of the first tube and the input capacitance of the second tube, respectively. Consequently the magnitude of α is decreased at high frequencies. There is also a decrease at low frequencies due to the increased reactance of condenser C_1. The phase angle of α is 180 degrees in the intermediate-frequency range and varies between plus or minus 90 degrees of this value between the high and low frequencies. The magnitude of the relative amplification and the phase angle are related in a manner as shown by Terman,[46] such that a gain of 70.7 per cent of the mid-frequency value occurs with a phase shift of 45 degrees from the mid-frequency value of 180 degrees. This idea has been applied by Spangenberg and Palmer[47] to a device for the rapid determination of audio-frequency amplifier characteristics.

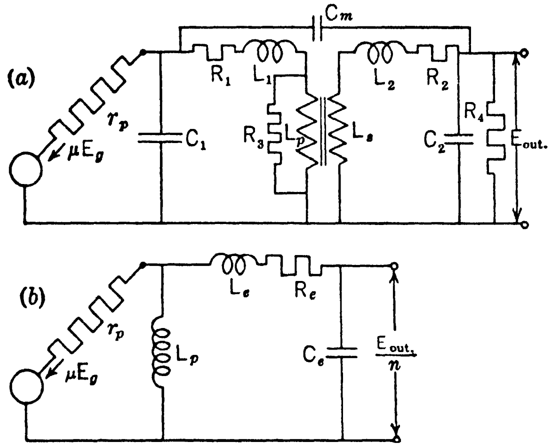

FIG. 866. Equivalent circuits for one stage of transformer-coupled amplifier.

R_3 = resistance equivalent to iron loss.
R_4 = resistance of grid circuit of succeeding tube.
r_p = plate resistance of tube.
$R_e = R_2/n^2 + R_1$.
n = transformer ratio.
L_1 = primary leakage inductance.
L_2 = secondary leakage inductance.
L_p = primary incremental inductance.
L_s = secondary incremental inductance.
$L_e = L_2/n^2 + L_1$.
C_1 = output and wiring capacitance of first tube.
C_2 = input and wiring capacitance of second tube.
C_m = capacitance between primary and secondary windings.
$C_e = n^2C_2 + C_m(n \pm 1)^2$.

Equivalent circuits for a transformer-coupled amplifier are shown in Fig. 866. From these it is seen that at low frequencies L_p, the primary inductance of the coupling transformer, is the determining factor in the calculation of the gain. The gain decreases rapidly at low frequencies owing to the decrease of ωL_p. The winding capacities results in a peak in the amplification curve, usually in the higher frequency range because of resonance produced by the equivalent capacitance C_e and the equivalent leakage inductance L_e. At still higher frequencies the gain decreases rapidly, owing to the shunting effect of C_e. Transformers for amplifiers with uniform gain over a wide range of frequencies must be designed with the conflicting requirements of large primary inductance and low winding capacitance.

---

[46] F. E. Terman, " Radio Engineering," p. 175, McGraw-Hill Book Co., 1937.

[47] Karl Spangenberg and Winslow Palmer, *Proc. I.R.E.*, vol. 27, No. 9, p. 555, September, 1939.

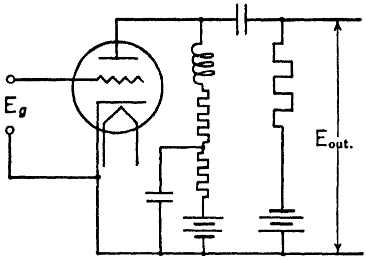

Fig. 867. One form of compensated amplifier for uniform amplification over a wide frequency range.

Amplifiers having uniform response over an extremely wide range of frequencies, such as that required of video amplifiers in television,[48] use a compensated resistance-capacitance coupling similar to that of Fig. 867. Tubes with high mutual conductance and low input and output capacitance have been developed to make such amplifiers possible.

1191. EXPERIMENT 59-K. — Measurement of Gain of a Resistance-Capacitance Coupled Amplifier. — A method of gain measurement is to be employed which is essentially a measurement of input and output voltages. Figure 868 shows the schematic diagram. A thermocouple connected to read the current to the input potentiometer is used to measure the input voltage. Many modifications of this idea are possible. R_1 may be replaced by a decade voltage divider arranged to have the total value of R_1 constant, and the adjustable point on the voltage divider connected to the grid lead of the first amplifier tube, or one of a number of types of "microvolters" may be used to measure input voltage.

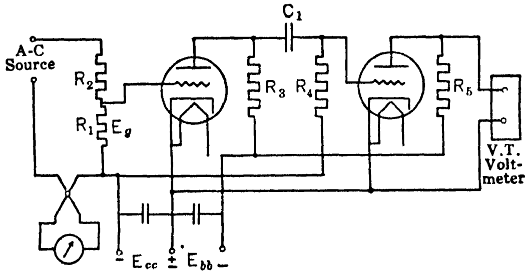

Fig. 868. Circuit for measuring the amplification of resistance-capacitance coupled amplifier.

---

[48] F. Alton Everest, *Electronics*, 1938, p. 16.

One stage of a resistance-capacitance coupled amplifier should be tested under typical operating conditions with proper provisions for conveniently changing some of the circuit constants. A general-purpose amplifier board, arranged with plugs and jacks for inserting plate and grid resistors and coupling condensers, is useful. Condensers of 8-μf capacitance or greater are used to by-pass the *B* and *C* power supplies and avoid unwanted coupling effects.

Variable-frequency runs should be made with constant input voltage or constant output voltage. If constant output voltage is used, the value should be low enough to prevent overloading the first stage at any time. The operating voltages and circuit constants may be taken from manufacturers' tube manuals. In general, for triodes with an amplification factor of about 10 and a plate resistance of about 10,000 ohms, R_5 may be varied from 50,000 to 250,000 ohms, R_4 from 50,000 ohms to 1 megohm, and C_1 from 0.001 to 0.1 μf. R_5 may be maintained at some constant value of about 100,000 ohms. Suggested values of frequency are 10, 20, 60, 100, 1000, 5000, 10,000, 30,000, 50,000, and 100,000 cycles per second.

The output voltage divided by the input voltage is the voltage amplification of both stages. To obtain the amplification of the first stage, the series of runs must be repeated with the input signal voltage applied to the grid of the second tube; i.e., C_1 and R_4 are removed and the input potentiometer connected so that R_1 occupies the position of R_4. The amplification of the second stage may thus be determined. The amplification of the first stage for a particular frequency is obtained by dividing the overall amplification by the amplification of the second stage, with the first stage operating under typical conditions.

Report. The magnitude of the voltage gain, $|\alpha|$, may be plotted as a function of frequency. It is better to use a logarithmic scale for frequency. To express gain or amplification in decibels:

$$N_{db} = 20 \log_{10}|\alpha| \qquad \ldots \ldots \ldots \quad (54)$$

For a consideration of the significance of the decibel and related units, the student is referred to Chapter LX, §1233.

1192. Amplifier Distortion. — The non-linearity of the tube characteristics has been neglected in developing amplifier equations and the resulting equivalent circuits thus far presented. This is possible because the operating point has been properly chosen, the a-c components of grid voltages have been small, and the external plate impedances have been high compared to plate resistances. A vacuum tube may be operated under conditions which make a more general type of analysis desirable. Starting with the general plate current equation for a triode:

$$i_b = f(e_b,\ e_c)$$

one may expand

$$i_b = I_{b0} + i_p = f(E_{b0} + e_p,\ E_{c0} + e_p) \quad . \ . \ . \ . \ . \quad (55)$$

in a Taylor series. For the details of this expansion, the student is referred to other sources.[49, 50] Assuming that μ is a constant $= -\left.\frac{\partial e_b}{\partial e_c}\right]_0 = \frac{\partial i_b/\partial e_c]_0}{\partial i_b/\partial e_b]_0}$ and $e_p = -i_p r_L$ the series becomes, for pure resistance in the external plate circuit:

$$\begin{aligned} I_{b0} + i_p = f(E_{b0}, E_{c0}) &+ \frac{\mu}{r_p + r_L}\, e_g - \frac{\mu^2 r_p}{2(r_p + r_L)^3} \left.\frac{\partial r_p}{\partial e_b}\right]_0 e_g^2 \\ &+ \frac{\mu^3 r_p}{6(r_p + r_L)^5} \left\{ (2r_p - r_L) \left(\left.\frac{\partial r_p}{\partial e_b}\right]_0 \right)^2 \right. \\ &\left. - r_p(r_p + r_L) \left.\frac{\partial^2 r_p}{\partial e_b^2}\right]_0 \right\} e_g^3 + \cdots \quad . \ . \ . \ . \quad (56) \end{aligned}$$

$\left.\frac{\partial r_p}{\partial e_b}\right]_0 \cdots$ means the partial derivative of r_p with respect to e_b evaluated at the operating point. If e_g is a sine wave, i.e., $e_g = E_{gM} \sin \omega t$,

$$e_g^2 = \frac{1 - E_{gM} \cos 2\omega t}{2} \quad . \ . \ . \ . \ . \ . \ . \ . \ . \quad (57)$$

$$e_g^3 = \frac{3E_{gM} \sin \omega t - E_{gM} \sin 3\omega t}{4} \quad . \ . \ . \ . \quad (58)$$

The plate current is thus given as a sum of sine and cosine terms. The first term is the d-c value at the operating point with no applied signal voltage. The second term is the undistorted output current. The other terms represent distortion and d-c increments. For most applications the four terms of eq. (56) are sufficient. Evaluation of the partial derivatives in this equation will permit the calculation of the percentage of second- and third-harmonic distortion when a single frequency is applied to the grid circuit. When more than one frequency is applied to the grid, the usual distortion terms appear with others, whose frequencies are the sum and difference frequencies of

---

[49] F. B. Llewellyn, *Bell System Tech. Jour.*, vol. 5 (1926), p. 433.

[50] Knox McIlwain and J. G. Brainerd, "High-Frequency Alternating Currents," Second Edition, pp. 108 et seq., John Wiley & Sons, 1939.

the input voltages and their harmonics. These latter distortion terms are the modulation products and are desired in certain modulation and demodulation processes.

Many graphical methods of making a harmonic analysis of the plate current have been developed.[51–54] Figure 845 shows the plate current obtained graphically, and the methods of Chapter LVIII could be applied to determine the harmonic components. As a rule, the percentage second and third harmonics indicate sufficiently the performance of an amplifier tube with regard to distortion.

The percentage second harmonic =

$$\frac{i_{b\max} + i_{b\min} - 2I_{b0}}{i_{b\max} - i_{b\min} + 1.41(i_{bx} - i_{by})} \times 100 \quad . \quad . \quad . \quad . \quad . \quad (59)$$

The percentage third harmonic =

$$\frac{i_{b\max} - i_{b\min} - 1.41(i_{bx} - i_{by})}{i_{b\max} - i_{b\min} + 1.41(i_{bx} - i_{by})} \times 100 \quad . \quad . \quad . \quad . \quad . \quad (60)$$

I_{b0} = plate current at intersection of the curve for dynamic load line and the curve for $e_c = E_{c0}$ on the plate characteristic.

i_{bx} = plate current at intersection of the dynamic load line and the curve for $e_c = E_{c0} + 0.707E_{gM}$ on the plate characteristic.

i_{by} = plate current at the intersection of the dynamic load line and the curve for $e_c = E_{c0} - 0.707E_{gM}$.

These formulas[55] may be proved by assuming that the current wave contains no harmonics beyond the third and summing up the Fourier series components at the selected ordinates.

1193. Power Amplifiers. — Class A amplifiers operated in a manner designed to deliver reasonably large power output will necessarily have greater distortion than voltage amplifiers. The operating conditions represent a compromise between allowable distortion and high power output. The vacuum-tube amplifier does not violate the principle that, for maximum power output, the impedance of the source must equal in magnitude the impedance of the receiver of energy. This means that r_p must equal r_L. The variation of power output with r_L for a given r_p is not critical near the maximum value, and the loss in power

---

[51] G. S. C. Lucas, *Wireless Eng'g*, vol. 8 (1931), p. 595; vol. 9 (1932), p. 75.

[52] D. C. Espley and L. I. Farren, *ibid.*, vol. 11 (1934), p. 183.

[53] J. A. Hutcheson, *Electronics*, January, 1936, p. 16.

[54] E. L. Chaffee, *Rev. Sci. Instruments*, vol. 7 (1936), p. 384.

[55] RCA Receiving Tube Manual RC-13, p. 19.

is not usually serious at the compromised value of r_L. Usually a limiting value of 5 per cent maximum distortion is chosen. For triodes, this results in $r_L \cong 2r_p$, and for pentodes and beam power tubes r_L is usually much less than r_p.

The operation of tubes in a push-pull scheme, as shown in Fig. 869, introduces a symmetry that theoretically eliminates even harmonics in the output wave form when the tubes are matched. Another practical advantage of the push-pull connection is a reduction in the effect of hum in the plate power supply. Distortion in a push-pull amplifier may be determined by a method due to B. J. Thompson[56] in which the plate characteristics of a tube are inverted with respect to that of a similar tube. A set of composite characteristics is obtained by adding (algebraically) the ordinates for the same grid voltages on the two sets of curves. The plate voltage axes are made to coincide at the point where $e_b = E_{bb}$. The composite curves obtained are nearly straight lines and may be used with a load line to determine the plate current in a manner similar to the single tube construction of Fig. 845. The slope of the load line is determined by a resistance $r_L/4$ (see Fig. 844), since the split choke in the plate circuit behaves like an auto-transformer with a ratio of 2/1. If a step-down transformer is used, the load line on the set of composite characteristics is determined by a resistance $a^2r_L/4$, where a is the primary-to-secondary turns ratio.

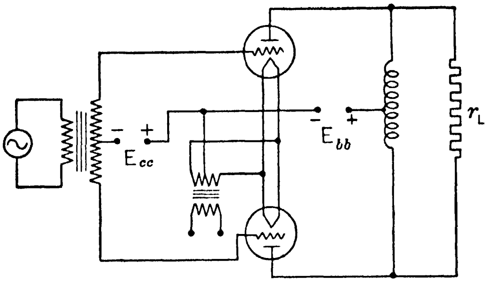

FIG. 869. Circuit of a push-pull amplifier.

1194. EXPERIMENT 59-L. — Measurement of Power Output and Distortion. — Two type-45 tubes in a push-pull connection as shown by Fig. 869 will provide a suitable circuit. Reasonable precautions should be taken to have the input transformer and output choke balanced with respect to the center tap. The output choke should also have low resistance and high coupling between halves. The voltages from each grid to center tap of the filament transformer may be measured by a vacuum-tube voltmeter. This will give an indication of the condition of balance in the input system. If it is desired to measure the a-c voltage from grid to grid or plate to plate, a vacuum-tube voltmeter with balanced input circuit must be employed. The output plate voltages may be measured from each plate to filament center tap and a check thus obtained on the balance in the plate circuit. The values of E_{cc} and E_{bb} may be varied over a range, but for type-45 tubes, suggested values are $E_{cc} = -55$ volts and $E_{bb} = 250$ volts.

---

[56] *Proc. I.R.E.*, vol. 21 (1933), p. 591.

With a constant input voltage (grid to filament center tap) of 55 volts peak, the plate-to-plate load resistance may be varied from about 2000 ohms to 10,000 ohms while readings of output plate voltage are taken. If a wave analyzer with a high input impedance is available, the second, third, and higher-harmonic components in the output may also be measured. For perfect balance even harmonics do not appear. The input grid signal voltage should be obtained from an oscillator low in harmonic content. A band-pass filter may be used to improve the wave form of the input grid voltage. An alternative method of measuring harmonic content, when a wave analyzer is not available, is the use of a full-wave square-law vacuum-tube voltmeter, an auxiliary variable audio-frequency source, and a scheme due to C. G. Suits.[57] The apparatus for this method is not elaborate or costly, but the procedure is tedious.

Data should also be taken with constant load resistance and variable grid bias. The input signal voltage is adjusted so that its peak value is equal to the grid bias in each case.

Report. Obviously the power·output may be calculated from the values of output voltage and load resistance (r_L). The power output should be plotted as a function of load resistance and also as a function of grid bias. Percentage harmonic distortion should also be plotted as a function of load resistance and power output. From these results optimum operating conditions may be determined.

1195. Gaseous Conduction. — *Ionization and excitation.* The passage of current through a gas is a more complicated process than conduction in solids or liquids because the current carriers (ions and electrons) are produced and caused to recombine at the electrodes of a tube and in the body of the gas. However, some of the more elementary phenomena may be explained quantitatively; and it is possible to have a qualitative understanding of the various types of gas discharge, because of the extensive investigations that have been made.

---

[57] C. G. Suits, *Proc. I.R.E.*, vol. 18 (1930), p. 178.

The structure of gas atoms, especially as it concerns the arrangement of extranuclear electrons and the possible energy levels of the atom, is important in the study of phenomena associated with gas discharges. The Bohr theory of the atom (§1148) supplies a satisfactory starting point and is adequate to explain certain elementary ideas about the simpler types of atoms. According to Bohr, the extranuclear electrons revolve in certain allowed orbits about the positive nucleus, each electron representing, in its state of motion, a contribution to the total energy of the atom. For the hydrogen atom, the total energy of its single revolving electron is given by

$$E = -\frac{2\pi^2 me^4}{h^2n^2} \text{ ergs} \quad . \quad . \qquad (61)$$

m = mass of electron.
e = charge of electron (esu).
h = Planck's constant.
n = an integer (1, 2, 3, etc.).

This formula was derived by Bohr, using the conventional definitions regarding potential and kinetic energy and the all-important and seemingly unusual idea that the moment of momentum was quantized in units of $nh/2\pi$, where n is an integer. Assigning different integral values to n gives different values of energy or energy levels. An energy-level diagram for hydrogen calculated on this basis is given in Fig. 870. The lowest energy level or zero level is taken for n = 1. The height of the horizontal lines representing allowed energy states is given by the difference between the energy for n = 1 and n = 2, 3, 4, etc. This is usually expressed in volts instead of ergs (an electron volt being 1.591×10^{-12} erg). When $n = \infty$, this process gives an energy difference which is the ionization potential. Other heights represent various excitation potentials. For hydrogen, the calculated excitation and ionization potentials check closely with those observed experimentally. Modifications in the Bohr theory are necessary for atoms with greater atomic number, and the theory is apparently inadequate to explain

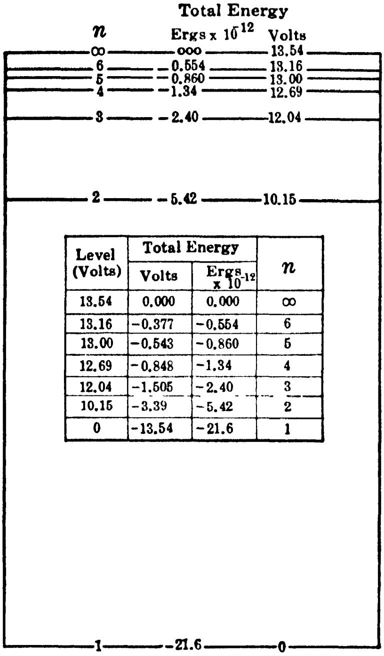

Level (Volts)	Total Energy		n
	Volts	Ergs x 10^{-12}	
13.54	0.000	0.000	∞
13.16	-0.377	-0.554	6
13.00	-0.543	-0.860	5
12.69	-0.848	-1.34	4
12.04	-1.505	-2.40	3
10.15	-3.39	-5.42	2
0	-13.54	-21.6	1

FIG. 870. Energy-level diagram for hydrogen.

atomic processes of a more complicated type. The energy released when an excited atom returns to a lower energy level appears in the form of light with a frequency given by

$$h\nu = E_1 - E_2 \quad . . \quad . . . . . . \quad (62)$$

where h is Planck's constant (6.55×10^{-27} erg sec), and ν is the light frequency. $E_1 - E_2$ is the change in energy in ergs. Spectroscopic observations may be used to construct the energy level diagrams of atoms. Figure 871 shows the energy level diagram for mercury, which is important in explaining the behavior of electron tubes containing mercury vapor.

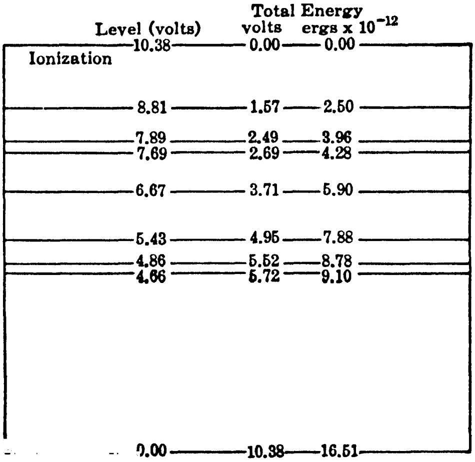

FIG. 871. Energy-level diagram for mercury (incomplete).

Ionization or the removal of one or more electrons from an atom may be accomplished directly by light energy, X-rays, cosmic rays, radioactivity, thermal and chemical effects, and " collisions " between moving particles. The removal of electrons from metals through the processes of photoelectric and thermionic emission is sometimes classed as a form of ionization. The amount of energy necessary to accomplish complete removal of one electron is known as the first ionization potential. This is usually expressed in electron volts. Ionization potentials for some of the common gases used in electron tubes are shown in Table IV. Ionizing agents in the form of X-rays, cosmic rays, ultra-violet light, etc., which are always present, account for the existence of a relatively small number of ions in a gas within any enclosure.

Discharge tube. A discharge tube with electrodes (Fig. 872) to which a potential difference is applied may be used to observe the varied phenomena associated with the passage of a current through a gas. With gas pressures of the order of 1000 microns,[58] the discharge will appear to be divided into regions as shown in the figure. For low applied voltages, the currents will be extremely small (less than 1 microampere) and will depend primarily upon the rate at which ions are formed by certain ever-present ionizing agents mentioned. An increase in voltage will result in an increased current (Fig. 873) up to the point where the ions are being swept from the field as rapidly as they are formed. The maximum value for the saturation current will vary widely with the location. Increase in voltage beyond this saturation condition soon leads to an unstable condition in which external resistance must be used to limit the current to a safe value. The elec-

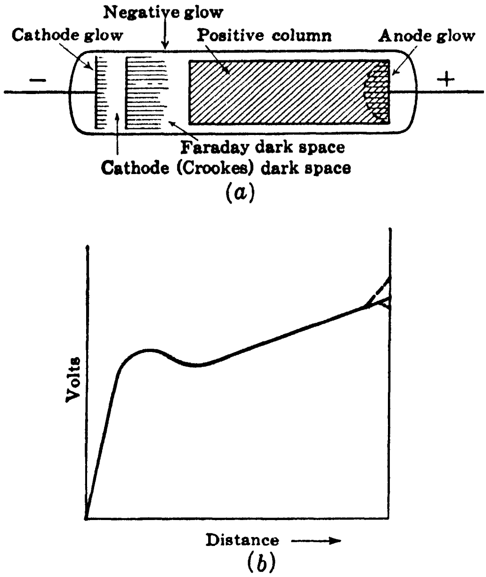

FIG. 872. (*a*) General appearance of a glow discharge; (*b*) potential distribution in a glow-discharge tube.

TABLE IV

IONIZATION POTENTIALS

Element	Atomic Number	Ionization Potential (volts)
Argon (A)	18	15.69 15.86
Krypton (Kr)	36	13.3
Xenon (Xe)	54	11.5
Neon (Ne)	10	21.47
Hydrogen (H)	1	13.54
Helium (He)	2	24.48
Mercury (Hg)	80	10.39
Oxygen (O)	8	13.55

---

[58] 1 micron = 10^{-6} meter of mercury = 1.333 baryes (dynes per square centimeter) = 1.315×10^{-6} atmosphere.

trons in the gas have now reached a sufficient velocity to produce appreciable ionization by "collision." The increase in current has been explained by Townsend, by assuming an initial source of electrons at the cathode and an ionizing constant α which is the number of new electrons that each electron releases by ionizing "collisions" per centimeter advance in the direction of the field. The anode current is then given by:[59]

$$i = i_0\epsilon^{\alpha l} \quad . \ . \ . \ . \ . \ . \ . \quad (63)$$

i_0 is the saturation current before ionization by collision becomes important, and l is the distance between anode and cathode. When positive ions are also considered to produce other ions by collision, the anode current is given by:[60]

$$i = i_0\frac{(\alpha - \beta)\epsilon^{(\alpha-\beta)l}}{\alpha - \beta\epsilon^{\alpha-\beta l}} \quad . \ . \ . \ . \ . \ . \ . \ . \ . \ . \quad (64)$$

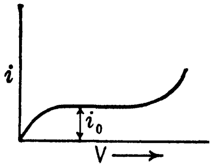

FIG. 873. Current flow in a discharge tube at low voltages.

β has the same meaning for positive ions that α has for electrons. Since α increases more rapidly than β with increased voltage, a critical value called the ignition voltage is reached when:

$$\alpha - \beta\epsilon^{(\alpha-\beta)} = 0$$

Beyond this point, the discharge is self-maintaining.

A similar theory developed by Thomson,[61] in which he assumed that positive ions produced secondary electrons by bombarding the cathode, results in a current given by:

$$i = i_0\frac{\epsilon^{\alpha l}}{1 + \gamma(1 - \epsilon^{\alpha l})} \quad . \ . \ . \ . \ . \ . \ . \ . \ . \ . \quad (65)$$

γ is the number of secondary electrons emitted at the cathode for each positive ion produced in the gas. The condition for a self-maintained discharge, i.e., a discharge which persists after the initial ionizing source has been removed, is reached when

$$(1 + \gamma)(1 - \epsilon^{\alpha l}) = 0 \quad \text{or} \quad \epsilon^{\alpha l} \geqq (1 + \gamma)/\gamma \quad . \ . \ . \quad (66)$$

An attempt to evaluate α and β in terms of other known factors leads immediately to a study of ionization probabilities. For a detailed account of this and other factors connected with the theory of discharges in gases, the reader is referred to previously cited works of Thomson, Townsend, and Slepian, as well as the articles and books by Langmuir,[62] Compton,[63] Darrow,[64] and others. A few of the concepts should be mentioned, however. Before a moving electron can convert its energy of motion in an ionizing "collision," it must have fallen through a potential difference equal to the ionization potential of the particular gas. Certain smaller electron energies are capable of excitation, but the probability of ionization is zero. It has been shown that the probability of ionization increases with electron energies above the ionization potential, and reaches a maximum at about ten times the energy required for ionization. The exact value depends upon the mean free path or the distance an electron will travel on the average before colliding with a gas molecule. From the kinetic theory of gases,[65] the mean free path for an electron among gas molecules is:

---

[59] J. Slepian, "Conduction of Electricity in Gases," p. 79, Educational Dept., Westinghouse Elec. & Mfg. Co.

[60] J. Slepian, *op. cit.*, p. 90.

[61] J. J. Thomson and G. P. Thomson, "Conduction of Electricity through Gases," Vol. II, p. 518.

$$\lambda = \frac{4}{N\pi\sigma^2}.$$

N is number of molecules per cubic centimeter.
σ is assumed diameter of molecule.

The mean free path is thus seen to be inversely proportional to the pressure.

An important relation known as Paschen's law[66] states that the ignition voltage or sparking voltage is a function of the product of pressure and distance, or $V_i = f(p \times d)$. Figure 874 shows the Paschen's law relation for helium, mercury, neon, and argon.[67]

Glow and arc discharges. When the voltage across a discharge tube is increased beyond that producing the so-called Townsend current, the current increases to a destructive value unless the tube has a resistance in series. By suitably limiting the current, the tube may be operated under the conditions of a glow discharge. The glow is characteristically divided into regions as shown in Fig. 872(a). Light from the tube is the result of excited atoms returning to lower energy levels.

---

[62] I. Langmuir, *Jour. Franklin Institute*, vol. 214, pp. 275–298, September, 1932.

[63] K. T. Compton and I. Langmuir, *Review of Modern Physics*, vol. 2 pp., 123–242, April, 1930; vol. 3, pp. 191–257, April, 1931.

[64] K. K. Darrow, "Electrical Phenomena in Gases," Williams & Wilkins, Baltimore, 1932.

[65] L. B. Loeb, "Nature of a Gas," John Wiley & Sons, 1931.

[66] F. Paschen, *Wiedemann Annalen*, vol. 37 (1889), p. 69.

[67] A. W. Hull, *Trans. A.I.E.E.*, vol. 53 (1934), p. 1439, "Some fundamental electrical properties of mercury vapor and monatomic gases."

The colors are characteristics of the particular gas or gases, and are determined by eq. (62). It will be noted from Fig. 870(*b*) that the greater portion of the total voltage drop occurs at the cathode. The potential distribution through the tube is influenced mainly by the space charge created by the presence of the positive ions. While the electrons are responsible for about 90 per cent or more of the current, their relatively greater velocity under the influence of the field minimizes their contribution to space-charge effects. Increasing the length of a discharge tube increases the length of the positive column without affecting the other regions appreciably. The tubes used for sign lighting are made extremely long to take advantage of this situation, and operate at an increased efficiency, since the illumination comes from the positive column and the cathode fall of potential is practically unaffected by the length of the positive column. A typical volt-ampere characteristic for a glow lamp is shown in Fig. 875. Most glow lamps, especially those used for voltage regulator applications, operate in the region *bc*, or the region of so-called normal glow where the cathode is not completely

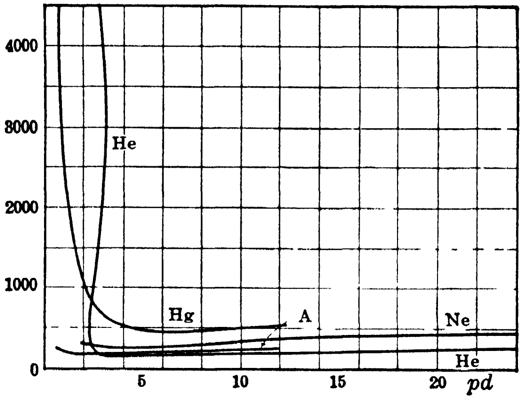

Fig. 874. Sparking potentials in gases as a function of the product, *pd*, of pressure and distance. Pressure, *p*, in millimeters of mercury; distance, *d*, in centimeters (A. W. Hull).

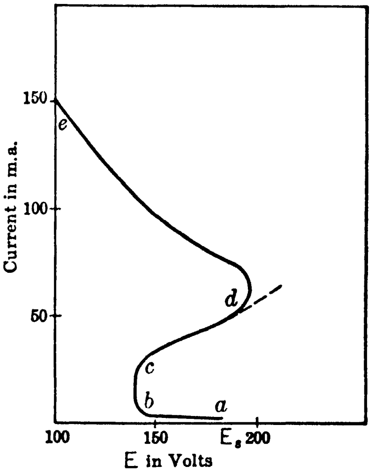

Fig. 875. Volt-ampere characteristics of a glow lamp.

covered. For higher current densities, there is the region of abnormal glow, represented by *cd* on the curve. As the current is increased beyond *d*, the glow is transformed into an arc and the cathode temperature becomes high enough to have appreciable thermionic emission, provided that the tube will withstand the severe service.

The transition from a glow to an arc is not always sharply defined. In general, arc discharges involve much higher current densities and lower voltage drops than glow discharges. The voltage drop for an arc is of the same order of magnitude as the ionization potential of the gas or vapor. The cathode supplies electrons which ionize the gas near the cathode with a resulting positive space charge and low voltage drop. In tubes employing the arc discharge, the cathode may be a thermionic emitter heated by a separate source of electrical energy, a mercury pool, or a cathode that is cold initially but becomes a thermionic emitter through the heat of positive-ion bombardment.

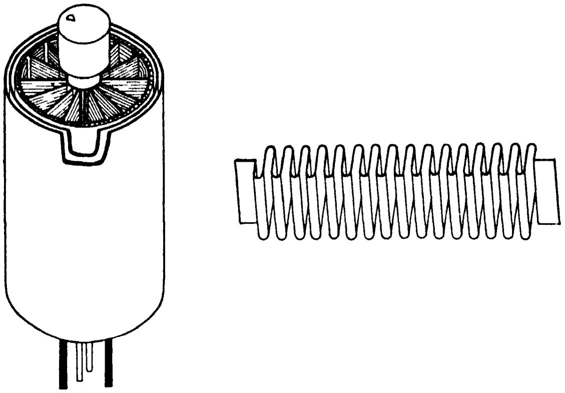

FIG. 876. Heat-shielded cathodes of two types.

1196. Gaseous Rectifiers. — Hot-cathode gaseous rectifiers are similar in many respects to the high-vacuum type. The principal difference consists in the presence of one of the inert gases or mercury vapor at a low pressure. The cathode is also of special design. Owing to the larger plate currents at low plate voltages, it becomes important to increase the efficiency of the thermionic cathode, since it must supply electrons for the entire plate current. The current carried by the positive ions is only a small fraction of the total current, owing to the greater mass and consequent slower motion of the positive ions. In mercury vapor the electrons move about 600 times as fast as the positive ions. Cathodes with high emission efficiency are constructed with heat shielding as shown in Fig. 876. This type of construction in high-vacuum tubes would result in serious negative space-charge limitation of current even at high plate voltages, but in a gaseous tube the positive ions neutralize this negative space charge at the cathode. It is important that the cathode of a gaseous tube be always operated at the proper temperature to prevent destruction by positive-ion bombardment. If at any time the plate current exceeds the total emission of the cathode, the tube drop increases and the positive ions strike the cathode with sufficient energy to knock off the oxide coating. The gaseous rectifier tube or phanotron thus has a peak plate current rating that is determined by cathode limitations rather than plate heating. The peak current rating is usually about four times the average current rating, and average plate current ratings as large as 50 amperes are not uncommon. The various manufacturers' catalogs should be consulted for typical tube ratings.

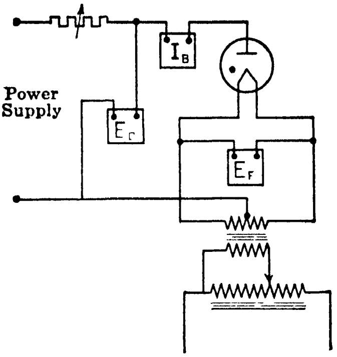

Fig. 877. Circuit for measuring the voltage drop through a gas or vapor rectifier tube.

1197. EXPERIMENT 59-M. — Measurement of the Voltage Drop through a Hot-Cathode Mercury-Vapor Tube. — The end of the useful life of a gaseous rectifier tube is generally indicated by an increase in the tube voltage drop. A simple test to determine the current-voltage characteristic of a tube may be made, using the schematic circuit diagram of Fig. 877. In a mercury tube the voltage drop is a function of the condensing mercury temperature, and the tube should be immersed in an oil bath with provisions for measuring the temperature and maintaining it at the desired value. The cathode should be carefully adjusted to the correct value, and sufficient time for the cathode to reach operating temperature should be given before plate voltage is applied. The plate current will be limited principally by the external plate resistance. Readings of tube voltage drop and plate current for plate currents from about 1/10 the rated value to not greater than 20 per cent above the rated average value should be obtained. The runs should be made for two or three constant temperatures of the oil bath in the operating range. The temperature of the bath is not exactly the condensing mercury temperature.

1198. — EXPERIMENT 59-N. — Measurement of Voltage Regulation and Hum Percentage in a Full-Wave Rectifier Using Phanotrons. — The circuit diagram and procedure are essentially the same as in

Experiment 59-E, with the following exceptions. The filament voltage should be carefully monitored and plate voltage applied to the tube or tubes only after the cathode has reached operating temperature. The filter should be of the choke input type to limit the peak plate current.

1199. Grid-Controlled Rectifiers. — *Thyratrons.* The current flow through two-electrode hot-cathode gaseous tubes is characterized by regions near electrodes and other surfaces where there is either a preponderance of positive ions or of electrons creating space-charge effects and known as sheaths, and another region (the plasma) where positive ions and electrons exist in about equal numbers, resulting in very low voltage gradients. If a third electrode is introduced, changing the potential of this electrode will have practically no effect on the current flow after the tube has started to conduct. If a negative voltage is applied, the electrode will attract positive ions and a positive-ion sheath will form, thus preventing the electrode potential from affecting the potential in regions outside the ion sheath. The sheath thickness may be calculated by Child's law equation (Art. 1168), since the electrode current will be space-charge limited. If a positive potential is applied to the electrode, electrons will be attracted and another sheath will be

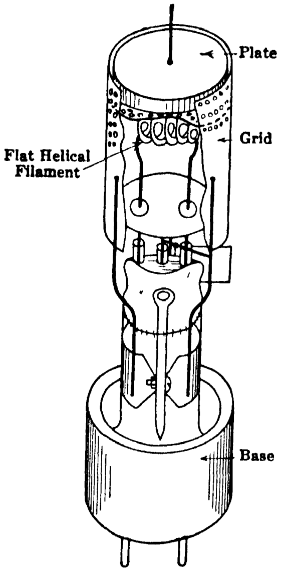

FIG. 878. Sketch showing construction of a Westinghouse thyratron tube, Type KU-628.

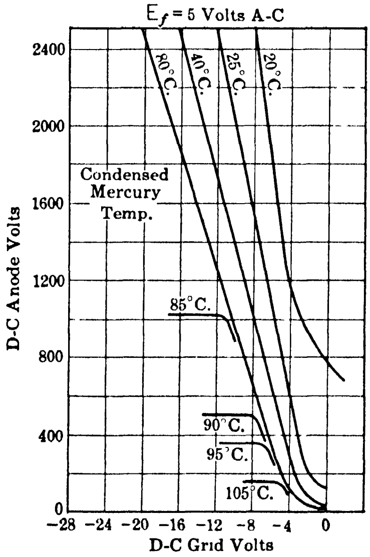

FIG. 879. Average control characteristics of a KU-628 thyratron (Westinghouse Electric and Mfg. Co.).

formed, with practically no effect on the plate current. Although a grid placed between plate and cathode has no effect on the plate current in a gas tube after the discharge has started, a grid that completely encloses the cathode will prevent the start of a discharge when its potential is only a few volts negative. If the enclosure is complete enough, a positive grid potential may be required to start the plate current. The relation between grid and plate voltages just necessary to prevent breakdown is known as a grid control characteristic. For mercury-vapor tubes, this is a function of the temperature. Figure 878 is a sketch showing the arrangement of grid, plate, and cathode in a KU-628 thyratron. The grid control characteristics for the KU-628 are given in Fig. 879. Voltages above and to the right of one of these curves for a particular temperature represent conditions permitting breakdown and plate current flow. Voltages below and to the left represent a condition of insulation and no plate current flow. The KU-628 is a negative control type. The curves for a positive control type (FG-67) are given in Fig. 880.

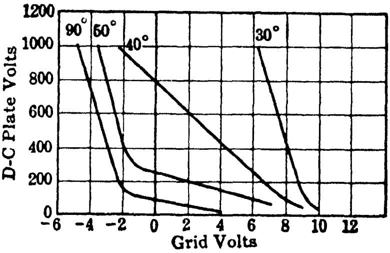

FIG 880. Characteristics of a FG-67 thyratron tube at various temperatures — degrees Centigrade (General Electric Co.).

1200. EXPERIMENT 59-O. — Determination of the Grid Control Characteristic of a Thyratron. — If the thyratron contains mercury vapor, the tube must be placed in an oil bath with provisions for adjusting and maintaining the temperature. A tube containing argon, neon, or another of the inert gases has a characteristic not affected much by change in temperature. A schematic circuit diagram suitable for testing an FG-57-type thyratron is shown in Fig. 881. Only slight modifications are necessary for testing any type of thyratron. Since anode or plate voltages will be high, due care should be exercised to prevent accidental contact with this part of the circuit. The plate power supply should be capable of delivering an output voltage of 1000 volts, although a maximum value of 500 volts will be sufficient to determine the grid control characteristic over the lower and perhaps most important part of the characteristic. The resistance R_1 will usually be chosen to limit the load on the power supply rather than the safe current for the thyratron. A value of 1000–5000 ohms should be satisfactory. If an adjustable plate supply voltage is available, the potentiometer in the plate circuit will not be necessary. It is important to have the filament voltage at the proper value, and the voltmeter should be connected as near the tube terminals as possible. The cathode should reach operating temperature before plate voltage is applied.

The grid voltage necessary to prevent breakdown should be measured for several plate voltages from about 25 volts to the maximum value. Breakdown and plate current flow will be indicated by a sudden drop in the plate voltage and by the appearance of a glow. After breakdown, the plate voltage must be removed to permit deionization and establishment of grid control. To determine the variation of grid current, the grid voltage should be varied from about -15 to a positive value sufficient to cause a maximum of 100 ma to flow. This should be performed for different plate currents from about $\frac{1}{3}$ rated plate current to the maximum rated value. It will be necessary to substitute a low-voltage plate supply with sufficient current capacity for the high-voltage supply previously used. The series plate resistor (R_1) must now be capable of carrying about 2.5 amperes and have a value of about 100 ohms if an FG-57 tube is being tested.

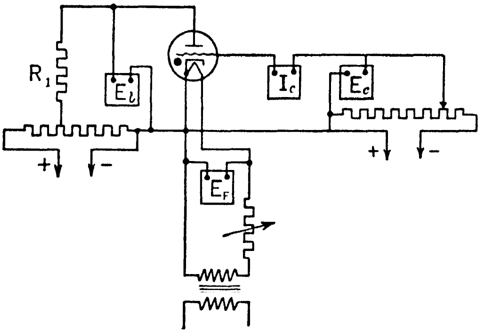

FIG 881. Circuit for determining the control characteristics of a thyratron tube.

1201. EXPERIMENT 59-P. — Determination of the Control Characteristic of a Cold-Cathode Grid-Glow Tube. — A test on a KU-618 cold-cathode grid-glow tube will illustrate the general procedure for tubes of this type.[68] The circuit diagram is given in Fig. 882. The anode in this tube is the end of a small rod, and the cathode is a comparatively large cylinder. The grid consists of a small ring surrounding the anode. A shield electrode surrounding the anode lead is also provided. This shield is normally connected to the cathode through a high resistance of 1 to 10 megohms. In the diagram, the anode is designated by *A*, the cathode by *C*, and the grid *G* and the shield *S*. The resistance R_1 should be about 1 megohm, R_2 about 5 megohms, and R_3 about 20,000 ohms. The measurement of E_G with respect to the anode rather than the cathode may seem a bit unconventional but is in accordance with the manufacturers' ratings and the way in which the tube is applied.

---

[68] Bohls and Thomas, *Electronics*, May, 1938, p. 14.

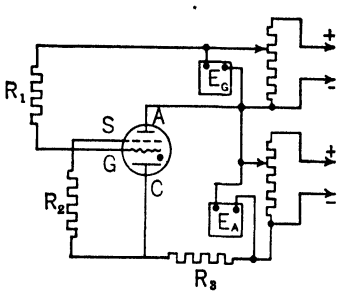

FIG. 882. Circuit for determining the control characteristics of a cold-cathode grid-glow tube.

With a plate voltage (E_A) of about 200 volts, the grid voltage (E_G) should be increased slowly until breakdown occurs, which will be indicated by the typical orange glow of a neon discharge. This should be repeated for several voltages between 200 and 500. For the higher plate voltages, the grid voltage for breakdown will be negative. For plate voltages lower than about 200 volts, the discharge occurs between grid and cathode and does not pass to the anode.

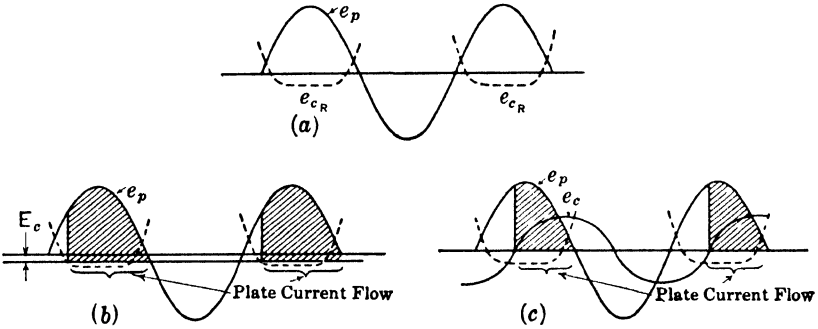

FIG. 883. (*a*) Instantaneous plate voltage and corresponding critical grid voltage obtained from control characteristics. (*b*) Plate current flow during portion of positive half-cycle with adjustable d-c grid voltage. (*c*) Plate current flow during portion of positive half-cycle with a-c grid voltage of adjustable phase.

1202. Operation of Thyratrons with A-C Plate Voltage Supply.—A majority of the applications of thyratrons employ an alternating voltage in the plate circuit. This permits deionization during the negative half-cycle when it is possible for the grid to regain control after passage of plate current. The exact point in the positive half-cycle when the tube conducts current is determined by the instantaneous plate and grid potentials in accordance with the control characteristics exemplified by Fig. 879. A construction shown in Fig. 883 is used to determine the part of the positive half-cycle during which plate current will flow. Figure 883(*a*) is a plot of the instantaneous sine-wave plate voltage and the corresponding critical grid voltage necessary just to prevent the start of plate current at any point in the positive half-cycle. An instantaneous grid voltage greater than the critical value will permit the tube to start conducting and continue to carry current through the remainder of the positive half-cycle. Figure 883(*b*) illustrates a steady d-c voltage applied to the grid. Adjustment of a d-c grid voltage will cause the tube to conduct from ¼ to a full half-cycle. Figure 883(*c*) shows an a-c grid voltage with adjustable phase. When the grid and plate voltage are 180 degrees out of phase, the tube does not conduct during any part of the cycle. When the grid voltage is in phase with the plate voltage, plate current flows for almost the entire positive half-cycle. The average plate current may also be varied by changing the magnitude of the a-c grid voltage or by any combination of the three methods.

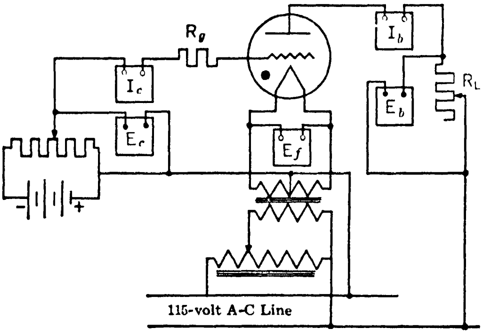

Fig. 884. Circuit for determining plate current variation with amplitude of d-c grid voltage.

1203. EXPERIMENT 59-Q. — Control of Average Plate Current in a Thyratron by Changing the D-C Grid Voltage.—The tube is connected according to the circuit of Fig. 884. If a KU-628 type is used, resistor R_L will have a maximum value of about 100 ohms and a current-carrying capacity of about 3 amperes. R_g should be about 50,000 ohms. The grid voltage may be supplied by a 6-volt battery. The filament should be brought up to the proper operating voltage and temperature before plate and grid circuits are closed. It should be remembered that if plate current flows it is limited to a safe value by the load resistor R_L. Starting with R_L at the maximum value and the grid voltage at the maximum negative value, the magnitude of the grid voltage is slowly reduced to zero, and values of plate current, plate voltage, grid voltage, and grid current recorded. The run may be repeated with a lower value of R_L adjusted to give about 2-ampere d-c plate current when the grid voltage is zero. A cathode-ray oscillograph, connected between plate and cathode center tap, will be of value.

Report. The d-c plate current should be plotted as a function of the d-c grid voltage, and several points on the curve should be calculated.

The effect of tube temperature on the results obtained should be analyzed.

1204. EXPERIMENT 59-R. — Control of Average Plate Current in a Thyratron by Changing the Phase of the A-C Grid Voltage. — The circuit diagram (Fig. 885*a*) is similar to that in the previous experiment (§1203) except for the grid circuit. The two grid transformers with secondaries in series could very well be replaced by a single transformer with center-tapped secondary. However, these may be 115/230 volt potential transformers, which are usually more generally available. The 230-volt winding of each transformer should be connected to the 115-volt line, and the secondaries connected series aiding. The student should prove by constructing a circle diagram that the voltage drop from *a* to *b* leads the voltage drop from 1 to 2 by an angle given by:

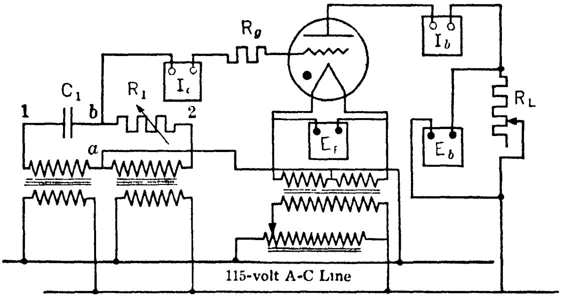

Fig. 885(*a*). Circuit for determining thyratron characteristics with phase-shift control.

$$\theta = 2 \tan^{-1} \frac{X_{c1}}{R_1}$$

when the grid does not take current. Grid current does not flow until the tube breaks down and becomes conducting. The angle θ or its supplement is the angle between the grid and plate voltage, assuming zero phase angle for the transformers. R_1 is an adjustable resistor of about 10,000 ohms maximum value. R_1 may be a decade resistor of sufficient current-carrying capacity, a number of fixed resistors of known value and arranged for series-parallel combinations, or a non-inductive slide-wire which must be measured for each setting. C_1 is a 2-μf condenser.

After the cathode has reached the correct operating temperature, the plate and grid circuits are closed. R_L should be about 100 ohms.

Readings of all quantities indicated on the circuit diagram are taken as R_1 is varied from zero to ∞. The grid supply voltage is then reversed by interchanging the transformer leads to points 1 and 2, and a similar run made. A cathode-ray oscillograph (Chapter LVII) or an electromagnetic oscillograph or both may be connected at different points in the circuit to observe the current and voltage wave forms. The above runs may be repeated with an inductance of about 0.1 henry connected in series with R_L.

Report. The plate current should be plotted as a function of the phase angle between plate and grid voltage. A typical curve is given in Fig. 885(*b*). The student should check by calculation one or two points on the curve with pure resistance in the plate circuit.

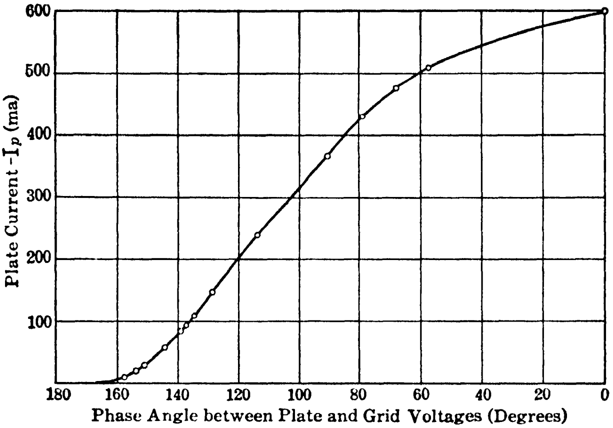

FIG. 885(*b*). Grid phase-shift control characteristics of thyratron tube KU-628 (R. L. Smithley).

1205. Principle of the Mercury-Arc Rectifier. — In the mercury-arc rectifier the cathode spot supplies a copious stream of electrons which is a primary requirement in the maintenance of an arc discharge. A high vapor pressure exists immediately above the cathode spot, tending to increase the probability of ionization and partly accounting for the low cathode drop of about 9 volts. This value is given by Güntherschulze,[69] who obtained other pertinent data on the mercury arc considered to be reliable.[70] Determinations also show that 7.2×10^{-3} gram of mercury is evaporated per second, per ampere, and that the current density at the cathode spot is about 4000 amperes per square centimeter. Owing to the high pressure over the spot, a depression is formed in the mercury surface at this point. The spot tends to climb the side of the depression, resulting in shift in the direction of the average force, which causes the cathode spot to dance rapidly over the mercury surface. The mercury-arc rectifier and its circuits are considered in Chapter LVI.

---

[69] Güntherschulze, *Engineering Progress*, August, 1925, pp. 251–256.

[70] Prince and Vogdes, "Principles of Mercury Arc Rectifiers and Rectifier Circuits."

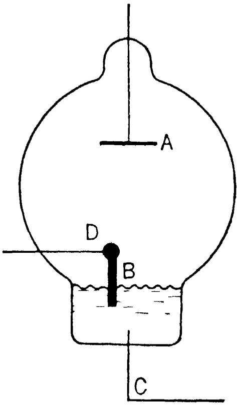

FIG. 886. Essential features of the ignitron.

The ignitron. A mercury-pool tube using the igniter principle[71] possesses definite advantages for certain power applications of tube rectifiers. The high peak current rating and overload capacity of the pool type is combined with the possibility of control. In a thyratron the grid controls the time in the positive half-cycle when the gas ionizes and the plate current starts. In an ignitron (Fig. 886), the initiation of a discharge is brought about by passage of current through a rod, *D*, of refractory material and into the surface of a mercury pool, *B*. The high potential gradient along the igniter causes minute sparks to occur at the entrance of the rod into the mercury surface. An arc cathode is thus formed with the metal part of the igniter as the anode. The discharge is immediately transferred to the main anode, *A*, when it is at a suitable positive potential. It has been shown that, with an igniter gradient of 85 volts per centimeter, the mean elapsed time between the flow of igniter current and the start of the discharge is between 1½ and 5 microseconds.[72]

The ignitron has definite advantages over the mercury-arc rectifier in more absolute freedom from arc-back and other difficulties of mercury-arc-rectifier operation. In polyphase rectifiers, the single-phase ignitron units eliminate the problem of ever-present ionization due to the operation of several anodes from one mercury pool. The deionization time of the ignitrons is still further reduced by using a water-cooled metal-clad construction. In simple rectifier circuits the igniter is connected to the anode through a resistor and rectifier. Far greater possibilities for application of the ignitron lie in the field of controlled rectification.

1206. EXPERIMENT 59-S. — Test of an Ignitron Controlled by a Thyratron. — The circuit arrangement is shown in Fig. 887. This shows a thyratron arranged for phase shift control of the average plate current as in Experiment 59-R. The plate of the tube is in series with the igniter, so that the phase of the grid voltage determines the time in the positive half-cycle when the igniter current is sufficient to start the discharge in the ignitron. Breakdown in the thyratron and the ignitron are not simultaneous, since the igniter current must rise to a sufficient value to initiate the cathode spot. This probably varies from cycle to cycle, and some instability may be expected for low igniter currents. The instability is reduced by operating at higher anode voltages.

---

[71] J. Slepian and L. R. Ludwig, *Trans. A.I.E.E.*, vol. 52 (1933), p. 693.

[72] W. G. Dow and W. H. Powers, *Elec. Eng'g*, vol. 54 (1935), p. 942.

With a KU-637 ignitron, resistor R_4 should be adjusted to give a load current (I_L) not greater than 5 amperes, when the phase of the grid voltage is adjusted for maximum I_L. R_2 should be about 50,000 ohms.

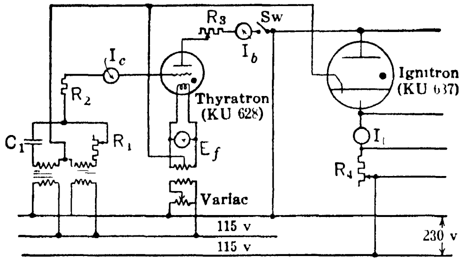

FIG. 887. Ignitron controlled by thyratron with phase-shift adjustment.

The best value for R_3 will vary considerably with different ignitrons. It should be low enough to permit positive firing and high enough to protect the igniter circuit, although a switch is provided to interrupt the igniter current, if for any reason the ignitron does not conduct. R_1 and C_1 in the phase shifter may be the same as used in Experiment 59-O.

A load run should be made by varying R_1 from zero to infinity and recording all meter readings. An oscillograph connected to show ignitron voltage drop, load current, and igniter current will assist in an understanding of the functioning of this circuit. The effect of changing the value of R_3 should be observed. For the circuit arrangement given it should be possible to reduce R_3 to zero. After some familiarity with the circuit is obtained, the load resistor R_4 may be replaced by the armature of a small d-c motor, whose speed may now be controlled by adjusting R_1. Typical curves of load current and igniter current as a function of phase angle between plate and grid voltage are shown in Fig. 888.

1207. Photoelectric Cells. — The fundamental surface photoelectric effect was discussed in §§1153 and 1154, and Experiment 59-B served to obtain some quantitative relations in connection with a high-vacuum cell operating on this principle. The sensitivity of the photoemissive cell may be increased about 10 times by introducing an inert gas at low pressure. The anode current is increased in accordance with Townsend's equation (eq. 63), and if a maximum anode voltage is not exceeded, stable operation is secured. The non-linearity and time lag introduced by gas amplification are not important in some applications such as relay operation, but may be disadvantageous in others such as sound reproduction.

Two other types of cells having operating characteristics different from the photoemissive cells have been classified. They are the *photovoltaic* or self-generating type of cell and the *photoconductive* cell. The photovoltaic cell is generally made up in a dry disk type using either the iron-selenium combination (photronic cell) or the copper-cuprous oxide principle (photox). The usual photoconductive cell consists of a thin layer of selenium deposited on a glass plate with electrodes at either end. The slower speed of response of photovoltaic and photoconductive cells limits their usefulness for some applications.

The photovoltaic cell is a low-impedance type, not adaptable to direct amplification by vacuum tubes, and should not be used with an external voltage supply. Average photronic cells produce about 1.4 microamperes per foot-candle of illumination uniformly distributed over the sensitive surface. Special cells with higher sensitivity are available. External resistance causes non-linearity in the current *vs.* illumination relation. This is due to the decreasing cell resistance with illumination. The emf generated for an illumination of 85 foot-candles is about 150 millivolts and is a non-linear function of the illumination.

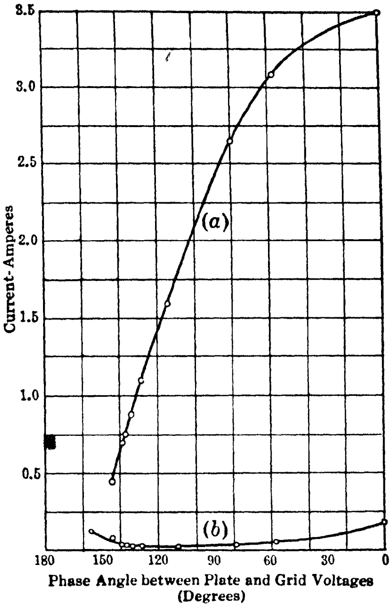

Fig. 888. Curves of tube current against phase angle; ignitron controlled by thyratron. (*a*) Ignitron current; (*b*) thyratron current. (R. L. Smithley.)

The photoconductive cell makes possible a larger amount of power than that available from other types, and a typical application is its use as the resistance element in a phase shifter for control of thyratron tubes. A typical cell (FJ-31) carries a maximum current of 0.5 milliampere, has a resistance of 0.75 megohm with 100 foot-candles illumination, and a ratio of light to dark resistance of 6.

1208. EXPERIMENT 59-T. — Determination of the Characteristics of a Gas-Filled Phototube. — This test may be made in accordance with the instructions for Experiment 59-B on the high-vacuum photoemissive cell using the same apparatus. A PJ-23, UX-868 or a similar type will be a suitable photocell for the test. The maximum rated anode voltage of 90 should not be exceeded on account of the danger of a glow discharge.

1209. EXPERIMENT 59-U. — Determination of the Characteristics of a Photovoltaic Cell. — The Weston photronic cell may be mounted by means of an adapter in the same apparatus used in Experiment 59-B on the photoemissive cell. An external supply voltage for the Weston cell should *not* be used, since the cell may be damaged. A meter with a maximum range of 500 microamperes will be suitable for measuring photocell currents.

The luminous flux should be varied from zero to about 2.5 lumens, and the corresponding photocell current observed for different values of external resistance to a maximum of about 5000 ohms. The meter resistance may constitute an appreciable part of the total external resistance. By a potentiometric method the generated emf in the cell should be determined as a function of the luminous flux in lumens and the illumination in foot-candles.

Report. In addition to the curves that should obviously be plotted to exhibit the data, the student should calculate and plot curves of power output for constant illuminations and variable external resistances. From the curve of emf *vs.* light flux and one of the curves of current *vs.* light flux, the curve of photocell current for zero external resistance should be determined.

1210. EXPERIMENT 59-V. — Measurement of the Spectral Response of a Photocell. — The phototube tested may be any one of the types employed in previous experiments or any similar type with appreciable response in the usual range. The light-bench arrangement of previous experiments may be used with an additional arrangement provided on the phototube housing to hold 2 in. by 2 in. light filters. The filters may be of the Wratten type (Eastman Kodak Company) or glass filters (Corning Glass Works), chosen with suitable transmission curves. By using single filters and combinations of filters, it is possible to secure several reasonably narrow transmission bands distributed over the visual and infra-red region. By assuming an average wavelength for each band selected and integrating the product, percentage transmission of the filter times the ordinates on a curve representing the spectral distribution of thermal radiation from tungsten (Table V), the

TABLE V

SPECTRAL DISTRIBUTION OF THERMAL RADIATION FROM TUNGSTEN*

A.u.	$E_2(\lambda)$(watt/cm^2)			
	2000°K	2500°K	2800°K	3000°K
2000	5.62×10^{-5}	7.15×10^{-2}	1.442	8.32
2500	2.31×10^{-2}	7.03	7.59×10^{1}	3.15×10^{2}
3000	1.08	1.25×10^{2}	9.20×10^{2}	2.98×10^{3}
3500	1.47×10^{1}	8.69×10^{2}	4.27×10^{3}	1.31×10^{4}
4000	9.51×10^{1}	3.36×10^{3}	1.50×10^{4}	3.59×10^{4}
4500	3.78×10^{2}	8.93×10^{3}	3.38×10^{4}	7.31×10^{4}
5000	1.08×10^{3}	1.84×10^{4}	6.07×10^{4}	1.22×10^{5}
5500	2.39×10^{3}	3.14×10^{4}	9.40×10^{4}	1.76×10^{5}
6000	4.50×10^{3}	4.76×10^{4}	1.29×10^{5}	2.30×10^{5}
6500	7.40×10^{3}	6.52×10^{4}	1.64×10^{5}	2.76×10^{5}
7000	1.10×10^{4}	8.27×10^{4}	1.93×10^{5}	3.15×10^{5}

NOTE: E_w (λ) is the rate of emission of energy in watts, from 1 cm^2 of surface, in a direction perpendicular to the surface, per unit solid angle, for 1 cm range of wavelengths. (The last specification is responsible for the magnitudes in the table; for a working range of, say, 10A, it would be necessary to divide by 10^7.)

* Taken from " Photoelectric Phenomena " by Hughes and DuBridge, p. 461, McGraw-Hill Book Co., 1932.

relative spectral response curve for the phototube may be determined. Owing to the relatively large amount of energy in the infra-red region from a tungsten lamp source, it is important that the infra-red filters used have sufficient absorbing power.

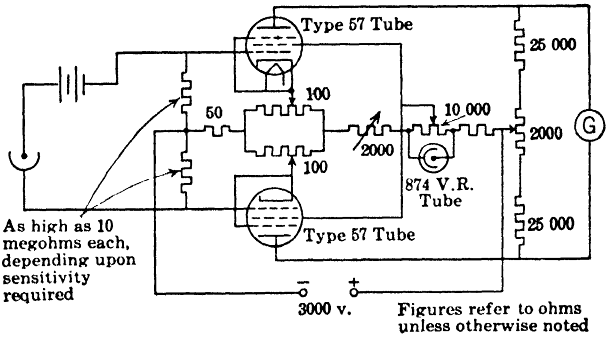
Type 57 Tube
25 000
100
50
10 000
2000
2000
100
874 V.R. Tube
25 000
Type 57 Tube
As high as 10 megohms each, depending upon sensitivity required
–
+
3000 v.
Figures refer to ohms unless otherwise noted

FIG. 889. Balanced amplifier for small photocell currents (Harnwell and Van Voorhes).

It will be necessary to employ a d-c vacuum tube amplifier in order to measure photocell currents. Figure 889 gives a circuit suitable for this purpose. More elaborate arrangements may be used.[73] A more accurate method of making this test is given in " Standards on Electronics for 1938 " (Institute of Radio Engineers), p. 51.

Much help in planning additional tests may be obtained from General Electric Company Bulletins G.E.T. 567, 568A, and 620; also Westinghouse Educational Department Courses 25 and 26. The current publications such as *Electronics*, *Proceedings of the Institute of Radio Engineers*, *Electrical Engineering*, *Experimental Wireless and Wireless Engineering*, and *General Radio Experimenter* also provide ideas and sometimes rather complete information on possible experiments. Footnotes throughout the chapter suggest an extensive bibliography of the subject of electronics, and these references need not be repeated here.

---

[73] G. P. Harnwell and S. N. Van Voorhes, *Rev. Sci. Inst.*, vol. 5, p. 244.

CHAPTER LX

HIGH-FREQUENCY MEASUREMENTS

BY PROFESSOR R. T. GABLER
Carnegie Institute of Technology

1211. Introduction. — High frequency is a relative term generally applied to measurements in a range where effects that are negligible at lower frequencies become important or ruling factors. The chart of Fig. 890 shows the frequency spectrum throughout which one might be interested in making electrical measurements. Naturally there is no sharp dividing line between high and low frequencies.

Circuits composed of lumped parameters so far as low frequencies are concerned may have distributed characteristics with non-uniform current and voltage distribution at higher frequencies. The general methods of analysis given in Chapter XXX are applicable in this case. Equivalent values of resistance, inductance, and/or capacitance may be determined for use at one frequency or over a very limited range of frequencies. To all the possible circuit losses that have been considered heretofore may be added another, that of radiation, especially for frequencies above 50 kilocycles and for circuits with distributed parameters.

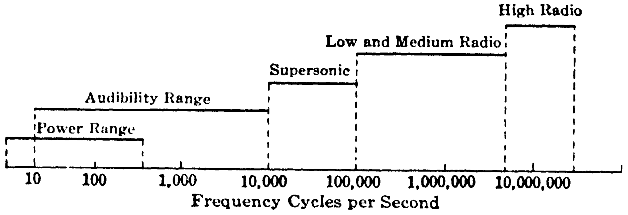

FIG. 890. General range of frequencies within which measurements are made.

The expected accuracy of a measurement made at a high frequency is not ordinarily so high as for a similar measurement at a lower frequency. Accordingly a healthy degree of skepticism about results is desirable until some familiarity with a given method is obtained. There is generally a tendency to underestimate the importance of proper circuit arrangement, grounding, and shielding (§632). Where possible, the use of an alternative method, if only for the purpose of checking, is desirable. Substitution methods are especially useful in high-frequency measurements, since they may be used in connection with resonance and null methods to eliminate many inherent errors.

Through the use of special measuring instruments, such as vacuum-tube voltmeters and special bridges, methods that are generally familiar at low frequencies may be extended to a higher frequency range. It is important to have an understanding of the limitations of the different devices used, since the general method may be quite familiar but the necessary technique decidedly different.

1212. Meters and Apparatus for High-Frequency Measurements.—(a) *Thermoelectric meters.* The thermocouple provides an extremely valuable means of measuring current at high frequencies. Thermocouple meters consist of a heater through which the current to be measured is passed, the thermocouple proper, and a d-c microammeter. The couple may be in direct contact with the heater wire (contact type) or insulated from it by a small glass bead (separate-heater type). The heater and couple are mounted in an evacuated glass bulb. The emf produced by a thermocouple is a function of the difference in temperature of the two junctions. Figure 891 shows the variation of couple emf with hot-junction temperature for two typical combinations used. This calibration is for a cold-junction temperature of 0°C. A correction must be made for other cold-junction temperatures. Figure 892 shows four thermojunctions connected in a bridge arrangement, a scheme used in high-frequency thermogalvanometers and thermomilliammeters. Figure 893 shows a schematic diagram representing a thermocouple meter. The d-c meter resistance should be the same as the couple resistance for maximum power delivered to the meter. In a typical thermocouple meter with a rated current of 10 milliamperes, the heater will have a resistance of 60 ohms, and the thermojunction a resistance of about 10 ohms. This will deflect full scale a 500-microampere meter with a resistance of 10 ohms when rated current flows through the

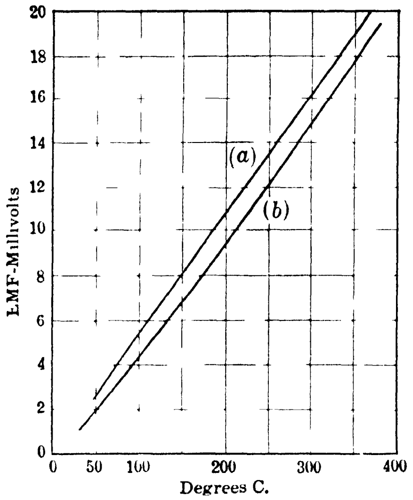

Fig. 891. Emf of thermocouples as a function of temperature difference between hot and cold junctions: (a) iron-constantan; (b) copper-constantan.

heater. The same type of thermocouple with a rating of 100 milliamperes has a heater resistance of 2 ohms and will deflect full scale the same 500-microampere meter with rated heater current. The deflection of the d-c meter is approximately proportional to the square of the rms heater current. For measuring large currents, some form of special shunt or current transformer must be used. The reader is referred to *Bureau of Standards, Circular 74,* for details. Thermocouple meters may be calibrated on direct current or at low frequencies and used at high frequencies.

(b) *Vacuum-tube voltmeter.* It is obvious that the thermocouple meter with a suitable resistance unit in series will constitute a high-frequency voltmeter. The power required to operate a thermocouple voltmeter is often too great, and some type of vacuum-tube voltmeter provides a better means of voltage measurement, especially in high-impedance circuits. Many forms have been developed.[1, 2, 3, 4] The circuit diagram for a full-wave square-law type is given in Fig. 894. When properly adjusted, the change in plate current read by the 200-microampere meter is proportional to the square of the input grid voltage. Maximum deflection occurs with an rms input voltage of about 2 volts. It can be shown that, if the change in plate current is directly proportional to the square of the input grid voltage, there is no wave-form error. Figure 895 illustrates the operating principle of this type of voltmeter. The range may be extended by increasing the value of resistance *R*. The square-law characteristic will then not be preserved, however, and where this is necessary a high-resistance input potentiometer must be used for the higher voltages. Some preliminary

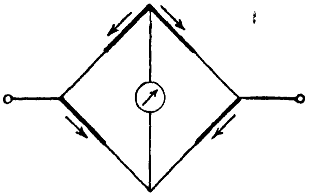

FIG. 892. Thermocouple meter using bridge circuit.

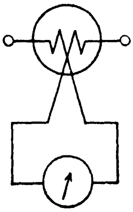

FIG. 893. Diagram of a thermoelectric meter.

---

[1] E. B. Moullin, "Radio Frequency Measurements," Second Edition, p. 140, 1931.

[2] F. E. Terman, "Measurements in Radio Engineering," pp. 22–30, McGraw-Hill Book Co., 1935.

[3] S. C. Hoare, *Trans. A.I.E.E.*, vol. 46 (1927), p. 541.

[4] A. Hund, "High Frequency Measurements," pp. 137–160, McGraw-Hill Book Co., 1933.

adjustment is necessary to secure square-law operation when the voltmeter is first put into operation. The grid bias obtained by a tap on the 25,000-ohm voltage divider is about −4.5 volts. Since all voltages are obtained from a common voltage divider, adjustment of the 10,000-ohm resistance in series with the plate battery will secure proper operating voltages throughout the useful life of the plate battery. A shunt on the 200-microampere meter will afford meter protection when the input terminals are not connected to a closed d-c circuit, to establish the operating grid bias, or when the meter is overloaded for any reason. It will be noted that one side of the meter is connected to the potential divider at a point which balances out the meter current when no voltage is applied to the input terminals. To measure the a-c component of a composite voltage, a condenser is placed in series with the grid input terminal to block the d-c component, and a high-leak resistance is connected across the input terminals.

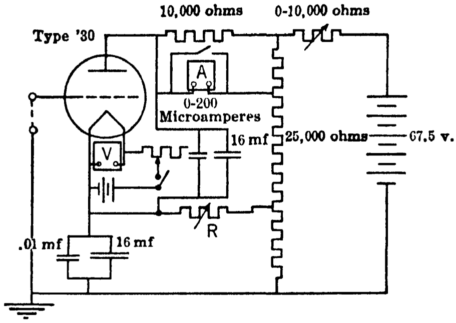

FIG. 894. Circuit diagram of a vacuum-tube voltmeter.

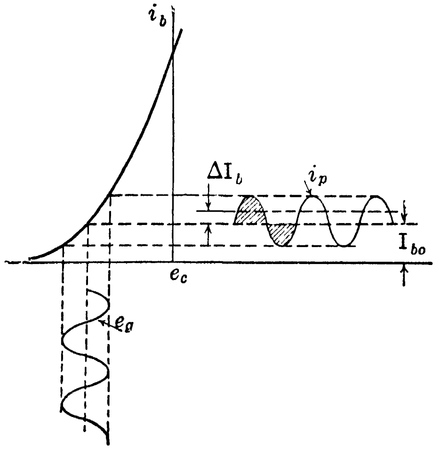

FIG. 895. Graphical illustration of the principle of the full-wave square-law vacuum-tube voltmeter.

Many types of vacuum-tube voltmeter are now commercially available. The rectifier type of peak vacuum-tube voltmeter lends itself well to the design of a high-frequency multirange instrument. The schematic circuit[5] for a meter of this type is shown in Fig. 896. The meter deflection is essentially proportional to the peak voltage, but the calibration is in terms of the rms value of the corresponding sine wave. The d-c feedback amplifier used gives a range of 0.1 to 150 volts in five steps.

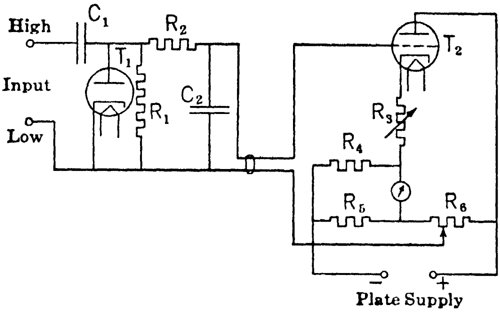

FIG. 896. Circuit diagram of the General Radio Type 726-A vacuum-tube voltmeter.

(c) *Rectifier-type meters.* The cuprous oxide-copper, so-called "copper oxide," rectifier may be used with a series resistance and suitable d-c meter to measure voltage for frequencies in the audio range. The full-wave bridge rectifier circuit is generally employed. Sensitivities of the order of 1000 ohms per volt are readily obtained. The design of multirange rectifier instruments for measuring current and voltage has been carried out by Terman.[6] For small currents the copper oxide meter has a square-law response and then, for larger currents, approaches a linear relation. The proportion of the scale over which the linear operating characteristic holds depends upon the current density in the rectifier element. Ordinarily, the copper oxide meter is considered to be a linear rectifier-type meter with a deflection proportional to the average value of the a-c wave, and accordingly has a wave-form error when used to measure rms values. The temperature error is also considerable, and commercial instruments have a specified accuracy not greater than about 5 per cent of full scale value. The frequency range is limited by the shunting effect of the rectifier capacitance.

(d) *Amplifiers.* Amplifiers may be used in connection with almost any of the meters described to increase the sensitivity or input impedance. The application of the negative feedback principle[7] to amplifiers has greatly increased their usefulness in connection with current- and voltage-measuring apparatus.[8]

---

[5] *General Radio Experimenter*, vol. 11, No. 12.

[6] F. E. Terman, *Proc. I.R.E.*, vol. 23 (1935), No. 3.

[7] H. S. Black, *Bell System Tech. Jour.*, vol. 13 (1934), No. 1, p. 1.

Although instruments have been developed for measuring power directly in high-frequency circuits, [9, 10, 11] this is usually accomplished by a knowledge of voltage, current, and impedance. Power level meters for measuring signal levels in telephone lines, broadcasting, and sound-recording systems, are essentially voltmeters with an adjustable attenuating network (see §1229) to change the range of the meter and maintain a constant input impedance. The calibration is usually in decibels above or below a certain reference level.

(e) *Oscillators.* Among the important items in a high-frequency-measurements laboratory are the oscillators providing sources of radio- and audio-frequency power. A simple circuit for a general-purpose radio-frequency oscillator having reasonably uniform output over a wide range (150 kilocycles to 20 megacycles) is given in Fig. 897. The plate and grid coils of the plug-in type are wound on a 3-inch form and spaced about 3 inches on centers. Plate and grid coils have the same number of turns. The plate and grid tuning condensers have a capacitance of 35–500 micro-microfarads, which determines the inductance of the coils used. The larger coils are bank-wound. A type-10 tube operated at a plate voltage of 250–500 volts will give sufficient output for many measurement purposes. Where high-frequency stability and good wave form are extremely important, automatic amplitude control as shown by Argimbau,[12] Terman,[13] and Groszkowski[14] may be applied. For some purposes it will be desirable to provide a shielded enclosure for the oscillator and employ link coupling to the measuring circuit.

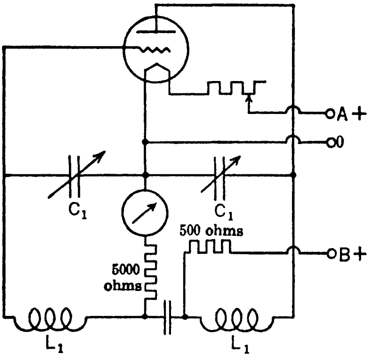

FIG. 897. Schematic diagram of a laboratory oscillator.

Oscillators with a low output and a degree of frequency stability sufficient for heterodyne frequency meters and similar duties may be designed by incorporating both the so-called " electron coupling " principle[15] and the stabilizing method of Llewellyn.[16] From Llewellyn's paper it will be seen that the Colpitt oscillator circuit may be stabilized for a range of frequencies. Employing these methods, it is quite easy to design oscillators for medium and low radio frequencies with a frequency stability determined almost entirely by the temperature changes in parts of the tuned circuit. Further improvement is obviously obtained by proper use of thermal insulation, automatic temperature control,[17] or temperature-compensating elements.[18, 19]

---

[8] Terman, Buss, Hewlett, and Cahill, *Proc. I.R.E.*, vol. 27 (1939), No. 10, p. 649.

[9] H. M. Turner and F. T. McNamara, *Proc. I.R.E.*, vol. 18, p. 1743, October, 1930.

[10] Harris J. Ryan, *Trans. A.I.E.E.*, vol. 30 (1911), part II, p. 1089.

[11] A. Hoyt Taylor, *Proc. I.R.E.*, vol. 24 (1936), No. 10, p. 1342.

[12] L. B. Argimbau, *ibid.*, vol. 21 (1935), No. 1, p. 14.

[13] F. E. Terman, "Measurements in Radio Engineering," p. 290, McGraw-Hill Book Co., 1935.

[14] Janusz Groszkowski, *Proc. I.R.E.*, vol. 22 (1934), p. 145.

Oscillators for use over the audio and supersonic ranges have generally been of the beat frequency type, but are now being rivaled by negative feedback oscillators,[20, 21] which generally have the advantage of better wave form and frequency stability. The resistance stabilized oscillator similar to the Bell Telephone Company's 8-A and 10-B oscillators are also used, especially when greater power output is desired.

(f) *Standard signal generators.* For testing radio receiving equipment and similar sensitive apparatus, a standard signal generator is an essential item. This consists of an elaborately shielded oscillator and attenuator with a provision for measuring the input voltage to the attenuator, usually by thermocouple or vacuum-tube voltmeter. Ordinarily the signal generator output may be modulated by an internal audio oscillator or by external means. The design information on signal generators is readily available[22, 23] if one wishes to build this equipment, although commercial instruments may now be obtained at a reasonable cost.

(g) *Power supplies.* Most high-frequency laboratory equipment may now be more conveniently operated from an a-c power supply, although the extra current capacity of a tapped storage battery with convenient outlets will be found worth while in a communication or electronics laboratory, especially since the storage-battery installation may be necessary for other measurements work. " B " power supplies either built into apparatus or provided separately should be, for most purposes, of the automatically regulated type. These may employ some modification of the scheme[24] using a neon tube or other voltage regulator tube in conjunction with a d-c amplifier and triode acting as an automatic rheostat. A voltage-regulating transformer[25] will provide automatic control of the secondary voltage when the input primary voltage is subject to fluctuation, and when inserted into power supplies will help to maintain constant filament as well as constant plate voltage.

---

[15] J. B. Dow, *ibid.*, vol. 19 (1931), p. 2095.

[16] F. B. Llewellyn, *ibid.*, vol. 19 (1931), p. 2063.

[17] J. D. Stranahan, *Rev. Sci. Instr.*, September, 1934.

[18] *Exper. Wireless & Wireless Engr.*, vol. 6, p. 23, January, 1929.

[19] W. H. F. Griffiths, *ibid.*, vol. 6, p. 543, October, 1929; also vol. 11, p. 305, June, 1934.

[20] H. H. Scott, *Proc. I.R.E.*, vol. 26, No. 2, p. 226, February, 1938.

[21] *Gen. Radio Experimenter*, vol. 13, No. 11, April, 1939.

[22] J. R. Bird, *Proc. I.R.E.*, vol. 19, p. 438, March, 1931.

[23] F. E. Terman, " Measurements in Radio Engineering," McGraw-Hill Book Co., 1935.

1213. Frequency Measurement. — (a) *Wave meters.* At radio frequencies, the standard measuring instrument was for a long time the tuned-circuit wavemeter. It is still used for measurements where it is sufficiently accurate and more convenient than other methods. This instrument depends for its operation upon the principle of series resonance. The usual high-grade wavemeter consists of a precision variable condenser and a coil connected in series with a current squared galvanometer as a resonance indicator. The setting of the condenser for resonance in the tuned circuit determines the frequency of the current being measured. The wavemeter is calibrated from a source of standard frequencies or by calculations based upon an accurate knowledge of the inductance and capacitance in the circuit. The former method is more generally used.

Resonance may be indicated in several ways, the principal ones being: maximum reading of a series current indicator, of a sensitive meter coupled inductively to the wavemeter, of a vacuum-tube voltmeter connected across the wavemeter condenser, or by a neon light connected in the same place. In all cases a standard wavemeter is calibrated with the particular resonance indicator in place because of its effect upon the constants of the circuit. The reaction of the wavemeter on a vacuum-tube oscillator plate or grid current when resonance is approached in the wavemeter circuit will frequently serve as an indicator.

Wavemeters should be coupled to the source very loosely, in some instances to prevent damage to the resonance indicator and in others to prevent reaction upon the source. The shield and rotor of the wavemeter condenser should be grounded both in calibrating and in using the instrument to insure the best accuracy. The overall accuracy of a frequency measurement by wavemeter depends upon the accuracy of calibration, the ability of the wavemeter to hold its calibration, and the precision with which a setting may be made and read. A wavemeter may be set merely for the maximum reading of the resonance indicator or more precisely by making two settings of the wavemeter condenser, one on each side of the resonance point where the currents are equal and slightly less than the maximum or resonance value. The true reading is then halfway between the two settings. This increases the accuracy, since the settings are made on the steep sides of the resonance curve instead of the relatively flat top.

---

[24] RCA Application Note No. 96, RCA Mfg. Co., Camden, N. J.

[25] K. J. Way, *Electronics*, vol. 10, No. 7, p. 14, July, 1937.

Resonant circuits are sometimes made the frequency-determining elements in a vacuum-tube oscillator to produce a " heterodyne wavemeter " Telephones connected in the vacuum-tube circuit indicate zero beat between the frequency being measured and the frequency generated by the " heterodyne frequency meter."

(b) *Standard-frequency service.* The advent of broadcasting and other radio communications services brought a demand for accurate measurement of radio frequencies and the development of standard frequency apparatus. Thanks to the work of the National Bureau of Standards in establishing and transmitting standard frequencies, it is possible to measure radio frequencies with an absolute accuracy of one part in a million without great difficulty. The standard frequency services of the Bureau of Standards have been and are being expanded to include more frequencies and a longer schedule.[26] Standard piezoelectric (quartz) oscillators are operated under controlled conditions, and their average frequency is measured in terms of standard time signals from the U. S. Naval Observatory at Arlington. Because of corrections for inexactness of time signals, the frequency of transmitted signals from WWV, the Bureau of Standards station, is now subject to an absolute error of about four parts in a hundred million. The average variation during a period of emission is about one part in a hundred million.

(c) *Secondary standards of frequency.* In order to utilize the Bureau of Standards transmission, some form of secondary standard of frequency is necessary. This may consist of a good temperature-controlled piezoelectric (quartz) oscillator, a frequency multiplying and dividing scheme, and an interpolation device. The accuracy of the secondary standard is controlled primarily by the piezo oscillator itself and will be sufficient for many purposes. The reader should consult other sources for methods of securing constant frequency from piezo oscillators.[27, 28, 29, 30, 31] The multivibrator provides a most satisfactory device for multiplying and dividing the standard frequency output of the piezo oscillator. In its simplest form, this is a resistance-capacitance coupled amplifier with the output circuit connected back to the input, as shown in Fig. 898. A type of relaxation oscillation takes place with a frequency given approximately by:

---

[26] The schedule of transmissions is obtainable from the Bureau of Standards and is announced from time to time in the *Proc. I.R.E.* and other publications.

[27] J. K. Clapp, *Proc. I.R.E.*, vol. 18, p. 2003, December, 1930.

[28] W. A. Morrison, *ibid.*, vol. 16, p. 976, July, 1928.

[29] Lack, Willard, and Fair, *Bell Sys. Tech. Jour.*, vol. 13, p. 453, July, 1934.

[30] H. R. Meahl, *Proc. I.R.E.*, p. 732, June, 1934.

[31] L. A. Meachan, *ibid.*, vol. 26, No. 10, p. 1278, October, 1938.

$$f = \frac{1}{R_1C_1 + R_2C_2} \quad \text{. . . . .} \quad (1)$$

In a qualitative manner, it is seen that any tendency for plate current in tube 1 to increase would cause a drop in the voltage applied to the grid of tube 2 and a corresponding decrease in plate current for tube 2. This would cause an increase in grid potential and a further increase in plate current for tube 1. The limit is reached when the plate current of tube 2 has been reduced to zero or cut off. This condition of zero plate current for tube 2 will continue until the excess charge in C_2 leaks off through R_2. The resumption of plate current in tube 2 is the beginning of a new cycle with tube 1 and tube 2 interchanging roles. The stopping of plate current in one tube and the starting in another occurs abruptly with a resulting plate-current curve that is almost rectangular in form. The fundamental frequency of a multivibrator is subject to control by an external voltage source. The controlling voltage is injected into the grid or plate circuit of either tube or into both tubes simultaneously, depending upon the ratio of controlling frequency to controlled multivibrator fundamental frequency. Multivibrators may be controlled by frequencies from one to ten times the multivibrator fundamental, the control frequency always being an integral multiple of the multivibrator frequency. Best results are secured when the uncontrolled multivibrator frequency is slightly less than the frequency under controlled operation.

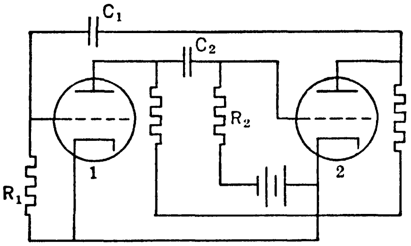

FIG. 898. Elementary diagram of a multivibrator circuit.

(d) *Comparison of frequencies.* In a typical standard frequency assembly, the piezo oscillator employs a quartz bar oscillating at a frequency of 50 kilocycles per second. This output controls a 10-kilocycle-per-second multivibrator which in turn controls a 1-kilocycle multivibrator. A 1000-cycle synchro-clock is operated from the fundamental frequency of the last multivibrator, thus providing a means of measuring the average crystal frequency and consequently any of the harmonics of the multivibrator in terms of standard time signals. A special dial on the synchro-clock enables one to check with time signals to within 1/100 second. In order to use the series of standard frequencies from the crystal oscillator and the different multivibrators, some auxiliary apparatus is necessary. A regenerative radio receiver or heterodyne detector is used to detect the beat note between one of the standard frequencies and the unknown frequency. This beat note is then measured by comparing with a standard audio oscillator, usually of the beat frequency type. The difference between the audio-oscillator frequency and the beat note being measured may be made less than one cycle by observing their combined effect on an audio amplifier connected to a copper oxide rectifier-type meter. The final accuracy depends somewhat on the accuracy of calibration of the audio oscillator. Whether the measured beat note frequency is to be added or subtracted may be determined by shifting the standard frequency slightly in a known direction by detuning the piezo oscillator. Another method of interpolating between standard frequency harmonics is through the use of a high-grade heterodyne frequency meter with a straight-line calibration. In a typical measurement of a radio frequency below 2.5 megacycles, the zero beat between the heterodyne frequency meter and the unknown frequency would be located by feeding the two frequencies into the heterodyne detector and tuning the heterodyne frequency meter. The reading of the heterodyne frequency meter is recorded as R_x. The output of the 10-kilocycle multivibrator is now substituted for the unknown frequency, and the zero beat between the 10-kilocycle harmonics and the heterodyne frequency meter output is noted. In particular, the reading R_1 for zero beat between the 10-kilocycle harmonic immediately below the unknown frequency and R_2, the reading of the heterodyne frequency meter for zero beat with the 10-kilocycle harmonic immediately above the unknown frequency, should be recorded. If the scale is straight-line, the unknown frequency is then given by:

$$f_x = f_1 + [(R_x - R_1)/(R_2 - R_1)](f_2 - f_1) \quad . \; . \; . \; . \; (2)$$

In this case

$$(f_2 - f_1) = 10 \text{ kc}$$

where f_1 and f_2 are the frequencies of the multivibrator harmonics corresponding to readings R_1 and R_2 on the heterodyne frequency meter.

1214. EXPERIMENT 60-A.—Calibration of a Heterodyne Frequency Meter or a Tuned-Circuit Wavemeter by a Standard-Frequency Source.—The exact procedure will depend upon the standard frequencies available and the type of frequency meter being calibrated. In general, provision must be made for observing beats between the standard source and the heterodyne frequency meter. If the standard source consists of a piezo oscillator with a fundamental frequency near the middle of the range over which the heterodyne frequency meter is to be calibrated, beats may be indicated by connecting audio amplifiers and telephones in the plate circuits of both the piezo oscillator and the frequency meter. A typical arrangement is shown in Fig. 899. A preliminary calibration of the heterodyne frequency meter (hfm) obtained by some approximate method, such as a calculation based upon the measured circuit constants, will be necessary. The standard oscillator and the heterodyne frequency meter are now coupled loosely by some convenient means and the dial of the heterodyne frequency meter turned slowly until an audio-frequency beat note is heard in the telephones. Careful adjustment of the dial will enable one to locate the point where the audio frequency appears to be of zero frequency. On either side of this point the audio beat note increases in pitch. Theoretically, zero beat may be located at points where

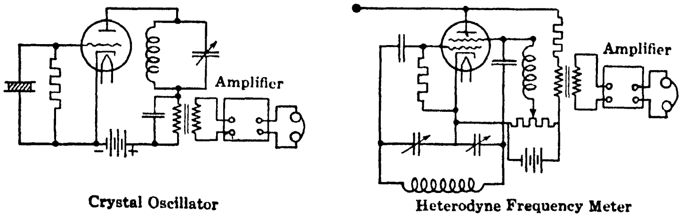

FIG. 899. Schematic circuit for calibration of a heterodyne frequency meter in terms of harmonics from a crystal.

$$n_1 f_1 = n_2 f_2, \quad \text{or} \quad f_1 = (n_2/n_1) f_2 \quad . \quad . \quad . \quad . \quad . \quad . \quad . \quad (3)$$

where f_1 = fundamental frequency of the hfm; f_2 = fundamental frequency of the standard piezo oscillator; n_1 = 1, 2, 3, 4, etc., order of harmonic of heterodyne frequency meter; n_2 = 1, 2, 3, 4, etc., the order of harmonic of piezo oscillator. The preliminary calibration curve will show the approximate value of f_1, from which the exact values of n_2, n_1, and f_1 may be determined, f_2, of course, being known. This process is repeated for as many beat notes as can be located within the range.

The loudest beat notes will be obtained when n_1 and n_2 are both small. For n_2 small and n_1 large, the points of zero beat can best be located by listening with the telephones connected to the heterodyne frequency meter. When n_2 is large, the telephones connected with the piezo oscillator should be used.

When a tuned-circuit wavemeter is being calibrated, the heterodyne frequency meter is replaced by an oscillator with power sufficient to operate the wavemeter and the above method is repeated. While the oscillator is maintained at zero beat with the standard frequency source, the wavemeter is tuned for resonance as shown by its resonance indicator, or by its reaction on the plate or grid current of the oscillator. The coupling should be kept as low as practicable.

If sufficient points for a calibration curve cannot be obtained with one piezo oscillator, another must be used, or the oscillator may be adapted to use more than one crystal. When a source of standard frequencies is available, such as those obtained from a controlled multivibrator, the beat notes may best be located by means of a radio receiver into which is fed radio-frequency energy from the standard source and from the oscillator or heterodyne frequency meter being calibrated. The very accurate "three-oscillator method"[32, 33] of locating the zero beat may be used if the radio receiver is provided with a regenerative detector that may be put into oscillation. The use of this method is warranted where one piezo oscillator is compared with another, or where frequency drifts are being measured.

1215. Methods of Measuring Frequencies in the Audio Range.— Any of the bridges discussed in Chapter XXVIII where the balance is a function of frequency may be used to measure audio frequencies. The Wien bridge circuit, Fig. 473, is the most advantageous, since no inductances are used. Since only the fundamental is balanced out, some difficulty due to harmonics may be experienced, unless a reasonably selective or discriminating detector is used. Telephone receivers are sufficiently selective over a limited range, usually about 800 to 1400 cycles per second. For higher and lower frequencies, an amplifier with a low-pass or band-pass filter and a rectifier instrument or vacuum-tube voltmeter as detector will be suitable.

Audio frequencies may be compared by applying the standard frequency and the unknown frequency to the two sets of plates of a cathode-ray oscillograph (Chapter LVII). When the two frequencies are exactly the same or have an integral ratio, a stationary pattern appears on the screen. For other ratios there is a movable pattern, making it necessary to adjust one frequency or the other until some recognizable

---

[32] "Frequency Measurement at Radio Frequencies," bulletin issued by General Radio Company.

[33] Hugh A. Brown, "Radio Frequency Electrical Measurements," McGraw-Hill Book Co.

Lissajous figure appears. Typical patterns may be obtained by plotting the intersections of the projections of sine waves of different frequency ratios and relative phases along the x and y axes, respectively. Treatises on the cathode-ray oscillograph[34] usually give typical Lissajous figures and their interpretation, as well as schemes for extending the method to higher frequency ratios.

Synchro-clocks similar to those designed for standard-frequency assemblies may be used to measure average frequency with a high degree of accuracy, provided that sufficient time for checking the clock against standard time intervals is permissible. If extremely high accuracy for the instantaneous value of a low frequency is desired, perhaps the best method is to have the low frequency control a multivibrator and then measure the frequency of one of the higher multivibrator harmonics, by a procedure similar to that followed in measuring radio frequencies with a standard-frequency assembly.

Stroboscopic disks turned by a synchronous motor running from a standard-frequency source may be used to measure frequencies in the audio range. The frequency to be measured is used to light a small neon lamp which illuminates the rotating disk. Assuming that the light flashes twice during each cycle, a stationary pattern is obtained when $f = kn/2m$, where

f = unknown frequency.
k = number of spokes or sectors on the disk.
n = revolutions per second.
m = 1, 2, 3, 4, etc., or $\frac{1}{2}$, $\frac{1}{3}$, $\frac{1}{4}$, etc.

The sharpest pattern is observed when $m = 1$. Other orders are not always discernible unless special provisions are made for peaking the waves.

1216. EXPERIMENT 60-B. — Calibration of an Audio-Frequency Oscillator Using a Standard-Frequency Source and a Cathode-Ray Oscillograph. — The standard-frequency source should be rich in harmonics if calibration over a wide range is desired. A multivibrator controlled by the output of a good electrically driven tuning fork or controlled by voltage from a standard-frequency assembly with piezo oscillator will be quite satisfactory. If the fundamental frequency of the multivibrator is 1000 cycles per second, no great difficulty should be experienced in calibrating the oscillator at the 1000-, 2000-, 3000-cycle, etc., points by the simple arrangement shown schematically in

---

[34] "RCA Cathode-Ray Tube Manual," Technical Series TS-2.

Fig. 900. To secure typical Lissajous figures, the multivibrator output should be fed through a selective amplifier which may be tuned successively to the different harmonics. It is commonly better to choose a standard harmonic not too far away from the frequency being measured to avoid error in the interpretation of a complicated figure. Sometimes a point may be checked by using more than one standard harmonic frequency. When either the standard or unknown frequency is considerably larger than the other, the figure may be spread out on the screen for easier interpretation by means of the circuit of Fig. 901, or the gear-wheel pattern may be obtained by the circuit of Fig. 902. In either case, the lower frequency provides a circular sweep through proper adjustment of the values of R and C in the phase-splitting circuit. The relative amplitudes of the two voltages may be adjusted by means of the gain controls on the oscillograph amplifiers or by means of potentiometers. If the transformer in the anode circuit of the cathode-ray tube has not already been provided, great care should be exercised in connecting it in this high-voltage circuit. The oscillograph power supply should be completely de-energized. If calibration for a particular frequency for which a completely stationary figure is not obtainable is desired, the rate at which loops pass a given point per second may serve as a correc-

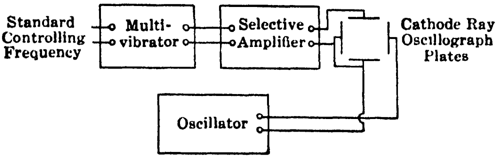

FIG. 900. Scheme for frequency calibration of an oscillator.

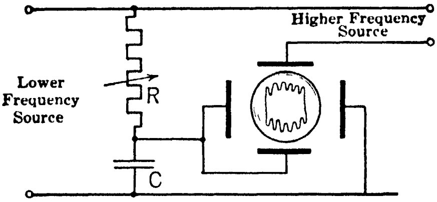

FIG. 901. Circuit giving Lissajous figures with one frequency materially higher than the other.

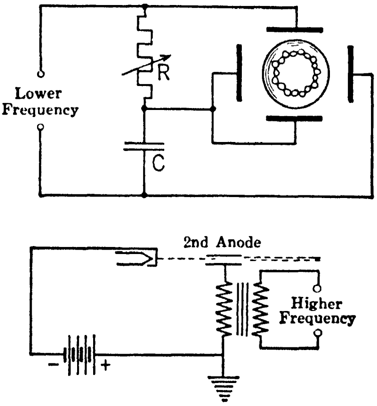

FIG. 902. Circuit similar to that of Fig. 901, but giving a gear-wheel pattern on the oscilloscope screen.

tion to the condition for a stationary pattern. Whether the correction is to be added or subtracted is determined by deliberately making a slight change in frequency and then noting whether the apparent speed of rotation is increased or decreased. Another method is to measure the change made in one of the circuit constants when frequency is changed from one stationary pattern to another, and then make the necessary interpolation.

1217. Measurement of Ultra-High Frequencies. — Ultra-high frequencies may be measured by an extension of the general methods employed in connection with a standard frequency assembly.[35, 36] Another method capable of yielding high accuracy with the proper precautions and corrections[37] is the measurement of wavelength or frequency using Lecher wires.[38, 39] Essentially, standing waves are produced on a transmission line, and the distance between successive nodes or antinodes, constituting half a wavelength, are measured.

1218. Measurement of Apparent Inductance in Iron-Cored Coils Carrying Direct Current. — In much high-frequency apparatus, use is made of iron cores in coils and transformers carrying both direct and alternating current. The apparent *incremental inductance* of a coil and the associated *incremental permeability*[40] of the core material will be considered here, not because the measurement is necessarily made at a high frequency, but because the phenomenon is important in equipment used at the higher frequencies. Incremental permeability may be defined by:

$$\mu_i = \Delta B/\Delta H \quad . \; . \; . \; . \; . \; . \; . \; . \; . \; . \quad (4)$$

where ΔB and ΔH are associated with a minor hysteresis loop. Incremental permeability can be measured by determining the associated incremental inductance of an iron-cored coil when an alternating current is superimposed on a direct current. Figure 903 shows the Hay bridge arranged to measure the effective a-c or incremental inductance of an iron-cored coil with d-c magnetization. It will be noted that condensers and choke coils are used to confine the d-c and a-c components to the proper paths. Resistor R_3 should be reasonably low in value, since it must have current-carrying capacity sufficient for the coil being meas-

---

[35] S. Sabaroff, *Proc. I.R.E.*, March, 1939, p. 208.

[36] *Electrician* (London), March 15, 1935.

[37] Dunmore and Engel, *Bur. of Stds. Sci. Paper* 469, 1933; also *Sci. Paper* 469, 1924.

[38] Aijaz Mohammed and S. R. Kantebet, *Proc. I.R.E.*, November, 1931, p. 1983.

[39] J. Barton Hoag, *ibid.*, vol. 18, p. 513, March, 1930.

[40] Thomas Spooner, *Trans. A.I.E.E.*, vol. 42 (1923), p. 340.

ured. When the bridge is balanced, the inductance is given by:

$$L_x = R_2R_3C_1/(1 + \omega^2R_1^2C_1^2) \quad . \quad . \quad . \quad . \quad . \quad . \quad . \quad (5)$$

and the coil resistance by:

$$R_x = (R_1R_2R_3\omega^2C_1^2)/(1 + \omega^2R_1^2C_1^2) \quad . \quad . \quad . \quad . \quad . \quad (6)$$

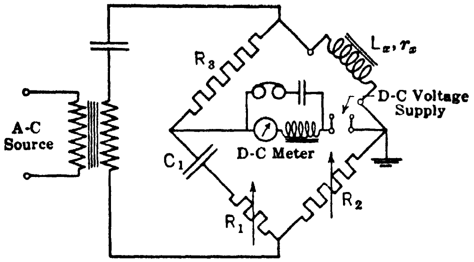

Fig. 903. Hay bridge arranged to measure effective inductance of an iron-cored coil carrying direct current.

The three-voltmeter method of impedance measurement may also be used to measure incremental inductance. Figure 904 shows the circuit and vector diagrams interpreting this method. The solution gives:

$$\cos\theta_x = (E_T^2 - E_R^2 - E_x^2)/(2E_RE_x) \quad . \quad . \quad . \quad . \quad . \quad (7)$$

$$L_x = (RE_x \sin\theta_x)/(\omega E_R) \quad . \quad . \quad . \quad . \quad . \quad . \quad . \quad . \quad . \quad (8)$$

$$r_x = (RE_x \cos\theta_x)/E_R \quad . \quad . \quad . \quad . \quad . \quad . \quad . \quad . \quad . \quad . \quad . \quad (9)$$

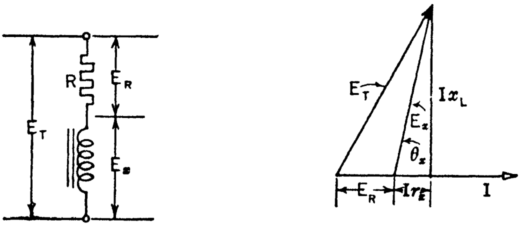

Fig. 904. Three-voltmeter method of impedance measurement.

1219. EXPERIMENT 60-C. — Measurement of the Inductance of an Iron-Cored Coil Carrying Direct Current (Voltmeter Method). — The general scheme involves connecting the coil in series with a known standard resistance and establishing proper values of direct current in the coil and alternating voltage across the coil. Voltages are measured by a vacuum-tube voltmeter affected only by a-c voltages. In most instances, the losses in the coil may be neglected when L_x is measured and the simple circuit of Fig. 905 may be used. The standard resistance value (R) is a compromise among the requirements of sufficient current-carrying capacity for the direct current, high enough value to give accuracy and low enough value to permit the necessary direct current to be obtained with a reasonably low d-c voltage supply. A wide-range vacuum-tube voltmeter will permit sufficient accuracy to be obtained with lower values of R, since it may be adapted to read accurately both the voltage E_x across the coil and the much lower voltage E_R across the standard resistor. A tuned amplifier connected to a copper oxide rectifier meter makes a satisfactory voltmeter, since it can be arranged with a condenser in series with one input terminal to measure a-c voltage only. A volume control on the amplifier will make it possible to measure a wide range of voltage. A calibrating arrangement must be provided, however, so that the readings for any volume control setting may be converted into volts.

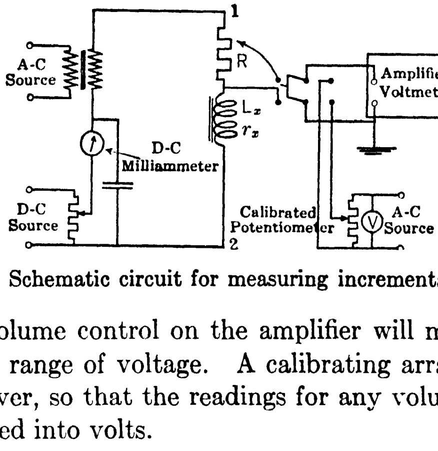

FIG. 905. Schematic circuit for measuring incremental inductance.

To measure the inductance using the circuit of Fig. 905, the d-c current through the coil and the a-c voltage across the coil are adjusted to the desired values. The a-c source may conveniently have a frequency of 60 cycles per second. The a-c voltages across the resistor R and the coil are now measured by the vacuum-tube amplifier voltmeter. The ungrounded voltmeter terminal is connected to point 1 to measure voltage across R and to point 2 for the coil voltage. A convenient reading is obtained on the indicating meter in each case by manipulation of the volume control, immediately after which the double-pole switch is thrown to the calibrating position and the potentiometer adjusted to give the same deflection. Readings should be taken in this way, maintaining the desired constant value of a-c voltage across the coil and varying the d-c current from zero to the maximum value. It should be noted that the incremental inductance will depend upon the magnetic history of the core material. The coil impedance is given by:

$$|Z_x| = (E_x R)/E_R$$

This is the reactance of the coil when r_x is neglected, as it may be in the vast majority of cases; and thus L_x may be calculated. The curve of L_x *vs.* d-c current may then be plotted.

When r_x is to be considered, the more elaborate circuit of Fig. 906 is used. This permits a measurement of L_x and r_x by the three-voltmeter method (see §1218). The commutating switch is necessary, since the voltmeter readings are taken with a vacuum-tube voltmeter with one terminal at ground potential. With the commutating switch in position A, the voltage across the coil (E_x), and the total voltage (E_T) are measured. The switch is then thrown to position B, when a check is made to maintain the same value of E_T, after which E_R is measured.

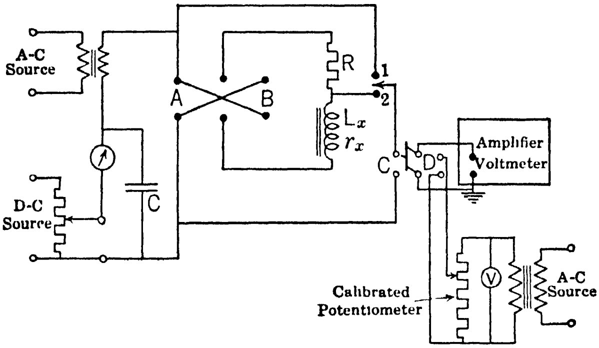

FIG. 906. Circuit for measuring incremental inductance when coil resistance is considered.

The amplifier voltmeter is connected to the calibrating network immediately after each reading. Equations (8) and (9) are used to solve for L_x and r_x.

1220. Inductance Coils. — The characteristics of a coil are subject to wide variation with frequency. Ordinary iron-core coils with the proper air-gap have satisfactory properties at low frequencies, but hysteresis and eddy-current losses limit their frequency range. Special alloy dust cores may be used for coils operating in the lower radio-frequency ranges.[41] At high radio frequencies, even air-core coils must be carefully designed to secure low losses and low distributed capacitance. Inductance coils are in general designed for a rather limited frequency range. A number of approximate formulas[42] have been developed for calculating the inductance of coils having special shapes, but one must eventually rely upon measurements to determine inductance coil characteristics in the frequency range desired. For preliminary design of single-layer coils, the Nagaoka formula:

---

[41] W. J. Polydoroff, *Proc. I.R.E.*, vol. 21, p. 690, May, 1933.

[42] Bureau of Standards, *Circular* 74; also *Sci. Paper* 169.

$$L = (0.03948a^2n^2)/bK \text{ microhenries} \quad . \; . \; . \; . \; . \quad (10)$$

is useful. a is the coil radius in centimeters measured from the axis to the center of any wire, b is the length of coil in centimeters, n is number of turns, and K is a function of $2a/b$ given in Fig. 907. The inductance of a multilayer coil with rectangular cross-section (Fig. 908) is given by:

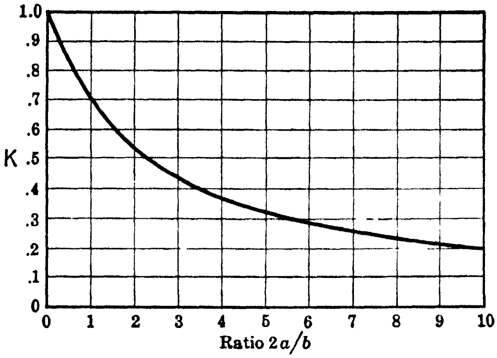

FIG. 907. The factor K as a function of the ratio $2a/b$.

$$L = (0.32a^2n^2)/(6a + 9b + 10c) \text{ microhenries} \quad . \; . \; . \quad (11)$$

The apparent inductance of a coil at high frequency is altered by skin effect and distributed capacity between coil turns. Over the limited operating frequency range of the coil, the effect of distributed capacitance is represented by a single capacitance connected across the coil terminals. For a single-layer coil, the value of this capacitance in micro-microfarads is of the order of magnitude of the radius of the coil in centimeters. Multilayer coils employ banked windings, honeycomb windings, or other means to lower the distributed capacitance. Over the usual working range, the inductance coil may be represented by the equivalent cir-

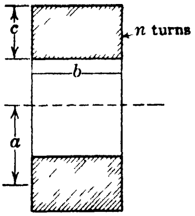

FIG. 908. Multilayer inductance coil; dimensions for eq. (11).

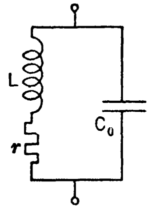

FIG. 909. Equivalent circuit of an inductance coil.

cuit of Fig. 909. The apparent inductance will then be:

$$L_a = \frac{L - C_0(r^2 + \omega^2 L^2)}{\omega^2 C_0^2 r^2 + (\omega^2 L C_0 - 1)^2} \quad . \; . \; . \; . \; . \; . \; . \; . \quad (12)$$

When r is negligible,

$$L_a = L/(1 - \omega^2 L C_0) \quad . \; . \; . \; . \; . \; . \; . \; . \; . \; . \quad (13)$$

and the apparent inductance will increase with frequency. At some frequency beyond the useful frequency range for the coil, the distributed capacity will cause the coil to behave more like a condenser. It is quite inaccurate to represent a coil over an extremely wide frequency range by the simple equivalent circuit of Fig. 909.

1221. EXPERIMENT 60-D. — Measurement of the Apparent Inductance, True Inductance, and Distributed Capacitance of a Coil. — The method comprises essentially a measurement of the capacitance necessary to produce series resonance with the coil for a number of frequencies over a range. Specific directions are given for frequencies in the audio and supersonic range, although the method may be used for other frequencies. Figure 910 shows the arrangement of apparatus. A sensitive resonance detector is desirable in order that L_x may be coupled loosely to the oscillator output coil. An amplifier and copper oxide rectifier meter will admirably serve the purpose for tests in the audio and supersonic frequency range. The amplifier pick-up coil is oriented to eliminate electromagnetic coupling with the oscillator output coil, but L_x is so placed as to have coupling with the oscillator output coil and with the amplifier pick-up coil. C is a high-grade decade-plus-air condenser with an accurate calibration.

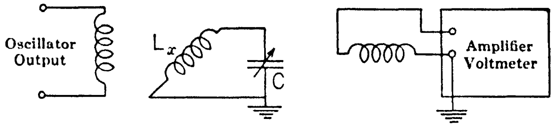

FIG. 910. Schematic arrangement for measurement of inductance coil parameters.

With the oscillator set for a frequency near the middle of the desired range, C is varied until resonance is obtained as indicated by maximum reading of the amplifier voltmeter. The amplifier volume control is manipulated to keep the indicator on scale. It is important to have resonance for the fundamental and not with some harmonic of the oscillator output. The value of C to produce resonance is approximately proportional to the inverse square of the frequency. This check will assure one that the fundamental and not a harmonic is being used, after one point has been definitely located. Readings of C to produce resonance should be obtained for frequencies at least over the range where the coil might be used. It is important to have accurate values for C and f.

From the data obtained, the value of apparent inductance $L_a = 1/(\omega^2 C)$ may be plotted as a function of frequency. The extrapolation of this curve to zero frequency will give the true coil inductance. If values of $1/f^2$ are plotted *vs.* C, the best straight line through the series of points will intercept the X axis at a point which determines the distributed capacity C_0, as shown by Fig. 911. From the slope of this straight line the value of L may also be calculated. The above statements follow from a consideration of the equation:

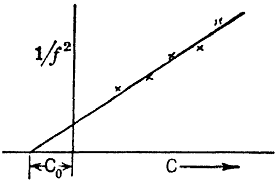

FIG. 911. Graphical method for evaluating the inductance and distributed capacitance of a coil.

$$1/f^2 = 4\pi^2 LC_0 + 4\pi^2 LC \quad . \quad . \quad . \quad (14)$$

which is a consequence of the resonance condition. The points used for the graphical determination should be limited to a frequency range where the coil is to be used. The distributed capacitance and consequently the inductance may be calculated from measurements at two frequencies, using the formula:

$$C_0 = \frac{C_1 - k^2 C_2}{k^2 - 1} \quad . \quad . \quad . \quad . \quad . \quad . \quad . \quad . \quad . \quad (15)$$

where C_1 is the capacitance of the standard condenser to produce resonance at a frequency f_1, C_2 is the capacitance at frequency f_2, and $k = f_2/f_1$. The student should derive this formula, using eq. (14) above. It is obvious that an accurate value for the two frequencies is not necessary when harmonics from a given source are used, since it is the frequency ratio that is important.

1222. Condensers at High Frequencies. — Of all high-frequency circuit elements, capacitance may be secured in the purest form. At audio frequencies and low radio frequencies, a condenser (§590) may be represented by the equivalent circuit of Fig. 912(a) or (b). At very high radio frequencies, the series inductance becomes important and must be included in the circuit.[43] The equivalent parallel conductance $g = 1/R_p$, or the equivalent series resistance R_s, represents losses due to both series lead resistance and dielectric loss, of which the latter is usually much more important. Analysis of the equivalent circuits gives:

---

[43] R. F. Field and D. B. Sinclair, *Proc. I.R.E.*, vol. 24, No. 2, p. 255, February, 1936.

$$C_p = (g^2 + \omega^2 C_s^2)/\omega^2 C_s \cong C_s \quad \ldots\ldots\ldots \quad (16)$$

and

$$R_s = g/(g^2 + \omega^2 C_s^2) \cong g/\omega^2 C_s^2 \quad \ldots\ldots \quad (17)$$

since $g^2 \ll \omega^2 C_s^2$.

The phase angle, which is the complement of the angle between the current and voltage in the condenser, is given by:

$$\tan \phi = g/\omega C_p = R_s \omega C_s \quad \ldots\ldots\ldots \quad (18)$$

For good condensers, this is seen to approximate the power factor quite closely. The power factor of good mica condensers is of the order of magnitude of 0.1 per cent, but is subject to variation with temperature and humidity. The power factor is almost constant, with frequency up to 1 or 2 megacycles. For air condensers where the losses are principally associated with the dielectric material in the stator supports, the quantity $R_s \omega C^2 = g/\omega = 1/R_p\omega = k$ is approximately a constant and is accordingly used as a figure of merit. For precision air condensers, the insulating material used is either " isolantite " with a resulting figure of merit of the order of 0.05×10^{-12}, or quartz with a figure of merit of 0.2×10^{-14}.

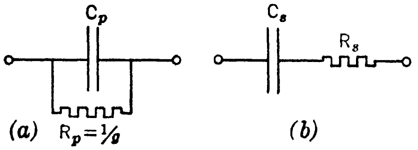

FIG. 912. Equivalent circuits of a defective condenser.

1223. EXPERIMENT 60-E. — Measurement of the Capacitance and Phase Angle of a Condenser by the Substitution Method. — One of the objects of this experiment is the illustration of the substitution method, and many variations from the specific procedure outlined are possible. An equal-arm capacitance bridge is used that is reasonably well shielded and that may be connected according to the circuit of the full-line diagram of Fig. 913, or including the shunting resistances, R_B and R_3, shown dotted. The former circuit has practical advantages for condensers that are not too large in value, and the latter is better for condensers of larger value. For the purposes of this experiment, a variable air condenser will be calibrated, using the full-line diagram of Fig. 913, and the capacitance and phase angle of a fixed condenser will be measured after the bridge is reconnected according to the circuit of Fig. 913 including R_B and R_3.

Referring to Fig. 913, C is a high-grade precision variable air condenser, C_B is a good variable condenser for which a calibration is not necessary, and R is a standard decade resistor with a maximum value of about 10,000 ohms, usually built into the shielded bridge. Stiff bare wire leads should be used to connect condensers to the bridge. Variable resistance R may be switched either in series with C_B or into the arm with C. When the bridge is balanced, the equivalent series capacitance of arm B is equal to the equivalent series capacitance of the arm containing C_x and C and likewise with the equivalent series resistances. With C_B at a fixed value, the sum $C_x + C$ must be constant for bridge balance. The balance may be disturbed by decreasing C_x, but may be restored by increasing C a corresponding amount, so that ΔC_x may be measured in terms of ΔC.

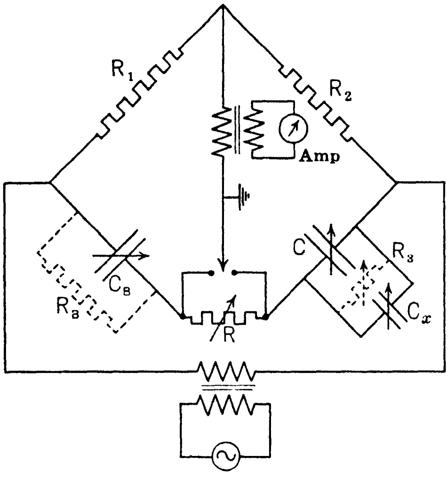

FIG. 913. Bridge circuit for the measurement of capacitance by substitution.

To proceed, C_x is set for its maximum value and C to a low value just sufficient to keep on the straight-line portion of its calibration curve. C_B is then adjusted for approximate bridge balance. More exact bridge balance is then obtained by alternately changing C and R. The reading of C_x is now lowered a fixed amount, and a new balance obtained by adjustment of C and R. This process of lowering the capacitance of C_x and increasing C, the substitution of ΔC for ΔC_x, to obtain bridge balance, is repeated until C has been increased to within 10 or 15 per cent of its maximum value, or until C_x has been reduced to its minimum reading. If the maximum value of C is reached before the minimum value of C_x, a new setting of C_B must be made. With C_x set at the point where bridge balance was last obtained, C is reduced to within about 15 per cent of its lowest scale reading, and C_B adjusted for approximate bridge balance. The final balancing is accomplished by adjusting C and R. The method following the start of the experiment is then continued. It will be noted that only the change in C_x is measured by this procedure. To secure the calibration curve for C_x the absolute value must be established for at least one point. This is usually done for the minimum or zero reading of the unknown condenser by adjusting C for balance when the lead to the high side of C_x has been disconnected and moved away from the terminal about ½ inch with as little disturbance to the remainder of the circuit as possible. The change in C necessary to restore bridge balance when C_x is connected and disconnected is the absolute value of C_x at the zero reading. The calibration curve for the unknown condenser may now be plotted. The change in R to maintain bridge balance when C_x is connected and disconnected may be used to determine the equivalent series resistance of the unknown condenser and consequently the phase angle of the condenser by considering:

$$R_x = \Delta R(C^2/C_x^2) \quad . \quad . \quad . \quad . \quad . \quad . \quad . \quad . \quad . \quad (19)$$

This is derived from a more exact expression by assuming that $\omega^2 R_x^2 C_x^2 C'$ is negligible compared to $C_x + C'$. C is the value of the standard condenser to obtain balance when C_x is disconnected, and C' is the value of the standard condenser when C_x is connected. The student should derive eq. (19).

When the bridge of Fig. 913 is reconnected to include R_B and R_3, R_B should be a 10,000-ohm standard resistance unit, and R_3 a high-grade decade resistance box. The procedure is essentially the same as for the first part of the experiment. With the unknown condenser connected, C is set to a low point on the scale and C_B is adjusted for approximate balance. The final balance is obtained by adjusting C and R_3. Another set of readings is obtained when the high side of C_x is disconnected and C and R_3 again adjusted for bridge balance. The results are:

$$C_x = C_2 - C_1 \quad . \quad . \quad . \quad . \quad . \quad . \quad . \quad . \quad . \quad (20)$$

where C_1 is the value of C with C_x connected, and C_2 is the value of C when C_x is disconnected. And

$$g_x = g_{s2} - g_{s1} = (R_{31} - R_{32})/R_{31}R_{32} \cong (R_{31} - R_{32}) \times 10^{-8} \text{ mho} \qquad (21)$$

where R_{31} is the value of R_3 when C_x is connected, and R_{32} is the value of R_3 when C_x is disconnected.

1224. Resistance of Conductors at High Frequencies. — The resistance of conductors is increased at high frequencies on account of skin effect, or the change in current distribution in the conductor. The effective resistance of a conductor system is also influenced by inductance and capacitance effects, but for a straight wire not too close to other conductors the skin effect in the conductor is the major factor in determining the resistance at high frequencies. The ratio of high-frequency resistance to d-c resistance, R/R_0, may be calculated by a method due to Lord Kelvin.[44] Tables of R/R_0 based on the Kelvin formula are given in *Scientific Paper* 169 of the U. S. Bureau of Standards and also in Bureau of Standards *Circular* 74. It should be noted that skin effect is greater for wires of large radius and high conductivity. A useful empirical relation[45] from which the skin-effect ratio for round wires may be calculated is given by:

$$\begin{aligned} R/R_0 &= 1 + 0.005M^4 && 0 < M < 2 \\ &= 1 + 0.078(M - 1)^2 && 2 < M < 4 \\ &= 0.355M + 0.256 && M > 4 \end{aligned}$$

where $M = 0.02768\sqrt{(\mu f)}/R_0$.

μ = the permeability of the conductor material.

f = the frequency, and R_0 is the d-c resistance in ohms per 1000 feet.

Calculations of the high-frequency resistance of simple coils may be made,[46] but for most circuit elements the effective resistance at a high frequency can best be determined by measurement. The effective resistance is the quantity which, when multiplied by the square of the current, gives the power dissipation. When effective resistance is to be determined accurately with an arbitrary wave form and frequency, the differential calorimeter method given by Hund[47] is the most reliable.

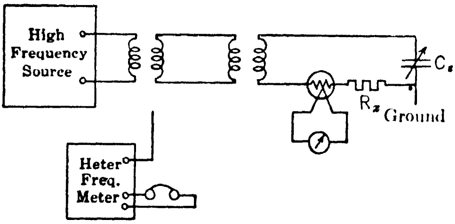

FIG. 914. Circuit arrangement for measuring high-frequency resistance.

1225. EXPERIMENT 60-F. — Measurement of Resistance by Reactance Variation and Resistance Variation. — The unknown resistance may be that of a coil, a meter, or other piece of apparatus, in which case it should be measured with some consideration for the conditions under which it is to be used. The circuit should in general be arranged in accordance with Fig. 914. Rigid connections should be used so that all parts of the circuit will maintain their positions. It is important that the coupling with the test circuit shall be entirely inductive, and the introduction of a Faraday shield between the test circuit and the link coupling may be necessary in some cases. The oscillator should have sufficient output so that loose coupling may be employed. A heterodyne frequency meter is used to monitor the oscillator frequency, so that it may be kept constant. The output voltage should also be constant. Current in the test circuit is measured by a thermocouple meter.

---

[44] Kelvin, "Mathematical and Physical Papers," vol. 3, p. 491.

[45] Due to Dr. W. R. Work.

[46] A. J. Palermo and F. W. Grover, *Proc. I.R.E.*, vol. 18 (1930), p. 2031.

[47] A. Hund, "High Frequency Measurements," pp. 86 and 276, McGraw-Hill Book Co.

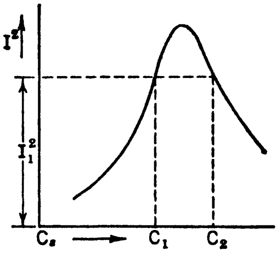

FIG. 915. The resonance curve used to calculate high-frequency resistance.

The test-circuit resistance with R_x short-circuited is first measured by the reactance-variation method. This consists in varying C through the range which passes through the resonance point and gives sufficient data to plot the curve of I^2 *vs.* C. By using particular values of I^2 from the resonance curve (see Fig. 915) it is possible to calculate the circuit resistance R_c. The particular values used are the resonance values where $I^2 = I_r^2 = E^2/R^2$ and $I^2 = I_1^2$ at two points on either side of the resonance point where C equals C_1 and C_2, respectively. Assuming that the voltage is constant and the equivalent series resistance in the condenser is negligible, or at least does not change, one arrives at the result:

$$R_c = \frac{C_2 - C_1}{2\omega C_2 C_1}\sqrt{\frac{I_1^2}{I_r^2 - I_1^2}} \quad . \; . \; . \; . \; . \quad (22)$$

If $I_1^2 = I_r^2/2$,

$$R_c = (C_2 - C_1)/(2\omega C_2 C_1) \quad . \; . \; . \; . \; . \; . \; . \; . \quad (23)$$

The student should carry through the derivation of eq. (22) as an exercise.

An unknown resistance (R_x) may now be inserted in the circuit and a new resonance curve obtained. The unknown resistance is given by the difference between the calculated circuit resistances in the two cases. It is important that the standard condenser be of a high-grade low-loss design, since this method depends upon the assumption of negligible condenser loss.

For successful use of the resistance variation method, standard resistance units whose values are known accurately are necessary. These may be conveniently uniform lengths of manganin or constantin resistance wire of small diameter to secure low skin-effect ratio. They may be mounted on an insulating strip provided with plugs to fit into jacks.

In this way different values of resistance may be plugged into the circuit without altering the circuit inductance. The d-c resistance of these units with their dimensions will enable one to calculate the skin-effect ratio and the high-frequency resistance. It will generally be possible to use a diameter small enough to give a negligible skin effect.

In making the measurement by resistance variation, the resonance current is noted when a short-circuiting link is inserted in the jacks provided for the standard-resistance links. The resonance current is again recorded when the short-circuiting link is replaced by one of the standard-resistance links. Since the resonance current is limited only by the total resistance of the circuit and the voltage is assumed to be constant, the circuit resistance is given by:

$$R_c = [I_1/(I_0 - I_1)]R_3$$

where I_0 is the resonance current with the short-circuiting link in place, and I_1 is the current with the standard-resistance link (R_3) inserted. To measure an unknown resistance, the circuit resistance R_c is measured again with the unknown connected in series in the circuit, and the difference between the two circuit resistances gives the value of the unknown resistance.

1226. EXPERIMENT 60-G. — Measurement of High Resistance (Low Conductance) at High Frequencies. — Obvious difficulties are encountered when an attempt is made to measure high resistances by the method of Experiment 60-F. Accordingly a method employing the parallel resonant circuit is used. For some of the details and derivations and a critical study of this method, as well as a rather complete bibliography, the reader is referred to an excellent article by D. B. Sinclair.[48] The circuit arrangement is given by Fig. 916. Rigid circuit connections should be employed. C_1 is a capacitance small enough to maintain essentially constant current to the parallel circuit when the admittance of this circuit is changed during the measurement. The vacuum-tube voltmeter should have an input impedance high compared to the parallel resonant impedance of the tuned circuit.

The conductance of the circuit is first measured with g_x disconnected by taking two sets of readings of voltage and capacitance, one with $C_s = C_r$ when $V = V_r$, the maximum or essentially the resonance value; and another when $C_s = C_1$, an arbitrary value, and $V = V_1$. Assuming that the current to the circuit does not change, the circuit conductance,

$$g = \frac{(C_1 - C_r)}{\sqrt{(V_r/V_1)^2 - 1}} \quad . \; . \; . \; . \; . \; . \; . \; . \; . \; . \quad (24)$$

---

[48] D. B. Sinclair, *Proc. I.R.E.*, vol. 26, No. 12, p. 1466, December, 1938.

When g_x is added, the new circuit conductance will be $g + g_x$, which may be measured in the same way; and consequently g_x may be determined.

If a standard conductance, g_s (high resistance) is available, the circuit conductance may be measured by taking two resonance voltage readings. The one reading, V_{r1}, is taken when g_s is disconnected; and the other, V_{r2}, is taken when g_s is connected. The circuit conductance is then given by:

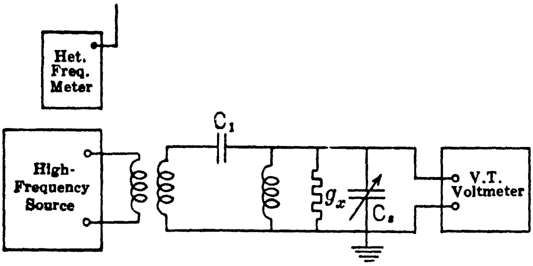

FIG. 916. Arrangement of apparatus for measuring a low conductance (or high resistance) at high frequencies.

$$g = \frac{g_s}{(V_{r1}/V_{r2}) - 1} \quad . \; . \; . \; . \; . \; . \; . \; . \; . \; . \quad (25)$$

The derivation of this formula is readily made if we assume C_1 small enough to keep the current constant irrespective of changes in the parallel resonant circuit impedance. An unknown conductance g_x is measured by making two measurements of circuit conductance, one with g_x connected and one with g_x disconnected.

1227. Properties of Lines and Filters. — The general theory of long lines with distributed parameters is developed in Chapter XXX. Some of these relations may be applied to filter sections and four-terminal networks in general. Consider the four-terminal network of Fig. 917. This may consist of any configuration of impedances between input and output terminals. Equations (34) and (35) on p. 81 will apply if it is a symmetrical network. If it is unsymmetrical, then the following similar equations may be written:

$$E_1 = AE_2 + BI_2 \quad . \; . \; . \; . \; . \; . \; . \; . \; . \; . \quad (26)$$

$$I_1 = DI_2 + CE_2 \quad . \; . \; . \; . \; . \; . \; . \; . \; . \; . \quad (27)$$

where A, B, C, and D are functions of the circuit parameters.

Three simple types of symmetrical networks that are frequently encountered in filters and other communication circuits are shown in

Fig. 918. The use of these networks, or at least the mathematical theory, is based upon operation into an infinite line of like sections or, what is equivalent, working into the iterative or characteristic impedance. The iterative impedance may be considered as the input impedance of a line made up of an infinite number of like sections, or the input impedance of a single section when it is terminated by an impedance equal to the input impedance. For the structures shown in Fig. 918, the characteristic impedances in terms of the circuit impedances are:

For the T section $Z_{KT} = \sqrt{Z_1Z_2 + (Z_1^2/4)}$ . . (28)

For the π section $Z_{K\pi} = (Z_1Z_2)/Z_{KT}$ . . . . (29)

For the lattice section $Z_{KL} = \sqrt{Z_1Z_2}$ . . . . . . (30)

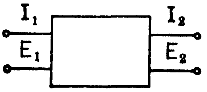

FIG. 917. A four-terminal network.

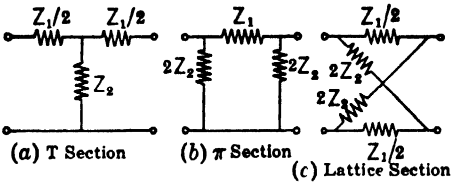

(a) T Section (b) π Section (c) Lattice Section

FIG. 918. Types of symmetrical four-terminal networks.

As shown in §652, the characteristic impedance of a transmission line may be determined by open- and short-circuit tests. This will also provide a basis for derivation of eqs. (28), (29), and (30).[49]

If the transmission line is terminated in its characteristic or surge impedance:

$$E_2/I_2 = Z_0$$

and this relation substituted in eqs. (28) and (29), Chapter XXX, yields the following important result:

$$E_1/E_2 = I_1/I_2 = \epsilon^{mS} \quad . \ . \ . \ . \ . \ . \ . \ . \ (31)$$

A corresponding relation may be given for a line of sections like Fig. 918*a*, *b*, or *c* terminated in their iterative impedance; i.e.:

$$E_1/E_2 = I_1/I_2 = \epsilon^{n\gamma} \quad . \ . \ . \ . \ . \ . \ . \ . \ (32)$$

This serves as a definition of complex "propagation constant" or propagation function, γ, where n is the number of sections. γ is used in the place of m to emphasize that it is evaluated per section rather than per unit length of line. For both the T and π sections of Fig. 918*a* and *b*, the propagation function is given by

---

[49] For an unsymmetrical network, the impedances which terminate each end of the structure and cause no reflection are known as image impedances. These may be determined by open- and short-circuit tests. See K. S. Johnson, "Transmission Circuits for Telephonic Communication," Western Electric Co., pp. 74–76.

$$\epsilon^{\gamma} = 1 + Z_1/2Z_2 + Z_{KT}/Z_2 \quad \ldots \quad (33)$$

or

$$\epsilon^{\gamma} = (1 + Z_1/2Z_2) + \sqrt{(1 + Z_1/2Z_2)^2 - 1} \quad \ldots \quad (34)$$

From this:

$$\cosh \gamma = 1 + Z_1/2Z_2 \quad \ldots \quad (35)$$

The lattice section of Fig. 918*c* has a propagation function given by:

$$\epsilon^{\gamma} = \frac{1 + \sqrt{Z_1/4Z_2}}{1 - \sqrt{Z_1/4Z_2}}$$

and

$$\tanh \gamma = \frac{\sqrt{Z_1 Z_2}}{Z_1/4 + Z_2} \quad \ldots \quad (36)$$

Equations (35) and (36) above are important as the starting point in establishing the pass and reject bands of electric wave filters. For the theory and design of filters, the reader is referred to other sources.[50, 51, 52]

To illustrate the meaning of γ, we may write:

$$\epsilon^{\gamma} = \epsilon^{\alpha}\epsilon^{j\beta} = A\epsilon^{j\beta}$$

and

$$\alpha = \log_{\epsilon} A = \log_{\epsilon} \left|\frac{E_1}{E_2}\right| = \log_{\epsilon} \left|\frac{I_1}{I_2}\right| \quad \ldots \quad (37)$$

The real part of the propagation function is thus seen to be the ratio of the magnitudes of input to output voltage or current expressed in logarithmic units. This unit has been designated as the *neper*. Another logarithmic unit used to represent current and voltage ratio is the *decibel*. The use of the decibel to measure current and voltage ratio is derived from the fundamental definition as a unit of power ratio. It may be expressed thus:

$$N = 10 \log_{10} P_1/P_2 \quad \ldots \quad (38)$$

---

[50] G. A. Campbell, "Collected Papers," American Telephone & Telegraph Co., 1937.

[51] T. E. Shea, "Transmission Networks and Wave Filters," D. Van Nostrand Co., 1929.

[52] O. J. Zobel, *Bell Sys. Tech. Jour.*, vol. 2, No. 1, p. 1, January, 1923; vol. 3, p. 567, October, 1924; vol. 10, p. 284, April, 1931.

where N is the number of decibels (db) and P_1/P_2 is the power ratio. When we choose to deal with identical impedances, this becomes:

$$N = 20 \log_{10} E_1/E_2 = 20 \log_{10} I_1/I_2 \quad . \; . \; . \; . \; . \quad (39)$$

If the impedances are not the same:

$$N = 20 \log_{10} E_1/E_2 - 10 \log_{10} (Z_1/Z_2) - 10 \log_{10} \cos \theta_1/\cos \theta_2 \quad (40)$$

Using (37) and (39), we may convert from nepers to decibels by writing:

$$N_{\text{db}} = 8.686\alpha_{(\text{nepers})} \quad . \; . \; . \; . \; . \; . \; . \; . \; . \quad (41)$$

1228. Equivalent Networks. — The use of equivalent structures is not only an aid in circuit analysis, but is also helpful in designing structures for attenuation purposes. The relations expressing equivalence between T and π networks are identical with those for " wye " and " delta " structures (see §747) when the proper nomenclature is adopted. A lattice may be converted to an equivalent T network by the relations shown in Fig. 919, and any symmetrical four-terminal network expressed in terms of its iterative impedance and complex propagation constant may be represented by the equivalent T of Fig. 920. This result may be obtained by following the general method of §652 for transmission lines, from which we will obtain:

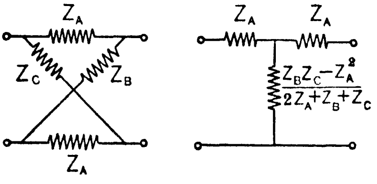

FIG. 919. Lattice network and its equivalent T network.

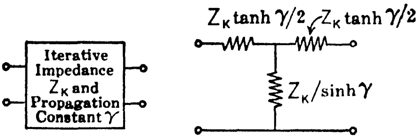

FIG. 920. General four-terminal network and its equivalent T.

$$Z_{oc} = Z_K \operatorname{cotanh} \gamma \quad . \; . \; . \; . \; . \; . \; . \; . \; . \quad (42)$$

and

$$Z_{sc} = Z_K \tanh \gamma \quad . \; . \; . \; . \; . \; . \; . \; . \; . \; . \quad (43)$$

If we consider open- and short-circuit impedances for the T section (see Fig. 918*a*), we have:

$$Z_{oc} = Z_1/2 + Z_2 \quad \ldots\ldots\ldots\ldots \quad (44)$$

$$Z_{sc} = Z_1/2 + Z_1Z_2/(Z_1 + 2Z_2) \quad \ldots\ldots \quad (45)$$

or

$$Z_1/2 = Z_{oc} - Z_2 \quad \ldots\ldots\ldots\ldots \quad (46a)$$

and

$$Z_2 = \sqrt{(Z_{oc} - Z_{sc})Z_{oc}} \quad \ldots\ldots\ldots \quad (46b)$$

Substituting (42) and (43) in (46*a*) and (46*b*), and using the necessary hyperbolic identities, we find:

$$Z_2 = Z_K/\sinh \gamma \quad \ldots\ldots\ldots\ldots \quad (47a)$$

and

$$Z_1/2 = Z_K \tanh \gamma/2 \quad \ldots\ldots\ldots\ldots \quad (47b)$$

This result applies to a transmission line if we replace γ by ml and to a line of n iterated sections if γ is replaced by γn.

The equivalence relations of Fig. 920 may be used advantageously in the design of resistance networks whose function is to introduce predetermined values of attenuation and have a definite characteristic or iterative impedance. These are known as attenuation boxes, attenuators, or pads. The design will be carried through for a simple T attenuator. Suppose that the attenuation desired is 15 db and the characteristic impedance into and out of which the attenuator must work is 500 ohms. With pure resistances in the network, $\beta = 0$, $\gamma = \alpha$

$$15 \text{ db} = \frac{15}{8.686} = 1.727 \text{ nepers}$$

$$Z_1/2 = R_1/2 = 500 \times \tanh \frac{1.727}{2} = 349.0 \text{ ohms}$$

$$Z_2 = R_2 = \frac{500}{\sinh 1.727} = \frac{500}{2.722} = 183.7 \text{ ohms}$$

and the T attenuator will have the values indicated in Fig. 921. If we designate the ratio $(I_1/I_2) = (E_1/E_2)$ by k, then $k = \log_{10}^{-1} (N/20)$, where N is the attenuation in decibels, and the T pad may be designed by using the formulas:

$$R_1/2 = (Z_K) \cdot (k - 1)/(k + 1) \quad \ldots\ldots \quad (48)$$

$$R_2 = (Z_K) \cdot (2k)/(k^2 - 1) \quad \ldots\ldots\ldots \quad (49)$$

The student may easily derive eqs. (48) and (49) by an elementary circuit analysis of the T network and then use them to check the results obtained for the example above. Convenient formulas and tables have been prepared for calculating the design of many different types of attenuators[53, 54] to work between equal or unequal impedances.

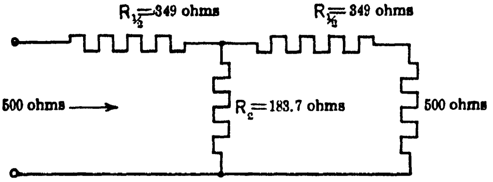

FIG. 921. A 15-db " T " attenuator to work into and out of 500 ohms.

1229. EXPERIMENT 60-H. — Calibration of an Attenuator and Design of a Power-Level Indicator. — Any type of attenuator available may be used to illustrate the design and use of these networks. If a variable attenuator is used, the value of the several resistances in the circuit should be measured by a Wheatstone bridge for three or four settings of the attenuator. From these readings, the attenuation should be calculated and compared with the nominal values. The attenuation should also be checked by measurement of input and output voltage when the attenuator is properly terminated. A vacuum-tube voltmeter, or at least a meter with an input impedance that is high compared to the terminating impedance of the attenuator, should be used. An alternative method is to use a calibrated potentiometer or resistors to form a potentiometer as shown in Fig. 922. The voltmeter need not have a calibration, but should have a high input impedance. When the voltmeter reads the same with the switch in either position, the attenuation through the attenuator is equal to that through the potentiometer, and the attenuation may be calculated from the potentiometer settings. An attenuator will have a frequency error due to distributed inductance and capacitance in the resistance units and in the box wiring. This may be checked by making a variable frequency run by the above methods with a vacuum-tube voltmeter having negligible frequency error or a potentiometer with a good frequency characteristic.

As part of this experiment, the student should design a power-level meter after the schematic circuit of Fig. 923. The meter proper is a 1-milliampere or 500-microampere d-c instrument connected to a full-

---

[53] P. K. McElroy, *Proc. I.R.E.*, vol. 23, No. 3, p. 213, March, 1935. Also correction, *Proc. I.R.E.*, vol. 23, No. 6, p. 682, June, 1935.

[54] R. E. Blakey, " Electronics Reference Sheets," Fourth Edition, McGraw-Hill Book Co.

wave copper oxide rectifier. The resistance R_m consists of the meter and rectifier resistance plus an external resistor having at least five times the rectifier meter resistance. This tends to mask the variable resistance characteristic of the copper oxide rectifier. The meter with its L-type attenuator is to be used to read power level in decibels above and below a certain reference level. A convenient zero level is 1.732 volts, which represents 6 milliwatts into a 500-ohm load. The meter is first calibrated as a voltmeter without R_1 and R_2 connected. The values of R_1 and R_2 are then calculated to give half-scale deflection on the meter when 1.732 volts is applied to the input terminals. A further requirement used in designing the attenuator is that the input resistance shall be maintained at a constant value, say 5000 ohms. Values of R_1 and R_2 should be calculated to give levels of 5–30 db in 5-db steps. The curve of decibels *vs.* actual scale reading of the meter should also be plotted. The calculations should be checked at a few points by setting up the circuit and making measurements.

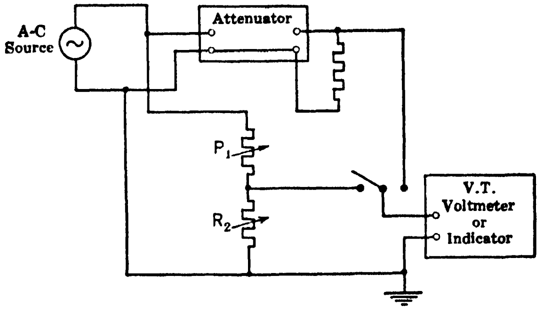

Fig. 922. Method of calibrating an attenuator.

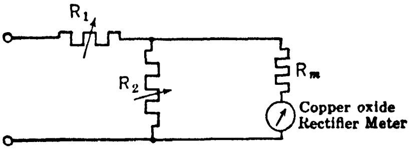

Fig. 923. Schematic circuit of power-level meter.

1230. EXPERIMENT 60-I. — Determination of the Characteristics of Four-Terminal Networks. — Some general methods apply to the measurement of the overall characteristics of four-terminal networks, whether they are filters, artificial lines, or other circuit elements. The exact method and procedure must be modified to suit the particular network and frequency range. Networks which normally operate with one side grounded should be measured with this condition satisfied by the measuring circuit. Four-terminal networks balanced to ground require a method of measurement that preserves this condition.

The open-circuit and short-circuit impedances may be used to calculate the characteristic or iterative impedance and propagation constant of a network from the relations:

$$Z_K = \sqrt{Z_{oc}Z_{sc}} \qquad (50)$$

and

$$\tanh \gamma = \sqrt{Z_{sc}/Z_{oc}} \qquad (51)$$

The value of $\gamma = \alpha + j\beta$ may be determined[55] from the consideration that if

$$\tanh \gamma = A + jB \qquad (52)$$

$$\tanh 2\alpha = 2A/(1 + A^2 + B^2)$$

$$\tan 2\beta = 2A/[1 - (A^2 + B^2)] \qquad (53)$$

To evaluate β from eq. (53), one must have some idea of its approximate value.

Impedance measurements are made between one pair of terminals, first when the pair at the opposite end are open-circuited and again when they are short-circuited. In a dissymmetrical network, measurements are made from both ends to determine the image impedances, which are given by:

$$Z_{I1} = \sqrt{Z_{oc}Z_{sc}} \qquad (54)$$

$$Z_{I2} = \sqrt{Z'_{oc}\,Z'_{sc}} \qquad (55)$$

These are the impedances between which the network may be used as a matching device (see note and reference at bottom of p. 788). In making the impedance measurements, a bridge method (see Chapter XXVIII) or the three-voltmeter method (described in §1218) may be used.

The attenuation as a function of frequency may be determined by a simple input and output voltage measurement with the network properly terminated. When tests are being made on filters or networks with highly selective characteristics, the wave form of the voltage source should be very good or a wave analyzer should be used to measure voltage to prevent serious error due to harmonic components. Attenuation may also be measured by a substitution method indicated schematically by Fig. 924. When the indicator or voltmeter reads the same with the switch in either position, the attenuation of the network is equal to that read on the adjustable attenuator.

---

[55] W. L. Everitt, "Communication Engineering," Second Edition, p. 169, McGraw-Hill Book Co.

The phase angle between input and output voltage of a network is not accurately measured by any simple method. Several schemes have been used,[56, 57, 58] some of which are more or less elaborate and have definite limitations. A method giving sufficient accuracy for many purposes is shown schematically by Fig. 925. It is essentially a substitution method. When the phase shifter is adjusted to give a straight line on the oscillograph screen, the phase change between input and output voltage of the four-terminal network is equal to that of the phase shifter. If the network is terminated in its characteristic impedance, this phase change is β, the imaginary part of the propagation function γ. The phase shifter shown in Fig. 925 includes an input transformer which

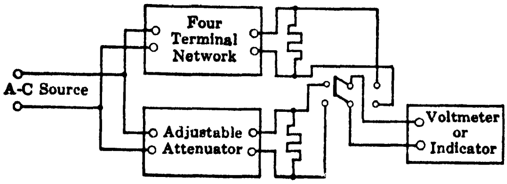

FIG. 924. Measurement of attenuation by substitution.

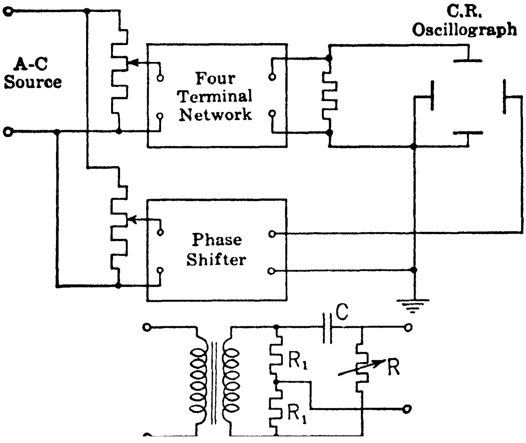

One Form of Phase Shifter

FIG. 925. Schematic arrangement for measurement of phase angle.

---

[56] W. L. Everitt, *op. cit.*, p. 311.

[57] J. L. Clarke, *Electronics*, July, 1938, p. 31.

[58] S. Bagno and A. Barnett, *ibid.*, January, 1938, p. 24.

must first be calibrated for phase shift. The phase change through the remainder of the network may be calculated. In some cases, an inductance may be employed instead of the condenser, C. If amplifiers are used on the horizontal and vertical plates of the oscillograph, they should be identical or at least should introduce identical phase shifts.

1231. Electromechanical Systems. — Owing to the similarity between the equations of motion for a mechanical system and the mesh equations for an electrical network, convenient analogies are possible. The following equations illustrate a typical set. A mechanical system with one degree of freedom will have the differential equation:

$$r_m \, dx/dt + m \, d^2x/dt^2 + x/C_m = f \quad \ldots\ldots \quad (56)$$

and a one-mesh electrical network has the equation:

$$r \, dq/dt + L \, d^2q/dt^2 + q/C = e \quad \ldots\ldots \quad (57)$$

Table I lists the data on the quantities in these equations which may be considered analogous. The units are chosen such that energy is measured in the same units in either system, which is especially advantageous when considering electromechanical systems. Other systems of units may be used,[59, 60] and in fact one may employ an entirely different set of analogies. The steady-state solution for mesh currents in a two-mesh network is obtained by solving the simultaneous equations:

$$I_1Z_{11} + I_2Z_{12} = E_1 \quad \ldots\ldots \quad (58)$$

$$I_1Z_{21} + I_2Z_{22} = E_2 \quad \ldots\ldots \quad (59)$$

where in general

$$Z_{11} = r_{11} + j\omega L_{11} - j/(\omega C_{11})$$

and

$$Z_{12} = r_{12} + j\omega L_{12} - j/(\omega C_{12}), \quad \text{etc.}$$

Also, the mutual impedances $Z_{12} = Z_{21}$, and in general $Z_{jk} = Z_{kj}$.

This scheme may be extended to an n-mesh network which will have n such Kirchhoff's law equations.[61] In a mechanical system such as an acoustic device, where the amplitudes are small enough to assume linearity in the impedances, the analogous equations would be:

$$\dot{X}_1Z_{11} + \dot{X}_2Z_{12} = F_1 \quad \ldots\ldots \quad (60)$$

$$\dot{X}_1Z_{21} + \dot{X}_2Z_{22} = F_2 \quad \ldots\ldots \quad (61)$$

---

[59] McIlwain and Brainerd, "High-Frequency Alternating Currents," Second Edition, p. 452, John Wiley & Sons, 1939.

[60] Olsen and Massa, "Applied Acoustics," p. 29, P. Blakiston's Son & Co.

[61] J. R. Carson, "Electric Circuit Theory," McGraw-Hill Book Co.; E. A. Guillemin, "Communication Networks," vol. 1, John Wiley & Sons.

TABLE I

QUANTITIES THAT MAY BE CONSIDERED ANALOGOUS IN MECHANICAL AND ELECTRICAL SYSTEMS

Mechanical System			Electrical Network		
Symbol	Quantity	Unit*	Symbol	Quantity	Unit
X	Displacement	cm	q	Charge	Coulomb
$\dot{X} = \frac{dx}{dt}$	Velocity	cm/sec	$i = \frac{dq}{dt}$	Current	Ampere
$\ddot{X} = \frac{d^2x}{dt^2}$	Acceleration	cm/sec²	$\frac{di}{dt} = \frac{d^2q}{dt^2}$	Time rate of change of current	amp/sec
f	Force	10^7 dynes	e	Voltage	Volt
m	Mass	10^7 grams	L	Inductance	Henry
r_m	Mechanical resistance	$10^7 \frac{\text{dyne sec}}{\text{cm}}$	r	Resistance	Ohm
C_m	Compliance	$10^{-7} \frac{\text{cm}}{\text{dyne}}$	C	Capacitance	Farad

There are many practical devices such as telephone receivers and vibration galvanometers in which a voltage is induced in an electrical circuit when a part of the mechanical system has a velocity and also a force is produced on a part of the mechanical system when current flows in the electrical circuit. Under these circumstances, for the steady-state condition, we have:

$$I_1Z_{11} + \dot{X}_2Z_{12} = E_1 \quad \text{. . . . .} \quad (62)$$

$$I_1Z_{21} + \dot{X}_2Z_{22} = F_2 \quad \text{. . . . .} \quad (63)$$

In the special case of pure electrostatic coupling, $Z_{12} = Z_{21}$, and for pure magnetic coupling, $Z_{12} = -Z_{21}$. For proof of this, see McIlwain and Brainerd, *op. cit.*, pp. 465–469.

The simple telephone receiver is an example of an electromechanical system with magnetic coupling. See Fig. 926. Since there is no externally applied mechanical force, F_2 in eq. (63) is zero. Solving eqs. (62) and (63) for the input impedance of the telephone receiver, we have:

$$Z_i = E_1/I_1 = Z_{11} + Z_{12}^2/Z_{22} \quad \text{. . . . .} \quad (64)$$

If $\dot{X}_2 = 0$, $Z_i = Z_{11}$. Therefore, the additional part of the input impedance Z_{12}^2/Z_{22} is known as the motional impedance, since it is due to the movement of the diaphragm. When the motional impedance is known as a function of frequency, an important part of the operating characteristics of telephone receivers and similar devices may be determined. If eddy currents are neglected, the motional impedance plotted as a vector (polar plot) is a circle with its center on the real axis. The eddy currents are usually small, and the actual plot is approximately a circle, but the center does not lie on the real axis. For a complete discussion of the telephone receiver, considering eddy currents, the reader is referred to an article by R. L. Wegel.[62]

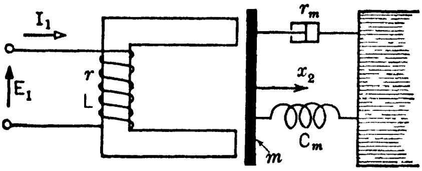

FIG. 926. Electromechanical system equivalent to a simple telephone receiver.

1232. EXPERIMENT 60-J. — Measurements on a Telephone Receiver. — The principal object will be the determination of the motional impedance as a function of frequency. Two runs are necessary: one with the receiver diaphragm free to move, and one with the diaphragm damped. The input impedance of the receiver with the diaphragm free is measured by a bridge method (see Chapter XXVIII) or by the three-voltmeter method (§1218) when the frequency is varied over a range which extends considerably above and below the resonant frequency of the diaphragm. The voltage on the receiver should be maintained constant at the normal value for all readings. Near the resonant frequency where the resistance and reactance components of the input impedance change rapidly, the frequency increments between readings should be smaller.

The diaphragm is then damped by fitting a tight plug into the hole in the receiver cap. The plug should be near the diaphragm, but should not touch since the diaphragm must remain in its equilibrium position. The data are plotted as a function of frequency, and the motional impedance of the telephone receiver is determined by taking the difference between input impedance with diaphragm free and the input impedance with diaphragm damped. Results obtained for a typical receiver are shown in Figs. 927 and 928.

---

[62] R. L. Wegel, *Jour. A.I.E.E.*, vol. 40, p. 791, October, 1921.

1233. Noise Measurement.[63] — Greater appreciation of the psychological and physiological effects of noise has concentrated an increasing amount of attention on noise measurements. The adoption of the A.S.A. Standards[64] covering terminology, methods, and measuring instruments made comparative studies possible for most applications. Noise measurements are of importance to the electrical engineer, not only because of the electrical principles used in the measuring instruments, but also because of the opportunity they afford of improving the design of machinery.

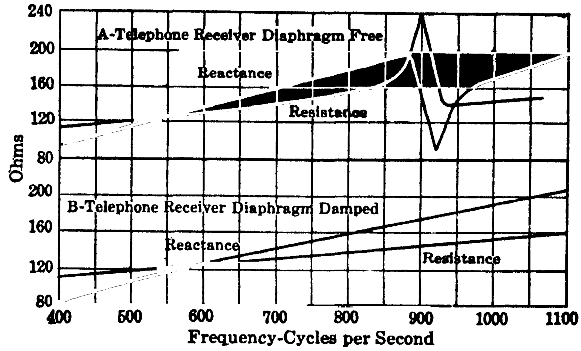

FIG. 927. Variation of telephone receiver impedance with frequency, for damped and undamped diaphragms.

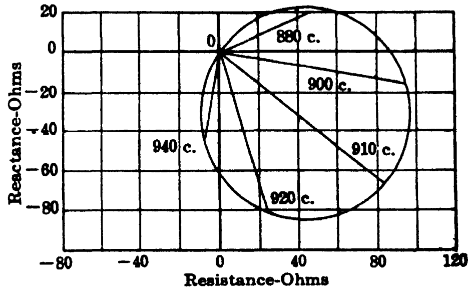

FIG. 928. Motional impedance diagram of a telephone receiver.

Sound levels are measured in decibels with the adopted reference level of 10^{-16} watt per square centimeter at 1000 cycles per second in a free progressive wave. A sound-level meter consists of a microphone, an amplifier, a frequency-weighting network, an attenuator, and an output meter. General specifications and recommendations for the sound-level meter are given in reference 64. For some measurements a vibration pickup is used instead of a microphone to reduce errors due to background noises and to locate more accurately points of origin and transmission of sounds. For most noise analysis the important considerations are location of the noise source, determining the method of transmission, and the cause of the vibration. The complete solution of a noise problem usually requires a knowledge of the amplitude of the different frequency components, necessitating the use of a wave analyzer in connection with the sound-level meter.

---

[63] For a bibliography on noise and noise measurement, see D. Silverman, *Electronics*, February, 1939, p. 34; and H. H. Scott, *General Radio Experimenter*, vol. 11, Nos. 2 and 3, July-August, 1936.

[64] "American Tentative Standards for Noise Measurement," Bulletin Z24.2, 1926, and "A.T.S. for Sound-Level Meters for Measurement of Noise and Other Sounds," Bulletin Z24.3, 1936, published by the American Standards Association.

1234. EXPERIMENT 60-K. — Measurement and Analysis of Machinery Noise. — Using a commercial noise-measuring instrument or one assembled from separate laboratory parts, the student should attempt to make an analysis of the type and cause of noise from some laboratory machine about which design data are available. If a small machine is tested, it should be located in a noise-free room. If the machine is too large to move or for some other reason background noise must be tolerated, either a vibration-type pickup should be used or a correction made. The error to be subtracted from the total noise reading is given by[65]

$$\text{Error in db} = \tfrac{1}{2}\left\{d - 20 \log_{10}\left[2 \sinh (0.1151\, d)\right]\right\} \quad . \; . \; (65)$$

where d is the difference in decibels between the readings for total noise and the reading for background noise alone. If a wave analyzer is available the amplitude of the different frequency components in the noise spectrum should be determined. An attempt should be made to determine the cause of the different noise frequencies and their means of transmission by correlating them with the speed of machine parts. If time permits, some remedial schemes should be tried.

1235. Antenna Measurements. — An antenna is used either as a receiver or as a radiator of electromagnetic energy, and we are accordingly interested in the efficiency with which these functions are performed. This not only is determined by characteristics of the antenna proper, but also is influenced by coupling apparatus. The inductance, capacitance, and resistance of an antenna are distributed, and only equivalent values are ordinarily defined. The resistance of an antenna is made up of the resistance of the antenna conductors, the resistance due to dielectric loss, and the radiation resistance. The last is used to account for the emission of power in the form of electromagnetic waves when current flows in the antenna. For a theoretical treatment of antennas and radiation resistance, the reader is referred to G. W. Pierce, " Electric Oscillation and Electric Waves," Chapter IX, or reference 66.

---

[65] L. E. Packard, *General Radio Experimenter*, vol. 12, No. 7, December, 1937.

The impedance measured between the antenna and ground, or between two points of the antenna, will show a variation between maxima and minima as the frequency is varied over a wide range. The minimum values for a grounded antenna occur when the antenna is approximately an odd multiple of quarter wavelengths long (slightly less for practical antennas). At about this point the antenna reactance passes through zero. The lowest frequency for which the reactance is zero is known as the antenna fundamental. The typical variation of resistance and reactance with frequency for frequencies near the fundamental is shown in Fig. 929.[66] The presence of trees, buildings, and other absorbing structures may alter these values considerably at certain frequencies.

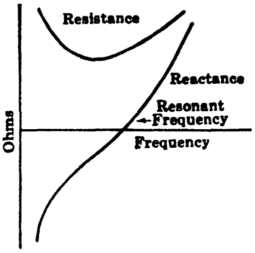

FIG. 929. Resistance and reactance curves for an antenna.

The loop antenna as given schematically by Fig. 930 is important in measurements work, since its constants may be calculated. The induced voltage in the loop is the vector difference of the two voltages induced in the vertical sides. The phase difference θ between E_1 and E_2 is given by:

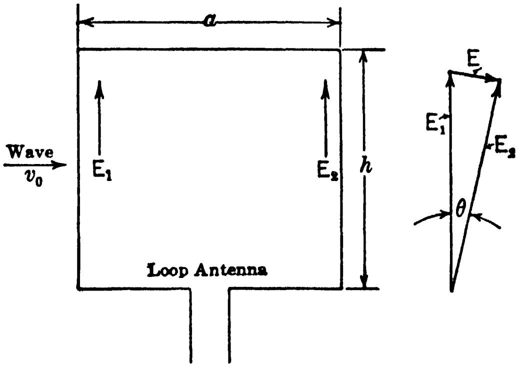

FIG. 930. Voltages induced in a loop aerial.

$$\theta = 2\pi a/\lambda \quad . \; . \; . \; . \; . \; . \; . \; . \; . \; . \; . \quad (66)$$

---

[66] McIlwain and Brainerd, " High-Frequency Alternating Currents," Second Edition, p. 393, John Wiley & Sons.

where λ (the wavelength) $= V_0/f$. By definition, the effective height (h_e) of an antenna is:

$$h_e = E/\varepsilon \quad . \; . \; . \; . \; . \; . \; . \; . \; . \; . \; . \; . \quad (67)$$

where E is the induced voltage and ε is the electrostatic field strength usually expressed in volts or microvolts per meter. For the loop antenna,[67] the effective height is

$$h_e = 2Nh \sin (1.045 \times 10^{-5} af) \quad . \; . \; . \; . \; . \; . \quad (68)$$

where h_e, h, and a are in meters, N is the number of coil turns, and f is the frequency in kilocycles. The loop may be used to measure the effective height of a more complicated type of antenna. With the loop located not less than about 10 wavelengths away from the sending antenna, it is pointed toward the direction of the signal and tuned for resonance. The effective height of the sending antenna is then:[67]

$$h_{es} = 796\ (drI_r)/(h_e f I_s) \quad . \; . \; . \; . \; . \; . \; . \; . \quad (69)$$

where d is distance to the sending antenna in meters, r is the total effective resistance of the loop, I_r is the current in the loop, and I_s is the current in the sending antenna.

1236. EXPERIMENT 60-L. — Measurement of Antenna Impedance. — While physically small antennas are more convenient for laboratory work, accurate measurements at the ultra-high frequencies sometimes require special techniques.[68] When the demonstration of measuring methods as well as typical characteristics are desired, it is well to compromise on the measurement of an antenna that might be suitable for operation at a frequency of about 10 megacycles.

Assuming that a grounded antenna is being measured, the impedance between the lower end of the antenna and ground is measured by a radio-frequency bridge or by measuring separately the resistance and reactance components over a wide frequency range. The reactance may be measured by determining the amount of capacitance or inductance necessary to secure resonance in the antenna at a particular frequency. Resonance may be indicated by a meter in the antenna circuit or by reaction on the oscillator grid or plate current, although the oscillator should not be coupled too closely. The antenna resistance may be measured by the reactance variation or resistance variation method of Experiment 60–F. When desired the results may be checked by using a substitution method described by Terman.[69] Sufficient information will thus be obtained to permit the resistance and reactance curves to be plotted and enable one to calculate the tuning and coupling units necessary to match[70] the antenna to its transmission line properly for a chosen mode of operation.

---

[67] A. Hund, "Phenomena in High Frequency Systems," pp. 468–70, McGraw-Hill Book Co., 1936.

[68] L. S. Nergaard, *RCA Rev.*, October, 1938, p. 139.

1237. Other Experiments. — Only those experiments have been presented here which seem to be of a fundamental nature and emphasize measurement of circuit properties at high frequencies. Many experiments involving applications of high-frequency apparatus require more or less elaborate arrangements and may necessitate several different measuring methods. It is expected that, after performing the experiments outlined in this chapter, the student will have acquired some familiarity with apparatus, a certain amount of technique, and possibly some of the philosophy associated with high-frequency measurements. This should permit the student gradually to assume more of the responsibility for planning his own experiments after a problem has been clearly defined. In view of the rapid developments in radio communication and associated fields, it is especially desirable that some flexibility be provided to permit the performance of a few more extensive investigations in connection with items of current importance.

The current literature provides abundant ideas for some of the more comprehensive laboratory problems. Sources such as *Proceedings of the Institute of Radio Engineers, Electrical Engineering, Wireless Engineer* (British), *Communications, Electronics, Q S T, RCA Review,* and *General Radio Experimenter* will be especially useful. The references throughout the chapter to books devoted particularly to high-frequency measurements should be consulted not only for the specific information cited, but also as a source of other experiments. The list is repeated here for convenience.

H. A. BROWN, Radio Frequency Electrical Measurements, McGraw-Hill Book Co., 1938.

A. HUND, High Frequency Measurements, McGraw-Hill Book Co., 1933.

E. B. MOULLIN, Radio Frequency Measurements, Charles Griffin & Co., 1937.

R. R. RAMSEY, Experimental Radio, Ramsey Publishing Co., 1935.

F. E. TERMAN, Measurements in Radio Engineering, McGraw-Hill Book Co., 1935.

MCILWAIN and BRAINERD, High-Frequency Alternating Currents, Second Edition, John Wiley & Sons, 1939.

---

[69] F. E. Terman, "Measurements in Radio Engineering," p. 273, McGraw-Hill Book Co.

[70] Carl G. Dietsch, *Electronics*, vol. 8, No. 9, p. 280, September, 1935.

INDEX

Numbers refer to pages

Allen and Gross fault locater, 131
Ammeter, phase-sequence, 180
Amplification factor, 714
  measurement of, 721, 729
Amplifiers, class A, 729.
  compensated, 732.
  distortion, 733–735
  gain measurement, 732–733
  impedance-coupled, 730
  meter amplifiers, 763–764
  photocell, 757.
  power measurement, 736
  push-pull, 736
Amplitudes of harmonics, determination of, 658
Anderson bridge, 50
Antennas, 800–802
  constants, 800–803
  loop, 801
  reactance, 801
  resistance, 801
Arc discharge, 744
Armature reaction in synchronous machines, *see* Synchronous machines, *see also* Converters, Motors
Artificial lines, *see* Transmission lines
Attenuation boxes, 791
Attenuators, 791
  calibration of, 792
Audio-frequency measurement, *see* Frequency measurement
Automatic equipment, *see the particular apparatus.*
Auto-transformers, *see* Transformers; Mercury-arc rectifiers, Controllers for induction motors

Beam power tubes, 727
Blondel diagram, 301–321
Blondelion, 309
Blow-out coils, *see* Contactor control
Bohr theory, 677, 738
Boltzmann's constant, 679
Booster, *see* Converter, synchronous
Braking, dynamic, 398, 555
  induction motor, 397
  motor counter-torque, 398
  " plugging," 398.
  regenerative, 398
Braun tube, 643
Breadth factor, 284.
Bridges, a-c, 39–61.
  Anderson, 50.
  balanced, 39–43.
    fundamental equations, 41.
    theory, 41.
  bibliography, 60.
  capacitance, 43, 781–783
  comparison of capacitance and inductance by means of, 49, 51
  comparison of mutual inductance and capacitance by means of, 52.
  comparison of two capacitances by means of, 48.
  comparison of two inductances by means of, 43
  comparison of two mutual inductances by means of, 53.
  Dawes and Hoover, 47.
  fault location method with, 123.
  frequency, 53–58.
    Leeds and Northrup, control of, by, 54.
    with capacitance only, 54.
    with mutual inductance and capacitance, 57.
  Hay, for measurement of iron-cored inductances, 775.
  mutual inductance, 51–53.
  parallel-resistance type, 44.
  Schering, 46.
  shielding in, 58
  triode parameters, 720
  Wagner ground in, 59.
  Wheatstone, 39.
Bullard's method of fault location, 129

Capacitance, 1–38.
  a-c circuits with inductance and, 21–28
  a-c circuits with resistance and, 23 27.
  inductance in parallel with, 29–35
  inductance in series with, 35–38.
  measurement, 9–20.
    a-c bridge method, 43–51.
    direct-discharge method, 9–12.
    loss of charge by leakage method, 17
    measurement by substitution, 781–783
    method of mixtures, 12.
    of a coil at high frequency, 779.
    Thomson zero method, 12.
  physical concept of, 1.
  resistance in series with, 15–17
  transmission line, 65, 75.
  unit of, 2.
  wave form and, 21.

Capacitors, 1.
  in practice, 2.
  capacitive reactance and susceptance, 22.
  relative permittivity, 3, 4.
Cascade connection, 424.
Cascade converters, 450.
Child's law, 690.
Circle diagrams, polyphase induction motor, 379, 407.
  repulsion motor, 508.
  Schrage motor, 541.
  single-phase induction motor, 487.
  single-phase series commutator motor, 493.
  synchronous machines, 277-280.
Commutating poles, high-reluctance, 374.
Commutation, *see* Motors, commutator; Converters, synchronous.
Commutation strips for repulsion-induction motors, 515.
Commutator machines, polyphase, for speed control of polyphase induction motors, 441.
Commutator motors, *see* Motors, commutator, single-phase and polyphase.
Concatenation, 424.
Condensers, absorption in, 9.
  air, 6.
  applications, 2.
  at high frequency, 780.
  calibration of, 12.
  capacitance and phase angle, 781-783.
  capacitance of, 3.
  comparison of, 9.
  connections, 5.
  construction, 1, 3, 18.
  dielectric hysteresis, 10.
  elastance, 8.
  electrolytic, 18-20.
  imperfect, 27, 33.
  loss of charge by leakage, 16-18.
  mica-insulated, 6.
  series and parallel, 6-8.
  standard, 3.
  synchronous, 327.
Contact-making voltmeter, 457.
Contactor control for d-c motors, magnetic, 551-572.
    accelerating switches, 552.
    blow-out, magnetic, 553.
    brake resistance in connection with, 555.
    clapper-type, 553.
    diagrams, how to read, 554.
    dynamic braking, 555.
    electronic devices, 568.
    functions of magnetic switches, 551.
    overload protection, 566.
    starting of motor, automatic, 552.
      lock-out switches, 557.
      push-button, 558, 561.
      various methods, 557.
        counter-emf, 557.
        drop-across resistance, 561.
        series relay, 560.
Contactor control for d-c motors, magnetic, starting of motor, various methods:
        time element, 562-566, 569.
    study of, 566.
    Thyratron speed controller, 570.
    time-delay relay, 568.
    under-voltage protection, 566.
Controllers for induction motors, 573-594.
  across-the-line starters, 573-576.
  auto-transformer starters, 578.
  magnetic-contactor type, 573, 577, 582.
  manually operated, 576, 581.
  protective resistance and reactances, 579.
  push-button control, 575, 584.
  resistance starters in primary circuit, 577.
    electrically operated, 577.
    manual, 576.
    operating coil, 578.
    push button, 578.
  rheostatic control in secondary circuit, 586-594.
    contactor type, 577, 588, 593.
    drum type, 586, 593.
    face-plate type, 576, 586.
    liquid rheostat, 590.
    protection against phase failure, 585.
    protection against phase reversal, 585.
    study of, 585.
    Y-connected type, 582.
Controllers for synchronous motors, 594-598.
  automatic starters, 594.
    full-voltage, 594.
    reduced-voltage, 597.
  bibliography, 598.
  field-application relay, 596.
  power factor removal relay, 595.
  typical circuit diagrams for, 596.
Converters, rotary, generalized, 438.
  synchronous, 350-377.
    armature reaction, 356.
    bibliography, 377.
    booster, 368.
    commutating poles, high-reluctance, 374.
    compounding, 364.
    dampers, 359.
    description, general, 350
    flashing, 374.
    hunting, 375.
    inducted voltages, 352, 359.
      ratio of a-c to d-c, 352-354.
    losses, 370-373.
    operation, inverted, 355.
      polyphase, from a-c side, 362.
    ratio of alternating and direct currents, 354.
    reactive current, 358.
    split-pole, 365.
    starting, 359.
      a-c side, 359-361.
      d-c side, 361.
      polarizing, 360.
      synchronizing, 361.
    voltage regulation and compounding, 364-370.
      booster, 368.
      series field and series-reactance, 365.

Converters, synchronous:
    wave form, 371.
Copper oxide meters, 873.
Coulomb, 1.
Counter-emf method of acceleration, 557.
Crystal oscillator, 767, 770.
Current flow in metals, 678.

Dampers in synchronous converters, 359.
Davisson coordinates, 681–682.
Decibel, definition of, 789.
Delta connection, *see* Polyphase systems.
Dielectric constant, 4.
Dielectric hysteresis, 4, 10.
Diode, parameters, measurement of, 701–702.
  rectification, 702.
Diodes, high-vacuum, definition, 697.
  plate current-voltage relation, 698.
  potential distribution, 698.
  types, 700–701.
Direct armature reaction, *see* Synchronous machines.
Discharge tube, 739–740.
Distributed winding and wave form, 285.
Dufour cathode-ray oscillograph, *see* Oscillographs.

Electrolytic condensers, 18.
Electromechanical systems, 796.
Electron gun, 693.
Electron mass, 677.
  change of, with velocity, 692.
  charge, 677.
Electron motion, in a uniform electric field, 688.
  in a uniform magnetic field, 688.
  in electric and magnetic fields, 688.
Electron optics, 692.
Electron oscillograph, *see* Oscillographs, cathode-ray type.
Electron paths, cycloidal, in electric and magnetic fields, 690.
  trochoidal, in electric and magnetic fields, 691.
Electron theory, *see* Mercury-arc rectifiers; Electronic devices.
Electron tube oscillators, *see* Oscillators.
Electronic devices, fundamentals of, 677–758.
Electrons, Fermi-Dirac distribution, 679.
  in metals, 677.

Farad, 1.
Fault location, 114–137.
  methods of, Allen and Gross, 131.
    Bullard's, 129.
    capacitance tests, 123–125.
    induction localizers, 126.
    Jamieson-Higgitt loop, 123.
    loop tests, *see* Loop tests.
    Lundin, 128.
    single-conductor tests, 115–118.
    tracing-current methods, *see* Tracing-current methods.
    varying-frequency, 131–136.
Filters, for rectifiers, 703.
  properties of, for communication, 787–789.
Fourier's theory, 656.
Four-terminal networks, 788.
Frequency bridges, 53–58.
Frequency converters, commutator-type, 441–443.
  induction-type, 450–455.
Frequency measurement, audio range, 771.
  a-c bridges, used for, 53–58.
  comparative, 768.
  standards, 767.
  standard frequency service for, 764.
  tuned frequency meter, 766.
  ultra high frequency, 774.
Frequency of waves, 657.
Fynn-Weichsel motor, 345–348.
  characteristics, 347.
  starting, 345.
  theory, 345.

Galvanometer, direct-deflection, insulation measurement by, 105.
Gaseous conduction, 737–744.
Geometric capacitance switch, 13.
Gliding field, *see* Revolving magnetic field.
Glow discharge, 742–743.
Grid-glow tube, control characteristics, 748.
Ground detectors, definition of, 95.
  electrostatic, 95–98.
    theoretical relationships, 96–98.
  lamps, 100.
  neon-tube, 98.
  vacuum-tube, 98.
  voltmeters as, 100.
Guard wire for insulation measurements, 110.

Harmonic analysis of periodic waves, 655–676.
  methods, analytical, 666–668.
    Chaffee simplified, 668.
    general, 655, 664.
    graphical, 668.
    instrumental or mechanical, 665.
    separation, experimental, 664.
    tables for, 673–676.
  theory, 656–664.
    amplitudes of harmonics, 658.
    coefficients, determination of, 661.
    equidistant ordinates, 662.
    fundamental rules, 660.
    integration of products, 660.
    sine and cosine components, 658–662.
    sines and cosines of angles, 663, 673–676.
    waves with odd harmonics only, 657.
Harmonics, 249–262.
  induction motors, 467.
  non-triplen, 252.
  oscillating neutral, 251.
  saturation of transformer core and, 253.
    core-type three-phase transformer, 255.
    shell-type three-phase transformer, 255.
    symmetrical *m*-phase system, 261.

Harmonics·
  triplen, 249
    delta-connected windings, currents in, 257
    neutral return, currents in, 256
    Y-connected system, and, 257
  See also Oscillographs, Harmonic analysis of periodic waves
Heterodyne frequency meter, calibration, 769
Higgitt-Jamieson loop 123
High-frequency measurements, 759–803
  meters and apparatus for, 760
High-reluctance interpoles, 374
Ho's circle diagram, *see* Motors, induction, polyphase
Hot-cathode tubes, *see* Oscillographs
Hot-wire vacuum gauges, 603
Hydrogen, energy level of, 738

Ignitron, construction, 753
  principle of, 623, 753
  test of, 753
Impedance, by the three-voltmeter method, 775
  image, 788
Inductance, apparent, measurement of, 779
  incremental, 774–777
  iron-cored coils carrying d-c, 774
  measurement, at high frequencies, 779
    by a-c bridges, *see* Bridges, a-c
  of coils, equivalent circuit including, 778
  resistance of inductance coils at high frequencies, 784
Induction generator, 393–397
  circle diagram, 396
  theory, 394
Induction localizers, 126
Induction machines, operation, abnormal conditions, 399, 460
    abnormal voltages, 399
    as frequency converter, 450
    flux harmonics, 467
    short circuit, 467
    single-phase primary, 475
    single-phase secondary, 461
    unsymmetrical terminal voltages, 399–404
    voltage harmonics, 467
  see also Motors, induction
Induction regulator, 455–461
Inductive coordination, 261
Indumor, 387
Insulation resistance, measurement of, 102–113
    by direct-deflection galvanometer, 105, 106
    by voltmeter, 102, 104, 106
    Megger insulation tester for, 107
    see also Ground detectors, Fault location
Interference, inductive, 261
Interphase transformer, *see* Mercury-arc rectifiers
Interpoles, high-reluctance, 374
Ionization, 739
  potentials, 739
  table, 740

Jamieson-Higgitt loop, 123
Joubertian voltage, 303

Kapp vibrator, 466.
Kraemer system of speed control, 432.

Latour motor, 508
Leakage conductance, 76
Leblanc-Sherbius phase advancer, 438
Line-drop compensator, 457
Loop tests, 118–124
  bridge-loop tests, 121–123
    Bridge-Meg," 123
    Murray loop, 121
    Varley loop, 122
  drop-of potential method, 119–121
  two-ammeter method, 120
  volt-ammeter method, 119
Losses, *see the particular apparatus*
Lundin fault locater, 128

Magnetic contactor control, *see* Contactor control
Magnetic field measured by magnetron, 697
Magnetron, 696
Mass spectrograph, 694
McLeod gauge, 603
Megger insulation tester, 107–112
  compensating coil, 110
  constant-pressure type, 108
  details of construction, 108–110
  fault location by, 123
  guard system, 110
  resistance measurement with, 111
  variable-pressure type, 109
Mercury, energy level, 739
Mercury-arc rectifiers, 600–630, 752
  arc stability, 605
  battery-charging, 607–611
    automatic, 608
    diagram of connections for, 609
    panel, 609
  bibliography, 630
  connections, fundamental, 600, 608
  control grids, 622
  degree of rectification, 606
  hot-wire gauge, 603
  ignitron-type, 623
  inductance, effect of, in anode circuit, 606, 620
  McLeod gauge, 603
  parallel operations, 616
  performance characteristics, 606, 611
    harmonic composition, 624–627
    output voltage, 618
    tables, 621, 625, 627
    transformer output and rating, 619
    voltage pulsations, 618, 622
    wave analysis, 625, 626
  polyphase, 613, 615, 617
  rectification, 602
    theory, advanced, 744, 752
      elementary, 602, 618
  starting, *or* ignition, 602, 608, 610, 614, 623

- Mercury-arc rectifiers:
  - steel-enclosed, 612.
  - temperature, 602.
  - utility factor, 619, 621.
  - vapor tube, voltage drop in, 745.
  - voltage control, 622.
  - voltage drop, 604.
  - voltage ratio, 618.
  - Vreeland oscillator, 627–630.
  - wave forms, 615, 619, 621.
- Merson diagram, 72.
- Metallic conduction, 678.
- Meters, copper oxide, 763.
  - power level, 764.
  - rectifier-type, 763.
  - thermocouple, 761.
  - vacuum-tube voltmeter, 761.
- Mixtures, method of, 14.
- Motors, commutator, polyphase, 524–550.
    - analytical theory, 529.
    - bibliography, 549.
    - Crocker-Wheeler adjustable-speed motor, 542–549.
      - characteristics, 543, 548.
      - emf in rotor, 543.
      - equivalent circuits, 546.
      - speed control, 542–543.
    - electrical connections, 524.
    - emf diagram, 527.
    - mmf diagram, 525.
    - parts, arrangement of, 524.
    - Schrage motor, 533–542.
      - brush shift, 533.
      - characteristics, 537.
        - current, 538.
        - speed range, 537.
        - starting torque, 538.
      - circle diagram, 541.
      - commutator emf, 535.
      - power factor, 536.
      - regeneration, 537.
      - reversing, 537.
      - shunt-connected motor, 525, 532.
      - speed, 536.
      - super-synchronous speed, 536.
      - theory, analytical, 541.
      - vector diagrams of, emf, 540; mmf, 538.
      - winding arrangement, 533.
    - series-connected motor, 525, 530.
    - shunt-connected motor, 532.
  - single-phase, 493–550.
    - commutator-type induction motor, 518–521.
      - phase compensation, 520.
      - reversing, 521.
      - speed control, by armature voltage, 519.
        - by field strength, 520.
      - starting, 521.
    - repulsion motor, compensated, 508–513.
        - analytical theory, 510.
        - armature excitation, 509.
        - brush shift, with, 511.
        - dynamic braking, 512.
- Motors. commutator, single-phase, repulsion motor, compensated:
        - Latour motor, 508.
        - Winter-Eichberg motor, 508.
      - plain, 502–508.
        - circle diagram, 506.
        - one field winding, 504.
        - reversing, 505.
        - starting conditions, 505.
        - theory, analytical, 506.
        - two field windings, 502.
    - repulsion-induction motor, 513–517.
      - commutator strips, 515.
      - power-factor improvement, 515.
      - speed range, 514.
      - vector diagram, 515.
    - series motors, 494–502.
      - armature reaction, composition, 495.
      - circle diagrams, 501.
      - commutation difficulties, 496.
        - emf of current reversal, 496.
        - transformer emf, 497.
      - compensating winding, 495.
      - interpoles, 496, 498.
      - performance, 498.
      - theory, analytical, 499.
      - vector diagram, 499.
    - shunt-type motor, with two sets of brushes, 517.
  - Fynn-Weichsel, 345–348.
  - induction, general, abnormal voltages, 399.
    - braking, 397.
      - dynamic, 398.
      - motor counter-torque, 398.
    - harmonics, 467.
    - starters, *see* Controllers for induction motors.
   - polyphase, 378–469.
     - abnormal voltages in, 467.
     - braking of, 397.
     - characteristics, 379, 386, 388, 390.
       - determination, by alignment chart, 387.
         - by circle diagram, approximate, 379.
           - exact, 413.
         - by equivalent diagram, 383, 399.
         - by Ho's circle diagram, 407.
         - by indumor, 387.
         - by method of tangents, 386.
         - by photographic method, 387.
     - circle diagram, approximate, 378–406.
         - bibliography, 406.
         - characteristics from, 379, 402.
         - primary ohmic drop, correction for, 417.
         - proof of, 378, 404.
       - exact, 407–423.
         - Ho's diagram, 407.
         - proof, 407–413.
         - vector algebra derivation, 415–421.
     - copper losses, 380.
     - power-factor control, 435–448.
       - external emf in secondary, 436.

- Motors, induction, polyphase, power-factor control, external emf in secondary:
          - explanation by equivalent diagrams, 437.
          - means of producing leading emf, 438.
        - Kapp vibrator, 446.
        - phase advancer, 443–447.
          - commutator-type, 441.
          - self-excited, 444.
          - separately excited, 445.
          - series-excited, 444.
      - rotor ohmic and effective resistances, 383.
      - single-phase operation, 475.
      - slip, 380.
      - speed control, 388, 424–449.
        - bibliography, 449.
        - cascade, 424.
          - cumulative, 425.
          - differential, 427.
        - commutator-type frequency converter, 441.
        - concatenation, 424.
        - electronic controller, 435.
        - external emf in secondary, 428–435.
          - classification of methods, 431.
          - explanation of equivalent diagram, 430.
          - generalized rotary converter, 438.
          - polyphase commutator machine, 433, 440.
        - Kraemer system, 432.
        - Sherbius system, 432.
      - single-phase rotor, operation with, 461–467.
      - synchronous watts, 414.
      - torque, 381.
      - unsymmetrical voltages, 399.
        - solution by symmetrical components, 399.
    - single-phase, 470–492.
      - bibliography, 492.
      - characteristics, 472.
      - circle diagram, 487–491.
        - equation of locus, 491.
        - fundamental equations, 488.
        - primary current, solution for, 490.
      - copper loss, secondary, 474.
      - commutator-type, 518.
      - magnetizing current, 473.
      - oppositely rotating mmf's, theory, 470.
      - quadrature-flux theory, 480–492.
        - emf's of pulsation and rotation, 481–484.
        - fundamental conditions, 487.
        - generator action, 485.
        - rotating magnetic field, 485.
        - transformer action, 484.
  - synchronous, 323–349.
    - bibliography, 348.
    - damper winding, 338.
    - circular loci, 328–330.
    - hunting, 337–339.
    - load characteristics, 325–332.
      - Potier diagram, 328.

- Motors, synchronous, load characteristics:
      - torque angle and synchronizing power, 334–336.
    - no-load characteristics, 325.
    - operating features, 325–332.
    - physical phenomena, explanation for, 323.
    - Potier diagram for, 328.
    - pull-out torque, 335.
    - reaction machine, 326.
    - simplex motor, 343.
    - squirrel-cage winding for, 338.
    - stability, 330.
    - starting, 339–345.
      - characteristics, 343.
      - connections, 342, 345.
      - induction start, 341, 344.
      - Korndorfer method, 343.
    - synchronous condenser, as, 327, 332.
    - theory, 323, 325.
    - torque angle, 334–337.
    - vector diagrams, 325–329.
    - V-curves, 327–332.
- Multielectrode tube, parameters of, 728.
  - types, 723.
- Multivibrator, 767.
- Murray loop, 121.
- Mutual conductance, definition, 715.
  - measurement of, 722.

- Nagaoka, formula for inductance, 778.
- Neon lamp, 98, 647.
- Neo-time relay, 569.
- Neper, definition, 789.
- Networks, four-terminal, 788–789.
  - characteristics of, 793–796.
  - equivalent, 790.
- Noise measurement, 799, 800.

- Optical pyrometer for cathode temperature, 683.
- Oscillators, audio frequency, 765.
  - laboratory-type, 764.
  - standard-frequency, 764.
  - vacuum-tube, 764.
- Oscillographs, 631–653.
  - applications, 631.
  - bibliography, 653.
  - cathode-ray type, 643–653.
    - Braun tube, 643.
    - Dufour type, 649.
    - General Radio type, 646.
    - hot-cathode type, 645.
    - Norinder relay, 651.
    - time-deflection control methods, 647, 652.
      - neon lamp, 647.
      - revolving mirror, 634, 636, 640.
      - sweep-frequency control, 647.
  - classification, 632.
  - demonstration oscillograph, 639.
  - Dufour cathode-ray type, 649.
  - electromagnetic type, 633–643.
    - circuits, electric, 636.
    - galvanometer, 633.
      - vibrating strips, 633.

Oscillographs, electromagnetic type:
    optical system, 634, 636.
    recording apparatus, 635.
    string-galvanometer, 637.
    study of, 642.
    transient visualizer, 638.
    vacuum-tube amplifier, 641.
    vibrator constants, 641.

Pascal's limaçon, 315.
Pentodes, 725, 726.
  static characteristics of, 726.
Permeability, incremental, 774.
Permittivity, relative, 4.
Phase advancer, 443–447.
  commutator-type, 441.
  Leblanc-Sherbius, 438, 443.
  self- or series-excited, 444.
  separately excited, 444.
Phase angle, of condenser, 781.
  of four-terminal networks, 795.
Phase modifier, 460.
Phase shifter, 460.
Pitch factor, 285.
Photocell, amplifier for, 757.
  high-vacuum characteristics, 687.
  measurement of spectral response, 756.
  test of gas-filled, 756.
  types, 754–755.
Photoelectric cell, characteristics, 686.
Photoelectric emission, Einstein photoelectric equation, 685.
  spectral sensitivity, 685.
  surface photoelectric effect, 684.
  threshold frequency, 685.
Phototube, *see* Photocell.
Photovoltaic cell, 755.
  test of, 756.
Photronic cell, 755, 756.
Piezo oscillators, 767, 770.
Planck's constant, 685.
Plate resistance of triode, definition, 715.
  measurement, 722.
  of multielectrode tube, 729.
Poisson's law, 699.
Polyphase commutator motors, *see* Motors, commutator, polyphase.
Polyphase induction motors, *see* Motors, induction, polyphase.
Polyphase systems, 138–262.
  advantages, 138.
  definition, 138.
  delta-connection, 205–211.
    equivalent balanced Y, 206.
    equivalent unbalanced Y, 209–211.
    notation, current and voltage, 205.
    tertiary winding, 231.
    theory, 205–209.
    unbalanced, 207–211.
      circulating currents, 208.
  diametrical connection, 242.
  double-delta connection, 242.
  double-T connection, 243.

Polyphase systems:
  double-V connection, 243.
  mesh connection, 241.
  open-delta connection, *see* Polyphase systems, V connection.
  phase sequence, negative or inverse, 167, 176.
    positive, 166, 175.
  power in three-phase systems, 190–203.
    measurement, reactive component wattmeter, 198–203.
      single-wattmeter method, 196.
      three-wattmeter method, 191.
      two-wattmeter method, 192–198.
      watt-ratio curve, 193–195.
    positive-sequence and negative-sequence, 186–188.
  quarter-phase systems, 227–229.
    mesh-connected, 228.
    star-connected, 227.
  T-connection, 216, 234–237, 243–245.
    generators with, 216.
    theory, 216.
    transformers with, 218–221.
    voltage unbalance, 219, 235.
  three-phase, advantages, 138.
    balanced load, 139.
    balanced voltages, 139.
    equivalent single-phase line, 141.
    paralleling three-phase transformers, 233.
    phase rotation, *see* phase sequence.
  phase sequence, 147, 160.
      ammeters, 180–185.
      determination by:
        inductive load, 147.
        oscillograph, 149.
        phase-sequence voltmeter, 174–180.
        wattmeter readings, by, 147.
        three-phase load, 148, 155.
      voltmeters, 147, 174–180.
    superimposed transmission, 259.
    turning operator, *h*, 162.
    types, 138.
    unbalanced three-phase system, 142–159.
      resolution into balanced components, 142, 161.
      components, determination of, 161.
      turning operator, *h*, 162.
      uniphase component, 160.
  transformations, 230–248.
    energy relations, 246.
    general transformations, 245.
    polyphase to single phase, or vice versa, 247.
    Scott connection, 234.
    six-phase system, 239–245.
    three-phase to three-phase, 230.
    two-phase or three-phase into six-phase or twelve-phase, 240–245.
      diametrical connection, 242.
      double-delta connection, 242.
      double-T connection, 243.
      double-V connection, 243.
      mesh connection, 241.
      star connection, 241.

Polyphase systems, transformations
    two-phase to three-phase, 234–239
        Scott connection, 234
        Taylor connection, 238
        unbalancing of voltages, 235
        various methods of, 237
  V-connection, 212–216
    generators with, 212
    relations in, 212
    solution by symmetrical components 215
    theory, 212–216
    transformers with, 213
    unbalanced, general case of, 214
  Y-connection, 139–159
    equivalent balanced delta, 206
    equivalent unbalanced delta, 145, 209, 211
    notation, current and voltage, 142
    symmetrical Y-system, 139
    unbalanced Y-system, 144–158
        mutual inductance, effect of, 157
        neutral-voltage method, 149–157
        principle of superposition, 151
        reversed neutral voltage method, 152
        solution by Kirchhoff's laws, 144
        study of symmetrical components in, 172
Potier diagram, 265–276
Potieron, 276
Power emission chart, 682
Power factor, *see the particular apparatus*
Power-factor correction, *see* Fynn-Weichsel motor, Motors, synchronous, Converters, synchronous
Power level indicator, 792, 793
Power level meters, 764
Power supplies, high-frequency, 765
Propagation constant, 80, 83
Propagation of waves, velocity of, 135

Quadrature-flux theory of single-phase induction motors, 480–492
Quarter-phase systems, *see* Polyphase systems

Radio, *see* Electronic devices, High-frequency measurements
Reactance, capacitive, 22
Reactance variation method of measuring resistance, 784
Reactors, current-limiting, 579
Rectifier circuits, single-phase, bridge type, 705
  single-phase full-wave, 703
  single-phase half-wave, 703
  three-phase, double-Y, 708
    full-wave, 709
    half-wave, 705
  voltage doubling, 705
Rectifiers, copper oxide, 350, 569, 595
  filter design, 706
  gaseous, 744
  grid-controlled, *see* Thyratron
  measurement of hum percentage, 745
  measurement of regulation, 745
  mercury-arc, *see* Mercury-arc rectifiers
  ripple voltage, 704
Rectifiers:
  steel-enclosed, *see* Mercury-arc rectifiers
  table, 707
  test of three-phase, 709
  thermionic, *see* Electronic devices
  vacuum-tube, *see* Electronic devices
Regenerative braking, 398
Regulation, *see special apparatus involved*
Regulators, induction, 455–461
  polyphase, 459
  single-phase, 455
Resistance, conductor at high frequencies, 783
  high-frequency, measurement of, 784
  high resistance at high frequencies, 786
Resonance, current, 29–35
    partial, 32
    perfect, 30
  voltage, 35–38
Revolving magnetic field, 286
  harmonics of, higher, 283
  polyphase, 286–289
  single-phase motors, in, 485, 518
  see also Motors, commutator, Motors, induction, Converters, synchronous
Richardson Dushman equation, 679
Rotary converter, generalized, 438
Rotary converters, 350–377, *see also* Converters, synchronous

Sherbius machine, 432
Schering impedance bridge, 46
Schrage motor, 533
Scott connection 234 *see also* Polyphase systems, transformations
Series a-c motors, polyphase, 525
  single-phase 494
Short-circuit tests, *see the particular apparatus*
Shunt-type a-c motors, polyphase, 532
  single-phase, 517
Six phase system, 239–245
Spark gap in surge generator, 651
Speed control, of commutator type induction motors, 519
  of polyphase induction motors, *see* Motors, induction, polyphase
Standard-frequency generators, 765
Standard-frequency service, 765
Standard-frequency source to calibrate frequency meter, 769
Starters, *see the particular apparatus*
Steel-enclosed rectifiers, *see* Mercury-arc rectifiers
Stroboscope to measure frequency, 772
Super-synchronous motor, 340
Superposition, principle of, proof of Ho's circle diagram by, 409
Surge impedance, 80, 93
Symmetrical components, analytical determination of, 163
  general case, 164
  generators, phase-sequence, 173
  graphical determination of, 165
  impedances, of, 168

Symmetrical components:
  methods of measurement, 174–189.
    bridge-type sequence network, 182.
    phase-sequence ammeters, 180.
    phase-sequence voltmeters, 174.
    simultaneous reading of opposite sequence components, 177.
    zero-sequence component of current, 185.
    zero-sequence component of voltage, 179.
  negative-sequence component, 160.
  positive-sequence component, 160, 180.
  problems, solution by, 179, 215, 399, 461, 475.
    parallel delta- and T-connected transformer banks, 219.
    three-phase motor with single-phase rotor, 461.
    three-phase motor with single-phase supply, 475.
  uniphase component, 160.
  unsymmetrical three-phase system in, 166.
  zero-sequence component, 160.
Synchronizing, *see the particular apparatus.*
Synchronizing power, 268.
Synchronous condensers, 327.
Synchronous converters, 350–377; *see also* Converters, synchronous.
Synchronous machines, with non-salient poles, 263–281.
    armature reaction of, 266.
    locus diagram of unsaturated machine, 271.
      armature current constant, 271.
      field current constant, 271.
      power, constant, 272.
        electric, 272.
        mechanical, 272.
      power factor, constant, 272.
      phase angle notation, 264.
      Potier diagrams, 265–276; transformation of, 270.
      torque angle and synchronizing power, 268, 308, 334.
    with salient poles, 282–322.
      armature reaction, 282–300.
      direct component, 289, 292, 296.
        experimental determination with d-c, 293.
      transverse component, 288–291.
        coefficient of, 292, 294.
        measurement of, 297.
    Blondel diagram, 301–326.
      analytical solution, 307.
      comparison with graphical, 306.
      special cases, 305.
      theory, 301–304.
    Blondelion, 309.
    locus diagrams of saturated machine, 311–321.
      armature current and excitation constant, 315.
      field current and direct armature reaction constant, 309.
      influence of armature resistance, 318.
      leakage reactance variable, 318.
Synchronous machines, with salient poles, armature reaction, locus diagrams of saturated machine:
      power constant, 316.
      sectionalized saturation curve, 311.
      torque angle as affecting power, 268, 308, 334.
Synchronous motors, 323, 349, *see also* Motors, synchronous.
Synchronous reactance and impedance, 271

Taylor connection, 238.
Teaser phase, 234.
Teaser transformer, 234
Telephone receiver, circle diagram of, 799.
  electromechanical system, 797.
  measurements on, 798, 799.
  motional impedance, 798.
Tertiary winding, 231.
Testing, *see the particular apparatus.*
Tetrodes, 723.
  static characteristics, 726.
Thermionic cathodes, *see* Cathodes.
Thermionic emission, 678
Thermocouples, emf as a function of temperature, 760.
  meters, *see* Meters.
Thompson theory of gaseous discharge, 741.
Thomson method of measuring capacitance, 12.
Thyratron, amplitude control, 750.
  construction, 746.
  control characteristics, 746.
  grid control, 747, 748.
  motor speed controlled by, 570.
  operation with a-c plate voltage, 749.
  phase control, 751.
  plate current flow, 749.
Torque angle, 268.
Torsance, term, 305.
Townsend, gaseous discharge, 741.
Tracing current methods of fault location, 125–131.
  Bullard's, 129.
  current transformer used in, 127.
  exploring coil, longitudinal, 128.
  Lundin fault locater, 128.
  magnetic needle, 126.
  sheath-potential, 126.
  shoes, metal, 126.
Transformers, circulating currents in, 208.
  general a-c, 452.
  paralleling three-phase, 219, 233.
  T-connection of, 234–237.
  tertiary delta winding, 231.
  V-connection of, 213–216.
Transient visualizer, 638.
Transmission lines, a-c, artificial, 74, 79, 90.
      tests, 74, 90.
    bibliography, 93.
    circular loci, 281.
    constants, attenuation, 84.
      capacitance, 65, 75.
      concentrated, 65, 75.
      determination of, 64, 89.

- Transmission lines, a-c, constants:
    - distributed, 76, 787.
    - leakage conductance, 76.
    - surge admittance, 81.
    - surge impedance, 80, 93.
    - wave-length constant, 84.
  - current along line, 76, 78.
  - fundamental equations, 78.
  - general relations, 63.
  - graphical methods of calculation, 70.
  - half-wave lines, 91–93.
  - hyperbolic functions replaced by series, 88.
  - line equivalent of load, 83.
  - long and short lines, 62.
  - methods of computation, 84.
  - nominal π and T circuits, 60.
  - Perrine-Baum diagram, 71.
  - propagation constant, 80, 83.
  - quarter-wave lines, 91–93.
  - summary of equations, 86.
  - superiority of three-phase, 62.
  - vector diagrams, constants lumped, 63, 66.
  - voltage along line, 78.
  - voltage regulation, analytical solution, 66, 84.
    - curves, 69, 70.
    - definition, 63.
    - factors involved, 63.
- d-c, artificial, tests, 82.
  - theory of, 82.
  - voltage regulation, 82.
- Transverse armature reaction, *see* Synchronous machines.
- Triodes, a-c plate resistance, 715.
  - d-c plate resistance, 715.
  - amplification factor, 714.
  - dynamic characteristics, 717.
  - graphical determination of plate current, 718.
  - high-vacuum, 710.
  - impedance load, 719, 720.
  - load line, 718.
  - measurement, of mutual conductance, 722.
    - of plate resistance, 722.
  - mutual conductance, 714.
  - parameters, definitions of, 714, 715.
  - plate current equation, 713, 714.
    - Taylor's series for, 734.
  - potential distribution in high-vacuum, 710.
  - static characteristic, 711, 715.
- Tungsten, distribution of free electrons in, 679.
  - spectral distribution of thermal radiation, 759.
- Two-phase systems, *see* Polyphase systems.

- V-connection, *see* Polyphase systems.
- V-curves, 327–332; *see also* Motors, synchronous.
- Vacuum-tube oscillators, *see* Oscillators.
- Vacuum tubes, *see* Diodes; Pentodes; Tetrodes; Triodes; Thyratrons.
  - multielectrode, 723.
  - symbols, 712.
- Varley loop, 122.
- Vector analysis, application, to circle diagram of the polyphase induction motor, 415–421.
    - to circle diagram of single-phase induction motors, 491.
    - to circle diagram of single-phase series commutator motors, 501.
    - to circle diagram of the repulsion motor, 506.
    - to theory of compensated repulsion motor, 510.
  - circle equation, 415.
  - definition, 415.
  - scalar product, 415.
- Vector diagrams, *see the particular apparatus.*
- Voltage regulation of transmission lines, 66, 84.
  - curves, 69, 70.
  - definition, 63.
- Voltmeter, contact-making, 457.
  - phase-sequence, 174–180.
- Vreeland oscillator, 627–630.

- Wattmeters, reactive-component, 198–203
- Wavemeters, 766, 767.
  - calibration of, 769.
- Wave shape, in converters, 371.
  - in mercury-arc rectifiers, 615, 619, 621.
- Wheatstone bridge, uses, a-c circuits, 39.
    - hot-wire vacuum gauges, 603.
    - Megger, 112.
    - phase-sequence ammeter, 182.
- Winter-Eichberg motor, 508.
- Work function, definition, 679.
  - table, 680.

- Y-connection, *see* Polyphase systems.